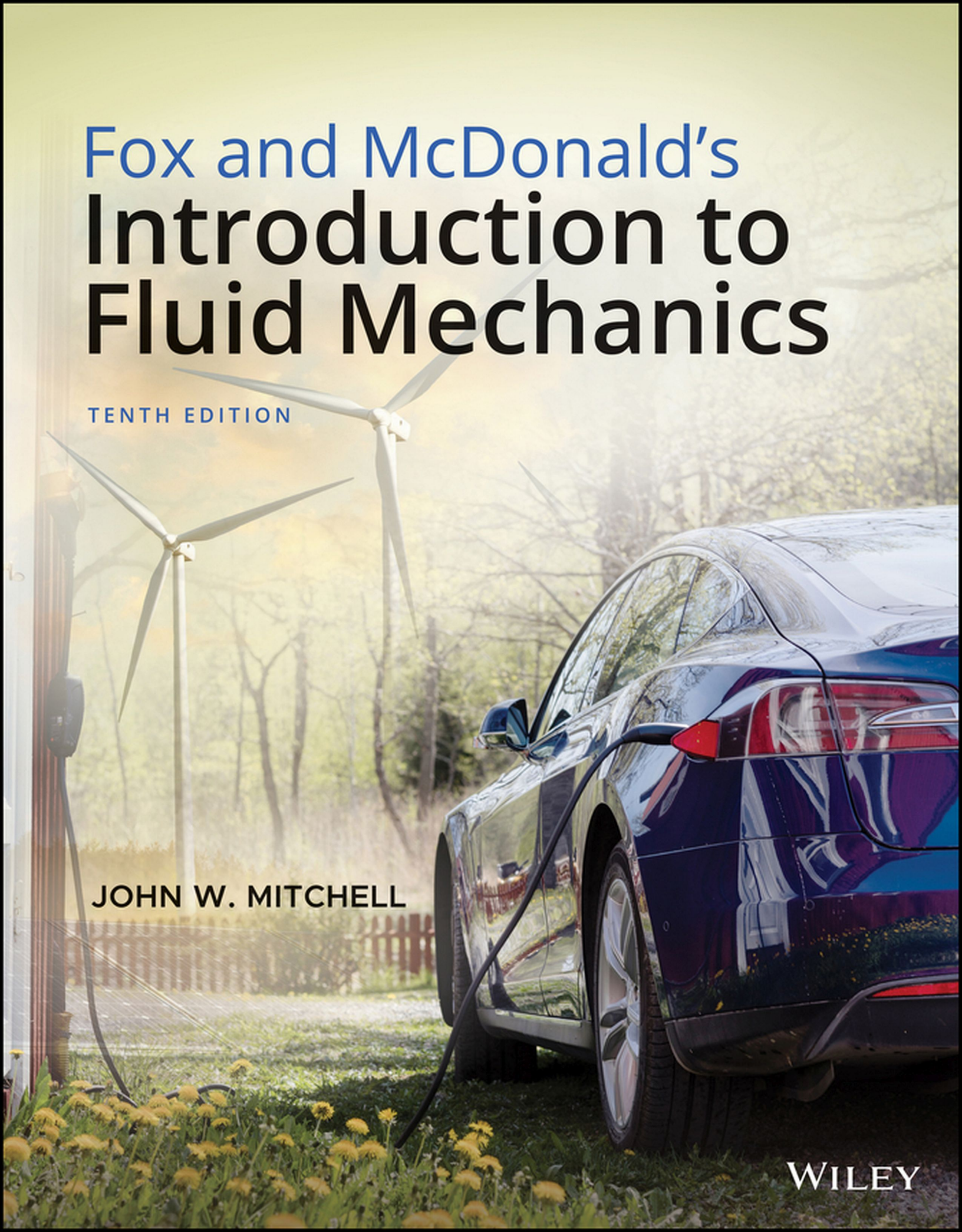


Fox and McDonald's Introduction to Fluid Mechanics

TENTH EDITION



JOHN W. MITCHELL

WILEY

FOX AND MCDONALD'S

Introduction to Fluid Mechanics

10th Edition

John W. Mitchell *University of Wisconsin-Madison*

WILEY

VICE PRESIDENT AND DIRECTOR Laurie Rosatone
SENIOR DIRECTOR Don Fowley
EDITOR Jennifer Brady
EDITORIAL MANAGER Judy Howarth
CONTENT MANAGEMENT DIRECTOR Lisa Wojcik
CONTENT MANAGER Nichole Urban
SENIOR CONTENT SPECIALIST Nicole Repasky
PRODUCTION EDITOR Padmapriya Soundararajan
COVER PHOTO CREDIT © Johner Images/Getty Images, © artjazz/Shutterstock

This book was set in 10/12 STIX SPi Global and printed and bound by Quad Graphics.

Founded in 1807, John Wiley & Sons, Inc. has been a valued source of knowledge and understanding for more than 200 years, helping people around the world meet their needs and fulfill their aspirations. Our company is built on a foundation of principles that include responsibility to the communities we serve and where we live and work. In 2008, we launched a Corporate Citizenship Initiative, a global effort to address the environmental, social, economic, and ethical challenges we face in our business. Among the issues we are addressing are carbon impact, paper specifications and procurement, ethical conduct within our business and among our vendors, and community and charitable support. For more information, please visit our website: www.wiley.com/go/citizenship.

Copyright © 2020, 2015, 2011, 2006 John Wiley & Sons, Inc. All rights reserved. No part of this publication may be reproduced, stored in a retrieval system, or transmitted in any form or by any means, electronic, mechanical, photocopying, recording, scanning or otherwise, except as permitted under Sections 107 or 108 of the 1976 United States Copyright Act, without either the prior written permission of the Publisher, or authorization through payment of the appropriate per-copy fee to the Copyright Clearance Center, Inc., 222 Rosewood Drive, Danvers, MA 01923 (Web site: www.copyright.com). Requests to the Publisher for permission should be addressed to the Permissions Department, John Wiley & Sons, Inc., 111 River Street, Hoboken, NJ 07030-5774, (201) 748-6011, fax (201) 748-6008, or online at: www.wiley.com/go/permissions.

Evaluation copies are provided to qualified academics and professionals for review purposes only, for use in their courses during the next academic year. These copies are licensed and may not be sold or transferred to a third party. Upon completion of the review period, please return the evaluation copy to Wiley. Return instructions and a free of charge return shipping label are available at: www.wiley.com/go/returnlabel. If you have chosen to adopt this textbook for use in your course, please accept this book as your complimentary desk copy. Outside of the United States, please contact your local sales representative.

ISBN: 978-1-119-61649-8 (PBK)
ISBN: 978-1-119-61657-3 (EVALC)

Library of Congress Cataloging in Publication Data:

Names: Fox, Robert W., 1934–2014, author. | Mitchell, John W., author.
Title: Fox and McDonald's introduction to fluid mechanics / John W. Mitchell, University of Wisconsin-Madison.
Other titles: Introduction to fluid mechanics
Description: 10th edition. | Hoboken : Wiley, 2020. | Includes bibliographical references and index.
Identifiers: LCCN 2019041375 (print) | LCCN 2019041376 (ebook) | ISBN 9781119616498 (paperback) | ISBN 9781119616566 (adobe pdf) | ISBN 9781119603764 (epub)
Subjects: LCSH: Fluid mechanics.
Classification: LCC TA357 .F69 2020 (print) | LCC TA357 (ebook) | DDC 620.1/06—dc23
LC record available at <https://lccn.loc.gov/2019041375>
LC ebook record available at <https://lccn.loc.gov/2019041376>

The inside back cover will contain printing identification and country of origin if omitted from this page. In addition, if the ISBN on the back cover differs from the ISBN on this page, the one on the back cover is correct.

Preface

Introduction

This text is written for an introductory course in fluid mechanics. Our approach to the subject emphasizes the physical concepts of fluid mechanics and methods of analysis that begin from basic principles. One primary objective of this text is to help users develop an orderly approach to problem solving. Thus, we always start from governing equations, state assumptions clearly, and try to relate mathematical results to corresponding physical behavior. We emphasize the use of control volumes to maintain a practical problem-solving approach that is also theoretically inclusive.

Proven Problem-Solving Methodology

The Fox-McDonald solution methodology used in this text is illustrated in numerous examples in each chapter, with each one picked to illustrate an important aspect. Solutions presented in the examples have been prepared to illustrate good solution technique and to explain difficult points of theory. Examples are set apart in format from the text so that they are easy to identify and follow. Additional important information about the text and our procedures is given in “Note to Students” in Section 1.1. We urge you to study this section carefully and to integrate the suggested procedures into your problem-solving and results-presentation approaches.

SI and English Units

SI units are used in about 70 percent of both example and end-of-chapter problems. English Engineering units are retained in the remaining problems to provide experience with this traditional system and to highlight conversions among unit systems.

Goals and Advantages of Using This Text

Complete explanations presented in the text, together with numerous detailed examples, make this book understandable for students, freeing the instructor to depart from conventional lecture teaching methods. Classroom time can be used to bring in outside material, expand on special topics (such as non-Newtonian flow, boundary-layer flow, lift and drag, or experimental methods), solve example problems, or explain difficult points of assigned homework problems. Thus, each

class period can be used in the manner most appropriate to meet student needs.

When students finish the fluid mechanics course, we expect them to be able to apply the governing equations to a variety of problems, including those they have not encountered previously. We particularly emphasize physical concepts throughout to help students model the variety of phenomena that occur in real fluid flow situations. Although we collect useful equations at the end of each chapter, we stress that our philosophy is to minimize the use of so-called “magic formulas” and emphasize the systematic and fundamental approach to problem-solving. By following this format, we believe students develop confidence in their ability to apply the material and to find that they can reason out solutions to rather challenging problems.

The book is well suited for independent study by students or practicing engineers. Its readability and clear examples help build confidence. Answers to selected problems are included, so students may check their own work.

Topical Coverage

The material has been selected carefully to include a broad range of topics suitable for a one- or two-semester course at the junior or senior level. We assume a background in rigid-body dynamics, mathematics through differential equations, and thermodynamics.

The text material is organized into broad topic areas:

- Introductory concepts, scope of fluid mechanics, and fluid statics (Chapters 1, 2, and 3)
- Development and application of control volume forms of basic equations (Chapter 4)
- Development and application of differential forms of basic equations (Chapters 5 and 6)
- Dimensional analysis and correlation of experimental data (Chapter 7)
- Applications for internal viscous incompressible flows (Chapter 8)
- Applications for external viscous incompressible flows (Chapter 9)
- Analysis of fluid machinery and system applications (Chapter 10)

- Analysis and applications of open-channel flows (Chapter 11)
- Analysis and applications of one-dimensional compressible flows (Chapter 12)

Chapter 4 deals with analysis using both finite and differential control volumes. The Bernoulli equation is derived as an example application of the basic equations to a differential control volume. Being able to use the Bernoulli equation in Chapter 4 allows us to include more challenging problems dealing with the momentum equation for finite control volumes.

Another derivation of the Bernoulli equation is presented in Chapter 6, where it is obtained by integrating Euler's equation along a streamline. If an instructor chooses to delay introducing the Bernoulli equation, the challenging problems from Chapter 4 may be assigned during study of Chapter 6.

Text Features

This edition incorporates a number of features that enhance learning:

- **Learning Objectives:** A set of specific Learning Objectives has been developed for the material in each chapter. These are a set of testable specific skills and knowledge that a student should be able to achieve after completing the material in the chapter. Representative questions designed to test whether the student has, in fact, achieved those skills and knowledge is on the Instructor Companion website.
- **Chapter Summary and Useful Equations:** At the end of each chapter, we summarize the major contributions the material has made to meeting the Learning Objectives. Also, as indicated previously, we provide a list of equations that are most commonly used in problem solving.
- **End-of-Chapter Problems:** Problems in each chapter are arranged by topic and grouped according to the chapter section headings. Within each topic they generally increase in complexity or difficulty. This makes it easy for the instructor to assign homework problems at the appropriate difficulty level for each section of the book.
- **Fluid Mechanics Concept Inventory:** The Fluid Mechanics Concept Inventory (FMCI) was developed under an NSF grant to the Foundation Coalition by faculty at the University of Wisconsin (J. Martin and J. Mitchell) and the University of Illinois (A. Jacobi and T. Newell). The inventory is used to a) evaluate whether students understand fluids concepts as opposed to be able to do calculations, and b) improve the teaching of fluids to correct student misconceptions.
- **Design and Open-ended Problems:** Where appropriate, we have provided open-ended design problems. Students could be assigned to work in teams to solve these problems. These problems encourage students to spend more time exploring applications of fluid mechanics principles to

the design of devices and systems. These design problems are available on the Instructor Companion website for many chapters.

New to This Edition

This edition has been edited significantly and incorporates a number of changes to previous editions:

- **End of Chapter Problems:** Approximately 5 new problems have been authored for each chapter and roughly 50% of the problems have been revised or updated. The number of problems at the end of each chapter has been significantly reduced and selected to illustrate the important aspects of the material. The end-of-chapter problems that have been removed from the previous edition are available on the Instructor Companion website.
- **Instructor-only Problems:** Approximately 25 % of the problems have been set aside as Instructor-only problems that can be assigned at the discretion of the instructor. These are mostly new problems developed for this edition.
- **Show/Hide Solutions:** Approximately 15 % of the problems in the enhanced ebook feature solutions behind show/hide buttons. This feature will allow students to check the intermediate steps of their work.
- **Case Study:** Each chapter is introduced with a Case Study that illustrates the application of the material in the chapter. Most of the case studies in the previous edition have been updated and replaced with more recent applications.
- **Videos:** For many of the chapter subjects, short videos are available that illustrate a specific phenomenon. These videos, which are available in the enhanced ebook, are indicated by an icon in the margin of the text. We also include references to much more extensive collections of videos on a wide range of fluid mechanics topics.
- **References:** The end-of-chapter references have been updated and edited to give the current references most relevant to the material.
- **Computational Fluid Dynamics (CFD):** The material on CFD has been updated to reflect the current state of the art and moved to an appendix with current references.

Additional Resources in the Enhanced Ebook:

The following resources are available for students enrolled in classes that use the enhanced ebook.

- **Excel Files:** The Excel files used to solve examples in the text are available on the Student Companion Website. These files can be used to explore the solution further or as a guide to the development of new solutions using Excel.
- **A Brief Review of Microsoft Excel:** This is an online tutorial prepared by Philip Pritchard that will aid students in using Excel to solve the end-of-chapter problems.

- **Supplemental Chapter 12 Content:** This is advanced material relevant to Chapter 12 Introduction to Compressible Fluid Flow.

Resources for Instructors

In addition to the materials available to students, the following resources are available to instructors who adopt this text on the Instructor Companion Website at www.wiley.com/go/mitchell/foxfluidmechanics10e

- **Solutions Manual:** The solutions manual contains a detailed solution for all homework problems. The expected solution difficulty is indicated, and each solution is prepared in the same systematic way as the example solutions in the printed text. Each solution begins from governing equations, clearly states assumptions, reduces governing equations to computing equations, obtains an algebraic result, and finally substitutes numerical values to obtain a quantitative answer. Solutions may be reproduced for classroom or library use, eliminating the labor of problem-solving for the instructor.
- **Learning Objective Assessment Questions:** These are questions designed to directly assess whether students have achieved the Learning Objectives of the chapter. These can be used in in-class discussions and assigned homework.
- **Problem Key:** The key provides the correspondence between the problems in this tenth edition and those that were renumbered from the ninth edition.
- **PowerPoint Lecture Slides:** Lecture slides outline the concepts in the book and include appropriate illustrations and equations.
- **Image Gallery:** Illustrations are taken from the text in a format appropriate to include in lecture presentations.
- **Sample Syllabi:** Syllabi appropriate for use in teaching a one-semester course in fluid mechanics are provided. First-time instructors will find these a helpful guide to creating an appropriate emphasis on the different topics.
- **Instructor-only Problems:** These are usually new problems that are available to the instructor only and that can be assigned as new challenges to the students.
- **Design Problems:** A set of open-ended design problems have been developed for appropriate chapters. They are designed to integrate material in the chapter and would

be expected to take one to two weeks of homework time for students working in small teams.

- **Supplemental Chapter 12 Content:** This is the material on Fanno flow, Rayleigh flow, and two-dimensional compressible flow that had been developed for previous editions.

Acknowledgments

This tenth edition continues the evolution of this classic text to meet the needs of students and instructors in fluid mechanics. It continues the tradition of providing a pedagogically sound introduction to the subject of fluids as created by the original authors, Robert Fox and Alan McDonald. Their focus on fundamentals provides a base for students who take only one course in fluids or who continue their studies. The basic aspects covered give students an introduction to the application of fluid mechanics in practice, and the focus on basic principles gives a solid foundation for further study.

Even though the original authors have not been involved with the later editions, we have tried to preserve their enthusiasm for the subject and their personal insights into fluid behavior. Their comments add a dimension not normally found in textbooks and enhance students' understanding of this important subject.

Over the years, many students and faculty have provided recommendations and insight that have shaped the subsequent editions of this book. The current edition thus contains the input of many instructors and researchers in the fluids field that supplements and supports the approach of the original authors.

It is not possible to acknowledge all of the contributors individually, but their collective efforts have been crucial to the success of this text. Most recently, Philip J. Pritchard, the author of the previous edition, introduced many significant improvements and developed the extensive Excel spreadsheets used for Example solutions. Valuable suggestions for updating the previous edition have been made by Tom Acker, Arindam Banerjee, Mark Cappelli; Eun Jung Chae, Melinda Keller, Christopher Pascual, Philippe Sucosky, Sindy KY Tang, and Pavlos Vlachos. We hope that colleagues and others who use this book continue to provide input, for their contributions are essential to maintaining the quality and relevance of this work.

John W. Mitchell
March, 2019

Contents

OC Content available in eBook.

SS Student solution available in interactive e-text.

CHAPTER 1 INTRODUCTION 1

1.1 Introduction to Fluid Mechanics 2

Note to Students 2

Scope of Fluid Mechanics 3

Definition of a Fluid 3

1.2 Basic Equations 4

1.3 Methods of Analysis 5

System and Control Volume 6

Differential versus Integral Approach 7

Methods of Description 7

1.4 Dimensions and Units 9

Systems of Dimensions 9

Systems of Units 10

Preferred Systems of Units 11

Dimensional Consistency and “Engineering”
Equations 11

1.5 Analysis of Experimental Error 13

1.6 Summary 14

References 14

CHAPTER 2 FUNDAMENTAL CONCEPTS 15

2.1 Fluid as a Continuum 16

2.2 Velocity Field 17

One-, Two-, and Three-Dimensional Flows 18

Timelines, Pathlines, Streaklines, and
Streamlines 19

2.3 Stress Field 23

2.4 Viscosity 25

Newtonian Fluid 26

Non-Newtonian Fluids 28

2.5 Surface Tension 29

2.6 Description and Classification of Fluid
Motions 30

Viscous and Inviscid Flows 32

Laminar and Turbulent Flows 34

Compressible and Incompressible Flows 34

Internal and External Flows 35

2.7 Summary and Useful Equations 36

References 37

CHAPTER 3 FLUID STATICS 38

3.1 The Basic Equation of Fluid Statics 39

3.2 The Standard Atmosphere 42

3.3 Pressure Variation in a Static Fluid 43

Incompressible Liquids: Manometers 43

Gases 48

3.4 Hydrostatic Force on Submerged Surfaces 50

Hydrostatic Force on a Plane Submerged
Surface 50

Hydrostatic Force on a Curved Submerged
Surface 57

3.5 Buoyancy and Stability 60

3.6 Fluids in Rigid-Body Motion 63

3.7 Summary and Useful Equations 68

References 69

CHAPTER 4 BASIC EQUATIONS IN INTEGRAL FORM FOR A CONTROL VOLUME 70

4.1 Basic Laws for a System 71

Conservation of Mass 71

Newton's Second Law 72

The Angular-Momentum Principle 72

The First Law of Thermodynamics 72

The Second Law of Thermodynamics 73

4.2 Relation of System Derivatives to the
Control Volume Formulation 73

Derivation 74

Physical Interpretation 76

4.3 Conservation of Mass 77

Special Cases 78

4.4 Momentum Equation for Inertial Control
Volume 82

Differential Control Volume Analysis 93

Control Volume Moving with Constant Velocity	97	Static, Stagnation, and Dynamic Pressures	169
4.5 Momentum Equation for Control Volume with Rectilinear Acceleration	99	Applications	171
4.6 Momentum Equation for Control Volume with Arbitrary Acceleration	105	Cautions on Use of the Bernoulli Equation	176
4.7 The Angular-Momentum Principle	110	6.3 The Bernoulli Equation Interpreted as an Energy Equation	177
Equation for Fixed Control Volume	110	6.4 Energy Grade Line and Hydraulic Grade Line	181
Equation for Rotating Control Volume	114	6.5 Unsteady Bernoulli Equation: Integration of Euler's Equation Along a Streamline	183
4.8 The First and Second Laws of Thermodynamics	118	6.6 Irrotational Flow	185
Rate of Work Done by a Control Volume	119	Bernoulli Equation Applied to Irrotational Flow	185
Control Volume Equation	121	Velocity Potential	186
4.9 Summary and Useful Equations	125	Stream Function and Velocity Potential for Two-Dimensional, Irrotational, Incompressible Flow: Laplace's Equation	187
CHAPTER 5 INTRODUCTION TO DIFFERENTIAL ANALYSIS OF FLUID MOTION	128	Elementary Plane Flows	189
5.1 Conservation of Mass	129	Superposition of Elementary Plane Flows	191
Rectangular Coordinate System	129	6.7 Summary and Useful Equations	200
Cylindrical Coordinate System	133	References	201
5.2 Stream Function for Two-Dimensional Incompressible Flow	135		
5.3 Motion of a Fluid Particle (Kinematics)	137	CHAPTER 7 DIMENSIONAL ANALYSIS AND SIMILITUDE	202
Fluid Translation: Acceleration of a Fluid Particle in a Velocity Field	138	7.1 Nondimensionalizing the Basic Differential Equations	204
Fluid Rotation	144	7.2 Buckingham Pi Theorem	206
Fluid Deformation	147	7.3 Significant Dimensionless Groups in Fluid Mechanics	212
5.4 Momentum Equation	151	7.4 Flow Similarity and Model Studies	214
Forces Acting on a Fluid Particle	151	Incomplete Similarity	216
Differential Momentum Equation	152	Scaling with Multiple Dependent Parameters	221
Newtonian Fluid: Navier–Stokes Equations	152	Comments on Model Testing	224
5.5 Summary and Useful Equations	160	7.5 Summary and Useful Equations	225
References	161	References	226

CHAPTER 6 INCOMPRESSIBLE INVISCID FLOW	162
6.1 Momentum Equation for Frictionless Flow: Euler's Equation	163
6.2 Bernoulli Equation: Integration of Euler's Equation Along a Streamline for Steady Flow	167
Derivation Using Streamline Coordinates	167
Derivation Using Rectangular Coordinates	168

CHAPTER 7 DIMENSIONAL ANALYSIS AND SIMILITUDE	202
7.1 Nondimensionalizing the Basic Differential Equations	204
7.2 Buckingham Pi Theorem	206
7.3 Significant Dimensionless Groups in Fluid Mechanics	212
7.4 Flow Similarity and Model Studies	214
Incomplete Similarity	216
Scaling with Multiple Dependent Parameters	221
Comments on Model Testing	224
7.5 Summary and Useful Equations	225
References	226

CHAPTER 8 INTERNAL INCOMPRESSIBLE VISCOUS FLOW	227
8.1 Internal Flow Characteristics	228
Laminar versus Turbulent Flow	228
The Entrance Region	229
PART A. FULLY DEVELOPED LAMINAR FLOW	230
8.2 Fully Developed Laminar Flow Between Infinite Parallel Plates	230
Both Plates Stationary	230

Upper Plate Moving with Constant Speed, U 236 8.3 Fully Developed Laminar Flow in a Pipe 241 PART B. FLOW IN PIPES AND DUCTS 245 8.4 Shear Stress Distribution in Fully Developed Pipe Flow 246 8.5 Turbulent Velocity Profiles in Fully Developed Pipe Flow 247 8.6 Energy Considerations in Pipe Flow 251 Kinetic Energy Coefficient 252 Head Loss 252 8.7 Calculation of Head Loss 253 Major Losses: Friction Factor 253 Minor Losses 258 Pumps, Fans, and Blowers in Fluid Systems 262 Noncircular Ducts 262 8.8 Solution of Pipe Flow Problems 263 Single-Path Systems 264 Multiple-Path Systems 276 PART C. FLOW MEASUREMENT 279 8.9 Restriction Flow Meters for Internal Flows 279 The Orifice Plate 282 The Flow Nozzle 286 The Venturi 286 The Laminar Flow Element 287 Linear Flow Meters 288 Traversing Methods 289 8.10 Summary and Useful Equations 290 References 292	PART B. FLUID FLOW ABOUT IMMERSED BODIES 316 9.6 Drag 316 Pure Friction Drag: Flow over a Flat Plate Parallel to the Flow 317 Pure Pressure Drag: Flow over a Flat Plate Normal to the Flow 320 Friction and Pressure Drag: Flow over a Sphere and Cylinder 320 Streamlining 326 9.7 Lift 328 9.8 Summary and Useful Equations 340 References 342 CHAPTER 10 FLUID MACHINERY 343 10.1 Introduction and Classification of Fluid Machines 344 Machines for Doing Work on a Fluid 344 Machines for Extracting Work (Power) from a Fluid 346 Scope of Coverage 348 10.2 Turbomachinery Analysis 348 The Angular Momentum Principle: The Euler Turbomachine Equation 348 Velocity Diagrams 350 Performance—Hydraulic Power 352 Dimensional Analysis and Specific Speed 353 10.3 Pumps, Fans, and Blowers 358 Application of Euler Turbomachine Equation to Centrifugal Pumps 358 Application of the Euler Equation to Axial Flow Pumps and Fans 359 Performance Characteristics 362 Similarity Rules 367 Cavitation and Net Positive Suction Head 371 Pump Selection: Applications to Fluid Systems 374 Blowers and Fans 380 10.4 Positive Displacement Pumps 384 10.5 Hydraulic Turbines 387 Hydraulic Turbine Theory 387 Performance Characteristics for Hydraulic Turbines 389 10.6 Propellers and Wind Turbines 395 Propellers 395 Wind Turbines 400
--	--

CHAPTER 9 EXTERNAL INCOMPRESSIBLE VISCOUS FLOW 293

PART A. BOUNDARY LAYERS 295 9.1 The Boundary Layer Concept 295 9.2 Laminar Flat Plate Boundary Layer: Exact Solution 299 9.3 Momentum Integral Equation 302 9.4 Use of the Momentum Integral Equation for Flow with Zero Pressure Gradient 306 Laminar Flow 307 Turbulent Flow 311 9.5 Pressure Gradients in Boundary Layer Flow 314
--

10.7	Compressible Flow Turbomachines	406
	Application of the Energy Equation to a Compressible Flow Machine	406
	Compressors	407
	Compressible-Flow Turbines	410
10.8	Summary and Useful Equations	410
	References	412

CHAPTER 11 FLOW IN OPEN CHANNELS 414

11.1	Basic Concepts and Definitions	416
	Simplifying Assumptions	416
	Channel Geometry	418
	Speed of Surface Waves and the Froude Number	419
11.2	Energy Equation for Open-Channel Flows	423
	Specific Energy	425
	Critical Depth: Minimum Specific Energy	426
11.3	Localized Effect of Area Change (Frictionless Flow)	431
	Flow over a Bump	431
11.4	The Hydraulic Jump	435
	Depth Increase Across a Hydraulic Jump	438
	Head Loss Across a Hydraulic Jump	439
11.5	Steady Uniform Flow	441
	The Manning Equation for Uniform Flow	443
	Energy Equation for Uniform Flow	448
	Optimum Channel Cross Section	450
11.6	Flow with Gradually Varying Depth	451
	Calculation of Surface Profiles	452
11.7	Discharge Measurement Using Weirs	455
	Suppressed Rectangular Weir	455
	Contracted Rectangular Weirs	456
	Triangular Weir	456
	Broad-Crested Weir	457
11.8	Summary and Useful Equations	458
	References	459

CHAPTER 12 INTRODUCTION TO COMPRESSIBLE FLOW 460

12.1	Review of Thermodynamics	461
12.2	Propagation of Sound Waves	467
	Speed of Sound	467
	Types of Flow—The Mach Cone	471
12.3	Reference State: Local Isentropic Stagnation Properties	473

	Local Isentropic Stagnation Properties for the Flow of an Ideal Gas	474
12.4	Critical Conditions	480
12.5	Basic Equations for One-Dimensional Compressible Flow	480
	Continuity Equation	481
	Momentum Equation	481
	First Law of Thermodynamics	481
	Second Law of Thermodynamics	482
	Equation of State	483
12.6	Isentropic Flow of an Ideal Gas: Area Variation	483
	Subsonic Flow, $M < 1$	485
	Supersonic Flow, $M > 1$	486
	Sonic Flow, $M = 1$	486
	Reference Stagnation and Critical Conditions for Isentropic Flow of an Ideal Gas	487
	Isentropic Flow in a Converging Nozzle	492
	Isentropic Flow in a Converging-Diverging Nozzle	496
12.7	Normal Shocks	501
	Basic Equations for a Normal Shock	501
	Normal-Shock Flow Functions for One-Dimensional Flow of an Ideal Gas	503
12.8	Supersonic Channel Flow with Shocks	507
12.9	Summary and Useful Equations	509
	References	511

Problems (Available in e-text for students) P-1

APPENDIX A FLUID PROPERTY DATA A-1

APPENDIX B VIDEOS FOR FLUID MECHANICS A-13

APPENDIX C SELECTED PERFORMANCE CURVES FOR PUMPS AND FANS A-15

APPENDIX D FLOW FUNCTIONS FOR COMPUTATION OF COMPRESSIBLE FLOW A-26

APPENDIX E ANALYSIS OF EXPERIMENTAL UNCERTAINTY A-29

APPENDIX F INTRODUCTION TO COMPUTATIONAL FLUID DYNAMICS A-35

Index I-1

Chapter 1 Problems

SS Student solution available in interactive e-text.

Definition of a Fluid: Basic Equations

1.1 Describe the conditions for which the following substances can be considered liquids.

Tar	Honey	Wax	Propane
Carbon dioxide	Sea water	Sand	Toothpaste

1.2 Give a word statement of each of the five basic conservation laws stated in Section 1.2 as they apply to a system.

Methods of Analysis

1.3 The barrel of a bicycle tire pump becomes quite warm during use. Explain the mechanisms responsible for the temperature increase.

SS 1.4 In a pollution control experiment, minute solid particles (typical mass 1×10^{-13} slug) are dropped in air. The terminal speed of the particles is measured to be 0.2 ft/s. The drag of these particles is given by $F_D = kV$, where V is the instantaneous particle speed. Find the value of the constant k . Find the time required to reach 99 percent of terminal speed.

1.5 A rocket payload with a weight on earth of 2000 lbf is sent to the moon. The acceleration due to gravity in the moon is $1/6^{\text{th}}$ that of the earth. Determine the mass of the payload on the earth and on the moon and the weight of the payload on the moon in SI, BG, EE units.

1.6 The English perfected the longbow as a weapon after the Medieval period. In the hands of a skilled archer, the longbow was reputed to be accurate at ranges to 100 m or more. If the maximum altitude of an arrow is less than $h = 10$ m while traveling to a target 100 m away from the archer, and neglecting air resistance, estimate the speed and angle at which the arrow must leave the bow. Plot the required release speed and angle as a function of height h .

1.7 Air at standard atmospheric conditions enters the 6 in. diameter inlet of an air compressor at a velocity of 20 ft/s. The air is compressed and leaves the compressor through a 6 in. diameter outlet at 80 psia and 150°F. Determine the mass flow rate of the air and the exit velocity.

1.8 A water flow of 4.5 slug/s at 60°F enters the condenser of steam turbine and leaves at 140°F. Determine the heat transfer rate (Btu/hr).

1.9 Determine the weight (N) and specific volume of a cubic meter of air at 101 kPa and 15°C. Determine the specific volume if the air is cooled to -10°C at constant pressure.

SS 1.10 Determine the specific weight, specific volume, and density of air at 40°F and 50 psia in BG units. Determine the specific weight, specific volume, and density when the air is then compressed isentropically to 100 psia.

Dimensions and Units

1.11 For each quantity listed, indicate dimensions using mass as a primary dimension, and give typical SI and English units:

- (a) Power
- (b) Pressure
- (c) Modulus of elasticity

(d) Angular velocity

(e) Energy

(f) Moment of a force

(g) Momentum

(h) Shear stress

(i) Strain

(j) Angular momentum

1.12 For each quantity listed, indicate dimensions using force as a **SS** primary dimension, and give typical SI and English units:

(a) Power

(b) Pressure

(c) Modulus of elasticity

(d) Angular velocity

(e) Energy

(f) Momentum

(g) Shear stress

(h) Specific heat

(i) Thermal expansion coefficient

(j) Angular momentum

1.13 The maximum theoretical flow rate (slug/s) for air flow through a supersonic nozzle is given as

$$\dot{m}_{\text{max}} = 2.38 \frac{A_t p_0}{\sqrt{T_0}},$$

where A_t is the nozzle throat area (ft^2), p_0 is the supply tank pressure (psia), and T_0 is the air temperature in the tank (°R). Determine the dimensions and units of the constant 2.38. Determine the equivalent equation in SI units.

1.14 The mean free path λ of a molecule of gas is the average distance it travels before collision with another molecule. It is given by

$$\lambda = C \frac{m}{\rho d^2}$$

where m and d are the molecule's mass and diameter, respectively, and ρ is the gas density. Determine the dimensions of constant C for a dimensionally consistent equation.

1.15 The density of a sample of sea water is 1.99 slug/ft³. Determine the value of density in SI and EE units, and the value of specific weight in SI, BG and EE units.

1.16 A fluid occupying 3.2 m³ has a mass of 4 mg. Calculate its density and specific volume in SI, EE, and BG units.

1.17 Derive the following conversion factors:

(a) Convert a pressure of 1 psi to kPa.

(b) Convert a volume of 1 liter to gallons.

(c) Convert a viscosity of 1 lbf·s/ft² to N·s/m².

1.18 Express the following in SI units:

(a) 100 cfm (ft³/min)

(b) 5 gal

(c) 65 mph

(d) 5.4 acres

P-2 Chapter 1 Problems

1.19 Express the following in BG units:

- (a) 50 m²
- (b) 250 cc
- (c) 100 kW
- (d) 5 kg/m²

1.20 Derive the conversion factors for the following quantities for volume flow rate

- (a) Converting in³/min to mm³/s.
- (b) Converting gallons per minute (gpm) to m³/s.
- (c) Converting gpm to liters/min.
- (d) Converting cubic feet per minute (cfm) to m³/s.

Analysis of Experimental Error

1.21 Calculate the density of standard air in a laboratory from the ideal gas equation of state. Estimate the experimental uncertainty in the air density calculated for standard conditions (29.9 in. of mercury and 59°F) if the uncertainty in measuring the barometer height is ± 0.1 in. of mercury and the uncertainty in measuring temperature is $\pm 0.5^\circ\text{F}$. (Note that 29.9 in. of mercury corresponds to 14.7 psia.)

1.22 A parameter that is often used in describing pump performance is the specific speed, $N_{S_{cu}}$, given by

$$N_{S_{cu}} = \frac{N(\text{rpm})[Q(\text{gpm})]^{1/2}}{[H(\text{ft})]^{3/4}}$$

Determine the units of specific speed. For a pump with a specific speed of 200, determine the specific speed in SI units with angular velocity in rad/S.

1.23 The mass flow rate in a water flow system determined by collecting the discharge over a timed interval is 0.2 kg/s. The scales used can be read to the nearest 0.05 kg and the stopwatch is accurate to 0.2 s. Estimate the precision with which the flow rate can be calculated for time intervals of (a) 10 s and (b) 1 min. SS

1.24 From Appendix A, the viscosity $\mu(\text{N}\cdot\text{s}/\text{m}^2)$ of water at temperature $T(\text{K})$ can be computed from $\mu = A10^{B/(T-C)}$, where $A = 2.414 \times 10^{-5} \text{ N}\cdot\text{s}/\text{m}^2$, $B = 247.8 \text{ K}$, and $C = 140 \text{ K}$. Determine the viscosity of water at 30°C, and estimate its uncertainty if the uncertainty in temperature measurement is $\pm 0.5^\circ\text{C}$.

1.25 The height of a building may be estimated by measuring the horizontal distance to a point on the ground and the angle from this point to the top of the building. Assuming that these measurements are $L = 100 \pm 0.5 \text{ ft}$ and $\theta = 30 \pm 0.2^\circ$, estimate the height H of the building and the uncertainty in the estimate. For the same building height and measurement uncertainties, use Excel's Solver to determine the angle (and the corresponding distance from the building) at which measurements should be made to minimize the uncertainty in estimated height. Evaluate and plot the optimum measurement angle as a function of building height for $50 \leq H \leq 1000 \text{ ft}$.

1.26 An American golf ball has a mass of $1.62 \pm 0.01 \text{ oz}$ and a nominal diameter of 1.68 in. Determine the precision that the diameter of the ball must be measured so that the uncertainty of the density of the ball is ± 1 percent.

CHAPTER 1

Introduction

- 1.1 Introduction to Fluid Mechanics
- 1.2 Basic Equations
- 1.3 Methods of Analysis

- 1.4 Dimensions and Units
- 1.5 Analysis of Experimental Error
- 1.6 Summary

Case Study

Wind generated electricity is increasingly becoming a major factor in meeting U.S. energy needs. In 2017, wind energy provided 254×10^9 kWh of electricity, or about 6.3 percent of the total electrical use (EIA, www.eia.gov/). In several states, over 10 percent of the electricity generated came from wind. The total production has increased by 30 percent over that of 2015, showing the rapid growth of wind power.

Electricity from the wind is produced in wind turbine farms, as shown in the figure. The individual turbines are large, with the height of the hub reaching to 70 m (220 ft) and the blades up to 35 m (120 ft) in diameter. The total weight of the blades, nacelle, and tower is about 165 tons. The nacelle contains the gearbox and the generator, with the transmission lines to the grid in the tower. A turbine this size is rated at 1.5 MW, which is enough electricity to supply about 250 U.S. homes.

The kinetic energy of the wind is the source of power for a wind turbine. Using the conservation of mass relation, the maximum efficiency of a wind turbine has been established at 59.3 percent. This maximum is known as Betz's law after the German physicist Albert Betz who derived the relation in 1919. Practical utility-scale wind turbines achieve 75–80 percent of the maximum, thus extracting about 45 percent of the available energy of the wind.

The design of turbine blades has evolved from the flat surfaces used on windmills to the propeller shapes seen on modern turbines. The pitch of the blade, which is the angle between the blade and the oncoming wind, is increased as the wind speed

increases. This is done to provide a match between the wind and the blade surface so that the wind flows smoothly over the blade. Because the velocity of the blade increases from the hub to the tip, the blade shape twists accordingly to maintain a constant pitch along the blade. Such designs allow the high efficiency attained in wind turbines. The basic fluid mechanics that we will study in this text provides the basis for the aerodynamic design of devices such as wind turbines.



Dale/Adobe Stock Photo

Wind turbine farm.

Learning Objectives

After completing this chapter, you should be able to

- Explain the definition of a fluid in physical terms.
- State and explain the basic laws of fluid mechanics.
- Define “system” and “control volume” and explain the difference.
- Describe the dimensions and units of the systems used in fluid mechanics.
- Estimate the uncertainty in a physical measurement.

1.1 Introduction to Fluid Mechanics

We decided to title this textbook “Introduction to ...” for the following reason: After studying the text, you will *not* be able to design the streamlining of a new car or an airplane, or design a new heart valve, or select the correct air extractors and ducting for a \$100 million building; however, you *will* have developed a good understanding of the concepts behind all of these, and many other applications, and have made significant progress toward being ready to work on such state-of-the-art fluid mechanics projects.

To start toward this goal, in this chapter we cover some very basic topics: a case study, what fluid mechanics encompasses, the standard engineering definition of a fluid, and the basic equations and methods of analysis. Finally, we discuss some common engineering student pitfalls in areas such as unit systems and experimental analysis.

Note to Students

This is a student-oriented book: We believe it is quite comprehensive for an introductory text, and a student can successfully self-teach from it. However, most students will use the text in conjunction with one or two undergraduate courses. In either case, we recommend a thorough reading of the relevant chapters. In fact, a good approach is to read a chapter quickly once, then reread more carefully a second and even a third time, so that concepts develop a context and meaning. While students often find fluid mechanics quite challenging, we believe this approach, supplemented by your instructor’s lectures that will hopefully amplify and expand upon the text material, will show fluid mechanics to be a fascinating and varied field of study.

There are some prerequisites for this text. We assume you have already studied introductory thermodynamics, as well as statics, dynamics, and calculus; however, as needed, we will review some of this material.

It is our strong belief that one learns best by *doing*. This is true whether the subject under study is fluid mechanics, or soccer. The fundamentals in any of these are few, and mastery of them comes through practice. *Thus it is extremely important that you solve problems.* The numerous problems included at the end of each chapter provide the opportunity to practice applying fundamentals to the solution of problems. Even though we provide for your convenience a summary of useful equations at the end of each chapter, you should avoid the temptation to adopt a so-called plug-and-chug approach to solving problems. Most of the problems are such that this approach simply will not work. In solving problems, we strongly recommend that you proceed using the following logical steps:

- 1 State briefly and concisely in your own words the information given.
- 2 State the information to be found.
- 3 Draw a schematic of the system or control volume to be used in the analysis. Be sure to label the boundaries of the system or control volume and label appropriate coordinate directions.
- 4 Give the appropriate mathematical formulation of the *basic* laws that you consider necessary to solve the problem.
- 5 List the simplifying assumptions that you feel are appropriate in the problem.

- 6 Complete the analysis algebraically before substituting numerical values. This is especially important if you are using software to solve the problem.
- 7 Substitute numerical values to obtain a numerical answer.
 - (a) Reference the source of values for any physical properties.
 - (b) Be sure the significant figures in the answer are consistent with the given data.
 - (c) Check the units of each term to be certain they are consistent.
- 8 Check the answer and review the assumptions made in the solution to make sure they are reasonable.
- 9 Label the answer.

In your initial work this problem format may seem unnecessary and even long-winded. However, it is our experience that this approach to problem solving is ultimately the most efficient. It will also prepare you to be a successful professional, for which a major prerequisite is to be able to communicate information and the results of an analysis clearly and precisely. *This format is used in all examples presented in this text; answers to examples are rounded to three significant figures.*

The problems at the end of each chapter range in degree of difficulty. For many, pencil and paper together with a calculator will suffice. This is especially true for those problems we have designed to illustrate a single principle or concept. However, there are many more complex problems, and we have found that using software tools is a more appropriate and satisfactory approach to obtaining a solution. We have provided an *Excel* tutorial and solutions for many of the book's examples on the website that can be used to help you get started with this tool. Additionally, there are a large number of other equation solvers that students have found very useful, including *EES*, *MATLAB*, and *Mathematica*. We encourage you to learn to use one of these tools as virtually all problems you will encounter in practice are complicated.

Scope of Fluid Mechanics

As the name implies, fluid mechanics is the study of fluids at rest or in motion. The subject has applications to a wide range of traditional subjects such as the design of dam systems, water delivery systems, pumps and compressors, and the aerodynamics of automobiles and airplanes. Fluid mechanics has facilitated the development of new technology in the environmental and energy area such as large-scale wind turbines and oil spill cleanups. Medical advances in the understanding and treatment of flow problems in the circulatory and respiratory system have been aided by fluid mechanics applications. The modeling of atmospheric circulation and ocean currents that aids understanding of climate change is based on fluid mechanics principles. Possibly the greatest advance in fluid mechanics in recent years is the ability to model extremely complex flows using software. The technique known as computational fluid dynamics (CFD) has at its heart the basic relations of fluid mechanics.

These are just a small sampling of the newer areas of fluid mechanics, but they illustrate how the discipline is still highly relevant, and increasingly diverse, even though it may be thousands of years old.

Definition of a Fluid

We are certain that you have a common-sense idea of what a fluid is, as opposed to a solid. Fluids tend to flow when we interact with them whereas solids tend to deform or bend. Engineers need a more formal and precise definition of a fluid: A *fluid* is a substance that deforms continuously under the application of a shear (tangential) stress no matter how small the shear stress may be. Because the fluid motion continues under the application of a shear stress, we can also define a fluid as any substance that cannot sustain a shear stress when at rest.

Hence liquids and gases (or vapors) are the forms, or phases, that fluids can take. We wish to distinguish these phases from the solid phase of matter. We can see the difference between solid and fluid behavior in Fig. 1.1. If we place a specimen of either substance between two plates (Fig. 1.1a) and then apply a shearing force F , each will initially deform (Fig. 1.1b); however, whereas a solid will then be at rest (assuming the force is not large enough to go beyond its elastic limit), a fluid will *continue* to deform (Fig. 1.1c, d, etc.) as long as the force is applied. Note that a fluid in contact with a solid surface

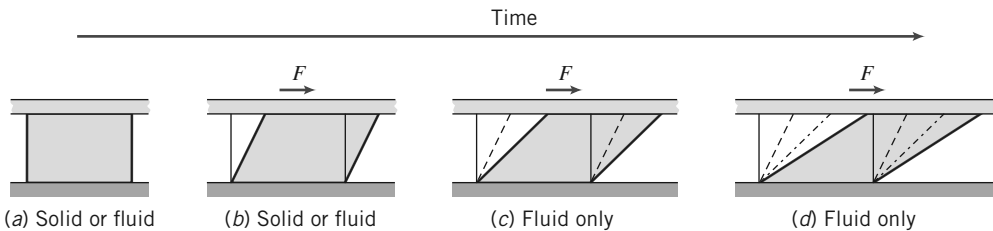


Fig. 1.1 Difference in behavior of a solid and a fluid due to a shear force.

does not slip. It has the same velocity as that surface because of the *no-slip* condition, which is a very important an experimental fact.

The amount of deformation of the solid depends on the solid's modulus of rigidity. In Chapter 2 we will learn that the *rate of deformation* of the fluid depends on the fluid's viscosity μ . We refer to solids as being *elastic* and fluids as being *viscous*. More informally, we say that solids exhibit "springiness." For example, when you drive over a pothole, the car bounces up and down due to the metal coil springs compressing and expanding. On the other hand, fluids exhibit friction effects so that the shock absorbers, which contain a fluid that is forced through a small opening, dissipate energy due to the fluid friction and stop the bouncing after a few oscillations.

The idea that substances can be categorized as being either a solid or a liquid holds for most substances, but a number of substances exhibit both springiness and friction. They are termed *viscoelastic*. Many biological tissues are viscoelastic. For example, the synovial fluid in human knee joints lubricates those joints but also absorbs some of the shock occurring during walking or running. Other examples of viscoelastic materials are some polymers, metals at very high temperatures, and bitumen material such as asphalt.

1.2 Basic Equations

Analysis of any problem in fluid mechanics necessarily includes statement of the basic laws governing the fluid motion. The basic laws, which are applicable to any fluid, are:

- 1 The conservation of mass
- 2 Newton's second law of motion (also termed the principle of linear momentum)
- 3 The principle of angular momentum
- 4 The first law of thermodynamics
- 5 The second law of thermodynamics

All basic laws are usually not required to solve any one problem. On the other hand, in many problems it is necessary to bring into the analysis additional relations that describe the behavior of physical properties of fluids under given conditions. For example, the *ideal gas* equation of state

$$p = \rho RT \quad (1.1)$$

is a model that relates density to pressure and temperature for many gases under normal conditions. In Eq. 1.1, R is the gas constant. Values of R are given in Appendix A for several common gases; p and T in Eq. 1.1 are the absolute pressure and absolute temperature, respectively and ρ is density (mass per unit volume). Example 1.1 illustrates use of the ideal gas equation of state.

It is obvious that the basic laws with which we shall deal are the same as those used in mechanics and thermodynamics. Our task will be to formulate these laws in suitable forms to solve fluid flow problems and to apply them to a wide variety of situations.

Example 1.1 FIRST LAW APPLICATION TO CLOSED SYSTEM

A piston-cylinder device contains 0.95 kg of oxygen initially at a temperature of 27°C and a pressure due to the weight of 150 kPa (abs). Heat is added to the gas until it reaches a temperature of 627°C. Determine the amount of heat added during the process.

Given: Piston-cylinder containing O₂, $m = 0.95 \text{ kg}$.

$$T_1 = 27^\circ\text{C} \quad T_2 = 627^\circ\text{C}$$

Find: $Q_{1 \rightarrow 2}$.

Solution: $p = \text{constant} = 150 \text{ kPa (abs)}$

We are dealing with a system, $m = 0.95 \text{ kg}$.

Governing equation: First law for the system, $Q_{12} - W_{12} = E_2 - E_1$

Assumptions: 1 $E = U$, since the system is stationary.

2 Ideal gas with constant specific heats.

Under the above assumptions,

$$E_2 - E_1 = U_2 - U_1 = m(u_2 - u_1) = mc_v(T_2 - T_1)$$

The work done during the process is moving boundary work

$$W_{12} = \int_{V_1}^{V_2} pdV = p(V_2 - V_1)$$

For an ideal gas, $pV = mRT$. Hence $W_{12} = mR(T_2 - T_1)$. Then from the first law equation,

$$Q_{12} = E_2 - E_1 + W_{12} = mc_v(T_2 - T_1) + mR(T_2 - T_1)$$

$$Q_{12} = m(T_2 - T_1)(c_v + R)$$

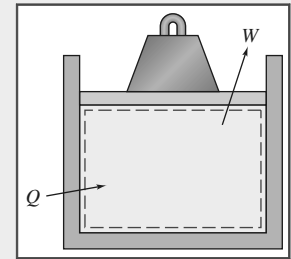
$$Q_{12} = mc_p(T_2 - T_1) \quad \{R = c_p - c_v\}$$

From Table A.6 in Appendix A, for O₂, $c_p = 909.4 \text{ J/(kg} \cdot \text{K)}$. Solving for Q_{12} , we obtain

$$Q_{12} = 0.95 \text{ kg} \times 909 \frac{\text{J}}{\text{kg} \cdot \text{K}} \times 600 \text{ K} = 518 \text{ kJ} \quad \xleftarrow{\hspace{1cm} Q_{12} \hspace{1cm}}$$

This problem:

- Was solved using the nine logical steps discussed earlier.
- Reviewed the use of the ideal gas equation and the first law of thermodynamics for a system.



1.3 Methods of Analysis

The first step in solving a problem is to define the system that you are attempting to analyze. In basic mechanics, we made extensive use of the *free-body diagram*. In fluid mechanics, we will use a *system* or a *control volume*, depending on the problem being studied. These concepts are identical to the ones you used in thermodynamics (also termed *closed system* and *open system*, respectively). We can use either one to get mathematical expressions for each of the basic laws. In thermodynamics we applied the conservation of mass and the first and second laws of thermodynamics in most problems. In our study of fluid mechanics, we will usually apply conservation of mass and Newton's second law of motion. In thermodynamics our focus was energy; in fluid mechanics it will mainly be forces and motion. We must always be aware of whether we are using a system or a control volume approach because each leads to

different mathematical expressions of these laws. At this point we review the definitions of systems and control volumes.

System and Control Volume

A *system* is defined as a fixed, identifiable quantity of mass with the system boundaries separating the system from the surroundings. The boundaries of the system may be fixed or movable; however, no mass crosses the system boundaries.

In the familiar piston-cylinder assembly from thermodynamics, Fig. 1.2, the gas in the cylinder is the system. If the gas is heated, the piston will lift the weight; the boundary of the system thus moves. Heat and work may cross the boundaries of the system, but the quantity of matter within the system boundaries remains fixed. No mass crosses the system boundaries.

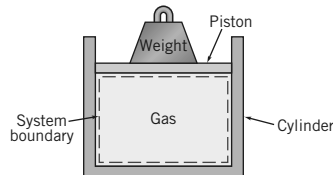


Fig. 1.2 Piston–cylinder assembly.

In solid body mechanics courses you used the free-body diagram (system approach) extensively. This was logical because you were dealing with an easily identifiable rigid body. However, in fluid mechanics we normally are concerned with the flow of fluids through devices such as compressors, turbines, pipelines, and nozzles. In these cases it is difficult to focus attention on a fixed identifiable quantity of mass. It is much more convenient, to focus attention on a volume in space through which the fluid flows. Consequently, we use the control volume approach.

A *control volume* is an arbitrary volume in space through which fluid flows. The geometric boundary of the control volume is called the control surface. The control surface may be real or imaginary; it may be at rest or in motion. Figure 1.3 shows flow through a pipe junction, with a control surface drawn on it. Note that some regions of the surface correspond to physical boundaries (the walls of the pipe) and others (at locations ①, ②, and ③) are parts of the surface that are imaginary. For the control volume defined by this surface, we could write equations for the basic laws and obtain results such as the flow rate at outlet ③ given the flow rates at inlet ① and outlet ② or the force required to hold the junction in place. Example 1.2 illustrates how we use a control volume to determine the mass flow rate in a section of a pipe. It is always important to take care in selecting a control volume, as the choice has a big effect on the mathematical form of the basic laws.

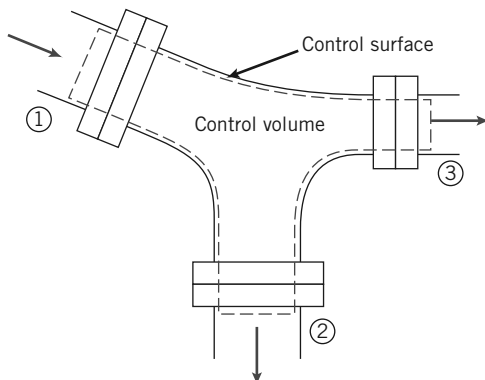


Fig. 1.3 Fluid flow through a pipe junction.

Example 1.2 MASS CONSERVATION APPLIED TO CONTROL VOLUME

A reducing water pipe section has an inlet diameter of 50 mm and exit diameter of 30 mm. If the steady inlet speed (averaged across the inlet area) is 2.5 m/s, find the exit speed.

Given: Pipe, inlet $D_i = 50$ mm, exit $D_e = 30$ mm.
Inlet speed, $V_i = 2.5$ m/s.

Find: Exit speed, V_e .

Solution:

Assumption: Water is incompressible (density $\rho = \text{constant}$).

The physical law we use here is the conservation of mass, which you learned in thermodynamics when studying turbines, boilers, and so on. You may have seen mass flow at an inlet or outlet expressed as either $\dot{m} = VA/v$ or $\dot{m} = \rho VA$ where V , A , v and ρ , are the speed, area, specific volume, and density, respectively. We will use the density form of the equation.

Hence the mass flow is:

$$\dot{m} = \rho VA$$

Applying mass conservation,

$$\rho V_i A_i = \rho V_e A_e$$

Note: $\rho_i = \rho_e = \rho$ by our first assumption.

Solving for V_e ,

$$V_e = V_i \frac{A_i}{A_e} = V_i \frac{\pi D_i^2 / 4}{\pi D_e^2 / 4} = V_i \left(\frac{D_i}{D_e} \right)^2$$

$$V_e = 2.7 \frac{\text{m}}{\text{s}} \left(\frac{50}{30} \right)^2 = 7.5 \frac{\text{m}}{\text{s}} \quad \longleftarrow V_e$$

This problem:

- Was solved using the nine logical steps.
- Demonstrated the use of a control volume and the mass conservation law.

Differential versus Integral Approach

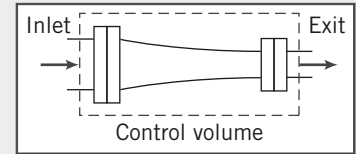
The basic laws that we apply in our study of fluid mechanics can be formulated in terms of systems or control volumes. As you might suspect, the equations will look different in the two cases. Both approaches are important in the study of fluid mechanics and both will be developed in the course of our work.

In the case of *infinitesimal* systems the resulting equations are differential equations. Solution of the differential equations of motion provides a means of determining the detailed behavior of the flow. An example might be the pressure distribution on a wing surface.

Frequently the information sought does not require a detailed knowledge of the flow. We often are interested in the gross behavior of a device; in such cases it is more appropriate to use integral formulations of the basic laws. An example might be the overall lift a wing produces. Integral formulations, using *finite* systems or control volumes, usually are easier to treat analytically. The basic laws of mechanics and thermodynamics, formulated in terms of finite systems, are the basis for deriving the control volume equations in Chapter 4.

Methods of Description

We use a method of description that follows the particle when we want to keep track of it. This sometime is referred to as the *Lagrangian* method of description. Consider, for example, the application of



Newton's second law to a particle of fixed mass. Mathematically, we can write Newton's second law for a system of mass m as

$$\Sigma \vec{F} = m\vec{a} = m\frac{d\vec{V}}{dt} = m\frac{d^2\vec{r}}{dt^2} \quad (1.2)$$

In Eq. 1.2, $\Sigma \vec{F}$ is the sum of all external forces acting on the system, \vec{a} is the acceleration of the center of mass of the system, \vec{V} is the velocity of the center of mass of the system, and \vec{r} is the position vector of the center of mass of the system relative to a fixed coordinate system. In Example 1.3, we show how Newton's second law is applied to a falling object to determine its speed.

Example 1.3 FREE FALL OF BALL IN AIR

The air resistance (drag force) on a 200 g ball in free flight is given by $F_D = 2 \times 10^{-4} V^2$, where F_D is in newtons and V is in meters per second. If the ball is dropped from rest 500 m above the ground, determine the speed at which it hits the ground. What percentage of the terminal speed is the result? (The *terminal speed* is the steady speed a falling body eventually attains.)

Given: Ball, $m = 0.2$ kg, released from rest at $y_0 = 500$ m.

Air resistance, $F_D = kV^2$, where $k = 2 \times 10^{-4}$ N·s²/m².

Units: F_D (N), V (m/s).

Find:

- (a) Speed at which the ball hits the ground.
- (b) Ratio of speed to terminal speed.

Solution:

Governing equation: $\Sigma \vec{F} = m\vec{a}$

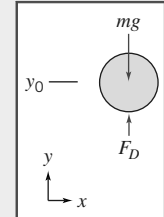
Assumption: Neglect buoyancy force.

The motion of the ball is governed by the equation

$$\Sigma F_y = ma_y = m\frac{dV}{dt}$$

Since $V = V(y)$, we write $\Sigma F_y = m\frac{dV}{dy}\frac{dy}{dt} = mV\frac{dV}{dy}$. Then,

$$\Sigma F_y = F_D - mg = kV^2 - mg = mV\frac{dV}{dy}$$



Separating variables and integrating,

$$\begin{aligned} \int_{y_0}^y dy &= \int_0^V \frac{mVdV}{kV^2 - mg} \\ y - y_0 &= \left[\frac{m}{2k} \ln(kV^2 - mg) \right]_0^V = \frac{m}{2k} \ln \frac{kV^2 - mg}{-mg} \end{aligned}$$

Taking antilogarithms, we obtain

$$kV^2 - mg = -mg e^{[(2k/m)(y-y_0)]}$$

Solving for V gives

$$V = \left\{ \frac{mg}{k} \left(1 - e^{[(2k/m)(y-y_0)]} \right) \right\}^{1/2}$$

Substituting numerical values with $y=0$ yields

$$V = \left\{ 0.2 \text{ kg} \times 9.81 \frac{\text{m}}{\text{s}^2} \times \frac{\text{m}^2}{2 \times 10^{-4} \text{ N} \cdot \text{s}^2} \times \frac{\text{N} \cdot \text{s}^2}{\text{kg} \cdot \text{m}} \left(1 - e^{[2 \times 2 \times 10^{-4} / 0.2(-500)]} \right) \right\}$$

$$V = 78.7 \text{ m/s} \xrightarrow{\hspace{10em}} V$$

At terminal speed, $a_y = 0$ and $\Sigma F_y = 0 = kV_t^2 - mg$.

$$\begin{aligned} \text{Then, } V_t &= \left[\frac{mg}{k} \right]^{1/2} = \left[0.2 \text{ kg} \times 9.81 \frac{\text{m}}{\text{s}^2} \times \frac{\text{m}^2}{2 \times 10^{-4} \text{ N} \cdot \text{s}^2} \times \frac{\text{N} \cdot \text{s}^2}{\text{kg} \cdot \text{m}} \right]^{1/2} \\ &= 99.0 \text{ m/s} \end{aligned}$$

The ratio of actual speed to terminal speed is

$$\frac{V}{V_t} = \frac{78.7}{99.0} = 0.795, \text{ or } 79.5\% \xrightarrow{\hspace{10em}} \frac{V}{V_t}$$

This problem:

- Reviewed the methods used in particle mechanics.
- Introduced a variable aerodynamic drag force.

We could use this Lagrangian approach to analyze a fluid flow by assuming the fluid to be composed of a very large number of particles whose motion must be described. However, keeping track of the motion of each fluid particle would become a horrendous bookkeeping problem. Consequently, a particle description becomes unmanageable. Often we find it convenient to use a different type of description. Particularly with control volume analyses, it is convenient to use the field, or *Eulerian*, method of description, which focuses attention on the properties of a flow at a given point in space as a function of time. In the Eulerian method of description, the properties of a flow field are described as functions of space coordinates and time. We shall see in Chapter 2 that this method of description is a logical outgrowth of the assumption that fluids may be treated as continuous media.

1.4 Dimensions and Units

Engineering problems are solved to answer specific questions. It goes without saying that the answer must include units, and it is very important to know what the units of a problem are. In 1999, NASA's Mars Climate Observer crashed because the JPL engineers assumed that a measurement was in meters, but the supplying company's engineers had actually made the measurement in feet. Consequently, it is appropriate to present a brief review of dimensions and units.

We refer to physical quantities such as length, time, mass, and temperature as *dimensions*. In terms of a particular system of dimensions, all measurable quantities are subdivided into the two groups of *primary* and *secondary* quantities. We refer to a small group of dimensions from which all others can be formed as primary quantities, and for which we set up arbitrary scales of measure. Secondary quantities are those quantities whose dimensions are expressible in terms of the dimensions of the primary quantities.

Units are the arbitrary names (and magnitudes) assigned to the primary dimensions adopted as standards for measurement. For example, the primary dimension of length may be measured in units of meters, feet, yards, or miles. These units of length are related to each other through unit conversion factors such as 1 mile = 5280 feet = 1609 meters.

Systems of Dimensions

Any valid equation that relates physical quantities must be dimensionally homogeneous; each term in the equation must have the same dimensions. We recognize that Newton's second law relates the four

dimensions, F , M , L , and t . Thus force and mass cannot both be selected as primary dimensions without introducing a constant of proportionality that has dimensions (and units).

Length and time are primary dimensions in all dimensional systems in common use. In some systems, mass is taken as a primary dimension. In others, force is selected as a primary dimension, whereas a third system chooses both force and mass as primary dimensions. Thus, we have three basic systems of dimensions, corresponding to the different ways of specifying the primary dimensions:

- (a) Mass [M], length [L], time [t], temperature [T]
- (b) Force [F], length [L], time [t], temperature [T]
- (c) Force [F], mass [M], length [L], time [t], temperature [T]

In system *a*, force [F] is a secondary dimension and the constant of proportionality in Newton's second law is dimensionless. In system *b*, mass [M] is a secondary dimension, and again the constant of proportionality in Newton's second law is dimensionless. In system *c*, both force [F] and mass [M] have been selected as primary dimensions. In this case the constant of proportionality is g_c and is not dimensionless. The dimensions of g_c must in fact be [ML/Ft^2] for the equation to be dimensionally homogeneous. The numerical value of the constant of proportionality depends on the units of measure chosen for each of the primary quantities.

Systems of Units

There is more than one way to select the unit of measure for each primary dimension. We shall present only the more common engineering systems of units for each of the basic systems of dimensions. Table 1.1 shows the basic units assigned to the primary dimensions for these systems. The units in parentheses are those assigned to that unit system's secondary dimension. Following the table is a brief description of each of them.

a. ML_tT dimensional system

SI, which is the official abbreviation in all languages for the Système International d'Unités [1] is an extension and refinement of the traditional metric system. More than 30 countries have declared it to be the only legally accepted system.

In the SI system of units, the unit of mass is the kilogram (kg), the unit of length is the meter (m), the unit of time is the second (s), and the unit of temperature is the kelvin (K). Force is a secondary dimension, and its unit, the newton (N), is defined from Newton's second law as the force required to accelerate a 1 kg mass at 1 m/s²

$$1 \text{ N} \equiv 1 \text{ kg} \cdot \text{m/s}^2$$

In the Absolute Metric system of units [2], the unit of mass is the gram, the unit of length is the centimeter, the unit of time is the second, and the unit of temperature is the kelvin. Since force is a secondary dimension, the unit of force, the dyne, is defined in terms of Newton's second law as

$$1 \text{ dyne} \equiv 1 \text{ g} \cdot \text{cm/s}^2$$

Table 1.1
Common Unit Systems

System of Dimensions	Unit System	Force F	Mass M	Length L	Time t	Temperature T
a. ML _t T	Système International d'Unités (SI)	(N)	kg	m	s	°K
b. FL _t T	British Gravitational (BG)	lbf	(slug)	ft	s	°R
c. FML _t T	English Engineering (EE)	lbf	lbm	ft	s	°R

b. FLtT dimensional system

In the British Gravitational system of units [3], the unit of force is the pound (lbf), the unit of length is the foot (ft), the unit of time is the second, and the unit of temperature is the degree Rankine ($^{\circ}\text{R}$). Since mass is a secondary dimension, the unit of mass, the slug, is defined in terms of Newton's second law as the mass that is accelerated 1 ft/s^2 by a force of 1 lbf.

$$1 \text{ slug} \equiv 1 \text{ lbf} \cdot \text{s}^2/\text{ft}$$

c. FMLtT dimensional system

In the English Engineering system of units [4], the unit of force is the pound force (lbf), the unit of mass is the pound mass (lbm), the unit of length is the foot, the unit of time is the second, and the unit of temperature is the degree Rankine. Since both force and mass are chosen as primary dimensions, Newton's second law is written as

$$\vec{F} = \frac{m\vec{a}}{g_c}$$

A force of one pound (1 lbf) is the force that gives a pound mass (1 lbm) an acceleration equal to the standard acceleration of gravity on Earth, 32.2 ft/s^2 . From Newton's second law we see that

$$1 \text{ lbf} \equiv \frac{1 \text{ lbm} \times 32.2 \text{ ft/s}^2}{g_c}$$

or

$$g_c \equiv 32.2 \text{ ft} \cdot \text{lbm}/(\text{lbf} \cdot \text{s}^2)$$

The constant of proportionality, g_c , has both dimensions and units. The dimensions arose because we selected both force and mass as primary dimensions; the units and the numerical value are a consequence of our choices for the standards of measurement.

Since a force of 1 lbf accelerates 1 lbm at 32.2 ft/s^2 , it would accelerate 32.2 lbm at 1 ft/s^2 . A slug also is accelerated at 1 ft/s^2 by a force of 1 lbf. Therefore,

$$1 \text{ slug} \equiv 32.2 \text{ lbm}$$

In this text, we distinguish the two uses of "pound" by using lbf for force and lbm for mass. In the English Engineering system then, the weight of an object is given by

$$W = m \frac{g}{g_c}$$

Preferred Systems of Units

In this text we shall use both the *SI* and the *British Gravitational* systems of units. In either case, the constant of proportionality in Newton's second law is dimensionless and has a value of unity. Consequently, Newton's second law is written as $\vec{F} = m\vec{a}$. In these systems, it follows that the weight of an object of mass m is given by $W = mg$.

SI units and prefixes, together with other defined units and useful conversion factors, are on the inside cover of the book. In Example 1.4, we show how we convert between mass and weight in the different unit systems that we use.

Dimensional Consistency and "Engineering" Equations

In engineering, we strive to make equations and formulas have consistent dimensions. That is, each term in an equation, should be reducible to the same dimensions. For example, a very important equation we will derive later on is the Bernoulli equation

$$\frac{p_1}{\rho} + \frac{V_1^2}{2} + gz_1 = \frac{p_2}{\rho} + \frac{V_2^2}{2} + gz_2$$

Example 1.4 USE OF UNITS

The label on a jar of peanut butter states its net weight is 510 g. Express its mass and weight in SI, BG, and EE units.

Given: Peanut butter “weight,” $m = 510 \text{ g}$.

Find: Mass and weight in SI, BG, and EE units.

Solution: This problem involves unit conversions and use of the equation relating weight and mass:

$$W = mg$$

The given “weight” is actually the mass because it is expressed in units of mass:

$$m_{\text{SI}} = 0.510 \text{ kg} \xrightarrow{\hspace{1cm}} m_{\text{SI}}$$

Using the conversions given inside the book cover,

$$m_{\text{EE}} = m_{\text{SI}} \left(\frac{1 \text{ lbm}}{0.454 \text{ kg}} \right) = 0.510 \text{ kg} \left(\frac{1 \text{ lbm}}{0.454 \text{ kg}} \right) = 1.12 \text{ lbm} \xrightarrow{\hspace{1cm}} m_{\text{EE}}$$

Using the fact that 1 slug = 32.2 lbm,

$$\begin{aligned} m_{\text{BG}} &= m_{\text{EE}} \left(\frac{1 \text{ slug}}{32.2 \text{ lbm}} \right) = 1.12 \text{ lbm} \left(\frac{1 \text{ slug}}{32.2 \text{ lbm}} \right) \\ &= 0.0349 \text{ slug} \xrightarrow{\hspace{1cm}} m_{\text{BG}} \end{aligned}$$

To find the weight, we use

$$W = mg$$

In SI units, and using the definition of a newton,

$$\begin{aligned} W_{\text{SI}} &= 0.510 \text{ kg} \times 9.81 \frac{\text{m}}{\text{s}^2} = 5.00 \left(\frac{\text{kg} \cdot \text{m}}{\text{s}^2} \right) \left(\frac{\text{N}}{\text{kg} \cdot \text{m}/\text{s}^2} \right) \\ &= 5.00 \text{ N} \xrightarrow{\hspace{1cm}} W_{\text{SI}} \end{aligned}$$

In BG units, and using the definition of a slug,

$$\begin{aligned} W_{\text{BG}} &= 0.0349 \text{ slug} \times 32.2 \frac{\text{ft}}{\text{s}^2} = 1.12 \frac{\text{slug} \cdot \text{ft}}{\text{s}^2} \\ &= 1.12 \left(\frac{\text{slug} \cdot \text{ft}}{\text{s}^2} \right) \left(\frac{\text{lbf} \cdot \text{ft}}{\text{slug}} \right) = 1.12 \text{ lbf} \xrightarrow{\hspace{1cm}} W_{\text{BG}} \end{aligned}$$

In EE units, we use the form $W = mg/g_c$, and using the definition of g_c ,

$$\begin{aligned} W_{\text{EE}} &= 1.12 \text{ lbm} \times 32.2 \frac{\text{ft}}{\text{s}^2} \times \frac{1}{g_c} = \frac{36.1}{g_c} \frac{\text{lbf} \cdot \text{ft}}{\text{s}^2} \\ &= 36.1 \left(\frac{\text{lbf} \cdot \text{ft}}{\text{s}^2} \right) \left(\frac{\text{lbf} \cdot \text{s}^2}{32.2 \text{ ft} \cdot \text{lbf}} \right) = 1.12 \text{ lbf} \xrightarrow{\hspace{1cm}} W_{\text{EE}} \end{aligned}$$

This problem illustrates:

- Conversions from SI to BG and EE systems.
- Use of g_c in the EE system.

Notes:

The student may feel this example involves a lot of unnecessary calculation details (e.g., a factor of 32.2 appears, then disappears), but it cannot be stressed enough that such steps should always be explicitly written out to minimize errors—if you do not write all steps and units down, it is just too easy, for example, to multiply by a conversion factor when you should be dividing by it. For the weights in SI, BG, and EE units, we could alternatively have looked up the conversion from newton to lbf.

which relates the pressure p , velocity V , and elevation z between points 1 and 2 along a streamline for a steady, frictionless incompressible flow. This equation is dimensionally consistent because each term in the equation can be reduced to dimensions of L^2/t^2 . The pressure term dimensions are FL/M , but from Newton’s law we find $F=M/Lt^2$, so $FL/M=ML^2/Mt^2=L^2/t^2$.

Almost all equations you are likely to encounter will be dimensionally consistent. However, you should be alert to some still commonly used equations that are not. These are often “engineering”

equations derived many years ago, or are empirical (based on experiment rather than theory), or are proprietary equations used in a particular industry or company. For example, civil engineers often use the semi-empirical Manning equation

$$V = \frac{R_h^{2/3} S_0^{1/2}}{n}$$

which gives the flow speed V in an open channel as a function of the hydraulic radius R_h (*which is a measure of the flow cross-section and contact surface area*), the channel slope S_0 , and the Manning resistance coefficient n . The value of this constant depends on the surface condition of the channel. This equation is dimensionally inconsistent. For the right side of the equation, R_h has dimensions L , and S_0 is dimensionless, so with a dimensionless constant n , we end up with dimensions of $L^{2/3}$. For the left side of the equation the dimensions must be L/t . A user of the equation needs to know that the values of n provided in most references will give correct results *only* if we ignore the dimensional inconsistency, always use R_h in meters, and interpret V to be in m/s. Because the equation is dimensionally inconsistent, using the *same* value for n with R_h in ft does *not* give the correct value for V in ft/s.

A second type of problem is one in which the dimensions of an equation are consistent but use of units is not. The commonly used *EER* of an air conditioner is

$$EER = \frac{\text{cooling rate}}{\text{electrical input}}$$

which indicates how efficiently the AC works. The equation *is* dimensionally consistent, with the *EER* being dimensionless as the cooling rate and electrical input are both measured in energy/time. However, the *units* traditionally used in it are not consistent. For example, an *EER* of 10 means you receive 10 *Btu/hr* of cooling for each 1 *W* of electrical power. Manufacturers, retailers, and customers all use the *EER*, in a sense, incorrectly in that they quote an *EER* of, say, 10, rather than the correct way, of 10 *Btu/hr/W*. (The *EER*, as used, is an everyday, inconsistent unit version of the coefficient of performance, *COP*, studied in thermodynamics.) *EER* has these units because the cooling effect is commonly expressed in terms of *Btu/hr* and the power input to the motor in *kW*.

The two examples above illustrate the dangers in using certain equations. Almost all the equations encountered in this text will be dimensionally consistent, but you should be aware of the occasional troublesome equation you will encounter in your engineering studies.

As a final note on units, we stated earlier that we will use SI and BG units in this text. You will become very familiar with their use through using this text but should be aware that many of the units used, although they are scientifically and engineering-wise correct, are nevertheless not units you will use in everyday activities.

1.5 Analysis of Experimental Error

Most consumers are unaware of it but, as with most foodstuffs, soft drink containers are filled to plus or minus a certain amount, as allowed by law. The allowable variation is typically 1 or 2.5 percent of the stated value. Because it is difficult to precisely measure the filling of a container in a rapid production process, a 12-fl-oz container may actually contain 12.1, or 12.3, fl oz. Similarly, the supplier of components for the interior of a car must satisfy minimum and maximum dimensions (tolerances) so that the final appearance of the interior is visually appealing. Engineers performing experiments must measure not just data but also the uncertainties in their measurements. They must also somehow determine how these uncertainties affect the uncertainty in the final result.

These examples illustrate the importance of *experimental uncertainty*, that is, the study of uncertainties in measurements and their effect on overall results. There is always a trade-off in experimental work or in manufacturing. We can reduce the uncertainties to a desired level, but the smaller the uncertainty (the more precise the measurement or experiment), the more expensive the procedure will be. Furthermore, in a complex manufacture or experiment, it is not always easy to see which measurement uncertainty has the biggest influence on the final outcome.

Anyone involved in experimental work should understand experimental uncertainties. Appendix E has details on this topic; there is a selection of problems on this topic at the end of this chapter.

1.6 Summary

In this chapter we introduced or reviewed a number of basic concepts and definitions, including:

- ✓ How fluids are defined, and the no-slip condition
- ✓ System/control volume concepts
- ✓ Lagrangian and Eulerian descriptions
- ✓ Units and dimensions (including SI, British Gravitational, and English Engineering systems)
- ✓ Experimental uncertainty

REFERENCES

1. A. Thompson and B. N. Taylor, *NIST Special Publication 811, 2008 Edition, Guide for the Use of the International System of Units (SI)*, NIST, Gaithersburg, MD, 2008. (<https://physics.nist.gov/cuu/Units/bibliography.html>)
2. American Society for Testing and Materials, *ASTM Standard for Metric Practice, E380-97*. Conshohocken, PA: ASTM, 1997.
3. F. Cardarelli, *Encyclopaedia of Scientific Units, Weights and Measures: Their SI Equivalences and Origins*, Google Books, Springer Science & Business Media, 2003.
4. E. W. Comings, English Engineering Units and Their Dimensions, *Ind. Eng. Chem.*, 1940.

Chapter 2 Problems

Velocity Field

2.1 Briefly state why the following flows are classified as either one-, two-, or three-dimensional, and as either steady or unsteady. The quantities a and b are constants.

1 $\vec{V} = [(ax+t)e^{by}]\hat{i}$

2 $\vec{V} = (ax-by)\hat{i}$

3 $\vec{V} = ax\hat{i} + [e^{bx}]\hat{j}$

4 $\vec{V} = ax\hat{i} + bx^2\hat{j} + ax\hat{k}$

5 $\vec{V} = ax\hat{i} + [e^{bt}]\hat{j}$

6 $\vec{V} = ax\hat{i} + bx^2\hat{j} + ay\hat{k}$

7 $\vec{V} = ax\hat{i} + [e^{bt}]\hat{j} + ay\hat{k}$

8 $\vec{V} = ax\hat{i} + [e^{by}]\hat{j} + az\hat{k}$

2.2 A fluid is contained between two parallel plates spaced a distance h apart. The lower plate moves at a constant velocity U and the upper plate is stationary. Determine which of the following velocity fields meets the appropriate boundary conditions, where x is the coordinate along the plates and y is the coordinate perpendicular to the plates with $y = 0$ at the lower plate.

(a) $u = U$

(b) $u = U \frac{y}{h}$

(c) $u = U \frac{h-y}{h}$

(d) $u = U \left(\frac{y}{h} - 1 \right)$

(e) $u = U \left(\frac{y}{h} \right)^2$

2.3 A fluid fills the space between two parallel disks. The lower one is stationary and the upper one rotates at a constant speed. The velocity field is given as $\vec{V} = \hat{e}_\theta r\omega z/h$, where the origin of the coordinate system is at the center of the stationary disks and h is the height of the rotating disk. Determine the dimensions of the velocity field. State the appropriate boundary conditions on the lower and upper disks and show that the velocity field meets these conditions.

2.4 For the velocity field $\vec{V} = Ax^2y\hat{i} + Bxy^2\hat{j}$, where $A = 2 \text{ m}^{-2}\text{s}^{-1}$ and $B = 1 \text{ m}^{-2}\text{s}^{-1}$, and the coordinates are measured in meters, obtain an equation for the flow streamlines. Plot the streamlines that pass through the points (1,1), (1,2), and (2,2).

2.5 When an incompressible, nonviscous fluid flows against a plate in a plane (two-dimensional) flow, an exact solution for the equations of motion for this flow is $u = Ax$, $v = -Ay$, with $A > 0$ for the sketch shown. The coordinate origin is located at the *stagnation point* 0, where the flow divides and the local velocity is zero. Plot the streamlines in the flow that pass through the points (1,1), (1,2), and (2,2).

2.6 For the *free vortex* flow the velocities are $v_t = 5/r$ and $v_r = 0$. Assume that lengths are in feet or meters and times are in seconds. Plot the streamlines of this flow that pass through the points (0,1), (0,2), and (0,3). Plot the velocity as a function of radius and determine the velocity at the origin (0,0).

2.7 For the *forced vortex* flow the velocities are $v_t = \omega r$ and $v_r = 0$. Plot the streamlines of this flow that pass through the points (0,1), (0,2), and (0,3). Plot the velocity as a function of radius and determine the velocity at the origin (0,0).

2.8 A velocity field is given by $\vec{V} = ax^3\hat{i} + bxy^3\hat{j}$, where $a = 1 \text{ m}^{-2}\text{s}^{-1}$ and $b = 1 \text{ m}^{-3}\text{s}^{-1}$. Find the equation of the streamlines. Plot the streamlines that pass through the points (2, 0.25), (2, 0.5) and (2,1).

2.9 A velocity field is given by $\vec{V} = a(1+bt)y\hat{i} + cx\hat{j}$, where x and y are in m and $a = 0.5 \text{ s}^{-1}$, $b = 1 \text{ s}^{-1}$, and $c = 4 \text{ s}^{-1}$. Determine an equation for the streamlines. Plot the streamlines that pass through the point (0,2) at $t = 0$ s and $t = 1$ s from $x = 0$ to $x = 1$ m.

2.10 Consider the velocity field $V = ax\hat{i} + by(1+ct)\hat{j}$, where **SS** $a = b = 2 \text{ s}^{-1}$ and $c = 0.4 \text{ s}^{-1}$. Coordinates are measured in meters. For the particle that passes through the point $(x,y) = (1,1)$ at the instant $t = 0$, plot the pathline during the interval from $t = 0$ to 1.5 s. Compare this pathline with the streamlines plotted through the same point at the instants $t = 0$, 1, and 1.5 s.

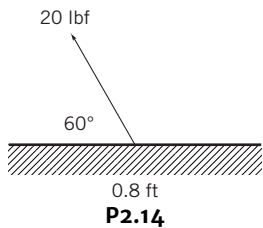
2.11 Consider the flow field given in Eulerian description by the expression $\vec{V} = ax\hat{i} + by\hat{j}$, where $a = 0.2 \text{ s}^{-1}$, $b = 0.04 \text{ s}^{-2}$, and the coordinates are measured in meters. Derive the Lagrangian position functions for the fluid particle that was located at the point $(x,y) = (1,1)$ at the instant $t = 0$. Obtain an algebraic expression for the pathline followed by this particle. Plot the pathline and compare with the streamlines plotted through the same point at the instants $t = 0$, 10, and 20 s.

P-4 Chapter 2 Problems

2.12 Consider the flow field $\vec{V} = ax\hat{i} + bj\hat{j}$, where $a = 1/4 \text{ s}^{-2}$ and $b = 1/3 \text{ m/s}$. Coordinates are measured in meters. For the particle that passes through the point $(x, y) = (1, 2)$ at the instant $t = 0$, plot the pathline during the time interval from $t = 0$ to 3 s. Compare this pathline with the streakline through the same point at the instant $t = 3$ s.

2.13 A flow is described by velocity field $\vec{V} = a\hat{i} + bx\hat{j}$, where $a = 2 \text{ m/s}$ and $b = 1 \text{ s}^{-1}$. Coordinates are measured in meters. Obtain the equation for the streamline passing through point $(2, 5)$. At $t = 2$ s, determine the coordinates of the particle that passed through point $(0, 4)$ at $t = 0$. At $t = 3$ s, determine the coordinates of the particle that passed through point $(1, 4.25)$ 2 s earlier. Draw some conclusions about the pathline, streamline, and streakline for this flow.

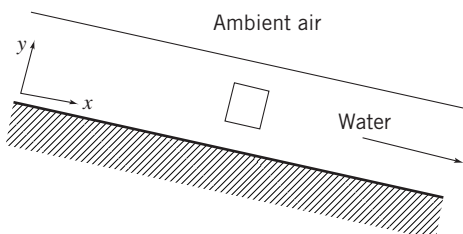
2.14 In a two-dimensional flow, a force of 20 lbf acts on a small square plate as shown below. Determine the normal stress σ_{xx} and the shear stress τ_{yx} .



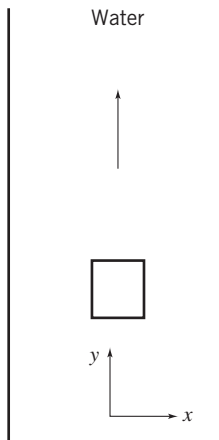
2.15 For each of the situations shown below, enter into the table whether the stresses on opposite sides are equal, unequal, or zero

Problem	Stress	Equal, unequal, or zero
a)	σ_{xx}	
	σ_{yy}	
	τ_{yx}	
	τ_{xy}	
b)	σ_{xx}	
	σ_{yy}	
	τ_{yx}	
	τ_{xy}	
c)	σ_{xx}	
	σ_{yy}	
	τ_{yx}	
	τ_{xy}	

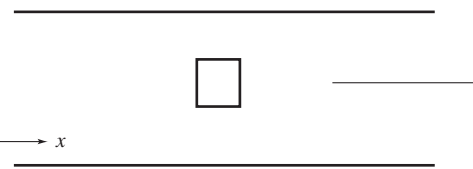
a) A sheet of water flowing down an inclined plane.



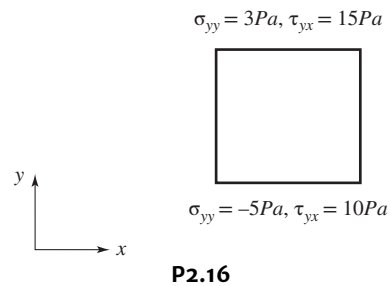
b) Water flowing between two vertical plates.



c) Air flowing between two horizontal plates.



2.16 A cubic element with sides 1 mm in length in a two-dimensional flow is shown below. The stresses on each of the faces are given on the diagram. Determine the net force on the element and the direction of the force.



Viscosity

2.17 The variation with temperature of the viscosity of air is represented well by the empirical Sutherland correlation

$$\mu = \frac{bT^{1/2}}{1 + S/T}$$

Best-fit values of b and S are given in Appendix A. Develop an equation in SI units for kinematic viscosity versus temperature for air at atmospheric pressure. Assume ideal gas behavior. Check by using the equation to compute the kinematic viscosity of air at 0°C and at 100°C and comparing to the data in Appendix A (Table A.10); plot the kinematic viscosity for a temperature range of 0°C to 100°C, using the equation and the data in Table A.10.

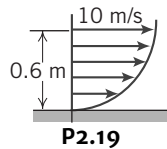
2.18 The velocity distribution for laminar flow between parallel plates is given by

$$\frac{u}{u_{\max}} = 1 - \left(\frac{2y}{h}\right)^2$$

where h is the distance separating the plates and the origin is placed midway between the plates. Consider a flow of water at 15°C, with $u_{\max} = 0.10 \text{ m/s}$ and $h = 0.1 \text{ mm}$. Calculate the shear stress on the upper plate and give its direction. Sketch the variation of shear stress across the channel.

2.19 Calculate velocity gradients and shear stress for $y=0, 0.2, 0.4$, and 0.6 m , if the velocity profile is a quarter-circle having its center 0.6 m from the boundary. The fluid viscosity is $7.5 \times 10^{-4} \text{ Ns/m}^2$.

The velocity profile is given by $\left(\frac{u}{10 \frac{m}{s}}\right)^2 + \left(\frac{y}{0.6 \text{ m}} - 1\right) = 1$



SS 2.20 A very large thin plate is centered in a gap of width 0.06 m with different oils of unknown viscosities above and below; one viscosity is twice the other. When the plate is pulled at a velocity of 0.3 m/s, the resulting force on one square meter of plate due to the viscous shear on both sides is 29 N. Assuming viscous flow and neglecting all end effects, calculate the viscosities of the oils.

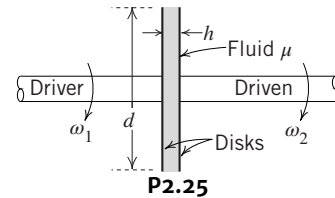
2.21 A vertical gap 25 mm wide of infinite extent contains oil of specific gravity 0.95 and viscosity 2.4 Pa·s. A metal plate $1.5 \text{ m} \times 1.5 \text{ m} \times 1.6 \text{ mm}$ weighing 45 N is to be lifted through the gap at a constant speed of 0.06 m/s. Estimate the force required.

2.22 A cylinder 8 in. in diameter and 3 ft long is concentric with a pipe of 8.25 in. i.d. Between the cylinder and pipe there is an oil film. Find the force required to move the cylinder along the pipe at a constant velocity of 3 fps. The kinematic viscosity of the oil is $0.006 \text{ ft}^2/\text{s}$; the specific gravity is 0.92.

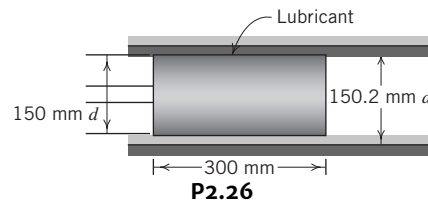
2.23 Crude oil at 20°C fills the space between two concentric cylinders 250 mm high and with diameters of 150 mm and 156 mm. Find the torque required to rotate the inner cylinder at 12 r/min, the outer cylinder remaining stationary.

2.24 A block 0.1 m square, with 5 kg mass, slides down a smooth incline, 30° below the horizontal, on a film of SAE 30 oil at 20°C that is 0.20 mm thick. If the block is released from rest at $t=0$, determine its initial acceleration. Derive an expression for the speed of the block as a function of time. Plot the curve for $V(t)$. Find the speed after 0.1 s. If we want the mass to instead reach a speed of 0.3 m/s at this time, find the viscosity μ of the oil we would have to use.

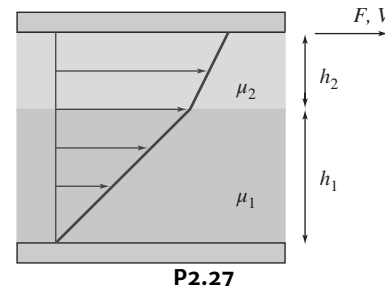
SS 2.25 The fluid drive shown transmits a torque T for steady-state conditions (ω_1 and ω_2 constant). Derive an expression for the slip ($\omega_1 - \omega_2$) in terms of T , μ , d , and h . For values $d = 6 \text{ in.}$, $h = 0.2 \text{ in.}$, SAE 30 oil at 75°F, a shaft rotation of 120 rpm, and a torque of 0.003 ft-lbf, determine the slip.



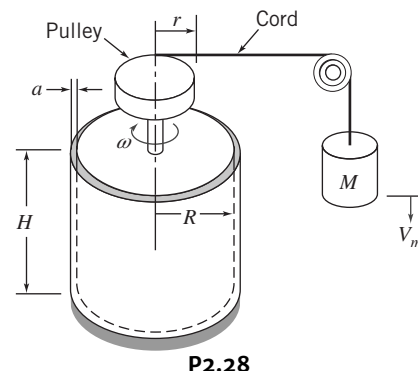
2.26 A piston-cylinder combination is shown in the figure. The piston velocity is 6 m/s and the oil has a kinematic viscosity of $2.8 \times 10^{-5} \text{ m}^2/\text{s}$ and a specific gravity of 0.92. Determine the power dissipated by the viscous friction.



2.27 Fluids of viscosities $\mu_1 = 0.1 \text{ N}\cdot\text{s}/\text{m}^2$ and $\mu_2 = 0.15 \text{ N}\cdot\text{s}/\text{m}^2$ are contained between two plates (each plate is 1 m^2 in area). The thicknesses are $h_1 = 0.5 \text{ mm}$ and $h_2 = 0.3 \text{ mm}$, respectively. And the upper plate moves at a velocity of 1.5 m/s. Determine the force required to move the upper plate and the fluid velocity at the interface between the two fluids.



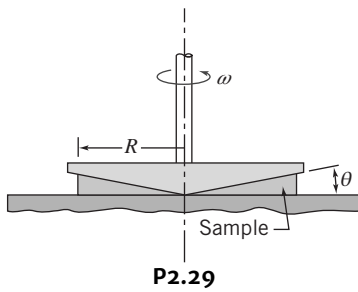
2.28 A concentric cylinder viscometer may be formed by rotating the inner member of a pair of closely fitting cylinders. The annular gap is small so that a linear velocity profile will exist in the liquid sample. Consider a viscometer with an inner cylinder of 4 in. diameter and 8 in. height, and a clearance gap width of 0.001 in., filled with castor oil at 90°F. Determine the torque required to turn the inner cylinder at 400 rpm.



P-6 Chapter 2 Problems

SS 2.29 The cone and plate viscometer shown is an instrument used frequently to characterize non-Newtonian fluids. It consists of a flat plate and a rotating cone with a very obtuse angle (typically θ is less than 0.5 degrees). The apex of the cone just touches the plate surface and the liquid to be tested fills the narrow gap formed by the cone and plate. The viscometer is used to measure the apparent viscosity of a fluid. The data below are obtained. Determine the kind of non-Newtonian fluid it is. Find the values of k and n used in Eqs. 2.16 and 2.17 in defining the apparent viscosity of a fluid. (Assume θ is 0.5 degrees.) Predict the viscosity at 90 and 100 rpm.

Speed (rpm)	10	20	30	40	50	60	70	80
$\mu(\text{N} \cdot \text{s}/\text{m}^2)$	0.121	0.139	0.153	0.159	0.172	0.172	0.183	0.185



2.30 A viscometer is used to measure the viscosity of a patient's blood. The deformation rate (shear rate)—shear stress data is shown below. Plot the apparent viscosity versus deformation rate. Find the value of k and n in Eq. 2.17

$\dot{\gamma} (\text{s}^{-1})$	5	10	25	50	100	200	300	400
$\tau (\text{Pa})$	0.0457	0.119	0.241	0.375	0.634	1.06	1.46	1.78

Surface Tension

2.31 Small gas bubbles form in soda when a bottle or can is opened. The average bubble diameter is about 0.1 mm. Estimate the pressure difference between the inside and outside of such a bubble.

2.32 Calculate the maximum capillary rise of water (20°C) to be expected between two vertical, clean glass plates spaced 1 mm apart.

2.33 Calculate the maximum capillary depression of mercury to be expected in a vertical glass tube 1 mm in diameter at 15.5°C .

Description and Classification of Fluid Motions

2.34 A supersonic aircraft travels at 2800 km/hr at an altitude of 27 km. Determine the Mach number for the airplane. The wing width (chord) is 7 m. Assume that the wing can be treated as a flat plate and determine the Reynolds number at the trailing edge and the position at which transition from a laminar to turbulent boundary layer occurs.

2.35 SAE 30 oil at 100°C flows through a 12-mm-diameter stainless-steel tube. Determine the specific gravity and specific weight of the oil. The oil discharged from the tube fills a 100-mL graduated cylinder in 9 seconds. Determine whether the flow is laminar or turbulent.

2.36 A seaplane flies at 80 mph in air at 45°F . The pontoons are 17 feet long. Assume that the flow over the underside of the pontoons can be treated as a flat plate and determine the Reynolds number for the air flow at the end of the pontoon. Determine the Reynolds number when the seaplane lands on water at 45°F .

2.37 The cruising speed of a military airplane is 700 km/hr. Determine the Mach number of the plane as it flies at this speed from an altitude of 1 km to 15 km and plot the Mach number as a function of altitude.

SS

CHAPTER 2

Fundamental Concepts

- 2.1 Fluid as a Continuum
- 2.2 Velocity Field
- 2.3 Stress Field
- 2.4 Viscosity

- 2.5 Surface Tension
- 2.6 Description and Classification of Fluid Motions
- 2.7 Summary and Useful Equations

Case Study

Airplane wings have constantly changed over the years as we have learned more about the flow of air over surfaces. Recent advances include the *winglet*, which is the tilted airfoil surface at the end of the wing as seen in the figure. The emphasis on fuel savings has motivated the design and development of winglets.

All winglets work the same way, but there are many different shapes to accomplish the same thing. When an airplane flies, the higher pressure air on the lower side of the wing flows upward at the wing tip to the region of lower pressure on top. This creates a *wingtip vortex*, and is a source of *lift-induced drag* that the engine needs to overcome. A winglet reduces this drag by recovering some of the energy in the wingtip vortex. It also changes the *aspect ratio* (ratio of the wing span squared divided by the wing area), which also reduces the drag.

In addition to reducing drag, winglets also generate lift at the tip, which is beneficial. Because they are at an angle, they also increase the bending moment at the wing root, which requires the airframe to be strengthened, which adds some weight. Newer winglets also have actively controlled surfaces added to the trailing edges to introduce aerodynamic instabilities into the eddies shed by the wing. Although this might seem undesirable, the instabilities help dissipate the vortices in the wake of an airplane

that prevent other airplanes from following too closely. Winglets are a good example of the application of the understanding of complex fluid behavior to making improvements.



Winglet at the end of an airline wing.

Elvis901/Adobe Stock Photo

Learning Objectives

After completing this chapter, you should be able to

- Explain in physical terms what is meant by “we treat fluid as a continuum.”
- Explain the difference between streamlines, streaklines, pathlines, and timelines.
- Explain the difference between a normal stress and a shear stress and give examples of each.
- Apply Newton’s law of viscosity in a flow problem.
- Describe the effects of the force produced by surface tension.
- Define the following terms used to classify fluid flow: inviscid, viscous, laminar, turbulent, incompressible, compressible, internal, and external.

In Chapter 1 we discussed in general terms what fluid mechanics is about, and described some of the approaches we will use in analyzing fluid mechanics problems. In this chapter we will be more specific in defining some important properties of fluids and ways in which flows can be described and characterized.

2.1 Fluid as a Continuum

We are all familiar with fluids, such as air and water, and we experience them as being “smooth,” i.e., as being a continuous medium. Unless we use specialized equipment, we are not aware of the underlying molecular nature of fluids. This molecular structure is one in which the mass is *not* continuously distributed in space, but is concentrated in molecules that are separated by relatively large regions of empty space. The sketch in Fig. 2.1a shows a schematic representation of this. A region of space “filled” by a stationary fluid (e.g., air, treated as a single gas) looks like a continuous medium, but if we zoom in on a very small cube of it, we can see that we mostly have empty space, with gas molecules scattered around, moving at high speed. Note that the size of the gas molecules is greatly exaggerated and that we have placed velocity vectors only on a small sample. We wish to determine the minimum volume, $\delta V'$, that a “point” C must be so that we can talk about continuous fluid properties such as the density at a point. In other words, under what circumstances can a fluid be treated as a *continuum*, for which, by definition, properties vary smoothly from point to point? This is an important question because the concept of a continuum is the basis of classical fluid mechanics.

Consider how we determine the density at a point. Density is defined as mass per unit volume; in Fig. 2.1a the mass δm will be given by the instantaneous number of molecules in δV and the mass of each molecule, so the average density in volume δV is given by $\rho = \delta m / \delta V$. We say “average” because the number of molecules in δV , and hence the density, fluctuates. For example, if the gas in Fig. 2.1a was air at standard temperature and pressure (STP) and the volume δV was a sphere of diameter $0.01\mu\text{m}$, there might be 15 molecules in δV , but an instant later there might be 17 (three might enter while one leaves). Hence the density at “point” C randomly fluctuates in time, as shown in Fig. 2.1b. In this figure, each vertical dashed line represents a specific chosen volume, δV , and each data point represents the measured density at an instant. For very small volumes, the density varies greatly, but above a certain volume, $\delta V'$, the density becomes stable as the volume now encloses a huge number of molecules. For example, if $\delta V = 0.001\text{ mm}^3$ (about the size of a grain of sand), there will on average be 2.5×10^{13} molecules present. Hence we can conclude that air at STP (and other gases and liquids) can be treated as a continuous medium as long as we consider a “point” to be no smaller than about this size; this is sufficiently precise for most engineering applications.

The concept of a continuum is the basis of classical fluid mechanics. The continuum assumption is valid in treating the behavior of fluids under normal conditions. It only breaks down when the mean free path of the molecules becomes the same order of magnitude as the smallest significant

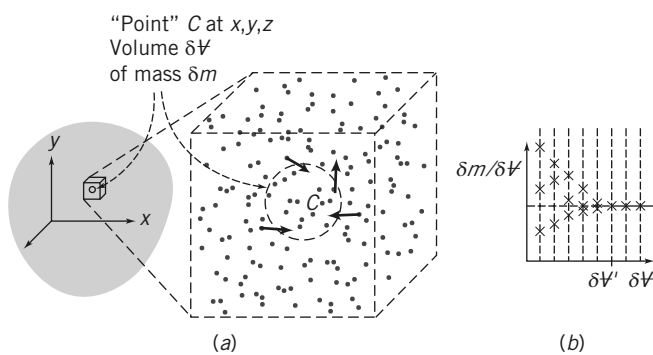


Fig. 2.1 Definition of density at a point.

characteristic dimension of the problem. This occurs in such specialized problems as rarefied gas flow such, as encountered in flights into the upper reaches of the atmosphere. For these specialized cases we must abandon the concept of a continuum in favor of the microscopic and statistical points of view.

As a consequence of the continuum assumption, each fluid property is assumed to have a definite value at every point in space. Thus fluid properties such as density, temperature, velocity, and so on are considered to be continuous functions of position and time. For example, we now have a workable definition of density at a point,

$$\rho \equiv \lim_{\delta V' \rightarrow \delta V} \frac{\delta m}{\delta V} \quad (2.1)$$

Since point C was arbitrary, the density at any other point in the fluid could be determined in the same manner. If density was measured simultaneously at an infinite number of points in the fluid, we would obtain an expression for the density distribution as a function of the space coordinates, $\rho = \rho(x, y, z)$, at the given instant.

The density at a point may also vary with time. Thus the complete representation of density (the *field* representation) is given by

$$\rho = \rho(x, y, z, t) \quad (2.2)$$

Since density is a scalar quantity, requiring only the specification of a magnitude for a complete description, the field represented by Eq. 2.2 is a scalar field.

An alternative way of expressing the density of a substance is to compare it to an accepted reference value, typically the maximum density of water, ρ_{H_2O} (1000 kg/m^3 at 4°C or 1.94 slug/ft^3 at 39°F). Thus, the *specific gravity*, SG, of a substance is expressed as

$$SG = \frac{\rho}{\rho_{H_2O}} \quad (2.3)$$

For example, the SG of mercury is typically 13.6; mercury is 13.6 times as dense as water. Appendix 1 contains specific gravity data for selected engineering materials. The specific gravity of liquids is a function of temperature; for most liquids specific gravity decreases with increasing temperature.

The *specific weight*, γ , of a substance is another useful material property. It is defined as the weight of a substance per unit volume and given as

$$\gamma = \frac{mg}{V} \rightarrow \gamma = \rho g \quad (2.4)$$

For example, the specific weight of water is approximately 9.81 kN/m^3 (62.4 lbf/ft^3).

2.2 Velocity Field

In the previous section we saw that the continuum assumption led directly to the notion of the density field. Other fluid properties also may be described by fields.

A very important property defined by a field is the velocity field, given by

$$\vec{V} = \vec{V}(x, y, z, t) \quad (2.5)$$

Velocity is a vector quantity, requiring a magnitude and direction for a complete description, so the velocity field (Eq. 2.5) is a vector field.

The velocity vector, \vec{V} , also can be written in terms of its three scalar components. Denoting the components in the x , y , and z directions by u , v , and w , then

$$\vec{V} = u\hat{i} + v\hat{j} + w\hat{k} \quad (2.6)$$

In general, each component, u , v , and w , will be a function of x , y , z , and t .

We need to be clear on what $\vec{V}(x,y,z,t)$ measures. It indicates the velocity of a fluid particle that is passing through the point x , y , z at time instant t , in the Eulerian sense. We conclude that $\vec{V}(x,y,z,t)$ should be thought of as the velocity field of all particles, not just the velocity of an individual particle.

If properties at every point in a flow field do not change with time, the flow is termed *steady*. Stated mathematically, the definition of steady flow is

$$\frac{\partial \eta}{\partial t} = 0$$

where η represents any fluid property. Hence, for steady flow,

$$\frac{\partial \rho}{\partial t} = 0 \text{ or } \rho = \rho(x,y,z)$$

and

$$\frac{\partial \vec{V}}{\partial t} = 0 \text{ or } \vec{V} = \vec{V}(x,y,z)$$

In steady flow, any property may vary from point to point in the field, but all properties remain constant with time at every point.

One-, Two-, and Three-Dimensional Flows

A flow is classified as one-, two-, or three-dimensional depending on the number of space coordinates required to specify the velocity field. Equation 2.5 indicates that the velocity field may be a function of three space coordinates and time. Such a flow field is termed *three-dimensional* because the velocity at any point in the flow field depends on the three coordinates required to locate the point in space.

Although most flow fields are inherently three-dimensional, analysis based on fewer dimensions is frequently appropriate. Consider, for example, the steady flow through a long straight pipe that has a divergent section, as shown in Fig. 2.2. In this example, we are using cylindrical coordinates (r, θ, x) . We will learn in Chapter 8 that under certain circumstances the velocity distribution may be described by

$$u = u_{\max} \left[1 - \left(\frac{r}{R} \right)^2 \right] \quad (2.7)$$

This is shown on the left of Fig. 2.2. The velocity $u(r)$ is a function of only one coordinate, and so the flow is one-dimensional. On the other hand, in the diverging section, the velocity decreases in the x direction, and the flow becomes two-dimensional: $u = u(r, x)$.

As you might suspect, the complexity of analysis increases considerably with the number of dimensions of the flow field. For many problems encountered in engineering, a one-dimensional analysis is adequate to provide approximate solutions of engineering accuracy.

Since all fluids satisfying the continuum assumption must have zero relative velocity at a solid surface (to satisfy the no-slip condition), most flows are inherently two- or three-dimensional. To simplify the analysis it is often convenient to use the notion of *uniform flow* at a given cross section. In a flow that

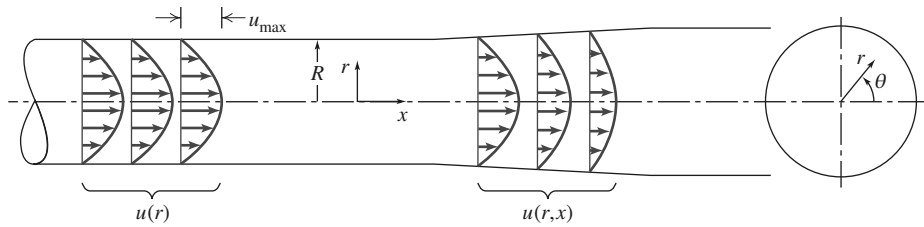


Fig. 2.2 Examples of one- and two-dimensional flows.

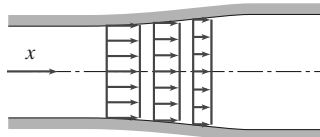


Fig. 2.3 Example of uniform flow at a section.

is uniform at a given cross section, the velocity is constant across any section normal to the flow. Under this assumption, the two-dimensional flow of Fig. 2.2 is modeled as the flow shown in Fig. 2.3. In the flow of Fig. 2.3, the velocity field is a function of x alone, and thus the flow model is one-dimensional. The term *uniform flow field* (as opposed to uniform flow at a cross section) is used to describe a flow in which the velocity is constant throughout the entire flow field.

Timelines, Pathlines, Streaklines, and Streamlines

Airplane and auto companies and college engineering laboratories, among others, frequently use wind tunnels to visualize flow fields [2]. Computational Fluid Dynamic software is becoming more extensively used also in flow visualization. For example, Fig. 2.4 shows a flow pattern for flow around a car mounted in a wind tunnel, generated by releasing smoke into the flow at five fixed upstream points. Flow patterns can be visualized using timelines, pathlines, streaklines, or streamlines.

If a number of adjacent fluid particles in a flow field are marked at a given instant, they form a line in the fluid at that instant called a *timeline*. Subsequent observations of the line may provide information about the flow field. For example, in discussing the behavior of a fluid under the action of a constant shear force, timelines were introduced to demonstrate the deformation of a fluid at successive instants.

A *pathline* is the path or trajectory traced out by a moving fluid particle. To make a pathline visible, we might identify a fluid particle at a given instant, e.g., by the use of dye or smoke, and then take a long exposure photograph of its subsequent motion. The line traced out by the particle is a pathline. This approach might be used to study, for example, the trajectory of a contaminant leaving a smokestack.

On the other hand, we might choose to focus our attention on a fixed location in space and identify, again by the use of dye or smoke, all fluid particles passing through this point. After a short period of time we would have a number of identifiable fluid particles in the flow, all of which had, at some time, passed through one fixed location in space. The line joining these fluid particles is defined as a *streakline*.

Streamlines are lines drawn in the flow field so that at a given instant they are tangent to the direction of flow at every point in the flow field. Since the streamlines are tangent to the velocity vector at every point in the flow field, there can be no flow across a streamline. Streamlines are the most commonly

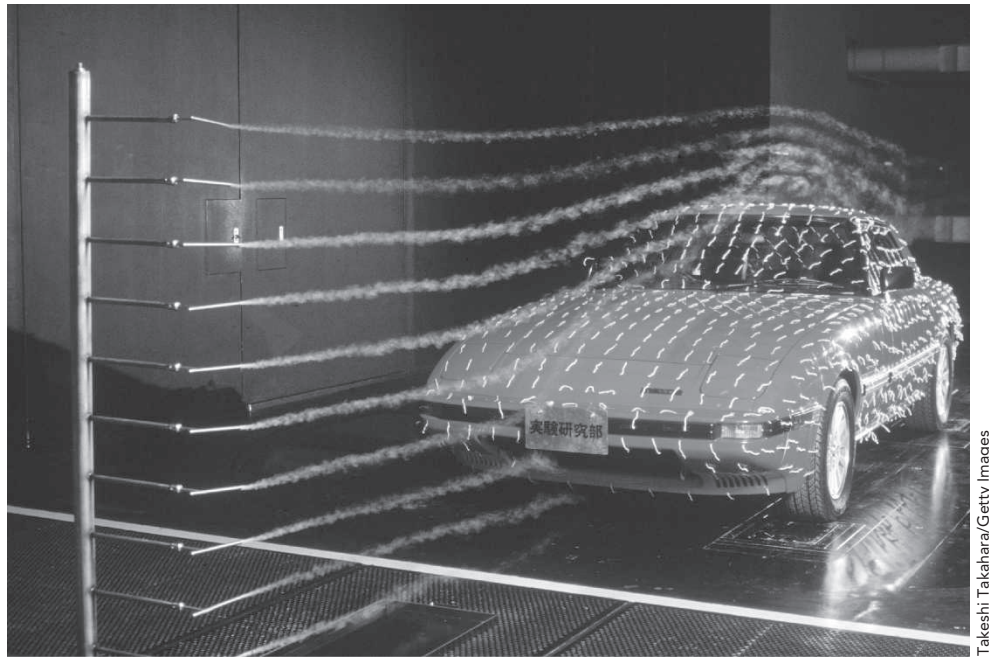


Fig. 2.4 Streaklines over an automobile in a wind tunnel.

Takeshi Takahara/Getty Images

used visualization technique. The procedure used to obtain the equation for a streamline in two-dimensional flow is illustrated in Example 2.1.

Figure 2.4 shows a photograph of the visualization of the flow over an automobile in a wind tunnel using smoke. In a steady flow such as in this photograph, the velocity at each point in the flow field remains constant with time and, consequently, the streamline shapes do not vary from one instant to the next. This implies that a particle located on a given streamline will always move along the same streamline. Furthermore, consecutive particles passing through a fixed point in space will be on the same streamline and, subsequently, will remain on this streamline. Thus in a steady flow, pathlines, streaklines, and streamlines are identical lines in the flow field.

For unsteady flow, streaklines, streamlines, and pathlines will in general have differing shapes. For example, consider holding a garden hose and swinging it side to side as water exits at high speed, as shown in Fig. 2.5. We obtain a continuous sheet of water. If we consider individual water particles, we see that each particle, once ejected, follows a straight-line path and so the pathlines are straight lines, as shown. On the other hand, if we start injecting dye into the water as it exits the hose, we will generate a streakline, and this takes the shape of an expanding sine wave, as shown. Clearly, pathlines and streaklines do not coincide for this unsteady flow.

We can use the velocity field to derive the shapes of streaklines, pathlines, and streamlines. Because the streamlines are parallel to the velocity vector, for a two-dimensional flow field we can write

$$\left. \frac{dy}{dx} \right)_{\text{streamline}} = \frac{v(x,y)}{u(x,y)} \quad (2.8)$$

Note that streamlines are obtained at an instant in time. If the flow is unsteady, time t is held constant in Eq. 2.8. Solution of this equation gives the equation $y = y(x)$, with an undetermined integration constant, the value of which determines the particular streamline.

For pathlines, we let $x = x_p(t)$ and $y = y_p(t)$, where $x_p(t)$ and $y_p(t)$ are the instantaneous coordinates of a specific particle. We then get

$$\left. \frac{dx}{dt} \right)_{\text{particle}} = u(x,y,t) \quad \left. \frac{dy}{dt} \right)_{\text{particle}} = v(x,y,t) \quad (2.9)$$

Example 2.1 STREAMLINES AND PATHLINES IN TWO-DIMENSIONAL FLOW

A velocity field is given by $\vec{V} = Ax\hat{i} - Ay\hat{j}$; the units of velocity are m/s; x and y are given in meters; $A = 0.3 \text{ s}^{-1}$.

- Obtain an equation for the streamlines in the xy plane.
- Plot the streamline passing through the point $(x_0, y_0) = (2, 8)$.
- Determine the velocity of a particle at the point $(2, 8)$.
- If the particle passing through the point (x_0, y_0) is marked at time $t = 0$, determine the location of the particle at time $t = 6 \text{ s}$.
- What is the velocity of this particle at time $t = 6 \text{ s}$?
- Show that the equation of the particle path (the pathline) is the same as the equation of the streamline.

Given: Velocity field, $\vec{V} = Ax\hat{i} - Ay\hat{j}$; x and y in meters; $A = 0.3 \text{ s}^{-1}$.

Find: (a) Equation of the streamlines in the xy plane.

- Streamline plot through point $(2, 8)$.
- Velocity of particle at point $(2, 8)$.
- Position at $t = 6 \text{ s}$ of particle located at $(2, 8)$ at $t = 0$.
- Velocity of particle at position found in (d).
- Equation of pathline of particle located at $(2, 8)$ at $t = 0$.

Solution:

- Streamlines are lines drawn in the flow field such that, at a given instant, they are tangent to the direction of flow at every point. Consequently,

$$\left. \frac{dy}{dx} \right|_{\text{streamline}} = \frac{v}{u} = \frac{-Ay}{Ax} = \frac{-y}{x}$$

Separating variables and integrating, we obtain

$$\int \frac{dy}{y} = - \int \frac{dx}{x}$$

or

$$\ln y = -\ln x + c_1$$

This can be written as $xy = c$

- For the streamline passing through the point $(x_0, y_0) = (2, 8)$ the constant, c , has a value of 16 and the equation of the streamline through the point $(2, 8)$ is

$$xy = x_0 y_0 = 16 \text{ m}^2$$

The plot is as sketched above.

- The velocity field is $\vec{V} = Ax\hat{i} - Ay\hat{j}$. At the point $(2, 8)$ the velocity is

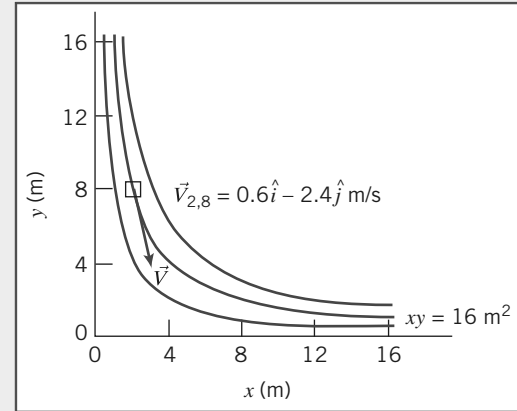
$$\vec{V} = A(x\hat{i} - y\hat{j}) = 0.3 \text{ s}^{-1}(2\hat{i} - 8\hat{j}) \text{ m} = 0.6\hat{i} - 2.4\hat{j} \text{ m/s}$$

- A particle moving in the flow field will have velocity given by

$$\vec{V} = Ax\hat{i} - Ay\hat{j}$$

Thus

$$u_p = \frac{dx}{dt} = Ax \quad \text{and} \quad v_p = \frac{dy}{dt} = -Ay$$



Separating variables and integrating (in each equation) gives

$$\int_{x_0}^x \frac{dx}{x} = \int_0^t A dt \quad \text{and} \quad \int_{y_0}^y \frac{dy}{y} = \int_0^t -A dt$$

Then

$$\ln \frac{x}{x_0} = At \quad \text{and} \quad \ln \frac{y}{y_0} = -At$$

or

$$x = x_0 e^{At} \quad \text{and} \quad y = y_0 e^{-At}$$

At $t = 6$ s,

$$x = 2 \text{ m } e^{(0.3)6} = 12.1 \text{ m} \quad \text{and} \quad y = 8 \text{ m } e^{-(0.3)6} = 1.32 \text{ m}$$

At $t = 6$ s, particle is at $(12.1, 1.32)$ m ←

(e) At the point $(12.1, 1.32)$ m,

$$\vec{V} = A(x\hat{i} - y\hat{j}) = 0.3 \text{ s}^{-1}(12.1\hat{i} - 1.32\hat{j}) \text{ m} \\ = 3.63\hat{i} - 0.396\hat{j} \text{ m/s} \leftarrow$$

(f) To determine the equation of the pathline, we use the parametric equations

$$x = x_0 e^{At} \quad \text{and} \quad y = y_0 e^{-At}$$

and eliminate t . Solving for e^{At} from both equations

$$e^{At} = \frac{y_0}{y} = \frac{x}{x_0}$$

Therefore $xy = x_0 y_0 = 16 \text{ m}^2 \leftarrow$

Notes:

- This problem illustrates the method for computing streamlines and pathlines.
- Because this is a steady flow, the streamlines and pathlines have the same shape—in an unsteady flow this would not be true.
- When we follow a particle (the Lagrangian approach), its position (x, y) and velocity $(u_p = dx/dt \text{ and } v_p = dy/dt)$ are functions of time, even though the flow is steady.

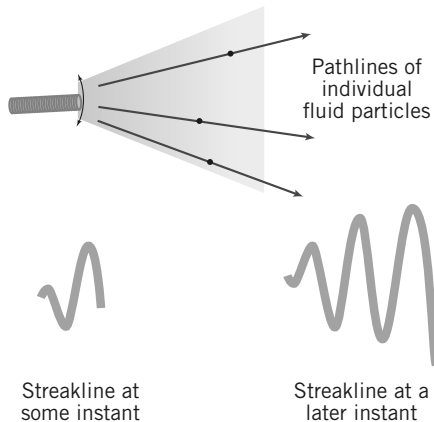


Fig. 2.5 Pathlines and streaklines for flow from the exit of an oscillating garden hose.

The simultaneous solution of these equations gives the path of a particle in parametric form $x_p(t), y_p(t)$.

The computation of streaklines is somewhat tricky. The first step is to compute the pathline of a particle (using Eqs. 2.9) that was released from the streak source point at x_0, y_0 at time t_0 , in the form

$$x_{\text{particle}}(t) = x(t, x_0, y_0, t_0) \quad y_{\text{particle}}(t) = y(t, x_0, y_0, t_0)$$

Then, instead of interpreting this as the position of a particle over time, we rewrite these equations as

$$x_{\text{streakline}}(t_0) = x(t, x_0, y_0, t_0) \quad y_{\text{streakline}}(t_0) = y(t, x_0, y_0, t_0) \quad (2.10)$$

Equations 2.10 give the line generated (by time t) from a streak source at point (x_0, y_0) . In these equations, t_0 (the release times of particles) is varied from 0 to t to show the instantaneous positions of all particles released up to time t !

2.3 Stress Field

In our study of fluid mechanics, we will need to understand what kinds of forces act on fluid particles. Each fluid particle can experience: *surface forces* (pressure, friction) that are generated by contact with other particles or a solid surface; and *body forces* (such as gravity and electromagnetic) that are experienced throughout the particle.

The gravitational body force acting on an element of volume, dV , is given by $\rho \vec{g} dV$, where ρ is the density and \vec{g} is the local gravitational acceleration. Thus the gravitational body force per unit volume is $\rho \vec{g}$ and the gravitational body force per unit mass is \vec{g} .

Surface forces on a fluid particle lead to *stresses*. The concept of stress is useful for describing how forces acting on the boundaries of a medium (fluid or solid) are transmitted throughout the medium. You have probably seen stresses discussed in solid mechanics. For example, when you stand on a diving board, stresses are generated within the board. On the other hand, when a body moves through a fluid, stresses are developed within the fluid. The difference between a fluid and a solid is, as we've seen, that stresses in a fluid are mostly generated by motion rather than by deflection.

Imagine the surface of a fluid particle in contact with other fluid particles, and consider the contact force being generated between the particles. Consider a portion, δA , of the surface at some point C . The orientation of δA is given by the unit vector, \hat{n} , shown in Fig. 2.6. The vector \hat{n} is the outwardly drawn unit normal with respect to the particle.

The force, $\delta \vec{F}$, acting on δA may be resolved into two components, one normal to and the other tangent to the area. A *normal stress* σ_n and a *shear stress* τ_n are then defined as

$$\sigma_n = \lim_{\delta A_n \rightarrow 0} \frac{\delta F_n}{\delta A_n} \quad (2.11)$$

and

$$\tau_n = \lim_{\delta A_n \rightarrow 0} \frac{\delta F_t}{\delta A_n} \quad (2.12)$$

Subscript n on the stress is included as a reminder that the stresses are associated with the surface δA through C , having an outward normal in the \hat{n} direction. The fluid is actually a continuum, so we could have imagined breaking it up any number of different ways into fluid particles around point C , and therefore obtained any number of different stresses at point C .

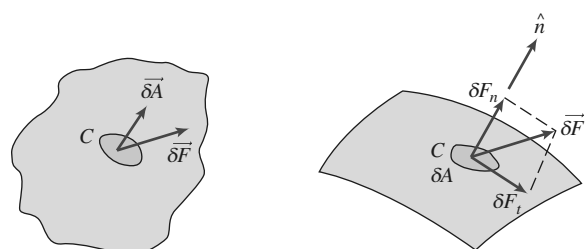


Fig. 2.6 The concept of stress in a continuum.

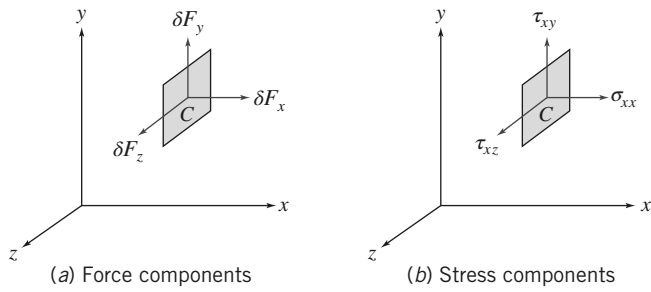


Fig. 2.7 Force and stress components on the element of area δA_x .

In dealing with vector quantities such as force, we usually consider components in an orthogonal coordinate system. In rectangular coordinates we might consider the stresses acting on planes whose outwardly drawn normals with respect to the material acted upon are in the x , y , or z directions. In Fig. 2.7 we consider the stress on the element δA_x , whose outwardly drawn normal is in the x direction. The force, $\delta \vec{F}$, has been resolved into components along each of the coordinate directions. Dividing the magnitude of each force component by the area, δA_x , and taking the limit as δA_x approaches zero, we define the three stress components shown in Fig. 2.7b:

$$\begin{aligned}\sigma_{xx} &= \lim_{\delta A_x \rightarrow 0} \frac{\delta F_x}{\delta A_x} \\ \tau_{xy} &= \lim_{\delta A_x \rightarrow 0} \frac{\delta F_y}{\delta A_x} \quad \tau_{xz} = \lim_{\delta A_x \rightarrow 0} \frac{\delta F_z}{\delta A_x}\end{aligned}\quad (2.13)$$

We have used a double subscript notation to label the stresses. The *first* subscript (in this case, x) indicates the *plane* on which the stress acts (in this case, a surface perpendicular to the x axis). The *second* subscript indicates the *direction* in which the stress acts.

Consideration of area element δA_y would lead to the definitions of the stresses, σ_{yy} , τ_{yx} , and τ_{yz} ; use of area element δA_z would similarly lead to the definitions of σ_{zz} , τ_{zx} , τ_{zy} .

Although we just looked at three orthogonal planes, an infinite number of planes can be passed through point C , resulting in an infinite number of stresses associated with planes through that point. Fortunately, the state of stress at a point can be described completely by specifying the stresses acting on *any* three mutually perpendicular planes through the point. The stress at a point is specified by the nine components

$$\begin{bmatrix} \sigma_{xx} & \tau_{xy} & \tau_{xz} \\ \tau_{yx} & \sigma_{yy} & \tau_{yz} \\ \tau_{zx} & \tau_{zy} & \sigma_{zz} \end{bmatrix}$$

where σ has been used to denote a normal stress, and τ to denote a shear stress. The notation for designating stress is shown in Fig. 2.8.

Referring to the infinitesimal element shown in Fig. 2.8, we see that there are six planes (two x planes, two y planes, and two z planes) on which stresses may act. In order to designate the plane of interest, we could use terms like front and back, top and bottom, or left and right. However, it is more logical to name the planes in terms of the coordinate axes. The planes are named and denoted as positive or negative according to the direction of the outwardly drawn normal to the plane. Thus the top plane, for example, is a positive y plane and the back plane is a negative z plane.

It also is necessary to adopt a sign convention for stress. A stress component is positive when the direction of the stress component and the plane on which it acts are both positive or both negative. Thus $\tau_{yx} = 5 \text{ lbf/in.}^2$ represents a shear stress on a positive y plane in the positive x direction or a shear stress on a negative y plane in the negative x direction. In Fig. 2.8 all stresses have been drawn as positive

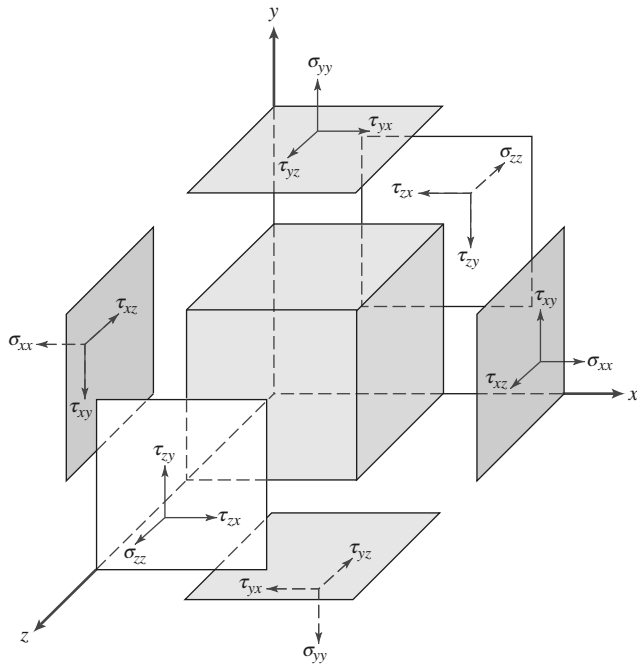


Fig. 2.8 Notation for stress.

stresses. Stress components are negative when the direction of the stress component and the plane on which it acts are of opposite sign.

2.4 Viscosity

Where do stresses come from? For a solid, stresses develop when the material is elastically deformed or strained; for a fluid, shear stresses arise due to viscous flow. Hence we say solids are *elastic*, and fluids are *viscous*. For a fluid at rest, there will be no shear stresses. We will see that each fluid can be categorized by examining the relation between the applied shear stresses and the flow of the fluid.

Consider the behavior of a fluid element between the two infinite plates shown in Fig. 2.9a. The rectangular fluid element is initially at rest at time t . Let us now suppose a constant rightward force δF_x is applied to the upper plate so that it is dragged across the fluid at constant velocity δu . The relative shearing action of the infinite plates produces a shear stress, τ_{yx} , which acts on the fluid element and is given by

$$\tau_{yx} = \lim_{\delta A_y \rightarrow 0} \frac{\delta F_x}{\delta A_y} = \frac{dF_x}{dA_y}$$

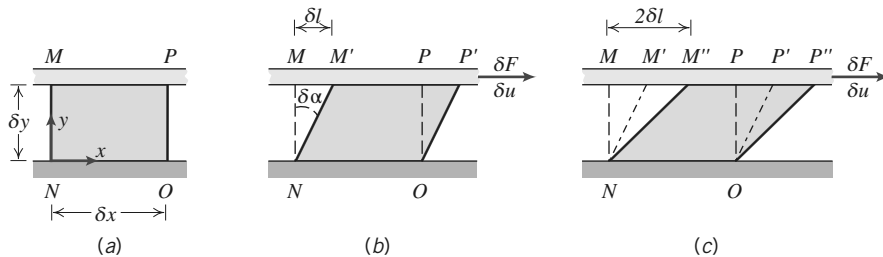


Fig. 2.9 (a) Fluid element at time t , (b) deformation of fluid element at time $t + \delta t$, and (c) deformation of fluid element at time $t + 2\delta t$.

where δA_y is the area of contact of the fluid element with the plate and δF_x is the force exerted by the plate on that element. Snapshots of the fluid element, shown in Figs. 2.9a–c, illustrate the deformation of the fluid element from position $MNOP$ at time t , to $M'NOP'$ at time $t + \delta t$, to $M''NOP''$ at time $t + 2\delta t$, due to the imposed shear stress. It is the fact that a fluid continually deforms in response to an applied shear stress that sets it apart from solids.

Focusing on the time interval δt (Fig. 2.9b), the deformation of the fluid is given by

$$\text{deformation rate} = \lim_{\delta t \rightarrow 0} \frac{\delta \alpha}{\delta t} = \frac{d\alpha}{dt}$$

We want to express $d\alpha/dt$ in terms of readily measurable quantities. The distance, δl , between the points M and M' is given by

$$\delta l = \delta u \delta t$$

Alternatively, for small angles,

$$\delta l = \delta y \delta \alpha$$

Equating these two expressions for δl gives

$$\frac{\delta \alpha}{\delta t} = \frac{\delta u}{\delta y}$$

Taking the limits of both sides of the equality, we obtain

$$\frac{d\alpha}{dt} = \frac{du}{dy}$$

Thus, the fluid element of Fig. 2.9, when subjected to shear stress τ_{yx} , experiences a rate of deformation (*shear rate*) given by du/dy . We have established that any fluid that experiences a shear stress will flow and thus have a shear rate. What is the relation between shear stress and shear rate? Fluids in which shear stress is directly proportional to rate of deformation are termed *Newtonian fluids*. The term *non-Newtonian* is used to classify all fluids in which shear stress is not directly proportional to shear rate.

Newtonian Fluid

Most common fluids such as water, air, and gasoline are Newtonian under normal conditions. If the fluid of Fig. 2.9 is Newtonian, then

$$\tau_{yx} \propto \frac{du}{dy} \quad (2.14)$$

We are familiar with the fact that some fluids resist motion more than others. For example, a container of SAE 30W oil is much harder to stir than one of water. Hence SAE 30W oil is much more viscous; it has a higher viscosity. The constant of proportionality in Eq. 2.14 is the *absolute* (or *dynamic*) *viscosity*, μ . Thus in terms of the coordinates of Fig. 2.9, Newton's law of viscosity is given for one-dimensional flow by

$$\tau_{yx} = \mu \frac{du}{dy} \quad (2.15)$$

Note that, since the dimensions of τ are $[F/L^2]$ and the dimensions of du/dy are $[1/t]$, μ has dimensions $[Ft/L^2]$. Since the dimensions of force, F , mass, M , length, L , and time, t , are related by Newton's

second law of motion, the dimensions of μ can also be expressed as $[M/Lt]$. In the British Gravitational system, the units of viscosity are $\text{lbf}\cdot\text{s}/\text{ft}^2$ or $\text{slug}/(\text{ft}\cdot\text{s})$. In the Absolute Metric system, the basic unit of viscosity is called a poise [1 poise $\equiv 1 \text{ g}/(\text{cm}\cdot\text{s})$]. In the SI system the units of viscosity are $\text{kg}/(\text{m}\cdot\text{s})$ or $\text{Pa}\cdot\text{s}$ ($1 \text{ Pa}\cdot\text{s} = 1 \text{ N}\cdot\text{s}/\text{m}^2$). The calculation of viscous shear stress is illustrated in Example 2.2.

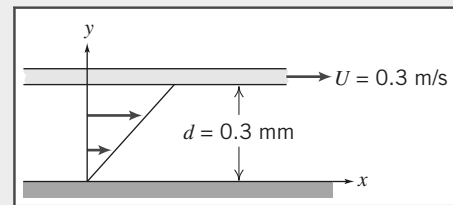
In fluid mechanics the ratio of absolute viscosity, μ , to density, ρ , often arises. This ratio is given the name *kinematic viscosity* and is represented by the symbol ν . Since density has dimensions $[M/L^3]$, the dimensions of ν are $[L^2/t]$. In the Absolute Metric system of units, the unit for ν is a stoke (1 stoke $\equiv 1 \text{ cm}^2/\text{s}$).

Viscosity data for a number of common Newtonian fluids are given in Appendix 1. For gases, viscosity increases with temperature, whereas for liquids, viscosity decreases with increasing temperature.

Example 2.2 VISCOSITY AND SHEAR STRESS IN NEWTONIAN FLUID

An infinite plate is moved over a second plate on a layer of liquid as shown. For small gap width, d , we assume a linear velocity distribution in the liquid. The liquid viscosity is 0.65 centipoise and its specific gravity is 0.88. Determine:

- The absolute viscosity of the liquid, in $\text{lbf}\cdot\text{s}/\text{ft}^2$.
- The kinematic viscosity of the liquid, in m^2/s .
- The shear stress on the upper plate, in lbf/ft^2 .
- The shear stress on the lower plate, in Pa.
- The direction of each shear stress calculated in parts (c) and (d).



Given: Linear velocity profile in the liquid between infinite parallel plates as shown.

$$\begin{aligned}\mu &= 0.65 \text{ cp} \\ \text{SG} &= 0.88\end{aligned}$$

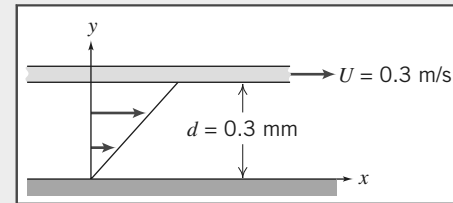
- Find:**
- μ in units of $\text{lbf}\cdot\text{s}/\text{ft}^2$.
 - ν in units of m^2/s .
 - τ on upper plate in units of lbf/ft^2 .
 - τ on lower plate in units of Pa.
 - Direction of stresses in parts (c) and (d).

Solution:

Governing equation: $\tau_{yx} = \mu \frac{du}{dy}$ **Definition:** $\nu = \frac{\mu}{\rho}$

Assumptions:

- Linear velocity distribution (given)
- Steady flow
- $\mu = \text{constant}$



$$\begin{aligned}(a) \mu &= 0.65 \text{ cp} \times \frac{\text{poise}}{100 \text{ cp}} \times \frac{\text{g}}{\text{cm} \cdot \text{s} \cdot \text{poise}} \times \frac{\text{lbf}}{454 \text{ g}} \times \frac{\text{slug}}{32.2 \text{ lbf}} \times 30.5 \frac{\text{cm}}{\text{ft}} \times \frac{\text{lbf} \cdot \text{s}^2}{\text{slug} \cdot \text{ft}} \\ \mu &= 1.36 \times 10^{-5} \text{ lbf} \cdot \text{s}/\text{ft}^2\end{aligned}$$

$$\begin{aligned}(b) \nu &= \frac{\mu}{\rho} = \frac{\mu}{\text{SG} \rho_{H_2O}} \\ &= 1.36 \times 10^{-5} \frac{\text{lbf} \cdot \text{s}}{\text{ft}^2} \times \frac{\text{ft}^3}{(0.88) 1.94 \text{ slug}} \times \frac{\text{slug} \cdot \text{ft}}{\text{lbf} \cdot \text{s}^2} \times (0.305)^2 \frac{\text{m}^2}{\text{ft}^2} \\ \nu &= 7.41 \times 10^{-7} \text{ m}^2/\text{s}\end{aligned}$$

$$(c) \tau_{\text{upper}} = \tau_{yx, \text{upper}} = \mu \frac{du}{dy} \Big|_{y=d}$$

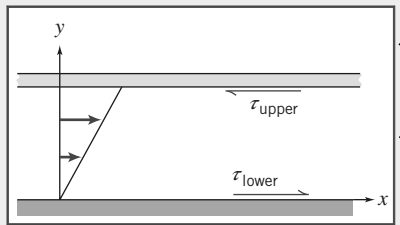
Since u varies linearly with y ,

$$\begin{aligned} \frac{du}{dy} &= \frac{\Delta u}{\Delta y} = \frac{U-0}{d-0} = \frac{U}{d} \\ &= 0.3 \frac{\text{m}}{\text{s}} \times \frac{1}{0.3 \text{ mm}} \times 1000 \frac{\text{mm}}{\text{m}} = 1000 \text{ s}^{-1} \end{aligned}$$

$$\tau_{\text{upper}} = \mu \frac{U}{d} = 1.36 \times 10^{-5} \frac{\text{lbf} \cdot \text{s}}{\text{ft}^2} \times \frac{1000}{\text{s}} = 0.0136 \text{ lbf}/\text{ft}^2 \xrightarrow{\tau_{\text{upper}}}$$

$$\begin{aligned} (d) \tau_{\text{lower}} &= \mu \frac{U}{d} = 0.0136 \frac{\text{lbf}}{\text{ft}^2} \times 4.45 \frac{\text{N}}{\text{lbf}} \times \frac{\text{ft}^2}{(0.305)^2 \text{m}^2} \times \frac{\text{Pa} \cdot \text{m}^2}{\text{N}} \\ &= 0.651 \text{ Pa} \xrightarrow{\tau_{\text{lower}}} \end{aligned}$$

(e) Directions of shear stresses on upper and lower plates.



- The upper plate is a negative y surface; so
 positive τ_{yx} acts in the negative x direction.
 The lower plate is a positive y surface; so
 positive τ_{yx} acts in the positive x direction.

(e)

Part (c) shows that the shear stress is:

- Constant across the gap for a linear velocity profile.
- Directly proportional to the speed of the upper plate (because of the linearity of Newtonian fluids).
- Inversely proportional to the gap between the plates.

Note that multiplying the shear stress by the plate area in such problems computes the force required to maintain the motion.

Non-Newtonian Fluids

Fluids in which shear stress is *not* directly proportional to deformation rate are non-Newtonian. Although we will not discuss these much in this text, many common fluids exhibit non-Newtonian behavior. Two familiar examples are toothpaste and paint. The latter is very “thick” when in the can, but becomes “thin” when sheared by brushing. Toothpaste behaves as a “fluid” when squeezed from the tube. However, it does not run out by itself when the cap is removed. There is a threshold or yield stress below which toothpaste behaves as a solid. Strictly speaking, our definition of a fluid is valid only for materials that have zero yield stress. Non-Newtonian fluids commonly are classified as having time-independent or time-dependent behavior. Examples of time-independent behavior are shown in the rheological diagram of Fig. 2.10.

Numerous empirical equations have been proposed [3, 4] to model the observed relations between τ_{yx} and du/dy for time-independent fluids. They may be adequately represented for many engineering applications by the power law model, which for one-dimensional flow becomes

$$\tau_{yx} = k \left(\frac{du}{dy} \right)^n \quad (2.16)$$

where the exponent, n , is called the flow behavior index and the coefficient, k , the consistency index. This equation reduces to Newton’s law of viscosity for $n=1$ with $k=\mu$.

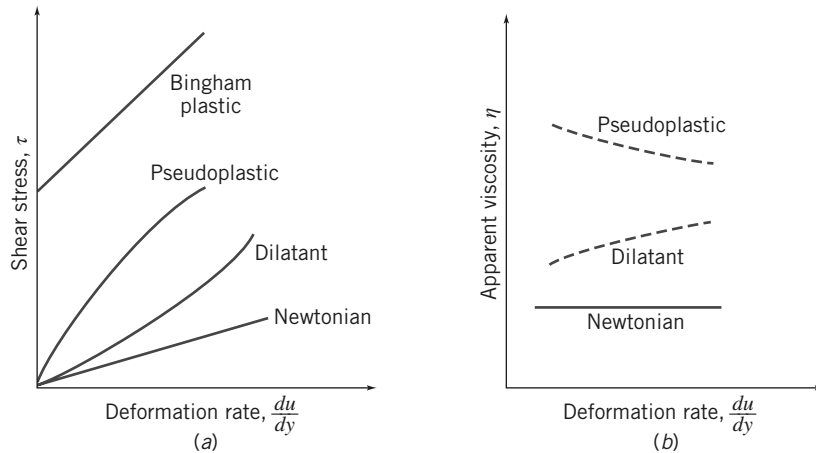


Fig. 2.10 (a) Shear stress, τ , and (b) apparent viscosity, η , as a function of deformation rate for one-dimensional flow of various non-Newtonian fluids.

To ensure that τ_{yx} has the same sign as du/dy , Eq. 2.16 is rewritten in the form

$$\tau_{yx} = k \left| \frac{du}{dy} \right|^{n-1} \frac{du}{dy} = \eta \frac{du}{dy} \quad (2.17)$$

The term $\eta = k|du/dy|^{n-1}$ is referred to as the *apparent viscosity*. The idea behind Eq. 2.17 is that we end up with a viscosity η that is used in a formula that is the same form as Eq. 2.15, in which the Newtonian viscosity μ is used. The big difference is that while μ is constant (except for temperature effects), η depends on the shear rate. Most non-Newtonian fluids have apparent viscosities that are relatively high compared with the viscosity of water.

Fluids in which the apparent viscosity decreases with increasing deformation rate ($n < 1$) are called *pseudoplastic* (or shear thinning) fluids. Most non-Newtonian fluids fall into this group; examples include polymer solutions, colloidal suspensions, and paper pulp in water. If the apparent viscosity increases with increasing deformation rate ($n > 1$) the fluid is termed *dilatant* (or shear thickening). Suspensions of starch and of sand are examples of dilatant fluids.

A “fluid” that behaves as a solid until a minimum yield stress, τ_y , is exceeded and subsequently exhibits a linear relation between stress and rate of deformation is referred to as an ideal or *Bingham plastic*. The corresponding shear stress model is

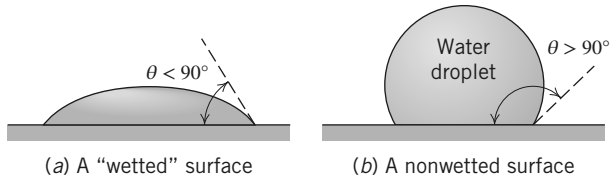
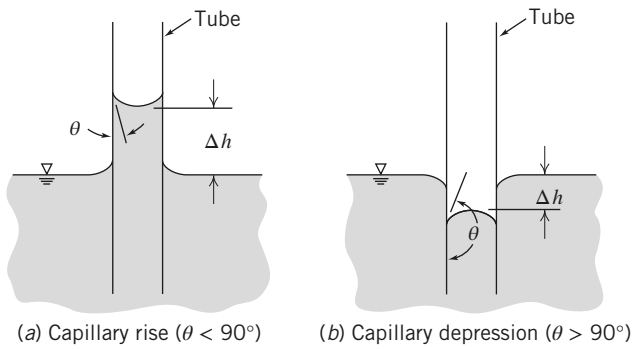
$$\tau_{yx} = \tau_y + \mu_p \frac{du}{dy} \quad (2.18)$$

Clay suspensions, drilling muds, and toothpaste are examples of substances exhibiting this behavior.

The study of non-Newtonian fluids is further complicated by the fact that the apparent viscosity may be time-dependent. *Thixotropic* fluids show a decrease in η with time under a constant applied shear stress; many paints are thixotropic. *Rheopectic* fluids show an increase in η with time. After deformation some fluids partially return to their original shape when the applied stress is released; such fluids are called *viscoelastic*. Many biological fluids exhibit this behavior.

2.5 Surface Tension

You have probably noticed that rain drops on a rain coat often remain as little drops, but flatten out on other surfaces. These two cases of a liquid on a surface are shown in Fig. 2.11. We define a liquid as “wetting” a surface when the *contact angle* $\theta < 90^\circ$. The behavior is due to *surface tension*. Whenever a liquid is in contact with other liquids or gases, or in this case a gas/solid surface, an interface develops

**Fig. 2.11** Surface tension effects on water droplets.**Fig. 2.12** Capillary rise and capillary depression inside and outside a circular tube.

that acts like a stretched elastic membrane, creating surface tension. There are two features to this membrane: the contact angle, θ , and the magnitude of the surface tension, σ (N/m or lbf/ft). Both of these depend on the type of liquid and the type of solid surface with which it shares an interface. Factors that affect the contact angle include the cleanliness of the surface and the purity of the liquid.

Appendix A contains data for surface tension and contact angle for common liquids in the presence of air and of water.

A force balance on a segment of interface shows that there is a pressure jump across the imagined elastic membrane whenever the interface is curved. For a water droplet in air, pressure in the water is higher than ambient; the same is true for a gas bubble in liquid. For a soap bubble in air, surface tension acts on both inside and outside interfaces between the soap film and air along the curved bubble surface. Surface tension also leads to the phenomena of capillary waves on a liquid surface [5], and capillary rise or depression, discussed below in Example 2.3.

In engineering, an important effect of surface tension is the creation of a curved *meniscus* that appears in manometers or barometers, leading to a *capillary rise* or depression, as shown in Fig. 2.12. This rise may be pronounced if the liquid is in a small-diameter tube or narrow gap, as shown in Example 2.3. The simple analysis of Example 2.3 gives reasonable results only for tube diameters less than 0.1 in. (2.54 mm) [6]. Over a diameter range $0.1 < D < 1.1$ in., experimental data for the capillary rise with a water-air interface are correlated by the empirical expression $\Delta h = 0.400/e^{4.37D}$. Manometer and barometer readings should be made at the level of the middle of the meniscus to minimize the effects of surface tension.

Impurities in the liquid, dirt on the surface, or surface inclination can cause an indistinct meniscus. Surfactant compounds reduce surface tension significantly when added to water [7] and have wide commercial application. Most detergents contain surfactants to help water penetrate and lift soil from surfaces. Automobile windows are often treated with surfactants so rain drops run off without using the wipers.

2.6 Description and Classification of Fluid Motions

Fluid mechanics is a huge discipline and covers everything from the aerodynamics of a supersonic airplane to the lubrication of human joints by synovial fluid. We need to break fluid mechanics down into manageable proportions. The two most difficult aspects of a fluid mechanics analysis to deal with

Example 2.3 ANALYSIS OF CAPILLARY EFFECT IN A TUBE

Create a graph showing the capillary rise or fall of a column of water or mercury, respectively, as a function of tube diameter D . Find the minimum diameter of each column required so that the height magnitude will be less than 1 mm.

Given: Tube dipped in liquid as in Fig. 2.12

Find: A general expression for Δh as a function of D .

Solution: Apply free-body diagram analysis, and sum vertical forces.

Governing equation:

$$\sum F_z = 0$$

Assumptions:

- 1 Measure to middle of meniscus
- 2 Neglect volume in meniscus region

Summing forces in the z direction:

$$\sum F_z = \sigma D \cos \theta - \rho g \Delta V = 0 \quad (1)$$

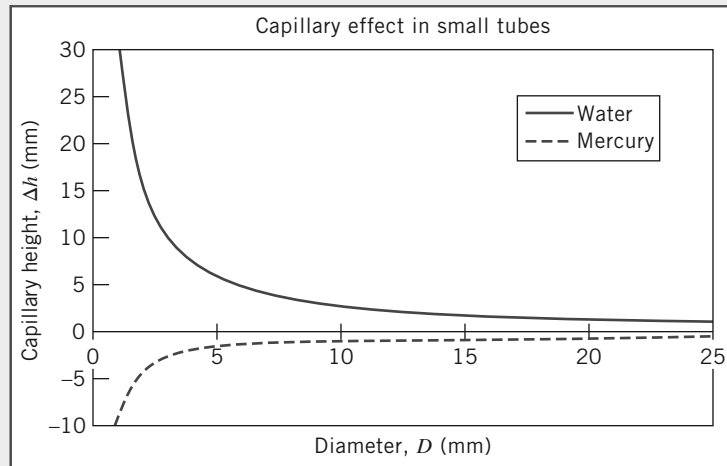
If we neglect the volume in the meniscus region:

$$\Delta V \approx \frac{\pi D^2}{4} \Delta h$$

Substituting in Eq. 1 and solving for Δh gives

$$\Delta h = \frac{4\sigma \cos \theta}{\rho g D} \quad \text{--- } \Delta h$$

For water, $\sigma = 72.8 \text{ mN/m}$ and $\theta \approx 0^\circ$, and for mercury, $\sigma = 484 \text{ mN/m}$ and $\theta = 140^\circ$ (Table A.4). Plotting,

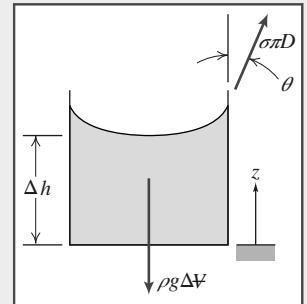


Using the above equation to compute D_{\min} for $\Delta h = 1 \text{ mm}$, we find for mercury and water

$$D_{M_{\min}} = 11.2 \text{ mm} \quad \text{and} \quad D_{W_{\min}} = 30 \text{ mm}$$

Notes:

- This problem reviewed use of the free-body diagram approach.
- It turns out that neglecting the volume in the meniscus region is only valid when Δh is large compared with D . However, in this problem we have the result that Δh is about 1 mm when D is 11.2 mm (or 30 mm); hence the results can only be very approximate.



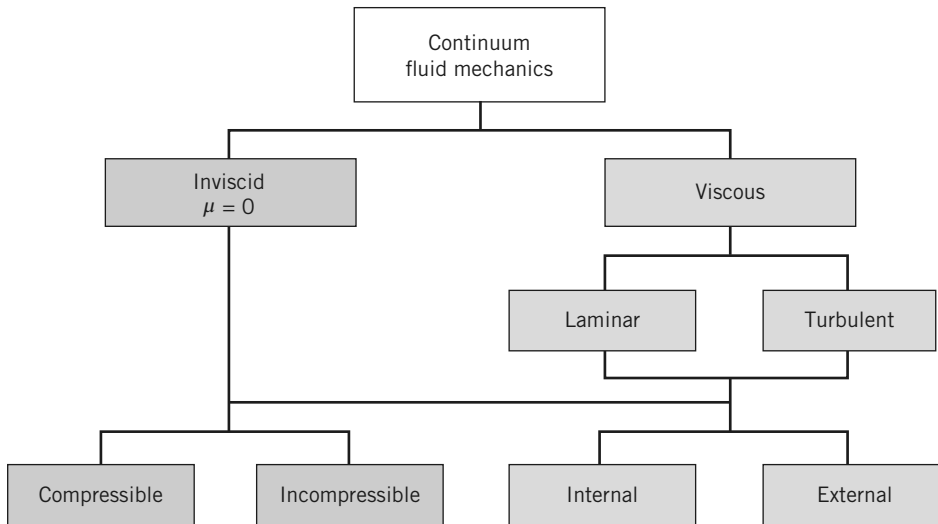


Fig. 2.13 Possible classification of continuum fluid mechanics.

are: (1) the fluid's viscous nature and (2) its compressibility. Fluid mechanics theory first became highly developed about 250 years ago and dealt with a frictionless, incompressible fluid. This theory, while extremely elegant, led to the famous result called d'Alembert's paradox. All bodies experience no drag as they move through such a fluid, which is not consistent with real behavior. The first significant efforts to deal with the viscous nature of fluids occurred in the early 1900s and led to the classification of fluids based on whether viscous effects and compressibility effects are present, as shown in Fig. 2.13. Also shown are classifications in terms of whether a flow is laminar or turbulent and internal or external. We will now discuss each of these.

Viscous and Inviscid Flows

An object moving through a fluid experiences gravity and, in addition, an aerodynamic drag force. The force is due in part to viscous friction and in part to pressure differences built up as the fluid is forced out of the way of the object. We can estimate whether or not viscous forces, as opposed to pressure forces, are negligible by simply computing the Reynolds number

$$Re = \rho \frac{VL}{\mu}$$

where ρ and μ are the fluid density and viscosity, respectively, and V and L are the typical or "characteristic" velocity and size scale of the flow, respectively. If the Reynolds number is "large," viscous effects will be small in most of the flow; if the Reynolds number is small, viscous effects will be dominant. Finally, if the Reynolds number is neither large nor small, both are important.

To illustrate this very powerful idea, consider two simple examples. First, consider a soccer ball (diameter = 8.75 in.) kicked so it moves at 60 mph. The Reynolds number is about 400,000, which is large, and so the drag on the soccer ball is almost entirely due to the pressure build-up in front of it. For our second example, consider a dust particle falling under gravity at a terminal velocity of 1 cm/s. In this case $Re \approx 0.7$, which is quite small, and the drag is mostly due to the friction of the air. Of course, in both of these examples, if we wish to *determine* the drag force, we would have to do substantially more analysis.

These examples illustrate an important point. A flow is considered to be friction dominated based not just on the fluid viscosity, but on the complete flow system. In these examples, the airflow was low friction for the soccer ball, but was high friction for the dust particle.

Let's return for a moment to the idealized notion of frictionless flow, called *inviscid flow*. This is the branch shown on the left in Fig. 2.13. This branch encompasses most aerodynamics, and among other things explains, for example, why sub- and supersonic aircraft have differing shapes and how a

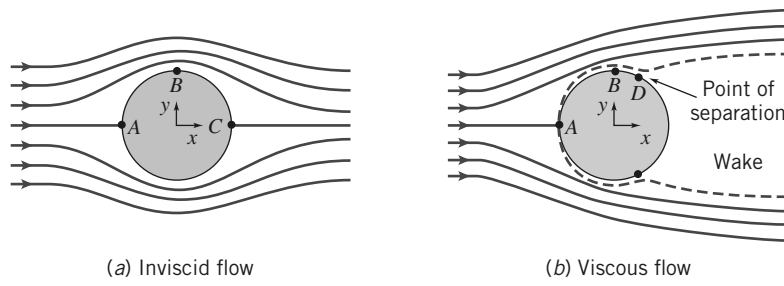


Fig. 2.14 Qualitative picture of incompressible flow over a sphere.

wing generates lift. If this theory is applied to the ball flying through the air, it predicts streamlines as shown in Fig. 2.14a.

The streamlines are symmetric front-to-back. Because the mass flow between any two streamlines is constant, wherever streamlines open up, the velocity must decrease, and vice versa. Hence we can see that the velocity in the vicinity of points A and C must be relatively low and at point B it will be high. In fact, the air comes to rest at points A and C and are termed *stagnation points*. The pressure in this flow is high wherever the velocity is low, and vice versa. Hence, points A and C have relatively large pressures and point B will be a point of low pressure. In fact, the pressure distribution on the sphere is symmetric front-to-back, and there is no net drag force due to pressure. Because we're assuming inviscid flow, there can be no drag due to friction either. This is the d'Alembert's paradox of 1752: the ball experiences no drag.

This is obviously unrealistic. It took about 150 years after the paradox first appeared for the answer, obtained by Prandtl in 1904. The no-slip condition requires that the velocity everywhere on the surface of the sphere be zero, but inviscid theory states that it's high at point B. Prandtl suggested that even though friction is negligible in general for high-Reynolds number flows, there will always be a thin *boundary layer*, in which friction is significant and across the width of which the velocity increases rapidly from zero at the surface to the value inviscid flow theory predicts on the outer edge of the boundary layer. This is shown in Fig. 2.14b from point A to point B, and in more detail in Fig. 2.15.

This boundary layer immediately allows us to reconcile theory and experiment. Once we have friction in a boundary layer we will have drag. However, this boundary layer has another important consequence. It often leads to bodies having a *wake*, as shown in Fig. 2.14b from point D onwards. Point D is a *separation point*, where fluid particles are pushed off the object and cause a wake to develop. Consider once again the original inviscid flow (Fig. 2.14a): As a particle moves along the surface from point B to C, it moves from low to high pressure. This *adverse pressure gradient* (a pressure change opposing fluid motion) causes the particles to slow down as they move along the rear of the sphere. If we now add to this the fact that the particles are moving in a boundary layer with friction that also slows down the fluid, the particles will eventually be brought to rest and then pushed off the sphere by the following particles, forming the wake. It turns out that the wake will always be relatively low pressure, but the front of the sphere will still have relatively high pressure. Hence, the sphere will now have a quite large *pressure or form drag*.

We can also now begin to see how *streamlining* of a body works. The drag force in most aerodynamics is due to the low-pressure wake. If we can reduce or eliminate the wake, drag will be greatly reduced. If we consider once again why the separation occurred, we recall two features. Boundary layer friction slowed down the particles, but so did the adverse pressure gradient. The pressure increased very rapidly across the back half of the sphere in Fig. 2.14a because the streamlines opened up so rapidly. If we make the sphere teardrop shaped, as in Fig. 2.16, the streamlines open up gradually, and hence the pressure will increase slowly, to such an extent that fluid particles are not forced to separate from the object until they almost reach the end of the object, as shown. The wake is much smaller leading to much less pressure drag. The only negative aspect of this streamlining is that the total surface area on which friction occurs is larger, so drag due to friction will increase a little. This discussion illustrates the very significant difference between inviscid flow ($\mu = 0$) and flows in which viscosity is negligible but not zero ($\mu \rightarrow 0$).

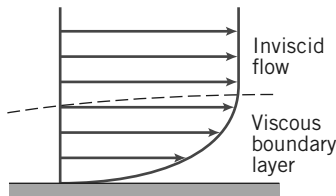


Fig. 2.15 Schematic of a boundary layer.

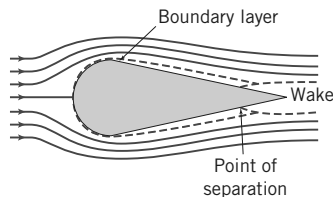


Fig. 2.16 Flow over a streamlined object.

Laminar and Turbulent Flows

If you turn on a faucet at a very low flow rate the water will flow out very smoothly. If you increase the flow rate, the water will exit in a churned-up, chaotic manner. These are examples of how a viscous flow can be laminar or turbulent, respectively. A *laminar* flow is one in which the fluid particles move in smooth layers, or *laminas*; a *turbulent* flow is one in which the fluid particles rapidly mix as they move along due to random three-dimensional velocity fluctuations. Typical examples of pathlines of each of these are illustrated in Fig. 2.17, which shows a one-dimensional flow. In most fluid mechanics problems, as for example, flow of water in a pipe, turbulence is an unwanted but often unavoidable phenomenon because it generates more resistance to flow. In other problems as for example, the flow of blood through blood vessels, it is desirable because the random mixing allows all of the blood cells to contact the walls of the blood vessels to exchange oxygen and other nutrients.

The velocity of the laminar flow is simply u . The velocity of the turbulent flow is given by the mean velocity \bar{u} plus the three components of randomly fluctuating velocity u' , v' , and w' . Although many turbulent flows of interest are steady in the mean the presence of the random, high-frequency velocity fluctuations makes the analysis of turbulent flows extremely difficult. In a one-dimensional laminar flow, the shear stress is related to the velocity gradient by the simple relation

$$\tau_{yx} = \mu \frac{du}{dy} \quad (2.15)$$

For a turbulent flow in which the mean velocity field is one-dimensional, no such simple relation is valid. Random, three-dimensional velocity fluctuations (u' , v' , and w') transport momentum across the mean flow streamlines, increasing the effective shear stress. Consequently, in turbulent flow there is no universal relationship between the stress field and the mean-velocity field. Thus in turbulent flows we must rely heavily on semi-empirical theories and on experimental data.

Compressible and Incompressible Flows

Flows in which variations in density are negligible are termed *incompressible* and those in which density variations are not negligible are called *compressible*. The most common example of compressible flow concerns the flow of gases, while the flow of liquids may frequently be treated as incompressible.

For many liquids, density is only a weak function of temperature. At modest pressures, liquids may be considered incompressible. However, at high pressures, compressibility effects in liquids can be

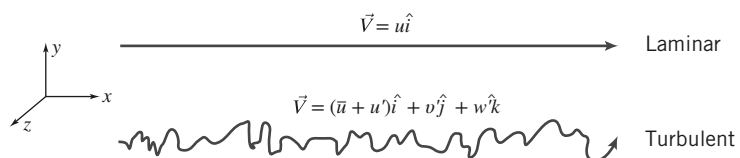


Fig. 2.17 Particle pathlines in one-dimensional laminar and turbulent flows.

important. Pressure and density changes in liquids are related by the *bulk compressibility modulus*, or modulus of elasticity,

$$E_v \equiv \frac{dp}{(d\rho/\rho)} \quad (2.19)$$

If the bulk modulus is independent of temperature, then density is only a function of pressure (the fluid is *barotropic*). Bulk modulus data for some common liquids are given in Appendix A.

Water hammer and cavitation are examples of the importance of compressibility effects in liquid flows. *Water hammer* is caused by acoustic waves propagating and reflecting in a confined liquid, for example, when a valve is closed abruptly. The resulting noise can be similar to “hammering” on the pipes, hence the term.

Cavitation occurs when vapor pockets form in a liquid flow because of local reductions in pressure (for example at the tip of a boat’s propeller blades). Depending on the number and distribution of particles in the liquid to which very small pockets of undissolved gas or air may attach, the local pressure at the onset of cavitation may be at or below the vapor pressure of the liquid. These particles act as nucleation sites to initiate vaporization.

Vapor pressure of a liquid is the partial pressure of the vapor in contact with the saturated liquid at a given temperature. When pressure in a liquid is reduced to less than the vapor pressure, the liquid may change phase suddenly and “flash” to vapor. The vapor pockets in a liquid flow may alter the geometry of the flow field substantially. When adjacent to a surface, the growth and collapse of vapor bubbles can cause serious damage by eroding the surface material. Very pure liquids can sustain large negative pressures, as much as -60 atmospheres for distilled water, before the liquid “ruptures” and vaporization occurs. Undissolved air is invariably present near the free surface of water or seawater, so cavitation occurs where the local total pressure is quite close to the vapor pressure.

Gas flows with negligible heat transfer also may be considered incompressible provided that the flow speeds are small relative to the speed of sound. The ratio of the flow speed, V , to the local speed of sound, c , in the gas is defined as the Mach number,

$$M \equiv \frac{V}{c}$$

For $M < 0.3$, the maximum density variation is less than 5 percent. Thus gas flows with $M < 0.3$ can be treated as incompressible; a value of $M = 0.3$ in air at standard conditions corresponds to a speed of approximately 100 m/s. For example, when you drive your car at 65 mph the air flowing around it has negligible change in density. As we shall see in Chapter 12, the speed of sound in an ideal gas is given by $c = \sqrt{kRT}$, where k is the ratio of specific heats, R is the gas constant, and T is the absolute temperature.

Compressible flows occur frequently in engineering applications. Common examples include compressed air systems used to power shop tools and dental drills, transmission of gases in pipelines at high pressure, and pneumatic or fluidic control and sensing systems. Compressibility effects are very important in the design of modern high-speed aircraft and missiles, power plants, fans, and compressors.

Internal and External Flows

Flows completely bounded by solid surfaces are called *internal* or *pipe* or *duct* flows. Flows over bodies immersed in an unbounded fluid are termed *external flows*. Both internal and external flows may be laminar or turbulent, compressible or incompressible.

The flow of water in a pipe is an example of internal flow. The Reynolds number for pipe flows is defined as $Re = \rho \bar{V} D / \mu$, where \bar{V} is the average flow velocity and D is the pipe diameter. This Reynolds number indicates whether a pipe flow will be laminar or turbulent. Flow will generally be laminar for $Re \leq 2300$ and turbulent for larger values: Flow in a pipe of constant diameter will be entirely laminar or entirely turbulent, depending on the value of the velocity \bar{V} . We will explore internal flows in detail in Chapter 8.

We already saw some examples of external flows when we discussed the flow over a sphere (Fig. 2.14b) and a streamlined object (Fig. 2.16). These flows could be laminar or turbulent and in addition, the boundary layers can be laminar or turbulent. When we discuss external flow in Chapter 9,

we'll learn that there is an overall Reynolds number for a plate $Re_L = \rho U_\infty L / \mu$ that indicates the relative significance of viscous forces. In addition, we'll find that the boundary layer will be laminar for $Re_x = \rho U_\infty x / \mu \leq 5 \times 10^5$ and turbulent for larger values: A boundary layer will start out laminar, and if the plate is long enough, the boundary layer will transition to become turbulent.

It is clear by now that computing a Reynolds number is often very informative for both internal and external flows. We will discuss this and other important *dimensionless groups* in Chapter 7.

The internal flow through fluid machines is considered in Chapter 10 and we will apply the principle of angular momentum to develop performance relations. Pumps, fans, blowers, compressors, and propellers that add energy to fluid streams are considered, as are turbines and windmills that extract energy. The chapter features detailed discussion of operation of fluid systems.

The internal flow of liquids in which there is a free surface exposed to the atmosphere termed *open-channel* flow. Common examples of open-channel flow include flow in rivers, irrigation ditches, and aqueducts. Open-channel flow will be treated in Chapter 11.

Both internal and external flows can be compressible or incompressible. Compressible flows can be divided into subsonic and supersonic regimes. We will study compressible flows in Chapter 12 and see among other things that *supersonic flows* ($M > 1$) will behave very differently than *subsonic flows* ($M < 1$). We will find that, for example, the shape of a nozzle for supersonic flow is different from that for subsonic flow. We will learn that there is a maximum flow rate for air flowing through a nozzle. Supersonic flows also have shock waves that affect the flow patterns significantly.

2.7 Summary and Useful Equations

In this chapter we have completed our review of some of the fundamental concepts we will utilize in our study of fluid mechanics. Some of these are:

- ✓ How to describe flows (timelines, pathlines, streamlines, streaklines).
- ✓ Forces (surface, body) and stresses (shear, normal).
- ✓ Types of fluids (Newtonian, non-Newtonian—dilatant, pseudoplastic, thixotropic, rheopectic, Bingham plastic) and viscosity (kinematic, dynamic, apparent).
- ✓ Types of flow (viscous/inviscid, laminar/turbulent, compressible/incompressible, internal/external).

We also briefly discussed some interesting phenomena, such as surface tension, boundary layers, wakes, and streamlining. Finally, we introduced two very useful dimensionless groups—the Reynolds number and the Mach number.

Note: Most of the equations in the table below have a number of constraints or limitations—*be sure to refer to their page numbers for details!*

Useful Equations

Definition of specific gravity:	$SG = \frac{\rho}{\rho_{H_2O}}$	(2.3)	Page 17
Definition of specific weight:	$\gamma = \frac{mg}{V} \rightarrow \gamma = \rho g$	(2.4)	Page 17
Definition of streamlines (2D):	$\frac{dy}{dx}_{\text{streamline}} = \frac{v(x,y)}{u(x,y)}$	(2.8)	Page 20
Definition of pathlines (2D):	$\frac{dx}{dt}_{\text{particle}} = u(x,y,t) \quad \frac{dy}{dt}_{\text{particle}} = v(x,y,t)$	(2.9)	Page 20
Definition of streaklines (2D):	$x_{\text{streakline}}(t_0) = x(t, x_0, y_0, t_0) \quad y_{\text{streakline}}(t_0) = y(t, x_0, y_0, t_0)$	(2.10)	Page 23
Newton's law of viscosity (1D flow):	$\tau_{yx} = \mu \frac{du}{dy}$	(2.15)	Page 26
Shear stress for a non-Newtonian fluid (1D flow):	$\tau_{yx} = k \left \frac{du}{dy} \right ^{n-1} \frac{du}{dy} = \eta \frac{du}{dy}$	(2.17)	Page 29

REFERENCES

1. Vincenti, W. G., and C. H. Kruger Jr., *Introduction to Physical Gas Dynamics*. New York: Wiley, 1965.
2. Merzkirch, W., *Flow Visualization*, 2nd ed. New York: Academic Press, 1987.
3. Tanner, R. I., *Engineering Rheology*. Oxford: Clarendon Press, 1985.
4. Macosko, C. W., *Rheology: Principles, Measurements, and Applications*. New York: VCH Publishers, 1994.
5. Loh, W. H. T., "Theory of the Hydraulic Analogy for Steady and Unsteady Gas Dynamics," in *Modern Developments in Gas Dynamics*, W. H. T. Loh, ed. New York: Plenum, 1969.
6. Folsom, R. G., "Manometer Errors Due to Capillarity, Instruments, 9, 1, 1937, pp. 36–37.
7. Waugh, J. G., and G. W. Stubstad, *Hydroballistics Modeling*. San Diego: Naval Undersea Center, ca. 1972.

Chapter 3 Problems

Standard Atmosphere

3.1 At standard atmospheric conditions, a gage measures the pressure in a tank as -2.1 psi . Determine the absolute pressure in psia and kPa.

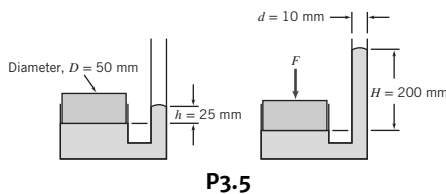
3.2 Atmospheric pressure decreases with altitude, which affects the boiling point of water and, consequently, the cooking times for some foods. Determine and plot the boiling temperature of water over the range of sea level to 4000 m assuming standard atmospheric conditions.

3.3 Ear “popping” occurs as air leaves the inner ear rapidly to accommodate a sudden change in the outside pressure. Determine the change in pressure if your ears “pop” when you are in a car and descend from 1000 m to 600 m. Determine the altitude change for the same pressure drop if the car descends from 3000 m.

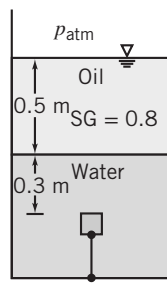
3.4 For a car parked at an altitude of 7000 ft, the tire is at atmospheric temperature and the tire pressure is indicated as 31 psi. Determine the absolute and gage pressures for the tire when the car is driven to sea level and the tire has warmed to 85°F .

Pressure Variation in a Static Fluid

3.5 A piston is placed on a tank filled with mercury at 20°C as shown below. A force is applied to the piston and the height of the mercury column rises. Determine the weight of the piston and the applied force.



3.6 A 125-mL cube of solid oak is held submerged by a tether as shown. Calculate the force of the water on the bottom surface of the cube and the tension in the tether.



3.7 Calculate the absolute and gage pressure in an open tank of crude oil 2.4 m below the liquid surface. If the tank is closed and pressurized to 130 kPa, what are the absolute and gage pressures at this location?

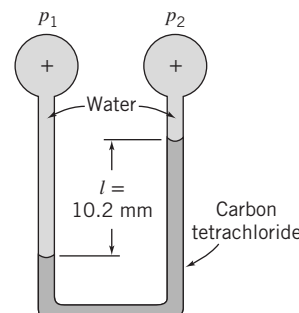
3.8 An open tank contains water to a depth of 6 ft and a layer of oil on top of the water that is 3 ft deep. Determine the pressure at the bottom of the tank.

3.9 The compressibility of sea water has a significant effect on the variation of density and pressure with depth. The density at sea level is 1020 kg/m^3 and the pressure is atmospheric. Determine the density

and pressure at a depth of 10,000 m assuming (a) a constant density and (b) a compressibility of $E = 2.07 \times 10^{-9} \text{ Pa}$.

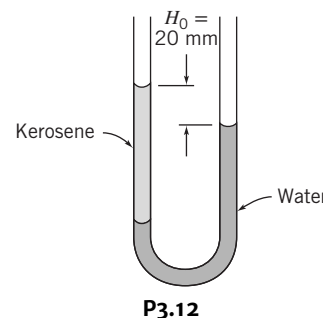
3.10 A water tank filled to a depth of 16 ft has a 1 in. \times 1 in. inspection cover at the base. The cover is held in place by a plastic bracket that can withstand a load of 9 lbf. Determine whether the bracket is strong enough under these conditions and the water depth that would cause the bracket to break.

3.11 Consider the two-fluid manometer shown. Calculate the applied pressure difference.

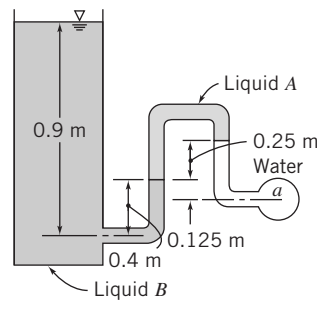


P3.11

3.12 The manometer shown contains water and kerosene. With both tubes open to the atmosphere, the free-surface elevations differ by $H_0 = 20.0 \text{ mm}$. Determine the elevation difference when a pressure of 98.0 Pa gage is applied to the right tube.

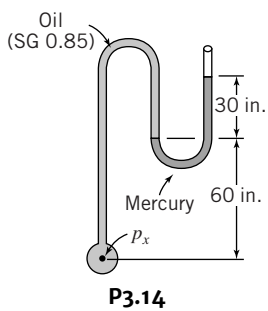


3.13 Determine the gage pressure in kPa at point *a*, if liquid *A* has SG = 1.20 and liquid *B* has SG = 0.75. The liquid surrounding point *a* is water, and the tank on the left is open to the atmosphere. SS



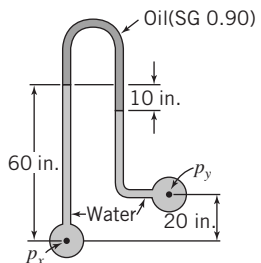
P3.13

3.14 Determine the pressure p_x in the bulb for the manometer readings shown.



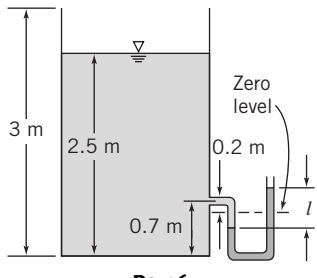
P3.14

3.15 Calculate $p_x - p_y$ for this inverted U-tube manometer.



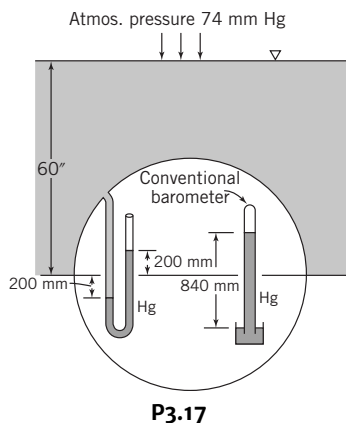
P3.15

3.16 A rectangular tank that is open to the atmosphere is filled to a depth of 2.5 m. A U-tube manometer filled with Meriam blue manometer fluid (SG = 1.75) is connected to the tank 0.7 m above the tank bottom. Before the manometer is connected to the tank, the zero level is 0.2 m below the connection. Determine the deflection ℓ after the manometer is connected.



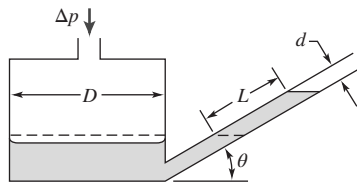
P3.16

SS 3.17 The figure shows a sectional view through a submarine. Calculate the depth of submergence, y . Assume the specific weight of seawater is 10.0 kN/m^3 .



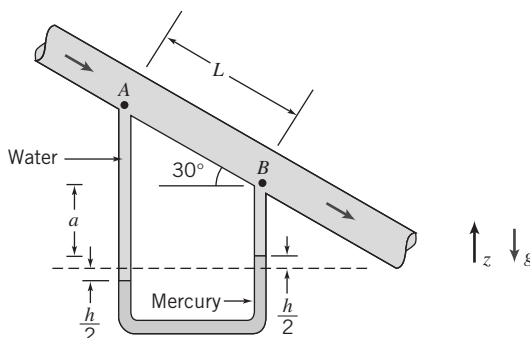
P3.17

3.18 The inclined-tube manometer shown has $D = 96 \text{ mm}$ and $d = 8 \text{ mm}$. Determine the angle θ that will give a deflection of 15 cm for a gage pressure in the tank of 25 mm water. Compare to the deflection for a vertical tube manometer.



P3.18

3.19 Water flows downward along a pipe that is inclined at 30° below the horizontal, as shown. Pressure difference $p_A - p_B$ is due partly to gravity and partly to friction. Derive an algebraic expression for the pressure difference. Evaluate the pressure difference if $L = 5 \text{ ft}$ and $h = 6 \text{ in}$.

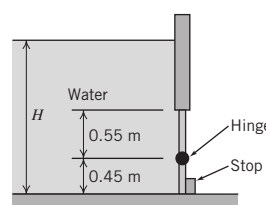


P3.19

3.20 The elevation of Tucson, AZ, is about 500 m, and Mt. Lemmon is about 2000 m higher. Assuming standard atmospheric conditions in Tucson, determine the pressure at the top of Mt. Lemmon assuming (a) an incompressible atmosphere and (b) an atmosphere for which the temperature varies linearly with altitude. Compare your result to the value for a standard atmosphere.

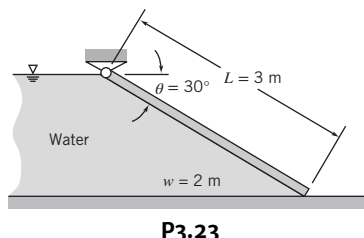
3.21 Compare the height due to capillary action of water exposed to air in a circular tube of diameter $D = 0.5 \text{ mm}$ with that between two infinite vertical parallel plates of gap $a = 0.5 \text{ mm}$.

3.22 A rectangular gate (width $w = 2 \text{ m}$) is hinged as shown, with a stop on the lower edge. Determine the depth H that will tip the gate.



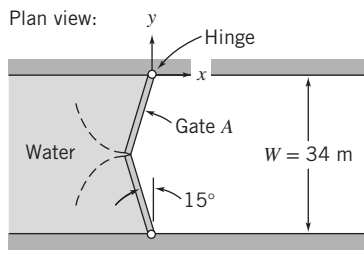
P3.22

3.23 A plane gate of uniform thickness holds back a depth of water as shown. Find the minimum weight needed to keep the gate closed.

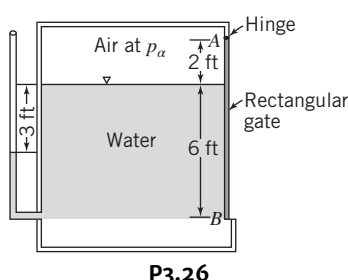


3.24 A vertical rectangular gate 2.4 m wide and 2.7 m high is subjected to water pressure on one side, the water surface being at the top of the gate. The gate is hinged at the bottom and is held by a horizontal chain at the top. Determine the tension in the chain.

3.25 Gates in the Poe Lock at Sault Ste. Marie, Michigan, close a channel $W = 34$ m wide, $L = 360$ m long, and $D = 10$ m deep. The geometry of one pair of gates is shown; each gate is hinged at the channel wall. When closed, the gate edges are forced together at the center of the channel by water pressure. Evaluate the force exerted by the water on gate A. Determine the magnitude and direction of the force components exerted by the gate on the hinge. Neglect the weight of the gate.

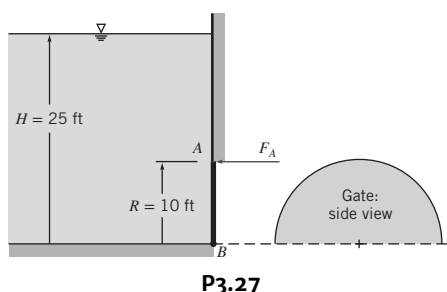


3.26 For the situation shown, find the air pressure in the tank in psi. Calculate the force exerted on the gate at the support B if the gate is 10 ft wide. Show a free body diagram of the gate with all the forces drawn in and their points of application located.

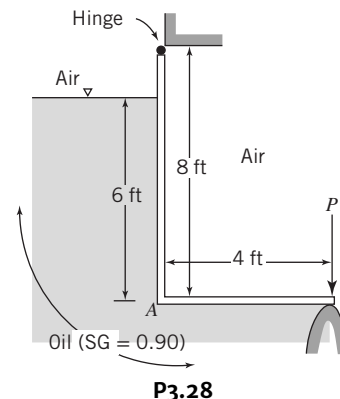


Hydrostatic Force on Submerged Surfaces

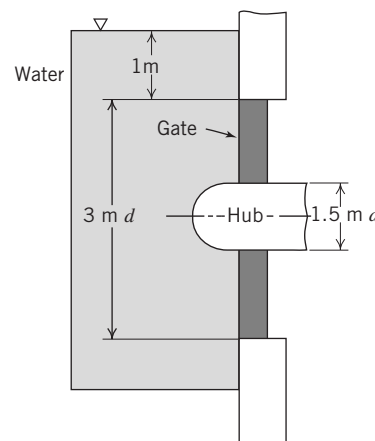
3.27 Semicircular plane gate AB is hinged along B and held by horizontal force F_A applied at A. The liquid to the left of the gate is water. Calculate the force F_A required for equilibrium.



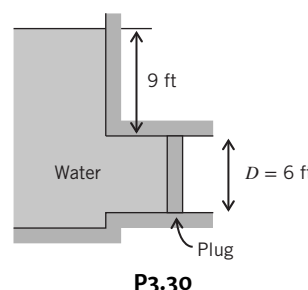
3.28 Determine the pressure at A. Draw a free body diagram of the 10-ft wide gate showing all forces and the locations of their lines of action. Calculate the minimum force P necessary to keep the gate closed. SS



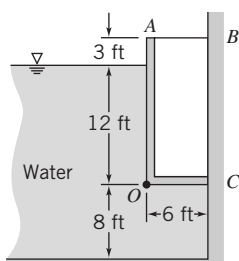
3.29 Calculate magnitude and location of the resultant force of water on this annular gate.



3.30 A large open tank contains water and is connected to a 6-ft-diameter conduit as shown. A circular plug is used to seal the conduit. Determine the magnitude, direction, and location of the force of the water on the plug.

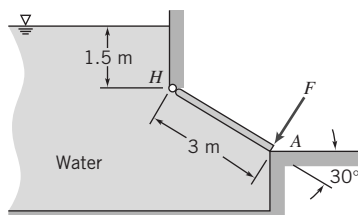


3.31 The gate AOC shown is 6 ft wide and is hinged along O. Neglecting the weight of the gate, determine the force in bar AB. The gate is sealed at C. SS



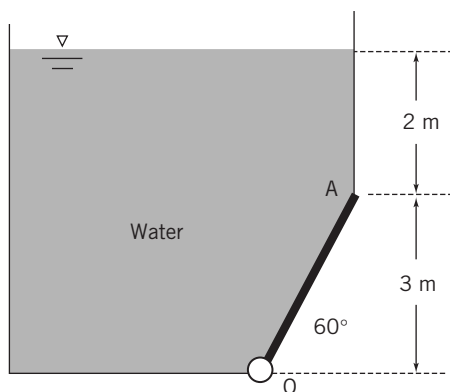
P3.31

- SS 3.32** The gate shown is hinged at H . The gate is 3 m wide normal to the plane of the diagram. Calculate the force required at A to hold the gate closed.



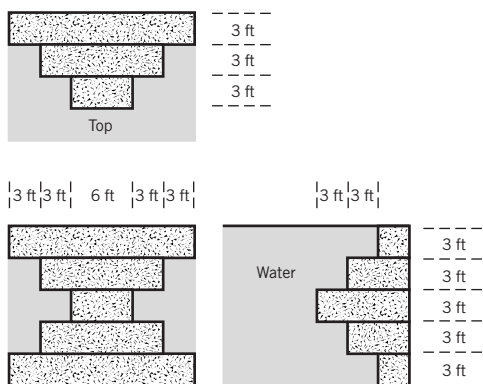
P3.32

- 3.33** A tank of water 4 m wide with a hinged gate is shown in the figure. Determine the magnitude and direction of the force at location A needed to hold the gate in the position shown and the moment around the hinge O . Determine what the moment would be if the hinge were at location A .



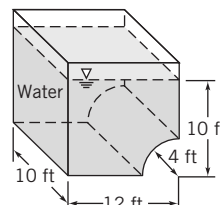
P3.33

- 3.34** Determine the vertical force on the dam shown.



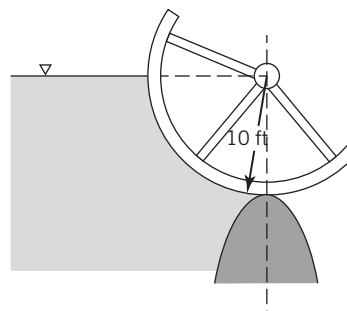
P3.34

- 3.35** An open tank is filled with water to the depth indicated. Atmospheric pressure acts on all outer surfaces of the tank. Determine the magnitude and line of action of the vertical component of the force of the water on the curved part of the tank bottom.



P3.35

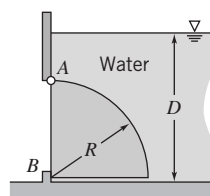
- 3.36** Calculate the magnitude, direction and line of action of the resultant force exerted by the water on the cylindrical gate 30 ft long.



P3.36

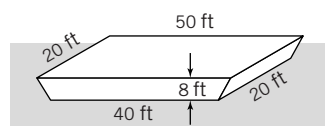
- 3.37** A hemispherical shell 1.2 m in diameter is connected to the vertical wall of a tank containing water. If the center of the shell is 1.8 m below the water surface, determine the vertical and horizontal force components on the shell as a whole and on the top half of the shell.

- 3.38** A gate, in the shape of a quarter-cylinder, hinged at A and sealed at B , is 3 m wide. The bottom of the gate is 4.5 m below the water surface. Determine the force on the stop at B if the gate is made of concrete; $R = 3$ m.



P3.38

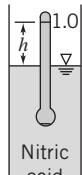
- 3.39** The barge shown in the figure weighs 40 tons and carries a cargo of 30 tons. Determine the draft (distance from the water level to the bottom of the barge) in freshwater. Determine the draft when the barge is towed into a salt water sea.



P3.39

Buoyancy and Stability

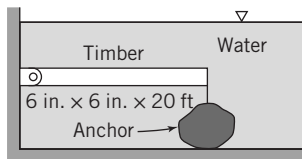
3.40 A hydrometer is a specific gravity indicator, the value being indicated by the level at which the free surface intersects the stem when floating in a liquid. The 1.0 mark is the level when in distilled water. For the unit shown, the immersed volume in distilled water is 15 cm^3 . The stem is 6 mm in diameter. Find the distance, h , from the 1.0 mark to the surface when the hydrometer is placed in a nitric acid solution of specific gravity 1.5.



P3.40

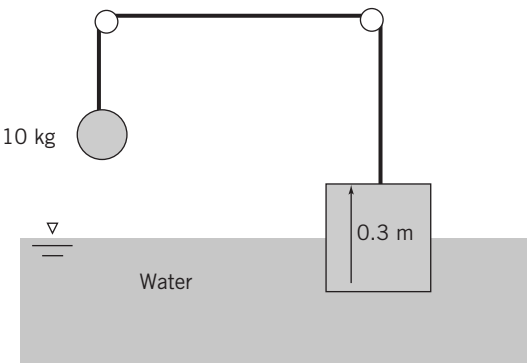
3.41 A cylindrical can 75 mm in diameter and 150 mm high is filled with water to a depth of 80 mm. The can weighs 1.1 N. Determine the depth the can will sink when placed in water.

SS 3.42 The timber weighs $40 \text{ lb}/\text{ft}^3$ and is held in a horizontal position by the concrete ($150 \text{ lb}/\text{ft}^3$) anchor. Calculate the minimum total weight which the anchor may have.



P3.42

3.43 Determine the specific weight of the cube when one-half is submerged as shown in the figure. Determine the position of the center of the cube relative to the water level when the weight is removed.

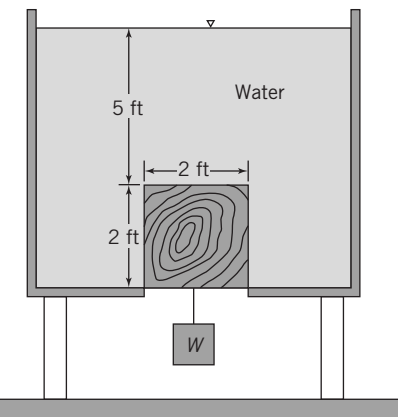


P3.43

3.44 The opening in the bottom of the tank is square and slightly less than 2 ft on each side. The opening is to be plugged with a wooden cube 2 ft on a side.

(a) Determine the weight W that will insure successful plugging of the hole. The wood weighs $40 \text{ lb}/\text{ft}^3$.

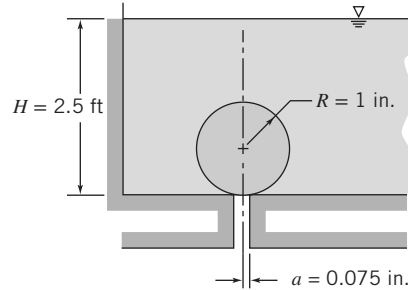
(b) Determine the upward force that must be exerted on the block to lift it and allow water to drain from the tank.



P3.44

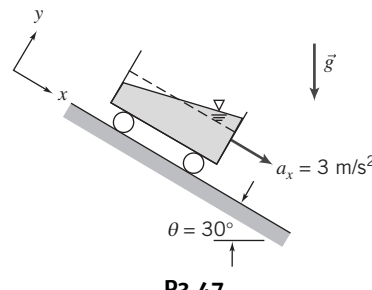
3.45 A balloon has a weight of 2.2 kN, not including gas, and a gas-bag capacity of 566 m^3 . At the ground, it is partially inflated with 445 N of helium. Determine how high the balloon will rise. Assume a Standard Atmosphere and that helium is always at the pressure and temperature of the atmosphere.

3.46 A sphere of 1-in.-radius made from material of specific gravity of $\text{SG} = 0.95$, is submerged in a tank of water. The sphere is placed over a hole of 0.075-in.-radius in the tank bottom. When the sphere is released, determine whether it stay on the bottom of the tank or float to the surface.



P3.46

3.47 A rectangular container of water undergoes constant acceleration down an incline as shown. Determine the slope of the free surface using the coordinate system shown.



P3.47

3.48 Cast iron or steel molds are used in a horizontal-spindle machine to make tubular castings such as liners and tubes. A charge of molten metal is poured into the spinning mold. The radial acceleration permits nearly uniformly thick wall sections to form. A steel liner, of length $L = 6 \text{ ft}$, outer radius $r_o = 6 \text{ in.}$, and inner radius $r_i = 4 \text{ in.}$, is to be formed by this process. To attain nearly uniform thickness, the angular velocity should be at least 300 rpm. Determine (a) the resulting radial acceleration on the inside surface of the liner and (b) the maximum and minimum pressures on the surface of the mold.

CHAPTER 3

Fluid Statics

- 3.1 The Basic Equation of Fluid Statics
- 3.2 The Standard Atmosphere
- 3.3 Pressure Variation in a Static Fluid
- 3.4 Hydrostatic Force on Submerged Surfaces

- 3.5 Buoyancy and Stability
- 3.6 Fluids in Rigid-Body Motion
- 3.7 Summary and Useful Equations

Case Study

Flood control is essential in the Netherlands as about two-thirds of the country could be flooded by the ocean or one of the three major European rivers that run through it. Over the centuries, a system of canals, dikes, and dams have been successful in preventing serious flooding, but the recent rises in sea level made it more imperative to develop methods to protect the land.

The Delta Works is a recent comprehensive approach that incorporates a storm surge barrier into the system of dikes, dams, and sluice gates. The Eastern Scheldt Storm Surge Barrier shown in the photograph is an important component in this barrier. It is 8 km in length and composed of 62 enormous sliding gates that are open during normal conditions to allow tidal flows in and out. This preserves the saltwater marine life behind the dam so that the traditional fishing and oyster catching can take place. However, under storm surge conditions, the gates can be closed in 75 min to keep high seas from encroaching and inundating the land inside the barrier.

The dam is controlled by human operators, but if they fail there is an electronic security system that takes over. By Dutch law, the level of the sea must be at least 3 m above normal before the gates can be completely shut. The dam has been closed twenty-seven

times since it was completed in 1986 due to water levels exceeding or being predicted to exceed the 3 m. The dam construction cost 2.5 billion Euros and the operating expenses are 17 million Euros per year. However, the dam is expected to protect the mainland of Holland for the next 200 years.



Storm Surge Gates in Holland Dam.

Will tilroe-otte/Adobe Stock Photo

Learning Objectives

After completing this chapter, you should be able to

- Calculate the absolute and gage pressures in a fluid at rest.
- Explain the variation of pressure with elevation for the Standard Atmosphere.
- Calculate pressure in a fluid as indicated by a manometer.
- Calculate the hydrostatic force on a submerged plane or curved object.
- Calculate the buoyancy force on an object immersed in a fluid.

In Chapter 1, we defined a fluid as any substance that continuously deforms when it experiences a shear stress. For a static fluid (or one undergoing “rigid-body” motion) only the normal stress due to pressure is present. We will study the topic of fluid statics in this chapter.

Although fluid statics problems are the simplest kind of fluid mechanics problems, this is not the only reason we will study them. The pressure generated within a static fluid is an important phenomenon in many practical situations. Using the principles of hydrostatics, we can compute forces on submerged objects, develop instruments for measuring pressures, and deduce properties of the atmosphere and oceans. The principles of hydrostatics also may be used to determine the forces developed by hydraulic systems in applications such as industrial presses or automobile brakes.

In a static, homogeneous fluid, or in a fluid undergoing rigid-body motion, a fluid particle retains its identity for all time, and fluid elements do not deform. We may apply Newton’s second law of motion to evaluate the forces acting on the particle.

3.1 The Basic Equation of Fluid Statics

The first objective of this chapter is to obtain an equation for computing the pressure field in a static fluid. We will deduce what we already know from everyday experience, that the pressure increases with depth. To do this, we apply Newton’s second law to a differential fluid element of mass $dm = \rho dV$, with sides dx , dy , and dz , as shown in Fig. 3.1. The fluid element is stationary relative to the stationary rectangular coordinate system shown.

From our previous discussion, recall that two general types of forces may be applied to a fluid: body forces and surface forces. The only body force that must be considered in most engineering problems is due to gravity. We will not consider body forces caused by electric or magnetic fields.

For a differential fluid element, the body force is

$$d\vec{F}_B = \vec{g} dm = \vec{g} \rho dV$$

where \vec{g} is the local gravity vector, ρ is the density, and dV is the volume of the element. In Cartesian coordinates $dV = dx dy dz$, so

$$d\vec{F}_B = \rho \vec{g} dx dy dz$$

In a static fluid there are no shear stresses, so the only surface force is the pressure force. Pressure is a scalar field, $p = p(x, y, z)$ and in general we expect the pressure to vary with position within the fluid. The net pressure force that results from this variation can be found by summing the forces that act on the six faces of the fluid element.

Let the pressure be p at the center, O , of the element. To determine the pressure at each of the six faces of the element, we use a Taylor series expansion of the pressure about point O . The pressure at the left face of the differential element is

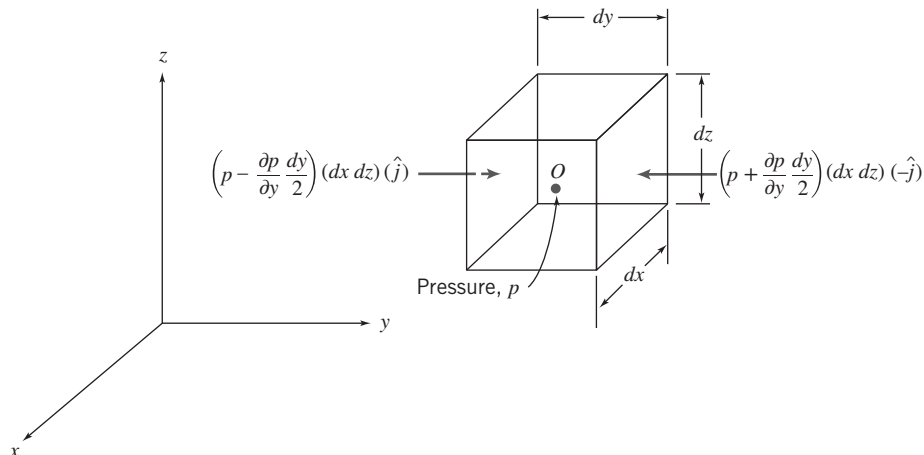


Fig. 3.1 Differential fluid element and pressure forces in the y direction.

$$p_L = p + \frac{\partial p}{\partial y} (y_L - y) = p + \frac{\partial p}{\partial y} \left(-\frac{dy}{2} \right) = p - \frac{\partial p}{\partial y} \frac{dy}{2}$$

Terms of higher order are omitted because they will vanish in the subsequent limiting process. The pressure on the right face of the differential element is

$$p_R = p + \frac{\partial p}{\partial y} (y_R - y) = p + \frac{\partial p}{\partial y} \frac{dy}{2}$$

The pressure *forces* acting on the two y surfaces of the differential element are shown in Fig. 3.1. Each pressure force is a product of three factors. The first is the magnitude of the pressure. This magnitude is multiplied by the area of the face to give the magnitude of the pressure force, and a unit vector is introduced to indicate direction. Note also in Fig. 3.1 that the pressure force on each face acts *against* the face. A positive pressure corresponds to a *compressive* normal stress.

Pressure forces on the other faces of the element are obtained in the same way. Combining all such forces gives the net surface force acting on the element. Thus

$$\begin{aligned} d\vec{F}_S &= \left(p - \frac{\partial p dx}{\partial x 2} \right) (dy dz) (\hat{i}) + \left(p + \frac{\partial p dx}{\partial x 2} \right) (dy dz) (-\hat{i}) \\ &\quad + \left(p - \frac{\partial p dy}{\partial y 2} \right) (dx dz) (\hat{j}) + \left(p + \frac{\partial p dy}{\partial y 2} \right) (dx dz) (-\hat{j}) \\ &\quad + \left(p - \frac{\partial p dz}{\partial z 2} \right) (dx dy) (\hat{k}) + \left(p + \frac{\partial p dz}{\partial z 2} \right) (dx dy) (-\hat{k}) \end{aligned}$$

Collecting and canceling terms, we obtain

$$d\vec{F}_S = - \left(\frac{\partial p}{\partial x} \hat{i} + \frac{\partial p}{\partial y} \hat{j} + \frac{\partial p}{\partial z} \hat{k} \right) dx dy dz \quad (3.1a)$$

The term in parentheses is called the gradient of the pressure or simply the pressure gradient and may be written $\text{grad } p$ or ∇p . In rectangular coordinates

$$\text{grad } p \equiv \nabla p \equiv \left(\hat{i} \frac{\partial p}{\partial x} + \hat{j} \frac{\partial p}{\partial y} + \hat{k} \frac{\partial p}{\partial z} \right) \equiv \left(\hat{i} \frac{\partial}{\partial x} + \hat{j} \frac{\partial}{\partial y} + \hat{k} \frac{\partial}{\partial z} \right) p$$

The gradient can be viewed as a vector operator; taking the gradient of a scalar field gives a vector field. Using the gradient designation, Eq. 3.1a can be written as

$$d\vec{F}_S = - \text{grad } p (dx dy dz) = - \nabla p dx dy dz \quad (3.1b)$$

Physically the gradient of pressure is the negative of the surface force per unit volume due to pressure. Note that the pressure magnitude itself is not relevant in computing the net pressure force; instead what counts is the rate of change of pressure with distance, the *pressure gradient*. We shall encounter this term throughout our study of fluid mechanics.

We combine the formulations for surface and body forces that we have developed to obtain the total force acting on a fluid element. Thus

$$d\vec{F} = d\vec{F}_S + d\vec{F}_B = (-\nabla p + \rho \vec{g}) dx dy dz = (-\nabla p + \rho \vec{g}) dV$$

or on a per unit volume basis

$$\frac{d\vec{F}}{dV} = - \nabla p + \rho \vec{g} \quad (3.2)$$

For a fluid particle, Newton's second law gives $\vec{F} = \vec{a} dm = \vec{a} \rho dV$. For a static fluid, $\vec{a} = 0$. Thus

$$\frac{d\vec{F}}{dV} = \rho \vec{a} = 0$$

Substituting for $d\vec{F}/dV$ from Eq. 3.2, we obtain

$$-\nabla p + \rho \vec{g} = 0 \quad (3.3)$$

Let us review this equation briefly. The physical significance of each term is

$$\begin{aligned} -\nabla p &+ \rho \vec{g} = 0 \\ \left\{ \begin{array}{l} \text{net pressure force} \\ \text{per unit volume} \\ \text{at a point} \end{array} \right\} + \left\{ \begin{array}{l} \text{body force per} \\ \text{unit volume} \\ \text{at a point} \end{array} \right\} = 0 \end{aligned}$$

This is a vector equation, which means that it is equivalent to three component equations that must be satisfied individually. The component equations are

$$\left. \begin{aligned} -\frac{\partial p}{\partial x} + \rho g_x &= 0 && x \text{ direction} \\ -\frac{\partial p}{\partial y} + \rho g_y &= 0 && y \text{ direction} \\ -\frac{\partial p}{\partial z} + \rho g_z &= 0 && z \text{ direction} \end{aligned} \right\} \quad (3.4)$$

Equations 3.4 describe the pressure variation in each of the three coordinate directions in a static fluid. It is convenient to choose a coordinate system such that the gravity vector is aligned with one of the coordinate axes. If the coordinate system is chosen with the z axis directed vertically upward, as in Fig. 3.1, then $g_x = 0$, $g_y = 0$, and $g_z = -g$. Under these conditions, the component equations become

$$\frac{\partial p}{\partial x} = 0 \quad \frac{\partial p}{\partial y} = 0 \quad \frac{\partial p}{\partial z} = -\rho g \quad (3.5)$$

Equations 3.5 indicate that, under the assumptions made, the pressure is independent of coordinates x and y and it depends on z alone. Thus since p is a function of a single variable, a total derivative may be used instead of a partial derivative. With these simplifications, Eq. 3.5 finally reduces to

$$\frac{dp}{dz} = -\rho g \equiv -\gamma \quad (3.6)$$

Restrictions:

- 1 Static fluid.
- 2 Gravity is the only body force.
- 3 The z axis is vertical and upward.

Equation 3.6 is the basic pressure-height relation of fluid statics. It is subject to the restrictions noted. Therefore it must be applied only where these restrictions are reasonable for the physical situation. To determine the pressure distribution in a static fluid, Eq. 3.6 may be integrated and appropriate boundary conditions applied.

Before considering specific applications of this equation, it is important to remember that pressure values must be stated with respect to a reference level. If the reference level is a vacuum, pressures are termed *absolute*, as shown in Fig. 3.2.

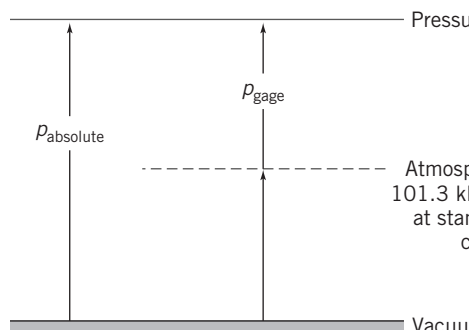


Fig. 3.2 Absolute and gage pressures, showing reference levels.

Most pressure gages indicate a pressure *difference* such as the difference between the measured pressure and the ambient level (usually atmospheric pressure). Pressure levels measured with respect to atmospheric pressure are termed *gage* pressures. Thus

$$p_{\text{gage}} = p_{\text{absolute}} - p_{\text{atmosphere}}$$

For example, a tire gage might indicate 30 psi, and absolute pressure would be about 44.7 psi. Absolute pressures must be used in all calculations with the ideal gas equation or other equations of state.

3.2 The Standard Atmosphere

Scientists and engineers sometimes need a numerical or analytical model of the Earth's atmosphere in order to simulate climate variations to study, for example, effects of global warming. Although there is no single standard model, in the United States the U.S. Standard Atmosphere [3] is the usual reference. In addition, there is an International Standard Atmosphere (ISA) [4] in use in many countries.

The temperature profile of the U.S. Standard Atmosphere is shown in Fig. 3.3. Additional property values are tabulated as functions of elevation in Appendix A. Sea level conditions of the U.S. Standard Atmosphere are summarized in Table 3.1.

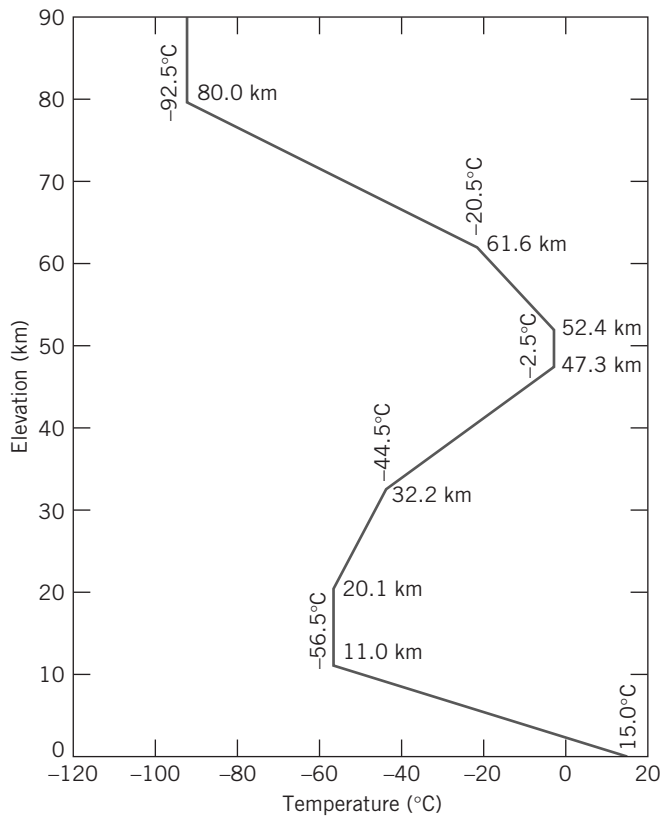


Fig. 3.3 Temperature variation with altitude in the U.S. Standard Atmosphere.

Table 3.1
Sea Level Conditions of the U.S. Standard Atmosphere

Property	Symbol	SI	English
Temperature	T	15°C	59°F
Pressure	p	101.3 kPa (abs)	14.696 psia
Density	ρ	1.225 kg/m ³	0.002377 slug/ft ³
Specific weight	γ	—	0.07651 lbf/ft ³
Viscosity	μ	1.789×10^{-5} kg/(m·s)(Pa·s)	3.737×10^{-7} lbf·s/ft ²

3.3 Pressure Variation in a Static Fluid

We proved that pressure variation in any static fluid is described by the basic pressure-height relation

$$\frac{dp}{dz} = -\rho g \quad (3.6)$$

Although ρg may be defined as the specific weight, γ , it has been written as ρg in Eq. 3.6 to emphasize that both ρ and g must be considered variables. In order to integrate Eq. 3.6 to find the pressure distribution, we need information about variations in both ρ and g .

For most practical engineering situations, the variation in g with elevation is negligible. Only for a purpose such as computing very precisely the pressure change over a large elevation difference would the variation in g need to be included. Unless we state otherwise, we shall assume g to be constant with elevation at any given location.

Incompressible Liquids: Manometers

For an incompressible fluid, $\rho = \text{constant}$. Then for constant gravity,

$$\frac{dp}{dz} = -\rho g = \text{constant}$$

To determine the pressure variation, we must integrate and apply appropriate boundary conditions. If the pressure at the reference level, z_0 , is designated as p_0 , then the pressure, p , at level z is found by integration:

$$\int_{p_0}^p dp = - \int_{z_0}^z \rho g dz$$

or

$$p - p_0 = -\rho g(z - z_0) = \rho g(z_0 - z)$$

For liquids, it is often convenient to take the origin of the coordinate system at the free surface (reference level) and to measure distances as positive downward from the free surface as in Fig. 3.4.

With the depth h measured positive downward, we have

$$z_0 - z = h$$

and obtain

$$p - p_0 = \Delta p = \rho gh \quad (3.7)$$

Equation 3.7 indicates that the pressure difference between two points in a static incompressible fluid can be determined by measuring the elevation difference between the two points. Devices used for this purpose are called *manometers*. Use of Eq. 3.7 for a manometer is illustrated in Example 3.1.

Manometers are simple and inexpensive devices used frequently for pressure measurements. Because the liquid level change is small at low pressure differential, a U-tube manometer may be

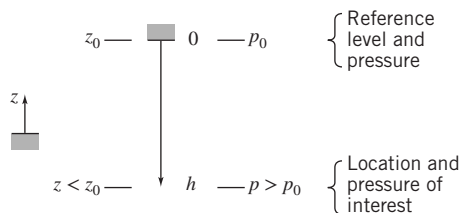


Fig. 3.4 Use of z and h coordinates.

Example 3.1 SYSTOLIC AND DIASTOLIC PRESSURE

Normal blood pressure for a human is 120/80 mm Hg. By modeling a sphygmomanometer pressure gage as a U-tube manometer, convert these pressures to psig.

Given: Gage pressures of 120 and 80 mm Hg.

Find: The corresponding pressures in psig.

Solution: Apply hydrostatic equation to points A, A', and B.

Governing equation:

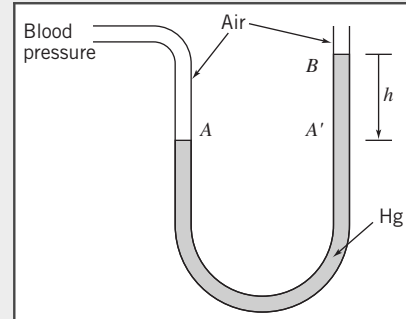
$$p - p_0 = \Delta p = \rho gh \quad (3.1)$$

Assumptions:

1 Static fluid.

2 Incompressible fluids.

3 Neglect air density (\ll Hg density).



Applying the governing equation between points A' and B (and p_B is atmospheric and therefore zero gage):

$$p_{A'} = p_B + \rho_{\text{Hg}}gh = SG_{\text{Hg}}\rho_{\text{H}_2\text{O}}gh$$

In addition, the pressure increases as we go downward from point A' to the bottom of the manometer, and decreases by an equal amount as we return up the left branch to point A. This means points A and A' have the same pressure, so we end up with

$$p_A = p_{A'} = SG_{\text{Hg}}\rho_{\text{H}_2\text{O}}gh$$

Substituting $SG_{\text{Hg}} = 13.6$ and $\rho_{\text{H}_2\text{O}} = 1.94 \text{ slug/ft}^3$ from Appendix A.1 yields for the systolic pressure ($h = 120 \text{ mm Hg}$)

$$\begin{aligned} p_{\text{systolic}} &= p_A = 13.6 \times 1.94 \frac{\text{slug}}{\text{ft}^3} \times 32.2 \frac{\text{ft}}{\text{s}^2} \times 120 \text{ mm} \times \frac{\text{in.}}{25.4 \text{ mm}} \\ &\quad \times \frac{\text{ft}}{12 \text{ in.}} \times \frac{\text{lbf} \cdot \text{s}^2}{\text{slug} \cdot \text{ft}} \\ p_{\text{systolic}} &= 334 \text{ lbf/ft}^2 = 2.32 \text{ psi} \end{aligned} \quad p_{\text{systolic}}$$

By a similar process, the diastolic pressure ($h = 80 \text{ mm Hg}$) is

$$p_{\text{diastolic}} = 1.55 \text{ psi} \quad p_{\text{diastolic}}$$

Notes:

- Two points at the same level in a continuous single fluid have the same pressure.
- In manometer problems we neglect change in pressure with depth for a gas: $\rho_{\text{gas}} \ll \rho_{\text{liquid}}$.
- This problem shows the conversion from mm Hg to psi, using Eq. 3.7: 120 mm Hg is equivalent to about 2.32 psi. More generally, $1 \text{ atm} = 14.7 \text{ psi} = 101 \text{ kPa} = 760 \text{ mm Hg}$.

difficult to read accurately. The *sensitivity* of a manometer is a measure of how sensitive it is compared to a simple water-filled U-tube manometer. Specifically, it is the ratio of the deflection of the manometer to that of a water-filled U-tube manometer due to the same applied pressure difference Δp . Sensitivity can be increased by changing the manometer design or by using two immiscible liquids of slightly different density. Analysis of an inclined manometer is illustrated in Example 3.2.

Students sometimes have trouble analyzing multiple-liquid manometer situations. The following rules of thumb are useful:

- Any two points at the same elevation in a continuous region of the same liquid are at the same pressure.
- Pressure increases as one goes *down* a liquid column.

Example 3.2 ANALYSIS OF INCLINED-TUBE MANOMETER

An inclined-tube reservoir manometer is constructed as shown. Derive a general expression for the liquid deflection, L , in the inclined tube, due to the applied pressure difference, Δp . Also obtain an expression for the manometer sensitivity, and discuss the effect on sensitivity of D , d , θ , and SG .

Given: Inclined-tube reservoir manometer.

Find: Expression for L in terms of Δp .

General expression for manometer sensitivity.

Effect of parameter values on sensitivity.

Solution: Use the equilibrium liquid level as a reference.

Governing equations:

$$p - p_0 = \Delta p = \rho g h \quad SG = \frac{\rho}{\rho_{H_2O}}$$

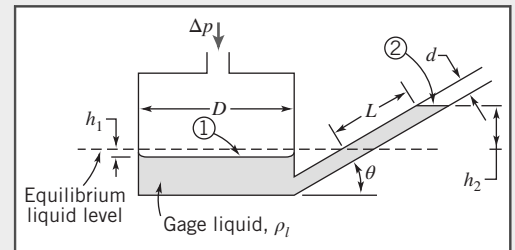
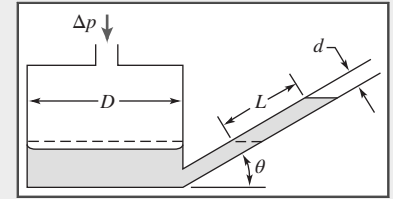
Assumptions:

1 Static fluid.

2 Incompressible fluid.

Applying the governing equation between points 1 and 2

$$p_1 - p_2 = \Delta p = \rho_l g (h_1 + h_2) \quad (1)$$



To eliminate h_1 , we recognize that the *volume* of manometer liquid remains constant; the volume displaced from the reservoir must equal the volume that rises in the tube, so

$$\frac{\pi D^2}{4} h_1 = \frac{\pi d^2}{4} L \quad \text{or} \quad h_1 = L \left(\frac{d}{D} \right)^2$$

In addition, from the geometry of the manometer, $h_2 = L \sin \theta$. Substituting into Eq. 1 gives

$$\Delta p = \rho_l g \left[L \sin \theta + L \left(\frac{d}{D} \right)^2 \right] = \rho_l g L \left[\sin \theta + \left(\frac{d}{D} \right)^2 \right]$$

Thus

$$L = \frac{\Delta p}{\rho_l g \left[\sin \theta + \left(\frac{d}{D} \right)^2 \right]} \quad \text{--- } L$$

To find the sensitivity of the manometer, we need to compare this to the deflection h a simple U-tube manometer, using water (density ρ), would experience,

$$h = \frac{\Delta p}{\rho g}$$

The sensitivity s is then

$$s = \frac{L}{h} = \frac{1}{SG_l \left[\sin \theta + \left(\frac{d}{D} \right)^2 \right]} \quad \text{--- } s$$

where we have used $SG_l = \rho_l / \rho$. This result shows that to increase sensitivity, SG_l , $\sin \theta$, and d/D each should be made as small as possible. Thus the designer must choose a gage liquid and two geometric parameters to complete a design, as discussed below.

Gage Liquid

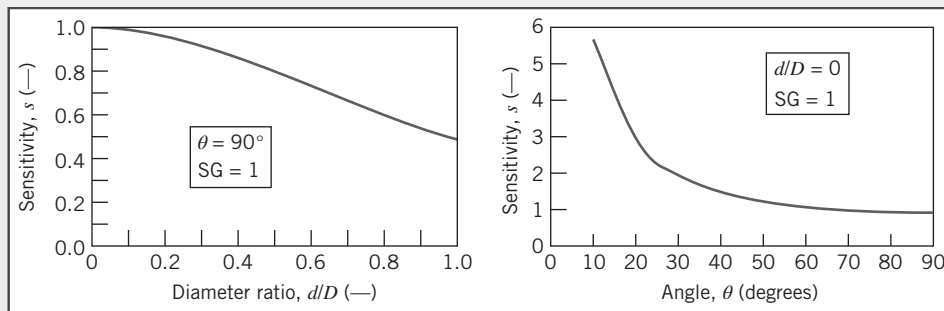
The gage liquid should have the smallest possible specific gravity to increase sensitivity. In addition, the gage liquid must be safe (without toxic fumes or flammability), be immiscible with the fluid being gaged, suffer minimal loss from evaporation, and develop a satisfactory meniscus. Thus the gage liquid should have relatively low surface tension and should accept dye to improve its visibility.

Tables A.1, A.2, and A.4 show that hydrocarbon liquids satisfy many of these criteria. The lowest specific gravity is about 0.8, which increases manometer sensitivity by 25 percent compared to water.

Diameter Ratio

The plot shows the effect of diameter ratio on sensitivity for a vertical reservoir manometer with gage liquid of unity specific gravity. Note that $d/D = 1$ corresponds to an ordinary U-tube manometer. Its sensitivity is 0.5 because for this case the total deflection will be h , and for each side it will be $h/2$, so $L = h/2$. Sensitivity doubles to 1.0 as d/D approaches zero because most of the level change occurs in the measuring tube.

The minimum tube diameter d must be larger than about 6 mm to avoid excessive capillary effect. The maximum reservoir diameter D is limited by the size of the manometer. If D is set at 60 mm, so that d/D is 0.1, then $(d/D)^2 = 0.01$, and the sensitivity increases to 0.99, very close to the maximum attainable value of 1.0.



Inclination Angle

The final plot shows the effect of inclination angle on sensitivity for $(d/D) = 0$. Sensitivity increases sharply as inclination angle is reduced below 30 degrees. A practical limit is reached at about 10 degrees: The meniscus becomes indistinct and the level hard to read for smaller angles.

Summary

Combining the best values ($SG = 0.8$, $d/D = 0.1$, and $\theta = 10$ degrees) gives a manometer sensitivity of 6.81. Physically this is the ratio of observed gage liquid deflection to equivalent water column height. Thus the deflection in the inclined tube is amplified 6.81 times compared to a vertical water column. With improved sensitivity, a small pressure difference can be read more accurately than with a water manometer, or a smaller pressure difference can be read with the same accuracy.

To find the pressure difference Δp between two points separated by a series of fluids, we can use the following modification of Eq. 3.1:

$$\Delta p = g \sum_i \rho_i h_i \quad (3.8)$$

where ρ_i and h_i represent the densities and depths of the various fluids, respectively. Use care in applying signs to the depths h_i ; they will be positive downwards, and negative upwards. Example 3.3 illustrates the use of a multiple-liquid manometer for measuring a pressure difference.

Example 3.3 MULTIPLE-LIQUID MANOMETER

Water flows through pipes A and B. Lubricating oil is in the upper portion of the inverted U. Mercury is in the bottom of the manometer bends. Determine the pressure difference, $p_A - p_B$, in units of lbf/in.²

Given: Multiple-liquid manometer as shown.

Find: Pressure difference, $p_A - p_B$, in lbf/in.²

Solution:

Governing equations:

$$\Delta p = g \sum_i \rho_i h_i \quad SG = \frac{\rho}{\rho_{H_2O}}$$

Assumptions:

1 Static fluid.

2 Incompressible fluid.

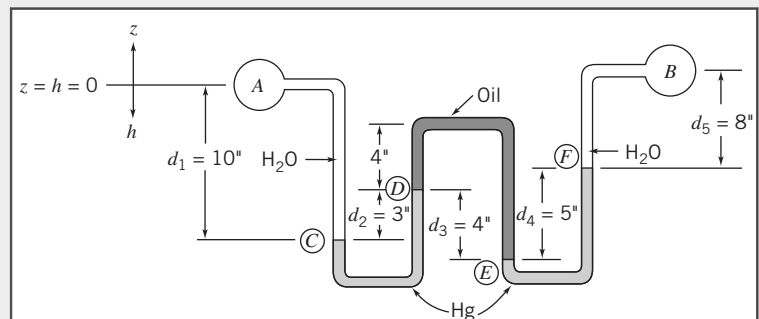
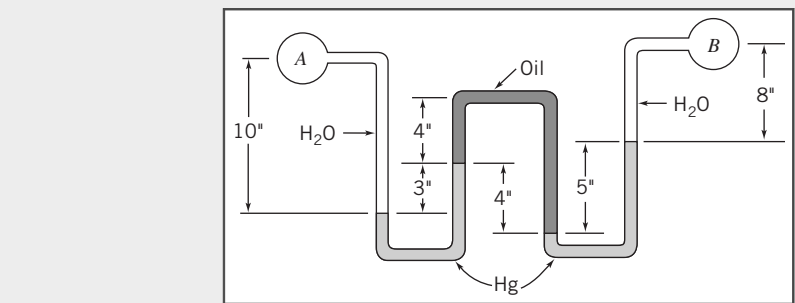
Applying the governing equation, working from point B to A

$$p_A - p_B = \Delta p = g(\rho_{H_2O}d_5 + \rho_{Hg}d_4 - \rho_{oil}d_3 + \rho_{Hg}d_2 - \rho_{H_2O}d_1) \quad (1)$$

This equation can also be derived by repeatedly using Eq. 3.1 in the following form:

$$p_2 - p_1 = \rho g(h_2 - h_1)$$

Beginning at point A and applying the equation between successive points along the manometer gives



Multiplying each equation by minus one and adding, we obtain Eq. 1

$$\begin{aligned} p_A - p_B &= (p_A - p_C) + (p_C - p_D) + (p_D - p_E) + (p_E - p_F) + (p_F - p_B) \\ &= -\rho_{H_2O}gd_1 + \rho_{Hg}gd_2 - \rho_{oil}gd_3 + \rho_{Hg}gd_4 + \rho_{H_2O}gd_5 \end{aligned}$$

Substituting $\rho = SG\rho_{H_2O}$ with $SG\rho_{Hg} = 13.6$ and $SG_{oil} = 0.88$ (Table A.2), yields

$$\begin{aligned} p_A - p_B &= g(-\rho_{H_2O}d_1 + 13.6\rho_{H_2O}d_2 - 0.88\rho_{H_2O}d_3 + 13.6\rho_{H_2O}d_4 + \rho_{H_2O}d_5) \\ &= g\rho_{H_2O}(-d_1 + 13.6d_2 - 0.88d_3 + 13.6d_4 + d_5) \end{aligned}$$

$$p_A - p_B = g\rho_{H_2O}(-10 + 40.8 - 3.52 + 68 + 8) \text{ in.}$$

$$p_A - p_B = g\rho_{H_2O} \times 103.3 \text{ in.}$$

$$= 32.2 \frac{\text{ft}}{\text{s}^2} \times 1.94 \frac{\text{slug}}{\text{ft}^3} \times 103.3 \text{ in.} \times \frac{\text{ft}}{12 \text{ in.}} \times \frac{\text{ft}^2}{144 \text{ in.}^2} \times \frac{\text{lbf} \cdot \text{s}^2}{\text{slug} \cdot \text{ft}}$$

$$p_A - p_B = 3.73 \text{ lbf/in.}^2$$

This problem shows use of both Eq. 3.1 and Eq. 3.8. Use of either equation is a matter of personal preference.

Atmospheric pressure may be obtained from a *barometer* in which the height of a mercury column is measured. The measured height may be converted to pressure using Eq. 3.1 and the data for specific gravity of mercury given in Appendix A. Although the vapor pressure of mercury may be neglected, for precise work, temperature and altitude corrections must be applied to the measured level and the effects of surface tension must be considered. The capillary effect in a tube caused by surface tension was illustrated in Example 2.3.

Gases

In many practical engineering problems density will vary appreciably with large changes in altitude, and accurate results will require that this variation be accounted for. Pressure variation in a compressible fluid can be evaluated by integrating Eq. 3.6 if the density can be expressed as a function of p or z . Property information or an equation of state may be used to obtain the required relation for density. Several types of property variation may be analyzed as shown in Example 3.4.

The density of gases depends on pressure and temperature. The ideal gas equation of state,

$$p = \rho RT \quad (1.1)$$

where R is the gas constant (see Appendix A) and T the absolute temperature, accurately models the behavior of most gases under engineering conditions. However, the use of Eq. 1.1 introduces the gas temperature as an additional variable. Therefore, an additional assumption must be made about temperature variation before Eq. 3.6 can be integrated.

In the U.S. Standard Atmosphere the temperature decreases linearly with altitude up to an elevation of 11.0 km. For a linear temperature variation with altitude given by $T = T_0 - mz$, we obtain, from Eq. 3.6,

$$dp = -\rho g dz = -\frac{pg}{RT} dz = -\frac{pg}{R(T_0 - mz)} dz$$

Separating variables and integrating from $z = 0$ where $p = p_0$ to elevation z where the pressure is p gives

$$\int_{p_0}^p \frac{dp}{p} = - \int_0^z \frac{gdz}{R(T_0 - mz)}$$

Then

$$\ln \frac{p}{p_0} = \frac{g}{mR} \ln \left(\frac{T_0 - mz}{T_0} \right) = \frac{g}{mR} \ln \left(1 - \frac{mz}{T_0} \right)$$

and the pressure variation, in a gas whose temperature varies linearly with elevation, is given by

$$p = p_0 \left(1 - \frac{mz}{T_0} \right)^{g/mR} = p_0 \left(\frac{T}{T_0} \right)^{g/mR} \quad (3.9)$$

Example 3.4 PRESSURE AND DENSITY VARIATION IN THE ATMOSPHERE

The maximum power output capability of a gasoline or diesel engine decreases with altitude because the air density and hence the mass flow rate of air decreases. A truck leaves Denver (elevation 5280 ft) on a day when the local temperature and barometric pressure are 80°F and 24.8 in. of mercury, respectively. It travels through Vail Pass (elevation 10,600 ft), where the temperature is 62°F. Determine the local barometric pressure at Vail Pass and the percent change in density.

Given: Truck travels from Denver to Vail Pass.

Denver: $z = 5280$ ft $p = 24.8$ in. Hg $T = 80^\circ\text{F}$	Vail Pass: $z = 10,600$ ft $T = 62^\circ\text{F}$
--	--

Find: Atmospheric pressure at Vail Pass.

Percent change in air density between Denver and Vail.

Solution:

$$\text{Governing equations: } \frac{dp}{dz} = -\rho g \quad p = \rho RT$$

Assumptions:

1 Static fluid.

2 Air behaves as an ideal gas.

We shall consider four assumptions for property variations with altitude.

(a) If we assume temperature varies linearly with altitude, Eq. 3.9 gives

$$\frac{p}{p_0} = \left(\frac{T}{T_0} \right)^{g/mR}$$

Evaluating the constant m gives

$$m = \frac{T_0 - T}{z - z_0} = \frac{(80 - 62)^\circ F}{(10.6 - 5.28)10^3 \text{ ft}} = 3.38 \times 10^{-3} \text{ }^\circ F/\text{ft}$$

and

$$\frac{g}{mR} = 32.2 \frac{\text{ft}}{\text{s}^2} \times \frac{\text{ft}}{3.38 \times 10^{-3} \text{ }^\circ \text{F}} \times \frac{\text{lbf} \cdot \text{R}}{53.3 \text{ ft} \cdot \text{lbf}} \times \frac{\text{slug}}{32.2 \text{ lbm}} \times \frac{\text{lbf} \cdot \text{s}^2}{\text{slug} \cdot \text{ft}} = 5.55$$

Thus

$$\frac{p}{p_0} = \left(\frac{T}{T_0} \right)^{g/mR} = \left(\frac{460 + 62}{460 + 80} \right)^{5.55} = (0.967)^{5.55} = 0.830$$

and

$$p = 0.830 p_0 = (0.830) 24.8 \text{ in. Hg} = 20.6 \text{ in. Hg} \xrightarrow[p]{}$$

Note that temperature must be expressed as an absolute temperature in the ideal gas equation of state.

The percent change in density is given by

$$\frac{\rho - \rho_0}{\rho_0} = \frac{\rho}{\rho_0} - 1 = \frac{p}{p_0} \frac{T_0}{T} - 1 = \frac{0.830}{0.967} - 1 = -0.142 \quad \text{or} \quad -14.2\% \xrightarrow[\rho_0]{\frac{\Delta\rho}{\rho_0}}$$

(b) For ρ assumed constant ($= \rho_0$),

$$p = p_0 - \rho_0 g(z - z_0) = p_0 - \frac{p_0 g(z - z_0)}{RT_0} = p_0 \left[1 - \frac{g(z - z_0)}{RT_0} \right]$$

$$p = 20.2 \text{ in. Hg} \quad \text{and} \quad \frac{\Delta\rho}{\rho_0} = 0 \xrightarrow[p, \frac{\Delta\rho}{\rho_0}]{} 0$$

(c) If we assume the temperature is constant, then

$$dp = -\rho g dz = -\frac{p}{RT} g dz$$

and

$$\int_{p_0}^p \frac{dp}{p} = - \int_{z_0}^z \frac{g}{RT} dz$$

$$p = p_0 \exp \left[\frac{-g(z-z_0)}{RT} \right]$$

For $T = \text{constant} = T_0$,

$$p = 20.6 \text{ in. Hg} \quad \text{and} \quad \frac{\Delta\rho}{\rho_0} = -16.9\% \quad \xrightarrow{p, \frac{\Delta\rho}{\rho_0}}$$

(d) For an adiabatic atmosphere $p/\rho^k = \text{constant}$,

$$p = p_0 \left(\frac{T}{T_0} \right)^{k/k-1} = 22.0 \text{ in. Hg} \quad \text{and} \quad \frac{\Delta\rho}{\rho_0} = -8.2\% \quad \xrightarrow{p, \frac{\Delta\rho}{\rho_0}}$$

We note that over the modest change in elevation the predicted pressure is not strongly dependent on the assumed property variation; values calculated under four different assumptions vary by a maximum of approximately 9 percent. There is considerably greater variation in the predicted percent change in density. The assumption of a linear temperature variation with altitude is the most reasonable assumption.

This problem shows use of the ideal gas equation with the basic pressure-height relation to obtain the change in pressure with height in the atmosphere under various atmospheric assumptions.

3.4 Hydrostatic Force on Submerged Surfaces

Now that we have determined how the pressure varies in a static fluid, we can examine the force on a surface submerged in a liquid.

In order to determine completely the resultant force acting on a submerged surface, we must specify:

- 1 The magnitude of the force.
- 2 The direction of the force.
- 3 The line of action of the force.

We shall consider both plane and curved submerged surfaces.

Hydrostatic Force on a Plane Submerged Surface

A plane submerged surface, on whose upper face we wish to determine the resultant hydrostatic force, is shown in Fig. 3.5. The coordinates are important and have been chosen so that the surface lies in the xy plane, and the origin O is located at the intersection of the plane surface (or its extension) and the free surface. As well as the magnitude of the force F_R , we wish to locate the point (with coordinates x', y') through which it acts on the surface.

Since there are no shear stresses in a static fluid, the hydrostatic force on any element of the surface acts normal to the surface. The pressure force acting on an element $dA = dx dy$ of the upper surface is given by

$$dF = p dA$$

The *resultant* force acting on the surface is found by summing the contributions of the infinitesimal forces over the entire area.

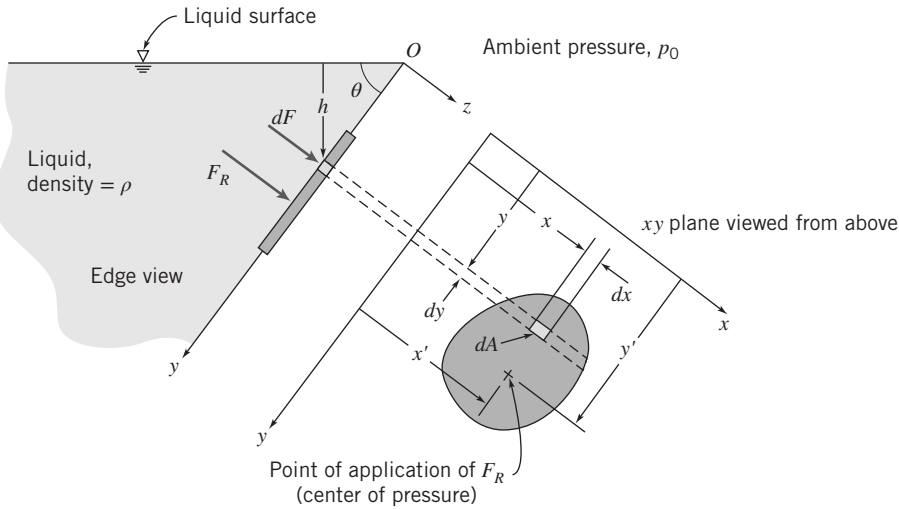


Fig. 3.5 Plane submerged surface.

Usually when we sum forces we must do so in a vectorial sense. However, in this case all of the infinitesimal forces are perpendicular to the plane, and hence so is the resultant force. Its magnitude is given by

$$F_R = \int_A p \, dA \quad (3.10a)$$

In order to evaluate the integral in Eq. 3.10a, both the pressure, p , and the element of area, dA , must be expressed in terms of the same variables.

We can use Eq. 3.7 to express the pressure p at depth h in the liquid as

$$p = p_0 + \rho gh$$

In this expression p_0 is the pressure at the free surface ($h=0$).

In addition, we have, from the system geometry, $h=y \sin \theta$. Using this expression and the above expression for pressure in Eq. 3.10a,

$$\begin{aligned} F_R &= \int_A p \, dA = \int_A (p_0 + \rho gh) \, dA = \int_A (p_0 + \rho gy \sin \theta) \, dA \\ F_R &= p_0 \int_A dA + \rho g \sin \theta \int_A y \, dA = p_0 A + \rho g \sin \theta \int_A y \, dA \end{aligned}$$

The integral is the first moment of the surface area about the x axis, which may be written

$$\int_A y \, dA = y_c A$$

where y_c is the y coordinate of the *centroid* of the area, A . Thus,

$$F_R = p_0 A + \rho g \sin \theta y_c A = (p_0 + \rho g h_c) A$$

or

$$F_R = p_c A \quad (3.10b)$$

where p_c is the absolute pressure in the liquid at the location of the centroid of area A . Equation 3.10b computes the resultant force due to the liquid, including the effect of the ambient pressure p_0 , on one

side of a submerged plane surface. It does not take into account whatever pressure or force distribution may be on the other side of the surface. However, if we have the *same* pressure, p_0 , on this side as we do at the free surface of the liquid, as shown in Fig. 3.6, its effect on F_R cancels out, and if we wish to obtain the *net* force on the surface we can use Eq. 3.10b with p_c expressed as a gage rather than absolute pressure.

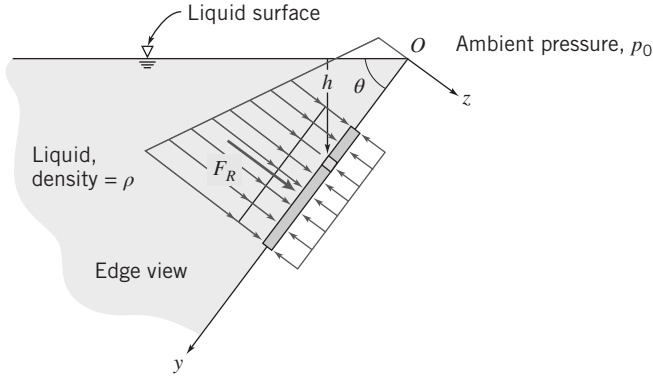


Fig. 3.6 Pressure distribution on plane submerged surface.

In computing F_R we can use either the integral of Eq. 3.10a or the resulting Eq. 3.10b. It is important to note that even though the force can be computed using the pressure at the center of the plate, this is *not* the point through which the force acts.

Our next task is to determine (x', y') , the location of the resultant force. Let's first obtain y' by recognizing that the moment of the resultant force about the x axis must be equal to the moment due to the distributed pressure force. Taking the sum (i.e., integral) of the moments of the infinitesimal forces dF about the x axis we obtain

$$y'F_R = \int_A yp \, dA \quad (3.11a)$$

We can integrate by expressing p as a function of y as before:

$$\begin{aligned} y'F_R &= \int_A yp \, dA = \int_A y(p_0 + \rho gh) \, dA = \int_A (p_0 y + \rho gy^2 \sin \theta) \, dA \\ &= p_0 \int_A y \, dA + \rho g \sin \theta \int_A y^2 \, dA \end{aligned}$$

The first integral is our familiar $y_c A$. The second integral, $\int_A y^2 \, dA$, is the second moment of area about the x axis, I_{xx} . We can use the parallel axis theorem, $I_{xx} = I_{\hat{x}\hat{x}} + Ay_c^2$, to replace I_{xx} with the standard second moment of area, about the centroidal \hat{x} axis. Using all of these, we find

$$\begin{aligned} y'F_R &= p_0 y_c A + \rho g \sin \theta (I_{\hat{x}\hat{x}} + Ay_c^2) = y_c (p_0 + \rho gy_c \sin \theta) A + \rho g \sin \theta I_{\hat{x}\hat{x}} \\ &= y_c (p_0 + \rho gh_c) A + \rho g \sin \theta I_{\hat{x}\hat{x}} = y_c F_R + \rho g \sin \theta I_{\hat{x}\hat{x}} \end{aligned}$$

Finally, we obtain for y' :

$$y' = y_c + \frac{\rho g \sin \theta I_{\hat{x}\hat{x}}}{F_R} \quad (3.11b)$$

Equation 3.11b is convenient for computing the location y' of the force on the submerged side of the surface when we include the ambient pressure p_0 . If we have the same ambient pressure acting on the other side of the surface we can use Eq. 3.10b with p_0 neglected to compute the net force,

$$F_R = p_{c_{\text{gage}}} A = \rho gh_c A = \rho gy_c \sin \theta A$$

and Eq. 3.11b becomes for this case

$$y' = y_c + \frac{I_{\hat{x}\hat{y}}}{Ay_c} \quad (3.11c)$$

Equation 3.11a is the integral equation for computing the location y' of the resultant force, Eq. 3.11b is a useful algebraic form for computing y' when we are interested in the resultant force on the submerged side of the surface, and Eq. 3.11c is for computing y' when we are interested in the net force for the case when the same p_0 acts at the free surface and on the other side of the submerged surface. For problems that have a pressure on the other side that is *not* p_0 , we can either analyze each side of the surface separately or reduce the two pressure distributions to one net pressure distribution, in effect creating a system to be solved using Eq. 3.10b with p_c expressed as a gage pressure.

Note that in any event, $y' > y_c$; the location of the force is always below the level of the plate centroid. This makes sense because, as Fig. 3.6 shows, the pressures will always be larger on the lower regions, moving the resultant force down the plate.

A similar analysis can be done to compute x' , the x location of the force on the plate. Taking the sum of the moments of the infinitesimal forces dF about the y axis we obtain

$$x'F_R = \int_A x p dA \quad (3.12a)$$

We can express p as a function of y as before:

$$\begin{aligned} x'F_R &= \int_A xp dA = \int_A x(p_0 + \rho gh) dA = \int_A (p_0x + \rho gxy \sin \theta) dA \\ &= p_0 \int_A x dA + \rho g \sin \theta \int_A xy dA \end{aligned}$$

The first integral is $x_c A$, where x_c is the distance of the centroid from y axis. The second integral is $\int_A xy dA = I_{xy}$. Using the parallel axis theorem, $I_{xy} = I_{\hat{x}\hat{y}} + Ax_c y_c$, we find

$$\begin{aligned} x'F_R &= p_0x_c A + \rho g \sin \theta(I_{\hat{x}\hat{y}} + Ax_c y_c) = x_c(p_0 + \rho gy_c \sin \theta)A + \rho g \sin \theta I_{\hat{x}\hat{y}} \\ &= x_c(p_0 + \rho g h_c)A + \rho g \sin \theta I_{\hat{x}\hat{y}} = x_c F_R + \rho g \sin \theta I_{\hat{x}\hat{y}} \end{aligned}$$

Finally, we obtain for x' :

$$x' = x_c + \frac{\rho g \sin \theta I_{\hat{x}\hat{y}}}{F_R} \quad (3.12b)$$

Equation 3.12b is convenient for computing x' when we include the ambient pressure p_0 . If we have ambient pressure also acting on the other side of the surface we can again use Eq. 3.10b with p_0 neglected to compute the net force and Eq. 3.12b becomes for this case

$$x' = x_c + \frac{I_{\hat{x}\hat{y}}}{Ay_c} \quad (3.12c)$$

Equation 3.12a is the integral equation for computing the location x' of the resultant force. Equation 3.12b can be used for computations when we are interested in the force on the submerged side only and Eq. 3.12c is useful when we have p_0 on the other side of the surface and we are interested in the net force.

In summary, Eqs. 3.10a through 3.12a constitute a complete set of equations for computing the magnitude and location of the force due to hydrostatic pressure on any submerged plane surface. The direction of the force will always be perpendicular to the plane.

We can now consider several examples using these equations. In Example 3.5 we use both the integral and algebraic sets of equations, and in Example 3.6 we use only the algebraic set.

Example 3.5 RESULTANT FORCE ON INCLINED PLANE SUBMERGED SURFACE

The inclined surface shown, hinged along edge A, is 5 m wide. Determine the resultant force, F_R , of the water and the air on the inclined surface.

Given: Rectangular gate, hinged along A, $w = 5 \text{ m}$.

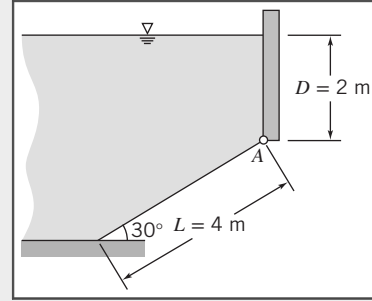
Find: Resultant force, F_R , of the water and the air on the gate.

Solution: In order to completely determine F_R , we need to find (a) the magnitude and (b) the line of action of the force (the direction of the force is perpendicular to the surface). We will solve this problem by using (i) direct integration and (ii) the algebraic equations.

Direct Integration

Governing equations:

$$p = p_0 + \rho gh \quad F_R = \int_A p dA \quad \eta' F_R = \int_A \eta p dA \quad x' F_R = \int_A x p dA$$

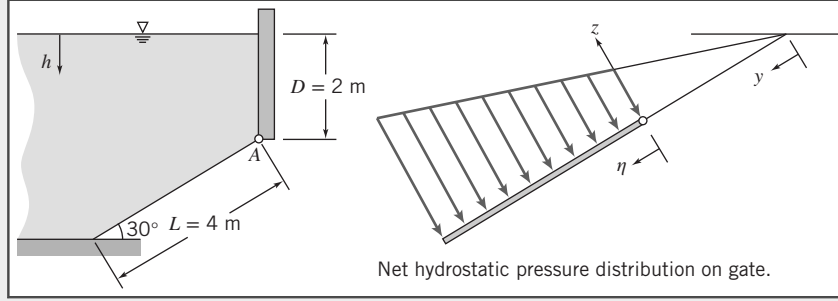


Because atmospheric pressure p_0 acts on both sides of the plate its effect cancels, and we can work in gage pressures ($p = \rho gh$). In addition, while we *could* integrate using the y variable, it will be more convenient here to define a variable η , as shown in the figure.

Using η to obtain expressions for h and dA , then

$$h = D + \eta \sin 30^\circ \quad \text{and} \quad dA = w d\eta$$

Applying these to the governing equation for the resultant force,



$$\begin{aligned} F_R &= \int_A p dA = \int_0^L \rho g(D + \eta \sin 30^\circ)w d\eta \\ &= \rho gw \left[D\eta + \frac{\eta^2}{2} \sin 30^\circ \right]_0^L = \rho gw \left[DL + \frac{L^2}{2} \sin 30^\circ \right] \\ &= 999 \frac{\text{kg}}{\text{m}^3} \times 9.81 \frac{\text{m}}{\text{s}^2} \times 5 \text{m} \left[2 \text{ m} \times 4 \text{ m} + \frac{16 \text{ m}^2}{2} \times \frac{1}{2} \right] \frac{\text{N} \cdot \text{s}^2}{\text{kg} \cdot \text{m}} \\ F_R &= 588 \text{ kN} \end{aligned}$$

For the location of the force we compute η' (the distance from the top edge of the plate),

$$\eta' F_R = \int_A \eta p dA$$

Then

$$\begin{aligned} \eta' &= \frac{1}{F_R} \int_A \eta p dA = \frac{1}{F_R} \int_0^L \eta \rho gw d\eta = \frac{\rho gw}{F_R} \int_0^L \eta (D + \eta \sin 30^\circ) d\eta \\ &= \frac{\rho gw}{F_R} \left[\frac{D\eta^2}{2} + \frac{\eta^3}{3} \sin 30^\circ \right]_0^L = \frac{\rho gw}{F_R} \left[\frac{DL^2}{2} + \frac{L^3}{3} \sin 30^\circ \right] \\ &= 999 \frac{\text{kg}}{\text{m}^3} \times 9.81 \frac{\text{m}}{\text{s}^2} \times \frac{5 \text{ m}}{5.88 \times 10^5 \text{ N}} \left[\frac{2 \text{ m} \times 16 \text{ m}^2}{2} + \frac{64 \text{ m}^3}{3} \times \frac{1}{2} \right] \frac{\text{N} \cdot \text{s}^2}{\text{kg} \cdot \text{m}} \\ \eta' &= 2.22 \text{ m} \quad \text{and} \quad y' = \frac{D}{\sin 30^\circ} + \eta' = \frac{2 \text{ m}}{\sin 30^\circ} + 2.22 \text{ m} = 6.22 \text{ m} \end{aligned}$$

Also, from consideration of moments about the y axis through edge A ,

$$x' = \frac{1}{F_R} \int_A xp \, dA$$

In calculating the moment of the distributed force (right side), recall, from your earlier courses in statics, that the centroid of the area element must be used for x . Since the area element is of constant width, then $x = w/2$, and

$$x' = \frac{1}{F_R} \int_A \frac{w}{2} p \, dA = \frac{w}{2F_R} \int_A p \, dA = \frac{w}{2} = 2.5 \text{ m} \quad \xleftarrow{x'}$$

Algebraic Equations

In using the algebraic equations we need to take care in selecting the appropriate set. In this problem we have $p_0 = p_{\text{atm}}$ on both sides of the plate, so Eq. 3.10b with p_c as a gage pressure is used for the net force:

$$\begin{aligned} F_R &= p_c A = \rho g h_i A = \rho g \left(D + \frac{L}{2} \sin 30^\circ \right) L w \\ F_R &= \rho g w \left[DL + \frac{L^2}{2} \sin 30^\circ \right] \end{aligned}$$

This is the same expression as was obtained by direct integration.

The y coordinate of the center of pressure is given by Eq. 3.11c:

$$y' = y_c + \frac{I_{\hat{x}\hat{x}}}{Ay_c} \quad (3.11c)$$

For the inclined rectangular gate

$$\begin{aligned} y_c &= \frac{D}{\sin 30^\circ} + \frac{L}{2} = \frac{2 \text{ m}}{\sin 30^\circ} + \frac{4 \text{ m}}{2} = 6 \text{ m} \\ A &= Lw = 4 \text{ m} \times 5 \text{ m} = 20 \text{ m}^2 \\ I_{\hat{x}\hat{x}} &= \frac{1}{12} w L^3 = \frac{1}{12} \times 5 \text{ m} \times (4 \text{ m})^3 = 26.7 \text{ m}^2 \\ y' &= y_c + \frac{I_{\hat{x}\hat{x}}}{Ay_c} = 6 \text{ m} + 26.7 \text{ m}^4 \times \frac{1}{20 \text{ m}^2} \times \frac{1}{6 \text{ m}^2} = 6.22 \text{ m} \quad \xleftarrow{y'} \end{aligned}$$

The x coordinate of the center of pressure is given by Eq. 3.12c:

$$x' = x_c + \frac{I_{\hat{x}\hat{y}}}{Ay_c} \quad (3.12c)$$

For the rectangular gate $I_{\hat{x}\hat{y}} = 0$ and $x' = x_c = 2.5 \text{ m}$. $\xleftarrow{x'}$

This problem shows:

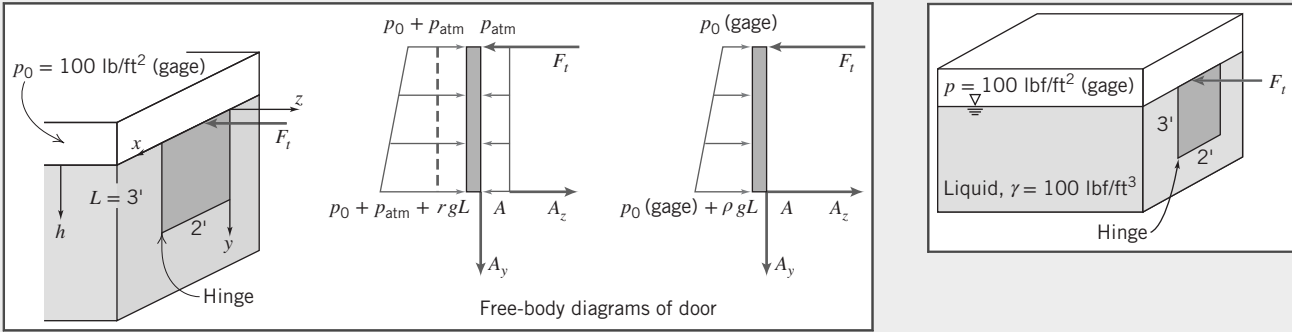
- Use of integral and algebraic equations.
- Use of the algebraic equations for computing the *net* force.

Example 3.6 FORCE ON VERTICAL PLANE SUBMERGED SURFACE WITH NONZERO GAGE PRESSURE AT FREE SURFACE

The door shown in the side of the tank is hinged along its bottom edge. A pressure of 100 psfg is applied to the liquid free surface. Find the force, F_t , required to keep the door closed.

Given: Door as shown in the figure.

Find: Force required to keep door shut.



Solution: This problem requires a free-body diagram (FBD) of the door. The pressure distributions on the inside and outside of the door will lead to a net force and its location that will be included in the FBD. We need to be careful in choosing the equations for computing the resultant force and its location. We can either use absolute pressures (as on the left FBD) and compute two forces (one on each side) or gage pressures and compute one force (as on the right FBD). For simplicity we will use gage pressures. The right-hand FBD makes clear we should use Eqs. 3.2 and 3.11b, which were derived for problems in which we wish to include the effects of an ambient pressure (p_0), or in other words, for problems when we have a nonzero gage pressure at the free surface. The components of force due to the hinge are A_y and A_z . The force F_t can be found by taking moments about A (the hinge).

Governing equations:

$$F_R = p_c A \quad y' = y_c + \frac{\rho g \sin \theta I_{\hat{x}\hat{x}}}{F_R} \quad \sum M_A = 0$$

The resultant force and its location are

$$F_R = (p_0 + \rho g h_c) A = \left(p_0 + \gamma \frac{L}{2} \right) b L \quad (1)$$

and

$$y' = y_c + \frac{\rho g \sin 90^\circ I_{\hat{x}\hat{x}}}{F_R} = \frac{L}{2} + \frac{\gamma b L^3 / 12}{\left(p_0 + \gamma \frac{L}{2} \right) b L} = \frac{L}{2} + \frac{\gamma L^2 / 12}{\left(p_0 + \gamma \frac{L}{2} \right)} \quad (2)$$

Taking moments about point A

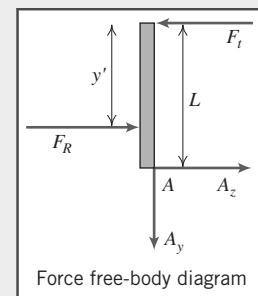
$$\sum M_A = F_t L - F_R (L - y') = 0 \quad \text{or} \quad F_t = F_R \left(1 - \frac{y'}{L} \right)$$

Using Eqs. 1 and 2 in this equation we find

$$F_t = \left(p_0 + \gamma \frac{L}{2} \right) b L \left[1 - \frac{1}{2} - \frac{\gamma L^2 / 12}{\left(p_0 + \gamma \frac{L}{2} \right)} \right]$$

$$\begin{aligned} F_t &= \left(p_0 + \gamma \frac{L}{2} \right) \frac{b L}{2} + \gamma \frac{b L^2}{12} = \frac{p_0 b L}{2} + \frac{\gamma b L^2}{6} \\ &= 100 \frac{\text{lbf}}{\text{ft}^2} \times 2 \text{ ft} \times 3 \text{ ft} \times \frac{1}{2} + 100 \frac{\text{lbf}}{\text{ft}^3} \times 2 \text{ ft} \times 9 \text{ ft}^2 \times \frac{1}{6} \end{aligned} \quad (3)$$

$$F_t = 600 \text{ lbf} \xrightarrow{F_t}$$



We could have solved this problem by considering the two separate pressure distributions on each side of the door, leading to two resultant forces and their locations. Summing moments about point A with these forces would also have yielded the same value for F_t . Note also that Eq. 3 could have been obtained directly without separately finding F_R and y' by using a direct integration approach:

$$\sum M_A = F_t L - \int_A y p dA = 0$$

This problem shows:

- Use of algebraic equations for nonzero gage pressure at the liquid free surface.
- Use of the moment equation from statics for computing the required applied force.

Hydrostatic Force on a Curved Submerged Surface

For curved surfaces, we will once again derive expressions for the resultant force by integrating the pressure distribution over the surface. However, unlike for the plane surface, we have a more complicated problem. The pressure force is normal to the surface at each point, but now the infinitesimal area elements point in varying directions because of the surface curvature. This means that instead of integrating over an element dA we need to integrate over vector element $d\vec{A}$. This will initially lead to a more complicated analysis, but we will see that a simple solution technique will be developed.

Consider the curved surface shown in Fig. 3.7. The pressure force acting on the element of area, $d\vec{A}$, is given by

$$d\vec{F} = -p d\vec{A}$$

where the minus sign indicates that the force acts on the area, in the direction opposite to the area normal. The resultant force is given by

$$\vec{F}_R = - \int_A p d\vec{A} \quad (3.13)$$

We can write

$$\vec{F}_R = \hat{i} F_{R_x} + \hat{j} F_{R_y} + \hat{k} F_{R_z}$$

where F_{R_x} , F_{R_y} , and F_{R_z} are the components of \vec{F}_R in the positive x , y , and z directions, respectively.

To evaluate the component of the force in a given direction, we take the dot product of the force with the unit vector in the given direction. For example, taking the dot product of each side of Eq. 3.13 with unit vector \hat{i} gives

$$F_{R_x} = \vec{F}_R \cdot \hat{i} = \int d\vec{F} \cdot \hat{i} = - \int_A p d\vec{A} \cdot \hat{i} = - \int_{A_x} p dA_x$$

where dA_x is the projection of $d\vec{A}$ on a plane perpendicular to the x axis (see Fig. 3.7), and the minus sign indicates that the x component of the resultant force is in the negative x direction.

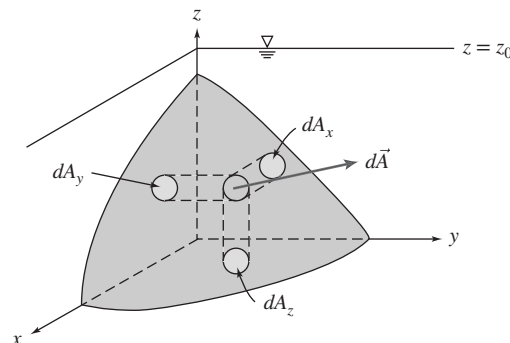


Fig. 3.7 Curved submerged surface.

Since, in any problem, the direction of the force component can be determined by inspection, the use of vectors is not necessary. In general, the magnitude of the component of the resultant force in the l direction is given by

$$F_{R_l} = \int_{A_l} p dA_l \quad (3.14)$$

where dA_l is the projection of the area element dA on a plane perpendicular to the l direction. The line of action of each component of the resultant force is found by recognizing that the moment of the resultant force component about a given axis must be equal to the moment of the corresponding distributed force component about the same axis.

Equation 3.14 can be used for the horizontal forces F_{R_x} and F_{R_y} . We have the interesting result that *the horizontal force and its location are the same as for an imaginary vertical plane surface of the same projected area*. This is illustrated in Fig. 3.8, where we have called the horizontal force F_H .

Figure 3.8 also illustrates how we can compute the vertical component of force. With atmospheric pressure at the free surface and on the other side of the curved surface *the net vertical force will be equal to the weight of fluid directly above the surface*. This can be seen by applying Eq. 3.14 to determine the magnitude of the vertical component of the resultant force, obtaining

$$F_{R_z} = F_V = \int p dA_z$$

Since $p = \rho gh$,

$$F_V = \int \rho gh dA_z = \int \rho g dV$$

where $\rho gh dA_z = \rho g dV$ is the weight of a differential cylinder of liquid above the element of surface area, dA_z , extending a distance h from the curved surface to the free surface. The vertical component of the resultant force is obtained by integrating over the entire submerged surface. Thus

$$F_V = \int \rho gh dA_z = \int \rho g dV = \rho g V$$

In summary, for a curved surface we can use two simple formulas for computing the horizontal and vertical force components due to the fluid only

$$F_H = p_c A \quad \text{and} \quad F_V = \rho g V \quad (3.15)$$

where p_c and A are the pressure at the center and the area, respectively, of a vertical plane surface of the same projected area, and V is the volume of fluid above the curved surface.

We have shown that the resultant hydrostatic force on a curved submerged surface is specified in terms of its components. We recall from our study of statics that the resultant of any force system can be represented by a force-couple system, i.e., the resultant force applied at a point and a couple about that point. If the force and the couple vectors are orthogonal, as is the case for a two-dimensional curved surface, the resultant can be represented as a pure force with a unique line of action.

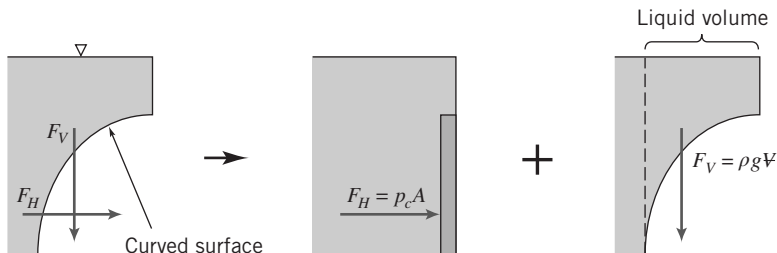


Fig. 3.8 Forces on curved submerged surface.

Example 3.7 FORCE COMPONENTS ON A CURVED SUBMERGED SURFACE

The gate shown is hinged at O and has constant width, $w = 5 \text{ m}$. The equation of the surface is $x = y^2/a$, where $a = 4 \text{ m}$. The depth of water to the right of the gate is $D = 4 \text{ m}$. Find the magnitude of the force, F_a , applied as shown, required to maintain the gate in equilibrium if the weight of the gate is neglected.

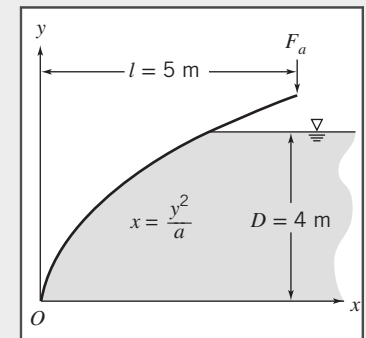
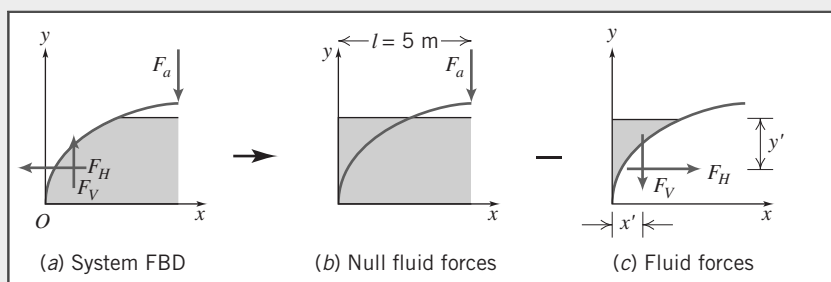
Given: Gate of constant width, $w = 5 \text{ m}$.

Equation of surface in xy plane is $x = y^2/a$, where $a = 4 \text{ m}$.

Water stands at depth $D = 4 \text{ m}$ to the right of the gate.

Force F_a is applied as shown, and weight of gate is to be neglected. (Note that for simplicity we do not show the reactions at O .)

Find: Force F_a required to maintain the gate in equilibrium.



Solution: We will take moments about point O after finding the magnitudes and locations of the horizontal and vertical forces due to the water. The free body diagram (FBD) of the system is shown above in part (a). In order to compute F_V , the vertical component of the fluid force, we imagine having a system with water on both sides of the gate (with null effect), minus a system with water directly above the gate (which generates fluid forces). This logic is demonstrated above: the system FBD(a) = the null FBD(b) – the fluid forces FBD(c). Thus the vertical and horizontal fluid forces on the system, FBD(a), are equal and opposite to those on FBD(c). In summary, the magnitude and location of the vertical fluid force F_V are given by the weight and location of the centroid of the fluid “above” the gate; the magnitude and location of the horizontal fluid force F_H are given by the magnitude and location of the force on an equivalent vertical flat plate.

Governing equations:

$$F_H = p_c A \quad y' = y_c + \frac{I_{\hat{x}\hat{x}}}{Ay_c} \quad F_V = \rho g V \quad x' = \text{water center of gravity}$$

For F_H , the centroid, area, and second moment of the equivalent vertical flat plate are, respectively, $y_c = h_c = D/2$, $A = Dw$, and $I_{\hat{x}\hat{x}} = wD^3/12$.

$$\begin{aligned} F_H &= p_c A = \rho g h_c A \\ &= \rho g \frac{D}{2} Dw = \rho g \frac{D^2}{2} w = 999 \frac{\text{kg}}{\text{m}^3} \times 9.81 \frac{\text{m}}{\text{s}^2} \times \frac{(4 \text{ m}^2)}{2} \times 5 \text{ m} \times \frac{\text{N} \cdot \text{s}^2}{\text{kg} \cdot \text{m}} \\ F_H &= 392 \text{ kN} \end{aligned} \quad (1)$$

and

$$\begin{aligned} y' &= y_c + \frac{I_{\hat{x}\hat{x}}}{Ay_c} \\ &= \frac{D}{2} + \frac{wD^3/12}{wDD/2} = \frac{D}{2} + \frac{D}{6} \\ y' &= \frac{2}{3}D = \frac{2}{3} \times 4 \text{ m} = 2.67 \text{ m} \end{aligned} \quad (2)$$

For F_V , we need to compute the weight of water “above” the gate. To do this we define a differential column of volume $(D-y)w dx$ and integrate

$$\begin{aligned} F_V &= \rho g V = \rho g \int_0^{D^{2/a}} (D-y)w dx = \rho gw \int_0^{D^{2/a}} (D - \sqrt{ax^{1/2}}) dx \\ &= \rho gw \left[Dx - \frac{2}{3} \sqrt{ax^{3/2}} \right]_0^{D^{2/a}} = \rho gw \left[\frac{D^3}{a} - \frac{2}{3} \sqrt{a} \frac{D^3}{a^{3/2}} \right] = \frac{\rho gw D^3}{3a} \\ F_V &= 999 \frac{\text{kg}}{\text{m}^3} \times 9.81 \frac{\text{m}}{\text{s}^2} \times 5 \text{ m} \times \frac{(4)^3 \text{m}^3}{3} \times \frac{1}{4 \text{ m}} \times \frac{\text{N} \cdot \text{s}^2}{\text{kg} \cdot \text{m}} = 261 \text{ kN} \end{aligned} \quad (3)$$

The location x' of this force is given by the location of the center of gravity of the water “above” the gate. We recall from statics that this can be obtained by using the notion that the moment of F_V and the moment of the sum of the differential weights about the y axis must be equal, so

$$\begin{aligned} x'F_V &= \rho g \int_0^{D^{2/a}} x(D-y)w dx = \rho gw \int_0^{D^{2/a}} (D - \sqrt{ax^{3/2}}) dx \\ x'F_V &= \rho gw \left[\frac{D}{2}x^2 - \frac{2}{5} \sqrt{ax^{5/2}} \right]_0^{D^{2/a}} = \rho gw \left[\frac{D^5}{2a^2} - \frac{2}{5} \sqrt{a} \frac{D^5}{a^{5/2}} \right] = \frac{\rho gw D^5}{10a^2} \\ x' &= \frac{\rho gw D^5}{10a^2 F_V} = \frac{3D^2}{10a} = \frac{3}{10} \times \frac{(4)^2 \text{m}^2}{4 \text{ m}} = 1.2 \text{ m} \end{aligned} \quad (4)$$

Now that we have determined the fluid forces, we can finally take moments about O (taking care to use the appropriate signs), using the results of Eqs. 1 through 4

$$\begin{aligned} \sum M_O &= -lF_a + x'F_V + (D-y')F_H = 0 \\ F_a &= \frac{1}{l}[x'F_V + (D-y')F_H] \\ &= \frac{1}{5 \text{ m}}[1.2 \text{ m} \times 261 \text{ kN} + (4-2.67)\text{m} \times 392 \text{ kN}] \\ F_a &= 167 \text{ kN} \end{aligned}$$

This problem shows:

- Use of vertical flat plate equations for the horizontal force, and fluid weight equations for the vertical force, on a curved surface.
- The use of “thought experiments” to convert a problem with fluid below a curved surface into an equivalent problem with fluid above.

3.5 Buoyancy and Stability

If an object is immersed in a liquid, or floating on its surface, the net vertical force acting on it due to liquid pressure is termed *buoyancy*. Consider an object totally immersed in static liquid, as shown in Fig. 3.9.

The vertical force on the body due to hydrostatic pressure may be found most easily by considering cylindrical volume elements similar to the one shown in Fig. 3.9.

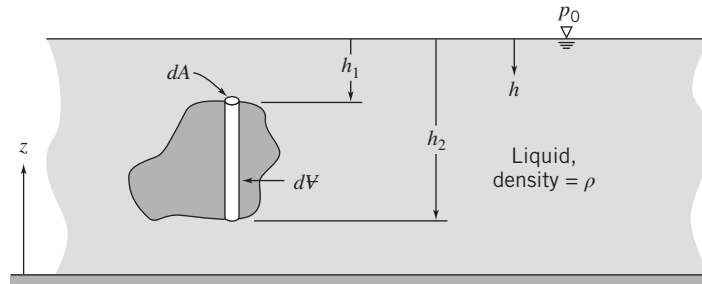


Fig. 3.9 Immersed body in static liquid.

We recall that we can use Eq. 3.7 for computing the pressure p at depth h in a liquid,

$$p = p_0 + \rho gh$$

The net vertical pressure force on the element is then

$$dF_z = (p_0 + \rho gh_2)dA - (p_0 + \rho gh_1)dA = \rho g(h_2 - h_1)dA$$

But $(h_2 - h_1)dA = dV$, the volume of the element. Thus

$$F_z = \int dF_z = \int_V \rho g dV = \rho g V$$

where V is the volume of the object. Hence we conclude that for a submerged body *the buoyancy force of the fluid is equal to the weight of displaced fluid*,

$$F_{\text{buoyancy}} = \rho g V \quad (3.16)$$

This relation reportedly was used by Archimedes in 220 b.c. to determine the gold content in the crown of King Hiero II. Consequently, it is often called “Archimedes’ Principle.” In more current technical applications, Eq. 3.16 is used to design displacement vessels, flotation gear, and submersibles [1].

The submerged object need not be solid. Hydrogen bubbles, used to visualize streaklines and timelines in water, are positively buoyant. They rise slowly as they are swept along by the flow. Conversely, water droplets in oil are negatively buoyant and tend to sink.

Airships and balloons are termed “lighter-than-air” craft. The density of an ideal gas is proportional to molecular weight, so hydrogen and helium are less dense than air at the same temperature and pressure. Hydrogen ($M_m = 2$) is less dense than helium ($M_m = 4$), but extremely flammable, whereas helium is inert. Hydrogen has not been used commercially since the disastrous explosion of the German passenger airship *Hindenburg* in 1937. The use of buoyancy force to generate lift is illustrated in Example 3.8.

Example 3.8 BUOYANCY FORCE IN A HOT AIR BALLOON

A hot air balloon (approximated as a sphere of diameter 50 ft) is to lift a basket load of 600 lbf. To what temperature must the air be heated in order to achieve liftoff?

Given: Atmosphere at STP, diameter of balloon $d = 50$ ft, and load $W_{\text{load}} = 600$ lbf.

Find: The hot air temperature to attain liftoff.

Solution: Apply the buoyancy equation to determine the lift generated by atmosphere, and apply the vertical force equilibrium equation to obtain the hot air density. Then use the ideal gas equation to obtain the hot air temperature.

Governing equations:

$$F_{\text{buoyancy}} = \rho g V \quad \sum F_y = 0 \quad p = \rho RT$$

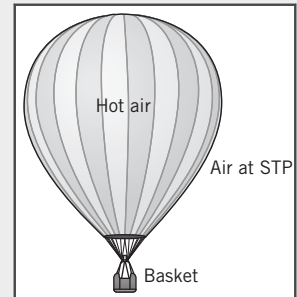
Assumptions:

- 1 Ideal gas.
- 2 Atmospheric pressure throughout.

Summing vertical forces

$$\sum F_y = F_{\text{buoyancy}} - W_{\text{hot air}} - W_{\text{load}} = \rho_{\text{atm}} g V - \rho_{\text{hot air}} g V - W_{\text{load}} = 0$$

Rearranging and solving for $\rho_{\text{hot air}}$ (using data from Appendix A),



$$\begin{aligned}\rho_{\text{hot air}} &= \rho_{\text{atm}} - \frac{W_{\text{load}}}{gV} = \rho_{\text{atm}} - \frac{6W_{\text{load}}}{\pi d^3 g} \\ &= 0.00238 \frac{\text{slug}}{\text{ft}^3} - 6 \times \frac{600 \text{lbf}}{\pi(50)^3 \text{ft}^3} \times \frac{\text{s}^2}{32.2 \text{ft}} \times \frac{\text{slug} \cdot \text{ft}}{\text{s}^2 \cdot \text{lbf}} \\ \rho_{\text{hot air}} &= (0.00238 - 0.000285) \frac{\text{slug}}{\text{ft}^3} = 0.00209 \frac{\text{slug}}{\text{ft}^3}\end{aligned}$$

Finally, to obtain the temperature of this hot air, we can use the ideal gas equation in the following form

$$\frac{P_{\text{hot air}}}{\rho_{\text{hot air}} RT_{\text{hot air}}} = \frac{P_{\text{atm}}}{\rho_{\text{atm}} RT_{\text{atm}}}$$

and with $p_{\text{hot air}} = p_{\text{atm}}$

$$\begin{aligned}T_{\text{hot air}} &= T_{\text{atm}} \frac{\rho_{\text{atm}}}{\rho_{\text{hot air}}} = (460 + 59)^\circ \text{R} \times \frac{0.00238}{0.00209} = 591^\circ \text{R} \\ T_{\text{hot air}} &= 131^\circ \text{F} \leftarrow \qquad \qquad \qquad T_{\text{hot air}}\end{aligned}$$

Notes:

- Absolute pressures and temperatures are always used in the ideal gas equation.
- This problem demonstrates that for lighter-than-air vehicles the buoyancy force exceeds the vehicle weight—that is, the weight of fluid (air) displaced exceeds the vehicle weight.

Equation 3.16 predicts the net vertical pressure force on a body that is totally submerged in a single liquid. In cases of partial immersion, a floating body displaces its own weight of the liquid in which it floats.

The line of action of the buoyancy force, which may be found using the methods of Section 3.4, acts through the centroid of the displaced volume. Since floating bodies are in equilibrium under body and buoyancy forces, the location of the line of action of the buoyancy force determines stability, as shown in Fig. 3.10.

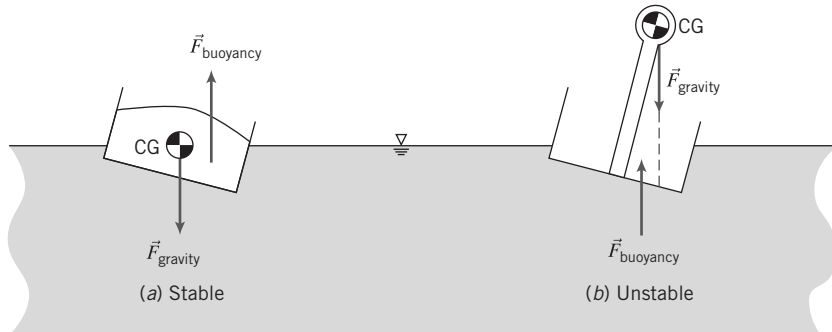


Fig. 3.10 Stability of floating bodies.

The weight of an object acts through its center of gravity, CG. In Fig. 3.10a, the lines of action of the buoyancy and the weight are offset in such a way as to produce a couple that tends to right the craft. In Fig. 3.10b, the couple tends to capsize the craft.

Ballast may be needed to achieve roll stability. Wooden warships carried stone ballast low in the hull to offset the weight of the heavy cannon on upper gun decks. Modern ships can have stability problems as well: overloaded ferry boats have capsized when passengers all gathered on one side of the upper deck, shifting the CG laterally. In stacking containers high on the deck of a container ship, care is needed to avoid raising the center of gravity to a level that may result in the unstable condition depicted in Fig. 3.10b.

For a vessel with a relatively flat bottom, as shown in Fig. 3.10a, the restoring moment increases as roll angle becomes larger. At some angle, typically that at which the edge of the deck goes below water level, the restoring moment peaks and starts to decrease. The moment may become zero at some large roll angle, known as the angle of vanishing stability. The vessel may capsize if the roll exceeds this angle.

The actual shape of the restoring moment curve depends on hull shape. A broad beam gives a large lateral shift in the line of action of the buoyancy force and thus a high restoring moment. High freeboard above the water line increases the angle at which the moment curve peaks, but may make the moment drop rapidly above this angle.

Sailing vessels are subjected to large lateral forces as wind engages the sails and in brisk winds typically operate at a considerable roll angle. The lateral wind force must be counteracted by a heavily weighted keel extended below the hull bottom. In small sailboats, crew members may lean far over the side to add additional restoring moment to prevent capsizing [2].

Within broad limits, the buoyancy of a surface vessel is adjusted automatically as the vessel rides higher or lower in the water. However, craft that operate fully submerged must actively adjust buoyancy and gravity forces to remain neutrally buoyant. For submarines this is accomplished using tanks which are flooded to reduce excess buoyancy or blown out with compressed air to increase buoyancy [1]. Airships may vent gas to descend or drop ballast to rise. Buoyancy of a hot-air balloon is controlled by varying the air temperature within the balloon envelope.

For deep ocean dives, use of compressed air becomes impractical because of the high pressures and a liquid such as gasoline, which is buoyant in seawater, may be used to provide buoyancy. However, because gasoline is more compressible than water, its buoyancy decreases as the dive gets deeper. Therefore it is necessary to carry and drop ballast to achieve positive buoyancy for the return trip to the surface.

The most structurally efficient hull shape for airships and submarines has a circular cross-section. The buoyancy force passes through the center of the circle. Therefore, for roll stability the CG must be located below the hull centerline.

3.6 Fluids in Rigid-Body Motion

There is one category of fluid motion that can be studied using fluid statics ideas: rigid-body motion. This is motion in which the entire fluid moves as if it were a rigid body, individual fluid particles, although they may be in motion, are not deforming. This means that, as in the case of a static fluid, there are no shear stresses. We will consider only constant acceleration (Example 3.9) and constant rotation (Example 3.10) in this section. As in the case of the static fluid, we may apply Newton's second law of motion to determine the pressure field that results from a specified rigid-body motion.

In Section 3.1 we derived an expression for the forces due to pressure and gravity acting on a fluid particle of volume dV . We obtained

$$d\vec{F} = (-\nabla p + \rho\vec{g})dV$$

or

$$\frac{d\vec{F}}{dV} = -\nabla p + \rho\vec{g} \quad (3.2)$$

Newton's second law was written

$$d\vec{F} = \vec{a} dm = \vec{a}\rho dV \quad \text{or} \quad \frac{d\vec{F}}{V} = \rho\vec{a}$$

Substituting from Eq. 3.2, we obtain

$$-\nabla p + \rho\vec{g} = \rho\vec{a} \quad (3.17)$$

If the acceleration \vec{a} is constant, we can combine it with \vec{g} and obtain an effective "acceleration of gravity," $\vec{g}_{eff} = \vec{g} - \vec{a}$, so that Eq. 3.17 has the same form as our basic equation for pressure distribution in a static fluid, Eq. 3.3:

$$-\nabla p + \rho\vec{g}_{eff} = 0 \quad [\text{Compare to } -\nabla p + \rho\vec{g} = 0 \quad (3.3)]$$

This means that we can use the results of previous sections of this chapter as long as we use \vec{g}_{eff} in place of \vec{g} . For example, for a liquid undergoing constant acceleration the pressure increases with depth in

the direction of \vec{g}_{eff} , and the rate of increase of pressure will be given by ρg_{eff} , where g_{eff} is the magnitude of \vec{g}_{eff} . Lines of constant pressure will be perpendicular to the direction of \vec{g}_{eff} . The physical significance of each term in Eq. 3.17 is as follows:

$$\left\{ \begin{array}{l} -\nabla p \\ \text{net pressure force} \\ \text{per unit volume} \\ \text{at a point} \end{array} \right\} + \left\{ \begin{array}{l} \rho \vec{g} \\ \text{body force per} \\ \text{unit volume} \\ \text{at a point} \end{array} \right\} = \left\{ \begin{array}{l} \rho \vec{a} \\ \text{mass per} \\ \text{unit} \\ \text{volume} \end{array} \right\} \times \left\{ \begin{array}{l} \text{acceleration} \\ \text{of fluid} \\ \text{particle} \end{array} \right\}$$

This vector equation consists of three component equations that must be satisfied individually. In rectangular coordinates the component equations are

$$\left. \begin{aligned} -\frac{\partial p}{\partial x} + \rho g_x &= \rho a_x && x \text{ direction} \\ -\frac{\partial p}{\partial y} + \rho g_y &= \rho a_y && y \text{ direction} \\ -\frac{\partial p}{\partial z} + \rho g_z &= \rho a_z && z \text{ direction} \end{aligned} \right\} \quad (3.18)$$

Component equations for other coordinate systems can be written using the appropriate expression for ∇p . In cylindrical coordinates the vector operator, ∇ , is given by

$$\nabla = \hat{e}_r \frac{\partial}{\partial r} + \hat{e}_\theta \frac{1}{r} \frac{\partial}{\partial \theta} + \hat{k} \frac{\partial}{\partial z} \quad (3.19)$$

where \hat{e}_r and \hat{e}_θ are unit vectors in the r and θ directions, respectively. Thus

$$\nabla p = \hat{e}_r \frac{\partial p}{\partial r} + \hat{e}_\theta \frac{1}{r} \frac{\partial p}{\partial \theta} + \hat{k} \frac{\partial p}{\partial z} \quad (3.20)$$

Example 3.9 LIQUID IN RIGID-BODY MOTION WITH LINEAR ACCELERATION

As a result of a promotion, you are transferred from your present location. You must transport a fish tank in the back of your minivan. The tank is 12 in. \times 24 in. \times 12 in. How much water can you leave in the tank and still be reasonably sure that it will not spill over during the trip?

Given: Fish tank 12 in. \times 24 in. \times 12 in. partially filled with water to be transported in an automobile.

Find: Allowable depth of water for reasonable assurance that it will not spill during the trip.

Solution: The first step in the solution is to formulate the problem by translating the general problem into a more specific one.

We recognize that there will be motion of the water surface as a result of the car's traveling over bumps in the road, going around corners, etc. However, we shall assume that the main effect on the water surface is due to linear accelerations (and decelerations) of the car; we shall neglect sloshing.

Thus we have reduced the problem to one of determining the effect of a linear acceleration on the free surface. We have not yet decided on the orientation of the tank relative to the direction of motion. Choosing the x coordinate in the direction of motion, should we align the tank with the long side parallel, or perpendicular, to the direction of motion?

If there will be no relative motion in the water, we must assume we are dealing with a constant acceleration, a_x . What is the shape of the free surface under these conditions?

Let us restate the problem to answer the original questions by idealizing the physical situation to obtain an approximate solution.

Given: Tank partially filled with water (to depth d) subject to constant linear acceleration, a_x . Tank height is 12 in.; length parallel to direction of motion is b . Width perpendicular to direction of motion is c .

- Find:**
- Shape of free surface under constant a_x .
 - Allowable water depth, d , to avoid spilling as a function of a_x and tank orientation.
 - Optimum tank orientation and recommended water depth.

Solution:

Governing equation: $-\nabla p + \rho \vec{g} = \rho \vec{a}$

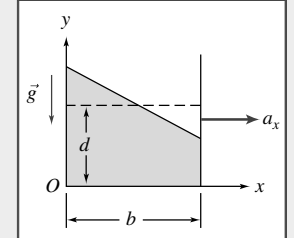
$$-\left(\hat{i}\frac{\partial p}{\partial x} + \hat{j}\frac{\partial p}{\partial y} + \hat{k}\frac{\partial p}{\partial z}\right) + \rho(\hat{i}g_x + \hat{j}g_y + \hat{k}g_z) = \rho(\hat{i}a_x + \hat{j}a_y + \hat{k}a_z)$$

Since p is not a function of z , $\partial p / \partial z = 0$. Also, $g_x = 0$, $g_y = -g$, $g_z = 0$, and $a_y = a_z = 0$.

$$\therefore -\hat{i}\frac{\partial p}{\partial x} - \hat{j}\frac{\partial p}{\partial y} - \hat{j}\rho g = \hat{i}\rho a_x$$

The component equations are:

$$\begin{aligned} \frac{\partial p}{\partial x} &= -\rho a_x \\ \frac{\partial p}{\partial y} &= -\rho g \end{aligned} \quad \left. \begin{array}{l} \text{Recall that a partial} \\ \text{derivative means that} \\ \text{all other independent} \\ \text{variables are held constant} \\ \text{in the differentiation.} \end{array} \right\}$$



The problem now is to find an expression for $p = p(x, y)$. This would enable us to find the equation of the free surface. But perhaps we do not have to do that.

Since the pressure is $p = p(x, y)$, the difference in pressure between two points (x, y) and $(x + dx, y + dy)$ is

$$dp = \frac{\partial p}{\partial x} dx + \frac{\partial p}{\partial y} dy$$

Since the free surface is a line of constant pressure, $p = \text{constant}$ along the free surface, so $dp = 0$ and

$$0 = \frac{\partial p}{\partial x} dx + \frac{\partial p}{\partial y} dy = -\rho a_x dx - \rho g dy$$

Therefore,

$$\left. \frac{dy}{dx} \right|_{\text{free surface}} = -\frac{a_x}{g} \quad \left. \begin{array}{l} \text{The free surface is a plane.} \end{array} \right\}$$

Note that we could have derived this result more directly by converting Eq. 3.17 into an equivalent “acceleration of gravity” problem,

$$-\nabla p + \rho \vec{g}_{eff} = 0$$

where $\vec{g}_{eff} = \vec{g} - \hat{i}a_x = -\hat{i}a_x - \hat{j}g$. Lines of constant pressure (including the free surface) will then be perpendicular to the direction of \vec{g}_{eff} , so that the slope of these lines will be $-1/(g/a_x) = -a_x/g$.

d = original depth

e = height above original depth

b = tank length parallel to direction of motion

$$e = \frac{b}{2} \tan \theta = \frac{b}{2} \left(-\frac{dy}{dx} \right)_{\text{free surface}} = \frac{ba_x}{2g} \quad \left. \begin{array}{l} \text{Only valid when the free surface intersects} \\ \text{the front wall at or above the floor} \end{array} \right\}$$

Since we want e to be smallest for a given a_x , the tank should be aligned so that b is as small as possible. We should align the tank with the long side perpendicular to the direction of motion.

That is, we should choose $b = 12$ in. $\leftarrow \underline{\hspace{1cm}} b$

With $b = 12$ in.,

$$e = 6 \frac{a_x}{g} \text{ in.}$$

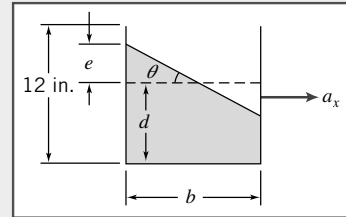
The maximum allowable value of $e = 12 - d$ in. Thus

$$12 - d = 6 \frac{a_x}{g} \quad \text{and} \quad d_{\max} = 12 - 6 \frac{a_x}{g}$$

If the maximum a_x is assumed to be $\frac{2}{3}g$, then allowable d equals 8 in.

To allow a margin of safety, perhaps we should select $d = 6$ in. $\leftarrow \underline{\hspace{1cm}} d$

Recall that a steady acceleration was assumed in this problem. The car would have to be driven *very* carefully and smoothly.



This problem shows that:

- Not all engineering problems are clearly defined, nor do they have unique answers.
- For constant linear acceleration, we effectively have a hydrostatics problem, with "gravity" redefined as the vector result of the acceleration and the actual gravity.

Example 3.10 LIQUID IN RIGID-BODY MOTION WITH CONSTANT ANGULAR SPEED

A cylindrical container, partially filled with liquid, is rotated at a constant angular speed, ω , about its axis as shown in the diagram. After a short time there is no relative motion; the liquid rotates with the cylinder as if the system were a rigid body. Determine the shape of the free surface.

Given: A cylinder of liquid in rigid-body rotation with angular speed ω about its axis.

Find: Shape of the free surface.

Solution:

Governing equation:

$$-\nabla p + \rho \vec{g} = \rho \vec{a}$$

It is convenient to use a cylindrical coordinate system, r, θ, z . Since $g_r = g_\theta = 0$ and $g_z = -g$, then

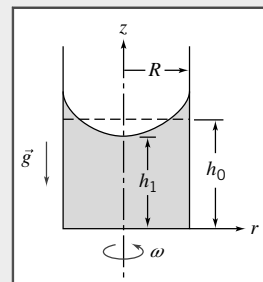
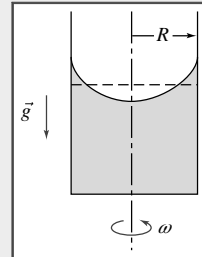
$$-\left(\hat{e}_r \frac{\partial p}{\partial r} + \hat{e}_\theta \frac{1}{r} \frac{\partial p}{\partial \theta} + \hat{k} \frac{\partial p}{\partial z}\right) - \hat{k} \rho g = \rho(\hat{e}_r a_r + \hat{e}_\theta a_\theta + \hat{k} a_z)$$

Also, $a_\theta = a_z = 0$ and $a_r = -\omega^2 r$.

$$\therefore -\left(\hat{e}_r \frac{\partial p}{\partial r} + \hat{e}_\theta \frac{1}{r} \frac{\partial p}{\partial \theta} + \hat{k} \frac{\partial p}{\partial z}\right) = -\hat{e}_r \rho \omega^2 r + \hat{k} \rho g$$

The component equations are:

$$\frac{\partial p}{\partial r} = \rho \omega^2 r \quad \frac{\partial p}{\partial \theta} = 0 \quad \frac{\partial p}{\partial z} = -\rho g$$



From the component equations we see that the pressure is not a function of θ ; it is a function of r and z only.

Since $p = p(r, z)$, the differential change, dp , in pressure between two points with coordinates (r, θ, z) and $(r + dr, \theta, z + dz)$ is given by

$$dp = \left(\frac{\partial p}{\partial r} \right)_z dr + \left(\frac{\partial p}{\partial z} \right)_r dz$$

Then

$$dp = \rho \omega^2 r dr - \rho g dz$$

To obtain the pressure difference between a reference point (r_1, z_1) , where the pressure is p_1 , and the arbitrary point (r, z) , where the pressure is p , we must integrate

$$\begin{aligned} \int_{p_1}^p dp &= \int_{r_1}^r \rho \omega^2 r dr - \int_{z_1}^z \rho g dz \\ p - p_1 &= \frac{\rho \omega^2}{2} (r^2 - r_1^2) - \rho g (z - z_1) \end{aligned}$$

Taking the reference point on the cylinder axis at the free surface gives

$$p_1 = p_{\text{atm}} \quad r_1 = 0 \quad z_1 = h_1$$

Then

$$p - p_{\text{atm}} = \frac{\rho \omega^2 r^2}{2} - \rho g (z - h_1)$$

Since the free surface is a surface of constant pressure ($p = p_{\text{atm}}$), the equation of the free surface is given by

$$0 = \frac{\rho \omega^2 r^2}{2} - \rho g (z - h_1)$$

or

$$z = h_1 + \frac{(\omega r)^2}{2g}$$

The equation of the free surface is a paraboloid of revolution with vertex on the axis at $z = h_1$.

We can solve for the height h_1 under conditions of rotation in terms of the original surface height, h_0 , in the absence of rotation. To do this, we use the fact that the volume of liquid must remain constant. With no rotation

$$V = \pi R^2 h_0$$

With rotation

$$\begin{aligned} V &= \int_0^R \int_0^z 2\pi r dz dr = \int_0^R 2\pi r dr = \int_0^R 2\pi \left(h_1 + \frac{\omega^2 r^2}{2g} \right) r dr \\ V &= 2\pi \left[h_1 \frac{r^2}{2} + \frac{\omega^2 r^4}{8g} \right]_0^R = \pi \left[h_1 R^2 + \frac{\omega^2 R^4}{4g} \right] \end{aligned}$$

Then

$$\pi R^2 h_0 = \pi \left[h_1 R^2 + \frac{\omega^2 R^4}{4g} \right] \quad \text{and} \quad h_1 = h_0 - \frac{(\omega R)^2}{4g}$$

Finally,

$$z = h_0 - \frac{(\omega R)^2}{4g} + \frac{(\omega r)^2}{2g} = h_0 - \frac{(\omega R)^2}{2g} \left[\frac{1}{2} - \left(\frac{r}{R} \right)^2 \right] \xleftarrow{\hspace{1cm}} z(r)$$

Note that the expression for z is valid only for $h_1 > 0$. Hence the maximum value of ω is given by $\omega_{\max} = 2\sqrt{gh_0}/R$.

This problem shows that:

- The effect of centripetal acceleration on the shape of constant pressure lines (isobars).
- Because the hydrostatic pressure variation and variation due to rotation each depend on fluid density, the final free surface shape is independent of fluid density.

3.7 Summary and Useful Equations

In this chapter we have reviewed the basic concepts of fluid statics. This included:

- ✓ Deriving the basic equation of fluid statics in vector form.
- ✓ Applying this equation to compute the pressure variation in a static fluid:
 - Incompressible liquids: pressure increases uniformly with depth.
 - Gases: pressure decreases nonuniformly with elevation (dependent on other thermodynamic properties).
- ✓ Study of:
 - Gage and absolute pressure.
 - Use of manometers and barometers.
- ✓ Analysis of the fluid force magnitude and location on submerged:
 - Plane surfaces.
 - Curved surfaces.
- ✓ Derivation and use of Archimedes' Principle of Buoyancy.
- ✓ Analysis of rigid-body fluid motion.

Note: Most of the equations in the table below have a number of constraints or limitations—*be sure to refer to their page numbers for details!*

Useful Equations

Hydrostatic pressure variation:	$\frac{dp}{dz} = -\rho g \equiv -\gamma$	(3.6)	Page 41
Hydrostatic pressure variation (incompressible fluid):	$p - p_0 = \Delta p = \rho gh$	(3.7)	Page 43
Hydrostatic pressure variation (several incompressible fluids):	$\Delta p = g \sum_i \rho_i h_i$	(3.8)	Page 46
Hydrostatic force on submerged plane (integral form):	$F_R = \int_A p dA$	(3.10a)	Page 51
Hydrostatic force on submerged plane:	$F_R = p_c A$	(3.10b)	Page 51
Location y' of hydrostatic force on submerged plane (integral):	$y' F_R = \int_A y p dA$	(3.11a)	Page 52
Location y' of hydrostatic force on submerged plane (algebraic):	$y' = y_c + \frac{\rho g \sin \theta I_{\hat{x}\hat{x}}}{F_R}$	(3.11b)	Page 52
Location y' of hydrostatic force on submerged plane (p_0 neglected):	$y' = y_c + \frac{I_{\hat{x}\hat{x}}}{A y_c}$	(3.11c)	Page 53
Location x' of hydrostatic force on submerged plane (integral):	$x' F_R = \int_A x p dA$	(3.12a)	Page 53
Location x' of hydrostatic force on submerged plane (algebraic):	$x' = x_c + \frac{\rho g \sin \theta I_{\hat{x}\hat{y}}}{F_R}$	(3.12b)	Page 53
Location x' of hydrostatic force on submerged plane (p_0 neglected):	$x' = x_c + \frac{I_{\hat{x}\hat{y}}}{A y_c}$	(3.12c)	Page 53
Horizontal and vertical hydrostatic forces on curved submerged surface:	$F_H = p_c A$ and $F_V = \rho g V$	(3.15)	Page 58
Buoyancy force on submerged object:	$F_{\text{buoyancy}} = \rho g V$	(3.16)	Page 61

We have now concluded our introduction to the fundamental concepts of fluid mechanics, and the basic concepts of fluid statics. In the next chapter we will begin our study of fluids in motion.

REFERENCES

1. Burcher, R., and L. Rydill, *Concepts in Submarine Design*. Cambridge, UK: Cambridge University Press, 1994.
2. Marchaj, C. A., *Aero-Hydrodynamics of Sailing*, rev. ed. Camden, ME: International Marine Publishing, 1988.
3. The U.S. Standard Atmosphere, Washington, DC: U.S. Government Printing Office, 1976.
4. International Organization for Standardization, *Standard Atmosphere*, ISO 2533:1975, 1975.

Chapter 4 Problems

Basic Laws for a System

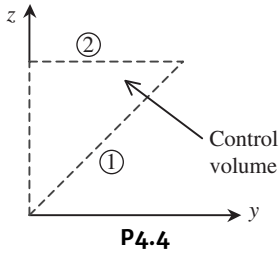
4.1 A hot air balloon with an initial volume of 2600 m^3 rises from sea level to 1000 m elevation. The temperature of the air inside the balloon is 100°C at the start and drops to 90°C at 1000 m. Determine the heat and work transferred between the balloon and the atmosphere. The atmospheric pressure varies linearly with altitude and the average pressure can be used to evaluate the work term.

4.2 A fully loaded Boeing 777-200 jet transport aircraft has a mass of 325,000 kg. The pilot brings the 2 engines to full takeoff thrust of 450 kN each before releasing the brakes. Neglecting aerodynamic and rolling resistance, estimate the minimum runway length and time needed to reach a takeoff speed of 225 km/hr. Assume that engine thrust remains constant during ground roll.

4.3 A block of copper of mass 5 kg is heated to 90°C and then plunged into an insulated container containing 4 L of water at 10°C . Find the final temperature of the system. For copper, the specific heat is $385 \text{ J/kg}\cdot\text{K}$, and for water the specific heat is $4186 \text{ J/kg}\cdot\text{K}$.

Conservation of Mass

SS 4.4 The velocity field in the region shown is given by $\vec{V} = (aj + by\hat{k})$ where $a = 10 \text{ m/s}$ and $b = 5 \text{ s}^{-1}$. For the $1 \text{ m} \times 1 \text{ m}$ triangular control volume (depth $w = 1 \text{ m}$ perpendicular to the diagram), an element of area ① may be represented by $dA_1 = wdz\hat{j} - wdy\hat{k}$ and an element of area ② by $dA_2 = -wdy\hat{k}$.



(a) Find an expression for $\vec{V} \cdot dA_1$.

(b) Evaluate $\int_{A_1} \vec{V} \cdot dA_1$.

(c) Find an expression for $\vec{V} \cdot dA_2$.

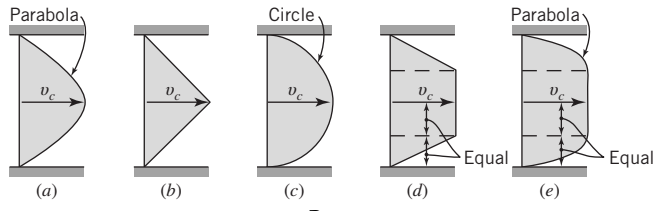
(d) Find an expression for $\vec{V}(\vec{V} \cdot dA_2)$.

(e) Evaluate $\int_{A_2} \vec{V}(\vec{V} \cdot dA_2)$.

4.5 A 0.3 m by 0.5 m rectangular air duct carries a flow of $0.45 \text{ m}^3/\text{s}$ at a density of 2 kg/m^3 . Calculate the mean velocity in the duct. If the duct tapers to 0.15 m by 0.5 m size, determine the mean velocity in this section if the density is 1.5 kg/m^3 in this section.

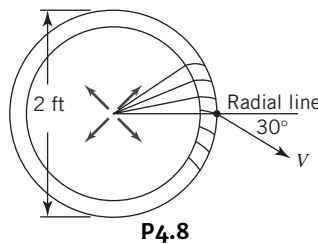
4.6 Across a shock wave in a gas flow there is a change in gas density ρ . If a shock wave occurs in a duct such that $V = 660 \text{ m/s}$ and $\rho = 1.0 \text{ kg/m}^3$ before the shock and $V = 250 \text{ m/s}$ after the shock, determine the density after the shock.

4.7 Calculate the mean velocities for these two-dimensional velocity profiles if $v_c = 3 \text{ m/s}$.



P4.7

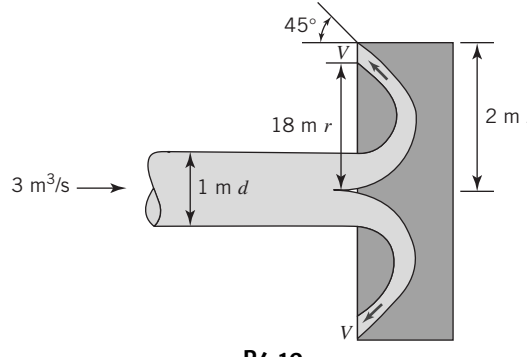
4.8 Fluid passes through this set of thin closely spaced blades. Determine flow rate q required for the velocity V to be 10 ft/s .



P4.8

4.9 A pipeline 0.3 m in diameter divides at a Y into two branches 200 mm and 150 mm in diameter. If the flow rate in the main line is $0.3 \text{ m}^3/\text{s}$ and the mean velocity in the 200-mm pipe is 2.5 m/s , determine the flow rate in the 150-mm pipe.

4.10 Find V for this mushroom cap on a pipeline.



P4.10

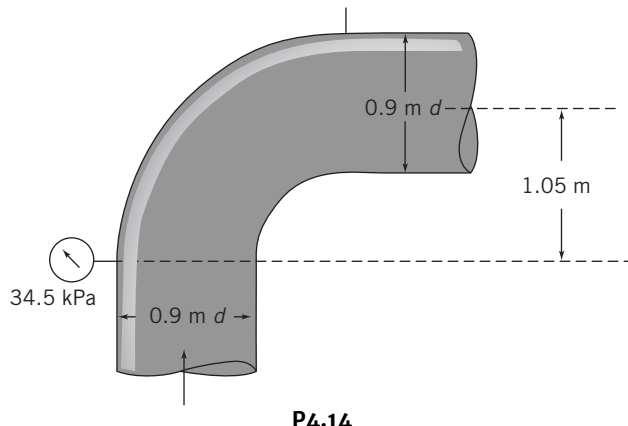
4.11 You are trying to pump stormwater out of your basement during a storm. The basement is $20 \text{ ft} \times 30 \text{ ft}$ and the pump extracts 27.5 gpm . The water level in the basement is dropping 4 in./hr . Determine the flow rate (gpm) from the storm into the basement.

4.12 A cylindrical tank, of diameter $D = 50 \text{ mm}$, drains through an opening, $d = 5 \text{ mm}$, in the bottom of the tank. The speed of the liquid leaving the tank is approximately $V = \sqrt{2gy}$ where y is the height from the tank bottom to the free surface. If the tank is initially

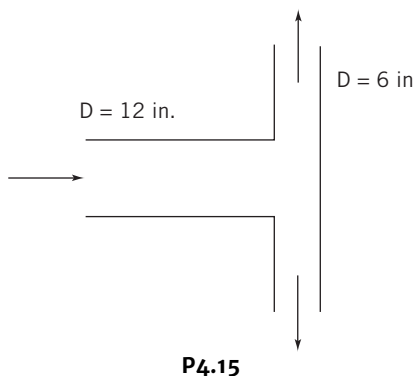
filled with water to $y_0 = 0.4$ m, determine the water depths at $t = 60$ sec, $t = 120$ sec, and $t = 180$ sec. Plot y (m) versus t for the first 180 sec.

4.13 A 100-mm nozzle is bolted with 6 bolts to the flange of a 300-mm-diameter horizontal pipeline and discharges water into the atmosphere. Calculate the tension load on each bolt when the gage pressure in the pipe is 600 kPa. Neglect vertical forces.

SS 4.14 The water flow rate through the vertical bend shown in the figure is $2.83 \text{ m}^3/\text{s}$. Calculate the magnitude, direction, and location of the resultant force of the water on the pipe bend.

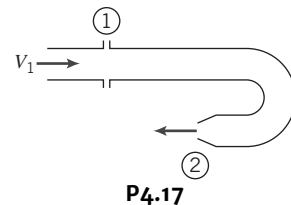


SS 4.15 Water flows through a tee in a horizontal pipe system as shown in the figure. The incoming velocity is 15 ft/s, the pressure is 20 psi, and the pipe diameter is 12 in. Each branch of the tee is 6 in. in diameter and the velocities in the branches are the same. Determine the magnitude and direction of the force of the water on the tee.

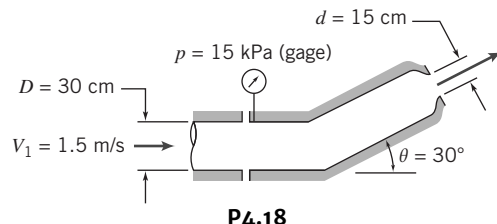


4.16 Water flows steadily through a fire hose and nozzle. The hose is 75-mm-ID, and the nozzle tip is 35-mm-ID; water gage pressure in the hose is 510 kPa, and the stream leaving the nozzle is uniform. The exit speed and pressure are 32 m/s and atmospheric, respectively. Find the force transmitted by the coupling between the nozzle and hose. Indicate whether the coupling is in tension or compression.

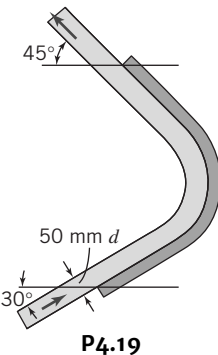
4.17 Water is flowing steadily through the 180° elbow shown. At the inlet to the elbow, the gage pressure is 103 psi. The water discharges to atmospheric pressure. Assume that properties are uniform over the inlet and outlet areas: $A_1 = 2500 \text{ mm}^2$, $A_2 = 650 \text{ mm}^2$, and $V_1 = 3 \text{ m/s}$. Find the horizontal component of force required to hold the elbow in place.



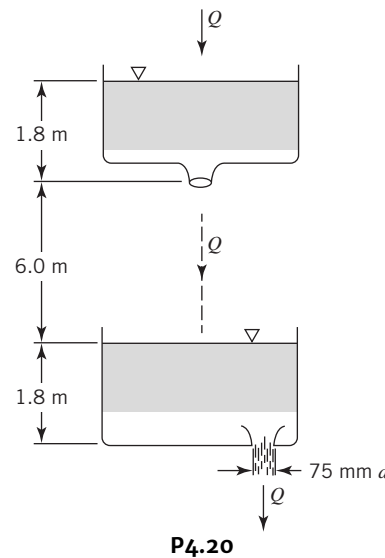
4.18 Water flows steadily through the nozzle shown, discharging to atmosphere. Calculate the horizontal component of force in the flanged joint. Indicate whether the joint is in tension or compression.



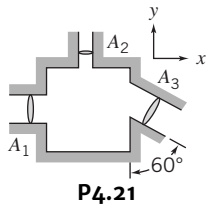
4.19 Calculate the magnitude and direction of the vertical and horizontal components and the total force exerted on this stationary blade by a 50 mm jet of water moving at 15 m/s.



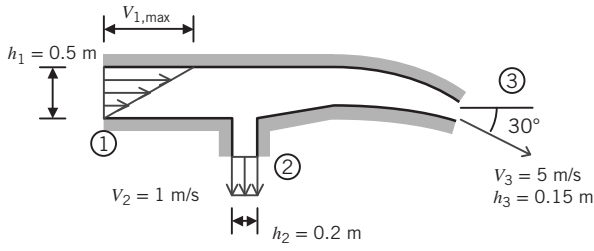
4.20 The lower tank weighs 224 N, and the water in it weighs **SS** 897 N. If this tank is on a platform scale, determine the weight that will register on the scale beam.



4.21 A fluid with a density of 1040 kg/m^3 density flows steadily through the rectangular box shown in the figure. The areas are $A_1 = 0.046 \text{ m}^2$, $A_2 = 0.009 \text{ m}^2$, and $A_3 = 0.056 \text{ m}^2$, and the velocities are $\vec{V}_1 = 3\hat{i} \text{ m/s}$ and $\vec{V}_2 = 6\hat{j} \text{ m/s}$. Determine the net rate of momentum flux out of the control volume.



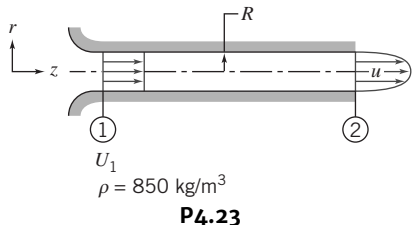
4.22 An incompressible fluid flows steadily through the two-dimensional reducing bend shown in the figure. The width of the bend is 1 m. The velocity profile is linear at section 1 and uniform at sections 2 and 3. Determine the net momentum flux through the bend.



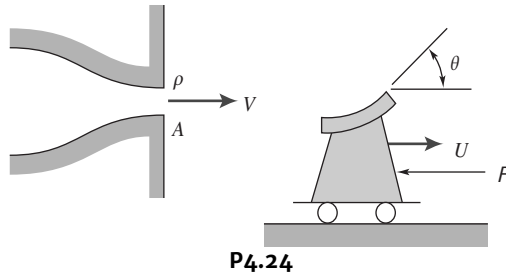
4.23 An incompressible fluid with a density of 850 kg/m^3 flows steadily in the entrance region of a circular tube of radius $R = 75 \text{ mm}$. The flow rate is $Q = 0.1 \text{ m}^3/\text{s}$. The velocity profile entering the tube is uniform and that leaving is given by

$$\frac{u}{u_{\max}} = 1 - \left(\frac{r}{R}\right)^2$$

Find the average velocity, which is also U_1 , and the maximum velocity at the exit. Determine the pressure drop due to the change in momentum of the flow.

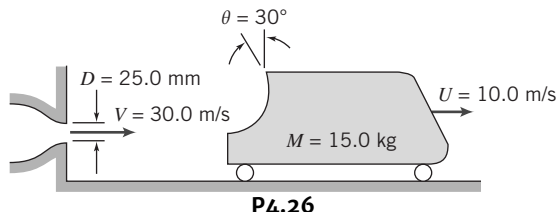


4.24 A water flow from a nozzle impinges on a moving vane as shown in the figure. The water leaves the nozzle at 30 m/s , and the exit area of the nozzle is 0.004 m^2 . The vane moves away from the nozzle with a constant speed, $U = 10 \text{ m/s}$. The angle θ is 60° . Determine the resisting force on the vane.

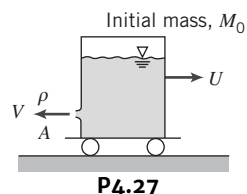


4.25 A inboard jet boat takes in water through side vents and ejects it through a nozzle at the stern. The drag on the boat is given by $F_{\text{drag}} = k V^2$, where V is the boat speed and k is a constant that is a function of boat size and shape. For a boat with a nozzle diameter of 75 mm , a jet speed of 15 m/s , and a boat speed of 10 m/s , determine the constant k . Determine the boat speed when the jet speed is increased to 20 m/s .

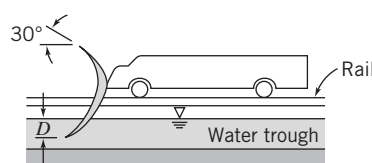
4.26 The cart in the figure below is accelerated along a level track by a jet of water that strikes the curved vane. Determine the time it takes to accelerate the cart from rest to $U = 10 \text{ m/s}$.



4.27 A pressurized tank of water is mounted on a cart as shown. A jet issues from a nozzle in the tank at a constant speed and propels the cart along a horizontal track. The initial mass of the cart and tank is 100 kg , and the nozzle area is 0.005 m^2 . Determine the jet speed required to accelerate the cart to 1.5 m/s in 30 s .



4.28 A sled used to test rockets is slowed lowering a scoop into a water trough. The scoop is 0.3 m wide and deflects water through 150° . The mass of the sled is 8000 kg . At the initial speed, it experiences an aerodynamic drag force of 90 kN . The aerodynamic force is proportional to the square of the sled speed. It is desired to slow the sled to 100 m/s . Determine the depth the scoop must be lowered into the water to slow the sled down from an initial speed of 300 m/s to 100 m/s in 800 m . (Note that using the chain rule the derivative can be expressed as $\frac{dU}{dt} = \frac{dU}{dx} \frac{dx}{dt} = \frac{dU}{dx} U$)

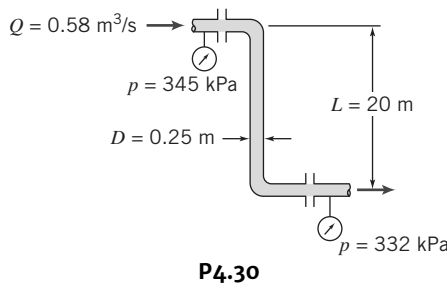


Momentum Equation for Control Volume with Arbitrary Acceleration

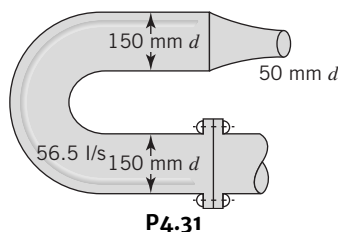
4.29 A solid-fuel rocket motor is fired on a test stand. The combustion chamber is circular, with 100 mm diameter. Fuel, of density 1660 kg/m^3 , burns uniformly at the rate of 12.7 mm/s . Measurements show that the exhaust gases leave the rocket at ambient pressure, at a speed of 2750 m/s . The absolute pressure and temperature in the combustion chamber are 7.0 MPa and 3610 K , respectively. Treat the combustion products as an ideal gas with molecular mass of 25.8. Determine the rate of change of mass and of linear momentum within the rocket motor. Determine the motor thrust and the percentage of the motor thrust that is due to the rate of change of linear momentum within the motor.

The Angular-Momentum Principle

4.30 Crude oil ($\text{SG} = 0.95$) from a tanker dock flows through a pipe of 0.25 m diameter in the configuration shown. The flow rate is $0.58 \text{ m}^3/\text{s}$, and the gage pressures are shown in the diagram. Determine the force and torque that are exerted by the pipe assembly on its supports.



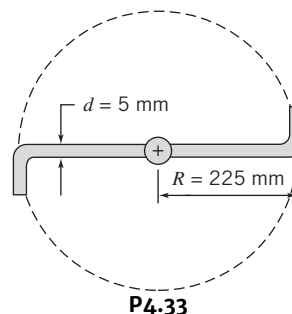
4.31 Calculate the torque about the pipe's centerline in the plane of the bolted flange that is caused by the flow through the nozzle. The nozzle centerline is 0.3 m above the flange centerline. Neglect the effects of the weights of the pipe and the fluid in the pipe.



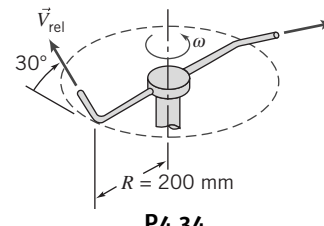
4.32 A fire truck is equipped with a 66 ft long extension ladder which is attached at a pivot and raised to an angle of 45° . A 4-in.-diameter fire hose is laid up the ladder and a 2-in.-diameter nozzle is attached to the top of the ladder so that the nozzle directs the stream horizontally into the window of a burning building. If the flow rate is $1 \text{ ft}^3/\text{s}$, compute the torque exerted about the ladder pivot point. The ladder, hose, and the water in the hose weigh 10 lb/ft .

4.33 The lawn sprinkler shown in the figure rotates in the horizontal plane. A water flow of 15 L/min of water enters the center vertically and discharges in the horizontal plane from the two jets.

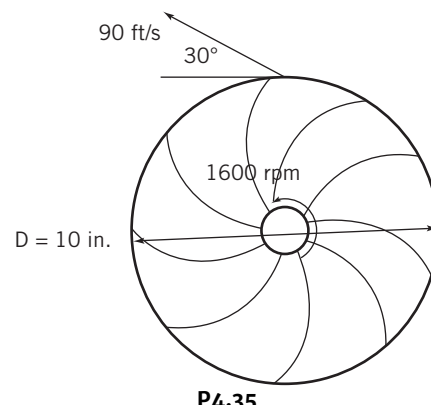
Determine (a) the torque needed to keep the sprinkler from rotating and (b) the rotating speed of the sprinkler when the torque is removed.



4.34 A water flow rate of 4 L/min enters the lawn sprinkler shown in the figure in a vertical direction. The velocity of the jets leaving the nozzles is 17 m/s relative to the sprinkler arm and inclined 30° above the horizontal. Friction in the bearing causes a torque of 0.18 N-m opposing rotation. Determine (a) the torque required to hold the sprinkler stationary, (b) the rotational speed if the torque is removed, and (c) the rotational speed if there is no torque due to the bearings.

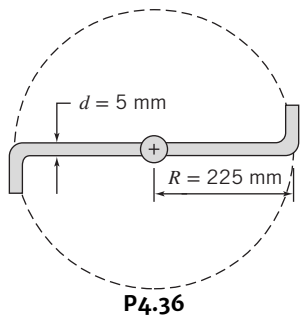


4.35 The impeller of a radial water pump has an outer diameter of 10 in. and rotates at 1600 rpm . A water flow of 1200 gpm enters the impeller axially and leaves at an absolute velocity of 90 ft/s and an angle of 30° relative to the impeller as shown in the figure. Determine the torque and power needed to drive the impeller.

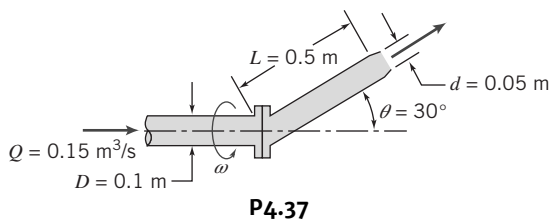


The Angular-Momentum Principle Equation for Rotating Control Volume

4.36 The simplified lawn sprinkler shown rotates in the horizontal plane. At the center pivot, $Q = 15 \text{ L/min}$ of water enters vertically. Water discharges in the horizontal plane from each jet. If the pivot is frictionless, calculate the torque needed to keep the sprinkler from rotating. Neglecting the inertia of the sprinkler itself, calculate the angular acceleration that results when the torque is removed.



4.37 Water flows at the rate of $0.15 \text{ m}^3/\text{s}$ through a nozzle assembly that rotates steadily at 30 rpm . The arm and nozzle masses are negligible compared with the water inside. Determine the torque required to drive the device and the reaction torques at the flange.



The First Law of Thermodynamics

4.38 A turbine is supplied with $0.6 \text{ m}^3/\text{s}$ of water from a 0.3 m diameter pipe; the discharge pipe has a 0.4 m diameter. Determine the pressure drop across the turbine if it delivers 60 kW .

4.39 Air is drawn from the atmosphere into a turbomachine. At the exit, conditions are 500 kPa gage and 130°C . The exit speed is 100 m/s and the mass flow rate is 0.8 kg/s . Flow is steady and there is no heat transfer. Compute the shaft work interaction with the surroundings.

4.40 Transverse thrusters are used to make large ships fully maneuverable at low speeds without tugboat assistance. A transverse thruster consists of a propeller mounted in a duct; the unit is then mounted below the waterline in the bow or stern of the ship. The duct runs completely across the ship. Calculate the thrust developed by a 1865 kW unit (supplied to the propeller) if the duct is 2.8 m in diameter and the ship is stationary.

4.41 All major harbors are equipped with fire boats for extinguishing ship fires. A 75-mm-diameter hose is attached to the discharge of a 11 kW pump on such a boat. The nozzle attached to the end of the hose has a diameter of 25 mm . If the nozzle discharge is held 3 m above the surface of the water, determine the volume flow rate through the nozzle, the maximum height to which the water will rise, and the force on the boat if the water jet is directed horizontally over the stern.

4.42 A pump draws water from a reservoir through a 150-mm-diameter suction pipe and delivers it to a 75-mm-diameter discharge pipe. The end of the suction pipe is 2 m below the free surface of the reservoir. The pressure gage on the discharge pipe, which is 2 m above the reservoir surface, reads 170 kPa . The average speed in the discharge pipe is 3 m/s . If the pump efficiency is 75 percent, determine the power required to drive it.

CHAPTER 4

Basic Equations in Integral Form for a Control Volume

4.1 Basic Laws for a System

4.2 Relation of System Derivatives to the Control Volume Formulation

4.3 Conservation of Mass

4.4 Momentum Equation for Inertial Control Volume

4.5 Momentum Equation for Control Volume with Rectilinear Acceleration

4.6 Momentum Equation for Control Volume with Arbitrary Acceleration

4.7 The Angular-Momentum Principle

4.8 The First and Second Laws of Thermodynamics

4.9 Summary and Useful Equations

Case Study

Long-distance trucking fuel use accounts for about 15 percent of all of the energy used in the United States. Traditional tractor-trailer combinations have not been streamlined and have a large aerodynamic resistance. The drag coefficient, which you will study in Chapter 9, is a relative measure of the aerodynamic resistance. For a typical tractor-trailer combination without any drag-reducing features, the drag coefficient is on the order of 0.8 to 1.0. Streamlining that incorporates deflectors on the top of the cab, skirts along the side of the trailer, and wake-reducing panels at the end of the trailer reduces the drag coefficient to the 0.4 to 0.5 range. At highway speeds, aerodynamic drag accounts for about 85 percent of the fuel use.

The all-electric Tesla truck shown in the figure has been intensively studied in an attempt to remove or modify all of the drag-producing components. The result is a drag coefficient of 0.36, or about one-third of that of an unmodified truck. This represents a significant fuel energy savings and a significant cost savings for the owner. The result is a 2 kWh/mile fuel cost for the all-electric truck. This converts to the equivalent of 18 miles/gallon (mpg) for the Tesla truck at highway speeds and compares to the current truck fleet average of about 6 mpg. The estimated annual fuel savings are stated to be \$200,000.

The electric truck has four independent motors on the rear axle, a range of 300 to 500 miles, and a speed of 60 mph on 5 percent grades. It comes equipped with a detection system that helps avoid collisions. The driver sits in the center of the cab which gives maximum visibility and control. The truck has a low center of gravity that provides rollover protection. All of these features, combined with the aerodynamic streamlining, give this style of truck the potential to change the long-distance trucking industry.



Streamlined highway tractor and trailer.

Alex Kondratenko/Adobe Stock Photo

Learning Objectives

After completing this chapter, you should be able to

- Solve a problem involving a system using the basic laws.
- Explain the physical meaning of each of the terms in the Reynolds Transport Equation
- Solve a flow problem using the control volume formulation of the conservation of mass principle.
- Solve a flow problem using the control volume formulation of the momentum principle
- Solve a flow problem using the control volume formulation of the angular momentum principle.
- Solve a flow problem using the control volume formulation of the conservation of energy principle.

We are now ready to study fluids in motion, so we have to decide how we are to examine a flowing fluid. There are two options available to us, discussed in Chapter 1:

- 1 We can study the motion of an *individual fluid particle or group of particles* as they move through space. This is the *system* approach, which has the advantage that the physical laws such as Newton's second law apply to matter and hence directly to the system. One disadvantage is that in practice the math associated with this approach can become somewhat complicated, usually leading to a set of partial differential equations. We will look at this approach in detail in Chapter 5. The system approach is needed if we are interested in studying the trajectory of particles over time.
- 2 We can study a *region of space* as fluid flows through it, which is the *control volume* approach. This is very often the method of choice, because it has widespread practical application; for example, in aerodynamics we are usually interested in the lift and drag on a wing rather than what happens to individual fluid particles. The disadvantage of this approach is that the physical laws apply to matter and not directly to regions of space, so we have to perform some math to convert physical laws from their system formulation to a control volume formulation.

We will examine the control volume approach in this chapter. This chapter has the word *integral* in its title, and Chapter 5 has the word *differential*. This is an important distinction as it indicates that we will study a finite region in this chapter and then study the motion of a particle in Chapter 5. The agenda for this chapter is to review the physical laws as they apply to a system (Section 4.1); develop some math to convert from a system to a control volume (Section 4.2) description; and obtain formulas for the physical laws for control volume analysis by combining the results of Sections 4.1 and 4.2.

4.1 Basic Laws for a System

The basic laws we will apply are conservation of mass, Newton's second law, the angular-momentum principle, and the first and second laws of thermodynamics. For converting these system equations to equivalent control volume formulas, it turns out we want to express each of the laws in terms of the property of the system (e.g. mass) in terms of the rates of flow in and out (a rate). These equations are termed *rate equations*.

Conservation of Mass

For a system (by definition a specified amount of matter, M , we have chosen) we have the simple result that $M = \text{constant}$. To express this law as a rate equation, we write

$$\frac{dM}{dt} \Big|_{\text{system}} = 0 \quad (4.1a)$$

where

$$M_{\text{system}} = \int_{M(\text{system})} dm = \int_{V(\text{system})} \rho dV \quad (4.1\text{b})$$

Newton's Second Law

For a system moving relative to an inertial reference frame, Newton's second law states that the sum of all external forces acting on the system is equal to the time rate of change of linear momentum of the system,

$$\vec{F} = \frac{d\vec{P}}{dt} \Bigg|_{\text{system}} \quad (4.2\text{a})$$

where the linear momentum of the system is given by

$$\vec{P}_{\text{system}} = \int_{M(\text{system})} \vec{V} dm = \int_{V(\text{system})} \vec{V} \rho dV \quad (4.2\text{b})$$

The Angular-Momentum Principle

The angular-momentum principle for a system states that the rate of change of angular momentum is equal to the sum of all torques acting on the system,

$$\vec{T} = \frac{d\vec{H}}{dt} \Bigg|_{\text{system}} \quad (4.3\text{a})$$

where the angular momentum of the system is given by

$$\vec{H}_{\text{system}} = \int_{M(\text{system})} \vec{r} \times \vec{V} dm = \int_{V(\text{system})} \vec{r} \times \vec{V} \rho dV \quad (4.3\text{b})$$

Torque can be produced by surface and body forces (here gravity) and also by shafts that cross the system boundary,

$$\vec{T} = \vec{r} \times \vec{F}_s + \int_{M(\text{system})} \vec{r} \times \vec{g} dm + \vec{T}_{\text{shaft}} \quad (4.3\text{c})$$

The First Law of Thermodynamics

The first law of thermodynamics is a statement of conservation of energy for a system,

$$\delta Q - \delta W = dE$$

The equation can be written in rate form as

$$\dot{Q} - \dot{W} = \frac{dE}{dt} \Bigg|_{\text{system}} \quad (4.4\text{a})$$

where the total energy of the system is given by

$$E_{\text{system}} = \int_{M(\text{system})} e dm = \int_{V(\text{system})} e \rho dV \quad (4.4\text{b})$$

and

$$e = u + \frac{V^2}{2} + gz \quad (4.4c)$$

In Eq. 4.4a, \dot{Q} (the rate of heat transfer) is positive when heat is added to the system from the surroundings; \dot{W} (the rate of work) is positive when work is done by the system on its surroundings. In Eq. 4.4c, u is the specific internal energy, V the speed, and z the height relative to a convenient datum of a particle of substance having mass dm .

The Second Law of Thermodynamics

If an amount of heat, δQ , is transferred to a system at temperature T , the second law of thermodynamics states that the change in entropy, dS , of the system satisfies

$$dS \geq \frac{\delta Q}{T}$$

On a rate basis we can write

$$\left. \frac{dS}{dt} \right)_{\text{system}} \geq \frac{1}{T} \dot{Q} \quad (4.5a)$$

where the total entropy of the system is given by

$$S_{\text{system}} = \int_{M(\text{system})} s dm = \int_{V(\text{system})} s \rho dV \quad (4.5b)$$

4.2 Relation of System Derivatives to the Control Volume Formulation

We now have the five basic laws expressed as system rate equations. Our task in this section is to develop a general expression for converting a system rate equation into an equivalent control volume equation. Instead of converting the equations for rates of change of M , \vec{P} , \vec{H} , E , and S (Eqs. 4.1a, 4.2a, 4.3a, 4.4a, and 4.5a) one by one, we let all of them be represented by the symbol N . Hence N represents the amount of mass, or momentum, or angular momentum, or energy, or entropy of the system. Corresponding to this extensive property, we will also need the intensive (i.e., per unit mass) property η . Thus

$$N_{\text{system}} = \int_{M(\text{system})} \eta dm = \int_{V(\text{system})} \eta \rho dV \quad (4.6)$$

Comparing Eq. 4.6 with Eqs. 4.1b, 4.2b, 4.3b, 4.4b, and 4.5b, we see that if:

$$\begin{aligned} N &= M, & \text{then } \eta &= 1 \\ N &= \vec{P}, & \text{then } \eta &= \vec{V} \\ N &= \vec{H}, & \text{then } \eta &= \vec{r} \times \vec{V} \\ N &= E, & \text{then } \eta &= e \\ N &= S, & \text{then } \eta &= s \end{aligned}$$

We will first explain how we derive a control volume description from a system description of a fluid flow in general terms. We imagine selecting an arbitrary piece of the flowing fluid at some time

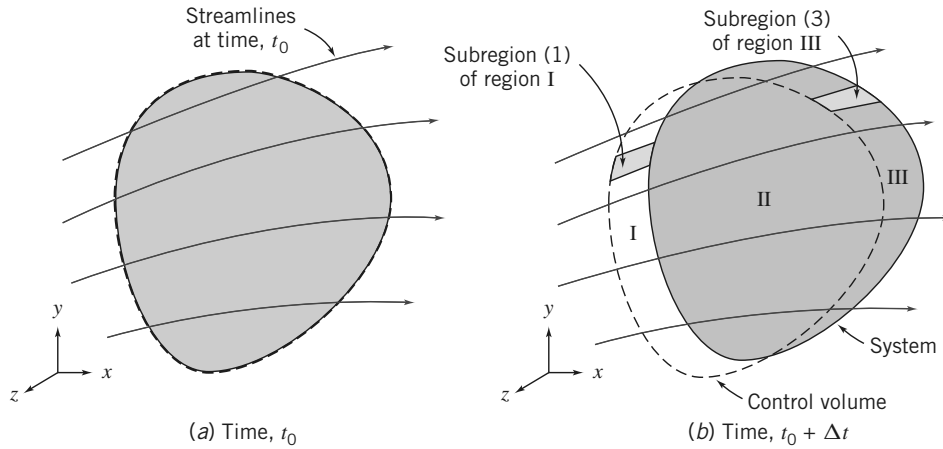


Fig. 4.1 System and control volume configuration.

t_0 , as shown in Fig. 4.1a, we could imagine dyeing this piece of fluid, say, blue. This initial shape of the fluid system is chosen as our control volume, which is fixed in space relative to coordinates xyz . After an infinitesimal time Δt the system will have moved to a new location, as shown in Fig. 4.1b, and possibly changed shape. The laws we discussed above apply to this piece of fluid; for example, its mass will be constant (Eq. 4.1a). By examining the geometry of the system/control volume pair at $t=t_0$ and at $t=t_0+\Delta t$, we will be able to obtain control volume formulations of the basic laws.

Derivation

From Fig. 4.1 we see that the system, which was entirely within the control volume at time t_0 , is partially out of the control volume at time $t_0+\Delta t$. In fact, three regions can be identified. These are: regions I and II, which together make up the control volume, and region III, which, with region II, is the location of the system at time $t_0+\Delta t$.

Recall that our objective is to relate the rate of change of any arbitrary extensive property, N , of the system to quantities associated with the control volume. From the definition of a derivative, the rate of change of N_{system} is given by

$$\left. \frac{dN}{dt} \right|_{\text{system}} \equiv \lim_{\Delta t \rightarrow 0} \frac{(N_s)_{t_0+\Delta t} - (N_s)_{t_0}}{\Delta t} \quad (4.7)$$

For convenience, subscript s has been used to denote the system in the definition of a derivative in Eq. 4.7.

From the geometry of Fig. 4.1,

$$(N_s)_{t_0+\Delta t} = (N_{\text{II}} + N_{\text{III}})_{t_0+\Delta t} = (N_{\text{CV}} - N_{\text{I}} + N_{\text{III}})_{t_0+\Delta t}$$

and

$$(N_s)_{t_0} = (N_{\text{CV}})_{t_0}$$

Substituting into the definition of the system derivative, Eq. 4.7, we obtain

$$\left. \frac{dN}{dt} \right|_{\text{s}} = \lim_{\Delta t \rightarrow 0} \frac{(N_{\text{CV}} - N_{\text{I}} + N_{\text{III}})_{t_0+\Delta t} - N_{\text{CV}})_{t_0}}{\Delta t}$$

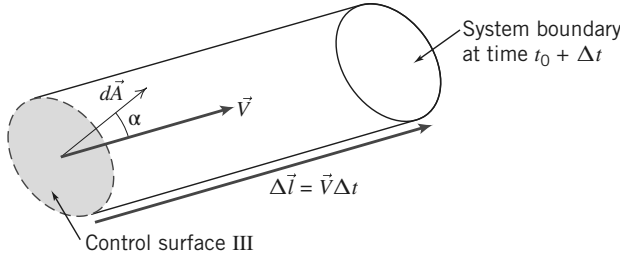


Fig. 4.2 Enlarged view of subregion (3) from Fig. 4.1.

Since the limit of a sum is equal to the sum of the limits, we can write

$$\frac{dN}{dt}_s = \lim_{\Delta t \rightarrow 0} \frac{N_{CV})_{t_0 + \Delta t} - N_{CV})_{t_0}}{\Delta t} + \lim_{\Delta t \rightarrow 0} \frac{N_{III})_{t_0 + \Delta t}}{\Delta t} - \lim_{\Delta t \rightarrow 0} \frac{N_I)_{t_0 + \Delta t}}{\Delta t} \quad (4.8)$$

① ② ③

We now evaluate each of the three terms in Eq. 4.8.

Term ① in Eq. 4.8 simplifies to

$$\lim_{\Delta t \rightarrow 0} \frac{N_{CV})_{t_0 + \Delta t} - N_{CV})_{t_0}}{\Delta t} = \frac{\partial N_{CV}}{\partial t} = \frac{\partial}{\partial t} \int_{CV} \eta \rho dV \quad (4.9a)$$

To evaluate term ② we first develop an expression for $N_{III})_{t_0 + \Delta t}$ by looking at the enlarged view of a typical subregion (subregion (3)) of region III shown in Fig. 4.2. The vector area element $d\vec{A}$ of the control surface has magnitude dA , and its direction is the *outward* normal of the area element. In general, the velocity vector \vec{V} will be at some angle α with respect to $d\vec{A}$.

For this subregion we have

$$dN_{III})_{t_0 + \Delta t} = (\eta \rho dV)_{t_0 + \Delta t}$$

We need to obtain an expression for the volume dV of this cylindrical element. The vector length of the cylinder is given by $\Delta l = \vec{V}\Delta t$. The volume of a prismatic cylinder, whose area $d\vec{A}$ is at an angle α to its length Δl , is given by $dV = \Delta l dA \cos \alpha = \Delta l \cdot d\vec{A} = \vec{V} \cdot d\vec{A} \Delta t$. Hence, for subregion (3) we can write

$$dN_{III})_{t_0 + \Delta t} = \eta \rho \vec{V} \cdot d\vec{A} \Delta t$$

Then, for the entire region III we can integrate and for term ② in Eq. 4.8 obtain

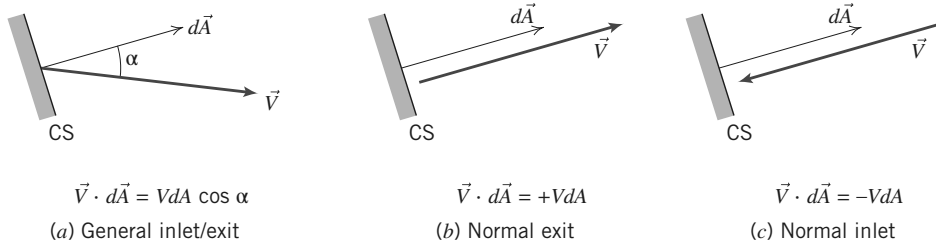
$$\lim_{\Delta t \rightarrow 0} \frac{N_{III})_{t_0 + \Delta t}}{\Delta t} = \lim_{\Delta t \rightarrow 0} \frac{\int_{CS_{III}} dN_{III})_{t_0 + \Delta t}}{\Delta t} = \lim_{\Delta t \rightarrow 0} \frac{\int_{CS_{III}} \eta \rho \vec{V} \cdot d\vec{A} \Delta t}{\Delta t} = \int_{CS_{III}} \eta \rho \vec{V} \cdot d\vec{A} \quad (4.9b)$$

We can perform a similar analysis for subregion (1) of region I, and obtain for term in Eq. 4.8

$$\lim_{\Delta t \rightarrow 0} \frac{N_I)_{t_0 + \Delta t}}{\Delta t} = - \int_{CS_I} \eta \rho \vec{V} \cdot d\vec{A} \quad (4.9c)$$

For subregion (1), the velocity vector acts *into* the control volume, but the area normal *always* (by convention) points outward (angle $\alpha > \pi/2$), so the scalar product in Eq. 4.9c is negative. Hence the minus sign in Eq. 4.9c is needed to cancel the negative result of the scalar product to make sure we obtain a positive result for the amount of matter that was in region I (we can't have negative matter).

This concept of the sign of the scalar product is illustrated in Fig. 4.3 for (a) the general case of an inlet or exit, (b) an exit velocity parallel to the surface normal, and (c) an inlet velocity parallel to the surface normal. Cases (b) and (c) are obviously convenient special cases of (a); the value of the cosine in case (a) automatically generates the correct sign of either an inlet or an exit.

**Fig. 4.3** Evaluating the scalar product.

We can finally use Eqs. 4.9a, 4.9b, and 4.9c in Eq. 4.8 to obtain

$$\frac{dN}{dt} \Big|_{\text{system}} = \frac{\partial}{\partial t} \int_{\text{CV}} \eta \rho dV + \int_{\text{CS}_I} \eta \rho \vec{V} \cdot d\vec{A} + \int_{\text{CS}_{III}} \eta \rho \vec{V} \cdot d\vec{A}$$

and the two last integrals can be combined because CS_I and CS_{III} constitute the entire control surface,

$$\frac{dN}{dt} \Big|_{\text{system}} = \frac{\partial}{\partial t} \int_{\text{CV}} \eta \rho dV + \int_{\text{CS}} \eta \rho \vec{V} \cdot d\vec{A} \quad (4.10)$$

Equation 4.10 is the fundamental relation between the rate of change of any arbitrary extensive property, N , of a system and the variations of this property associated with a control volume. Some authors refer to Eq. 4.10 as the *Reynolds Transport Theorem*.

Physical Interpretation

We now have a formula (Eq. 4.10) that we can use to convert the rate of change of any extensive property N of a system to an equivalent formulation for use with a control volume. We can now use Eq. 4.10 in the various basic physical law equations (Eqs. 4.1a, 4.2a, 4.3a, 4.4a, and 4.5a) one by one, with N replaced with each of the properties M , \bar{P} , \bar{H} , E , and S (with corresponding symbols for η), to replace system derivatives with control volume expressions. Because we consider the equation itself to be “basic” we repeat it to emphasize its importance:

$$\frac{dN}{dt} \Big|_{\text{system}} = \frac{\partial}{\partial t} \int_{\text{CV}} \eta \rho dV + \int_{\text{CS}} \eta \rho \vec{V} \cdot d\vec{A} \quad (4.10)$$

We need to be clear here: The system is the matter that happens to be passing through the chosen control volume, at the instant we chose. For example, if we chose as a control volume the region contained by an airplane wing and an imaginary rectangular boundary around it, the system would be the mass of the air that is instantaneously contained between the rectangle and the airfoil. Before applying Eq. 4.10 to the physical laws, let’s discuss the meaning of each term of the equation:

$\frac{dN}{dt} \Big|_{\text{system}}$ is the rate of change of the system extensive property N . For example, if $N = \vec{P}$, we obtain the rate of change of momentum.

$\frac{\partial}{\partial t} \int_{\text{CV}} \eta \rho dV$ is the rate of change of the amount of property N in the control volume. The term $\int_{\text{CV}} \eta \rho dV$ computes the instantaneous value of N in the control volume where $\int_{\text{CV}} \rho dV$ is the instantaneous mass in the control volume. For example, if $N = \vec{P}$, then $\eta = \vec{V}$ and $\int_{\text{CV}} \vec{V} \rho dV$ computes the instantaneous amount of momentum in the control volume.

$\int_{\text{CS}} \eta \rho \vec{V} \cdot d\vec{A}$ is the rate at which property N is exiting the surface of the control volume. The term $\rho \vec{V} \cdot d\vec{A}$ computes the rate of mass transfer leaving across control surface area element $d\vec{A}$. Multiplying by η computes the rate of flux of property N across the element and integrating therefore computes the net flux of N out of the control volume. For example, if $N = \vec{P}$, then $\eta = \vec{V}$ and $\int_{\text{CS}} \vec{V} \rho \vec{V} \cdot d\vec{A}$ computes the net flux of momentum out of the control volume.

We make two comments about velocity \vec{V} in Eq. 4.10. First, we reiterate the discussion for Fig. 4.3 that care should be taken in evaluating the dot product. Because \vec{A} is always directed outwards, the dot product will be positive when \vec{V} is outward and negative when \vec{V} is inward. Second, \vec{V} is measured with respect to the control volume. When the control volume coordinates xyz are stationary or moving with a constant linear velocity, the control volume will constitute an inertial frame and the physical laws we have described will apply.

With these comments we are ready to combine the physical laws (Eqs. 4.1a, 4.2a, 4.3a, 4.4a, and 4.5a) with Eq. 4.10 to obtain some useful control volume equations.

4.3 Conservation of Mass

The first physical principle to which we apply this conversion from a system to a control volume description is the mass conservation principle: The mass of the system remains constant,

$$\frac{dM}{dt} \Big|_{\text{system}} = 0 \quad (4.1a)$$

where

$$M_{\text{system}} = \int_{M(\text{system})} dm = \int_{V(\text{system})} \rho dV \quad (4.1b)$$

The system and control volume formulations are related by Eq. 4.10,

$$\frac{dN}{dt} \Big|_{\text{system}} = \frac{\partial}{\partial t} \int_{CV} \eta \rho dV + \int_{CS} \eta \rho \vec{V} \cdot d\vec{A} \quad (4.10)$$

where

$$N_{\text{system}} = \int_{M(\text{system})} \eta dm = \int_{V(\text{system})} \eta \rho dV \quad (4.6)$$

To derive the control volume formulation of conservation of mass, we set

$$N = M \quad \text{and} \quad \eta = 1$$

With this substitution, we obtain

$$\frac{dM}{dt} \Big|_{\text{system}} = \frac{\partial}{\partial t} \int_{CV} \rho dV + \int_{CS} \rho \vec{V} \cdot d\vec{A} \quad (4.11)$$

Comparing Eqs. 4.1a and 4.11, we arrive after rearranging at the control volume formulation of the conservation of mass:

$$\frac{\partial}{\partial t} \int_{CV} \rho dV + \int_{CS} \rho \vec{V} \cdot d\vec{A} = 0 \quad (4.12)$$

In Eq. 4.12 the first term represents the rate of change of mass within the control volume and the second term represents the net rate of mass flux out through the control surface. Equation 4.12 indicates that the rate of change of mass in the control volume plus the net outflow is zero. The mass conservation equation is also called the *continuity* equation. In common-sense terms, the rate of increase of mass in the control volume is due to the net inflow of mass:

$$\begin{aligned} \text{Rate of increase} &= \text{Net influx of} \\ \text{of mass in CV} &= \text{mass} \\ \frac{\partial}{\partial t} \int_{CV} \rho dV &= - \int_{CS} \rho \vec{V} \cdot d\vec{A} \end{aligned}$$

Once again, we note that in using Eq. 4.12, care should be taken in evaluating the scalar product $\vec{V} \cdot d\vec{A} = VdA \cos \alpha$: It could be positive (outflow, $\alpha < \pi/2$), negative (inflow, $\alpha > \pi/2$), or even zero ($\alpha = \pi/2$). Recall that Fig. 4.3 illustrates the general case as well as the convenient cases $\alpha = 0$ and $\alpha = \pi$.

Special Cases

In special cases it is possible to simplify Eq. 4.12. Consider first the case of an incompressible fluid. When ρ is constant, it is not a function of space or time. Consequently, for *incompressible fluids*, Eq. 4.12 may be written as

$$\rho \frac{\partial}{\partial t} \int_{CV} dV + \rho \int_{CS} \vec{V} \cdot d\vec{A} = 0$$

The integral of dV over the control volume is simply the volume of the control volume. Thus, on dividing through by ρ , we write

$$\frac{\partial V}{\partial t} + \int_{CS} \vec{V} \cdot d\vec{A} = 0$$

For a nondeformable control volume of fixed size and shape, $V = \text{constant}$. The conservation of mass for incompressible flow through a fixed control volume becomes

$$\int_{CS} \vec{V} \cdot d\vec{A} = 0 \quad (4.13a)$$

A useful special case is when we have uniform velocity at each inlet and exit. In this case Eq. 4.13a simplifies to

$$\sum_{CS} \vec{V} \cdot \vec{A} = 0 \quad (4.13b)$$

Note that we have not assumed the flow to be steady in reducing Eq. 4.12 to the forms 4.13a and 4.13b. We have only imposed the restriction of incompressible fluid. Thus Eqs. 4.13a and 4.13b are statements of conservation of mass for flow of an incompressible fluid that may be steady or unsteady.

The dimensions of the integrand in Eq. 4.13a are L^3/t . The integral of $\vec{V} \cdot d\vec{A}$ over a section of the control surface is commonly called the *volume flow rate* or *volume rate of flow*. Thus, for incompressible flow, the volume flow rate into a fixed control volume must be equal to the volume flow rate out of the control volume. The volume flow rate Q , through a section of a control surface of area A , is given by

$$Q = \int_A \vec{V} \cdot d\vec{A} \quad (4.14a)$$

The average velocity magnitude, \bar{V} , at a section is defined as

$$\bar{V} = \frac{Q}{A} = \frac{1}{A} \int_A \vec{V} \cdot d\vec{A} \quad (4.14b)$$

Consider now the general case of *steady, compressible flow* through a fixed control volume. Since the flow is steady, this means that at most $\rho = \rho(x, y, z)$. By definition, no fluid property varies with time in a steady flow. Consequently, the first term of Eq. 4.12 must be zero and, hence, for steady flow, the statement of conservation of mass reduces to

$$\int_{CS} \rho \vec{V} \cdot d\vec{A} = 0 \quad (4.15a)$$

A useful special case is when we have uniform velocity at each inlet and exit. In this case, Eq. 4.15a simplifies to

$$\sum_{CS} \rho \vec{V} \cdot \vec{A} = 0 \quad (4.15b)$$

Thus, for steady flow, the mass flow rate into a control volume must be equal to the mass flow rate out of the control volume.

We will now look at three examples to illustrate some features of the various forms of the conservation of mass equation for a control volume. Example 4.1 involves a problem in which we have uniform flow at each section, Example 4.2 involves a problem in which we do not have uniform flow at a location, and Example 4.3 involves a problem in which we have unsteady flow.

Example 4.1 MASS FLOW AT A PIPE JUNCTION

Consider the steady flow in a water pipe joint shown in the diagram. The areas are: $A_1 = 0.2 \text{ m}^2$, $A_2 = 0.2 \text{ m}^2$, and $A_3 = 0.15 \text{ m}^2$. In addition, fluid is lost out of a hole at ④, estimated at a rate of $0.1 \text{ m}^3/\text{s}$. The average speeds at sections ① and ③ are $V_1 = 5 \text{ m/s}$ and $V_3 = 12 \text{ m/s}$, respectively. Find the velocity at section ②.

Given: Steady flow of water through the device.

$$A_1 = 0.2 \text{ m}^2 \quad A_2 = 0.2 \text{ m}^2 \quad A_3 = 0.15 \text{ m}^2 \\ V_1 = 5 \text{ m/s} \quad V_3 = 12 \text{ m/s} \quad \rho = 999 \text{ kg/m}^3$$

$$\text{Volume flow rate at } ④ = 0.1 \text{ m}^3/\text{s}$$

Find: Velocity at section ②.

Solution: Choose a fixed control volume as shown. Make an assumption that the flow at section ② is outwards, and label the diagram accordingly. If this assumption is incorrect our final result will tell us.

Governing equation: The general control volume equation is Eq. 4.12, but we can go immediately to Eq. 4.13b because of assumptions (2) and (3) below,

$$\sum_{\text{CS}} \vec{V} \cdot \vec{A} = 0$$

Assumptions:

- 1 Steady flow (given).
- 2 Incompressible flow.
- 3 Uniform properties at each section.

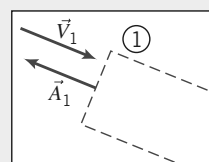
Hence

$$\vec{V}_1 \cdot \vec{A}_1 + \vec{V}_2 \cdot \vec{A}_2 + \vec{V}_3 \cdot \vec{A}_3 + Q_4 = 0 \quad (1)$$

where Q_4 is the flow rate out of the leak.

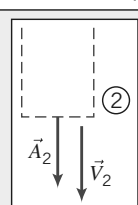
Let us examine the first three terms in Eq. 1 in light of the discussion of Fig. 4.3 and the directions of the velocity vectors:

$$\vec{V}_1 \cdot \vec{A}_1 = -V_1 A_1$$

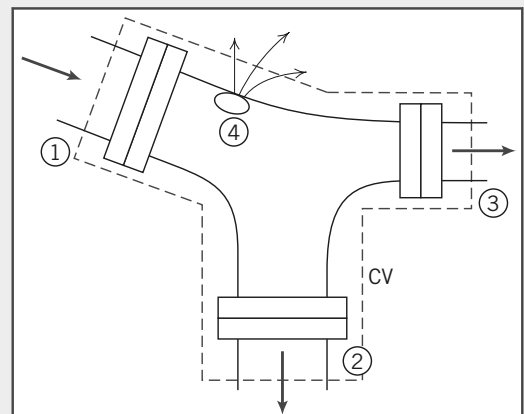
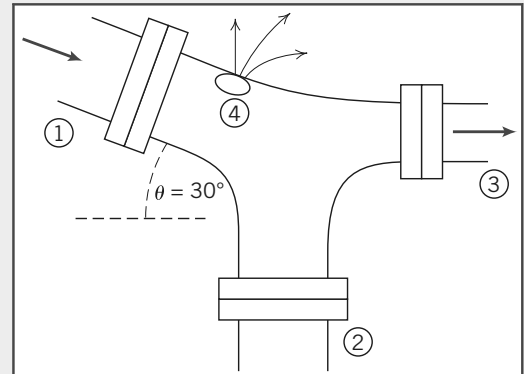


$\left\{ \begin{array}{l} \text{Sign of } \vec{V}_1 \cdot \vec{A}_1 \text{ is} \\ \text{negative at surface } ① \end{array} \right\}$

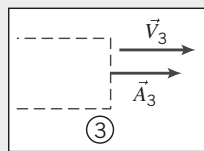
$$\vec{V}_2 \cdot \vec{A}_2 = +V_2 A_2$$



$\left\{ \begin{array}{l} \text{Sign of } \vec{V}_2 \cdot \vec{A}_2 \text{ is} \\ \text{positive at surface } ② \end{array} \right\}$



$$\vec{V}_3 \cdot \vec{A}_3 = +V_3 A_3$$



{ Sign of $\vec{V}_3 \cdot \vec{A}_3$ is positive at surface ③ }

Using these results in Eq. 1,

$$-V_1 A_1 + V_2 A_2 + V_3 A_3 + Q_4 = 0$$

or

$$\begin{aligned} V_2 &= \frac{V_1 A_1 - V_3 A_3 - Q_4}{A_2} \\ &= \frac{5 \frac{\text{m}}{\text{s}} \times 0.2 \text{ m}^2 - 12 \frac{\text{m}}{\text{s}} \times 0.15 \text{ m}^2 - \frac{0.1 \text{ m}^3}{\text{s}}}{0.2 \text{ m}^2} \\ &= -4.5 \text{ m/s}, \quad V_2 \end{aligned}$$

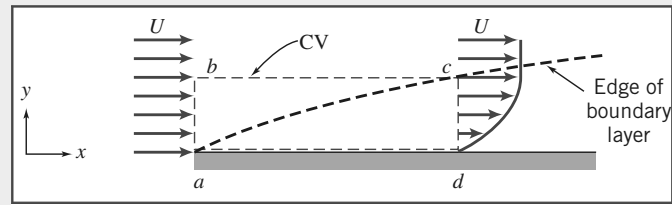
Recall that V_2 represents the magnitude of the velocity, which we assumed was outwards from the control volume. The fact that V_2 is negative means that in fact we have an *inflow* at location ②—our initial assumption was invalid.

This problem demonstrates use of the sign convention for evaluating $\int_A \vec{V} \cdot d\vec{A}$ or $\sum_{CS} \vec{V} \cdot \vec{A}$. In particular, the area normal is *always drawn outwards from the control surface*.

Example 4.2 MASS FLOW RATE IN BOUNDARY LAYER

The fluid in direct contact with a stationary solid boundary has zero velocity; there is no slip at the boundary. Thus the flow over a flat plate adheres to the plate surface and forms a boundary layer, as depicted below. The flow ahead of the plate is uniform with velocity $\vec{V} = U\hat{i}$; $U = 30 \text{ m/s}$. The velocity distribution within the boundary layer ($0 \leq y \leq \delta$) along cd is approximated as $u/U = 2(y/\delta) - (y/\delta)^2$.

The boundary-layer thickness at location d is $\delta = 5 \text{ mm}$. The fluid is air with density $\rho = 1.24 \text{ kg/m}^3$. Assuming the plate width perpendicular to the paper to be $w = 0.6 \text{ m}$, calculate the mass flow rate across surface bc of control volume $abcd$.



Given: Steady, incompressible flow over a flat plate, $\rho = 1.24 \text{ kg/m}^3$. Width of plate, $w = 0.6 \text{ m}$

Velocity ahead of plate is uniform: $\vec{V} = U\hat{i}$, $U = 30 \text{ m/s}$.

At $x = x_d$:

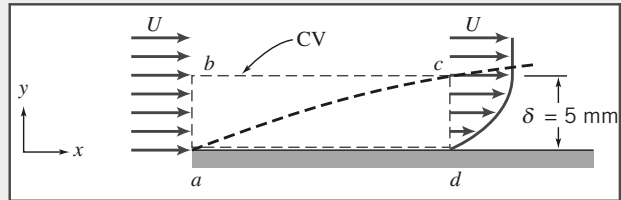
$$\delta = 5 \text{ mm}$$

$$\frac{u}{U} = 2\left(\frac{y}{\delta}\right) - \left(\frac{y}{\delta}\right)^2$$

Find: Mass flow rate across surface bc .

Solution: The fixed control volume is shown by the dashed lines.

Governing equation: The general control volume equation is Eq. 4.12, but we can go immediately to Eq. 4.15a because of assumption (1) below,



$$\int_{CS} \rho \vec{V} \cdot d\vec{A} = 0$$

Assumptions:

- 1 Steady flow (given).
- 2 Incompressible flow (given).
- 3 Two-dimensional flow, given properties are independent of z .

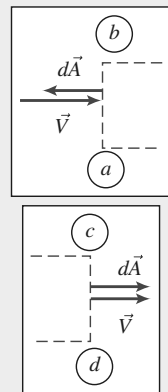
Assuming that there is no flow in the z direction, then

$$\begin{aligned} \int_{A_{ab}} \rho \vec{V} \cdot d\vec{A} + \int_{A_{bc}} \rho \vec{V} \cdot d\vec{A} + \int_{A_{cd}} \rho \vec{V} \cdot d\vec{A} + \int_{A_{da}} \rho \vec{V} \cdot d\vec{A} &= 0 \\ \therefore \dot{m}_{bc} = \int_{A_{bc}} \rho \vec{V} \cdot d\vec{A} &= - \int_{A_{ab}} \rho \vec{V} \cdot d\vec{A} - \int_{A_{cd}} \rho \vec{V} \cdot d\vec{A} \end{aligned} \quad (1)$$

We need to evaluate the integrals on the right side of the equation.

For depth w in the z direction, we obtain

$$\begin{aligned} \int_{A_{ab}} \rho \vec{V} \cdot d\vec{A} &= - \int_{A_{ab}} \rho u \, dA = - \int_{y_a}^{y_b} \rho uw \, dy \\ &= - \int_0^\delta \rho uw \, dy = - \int_0^\delta \rho Uw \, dy \\ \int_{A_{ab}} \rho \vec{V} \cdot d\vec{A} &= -[\rho Uwy]_0^\delta = -\rho Uw\delta \\ \int_{A_{cd}} \rho \vec{V} \cdot d\vec{A} &= \int_{A_{cd}} \rho u \, dA = \int_{y_d}^{y_c} \rho uw \, dy \\ &= \int_0^\delta \rho uw \, dy = \int_0^\delta \rho wU \left[2\left(\frac{y}{\delta}\right) - \left(\frac{y}{\delta}\right)^2 \right] dy \\ \int_{A_{cd}} \rho \vec{V} \cdot d\vec{A} &= \rho wU \left[\frac{y^2}{\delta} - \frac{y^3}{3\delta^2} \right]_0^\delta = \rho wU\delta \left[1 - \frac{1}{3} \right] = \frac{2\rho Uw\delta}{3} \end{aligned}$$



$$\left\{ \begin{array}{l} \vec{V} \cdot d\vec{A} \text{ is negative} \\ dA = wdy \\ u = U \text{ over area } ab \end{array} \right\}$$

$$\left\{ \begin{array}{l} \vec{V} \cdot d\vec{A} \text{ is positive} \\ dA = wdy \end{array} \right\}$$

Substituting into Eq. 1, we obtain

$$\begin{aligned} \therefore \dot{m}_{bc} &= \rho Uw\delta - \frac{2\rho Uw\delta}{3} = \frac{\rho Uw\delta}{3} \\ &= \frac{1}{3} \times 1.24 \frac{\text{kg}}{\text{m}^3} \times 30 \frac{\text{m}}{\text{s}} \times 0.6 \text{ m} \times 5 \text{ mm} \times \frac{\text{m}}{1000 \text{ mm}} \\ \dot{m}_{bc} &= 0.0372 \text{ kg/s} \quad \left\{ \begin{array}{l} \text{Positive sign indicates flow} \\ \text{out across surface } bc. \end{array} \right\} \quad \dot{m}_b \end{aligned}$$

This problem demonstrates use of the conservation of mass equation when we have nonuniform flow at a section.

Example 4.3 DENSITY CHANGE IN VENTING TANK

A tank of 0.05 m^3 volume contains air at 800 kPa (absolute) and 15°C . At $t = 0$, air begins escaping from the tank through a valve with a flow area of 65 mm^2 . The air passing through the valve has a speed of 300 m/s and a density of 6 kg/m^3 . Determine the instantaneous rate of change of density in the tank at $t = 0$.

Given: Tank of volume $V = 0.05 \text{ m}^3$ contains air at $p = 800 \text{ kPa}$ (absolute), $T = 15^\circ\text{C}$. At $t = 0$, air escapes through a valve. Air leaves with speed $V = 300 \text{ m/s}$ and density $\rho = 6 \text{ kg/m}^3$ through area $A = 65 \text{ mm}^2$.

Find: Rate of change of air density in the tank at $t=0$.

Solution: Choose a fixed control volume as shown by the dashed line.

Governing equation:

$$\frac{\partial}{\partial t} \int_{CV} \rho dV + \int_{CS} \rho \vec{V} \cdot d\vec{A} = 0$$

Assumptions:

- 1 Properties in the tank are uniform, but time-dependent.
- 2 Uniform flow at section ①.

Since properties are assumed uniform in the tank at any instant, we can take ρ out from within the volume integral of the first term,

$$\frac{\partial}{\partial t} \left[\rho_{CV} \int_{CV} dV \right] + \int_{CS} \rho \vec{V} \cdot d\vec{A} = 0$$

Now, $\int_{CV} dV = V$, and hence

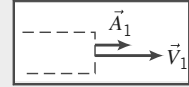
$$\frac{\partial}{\partial t} (\rho V)_{CV} + \int_{CS} \rho \vec{V} \cdot d\vec{A} = 0$$

The only place where mass crosses the boundary of the control volume is at surface ①. Hence

$$\int_{CS} \rho \vec{V} \cdot d\vec{A} = \int_{A_1} \rho \vec{V} \cdot d\vec{A} \quad \text{and} \quad \frac{\partial}{\partial t} (\rho V) + \int_{A_1} \rho \vec{V} \cdot d\vec{A} = 0$$

At surface ① the sign of $\rho \vec{V} \cdot d\vec{A}$ is positive, so

$$\frac{\partial}{\partial t} (\rho V) + \int_{A_1} \rho V dA = 0$$



Since flow is assumed uniform over surface ①, then

$$\frac{\partial}{\partial t} (\rho V) + \rho_1 V_1 A_1 = 0 \quad \text{or} \quad \frac{\partial}{\partial t} (\rho V) = -\rho_1 V_1 A_1$$

Since the volume, V , of the tank is not a function of time,

$$V \frac{\partial \rho}{\partial t} = -\rho_1 V_1 A_1$$

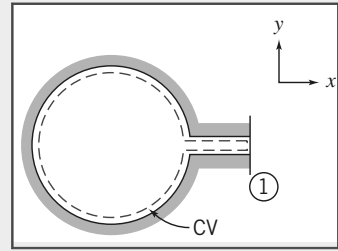
and

$$\frac{\partial \rho}{\partial t} = -\frac{\rho_1 V_1 A_1}{V}$$

At $t=0$,

$$\begin{aligned} \frac{\partial \rho}{\partial t} &= -6 \frac{\text{kg}}{\text{m}^3} \times 300 \frac{\text{m}}{\text{s}} \times 65 \text{ mm}^3 \times \frac{1}{0.05 \text{ m}^3} \times \frac{\text{m}^2}{10^6 \text{ mm}^2} \\ \frac{\partial \rho}{\partial t} &= -2.34(\text{kg/m}^3)/\text{s} \end{aligned} \quad \{ \text{The density is decreasing.} \} \quad \frac{\partial \rho}{\partial t}$$

This problem demonstrates use of the conservation of mass equation for unsteady flow problems.



4.4 Momentum Equation for Inertial Control Volume

We now obtain a control volume form of Newton's second law. We use the same procedure we just used for mass conservation, with one note of caution: the control volume coordinates (with respect to which we measure all velocities) are inertial; that is, the control volume coordinates xyz are either at rest or moving at constant speed with respect to an "absolute" set of coordinates XYZ . We begin with the mathematical formulation for a system and then use Eq. 4.10 to go from the system to the control volume formulation.

Recall that Newton's second law for a system moving relative to an inertial coordinate system was given by Eq. 4.2a as

$$\vec{F} = \frac{d\vec{P}}{dt} \Bigg|_{\text{system}} \quad (4.2a)$$

where the linear momentum of the system is given by

$$\vec{P}_{\text{system}} = \int_{M(\text{system})} \vec{V} dm = \int_{V(\text{system})} \vec{V} \rho dV \quad (4.2b)$$

and the resultant force, \vec{F} , includes all surface and body forces acting on the system,

$$\vec{F} = \vec{F}_S + \vec{F}_B$$

The system and control volume formulations are related using Eq. 4.10,

$$\frac{dN}{dt} \Bigg|_{\text{system}} = \frac{\partial}{\partial t} \int_{CV} \eta \rho dV + \int_{CS} \eta \rho \vec{V} \cdot d\vec{A} \quad (4.10)$$

To derive the control volume formulation of Newton's second law, we set

$$N = \vec{P} \quad \text{and} \quad \eta = \vec{V}$$

From Eq. 4.10, with this substitution, we obtain

$$\frac{d\vec{P}}{dt} \Bigg|_{\text{system}} = \frac{\partial}{\partial t} \int_{CV} \vec{V} \rho dV + \int_{CS} \vec{V} \rho \vec{V} \cdot d\vec{A} \quad (4.16)$$

From Eq. 4.2a

$$\frac{d\vec{P}}{dt} \Bigg|_{\text{system}} = \vec{F} \Big|_{\text{on system}} \quad (4.2a)$$

Since, in deriving Eq. 4.10, the system and the control volume coincided at t_0 , then

$$\vec{F} \Big|_{\text{on system}} = \vec{F} \Big|_{\text{on control volume}}$$

In light of this, Eqs. 4.2a and 4.16 may be combined to yield the control volume formulation of Newton's second law for a nonaccelerating control volume

$$\vec{F} = \vec{F}_S + \vec{F}_B = \frac{\partial}{\partial t} \int_{CV} \vec{V} \rho dV + \int_{CS} \vec{V} \rho \vec{V} \cdot d\vec{A} \quad (4.17a)$$

For cases when we have uniform flow at each inlet and exit, we can use

$$\vec{F} = \vec{F}_S + \vec{F}_B = \frac{\partial}{\partial t} \int_{CV} \vec{V} \rho dV + \sum_{CS} \vec{V} \rho \vec{V} \cdot \vec{A} \quad (4.17b)$$

Equations 4.17a and 4.17b are our nonaccelerating control volume forms of Newton's second law. It states that the total force due to surface and body forces acting on the control volume leads to a rate of change of momentum within the control volume (the volume integral) and/or a net rate at which momentum is leaving the control volume through the control surface.

We must be a little careful in applying Eqs. 4.17a. The first step will always be to carefully choose a control volume and its control surface so that we can evaluate the volume integral and the surface integral. In fluid mechanics the body force is usually gravity, so

$$\vec{F}_B = \int_{CV} \rho \vec{g} dV = \vec{W}_{CV} = Mg$$

where \vec{g} is the acceleration of gravity and \vec{W}_{CV} is the instantaneous weight of the entire control volume. In many applications the surface force is due to pressure,

$$\vec{F}_S = \int_A -pd\vec{A}$$

Note that the minus sign is to ensure that we always compute pressure forces acting *onto* the control surface (recall $d\vec{A}$ was chosen to be a vector pointing *out* of the control volume). It is worth stressing that *even at points on the surface that have an outflow*, the pressure force acts *onto* the control volume.

In Eqs. 4.17 we must also be careful in evaluating $\int_{CS} \vec{V} \rho \vec{V} \cdot d\vec{A}$ or $\Sigma_{CS} \vec{V} \rho \vec{V} \cdot \vec{A}$. This may be easier to do if we write them with the implied parentheses, $\int_{CS} \vec{V} \rho (\vec{V} \cdot d\vec{A})$ or $\Sigma_{CS} \vec{V} \rho (\vec{V} \cdot \vec{A})$. The velocity \vec{V} must be measured with respect to the control volume coordinates xyz , with the appropriate signs for its vector components u , v , and w . Recall also that the scalar product will be positive for outflow and negative for inflow (refer to Fig. 4.3).

The momentum equation (Eqs. 4.17) is a vector equation. We will usually write the three scalar components, as measured in the xyz coordinates of the control volume,

$$F_x = F_{S_x} + F_{B_x} = \frac{\partial}{\partial t} \int_{CV} u \rho dV + \int_{CS} u \rho \vec{V} \cdot d\vec{A} \quad (4.18a)$$

$$F_y = F_{S_y} + F_{B_y} = \frac{\partial}{\partial t} \int_{CV} v \rho dV + \int_{CS} v \rho \vec{V} \cdot d\vec{A} \quad (4.18b)$$

$$F_z = F_{S_z} + F_{B_z} = \frac{\partial}{\partial t} \int_{CV} w \rho dV + \int_{CS} w \rho \vec{V} \cdot d\vec{A} \quad (4.18c)$$

or, for uniform flow at each inlet and exit,

$$F_x = F_{S_x} + F_{B_x} = \frac{\partial}{\partial t} \int_{CV} u \rho dV + \sum_{CS} u \rho \vec{V} \cdot \vec{A} \quad (4.18d)$$

$$F_y = F_{S_y} + F_{B_y} = \frac{\partial}{\partial t} \int_{CV} v \rho dV + \sum_{CS} v \rho \vec{V} \cdot \vec{A} \quad (4.18e)$$

$$F_z = F_{S_z} + F_{B_z} = \frac{\partial}{\partial t} \int_{CV} w \rho dV + \sum_{CS} w \rho \vec{V} \cdot \vec{A} \quad (4.18f)$$

Note that, as we found for the mass conservation equation (Eq. 4.12), for steady flow the first term on the right in Eqs. 4.17 and 4.18 is zero.

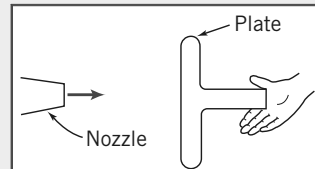
We will now look at five examples to illustrate some features of the various forms of the momentum equation for a control volume. Example 4.4 demonstrates how intelligent choice of the control volume can simplify analysis of a problem, Example 4.5 involves a problem in which we have significant body forces, Example 4.6 explains how to simplify surface force evaluations by working in gage pressures, Example 4.7 involves nonuniform surface forces, and Example 4.8 involves a problem in which we have unsteady flow.

Example 4.4 CHOICE OF CONTROL VOLUME FOR MOMENTUM ANALYSIS

Water from a stationary nozzle strikes a flat plate as shown. The water leaves the nozzle at 15 m/s; the nozzle area is 0.01 m². Assuming the water is directed normal to the plate, and flows along the plate, determine the horizontal force you need to resist to hold it in place.

Given: Water from a stationary nozzle is directed normal to the plate; subsequent flow is parallel to plate.

$$\begin{aligned} \text{Jet velocity, } \vec{V} &= 15\hat{i} \text{ m/s} \\ \text{Nozzle area, } A_n &= 0.01 \text{ m}^2 \end{aligned}$$



Find: Horizontal force on your hand.

Solution: We chose a coordinate system in defining the problem above. We must now choose a suitable control volume. Two possible choices are shown by the dashed lines below.

In both cases, water from the nozzle crosses the control surface through area A_1 (assumed equal to the nozzle area) and is assumed to leave the control volume tangent to the plate surface in the $+y$ or $-y$ direction. Before trying to decide which is the “best” control volume to use, let us write the governing equations.

$$\vec{F} = \vec{F}_S + \vec{F}_B = \frac{\partial}{\partial t} \int_{CV} \vec{V} \rho dV + \int_{CS} \vec{V} \rho \vec{V} \cdot d\vec{A} \quad \text{and} \quad \frac{\partial}{\partial t} \int_{CV} \rho dV + \int_{CS} \rho \vec{V} \cdot d\vec{A} = 0$$

Assumptions:

- 1 Steady flow.
- 2 Incompressible flow.
- 3 Uniform flow at each section where fluid crosses the CV boundaries.

Regardless of our choice of control volume, assumptions (1), (2), and (3) lead to

$$\vec{F} = \vec{F}_S + \vec{F}_B = \sum_{CS} \vec{V} \rho \vec{V} \cdot \vec{A} \quad \text{and} \quad \sum_{CS} \rho \vec{V} \cdot \vec{A} = 0$$

Evaluating the momentum flux term will lead to the same result for both control volumes. We should choose the control volume that allows the most straightforward evaluation of the forces.

Remember in applying the momentum equation that the force, \vec{F} , represents all forces acting *on* the control volume.

Let us solve the problem using each of the control volumes.

CV_I

The control volume has been selected so that the area of the left surface is equal to the area of the right surface. Denote this area by A .

The control volume cuts through your hand. We denote the components of the reaction force of your hand on the control volume as R_x and R_y and assume both to be positive. (The force of the control volume on your hand is equal and opposite to R_x and R_y)

Atmospheric pressure acts on all surfaces of the control volume. Note that *the pressure in a free jet is ambient*, i.e., in this case atmospheric. The distributed force due to atmospheric pressure has been shown on the vertical faces only.

The body force on the control volume is denoted as W .

Since we are looking for the horizontal force, we write the x component of the steady flow momentum equation

$$F_{S_x} + F_{B_x} = \sum_{CS} u \rho \vec{V} \cdot \vec{A}$$

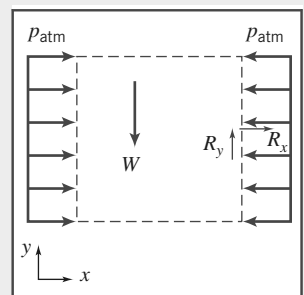
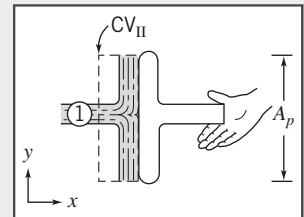
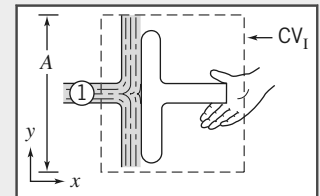
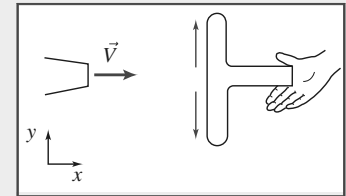
There are no body forces in the x direction, so $F_{B_x} = 0$, and

$$F_{S_x} = \sum_{CS} u \rho \vec{V} \cdot \vec{A}$$

To evaluate F_{S_x} , we must include all surface forces acting on the control volume

$$F_{S_x} = p_{atm} A - p_{atm} A + R_x$$

force due to atmospheric pressure acts to right (positive direction) on left surface force due to atmospheric pressure acts to left (negative direction) on right surface force of your hand on control volume (assumed positive)



Consequently, $F_{S_x} = R_x$, and

$$R_x = \sum_{CS} u \rho \vec{V} \cdot \vec{A} = u \rho \vec{V} \cdot \vec{A}|_1$$

{For top and bottom surfaces, $u = 0$ }

At ①, $\rho \vec{V}_1 \cdot \vec{A}_1 = \rho (-V_1 A_1)$ since

$$R_x = -u_1 \rho V_1 A_1$$

\vec{V}_1 and \vec{A}_1 are 180° apart.

Note that $u_1 = V_1$

$$R_x = -15 \frac{\text{m}}{\text{s}} \times 999 \frac{\text{kg}}{\text{m}^3} \times 15 \frac{\text{m}}{\text{s}} \times 0.01 \text{ m}^2 \times \frac{\text{N} \cdot \text{s}^2}{\text{kg} \cdot \text{m}}$$

{ $u_1 = 15 \text{ m/s}$ }

$$R_x = -2.25 \text{ kN}$$

{ R_x acts opposite to positive direction assumed.}

The horizontal force on your hand is

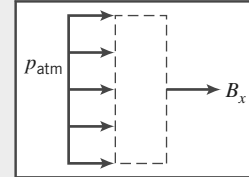
$$K_x = -R_x = 2.25 \text{ kN} \xleftarrow{\text{force on your hand acts to the right}} K_x$$

CV_{II} with Horizontal Forces Shown

The control volume has been selected so the areas of the left surface and of the right surface are equal to the area of the plate. Denote this area by A_p .

The control volume is in contact with the plate over the entire plate surface. We denote the horizontal reaction force from the plate on the control volume as B_x and assume it to be positive.

Atmospheric pressure acts on the left surface of the control volume and on the two horizontal surfaces.



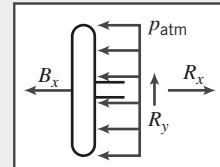
The body force on this control volume has no component in the x direction.

Then the x component of the momentum equation,

$$F_{S_x} = \sum_{CS} u \rho \vec{V} \cdot \vec{A}$$

yields

$$F_{S_x} = p_{atm} A_p + B_x = u \rho \vec{V} \cdot \vec{A}|_1 = -u_1 V_1 A_1 = -2.25 \text{ kN}$$



Then

$$B_x = -p_{atm} A_p - 2.25 \text{ kN}$$

To determine the net force on the plate, we need a free-body diagram of the plate:

$$\sum F_x = 0 = -B_x - p_{atm} A_p + R_x$$

$$R_x = p_{atm} A_p + B_x$$

$$R_x = p_{atm} A_p + (-p_{atm} A_p - 2.25 \text{ kN}) = -2.25 \text{ kN}$$

Then the horizontal force on your hand is $K_x = -R_x = 2.25 \text{ kN}$.

Note that the choice of CV_{II} meant we needed an additional free-body diagram. In general it is best to select the control volume so that the force sought acts explicitly on the control volume.

Notes:

- This problem demonstrates how thoughtful choice of the control volume can simplify use of the momentum equation.
- The analysis would have been greatly simplified if we had worked in gage pressures (see Example 4.6).
- For this problem the force generated was entirely due to the plate absorbing the jet's horizontal momentum.

Example 4.5 TANK ON SCALE: BODY FORCE

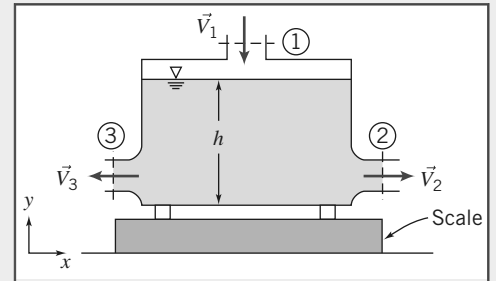
A metal container 0.61 m high, with an inside cross-sectional area of 0.09 m^2 , weighs 22.2 N when empty. The container is placed on a scale and water flows in through an opening in the top and out through the two equal-area openings in the sides, as shown in the diagram. Under steady flow conditions, the height of the water in the tank is 0.58 m.

$$A_1 = 0.009 \text{ m}^2$$

$$\vec{V}_1 = -3\hat{j} \text{ m/s}$$

$$A_2 = A_3 = 0.009 \text{ m}^2$$

Your boss claims that the scale will read the weight of the volume of water in the tank plus the tank weight, i.e., that we can treat this as a simple statics problem. You disagree, claiming that a fluid flow analysis is required. Who is right, and what does the scale indicate?



Given: Metal container, of height 0.61 m and cross-sectional area $A = 0.09 \text{ m}^2$, weighs 22.2 lbf when empty. Container rests on scale. Under steady flow conditions water depth is $h = 0.58 \text{ m}$. Water enters vertically at section ① and leaves horizontally through sections ② and ③

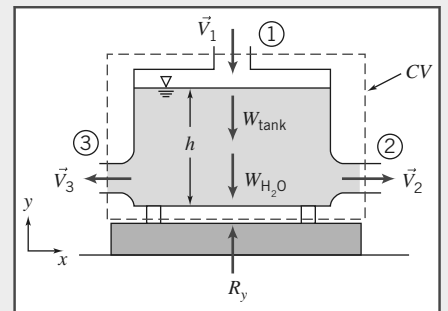
$$A_1 = 0.009 \text{ m}^2$$

$$\vec{V}_1 = -3\hat{j} \text{ m/s}$$

$$A_2 = A_3 = 0.009 \text{ m}^2$$

Find: Scale reading.

Solution: Choose a control volume as shown; R_y is the force of the scale on the control volume (exerted on the control volume through the supports) and is assumed positive.



The weight of the tank is designated W_{tank} ; the weight of the water in the tank is $W_{\text{H}_2\text{O}}$.

Atmospheric pressure acts uniformly on the entire control surface, and therefore has no net effect on the control volume. Because of this null effect we have not shown the pressure distribution in the diagram.

Governing equations: The general control volume momentum and mass conservation equations are Eqs. 4.17 and 4.12, respectively,

$$= 0(1)$$

$$\vec{F}_S + \vec{F}_B = \frac{\partial}{\partial t} \int_{\text{CV}} \vec{V} \rho dV + \int_{\text{CS}} \vec{V} \rho \vec{V} \cdot d\vec{A}$$

$$= 0(1)$$

$$\frac{\partial}{\partial t} \int_{\text{CV}} \rho dV + \int_{\text{CS}} \rho \vec{V} \cdot d\vec{A} = 0$$

Note that we usually start with the simplest forms based on the problem assumptions, (e.g., steady flow) of the mass conservation and momentum equations. However, in this problem, for illustration purposes, we start with the most general forms of the equations.

Assumptions:

- 1 Steady flow (given).
- 2 Incompressible flow.
- 3 Uniform flow at each section where fluid crosses the CV boundaries.

We are only interested in the y component of the momentum equation

$$\begin{aligned}
 F_{S_y} + F_{B_y} &= \int_{CS} v \rho \vec{V} \cdot d\vec{A} && (1) \\
 F_{S_y} &= R_y && \{\text{There is no net force due to atmosphere pressure.}\} \\
 F_{B_y} &= -W_{\text{tank}} - W_{H_2O} && \{\text{Both body forces act in negative } y \text{ direction.}\} \\
 W_{H_2O} &= \rho g V = \gamma Ah \\
 \int_{CS} v \rho \vec{V} \cdot d\vec{A} &= \int_{A_1} v \rho \vec{V} \cdot d\vec{A} = \int_{A_1} v (-\rho V_1 dA_1) && \left. \begin{array}{l} \vec{V} \cdot d\vec{A} \text{ is negative at } \textcircled{1} \\ v = 0 \text{ at sections } \textcircled{2} \text{ and } \textcircled{3} \end{array} \right\} \\
 &= v_1 (-\rho V_1 A_1) && \left. \begin{array}{l} \text{We are assuming uniform} \\ \text{properties at } \textcircled{1} \end{array} \right\}
 \end{aligned}$$

Using these results in Eq. 1 gives

$$R_y - W_{\text{tank}} - \gamma Ah = v_1 (-\rho V_1 A_1)$$

Note that v_1 is the y component of the velocity, so that $v_1 = -V_1$, where we recall that $V_1 = 3 \text{ m/s}$ is the magnitude of velocity \vec{V}_1 . Hence, solving for R_y ,

$$\begin{aligned}
 R_y &= W_{\text{tank}} + \gamma Ah + \rho V_1^2 A_1 \\
 &= 22.2 \text{ N} + 9800 \frac{\text{N}}{\text{m}^3} \times 0.09 \text{ m}^2 \times 0.58 \text{ m} + 1000 \frac{\text{kg}}{\text{m}^3} \times 9 \frac{\text{m}^2}{\text{s}^2} \times 0.009 \text{ m}^2 \times \frac{\text{N} \cdot \text{s}^2}{\text{kg} \cdot \text{m}} \\
 &= 22.2 \text{ N} + 511.6 \text{ N} + 81 \text{ N} \\
 R_y &= 614.8 \text{ N}
 \end{aligned}$$

Note that this is the force of the scale on the control volume and is also the reading on the scale. We can see that the scale reading is due to: the tank weight (22.2 N), the weight of water instantaneously in the tank (511.6 N), and the force involved in absorbing the downward momentum of the fluid at section $\textcircled{1}$ (81 N). Hence neglecting the momentum results in an error of almost 13 percent.

This problem illustrates use of the momentum equation including significant body forces.

Example 4.6 FLOW THROUGH ELBOW: USE OF GAGE PRESSURES

Water flows steadily through the 90° reducing elbow shown in the diagram. At the inlet to the elbow, the absolute pressure is 220 kPa and the cross-sectional area is 0.01 m^2 . At the outlet, the cross-sectional area is 0.0025 m^2 and the velocity is 16 m/s . The elbow discharges to the atmosphere. Determine the force required to hold the elbow in place.

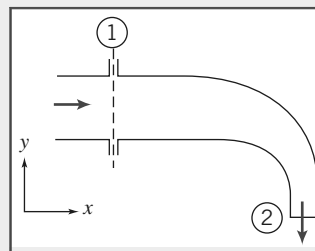
Given: Steady flow of water through 90° reducing elbow.

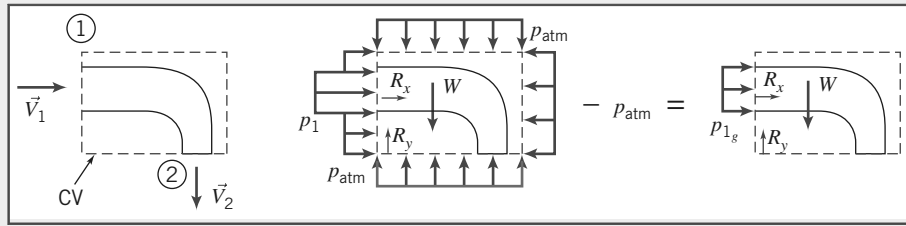
$$p_1 = 220 \text{ kPa (abs)} \quad A_1 = 0.01 \text{ m}^2 \quad \vec{V}_2 = -16 \hat{j} \text{ m/s} \quad A_2 = 0.0025 \text{ m}^2$$

Find: Force required to hold elbow in place.

Solution: Choose a fixed control volume as shown. Note that we have several surface force computations: p_1 on area A_1 and p_{atm} everywhere else. The exit at section $\textcircled{2}$ is to a free jet, and so at ambient (i.e., atmospheric) pressure. We can use a simplification here. If we subtract p_{atm} from the entire surface (a null effect as far as forces are concerned) we can work in gage pressures, as shown.

Note that since the elbow is anchored to the supply line, in addition to the reaction forces R_x and R_y (shown), there would also be a reaction moment (not shown).





Governing equations:

$$\begin{aligned} \vec{F} &= \vec{F}_S + \vec{F}_B = \frac{\partial}{\partial t} \int_{CV} \vec{V} \rho dV + \int_{CS} \vec{V} \rho \vec{V} \cdot dA \\ &= 0(4) \\ \frac{\partial}{\partial t} \int_{CV} \rho dV + \int_{CS} \rho \vec{V} \cdot dA &= 0 \end{aligned}$$

Assumptions:

- 1 Uniform flow at each section.
- 2 Atmospheric pressure, $p_{atm} = 101$ kPa (abs).
- 3 Incompressible flow.
- 4 Steady flow (given).
- 5 Neglect weight of elbow and water in elbow.

Once again we started with the most general form of the governing equations. Writing the x component of the momentum equation results in

$$\begin{aligned} F_{S_x} &= \int_{CS} u \rho \vec{V} \cdot d\vec{A} = \int_{A_1} u \rho \vec{V} \cdot d\vec{A} & \{ F_{B_x} = 0 \text{ and } u_2 = 0 \} \\ p_{1g} A_1 + R_x &= \int_{A_1} u \rho \vec{V} \cdot d\vec{A} \end{aligned}$$

so

$$\begin{aligned} R_x &= -p_{1g} A_1 + \int_{A_1} u \rho \vec{V} \cdot d\vec{A} \\ &= -p_{1g} A_1 + u_1 (-\rho V_1 A_1) \\ R_x &= -p_{1g} A_1 - \rho V_1^2 A_1 \end{aligned}$$

Note that u_1 is the x component of the velocity, so that $u_1 = V_1$. To find V_1 , use the mass conservation equation:

$$\begin{aligned} \int_{CS} \rho \vec{V} \cdot d\vec{A} &= \int_{A_1} \rho \vec{V} \cdot d\vec{A} + \int_{A_2} \rho \vec{V} \cdot d\vec{A} = 0 \\ \therefore (-\rho V_1 A_1) + (\rho V_2 A_2) &= 0 \end{aligned}$$

and

$$V_1 = V_2 \frac{A_2}{A_1} = 16 \frac{\text{m}}{\text{s}} \times \frac{0.0025}{0.01} = 4 \text{ m/s}$$

We can now compute R_x

$$\begin{aligned} R_x &= -p_{1g} A_1 - \rho V_1^2 A_1 \\ &= -1.19 \times 10^5 \frac{\text{N}}{\text{m}^2} \times 0.01 \text{ m}^2 - 999 \frac{\text{kg}}{\text{m}^3} \times 16 \frac{\text{m}^2}{\text{s}^2} \times 0.01 \text{ m}^2 \times \frac{\text{N} \cdot \text{s}^2}{\text{kg} \cdot \text{m}} \\ R_x &= -1.35 \text{ kN} \end{aligned}$$

Writing the y component of the momentum equation gives

$$F_{S_y} + F_{B_y} = R_y + F_{B_y} = \int_{CS} v \rho \vec{V} \cdot d\vec{A} = \int_{A_2} v \rho \vec{V} \cdot d\vec{A} \quad \{v_1 = 0\}$$

or

$$\begin{aligned} R_y &= -F_{B_y} + \int_{A_2} v \rho \vec{V} \cdot d\vec{A} \\ &= -F_{B_y} + v_2 (\rho V_2 A_2) \\ R_y &= -F_{B_y} - \rho V_2^2 A_2 \end{aligned}$$

Note that v_2 is the y component of the velocity, so that $v_2 = -V_2$, where V_2 is the magnitude of the exit velocity.

Substituting known values

$$\begin{aligned} R_y &= -F_{B_y} - \rho V_2^2 A_2 \\ &= -F_{B_y} - 999 \frac{\text{kg}}{\text{m}^3} \times (16)^2 \frac{\text{m}^2}{\text{s}^2} \times 0.0025 \text{ m}^2 \times \frac{\text{N} \cdot \text{s}^2}{\text{kg} \cdot \text{m}} \\ &= -F_{B_y} - 639 \text{ N} \end{aligned}$$

Neglecting F_{B_y} gives

$$R_y = -639 \text{ N}$$

This problem illustrates how using gage pressures simplifies evaluation of the surface forces in the momentum equation.

Example 4.7 FLOW UNDER A SLUICE GATE: HYDROSTATIC PRESSURE FORCE

Water in an open channel is held in by a sluice gate. Compare the horizontal force of the water on the gate (a) when the gate is closed and (b) when it is open and the flow is steady. Assume the flow at sections ① and ② is incompressible and uniform, and that, because the streamlines are straight there, the pressure distributions are hydrostatic.

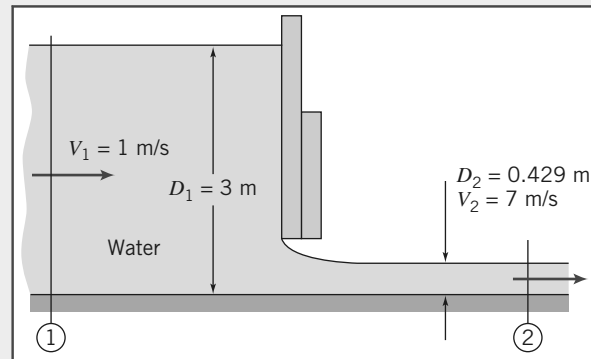
Given: Flow under sluice gate. Width = w .

Find: Horizontal force (per unit width) on the closed and open gate.

Solution: Choose a control volume as shown for the open gate. Note that it is much simpler to work in gage pressures, as we learned in Example 4.6.

The forces acting on the control volume include:

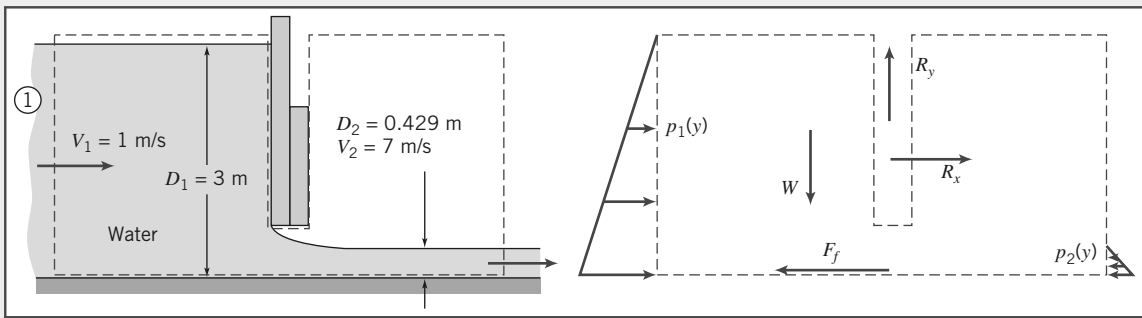
- Force of gravity W .
- Friction force F_f .
- Components R_x and R_y of reaction force from gate.
- Hydrostatic pressure distribution on vertical surfaces, assumption (6).
- Pressure distribution $p_b(x)$ along bottom surface (not shown).



Apply the x component of the momentum equation.

Governing equation:

$$\begin{aligned} &= 0(2) = 0(3) \\ F_{S_x} + \cancel{F_{B_x}} = \cancel{\frac{\partial}{\partial t} \int_{CV} u \rho dV} + \int_{CS} u \rho \vec{V} \cdot d\vec{A} \end{aligned}$$



Assumptions:

- 1 F_f negligible (neglect friction on channel bottom).
- 2 $F_{B_x} = 0$.
- 3 Steady flow.
- 4 Incompressible flow (given).
- 5 Uniform flow at each section (given).
- 6 Hydrostatic pressure distributions at ① and ② (given).

Then

$$F_{S_x} = F_{R_1} + F_{R_2} + R_x = u_1(-\rho V_1 w D_1) + u_2(\rho V_2 w D_2)$$

The surface forces acting on the CV are due to the pressure distributions and the unknown force R_x . From assumption (6), we can integrate the gage pressure distributions on each side to compute the hydrostatic forces F_{R_1} and F_{R_2} ,

$$F_{R_1} = \int_0^{D_1} p_1 dA = w \int_0^{D_1} \rho gy dy = \rho gw \frac{y^2}{2} \Big|_0^{D_1} = \frac{1}{2} \rho gw D_1^2$$

where y is measured downward from the free surface of location ①, and

$$F_{R_2} = \int_0^{D_2} p_2 dA = w \int_0^{D_2} \rho gy dy = \rho gw \frac{y^2}{2} \Big|_0^{D_2} = \frac{1}{2} \rho gw D_2^2$$

where y is measured downward from the free surface of location ②. (Note that we could have used the hydrostatic force equation, Eq. 3.10b, directly to obtain these forces.)

Evaluating F_{S_x} gives

$$F_{S_x} = R_x + \frac{\rho gw}{2} (D_1^2 - D_2^2)$$

Substituting into the momentum equation, with $u_1 = V_1$ and $u_2 = V_2$, gives

$$R_x + \frac{\rho gw}{2} (D_1^2 - D_2^2) = -\rho V_1^2 w D_1 + \rho V_2^2 w D_2$$

or

$$R_x = \rho w (V_2^2 D_2 - V_1^2 D_1) - \frac{\rho gw}{2} (D_1^2 - D_2^2)$$

The second term on the right is the net hydrostatic force on the gate; the first term “corrects” this for the case when the gate is open. What is the nature of this “correction”? The pressure in the fluid far away from the gate in either direction is hydrostatic, but because we have significant velocity variations close to the gate, the pressure distributions deviate significantly from hydrostatic. For example, as the fluid accelerates under the gate there will be a significant pressure drop on the lower left side of the gate. Deriving this pressure field would be a difficult task, but by careful choice of our CV we have avoided having to do so.

We can now compute the horizontal force per unit width,

$$\begin{aligned}\frac{R_x}{w} &= \rho(V_2^2 D_2 - V_1^2 D_1) - \frac{\rho g}{2}(D_1^2 - D_2^2) \\ &= 999 \frac{\text{kg}}{\text{m}^3} \times [(7)^2(0.429) - (1)^2(3)] \frac{\text{m}^2}{\text{s}^2} \text{m} \times \frac{\text{N} \cdot \text{s}^2}{\text{kg} \cdot \text{m}} \\ &\quad - \frac{1}{2} \times 999 \frac{\text{kg}}{\text{m}^3} \times 9.81 \frac{\text{m}}{\text{s}^2} \times [(3)^2 - (0.429)^2] \text{m}^2 \times \frac{\text{N} \cdot \text{s}^2}{\text{kg} \cdot \text{m}} \\ \frac{R_x}{w} &= 18.0 \text{ kN/m} - 43.2 \text{ kN/m} \\ \frac{R_x}{w} &= -25.2 \text{ kN/m}\end{aligned}$$

R_x is the external force acting on the control volume, applied to the CV by the gate. Therefore, the force of the water on the gate is K_x , where $K_x = -R_x$. Thus,

$$\frac{K_x}{w} = -\frac{R_x}{w} = 25.2 \text{ kN/m} \leftarrow \frac{K_x}{w}$$

This force can be compared to the force on the closed gate of 44.1 kN (obtained from the second term on the right in the equation above, evaluated with D_2 set to zero because for the closed gate there is no fluid on the right of the gate)—the force on the open gate is significantly less as the water accelerates out under the gate.

This problem illustrates the application of the momentum equation to a control volume for which the pressure is not uniform on the control surface.

Example 4.8 CONVEYOR BELT FILLING: RATE OF CHANGE OF MOMENTUM IN CONTROL VOLUME

A horizontal conveyor belt moving at 0.9 m/s receives sand from a hopper. The sand falls vertically from the hopper to the belt at a speed of 1.5 m/s and a flow rate of 225 kg/s (the density of sand is approximately 1580 kg/m³). The conveyor belt is initially empty but begins to fill with sand. If friction in the drive system and rollers is negligible, find the tension required to pull the belt while the conveyor is filling.

Given: Conveyor and hopper shown in sketch.

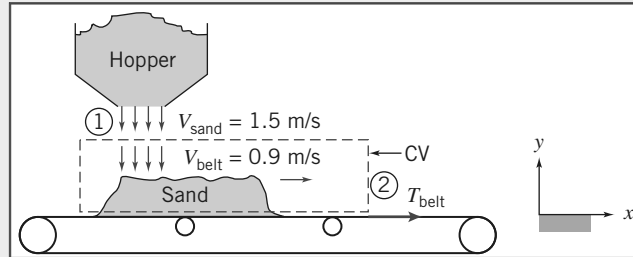
Find: T_{belt} at the instant shown.

Solution: Use the control volume and coordinates shown. Apply the x component of the momentum equation.

Governing equations:

$$= 0(2)$$

$$F_{S_x} + \oint_{CV} \frac{\partial}{\partial t} \int_{CV} u \rho dV + \int_{CS} u \rho \vec{V} \cdot d\vec{A} = \frac{\partial}{\partial t} \int_{CV} \rho dV + \int_{CS} \rho \vec{V} \cdot d\vec{A} = 0$$



Assumptions:

- 1 $F_{S_x} = T_{\text{belt}} = T$.
- 2 $F_{B_x} = 0$.
- 3 Uniform flow at section ①.
- 4 All sand on belt moves with $V_{\text{belt}} = V_b$.

Then

$$T = \frac{\partial}{\partial t} \int_{CV} u\rho dV + u_1(-\rho V_1 A_1) + u_2(\rho V_2 A_2)$$

Since $u_1 = 0$, and there is no flow at section ②,

$$T = \frac{\partial}{\partial t} \int_{CV} u\rho dV$$

From assumption (4), inside the CV, $u = V_b = \text{constant}$, and hence

$$T = V_b \frac{\partial}{\partial t} \int_{CV} \rho dV = V_b \frac{\partial M_s}{\partial t}$$

where M_s is the mass of sand on the belt and inside the control volume. This result is perhaps not surprising—the tension in the belt is the force required to increase the momentum inside the CV. The tension is increasing because even though the velocity of the mass in the CV is constant, the mass is not. From the continuity equation,

$$\frac{\partial}{\partial t} \int_{CV} \rho dV = \frac{\partial}{\partial t} M_s = - \int_{CS} \rho \vec{V} \cdot d\vec{A} = \dot{m}_s = 225 \text{ kg/s}$$

Then

$$T = V_b \dot{m}_s = 0.9 \frac{\text{m}}{\text{s}} \times 225 \frac{\text{kg}}{\text{s}} \times \frac{\text{N} \cdot \text{s}^2}{\text{kg} \cdot \text{m}}$$

$$T = 203.4 \text{ N} \xrightarrow{\hspace{10em}} T$$

This problem illustrates application of the momentum equation to a control volume in which the momentum is changing.

Differential Control Volume Analysis

The control volume approach, as we have seen in the previous examples, provides useful results when applied to a finite region.

If we apply the approach to a differential control volume, we can obtain differential equations describing a flow field. In this section, we will apply the conservation of mass and momentum equations to such a control volume to obtain a simple differential equation describing flow in a steady, incompressible, frictionless flow, and integrate it along a streamline to obtain the famous Bernoulli equation.

Let us apply the continuity and momentum equations to a steady incompressible flow without friction, as shown in Fig. 4.4. The control volume chosen is fixed in space and bounded by flow streamlines, and is thus an element of a stream tube. The length of the control volume is ds .

Because the control volume is bounded by streamlines, flow across the bounding surfaces occurs only at the end sections. These are located at coordinates s and $s + ds$, measured along the central streamline.

Properties at the inlet section are assigned arbitrary symbolic values. Properties at the outlet section are assumed to increase by differential amounts. Thus at $s + ds$, the flow speed is assumed to be $V_s + dV_s$, and so on. The differential changes, dp , dV_s , and dA , all are assumed to be positive in setting up the problem. As in a free-body analysis in statics or dynamics, the actual algebraic sign of each differential change will be determined from the results of the analysis.

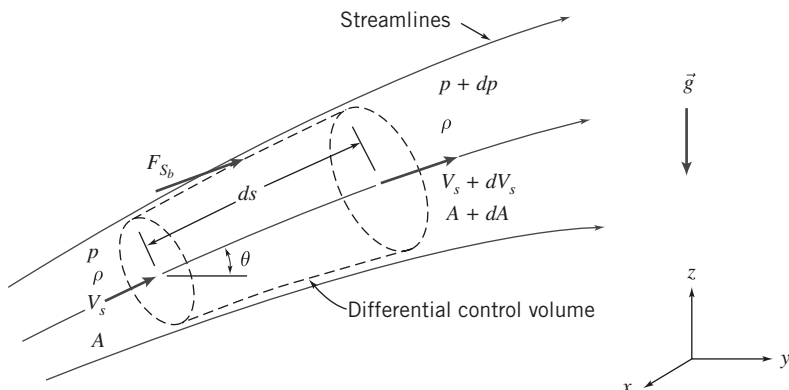


Fig. 4.4 Differential control volume for momentum analysis of flow through a stream tube.

Now let us apply the continuity equation and the s component of the momentum equation to the control volume of Fig. 4.4.

a. Continuity Equation

$$\text{Basic equation : } \frac{\partial}{\partial t} \int_{CV} \rho dV + \int_{CS} \rho \vec{V} \cdot d\vec{A} = 0 \quad (4.12)$$

Assumptions:

- 1 Steady flow.
- 2 No flow across bounding streamlines.
- 3 Incompressible flow, $\rho = \text{constant}$.

Then

$$(-\rho V_s A) + \{\rho(V_s + dV_s)(A + dA)\} = 0$$

so

$$\rho(V_s + dV_s)(A + dA) = \rho V_s A \quad (4.19a)$$

On expanding the left side and simplifying, we obtain

$$V_s dA + A dV_s + dA dV_s = 0$$

But $dA dV_s$ is a product of differentials, which may be neglected compared with $V_s dA$ or $A dV_s$. Thus

$$V_s dA + A dV_s = 0 \quad (4.19b)$$

b. Streamwise Component of the Momentum Equation

$$\text{Basic equation : } F_{S_s} + F_{B_s} = \frac{\partial}{\partial t} \int_{CV} u_s \rho dV + \int_{CS} u_s \rho \vec{V} \cdot d\vec{A} \quad (4.20)$$

Assumption: (4) No friction, so F_{S_b} is due to pressure forces only.

The surface force (due only to pressure) will have three terms:

$$F_{S_s} = pA - (p + dp)(A + dA) + \left(p + \frac{dp}{2} \right) dA \quad (4.21a)$$

The first and second terms in Eq. 4.21a are the pressure forces on the end faces of the control surface. The third term is F_{s_b} , the pressure force acting in the s direction on the bounding stream surface of the control volume. Its magnitude is the product of the average pressure acting on the stream surface, $p + \frac{1}{2}dp$, times the area component of the stream surface in the s direction, dA . Equation 4.21a simplifies to

$$F_{S_s} = -A dp - \frac{1}{2}dp dA \quad (4.21b)$$

The body force component in the s direction is

$$F_{B_s} = \rho g_s dV = \rho(-g \sin \theta) \left(A + \frac{dA}{2} \right) ds$$

But $\sin \theta ds = dz$, so that

$$F_{B_s} = -\rho g \left(A + \frac{dA}{2} \right) dz \quad (4.21c)$$

The momentum flux will be

$$\int_{CS} u_s \rho \vec{V} \cdot d\vec{A} = V_s (-\rho V_s A) + (V_s + dV_s) \{\rho(V_s + dV_s)(A + dA)\}$$

since there is no mass flux across the bounding stream surfaces. The mass flux factors in parentheses and braces are equal from continuity, Eq. 4.19a, so

$$\int_{CS} u_s \rho \vec{V} \cdot d\vec{A} = V_s (-\rho V_s A) + (V_s + dV_s)(\rho V_s A) = \rho V_s A dV_s \quad (4.22)$$

Substituting Eqs. 4.21b, 4.21c, and 4.22 into Eq. 4.20 (the momentum equation) gives

$$-A dp - \frac{1}{2} dp dA - \rho g A dz - \frac{1}{2} \rho g dA dz = \rho V_s A dV_s$$

Dividing by ρA and noting that products of differentials are negligible compared with the remaining terms, we obtain

$$-\frac{dp}{\rho} - g dz = V_s dV_s = d\left(\frac{V_s^2}{2}\right)$$

or

$$\frac{dp}{\rho} + d\left(\frac{V_s^2}{2}\right) + g dz = 0 \quad (4.23)$$

Because the flow is incompressible, this equation may be integrated to obtain

$$\frac{p}{\rho} + \frac{V_s^2}{2} + gz = \text{constant} \quad (4.24)$$

or, dropping subscript s ,

$$\frac{p}{\rho} + \frac{V_s^2}{2} + gz = \text{constant} \quad (4.24)$$

This equation is subject to the restrictions:

- 1 Steady flow.
- 2 No friction.
- 3 Flow along a streamline.
- 4 Incompressible flow.

We have derived one form of perhaps the most famous (and misused) equation in fluid mechanics—the Bernoulli equation. It can be used *only* when the four restrictions listed above apply. Although no real flow satisfies all these restrictions (especially the second), we can approximate the behavior of many flows with Eq. 4.24.

For example, the equation is widely used in aerodynamics to relate the pressure and velocity in a flow (e.g., it explains the lift of a subsonic wing). It could also be used to find the pressure at the inlet of the reducing elbow analyzed in Example 4.6 or to determine the velocity of water leaving the sluice gate of Example 4.7 (both of these flows approximately satisfy the four restrictions). On the other hand, Eq. 4.24 does *not* correctly describe the variation of water pressure in pipe flow. According to it, for a horizontal pipe of constant diameter, the pressure will be constant, but in fact the pressure drops significantly along the pipe.

The Bernoulli equation and the limits on its use, are so important we will derive it again and discuss its limitations in detail in Chapter 6. In Example 4.9 we will show the use of the Bernoulli equation for a situation in which all of the limitations apply.

Example 4.9 NOZZLE FLOW: APPLICATION OF BERNOULLI EQUATION

Water flows steadily through a horizontal nozzle, discharging to the atmosphere. At the nozzle inlet the diameter is D_1 ; at the nozzle outlet the diameter is D_2 . Derive an expression for the minimum gage pressure required at the nozzle inlet to produce a given volume flow rate, Q . Evaluate the inlet gage pressure if $D_1 = 75$ mm, $D_2 = 25$ mm, and the desired flow rate is $0.02 \text{ m}^3/\text{s}$.

Given: Steady flow of water through a horizontal nozzle, discharging to the atmosphere.

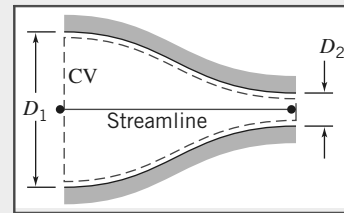
$$D_1 = 75 \text{ mm} \quad D_2 = 25 \text{ mm} \quad p_2 = p_{\text{atm}}$$

Find: (a) p_{1g} as a function of volume flow rate, Q .
 (b) p_{1g} for $Q = 0.7 \text{ ft}^3/\text{s}$.

Solution:

Governing equations:

$$\begin{aligned} \frac{p_1}{\rho} + \frac{V_1^2}{2} + gz_1 &= \frac{p_2}{\rho} + \frac{V_2^2}{2} + gz_2 \\ &= 0(1) \\ \oint_C \rho d\psi + \int_{CS} \rho \vec{V} \cdot d\vec{A} &= 0 \end{aligned}$$



Assumptions:

- 1 Steady flow (given).
- 2 Incompressible flow.
- 3 Frictionless flow.
- 4 Flow along a streamline.
- 5 $z_1 = z_2$.
- 6 Uniform flow at sections ① and ②.

Apply the Bernoulli equation along a streamline between points ① and ② to evaluate p_1 . Then

$$p_{1g} = p_1 - p_{\text{atm}} = p_1 - p_2 = \frac{\rho}{2}(V_2^2 - V_1^2) = \frac{\rho}{2}V_1^2 \left[\left(\frac{V_2}{V_1} \right)^2 - 1 \right]$$

Apply the continuity equation

$$(-\rho V_1 A_1) + (\rho V_2 A_2) = 0 \quad \text{or} \quad V_1 A_1 = V_2 A_2 = Q$$

so that

$$\frac{V_2}{V_1} = \frac{A_1}{A_2} \quad \text{and} \quad V_1 = \frac{Q}{A_1}$$

Then

$$p_{1g} = \frac{\rho Q^2}{2A_1^2} \left[\left(\frac{A_1}{A_2} \right)^2 - 1 \right]$$

Since $A = \pi D^2/4$, then

$$p_{1g} = \frac{8\rho Q^2}{\pi^2 D_1^4} \left[\left(\frac{D_1}{D_2} \right)^4 - 1 \right] \xrightarrow{p_{1g}}$$

Note that for a given nozzle the pressure required is proportional to the square of the flow rate, which is consistent with Eq. 4.24, which shows that $p \sim V^2 \sim Q^2$. With $D_1 = 75 \text{ mm}$, $D_2 = 25 \text{ mm}$, and $\rho = 1000 \text{ kg/m}^3$,

$$p_{1g} = \frac{8}{\pi^2} \times 1000 \frac{\text{kg}}{\text{m}^3} \times \frac{1}{(0.075)^4 \text{m}^4} \times Q^2 [(3.0)^4 - 1] \frac{\text{N} \cdot \text{s}^2}{\text{kg} \cdot \text{m}} \times \frac{\text{Pa} \cdot \text{m}^2}{\text{N}^2}$$

$$p_{1g} = 2049.44 \times 10^6 Q^2 \frac{\text{N} \cdot \text{s}^2}{\text{m}^8} \times \frac{\text{Pa} \cdot \text{m}^2}{\text{N}}$$

With $Q = 0.02 \text{ m}^3/\text{s}$ then

$$p_1 = 819,776 \text{ kPa} \xrightarrow{p_{1g}}$$

This problem illustrates application of the Bernoulli equation to a flow where the restrictions of steady, incompressible, frictionless flow along a streamline are reasonable.

Control Volume Moving with Constant Velocity

In the preceding problems, which illustrate applications of the momentum equation to inertial control volumes, we have considered only stationary control volumes. Suppose we have a control volume moving at constant speed. We can set up two coordinate systems: *XYZ*, “absolute,” or stationary (inertial), coordinates, and the *xyz* coordinates attached to the control volume.

Equation 4.10, which expresses system derivatives in terms of control volume variables, is valid for any motion of the control volume coordinate system *xyz*, provided that all velocities are measured *relative* to the control volume. To emphasize this point, we rewrite Eq. 4.10 as

$$\frac{dN}{dt} \Big|_{\text{system}} = \frac{\partial}{\partial t} \int_{CV} \eta \rho dV + \int_{CS} \eta \rho \vec{V}_{xyz} \cdot dA \quad (4.25)$$

Since all velocities must be measured relative to the control volume, in using this equation to obtain the momentum equation for an inertial control volume from the system formulation, we must set

$$N = \vec{P}_{xyz} \quad \text{and} \quad \eta = \vec{V}_{xyz}$$

The control volume equation is then written as

$$\vec{F} = \vec{F}_S + \vec{F}_B = \frac{\partial}{\partial t} \int_{CV} \vec{V}_{xyz} \rho dV + \int_{CS} \vec{V}_{xyz} \rho \vec{V}_{xyz} \cdot dA \quad (4.26)$$

Equation 4.26 is the formulation of Newton’s second law applied to any inertial control volume (stationary or moving with a constant velocity). It is identical to Eq. 4.17a except that we have included subscript *xyz* to emphasize that velocities must be measured relative to the control volume. These are the velocities that would be seen by an observer moving with the control volume. Example 4.10 illustrates the use of Eq. 4.26 for a control volume moving at constant velocity.

Example 4.10 VANE MOVING WITH CONSTANT VELOCITY

The sketch shows a vane with a turning angle of 60° . The vane moves at constant speed, $U = 10 \text{ m/s}$, and receives a jet of water that leaves a stationary nozzle with speed $V = 30 \text{ m/s}$. The nozzle has an exit area of 0.003 m^2 . Determine the force components that act on the vane.

Given: Vane, with turning angle $\theta = 60^\circ$, moves with constant velocity, $\vec{U} = 10\hat{i} \text{ m/s}$. Water from a constant area nozzle, $A = 0.003 \text{ m}^2$, with velocity $\vec{V} = 30\hat{i} \text{ m/s}$, flows over the vane as shown.

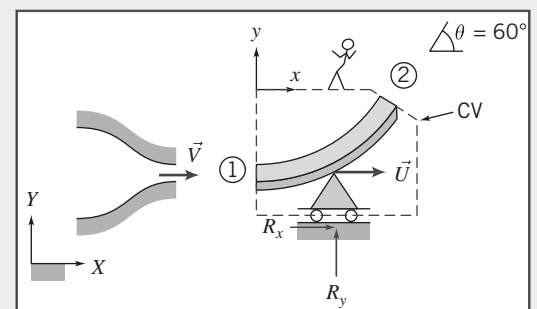
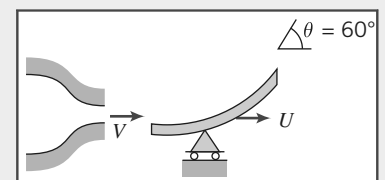
Find: Force components acting on the vane.

Solution: Select a control volume moving with the vane at constant velocity, \vec{U} , as shown by the dashed lines. R_x and R_y are the components of force required to maintain the velocity of the control volume at $10\hat{i} \text{ m/s}$.

The control volume is inertial since it is not accelerating ($U = \text{constant}$). Remember that all velocities must be measured relative to the control volume in applying the basic equations.

Governing equations:

$$\begin{aligned} \vec{F}_S + \vec{F}_B &= \frac{\partial}{\partial t} \int_{CV} \vec{V}_{xyz} \rho dV + \int_{CS} \vec{V}_{xyz} \rho \vec{V}_{xyz} \cdot dA \\ \frac{\partial}{\partial t} \int_{CV} \rho dV + \int_{CS} \rho \vec{V}_{xyz} \cdot dA &= 0 \end{aligned}$$



Assumptions:

- 1 Flow is steady relative to the vane.
- 2 Magnitude of relative velocity along the vane is constant: $|\vec{V}_1| = |\vec{V}_2| = V - U$.
- 3 Properties are uniform at sections ① and ②.
- 4 $F_{B_x} = 0$.
- 5 Incompressible flow.

The x component of the momentum equation is

$$F_{S_x} + F_{B_x}^{\wedge} = \cancel{\frac{\partial}{\partial t}} \int_{CV} u_{xyz} \rho dV + \int_{CS} u_{xyz} \rho \vec{V}_{xyz} \cdot d\vec{A} = 0 \quad (1)$$

There is no net pressure force, since p_{atm} acts on all sides of the CV. Thus

$$R_x = \int_{A_1} u(-\rho V dA) + \int_{A_2} u(\rho V dA) = +u_1(-\rho V_1 A_1) + u_2(\rho V_2 A_2)$$

From the continuity equation

$$\int_{A_1} (-\rho V dA) + \int_{A_2} (\rho V dA) = (-\rho V_1 A_1) + (\rho V_2 A_2) = 0$$

or

$$\rho V_1 A_1 = \rho V_2 A_2$$

Therefore,

$$R_x = (u_2 - u_1)(\rho V_1 A_1)$$

All velocities must be measured relative to the CV, so we note that

$$\begin{aligned} V_1 &= V - U & V_2 &= V - U \\ u_1 &= V - U & u_2 &= (V - U)\cos \theta \end{aligned}$$

Substituting yields

$$\begin{aligned} R_x &= [(V - U)\cos \theta - (V - U)](\rho(V - U)A_1) = (V - U)(\cos \theta - 1)\{\rho(V - U)A_1\} \\ &= (30 - 10)\frac{m}{s} \times (0.50 - 1) \times \left(999 \frac{kg}{m^3} (30 - 10) \frac{m}{s} \times 0.003 m^2 \right) \times \frac{N \cdot s^2}{kg \cdot m} \end{aligned}$$

$$R_x = -599 N \quad \{ \text{to the left} \}$$

Writing the y component of the momentum equation, we obtain

$$F_{S_y} + F_{B_y}^{\wedge} = \cancel{\frac{\partial}{\partial t}} \int_{CV} v_{xyz} \rho dV + \int_{CS} v_{xyz} \rho \vec{V}_{xyz} \cdot d\vec{A} = 0 \quad (1)$$

Denoting the mass of the CV as M gives

$$\begin{aligned} R_y - Mg &= \int_{CS} v \rho \vec{V} \cdot d\vec{A} = \int_{A_2} v \rho \vec{V} \cdot d\vec{A} \quad \{v_1 = 0\} \\ &= \int_{A_2} v(\rho V dA) = v_2(\rho V_2 A_2) = v_2(\rho V_1 A_1) \\ &= (V - U)\sin \theta \{\rho(V - U)A_1\} \\ &= (30 - 10)\frac{m}{s} \times (0.866) \times \left((999) \frac{kg}{m^3} (30 - 10) \frac{m}{s} \times 0.003 m^2 \right) \times \frac{N \cdot s^2}{kg \cdot m} \end{aligned}$$

$$\left. \begin{aligned} &\text{All velocities are} \\ &\text{measured relative to} \\ &xyz. \\ &\text{Recall } \rho V_2 A_2 = \rho V_1 A_1. \end{aligned} \right\}$$

$$R_y - Mg = 1.04 \text{ kN} \quad \{\text{upward}\}$$

Thus the vertical force is

$$R_y = 1.04 \text{ kN} + Mg \quad \{\text{upward}\}$$

Then the net force on the vane, neglecting the weight of the vane and water within the CV, is

$$\vec{R} = -0.599\hat{i} + 1.04\hat{j} \text{ kN} \quad \vec{R}$$

This problem illustrates how to apply the momentum equation for a control volume in constant velocity motion by evaluating all velocities relative to the control volume.

4.5 Momentum Equation for Control Volume with Rectilinear Acceleration

For an inertial control volume, the appropriate formulation of Newton's second law is given by Eq. 4.26,

$$\vec{F} = \vec{F}_S + \vec{F}_B = \frac{\partial}{\partial t} \int_{CV} \vec{V}_{xyz} \rho dV + \int_{CS} \vec{V}_{xyz} \rho \vec{V}_{xyz} \cdot d\vec{A} \quad (4.26)$$

Not all control volumes are inertial; for example, a rocket must accelerate if it is to get off the ground. Since we are interested in analyzing control volumes that may accelerate relative to inertial coordinates, we can determine whether Eq. 4.26 can be used for an accelerating control volume. To answer this let us briefly review the two major elements used in developing Eq. 4.26.

First, in relating the system derivatives to the control volume formulation (Eq. 4.25 or 4.10), the flow field, $\vec{V}(x, y, z, t)$, was specified relative to the control volume's coordinates x , y , and z . No restriction was placed on the motion of the xyz reference frame. Consequently, Eq. 4.25 (or Eq. 4.10) is valid at any instant for any arbitrary motion of the coordinates x , y , and z provided that all velocities in the equation are measured relative to the control volume.

Second, the system equation

$$\vec{F} = \left. \frac{d\vec{P}}{dt} \right|_{\text{system}} \quad (4.2a)$$

where the linear momentum of the system is given by

$$\vec{P}_{\text{system}} = \int_{M(\text{system})} \vec{V} dm = \int_{V(\text{system})} \vec{V} \rho dV \quad (4.2b)$$

is valid only for velocities measured relative to an inertial reference frame. Thus, if we denote the inertial reference frame by XYZ , then Newton's second law states that

$$\vec{F} = \left. \frac{d\vec{P}_{XYZ}}{dt} \right|_{\text{system}} \quad (4.27)$$

Since the time derivatives of \vec{P}_{XYZ} and \vec{P}_{xyz} are not equal when the control volume reference frame xyz is accelerating relative to the inertial reference frame, Eq. 4.26 is not valid for an accelerating control volume.

To develop the momentum equation for a linearly accelerating control volume, it is necessary to relate \vec{P}_{XYZ} of the system to \vec{P}_{xyz} of the system. The system derivative $d\vec{P}_{xyz}/dt$ can then be related to control volume variables through Eq. 4.25. We begin by writing Newton's second law for a system, remembering that the acceleration must be measured relative to an inertial reference frame that we have designated XYZ . We write

$$\vec{F} = \left. \frac{d\vec{P}_{XYZ}}{dt} \right|_{\text{system}} = \frac{d}{dt} \int_{M(\text{system})} \vec{V}_{XYZ} dm = \int_{M(\text{system})} \frac{d\vec{V}_{XYZ}}{dt} dm \quad (4.28)$$

The velocities with respect to the inertial (XYZ) and the control volume coordinates (xyz) are related by the relative-motion equation

$$\vec{V}_{XYZ} = \vec{V}_{xyz} + \vec{V}_{rf} \quad (4.29)$$

where \vec{V}_{rf} is the velocity of the control volume coordinates xyz with respect to the “absolute” stationary coordinates XYZ .

Since we are assuming the motion of xyz is pure translation, without rotation, relative to inertial reference frame XYZ , then

$$\frac{d\vec{V}_{XYZ}}{dt} = \vec{a}_{XYZ} = \frac{d\vec{V}_{xyz}}{dt} + \frac{d\vec{V}_{rf}}{dt} = \vec{a}_{xyz} + \vec{a}_{rf} \quad (4.30)$$

where

- \vec{a}_{XYZ} is the rectilinear acceleration of the system relative to inertial reference frame XYZ ,
- \vec{a}_{xyz} is the rectilinear acceleration of the system relative to noninertial reference frame xyz (i.e., relative to the control volume), and
- \vec{a}_{rf} is the rectilinear acceleration of noninertial reference frame xyz (i.e., of the control volume) relative to inertial frame XYZ .

Substituting from Eq. 4.30 into Eq. 4.28 gives

$$\vec{F} = \int_{M(\text{system})} \vec{a}_{rf} dm + \int_{M(\text{system})} \frac{d\vec{V}_{xyz}}{dt} dm$$

or

$$\vec{F} - \int_{M(\text{system})} \vec{a}_{rf} dm = \left. \frac{d\vec{P}_{xyz}}{dt} \right|_{\text{system}} \quad (4.31a)$$

where the linear momentum of the system is given by

$$\vec{P}_{xyz}|_{\text{system}} = \int_{M(\text{system})} \vec{V}_{xyz} dm = \int_{V(\text{system})} \vec{V}_{xyz} \rho dV \quad (4.31b)$$

and the force, \vec{F} , includes all surface and body forces acting on the system.

To derive the control volume formulation of Newton’s second law, we set

$$N = \vec{P}_{xyz} \quad \text{and} \quad \eta = \vec{V}_{xyz}$$

From Eq. 4.25, with this substitution, we obtain

$$\left. \frac{d\vec{P}_{xyz}}{dt} \right|_{\text{system}} = \frac{\partial}{\partial t} \int_{CV} \vec{V}_{xyz} \rho dV + \int_{CS} \vec{V}_{xyz} \rho \vec{V}_{xyz} \cdot d\vec{A} \quad (4.32)$$

Combining Eq. 4.31a (the linear momentum equation for the system) and Eq. 4.32 (the system-control volume conversion), and recognizing that at time t_0 the system and control volume coincide, Newton’s second law for a control volume accelerating, without rotation, relative to an inertial reference frame is

$$\vec{F} - \int_{CV} \vec{a}_{rf} \rho dV = \frac{\partial}{\partial t} \int_{CV} \vec{V}_{xyz} \rho dV + \int_{CS} \vec{V}_{xyz} \rho \vec{V}_{xyz} \cdot d\vec{A}$$

Since $\vec{F} = \vec{F}_S + \vec{F}_B$, this equation becomes

$$\vec{F}_S + \vec{F}_B - \int_{CV} \vec{a}_{rf} \rho dV = \frac{\partial}{\partial t} \int_{CV} \vec{V}_{xyz} \rho dV + \int_{CS} \vec{V}_{xyz} \rho \vec{V}_{xyz} \cdot d\vec{A} \quad (4.33)$$

Comparing this momentum equation for a control volume with rectilinear acceleration to that for a non-accelerating control volume, Eq. 4.26, we see that the only difference is the presence of one additional term in Eq. 4.33. When the control volume is not accelerating relative to inertial reference frame XYZ , then $\vec{a}_{rf} = 0$, and Eq. 4.33 reduces to Eq. 4.26.

The precautions concerning the use of Eq. 4.26 also apply to the use of Eq. 4.33. Before attempting to apply either equation, one must draw the boundaries of the control volume and label appropriate coordinate directions. For an accelerating control volume, one must label two coordinate systems: one (xyz) on the control volume and the other (XYZ) an inertial reference frame.

In Eq. 4.33, \vec{F}_S represents all surface forces acting on the control volume. Since the mass within the control volume may vary with time, both the remaining terms on the left side of the equation may be functions of time. Furthermore, the acceleration, \vec{a}_{rf} , of the reference frame xyz relative to an inertial frame will in general be a function of time.

All velocities in Eq. 4.33 are measured relative to the control volume. The momentum flux, $\vec{V}_{xyz}\rho\vec{V}_{xyz} \cdot d\vec{A}$, through an element of the control surface area, $d\vec{A}$, is a vector. As we saw for the non-accelerating control volume, the sign of the scalar product, $\rho\vec{V}_{xyz} \cdot d\vec{A}$, depends on the direction of the velocity vector, \vec{V}_{xyz} , relative to the area vector, $d\vec{A}$.

The momentum equation is a vector equation. As with all vector equations, it may be written as three scalar component equations. The scalar components of Eq. 4.33 are

$$F_{S_x} + F_{B_x} - \int_{CV} a_{rf_x} \rho dV = \frac{\partial}{\partial t} \int_{CV} u_{xyz} \rho dV + \int_{CS} u_{xyz} \rho \vec{V}_{xyz} \cdot d\vec{A} \quad (4.34a)$$

$$F_{S_y} + F_{B_y} - \int_{CV} a_{rf_y} \rho dV = \frac{\partial}{\partial t} \int_{CV} v_{xyz} \rho dV + \int_{CS} v_{xyz} \rho \vec{V}_{xyz} \cdot d\vec{A} \quad (4.34b)$$

$$F_{S_z} + F_{B_z} - \int_{CV} a_{rf_z} \rho dV = \frac{\partial}{\partial t} \int_{CV} w_{xyz} \rho dV + \int_{CS} w_{xyz} \rho \vec{V}_{xyz} \cdot d\vec{A} \quad (4.34c)$$

We will consider two applications of the linearly accelerating control volume. Example 4.11 will analyze an accelerating control volume in which the mass contained in the control volume is constant and Example 4.12 will analyze an accelerating control volume in which the mass contained varies with time.

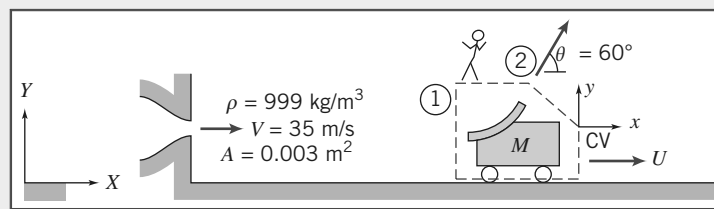
Example 4.11 VANE MOVING WITH RECTILINEAR ACCELERATION

A vane, with turning angle $\theta = 60^\circ$, is attached to a cart. The cart and vane, of mass $M = 75 \text{ kg}$, roll on a level track. Friction and air resistance may be neglected. The vane receives a jet of water, which leaves a stationary nozzle horizontally at $V = 35 \text{ m/s}$. The nozzle exit area is $A = 0.003 \text{ m}^2$. Determine the velocity of the cart as a function of time and plot the results.

Given: Vane and cart as sketched, with $M = 75 \text{ kg}$.

Find: $U(t)$ and plot results.

Solution: Choose the control volume and coordinate systems shown for the analysis. Note that XY is a fixed frame, while frame xy moves with the cart. Apply the x component of the momentum equation.



Governing equations:

$$= 0(1) = 0(2) \quad \simeq 0(4)$$

$$\int_{CV} F_{S_x} + \int_{CV} F_{B_x} - \int_{CV} a_{rf_x} \rho dV = \frac{\partial}{\partial t} \int_{CV} u_{xyz} \rho dV + \int_{CS} u_{xyz} \rho \vec{V}_{xyz} \cdot d\vec{A}$$

Assumptions:

1 $F_{S_x} = 0$, since no resistance is present.

2 $F_{B_x} = 0$.

3 Neglect the mass of water in contact with the vane compared to the cart mass.

4 Neglect rate of change of momentum of liquid inside the CV.

$$\frac{\partial}{\partial t} \int_{CV} u_{xyz} \rho dV \simeq 0$$

5 Uniform flow at sections ① and ②.

6 Speed of water stream is not slowed by friction on the vane, so $|\vec{V}_{xyz_1}| = |\vec{V}_{xyz_2}|$.

7 $A_2 = A_1 = A$.

Then, dropping subscripts *rf* and *xyz* for clarity but remembering that all velocities are measured relative to the moving coordinates of the control volume,

$$\begin{aligned} - \int_{CV} a_x \rho dV &= u_1(-\rho V_1 A_1) + u_2(\rho V_2 A_2) \\ &= (V-U)\{-\rho(V-U)A\} + (V-U)\cos\theta\{\rho(V-U)A\} \\ &= -\rho(V-U)^2 A + \rho(V-U)^2 A \cos\theta \end{aligned}$$

For the left side of this equation we have

$$- \int_{CV} a_x \rho dV = -a_x M_{CV} = -a_x M = -\frac{dU}{dt} M$$

so that

$$-M \frac{dU}{dt} = -\rho(V-U)^2 A + \rho(V-U)^2 A \cos\theta$$

or

$$M \frac{dU}{dt} = (1-\cos\theta)\rho(V-U)^2 A$$

Separating variables, we obtain

$$\frac{dU}{(V-U)^2} = \frac{(1-\cos\theta)\rho A}{M} dt \quad \text{where } b = \frac{(1-\cos\theta)\rho A}{M}$$

Note that since $V = \text{constant}$, $dU = -d(V-U)$. Integrating between limits $U=0$ at $t=0$, and $U=U$ at $t=t$,

$$\int_0^U \frac{dU}{(V-U)^2} = \int_0^U \frac{-d(V-U)}{(V-U)^2} = \frac{1}{(V-U)} \Big|_0^U = \int_0^t b dt = bt$$

or

$$\frac{1}{(V-U)} - \frac{1}{V} = \frac{U}{V(V-U)} = bt$$

Solving for U , we obtain

$$\frac{U}{V} = \frac{Vbt}{1+Vbt}$$

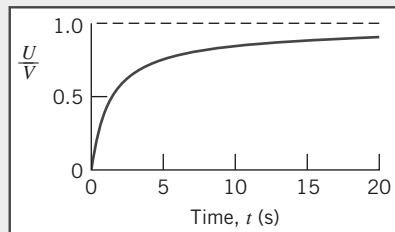
Evaluating Vb gives

$$\begin{aligned} Vb &= V \frac{(1-\cos\theta)\rho A}{M} \\ Vb &= 35 \frac{\text{m}}{\text{s}} \times \frac{(1-0.5)}{75 \text{ kg}} \times 999 \frac{\text{kg}}{\text{m}^3} \times 0.003 \text{ m}^2 = 0.699 \text{ s}^{-1} \end{aligned}$$

Thus

$$\frac{U}{V} = \frac{0.699t}{1+0.699t} \quad \begin{array}{l} (t \text{ in seconds}) \\ \hline U(t) \end{array}$$

Plot:



Example 4.12 ROCKET DIRECTED VERTICALLY

A small rocket, with an initial mass of 400 kg, is to be launched vertically. Upon ignition the rocket consumes fuel at the rate of 5 kg/s and ejects gas at atmospheric pressure with a speed of 3500 m/s relative to the rocket. Determine the initial acceleration of the rocket and the rocket speed after 10 s, if air resistance is neglected.

Given: Small rocket accelerates vertically from rest.

Initial mass, $M_0 = 400 \text{ kg}$.

Air resistance may be neglected.

Rate of fuel consumption, $\dot{m}_e = 5 \text{ kg/s}$.

Exhaust velocity, $V_e = 3500 \text{ m/s}$, relative to rocket, leaving at atmospheric pressure.

Find: (a) Initial acceleration of the rocket.
 (b) Rocket velocity after 10 s.

Solution: Choose a control volume as shown by dashed lines. Because the control volume is accelerating, define inertial coordinate system XY and coordinate system xy attached to the CV. Apply the y component of the momentum equation.

Governing equation:

$$F_{S_y} + F_{B_y} - \int_{CV} a_{rfy} \rho dV = \frac{\partial}{\partial t} \int_{CV} v_{xyz} \rho dV + \int_{CV} v_{xyz} \rho \vec{V}_{xyz} \cdot d\vec{A}$$

Assumptions:

1 Atmospheric pressure acts on all surfaces of the CV; since air resistance is neglected, $F_{S_y} = 0$.

2 Gravity is the only body force; g is constant.

3 Flow leaving the rocket is uniform, and V_e is constant.

Under these assumptions the momentum equation reduces to

$$F_{B_y} - \int_{CV} a_{rfy} \rho dV = \frac{\partial}{\partial t} \int_{CV} v_{xyz} \rho dV + \int_{CS} v_{xyz} \rho \vec{V}_{xyz} \cdot d\vec{A} \quad (1)$$

Ⓐ Ⓑ Ⓒ Ⓓ

Let us look at the equation term by term:

$$\textcircled{A} \quad F_{B_y} = - \int_{CV} g \rho dV = -g \int_{CV} \rho dV = -g M_{CV} \quad \{ \text{since } g \text{ is constant} \}$$

The mass of the CV will be a function of time because mass is leaving the CV at rate \dot{m}_e . To determine M_{CV} as a function of time, we use the conservation of mass equation

$$\frac{\partial}{\partial t} \int_{CV} \rho dV + \int_{CS} \rho \vec{V} \cdot d\vec{A} = 0$$

Then

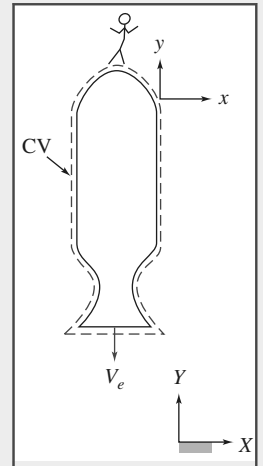
$$\frac{\partial}{\partial t} \int_{CV} \rho dV = - \int_{CS} \rho \vec{V} \cdot d\vec{A} = - \int_{CS} (\rho V_{xyz} dA) = -\dot{m}_e$$

The minus sign indicates that the mass of the CV is decreasing with time. Since the mass of the CV is only a function of time, we can write

$$\frac{dM_{CV}}{dt} = -\dot{m}_e$$

To find the mass of the CV at any time, t , we integrate

$$\int_{M_0}^M dM_{CV} = \int_0^t \dot{m}_e dt \quad \text{where at } t=0, M_{CV}=M_0, \text{ and at } t=t, M_{CV}=M$$



Then, $M - M_0 = -\dot{m}_e t$, or $M = M_0 - \dot{m}_e t$.

Substituting the expression for M into term (B), we obtain

$$F_{B_y} = - \int_{CV} g \rho dV = -gM_{CV} = -g(M_0 - \dot{m}_e t)$$

$$(B) \quad - \int_{CV} a_{rfy} \rho dV$$

The acceleration, a_{rfy} , of the CV is that seen by an observer in the XY coordinate system. Thus a_{rfy} is not a function of the coordinates xyz , and

$$- \int_{CV} a_{rfy} \rho dV = -a_{rfy} \int_{CV} \rho dV = -a_{rfy} M_{CV} = -a_{rfy} (M_0 - \dot{m}_e t)$$

$$(C) \quad \frac{\partial}{\partial t} \int_{CV} v_{xyz} \rho dV$$

This is the time rate of change of the y momentum of the fluid in the control volume measured relative to the control volume.

Even though the y momentum of the fluid inside the CV, measured relative to the CV, is a large number, it does not change appreciably with time. To see this, we must recognize that:

- 1 The unburned fuel and the rocket structure have zero momentum relative to the rocket.
- 2 The velocity of the gas at the nozzle exit remains constant with time as does the velocity at various points in the nozzle.

Consequently, it is reasonable to assume that

$$\frac{\partial}{\partial t} \int_{CV} v_{xyz} \rho dV \approx 0$$

$$(D) \quad \int_{CS} v_{xyz} \rho \vec{V}_{xyz} \cdot d\vec{A} = \int_{CS} v_{xyz} (\rho V_{xyz} dA) = -V_e \int_{CS} (\rho V_{xyz} dA)$$

The velocity v_{xyz} (relative to the control volume) is $-V_e$ (it is in the negative y direction), and is a constant, so was taken outside the integral. The remaining integral is simply the mass flow rate at the exit (positive because flow is out of the control volume),

$$\int_{CS} (\rho V_{xyz} dA) = \dot{m}_e$$

and so

$$\int_{CS} v_{xyz} \rho \vec{V}_{xyz} \cdot d\vec{A} = -V_e \dot{m}_e$$

Substituting terms (A) through (D) into Eq. 1, we obtain

$$-g(M_0 - \dot{m}_e t) - a_{rfy}(M_0 - \dot{m}_e t) = -V_e \dot{m}_e$$

or

$$a_{rfy} = \frac{V_e \dot{m}_e}{M_0 - \dot{m}_e t} - g \quad (2)$$

At time $t = 0$,

$$a_{rfy}|_{t=0} = \frac{V_e \dot{m}_e}{M_0} - g = 3500 \frac{\text{m}}{\text{s}} \times 5 \frac{\text{kg}}{\text{s}} \times \frac{1}{400 \text{ kg}} - 9.81 \frac{\text{m}}{\text{s}^2}$$

$$a_{rfy}|_{t=0} = 33.9 \text{ m/s}^2$$

The acceleration of the CV is by definition

$$a_{rfy} = \frac{dV_{CV}}{dt}$$

Substituting from Eq. 2,

$$\frac{dV_{CV}}{dt} = \frac{V_e \dot{m}_e}{M_0 - \dot{m}_e t} - g$$

Separating variables and integrating gives

$$V_{CV} = \int_0^{V_{CV}} dV_{CV} = \int_0^t \frac{V_e \dot{m}_e dt}{M_0 - \dot{m}_e t} - \int_0^t g dt = -V_e \ln \left[\frac{M_0 - \dot{m}_e t}{M_0} \right] - gt$$

At $t = 10$ s,

$$V_{CV} = -3500 \frac{\text{m}}{\text{s}} \times \ln \left[\frac{350 \text{ kg}}{400 \text{ kg}} \right] - 9.81 \frac{\text{m}}{\text{s}^2} \times 10 \text{ s}$$

$$V_{CV} = 369 \text{ m/s} \quad V_{CV})_{t=10 \text{ s}}$$

4.6 Momentum Equation for Control Volume with Arbitrary Acceleration

In Section 4.5 we obtained a momentum equation for a control volume with rectilinear acceleration. The purpose of this section is to extend this for completeness to include rotation and angular acceleration of the control volume.

First, we develop an expression for Newton's second law in an arbitrary, noninertial coordinate system. Then we use Eq. 4.25 to complete the formulation for a control volume. Newton's second law for a system moving relative to an inertial coordinate system is given by

$$\vec{F} = \frac{d\vec{P}_{XYZ}}{dt} \Big|_{\text{system}} \quad (4.27)$$

where, as in the Section 4.5, XYZ denotes the inertial (e.g., stationary) reference frame. Since

$$\vec{P}_{XYZ})_{\text{system}} = \int_{M(\text{system})} \vec{V}_{XYZ} dm$$

and $M(\text{system})$ is constant,

$$\vec{F} = \frac{d}{dt} \int_{M(\text{system})} \vec{V}_{XYZ} dm = \int_{M(\text{system})} \frac{d\vec{V}_{XYZ}}{dt} dm$$

or

$$\vec{F} = \int_{M(\text{system})} \vec{a}_{XYZ} dm \quad (4.35)$$

The basic problem is to relate \vec{a}_{XYZ} to the acceleration \vec{a}_{xyz} , measured relative to a noninertial coordinate system. For this purpose, consider the noninertial reference frame, xyz , shown in Fig. 4.5.

The noninertial frame, xyz , itself is located by position vector \vec{R} relative to the fixed frame XYZ . The noninertial frame is assumed to rotate with angular velocity $\vec{\omega}$. A particle is instantaneously located relative to the moving frame by position vector $\vec{r} = \hat{i}\dot{x} + \hat{j}\dot{y} + \hat{k}\dot{z}$. Relative to inertial reference frame XYZ , the position of the particle is denoted by position vector \vec{X} . From the geometry of the figure, $\vec{X} = \vec{R} + \vec{r}$.

The velocity of the particle relative to an observer in the XYZ system is

$$\vec{V}_{XYZ} = \frac{d\vec{X}}{dt} = \frac{d\vec{R}}{dt} + \frac{d\vec{r}}{dt} = \vec{V}_{rf} + \frac{d\vec{r}}{dt} \quad (4.36)$$

where, as in the previous section, \vec{V}_{rf} is the instantaneous velocity of the control volume frame itself relative to the inertial XYZ reference frame.

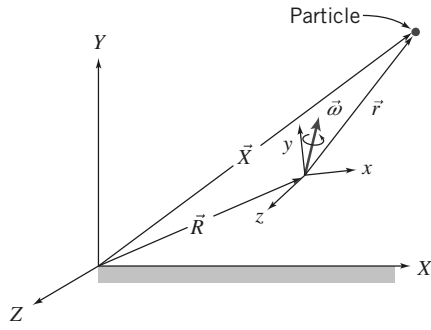


Fig. 4.5 Location of a particle in inertial (XYZ) and noninertial (xyz) reference frames.

We must be careful in evaluating $d\vec{r}/dt$ because both the magnitude, $|\vec{r}|$, and the orientation of the unit vectors, \hat{i} , \hat{j} , and \hat{k} , are functions of time. Thus

$$\frac{d\vec{r}}{dt} = \frac{d}{dt}(x\hat{i} + y\hat{j} + z\hat{k}) = \hat{i}\frac{dx}{dt} + x\frac{d\hat{i}}{dt} + \hat{j}\frac{dy}{dt} + y\frac{d\hat{j}}{dt} + \hat{k}\frac{dz}{dt} + z\frac{d\hat{k}}{dt} \quad (4.37a)$$

The terms dx/dt , dy/dt , and dz/dt are the velocity components of the particle relative to xyz. Thus

$$\vec{V}_{xyz} = \hat{i}\frac{dx}{dt} + \hat{j}\frac{dy}{dt} + \hat{k}\frac{dz}{dt} \quad (4.37b)$$

You may recall from dynamics that for a rotating coordinate system

$$\vec{\omega} \times \vec{r} = x\frac{d\hat{i}}{dt} + y\frac{d\hat{j}}{dt} + z\frac{d\hat{k}}{dt} \quad (4.37c)$$

Combining Eqs. 4.37a, 4.37b, and 4.37c, we obtain

$$\frac{d\vec{r}}{dt} = \vec{V}_{xyz} + \vec{\omega} \times \vec{r} \quad (4.37d)$$

Substituting into Eq. 4.36 gives

$$\vec{V}_{XYZ} = \vec{V}_{rf} + \vec{V}_{xyz} + \vec{\omega} \times \vec{r} \quad (4.38)$$

The acceleration of the particle relative to an observer in the inertial XYZ system is then

$$\vec{a}_{XYZ} = \frac{d\vec{V}_{XYZ}}{dt} = \frac{d\vec{V}_{rf}}{dt} + \left. \frac{d\vec{V}_{xyz}}{dt} \right|_{XYZ} + \frac{d}{dt}(\vec{\omega} \times \vec{r})$$

or

$$\vec{a}_{XYZ} = \vec{a}_{rf} + \left. \frac{d\vec{V}_{xyz}}{dt} \right|_{XYZ} + \frac{d}{dt}(\vec{\omega} \times \vec{r}) \quad (4.39)$$

Both \vec{V}_{xyz} and \vec{r} are measured relative to xyz, so the same caution observed in developing Eq. 4.37d applies. Thus

$$\left. \frac{d\vec{V}_{xyz}}{dt} \right|_{XYZ} = \hat{i}\frac{du}{dt} + \hat{j}\frac{dv}{dt} + \hat{k}\frac{dw}{dt} + \vec{\omega} \times \vec{V}_{xyz} = \vec{a}_{xyz} + \vec{\omega} \times \vec{V}_{xyz} \quad (4.40a)$$

and

$$\begin{aligned} \frac{d}{dt}(\vec{\omega} \times \vec{r}) &= \frac{d\vec{\omega}}{dt} \times \vec{r} + \vec{\omega} \times \frac{d\vec{r}}{dt} \\ &= \vec{\omega} \times \vec{r} + \vec{\omega} \times (\vec{V}_{xyz} + \vec{\omega} \times \vec{r}) \end{aligned}$$

or

$$\frac{d}{dt}(\vec{\omega} \times \vec{r}) = \dot{\vec{\omega}} \times \vec{r} + \vec{\omega} \times \vec{V}_{xyz} + \vec{\omega} \times (\vec{\omega} \times \vec{r}) \quad (4.40b)$$

Substituting Eqs. 4.40a and 4.40b into Eq. 4.39, we obtain

$$\vec{a}_{XYZ} = \vec{a}_{rf} + \vec{a}_{xyz} + 2\vec{\omega} \times \vec{V}_{xyz} + \vec{\omega} \times (\vec{\omega} \times \vec{r}) + \dot{\vec{\omega}} \times \vec{r} \quad (4.41)$$

Equation 4.41 relates the acceleration of a fluid particle as measured in the two frames (the inertial frame XYZ and the noninertial frame xyz). The terms in the equations are

- \vec{a}_{XYZ} : Absolute rectilinear acceleration of a particle relative to fixed reference frame XYZ .
- \vec{a}_{rf} : Absolute rectilinear acceleration of origin of moving reference frame xyz relative to fixed frame XYZ .
- \vec{a}_{xyz} : Rectilinear acceleration of a particle *relative* to moving reference frame xyz (this acceleration would be that “seen” by an observer on moving frame xyz ; $\vec{a}_{xyz} = d\vec{V}_{xyz}/dt$).
- $2\vec{\omega} \times \vec{V}_{xyz}$: Coriolis acceleration due to motion of the particle *within* moving frame xyz .
- $\vec{\omega} \times (\vec{\omega} \times \vec{r})$: Centripetal acceleration due to rotation of moving frame xyz .
- $\dot{\vec{\omega}} \times \vec{r}$: Tangential acceleration due to angular acceleration of moving reference frame xyz .

Substituting \vec{a}_{XYZ} , as given by Eq. 4.41, into Eq. 4.35, we obtain

$$\vec{F}_{\text{system}} = \int_{M(\text{system})} [\vec{a}_{rf} + \vec{a}_{xyz} + 2\vec{\omega} \times \vec{V}_{xyz} + \vec{\omega} \times (\vec{\omega} \times \vec{r}) + \dot{\vec{\omega}} \times \vec{r}] dm$$

or

$$\vec{F} - \int_{M(\text{system})} [\vec{a}_{rf} + 2\vec{\omega} \times \vec{V}_{xyz} + \vec{\omega} \times (\vec{\omega} \times \vec{r}) + \dot{\vec{\omega}} \times \vec{r}] dm = \int_{M(\text{system})} \vec{a}_{xyz} dm \quad (4.42a)$$

But

$$\int_{M(\text{system})} \vec{a}_{xyz} dm = \int_{M(\text{system})} \frac{d\vec{V}_{xyz}}{dt} dm = \frac{d}{dt} \left(\int_{M(\text{system})} \vec{V}_{xyz} dm \right)_{xyz} = \frac{d\vec{P}_{xyz}}{dt} \Big|_{\text{system}} \quad (4.42b)$$

Combining Eqs. 4.42a and 4.42b, we obtain

$$\vec{F} - \int_{M(\text{system})} \left[\vec{a}_{rf} + 2\vec{\omega} \times \vec{V}_{xyz} + \vec{\omega} \times (\vec{\omega} \times \vec{r}) + \dot{\vec{\omega}} \times \vec{r} \right] dm = \frac{d\vec{P}_{xyz}}{dt} \Big|_{\text{system}}$$

or

$$\vec{F}_S + \vec{F}_B - \int_{V(\text{system})} \left[\vec{a}_{rf} + 2\vec{\omega} \times \vec{V}_{xyz} + \vec{\omega} \times (\vec{\omega} \times \vec{r}) + \dot{\vec{\omega}} \times \vec{r} \right] \rho dV = \frac{d\vec{P}_{xyz}}{dt} \Big|_{\text{system}} \quad (4.43)$$

Equation 4.43 is a statement of Newton’s second law for a system. The system derivative, $d\vec{P}_{xyz}/dt$, represents the rate of change of momentum, \vec{P}_{xyz} , of the system measured relative to xyz , as seen by an observer in xyz . This system derivative can be related to control volume variables through Eq. 4.25,

$$\frac{dN}{dt} \Big|_{\text{system}} = \frac{\partial}{\partial t} \int_{CV} \eta \rho dV + \int_{CS} \eta \rho \vec{V}_{xyz} \cdot d\vec{A} \quad (4.25)$$

To obtain the control volume formulation, we set $N = \vec{P}_{xyz}$, and $\eta = \vec{V}_{xyz}$. Then Eqs. 4.25 and 4.43 may be combined to give

$$\begin{aligned} \vec{F}_S + \vec{F}_B - \int_{CV} \left[\vec{a}_{rf} + 2\vec{\omega} \times \vec{V}_{xyz} + \vec{\omega} \times (\vec{\omega} \times \vec{r}) + \dot{\vec{\omega}} \times \vec{r} \right] \rho dV \\ = \frac{\partial}{\partial t} \int_{CV} \vec{V}_{xyz} \rho dV + \int_{CS} \vec{V}_{xyz} \rho \vec{V}_{xyz} \cdot d\vec{A} \end{aligned} \quad (4.44)$$

Equation 4.44 is the most general control volume form of Newton's second law. Comparing the momentum equation for a control volume moving with arbitrary acceleration, Eq. 4.44, with that for a control volume moving with rectilinear acceleration, Eq. 4.33, we see that the only difference is the presence of three additional terms on the left side of Eq. 4.44. These terms result from the *angular motion* of noninertial reference frame xyz . In dynamics these terms are often referred to as "fictitious" forces that arise due to inertia effects present when we use a noninertial xyz coordinate system. These are the Coriolis force due to particle motion within the xyz coordinates and centripetal and tangential forces due to the xyz coordinate system's rotational motion, respectively. As we should expect, the general form, Eq. 4.44, reduces to the rectilinear acceleration form, Eq. 4.33, when the angular terms are zero, and to the inertial control volume form, Eq. 4.26, when all of the terms for the control volume motion (\vec{a}_{rf} , $\vec{\omega}$, and $\dot{\vec{\omega}}$) are zero.

The precautions concerning the use of Eqs. 4.26 and 4.33 also apply to the use of Eq. 4.44. Before attempting to apply this equation, one must draw the boundaries of the control volume and label appropriate coordinate directions. For a control volume moving with arbitrary acceleration, one must label a coordinate system xyz on the control volume and an inertial reference frame XYZ . Example 4.13 shows how the absolute velocity of a particle is determined with respect to a moving reference frame.

Example 4.13 VELOCITY IN FIXED AND NONINERTIAL REFERENCE FRAMES

A reference frame, xyz , moves arbitrarily with respect to a fixed frame, XYZ . A particle moves with velocity $\vec{V}_{xyz} = (dx/dt)\hat{i} + (dy/dt)\hat{j} + (dz/dt)\hat{k}$, relative to frame xyz . Show that the absolute velocity of the particle is given by

$$\vec{V}_{XYZ} = \vec{V}_{rf} + \vec{V}_{xyz} + \vec{\omega} \times \vec{r}$$

Given: Fixed and noninertial frames as shown.

Find: \vec{V}_{XYZ} in terms of \vec{V}_{xyz} , $\vec{\omega}$, \vec{r} , and \vec{V}_{rf} .

Solution: From the geometry of the sketch, $\vec{X} = \vec{R} + \vec{r}$, so

$$\vec{V}_{XYZ} = \frac{d\vec{X}}{dt} = \frac{d\vec{R}}{dt} + \frac{d\vec{r}}{dt} = \vec{V}_{rf} + \frac{d\vec{r}}{dt}$$

Since

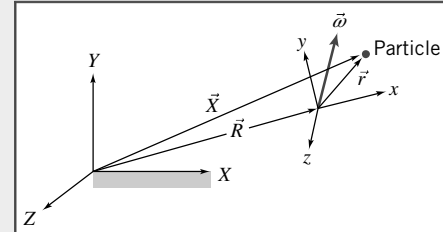
$$\vec{r} = x\hat{i} + y\hat{j} + z\hat{k}$$

we have

$$\frac{d\vec{r}}{dt} = \frac{dx}{dt}\hat{i} + \frac{dy}{dt}\hat{j} + \frac{dz}{dt}\hat{k} + x\frac{d\hat{i}}{dt} + y\frac{d\hat{j}}{dt} + z\frac{d\hat{k}}{dt}$$

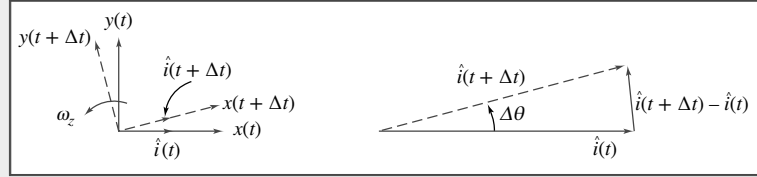
or

$$\frac{d\vec{r}}{dt} = \vec{V}_{xyz} + x\frac{d\hat{i}}{dt} + y\frac{d\hat{j}}{dt} + z\frac{d\hat{k}}{dt}$$



The problem now is to evaluate $d\hat{i}/dt$, $d\hat{j}/dt$, and $d\hat{k}/dt$ that result from the angular motion of frame xyz . To evaluate these derivatives, we must consider the rotation of each unit vector caused by the three components of the angular velocity, $\vec{\omega}$, of frame xyz .

Consider the unit vector \hat{i} . It will rotate in the xy plane because of ω_z , as follows:



Now from the diagram

$$\hat{i}(t + \Delta t) - \hat{i}(t) = (1)\sin\Delta\theta\hat{j} + (1)(1 - \cos\Delta\theta)(-\hat{i})$$

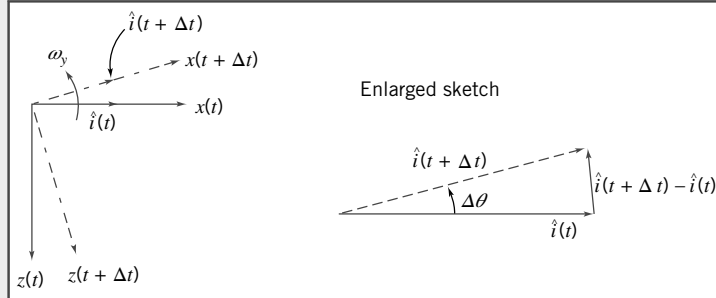
But for small angles $\cos\Delta\theta \approx 1 - [\Delta\theta]^2/2$ and $\sin\Delta\theta \approx \Delta\theta$, so

$$\hat{i}(t + \Delta t) - \hat{i}(t) = (1)\Delta\theta\hat{j} + (1)\frac{(\Delta\theta)^2}{2}(-\hat{i}) = (1)\Delta\theta\left[\hat{j} - \frac{\Delta\theta}{2}\hat{i}\right]$$

In the limit as $\Delta t \rightarrow 0$, since $\Delta\theta = \omega_z \Delta t$,

$$\begin{aligned} \frac{d\hat{i}}{dt} \Big|_{\text{due to } \omega_z} &= \lim_{\Delta t \rightarrow 0} \frac{[\hat{i}(t + \Delta t) - \hat{i}(t)]}{\Delta t} = \lim_{\Delta t \rightarrow 0} \left[\frac{(1)\omega_z \Delta t \left[\hat{j} - \frac{\omega_z \Delta t}{2} \hat{i} \right]}{\Delta t} \right] \\ &= \frac{d\hat{i}}{dt} \Big|_{\text{due to } \omega_z} = \hat{j}\omega_z \end{aligned}$$

Similarly, \hat{i} will rotate in the xz plane because of ω_y .



Then from the diagram

$$\hat{i}(t + \Delta t) - \hat{i}(t) = (1)\sin\Delta\theta(-\hat{k}) + (1)(1 - \cos\Delta\theta)(-\hat{i})$$

For small angles

$$\hat{i}(t + \Delta t) - \hat{i}(t) = (1)\Delta\theta(-\hat{k}) + (1)\frac{(\Delta\theta)^2}{2}(-\hat{i}) = (1)\Delta\theta\left(-\hat{k} - \frac{\Delta\theta}{2}\hat{i}\right)$$

In the limit as $\Delta t \rightarrow 0$, since $\Delta\theta = \omega_y \Delta t$,

$$\begin{aligned} \frac{d\hat{i}}{dt} \Big|_{\text{due to } \omega_y} &= \lim_{\Delta t \rightarrow 0} \frac{[\hat{i}(t + \Delta t) - \hat{i}(t)]}{\Delta t} = \lim_{\Delta t \rightarrow 0} \left[\frac{(1)\omega_y \Delta t \left[-\hat{k} - \frac{\omega_y \Delta t}{2} \hat{i} \right]}{\Delta t} \right] \\ &= \frac{d\hat{i}}{dt} \Big|_{\text{due to } \omega_y} = -\hat{k}\omega_y \end{aligned}$$

Rotation in the yz plane because of ω_x does not affect \hat{i} . Combining terms,

$$\frac{d\hat{i}}{dt} = \omega_z \hat{j} - \omega_y \hat{k}$$

By similar reasoning,

$$\frac{d\hat{j}}{dt} = \omega_x \hat{k} - \omega_z \hat{i} \quad \text{and} \quad \frac{d\hat{k}}{dt} = \omega_y \hat{i} - \omega_x \hat{j}$$

Thus

$$x \frac{d\hat{i}}{dt} + y \frac{d\hat{j}}{dt} + z \frac{d\hat{k}}{dt} = (z\omega_y - y\omega_z)\hat{i} + (x\omega_z - z\omega_x)\hat{j} + (y\omega_x - x\omega_y)\hat{k}$$

But

$$\vec{\omega} \times \vec{r} = \begin{vmatrix} \hat{i} & \hat{j} & \hat{k} \\ \omega_x & \omega_y & \omega_z \\ x & y & z \end{vmatrix} = (z\omega_y - y\omega_z)\hat{i} + (x\omega_z - z\omega_x)\hat{j} + (y\omega_x - x\omega_y)\hat{k}$$

Combining these results, we obtain

$$\vec{V}_{XYZ} = \vec{V}_{rf} + \vec{V}_{xyz} + \vec{\omega} \times \vec{r} \xrightarrow{\hspace{10cm}} \vec{V}_{XYZ}$$

4.7 The Angular-Momentum Principle

We will now derive a control volume form of the angular-momentum principle. There are two obvious approaches we can use to express the angular-momentum principle: We can use an inertial (fixed) XYZ control volume; we can also use a rotating xyz control volume. For each approach we will start with the principle in its system form (Eq. 4.3a), then write the system angular momentum in terms of XYZ or xyz coordinates, and finally use Eq. 4.10 (or its slightly different form, Eq. 4.25) to convert from a system to a control volume formulation. To verify that these two approaches are equivalent, we will use each approach to solve the same problem, in Examples 4.14 and 4.15.

There are two reasons for the material of this section. We wish to develop a control volume equation for each of the basic physical laws of Section 4.2 and we will need the results for use in Chapter 10, where we discuss rotating machinery.

Equation for Fixed Control Volume

The angular-momentum principle for a system in an inertial frame is

$$\vec{T} = \left. \frac{d\vec{H}}{dt} \right)_{\text{system}} \quad (4.3a)$$

where

\vec{T} = total torque exerted on the system by its surroundings, and

\vec{H} = angular momentum of the system.

$$\vec{H} = \int_{M(\text{system})} \vec{r} \times \vec{V} dm = \int_{V(\text{system})} \vec{r} \times \vec{V} \rho dV \quad (4.3b)$$

All quantities in the system equation must be formulated with respect to an inertial reference frame. Reference frames at rest, or translating with constant linear velocity, are inertial, and Eq. 4.12 can be used directly to develop the control volume form of the angular-momentum principle.

The position vector, \vec{r} , locates each mass or volume element of the system with respect to the coordinate system. The torque, \vec{T} , applied to a system may be written

$$\vec{T} = \vec{r} \times \vec{F}_s + \int_{M(\text{system})} \vec{r} \times \vec{g} dm + \vec{T}_{\text{shaft}} \quad (4.3c)$$

where \vec{F}_s is the surface force exerted on the system.

The relation between the system and fixed control volume formulations is

$$\frac{dN}{dt} \Big|_{\text{system}} = \frac{\partial}{\partial t} \int_{\text{CV}} \eta \rho dV + \int_{\text{CS}} \eta \rho \vec{V} \cdot d\vec{A} \quad (4.10)$$

where

$$N_{\text{system}} = \int_{M(\text{system})} \eta dm$$

If we set $N = \vec{H}$, then $\eta = \vec{r} \times \vec{V}$, and

$$\frac{d\vec{H}}{dt} \Big|_{\text{system}} = \frac{\partial}{\partial t} \int_{\text{CV}} \vec{r} \times \vec{V} \rho dV + \int_{\text{CS}} \vec{r} \times \vec{V} \rho \vec{V} \cdot d\vec{A} \quad (4.45)$$

Combining Eqs. 4.3a, 4.20, and 4.45, we obtain

$$\vec{r} \times \vec{F}_s + \int_{M(\text{system})} \vec{r} \times \vec{g} dm + \vec{T}_{\text{shaft}} = \frac{\partial}{\partial t} \int_{\text{CV}} \vec{r} \times \vec{V} \rho dV + \int_{\text{CS}} \vec{r} \times \vec{V} \rho \vec{V} \cdot d\vec{A}$$

Since the system and control volume coincide at time t_0 ,

$$\vec{T} = \vec{T}_{\text{CV}}$$

and

$$\vec{r} \times \vec{F}_s + \int_{\text{CV}} \vec{r} \times \vec{g} \rho dV + \vec{T}_{\text{shaft}} = \frac{\partial}{\partial t} \int_{\text{CV}} \vec{r} \times \vec{V} \rho dV + \int_{\text{CS}} \vec{r} \times \vec{V} \rho \vec{V} \cdot d\vec{A} \quad (4.46)$$

Equation 4.46 is a general formulation of the angular-momentum principle for an inertial control volume. The left side of the equation is an expression for all the torques that act on the control volume. Terms on the right express the rate of change of angular momentum within the control volume and the net rate of flux of angular momentum from the control volume. All velocities in Eq. 4.46 are measured relative to the fixed control volume.

For analysis of rotating machinery, Eq. 4.46 is often used in scalar form by considering only the component directed along the axis of rotation. This equation is applied to turbomachinery in Chapter 10.

The application of Eq. 4.46 to the analysis of a simple lawn sprinkler is illustrated in Example 4.14. This same problem is considered in Example 4.15 using a *rotating* control volume.

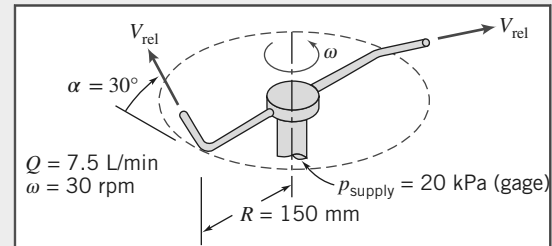
Example 4.14 LAWN SPRINKLER: ANALYSIS USING FIXED CONTROL VOLUME

A small lawn sprinkler is shown in the sketch at right. At an inlet gage pressure of 20 kPa, the total volume flow rate of water through the sprinkler is 7.5 liters per minute and it rotates at 30 rpm. The diameter of each jet is 4 mm. Calculate the jet speed relative to each sprinkler nozzle. Evaluate the friction torque at the sprinkler pivot.

Given: Small lawn sprinkler as shown.

Find: (a) Jet speed relative to each nozzle.
(b) Friction torque at pivot.

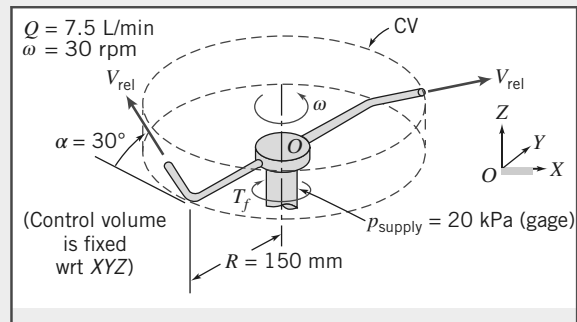
Solution: Apply continuity and angular momentum equations using fixed control volume enclosing sprinkler arms.



Governing equations:

$$\begin{aligned} &= 0(1) \\ &\frac{\partial}{\partial t} \int_{CV} \rho dV + \int_{CS} \rho \vec{V} \cdot d\vec{A} = 0 \\ \vec{r} \times \vec{F}_s + \int_{CV} \vec{r} \times \vec{g} \rho dV + \vec{T}_{\text{shaft}} &= \frac{\partial}{\partial t} \int_{CV} \vec{r} \times \vec{V} \rho dV + \int_{CS} \vec{r} \times \vec{V} \rho \vec{V} \cdot d\vec{A} \end{aligned} \quad (1)$$

where all velocities are measured relative to the inertial coordinates XYZ .



Assumptions:

- 1 Incompressible flow.
- 2 Uniform flow at each section.
- 3 $\vec{\omega}$ = constant.

From continuity, the jet speed relative to the nozzle is given by

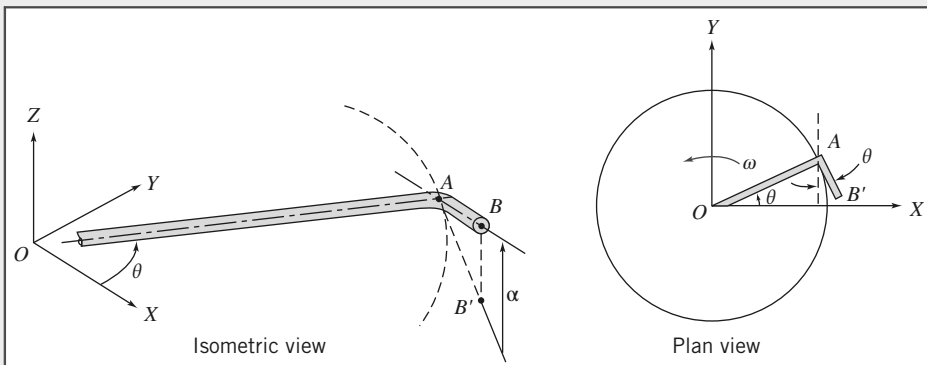
$$\begin{aligned} V_{\text{rel}} &= \frac{Q}{2A_{\text{jet}}} = \frac{Q}{2\pi D_{\text{jet}}^2} \frac{4}{4} \\ &= \frac{1}{2} \times 7.5 \frac{L}{\text{min}} \times \frac{4}{\pi} \frac{1}{(4)^2 \text{ mm}^2} \times \frac{\text{m}^3}{1000 L} \times 10^6 \frac{\text{mm}^2}{\text{m}^2} \times \frac{\text{min}}{60 \text{ s}} \\ V_{\text{rel}} &= 4.97 \text{ m/s} \end{aligned} \quad \underline{V_{\text{rel}}}$$

Consider terms in the angular momentum equation separately. Since atmospheric pressure acts on the entire control surface, and the pressure force at the inlet causes no moment about O , $\vec{r} \times \vec{F}_s = 0$. The moments of the body (i.e., gravity) forces in the two arms are equal and opposite and hence the second term on the left side of the equation is zero. The only external torque acting on the CV is friction in the pivot. It opposes the motion, so

$$\vec{T}_{\text{shaft}} = -T_f \hat{K} \quad (2)$$

Our next task is to determine the two angular momentum terms on the right side of Eq. 1. Consider the unsteady term. This is the rate of change of angular momentum in the control volume. It is clear that although the position \vec{r} and velocity \vec{V} of fluid particles are functions of time in XYZ coordinates, because the sprinkler rotates at constant speed the control volume angular momentum is constant in XYZ coordinates this term is zero. However as an exercise in manipulating vector quantities, let us derive this result. Before we can evaluate the control volume integral, we need to develop expressions for the instantaneous position vector, \vec{r} , and velocity vector, \vec{V} (measured relative to the fixed coordinate system XYZ) of each element of fluid in the control volume. OA lies in the XY plane; AB is inclined at angle α to the XY plane; point B' is the projection of point B on the XY plane.

We assume that the length, L , of the tip AB is small compared with the length, R , of the horizontal arm OA . Consequently we neglect the angular momentum of the fluid in the tips compared with the angular momentum in the horizontal arms.



Consider flow in the horizontal tube OA of length R . Denote the radial distance from O by r . At any point in the tube the fluid velocity relative to fixed coordinates XYZ is the sum of the velocity relative to the tube \vec{V}_t and the tangential velocity $\vec{\omega} \times \vec{r}$. Thus

$$\vec{V} = \hat{I}(V_t \cos \theta - r\omega \sin \theta) + \hat{J}(V_t \sin \theta + r\omega \cos \theta)$$

The angle θ is a function of time. The position vector is

$$\vec{r} = \hat{I}r \cos \theta + \hat{J}r \sin \theta$$

and

$$\vec{r} \times \vec{V} = \hat{K}(r^2\omega \cos^2 \theta + r^2\omega \sin^2 \theta) = \hat{K}r^2\omega$$

Then

$$\int_{V_{OA}} \vec{r} \times \vec{V} \rho dV = \int_0^R \hat{K}r^2\omega \rho A dr = \hat{K} \frac{R^3}{3} \omega \rho A$$

and

$$\frac{\partial}{\partial t} \int_{V_{OA}} \vec{r} \times \vec{V} \rho dV = \frac{\partial}{\partial t} \left[\hat{K} \frac{R^3}{3} \omega \rho A \right] = 0 \quad (3)$$

where A is the cross-sectional area of the horizontal tube. Identical results are obtained for the other horizontal tube in the control volume. We have confirmed our insight that the angular momentum within the control volume does not change with time.

Now we need to evaluate the second term on the right, the flux of momentum across the control surface. There are three surfaces through which we have mass and therefore momentum flux: the supply line (for which $\vec{r} \times \vec{V} = 0$) because $\vec{r} = 0$ and the two nozzles. Consider the nozzle at the end of branch OAB . For $L \ll R$, we have

$$\vec{r}_{jet} = \vec{r}_B \approx \vec{r}|_{r=R} = (\hat{I}r \cos \theta + \hat{J}r \sin \theta)|_{r=R} = \hat{I}R \cos \theta + \hat{J}R \sin \theta$$

and for the instantaneous jet velocity \vec{V}_j we have

$$\begin{aligned} \vec{V}_j &= \vec{V}_{rel} + \vec{V}_{tip} = \hat{I}V_{rel} \cos \alpha \sin \theta - \hat{J}V_{rel} \cos \alpha \cos \theta + \hat{K}V_{rel} \sin \alpha \sin \theta - \hat{I}\omega R \sin \theta + \hat{J}\omega R \cos \theta \\ \vec{V}_j &= \hat{I}(V_{rel} \cos \alpha - \omega R) \sin \theta - \hat{J}(V_{rel} \cos \alpha - \omega R) \cos \theta + \hat{K}V_{rel} \sin \alpha \\ \vec{r}_B \times \vec{V}_j &= \hat{I}RV_{rel} \sin \alpha \sin \theta - \hat{J}RV_{rel} \sin \alpha \cos \theta - \hat{K}R(V_{rel} \cos \alpha - \omega R)(\sin^2 \theta + \cos^2 \theta) \\ \vec{r}_B \times \vec{V}_j &= \hat{I}RV_{rel} \sin \alpha \sin \theta - \hat{J}RV_{rel} \sin \alpha \cos \theta - \hat{K}R(V_{rel} \cos \alpha - \omega R) \end{aligned}$$

The flux integral evaluated for flow crossing the control surface at location B is then

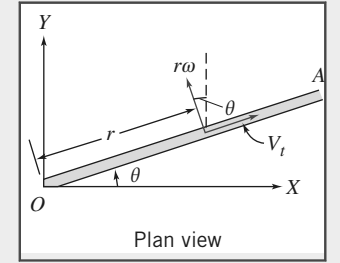
$$\int_{CS} \vec{r} \times \vec{V}_j \rho \vec{V} \cdot d\vec{A} = [\hat{I}RV_{rel} \sin \alpha \sin \theta - \hat{J}RV_{rel} \sin \alpha \cos \theta - \hat{K}R(V_{rel} \cos \alpha - \omega R)] \rho \frac{Q}{2}$$

The velocity and radius vectors for flow in the left arm must be described in terms of the same unit vectors used for the right arm. In the left arm the \hat{I} and \hat{J} components of the cross product are of opposite sign since $\sin(\theta + \pi) = -\sin(\theta)$ and $\cos(\theta - \pi) = -\cos(\theta)$. Thus for the complete CV,

$$\int_{CS} \vec{r} \times \vec{V}_j \rho \vec{V} \cdot d\vec{A} = -\hat{K}R(V_{rel} \cos \alpha - \omega R) \rho Q \quad (4)$$

Substituting terms (2), (3), and (4) into Eq. 1, we obtain

$$-T_f \hat{K} = -\hat{K}R(V_{rel} \cos \alpha - \omega R) \rho Q$$



or

$$T_f = R(V_{\text{rel}} \cos \alpha - \omega R) \rho Q$$

This expression indicates that when the sprinkler runs at constant speed the friction torque at the sprinkler pivot just balances the torque generated by the angular momentum of the two jets.

From the data given,

$$\omega R = 30 \frac{\text{rev}}{\text{min}} \times 150 \text{ mm} \times 2\pi \frac{\text{rad}}{\text{rev}} \times \frac{\text{min}}{60 \text{ s}} \times \frac{\text{m}}{1000 \text{ mm}} = 0.471 \text{ m/s}$$

Substituting gives

$$\begin{aligned} T_f &= 150 \text{ mm} \times \left(4.97 \frac{\text{m}}{\text{s}} \times \cos 30^\circ - 0.471 \frac{\text{m}}{\text{s}} \right) 999 \frac{\text{kg}}{\text{m}^3} \times 7.5 \frac{\text{L}}{\text{min}} \\ &\quad \times \frac{\text{m}^3}{1000 \text{ L}} \times \frac{\text{min}}{60 \text{ s}} \times \frac{\text{N} \cdot \text{s}^3}{\text{kg} \cdot \text{m}} \times \frac{\text{m}}{1000 \text{ mm}} \\ T_f &= 0.0718 \text{ N} \cdot \text{m} \end{aligned}$$

This problem illustrates use of the angular-momentum principle for an inertial control volume. Note that in this example the fluid particle position vector \vec{r} and velocity vector \vec{V} are time-dependent (through θ) in XYZ coordinates. This problem is also solved using a noninertial (rotating) xyz coordinate system in Example 4.15.

Equation for Rotating Control Volume

In problems involving rotating components, such as the rotating sprinkler of Example 4.14, it is often convenient to express all fluid velocities relative to the rotating component. The most convenient control volume is a noninertial one that rotates with the component. In this section we develop a form of the angular-momentum principle for a noninertial control volume rotating about an axis fixed in space.

Inertial and noninertial reference frames were related in Section 4.6. Figure 4.5 showed the notation used. For a system in an inertial frame,

$$\vec{T}_{\text{system}} = \frac{d\vec{H}}{dt} \Bigg|_{\text{system}} \quad (4.3a)$$

The angular momentum of a system in general motion must be specified relative to an inertial reference frame. Using the notation of Fig. 4.5,

$$\vec{H}_{\text{system}} = \int_{M(\text{system})} (\vec{R} + \vec{r}) \times \vec{V}_{XYZ} dm = \int_{\Psi(\text{system})} (\vec{R} + \vec{r}) \times \vec{V}_{XYZ} \rho dV$$

With $\vec{R} = 0$ the xyz frame is restricted to rotation within XYZ, and the equation becomes

$$\vec{H}_{\text{system}} = \int_{M(\text{system})} \vec{r} \times \vec{V}_{XYZ} dm = \int_{\Psi(\text{system})} \vec{r} \times \vec{V}_{XYZ} \rho dV$$

so that

$$\vec{T}_{\text{system}} = \frac{d}{dt} \int_{M(\text{system})} \vec{r} \times \vec{V}_{XYZ} dm$$

Since the mass of a system is constant,

$$\vec{T}_{\text{system}} = \int_{M(\text{system})} \frac{d}{dt} (\vec{r} \times \vec{V}_{XYZ}) dm$$

or

$$\vec{T}_{\text{system}} = \int_{M(\text{system})} \left(\frac{d\vec{r}}{dt} \times \vec{V}_{XYZ} + \vec{r} \times \frac{d\vec{V}_{XYZ}}{dt} \right) dm \quad (4.47)$$

From the analysis of Section 4.6,

$$\vec{V}_{XYZ} = \vec{V}_{rf} + \frac{d\vec{r}}{dt} \quad (4.36)$$

With xyz restricted to pure rotation, $\vec{V}_{rf} = 0$. The first term under the integral on the right side of Eq. 4.47 is then

$$\frac{d\vec{r}}{dt} \times \frac{d\vec{r}}{dt} = 0$$

Thus Eq. 4.47 reduces to

$$\vec{T}_{\text{system}} = \int_{M(\text{system})} \vec{r} \times \frac{d\vec{V}_{XYZ}}{dt} dm = \int_{M(\text{system})} \vec{r} \times \vec{a}_{XYZ} dm \quad (4.48)$$

From Eq. 4.41 with $\vec{a}_{rf} = 0$ (since xyz does not translate),

$$\vec{a}_{XYZ} = \vec{a}_{xyz} + 2\vec{\omega} \times \vec{V}_{xyz} + \vec{\omega} \times (\vec{\omega} \times \vec{r}) + \dot{\vec{\omega}} \times \vec{r}$$

Substituting into Eq. 4.48, we obtain

$$\vec{T}_{\text{system}} = \int_{M(\text{system})} \vec{r} \times \left[\vec{a}_{xyz} + 2\vec{\omega} \times \vec{V}_{xyz} + \vec{\omega} \times (\vec{\omega} \times \vec{r}) + \dot{\vec{\omega}} \times \vec{r} \right] dm$$

or

$$\begin{aligned} \vec{T}_{\text{system}} &= \int_{M(\text{system})} \vec{r} \times \left[2\vec{\omega} \times \vec{V}_{xyz} + \vec{\omega} \times (\vec{\omega} \times \vec{r}) + \dot{\vec{\omega}} \times \vec{r} \right] dm \\ &= \int_{M(\text{system})} \vec{r} \times \vec{a}_{xyz} dm = \int_{M(\text{system})} \vec{r} \times \frac{d\vec{V}_{xyz}}{dt} \Big|_{xyz} dm \end{aligned} \quad (4.49)$$

We can write the last term as

$$\int_{M(\text{system})} \vec{r} \times \frac{d\vec{V}_{xyz}}{dt} \Big|_{xyz} dm = \frac{d}{dt} \left(\int_{M(\text{system})} \vec{r} \times \vec{V}_{xyz} dm \right) xyz = \frac{d\vec{H}_{xyz}}{dt} \Big|_{\text{system}} \quad (4.50)$$

The torque on the system is given by

$$\vec{T}_{\text{system}} = \vec{r} \times \vec{F}_s + \int_{M(\text{system})} \vec{r} \times \vec{g} dm + \vec{T}_{\text{shaft}} \quad (4.3c)$$

The relation between the system and control volume formulations is

$$\frac{dN}{dt} \Big|_{\text{system}} = \frac{\partial}{\partial t} \int_{CV} \eta \rho dV + \int_{CS} \eta \rho \vec{V}_{xyz} \cdot d\vec{A} \quad (4.25)$$

where

$$N_{\text{system}} = \int_{M(\text{system})} \eta dm$$

Setting N equal to \vec{H}_{xyz})_{system} and $\eta = \vec{r} \times \vec{V}_{xyz}$ yields

$$\left. \frac{d\vec{H}_{xyz}}{dt} \right)_{\text{system}} = \frac{\partial}{\partial t} \int_{\text{CV}} \vec{r} \times \vec{V}_{xyz} \rho dV + \int_{\text{CS}} \vec{r} \times \vec{V}_{xyz} \rho \vec{V}_{xyz} \cdot d\vec{A} \quad (4.51)$$

Combining Eqs. 4.49, 4.50, 4.51, and 4.3c, we obtain

$$\begin{aligned} & \vec{r} \times \vec{F}_s + \int_{M(\text{system})} \vec{r} \times \vec{g} dm + \vec{T}_{\text{shaft}} \\ & - \int_{M(\text{system})} \vec{r} \times [2\vec{\omega} \times \vec{V}_{xyz} + \vec{\omega} \times (\vec{\omega} \times \vec{r}) + \dot{\vec{\omega}} \times \vec{r}] dm \\ & = \frac{\partial}{\partial t} \int_{\text{CV}} \vec{r} \times \vec{V}_{xyz} \rho dV + \int_{\text{CS}} \vec{r} \times \vec{V}_{xyz} \rho \vec{V}_{xyz} \cdot d\vec{A} \end{aligned}$$

Since the system and control volume coincided at t_0 ,

$$\begin{aligned} & \vec{r} \times \vec{F}_s + \int_{\text{CV}} \vec{r} \times \vec{g} \rho dV + \vec{T}_{\text{shaft}} \\ & - \int_{\text{CV}} \vec{r} \times [2\vec{\omega} \times \vec{V}_{xyz} + \vec{\omega} \times (\vec{\omega} \times \vec{r}) + \dot{\vec{\omega}} \times \vec{r}] \rho dV \\ & = \frac{\partial}{\partial t} \int_{\text{CV}} \vec{r} \times \vec{V}_{xyz} \rho dV + \int_{\text{CS}} \vec{r} \times \vec{V}_{xyz} \rho \vec{V}_{xyz} \cdot d\vec{A} \end{aligned} \quad (4.52)$$

Equation 4.52 is the formulation of the angular-momentum principle for a noninertial control volume rotating about an axis fixed in space. All fluid velocities in Eq. 4.52 are evaluated relative to the control volume. Comparing Eq. 4.52 with Eq. 4.46 (for inertial XYZ coordinates) we see that the noninertial, rotating xyz coordinates have an extra “moment” term on the left side that includes three components. As we discussed following Eq. 4.44, these components arise because of “fictitious” forces: the Coriolis force because of fluid particle motion within the xyz coordinates, and centripetal and tangential forces because of the xyz coordinates’ rotational motion, respectively. Equation 4.52 reduces to Eq. 4.46 when the control volume is not in motion (when $\vec{\omega}$ and $\dot{\vec{\omega}}$ are zero). Even though we have the extra term to evaluate, Eq. 4.52 is sometimes simpler to use than Eq. 4.44 because a problem that is unsteady in XYZ coordinates becomes steady state in xyz coordinates, as we will see in Example 4.15.

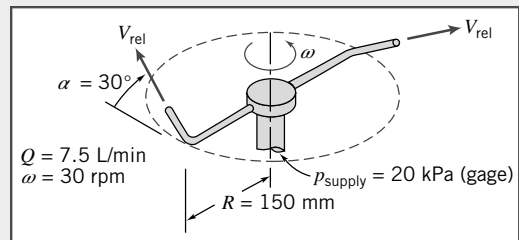
Example 4.15 LAWN SPRINKLER: ANALYSIS USING ROTATING CONTROL VOLUME

A small lawn sprinkler is shown in the sketch at right. At an inlet gage pressure of 20 kPa, the total volume flow rate of water through the sprinkler is 7.5 liters per minute and it rotates at 30 rpm. The diameter of each jet is 4 mm. Calculate the jet speed relative to each sprinkler nozzle. Evaluate the friction torque at the sprinkler pivot.

Given: Small lawn sprinkler as shown.

Find: (a) Jet speed relative to each nozzle.
(b) Friction torque at pivot.

Solution: Apply continuity and angular momentum equations using rotating A control volume enclosing sprinkler arms.



Governing equations:

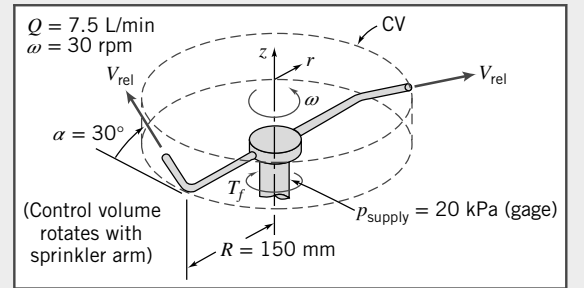
$$\begin{aligned}
 &= 0(1) \\
 &\frac{\partial}{\partial t} \int_{CV} \rho dV + \int_{CS} \rho \vec{V}_{xyz} \cdot d\vec{A} = 0 \\
 &\vec{r} \times \vec{F}_S + \int_{CV} \vec{r} \times \vec{g} \rho dV + \vec{T}_{\text{shaft}} - \int_{CV} \vec{r} \times \left[2\vec{\omega} \times \vec{V}_{xyz} + \vec{\omega} \times (\vec{\omega} \times \vec{r}) + \cancel{\dot{\vec{\omega}} \times \vec{r}} \right] \rho dV = 0(3) \\
 &= 0(1) \\
 &= \frac{\partial}{\partial t} \int_{CV} \vec{r} \times \vec{V}_{xyz} \rho dV + \int_{CV} \vec{r} \times \vec{V}_{xyz} \rho \vec{V}_{xyz} \cdot d\vec{A}
 \end{aligned} \tag{4.52}$$

Assumptions:

- 1 Steady flow relative to the rotating CV.
- 2 Uniform flow at each section.
- 3 $\omega = \text{constant}$.

From continuity

$$\begin{aligned}
 V_{\text{rel}} &= \frac{Q}{2A_{\text{jet}}} = \frac{Q}{2\pi D_{\text{jet}}^2} \\
 &= \frac{1}{2} \times 7.5 \frac{\text{L}}{\text{min}} \times \frac{4}{\pi(4)^2 \text{mm}^2} \times \frac{\text{m}^3}{1000 \text{L}} \times 10^6 \frac{\text{mm}^2}{\text{m}^2} \times \frac{\text{min}}{60 \text{s}} \\
 V_{\text{rel}} &= 4.97 \text{ m/s}
 \end{aligned}$$



Consider terms in the angular-momentum equation separately. As in Example 4.13, the only external torque acting on the CV is friction in the pivot. It opposes the motion, so

$$\vec{T}_{\text{shaft}} = -T_f \hat{k} \tag{1}$$

The second integral on the left of Eq. 4.52 is evaluated for flow *within* the CV. Let the velocity and area within the sprinkler tubes be V_{CV} and A_{CV} , respectively. Then, for *one side*, the first term (a Coriolis effect) is

$$\begin{aligned}
 \int_{CV} \vec{r} \times [2\vec{\omega} \times \vec{V}_{xyz}] \rho dV &= \int_0^R r \hat{e}_r \times [2\omega \hat{k} \times V_{\text{CV}} \hat{e}_r] \rho A_{\text{CV}} dr \\
 &= \int_0^R r \hat{e}_r \times 2\omega V_{\text{CV}} \hat{e}_\theta \rho A_{\text{CV}} dr \\
 &= \int_0^R 2\omega V_{\text{CV}} \rho A_{\text{CV}} r dr \hat{k} = \omega R^2 \rho V_{\text{CV}} A_{\text{CV}} \hat{k} \quad \{\text{one side}\}
 \end{aligned}$$

The flow in the bent portion of the tube has no radial component of velocity, so it does not contribute to the integral.

From continuity, $Q = 2 V_{\text{CV}} A_{\text{CV}}$, so for *both sides* the integral becomes

$$\int_{CV} \vec{r} \times [2\vec{\omega} \times \vec{V}_{xyz}] \rho dV = \omega R^2 \rho Q \hat{k} \tag{2}$$

The second term in the integral (a moment generated by centripetal acceleration) is evaluated as

$$\begin{aligned}
 \int_{CV} \vec{r} \times [\vec{\omega} \times (\vec{\omega} \times \vec{r})] \rho dV &= \int_{CV} r \hat{e}_r \times [\omega \hat{k} \times (\omega \hat{k} \times r \hat{e}_r)] \rho dV \\
 &= \int_{CV} r \hat{e}_r \times [\omega \hat{k} \times \omega r \hat{e}_\theta] \rho dV = \int_{CV} r \hat{e}_r \times \omega^2 r (-\hat{e}_r) \rho dV = 0
 \end{aligned}$$

so it contributes no torque. The force generated by centripetal acceleration is radial, so it generates no moment.

The integral on the right side of Eq. 4.52 is evaluated for flow crossing the control surface. For the right arm of the sprinkler,

$$\begin{aligned}\int_{CS} \vec{r} \times \vec{V}_{xyz} \rho \vec{V}_{xyz} \cdot d\vec{A} &= R \hat{e}_r \times V_{rel} [\cos \alpha (-\hat{e}_\theta) + \sin \alpha \hat{k}] \{ + \rho V_{rel} A_{jet} \} \\ &= RV_{rel} [\cos \alpha (-\hat{k}) + \sin \alpha (-\hat{e}_\theta)] \rho \frac{Q}{2}\end{aligned}$$

The velocity and radius vectors for flow in the left arm must be described in terms of the same unit vectors used for the right arm. In the left sprinkler arm, the θ component has the same magnitude but opposite sign, so it cancels. For the complete CV,

$$\int_{CV} \vec{r} \times \vec{V}_{xyz} \rho \vec{V}_{xyz} \cdot d\vec{A} = -RV_{rel} \cos \alpha \rho Q \hat{k} \quad (3)$$

Combining terms (1), (2), and (3), we obtain

$$-T_f \hat{k} - \omega R^2 \rho Q \hat{k} = -RV_{rel} \cos \alpha \rho Q \hat{k}$$

or

$$T_f = R(V_{rel} \cos \alpha - \omega R) \rho Q$$

From the data given,

$$\omega R = 30 \frac{\text{rev}}{\text{min}} \times 150 \text{ mm} \times 2\pi \frac{\text{rad}}{\text{rev}} \times \frac{\text{min}}{60 \text{ s}} \times \frac{\text{m}}{1000 \text{ mm}} = 0.471 \text{ m/s}$$

Substituting gives

$$\begin{aligned}T_f &= 150 \text{ mm} \left(4.97 \frac{\text{m}}{\text{s}} \times \cos 30^\circ - 0.471 \frac{\text{m}}{\text{s}} \right) 999 \frac{\text{kg}}{\text{m}^3} \times 7.5 \frac{\text{L}}{\text{min}} \\ &\quad \times \frac{\text{m}^3}{1000 \text{ L}} \times \frac{\text{min}}{60 \text{ s}} \times \frac{\text{N} \cdot \text{s}^2}{\text{kg} \cdot \text{m}} \times \frac{\text{m}}{1000 \text{ mm}} \\ T_f &= 0.0718 \text{ N} \cdot \text{m} \end{aligned}$$

This problem illustrates use of the angular-momentum principle for a noninertial (rotating) control volume. Note that in this approach, unlike the inertial control volume of Example 4.14, the fluid particle position vector \vec{r} and velocity vector \vec{V} are *not* time-dependent. As we should expect, the results agree using either an inertial or noninertial control volume.

4.8 The First and Second Laws of Thermodynamics

The first law of thermodynamics is a statement of conservation of energy. Recall that the system formulation of the first law was

$$\dot{Q} - \dot{W} = \frac{dE}{dt} \Big|_{\text{system}} \quad (4.4a)$$

where the total energy of the system is given by

$$E_{\text{system}} = \int_{M(\text{system})} e dm = \int_{V(\text{system})} e \rho dV \quad (4.4b)$$

and

$$e = u + \frac{V^2}{2} + gz$$

In Eq. 4.4a, the rate of heat transfer, \dot{Q} , is positive when heat is added *to* the system from the surroundings; the rate of work, \dot{W} , is positive when work is done *by* the system on its surroundings. (Note that some texts use the opposite notation for work.)

To derive the control volume formulation of the first law of thermodynamics, we set

$$N = E \quad \text{and} \quad \eta = e$$

in Eq. 4.10 and obtain

$$\frac{dE}{dt} \Big|_{\text{system}} = \frac{\partial}{\partial t} \int_{\text{CV}} e \rho dV + \int_{\text{CS}} e \rho \vec{V} \cdot d\vec{A} \quad (4.53)$$

Since the system and the control volume coincide at t_0 ,

$$[\dot{Q} - \dot{W}]_{\text{system}} = [\dot{Q} - \dot{W}]_{\text{control volume}}$$

In light of this, Eqs. 4.4a and 4.53 yield the control volume form of the first law of thermodynamics,

$$\dot{Q} - \dot{W} = \frac{\partial}{\partial t} \int_{\text{CV}} e \rho dV + \int_{\text{CS}} e \rho \vec{V} \cdot d\vec{A} \quad (4.54)$$

where

$$e = u + \frac{V^2}{2} + gz$$

Note that for steady flow the first term on the right side of Eq. 4.54 is zero.

Eq. 4.54 is not quite the same form used in applying the first law to control volume problems. To obtain a formulation suitable and convenient for problem solutions, let us take a closer look at the work term, \dot{W} .

Rate of Work Done by a Control Volume

The term \dot{W} in Eq. 4.54 has a positive numerical value when work is done by the control volume on the surroundings. The rate of work done *on* the control volume is of opposite sign to the work done *by* the control volume.

The rate of work done by the control volume is conveniently subdivided into four classifications,

$$\dot{W} = \dot{W}_s + \dot{W}_{\text{normal}} + \dot{W}_{\text{shear}} + \dot{W}_{\text{other}}$$

Let us consider these separately:

1. Shaft Work

We shall designate shaft work W_s and hence the rate of work transferred out through the control surface by shaft work is designated \dot{W}_s . Examples of shaft work are the work produced by the steam turbine (positive shaft work) of a power plant, and the work input required to run the compressor of a refrigerator (negative shaft work).

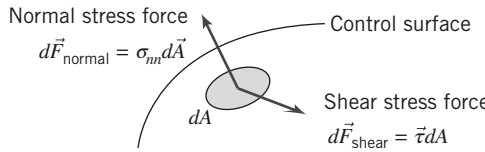
2. Work Done by Normal Stresses at the Control Surface

Recall that work requires a force to act through a distance. Thus, when a force, \vec{F} , acts through an infinitesimal displacement, $d\vec{s}$, the work done is given by

$$\delta W = \vec{F} \cdot d\vec{s}$$

To obtain the rate at which work is done by the force, divide by the time increment, Δt , and take the limit as $\Delta t \rightarrow 0$. Thus the rate of work done by the force, \vec{F} , is

$$\dot{W} = \lim_{\Delta t \rightarrow 0} \frac{\delta W}{\Delta t} = \lim_{\Delta t \rightarrow 0} \frac{\vec{F} \cdot d\vec{s}}{\Delta t} \quad \text{or} \quad \dot{W} = \vec{F} \cdot \vec{V}$$

**Fig. 4.6** Normal and shear stress forces.

We can use this to compute the rate of work done by the normal and shear stresses. Consider the segment of control surface shown in Fig. 4.6. For an element of area $d\vec{A}$ we can write an expression for the normal stress force $d\vec{F}_{\text{normal}}$: It will be given by the normal stress σ_{nn} multiplied by the vector area element $d\vec{A}$ (normal to the control surface).

Hence the rate of work done on the area element is

$$d\vec{F}_{\text{normal}} \cdot \vec{V} = \sigma_{nn} d\vec{A} \cdot \vec{V}$$

Since the work out across the boundaries of the control volume is the negative of the work done on the control volume, the total rate of work out of the control volume due to normal stresses is

$$\dot{W}_{\text{normal}} = - \int_{\text{CS}} \sigma_{nn} d\vec{A} \cdot \vec{V} = - \int_{\text{CS}} \sigma_{nn} \vec{V} \cdot d\vec{A}$$

3. Work Done by Shear Stresses at the Control Surface

Just as work is done by the normal stresses at the boundaries of the control volume, so may work be done by the shear stresses.

As shown in Fig. 4.6, the shear force acting on an element of area of the control surface is given by

$$d\vec{F}_{\text{shear}} = \vec{\tau} dA$$

where the shear stress vector, $\vec{\tau}$, is the shear stress acting in some direction in the plane of dA .

The rate of work done on the entire control surface by shear stresses is given by

$$\int_{\text{CS}} \vec{\tau} dA \cdot \vec{V} = \int_{\text{CS}} \vec{\tau} \cdot \vec{V} dA$$

Since the work out across the boundaries of the control volume is the negative of the work done on the control volume, the rate of work out of the control volume due to shear stresses is given by

$$\dot{W}_{\text{shear}} = - \int_{\text{CS}} \vec{\tau} \cdot \vec{V} dA$$

This integral is better expressed as three terms

$$\begin{aligned} \dot{W}_{\text{shear}} &= - \int_{\text{CS}} \vec{\tau} \cdot \vec{V} dA \\ &= - \int_{A(\text{shafts})} \vec{\tau} \cdot \vec{V} dA - \int_{A(\text{solid surface})} \vec{\tau} \cdot \vec{V} dA - \int_{A(\text{ports})} \vec{\tau} \cdot \vec{V} dA \end{aligned}$$

We have already accounted for the first term, since we included \dot{W}_s previously. At solid surfaces, $\vec{V} = 0$, so the second term is zero (for a fixed control volume). Thus,

$$\dot{W}_{\text{shear}} = - \int_{A(\text{ports})} \vec{\tau} \cdot \vec{V} dA$$

This last term can be made zero by proper choice of control surfaces. If we choose a control surface that cuts across each port perpendicular to the flow, then $d\vec{A}$ is parallel to \vec{V} . Since $\vec{\tau}$ is in the plane of dA , $\vec{\tau}$ is perpendicular to \vec{V} . Thus, for a control surface perpendicular to \vec{V} ,

$$\vec{\tau} \cdot \vec{V} = 0 \quad \text{and} \quad \dot{W}_{\text{shear}} = 0$$

4. Other Work

Electrical energy could be added to the control volume and electromagnetic energy could be absorbed. In most problems, such contributions will be absent, but we should note them in our general formulation.

With all of the terms in \dot{W} evaluated, we obtain

$$\dot{W} = \dot{W}_s - \int_{\text{CS}} \sigma_{nn} \vec{V} \cdot d\vec{A} + \dot{W}_{\text{shear}} + \dot{W}_{\text{other}} \quad (4.55)$$

Control Volume Equation

Substituting the expression for \dot{W} from Eq. 4.55 into Eq. 4.54 gives

$$\dot{Q} - \dot{W}_s + \int_{\text{CS}} \sigma_{nn} \vec{V} \cdot d\vec{A} - \dot{W}_{\text{shear}} - \dot{W}_{\text{other}} = \frac{\partial}{\partial t} \int_{\text{CV}} e \rho dV + \int_{\text{CS}} e \rho \vec{V} \cdot d\vec{A}$$

Rearranging this equation, we obtain

$$\dot{Q} - \dot{W}_s - \dot{W}_{\text{shear}} - \dot{W}_{\text{other}} = \frac{\partial}{\partial t} \int_{\text{CV}} e \rho dV + \int_{\text{CS}} e \rho \vec{V} \cdot d\vec{A} - \int_{\text{CS}} \sigma_{nn} \vec{V} \cdot d\vec{A}$$

Since $\rho = 1/v$, where v is *specific volume*, then

$$\int_{\text{CS}} \sigma_{nn} \vec{V} \cdot d\vec{A} = \int_{\text{CS}} \sigma_{nn} v \rho \vec{V} \cdot d\vec{A}$$

Hence

$$\dot{Q} - \dot{W}_s - \dot{W}_{\text{shear}} - \dot{W}_{\text{other}} = \frac{\partial}{\partial t} \int_{\text{CV}} e \rho dV + \int_{\text{CS}} (e - \sigma_{nn} v) \rho \vec{V} \cdot d\vec{A}$$

Viscous effects can make the normal stress, σ_{nn} , different from the negative of the thermodynamic pressure, $-p$. However, for most flows of common engineering interest, $\sigma_{nn} \approx -p$. Then

$$\dot{Q} - \dot{W}_s - \dot{W}_{\text{shear}} - \dot{W}_{\text{other}} = \frac{\partial}{\partial t} \int_{\text{CV}} e \rho dV + \int_{\text{CS}} (e + pv) \rho \vec{V} \cdot d\vec{A}$$

Finally, substituting $e = u + V^2/2 + gz$ into the last term, we obtain the familiar form of the first law for a control volume,

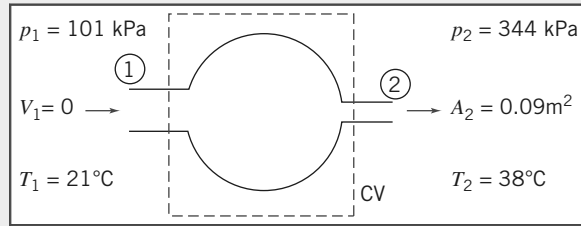
$$\dot{Q} - \dot{W}_s - \dot{W}_{\text{shear}} - \dot{W}_{\text{other}} = \frac{\partial}{\partial t} \int_{\text{CV}} e \rho dV + \int_{\text{CS}} \left(u + pv + \frac{V^2}{2} + gz \right) \rho \vec{V} \cdot d\vec{A} \quad (4.56)$$

Each work term in Eq. 4.56 represents the rate of work done by the control volume on the surroundings. Note that in thermodynamics, for convenience, the combination $u + pv$ (the fluid internal energy plus what is often called the “flow work”) is usually replaced with enthalpy, $h \equiv u + pv$. Example 4.16 illustrates the application of the first law to a steady flow system, and Example 4.17 shows how to apply the first law to a system in which the flow is unsteady.

Example 4.16 COMPRESSOR: FIRST LAW ANALYSIS

Air at 101 kPa, 21°C, enters a compressor with negligible velocity and is discharged at 344 kPa, 38°C through a pipe with 0.09 m² area. The flow rate is 9 kg/s. The power input to the compressor is 447 kW. Determine the rate of heat transfer.

Given: Air enters a compressor at ① and leaves at ② with conditions as shown. The air flow rate is 9 kg/s and the power input to the compressor is 447 kW.



Find: Rate of heat transfer.

Solution:

Governing equations:

$$\begin{aligned} &= 0(1) \\ &\frac{\partial}{\partial t} \int_{CV} \rho dV + \int_{CS} \rho \vec{V} \cdot d\vec{A} = 0 \\ &= 0(4) = 0(1) \\ \dot{Q} - \dot{W}_s - \dot{W}_{shear} &= \frac{\partial}{\partial t} \int_{CV} e \rho dV + \int_{CS} \left(u + pv + \frac{V^2}{2} + gz \right) \rho \vec{V} \cdot d\vec{A} \end{aligned}$$

Assumptions:

- 1 Steady flow.
- 2 Properties uniform over inlet and outlet sections.
- 3 Treat air as an ideal gas, $p = \rho RT$.
- 4 Area of CV at ① and ② perpendicular to velocity, thus $\dot{W}_{shear} = 0$.
- 5 $z_1 = z_2$.
- 6 Inlet kinetic energy is negligible.

Under the assumptions listed, the first law becomes

$$\begin{aligned} \dot{Q} - \dot{W}_s &= \int_{CV} \left(u + pv + \frac{V^2}{2} + gz \right) \rho \vec{V} \cdot d\vec{A} \\ \dot{Q} - \dot{W}_s &= \int_{CS} \left(h + \frac{V^2}{2} + gz \right) \rho \vec{V} \cdot d\vec{A} \end{aligned}$$

or

$$\dot{Q} = \dot{W}_s + \int_{CS} \left(h + \frac{V^2}{2} + gz \right) \rho \vec{V} \cdot d\vec{A}$$

For uniform properties, assumption (2), we can write

$$\begin{aligned} &\approx 0(6) \\ \dot{Q} &= \dot{W}_s + \left(h_1 + \frac{V_1^2}{2} + gz_1 \right) (-\rho_1 V_1 A_1) + \left(h_2 + \frac{V_2^2}{2} + gz_2 \right) (\rho_2 V_2 A_2) \end{aligned}$$

For steady flow, from conservation of mass,

$$\int_{CS} \rho \vec{V} \cdot d\vec{A} = 0$$

Therefore, $-(\rho_1 V_1 A_1) + (\rho_2 V_2 A_2) = 0$, or $\rho_1 V_1 A_1 = \rho_2 V_2 A_2 = \dot{m}$. Hence we can write

$$\dot{Q} = \dot{W}_s + \dot{m} \left[(h_2 - h_1) + \frac{V_2^2}{2} + g(z_2 - z_1) \right] = 0 \quad (5)$$

Assume that air behaves as an ideal gas with constant c_p . Then $h_2 - h_1 = c_p(T_2 - T_1)$, and

$$\dot{Q} = \dot{W}_s + \dot{m} \left[c_p(T_2 - T_1) + \frac{V_2^2}{2} \right]$$

From continuity $V_2 = \dot{m}/\rho_2 A_2$. Since $p_2 = \rho_2 R T_2$,

$$V_2 = \frac{\dot{m} R T_2}{A_2 p_2} = \frac{9 \text{ kg}}{\text{s}} \times \frac{1}{0.09 \text{ m}^2} \times 287 \frac{\text{J}}{\text{kg} \cdot \text{K}} \times (38 + 273)^\circ \text{K} \times \frac{1}{344,000 \text{ Pa}} \times \frac{\text{Pa} \cdot \text{m}^2}{\text{N}} \times \frac{\text{N} \cdot \text{m}}{\text{J}}$$

$$V_2 = 25.9 \text{ m/s}$$

Note that power input is to the CV, so $\dot{W}_s = -447 \text{ kW}$, and

$$\begin{aligned} \dot{Q} &= \dot{W}_s + \dot{m} c_p (T_2 - T_1) + \dot{m} \frac{V_2^2}{2} \\ \dot{Q} &= -447,000 \text{ W} \times 9 \frac{\text{kg}}{\text{s}} \times 1005 \frac{\text{J}}{\text{kg} \cdot \text{K}} \times [(273 + 38) - (273 + 21)]^\circ \text{K} \times \frac{\text{W} \cdot \text{s}}{\text{J}} \\ &\quad + 9 \frac{\text{kg}}{\text{s}} \times \frac{(25.9)^2 \text{ m}^2}{2 \text{ s}^2} \times \frac{\text{N} \cdot \text{s}^2}{\text{kg} \cdot \text{m}} \times \frac{\text{W} \cdot \text{s}^2}{\text{N} \cdot \text{m}} \\ \dot{Q} &= -290.2 \text{ kW} \xrightarrow{\text{heat rejection}} \dot{Q} \end{aligned}$$

This problem illustrates use of the first law of thermodynamics for a control volume. It is also an example of the care that must be taken with unit conversions for mass, energy, and power.

Example 4.17 TANK FILLING: FIRST LAW ANALYSIS

A tank of 0.1 m^3 volume is connected to a high-pressure air line; both line and tank are initially at a uniform temperature of 20°C . The initial tank gage pressure is 100 kPa . The absolute line pressure is 2.0 MPa ; the line is large enough so that its temperature and pressure may be assumed constant. The tank temperature is monitored by a fast-response thermocouple. At the instant after the valve is opened, the tank temperature rises at the rate of 0.05°C/s . Determine the instantaneous flow rate of air into the tank if heat transfer is neglected.

Given: Air supply pipe and tank as shown. At $t = 0^+$, $\partial T / \partial t = 0.05^\circ \text{C/s}$.

Find: \dot{m} at $t = 0^+$.

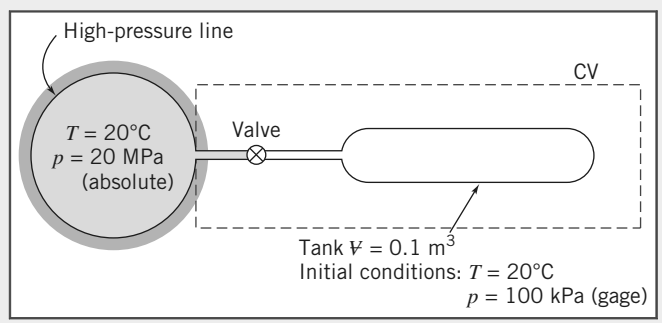
Solution: Choose CV shown, apply energy equation.

Governing equations:

$$= 0(1) = 0(2) = 0(3) = 0(4)$$

$$\begin{aligned} \cancel{\dot{Q}} - \cancel{\dot{W}_s} - \cancel{\dot{W}_{shear}} - \cancel{\dot{W}_{other}} &= \frac{\partial}{\partial t} \int_{\text{CV}} e \rho dV + \int_{\text{CS}} (e + pv) \rho \vec{V} \cdot d\vec{A} \\ &\simeq 0(5) \simeq 0(6) \end{aligned}$$

$$e = u + \frac{V^2}{2} + gz$$



Assumptions:

- 1 $\dot{Q} = 0$ (given).
- 2 $\dot{W}_s = 0$.
- 3 $\dot{W}_{\text{shear}} = 0$.
- 4 $\dot{W}_{\text{other}} = 0$.
- 5 Velocities in line and tank are small.
- 6 Neglect potential energy.
- 7 Uniform flow at tank inlet.
- 8 Properties uniform in tank.
- 9 Ideal gas, $p = \rho RT$, $du = c_v dT$.

Then

$$\frac{\partial}{\partial t} \int_{\text{CV}} u_{\text{tank}} \rho \, dV + (u + pv)|_{\text{line}} (-\rho VA) = 0$$

This expresses the fact that the gain in energy in the tank is due to influx of fluid energy (in the form of enthalpy $h = u + pv$) from the line. We are interested in the initial instant, when T is uniform at 20°C, so $u_{\text{tank}} = u_{\text{line}} = u$, the internal energy at T ; also, $p v_{\text{line}} = R T_{\text{line}} = R T$, and

$$\frac{\partial}{\partial t} \int_{\text{CV}} u \rho \, dV + (u + RT)(-\rho VA) = 0$$

Since tank properties are uniform, $\partial/\partial t$ may be replaced by d/dt , and

$$\frac{d}{dt}(uM) = (u + RT)\dot{m}$$

where M is the instantaneous mass in the tank and $\dot{m} = \rho VA$ is the mass flow rate, or

$$u \frac{dM}{dt} + M \frac{du}{dt} = u\dot{m} + RT\dot{m} \quad (1)$$

The term dM/dt may be evaluated from continuity:

Governing equation:

$$\begin{aligned} \frac{\partial}{\partial t} \int_{\text{CV}} \rho dV + \int_{\text{CS}} \rho \vec{V} \cdot d\vec{A} &= 0 \\ \frac{dM}{dt} + (-\rho VA) &= 0 \quad \text{or} \quad \frac{dM}{dt} = \dot{m} \end{aligned}$$

Substituting in Eq. 1 gives

$$u\dot{m} + M c_v \frac{dT}{dt} = u\dot{m} + RT\dot{m}$$

or

$$\dot{m} = \frac{Mc_v(dT/dt)}{RT} = \frac{\rho V c_v (dT/dt)}{RT} \quad (2)$$

But at $t = 0$, $p_{\text{tank}} = 100 \text{ kPa}$ (gage), and

$$\begin{aligned} \rho &= \rho_{\text{tank}} = \frac{p_{\text{tank}}}{RT} = (1.00 + 1.01)10^5 \frac{\text{N}}{\text{m}^2} \times \frac{\text{kg} \cdot \text{K}}{287 \text{ N} \cdot \text{m}} \times \frac{1}{293 \text{ K}} \\ &= 2.39 \text{ kg/m}^3 \end{aligned}$$

Substituting into Eq. 2, we obtain

$$\begin{aligned}\dot{m} &= 2.39 \frac{\text{kg}}{\text{m}^3} \times 0.1 \text{ m}^3 \times 717 \frac{\text{N} \cdot \text{m}}{\text{kg} \cdot \text{K}} \times 0.05 \frac{\text{K}}{\text{s}} \\ &\quad \times \frac{\text{kg} \cdot \text{K}}{287 \text{ N} \cdot \text{m}} \times \frac{1}{293 \text{ K}} \times 1000 \frac{\text{g}}{\text{kg}} \\ \dot{m} &= 0.102 \text{ g/s} \end{aligned}$$

This problem illustrates use of the first law of thermodynamics for a control volume. It is also an example of the care that must be taken with unit conversions for mass, energy, and power.

The second law of thermodynamics applies to all fluid systems. Recall that the system formulation of the second law is

$$\left. \frac{dS}{dt} \right)_{\text{system}} \geq \frac{1}{T} \dot{Q} \quad (4.5a)$$

where the total entropy of the system is given by

$$S_{\text{system}} = \int_{M(\text{system})} s dm = \int_{V(\text{system})} s \rho dV \quad (4.5b)$$

To derive the control volume formulation of the second law of thermodynamics, we set

$$N = S \quad \text{and} \quad \eta = s$$

in Eq. 4.10 and obtain

$$\left. \frac{dS}{dt} \right)_{\text{system}} = \frac{\partial}{\partial t} \int_{CV} s \rho dV + \int_{CS} s \rho \vec{V} \cdot d\vec{A} \quad (4.57)$$

The system and the control volume coincide at t_0 ; thus in Eq. 4.5a,

$$\left. \frac{1}{T} \dot{Q} \right)_{\text{system}} = \left. \frac{1}{T} \dot{Q} \right)_{CV} = \int_{CS} \frac{1}{T} \left(\frac{\dot{Q}}{A} \right) dA$$

In light of this, Eqs. 4.5a and 4.57 yield the control volume formulation of the second law of thermodynamics

$$\frac{\partial}{\partial t} \int_{CV} s \rho dV + \int_{CS} s \rho \vec{V} \cdot d\vec{A} \geq \int_{CS} \frac{1}{T} \left(\frac{\dot{Q}}{A} \right) dA \quad (4.58)$$

In Eq. 4.58, the factor (\dot{Q}/A) represents the heat flux per unit area into the control volume through the area element dA . To evaluate the term

$$\int_{CS} \frac{1}{T} \left(\frac{\dot{Q}}{A} \right) dA$$

both the local heat flux, (\dot{Q}/A) , and local temperature, T , must be known for each area element of the control surface.

4.9 Summary and Useful Equations

In this chapter we wrote the basic laws for a system: mass conservation (or continuity), Newton's second law, the angular-momentum equation, the first law of thermodynamics, and the second law of thermodynamics. We then developed an equation (sometimes called the Reynolds

Transport Theorem) for relating system formulations to control volume formulations. Using this we derived control volume forms of:

- ✓ The mass conservation equation (sometimes called the continuity equation).
- ✓ Newton's second law (in other words, a momentum equation) for:
 - An inertial control volume.
 - A control volume with rectilinear acceleration.
 - A control volume with arbitrary acceleration.
- ✓ The angular-momentum equation for:
 - A fixed control volume.
 - A rotating control volume.
- ✓ The first law of thermodynamics (or energy equation).
- ✓ The second law of thermodynamics.

We discussed the physical meaning of each term appearing in these control volume equations, and used the equations for the solution of a variety of flow problems. In particular, we used a differential control volume to derive a famous equation in fluid mechanics—the Bernoulli equation—and while doing so learned about the restrictions on its use in solving problems.

Note: Most of the equations in the table below have a number of constraints or limitations—*be sure to refer to their page numbers for details!*

Useful Equations

Continuity (mass conservation), incompressible fluid:	$\int_{CS} \vec{V} \cdot d\vec{A} = 0$	(4.13a)	Page 78
Continuity (mass conservation), incompressible fluid, uniform flow:	$\sum_{CS} \vec{V} \cdot \vec{A} = 0$	(4.13b)	Page 78
Continuity (mass conservation), steady flow:	$\int_{CS} \rho \vec{V} \cdot d\vec{A} = 0$	(4.15a)	Page 78
Continuity (mass conservation), steady flow, uniform flow:	$\sum_{CS} \rho \vec{V} \cdot \vec{A} = 0$	(4.15b)	Page 78
Momentum (Newton's second law):	$\vec{F} = \vec{F}_S + \vec{F}_B = \frac{\partial}{\partial t} \int_{CV} \vec{V} \rho dV + \int_{CS} \vec{V} \rho \vec{V} \cdot d\vec{A}$	(4.17a)	Page 83
Momentum (Newton's second law), uniform flow:	$\vec{F} = \vec{F}_S + \vec{F}_B = \frac{\partial}{\partial t} \int_{CV} \vec{V} \rho dV + \sum_{CS} \vec{V} \rho \vec{V} \cdot \vec{A}$	(4.17b)	Page 83
Momentum (Newton's second law), scalar components:	$F_x = F_{S_x} + F_{B_x} = \frac{\partial}{\partial t} \int_{CV} u \rho dV + \int_{CS} u \rho \vec{V} \cdot d\vec{A}$ $F_y = F_{S_y} + F_{B_y} = \frac{\partial}{\partial t} \int_{CV} v \rho dV + \int_{CS} v \rho \vec{V} \cdot d\vec{A}$ $F_z = F_{S_z} + F_{B_z} = \frac{\partial}{\partial t} \int_{CV} w \rho dV + \int_{CS} w \rho \vec{V} \cdot d\vec{A}$	(4.18a) (4.18b) (4.18c)	Page 84
Momentum (Newton's second law), uniform flow, scalar components:	$F_x = F_{S_x} + F_{B_x} = \frac{\partial}{\partial t} \int_{CV} u \rho dV + \sum_{CS} u \rho \vec{V} \cdot \vec{A}$ $F_y = F_{S_y} + F_{B_y} = \frac{\partial}{\partial t} \int_{CV} v \rho dV + \sum_{CS} v \rho \vec{V} \cdot \vec{A}$ $F_z = F_{S_z} + F_{B_z} = \frac{\partial}{\partial t} \int_{CV} w \rho dV + \sum_{CS} w \rho \vec{V} \cdot \vec{A}$	(4.18d) (4.18e) (4.18f)	Page 84

Table (Continued)

Bernoulli equation (steady, incompressible, frictionless, flow along a streamline):	$\frac{p}{\rho} + \frac{V^2}{2} + gz = \text{constant}$	(4.24)	Page 95
Momentum (Newton's second law), inertial control volume (stationary or constant speed):	$\vec{F} = \vec{F}_S + \vec{F}_B = \frac{\partial}{\partial t} \int_{CV} \vec{V}_{xyz} \rho dV + \int_{CS} \vec{V}_{xyz} \rho \vec{V}_{xyz} \cdot d\vec{A}$	(4.26)	Page 97
Momentum (Newton's second law), rectilinear acceleration of control volume:	$\vec{F}_S + \vec{F}_B - \int_{CV} \vec{a}_{rf} \rho dV = \frac{\partial}{\partial t} \int_{CV} \vec{V}_{xyz} \rho dV + \int_{CS} \vec{V}_{xyz} \rho \vec{V}_{xyz} \cdot d\vec{A}$	(4.33)	Page 100
Angular-momentum principle:	$\vec{r} \times \vec{F}_s + \int_{CV} \vec{r} \times \vec{g} \rho dV + \vec{T}_{\text{shaft}} = \frac{\partial}{\partial t} \int_{CV} \vec{r} \times \vec{V} \rho dV + \int_{CS} \vec{r} \times \vec{V} \rho \vec{V} \cdot d\vec{A}$	(4.46)	Page 111
First law of thermodynamics:	$\dot{Q} - \dot{W}_s - \dot{W}_{\text{shear}} - \dot{W}_{\text{other}} \\ = \frac{\partial}{\partial t} \int_{CV} e \rho dV + \int_{CS} \left(u + pv + \frac{V^2}{2} + gz \right) \rho \vec{V} \cdot d\vec{A}$	(4.56)	Page 121
Second law of thermodynamics:	$\frac{\partial}{\partial t} \int_{CV} s \rho dV + \int_{CS} s \rho \vec{V} \cdot d\vec{A} \geq \int_{CS} \frac{1}{T} (\dot{Q} A) dA$	(4.58)	Page 125

Chapter 5 Problems

Conservation of Mass

5.1 Determine which of the following velocity distributions are possible three-dimensional incompressible flows.

(a) $u = 2y^2 + 2xz; v = -2xy + 6x^2yz; w = 3x^2z^2 + x^3y^4$

(b) $u = xyzt; v = -xyzt^2; w = z^2(xt^2 - yt)$

(c) $u = x^2 + 2y + z^2; v = x - 2y + z; w = -2xz + y^2 + 2z$

5.2 Determine which of the following flow fields represent a possible incompressible flow.

(a) $V_r = U \cos \theta; V_\theta = -U \sin \theta$

(b) $V_r = -q/2\pi r; V_\theta = K/2\pi r$

(c) $V_r = U \cos \theta [1 - (a/r)^2]; V_\theta = -U \sin \theta [1 + (a/r)^2]$

5.3 The x component of velocity in a steady, incompressible flow field in the xy plane is $u = A/x$, where $A = 2 \text{ m}^2/\text{s}$, and x is measured in meters. Find the simplest y component of velocity for this flow field.

5.4 The velocity components for an incompressible steady flow field are $u = A(x^2 + z^2)$ and $v = B(xy + yz)$. Determine the z component of velocity for steady and for unsteady flow.

SS 5.5 For the laminar boundary layer flow of an incompressible fluid, the x component of velocity can be approximated as a linear variation from $u = 0$ at the surface to the $u = U$ at the boundary-layer edge, δ , where U is the freestream velocity. The equation for the profile is then $u = U \frac{y}{\delta}$ where $\delta = cx^{1/2}$ and c is a constant. Show that v is given by $v = \frac{Uy}{4x}$. At a location where $x = 0.5 \text{ m}$ and $d = 5 \text{ mm}$, evaluate the ratio $\frac{v}{U}$ at the wall, at $\delta/2$, and at δ .

5.6 The x component of velocity for a flow field is given as $u = Ax^2y^2$ where $A = 0.3 \text{ m}^{-3} \text{ s}^{-1}$ and x and y are in meters. Determine the y component of velocity for a steady incompressible flow. Determine the equation of the streamline and plot the streamline that goes through the point $(x, y) = (1, 4)$.

5.7 A viscous liquid is sheared between two parallel disks of radius R , one of which rotates while the other is fixed. The velocity field is purely tangential, and the velocity varies linearly with z from $V_\theta = 0$ at $z = 0$ (the fixed disk) to the velocity of the rotating disk at its surface ($z = h$). Derive an expression for the velocity field between the disks.

Stream Function for Two-Dimensional Incompressible Flow

5.8 Determine the stream function ψ that will yield the velocity field $\vec{V} = 2y(2x+1)\hat{i} + [x(x+1) - 2y^2]\hat{j}$

SS 5.9 The stream function for a certain incompressible flow field is given by the expression $\psi = -Ur \sin \theta + q\theta/2\pi$. Obtain an expression for the velocity field. Find the stagnation point(s) where $|\vec{V}| = 0$, and show that $\psi = 0$ there.

5.10 An incompressible frictionless flow field is specified by the stream function $\psi = 5Ax - 2Ay$ where $A = 2 \text{ m/s}$, and x and y are in

meters. Determine the velocity field. Plot the streamlines passing between the points $(x, y) = (2, 2)$ and $(4, 1)$ and determine the flow rate between the two streamlines.

5.11 Determine the stream function for the flow field specified by $u = 4y$; $v = -4x$, where x and y are in meters and u and v are in m/s . Plot the streamlines passing between the points $(x, y) = (0, 0)$ and $(1, 1)$ and determine the flow rate between the two streamlines.

5.12 The velocity in a parallel one-dimensional flow in the positive x direction varies linearly from zero at $y = 0$ to 30 m/s at $y = 1.5 \text{ m}$. Determine the stream function. Calculate the volume flow rate and the value of y at one-half of the total flow.

Motion of a Fluid Particle (Kinematics)

5.13 A flow field given by $\vec{V} = xy^2\hat{i} - \frac{1}{3}y^3\hat{j} + xy\hat{k}$. Determine (a) whether this is a one-, two-, or three-dimensional flow and (b) whether it is a possible incompressible flow. Determine the acceleration of a fluid particle at the location $(x, y, z) = (1, 2, 3)$.

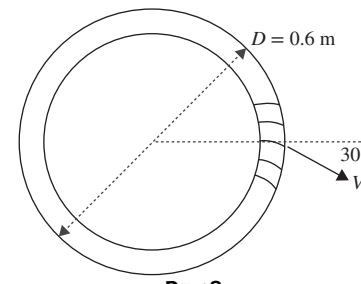
5.14 The velocity field within a laminar boundary layer is represented by the expression $\vec{V} = AU \frac{y}{x^{1/2}}\hat{i} + \frac{AU}{4} \frac{y^2}{x^{3/2}}\hat{j}$, where $A = 141 \text{ m}^{-1/2}$ and the free stream velocity is $U = 0.240 \text{ m/s}$. Demonstrate that this is a possible incompressible velocity field. Determine the acceleration of a fluid particle at the point $(x, y) = (5 \text{ m}, 0.5 \text{ mm})$.

5.15 A 4 m diameter tank is filled with water and then rotated at a rate of $\omega = 2\pi(1 - e^{-t}) \text{ rad/s}$. At the tank walls, viscosity prevents relative motion between the fluid and the wall. Determine the speed and acceleration of the fluid particles next to the tank walls as a function of time.

5.16 A fluid flows parallel to the x axis with a constant shear rate given by $\frac{du}{dy} = A$ where $A = 0.1 \text{ s}^{-1}$. Determine an expression for the velocity field \vec{V} . Determine the rate of rotation and the stream function for this flow field.

5.17 The velocity field given by $\vec{V} = Ax\hat{i} - Ay\hat{j}$ represents flow in a rectangular corner. Evaluate the circulation around the unit square with corners at $(x, y) = (1, 1), (1, 2), (2, 2)$ and $(2, 1)$ for the value of $A = 0.3 \text{ s}^{-1}$.

5.18 Fluid passes through the set of thin, closely spaced blades at a velocity of 3 m/s . Determine the circulation for the flow.



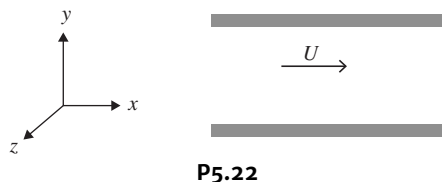
P5.18

5.19 A velocity field is given by $\vec{V} = 2\hat{i} - 4x\hat{j}$ m/s. Determine an equation for the streamline. Calculate the vorticity of the flow.

5.20 The flow between stationary parallel plates separated by distance $2b$ is driven by a pressure gradient. The velocity field is given by $u = U \left[1 - \left(\frac{y}{b} \right)^2 \right]$, where U is the centerline velocity and y is measured from the centerline. Evaluate the rates of linear and angular deformation. Obtain an expression for the vorticity vector, $\vec{\zeta}$, and find the location where the vorticity is a maximum.

5.21 As a weather reconnaissance airplane flies through a cold front, the outside air temperature instrument measures a rate of change of $-0.7^{\circ}\text{F}/\text{min}$. The air speed is 400 mph and the airplane is climbing at a rate of 2500 ft/min. Assume that the front is stationary and vertically uniform. Determine the rate of change of temperature with respect to horizontal distance through the cold front.

5.22 Consider a steady, laminar, fully developed incompressible flow between two infinite parallel plates as shown. The flow is due to a pressure gradient applied in the x direction. Given that $\vec{V} \neq \vec{V}(z)$, $w = 0$ and that gravity points in the negative y direction, prove that $v = 0$ and that the pressure gradients in the x and y directions are constant.



P5.22

5.23 There is a fully developed laminar flow of an incompressible fluid between two infinite parallel plates separated by a distance $2h$ as shown in the figure. The top plate moves with a velocity V_0 and there is a negative pressure gradient $\frac{dp}{dx}$ (pressure decreases in the x -direction). Derive an expression for the velocity profile. Determine the pressure gradient and the rate of rotation for which the flow rate is zero.

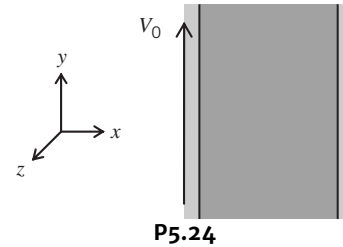


P5.23

Momentum Equation

5.24 There is a fully developed laminar flow of an incompressible fluid between two vertical infinite parallel plates due to a negative

pressure gradient in the y direction. Show that the velocity is a function of y only ($u = 0$) and that the pressure gradient in the y direction is constant.

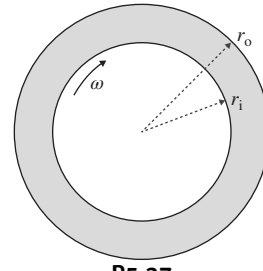


P5.24

5.25 A liquid film flows on a horizontal surface due to a constant shear stress on the top surface. The liquid film is thin, the flow is fully developed, and the thickness is constant in the flow direction. Determine the velocity profile $u(x)$ and the pressure gradient $\frac{dp}{dx}$.

5.26 The flow in a laminar incompressible boundary layer can be modeled as a linear profile $u = U \frac{y}{\delta}$ where δ is the boundary thickness and varies with x as $\delta = cx^{1/2}$. Determine the rotation of a fluid particle and the location of the maximum rate of rotation. Determine the rates of angular and linear deformation and the positions of the maximum values.

5.27 A cylinder of radius r_i rotates at a speed ω coaxially inside a fixed cylinder of radius r_o . A viscous fluid fills the space between the two cylinders. Determine the velocity profile in the space between the cylinders and the shear stress on the surface of each cylinder. Explain why the shear stresses are not equal. SS



P5.27

5.28 The velocity profile for fully developed laminar flow in a circular tube is $u = u_{\max} [1 - (r/R)^2]$. Obtain an expression for the shear force per unit volume in the x direction for this flow. Evaluate its maximum value for a pipe radius of 75 mm and a maximum velocity of 3 m/s for water.

CHAPTER 5

Introduction to Differential Analysis of Fluid Motion

5.1 Conservation of Mass

5.2 Stream Function for Two-Dimensional Incompressible Flow

5.3 Motion of a Fluid Particle (Kinematics)

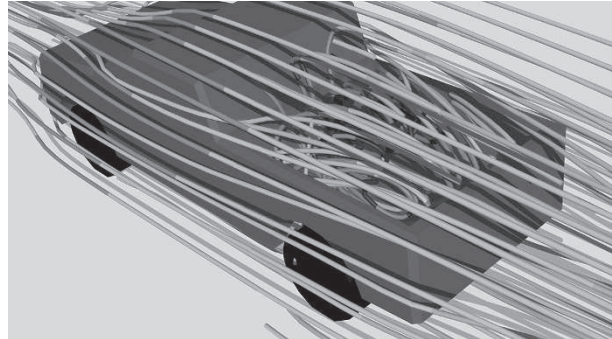
5.4 Momentum Equation

5.5 Summary and Useful Equations

Case Study

Computational fluid dynamics (CFD) represents one of the most important advances in the area of fluid mechanics in the last few decades. In CFD, the equations that govern the flow of fluids are formulated numerically and programmed into software. CFD techniques then allow the solution of many problems that were either too difficult to solve analytically or too expensive to investigate experimentally. CFD software essentially produces a video-camera-like tool that provides detailed pictures for fluid flowing over an object, as in the case of the pickup truck shown in the figure. CFD has had extensive use in a wide range of engineering studies ranging from the pressure drop for water flow through a pipe valve to the lift produced by air flowing over a wing. Basic scientific studies such as the dispersal of particulates in an airstream have also been studied using CFD.

The basic approach to formulating a CFD program is to divide the fluid up into many small cells; a typical problem might have a million cells. The basic equations, which we will study in this chapter, are then put in numerical form and programmed. The equations are difficult/impossible to solve analytically, and even the numerical formulation of them is difficult. It is only through the advances in computational power of the last several years has it been possible to solve these equations.



Courtesy of Symscape, www.symscape.com

CFD solution for the airflow over a pickup truck.

As with any computer program, it is essential to validate the results against reality. For this case of airflow over a pickup truck, tests on a scale model could be performed in a wind tunnel and the results compared to this picture. If there is good agreement, the maker of the pickup can then modify the software to study a variety of alternatives such as whether a deflector on top of the cab or opening the tailgate while driving would make the airflow more smooth and increase fuel economy.

Learning Objectives

After completing this chapter, you should be able to

- Solve a flow problem using the differential continuity equation (conservation of mass).
- Determine the stream function and flow rate for a flow problem.
- Determine the motion of a fluid particle in a flow problem.
- Solve a flow problem using the differential momentum equation (Navier–Stokes equation).

In Chapter 4, we developed the basic equations in integral form for a control volume. Integral equations are useful when we are interested in the gross behavior of a flow field and its effect on various devices. However, the integral approach does not enable us to obtain detailed point-by-point knowledge of the flow field. For example, the integral approach could provide information on the lift generated by a wing; it could not be used to determine the pressure distribution that produced the lift on the wing.

To see what is happening in a flow in detail, we need differential forms of the equations of motion. In this chapter we shall develop differential equations for the conservation of mass and Newton's second law of motion. Since we are interested in developing differential equations, we will need to analyze infinitesimal systems and control volumes. References 1 and 2 also provide details on the development of the differential equations.

5.1 Conservation of Mass

In Chapter 2, we developed the field representation of fluid properties. The property fields are defined by continuous functions of the space coordinates and time. The density and velocity fields were related through conservation of mass in integral form in Chapter 4 (Eq. 4.12). In this chapter, we shall derive the differential equation for conservation of mass in rectangular and in cylindrical coordinates. In both cases the derivation is carried out by applying conservation of mass to a differential control volume.

Rectangular Coordinate System

In rectangular coordinates, the control volume chosen is an infinitesimal cube with sides of length dx, dy, dz as shown in Fig. 5.1. The density at the center, O , of the control volume is assumed to be ρ and the velocity there is assumed to be $\vec{V} = \hat{i}u + \hat{j}v + \hat{k}w$.

To evaluate the properties at each of the six faces of the control surface, we use a Taylor series expansion about point O . For example, at the right face,

$$\rho_{x+dx/2} = \rho + \left(\frac{\partial \rho}{\partial x}\right) \frac{dx}{2} + \left(\frac{\partial^2 \rho}{\partial x^2}\right) \frac{1}{2!} \left(\frac{dx}{2}\right)^2 + \dots$$

Neglecting higher-order terms, we can write

$$\rho_{x+dx/2} = \rho + \left(\frac{\partial \rho}{\partial x}\right) \frac{dx}{2}$$

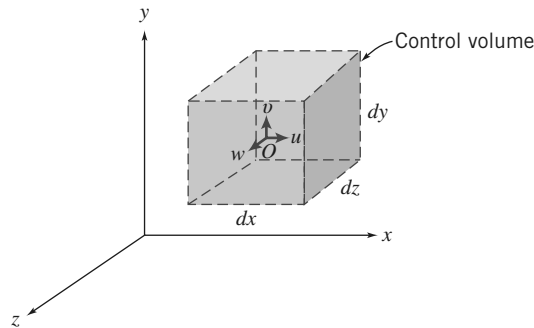


Fig. 5.1 Differential control volume in rectangular coordinates.

and

$$u)_{x+dx/2} = u + \left(\frac{\partial u}{\partial x} \right) \frac{dx}{2}$$

where $\rho, u, \partial\rho/\partial x$, and $\partial u/\partial x$ are all evaluated at point O . The corresponding terms at the left face are

$$\begin{aligned} \rho)_{x-dx/2} &= \rho + \left(\frac{\partial \rho}{\partial x} \right) \left(-\frac{dx}{2} \right) = \rho - \left(\frac{\partial \rho}{\partial x} \right) \frac{dx}{2} \\ u)_{x-dx/2} &= u + \left(\frac{\partial u}{\partial x} \right) \left(-\frac{dx}{2} \right) = u - \left(\frac{\partial u}{\partial x} \right) \frac{dx}{2} \end{aligned}$$

We can write similar expressions involving ρ and v for the front and back faces and ρ and w for the top and bottom faces of the infinitesimal cube $dx dy dz$. These can then be used to evaluate the surface integral in Eq. 4.12 (recall that $\int_{CS} \rho \vec{V} \cdot d\vec{A}$ is the net flux of mass out of the control volume):

$$\frac{\partial}{\partial t} \int_{CV} \rho dV + \int_{CS} \rho \vec{V} \cdot d\vec{A} = 0 \quad (4.12)$$

Table 5.1 shows the details of this evaluation. Note: We assume that the velocity components u, v , and w are positive in the x, y , and z directions, respectively; the area normal is by convention positive out of the cube; and higher-order terms [e.g., $(dx)^2$] are neglected in the limit as dx, dy , and $dz \rightarrow 0$.

The result of all this work is

$$\left[\frac{\partial \rho u}{\partial x} + \frac{\partial \rho v}{\partial x} + \frac{\partial \rho w}{\partial x} \right] dx dy dz$$

This expression is the surface integral evaluation for our differential cube. To complete Eq. 4.12, we need to evaluate the volume integral (recall that $\partial/\partial t \int_{CV} \rho dV$ is the rate of change of mass in the control volume):

$$\frac{\partial}{\partial t} \int_{CV} \rho dV \rightarrow \frac{\partial}{\partial t} [\rho dx dy dz] = \frac{\partial \rho}{\partial t} dx dy dz$$

Table 5.1
Mass Flux Through the Control Surface of a Rectangular Differential Control Volume

Surface	Evaluation of $\int \rho \vec{V} \cdot d\vec{A}$
Left $(-x)$	$-\left[\rho - \left(\frac{\partial \rho}{\partial x} \right) \frac{dx}{} \right] \left[u - \left(\frac{\partial u}{\partial x} \right) \frac{dx}{} \right] dy dz = -\rho u dy dz + \frac{1}{2} \left[u \left(\frac{\partial \rho}{\partial x} \right) + \rho \left(\frac{\partial u}{\partial x} \right) \right] dx dy dz$
Right $(+x)$	$\left[\rho + \left(\frac{\partial \rho}{\partial x} \right) \frac{dx}{} \right] \left[u + \left(\frac{\partial u}{\partial x} \right) \frac{dx}{} \right] dy dz = \rho u dy dz + \frac{1}{2} \left[u \left(\frac{\partial \rho}{\partial x} \right) + \rho \left(\frac{\partial u}{\partial x} \right) \right] dx dy dz$
Bottom $(-y)$	$-\left[\rho - \left(\frac{\partial \rho}{\partial y} \right) \frac{dy}{} \right] \left[v - \left(\frac{\partial v}{\partial y} \right) \frac{dy}{} \right] dx dz = -\rho v dx dz + \frac{1}{2} \left[v \left(\frac{\partial \rho}{\partial y} \right) + \rho \left(\frac{\partial v}{\partial y} \right) \right] dx dy dz$
Top $(+y)$	$\left[\rho + \left(\frac{\partial \rho}{\partial y} \right) \frac{dy}{} \right] \left[v + \left(\frac{\partial v}{\partial y} \right) \frac{dy}{} \right] dx dz = \rho v dx dz + \frac{1}{2} \left[v \left(\frac{\partial \rho}{\partial y} \right) + \rho \left(\frac{\partial v}{\partial y} \right) \right] dx dy dz$
Back $(-z)$	$-\left[\rho - \left(\frac{\partial \rho}{\partial z} \right) \frac{dz}{} \right] \left[w - \left(\frac{\partial w}{\partial z} \right) \frac{dz}{} \right] dx dy = -\rho w dx dy + \frac{1}{2} \left[w \left(\frac{\partial \rho}{\partial z} \right) + \rho \left(\frac{\partial w}{\partial z} \right) \right] dx dy dz$
Front $(+z)$	$\left[\rho + \left(\frac{\partial \rho}{\partial z} \right) \frac{dz}{} \right] \left[w + \left(\frac{\partial w}{\partial z} \right) \frac{dz}{} \right] dx dy = \rho w dx dy + \frac{1}{2} \left[w \left(\frac{\partial \rho}{\partial z} \right) + \rho \left(\frac{\partial w}{\partial z} \right) \right] dx dy dz$
Adding the results for all six faces,	
$\int_{CS} \rho \vec{V} \cdot d\vec{A} = \left[\left\{ u \left(\frac{\partial \rho}{\partial x} \right) + \rho \left(\frac{\partial u}{\partial x} \right) \right\} + \left\{ v \left(\frac{\partial \rho}{\partial y} \right) + \rho \left(\frac{\partial v}{\partial y} \right) \right\} + \left\{ w \left(\frac{\partial \rho}{\partial z} \right) + \rho \left(\frac{\partial w}{\partial z} \right) \right\} \right] dx dy dz$	
or	
$\int_{CS} \rho \vec{V} \cdot d\vec{A} = \left[\frac{\partial \rho u}{\partial x} + \frac{\partial \rho v}{\partial y} + \frac{\partial \rho w}{\partial z} \right] dx dy dz$	

Hence, we obtain (after canceling $dx dy dz$) from Eq. 4.12 a differential form of the mass conservation law

$$\frac{\partial \rho u}{\partial x} + \frac{\partial \rho v}{\partial y} + \frac{\partial \rho w}{\partial z} + \frac{\partial \rho}{\partial t} = 0 \quad (5.1a)$$

Equation 5.1a is frequently called the *continuity equation*.

Since the vector operator, ∇ , in rectangular coordinates, is given by

$$\nabla = \hat{i} \frac{\partial}{\partial x} + \hat{j} \frac{\partial}{\partial y} + \hat{k} \frac{\partial}{\partial z}$$

then

$$\frac{\partial \rho u}{\partial x} + \frac{\partial \rho v}{\partial y} + \frac{\partial \rho w}{\partial z} = \nabla \cdot \rho \vec{V}$$

Note that the del operator ∇ acts on ρ and \vec{V} . Think of it as $\nabla \cdot (\rho \vec{V})$. The conservation of mass may be written as

$$\nabla \cdot \rho \vec{V} + \frac{\partial \rho}{\partial t} = 0 \quad (5.1b)$$

Two flow cases for which the differential continuity equation may be simplified are worthy of note.

For an *incompressible* fluid, $\rho = \text{constant}$; density is neither a function of space coordinates nor a function of time. For an incompressible fluid, the continuity equation simplifies to

$$\frac{\partial u}{\partial x} + \frac{\partial v}{\partial y} + \frac{\partial w}{\partial z} = \nabla \cdot \vec{V} = 0 \quad (5.1c)$$

Thus the velocity field, $\vec{V}(x, y, z, t)$, for incompressible flow must satisfy $\nabla \cdot \vec{V} = 0$.

For *steady* flow, all fluid properties are, by definition, independent of time. Thus $\partial \rho / \partial t = 0$ and at most $\rho = \rho(x, y, z)$. For steady flow, the continuity equation can be written as

$$\frac{\partial \rho u}{\partial x} + \frac{\partial \rho v}{\partial y} + \frac{\partial \rho w}{\partial z} = \nabla \cdot \rho \vec{V} = 0 \quad (5.1d)$$

where the del operator ∇ acts on ρ and \vec{V} . Example 5.1 show the integration of the continuity equation for an incompressible flow, and Example 5.2 shows its application to a compressible unsteady flow.

Example 5.1 INTEGRATION OF TWO-DIMENSIONAL DIFFERENTIAL CONTINUITY EQUATION

For a two-dimensional flow in the xy plane, the x component of velocity is given by $u = Ax$. Determine a possible y component for incompressible flow. How many y components are possible?

Given: Two-dimensional flow in the xy plane for which $u = Ax$.

Find: (a) Possible y component for incompressible flow.
(b) Number of possible y components.

Solution:

Governing equation: $\nabla \cdot \rho \vec{V} + \frac{\partial \rho}{\partial t} = 0$

For incompressible flow this simplifies to $\nabla \cdot \vec{V} = 0$. In rectangular coordinates

$$\frac{\partial u}{\partial x} + \frac{\partial v}{\partial y} + \frac{\partial w}{\partial z} = 0$$

For two-dimensional flow in the xy plane, $\vec{V} = \vec{V}(x, y)$. Then partial derivatives with respect to z are zero, and

$$\frac{\partial u}{\partial x} + \frac{\partial v}{\partial y} = 0$$

Then

$$\frac{\partial v}{\partial y} = -\frac{\partial u}{\partial x} = -A$$

which gives an expression for the rate of change of v holding x constant. This equation can be integrated to obtain an expression for v . The result is

$$v = \int \frac{\partial v}{\partial y} dy + f(x, t) = -Ay + f(x, t) \quad \text{---} \quad v$$

The function of x and t appears because we had a partial derivative of v with respect to y .

Any function $f(x, t)$ is allowable, since $\partial/\partial y f(x, t) = 0$. Thus any number of expressions for v could satisfy the differential continuity equation under the given conditions. The simplest expression for v would be obtained by setting $f(x, t) = 0$. Then $v = -Ay$, and

$$\vec{V} = Ax\hat{i} - Ay\hat{j} \quad \text{---} \quad \vec{V}$$

This problem:

- Shows use of the differential continuity equation for obtaining information on a flow field.
- Demonstrates integration of a partial derivative.
- Proves that the flow originally discussed in Example 2.1 is indeed incompressible.

Example 5.2 UNSTEADY DIFFERENTIAL CONTINUITY EQUATION

A gas-filled pneumatic strut in an automobile suspension system behaves like a piston-cylinder apparatus. At one instant when the piston is $L = 0.15$ m away from the closed end of the cylinder, the gas density is uniform at $\rho = 18 \text{ kg/m}^3$ and the piston begins to move away from the closed end at $V = 12 \text{ m/s}$. Assume as a simple model that the gas velocity is one-dimensional and proportional to distance from the closed end; it varies linearly from zero at the end to $u = V$ at the piston. Find the rate of change of gas density at this instant. Obtain an expression for the average density as a function of time.

Given: Piston-cylinder as shown.

Find: (a) Rate of change of density.
(b) $\rho(t)$.

Solution:

Governing equation: $\nabla \cdot \rho \vec{V} + \frac{\partial \rho}{\partial t} = 0$

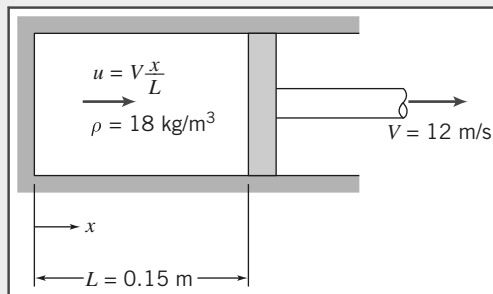
In rectangular coordinates, $\frac{\partial \rho u}{\partial x} + \frac{\partial \rho v}{\partial y} + \frac{\partial \rho w}{\partial z} + \frac{\partial \rho}{\partial t} = 0$

Since $u = u(x)$, partial derivatives with respect to y and z are zero, and

$$\frac{\partial \rho u}{\partial x} + \frac{\partial \rho}{\partial t} = 0$$

Then

$$\frac{\partial \rho}{\partial t} = -\frac{\partial \rho u}{\partial x} = -\rho \frac{\partial u}{\partial x} - u \frac{\partial \rho}{\partial x}$$



Since ρ is assumed uniform in the volume, $\frac{\partial \rho}{\partial x} = 0$, and $\frac{\partial \rho}{\partial t} = \frac{d\rho}{dt} = -\rho \frac{\partial u}{\partial x}$.

Since $u = V \frac{x}{L}, \frac{\partial u}{\partial x} = \frac{V}{L}$, then $\frac{d\rho}{dt} = -\rho \frac{V}{L}$. However, note that $L = L_0 + Vt$.

Separate variables and integrate,

$$\int_{\rho_0}^{\rho} \frac{d\rho}{\rho} = - \int_0^t \frac{V}{L} dt = - \int_0^t \frac{V dt}{L_0 + Vt}$$

$$\ln \frac{\rho}{\rho_0} = \ln \frac{L_0}{L_0 + Vt} \quad \text{and} \quad \rho(t) = \rho_0 \left[\frac{1}{1 + Vt/L_0} \right] \xrightarrow{\rho(t)}$$

At $t = 0$,

$$\frac{\partial \rho}{\partial t} = -\rho_0 \frac{V}{L} = -18 \frac{\text{kg}}{\text{m}^3} \times 12 \frac{\text{m}}{\text{s}} \times \frac{1}{0.15 \text{ m}} = -1440 \frac{\text{kg}}{(\text{m}^3 \cdot \text{s})} \xrightarrow{\frac{\partial \rho}{\partial t}}$$

This problem demonstrates use of the differential continuity equation for obtaining the density variation with time for an unsteady flow.

Cylindrical Coordinate System

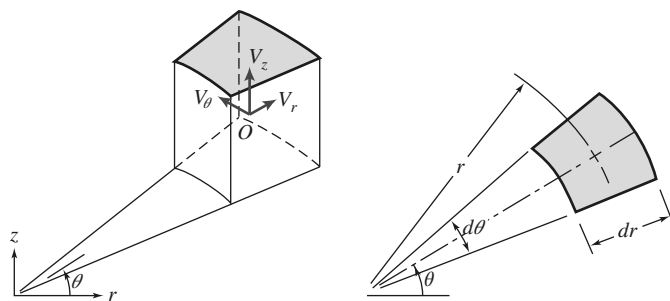
A suitable differential control volume for cylindrical coordinates is shown in Fig. 5.2. The density at the center, O , of the control volume is assumed to be ρ and the velocity there is assumed to be $\vec{V} = \hat{e}_r V_r + \hat{e}_\theta V_\theta + \hat{k} V_z$, where \hat{e}_r , \hat{e}_θ , and \hat{k} are unit vectors in the r , θ , and z directions, respectively, and V_r , V_θ , and V_z are the velocity components in the r , θ , and z directions, respectively. To evaluate $\int_{CS} \rho \vec{V} \cdot d\vec{A}$, we must consider the mass flux through each of the six faces of the control surface. The properties at each of the six faces of the control surface are obtained from a Taylor series expansion about point O . The details of the mass flux evaluation are shown in Table 5.2. Velocity components V_r , V_θ , and V_z are all assumed to be in the positive coordinate directions and we have again used the convention that the area normal is positive outwards on each face, and higher-order terms have been neglected.

We see that the net rate of mass flux out through the control surface (the term $\int_{CS} \rho \vec{V} \cdot d\vec{A}$ in Eq. 4.12) is given by

$$\left[\rho V_r + r \frac{\partial \rho V_r}{\partial r} + \frac{\partial \rho V_\theta}{\partial \theta} + r \frac{\partial \rho V_z}{\partial z} \right] dr d\theta dz$$

The mass inside the control volume at any instant is the product of the mass per unit volume, ρ , and the volume, $rd\theta dr dz$. Thus the rate of change of mass inside the control volume (the term $\partial/\partial t \int_{CV} \rho dV$ in Eq. 4.12) is given by

$$\frac{\partial \rho}{\partial t} r d\theta dr dz$$



(a) Isometric view

(b) Projection on $r\theta$ plane

Fig. 5.2 Differential control volume in cylindrical coordinates.

Table 5.2

Mass Flux Through the Control Surface of a Cylindrical Differential Control Volume

Surface	Evaluation of $\int \rho \vec{V} \cdot d\vec{A}$
Inside $(-r)$	$-\left[\rho - \left(\frac{\partial \rho}{\partial r}\right) \frac{dr}{2}\right] \left[V_r - \left(\frac{\partial V_r}{\partial r}\right) \frac{dr}{2}\right] \left(r - \frac{dr}{2}\right) d\theta dz = -\rho V_r r d\theta dz + \rho V_r \frac{dr}{2} d\theta dz + \rho \left(\frac{\partial V_r}{\partial r}\right) r \frac{dr}{2} d\theta dz + V_r \left(\frac{\partial \rho}{\partial r}\right) r \frac{dr}{2} d\theta dz$
Outside $(+r)$	$\left[\rho + \left(\frac{\partial \rho}{\partial r}\right) \frac{dr}{2}\right] \left[V_r + \left(\frac{\partial V_r}{\partial r}\right) \frac{dr}{2}\right] \left(r + \frac{dr}{2}\right) d\theta dz = \rho V_r r d\theta dz + \rho V_r \frac{dr}{2} d\theta dz + \rho \left(\frac{\partial V_r}{\partial r}\right) r \frac{dr}{2} d\theta dz + V_r \left(\frac{\partial \rho}{\partial r}\right) r \frac{dr}{2} d\theta dz$
Front $(-\theta)$	$-\left[\rho - \left(\frac{\partial \rho}{\partial \theta}\right) \frac{d\theta}{2}\right] \left[V_\theta - \left(\frac{\partial V_\theta}{\partial \theta}\right) \frac{d\theta}{2}\right] dr dz = -\rho V_\theta dr dz + \rho \left(\frac{\partial V_\theta}{\partial \theta}\right) \frac{d\theta}{2} dr dz + V_\theta \left(\frac{\partial \rho}{\partial \theta}\right) \frac{d\theta}{2} dr dz$
Back $(+\theta)$	$\left[\rho + \left(\frac{\partial \rho}{\partial \theta}\right) \frac{d\theta}{2}\right] \left[V_\theta + \left(\frac{\partial V_\theta}{\partial \theta}\right) \frac{d\theta}{2}\right] dr dz = \rho V_\theta dr dz + \rho \left(\frac{\partial V_\theta}{\partial \theta}\right) \frac{d\theta}{2} dr dz + V_\theta \left(\frac{\partial \rho}{\partial \theta}\right) \frac{d\theta}{2} dr dz$
Bottom $(-z)$	$-\left[\rho - \left(\frac{\partial \rho}{\partial z}\right) \frac{dz}{2}\right] \left[V_z - \left(\frac{\partial V_z}{\partial z}\right) \frac{dz}{2}\right] rd\theta dr = -\rho V_z rd\theta dr + \rho \left(\frac{\partial V_z}{\partial z}\right) \frac{dz}{2} rd\theta dr + V_z \left(\frac{\partial \rho}{\partial z}\right) \frac{dz}{2} rd\theta dr$
Top $(+z)$	$\left[\rho + \left(\frac{\partial \rho}{\partial z}\right) \frac{dz}{2}\right] \left[V_z + \left(\frac{\partial V_z}{\partial z}\right) \frac{dz}{2}\right] rd\theta dr = \rho V_z r d\theta dr + \rho \left(\frac{\partial V_z}{\partial z}\right) \frac{dz}{2} rd\theta dr + V_z \left(\frac{\partial \rho}{\partial z}\right) \frac{dz}{2} rd\theta dr$

Adding the results for all six faces,

$$\int_{CS} \rho \vec{V} \cdot d\vec{A} = \left[\rho V_r + r \left\{ \rho \left(\frac{\partial V_r}{\partial r} \right) + V_r \left(\frac{\partial \rho}{\partial r} \right) \right\} + \left\{ \rho \left(\frac{\partial V_\theta}{\partial \theta} \right) + V_\theta \left(\frac{\partial \rho}{\partial \theta} \right) \right\} + r \left\{ \rho \left(\frac{\partial V_z}{\partial z} \right) + V_z \left(\frac{\partial \rho}{\partial z} \right) \right\} \right] dr d\theta dz$$

or

$$\int_{CS} \rho \vec{V} \cdot d\vec{A} = \left[\rho V_r + r \frac{\partial \rho V_r}{\partial r} + \frac{\partial \rho V_\theta}{\partial \theta} + r \frac{\partial \rho V_z}{\partial z} \right] dr d\theta dz$$

In cylindrical coordinates the differential equation for conservation of mass is then

$$\rho V_r + r \frac{\partial \rho V_r}{\partial r} + \frac{\partial \rho V_\theta}{\partial \theta} + r \frac{\partial \rho V_z}{\partial z} + r \frac{\partial \rho}{\partial t} = 0$$

or

$$\frac{\partial(r\rho V_r)}{\partial r} + \frac{\partial \rho V_\theta}{\partial \theta} + r \frac{\partial \rho V_z}{\partial z} + r \frac{\partial \rho}{\partial t} = 0$$

Dividing by r gives

$$\frac{1}{r} \frac{\partial(r\rho V_r)}{\partial r} + \frac{1}{r} \frac{\partial(\rho V_\theta)}{\partial \theta} + \frac{\partial(\rho V_z)}{\partial z} + \frac{\partial \rho}{\partial t} = 0 \quad (5.2a)$$

In cylindrical coordinates the vector operator ∇ is given by

$$\nabla = \hat{e}_r \frac{\partial}{\partial r} + \hat{e}_\theta \frac{1}{r} \frac{\partial}{\partial \theta} + \hat{k} \frac{\partial}{\partial z} \quad (3.19)$$

where

$$\frac{\partial \hat{e}_r}{\partial \theta} = \hat{e}_\theta \quad \text{and} \quad \frac{\partial \hat{e}_\theta}{\partial \theta} = -\hat{e}_r$$

Equation 5.2a also may be written in vector notation as

$$\nabla \cdot \rho \vec{V} + \frac{\partial \rho}{\partial t} = 0 \quad (5.1b)$$

For an *incompressible* fluid, $\rho = \text{constant}$, and Eq. 5.2a reduces to

$$\frac{1}{r} \frac{\partial(rV_r)}{\partial r} + \frac{1}{r} \frac{\partial V_\theta}{\partial \theta} + \frac{\partial V_z}{\partial z} = \nabla \cdot \vec{V} = 0 \quad (5.2b)$$

Thus the velocity field, $\vec{V}(x, y, z, t)$, for incompressible flow must satisfy $\nabla \cdot \vec{V} = 0$. For *steady* flow, Eq. 5.2a reduces to

$$\frac{1}{r} \frac{\partial(r\rho V_r)}{\partial r} + \frac{1}{r} \frac{\partial(\rho V_\theta)}{\partial \theta} + \frac{\partial(\rho V_z)}{\partial z} = \nabla \cdot \rho \vec{V} = 0 \quad (5.2c)$$

When written in vector form, the differential continuity equation (the mathematical statement of conservation of mass), Eq. 5.1b, may be applied in any coordinate system. We simply substitute the appropriate expression for the vector operator ∇ . In retrospect, this result is not surprising since mass must be conserved regardless of our choice of coordinate system. Example 5.3 illustrates the application of the continuity equation in cylindrical coordinates.

Example 5.3 DIFFERENTIAL CONTINUITY EQUATION IN CYLINDRICAL COORDINATES

Consider a one-dimensional radial flow in the $r\theta$ plane, given by $V_r = f(r)$ and $V_\theta = 0$. Determine the conditions on $f(r)$ required for the flow to be incompressible.

Given: One-dimensional radial flow in the $r\theta$ plane: $V_r = f(r)$ and $V_\theta = 0$.

Find: Requirements on $f(r)$ for incompressible flow.

Solution:

Governing equation: $\nabla \cdot \rho \vec{V} + \frac{\partial \rho}{\partial t} = 0$

For incompressible flow in cylindrical coordinates this reduces to Eq. 5.2b,

$$\frac{1}{r} \frac{\partial}{\partial r} (rV_r) + \frac{1}{r} \frac{\partial V_\theta}{\partial \theta} + \frac{\partial V_z}{\partial z} = 0$$

For the given velocity field, $\vec{V} = \vec{V}(r) \cdot V_\theta = 0$ and partial derivatives with respect to z are zero, so

$$\frac{1}{r} \frac{\partial}{\partial r} (rV_r) = 0$$

Integrating with respect to r gives

$$rV_r = \text{constant}$$

Thus the continuity equation shows that the radial velocity must be $V_r = f(r) = C/r$ for one-dimensional radial flow of an incompressible fluid. This is not a surprising result: As the fluid moves outwards from the center, the volume flow rate (per unit depth in the z direction) $Q = 2\pi rV$ at any radius r is constant.

5.2 Stream Function for Two-Dimensional Incompressible Flow

We discussed streamlines in Chapter 2, where we stated that they were lines tangent to the velocity vectors in a flow at an instant

$$\left. \frac{dy}{dx} \right|_{\text{streamline}} = \frac{v}{u} \quad (2.8)$$

We can now develop a more formal definition of streamlines by introducing the *stream function*, ψ . This will allow us to represent two entities—the velocity components $u(x,y,t)$ and $v(x,y,t)$ of a two-dimensional incompressible flow—with a single function $\psi(x,y,t)$.

There are various ways to define the stream function. We start with the two-dimensional version of the continuity equation for incompressible flow (Eq. 5.1c):

$$\frac{\partial u}{\partial x} + \frac{\partial v}{\partial y} = 0 \quad (5.3)$$

We use what looks at first like a purely mathematical exercise (we will see a physical basis for it later) and define the stream function by

$$u \equiv \frac{\partial \psi}{\partial y} \quad \text{and} \quad v \equiv -\frac{\partial \psi}{\partial x} \quad (5.4)$$

so that Eq. 5.3 is *automatically* satisfied for *any* $\psi(x,y,t)$. To see this, use Eq. 5.4 in Eq. 5.3:

$$\frac{\partial u}{\partial x} + \frac{\partial v}{\partial y} = \frac{\partial^2 \psi}{\partial x \partial y} - \frac{\partial^2 \psi}{\partial y \partial x} = 0$$

Using Eq. 2.8, we can obtain an equation valid only *along* a streamline

$$udy - vdx = 0$$

or, using the definition of our stream function,

$$\frac{\partial \psi}{\partial x} dx + \frac{\partial \psi}{\partial y} dy = 0 \quad (5.5)$$

On the other hand, from a strictly mathematical point of view, at any instant in time t the variation in a function $\psi(x,y,t)$ in space (x,y) is given by

$$d\psi = \frac{\partial \psi}{\partial x} dx + \frac{\partial \psi}{\partial y} dy \quad (5.6)$$

Comparing Eqs. 5.5 and 5.6, we see that along an instantaneous streamline, $d\psi = 0$; in other words, ψ is a constant along a streamline. Hence we can specify individual streamlines by their stream function values: $\psi = 0, 1, 2$, etc. The significance of the ψ values is that they can be used to obtain the volume flow rate between any two streamlines. Consider the streamlines shown in Fig. 5.3. We can compute the volume flow rate between streamlines ψ_1 and ψ_2 by using line AB, BC, DE , or EF (recall that there is no flow *across* a streamline).

Let us compute the flow rate by using line AB , and also by using line BC —they should be the same! For a unit depth (dimension perpendicular to the xy plane), the flow rate across AB is

$$Q = \int_{y_1}^{y_2} u dy = \int_{y_1}^{y_2} \frac{\partial \psi}{\partial y} dy$$

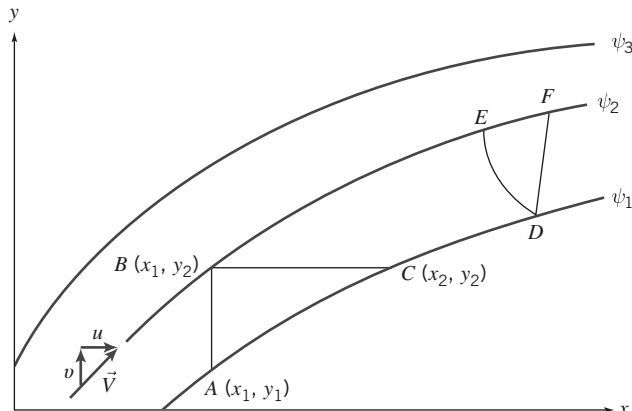


Fig. 5.3 Instantaneous streamlines in a two-dimensional flow.

But along AB , $x = \text{constant}$, and (from Eq. 5.6) $d\psi = \partial\psi/\partial y dy$. Therefore,

$$Q = \int_{y_1}^{y_2} \frac{\partial\psi}{\partial y} dy = \int_{\psi_1}^{\psi_2} d\psi = \psi_2 - \psi_1$$

For a unit depth, the flow rate across BC , is

$$Q = \int_{x_1}^{x_2} v dx = - \int_{x_1}^{x_2} \frac{\partial\psi}{\partial x} dx$$

Along BC , $y = \text{constant}$, and (from Eq. 5.6) $d\psi = \partial\psi/\partial y dy$. Therefore,

$$Q = - \int_{x_1}^{x_2} \frac{\partial\psi}{\partial x} dx = - \int_{\psi_2}^{\psi_1} d\psi = \psi_2 - \psi_1$$

Hence, whether we use line AB or line BC (or for that matter lines DE or DF), we find that *the volume flow rate (per unit depth) between two streamlines is given by the difference between the two stream function values.*

For two-dimensional steady compressible flow in the xy plane, the stream function, ψ , can be defined such that

$$\rho u \equiv \frac{\partial\psi}{\partial y} \quad \text{and} \quad \rho v \equiv - \frac{\partial\psi}{\partial x}$$

The difference between the constant values of ψ defining two streamlines is then the mass flow rate per unit depth between the two streamlines.

If the streamline through the origin is designated $\psi = 0$, then the ψ value for any other streamline represents the flow between the origin and that streamline. We are free to select any streamline as the zero streamline because the stream function is defined as a differential (Eq. 5.3); also, the flow rate will always be given by a *difference of ψ values*. Note that because the volume flow between any two streamlines is constant, *the velocity will be relatively high wherever the streamlines are close together, and relatively low wherever the streamlines are far apart*.

For a two-dimensional, incompressible flow in the $r\theta$ plane, conservation of mass, Eq. 5.2b, can be written as

$$\frac{\partial(rV_r)}{\partial r} + \frac{\partial V_\theta}{\partial \theta} = 0 \quad (5.7)$$

Using a logic similar to that used for Eq. 5.4, the stream function, $\psi(r, \theta, t)$, then is defined such that

$$V_r \equiv \frac{1}{r} \frac{\partial\psi}{\partial\theta} \quad \text{and} \quad V_\theta \equiv - \frac{\partial\psi}{\partial r} \quad (5.8)$$

With ψ defined according to Eq. 5.8, the continuity equation, Eq. 5.7, is satisfied exactly.

5.3 Motion of a Fluid Particle (Kinematics)

Figure 5.4 shows a typical finite fluid element, within which we have selected an infinitesimal particle of mass dm and initial volume $dx dy dz$, at time t , and as it may appear after a time interval dt . The finite element has moved and changed its shape and orientation. Note that while the finite element has quite severe distortion, the infinitesimal particle has changes in shape limited to stretching/shrinking and rotation of the element's sides. This is because we are considering both an infinitesimal time step and particle, so that the sides remain straight. We will examine the infinitesimal particle so that we will eventually obtain results applicable to a point. We can decompose this particle's motion into four components: *translation*, in which the particle moves from one point to another; *rotation* of the particle, which can occur about any or all of the x , y or z axes; *linear deformation*, in which the particle's sides stretch or contract; and *angular deformation*, in which the angles that were initially 90° for our particle between the sides change.

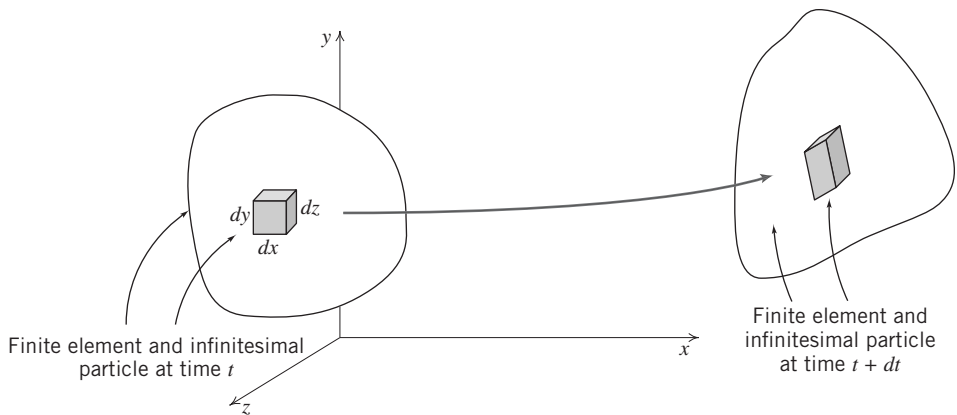


Fig. 5.4 Finite fluid element and infinitesimal particle at times t and $t + dt$.

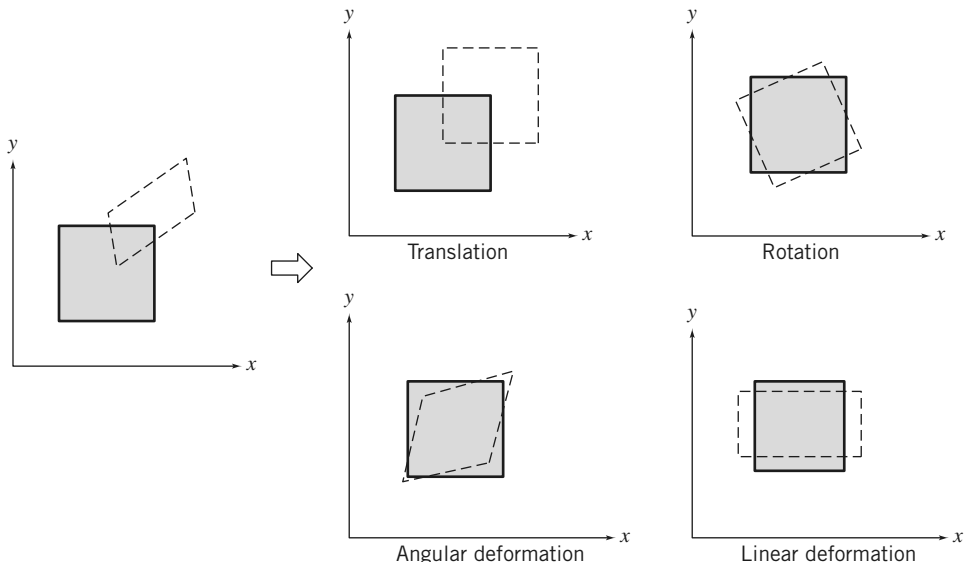


Fig. 5.5 Pictorial representation of the components of fluid motion.

It may seem difficult by looking at Fig. 5.4 to distinguish between rotation and angular deformation of the infinitesimal fluid particle. It is important to do so, because pure rotation involves no deformation but angular deformation does and, as we learned in Chapter 5, fluid deformation generates shear stresses. Figure 5.5 shows a typical xy plane motion decomposed into the four components described above, and as we examine each of these four components in turn we will see that we *can* distinguish between rotation and angular deformation.

Fluid Translation: Acceleration of a Fluid Particle in a Velocity Field

The translation of a fluid particle is obviously connected with the velocity field $\vec{V} = \vec{V}(x, y, z, t)$ that we previously discussed in Section 2.2. We will need the acceleration of a fluid particle for use in Newton's second law. It might seem that we could simply compute this as $\vec{a} = \partial \vec{V} / \partial t$. This is incorrect, because \vec{V} is a *field*, i.e., it describes the whole flow and not just the motion of an individual particle. We will see that this way of computing is incorrect by examining Example 5.4, in which particles are clearly accelerating and decelerating so $\vec{a} \neq 0$, but $\partial \vec{V} / \partial t = 0$.

Example 5.4 STREAM FUNCTION FOR FLOW IN A CORNER

Given the velocity field for steady, incompressible flow in a corner (Example 2.1), $\vec{V} = Ax\hat{i} - Ay\hat{j}$, with $A = 0.3 \text{ s}^{-1}$, determine the stream function that will yield this velocity field. Plot and interpret the streamline pattern in the first and second quadrants of the xy plane.

Given: Velocity field, $\vec{V} = Ax\hat{i} - Ay\hat{j}$, with $A = 0.3 \text{ s}^{-1}$.

Find: Stream function ψ and plot in first and second quadrants; interpret the results.

Solution: The flow is incompressible, so the stream function satisfies Eq. 5.4.

From Eq. 5.4, $u = \frac{\partial \psi}{\partial y}$ and $v = -\frac{\partial \psi}{\partial x}$. From the given velocity field,

$$u = Ax = \frac{\partial \psi}{\partial y}$$

Integrating with respect to y gives

$$\psi = \int \frac{\partial \psi}{\partial y} dy + f(x) = Axy + f(x) \quad (1)$$

where $f(x)$ is arbitrary. The function $f(x)$ may be evaluated using the equation for v . Thus, from Eq. 1,

$$v = -\frac{\partial \psi}{\partial x} = -Ay - \frac{df}{dx} \quad (2)$$

From the given velocity field, $v = -Ay$. Comparing this with Eq. 2 shows that $\frac{df}{dx} = 0$, or $f(x) = \text{constant}$. Therefore, Eq. 1 becomes

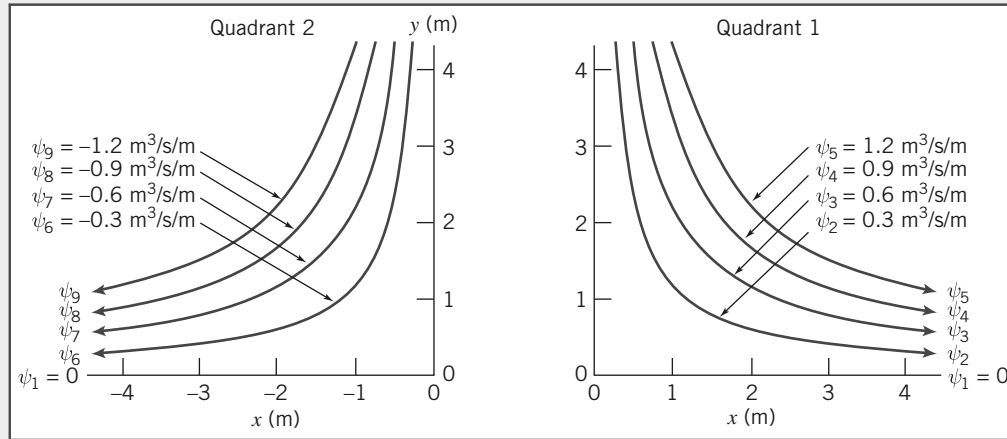
$$\psi = Axy + c \xleftarrow{\psi} \psi$$

Lines of constant ψ represent streamlines in the flow field. The constant c may be chosen as any convenient value for plotting purposes. The constant is chosen as zero in order that the streamline through the origin be designated as $\psi = \psi_1 = 0$. Then the value for any other streamline represents the flow between the origin and that streamline. With $c = 0$ and $A = 0.3 \text{ s}^{-1}$, then

$$\psi = 0.3xy \quad (\text{m}^3/\text{s}/\text{m})$$

This equation of a streamline is identical to the result ($xy = \text{constant}$), obtained in Example 2.1.

Separate plots of the streamlines in the first and second quadrants are presented below. Note that in quadrant 1, $u > 0$, so ψ values are positive. In quadrant 2, $u < 0$, so ψ values are negative.



In the first quadrant, since $u > 0$ and $v < 0$, the flow is from left to right and down. The volume flow rate between the streamline $\psi = \psi_1$ through the origin and the streamline $\psi = \psi_2$ is

$$Q_{12} = \psi_2 - \psi_1 = 0.3 \text{ m}^3/\text{s}/\text{m}$$

In the second quadrant, since $u < 0$ and $v < 0$, the flow is from right to left and down. The volume flow rate between streamlines ψ_7 and ψ_9 is

$$Q_{79} = \psi_9 - \psi_7 = [-1.2 - (-0.6)] \text{ m}^3/\text{s}/\text{m} = -0.6 \text{ m}^3/\text{s}/\text{m}$$

The negative sign is consistent with flow having $u < 0$.

As both the streamline spacing in the graphs and the equation for \bar{V} indicate, the velocity is smallest near the origin (a “corner”).

The problem, then, is to retain the field description for fluid properties and obtain an expression for the acceleration of a fluid particle as it moves in a flow field.

Consider a particle moving in a velocity field. At time t , the particle is at the position x, y, z and has a velocity corresponding to the velocity at that point in space at time t ,

$$\vec{V}_p \Big|_t = \vec{V}(x, y, z, t)$$

At $t + dt$, the particle has moved to a new position, with coordinates $x + dx, y + dy, z + dz$, and has a velocity given by

$$\vec{V}_p \Big|_{t+dt} = \vec{V}(x + dx, y + dy, z + dz, t + dt)$$

This is shown pictorially in Fig. 5.6.

The particle velocity at time t (position \vec{r}) is given by $\vec{V}_p = \vec{V}(x, y, z, t)$. Then $d\vec{V}_p$, the change in the velocity of the particle, in moving from location \vec{r} to $\vec{r} + d\vec{r}$, in time dt , is given by the chain rule,

$$d\vec{V}_p = \frac{\partial \vec{V}}{\partial x} dx_p + \frac{\partial \vec{V}}{\partial y} dy_p + \frac{\partial \vec{V}}{\partial z} dz_p + \frac{\partial \vec{V}}{\partial t} dt$$

The total acceleration of the particle is given by

$$\vec{a}_p = \frac{d\vec{V}_p}{dt} = \frac{\partial \vec{V}}{\partial x} \frac{dx_p}{dt} + \frac{\partial \vec{V}}{\partial y} \frac{dy_p}{dt} + \frac{\partial \vec{V}}{\partial z} \frac{dz_p}{dt} + \frac{\partial \vec{V}}{\partial t}$$

Since

$$\frac{dx_p}{dt} = u, \quad \frac{dy_p}{dt} = v, \quad \text{and} \quad \frac{dz_p}{dt} = w,$$

we have

$$\vec{a}_p = \frac{d\vec{V}_p}{dt} = u \frac{\partial \vec{V}}{\partial x} + v \frac{\partial \vec{V}}{\partial y} + w \frac{\partial \vec{V}}{\partial z} + \frac{\partial \vec{V}}{\partial t}$$

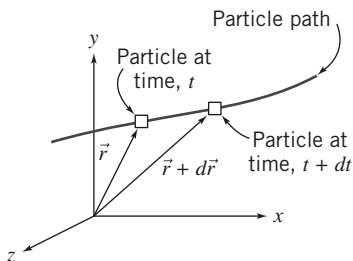


Fig. 5.6 Motion of a particle in a flow field.

To remind us that calculation of the acceleration of a fluid particle in a velocity field requires a special derivative, it is given the symbol $D\vec{V}/Dt$. Thus

$$\frac{D\vec{V}}{Dt} \equiv \vec{a}_p = u \frac{\partial \vec{V}}{\partial x} + v \frac{\partial \vec{V}}{\partial y} + w \frac{\partial \vec{V}}{\partial z} + \frac{\partial \vec{V}}{\partial t} \quad (5.9)$$

The derivative, D/Dt , defined by Eq. 5.9, is commonly called the *substantial derivative* to remind us that it is computed for a particle of “substance.” It also is called the *material derivative* or *particle derivative*.

The physical significance of the terms in Eq. 5.9 is

$$\vec{a}_p = \frac{D\vec{V}}{Dt} = \underbrace{u \frac{\partial \vec{V}}{\partial x} + v \frac{\partial \vec{V}}{\partial y} + w \frac{\partial \vec{V}}{\partial z}}_{\substack{\text{total} \\ \text{acceleration} \\ \text{of a particle}}} + \underbrace{\frac{\partial \vec{V}}{\partial t}}_{\substack{\text{convective} \\ \text{acceleration} \\ \text{local} \\ \text{acceleration}}}$$

From Eq. 5.9 we recognize that a fluid particle moving in a flow field may undergo acceleration for either of two reasons. As an illustration, refer to Example 5.4. This is a steady flow in which particles are *convected* toward the low-velocity region (near the “corner”), and then away to a high-velocity region. If a flow field is unsteady a fluid particle will undergo an additional *local* acceleration, because the velocity field is a function of time.

The convective acceleration may be written as a single vector expression using the gradient operator ∇ . Thus

$$u \frac{\partial \vec{V}}{\partial x} + v \frac{\partial \vec{V}}{\partial y} + w \frac{\partial \vec{V}}{\partial z} = (\vec{V} \cdot \nabla) \vec{V}$$

Thus Eq. 5.9 may be written as

$$\frac{D\vec{V}}{Dt} \equiv \vec{a}_p = (\vec{V} \cdot \nabla) \vec{V} + \frac{\partial \vec{V}}{\partial t} \quad (5.10)$$

For a *two-dimensional flow*, say $\vec{V} = \vec{V}(x, y, t)$, Eq. 5.9 reduces to

$$\frac{D\vec{V}}{Dt} = u \frac{\partial \vec{V}}{\partial x} + v \frac{\partial \vec{V}}{\partial y} + \frac{\partial \vec{V}}{\partial t}$$

For a *one-dimensional flow*, say $\vec{V} = \vec{V}(x, t)$, Eq. 5.9 becomes

$$\frac{D\vec{V}}{Dt} = u \frac{\partial \vec{V}}{\partial x} + \frac{\partial \vec{V}}{\partial t}$$

Finally, for a *steady flow in three dimensions*, Eq. 5.9 becomes

$$\frac{D\vec{V}}{Dt} = u \frac{\partial \vec{V}}{\partial x} + v \frac{\partial \vec{V}}{\partial y} + w \frac{\partial \vec{V}}{\partial z}$$

which, as we have seen, is not necessarily zero even though the flow is steady. Thus a fluid particle may undergo a convective acceleration due to its motion, even in a steady velocity field.

Equation 5.9 is a vector equation. As with all vector equations, it may be written in scalar component equations. Relative to an xyz coordinate system, the scalar components of Eq. 5.9 are written

$$a_{x_p} = \frac{Du}{Dt} = u \frac{\partial u}{\partial x} + v \frac{\partial u}{\partial y} + w \frac{\partial u}{\partial z} + \frac{\partial u}{\partial t} \quad (5.11a)$$

$$a_{y_p} = \frac{Dv}{Dt} = u \frac{\partial v}{\partial x} + v \frac{\partial v}{\partial y} + w \frac{\partial v}{\partial z} + \frac{\partial v}{\partial t} \quad (5.11b)$$

$$a_{z_p} = \frac{Dw}{Dt} = u \frac{\partial w}{\partial x} + v \frac{\partial w}{\partial y} + w \frac{\partial w}{\partial z} + \frac{\partial w}{\partial t} \quad (5.11c)$$

The components of acceleration in cylindrical coordinates may be obtained from Eq. 5.10 by expressing the velocity, \vec{V} , in cylindrical coordinates (Section 5.1) and utilizing the appropriate expression (Eq. 3.19, on the web) for the vector operator ∇ . Thus,

$$a_{r_p} = V_r \frac{\partial V_r}{\partial r} + \frac{V_\theta \partial V_r}{r} - \frac{V_\theta^2}{r} + V_z \frac{\partial V_r}{\partial z} + \frac{\partial V_r}{\partial t} \quad (5.12a)$$

$$a_{\theta_p} = V_r \frac{\partial V_\theta}{\partial r} + \frac{V_\theta \partial V_\theta}{r} + \frac{V_r V_\theta}{r} + V_z \frac{\partial V_\theta}{\partial z} + \frac{\partial V_\theta}{\partial t} \quad (5.12b)$$

$$a_{z_p} = V_r \frac{\partial V_z}{\partial r} + \frac{V_\theta \partial V_z}{r} + V_z \frac{\partial V_z}{\partial z} + \frac{\partial V_z}{\partial t} \quad (5.12c)$$

Equations 5.9, 5.11, and 5.12 are useful for computing the acceleration of a fluid particle anywhere in a flow from the velocity field (a function of x , y , z , and t); this is the *Eulerian* method of description, the most-used approach in fluid mechanics.

As an alternative if we wish to track an individual particle's motion we sometimes use the *Lagrangian* description of particle motion, in which the acceleration, position, and velocity of a particle are specified as a function of time only. Both descriptions are illustrated in Example 5.5.

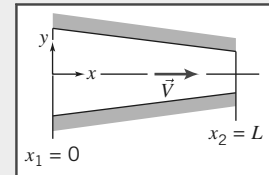
Example 5.5 PARTICLE ACCELERATION IN EULERIAN AND LAGRANGIAN DESCRIPTIONS

Consider two-dimensional, steady, incompressible flow through the plane converging channel shown. The velocity on the horizontal centerline (x axis) is given by $\vec{V} = V_1[1 + (x/L)]\hat{i}$. Find an expression for the acceleration of a particle moving along the centerline using (a) the Eulerian approach and (b) the Lagrangian approach. Evaluate the acceleration when the particle is at the beginning and at the end of the channel.

Given: Steady, two-dimensional, incompressible flow through the converging channel shown.

$$\vec{V} = V_1 \left(1 + \frac{x}{L}\right) \hat{i} \quad \text{on } x \text{ axis}$$

Find: (a) The acceleration of a particle moving along the centerline using the Eulerian approach.
(b) The acceleration of a particle moving along the centerline using the Lagrangian approach.
(c) Evaluate the acceleration when the particle is at the beginning and at the end of the channel.



Solution:

(a) The Eulerian approach

The governing equation for acceleration of a fluid particle is Eq. 5.9:

$$\vec{a}_p(x, y, z, t) = \frac{D\vec{V}}{Dt} = u \frac{\partial \vec{V}}{\partial x} + v \frac{\partial \vec{V}}{\partial y} + w \frac{\partial \vec{V}}{\partial z} + \frac{\partial \vec{V}}{\partial t}$$

In this case we are interested in the x component of acceleration (Eq. 5.11a):

$$a_{x_p}(x, y, z, t) = \frac{Du}{Dt} = u \frac{\partial u}{\partial x} + v \frac{\partial u}{\partial y} + w \frac{\partial u}{\partial z} + \frac{\partial u}{\partial t} \quad (5.11a)$$

On the x axis, $v = w = 0$ and $u = V_1 \left(1 + \frac{x}{L}\right)$, so for steady flow we obtain

$$a_{x_p}(x) = \frac{Du}{Dt} = u \frac{\partial u}{\partial x} = V_1 \left(1 + \frac{x}{L}\right) \frac{V_1}{L}$$

or

$$a_{x_p}(x) = \frac{V_1^2}{L} \left(1 + \frac{x}{L}\right) \xleftarrow{a_{x_p}(x)}$$

This expression gives the acceleration of *any* particle that is at point x at an instant.

(b) The Lagrangian approach

In this approach we need to obtain the motion of a fluid particle as we would in particle mechanics; that is, we need the position $\vec{x}_p(t)$, and then we can obtain the velocity $\vec{V}_p(t) = d\vec{x}_p/dt$ and acceleration $\vec{a}_p(t) = d\vec{V}_p/dt$. Actually, we are considering motion along the x axis, so we want $x_p(t)$, $u_p(t) = dx_p/dt$, and $a_{x_p}(t) = du_p/dt$. We are not given $x_p(t)$, but we do have

$$u_p = \frac{dx_p}{dt} = V_1 \left(1 + \frac{x_p}{L}\right)$$

Separating variables, and using limits $x_p(t=0) = 0$ and $x_p(t=t) = x_p$,

$$\int_0^{x_p} \frac{dx_p}{\left(1 + \frac{x_p}{L}\right)} = \int_0^1 V_1 dt \quad \text{and} \quad L \ln\left(1 + \frac{x_p}{L}\right) = V_1 t \quad (1)$$

We can then solve for $x_p(t)$:

$$x_p(t) = L(e^{V_1 t/L} - 1)$$

The velocity and acceleration are then

$$u_p(t) = \frac{dx_p}{dt} = V_1 e^{V_1 t/L}$$

and

$$a_{x_p}(t) = \frac{du_p}{dt} = \frac{V_1^2}{L} e^{V_1 t/L} \xleftarrow{a_{x_p}(t)} \quad (2)$$

This expression gives the acceleration at any time t of the particle that was initially at $x=0$.

(c) We wish to evaluate the acceleration when the particle is at $x=0$ and $x=L$. For the Eulerian approach this is straightforward:

$$a_{z_p}(x=0) = \frac{V_1^2}{L}, \quad a_{x_p}(x=L) = 2 \frac{V_1^2}{L} \xleftarrow{a_{x_p}}$$

For the Lagrangian approach, we need to find the times at which $x=0$ and $x=L$. Using Eq. 1, these are

$$t(x_p=0) = \frac{L}{V_1} \quad t(x_p=L) = \frac{L}{V_1} \ln(2)$$

Then, from Eq. 5.1,

$$a_{z_p}(t=0) = \frac{V_1^2}{L}, \quad \text{and} \\ a_{x_p}\left(t = \frac{L}{V_1} \ln(2)\right) = \frac{V_1^2}{L} e^{\ln(2)} = 2 \frac{V_1^2}{L} \xleftarrow{a_{x_p}}$$

Note that both approaches yield the same results for particle acceleration, as they should.

This problem illustrates use of the Eulerian and Lagrangian descriptions of the motion of a fluid particle.

Fluid Rotation

A fluid particle moving in a general three-dimensional flow field may rotate about all three coordinate axes. Thus particle rotation is a vector quantity and, in general,

$$\vec{\omega} = \hat{i}\omega_x + \hat{j}\omega_y + \hat{k}\omega_z$$

where ω_x is the rotation about the x axis, ω_y is the rotation about the y axis, and ω_z is the rotation about the z axis. The positive sense of rotation is given by the right-hand rule.

We now see how we can extract the rotation component of the particle motion. Consider the xy plane view of the particle at time t . The left and lower sides of the particle are given by the two perpendicular line segments oa and ob of lengths Δx and Δy , respectively, shown in Fig. 5.7a. In general, after an interval Δt the particle will have translated to some new position, and also have rotated and deformed. A possible instantaneous orientation of the lines at time $t + \Delta t$ is shown in Fig. 5.7b.

We need to be careful here with our signs for angles. Following the right-hand rule, *counterclockwise rotation is positive*, and we have shown side oa rotating counterclockwise through angle $\Delta\alpha$, but be aware that we have shown edge ob rotating at a *clockwise* angle $\Delta\beta$. Both angles are obviously arbitrary, but it will help visualize the discussion if we assign values to these angles, e.g., let $\Delta\alpha = 6^\circ$ and $\Delta\beta = 4^\circ$.

How do we extract from $\Delta\alpha$ and $\Delta\beta$ a measure of the particle's rotation? The answer is that we take an average of the rotations $\Delta\alpha$ and $\Delta\beta$, so that the particle's rigid body counterclockwise rotation is $\frac{1}{2}(\Delta\alpha - \Delta\beta)$, as shown in Fig. 5.7c. The minus sign is needed because the *counterclockwise* rotation of ob is $-\Delta\beta$. Using the assigned values, the rotation of the particle is then $\frac{1}{2}(6^\circ - 4^\circ) = 1^\circ$.

Now we can determine from $\Delta\alpha$ and $\Delta\beta$ a measure of the particle's angular deformation, as shown in Fig. 5.7d. To obtain the deformation of side oa in Fig. 5.7d, we use Fig. 5.7b and c: If we subtract the particle rotation $\frac{1}{2}(\Delta\alpha - \Delta\beta)$, in Fig. 5.7c, from the actual rotation of oa , $\Delta\alpha$, in Fig. 5.7b, what remains must be pure deformation [$\Delta\alpha - \frac{1}{2}(\Delta\alpha - \Delta\beta) = \frac{1}{2}(\Delta\alpha + \Delta\beta)$, in Fig. 5.7d]. Using the assigned values, the deformation of side oa is $6^\circ - \frac{1}{2}(6^\circ - 4^\circ) = 5^\circ$. By a similar process, for side ob we end with $\Delta\beta - \frac{1}{2}(\Delta\alpha - \Delta\beta) = \frac{1}{2}(\Delta\alpha + \Delta\beta)$, or a *clockwise* deformation $\frac{1}{2}(\Delta\alpha + \Delta\beta)$, as shown in Fig. 5.7d. The total deformation of the particle is the sum of the deformations of the sides, or $(\Delta\alpha + \Delta\beta)$ (with our example values, 10°). We verify that this leaves us with the correct value for the particle's deformation: Recall that in Section 2.4 we saw that deformation is measured by the change in a 90° angle. In Fig. 5.7a we see this is angle aob , and in Fig. 5.7d we see the total change of this angle is indeed $\frac{1}{2}(\Delta\alpha + \Delta\beta) + \frac{1}{2}(\Delta\alpha + \Delta\beta) = (\Delta\alpha + \Delta\beta)$.

We need to convert these angular measures to quantities obtainable from the flow field. To do this, we recognize that (for small angles) $\Delta\alpha = \Delta\eta/\Delta x$, and $\Delta\beta = \Delta\xi/\Delta y$. But $\Delta\xi$ arises because, if in interval Δt point o moves horizontally distance $u\Delta t$, then point b will have moved distance $(u + [\partial u/\partial y]\Delta y)\Delta t$ (using a Taylor series expansion). Likewise, $\Delta\eta$ arises because, if in interval Δt point o moves vertically distance $v\Delta t$, then point a will have moved distance $(v + [\partial v/\partial x]\Delta x)\Delta t$. Hence,

$$\Delta\xi = \left(u + \frac{\partial u}{\partial y} \Delta y \right) \Delta t - u \Delta t = \frac{\partial u}{\partial y} \Delta y \Delta t$$

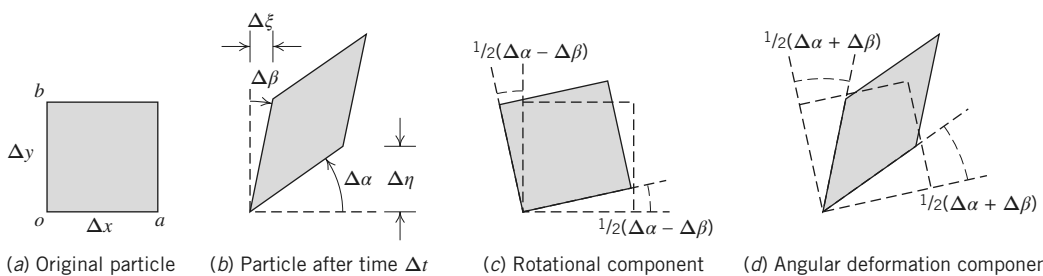


Fig. 5.7 Rotation and angular deformation of perpendicular line segments in a two-dimensional flow.

and

$$\Delta\eta = \left(v + \frac{\partial v}{\partial x} \Delta x \right) \Delta t - v \Delta t = \frac{\partial v}{\partial x} \Delta x \Delta t$$

We can now compute the angular velocity of the particle about the z axis, ω_z , by combining all these results:

$$\begin{aligned}\omega_z &= \lim_{\Delta t \rightarrow 0} \frac{1}{2} \frac{(\Delta\alpha - \Delta\beta)}{\Delta t} = \lim_{\Delta t \rightarrow 0} \frac{\frac{1}{2} \left(\frac{\Delta\eta}{\Delta x} - \frac{\Delta\xi}{\Delta y} \right)}{\Delta t} = \lim_{\Delta t \rightarrow 0} \frac{\frac{1}{2} \left(\frac{\partial v \Delta x}{\partial x \Delta x} \Delta t - \frac{\partial u \Delta y}{\partial y \Delta y} \Delta t \right)}{\Delta t} \\ \omega_z &= \frac{1}{2} \left(\frac{\partial v}{\partial x} - \frac{\partial u}{\partial y} \right)\end{aligned}$$

By considering the rotation of pairs of perpendicular line segments in the yz and xy planes, one can show similarly that

$$\omega_x = \frac{1}{2} \left(\frac{\partial w}{\partial y} - \frac{\partial v}{\partial z} \right) \quad \text{and} \quad \omega_y = \frac{1}{2} \left(\frac{\partial u}{\partial z} - \frac{\partial w}{\partial x} \right)$$

Then $\vec{\omega} = \hat{i}\omega_x + \hat{j}\omega_y + \hat{k}\omega_z$ becomes

$$\vec{\omega} = \frac{1}{2} \left[\hat{i} \left(\frac{\partial w}{\partial y} - \frac{\partial v}{\partial z} \right) + \hat{j} \left(\frac{\partial u}{\partial z} - \frac{\partial w}{\partial x} \right) + \hat{k} \left(\frac{\partial v}{\partial x} - \frac{\partial u}{\partial y} \right) \right] \quad (5.13)$$

We recognize the term in the square brackets as

$$\operatorname{curl} \vec{V} = \nabla \times \vec{V}$$

Then, in vector notation, we can write

$$\vec{\omega} = \frac{1}{2} \nabla \times \vec{V} \quad (5.14)$$

It is worth noting here that we should not confuse rotation of a fluid particle with flow consisting of circular streamlines, or *vortex* flow. As we will see in Example 5.6, in such a flow the particles *could* rotate as they move in a circular motion, but they do not have to.

Example 5.6 FREE AND FORCED VORTEX FLOWS

Consider flow fields with purely tangential motion (circular streamlines): $V_r = 0$ and $V_\theta = f(r)$. Evaluate the rotation, vorticity, and circulation for rigid-body rotation, a *forced vortex*. Show that it is possible to choose $f(r)$ so that flow is irrotational, i.e., to produce a *free vortex*.

Given: Flow fields with tangential motion, $V_r = 0$ and $V_\theta = f(r)$.

Find: (a) Rotation, vorticity, and circulation for rigid-body motion (a *forced vortex*).
(b) $V_\theta = f(r)$ for irrotational motion (a *free vortex*).

Solution:

Governing equation:

$$\vec{\zeta} = 2\vec{\omega} = \nabla \times \vec{V} \quad (5.15)$$

For motion in the $r\theta$ plane, the only components of rotation and vorticity are in the z direction,

$$\zeta_z = 2\omega_z = \frac{1}{r} \frac{\partial rV_\theta}{\partial r} - \frac{1}{r} \frac{\partial V_r}{\partial \theta}$$

Because $V_r = 0$ everywhere in these fields, this reduces to $\zeta_z = 2\omega_z = \frac{1}{r} \frac{\partial rV_\theta}{\partial r}$.

(a) For rigid-body rotation, $V_\theta = \omega r$

$$\text{Then } \omega_z = \frac{1}{2} \frac{1}{r} \frac{\partial r V_\theta}{\partial r} = \frac{1}{2} \frac{1}{r} \frac{\partial}{\partial r} (\omega r^2) = \frac{1}{2r} (2\omega r) = \omega \quad \text{and} \quad \zeta_z = 2\omega.$$

The circulation is

$$\Gamma = \oint_c \vec{V} \cdot d\vec{s} = \int_A 2\omega_z dA. \quad (18)$$

Since $\omega_z = \omega = \text{constant}$, the circulation about any closed contour is given by $\Gamma = 2\omega A$, where A is the area enclosed by the contour. Thus for rigid-body motion (a forced vortex), the rotation and vorticity are constants; the circulation depends on the area enclosed by the contour.

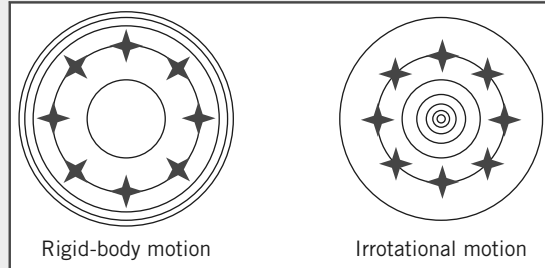
(b) For irrotational flow, $\omega_z = \frac{1}{r} \frac{\partial}{\partial r} r V_\theta = 0$. Integrating, we find

$$r V_\theta = \text{constant} \quad \text{or} \quad V_\theta = f(r) = \frac{C}{r}$$

For this flow, the origin is a singular point where $V_\theta \rightarrow \infty$. The circulation for any contour enclosing the origin is

$$\Gamma = \oint_c \vec{V} \cdot d\vec{s} = \int_0^{2\pi} \frac{C}{r} r d\theta = 2\pi C$$

It turns out that the circulation around any contour *not* enclosing the singular point at the origin is zero. Streamlines for the two vortex flows are shown below, along with the location and orientation at different instants of a cross marked in the fluid that was initially at the 12 o'clock position. For the rigid-body motion, the cross rotates as it moves in a circular motion; also, the streamlines are closer together as we move away from the origin. For the irrotational motion the cross does not rotate as it moves in a circular motion; also, the streamlines are farther apart as we move away from the origin.



When might we expect to have a flow in which the particles rotate as they move ($\vec{\omega} \neq 0$)? One possibility is that we start out with a flow in which (for whatever reason) the particles already have rotation. On the other hand, if we assumed the particles are not initially rotating, particles will only begin to rotate if they experience a torque caused by surface shear stresses; the particle body forces and normal (pressure) forces may accelerate and deform the particle, but cannot generate a torque. We can conclude that rotation of fluid particles will *always* occur for flows in which we have shear stresses. We have already learned in Chapter 2 that shear stresses are present whenever we have a viscous fluid that is experiencing angular deformation (shearing). Hence we conclude that rotation of fluid particles only occurs in viscous flows unless the particles are initially rotating, as in Example 3.10.

Flows for which no particle rotation occurs are called *irrotational* flows. Although no real flow is truly irrotational because all fluids have viscosity, it turns out that many flows can be successfully studied by assuming they are inviscid and irrotational, because viscous effects are often negligible. As we discussed in Chapter 1, and will again in Chapter 6, much of aerodynamics theory assumes inviscid flow. We just need to be aware that in any flow there will always be regions (e.g., the boundary layer for flow over a wing) in which viscous effects cannot be ignored.

The factor of $\frac{1}{2}$ can be eliminated from Eq. 5.14 by defining the *vorticity*, $\vec{\zeta}$, to be twice the rotation,

$$\vec{\zeta} \equiv 2\vec{\omega} = \nabla \times \vec{V} \quad (5.15)$$

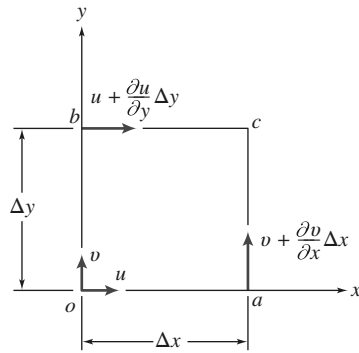


Fig. 5.8 Velocity components on the boundaries of a fluid element.

The vorticity is a measure of the rotation of a fluid element as it moves in the flow field. In cylindrical coordinates the vorticity is

$$\nabla \times \vec{V} = \hat{e}_r \left(\frac{1}{r} \frac{\partial V_z}{\partial \theta} - \frac{\partial V_\theta}{\partial z} \right) + \hat{e}_\theta \left(\frac{\partial V_r}{\partial z} - \frac{\partial V_z}{\partial r} \right) + \hat{k} \left(\frac{1}{r} \frac{\partial r V_\theta}{\partial r} - \frac{1}{r} \frac{\partial V_r}{\partial \theta} \right) \quad (5.16)$$

The *circulation*, Γ (which we will revisit in Example 6.12), is defined as the line integral of the tangential velocity component about any closed curve fixed in the flow,

$$\Gamma = \oint_c \vec{V} \cdot d\vec{s} \quad (5.17)$$

where $d\vec{s}$ is an elemental vector tangent to the curve and having length ds of the element of arc; a positive sense corresponds to a counterclockwise path of integration around the curve. We can develop a relationship between circulation and vorticity by considering the rectangular circuit shown in Fig. 5.8, where the velocity components at o are assumed to be (u, v) , and the velocities along segments bc and ac can be derived using Taylor series approximations.

For the closed curve $oacb$,

$$\begin{aligned} \Delta\Gamma &= u\Delta x + \left(v + \frac{\partial v}{\partial x} \Delta x \right) \Delta y - \left(u + \frac{\partial u}{\partial y} \Delta y \right) \Delta x - v \Delta y \\ \Delta\Gamma &= \left(\frac{\partial v}{\partial x} - \frac{\partial u}{\partial y} \right) \Delta x \Delta y \\ \Delta\Gamma &= 2\omega_z \Delta x \Delta y \end{aligned}$$

Then,

$$\Gamma = \oint_c \vec{V} \cdot d\vec{s} = \int_A 2\omega_z dA = \int_A (\nabla \times \vec{V})_z dA \quad (5.18)$$

Equation 5.18 is a statement of the Stokes Theorem in two dimensions. Thus the circulation around a closed contour is equal to the total vorticity enclosed within it.

Fluid Deformation

a. Angular Deformation

As we discussed earlier (and as shown in Fig. 5.7d), the *angular deformation* of a particle is given by the sum of the two angular deformations, or in other words by $(\Delta\alpha + \Delta\beta)$.

We also recall that $\Delta\alpha = \Delta\eta/\Delta x$, $\Delta\beta = \Delta\xi/\Delta y$, and $\Delta\xi$ and $\Delta\eta$ are given by

$$\Delta\xi = \left(u + \frac{\partial u}{\partial y} \Delta y \right) \Delta t - u \Delta t = \frac{\partial u}{\partial y} \Delta y \Delta t$$

and

$$\Delta\eta = \left(v + \frac{\partial v}{\partial x} \Delta x \right) \Delta t - v \Delta t = \frac{\partial v}{\partial x} \Delta x \Delta t$$

We can now compute the rate of angular deformation of the particle in the xy plane by combining these results,

$$\begin{aligned} \text{Rate of angular deformation in } xy \text{ plane} &= \lim_{\Delta t \rightarrow 0} \frac{(\Delta\alpha + \Delta\beta)}{\Delta t} = \lim_{\Delta t \rightarrow 0} \frac{\left(\frac{\Delta\eta}{\Delta x} + \frac{\Delta\xi}{\Delta y} \right)}{\Delta t} \\ \text{Rate of angular deformation in } xy \text{ plane} &= \lim_{\Delta t \rightarrow 0} \frac{\left(\frac{\partial v}{\partial x} \frac{\Delta x}{\Delta x} \Delta t + \frac{\partial u}{\partial y} \frac{\Delta y}{\Delta y} \Delta t \right)}{\Delta t} = \left(\frac{\partial v}{\partial x} + \frac{\partial u}{\partial y} \right) \end{aligned} \quad (5.19a)$$

Similar expressions can be written for the rate of angular deformation of the particle in the yz and zx planes,

$$\text{Rate of angular deformation in } yz \text{ plane} = \left(\frac{\partial w}{\partial y} + \frac{\partial v}{\partial z} \right) \quad (5.19b)$$

$$\text{Rate of angular deformation in } zx \text{ plane} = \left(\frac{\partial w}{\partial x} + \frac{\partial u}{\partial z} \right) \quad (5.19c)$$

We saw in Chapter 2 that for one-dimensional laminar Newtonian flow the shear stress is given by the rate of deformation (du/dy) of the fluid particle,

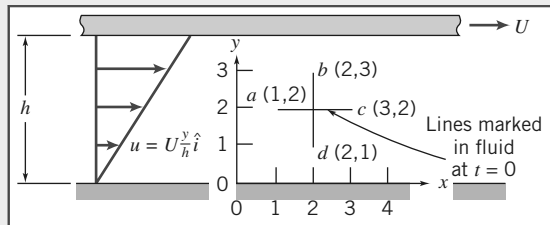
$$\tau_{yx} = \mu \frac{du}{dy} \quad (2.15)$$

We will see shortly that we can generalize Eq. 2.15 to the case of three-dimensional laminar flow; this will lead to expressions for three-dimensional shear stresses involving the three rates of angular deformation given above. (Eq. 2.15 is a special case of Eq. 5.19a.)

Calculation of angular deformation is illustrated for a simple flow field in Example 5.7.

Example 5.7 ROTATION IN VISCOMETRIC FLOW

A viscometric flow in the narrow gap between large parallel plates is shown. The velocity field in the narrow gap is given by $\vec{V} = U(y/h)\hat{i}$, where $U = 4 \text{ mm/s}$ and $h = 4 \text{ mm}$. At $t = 0$ line segments ac and bd are marked in the fluid to form a cross as shown. Evaluate the positions of the marked points at $t = 1.5 \text{ s}$ and sketch for comparison. Calculate the rate of angular deformation and the rate of rotation of a fluid particle in this velocity field. Comment on your results.



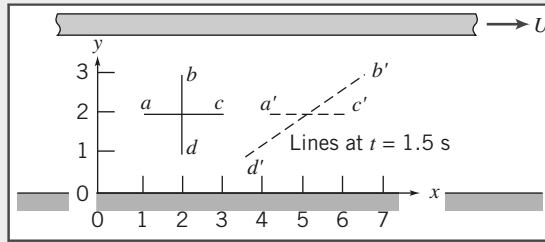
Given: Velocity field, $\vec{V} = U(y/h)\hat{i}$; $U = 4 \text{ mm/s}$, and $h = 4 \text{ mm}$. Fluid particles marked at $t = 0$ to form cross as shown.

- Find:**
- Positions of points a' , b' , c' , and d' at $t = 1.5 \text{ s}$; plot.
 - Rate of angular deformation.
 - Rate of rotation of a fluid particle.
 - Significance of these results.

Solution: For the given flow field $v = 0$, so there is no vertical motion. The velocity of each point stays constant, so $\Delta x = u\Delta t$ for each point. At point b , $u = 3 \text{ mm/s}$, so

$$\Delta x_b = 3 \frac{\text{mm}}{\text{s}} \times 1.5 \text{ s} = 4.5 \text{ mm}$$

Similarly, points *a* and *c* each move 3 mm, and point *d* moves 1.5 mm. Hence the plot at $t = 1.5$ s is



The rate of angular deformation is

$$\frac{\partial u}{\partial y} + \frac{\partial v}{\partial x} = U \frac{1}{h} + 0 = \frac{U}{h} = 4 \frac{\text{mm}}{\text{s}} \times \frac{1}{4 \text{ mm}} = 1 \text{ s}^{-1}$$

The rate of rotation is

$$\omega_z = \frac{1}{2} \left(\frac{\partial v}{\partial x} - \frac{\partial u}{\partial y} \right) = \frac{1}{2} \left(0 - \frac{U}{h} \right) = -\frac{1}{2} \times 4 \frac{\text{mm}}{\text{s}} \times \frac{1}{4 \text{ mm}} = -0.5 \text{ s}^{-1}$$

In this problem we have a viscous flow, and hence should have expected both angular deformation and particle rotation.

b. Linear Deformation

During linear deformation, the shape of the fluid element, described by the angles at its vertices, remains unchanged, since all right angles continue to be right angles (see Fig. 5.5). The element will change length in the *x* direction only if $\partial u / \partial x$ is other than zero. Similarly, a change in the *y* dimension requires a nonzero value of $\partial v / \partial y$ and a change in the *z* dimension requires a nonzero value of $\partial w / \partial z$. These quantities represent the components of longitudinal rates of strain in the *x*, *y*, and *z* directions, respectively.

Changes in length of the sides may produce changes in volume of the element. The rate of local instantaneous *volume dilation* is given by

$$\text{Volume dilation rate} = \frac{\partial u}{\partial x} + \frac{\partial v}{\partial y} + \frac{\partial w}{\partial z} = \nabla \cdot \vec{V} \quad (5.20)$$

For incompressible flow, the rate of volume dilation is zero (Eq. 5.1c).

We have shown in this section that the velocity field can be used to find the acceleration, rotation, angular deformation, and linear deformation of a fluid particle in a flow field. Evaluation of the rate of deformation for flow near a corner is illustrated in Example 5.8.

Example 5.8 DEFORMATION RATES FOR FLOW IN A CORNER

The velocity field $\vec{V} = Ax\hat{i} - Ay\hat{j}$ represents flow in a “corner,” as shown in Example 5.4, where $A = 0.3 \text{ s}^{-1}$ and the coordinates are measured in meters. A square is marked in the fluid as shown at $t = 0$. Evaluate the new positions of the four corner points when point *a* has moved to $x = \frac{3}{2} \text{ m}$ after τ seconds. Evaluate the rates of linear deformation in the *x* and *y* directions. Compare area $a'b'c'd'$ at $t = \tau$ with area $abcd$ at $t = 0$. Comment on the significance of this result.

Given: $\vec{V} = Ax\hat{i} - Ay\hat{j}; A = 0.3 \text{ s}^{-1}$, *x* and *y* in meters.

Find: (a) Position of square at $t = \tau$ when *a* is at *a'* at $x = \frac{3}{2} \text{ m}$.
 (b) Rates of linear deformation.
 (c) Area $a'b'c'd'$ compared with area $abcd$.
 (d) Significance of the results.

Solution: First we must find τ , so we must follow a fluid particle using a Lagrangian description. Thus

$$u = \frac{dx_p}{dt} = Ax_p, \quad \frac{dx}{x} = A dt, \text{ so } \int_{x_0}^x \frac{dx}{x} = \int_0^\tau A dt \quad \text{and} \quad \ln \frac{x}{x_0} = A\tau$$

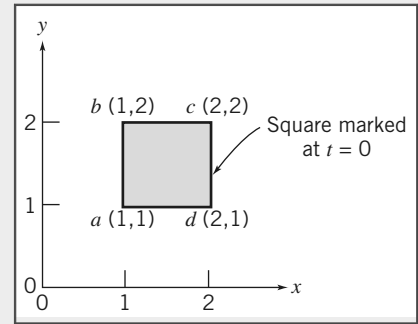
$$\tau = \frac{\ln x/x_0}{A} = \frac{\ln \left(\frac{3}{2}\right)}{0.3 \text{ s}^{-1}} = 1.35 \text{ s}$$

In the y direction

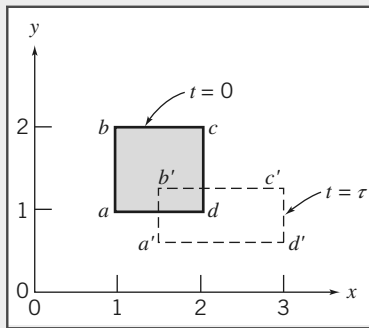
$$v = \frac{dy_p}{dt} = -Ay_p \quad \frac{dy}{y} = -A dt \quad \frac{y}{y_0} = e^{-At}$$

The point coordinates at τ are:

Point	$t=0$	$t=\tau$
a	(1, 1)	$\left(\frac{3}{2}, \frac{2}{3}\right)$
b	(1, 2)	$\left(\frac{3}{2}, \frac{4}{3}\right)$
c	(2, 2)	$\left(3, \frac{4}{3}\right)$
d	(2, 1)	$\left(3, \frac{2}{3}\right)$



The plot is:



The rates of linear deformation are:

$$\frac{\partial u}{\partial x} = \frac{\partial}{\partial x} Ax = A = 0.3 \text{ s}^{-1} \quad \text{in the } x \text{ direction}$$

$$\frac{\partial v}{\partial y} = \frac{\partial}{\partial y} (-Ay) = -A = -0.3 \text{ s}^{-1} \quad \text{in the } y \text{ direction}$$

The rate of volume dilation is

$$\nabla \cdot \vec{V} = \frac{\partial u}{\partial x} + \frac{\partial v}{\partial y} = A - A = 0$$

$$\text{Area } abcd = 1 \text{ m}^2 \text{ and area } a'b'c'd' = \left(3 - \frac{3}{2}\right) \left(\frac{4}{3} - \frac{2}{3}\right) = 1 \text{ m}^2.$$

Notes:

- Parallel planes remain parallel; there is linear deformation but no angular deformation.
- The flow is irrotational ($\partial v / \partial x - \partial u / \partial y = 0$).
- Volume is conserved because the two rates of linear deformation are equal and opposite.
- The NCFMF video *Flow Visualization* (see <http://web.mit.edu/fluids/www/Shapiro/ncfmf.html> for free online viewing of this film) uses hydrogen bubble time-streak markers to demonstrate experimentally that the area of a marked fluid square is conserved in two-dimensional incompressible flow.

5.4 Momentum Equation

A dynamic equation describing fluid motion may be obtained by applying Newton's second law to a particle. To derive the differential form of the momentum equation, we shall apply Newton's second law to an infinitesimal fluid particle of mass dm .

Recall that Newton's second law for a finite system is given by

$$\vec{F} = \frac{d\vec{P}}{dt} \Bigg|_{\text{system}} \quad (4.2a)$$

where the linear momentum, \vec{P} , of the system is given by

$$\vec{P}_{\text{system}} = \int_{\text{mass (system)}} \vec{V} dm \quad (4.2b)$$

Then, for an infinitesimal system of mass dm , Newton's second law can be written

$$d\vec{F} = dm \frac{d\vec{V}}{dt} \Bigg|_{\text{system}} \quad (5.21)$$

Having obtained an expression for the acceleration of a fluid element of mass dm , moving in a velocity field (Eq. 5.9), we can write Newton's second law as the vector equation

$$d\vec{F} = dm \frac{D\vec{V}}{Dt} = dm \left[u \frac{\partial \vec{V}}{\partial x} + v \frac{\partial \vec{V}}{\partial y} + w \frac{\partial \vec{V}}{\partial z} + \frac{\partial \vec{V}}{\partial t} \right] \quad (5.22)$$

We now need to obtain a suitable formulation for the force, $d\vec{F}$, or its components, dF_x , dF_y , and dF_z , acting on the element.

Forces Acting on a Fluid Particle

Recall that the forces acting on a fluid element may be classified as body forces and surface forces; surface forces include both normal forces and tangential (shear) forces.

We shall consider the x component of the force acting on a differential element of mass dm and volume $dV = dx dy dz$. Only those stresses that act in the x direction will give rise to surface forces in the x direction. If the stresses at the center of the differential element are taken to be σ_{xx} , τ_{yx} , and τ_{zx} , then the stresses acting in the x direction on all faces of the element (obtained by a Taylor series expansion about the center of the element) are as shown in Fig. 5.9.

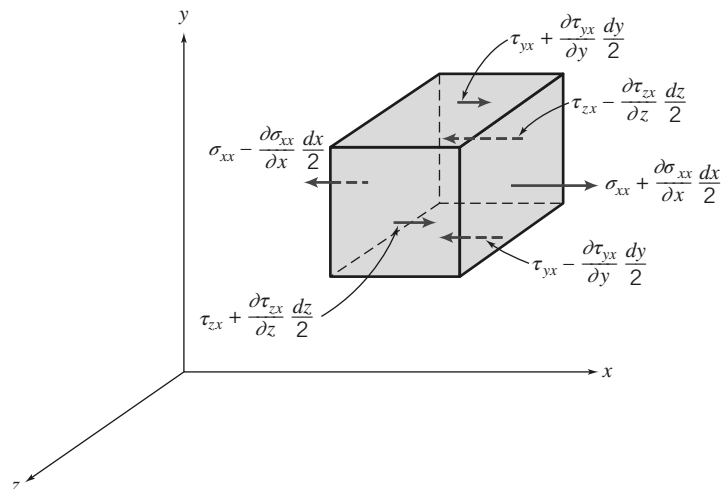


Fig. 5.9 Stresses in the x direction on an element of fluid.

To obtain the net surface force in the x direction, dF_{S_x} , we must sum the forces in the x direction. Thus,

$$\begin{aligned} dF_{S_x} &= \left(\sigma_{xx} + \frac{\partial \sigma_{xx}}{\partial x} \frac{dx}{2} \right) dy dz - \left(\sigma_{xx} - \frac{\partial \sigma_{xx}}{\partial x} \frac{dx}{2} \right) dy dz \\ &\quad + \left(\tau_{yx} + \frac{\partial \tau_{yx}}{\partial y} \frac{dy}{2} \right) dx dz - \left(\tau_{yx} - \frac{\partial \tau_{yx}}{\partial y} \frac{dy}{2} \right) dx dz \\ &\quad + \left(\tau_{zx} + \frac{\partial \tau_{zx}}{\partial z} \frac{dz}{2} \right) dx dy - \left(\tau_{zx} - \frac{\partial \tau_{zx}}{\partial z} \frac{dz}{2} \right) dx dy \end{aligned}$$

On simplifying, we obtain

$$dF_{S_x} = \left(\frac{\partial \sigma_{xx}}{\partial x} + \frac{\partial \tau_{yx}}{\partial y} + \frac{\partial \tau_{zx}}{\partial z} \right) dx dy dz$$

When the force of gravity is the only body force acting, then the body force per unit mass is \vec{g} . The net force in the x direction, dF_x , is given by

$$dF_x = dF_{B_x} + dF_{S_x} = \left(\rho g_x + \frac{\partial \sigma_{xx}}{\partial x} + \frac{\partial \tau_{yx}}{\partial y} + \frac{\partial \tau_{zx}}{\partial z} \right) dx dy dz \quad (5.23a)$$

We can derive similar expressions for the force components in the y and z directions:

$$dF_y = dF_{B_y} + dF_{S_y} = \left(\rho g_y + \frac{\partial \tau_{xy}}{\partial x} + \frac{\partial \sigma_{yy}}{\partial y} + \frac{\partial \tau_{zy}}{\partial z} \right) dx dy dz \quad (5.23b)$$

$$dF_z = dF_{B_z} + dF_{S_z} = \left(\rho g_z + \frac{\partial \tau_{xz}}{\partial x} + \frac{\partial \tau_{yz}}{\partial y} + \frac{\partial \sigma_{zz}}{\partial z} \right) dx dy dz \quad (5.23c)$$

Differential Momentum Equation

We have now formulated expressions for the components, dF_x , dF_y , and dF_z , of the force, $d\vec{F}$, acting on the element of mass dm . If we substitute these expressions (Eqs. 5.23) for the force components into the x , y , and z components of Eq. 5.22, we obtain the differential equations of motion,

$$\rho g_x + \frac{\partial \sigma_{xx}}{\partial x} + \frac{\partial \tau_{yx}}{\partial y} + \frac{\partial \tau_{zx}}{\partial z} = \rho \left(\frac{\partial u}{\partial t} + u \frac{\partial u}{\partial x} + v \frac{\partial u}{\partial y} + w \frac{\partial u}{\partial z} \right) \quad (5.24a)$$

$$\rho g_y + \frac{\partial \tau_{xy}}{\partial x} + \frac{\partial \sigma_{yy}}{\partial y} + \frac{\partial \tau_{zy}}{\partial z} = \rho \left(\frac{\partial v}{\partial t} + u \frac{\partial v}{\partial x} + v \frac{\partial v}{\partial y} + w \frac{\partial v}{\partial z} \right) \quad (5.24b)$$

$$\rho g_z + \frac{\partial \tau_{xz}}{\partial x} + \frac{\partial \tau_{yz}}{\partial y} + \frac{\partial \sigma_{zz}}{\partial z} = \rho \left(\frac{\partial w}{\partial t} + u \frac{\partial w}{\partial x} + v \frac{\partial w}{\partial y} + w \frac{\partial w}{\partial z} \right) \quad (5.24c)$$

Equations 5.24 are the differential equations of motion for any fluid satisfying the continuum assumption. Before the equations can be used to solve for u , v , and w , suitable expressions for the stresses must be obtained in terms of the velocity and pressure fields.

Newtonian Fluid: Navier–Stokes Equations

For a Newtonian fluid the viscous stress is directly proportional to the rate of shearing strain (angular deformation rate). We saw in Chapter 2 that for one-dimensional laminar Newtonian flow the shear stress is proportional to the rate of angular deformation: $\tau_{yx} = du/dy$ (Eq. 2.15). For a three-dimensional flow the situation is a bit more complicated as we need to use the more complicated expressions for rate of angular deformation, Eq. 5.19. The stresses may be expressed in terms of velocity gradients and fluid properties in rectangular coordinates as follows:

$$\tau_{xy} = \tau_{yx} = \mu \left(\frac{\partial v}{\partial x} + \frac{\partial u}{\partial y} \right) \quad (5.25a)$$

$$\tau_{yz} = \tau_{zy} = \mu \left(\frac{\partial w}{\partial y} + \frac{\partial v}{\partial z} \right) \quad (5.25b)$$

$$\tau_{zx} = \tau_{xz} = \mu \left(\frac{\partial u}{\partial z} + \frac{\partial w}{\partial x} \right) \quad (5.25c)$$

$$\sigma_{xx} = -p - \frac{2}{3}\mu \nabla \cdot \vec{V} + 2\mu \frac{\partial u}{\partial x} \quad (5.25d)$$

$$\sigma_{yy} = -p - \frac{2}{3}\mu \nabla \cdot \vec{V} + 2\mu \frac{\partial v}{\partial y} \quad (5.25e)$$

$$\sigma_{zz} = -p - \frac{2}{3}\mu \nabla \cdot \vec{V} + 2\mu \frac{\partial w}{\partial z} \quad (5.25f)$$

where p is the local thermodynamic pressure. Thermodynamic pressure is related to the density and temperature by the thermodynamic relation usually called the equation of state.

If these expressions for the stresses are introduced into the differential equations of motion (Eq. 5.24), we obtain

$$\begin{aligned} \rho \frac{Du}{Dt} &= \rho g_x - \frac{\partial p}{\partial x} + \frac{\partial}{\partial x} \left[\mu \left(2 \frac{\partial u}{\partial x} - \frac{2}{3} \nabla \cdot \vec{V} \right) \right] + \frac{\partial}{\partial y} \left[\mu \left(\frac{\partial u}{\partial y} + \frac{\partial v}{\partial x} \right) \right] \\ &\quad + \frac{\partial}{\partial z} \left[\mu \left(\frac{\partial w}{\partial x} + \frac{\partial u}{\partial z} \right) \right] \end{aligned} \quad (5.26a)$$

$$\begin{aligned} \rho \frac{Dv}{Dt} &= \rho g_y - \frac{\partial p}{\partial y} + \frac{\partial}{\partial x} \left[\mu \left(\frac{\partial u}{\partial y} + \frac{\partial v}{\partial x} \right) \right] + \frac{\partial}{\partial y} \left[\mu \left(2 \frac{\partial v}{\partial y} - \frac{2}{3} \nabla \cdot \vec{V} \right) \right] \\ &\quad + \frac{\partial}{\partial z} \left[\mu \left(\frac{\partial v}{\partial z} + \frac{\partial w}{\partial y} \right) \right] \end{aligned} \quad (5.26b)$$

$$\begin{aligned} \rho \frac{Dw}{Dt} &= \rho g_z - \frac{\partial p}{\partial z} + \frac{\partial}{\partial x} \left[\mu \left(\frac{\partial w}{\partial x} + \frac{\partial u}{\partial z} \right) \right] + \frac{\partial}{\partial y} \left[\mu \left(\frac{\partial w}{\partial z} + \frac{\partial v}{\partial y} \right) \right] \\ &\quad + \frac{\partial}{\partial z} \left[\mu \left(2 \frac{\partial w}{\partial z} - \frac{2}{3} \nabla \cdot \vec{V} \right) \right] \end{aligned} \quad (5.26c)$$

These equations of motion are called the *Navier–Stokes* equations. The equations are greatly simplified when applied to *incompressible flow* with *constant viscosity*. Under these conditions the equations reduce to

$$\rho \left(\frac{\partial u}{\partial t} + u \frac{\partial u}{\partial x} + v \frac{\partial u}{\partial y} + w \frac{\partial u}{\partial z} \right) = \rho g_x - \frac{\partial p}{\partial x} + \mu \left(\frac{\partial^2 u}{\partial x^2} + \frac{\partial^2 u}{\partial y^2} + \frac{\partial^2 u}{\partial z^2} \right) \quad (5.27a)$$

$$\rho \left(\frac{\partial v}{\partial t} + u \frac{\partial v}{\partial x} + v \frac{\partial v}{\partial y} + w \frac{\partial v}{\partial z} \right) = \rho g_y - \frac{\partial p}{\partial y} + \mu \left(\frac{\partial^2 v}{\partial x^2} + \frac{\partial^2 v}{\partial y^2} + \frac{\partial^2 v}{\partial z^2} \right) \quad (5.27b)$$

$$\rho \left(\frac{\partial w}{\partial t} + u \frac{\partial w}{\partial x} + v \frac{\partial w}{\partial y} + w \frac{\partial w}{\partial z} \right) = \rho g_z - \frac{\partial p}{\partial z} + \mu \left(\frac{\partial^2 w}{\partial x^2} + \frac{\partial^2 w}{\partial y^2} + \frac{\partial^2 w}{\partial z^2} \right) \quad (5.27c)$$

This form of the Navier–Stokes equations is one of the most famous set of equations in fluid mechanics, and has been widely studied. These equations, with the continuity equation (Eq. 5.1c), form a set of four coupled nonlinear partial differential equations for u , v , w , and p . In principle, these four equations describe many common flows. The only restrictions are that the fluid be Newtonian (with a constant viscosity) and incompressible. For example, lubrication theory, pipe flows, and even the motion of your coffee as you stir it are explained by these equations. Unfortunately, they are impossible to solve analytically, except for the most basic cases [1] in which we have simple boundaries and initial or boundary conditions. We will solve the equations for such a simple problem in Example 5.9.

Example 5.9 ANALYSIS OF FULLY DEVELOPED LAMINAR FLOW DOWN AN INCLINED PLANE SURFACE

A liquid flows down an inclined plane surface in a steady, fully developed laminar film of thickness h . Simplify the continuity and Navier–Stokes equations to model this flow field. Obtain expressions for the liquid velocity profile, the shear stress distribution, the volume flow rate, and the average velocity. Relate the liquid film thickness to the volume flow rate per unit depth of surface normal to the flow. Calculate the volume flow rate in a film of water $h = 1$ mm thick, flowing on a surface $b = 1$ m wide, inclined at $\theta = 15^\circ$ to the horizontal.

Given: Liquid flow down an inclined plane surface in a steady, fully developed laminar film of thickness h .

Find: (a) Continuity and Navier–Stokes equations simplified to model this flow field.

(b) Velocity profile.

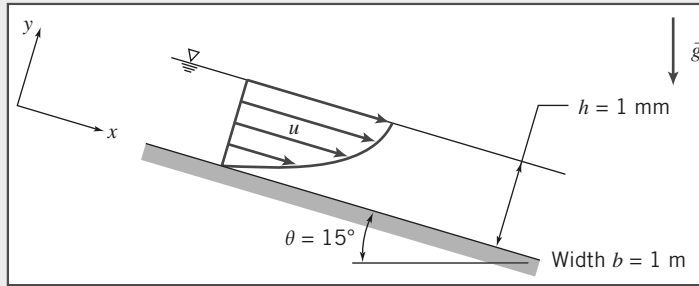
(c) Shear stress distribution.

(d) Volume flow rate per unit depth of surface normal to diagram.

(e) Average flow velocity.

(f) Film thickness in terms of volume flow rate per unit depth of surface normal to diagram.

(g) Volume flow rate in a film of water 1 mm thick on a surface 1 m wide, inclined at 15° to the horizontal.



Solution: The geometry and coordinate system used to model the flow field are shown. It is convenient to align one coordinate with the flow down the plane surface.

The governing equations written for incompressible flow with constant viscosity are

$$\frac{\partial u}{\partial x} + \frac{\partial v}{\partial y} + \frac{\partial w}{\partial z} = 0 \quad (5.1c)$$

$$\rho \left(\frac{\partial u}{\partial t} + u \frac{\partial u}{\partial x} + v \frac{\partial u}{\partial y} + w \frac{\partial u}{\partial z} \right) = \rho g_x - \frac{\partial p}{\partial x} + \mu \left(\frac{\partial^2 u}{\partial x^2} + \frac{\partial^2 u}{\partial y^2} + \frac{\partial^2 u}{\partial z^2} \right) \quad (5.27a)$$

$$\rho \left(\frac{\partial v}{\partial t} + u \frac{\partial v}{\partial x} + v \frac{\partial v}{\partial y} + w \frac{\partial v}{\partial z} \right) = \rho g_y - \frac{\partial p}{\partial y} + \mu \left(\frac{\partial^2 v}{\partial x^2} + \frac{\partial^2 v}{\partial y^2} + \frac{\partial^2 v}{\partial z^2} \right) \quad (5.27b)$$

$$\rho \left(\frac{\partial w}{\partial t} + u \frac{\partial w}{\partial x} + v \frac{\partial w}{\partial y} + w \frac{\partial w}{\partial z} \right) = \rho g_z - \frac{\partial p}{\partial z} + \mu \left(\frac{\partial^2 w}{\partial x^2} + \frac{\partial^2 w}{\partial y^2} + \frac{\partial^2 w}{\partial z^2} \right) \quad (5.27c)$$

The terms canceled to simplify the basic equations are keyed by number to the assumptions listed below. The assumptions are discussed in the order in which they are applied to simplify the equations.

Assumptions:

- 1 Steady flow (given).
- 2 Incompressible flow; $\rho = \text{constant}$.
- 3 No flow or variation of properties in the z direction; $w = 0$ and $\partial/\partial z = 0$.
- 4 Fully developed flow, so no properties vary in the x direction; $\partial/\partial x = 0$.

Assumption 1 eliminates time variations in any fluid property.

Assumption 2 eliminates space variations in density.

Assumption 3 states that there is no z component of velocity and no property variations in the z direction. All terms in the z component of the Navier–Stokes equation cancel.

After assumption 4 is applied, the continuity equation reduces to $\partial v / \partial y = 0$. Assumptions 3 and 4 also indicate that $\partial v / \partial z = 0$ and $\partial v / \partial x = 0$. Therefore, v must be constant. Since v is zero at the solid surface, then v must be zero everywhere.

The fact that $v = 0$ reduces the Navier–Stokes equations further, as indicated by (5) in Eqs. 5.27a and 5.27b. The final simplified equations are

$$0 = \rho g_x + \mu \frac{\partial^2 u}{\partial y^2} \quad (1)$$

$$0 = \rho g_y - \frac{\partial p}{\partial y} \quad (2)$$

Since $\partial u / \partial z = 0$ (assumption 3) and $\partial u / \partial x = 0$ (assumption 4), then u is at most a function of y , and $\partial^2 u / \partial y^2 = d^2 u / dy^2$, and from Eq. 1, then

$$\frac{d^2 u}{dy^2} = -\frac{\rho g_x}{\mu} = -\rho g \frac{\sin \theta}{\mu}$$

Integrating,

$$\frac{du}{dy} = -\rho g \frac{\sin \theta}{\mu} y + c_1 \quad (3)$$

and integrating again,

$$u = -\rho g \frac{\sin \theta}{\mu} \frac{y^2}{2} + c_1 y + c_2 \quad (4)$$

The boundary conditions needed to evaluate the constants are the no-slip condition at the solid surface ($u = 0$ at $y = 0$) and the zero-shear-stress condition at the liquid free surface ($du/dy = 0$ at $y = h$).

Evaluating Eq. 4 at $y = 0$ gives $c_2 = 0$. From Eq. 3 at $y = h$,

$$0 = -\rho g \frac{\sin \theta}{\mu} h + c_1$$

or

$$c_1 = \rho g \frac{\sin \theta}{\mu} h$$

Substituting into Eq. 4 we obtain the velocity profile

$$u = -\rho g \frac{\sin \theta}{\mu} \frac{y^2}{2} + \rho g \frac{\sin \theta}{\mu} h y$$

or

$$u = \rho g \frac{\sin \theta}{\mu} \left(h y - \frac{y^2}{2} \right) \xrightarrow{u(y)}$$

The shear stress distribution is (from Eq. 5.25a after setting $\partial v / \partial x$ to zero, or alternatively, for one-dimensional flow, from Eq. 2.15)

$$\tau_{yx} = \mu \frac{du}{dy} = \rho g \sin \theta (h - y) \xrightarrow{\tau_{yx}(y)}$$

The shear stress in the fluid reaches its maximum value at the wall ($y = 0$); as we expect, it is zero at the free surface ($y = h$). At the wall the shear stress τ_{yx} is positive but the surface normal for the fluid is in the negative y direction; hence the shear force acts in the negative x direction, and just balances the x component of the body force acting on the fluid. The volume flow rate is

$$Q = \int_A u \, dA = \int_0^h u \, b \, dy$$

where b is the surface width in the z direction. Substituting,

$$Q = \int_0^h \frac{\rho g \sin \theta}{\mu} \left(hy - \frac{y^2}{2} \right) b dy = \rho g \frac{\sin \theta b}{\mu} \left[\frac{hy^2}{2} - \frac{y^3}{6} \right]_0^h$$

$$Q = \frac{\rho g \sin \theta b}{\mu} \frac{h^3}{3} \quad \text{---} \quad Q \quad (5)$$

The average flow velocity is $\bar{V} = Q/A = Q/bh$. Thus

$$\bar{V} = \frac{Q}{bh} = \frac{\rho g \sin \theta}{\mu} \frac{h^2}{3} \quad \text{---} \quad \bar{V}$$

Solving for film thickness gives

$$h = \left[\frac{3\mu Q}{\rho g \sin \theta b} \right]^{1/3} \quad h \quad (6)$$

A film of water $h = 1$ mm thick on a plane $b = 1$ m wide, inclined at $\theta = 15^\circ$, would carry

$$Q = 999 \frac{\text{kg}}{\text{m}^3} \times 9.81 \frac{\text{m}}{\text{s}^2} \times \sin(15^\circ) \times 1 \text{ m} \times \frac{\text{m} \cdot \text{s}}{1.00 \times 10^{-3} \text{ kg}}$$

$$\times \frac{(0.001)^3 \text{ m}^3}{3} \times 1000 \frac{\text{L}}{\text{m}^3}$$

$$Q = 0.846 \text{ L/s} \quad Q$$

Notes:

- This problem illustrates how the full Navier–Stokes equations (Eqs. 5.27a–5.27c) can sometimes be reduced to a set of solvable equations (Eqs. 1 and 2 in this problem).
- After integration of the simplified equations, boundary (or initial) conditions are used to complete the solution.
- Once the velocity field is obtained, other useful quantities (e.g., shear stress, volume flow rate) can be found.
- Equations 5 and 6 show that even for fairly simple problems the results can be quite complicated: The depth of the flow depends in a nonlinear way on flow rate ($h \propto Q^{1/3}$).

The Navier–Stokes equations for constant density and viscosity are given in cylindrical coordinates in Example 5.10. They have also been derived for spherical coordinates [1, 2]. We will apply the cylindrical coordinate form in solving Example 5.10.

Example 5.10 ANALYSIS OF LAMINAR VISCOMETRIC FLOW BETWEEN COAXIAL CYLINDERS

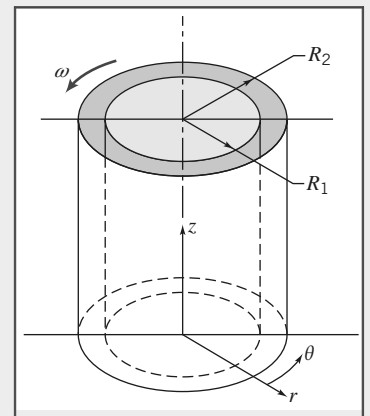
A viscous liquid fills the annular gap between vertical concentric cylinders. The inner cylinder is stationary, and the outer cylinder rotates at constant speed. The flow is laminar. Simplify the continuity, Navier–Stokes, and tangential shear stress equations to model this flow field. Obtain expressions for the liquid velocity profile and the shear stress distribution. Compare the shear stress at the surface of the inner cylinder with that computed from a planar approximation obtained by “unwrapping” the annulus into a plane and assuming a linear velocity profile across the gap. Determine the ratio of cylinder radii for which the planar approximation predicts the correct shear stress at the surface of the inner cylinder within 1 percent.

Given: Laminar viscometric flow of liquid in annular gap between vertical concentric cylinders. The inner cylinder is stationary, and the outer cylinder rotates at constant speed.

- Find:**
- Continuity and Navier–Stokes equations simplified to model this flow field.
 - Velocity profile in the annular gap.
 - Shear stress distribution in the annular gap.
 - Shear stress at the surface of the inner cylinder.
 - Comparison with “planar” approximation for constant shear stress in the narrow gap between cylinders.
 - Ratio of cylinder radii for which the planar approximation predicts shear stress within 1 percent of the correct value.

Solution: The geometry and coordinate system used to model the flow field are shown. The z coordinate is directed vertically upward; as a consequence, $g_r = g_\theta = 0$ and $g_z = -g$.

The continuity, Navier–Stokes, and tangential shear stress equations written in cylindrical coordinates for incompressible flow with constant viscosity are



$$\frac{1}{r} \frac{\partial}{\partial r} (r v_r) + \frac{1}{r} \frac{\partial v_\theta}{\partial \theta} + \frac{\partial v_z}{\partial z} = 0 \quad (1)$$

r component:

$$\begin{aligned} & \rho \left(\frac{\partial v_r^1}{\partial t} + v_r \frac{\partial v_r^5}{\partial r} + \frac{v_\theta}{r} \frac{\partial v_r^4}{\partial \theta} - \frac{v_\theta^2}{r} + v_z \frac{\partial v_r^3}{\partial z} \right) \\ &= \rho g_r^0 - \frac{\partial p}{\partial r} + \mu \left\{ \frac{\partial}{\partial r} \left(\frac{1}{r} \frac{\partial}{\partial r} \left[r v_r^5 \right] \right) + \frac{1}{r^2} \frac{\partial^2 v_r^4}{\partial \theta^2} - \frac{2}{r^2} \frac{\partial v_\theta^4}{\partial \theta} + \frac{\partial^2 v_r^3}{\partial z^2} \right\} \end{aligned}$$

θ component:

$$\begin{aligned} & \rho \left(\frac{\partial v_\theta^1}{\partial t} + v_r^5 \frac{\partial v_\theta}{\partial r} + \frac{v_\theta}{r} \frac{\partial v_\theta^4}{\partial \theta} + \frac{v_r v_\theta^5}{r} + v_z \frac{\partial v_\theta^3}{\partial z} \right) \\ &= \rho g_\theta^0 - \frac{1}{r} \frac{\partial p^4}{\partial \theta} + \mu \left\{ \frac{\partial}{\partial r} \left(\frac{1}{r} \frac{\partial}{\partial r} [r v_\theta] \right) + \frac{1}{r^2} \frac{\partial^2 v_\theta^4}{\partial \theta^2} + \frac{2}{r^2} \frac{\partial v_\theta^4}{\partial \theta} + \frac{\partial^2 v_\theta^3}{\partial z^2} \right\} \end{aligned}$$

z component:

$$\begin{aligned} & \rho \left(\frac{\partial v_z^1}{\partial t} + v_r^5 \frac{\partial v_z}{\partial r} + \frac{v_\theta}{r} \frac{\partial v_z^4}{\partial \theta} + v_z \frac{\partial v_z^3}{\partial z} \right) = \rho g_z - \frac{\partial p}{\partial z} + \mu \left\{ \frac{1}{r} \frac{\partial}{\partial r} \left(r \frac{\partial v_z^3}{\partial r} \right) + \frac{1}{r^2} \frac{\partial^2 v_z^3}{\partial \theta^2} + \frac{\partial^2 v_z^3}{\partial z^2} \right\} \\ & \tau_{r\theta} = \mu \left[r \frac{\partial}{\partial r} \left(\frac{v_\theta}{r} \right) + \frac{1}{r} \frac{\partial v_\theta^4}{\partial \theta} \right] \end{aligned}$$

The terms canceled to simplify the basic equations are keyed by number to the assumptions listed below. The assumptions are discussed in the order in which they are applied to simplify the equations.

Assumptions:

- 1 Steady flow; angular speed of outer cylinder is constant.
- 2 Incompressible flow; $\rho = \text{constant}$.
- 3 No flow or variation of properties in the z direction; $v_z = 0$ and $\partial/\partial z = 0$.
- 4 Circumferentially symmetric flow, so properties do not vary with θ , so $\partial/\partial\theta = 0$.

Assumption 1 eliminates time variations in fluid properties.

Assumption 2 eliminates space variations in density.

Assumption 3 causes all terms in the z component of the Navier–Stokes equation to cancel, except for the hydrostatic pressure distribution.

After assumptions 3 and 4 are applied, the continuity equation reduces to

$$\frac{1}{r} \frac{\partial}{\partial r} (r v_r) = 0$$

Because $\partial/\partial\theta=0$ and $\partial/\partial z=0$ by assumptions 3 and 4, then $\frac{\partial}{\partial r} \rightarrow \frac{d}{dr}$, so integrating gives

$$r v_r = \text{constant}$$

Since v_r is zero at the solid surface of each cylinder, then v_r must be zero everywhere.

The fact that $v_r=0$ reduces the Navier-Stokes equations further. The r - and θ -component equations reduce to

$$\begin{aligned} -\rho \frac{v_\theta^2}{r} &= -\frac{\partial p}{\partial r} \\ 0 &= \mu \left\{ \frac{\partial}{\partial r} \left(\frac{1}{r} \frac{\partial}{\partial r} [r v_\theta] \right) \right\} \end{aligned}$$

But since $\partial/\partial\theta=0$ and $\partial/\partial z=0$ by assumptions 3 and 4, then v_θ is a function of radius only, and

$$\frac{d}{dr} \left(\frac{1}{r} \frac{d}{dr} [r v_\theta] \right) = 0$$

Integrating once,

$$\frac{1}{r} \frac{d}{dr} [r v_\theta] = c_1$$

or

$$\frac{d}{dr} [r v_\theta] = c_1 r$$

Integrating again,

$$r v_\theta = c_1 \frac{r^2}{2} + c_2 \quad \text{or} \quad v_\theta = c_1 \frac{r}{2} + c_2 \frac{1}{r}$$

Two boundary conditions are needed to evaluate constants c_1 and c_2 . The boundary conditions are

$$\begin{aligned} v_\theta &= \omega R_2 & \text{at} & \quad r = R_2 & \quad \text{and} \\ v_\theta &= 0 & \text{at} & \quad r = R_1 \end{aligned}$$

Substituting

$$\begin{aligned} \omega R_2 &= c_1 \frac{R_2}{2} + c_2 \frac{1}{R_2} \\ 0 &= c_1 \frac{R_1}{2} + c_2 \frac{1}{R_1} \end{aligned}$$

After considerable algebra

$$c_1 = \frac{2\omega}{1 - \left(\frac{R_1}{R_2}\right)^2} \quad \text{and} \quad c_2 = \frac{-\omega R_1^2}{1 - \left(\frac{R_1}{R_2}\right)^2}$$

Substituting into the expression for v_θ ,

$$v_\theta = \frac{\omega r}{1 - \left(\frac{R_1}{R_2}\right)^2} - \frac{\omega R_1^2/r}{1 - \left(\frac{R_1}{R_2}\right)^2} = \frac{\omega R_1}{1 - \left(\frac{R_1}{R_2}\right)^2} \left[\frac{r}{R_1} - \frac{R_1}{r} \right] \xleftarrow{\hspace{10cm}} v_\theta(r)$$

The shear stress distribution, using assumption 4, is:

$$\tau_{r\theta} = \mu r \frac{d}{dr} \left(\frac{v_\theta}{r} \right) = \mu r \frac{d}{dr} \left\{ \frac{\omega R_1}{1 - \left(\frac{R_1}{R_2} \right)^2} \left[\frac{1}{R_1} - \frac{R_1}{r^2} \right] \right\} = \mu r \frac{\omega R_1}{1 - \left(\frac{R_1}{R_2} \right)^2} (-2) \left(-\frac{R_1}{r^3} \right)$$

$$\tau_{r\theta} = \mu \frac{2\omega R_1^2}{1 - \left(\frac{R_1}{R_2} \right)^2} \frac{1}{r^2} \quad \xrightarrow{\tau_{r\theta}}$$

At the surface of the inner cylinder, $r = R_1$, so

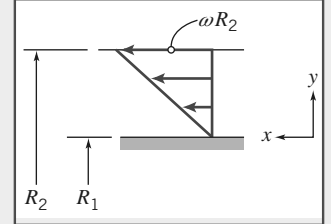
$$\tau_{\text{surface}} = \mu \frac{2\omega}{1 - \left(\frac{R_1}{R_2} \right)^2} \quad \xrightarrow{\tau_{\text{surface}}}$$

For a “planar” gap

$$\tau_{\text{planar}} = \mu \frac{\Delta v}{\Delta y} = \mu \frac{\omega R_2}{R_2 - R_1}$$

or

$$\tau_{\text{planar}} = \mu \frac{\omega}{1 - \frac{R_1}{R_2}} \quad \xrightarrow{\tau_{\text{planar}}}$$



Factoring the denominator of the exact expression for shear stress at the surface gives

$$\tau_{\text{surface}} = \mu \frac{2\omega}{\left(1 - \frac{R_1}{R_2} \right) \left(1 + \frac{R_1}{R_2} \right)} = \mu \frac{\omega}{1 - \frac{R_1}{R_2}} \cdot \frac{2}{1 + \frac{R_1}{R_2}}$$

Thus

$$\frac{\tau_{\text{surface}}}{\tau_{\text{planar}}} = \frac{2}{1 + \frac{R_1}{R_2}}$$

For 1 percent accuracy,

$$1.01 = \frac{2}{1 + \frac{R_1}{R_2}}$$

or

$$\frac{R_1}{R_2} = \frac{1}{1.01} (2 - 1.01) = 0.980 \quad \xrightarrow{\frac{R_1}{R_2}}$$

The accuracy criterion is met when the gap width is less than 2 percent of the cylinder radius.

Notes:

- This problem illustrates how the full Navier–Stokes equations in cylindrical coordinates (Eqs. 1–5) can sometimes be reduced to a set of solvable equations.
- As in Example 5.9, after integration of the simplified equations, boundary (or initial) conditions are used to complete the solution.
- Once the velocity field is obtained, other useful quantities (in this problem, shear stress) can be found.

5.5 Summary and Useful Equations

In this chapter we have:

- ✓ Derived the differential form of the conservation of mass (continuity) equation in vector form as well as in rectangular and cylindrical coordinates.
- ✓ *Defined the stream function ψ for a two-dimensional incompressible flow and learned how to derive the velocity components from it, as well as to find ψ from the velocity field.
- ✓ Learned how to obtain the total, local, and convective accelerations of a fluid particle from the velocity field.
- ✓ Presented examples of fluid particle translation and rotation, and both linear and angular deformation.
- ✓ Defined vorticity and circulation of a flow.
- ✓ Derived, and solved for simple cases, the Navier–Stokes equations, and discussed the physical meaning of each term.

We have also explored such ideas as how to determine whether a flow is incompressible by using the velocity field and, given one velocity component of a two-dimensional incompressible flow field, how to derive the other velocity component.

In this chapter we studied the effects of viscous stresses on fluid particle deformation and rotation; in the next chapter we examine flows for which viscous effects are negligible.

Note: Most of the equations in the table below have a number of constraints or limitations—*be sure to refer to their page numbers for details!*

Useful Equations

Continuity equation (general, rectangular coordinates):	$\frac{\partial \rho u}{\partial x} + \frac{\partial \rho v}{\partial y} + \frac{\partial \rho w}{\partial z} + \frac{\partial \rho}{\partial t} = 0$ $\nabla \cdot \rho \vec{V} + \frac{\partial \rho}{\partial t} = 0$	(5.1a) (5.1b)	Page 131
Continuity equation (incompressible, rectangular coordinates):	$\frac{\partial u}{\partial x} + \frac{\partial v}{\partial y} + \frac{\partial w}{\partial z} = \nabla \cdot \vec{V} = 0$	(5.1c)	Page 131
Continuity equation (steady, rectangular coordinates):	$\frac{\partial \rho u}{\partial x} + \frac{\partial \rho v}{\partial y} + \frac{\partial \rho w}{\partial z} = \nabla \cdot \rho \vec{V} = 0$	(5.1d)	Page 131
Continuity equation (general, cylindrical coordinates):	$\frac{1}{r} \frac{\partial(r\rho V_r)}{\partial r} + \frac{1}{r} \frac{\partial(\rho V_\theta)}{\partial \theta} + \frac{\partial(\rho V_z)}{\partial z} + \frac{\partial \rho}{\partial t} = 0$ $\nabla \cdot \rho \vec{V} + \frac{\partial \rho}{\partial t} = 0$	(5.2a) (5.1b)	Page 134
Continuity equation (incompressible, cylindrical coordinates):	$\frac{1}{r} \frac{\partial(rV_r)}{\partial r} + \frac{1}{r} \frac{\partial V_\theta}{\partial \theta} + \frac{\partial V_z}{\partial z} = \nabla \cdot \vec{V} = 0$	(5.2b)	Page 135
Continuity equation (steady, cylindrical coordinates):	$\frac{1}{r} \frac{\partial(r\rho V_r)}{\partial r} + \frac{1}{r} \frac{\partial(\rho V_\theta)}{\partial \theta} + \frac{\partial(\rho V_z)}{\partial z} = \nabla \cdot \rho \vec{V} = 0$	(5.2c)	Page 135
Continuity equation (2D, incompressible, rectangular coordinates):	$\frac{\partial u}{\partial x} + \frac{\partial v}{\partial y} = 0$	(5.3)	Page 136
Stream function (2D, incompressible, rectangular coordinates):	$u \equiv \frac{\partial \psi}{\partial y} \quad \text{and} \quad v \equiv -\frac{\partial \psi}{\partial x}$	(5.4)	Page 136
Continuity equation (2D, incompressible, cylindrical coordinates):	$\frac{\partial(rV_r)}{\partial r} + \frac{\partial V_\theta}{\partial \theta} = 0$	(5.7)	Page 137

Table (Continued)

Stream function (2D, incompressible, cylindrical coordinates):	$V_r \equiv \frac{1}{r} \frac{\partial \psi}{\partial \theta}$ and $V_\theta \equiv -\frac{\partial \psi}{\partial r}$	(5.8)	Page 137
Particle acceleration (rectangular coordinates):	$\frac{D\vec{V}}{Dt} \equiv \vec{a}_p = u \frac{\partial \vec{V}}{\partial x} + v \frac{\partial \vec{V}}{\partial y} + w \frac{\partial \vec{V}}{\partial z} + \frac{\partial \vec{V}}{\partial t}$	(5.9)	Page 141
Particle acceleration components in rectangular coordinates:	$a_{x_p} = \frac{Du}{Dt} = u \frac{\partial u}{\partial x} + v \frac{\partial u}{\partial y} + w \frac{\partial u}{\partial z} + \frac{\partial u}{\partial t}$ $a_{y_p} = \frac{Dv}{Dt} = u \frac{\partial v}{\partial x} + v \frac{\partial v}{\partial y} + w \frac{\partial v}{\partial z} + \frac{\partial v}{\partial t}$ $a_{z_p} = \frac{Dw}{Dt} = u \frac{\partial w}{\partial x} + v \frac{\partial w}{\partial y} + w \frac{\partial w}{\partial z} + \frac{\partial w}{\partial t}$	(5.11a) (5.11b) (5.11c)	Page 141
Particle acceleration components in cylindrical coordinates:	$a_{r_p} = V_r \frac{\partial V_r}{\partial r} + \frac{V_\theta}{r} \frac{\partial V_r}{\partial \theta} - \frac{V_\theta^2}{r} + V_z \frac{\partial V_r}{\partial z} + \frac{\partial V_r}{\partial t}$ $a_{\theta_p} = V_r \frac{\partial V_\theta}{\partial r} + \frac{V_\theta}{r} \frac{\partial V_\theta}{\partial \theta} + \frac{V_r V_\theta}{r} + V_z \frac{\partial V_\theta}{\partial z} + \frac{\partial V_\theta}{\partial t}$ $a_{z_p} = V_r \frac{\partial V_z}{\partial r} + \frac{V_\theta}{r} \frac{\partial V_z}{\partial \theta} + V_z \frac{\partial V_z}{\partial z} + \frac{\partial V_z}{\partial t}$	(5.12a) (5.12b) (5.12c)	Page 142
Navier–Stokes equations (incompressible, constant viscosity):	$\rho \left(\frac{\partial u}{\partial t} + u \frac{\partial u}{\partial x} + v \frac{\partial u}{\partial y} + w \frac{\partial u}{\partial z} \right) = \rho g_x - \frac{\partial p}{\partial x} + \mu \left(\frac{\partial^2 u}{\partial x^2} + \frac{\partial^2 u}{\partial y^2} + \frac{\partial^2 u}{\partial z^2} \right)$ $\rho \left(\frac{\partial v}{\partial t} + u \frac{\partial v}{\partial x} + v \frac{\partial v}{\partial y} + w \frac{\partial v}{\partial z} \right) = \rho g_y - \frac{\partial p}{\partial y} + \mu \left(\frac{\partial^2 v}{\partial x^2} + \frac{\partial^2 v}{\partial y^2} + \frac{\partial^2 v}{\partial z^2} \right)$ $\rho \left(\frac{\partial w}{\partial t} + u \frac{\partial w}{\partial x} + v \frac{\partial w}{\partial y} + w \frac{\partial w}{\partial z} \right) = \rho g_z - \frac{\partial p}{\partial z} + \mu \left(\frac{\partial^2 w}{\partial x^2} + \frac{\partial^2 w}{\partial y^2} + \frac{\partial^2 w}{\partial z^2} \right)$	(5.27a) (5.27b) (5.27c)	Page 153

REFERENCES

1. Schlichting, H., and K. Gersten, *Boundary-Layer Theory*, 9th ed. Springer-Verlag, Berlin, Heidelberg, 2017, ISBN 978-3-662-52917-1.
2. Gerhart, P. M., A. L. Gerhart, and J. I. Hochstein, Munson's Fluid Mechanics, John Wiley & Sons, Inc., Hoboken, NJ 07030, 2017, ISBN: 978-1-119-24898-9.

Chapter 6 Problems

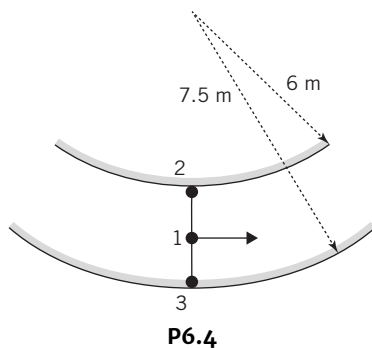
Euler's Equation

6.1 An incompressible frictionless flow field is given by $\vec{V} = (Ax + By)\hat{i} + (Bx - Ay)\hat{j}$ where $A = 2 \text{ s}^{-1}$ and $B = 2 \text{ s}^{-1}$ and x and y are in meters. The fluid is water and $\vec{g} = g\hat{j}$. Determine the magnitude and acceleration of a fluid particle and the pressure gradient at $(x,y) = (2,2)$.

6.2 The velocity field for a two-dimensional downward flow of water against a plate is given by $\vec{V} = Ax\hat{i} - Ay\hat{j}$. Plot the pressure gradient along the centerline and determine the pressure gradient at $(x,y) = (0,2)$, $(0,0)$ and $(2,0)$.

6.3 For a water flow in a pipe, determine the pressure gradient required to accelerate the water at 20 ft/s^2 for (a) a horizontal pipe, (b) a vertical pipe with the water flowing upward, and (c) a vertical pipe with the water flowing downward. Explain why the pressure gradient differs in sign between case (b) and case (c).

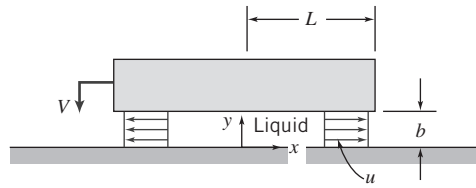
6.4 Water flows in a circular channel as shown in the figure. The velocity is 12 m/s and uniform across the channel. The pressure is 120 kPa at the centerline (point 1). Determine the pressures at points 2 and 3 for the case of (a) flow in the horizontal plane and (b) flow in the vertical plane with gravity acting in the direction of 2 to 3.



P6.4

6.5 A tornado moves in a circular pattern with a vertical axis. The wind speed is 200 mph , and the diameter of the tornado is 200 ft . Determine the radial pressure gradient. If it is desired to model the tornado using water in a 6 in. diameter tube, determine the speed needed to give the same radial pressure gradient.

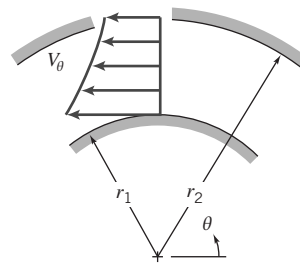
6.6 The y component of velocity in a two-dimensional incompressible flow field is given by $v = -Axy$, where v is in m/s , the coordinates are measured in meters, and $A = 1/\text{m s}$. There is no velocity component or variation in the z direction. Calculate the acceleration of a fluid particle at point $(x,y) = (1,2)$. Estimate the radius of curvature of the streamline passing through this point. Plot the streamline and show both the velocity vector and the acceleration vector on the plot. (Assume the simplest form of the x component of velocity.)



P6.6

6.7 Air flows in a two-dimensional bend of width w in a duct as shown in the figure. The velocity profile is similar to a free vortex (irrotational) profile given by $V_\theta = cr$, where c is a constant. Following Example 6.1, show that the flow rate is given by $Q = k\sqrt{\Delta p}$

$$\text{where } k \text{ is a constant and given by } k = w \ln\left(\frac{r_2}{r_1}\right) \sqrt{\frac{2r_1 r_2}{\rho(r_2^2 - r_1^2)}}$$

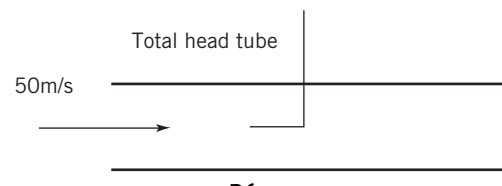


P6.7

6.8 Determine the dynamic and stagnation pressure of water flowing at a speed of 25 ft/s . Express your answer in psi, kPa, and inches of mercury.

6.9 In a pipe 0.3 m in diameter, $0.3 \text{ m}^3/\text{s}$ of water are pumped up a hill. On the hilltop (elevation 48), the line reduces to 0.2 m diameter. If the pump maintains a pressure of 690 kPa at elevation 21, calculate the pressure in the pipe on the hilltop.

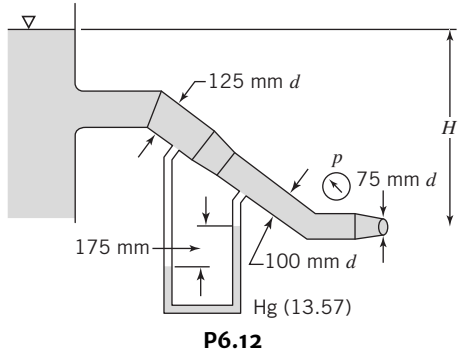
6.10 The flow section of a laboratory wind tunnel is shown in the figure. A total head tube pointed upstream indicates that the stagnation pressure on the test section centerline is 10 mm of water below atmospheric. The laboratory is maintained at atmospheric pressure and a temperature of -5°C . Determine the dynamic and static pressures at the wind tunnel test section.



P6.10

6.11 An open-circuit wind tunnel draws in air from the atmosphere through a well-contoured nozzle. In the test section, where the flow is straight and nearly uniform, a static pressure tap is drilled into the tunnel wall. A manometer connected to the tap shows that static pressure within the tunnel is 45 mm of water below atmospheric. Assume that the air is incompressible, and at 25°C, 100 kPa absolute. Calculate the air speed in the wind-tunnel test section.

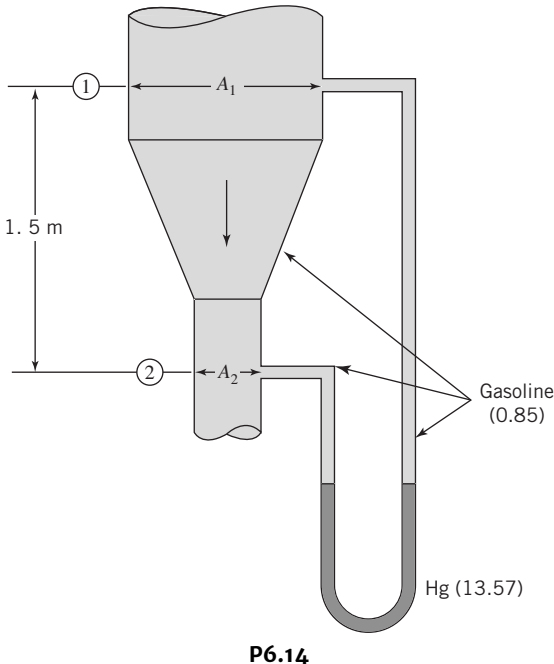
SS 6.12 Determine the height H (m) and the pressure p (kPa) for the water flow in the system shown in the figure.



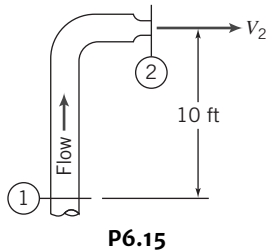
The Bernoulli Equation

SS 6.13 Water flows in a pipeline. At a point in the line where the diameter is 7 in., the velocity is 12 fps and the pressure is 50 psi. At a point 40 ft away the diameter reduces to 3 in. Calculate the pressure here when the pipe is (a) horizontal, (b) vertical with flow downward, and (c) vertical with the flow upward. Explain why there is a difference in the pressure for the different situations.

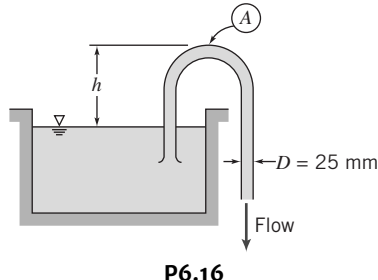
6.14 Determine the relation between A_1 and A_2 so that for a flow rate of 0.28 m^3/s the static pressure will be the same at sections 1 and 2. Determine the manometer reading for this condition and state which leg has the higher mercury column.'



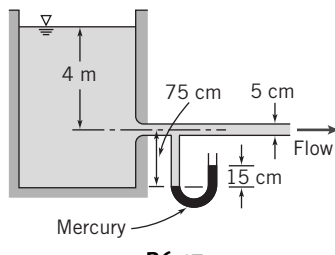
6.15 Water flows steadily through the vertical 1-in.-diameter pipe and out the 0.5 in. in diameter nozzle to the atmosphere. Determine the minimum gage pressure required at section 1 to produce a velocity at the nozzle exit of 30 ft/s. Determine the required minimum pressure at section 1 that maintains the same exit velocity when the system is inverted.



6.16 The water flow rate through the siphon is 5 L/s, its temperature is 20°C, and the pipe diameter is 25 mm. Compute the maximum allowable height, h , so that the pressure at point A is above the vapor pressure of the water. Assume the flow is frictionless.

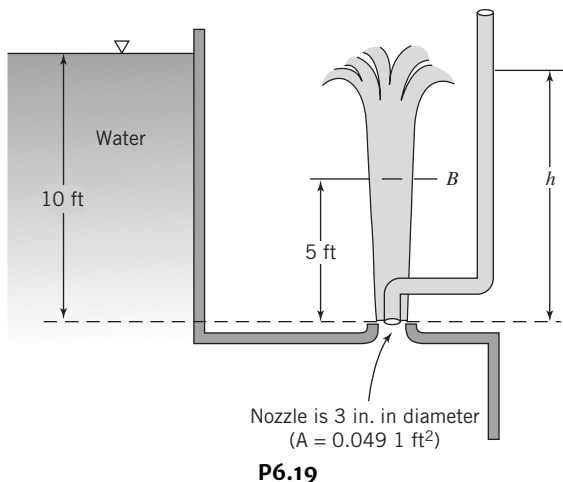


6.17 Water flows from a very large tank through a 5 cm diameter tube. The dark liquid in the manometer is mercury. Estimate the velocity in the pipe and the rate of discharge from the tank. Assume the flow is frictionless.

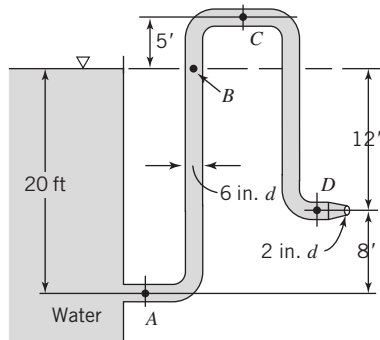


6.18 Consider frictionless, incompressible flow of air over the wing of an airplane flying at 200 km/hr. The air approaching the wing is at 65 kPa and -10°C . At a certain point in the flow, the pressure is 60 kPa. Calculate the speed of the air relative to the wing at this point and the absolute air speed.

6.19 The water jet is directed upward through a 3-in.-diameter nozzle under a head of 10 ft as shown in the figure. Determine the height h of the liquid in the pitot tube. Determine the cross-sectional area of the jet at section B.



- SS 6.20** Determine the flow rate through the pipeline shown in the figure and the pressures at A, B, C, and D.



6.21 A smoothly contoured nozzle, with outlet diameter $d = 20 \text{ mm}$, is coupled to a straight pipe by means of flanges. Water flows in the pipe, of diameter $D = 50 \text{ mm}$, and the nozzle discharges to the atmosphere. For steady flow and neglecting the effects of viscosity, find the volume flow rate in the pipe corresponding to a calculated axial force of 45.5 N needed to keep the nozzle attached to the pipe.

6.22 Water flows steadily through a 3.25-in.-diameter pipe and discharges through a 1.25-in.-diameter nozzle to atmospheric pressure. The flow rate is 24.5 gpm. Calculate the minimum static pressure required in the pipe to produce this flow rate. Evaluate the axial force of the nozzle assembly on the pipe flange.

SS 6.23 Two water reservoirs at a 30 m elevation each have discharge pipes that are connected at a “tee” junction. One pipe has a 200-mm diameter and the other a 150-mm diameter. The outlet pipe from the “tee” is 300-mm in diameter and discharges to the atmosphere at an elevation of 20 m. Determine the total flow rate and the flow rate in each pipe.

6.24 A horizontal jet of air with 0.4-in.-diameter and a speed of speed 225 ft/s strikes a 7.5 in. diameter stationary vertical disk. A manometer is connected to a hole at the center of the disk. Determine

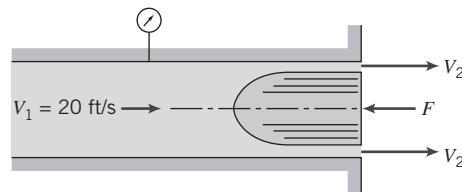
the height of the manometer liquid, which has a specific gravity of 1.75. Determine the force exerted by the jet on the disk.

6.25 An air-supported structure is used to enclose a set of tennis courts. It is a semi-cylinder structure with a diameter of 50 ft and a length of 50 ft. The blowers used to inflate the structure can maintain the air pressure inside the structure at 0.75 in. of water above ambient pressure. At design conditions, the wind blows at 35 mph perpendicular to the axis of the semi-cylindrical shape. The resulting pressure distribution is expressed as

$$\frac{p - p_\infty}{\frac{1}{2}\rho V_\infty^2} = 1 - 4\sin^2\theta$$

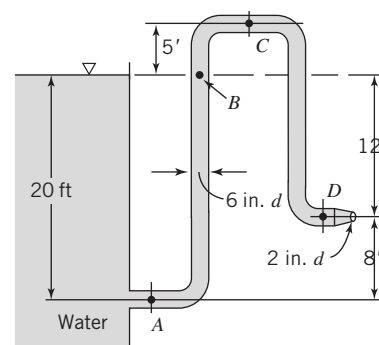
Where the angle θ is measured from the ground on the upwind side of the structure, p is the pressure at the surface, p_∞ the atmospheric pressure, and V_∞ the wind speed. Determine the net vertical force exerted on the structure.

6.26 Water flows at low speed through a circular tube with inside diameter of 2 in. A smoothly contoured body of 1.5 in. diameter is held in the end of the tube where the water discharges to atmosphere. Neglect frictional effects and assume uniform velocity profiles at each section. Determine the pressure measured by the gauge and the force required to hold the body.

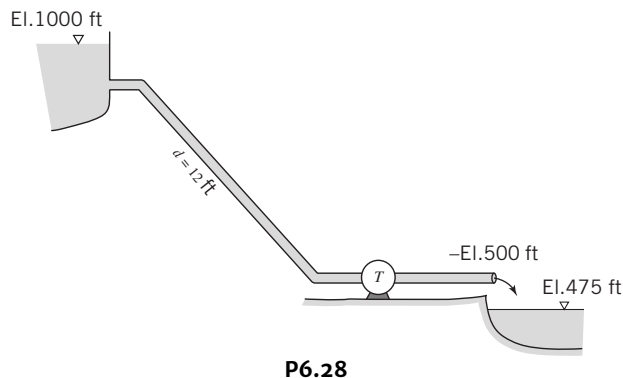


Energy Grade Line and Hydraulic Grade Line

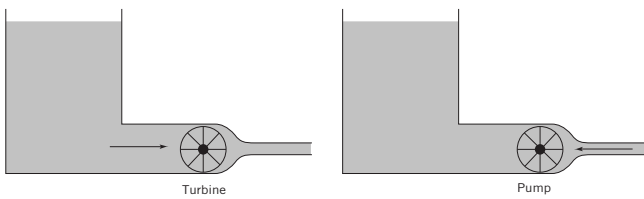
6.27 Sketch the energy (EGL) and hydraulic (HGL) grade lines for the system shown in the figure below.



6.28 The turbine extracts power from the water flowing from the reservoir. Find the horsepower extracted if the flow through the system is 1000 cfs. Draw the energy line and the hydraulic grade line.



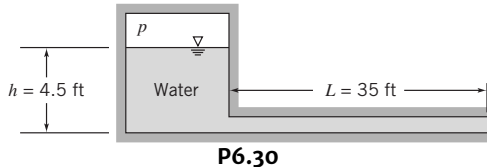
6.29 Sketch the energy grade lines (EGL) and hydraulic grade lines (HGL) for the two systems shown in the figure below.



P6.29

Irrational Flow

6.30 Compressed air is used to accelerate water from a tube. Neglect the velocity in the reservoir and assume the flow in the tube is uniform at any section. At a particular instant, it is known that $V = 6 \text{ ft/s}$ and $dV/dt = 7.5 \text{ ft/s}^2$. The cross-sectional area of the tube is $A = 32 \text{ in.}^2$. Determine the pressure in the tank at this instant.



6.31 The velocity field for a two-dimensional flow is $\vec{V} = (Ax - By)\hat{i} - (Bx + Ay)\hat{j}$ where $A = 1 \text{ s}^{-2}$, $B = 2 \text{ s}^{-2}$, t is in seconds, and the coordinates are measured in meters. Determine whether this is a possible incompressible flow and whether it is steady. Show that the flow is irrotational and derive an expression for the velocity potential.

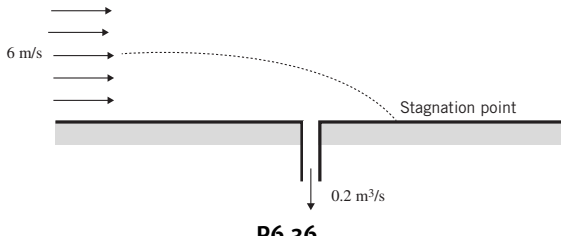
6.32 A flow field is characterized by the stream function $\psi = Axy$, where $A = 2 \text{ s}^{-1}$ and the coordinates are measured in feet. Verify that the flow is irrotational and determine the velocity potential ϕ . Plot the streamlines and potential lines and visually verify that they are orthogonal. SS

6.33 The stream function of a flow field is $\psi = Ax^3 - Bxy^2$ where $A = 1 \text{ m}^{-1} \text{ s}^{-1}$ and $B = 3 \text{ m}^{-1} \text{ s}^{-1}$, and the coordinates are measured in meters. Find expressions for the velocity field, the velocity potential, and the pressure gradient.

6.34 A flow field is represented by the stream function $\psi = x^5 - 15x^4y^2 + 15x^2y^4 - y^6$. Find the corresponding velocity field. Show that this flow field is irrotational and obtain the potential function.

6.35 Consider the flow field represented by the velocity potential $\phi = Ax + Bx^2 - By^2$, where $A = 1 \text{ m} \cdot \text{s}^{-1}$, $B = 1 \text{ m}^{-1} \cdot \text{s}^{-1}$, and the coordinates are measured in meters. Obtain expressions for the velocity field and the stream function. Calculate the pressure difference between the origin and point $(x, y) = (1, 2)$.

6.36 Consider an air flow over a flat wall with an upstream velocity of 6 m/s . There is a narrow slit through which air is drawn in at a flow rate of $0.2 \text{ m}^3/\text{s}$ per meter of width. Represent the flow as a combination of a uniform flow and a sink. Determine the location of the stagnation point. Sketch the dividing line between the air that enters the slit and the air that continues downstream.



P6.36

6.37 A source with a strength of $q = 3\pi \text{ m}^2/\text{s}$ and a sink with a strength of $q = \pi \text{ m}^2/\text{s}$ are located on the x axis at $x = -1 \text{ m}$ and $x = 1 \text{ m}$, respectively. Determine the stream function and velocity potential for the combined flow and sketch the streamlines.

6.38 The flow in a corner with an angle α can be described in radial coordinates by the stream function as $\psi = Ar^{\frac{1}{2}}\sin\frac{\pi\theta}{\alpha}$. Determine the velocity potential for the flow and plot streamlines for flow for $\alpha = 60^\circ$.

6.39 A flow field is formed by combining a uniform flow in the positive x direction with $U = 10 \text{ m/s}$, and a counterclockwise vortex with strength $K = 16\pi \text{ m}^2/\text{s}$ located at the origin. Determine the stream function, velocity potential, and velocity field for the combined flow.

CHAPTER 6

Incompressible Inviscid Flow

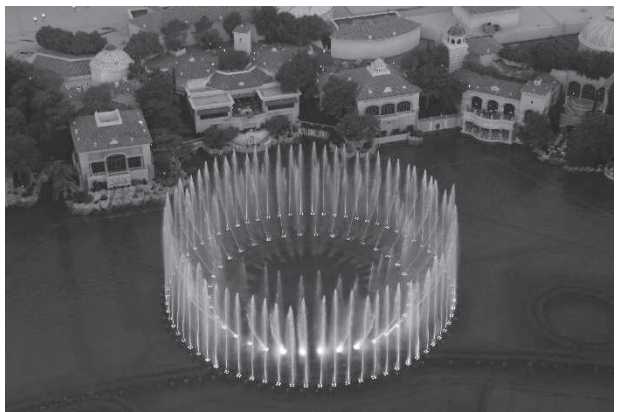
- 6.1 Momentum Equation for Frictionless Flow: Euler's Equation
- 6.2 Bernoulli Equation: Integration of Euler's Equation Along a Streamline for Steady Flow
- 6.3 The Bernoulli Equation Interpreted as an Energy Equation

- 6.4 Energy Grade Line and Hydraulic Grade Line
- 6.5 Unsteady Bernoulli Equation: Integration of Euler's Equation Along a Streamline
- 6.6 Irrotational Flow
- 6.7 Summary and Useful Equations

Case Study

The Fountains at the Bellagio in Las Vegas

The water fountains at the Bellagio in Las Vegas are spectacular. They are choreographed to vary the strength and direction of the water jets in time with the music. The production of this system of plumbing and control is also a spectacular fluid mechanics achievement. The WET Design Company was responsible for the design and construction of the system that produces the extraordinary visual display.



The fountains at the Bellagio in Las Vegas.

WET developed many innovations to make the fountains. Traditional fountains use pumps and pipes, which must be matched for optimum flow. Many of WET's designs use compressed air instead of water pumps, which allows energy to be continuously generated and accumulated, ready for instant output. This innovative use of compressed air allowed the fountains to become a reality—with the traditional systems of pipes or pumps, a fountain such as the Bellagio's would be impractical and expensive. For example, it would be difficult to obtain the 240-foot heights the fountains achieve without expensive, large, and noisy water pumps. The “Shooter” that WET developed works on the principle of introducing a large bubble of compressed air into the piping, which forces trapped water through a nozzle at high pressure. The ones installed at the Bellagio are able to shoot about 75 gallons per second of water over 240 feet in the air. In addition to providing a spectacular effect, they require only about 1/10th the energy of traditional water pumps to produce the same effect. Other air-powered devices produce pulsing water jets, achieving a maximum height of 125 feet. In addition to their power, these innovations lead to a saving of 80 percent or more in energy costs and have project construction costs that are about 50 percent less than traditional pipe-pump fountains.

Fountains such as the one at the Bellagio are designed using the relations for the flow of water with friction in pipes. The tradeoffs among pumping power, the cost of equipment, and the desired fountain effects bring in the techniques presented in this chapter.

Learning Objectives

After completing this chapter, you should be able to

- Solve an incompressible, inviscid flow problem using Euler's equation.
- Solve a steady incompressible frictionless flow problem using the Bernoulli equation.
- Explain the conditions under which the energy equation reduces to the Bernoulli equation.
- Determine the energy and hydraulic grade lines for a flow problem.
- Determine the stream function, potential function, and circulation for a flow problem.

In Chapter 5 we derived the differential equations (Eqs. 5.24) that describe the behavior of any fluid satisfying the continuum assumption. We also saw how these equations reduced to various particular forms—the most well known being the Navier–Stokes equations for an incompressible, constant viscosity fluid (Eqs. 5.27). Although Eqs. 5.27 describe the behavior of common fluids (e.g., water, air, lubricating oil) for a wide range of problems, as we discussed in Chapter 5, they are unsolvable analytically except for the simplest of geometries and flows. For example, even using the equations to predict the motion of your coffee as you slowly stir it would require the use of an advanced computational fluid dynamics computer application, and the prediction would take a lot. In this chapter, instead of the Navier–Stokes equations, we will study Euler's equation, which applies to an inviscid fluid. Although truly inviscid fluids do not exist, many flow problems, especially in aerodynamics, can be successfully analyzed with the approximation that $\mu = 0$.

6.1 Momentum Equation for Frictionless Flow: Euler's Equation

Euler's equation obtained from Eqs. 5.27 after neglecting the viscous terms is

$$\rho \frac{D\vec{V}}{Dt} = \rho \vec{g} - \nabla p \quad (6.1)$$

This equation states that for an inviscid fluid the change in momentum of a fluid particle is caused by the body force (assumed to be gravity only) and the net pressure force. For convenience we recall that the particle acceleration is

$$\frac{D\vec{V}}{Dt} = \frac{\partial \vec{V}}{\partial t} + (\vec{V} \cdot \nabla) \vec{V} \quad (5.10)$$

In this chapter we will apply Eq. 6.1 to the solution of incompressible, inviscid flow problems. In addition to Eq. 6.1 we have the incompressible form of the mass conservation equation,

$$\nabla \cdot \vec{V} = 0 \quad (5.1c)$$

Equation 6.1 expressed in rectangular coordinates is

$$\rho \left(\frac{\partial u}{\partial t} + u \frac{\partial u}{\partial x} + v \frac{\partial u}{\partial y} + w \frac{\partial u}{\partial z} \right) = \rho g_x - \frac{\partial p}{\partial x} \quad (6.2a)$$

$$\rho \left(\frac{\partial v}{\partial t} + u \frac{\partial v}{\partial x} + v \frac{\partial v}{\partial y} + w \frac{\partial v}{\partial z} \right) = \rho g_y - \frac{\partial p}{\partial y} \quad (6.2b)$$

$$\rho \left(\frac{\partial w}{\partial t} + u \frac{\partial w}{\partial x} + v \frac{\partial w}{\partial y} + w \frac{\partial w}{\partial z} \right) = \rho g_z - \frac{\partial p}{\partial z} \quad (6.2c)$$

If the z axis is assumed vertical, then $g_x = 0$, $g_y = 0$, and $g_z = -g$, so $\vec{g} = -g\hat{k}$.

In cylindrical coordinates, the equations in component form, with gravity the only body force, are

$$\rho a_r = \rho \left(\frac{\partial V_r}{\partial t} + V_r \frac{\partial V_r}{\partial r} + \frac{V_\theta}{r} \frac{\partial V_r}{\partial \theta} + V_z \frac{\partial V_r}{\partial z} - \frac{V_\theta^2}{r} \right) = \rho g_r - \frac{\partial p}{\partial r} \quad (6.3a)$$

$$\rho a_\theta = \rho \left(\frac{\partial V_\theta}{\partial t} + V_r \frac{\partial V_\theta}{\partial r} + \frac{V_\theta}{r} \frac{\partial V_\theta}{\partial \theta} + V_z \frac{\partial V_\theta}{\partial z} + \frac{V_r V_\theta}{r} \right) = \rho g_\theta - \frac{1}{r} \frac{\partial p}{\partial \theta} \quad (6.3b)$$

$$\rho a_z = \rho \left(\frac{\partial V_z}{\partial t} + V_r \frac{\partial V_z}{\partial r} + \frac{V_\theta}{r} \frac{\partial V_z}{\partial \theta} + V_z \frac{\partial V_z}{\partial z} \right) = \rho g_z - \frac{\partial p}{\partial z} \quad (6.3c)$$

If the z axis is directed vertically upward, then $g_r = g_\theta = 0$ and $g_z = -g$.

Equations 6.1, 6.2, and 6.3 apply to problems in which there are no viscous stresses. Before continuing with the main topic of this chapter, which is inviscid flow, let's consider for a moment when we have no viscous stresses, other than when $\mu = 0$. We recall from previous discussions that, in general, viscous stresses are present when we have fluid deformation. When we have no fluid deformation, i.e., when we have *rigid-body* motion, no viscous stresses will be present, even if $\mu \neq 0$. Hence Euler's equations apply to rigid-body motions as well as to inviscid flows. We discussed rigid-body motion in detail in the online Section 3.6 as a special case of fluid statics.

In Chapters 2 and 5 we pointed out that streamlines, drawn tangent to the velocity vectors at every point in the flow field, provide a convenient graphical representation. In steady flow a fluid particle will move along a streamline because, for steady flow, pathlines and streamlines coincide. Thus, in describing the motion of a fluid particle in a steady flow, in addition to using orthogonal coordinates x, y, z , the distance along a streamline is a logical coordinate to use in writing the equations of motion. "Streamline coordinates" also may be used to describe unsteady flow. Streamlines in unsteady flow give a graphical representation of the instantaneous velocity field.

For simplicity, consider the flow in the yz plane shown in Fig. 6.1. We wish to write the equations of motion in terms of the coordinate s , distance along a streamline, and the coordinate n , distance normal to the streamline. The pressure at the center of the fluid element is p . If we apply Newton's second law in the direction s of the streamline, to the fluid element of volume $ds dn dx$, then neglecting viscous forces we obtain

$$\left(p - \frac{\partial p}{\partial s} \frac{ds}{2} \right) dn dx - \left(p + \frac{\partial p}{\partial s} \frac{ds}{2} \right) dn dx - \rho g \sin \beta ds dn dx = \rho a_s ds dn dx$$

where β is the angle between the tangent to the streamline and the horizontal, and a_s is the acceleration of the fluid particle along the streamline. Simplifying the equation, we obtain

$$-\frac{\partial p}{\partial s} - \rho g \sin \beta = \rho a_s$$

Since $\sin \beta = dz/ds$, we can write

$$-\frac{1}{\rho} \frac{\partial p}{\partial s} - g \frac{\partial z}{\partial s} = a_s$$

Along any streamline $V = V(s, t)$, and the material or total acceleration of a fluid particle in the streamwise direction is given by

$$a_s = \frac{DV}{Dt} = \frac{\partial V}{\partial t} + V \frac{\partial V}{\partial s}$$

Euler's equation in the streamwise direction with the z axis directed vertically upward is then

$$-\frac{1}{\rho} \frac{\partial p}{\partial s} - g \frac{\partial z}{\partial s} = \frac{\partial V}{\partial t} + V \frac{\partial V}{\partial s} \quad (6.4a)$$

For steady flow Euler's equation in the streamwise direction reduces to

$$\frac{1}{\rho} \frac{\partial p}{\partial s} = -g \frac{\partial z}{\partial s} - V \frac{\partial V}{\partial s} \quad (6.4b)$$

Equation 6.4b indicates that the pressure along a streamline is influenced by both the gravitational field and the velocity. The first effect is the hydrostatic effect that we studied in Chapter 3, which shows that in the absence of velocity, the pressure increases directly with the change in elevation. If we were to apply the Euler's equation to flow in the xy plane, in which there is no influence of gravity, Eq. 6.4b would become

$$\frac{1}{\rho} \frac{\partial p}{\partial s} = -V \frac{\partial V}{\partial s} \quad (6.4c)$$

which indicates that for an incompressible, inviscid flow *a decrease in velocity is accompanied by an increase in pressure* and conversely. This makes sense: the only force experienced by the particle is the net pressure force, so the particle accelerates toward low-pressure regions and decelerates when approaching high-pressure regions.

To obtain Euler's equation in a direction normal to the streamlines, we apply Newton's second law in the n direction to the fluid element. Again, neglecting viscous forces, we obtain

$$\left(p - \frac{\partial p}{\partial n} \frac{dn}{2} \right) ds dx - \left(p + \frac{\partial p}{\partial n} \frac{dn}{2} \right) ds dx - \rho g \cos \beta dn dx ds = \rho a_n dn dx ds$$

where β is the angle between the n direction and the vertical, and a_n is the acceleration of the fluid particle in the n direction. Simplifying the equation, we obtain

$$-\frac{\partial p}{\partial n} - \rho g \cos \beta = \rho a_n$$

Since $\cos \beta = \partial z / \partial n$, we write

$$-\frac{1}{\rho} \frac{\partial p}{\partial n} - g \frac{\partial z}{\partial n} = a_n$$

The normal acceleration of the fluid element is toward the center of curvature of the streamline, in the minus n direction; thus in the coordinate system of Fig. 6.1, the familiar centripetal acceleration is written

$$a_n = -\frac{V^2}{R}$$

for steady flow, where R is the radius of curvature of the streamline at the point chosen. Then, Euler's equation normal to the streamline is written for steady flow as

$$\frac{1}{\rho} \frac{\partial p}{\partial n} + g \frac{\partial z}{\partial n} = \frac{V^2}{R} \quad (6.5a)$$

For steady flow in a horizontal plane, Euler's equation normal to a streamline becomes

$$\frac{1}{\rho} \frac{\partial p}{\partial n} = \frac{V^2}{R} \quad (6.5b)$$

Equation 6.5 indicates that *pressure increases in the direction outward from the center of curvature of the streamlines*. This also makes sense. Because the only force experienced by the particle is the net pressure force, the pressure field creates the centripetal acceleration. In regions where the streamlines are straight, the radius of curvature, R , is infinite so *there is no pressure variation normal to straight streamlines*. Example 6.1 shows how Eq. 6.5b can be used to compute the velocity from the pressure gradient in the normal direction.

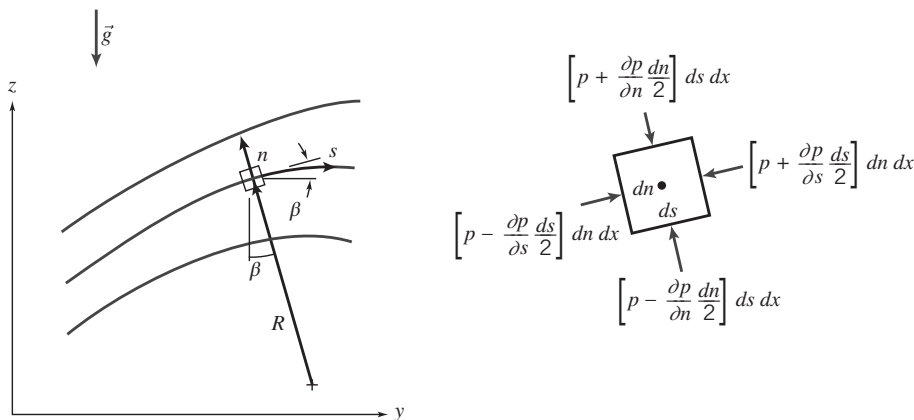


Fig. 6.1 Fluid particle moving along a streamline.

Example 6.1 FLOW IN A BEND

The flow rate of air at standard conditions in a flat duct is to be determined by installing pressure taps across a bend. The duct is 0.3 m deep and 0.1 m wide. The inner radius of the bend is 0.25 m. If the measured pressure difference between the taps is 40 mm of water, compute the approximate flow rate.

Given: Flow through duct bend as shown.

$$p_2 - p_1 = \rho_{\text{H}_2\text{O}} g \Delta h$$

where $\Delta h = 40 \text{ mm H}_2\text{O}$. Air is at STP.

Find: Volume flow rate, Q .

Solution: Apply Euler's n component equation across flow streamlines.

$$\text{Governing equation: } \frac{\partial p}{\partial r} = \frac{\rho V^2}{r}$$

Assumptions:

- 1 Frictionless flow.
- 2 Incompressible flow.
- 3 Uniform flow at measurement section.

For this flow, $p = p(r)$, so

$$\frac{\partial p}{\partial r} = \frac{dp}{dr} = \frac{\rho V^2}{r}$$

or

$$dp = \rho V^2 \frac{dr}{r}$$

Integrating gives

$$p_2 - p_1 = \rho V^2 \ln r_2 - \rho V^2 \ln r_1 = \rho V^2 \ln \frac{r_2}{r_1}$$

and hence

$$V = \left[\frac{p_2 - p_1}{\rho \ln(r_2/r_1)} \right]^{1/2}$$

$$\text{But } \Delta p = p_2 - p_1 = \rho_{\text{H}_2\text{O}} g \Delta h, \text{ so } V = \left[\frac{\rho_{\text{H}_2\text{O}} g \Delta h}{\rho \ln(r_2/r_1)} \right]^{1/2}$$

Substituting numerical values,

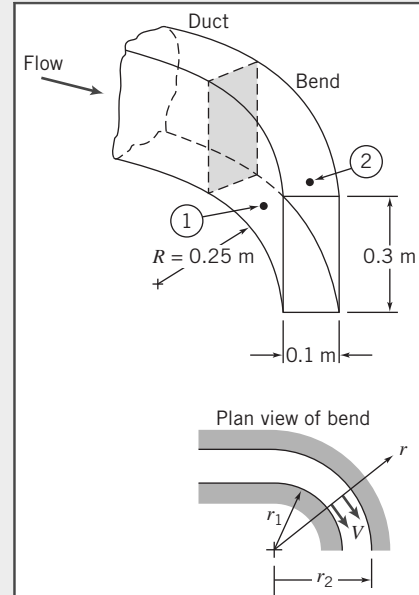
$$V = \left[999 \frac{\text{kg}}{\text{m}^3} \times 9.81 \frac{\text{m}}{\text{s}^2} \times 0.04 \text{ m} \times \frac{\text{m}^3}{1.23 \text{ kg}} \times \frac{1}{\ln(0.35 \text{ m}/0.25 \text{ m})} \right]^{1/2}$$

$$= 30.8 \text{ m/s}$$

For uniform flow

$$Q = VA = 30.8 \frac{\text{m}}{\text{s}} \times 0.1 \text{ m} \times 0.3 \text{ m}$$

$$Q = 0.924 \text{ m}^3/\text{s} \longleftarrow$$



In this problem we assumed that the velocity is uniform across the section. In fact, the velocity in the bend approximates a free vortex (irrotational) profile in which $V \propto 1/r$ (where r is the radius) instead of $V = \text{const}$. Hence, this flow-measurement device could only be used to obtain approximate values of the flow rate (see Problem 6.7).

6.2 Bernoulli Equation: Integration of Euler's Equation Along a Streamline for Steady Flow

Compared to the viscous-flow equivalents, the momentum or Euler's equation for incompressible, inviscid flow, Eq. 6.1, is simpler mathematically, but its solution in conjunction with the mass conservation equation, Eq. 5.1c, still presents formidable difficulties in all but the most basic flow problems. One convenient approach for a steady flow is to integrate Euler's equation along a streamline. We will do this below using two different mathematical approaches, and each will result in the Bernoulli equation. Recall that in Section 4.4 we derived the Bernoulli equation by starting with a differential control volume. These two additional derivations will give us more insight into the restrictions inherent in use of the Bernoulli equation.

Derivation Using Streamline Coordinates

Euler's equation for steady flow along a streamline from Eq. 6.4a is

$$-\frac{1}{\rho} \frac{\partial p}{\partial s} - g \frac{\partial z}{\partial s} = V \frac{\partial V}{\partial s} \quad (6.6)$$

If a fluid particle moves a distance, ds , along a streamline, then

$$\frac{\partial p}{\partial s} ds = dp \quad (\text{the change in pressure along } s)$$

$$\frac{\partial z}{\partial s} ds = dz \quad (\text{the change in elevation along } s)$$

$$\frac{\partial V}{\partial s} ds = dV \quad (\text{the change in speed along } s)$$

Thus, after multiplying Eq. 6.6 by ds , we can write

$$-\frac{dp}{\rho} - g dz = V dV \quad \text{or} \quad \frac{dp}{\rho} + V dV + g dz = 0 \quad (\text{along } s)$$

Integration of this equation gives

$$\int \frac{dp}{\rho} + \frac{V^2}{2} + gz = \text{constant} \quad (\text{along } s) \quad (6.7)$$

Before Eq. 6.7 can be applied, we must specify the relation between pressure and density. For the special case of incompressible flow, $\rho = \text{constant}$, and Eq. 6.7 becomes the Bernoulli equation,

$$\frac{p}{\rho} + \frac{V^2}{2} + gz = \text{constant} \quad (6.8)$$

Restrictions:

- 1 Steady flow.
- 2 Incompressible flow.
- 3 Frictionless flow.
- 4 Flow along a streamline.

The Bernoulli equation is probably the most famous, and abused, equation in all of fluid mechanics. It is always tempting to use because it is a simple algebraic equation for relating the pressure, velocity, and elevation in a fluid. For example, it is used to explain the lift of a wing. In aerodynamics the gravity term is usually negligible, so Eq. 6.8 indicates that wherever the velocity is relatively high (e.g., on the upper surface of a wing), the pressure must be relatively low, and wherever the velocity is relatively low (e.g., on the lower surface of a wing), the pressure must be relatively high, generating substantial lift. Equation 6.8 indicates that, in general if a particle increases its elevation ($z \uparrow$) or moves into a higher pressure region ($p \uparrow$), it will tend to decelerate ($V \downarrow$). This makes sense from a momentum point of view. These comments *only* apply if the four restrictions listed are reasonable. For example, Eq. 6.8 cannot be

used to explain the pressure drop in a horizontal constant diameter pipe flow: according to it, for $z = \text{constant}$ and $V = \text{constant}$, $p = \text{constant}$. We cannot stress enough that you should *keep the restrictions firmly in mind whenever you consider using the Bernoulli equation!*

Derivation Using Rectangular Coordinates

The vector form of Euler's equation, Eq. 6.1, also can be integrated along a streamline. We shall restrict the derivation to steady flow; thus, the end result of our effort should be Eq. 6.7.

For steady flow, Euler's equation in rectangular coordinates can be expressed as

$$\frac{D\vec{V}}{Dt} = u \frac{\partial \vec{V}}{\partial x} + v \frac{\partial \vec{V}}{\partial y} + w \frac{\partial \vec{V}}{\partial z} = (\vec{V} \cdot \nabla) \vec{V} = -\frac{1}{\rho} \nabla p - g\hat{k} \quad (6.9)$$

For steady flow the velocity field is given by $\vec{V} = \vec{V}(x, y, z)$. The streamlines are lines drawn in the flow field tangent to the velocity vector at every point. Recall again that for steady flow, streamlines, pathlines, and streaklines coincide. The motion of a particle along a streamline is governed by Eq. 6.9. During time interval dt the particle has vector displacement $d\vec{s}$ along the streamline.

If we take the dot product of the terms in Eq. 6.9 with displacement $d\vec{s}$ along the streamline, we obtain a scalar equation relating pressure, speed, and elevation along the streamline. Taking the dot product of $d\vec{s}$ with Eq. 6.9 gives

$$(\vec{V} \cdot \nabla) \vec{V} \cdot d\vec{s} = -\frac{1}{\rho} \nabla p \cdot d\vec{s} - g\hat{k} \cdot d\vec{s} \quad (6.10)$$

where

$$d\vec{s} = dx\hat{i} + dy\hat{j} + dz\hat{k} \quad (\text{along } s)$$

Now we evaluate each of the three terms in Eq. 6.10, starting on the right,

$$\begin{aligned} -\frac{1}{\rho} \nabla p \cdot d\vec{s} &= -\frac{1}{\rho} \left[\hat{i} \frac{\partial p}{\partial x} + \hat{j} \frac{\partial p}{\partial y} + \hat{k} \frac{\partial p}{\partial z} \right] \cdot [dx\hat{i} + dy\hat{j} + dz\hat{k}] \\ &= -\frac{1}{\rho} \left[\frac{\partial p}{\partial x} dx + \frac{\partial p}{\partial y} dy + \frac{\partial p}{\partial z} dz \right] \quad (\text{along } s) \\ -\frac{1}{\rho} \nabla p \cdot d\vec{s} &= -\frac{1}{\rho} dp \quad (\text{along } s) \end{aligned}$$

and

$$\begin{aligned} -g\hat{k} \cdot d\vec{s} &= -g\hat{k} \cdot [dx\hat{i} + dy\hat{j} + dz\hat{k}] \\ &= -g dz \quad (\text{along } s) \end{aligned}$$

Using a vector identity, we can write the third term as

$$\begin{aligned} (\vec{V} \cdot \nabla) \vec{V} \cdot d\vec{s} &= \left[\frac{1}{2} \nabla(\vec{V} \cdot \vec{V}) - \vec{V} \times (\nabla \times \vec{V}) \right] \cdot d\vec{s} \\ &= \left\{ \frac{1}{2} \nabla(\vec{V} \cdot \vec{V}) \right\} \cdot d\vec{s} - \left\{ \vec{V} \times (\nabla \times \vec{V}) \right\} \cdot d\vec{s} \end{aligned}$$

The last term on the right side of this equation is zero, since \vec{V} is parallel to $d\vec{s}$ [recall from vector math that $\vec{V} \times (\nabla \times \vec{V}) \cdot d\vec{s} = -(\nabla \times \vec{V}) \times \vec{V} \cdot d\vec{s} = -(\nabla \times \vec{V}) \cdot \vec{V} \times d\vec{s}$]. Consequently,

$$\begin{aligned} (\vec{V} \cdot \nabla) \vec{V} \cdot d\vec{s} &= \frac{1}{2} \nabla(\vec{V} \cdot \vec{V}) \cdot d\vec{s} = \frac{1}{2} \nabla(V^2) \cdot d\vec{s} \quad (\text{along } s) \\ &= \frac{1}{2} \left[\hat{i} \frac{\partial V^2}{\partial x} + \hat{j} \frac{\partial V^2}{\partial y} + \hat{k} \frac{\partial V^2}{\partial z} \right] \cdot [dx\hat{i} + dy\hat{j} + dz\hat{k}] \\ &= \frac{1}{2} \left[\frac{\partial V^2}{\partial x} dx + \frac{\partial V^2}{\partial y} dy + \frac{\partial V^2}{\partial z} dz \right] \\ (\vec{V} \cdot \nabla) \vec{V} \cdot d\vec{s} &= \frac{1}{2} d(V^2) \quad (\text{along } s) \end{aligned}$$

Substituting these three terms into Eq. 6.10 yields

$$\frac{dp}{\rho} + \frac{1}{2}d(V^2) + g dz = 0 \quad (\text{along } s)$$

Integrating this equation, we obtain

$$\int \frac{dp}{\rho} + \frac{V^2}{2} + gz = \text{constant} \quad (\text{along } s)$$

If the density is constant, we obtain the Bernoulli equation

$$\frac{p}{\rho} + \frac{V^2}{2} + gz = \text{constant}$$

As expected, we see that the last two equations are identical to Eqs. 6.7 and 6.8 derived previously using streamline coordinates. The Bernoulli equation, derived using rectangular coordinates, is still subject to the restrictions: (1) steady flow, (2) incompressible flow, (3) frictionless flow, and (4) flow along a streamline.

Static, Stagnation, and Dynamic Pressures

The pressure, p , which we have used in deriving the Bernoulli equation, Eq. 6.8, is the thermodynamic pressure and is commonly called the *static pressure*. The static pressure is the pressure measured by an observer riding along with the fluid. We also have the stagnation and dynamic pressures, which we will define shortly. How do we measure the pressure in a fluid in motion?

In Section 6.1 we showed that there is no pressure variation normal to straight streamlines. This fact makes it possible to measure the static pressure in a flowing fluid using a wall pressure “tap,” placed in a region where the flow streamlines are straight, as shown in Fig. 6.2a. The pressure tap is a small hole, drilled carefully in the wall, with its axis perpendicular to the surface. If the hole is perpendicular to the duct wall and free from burrs, accurate measurements of static pressure can be made by connecting the tap to a suitable pressure-measuring instrument [1].

In a fluid stream far from a wall, or where streamlines are curved, accurate static pressure measurements can be made by careful use of a static pressure probe, shown in Fig. 6.2b. Such probes must be designed so that the measuring holes are placed correctly with respect to the probe tip and stem to avoid erroneous results [2]. In use, the measuring section must be aligned with the local flow direction. Static pressure probes, such as that shown in Fig 6.2b, and in a variety of other forms, are available commercially in sizes as small as 1.5 mm ($\frac{1}{16}$ in.) in diameter [3].

The *stagnation pressure* is obtained when a flowing fluid is decelerated to zero speed by a frictionless process. For incompressible flow, the Bernoulli equation can be used to relate changes in speed and pressure along a streamline for such a process. Neglecting elevation differences, Eq. 6.8 becomes

$$\frac{p}{\rho} + \frac{V^2}{2} = \text{constant}$$

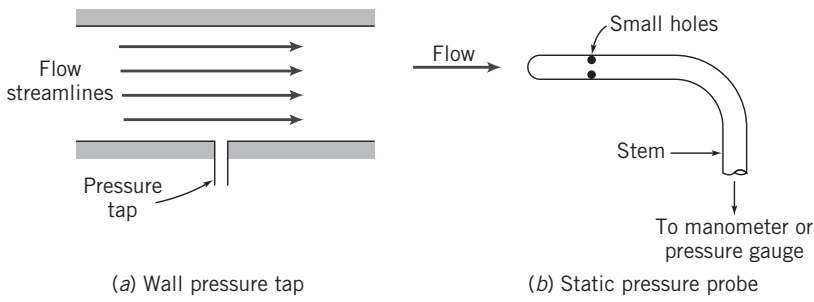
If the static pressure is p at a point in the flow where the speed is V , then the stagnation pressure, p_0 , where the stagnation speed, V_0 , is zero, may be computed from

$$\frac{P_0}{\rho} + \frac{\overset{=}0}{\cancel{\rho}} = \frac{P}{\rho} + \frac{V^2}{2}$$

or

$$p_0 = p + \frac{1}{2}\rho V^2 \quad (6.11)$$

Equation 6.11 is a mathematical statement of the definition of stagnation pressure, valid for incompressible flow. The term $\frac{1}{2}\rho V^2$ generally is called the *dynamic pressure*. Equation 6.11 states that the stagnation (or *total*) pressure equals the static pressure plus the dynamic pressure. One way to picture the three pressures is to imagine you are standing in a steady wind holding up your hand. The static pressure will be atmospheric pressure; the larger pressure you feel at the center of your hand will be

**Fig. 6.2** Measurement of static pressure.

the stagnation pressure; and the buildup of pressure (the difference between the stagnation and static pressures) will be the dynamic pressure. Solving Eq. 6.11 for the speed,

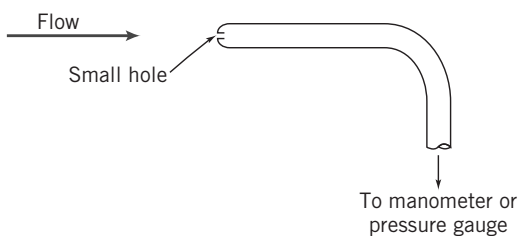
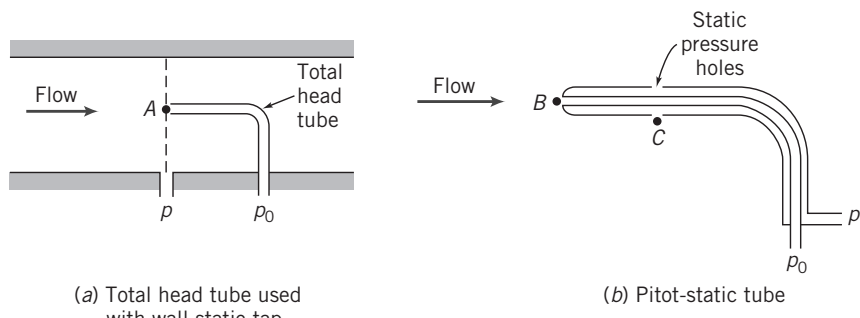
$$V = \sqrt{\frac{2(p_0 - p)}{\rho}} \quad (6.12)$$

Thus, if the stagnation pressure and the static pressure could be measured at a point, Eq. 6.12 would give the local flow speed.

Stagnation pressure is measured in the laboratory using a probe with a hole that faces directly upstream as shown in Fig. 6.3. Such a probe is called a stagnation pressure probe, or pitot tube. Again, the measuring section must be aligned with the local flow direction.

We have seen that static pressure at a point can be measured with a static pressure tap or probe (Fig. 6.2). If we knew the stagnation pressure at the same point, then the flow speed could be computed from Eq. 6.12. Two possible experimental setups are shown in Fig. 6.4.

In Fig. 6.4a, the static pressure corresponding to point A is read from the wall static pressure tap. The stagnation pressure is measured directly at A by the total head tube, as shown. The stem of the total head tube is placed downstream from the measurement location to minimize disturbance of the local flow. The use of a total head tube and a wall static pressure tap to determine the flow velocity is shown in Example 6.2.

**Fig. 6.3** Measurement of stagnation pressure.**Fig. 6.4** Simultaneous measurement of stagnation and static pressures.

Example 6.2 PITOT TUBE

A pitot tube is inserted in an air flow (at STP) to measure the flow speed. The tube is inserted so that it points upstream into the flow and the pressure sensed by the tube is the stagnation pressure. The static pressure is measured at the same location in the flow, using a wall pressure tap. If the pressure difference is 30 mm of mercury, determine the flow speed.

Given: A pitot tube inserted in a flow as shown. The flowing fluid is air and the manometer liquid is mercury.

Find: The flow speed.

Solution:

$$\text{Governing equation: } \frac{p}{\rho} + \frac{V^2}{2} + gz = \text{constant}$$

Assumptions:

- 1 Steady flow.
- 2 Incompressible flow.
- 3 Flow along a streamline.
- 4 Frictionless deceleration along stagnation streamline.

Writing Bernoulli's equation along the stagnation streamline (with $\Delta z = 0$) yields Eq. 6.11

$$\frac{p_0}{\rho} = \frac{p}{\rho} + \frac{V^2}{2}$$

p_0 is the stagnation pressure at the tube opening where the speed has been reduced, without friction, to zero. Solving for V gives

$$V = \sqrt{\frac{2(p_0 - p)}{\rho_{\text{air}}}}$$

From the diagram,

$$p_0 - p = \rho_{\text{Hg}}gh = \rho_{\text{H}_2\text{O}}ghSG_{\text{Hg}}$$

and

$$\begin{aligned} V &= \sqrt{\frac{2\rho_{\text{H}_2\text{O}}ghSG_{\text{Hg}}}{\rho_{\text{air}}}} \\ &= \sqrt{2 \times 1000 \frac{\text{kg}}{\text{m}^3} \times 9.81 \frac{\text{m}}{\text{s}^2} \times 30 \text{ mm} \times 13.6 \times \frac{\text{m}^3}{1.23 \text{ kg}} \times \frac{1 \text{ m}}{1000 \text{ mm}}} \\ V &= 80.8 \text{ m/s} \end{aligned}$$

At $T = 20^\circ\text{C}$, the speed of sound in air is 343 m/s. Hence, $M = 0.236$ and the assumption of incompressible flow is valid.

This problem illustrates use of a pitot tube to determine flow speed. Pitot (or pitot-static) tubes are often placed on the exterior of aircraft to indicate air speed relative to the aircraft, and hence aircraft speed relative to the air.

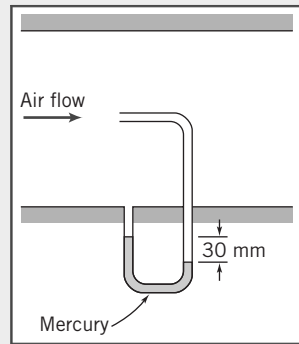
Two probes often are combined, as in the pitot-static tube shown in Fig. 6.4b. The inner tube is used to measure the stagnation pressure at point B , while the static pressure at C is sensed using the small holes in the outer tube. In flow fields where the static pressure variation in the streamwise direction is small, the pitot-static tube may be used to infer the speed at point B in the flow by assuming $p_B = p_C$ and using Eq. 6.12. (Note that when $p_B \neq p_C$, this procedure will give erroneous results.)

Remember that the Bernoulli equation applies only for incompressible flow (Mach number $M \leq 0.3$). The definition and calculation of the stagnation pressure for compressible flow will be discussed in Section 12.3.

Applications

The Bernoulli equation can be applied between any two points on a streamline provided that the other three restrictions are satisfied. The result is

$$\frac{p_1}{\rho} + \frac{V_1^2}{2} + gz_1 = \frac{p_2}{\rho} + \frac{V_2^2}{2} + gz_2 \quad (6.13)$$



where subscripts 1 and 2 represent any two points on a streamline. Applications of Eqs. 6.8 and 6.13 to typical flow problems are illustrated in Examples 6.3 through 6.5. In some situations, the flow appears unsteady from one reference frame, but steady from another, which translates with the flow. Since the Bernoulli equation was derived by integrating Newton's second law for a fluid particle, it can be applied in any inertial reference frame. The procedure is illustrated in Example 6.6.

Example 6.3 NOZZLE FLOW

Air flows steadily at low speed through a horizontal *nozzle* (by definition a device for accelerating a flow), discharging to atmosphere. The area at the nozzle inlet is 0.1 m^2 . At the nozzle exit, the area is 0.02 m^2 . Determine the gage pressure required at the nozzle inlet to produce an outlet speed of 50 m/s .

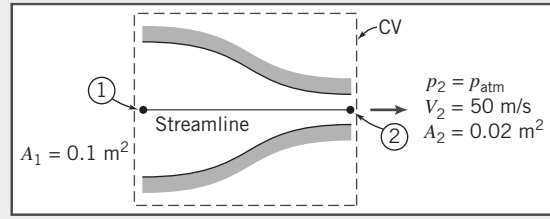
Given: Flow through a nozzle, as shown.

Find: $p_1 - p_{\text{atm}}$.

Solution:

Governing equations:

$$\frac{p_1}{\rho} + \frac{V_1^2}{2} + gz_1 = \frac{p_2}{\rho} + \frac{V_2^2}{2} + gz_2 \quad (6.13)$$



Continuity for incompressible and uniform flow:

$$\sum_{\text{CS}} \vec{V} \cdot \vec{A} = 0 \quad (4.13b)$$

Assumptions:

- 1 Steady flow.
- 2 Incompressible flow.
- 3 Frictionless flow.
- 4 Flow along a streamline.
- 5 $z_1 = z_2$.
- 6 Uniform flow at sections ① and ②.

The maximum speed of 50 m/s is well below 100 m/s , which corresponds to Mach number $M \approx 0.3$ in standard air. Hence, the flow may be treated as incompressible.

Apply the Bernoulli equation along a streamline between points ① and ② to evaluate p_1 . Then

$$p_1 - p_{\text{atm}} = p_1 - p_2 = \frac{\rho}{2}(V_2^2 - V_1^2)$$

Apply the continuity equation to determine V_1 ,

$$(-\rho V_1 A_1) + (\rho V_2 A_2) = 0 \quad \text{or} \quad V_1 A_1 = V_2 A_2$$

so that

$$V_1 = V_2 \frac{A_2}{A_1} = 50 \frac{\text{m}}{\text{s}} \times \frac{0.02 \text{ m}^2}{0.1 \text{ m}^2} = 10 \text{ m/s}$$

For air at standard conditions, $\rho = 1.23 \text{ kg/m}^3$. Then

$$\begin{aligned} p_1 - p_{\text{atm}} &= \frac{\rho}{2}(V_2^2 - V_1^2) \\ &= \frac{1}{2} \times 1.23 \frac{\text{kg}}{\text{m}^3} \left[(50)^2 \frac{\text{m}^2}{\text{s}^2} - (10)^2 \frac{\text{m}^2}{\text{s}^2} \right] \frac{\text{N} \cdot \text{s}^2}{\text{kg} \cdot \text{m}} \\ p_1 - p_{\text{atm}} &= 1.48 \text{ kPa} \end{aligned}$$

Notes:

- This problem illustrates a typical application of the Bernoulli equation.
- The streamlines must be straight at the inlet and exit in order to have uniform pressures at those locations.

Example 6.4 FLOW THROUGH A SIPHON

A U-tube acts as a water siphon. The bend in the tube is 1 m above the water surface; the tube outlet is 7 m below the water surface. The water issues from the bottom of the siphon as a free jet at atmospheric pressure. Determine the speed of the free jet and the minimum absolute pressure of the water in the bend.

Given: Water flowing through a siphon as shown.

Find: (a) Speed of water leaving as a free jet.
(b) Pressure at point \textcircled{A} (the minimum pressure point) in the flow.

Solution:

Governing equation:

$$\frac{p}{\rho} + \frac{V^2}{2} + gz = \text{constant}$$

Assumptions:

- 1 Neglect friction.
- 2 Steady flow.
- 3 Incompressible flow.
- 4 Flow along a streamline.
- 5 Reservoir is large compared with pipe.

Apply the Bernoulli equation between points $\textcircled{1}$ and $\textcircled{2}$.

$$\frac{p_1}{\rho} + \frac{V_1^2}{2} + gz_1 = \frac{p_2}{\rho} + \frac{V_2^2}{2} + gz_2$$

Since $\text{area}_{\text{reservoir}} \gg \text{area}_{\text{pipe}}$, then $V_1 \approx 0$. Also $p_1 = p_2 = p_{\text{atm}}$, so

$$gz_1 = \frac{V_2^2}{2} + gz_2 \quad \text{and} \quad V_2^2 = 2g(z_1 - z_2)$$

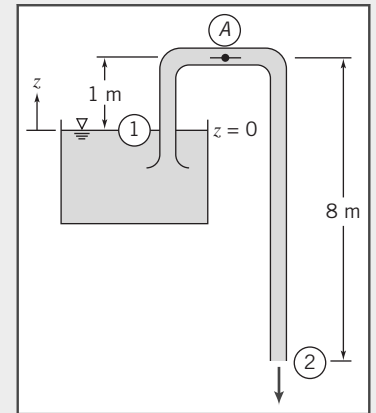
$$V_2 = \sqrt{2g(z_1 - z_2)} = \sqrt{2 \times 9.81 \frac{\text{m}}{\text{s}^2} \times 7 \text{ m}} \\ = 11.7 \text{ m/s} \xrightarrow{V_2}$$

To determine the pressure at location \textcircled{A} , we write the Bernoulli equation between $\textcircled{1}$ and \textcircled{A} .

$$\frac{p_1}{\rho} + \frac{V_1^2}{2} + gz_1 = \frac{p_A}{\rho} + \frac{V_A^2}{2} + gz_A$$

Again $V_1 \approx 0$ and from conservation of mass $V_A = V_2$. Hence

$$\begin{aligned} \frac{p_A}{\rho} &= \frac{p_1}{\rho} + gz_1 - \frac{V_2^2}{2} - gz_A = \frac{p_1}{\rho} + g(z_1 - z_A) - \frac{V_2^2}{2} \\ p_A &= p_1 + \rho g(z_1 - z_A) - \rho \frac{V_2^2}{2} \\ &= 1.01 \times 10^5 \frac{\text{N}}{\text{m}^2} + 999 \frac{\text{kg}}{\text{m}^3} \times 9.81 \frac{\text{m}}{\text{s}^2} \times (-1 \text{ m}) \frac{\text{N} \cdot \text{s}^2}{\text{kg} \cdot \text{m}} \\ &\quad - \frac{1}{2} \times 999 \frac{\text{kg}}{\text{m}^3} \times (11.7)^2 \frac{\text{m}^2}{\text{s}^2} \times \frac{\text{N} \cdot \text{s}^2}{\text{kg} \cdot \text{m}} \\ p_A &= 22.8 \text{ kPa (abs)} \text{ or } -78.5 \text{ kPa (gage)} \end{aligned}$$



Notes:

- This problem illustrates an application of the Bernoulli equation that includes elevation changes.
- It is interesting to note that when the Bernoulli equation applies between a reservoir and a free jet that it feeds at a location h below the reservoir surface, the jet speed will be $V = \sqrt{2gh}$; this is the same velocity a droplet (or stone) falling without friction from the reservoir level would attain if it fell a distance h .
- Always take care when neglecting friction in any internal flow. In this problem, neglecting friction is reasonable if the pipe is smooth-surfaced and is relatively short. In Chapter 8 we will study frictional effects in internal flows.

Example 6.5 FLOW UNDER A SLUICE GATE

Water flows under a sluice gate on a horizontal bed at the inlet to a flume. Upstream from the gate, the water depth is 1.5 ft and the speed is negligible. At the vena contracta downstream from the gate, the flow streamlines are straight and the depth is 2 in. Determine the flow speed downstream from the gate and the discharge in cubic feet per second per foot of width.

Given: Flow of water under a sluice gate.

Find: (a) V_2 .
 (b) Q in $\text{ft}^3/\text{s}/\text{ft}$ of width.

Solution: Under the assumptions listed below, the flow satisfies all conditions necessary to apply the Bernoulli equation. The question is, what streamline do we use?

$$\text{Governing equation: } \frac{p_1}{\rho} + \frac{V_1^2}{2} + gz_1 = \frac{p_2}{\rho} + \frac{V_2^2}{2} + gz_2$$

Assumption:

- 1 Steady flow.
- 2 Incompressible flow.
- 3 Frictionless flow.
- 4 Flow along a streamline.
- 5 Uniform flow at each section.
- 6 Hydrostatic pressure distribution (at each location, pressure increases linearly with depth).

If we consider the streamline that runs along the bottom of the channel ($z=0$), because of assumption 6 the pressures at ① and ② are

$$p_1 = p_{\text{atm}} + \rho g D_1 \quad \text{and} \quad p_2 = p_{\text{atm}} + \rho g D_2$$

so that the Bernoulli equation for this streamline is

$$\frac{(p_{\text{atm}} + \rho g D_1)}{\rho} + \frac{V_1^2}{2} = \frac{(p_{\text{atm}} + \rho g D_2)}{\rho} + \frac{V_2^2}{2}$$

or

$$\frac{V_1^2}{2} + gD_1 = \frac{V_2^2}{2} + gD_2 \quad (1)$$

On the other hand, consider the streamline that runs along the free surface on both sides and down the inner surface of the gate. For this streamline

$$\frac{p_{\text{atm}}}{\rho} + \frac{V_1^2}{2} + gD_1 = \frac{p_{\text{atm}}}{\rho} + \frac{V_2^2}{2} + gD_2$$

or

$$\frac{V_1^2}{2} + gD_1 = \frac{V_2^2}{2} + gD_2 \quad (1)$$

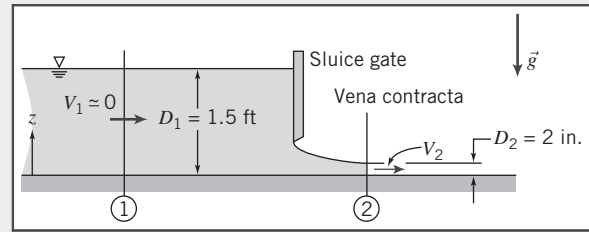
We have arrived at the same equation (Eq. 1) for the streamline at the bottom and the streamline at the free surface, implying the Bernoulli constant is the same for both streamlines. We will see in Section 6.5 that this flow is one of a family of flows for which this is the case. Solving for V_2 yields

$$V_2 = \sqrt{2g(D_1 - D_2) + V_1^2}$$

But $V_1^2 \approx 0$, so

$$V_2 = \sqrt{2g(D_1 - D_2)} = \sqrt{2 \times 32.2 \frac{\text{ft}}{\text{s}^2} \times \left(1.5 \text{ ft} - 2 \text{ in.} \times \frac{\text{ft}}{12 \text{ in.}} \right)}$$

$$V_2 = 9.27 \text{ ft/s} \quad \xrightarrow{V_2}$$



For uniform flow, $Q = VA = VDw$, or

$$\frac{Q}{w} = VD = V_2 D_2 = 9.27 \frac{\text{ft}}{\text{s}} + 2 \text{ in.} \times \frac{\text{ft}}{12 \text{ in.}} = 1.55 \text{ ft}^2/\text{s}$$

$$\frac{Q}{w} = 1.55 \text{ ft}^3/\text{s}/\text{foot of width} \xrightarrow{\quad} \frac{Q}{w}$$

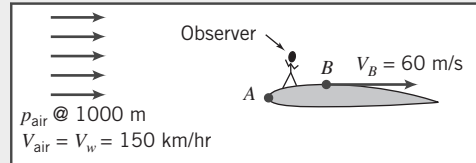
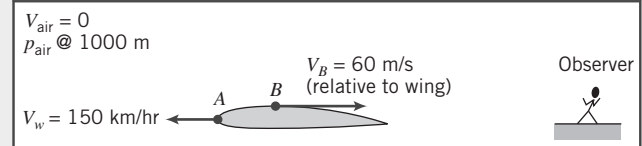
Example 6.6 BERNOULLI EQUATION IN TRANSLATING REFERENCE FRAME

A light plane flies at 150 km/hr in standard air at an altitude of 1000 m. Determine the stagnation pressure at the leading edge of the wing. At a certain point close to the wing, the air speed *relative* to the wing is 60 m/s. Compute the pressure at this point.

Given: Aircraft in flight at 150 km/hr at 1000 m altitude in standard air.

Find: Stagnation pressure, p_{0A} , at point A and static pressure, p_B , at point B.

Solution: Flow is unsteady when observed from a fixed frame, that is, by an observer on the ground. However, an observer *on* the wing sees the following steady flow:



At $z = 1000$ m in standard air, the temperature is 281 K and the speed of sound is 336 m/s. Hence at point B, $M_B = V_{B/C} = 0.178$. This is less than 0.3, so the flow may be treated as incompressible. Thus the Bernoulli equation can be applied along a streamline in the moving observer's inertial reference frame.

Governing equation:

$$\frac{p_{\text{air}}}{\rho} + \frac{V_{\text{air}}^2}{2} + gz_{\text{air}} = \frac{p_A}{\rho} + \frac{V_A^2}{2} + gz_A = \frac{p_B}{\rho} + \frac{V_B^2}{2} + gz_B$$

Assumptions:

- 1 Steady flow.
- 2 Incompressible flow ($V < 100$ m/s).
- 3 Frictionless flow.
- 4 Flow along a streamline.
- 5 Neglect Δz .

Values for pressure and density may be found from Table A.3. Thus, at 1000 m, $p/p_{SL} = 0.8870$ and $\rho/\rho_{SL} = 0.9075$. Consequently,

$$p = 0.8870 p_{SL} = 0.8870 \times 1.01 \times 10^5 \frac{\text{N}}{\text{m}^2} = 8.96 \times 10^4 \text{ N/m}^2$$

and

$$\rho = 0.9075 \rho_{SL} = 0.9075 \times 1.23 \frac{\text{kg}}{\text{m}^3} = 1.12 \text{ kg/m}^3$$

Since the speed is $V_A = 0$ at the stagnation point,

$$\begin{aligned} p_{0A} &= p_{\text{air}} + \frac{1}{2}\rho V_{\text{air}}^2 \\ &= 8.96 \times 10^4 \frac{\text{N}}{\text{m}^2} + \frac{1}{2} \times 1.12 \frac{\text{kg}}{\text{m}^3} \left(150 \frac{\text{km}}{\text{hr}} \times 1000 \frac{\text{m}}{\text{km}} \times \frac{\text{hr}}{3600 \text{ s}} \right)^2 \times \frac{\text{N} \cdot \text{s}^2}{\text{kg} \cdot \text{m}} \\ p_{0A} &= 90.6 \text{ kPa (abs)} \xrightarrow{p_{0A}} \end{aligned}$$

Solving for the static pressure at B , we obtain

$$\begin{aligned} p_B &= p_{\text{air}} + \frac{1}{2}\rho(V_{\text{air}}^2 - V_B^2) \\ p_B &= 8.96 \times 10^4 \frac{\text{N}}{\text{m}^2} + \frac{1}{2} \times 1.12 \frac{\text{kg}}{\text{m}^3} \left[\left(150 \frac{\text{km}}{\text{hr}} \times 1000 \frac{\text{m}}{\text{km}} \times \frac{\text{hr}}{3600 \text{ s}} \right)^2 - (60)^2 \frac{\text{m}^2}{\text{s}^2} \right] \times \frac{\text{N} \cdot \text{s}^2}{\text{kg} \cdot \text{m}} \\ p_B &= 88.6 \text{ kPa (abs)} \xrightarrow{p_B} \end{aligned}$$

This problem gives a hint as to how a wing generates lift. The incoming air has a velocity $V_{\text{air}} = 150 \text{ km/hr} = 41.7 \text{ m/s}$ and accelerates to 60 m/s on the upper surface. This leads, through the Bernoulli equation, to a pressure drop of 1 kPa (from 89.6 kPa to 88.6 kPa). It turns out that the flow decelerates on the lower surface, leading to a pressure rise of about 1 kPa . Hence, the wing experiences a net upward pressure difference of about 2 kPa , a significant effect.

Cautions on Use of the Bernoulli Equation

In Examples 6.3 through 6.7, we have seen several situations where the Bernoulli equation may be applied because the restrictions on its use led to a reasonable flow model. However, in some situations you might be tempted to apply the Bernoulli equation where the restrictions are not satisfied. Some subtle cases that violate the restrictions are discussed briefly in this section.

Example 6.3 examined flow in a nozzle. In a *subsonic nozzle* (a converging section) the pressure drops, accelerating a flow. Because the pressure drops and the walls of the nozzle converge, there is no flow separation from the walls and the boundary layer remains thin. In addition, a nozzle is usually relatively short so frictional effects are not significant. All of this leads to the conclusion that the Bernoulli equation is suitable for use for subsonic nozzles.

Sometimes we need to decelerate a flow. This can be accomplished using a *subsonic diffuser* (e.g., a diverging section), or by using a sudden expansion (e.g., from a pipe into a reservoir). In these devices the flow decelerates because of an adverse pressure gradient. As we discussed in Section 2.6, an adverse pressure gradient tends to lead to rapid growth of the boundary layer and its separation. Hence, we should be careful in applying the Bernoulli equation in such devices—at best, it will be an approximation. Because of area blockage caused by boundary-layer growth, pressure rise in actual diffusers always is less than that predicted for inviscid one-dimensional flow.

The Bernoulli equation was a reasonable model for the siphon of Example 6.4 because the entrance was well rounded, the bends were gentle, and the overall length was short. Flow separation, which can occur at inlets with sharp corners and in abrupt bends, causes the flow to depart from that predicted by a one-dimensional model and the Bernoulli equation. Frictional effects would not be negligible if the tube were long.

Example 6.5 presented an open-channel flow analogous to that in a nozzle, for which the Bernoulli equation is a good flow model. The hydraulic jump is an example of an open-channel flow with adverse pressure gradient. Flow through a hydraulic jump is mixed violently, making it impossible to identify streamlines. Thus the Bernoulli equation cannot be used to model flow through a hydraulic jump. We will see a more detailed presentation of open channel flows in Chapter 11.

The Bernoulli equation cannot be applied *through* a machine such as a propeller, pump, turbine, or windmill. The equation was derived by integrating along a stream tube (Section 4.4) or a streamline (Section 6.2) in the absence of moving surfaces such as blades or vanes. It is impossible to have locally steady flow or to identify streamlines during flow through a machine. Hence, while the Bernoulli equation may be applied between points *before* a machine, or between points *after* a machine (assuming its

restrictions are satisfied), it cannot be applied *through* the machine. In effect, a machine will change the value of the Bernoulli constant.

Finally, compressibility must be considered for flow of gases. Density changes caused by dynamic compression due to motion may be neglected for engineering purposes if the local Mach number remains below about $M \approx 0.3$, as noted in Examples 6.4 and 6.7. Temperature changes can cause significant changes in density of a gas, even for low-speed flow. Thus the Bernoulli equation could not be applied to air flow through a heating element (e.g., of a hand-held hair dryer) where temperature changes are significant.

6.3 The Bernoulli Equation Interpreted as an Energy Equation

The Bernoulli equation, Eq. 6.8, was obtained by integrating Euler's equation along a streamline for steady, incompressible, frictionless flow. Thus Eq. 6.8 was derived from the momentum equation for a fluid particle.

An equation identical in form to Eq. 6.8, although requiring very different restrictions, may be obtained from the first law of thermodynamics. Our objective in this section is to reduce the energy equation to the form of the Bernoulli equation given by Eq. 6.8. Having arrived at this form, we then compare the restrictions on the two equations to help us understand more clearly the restrictions on the use of Eq. 6.8.

Consider steady flow in the absence of shear forces. We choose a control volume bounded by streamlines along its periphery. Such a boundary, shown in Fig. 6.5, often is called a *stream tube*.

Basic equation:

$$\begin{aligned} &= 0(1) = 0(2) = 0(3) = 0(4) \\ \dot{Q} - \dot{W}_s - \dot{W}_{\text{shear}} - \dot{W}_{\text{other}} &= \frac{\partial}{\partial t} \int_{\text{CV}} e \rho dV + \int_{\text{CS}} (e + pv) \rho \vec{V} \cdot d\vec{A} \\ e &= u + \frac{V^2}{2} + gz \end{aligned} \quad (4.56)$$

Restrictions

- 1 $\dot{W}_s = 0$.
- 2 $\dot{W}_{\text{shear}} = 0$.
- 3 $\dot{W}_{\text{other}} = 0$.
- 4 Steady flow.
- 5 Uniform flow and properties at each section.

Under these restrictions, Eq. 4.56 becomes

$$\left(u_1 + p_1 v_1 + \frac{V_1^2}{2} + gz_1 \right) (-\rho_1 V_1 A_1) + \left(u_2 + p_2 v_2 + \frac{V_2^2}{2} + gz_2 \right) (\rho_2 V_2 A_2) - \dot{Q} = 0$$

From continuity, with restrictions (4) and (5):

$$\sum_{\text{CS}} \rho \vec{V} \cdot \vec{A} = 0 \quad (4.15b)$$

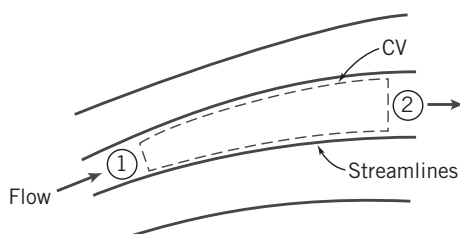


Fig. 6.5 Flow through a stream tube.

or

$$(-\rho_1 V_1 A_1) + (\rho_2 V_2 A_2) = 0$$

That is,

$$\dot{m} = \rho_1 V_1 A_1 = \rho_2 V_2 A_2$$

Also

$$\dot{Q} = \frac{\delta Q}{dt} = \frac{\delta Q}{dm} \frac{dm}{dt} = \frac{\delta Q}{dm} \dot{m}$$

Thus, from the energy equation, after rearranging

$$\left[\left(p_2 v_2 + \frac{V_2^2}{2} + gz_2 \right) - \left(p_1 v_1 + \frac{V_1^2}{2} + gz_1 \right) \right] \dot{m} + \left(u_2 - u_1 - \frac{\delta Q}{dm} \right) \dot{m} = 0$$

or

$$p_1 v_1 + \frac{V_1^2}{2} + gz_1 = p_2 v_2 + \frac{V_2^2}{2} + gz_2 + \left(u_2 - u_1 - \frac{\delta Q}{dm} \right)$$

Under the additional assumption (6) of incompressible flow, $v_1 = v_2 = 1/\rho$ and hence

$$\frac{p_1}{\rho} + \frac{V_1^2}{2} + gz_1 = \frac{p_2}{\rho} + \frac{V_2^2}{2} + gz_2 + \left(u_2 - u_1 - \frac{\delta Q}{dm} \right) \quad (6.14)$$

Equation 6.14 would reduce to the Bernoulli equation if the term in parentheses were zero. Thus, under the further restriction,

$$(7) \quad \left(u_2 - u_1 - \frac{\delta Q}{dm} \right) = 0$$

the energy equation reduces to

$$\frac{p_1}{\rho} + \frac{V_1^2}{2} + gz_1 = \frac{p_2}{\rho} + \frac{V_2^2}{2} + gz_2$$

or

$$\frac{p}{\rho} + \frac{V^2}{2} + gz = \text{constant} \quad (6.15)$$

Equation 6.15 is identical in form to the Bernoulli equation, Eq. 6.8. The Bernoulli equation was derived from momentum considerations (Newton's second law), and is valid for steady, incompressible, frictionless flow along a streamline. Equation 6.15 was obtained by applying the first law of thermodynamics to a stream tube control volume, subject to restrictions 1 through 7 above. Thus the Bernoulli equation (Eq. 6.8) and the identical form of the energy equation (Eq. 6.15) were developed from entirely different models, coming from entirely different basic concepts, and involving different restrictions.

It may appear that we needed restriction (7), the relation between the heat transfer and internal thermal energy change, to finally transform the energy equation into the Bernoulli equation. It really isn't a restriction because for an incompressible and frictionless flow without shear forces, heat transfer results only in a temperature change and does not affect pressure or velocity.

For the steady, frictionless, and incompressible flow, it is true that the first law of thermodynamics reduces to the Bernoulli equation. Each term in Eq. 6.15 has dimensions of energy per unit mass and we sometimes refer to the three terms in the equation as the "pressure" energy, kinetic energy, and potential energy per unit mass of the fluid. It is not surprising that Eq. 6.15 contains energy terms because we used the first law of thermodynamics in deriving it. We ended up with the same energy-like terms in the Bernoulli equation, which we derived from the momentum equation because we integrated the momentum equation (which involves force terms) along a streamline (which involves distance), and by doing so ended up with work or energy terms (work being defined as force times distance). The work of gravity and pressure forces leads to a kinetic energy change (which came from integrating momentum over

Example 6.7 INTERNAL ENERGY AND HEAT TRANSFER IN FRICTIONLESS INCOMPRESSIBLE FLOW

Consider frictionless, incompressible flow with heat transfer. Show that

$$u_2 - u_1 = \frac{\delta Q}{dm}$$

Given: Frictionless, incompressible flow with heat transfer.

Show: $u_2 - u_1 = \frac{\delta Q}{dm}$.

Solution: In general, internal energy can be expressed as $u = u(T, v)$. For incompressible flow, $v = \text{constant}$, and $u = u(T)$. Thus the thermodynamic state of the fluid is determined by the single thermodynamic property, T . For any process, the internal energy change, $u_2 - u_1$, depends only on the temperatures at the end states.

From the Gibbs equation, $Tds = du + \rho dv$, valid for a pure substance undergoing any process, we obtain

$$Tds = du$$

for incompressible flow, since $dv = 0$. Since the internal energy change, du , between specified end states, is independent of the process, we take a reversible process, for which $Tds = d(\delta Q/dm) = du$. Therefore,

$$u_2 - u_1 = \frac{\delta Q}{dm} \leftarrow$$

This example shows that for an incompressible fluid, heat transfer only changes the temperature and entropy, and not any other properties.

distance). In this context, we can think of the Bernoulli equation as a *mechanical energy balance*—the mechanical energy (“pressure” plus potential plus kinetic) will be constant. We must always bear in mind that for the Bernoulli equation to be valid along a streamline requires an incompressible inviscid steady flow. The two properties of the flow, compressibility and friction, are what “link” thermodynamic and mechanical energies. If a fluid is compressible, any flow-induced pressure changes will compress or expand the fluid, thereby doing work and changing the particle thermal energy. Friction as we know from everyday experience, always converts mechanical to thermal energy. Their absence, therefore, breaks the link between the mechanical and thermal energies, and they are independent.

In summary, when the conditions are satisfied for the Bernoulli equation to be valid, we can consider separately the mechanical energy and the internal thermal energy of a fluid particle as illustrated in Example 6.8 and when they are not satisfied, there will be an interaction between these energies, the Bernoulli equation becomes invalid, and we must use the full first law of thermodynamics.

Example 6.8 FRICTIONLESS FLOW WITH HEAT TRANSFER

Water flows steadily from a large open reservoir through a short length of pipe and a nozzle with cross-sectional area $A = 0.864 \text{ in.}^2$. A well-insulated 10 kW heater surrounds the pipe. Find the temperature rise of the water.

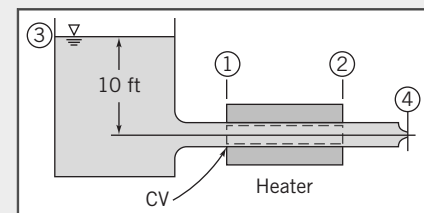
Given: Water flows from a large reservoir through the system shown and discharges to atmospheric pressure. The heater is 10 kW; $A_4 = 0.864 \text{ in.}^2$

Find: The temperature rise of the water between points ① and ②.

Solution:

Governing equations:

$$\frac{p}{\rho} + \frac{V^2}{2} + gz = \text{constant} \quad (6.8)$$



$$\sum_{\text{CS}} \vec{V} \cdot \vec{A} = 0 \quad (4.13b)$$

$$\dot{Q} - \dot{W}_s - \dot{W}_{\text{shear}} = \frac{\partial}{\partial t} \int_{\text{CV}} e \rho dV + \int_{\text{CS}} \left(u + pv + \frac{V^2}{2} + gz \right) \rho \vec{V} \cdot d\vec{A} \quad (4.56)$$

Assumptions:

- 1 Steady flow.
- 2 Frictionless flow.
- 3 Incompressible flow.
- 4 No shaft work, no shear work.
- 5 Flow along a streamline.
- 6 Uniform flow at each section [a consequence of assumption (2)].

Under the assumptions listed, the first law of thermodynamics for the CV shown becomes

$$\begin{aligned} \dot{Q} &= \int_{\text{CS}} \left(u + pv + \frac{V^2}{2} + gz \right) \rho \vec{V} \cdot d\vec{A} \\ &= \int_{A_1} \left(u + pv + \frac{V^2}{2} + gz \right) \rho \vec{V} \cdot d\vec{A} + \int_{A_2} \left(u + pv + \frac{V^2}{2} + gz \right) \rho \vec{V} \cdot d\vec{A} \end{aligned}$$

For uniform properties at ① and ②

$$\dot{Q} = -(\rho V_1 A_1) \left(u_1 + p_1 v + \frac{V_1^2}{2} + g z_1 \right) + (\rho V_2 A_2) \left(u_2 + p_2 v + \frac{V_2^2}{2} + g z_2 \right)$$

From conservation of mass, $\rho V_1 A_1 = \rho V_2 A_2 = \dot{m}$, so

$$\dot{Q} = \dot{m} \left[u_2 - u_1 + \left(\frac{p_2}{\rho} + \frac{V_2^2}{2} + g z_2 \right) - \left(\frac{p_1}{\rho} + \frac{V_1^2}{2} + g z_1 \right) \right]$$

For frictionless, incompressible, steady flow, along a streamline,

$$\frac{p}{\rho} + \frac{V^2}{2} + gz = \text{constant}$$

Therefore,

$$\dot{Q} = \dot{m}(u_2 - u_1)$$

Since, for an incompressible fluid, $u_2 - u_1 = c(T_2 - T_1)$, then

$$T_2 - T_1 = \frac{\dot{Q}}{\dot{m}c}$$

From continuity,

$$\dot{m} = \rho V_4 A_4$$

To find V_4 , write the Bernoulli equation between the free surface at ③ and point ④.

$$\frac{p_3}{\rho} + \frac{V_3^2}{2} + gz_3 = \frac{p_4}{\rho} + \frac{V_4^2}{2} + gz_4$$

Since $p_3 = p_4$ and $V_3 \approx 0$, then

$$V_4 = \sqrt{2g(z_3 - z_4)} = \sqrt{2 \times 32.2 \frac{\text{ft}}{\text{s}^2} \times 10 \text{ ft}} = 25.4 \text{ ft/s}$$

and

$$\dot{m} = \rho V_4 A_4 = 1.94 \frac{\text{slug}}{\text{ft}^3} \times 25.4 \frac{\text{ft}}{\text{s}} \times 0.864 \text{ in.}^2 \times \frac{\text{ft}^2}{144 \text{ in.}^2} = 0.296 \text{ slug/s}$$

Assuming no heat loss to the surroundings, we obtain

$$\begin{aligned} T_2 - T_1 &= \frac{\dot{Q}}{\dot{m}c} = 10 \text{ kW} \times 3413 \frac{\text{Btu}}{\text{kW} \cdot \text{hr}} \times \frac{\text{hr}}{3600 \text{ s}} \\ &\quad \times \frac{\text{s}}{0.296 \text{ slug}} \times \frac{\text{slug}}{32.2 \text{ lbm}} \times \frac{\text{lbm} \cdot {}^\circ\text{R}}{1 \text{ Btu}} \\ T_2 - T_1 &= 0.995 {}^\circ\text{R} \xleftarrow{\hspace{10em}} T_2 - T_1 \end{aligned}$$

This problem illustrates that:

- In general, the first law of thermodynamics and the Bernoulli equation are independent equations.
- For an incompressible, inviscid flow the internal thermal energy is only changed by a heat transfer process, and is independent of the fluid mechanics.

6.4 Energy Grade Line and Hydraulic Grade Line

We have learned that for a steady, incompressible, frictionless flow, we may use the Bernoulli equation, Eq. 6.8, derived from the momentum equation, and also Eq. 6.15, derived from the energy equation:

$$\frac{p}{\rho} + \frac{V^2}{2} + gz = \text{constant} \quad (6.15)$$

We also interpreted the three terms comprised of “pressure,” kinetic, and potential energies to make up the total mechanical energy, per unit mass, of the fluid. If we divide Eq. 6.15 by g , we obtain another form,

$$\frac{p}{\rho g} + \frac{V^2}{2g} + z = H \quad (6.16a)$$

Here H is the *total head* of the flow and measures the total mechanical energy in units of meters or feet. We will learn in Chapter 8 that in a fluid flow with friction this head will *not* be constant but will continuously decrease in value as mechanical energy is converted to thermal. We can go one step further here and get a very useful graphical approach if we also define this to be the *energy grade line* (EGL),

$$EGL = \frac{p}{\rho g} + \frac{V^2}{2g} + z \quad (6.16b)$$

This can be measured using the pitot (total head) tube shown in Fig. 6.3. Placing such a tube in a flow measures the total pressure, $p_0 = p + \frac{1}{2}\rho V^2$, so this will cause the height of a column of *the same fluid* to rise to a height $h = p_0/\rho g = p/\rho g + V^2/2g$. If the vertical location of the pitot tube is measured from some datum (e.g., the ground), the height of column of fluid *measured from the datum* will then be $h + z = p/\rho g + V^2/2g + z = EGL = H$. In summary, the height of the column, measured from the datum, attached to a pitot tube directly indicates the EGL.

We can also define the *hydraulic grade line* (HGL),

$$HGL = \frac{p}{\rho g} + z \quad (6.16c)$$

This can be measured using the static pressure tap shown in Fig. 6.2a. Placing such a tube in a flow measures the static pressure, p , so this will cause the height of a column of *the same fluid* to rise to a height $h = p/\rho g$. If the vertical location of the tap is also at z , measured from some datum, the height

of column of fluid *measured from the datum* will then be $h + z = p/\rho g + z = HGL$. The height of the column attached to a static pressure tap thus directly indicates the HGL.

From Eqs. 6.16b and 6.16c we obtain

$$EGL - HGL = \frac{V^2}{2g} \quad (6.16d)$$

which shows that the difference between the EGL and HGL is always the dynamic pressure term.

To see a graphical interpretation of the EGL and HGL, refer to Fig. 6.6, which shows frictionless flow from a reservoir, through a pipe reducer. At all locations the EGL is the same because there is no loss of mechanical energy. Station ① is at the reservoir, and here the EGL and HGL coincide with the free surface: in Eqs. 6.16b and 6.16c $p = 0$ (gage), $V = 0$, and $z = z_1$, so $EGL_1 = HGL_1 = H = z_1$; all of the mechanical energy is potential.

At station ② we have a pitot (total head) tube and a static head tap. The pitot tube's column indicates the correct value of the EGL ($EGL_1 = EGL_2 = H$), but *something* changed between the two stations: The fluid now has significant kinetic energy and has lost some potential energy. From Eq. 6.16d, we can see that the HGL is lower than the EGL by $V_2^2/2g$; the HGL at station ② shows this.

From station ② to station ③ there is a reduction in diameter, so continuity requires that $V_3 > V_2$; hence the gap between the EGL and HGL increases further, as shown.

Station ④ is at the exit to the atmosphere. Here the pressure is zero gage, so the EGL consists entirely of kinetic and potential energy terms, and $HGL_4 = EGL_4$. We can summarize two important ideas when sketching EGL and HGL curves:

- 1 The EGL is constant for incompressible, inviscid flow in the absence of work devices. We will see in Chapter 8 that work devices may increase or decrease the EGL, and friction will always lead to a fall in the EGL.

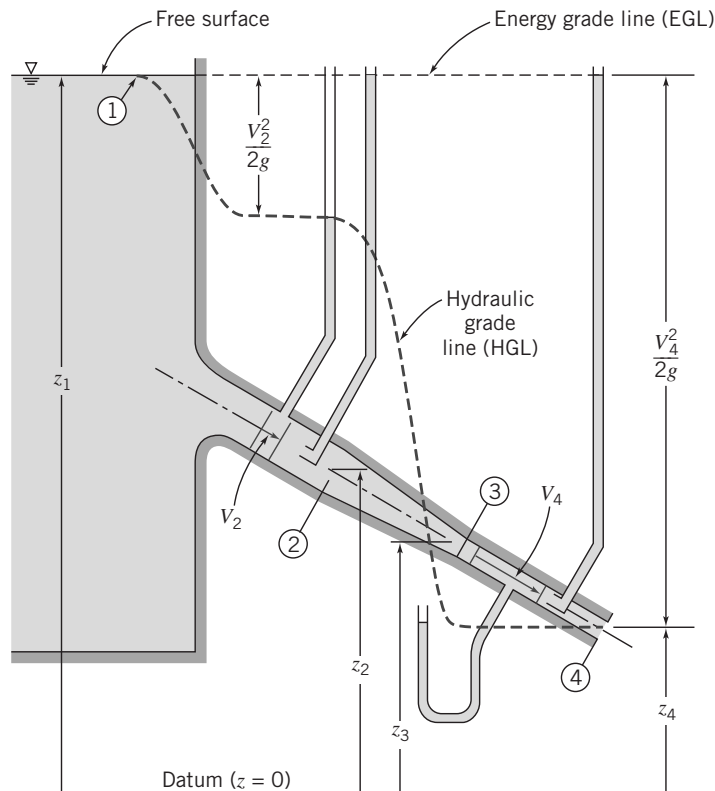


Fig. 6.6 Energy and hydraulic grade lines for frictionless flow.

- 2 The HGL is always lower than the EGL by distance $V^2/2g$. Note that the value of velocity V depends on the overall system (e.g., reservoir height, pipe diameter, etc.), but *changes* in velocity *only* occur when the diameter changes.

6.5 Unsteady Bernoulli Equation: Integration of Euler's Equation Along a Streamline

It is not necessary to restrict the development of the Bernoulli equation to steady flow. The purpose of this section is to develop the corresponding equation for unsteady flow along a streamline and to illustrate its use.

The momentum equation for frictionless flow (Eq. 6.1) can be written (with \vec{g} in the negative z direction) as

$$\frac{D\vec{V}}{Dt} = -\frac{1}{\rho} \nabla p - g\hat{k} \quad (6.17)$$

Equation 6.17 is a vector equation. It can be converted to a scalar equation by taking the dot product with $d\vec{s}$, where $d\vec{s}$ is an element of distance along a streamline. Thus

$$\frac{D\vec{V}}{Dt} \cdot d\vec{s} = \frac{DV}{Dt} ds = V \frac{\partial V}{\partial s} ds + \frac{\partial V}{\partial t} ds = -\frac{1}{\rho} \nabla p \cdot d\vec{s} - g\hat{k} \cdot d\vec{s} \quad (6.18)$$

Examining the terms in Eq. 6.18, we note that

$$\begin{aligned} \frac{\partial V}{\partial s} ds &= dV && \text{(the change in } V \text{ along } s\text{)} \\ \nabla p \cdot d\vec{s} &= dp && \text{(the change in pressure along } s\text{)} \\ \hat{j} \cdot d\vec{s} &= dz && \text{(the change in } z \text{ along } s\text{)} \end{aligned}$$

Substituting into Eq. 6.18, we obtain

$$V dV + \frac{\partial V}{\partial t} ds = -\frac{dp}{\rho} - g dz \quad (6.19)$$

Integrating along a streamline from point 1 to point 2 yields

$$\int_1^2 \frac{dp}{\rho} + \frac{V_2^2 - V_1^2}{2} + g(z_2 - z_1) + \int_1^2 \frac{\partial V}{\partial t} ds = 0 \quad (6.20)$$

For incompressible flow, the density is constant. For this special case, Eq. 6.20 becomes

$$\frac{p_1}{\rho} + \frac{V_1^2}{2} + gz_1 = \frac{p_2}{\rho} + \frac{V_2^2}{2} + gz_2 + \int_1^2 \frac{\partial V}{\partial t} ds \quad (6.21)$$

Restrictions:

- 1 Incompressible flow.
- 2 Frictionless flow.
- 3 Flow along a streamline.

This is a form of the Bernoulli equation for unsteady flows. It differs from the Bernoulli equation Eq. 6.8 by the factor $\int_1^2 \partial V / \partial t ds$. We can interpret this factor as the work involved in the rate of increase of momentum of the fluid on the streamline over time, as opposed to the change in momentum over distance, represented by the change in velocity from V_1 to V_2 . Example 6.9 will demonstrate this idea. Equation 6.21 may be applied to any flow in which the restrictions are compatible with the physical situation.

Example 6.9 UNSTEADY BERNOULLI EQUATION

A long pipe is connected to a large reservoir that initially is filled with water to a depth of 3 m. The pipe is 150 mm in diameter and 6 m long. Determine the flow velocity leaving the pipe as a function of time after a cap is removed from its free end.

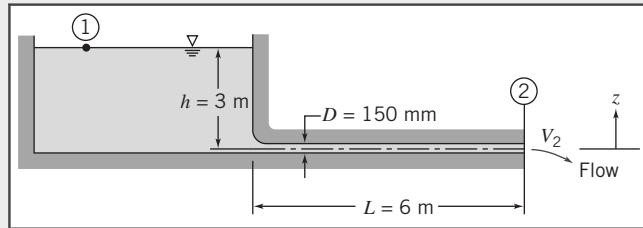
Given: Pipe and large reservoir as shown.

Find: $V_2(t)$.

Solution: Apply the Bernoulli equation to the unsteady flow along a streamline from point ① to point ②.

Governing equation:

$$\frac{p_1}{\rho} + \frac{V_1^2}{2} + gz_1 = \frac{p_2}{\rho} + \frac{V_2^2}{2} + gz_2 + \int_1^2 \frac{\partial V}{\partial t} ds \quad \begin{matrix} \simeq 0(5) \\ = 0(6) \end{matrix}$$



Assumptions:

- 1 Incompressible flow.
- 2 Frictionless flow.
- 3 Flow along a streamline from ① to ②.
- 4 $p_1 = p_2 = p_{atm}$.
- 5 $V_1^2 \simeq 0$.
- 6 $z_2 = 0$.
- 7 $z_1 = h = \text{constant}$.
- 8 Neglect velocity in reservoir, except for small region near the inlet to the tube.

Then

$$gz_1 = gh = \frac{V_2^2}{2} + \int_1^2 \frac{\partial V}{\partial t} ds$$

In view of assumption (8), the integral becomes

$$\int_1^2 \frac{\partial V}{\partial t} ds \approx \int_0^L \frac{\partial V}{\partial t} ds$$

In the tube, $V = V_2$ everywhere, so that

$$\int_0^L \frac{\partial V}{\partial t} ds = \int_0^L \frac{dV_2}{dt} ds = L \frac{dV_2}{dt}$$

This is the rate of change over time of the momentum (per unit mass) within the pipe; in the long term it will approach zero. Substituting gives

$$gh = \frac{V_2^2}{2} + L \frac{dV_2}{dt}$$

Separating variables, we obtain

$$\frac{dV_2}{2gh - V_2^2} = \frac{dt}{2L}$$

Integrating between limits $V = 0$ at $t = 0$ and $V = V_2$ at $t = t$,

$$\int_0^{V_2} \frac{dV}{2gh - V^2} = \left[\frac{1}{\sqrt{2gh}} \tanh^{-1} \left(\frac{V}{\sqrt{2gh}} \right) \right]_0^{V_2} = \frac{t}{2L}$$

Since $\tanh^{-1}(0) = 0$, we obtain

$$\frac{1}{\sqrt{2gh}} \tanh^{-1} \left(\frac{V_2}{\sqrt{2gh}} \right) = \frac{t}{2L} \quad \text{or} \quad \frac{V_2}{\sqrt{2gh}} = \tanh \left(\frac{1}{2L} \sqrt{2gh} \right) \xrightarrow{\text{V}_2(t)}$$

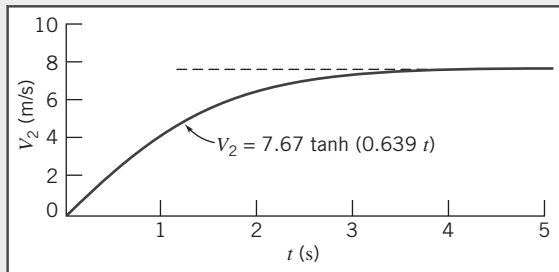
For the given conditions,

$$\sqrt{2gh} = \sqrt{2 \times 9.81 \frac{\text{m}}{\text{s}^2} \times 3 \text{ m}} = 7.67 \text{ m/s}$$

and

$$\frac{t}{2L} \sqrt{2gh} = \frac{t}{2} \times \frac{1}{6 \text{ m}} \times 7.67 \frac{\text{m}}{\text{s}} = 0.639t$$

The result is then $V_2 = 7.67 \tanh(0.639t)$ m/s, as shown:



Notes:

- This problem illustrates use of the unsteady Bernoulli equation.
- Initially the head available at state is used to accelerate the fluid in the pipe; eventually the head at state equals the head at state.
- In reality, friction would be important and reduce the velocity significantly.

6.6 Irrotational Flow

We have already discussed irrotational flows in Section 5.3. These are flows in which the fluid particles do not rotate ($\vec{\omega} = 0$). We recall that the only stresses that can generate particle rotation are shear stresses; hence, inviscid flows (i.e., those with zero shear stresses) will be irrotational unless the particles were initially rotating. Using Eq. 5.14, we obtain the irrotationality condition

$$\nabla \times \vec{V} = 0 \quad (6.22)$$

leading to

$$\frac{\partial w}{\partial y} - \frac{\partial v}{\partial z} = \frac{\partial u}{\partial z} - \frac{\partial w}{\partial x} = \frac{\partial v}{\partial x} - \frac{\partial u}{\partial y} = 0 \quad (6.23)$$

In cylindrical coordinates, from Eq. 5.16, the irrotationality condition requires that

$$\frac{1}{r} \frac{\partial V_z}{\partial \theta} - \frac{\partial V_\theta}{\partial z} = \frac{\partial V_r}{\partial z} - \frac{\partial V_z}{\partial r} = \frac{1}{r} \frac{\partial r V_\theta}{\partial r} - \frac{1}{r} \frac{\partial V_r}{\partial \theta} = 0 \quad (6.24)$$

Bernoulli Equation Applied to Irrotational Flow

In Section 6.2, we integrated Euler's equation along a streamline for steady, incompressible, inviscid flow to obtain the Bernoulli equation

$$\frac{p}{\rho} + \frac{V^2}{2} + gz = \text{constant} \quad (6.8)$$

Equation 6.8 can be applied between any two points on the *same* streamline. In general, the value of the constant will vary from streamline to streamline.

If, in addition to being inviscid, steady, and incompressible, the flow field is also irrotational (i.e., the particles had no initial rotation), so that $\nabla \times \vec{V} = 0$ (Eq. 6.22), we can show that Bernoulli's equation can be applied between any and all points in the flow. Then the value of the constant in Eq. 6.8 is the same for all streamlines. To illustrate this, we start with Euler's equation in vector form,

$$(\vec{V} \cdot \nabla) \vec{V} = -\frac{1}{\rho} \nabla p - g \hat{k} \quad (6.9)$$

Using the vector identity

$$(\vec{V} \cdot \nabla) \vec{V} = \frac{1}{2} \nabla (\vec{V} \cdot \vec{V}) - \vec{V} \times (\nabla \times \vec{V})$$

we see for irrotational flow, where $\nabla \times \vec{V} = 0$, that

$$(\vec{V} \cdot \nabla) \vec{V} = \frac{1}{2} \nabla (\vec{V} \cdot \vec{V})$$

and Euler's equation for irrotational flow can be written as

$$\frac{1}{2} \nabla (\vec{V} \cdot \vec{V}) = \frac{1}{2} \nabla (V^2) = -\frac{1}{\rho} \nabla p - g \hat{k} \quad (6.25)$$

Consider a displacement in the flow field from position \vec{r} to position $\vec{r} + d\vec{r}$; the displacement $d\vec{r}$ is an arbitrary infinitesimal displacement in *any* direction, not necessarily along a streamline. Taking the dot product of $d\vec{r} = dx\hat{i} + dy\hat{j} + dz\hat{k}$ with each of the terms in Eq. 6.25, we have

$$\frac{1}{2} \nabla (V^2) \cdot d\vec{r} = -\frac{1}{\rho} \nabla p \cdot d\vec{r} - g \hat{k} \cdot d\vec{r}$$

and hence

$$\frac{1}{2} d(V^2) = -\frac{dp}{\rho} - gdz$$

or

$$\frac{dp}{\rho} + \frac{1}{2} d(V^2) + gdz = 0$$

Integrating this equation for incompressible flow gives

$$\frac{p}{\rho} + \frac{V^2}{2} + gz = \text{constant} \quad (6.26)$$

Since $d\vec{r}$ was an arbitrary displacement, Eq. 6.26 is valid between *any* two points (i.e., not just along a streamline) in a steady, incompressible, inviscid flow that is also irrotational (see Example 6.5).

Velocity Potential

Section 5.2 provides the necessary background for the development of the stream function ψ for a two-dimensional incompressible flow. For irrotational flow we can introduce a companion function, the *potential function* ϕ , defined by

$$\vec{V} = -\nabla \phi \quad (6.27)$$

This definition guarantees that *any* continuous scalar function $\phi(x, y, z, t)$ *automatically* satisfies the irrotationality condition (Eq. 6.22) because of a fundamental identity:

$$\nabla \times \vec{V} = -\nabla \times \nabla \phi = -\text{curl}(\text{grad } \phi) \equiv 0 \quad (6.28)$$

The minus sign is inserted simply so that ϕ decreases in the flow direction. Thus,

$$u = -\frac{\partial \phi}{\partial x}, \quad v = -\frac{\partial \phi}{\partial y}, \quad \text{and} \quad w = -\frac{\partial \phi}{\partial z} \quad (6.29)$$

The irrotationality condition, Eq. 6.22, is satisfied identically.

In cylindrical coordinates,

$$\nabla = \hat{e}_r \frac{\partial}{\partial r} + \hat{e}_\theta \frac{1}{r} \frac{\partial}{\partial \theta} + \hat{k} \frac{\partial}{\partial z} \quad (3.19)$$

From Eq. 6.27, then, in cylindrical coordinates

$$V_r = -\frac{\partial \phi}{\partial r} \quad V_\theta = -\frac{1}{r} \frac{\partial \phi}{\partial \theta} \quad V_z = -\frac{\partial \phi}{\partial z} \quad (6.30)$$

Because $\nabla \times \nabla \phi \equiv 0$ for all ϕ , the velocity potential exists only for irrotational flow.

Irrotationality may be a valid assumption for those regions of a flow in which viscous forces are negligible. The theory for irrotational flow is developed in terms of an imaginary ideal fluid whose viscosity is identically zero. Since, in an irrotational flow, the velocity field may be defined by the potential function ϕ , the theory is often referred to as potential flow theory.

All real fluids possess viscosity, but there are many situations in which the assumption of inviscid flow considerably simplifies the analysis and, at the same time, gives meaningful results. Because of its relative simplicity and mathematical beauty, potential flow has been studied extensively [4], [5], and [6].

Stream Function and Velocity Potential for Two-Dimensional, Irrotational, Incompressible Flow: Laplace's Equation

For a two-dimensional, incompressible, irrotational flow we have expressions for the velocity components, u and v , in terms of both the stream function ψ , and the velocity potential ϕ ,

$$u = \frac{\partial \psi}{\partial y} \quad v = -\frac{\partial \psi}{\partial x} \quad (5.4)$$

$$u = -\frac{\partial \phi}{\partial x} \quad v = -\frac{\partial \phi}{\partial y} \quad (6.29)$$

Substituting for u and v from Eq. 5.4 into the irrotationality condition,

$$\frac{\partial v}{\partial x} - \frac{\partial u}{\partial y} = 0 \quad (6.23)$$

we obtain

$$\frac{\partial^2 \psi}{\partial x^2} + \frac{\partial^2 \psi}{\partial y^2} = \nabla^2 \psi = 0 \quad (6.31)$$

Substituting for u and v from Eq. 6.29 into the continuity equation,

$$\frac{\partial u}{\partial x} + \frac{\partial v}{\partial y} = 0 \quad (5.3)$$

we obtain

$$\frac{\partial^2 \phi}{\partial x^2} + \frac{\partial^2 \phi}{\partial y^2} = \nabla^2 \phi = 0 \quad (6.32)$$

Equations 6.31 and 6.32 are forms of Laplace's equation, which is an equation that arises in many areas of the physical sciences and engineering. Any function ψ or ϕ that satisfies Laplace's equation represents a possible two-dimensional, incompressible, irrotational flow field.

Table 6.1 summarizes the results of our discussion of the stream function and velocity potential for two-dimensional flows.

The same rules for when incompressibility and irrotationality apply are valid for the stream function and velocity potential when expressed in cylindrical coordinates,

$$V_r = \frac{1}{r} \frac{\partial \psi}{\partial \theta} \quad \text{and} \quad V_\theta = -\frac{\partial \psi}{\partial r} \quad (5.8)$$

and

$$V_r = -\frac{\partial \phi}{\partial r} \quad \text{and} \quad V_\theta = -\frac{1}{r} \frac{\partial \phi}{\partial \theta} \quad (6.33)$$

Table 6.1Definitions of ψ and ϕ , and Conditions Necessary for Satisfying Laplace's Equation

Definition	Always satisfies ...	Satisfies Laplace equation ... $\frac{\partial^2(\cdot)}{\partial x^2} + \frac{\partial^2(\cdot)}{\partial y^2} = \nabla^2(\cdot) = 0$
Stream function ψ	... incompressibility: $u = \frac{\partial \psi}{\partial y}, v = -\frac{\partial \psi}{\partial x}$ $\frac{\partial u}{\partial x} + \frac{\partial v}{\partial y} = \frac{\partial^2 \psi}{\partial x \partial y} - \frac{\partial^2 \psi}{\partial y \partial x} \equiv 0$... only if irrotational: $\frac{\partial v}{\partial x} - \frac{\partial u}{\partial y} = -\frac{\partial^2 \psi}{\partial x \partial x} - \frac{\partial^2 \psi}{\partial y \partial y} = 0$
Velocity potential ϕ	... irrotationality: $u = -\frac{\partial \phi}{\partial x}, v = -\frac{\partial \phi}{\partial y}$ $\frac{\partial v}{\partial x} - \frac{\partial u}{\partial y} = -\frac{\partial^2 \phi}{\partial x \partial y} - \frac{\partial^2 \phi}{\partial y \partial x} \equiv 0$... only if incompressible: $\frac{\partial u}{\partial x} + \frac{\partial v}{\partial y} = -\frac{\partial^2 \phi}{\partial x \partial x} - \frac{\partial^2 \phi}{\partial y \partial y} = 0$

In Section 5.2 we showed that the stream function ψ is constant along any streamline. For $\psi = \text{constant}$, $d\psi = 0$ and

$$d\psi = \frac{\partial \psi}{\partial x} dx + \frac{\partial \psi}{\partial y} dy = 0$$

The slope of a streamline, which is a line of constant ψ , is given by

$$\left. \frac{dy}{dx} \right|_{\psi} = -\frac{\partial \psi / \partial x}{\partial \psi / \partial y} = -\frac{-v}{u} = \frac{v}{u} \quad (6.34)$$

Along a line of constant ϕ , $d\phi = 0$ and

$$d\phi = \frac{\partial \phi}{\partial x} dx + \frac{\partial \phi}{\partial y} dy = 0$$

Consequently, the slope of a potential line, which is a line of constant ϕ , is given by

$$\left. \frac{dy}{dx} \right|_{\phi} = -\frac{\partial \phi / \partial x}{\partial \phi / \partial y} = -\frac{u}{v} \quad (6.35)$$

The last equality of Eq. 6.35 follows from use of Eq. 6.29.

Comparing Eqs. 6.34 and 6.35, we see that the slope of a constant ψ line at any point is the negative reciprocal of the slope of the constant ϕ line at that point; this means that *lines of constant ψ and constant ϕ are orthogonal*. This property of potential lines and streamlines is useful in graphical analyses of flow fields. Example 6.10 shows how the velocity potential is computed from the stream function.

Example 6.10 VELOCITY POTENTIAL

Consider the flow field given by $\psi = ax^2 - ay^2$, where $a = 3 \text{ s}^{-1}$. Show that the flow is irrotational. Determine the velocity potential for this flow.

Given: Incompressible flow field with $\psi = ax^2 - ay^2$, where $a = 3 \text{ s}^{-1}$.

Find: (a) Whether or not the flow is irrotational.
(b) The velocity potential for this flow.

Solution: If the flow is irrotational, $\nabla^2 \psi = 0$. Checking for the given flow,

$$\nabla^2 \psi = \frac{\partial^2}{\partial x^2}(ax^2 - ay^2) + \frac{\partial^2}{\partial y^2}(ax^2 - ay^2) = 2a - 2a = 0$$

so that the flow is irrotational. As an alternative proof, we can compute the fluid particle rotation (in the xy plane, the only component of rotation is ω_z):

$$2\omega_z = \frac{\partial v}{\partial x} - \frac{\partial u}{\partial y} \quad \text{and} \quad u = \frac{\partial \psi}{\partial y} \quad v = -\frac{\partial \psi}{\partial x}$$

then

$$u = \frac{\partial}{\partial y}(ax^2 - ay^2) = -2ay \quad \text{and} \quad v = -\frac{\partial}{\partial x}(ax^2 - ay^2) = -2ax$$

so

$$2\omega_z = \frac{\partial v}{\partial x} - \frac{\partial u}{\partial y} = \frac{\partial}{\partial x}(-2ax) - \frac{\partial}{\partial y}(-2ay) = -2a + 2a = 0 \xrightarrow{2\omega_z}$$

Once again, we conclude that the flow is irrotational. Because it is irrotational, ϕ must exist, and

$$u = -\frac{\partial \phi}{\partial x} \quad \text{and} \quad v = -\frac{\partial \phi}{\partial y}$$

Consequently, $u = -\frac{\partial \phi}{\partial x} = -2ay$ and $\frac{\partial \phi}{\partial x} = 2ay$. Integrating with respect to x gives $\phi = 2axy + f(y)$, where $f(y)$ is an arbitrary function of y . Then

$$v = -2ax = -\frac{\partial \phi}{\partial y} = -\frac{\partial}{\partial x}[2axy + f(y)]$$

Therefore, $-2ax = -2ax - \frac{df(y)}{dy} = -2ax - \frac{df}{dy}$, so $\frac{df}{dy} = 0$ and $f = \text{constant}$. Thus

$$\phi = 2axy + \text{constant} \xrightarrow{\phi}$$

We also can show that lines of constant ψ and constant ϕ are orthogonal.

$$\psi = ax^2 - ay^2 \quad \text{and} \quad \phi = 2axy$$

For $\psi = \text{constant}$, $d\psi = 0 = 2axdx - 2aydy$; hence $\frac{dy}{dx}_{\psi=c} = \frac{x}{y}$

For $\phi = \text{constant}$, $d\phi = 0 = 2aydx + 2axdy$; hence $\frac{dy}{dx}_{\phi=c} = -\frac{y}{x}$

The slopes of lines of constant ϕ and constant ψ are negative reciprocals. Therefore lines of constant ϕ are orthogonal to lines of constant ψ .

This problem illustrates the relations among the stream function, velocity potential, and velocity field.

Elementary Plane Flows

The ψ and ϕ functions for the five elementary two-dimensional flows of a uniform flow, a source, a sink, a vortex, and a doublet are summarized in Table 6.2. The ψ and ϕ functions can be obtained from the velocity field for each elementary flow.

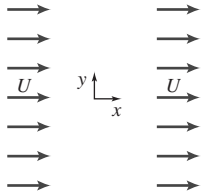
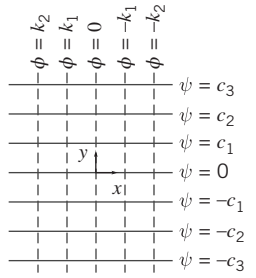
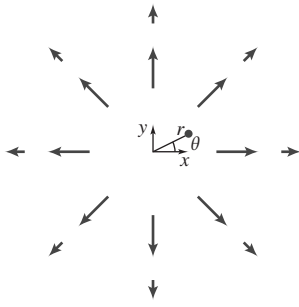
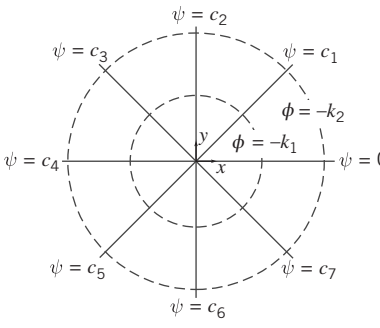
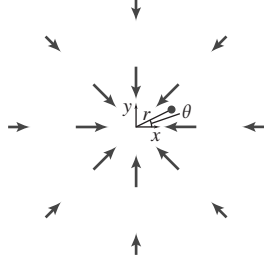
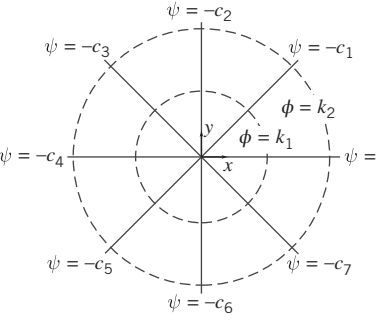
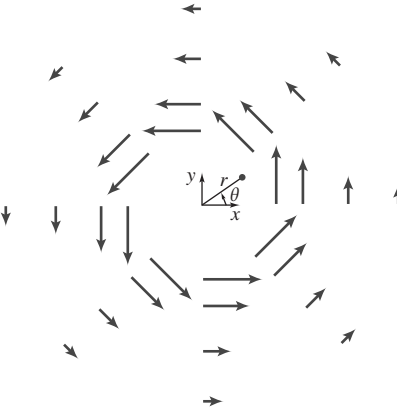
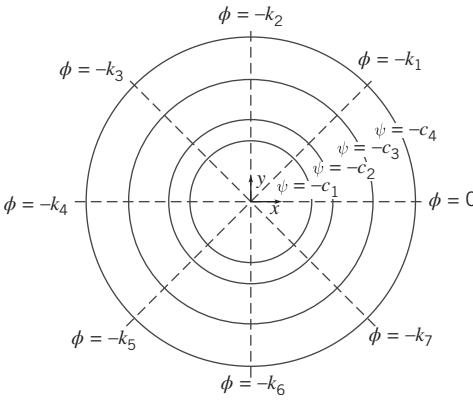
A *uniform flow* of constant velocity parallel to the x axis satisfies the continuity equation and the irrotationality condition identically. In Table 6.2 we have shown the ψ and ϕ functions for a uniform flow in the positive x direction.

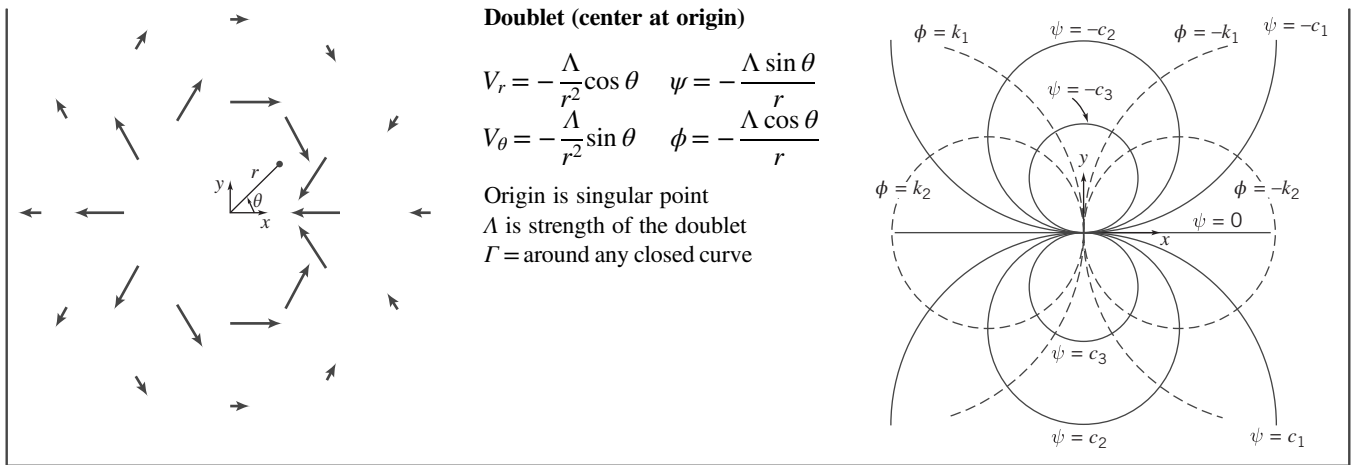
For a uniform flow of constant magnitude V , inclined at angle α to the x axis,

$$\begin{aligned} \psi &= (V \cos \alpha)y - (V \sin \alpha)x \\ \phi &= -(V \sin \alpha)y - (V \cos \alpha)x \end{aligned}$$

A simple *source* is a flow pattern in the xy plane in which flow is radially outward from the z axis and symmetrical in all directions. The strength, q , of the source is the volume flow rate per unit depth. At any radius, r , from a source, the tangential velocity, V_θ , is zero; the radial velocity, V_r , is the volume flow rate per unit depth, q , divided by the flow area per unit depth, $2\pi r$. Thus $V_r = q/2\pi r$ for a source. Knowing V_r and V_θ , obtaining ψ and ϕ from Eqs. 5.8 and 6.33, respectively, is straightforward.

Table 6.2
Elementary Plane Flows

 Uniform Flow (positive x direction) $u = U \quad \psi = Uy$ $v = 0 \quad \phi = -Ux$ $\Gamma = 0$ around any closed curve	
 Source Flow (from origin) $V_r = \frac{q}{2\pi r} \quad \psi = \frac{q}{2\pi} \theta$ $V_\theta = 0 \quad \phi = -\frac{q}{2\pi} \ln r$ Origin is singular point q is volume flow rate per unit depth $\Gamma = 0$ around any closed curve	
 Sink Flow (toward origin) $V_r = -\frac{q}{2\pi r} \quad \psi = -\frac{q}{2\pi} \theta$ $V_\theta = 0 \quad \phi = \frac{q}{2\pi} \ln r$ Origin is singular point q is volume flow rate per unit depth $\Gamma = 0$ around any closed curve	
 Irrotational Vortex (counterclockwise, center at origin) $V_r = 0 \quad \psi = -\frac{K}{2\pi} \ln r$ $V_\theta = \frac{K}{2\pi r} \quad \phi = -\frac{K}{2\pi} \theta$ Origin is singular point K is strength of the vortex $\Gamma = K$ around any closed curve enclosing origin $\Gamma = 0$ around any closed curve not enclosing origin	



In a simple *sink*, flow is radially inward; a sink is a negative source. The ψ and ϕ functions for a sink shown in Table 6.2 are the negatives of the corresponding functions for a source flow.

The origin of either a sink or a source is a singular point, since the radial velocity approaches infinity as the radius approaches zero. Thus, while an actual flow may resemble a source or a sink for some values of r , sources and sinks have no exact physical counterparts. The primary value of the concept of sources and sinks is that, when combined with other elementary flows, they produce flow patterns that adequately represent realistic flows.

A flow pattern in which the streamlines are concentric circles is a vortex. In a *free (irrotational) vortex*, fluid particles do not rotate as they translate in circular paths around the vortex center. There are a number of ways of obtaining the velocity field, for example, by combining the equation of motion (Euler's equation) and the Bernoulli equation to eliminate the pressure. Here, though, for circular streamlines, we have $V_r = 0$ and $V_\theta = f(\theta)$ only. We also have previously introduced the condition of irrotationality in cylindrical coordinates,

$$\frac{1}{r} \frac{\partial r V_\theta}{\partial r} - \frac{1}{r} \frac{\partial V_r}{\partial \theta} = 0 \quad (6.24)$$

Hence, using the known forms of V_r and V_θ , we obtain

$$\frac{1}{r} \frac{d(r V_\theta)}{dr} = 0$$

Integrating this equation gives

$$V_\theta r = \text{constant}$$

The strength, K , of the vortex is defined as $K = 2\pi r V_\theta$; the dimensions of K are L^2/t (volume flow rate per unit depth). Once again, knowing V_r and V_θ , obtaining ψ and ϕ from Eqs. 5.8 and 6.33, respectively, is straightforward. The irrotational vortex is a reasonable approximation to the flow field in a tornado except in the region of the origin, which is a singular point.

The final "elementary" flow listed in Table 6.2 is the *doublet* of strength Λ . This flow is produced mathematically by allowing a source and a sink of numerically equal strengths to merge. In the limit, as the distance, δs , between them approaches zero, their strengths increase so the product $q\delta s/2\pi$ tends to a finite value, Λ , which is termed the strength of the doublet.

Superposition of Elementary Plane Flows

We saw earlier that both ϕ and ψ satisfy Laplace's equation for flow that is both incompressible and irrotational. Since Laplace's equation is a linear, homogeneous partial differential equation, solutions may be superposed (added together) to develop more complex and interesting patterns of flow. Thus if ψ_1 and ψ_2 satisfy Laplace's equation, then so does $\psi_3 = \psi_1 + \psi_2$. The elementary plane flows are the building blocks in this superposition process. There is one note of caution: while Laplace's equation for the stream function, and the stream function-velocity field equations (Eq. 5.3) are linear, the Bernoulli

equation is not. Hence, in the superposition process we will have $\psi_3 = \psi_1 + \psi_2$, $u_3 = u_1 + u_2$, and $v_3 = v_1 + v_2$, but $p_3 \neq p_1 + p_2$. We must use the Bernoulli equation, which is nonlinear in V , to find p_3 .

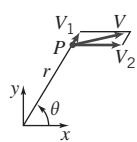
We can add together elementary flows to try and generate recognizable flow patterns. The simplest superposition approach is called the *direct* method, in which we try different combinations of elementary flows and see what kinds of flow patterns are produced. For example, look at some of the classic examples listed in Table 6.3. The source and uniform flow combination makes sense as we would intuitively expect a source to partially push its way upstream, and to divert the flow around it. The source, sink, and uniform flow (generating what is called a Rankine body) is also not surprising. The entire flow out of the source makes its way into the sink, leading to a closed streamline. *Any streamline can be interpreted as a solid surface because there is no flow across it*; we can therefore pretend that this closed streamline represents a solid. We could easily generalize this source-sink approach to any number of sources and sinks distributed along the x axis, and as long as the sum of the source and sink strengths added up to zero, we would generate a closed streamline body shape.

The doublet-uniform flow (with or without a vortex) generates a very interesting result: flow over a cylinder (with or without circulation). We first saw the flow without circulation in Fig. 2.12a. The flow with a clockwise vortex produces a top-to-bottom asymmetry. This is because in the region above the cylinder the velocities due to the uniform flow and vortex are in the same overall direction and lead to a high velocity; below the cylinder they are in opposite directions and therefore lead to a low velocity. As we have learned, whenever velocities are high, streamlines will be close together, and vice versa. More importantly, from the Bernoulli equation we know that whenever the velocity is high the pressure will be low, and vice versa. Hence, we can anticipate that the cylinder with circulation will experience a net upward force (lift) due to pressure. This approach, of looking at streamline patterns to see where we have regions of high or low velocity and hence low or high pressure, is very useful. We will examine these last two flows in Examples 6.11 and 6.12.

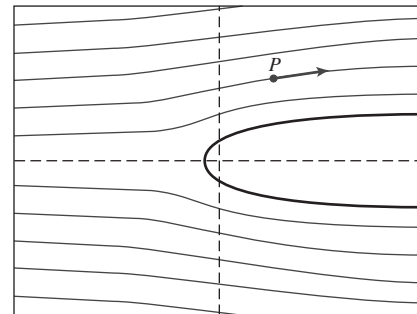
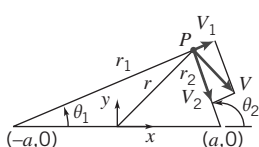
The last example in Table 6.3, the vortex pair, hints at a way to create flows that simulate the presence of a wall or walls: for the y axis to be a streamline (and thus a wall), simply make sure that any objects (e.g., a source, a vortex) in the positive x quadrants have mirror-image objects in the negative x quadrants; the y axis will thus be a line of symmetry. For a flow pattern in a 90° corner, we need to place objects so that we have symmetry with respect to both the x and y axes. For flow in a corner whose angle is a fraction of 90° (e.g., 30°), we need to place objects in a radially symmetric fashion.

Table 6.3

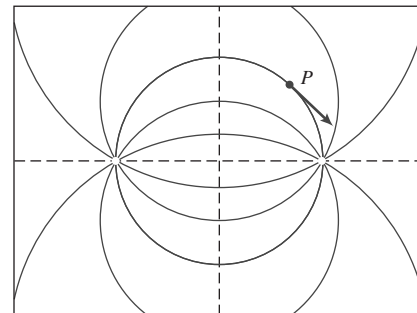
Superposition of Elementary Plane Flows

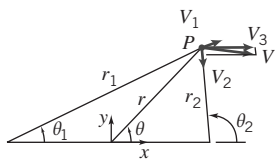
Source and Uniform Flow (flow past a half-body)

$$\begin{aligned}\psi &= \psi_{so} + \psi_{uf} = \psi_1 + \psi_2 = \frac{q}{2\pi}\theta + Uy \\ \psi &= \frac{q}{2\pi}\theta + Ur \sin\theta \\ \phi &= \phi_{so} + \phi_{uf} = \phi_1 + \phi_2 = -\frac{q}{2\pi}\ln r - Ux \\ \phi &= -\frac{q}{2\pi}\ln r - Ur \cos\theta\end{aligned}$$

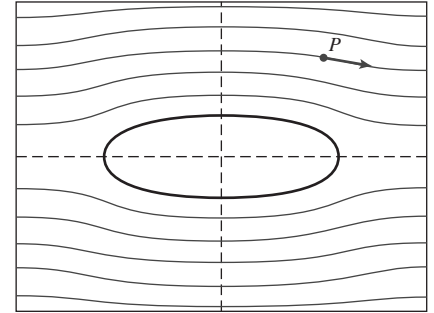
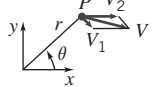
**Source and Sink (equal strength, separation distance on x axis = 2a)**

$$\begin{aligned}\psi &= \psi_{so} + \psi_{si} = \psi_1 + \psi_2 = \frac{q}{2\pi}\theta_1 - \frac{q}{2\pi}\theta_2 \\ \psi &= \frac{q}{2\pi}(\theta_1 - \theta_2) \\ \phi &= \phi_{so} + \phi_{si} = \phi_1 + \phi_2 = -\frac{q}{2\pi}\ln r_1 + \frac{q}{2\pi}\ln r_2 \\ \phi &= \frac{q}{2\pi}\ln \frac{r_2}{r_1}\end{aligned}$$

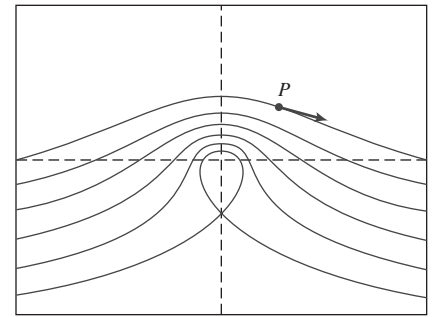
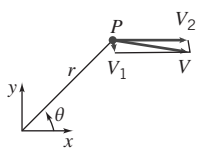


Source, Sink, and Uniform Flow (flow past a Rankine body)

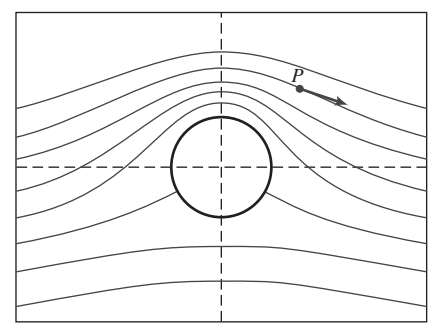
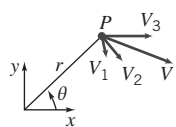
$$\begin{aligned}\psi &= \psi_{so} + \psi_{si} + \psi_{uf} = \psi_1 + \psi_2 + \psi_3 \\ &= \frac{q}{2\pi} \theta_1 - \frac{q}{2\pi} \theta_2 + Uy \\ \psi &= \frac{q}{2\pi} (\theta_1 - \theta_2) + Ur \sin \theta \\ \phi &= \phi_{so} + \phi_{si} + \phi_{uf} = \phi_1 + \phi_2 + \phi_3 \\ &= -\frac{q}{2\pi} \ln r_1 + \frac{q}{2\pi} \ln r_2 - Ux \\ \phi &= \frac{q}{2\pi} \ln \frac{r_2}{r_1} - Ur \cos \theta\end{aligned}$$

**Vortex (clockwise) and Uniform Flow**

$$\begin{aligned}\psi &= \psi_v + \psi_{uf} = \psi_1 + \psi_2 = \frac{K}{2\pi} \ln r + Uy \\ \psi &= \frac{K}{2\pi} \ln r + Ur \sin \theta \\ \phi &= \phi_v + \phi_{uf} = \phi_1 + \phi_2 = \frac{K}{2\pi} \theta - Ux \\ \phi &= \frac{K}{2\pi} \theta - Ur \cos \theta\end{aligned}$$

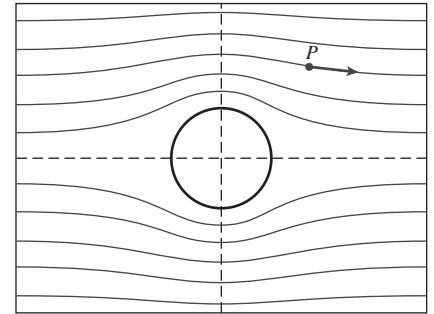
**Doublet and Uniform Flow (flow past a cylinder)**

$$\begin{aligned}\psi &= \psi_d + \psi_{uf} = \psi_1 + \psi_2 = -\frac{\Lambda \sin \theta}{r} + Uy \\ &= -\frac{\Lambda \sin \theta}{r} + Ur \sin \theta \\ \psi &= U \left(r - \frac{\Lambda}{Ur} \right) \sin \theta \\ \psi &= Ur \left(1 - \frac{a^2}{r^2} \right) \sin \theta \quad a = \sqrt{\frac{\Lambda}{U}} \\ \phi &= \phi_d + \phi_{uf} = \phi_1 + \phi_2 = -\frac{\Lambda \cos \theta}{r} - Ux \\ &= -\frac{\Lambda \cos \theta}{r} - Ur \cos \theta \\ \phi &= -U \left(r + \frac{\Lambda}{Ur} \right) \cos \theta = -Ur \left(1 + \frac{a^2}{r^2} \right) \cos \theta\end{aligned}$$

**Doublet, Vortex (clockwise), and Uniform Flow (flow past a cylinder with circulation)**

$$a = \sqrt{\frac{\Lambda}{U}}; K < 4\pi a U$$

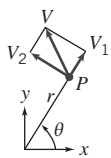
$$\begin{aligned}\psi &= \psi_d + \psi_v + \psi_{uf} = \psi_1 + \psi_2 + \psi_3 \\ &= -\frac{\Lambda \sin \theta}{r} + \frac{K}{2\pi} \ln r + Uy \\ \psi &= -\frac{\Lambda \sin \theta}{r} + \frac{K}{2\pi} \ln r + Ur \sin \theta \\ \psi &= Ur \left(1 - \frac{a^2}{r^2} \right) \sin \theta + \frac{K}{2\pi} \ln r \\ \phi &= \phi_d + \phi_v + \phi_{uf} = \phi_1 + \phi_2 + \phi_3 \\ &= -\frac{\Lambda \cos \theta}{r} + \frac{K}{2\pi} \theta - Ux \\ \phi &= -\frac{\Lambda \cos \theta}{r} + \frac{K}{2\pi} \theta - Ur \cos \theta \\ \phi &= -Ur \left(1 + \frac{a^2}{r^2} \right) \cos \theta + \frac{K}{2\pi} \theta\end{aligned}$$



(Continued)

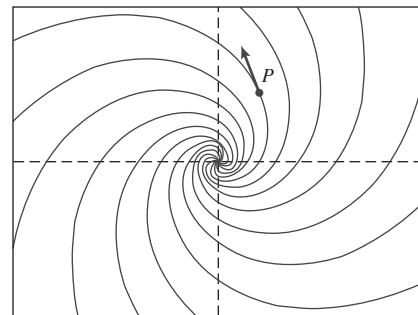
Table 6.3
Superposition of Elementary Plane Flows (Continued)

Source and Vortex (spiral vortex)

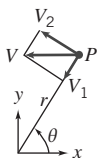


$$\psi = \psi_{so} + \psi_v = \psi_1 + \psi_2 = \frac{q}{2\pi} \theta - \frac{K}{2\pi} \ln r$$

$$\phi = \phi_{so} + \phi_v = \phi_1 + \phi_2 = -\frac{q}{2\pi} \ln r - \frac{K}{2\pi} \theta$$

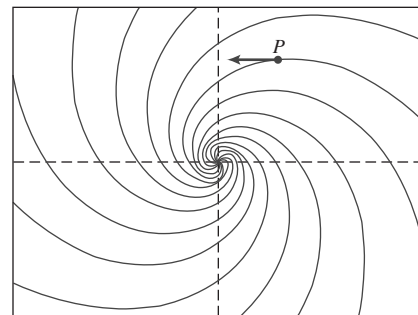


Sink and Vortex

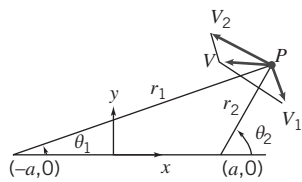


$$\psi = \psi_{si} + \psi_v = \psi_1 + \psi_2 = -\frac{q}{2\pi} \theta - \frac{K}{2\pi} \ln r$$

$$\phi = \phi_{si} + \phi_v = \phi_1 + \phi_2 = \frac{q}{2\pi} \ln r - \frac{K}{2\pi} \theta$$



Vortex Pair (equal strength, opposite rotation, separation distance on x axis = 2a)

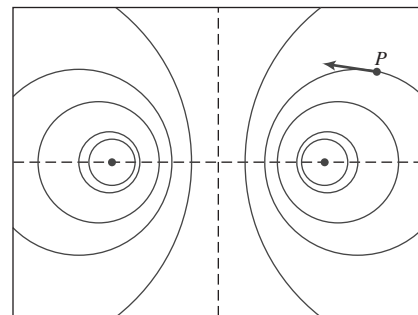


$$\psi = \psi_{v1} + \psi_{v2} = \psi_1 + \psi_2 = -\frac{K}{2\pi} \ln r_1 + \frac{K}{2\pi} \ln r_2$$

$$\psi = \frac{K}{2\pi} \ln \frac{r_2}{r_1}$$

$$\phi = \phi_{v1} + \phi_{v2} = \phi_1 + \phi_2 = -\frac{K}{2\pi} \theta_1 + \frac{K}{2\pi} \theta_2$$

$$\phi = \frac{K}{2\pi} (\theta_2 - \theta_1)$$



Example 6.11 FLOW OVER A CYLINDER: SUPERPOSITION OF DOUBLET AND UNIFORM FLOW

For two-dimensional, incompressible, irrotational flow, the superposition of a doublet and a uniform flow represents flow around a circular cylinder. Obtain the stream function and velocity potential for this flow pattern. Find the velocity field, locate the stagnation points and the cylinder surface, and obtain the surface pressure distribution. Integrate the pressure distribution to obtain the drag and lift forces on the circular cylinder.

Given: Two-dimensional, incompressible, irrotational flow formed from superposition of a doublet and a uniform flow.

- Find:**
- (a) Stream function and velocity potential.
 - (b) Velocity field.
 - (c) Stagnation points.
 - (d) Cylinder surface.
 - (e) Surface pressure distribution.
 - (f) Drag force on the circular cylinder.
 - (g) Lift force on the circular cylinder.

Solution: Stream functions may be added because the flow field is incompressible and irrotational. Thus from Table 6.2, the stream function for the combination is

$$\psi = \psi_d + \psi_{uf} = -\frac{\Lambda \sin \theta}{r} + Ur \sin \theta \xrightarrow{\quad} \psi$$

The velocity potential is

$$\phi = \phi_d + \phi_{uf} = -\frac{\Lambda \cos \theta}{r} - Ur \cos \theta \xrightarrow{\quad} \phi$$

The corresponding velocity components are obtained using Eqs. 6.30 as

$$V_r = -\frac{\partial \phi}{\partial r} = -\frac{\Lambda \cos \theta}{r^2} + U \cos \theta$$

$$V_\theta = -\frac{1}{r} \frac{\partial \phi}{\partial \theta} = -\frac{\Lambda \sin \theta}{r^2} - U \sin \theta$$

The velocity field is

$$\vec{V} = V_r \hat{e}_r + V_\theta \hat{e}_\theta = \left(-\frac{\Lambda \cos \theta}{r^2} + U \cos \theta \right) \hat{e}_r + \left(-\frac{\Lambda \sin \theta}{r^2} - U \sin \theta \right) \hat{e}_\theta \xrightarrow{\quad} \vec{V}$$

Stagnation points are where $\vec{V} = V_r \hat{e}_r + V_\theta \hat{e}_\theta = 0$

$$V_r = -\frac{\Lambda \cos \theta}{r^2} + U \cos \theta = \cos \theta \left(U - \frac{\Lambda}{r^2} \right)$$

Thus $V_r = 0$ when $r = \sqrt{\frac{\Lambda}{U}} = a$. Also,

$$V_\theta = -\frac{\Lambda \sin \theta}{r^2} - U \sin \theta = -\sin \theta \left(U + \frac{\Lambda}{r^2} \right)$$

Thus $V_\theta = 0$ when $\theta = 0, \pi$.

Stagnation points are $(r, \theta) = (a, 0), (a, \pi)$.

Stagnation points

Note that $V_r = 0$ along $r = a$, so this represents flow around a circular cylinder, as shown in Table 6.3. Flow is irrotational, so the Bernoulli equation may be applied between any two points. Applying the equation between a point far upstream and a point on the surface of the cylinder (neglecting elevation differences), we obtain

$$\frac{p_\infty}{\rho} + \frac{U^2}{2} = \frac{p}{\rho} + \frac{V^2}{2}$$

Thus,

$$p - p_\infty = \frac{1}{2} \rho (U^2 - V^2)$$

Along the surface, $r = a$, and

$$V^2 = V_\theta^2 = \left(-\frac{\Lambda}{a^2} - U \right)^2 \sin^2 \theta = 4U^2 \sin^2 \theta$$

since $\Lambda = Ua^2$. Substituting yields

$$p - p_\infty = \frac{1}{2} \rho (U^2 - 4U^2 \sin^2 \theta) = \frac{1}{2} \rho U^2 (1 - 4 \sin^2 \theta)$$

or

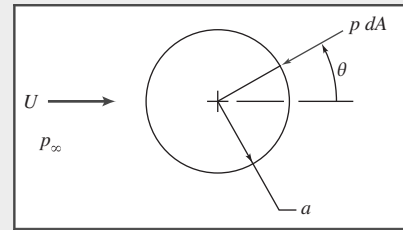
$$\frac{p - p_\infty}{\frac{1}{2} \rho U^2} = 1 - 4 \sin^2 \theta \xrightarrow{\quad} \text{Pressure distribution}$$

Drag is the force component parallel to the freestream flow direction. The drag force is given by

$$F_D = \int_A -p dA \cos \theta = \int_0^{2\pi} -pa d\theta b \cos \theta$$

since $dA = a d\theta b$, where b is the length of the cylinder normal to the diagram.

Substituting $p = p_\infty + \frac{1}{2}\rho U^2(1 - 4 \sin^2 \theta)$,



$$\begin{aligned} F_D &= \int_0^{2\pi} -p_\infty ab \cos \theta d\theta + \int_0^{2\pi} -\frac{1}{2}\rho U^2(1 - 4 \sin^2 \theta)ab \cos \theta d\theta \\ &= -p_\infty ab \sin \theta \Big|_0^{2\pi} - \frac{1}{2}\rho U^2 ab \sin \theta \Big|_0^{2\pi} + \frac{1}{2}\rho U^2 ab \frac{4}{3} \sin^3 \theta \Big|_0^{2\pi} \end{aligned}$$

$$F_D = 0 \xleftarrow{\quad} F_D$$

Lift is the force component normal to the freestream flow direction. (By convention, positive lift is an upward force.) The lift force is given by

$$F_L = \int_A p dA (-\sin \theta) = - \int_0^{2\pi} pa d\theta b \sin \theta$$

Substituting for p gives

$$\begin{aligned} F_L &= - \int_0^{2\pi} p_\infty ab \sin \theta d\theta - \int_0^{2\pi} \frac{1}{2}\rho U^2(1 - 4 \sin^2 \theta)ab \sin \theta d\theta \\ &= p_\infty ab \cos \theta \Big|_0^{2\pi} + \frac{1}{2}\rho U^2 ab \cos \theta \Big|_0^{2\pi} + \frac{1}{2}\rho U^2 ab \left[\frac{4 \cos^3 \theta}{3} - 4 \cos \theta \right]_0^{2\pi} \\ F_L &= 0 \xleftarrow{\quad} F_L \end{aligned}$$

This problem illustrates:

- How elementary plane flows can be combined to generate interesting and useful flow patterns.
- d'Alembert's paradox, that potential flows over a body do not generate drag.

Example 6.12 FLOW OVER A CYLINDER WITH CIRCULATION: SUPERPOSITION OF DOUBLET, UNIFORM FLOW, AND CLOCKWISE FREE VORTEX

For two-dimensional, incompressible, irrotational flow, the superposition of a doublet, a uniform flow, and a free vortex represents the flow around a circular cylinder with circulation. Obtain the stream function and velocity potential for this flow pattern, using a clockwise free vortex. Find the velocity field, locate the stagnation points and the cylinder surface, and obtain the surface pressure distribution. Integrate the pressure distribution to obtain the drag and lift forces on the circular cylinder. Relate the lift force on the cylinder to the circulation of the free vortex.

Given: Two-dimensional, incompressible, irrotational flow formed from superposition of a doublet, a uniform flow, and a clockwise free vortex.

Find: (a) Stream function and velocity potential.

- (b) Velocity field.
- (c) Stagnation points.
- (d) Cylinder surface.
- (e) Surface pressure distribution.
- (f) Drag force on the circular cylinder.
- (g) Lift force on the circular cylinder.
- (h) Lift force in terms of circulation of the free vortex.

Solution: Stream functions may be added because the flow field is incompressible and irrotational. From Table 6.2, the stream function and velocity potential for a clockwise free vortex are

$$\psi_{fv} = \frac{K}{2\pi} \ln r \quad \phi_{fv} = \frac{K}{2\pi} \theta$$

Using the results of Example 6.11, the stream function for the combination is

$$\begin{aligned} \psi &= \psi_d + \psi_{uf} + \psi_{fv} \\ \psi &= -\frac{\Lambda \sin \theta}{r} + Ur \sin \theta + \frac{K}{2\pi} \ln r \end{aligned} \quad \psi$$

The velocity potential for the combination is

$$\begin{aligned} \phi &= \phi_d + \phi_{uf} + \phi_{fv} \\ \phi &= -\frac{\Lambda \cos \theta}{r} - Ur \cos \theta + \frac{K}{2\pi} \theta \end{aligned} \quad \phi$$

The corresponding velocity components are obtained using Eqs. 6.30 as

$$V_r = -\frac{\partial \phi}{\partial r} = -\frac{\Lambda \cos \theta}{r^2} + U \cos \theta \quad (1)$$

$$V_\theta = -\frac{1}{r} \frac{\partial \phi}{\partial \theta} = -\frac{\Lambda \sin \theta}{r^2} - U \sin \theta - \frac{K}{2\pi r} \quad (2)$$

The velocity field is

$$\begin{aligned} \vec{V} &= V_r \hat{e}_r + V_\theta \hat{e}_\theta \\ \vec{V} &= \left(-\frac{\Lambda \cos \theta}{r^2} + U \cos \theta \right) \hat{e}_r + \left(-\frac{\Lambda \sin \theta}{r^2} - U \sin \theta - \frac{K}{2\pi r} \right) \hat{e}_\theta \end{aligned} \quad \vec{V}$$

Stagnation points are located where $\vec{V} = V_r \hat{e}_r + V_\theta \hat{e}_\theta = 0$. From Eq. 1,

$$V_r = -\frac{\Lambda \cos \theta}{r^2} + U \cos \theta = \cos \theta \left(U - \frac{\Lambda}{r^2} \right)$$

Thus $V_r = 0$ when $r = \sqrt{\Lambda/U} = a$ Cylinder surface

The stagnation points are located on $r = a$. Substituting into Eq. 2 with $r = a$,

$$\begin{aligned} V_\theta &= -\frac{\Lambda \sin \theta}{a^2} - U \sin \theta - \frac{K}{2\pi a} \\ &= -\frac{\Lambda \sin \theta}{\Lambda/U} - U \sin \theta - \frac{K}{2\pi a} \\ V_\theta &= -2U \sin \theta - \frac{K}{2\pi a} \end{aligned}$$

Thus $V_\theta = 0$ along $r = a$ when

$$\sin \theta = -\frac{K}{4\pi U a} \quad \text{or} \quad \theta = \sin^{-1} \left[\frac{-K}{4\pi U a} \right]$$

Stagnation points: $r = a \quad \theta = \sin^{-1} \left[\frac{-K}{4\pi U a} \right]$ Stagnation points

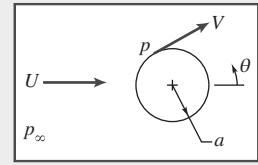
As in Example 6.11, $V_r = 0$ along $r = a$, so this flow field once again represents flow around a circular cylinder, as shown in Table 6.3. For $K = 0$ the solution is identical to that of Example 6.11.

The presence of the free vortex ($K > 0$) moves the stagnation points below the center of the cylinder. Thus the free vortex alters the vertical symmetry of the flow field. The flow field has two stagnation points for a range of vortex strengths between $K = 0$ and $K = 4\pi U a$.

A single stagnation point is located at $\theta = -\pi/2$ when $K = 4\pi U a$.

Even with the free vortex present, the flow field is irrotational, so the Bernoulli equation may be applied between any two points. Applying the equation between a point far upstream and a point on the surface of the cylinder we obtain

$$\frac{p_\infty}{\rho} + \frac{U^2}{2} + g z = \frac{p}{\rho} + \frac{V^2}{2} + gz$$



Thus, neglecting elevation differences,

$$p - p_\infty = \frac{1}{2}\rho(U^2 - V^2) = \frac{1}{2}\rho U^2 \left[1 - \left(\frac{U}{V} \right)^2 \right]$$

Along the surface $r=a$ and $V_r=0$, so

$$V^2 = V_\theta^2 = \left(-2U \sin \theta - \frac{K}{2\pi a} \right)^2$$

and

$$\left(\frac{V}{U} \right)^2 = 4 \sin^2 \theta + \frac{2K}{\pi U a} \sin \theta + \frac{K^2}{4\pi^2 U^2 a^2}$$

Thus

$$p = p_\infty + \frac{1}{2}\rho U^2 \left(1 - 4 \sin^2 \theta - \frac{2K}{\pi U a} \sin \theta - \frac{K^2}{4\pi^2 U^2 a^2} \right) \xrightarrow{\hspace{10cm}} p(\theta)$$

Drag is the force component parallel to the freestream flow direction. As in Example 6.11, the drag force is given by

$$F_D = \int_A -p dA \cos \theta = \int_0^{2\pi} -pa d\theta b \cos \theta$$

since $dA = a d\theta b$, where b is the length of the cylinder normal to the diagram.

Comparing pressure distributions, the free vortex contributes only to the terms containing the factor K . The contribution of these terms to the drag force is

$$\frac{F_{D_{fv}}}{\frac{1}{2}\rho U^2} = \int_0^{2\pi} \left(\frac{2K}{\pi U a} \sin \theta + \frac{K^2}{4\pi^2 U^2 a^2} \right) ab \cos \theta d\theta \quad (3)$$

$$\frac{F_{D_{fv}}}{\frac{1}{2}\rho U^2} = \frac{2K}{\pi U a} ab \left[\frac{\sin^2 \theta}{2} \right]_0^{2\pi} + \frac{K^2}{4\pi^2 U^2 a^2} ab \left[\sin \theta \right]_0^{2\pi} = 0 \quad \xrightarrow{\hspace{10cm}} F_D$$

Lift is the force component normal to the freestream flow direction. (Upward force is defined as positive lift.) The lift force is given by

$$F_L = \int_A -p dA \sin \theta = \int_0^{2\pi} -pa d\theta b \sin \theta$$

Comparing pressure distributions, the free vortex contributes only to the terms containing the factor K . The contribution of these terms to the lift force is

$$\begin{aligned} \frac{F_{L_{fv}}}{\frac{1}{2}\rho U^2} &= \int_0^{2\pi} \left(\frac{2K}{\pi U a} \sin \theta + \frac{K^2}{4\pi^2 U^2 a^2} \right) ab \sin \theta d\theta \\ &= \frac{2K}{\pi U a} \int_0^{2\pi} ab \sin^2 \theta d\theta + \frac{K^2}{4\pi^2 U^2 a^2} \int_0^{2\pi} ab \sin \theta d\theta \\ &= \frac{2Kb}{\pi U} \left[\frac{\theta}{2} - \frac{\sin^2 \theta}{4} \right]_0^{2\pi} - \frac{K^2 b}{4\pi^2 U^2 a} \cos \theta \Big|_0^{2\pi} \\ \frac{F_{L_{fv}}}{\frac{1}{2}\rho U^2} &= \frac{2Kb}{\pi U} \left[\frac{2\pi}{2} \right] = \frac{2Kb}{U} \end{aligned}$$

Then $F_{L_{f_0}} = \rho UKb$

F_L

The circulation is defined by Eq. 5.18 as

$$\Gamma \equiv \oint \vec{V} \cdot d\vec{s}$$

On the cylinder surface, $r=a$, and $\vec{V} = V_\theta \hat{e}_\theta$, so

$$\begin{aligned}\Gamma &= \int_0^{2\pi} \left(-2U \sin \theta - \frac{K}{2\pi a} \right) \hat{e}_\theta \cdot a \, d\theta \, \hat{e}_\theta \\ &= - \int_0^{2\pi} 2Ua \sin \theta \, d\theta - \int_0^{2\pi} \frac{K}{2\pi} \, d\theta \\ \Gamma &= -K\end{aligned}\quad \text{Circulation}$$

Substituting into the expression for lift,

$$F_L = \rho UKb = \rho U(-\Gamma)b = -\rho U \Gamma b$$

or the lift force per unit length of cylinder is

$$\frac{F_L}{b} = -\rho U \Gamma$$

This problem illustrates:

- Once again d'Alembert's paradox, that potential flows do not generate drag on a body.
- That the lift per unit length is $-\rho U \Gamma$. It turns out that this expression for lift is the same for all bodies in an ideal fluid flow, regardless of shape!

Because Laplace's equation appears in many engineering and physics applications, it has been extensively studied. For analytic solutions, one approach is to use conformal mapping with complex notation. It turns out that any continuous complex function $f(z)$ (where $z=x+iy$, and $i=\sqrt{-1}$) is a solution of Laplace's equation, and can therefore represent both ϕ and ψ . With this approach many elegant mathematical results have been derived [4–7]. We mention only two: the circle theorem, which enables any given flow [e.g., from a source at some point (a,b)] to be easily transformed to allow for the presence of a cylinder at the origin, and the Schwarz-Christoffel theorem, which enables a given flow to be transformed to allow for the presence of virtually unlimited stepwise linear boundaries (e.g., the presence on the x axis of the silhouette of a building).

Much of this analytical work was done centuries ago, when it was called “hydrodynamics” instead of potential theory. A list of famous contributors includes Bernoulli, Lagrange, d’Alembert, Cauchy, Rankine, and Euler [8]. As we discussed in Section 2.6, the theory immediately ran into difficulties: in an ideal fluid flow no body experiences drag, termed the d’Alembert paradox of 1752. Prandtl, in 1904, resolved this discrepancy by describing how real flows may be essentially inviscid almost everywhere, but there is always a “boundary layer” adjacent to the body. In this layer significant viscous effects occur, and the no-slip condition is satisfied. In potential flow theory the no-slip condition is not satisfied. We will study boundary layers in detail in Chapter 9, where we will see that their existence leads to drag on bodies, and also affects the lift of bodies.

An alternative superposition approach is the *inverse* method in which distributions of objects such as sources, sinks, and vortices are used to model a body [9]. It is called inverse because the body shape is deduced based on a desired pressure distribution. Both the direct and inverse methods, including three-dimensional space, are today mostly analyzed using Computational Fluid Dynamics software.

6.7 Summary and Useful Equations

In this chapter we have:

- ✓ Derived Euler's equations in vector form and in rectangular, cylindrical, and streamline coordinates.
- ✓ Obtained Bernoulli's equation by integrating Euler's equation along a steady-flow streamline, and discussed its restrictions. We have also seen how for a steady, incompressible flow through a stream tube the first law of thermodynamics reduces to the Bernoulli equation if certain restrictions apply.
- ✓ Defined the static, dynamic, and stagnation (or total) pressures.
- ✓ Defined the energy and hydraulic grade lines.
- ✓ Derived an unsteady flow Bernoulli equation, and discussed its restrictions.
- ✓ Observed that for an irrotational flow that is steady and incompressible, the Bernoulli equation applies between *any* two points in the flow.
- ✓ Defined the velocity potential ϕ and discussed its restrictions.

We have also explored in detail two-dimensional, incompressible, and irrotational flows, and learned that for these flows: the stream function ψ and the velocity potential ϕ satisfy Laplace's equation; ψ and ϕ can be derived from the velocity components, and vice versa, and the iso-lines of the stream function ψ and the velocity potential ϕ are orthogonal. We explored for such flows how to combine potential flows to generate various flow patterns, and how to determine the pressure distribution and lift and drag on, for example, a cylindrical shape.

Note: Most of the equations in the table below have a number of constraints or limitations—*be sure to refer to their page numbers for details!*

Useful Equations

The Euler equation for incompressible, inviscid flow:	$\rho \frac{D\vec{V}}{Dt} = \rho \vec{g} - \nabla p$	(6.1)	Page 163
The Euler equation (rectangular coordinates):	$\rho \left(\frac{\partial u}{\partial t} + u \frac{\partial u}{\partial x} + v \frac{\partial u}{\partial y} + w \frac{\partial u}{\partial z} \right) = \rho g_x - \frac{\partial p}{\partial x}$ $\rho \left(\frac{\partial v}{\partial t} + u \frac{\partial v}{\partial x} + v \frac{\partial v}{\partial y} + w \frac{\partial v}{\partial z} \right) = \rho g_y - \frac{\partial p}{\partial y}$ $\rho \left(\frac{\partial w}{\partial t} + u \frac{\partial w}{\partial x} + v \frac{\partial w}{\partial y} + w \frac{\partial w}{\partial z} \right) = \rho g_z - \frac{\partial p}{\partial z}$	(6.2a) (6.2b) (6.2c)	Page 163
The Euler equation (cylindrical coordinates):	$\rho a_r = \rho \left(\frac{\partial V_r}{\partial t} + V_r \frac{\partial V_r}{\partial r} + \frac{V_\theta}{r} \frac{\partial V_r}{\partial \theta} + V_z \frac{\partial V_r}{\partial z} - \frac{V_\theta^2}{r} \right) = \rho g_r - \frac{\partial p}{\partial r}$ $\rho a_\theta = \rho \left(\frac{\partial V_\theta}{\partial t} + V_r \frac{\partial V_\theta}{\partial r} + \frac{V_\theta}{r} \frac{\partial V_\theta}{\partial \theta} + V_z \frac{\partial V_\theta}{\partial z} + \frac{V_r V_\theta}{r} \right) = \rho g_\theta - \frac{1}{r} \frac{\partial p}{\partial \theta}$ $\rho a_z = \rho \left(\frac{\partial V_z}{\partial t} + V_r \frac{\partial V_z}{\partial r} + \frac{V_\theta}{r} \frac{\partial V_z}{\partial \theta} + V_z \frac{\partial V_z}{\partial z} \right) = \rho g_z - \frac{\partial p}{\partial z}$	(6.3a) (6.3b) (6.3c)	Page 163 Page 164 Page 164
The Bernoulli equation (steady, incompressible, inviscid, along a streamline):	$\frac{p}{\rho} + \frac{V^2}{2} + gz = \text{constant}$	(6.8)	Page 167
Definition of total head of a flow:	$\frac{p}{\rho g} + \frac{V^2}{2g} + z = H$	(6.16a)	Page 181

Table (Continued)

Definition of energy grade line (EGL):	$EGL = \frac{p}{\rho g} + \frac{V^2}{2g} + z$	(6.16b)	Page 181
Definition of hydraulic grade line (HGL):	$HGL = \frac{p}{\rho g} + z$	(6.16c)	Page 181
Relation between EGL, HGL, and dynamic pressure:	$EGL - HGL = \frac{V^2}{2g}$	(6.16d)	Page 182
Definition of stream function (2D, incompressible flow):	$u = \frac{\partial \psi}{\partial y} \quad v = -\frac{\partial \psi}{\partial x}$	(5.4)	Page 187
Definition of velocity potential (2D irrotational flow):	$u = -\frac{\partial \phi}{\partial x} \quad v = -\frac{\partial \phi}{\partial y}$	(6.29)	Page 187
Definition of stream function (2D, incompressible flow, cylindrical coordinates):	$V_r = \frac{1}{r} \frac{\partial \psi}{\partial \theta} \quad \text{and} \quad V_\theta = -\frac{\partial \psi}{\partial r}$	(5.8)	Page 187
Definition of velocity potential (2D irrotational flow, cylindrical coordinates):	$V_r = -\frac{\partial \phi}{\partial r} \quad \text{and} \quad V_\theta = -\frac{1}{r} \frac{\partial \phi}{\partial \theta}$	(6.33)	Page 187

REFERENCES

1. Shaw, R., "The Influence of Hole Dimensions on Static Pressure Measurements," *J. Fluid Mech.*, 7, Part 4, April 1960, pp. 550–564.
2. Chue, S. H., "Pressure Probes for Fluid Measurement," *Progress in Aerospace Science*, 16, 2, 1975, pp. 147–223.
3. United Sensor Corporation, 3 Northern Blvd., Amherst, NH 03031.
4. Lamb, H., *Hydrodynamics*. New York: Dover, 1945.
5. Milne-Thomson, L. M., *Theoretical Hydrodynamics*, 4th ed. New York: Macmillan, 1960.
6. Karamcheti, K., *Principles of Ideal-Fluid Aerodynamics*. New York: Wiley, 1966.
7. Kirchhoff, R. H., *Potential Flows: Computer Graphic Solutions*. New York: Marcel Dekker, 1985.
8. Rouse, H., and S. Ince, *History of Hydraulics*. New York: Dover, 1957.
9. Kuethe, A. M., and C.-Y. Chow, *Foundations of Aerodynamics: Bases of Aerodynamic Design*, 4th ed. New York: Wiley, 1986.

Chapter 7 Problems

Nondimensionalizing the Basic Differential Equations

7.1 The slope of the height h of a surface wave moving in a shallow pool of liquid is related to the speed of the wave u and gravity g by the equation

$$\frac{\partial h}{\partial x} = -\frac{u}{g} \frac{\partial u}{\partial x}$$

Use a length scale L and a velocity scale V_0 to put the equation in nondimensional terms and obtain the dimensionless groups that characterize the situation.

7.2 One-dimensional unsteady flow in a thin liquid layer is described by the equation

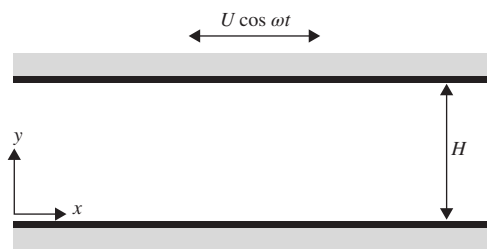
$$\frac{\partial u}{\partial t} + u \frac{\partial u}{\partial x} = -g \frac{\partial h}{\partial x}$$

Use a length scale, L , and a velocity scale, V_0 , to nondimensionalize this equation. Obtain the dimensionless groups that characterize this flow.

7.3 Fluid fills the space between two parallel plates. The differential equation that describes the instantaneous fluid velocity for unsteady flow with the fluid moving parallel to the walls is

$$\rho \frac{\partial u}{\partial t} = \mu \frac{\partial^2 u}{\partial y^2}$$

The lower plate is stationary and the upper plate oscillates in the x -direction with a frequency ω and an amplitude in the plate velocity of U . Use the characteristic dimensions to normalize the differential equation and obtain the dimensionless groups that characterize the flow.



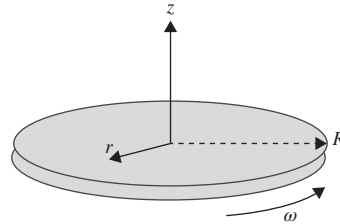
P7.3

7.4 Consider a disk of radius R rotating in an incompressible fluid at a speed ω . The equations that describe the boundary layer on the disk are:

$$\frac{1}{r} \left(\frac{\partial(rv_r)}{\partial r} \right) + \frac{\partial v_z}{\partial z} = 0$$

$$\rho \left(v_r \frac{\partial v_r}{\partial r} - \frac{v_\theta^2}{r} + v_z \frac{\partial v_r}{\partial z} \right) = \mu \frac{\partial^2 v_r}{\partial z^2}$$

Use the characteristic dimensions to normalize the differential equation and obtain the dimensionless groups that characterize the flow.



P7.4

7.5 The transient temperature change T in a plane wall of thickness L is given by the differential equation

$$\frac{\partial^2 T}{\partial x^2} = \frac{1}{\alpha} \frac{\partial T}{\partial t}$$

Where α is the thermal diffusivity with units of $L^2 t^{-1}$. Determine the nondimensional groups that characterize the situation for a plane wall with a fixed temperature at T_L at $x = L$ and a periodic surface temperature variation at $x = 0$ given by $(T - T_L) = (T_0 - T_L) \cos \omega t$ where ω is the frequency of the oscillation and T_0 is a temperature higher than T_L . Nondimensional temperature parameters use a temperature difference rather than temperature alone. The reference value of time comes from nondimensionalizing the boundary condition.

Buckingham Pi Theorem

7.6 Experiments on flow through an orifice plate of diameter d mounted in a length of pipe of diameter D show that the pressure drop is a function of the orifice diameter, pipe diameter, fluid velocity, and fluid density and viscosity. Determine the dimensionless parameters that represent this situation.

7.7 The speed, V , of a free-surface wave in shallow liquid is a function of depth, D , density, ρ , gravity, g , and surface tension, σ . Use dimensional analysis to find the functional dependence of V on the other variables. Express V in the simplest form possible.

7.8 The speed, V , of a free-surface gravity wave in deep water is a function of wavelength, λ , depth, D , density, ρ , and acceleration of gravity, g . Use dimensional analysis to find the functional dependence of V on the other variables. Express V in the simplest form possible.

7.9 Experiments have shown that axial thrust exerted by a propeller depends on the forward speed of the ship, angular speed and size of the propeller, and viscosity and density of the fluid. Determine the dimensionless representation of the situation. Determine how the expression would change if gravity were also a relevant variable.

7.10 A weir is a submerged gate extending across the width of a channel in which water is flowing. The depth of the water upstream of the weir can be used to determine the flow rate. Assume that the volume flow depends on the upstream depth, channel width, and gravity to find the nondimensional parameters for this situation and determine the dependency of flow rate on the other variables.

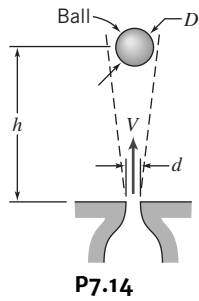
SS

7.11 A circular disk of diameter d and of negligible thickness is rotated at a constant angular speed, ω , in a cylindrical casing filled with a liquid of viscosity μ and density ρ . The casing has an internal diameter D , and there is a clearance y between the surfaces of disk and casing. Derive an expression for the torque required to maintain this speed if it depends only on the foregoing variables.

SS 7.12 Derive relation for the dependency of the frictional torque exerted on a journal of a bearing. The torque depends on the diameters of the journal and bearing, the length of the bearing, the angular speed of the journal, the transverse load (force), and the viscosity of the lubricant.

7.13 The power, \mathcal{P} , required to drive a fan is believed to depend on fluid density, ρ , volume flow rate, Q , impeller diameter, D , and angular velocity, ω . Use dimensional analysis to determine the dependence of \mathcal{P} on the other variables.

SS 7.14 A ball is suspended in an air jet in a stable position as shown in the figure. Experiments show that the equilibrium height of the ball is found to depend on the ball diameter and weight, jet diameter and velocity, and the air density and viscosity. Determine the dimensionless parameters that characterize this experiment.



P7.14

7.15 A large tank of liquid under pressure is drained through a smoothly contoured nozzle of area A . The mass flow rate is thought to depend on nozzle area, A , liquid density, ρ , difference in height between the liquid surface and nozzle, h , tank gage pressure, Δp , and gravitational acceleration, g . Determine how many independent Π parameters can be formed for this problem. Find the dimensionless parameters. State the functional relationship for the mass flow rate in terms of the dimensionless parameters.

7.16 Spin plays an important role in the flight trajectory of golf, ping-pong, and tennis balls. Therefore, it is important to know the rate at which spin decreases for a ball in flight. The aerodynamic torque, T , acting on a ball in flight, is thought to depend on flight speed, V , air density, ρ , air viscosity, μ , ball diameter, D , spin rate (angular speed), ω , and diameter of the dimples on the ball, d . Determine the dimensionless parameters that result.

SS 7.17 The rate $\frac{dT}{dt}$ at which the temperature T at the center of a rice kernel falls during cooking is critical, as too high a value leads to cracking of the kernel and too low a value makes the process slow and costly. The cooling rate depends on the rice specific heat, c , thermal conductivity, k , and size, L , the cooling air flow specific heat, c_p , density, ρ , viscosity, μ , and speed, V . Determine the dimensionless parameters for this problem.

7.18 There are various applications such as the freezing of food, combustion of small particles, or some chemical reactions in which a fluid flows through a matrix of particles, called a fluidized bed. The fluid pressure drop is a function of the diameter of the particles d , the

flow length of the bed L , the fluid velocity V , fluid density ρ , and fluid viscosity μ . Use dimensional analysis to find the functional dependence of pressure drop on the other variables.

7.19 The summer water flow rate in the Wisconsin River is 6,000 cfs. At the Highway 23 bridge, the river is 150 ft wide and an average of 8 ft deep. The relevant dimensionless groups are the Reynolds number (based on river depth), Froude number, and Weber number. Compute these parameters for the river.

7.20 The pressure drop in air-conditioning ducts is an important factor in performance. For a circular 4 ft diameter duct carrying 1,000 cfm of air at 55°F, the design pressure drop is 0.1 in. of water per 100 ft of length. Compute the value of the relevant dimensionless parameters [pressure coefficient and Reynolds number] for a duct.

Flow Similarity and Model Studies

7.21 A drone is designed to operate at 20 m/s in air at standard conditions. A model is constructed to 1:20 scale and tested in a variable-pressure wind tunnel at the same air temperature to determine the drag on the drone. Determine the groups necessary to obtain dynamic similarity. Determine the wind tunnel pressure necessary for model tests at 75 m/s. Determine drag of the prototype if the measured model drag force is 250 N.

7.22 A flat plate 1.5 m long and 0.3 m wide is towed at 3 m/s in a towing basin containing water at 20°C. The measured drag force is 14 N. Calculate the dimensions of a similar plate that will yield dynamically similar conditions in an airstream at a velocity of 18 m/s, 101.4 kPa, and 15°C. Determine the expected drag force plate in the air stream.

7.23 A 1:3 scale model of a torpedo is tested in a wind tunnel to determine the drag force. The prototype operates in water at 28 m/s. It has a diameter of 533 mm and is 6.7 m long. The maximum wind tunnel speed is 110 m/s but the air pressure can be varied. The air temperature is constant at 20°C. Determine the air pressure in the wind tunnel necessary to achieve a dynamically similar test. At these conditions, the drag force on the model is measured as 618 N. Determine the drag force expected on the full-scale torpedo.

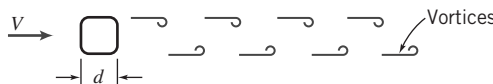
7.24 A flow rate of 0.18 m³/s of water at 20°C discharges from a 0.3 m pipe through a 0.15 m nozzle into the atmosphere. The axial force component exerted by water on the nozzle is 3 kN. Determine the corresponding force exerted on a 4:1 prototype of nozzle and pipe discharging 1:13 m³/s of air at 101.4 kPa and 15°C to the atmosphere.

7.25 An airplane wing, with chord length of 1.5 m and span of 9 m is designed to move through standard air at a speed of 7.5 m/s. A 1:10 scale model of this wing is to be tested in a water tunnel. Determine the speed necessary in the water tunnel to achieve dynamic similarity. Determine the ratio of forces measured in the model flow to those on the prototype wing.

7.26 A model hydrofoil is to be tested at 1:20 scale. The test speed is chosen to duplicate the Froude number corresponding to the 60-knot prototype speed in 45°F water. To model cavitation correctly, the cavitation number also must be duplicated. Determine the ambient pressure at which the tests must be run. The water in the model test basin can be heated to 130°F.

7.27 In some speed ranges, vortices are shed from the rear of bluff cylinders placed across a flow. The vortices alternately leave the top and bottom of the cylinder, as shown, causing an alternating force normal to the freestream velocity. The vortex shedding frequency, f , is thought to depend on ρ , d , V , and μ . Use dimensional analysis to develop a functional relationship for f . Vortex shedding occurs in

standard air on two cylinders with a diameter ratio of 2. Determine the velocity ratio for dynamic similarity, and the ratio of vortex shedding frequencies.



P7.27

7.28 A 0.25 mm diameter sphere with a specific gravity of 5.54 is dropped in water at 25°C and attains a constant velocity of 0.07 m/s. Determine the specific gravity a 2.5 mm diameter sphere dropped in crude oil at 25°C must have so that the two flows will be dynamically similar at terminal velocity.

7.29 A 150 mm artillery projectile that travels at 600 m/s through still air at 30°C and air pressure of 101.4 kPa is to be modeled in a high-speed wind tunnel with a 1:6 scale model. The wind tunnel air has a temperature of -18°C and a pressure of 68.9 kPa. Determine the velocity required for dynamic similarity. Determine the drag force on the prototype for a drag force on the model of 35 N.

7.30 A 1:50-scale model of a submarine is to be tested in a towing tank under two conditions: motion at the free surface and motion far below the surface. The tests are performed in freshwater. On the surface, the submarine cruises at 24 knots. Determine the speed the model should be towed to ensure dynamic similarity. The sub cruises at 0.35 knot below the surface. Determine the speed should the model should be towed to ensure dynamic similarity under the surface. Determine the factor the drag of the model needs to be multiplied by under each condition to give the drag of the full scale submarine.

SS 7.31 The power, \mathcal{P} , required to drive a fan is depends on fluid density ρ , volume flow rate Q , impeller diameter D , and angular speed ω . A fan with a diameter of 8 in. rotating at 2500 rpm delivers 15 ft³/s of air. Determine the diameter of a geometrically and dynamically similar fan rotating at 1800 rpm that delivers 88 ft³/s of air.

7.32 Over a certain range of air speeds, V , the lift, F_L , produced by a model of a complete aircraft in a wind tunnel depends on the air speed, air density, ρ , and a characteristic length (the wing base chord length, $c = 150$ mm). The following experimental data is obtained for air at standard atmospheric conditions:

V (m/s)	10	15	20	25	30	35	40	45	50
F_L (N)	2.2	4.8	8.7	13.3	19.6	26.5	34.5	43.8	54

Plot the lift as a function of the air speed. Determine the lift coefficient defined as $C_L = \frac{F_L}{\frac{1}{2} \rho V^2 c^2}$ and plot the lift coefficient as a function of

air speed. The prototype has a wing base chord length of 5 m. Determine the lift produced by the prototype over a speed range of 75 m/s to 250 m/s.

7.33 An axial-flow pump is required to deliver 0.75 m³/s of water at a head of 15 J/kg. The diameter of the rotor is 0.25 m, and it is to be driven at 500 rpm. The prototype is to be modeled on a small test apparatus having a 2.25 kW, 1000 rpm power supply. For similar performance between the prototype and the model, calculate the head, volume flow rate, and diameter of the model.

7.34 A model propeller 1 m in diameter is tested in a wind tunnel. Air approaches the propeller at 50 m/s when it rotates at 1800 rpm. The thrust and torque measured under these conditions are 100 N and 10 N·m, respectively. A prototype eight times as large as the model is to be built. At a dynamically similar operating point, the approach air speed is to be 130 m/s. Calculate the speed, thrust, and torque of the prototype propeller under these conditions, neglecting the effect of viscosity but including density.

7.35 A 1:16 model of a bus is tested in a wind tunnel in standard air. The model is 152 mm wide, 200 mm high, and 762 mm long. The measured drag force at 26.5 m/s wind speed is 6.09 N. The longitudinal pressure gradient in the wind tunnel test section is -11.8 N/m²/m. Estimate the correction that should be made to the measured drag force to correct for horizontal buoyancy caused by the pressure gradient in the test section. Calculate the drag coefficient for the model. Evaluate the aerodynamic drag force on the prototype at 100 km/hr on a calm day.

7.36 Tests on the established flow of six different liquids in smooth pipes of various sizes yield the following data:

Diameter mm	Velocity m/s	Viscosity mPa·s	Density kg/m ³	Wall Shear Pa
300	2.26	862.0	1247	51.2
250	2.47	431.0	1031	33.5
150	1.22	84.3	907	5.41
100	1.39	44.0	938	9.67
50	0.20	1.5	861	0.162
25	0.36	1.0	1000	0.517

Make a dimensional analysis of this problem and a plot of the resulting dimensionless numbers as ordinate and abscissa. Describe the plot and draw some conclusions.

CHAPTER 7

Dimensional Analysis and Similitude

- 7.1 Nondimensionalizing the Basic Differential Equations
- 7.2 Buckingham Pi Theorem
- 7.3 Significant Dimensionless Groups in Fluid Mechanics

- 7.4 Flow Similarity and Model Studies
- 7.5 Summary and Useful Equations

Case Study

Performance in a bicycle race such as the Tour de France depends on both the bicycle and the rider. The rider needs to overcome the aerodynamic force of the wind and the friction forces of the tires and bearings, and at race speeds, the force to move against the surrounding air predominates. A great deal of attention has been paid to improving the aerodynamics of the bicycle. As shown in the picture, the bicycle and rider are very streamlined in an effort to reduce the aerodynamic drag as much as possible.

One way to evaluate the effect on drag of modifying a bicycle is to test the full-scale bicycle and rider in a wind tunnel. This requires a facility large enough to accommodate both without aerodynamic interference from the walls. As we will learn in this chapter, it is feasible to perform testing on a model of the bicycle and then scale the results up to the full-size system. The approach of *dimensional analysis* allows models to be tested and the results scaled to accurately predict the effect of changes on the full-size bicycle.

A large number of improvements have been made to bicycles that reduce drag and make riding faster with less effort. Some of these are sweeping the handle bars forward, eliminating the crossbar, tapering the seat post and all other tubing, and making the spokes bladelike instead of round. Replacing the spoked rear wheel with a solid disk has a significant effect, but the disk wheel

is a disadvantage in cross winds. Also, as shown in the photograph, the helmet can be streamlined to reduce the wake and turbulence behind the rider. In a time trial, the rider races alone and does not receive any benefit from surrounding riders. Currently, the time trial record in the Tour de France is 58.9 km/hr (36.6 mph) for a 7.6 km (4.7 mi) course.



Streamlined bicycle and rider.

Mariadav/Adobe Stock Photo

Learning Objectives

After completing this chapter, you should be able to

- Determine the dimensionless groups for a differential equation.
- Determine the dimensionless groups for a problem using the Buckingham Pi Theorem.
- Explain the meaning of the important dimensionless groups used in fluid mechanics.
- Use dimensional analysis to scale results from one flow situation to another.

Most phenomena in fluid mechanics depend in a complex way on geometric and flow parameters. For example, consider the drag force on a stationary smooth sphere immersed in a uniform stream. What experiments must be conducted to determine the drag force on the sphere? To answer this question, we must specify what we believe are the parameters that are important in determining the drag force. Clearly, we would expect the drag force to depend on the size of the sphere (characterized by the diameter, D), the fluid speed, V , and the fluid viscosity, μ . In addition, the density of the fluid, ρ , also might be important. Representing the drag force by F , we can write the symbolic equation

$$F = f(D, V, \rho, \mu)$$

Although we may have neglected parameters on which the drag force depends, such as surface roughness, we have set up the problem of determining the drag force for a stationary sphere in terms of quantities that are both controllable and measurable in the laboratory.

We could set up an experimental procedure for finding the dependence of F on V , D , ρ , and μ . To see how the drag, F , is affected by fluid speed, V , we could place a sphere in a wind tunnel and measure F for a range of V values. We could then run more tests in which we explore the effect on F of sphere diameter, D , by using different diameter spheres. We are already generating a lot of data. If we ran the wind tunnel at, say, 10 different speeds, for 10 different sphere sizes, we'd have 100 data points. We could plot 10 curves of F vs. V , one for each sphere size, but acquiring the data would be time consuming. In principle, we would next have to search out a way to use other fluids to be able to do experiments for a range of ρ and μ values. Then we would have to try and make sense of the data: How do we plot, say, curves of F vs. V , with D , ρ , and μ all being parameters? This is a daunting task, even for such a seemingly simple phenomenon as the drag on a sphere!

Fortunately we do not have to do all this work. As we will see in Example 7.1, using dimensional analysis, all the data for drag on a smooth sphere can be plotted as a single relationship between two nondimensional parameters in the form

$$\frac{F}{\rho V^2 D^2} = f\left(\frac{\rho V D}{\mu}\right)$$

The form of the function f still must be determined experimentally, but the point is that all spheres, in all fluids, for most velocities will fall on the same curve. Rather than needing to conduct 10^4 experiments, we could establish the nature of the function as accurately with only about 10 tests. The time saved in performing only 10 rather than 10^4 tests is obvious. Even more important is the greater experimental convenience. No longer must we find fluids with 10 different values of density and viscosity. Nor must we make 10 spheres of different diameters. Instead, only the parameter $\rho V D / \mu$ must be varied. This can be accomplished simply by using *one* sphere (e.g., 1 in. diameter), in *one* fluid (e.g., air), and only changing the speed, for example.

Figure 7.1 shows some classic data for flow over a sphere. The factors $\frac{1}{2}$ and $\pi/4$ have been added to the denominator of the parameter on the left to make it take the form of a commonly used nondimensional group, the drag coefficient, C_D , that we will discuss in detail in Chapter 9. If we performed the experiments as outlined above, our results would fall on the same curve, within experimental error. The data points represent results obtained by various workers for several different fluids and spheres. Note that we end up with a curve that can be used to obtain the drag force on a very wide range of sphere/fluid combinations. For example, it could be used to obtain the drag on a hot-air balloon due to a crosswind, or on a red blood cell as it moves through the aorta. In either case, given the fluid (ρ and μ), the flow speed V , and the sphere diameter D , we could compute a value for $\rho V D / \mu$, then read the corresponding value for C_D , and finally compute the drag force F .

In Section 7.1, we examine the governing differential equation to see what we can learn about dimensionless groups. These equations contain the physics of the situation and so are an important source of information. Next, in Section 7.2 we introduce the *Buckingham Pi* theorem, a formalized procedure for deducing the dimensionless groups appropriate for a given fluid mechanics or other engineering problem. We suggest you read it once, then study Examples 7.1, 7.2, and 7.3 to see how practical and useful the method in fact is, before returning to reread the section. The Buckingham Pi theorem is a

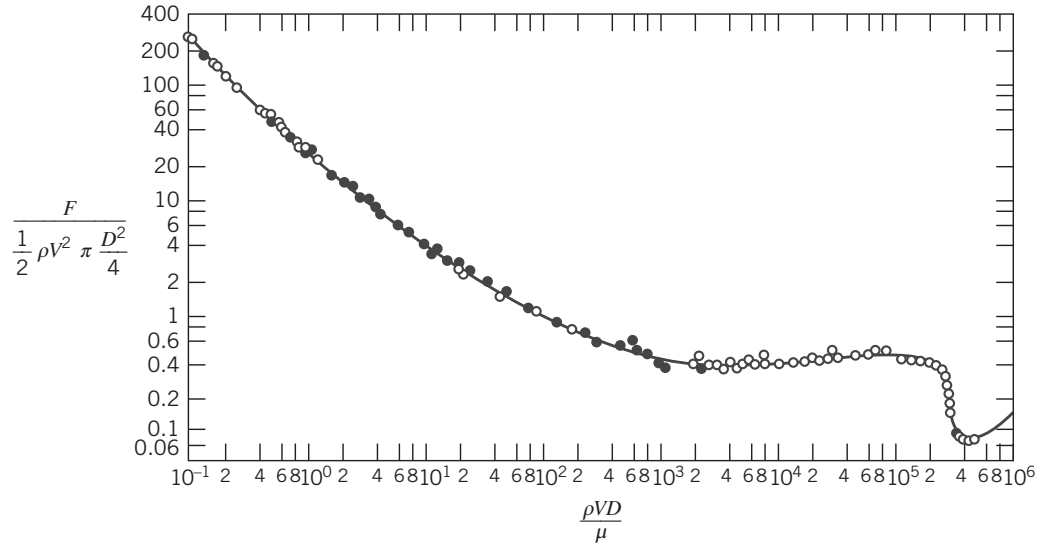


Fig. 7.1 Experimentally derived relation between the nondimensional parameters [3, 15, 16].

statement of the relation between a function expressed in terms of dimensional parameters and a related function expressed in terms of nondimensional parameters. The Buckingham Pi theorem allows us to develop the important nondimensional parameters quickly and easily.

7.1 Nondimensionalizing the Basic Differential Equations

Before developing a general approach to dimensional analysis let us see what we can learn from our previous analytical descriptions of fluid flow. Consider, for example, a steady incompressible two-dimensional flow of a Newtonian fluid with constant viscosity. The mass conservation equation (Eq. 5.1c) becomes

$$\frac{\partial u}{\partial x} + \frac{\partial v}{\partial y} = 0 \quad (7.1)$$

and the Navier–Stokes equations (Eqs. 5.27) reduce to

$$\rho \left(u \frac{\partial u}{\partial x} + v \frac{\partial u}{\partial y} \right) = - \frac{\partial p}{\partial x} + \mu \left(\frac{\partial^2 u}{\partial x^2} + \frac{\partial^2 u}{\partial y^2} \right) \quad (7.2)$$

and

$$\rho \left(u \frac{\partial v}{\partial x} + v \frac{\partial v}{\partial y} \right) = - \rho g - \frac{\partial p}{\partial y} + \mu \left(\frac{\partial^2 v}{\partial x^2} + \frac{\partial^2 v}{\partial y^2} \right) \quad (7.3)$$

As we discussed in Section 5.4, these equations form a set of coupled nonlinear partial differential equations for u , v , and p , and are difficult to solve for most flows. Equation 7.1 has dimensions of 1/time, and Eqs. 7.2 and 7.3 have dimensions of force/volume. Let us see what happens when we convert them into dimensionless equations.

To nondimensionalize these equations, divide all lengths by a reference length, L , and all velocities by a reference speed, V_∞ , which usually is taken as the freestream velocity. Make the pressure nondimensional by dividing by ρV_∞^2 (twice the freestream dynamic pressure). Denoting nondimensional quantities with asterisks, we obtain

$$x^* = \frac{x}{L}, \quad y^* = \frac{y}{L}, \quad u^* = \frac{u}{V_\infty}, \quad v^* = \frac{v}{V_\infty}, \quad \text{and} \quad p^* = \frac{p}{\rho V_\infty^2} \quad (7.4)$$

so that $x = x^*L$, $y = y^*L$, $u = u^*V_\infty$, and so on. We can then substitute into Eqs. 7.1 through 7.3; here we show two representative substitutions:

$$u \frac{\partial u}{\partial x} = u^* V_\infty \frac{\partial(u^* V_\infty)}{\partial(x^* L)} = \frac{V_\infty^2}{L} u^* \frac{\partial u^*}{\partial x^*}$$

and

$$\frac{\partial^2 u}{\partial x^2} = \frac{\partial(u^* V_\infty)}{\partial(x^* L)^2} = \frac{V_\infty}{L^2} \frac{\partial^2 u^*}{\partial x^{*2}}$$

Using this procedure, the equations become

$$\frac{V_\infty}{L} \frac{\partial u^*}{\partial x^*} + \frac{V_\infty}{L} \frac{\partial v^*}{\partial y^*} = 0 \quad (7.5)$$

$$\frac{\rho V_\infty^2}{L} \left(u^* \frac{\partial u^*}{\partial x^*} + v^* \frac{\partial u^*}{\partial y^*} \right) = -\frac{\rho V_\infty^2}{L} \frac{\partial p^*}{\partial x^*} + \frac{\mu V_\infty}{L^2} \left(\frac{\partial^2 u^*}{\partial x^{*2}} + \frac{\partial^2 u^*}{\partial y^{*2}} \right) \quad (7.6)$$

$$\frac{\rho V_\infty^2}{L} \left(u^* \frac{\partial v^*}{\partial x^*} + v^* \frac{\partial v^*}{\partial y^*} \right) = -\rho g - \frac{\rho V_\infty^2}{L} \frac{\partial p^*}{\partial y^*} + \frac{\mu V_\infty}{L^2} \left(\frac{\partial^2 v^*}{\partial x^{*2}} + \frac{\partial^2 v^*}{\partial y^{*2}} \right) \quad (7.7)$$

Dividing Eq. 7.5 by V_∞/L and Eqs. 7.6 and 7.7 by $\rho V_\infty^2/L$ gives

$$\frac{\partial u^*}{\partial x^*} + \frac{\partial v^*}{\partial y^*} = 0 \quad (7.8)$$

$$u^* \frac{\partial u^*}{\partial x^*} + v^* \frac{\partial u^*}{\partial y^*} = -\frac{\partial p^*}{\partial x^*} + \frac{\mu}{\rho V_\infty L} \left(\frac{\partial^2 u^*}{\partial x^{*2}} + \frac{\partial^2 u^*}{\partial y^{*2}} \right) \quad (7.9)$$

$$u^* \frac{\partial v^*}{\partial x^*} + v^* \frac{\partial v^*}{\partial y^*} = -\frac{gL}{V_\infty^2} - \frac{\partial p^*}{\partial y^*} + \frac{\mu}{\rho V_\infty L} \left(\frac{\partial^2 v^*}{\partial x^{*2}} + \frac{\partial^2 v^*}{\partial y^{*2}} \right) \quad (7.10)$$

Equations 7.8, 7.9, and 7.10 are the nondimensional forms of our original equations (Eqs. 7.1, 7.2, 7.3). As such, we can think about their solution (with appropriate boundary conditions) as an exercise in applied mathematics. Equation 7.9 contains a dimensionless coefficient $\mu/\rho V_\infty L$ (which we recognize as the inverse of the Reynolds number) in front of the second-order (viscous) terms; Eq. 7.10 contains this and another dimensionless coefficient, gL/V_∞^2 the gravity force term. We recall from the theory of differential equations that the mathematical form of the solution of such equations is very sensitive to the values of the coefficients in the equations.

These equations tell us that the solution, and hence the actual flow pattern they describe, depends on the values of the two coefficients. For example, if $\mu/\rho V_\infty L$ is very small (i.e., we have a high Reynolds number), the second-order differentials, representing viscous forces, can be neglected, at least in most of the flow, and we end up with a form of Euler's equations (Eqs. 6.2). We say "in most of the flow" because we have already learned that in reality for this case we will have a boundary layer in which there is significant effect of viscosity. In addition, from a mathematical point of view, it is always dangerous to neglect higher-order derivatives, even if their coefficients are small, because reduction to a lower-order equation means we lose a boundary condition (specifically the no-slip condition). We can predict that if $\mu/\rho V_\infty L$ is large or small, then viscous forces will be significant or not, respectively; if gL/V_∞^2 is large or small, we can predict that gravity forces will be significant or not, respectively. We can thus gain insight even before attempting a solution to the differential equations. Note that for completeness, we would have to apply the same nondimensionalizing approach to the boundary conditions of the problem, which often introduce further dimensionless coefficients.

Writing nondimensional forms of the governing equations, then, can yield insight into the underlying physical phenomena, and indicate which forces are dominant. If we had two geometrically similar

but different scale flows satisfying Eqs. 7.8, 7.9, and 7.10 (e.g., a model and a prototype), the equations would only yield the same mathematical results if the two flows had the same values for the two coefficients (i.e., had the same relative importance of gravity, viscous, and inertia forces). This nondimensional form of the equations is also the starting point in numerical methods, which is very often the only way of obtaining their solution. Additional derivations and examples of establishing similitude from the governing equations of a problem are presented in Kline [1] and Hansen [2].

We will now see how the method of dimensional analysis can be used instead of the above procedure to find appropriate dimensionless groupings of physical parameters. As we have mentioned, using dimensionless groupings is very useful for experimental measurements, and we will see in the next two sections that we can obtain them even when we do not have the governing equations such as Eqs. 7.1, 7.2, and 7.3 to work from.

7.2 Buckingham Pi Theorem

In the Introduction we discussed how the drag F on a sphere depends on the sphere diameter D , fluid density ρ and viscosity μ , and fluid speed V , or

$$F = F(D, \rho, \mu, V)$$

with theory or experiment being needed to determine the nature of function f . More formally, we write

$$g(F, D, \rho, \mu, V) = 0$$

where g is an unspecified function, different from f . The Buckingham Pi theorem [4] states that we can transform a relationship between n parameters of the form

$$g(q_1, q_2, \dots, q_n) = 0$$

into a corresponding relationship between $n-m$ independent dimensionless Π parameters in the form

$$G(\Pi_1, \Pi_2, \dots, \Pi_{n-m}) = 0$$

or

$$\Pi_1 = G_1(\Pi_2, \dots, \Pi_{n-m})$$

where m is usually the minimum number, r , of independent dimensions (e.g., mass, length, time) required to define the dimensions of all the parameters q_1, q_2, \dots, q_n . For example, for the sphere problem, we will see in Example 7.1 that

$$g(F, D, \rho, \mu, V) = 0 \quad \text{or} \quad F = F(D, \rho, \mu, V)$$

leads to

$$G\left(\frac{F}{\rho V^2 D^2}, \frac{\mu}{\rho V D}\right) = 0 \quad \text{or} \quad \frac{F}{\rho V^2 D^2} = G_1\left(\frac{\mu}{\rho V D}\right)$$

The theorem does not predict the functional form of G or G_1 . The functional relation among the independent dimensionless Π parameters must be determined experimentally.

The $n-m$ dimensionless Π parameters obtained from the procedure are independent. A Π parameter is not independent if it can be formed from any combination of one or more of the other Π parameters. For example, if

$$\Pi_5 = \frac{2\Pi_1}{\Pi_2 \Pi_3} \quad \text{or} \quad \Pi_6 = \frac{\Pi_1^{3/4}}{\Pi_3^2}$$

then neither Π_5 nor Π_6 is independent of the other dimensionless parameters.

Several methods for determining the dimensionless parameters are available. A detailed procedure is presented in the rest of this section.

Regardless of the method to be used to determine the dimensionless parameters, one begins by listing all dimensional parameters that are believed to affect the given flow phenomenon. Some

experience admittedly is helpful in compiling the list. Students, who do not have this experience, often are troubled by the need to apply engineering judgment in an apparent massive dose. However, it is difficult to go wrong if a generous selection of parameters is made.

If you suspect that a phenomenon depends on a given parameter, include it. If your suspicion is correct, experiments will show that the parameter must be included to get consistent results. If the parameter is extraneous, an extra Π parameter may result, but experiments will later show that it may be eliminated. Therefore, do not be afraid to include *all* the parameters that you feel are important.

The six steps listed below outline a recommended procedure for determining the Π parameters:

- Step 1.** *List all the dimensional parameters involved.* Let n be the number of parameters. If all of the pertinent parameters are not included, a relation may be obtained, but it will not give the complete story. If parameters that actually have no effect on the physical phenomenon are included, either the process of dimensional analysis will show that these do not enter the relation sought, or one or more dimensionless groups will be obtained that experiments will show to be extraneous.
- Step 2.** *Select a set of fundamental (primary) dimensions, e.g., MLt or FLt .* For a heat transfer problems you may also need T for temperature, and in electrical systems, q for charge.
- Step 3.** *List the dimensions of all parameters in terms of primary dimensions.* Let r be the number of primary dimensions. Either force or mass may be selected as a primary dimension.
- Step 4.** *Select a set of r dimensional parameters that includes all the primary dimensions.* These parameters will all be combined with each of the remaining parameters, one of those at a time, and so will be called repeating parameters. No repeating parameter should have dimensions that are a power of the dimensions of another repeating parameter; for example, do not include both an area (L^2) and a second moment of area (L^4) as repeating parameters. The repeating parameters chosen may appear in all the dimensionless groups obtained; consequently, do *not* include the dependent parameter among those selected in this step.
- Step 5.** *Set up dimensional equations, combining the parameters selected in Step 4 with each of the other parameters in turn, to form dimensionless groups.* There will be $n-m$ equations. Solve the dimensional equations to obtain the $n-m$ dimensionless groups.
- Step 6.** *Check to see that each group obtained is dimensionless.* If mass was initially selected as a primary dimension, it is wise to check the groups using force as a primary dimension, or vice versa.

The functional relationship among the Π parameters must be determined experimentally. The detailed procedure for determining the dimensionless Π parameters is illustrated in Examples 7.1 and 7.2.

Example 7.1 DRAG FORCE ON A SMOOTH SPHERE

As noted in Section 7.2, the drag force, F , on a smooth sphere depends on the relative speed, V , the sphere diameter, D , the fluid density, ρ , and the fluid viscosity, μ . Obtain a set of dimensionless groups that can be used to correlate experimental data.

Given: $F=f(\rho, V, D, \mu)$ for a smooth sphere.

Find: An appropriate set of dimensionless groups.

Solution: (Circled numbers refer to steps in the procedure for determining dimensionless Π parameters.)

$$\textcircled{1} \quad F \quad V \quad D \quad \rho \quad \mu \quad n = 5 \text{ dimensional parameters}$$

$\textcircled{2}$ Select primary dimensions M, L , and t .

$$\textcircled{3} \quad F \quad V \quad D \quad \rho \quad \mu$$

$$\frac{ML}{t^2} \quad \frac{L}{t} \quad L \quad \frac{M}{L^3} \quad \frac{M}{Lt} \quad r = 3 \text{ primary dimensions}$$

- ④ Select repeating parameters ρ, V, D . $m=r=3$ repeating parameters
 ⑤ Then $n-m=2$ dimensionless groups will result. Setting up dimensional equations, we obtain

$$\Pi_1 = \rho^a V^b D^c F \quad \text{and} \quad \left(\frac{M}{L^3}\right)^a \left(\frac{L}{t}\right)^b (L)^c \left(\frac{ML}{t^2}\right) = M^0 L^0 t^0$$

Equating the exponents of M, L , and t results in

$$\begin{aligned} M: & \quad a+1=0 & a=-1 \\ L: & \quad -3a+b+c+1=0 & c=-2 \\ t: & \quad -b-2=0 & b=-2 \end{aligned} \quad \text{Therefore, } \Pi_1 = \frac{F}{\rho V^2 D^2}$$

Similarly,

$$\begin{aligned} \Pi_2 = \rho^d V^e D^f \mu & \quad \text{and} \quad \left(\frac{M}{L^3}\right)^d \left(\frac{L}{t}\right)^e (L)^f \left(\frac{M}{Lt}\right) = M^0 L^0 t^0 \\ M: & \quad d+1=0 & d=-1 \\ L: & \quad -3d+e+f-1=0 & f=-1 \\ t: & \quad -e-1=0 & e=-1 \end{aligned} \quad \text{Therefore, } \Pi_2 = \frac{\mu}{\rho V D}$$

- ⑥ Check using F, L, t dimensions

$$[\Pi_1] = \left[\frac{F}{\rho V^2 D^2} \right] \quad \text{and} \quad F \frac{L^4}{F t^2} \left(\frac{t}{L} \right)^2 \frac{1}{L^2} = 1$$

where $[]$ means “has dimensions of,” and

$$[\Pi_2] = \left[\frac{\mu}{\rho V D} \right] \quad \text{and} \quad \frac{F t}{L^2} \frac{L^4}{F t^2} \frac{t}{L} \frac{1}{L} = 1$$

The functional relationship is $\Pi_1 = f(\Pi_2)$, or

$$\frac{F}{\rho V^2 D^2} = f \left(\frac{\mu}{\rho V D} \right)$$

as noted before. The form of the function, f , must be determined experimentally (see Fig. 7.1).

Note:

This example illustrates the use of the Pi theorem to develop the dimensionless groups for a problem.

Example 7.2 PRESSURE DROP IN PIPE FLOW

The pressure drop, Δp , for steady, incompressible viscous flow through a straight horizontal pipe depends on the pipe length, l , the average velocity, \bar{V} , the fluid viscosity, μ , the pipe diameter, D , the fluid density, ρ , and the average “roughness” height, e . Determine a set of dimensionless groups that can be used to correlate data.

Given: $\Delta p = f(\rho, \bar{V}, D, l, \mu, e)$ for flow in a circular pipe.

Find: A suitable set of dimensionless groups.

Solution: (Circled numbers refer to steps in the procedure for determining dimensionless Π parameters.)

$$\textcircled{1} \quad \Delta p \quad \rho \quad \mu \quad \bar{V} \quad l \quad D \quad e \quad n=7 \text{ dimensional parameters}$$

\textcircled{2} Choose primary dimensions M, L , and t .

$$\textcircled{3} \quad \Delta p \quad \rho \quad \mu \quad \bar{V} \quad l \quad D \quad e$$

$$\frac{M}{L^2} \quad \frac{M}{L^3} \quad \frac{M}{Lt} \quad \frac{L}{t} \quad L \quad L \quad L \quad r=3 \text{ primary dimensions}$$

$$\textcircled{4} \quad \text{Select repeating parameters } \rho, \bar{V}, D. \quad m=r=3 \text{ repeating parameters}$$

\textcircled{5} Then $n-m=4$ dimensionless groups will result. Setting up dimensional equations we have:

$$\begin{aligned} \Pi_1 &= \rho^a \bar{V}^b D^c \Delta p \quad \text{and} \\ \left(\frac{M}{L^3}\right)^a \left(\frac{L}{t}\right)^b (L)^c \left(\frac{M}{L^2}\right) &= M^0 L^0 t^0 \\ \left\{ \begin{array}{l} M: 0=a+1 \\ L: 0=-3a+b+c-1 \\ t: 0=-b-2 \end{array} \right. & \left. \begin{array}{l} a=-1 \\ b=-2 \\ c=0 \end{array} \right. \end{aligned}$$

$$\text{Therefore, } \Pi_1 = \rho^{-1} \bar{V}^{-2} D^0 \Delta p = \frac{\Delta p}{\rho \bar{V}^2}$$

$$\begin{aligned} \Pi_3 &= \rho^g \bar{V}^h D^i l \quad \text{and} \\ \left(\frac{M}{L^3}\right)^g \left(\frac{L}{t}\right)^h (L)^i L &= M^0 L^0 t^0 \\ \left\{ \begin{array}{l} M: 0=g \\ L: 0=-3g+h+i+1 \\ t: 0=-h \end{array} \right. & \left. \begin{array}{l} g=0 \\ h=0 \\ i=-1 \end{array} \right. \end{aligned}$$

$$\text{Therefore, } \Pi_3 = \frac{l}{D}$$

$$\begin{aligned} \Pi_2 &= \rho^d \bar{V}^e D^f \mu \quad \text{and} \\ \left(\frac{M}{L^3}\right)^d \left(\frac{L}{t}\right)^e (L)^f \frac{M}{Lt} &= M^0 L^0 t^0 \\ \left\{ \begin{array}{l} M: 0=d+1 \\ L: 0=-3d+e+f-1 \\ t: 0=-e-1 \end{array} \right. & \left. \begin{array}{l} d=-1 \\ e=-1 \\ f=-1 \end{array} \right. \end{aligned}$$

$$\text{Therefore, } \Pi_2 = \frac{\mu}{\rho \bar{V} D}$$

$$\begin{aligned} \Pi_4 &= \rho^j \bar{V}^k D^l e \quad \text{and} \\ \left(\frac{M}{L^3}\right)^j \left(\frac{L}{t}\right)^k (L)^l L &= M^0 L^0 t^0 \\ \left\{ \begin{array}{l} M: 0=j \\ L: 0=-3j+k+l+1 \\ t: 0=-k \end{array} \right. & \left. \begin{array}{l} j=0 \\ k=0 \\ l=-1 \end{array} \right. \end{aligned}$$

$$\text{Therefore, } \Pi_4 = \frac{e}{D}$$

\textcircled{6} Check, using F, L, t dimensions

$$[\Pi_1] = \left[\frac{\Delta p}{\rho \bar{V}^2} \right] \quad \text{and} \quad \frac{F}{L^2} \frac{L^4}{Ft^2} \frac{t^2}{L^2} = 1 \quad [\Pi_3] = \left[\frac{l}{D} \right] \quad \text{and} \quad \frac{L}{L} = 1$$

$$[\Pi_2] = \left[\frac{\mu}{\rho \bar{V} D} \right] \quad \text{and} \quad \frac{Ft}{L^2} \frac{L^4}{Ft^2} \frac{t}{L} \frac{1}{L} = 1 \quad [\Pi_4] = \left[\frac{e}{D} \right] \quad \text{and} \quad \frac{L}{L} = 1$$

Finally, the functional relationship is

$$\Pi_1 = f(\Pi_2, \Pi_3, \Pi_4)$$

or

$$\frac{\Delta p}{\rho \bar{V}^2} = f\left(\frac{\mu}{\rho \bar{V} D}, \frac{l}{D}, \frac{e}{D}\right)$$

Notes:

- As we shall see when we study pipe flow in detail in Chapter 8, this relationship correlates the data well.
- Each Π group is unique (e.g., there is only one possible dimensionless grouping of μ, ρ, \bar{V} , and D).
- We can often deduce Π groups by inspection, e.g., l/D is the obvious unique grouping of l with ρ, \bar{V} , and D .

The procedure outlined above, where m is taken equal to r (the fewest independent dimensions required to specify the dimensions of all parameters involved), almost always produces the correct number of dimensionless Π parameters. In a few cases, trouble arises because the number of primary dimensions differs when variables are expressed in terms of different systems of dimensions (e.g., MLt or FLt). The value of m can be established with certainty by determining the rank of the dimensional matrix; that rank is m . Although not needed in most applications, for completeness, this procedure is illustrated in Example 7.3.

Example 7.3 CAPILLARY EFFECT: USE OF DIMENSIONAL MATRIX

When a small tube is dipped into a pool of liquid, surface tension causes a meniscus to form at the free surface, which is elevated or depressed depending on the contact angle at the liquid–solid–gas interface. Experiments indicate that the magnitude of this capillary effect, Δh , is a function of the tube diameter, D , liquid specific weight, γ , and surface tension, σ . Determine the number of independent Π parameters that can be formed and obtain a set.

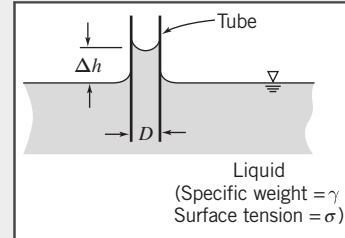
Given: $\Delta h = f(D, \gamma, \sigma)$

Find: (a) Number of independent Π parameters.
 (b) One set of Π parameters.

Solution: Circled numbers refer to steps in the procedure for determining dimensionless Π parameters.

① $\Delta h \quad D \quad \gamma \quad \sigma \quad n=4$ dimensional parameters

② Choose primary dimensions (use both M, L, t and F, L, t dimensions to illustrate the problem in determining m).



③ (a) M, L, t

$$\begin{array}{cccc} \Delta h & D & \gamma & \sigma \\ L & L & \frac{M}{L^2 t^2} & M \\ & & & t^2 \end{array}$$

$$r=3 \text{ primary dimensions}$$

(b) F, L, t

$$\begin{array}{cccc} \Delta h & D & \gamma & \sigma \\ L & L & F & F \\ & & L^3 & L \end{array}$$

$$r=2 \text{ primary dimensions}$$

Thus for each set of primary dimensions we ask, "Is m equal to r ?" Let us check each dimensional matrix to find out. The dimensional matrices are

	Δh	D	γ	σ
M	0	0	1	1
L	1	1	-2	0
t	0	0	-2	-2

	Δh	D	γ	σ
F	0	0	1	1
L	1	1	-3	-1

The rank of a matrix is equal to the order of its largest nonzero determinant.

$$\begin{vmatrix} 0 & 1 & 1 \\ 1 & -2 & 0 \\ 0 & -2 & -2 \end{vmatrix} = 0 - (1)(-2) + (1)(-2) = 0$$

$$\begin{vmatrix} -2 & 0 \\ -2 & -2 \end{vmatrix} = 4 \neq 0 \quad \therefore m=2$$

$$\begin{vmatrix} 1 & 1 \\ -3 & -1 \end{vmatrix} = -1 + 3 = 2 \neq 0$$

$$\therefore m=2$$

$m=2$. Choose D, γ as repeating parameters.
 $n-m=2$ dimensionless groups will result.

$$\Pi_1 = D^a \gamma^b \Delta h \text{ and}$$

$$(L)^a \left(\frac{M}{L^2 t^2} \right)^b (L) = M^0 L^0 t^0$$

$$\Pi_1 = D^e \gamma^f \Delta h \text{ and}$$

$$(L)^e \left(\frac{F}{L^3} \right)^f L = F^0 L^0 t^0$$

$$\left. \begin{array}{l} M: b+0=0 \\ L: a-2b+1=0 \\ t: -2b+0=0 \end{array} \right\} \quad \begin{array}{l} b=0 \\ a=-1 \end{array}$$

$$\text{Therefore, } \Pi_1 = \frac{\Delta h}{D}$$

$$\Pi_2 = D^c \gamma^d \sigma \text{ and}$$

$$(L)^c \left(\frac{M}{L^2 t^2} \right)^d \frac{M}{t^2} = M^0 L^0 t^0$$

$$\left. \begin{array}{l} M: d+1=0 \\ L: c-2d=0 \\ t: -2d-2=0 \end{array} \right\} \quad \begin{array}{l} d=-1 \\ c=-2 \end{array}$$

$$\text{Therefore, } \Pi_2 = \frac{\sigma}{D^2 \gamma}$$

⑥ Check, using F, L, t dimensions

$$[\Pi_1] = \left[\frac{\Delta h}{D} \right] \quad \text{and} \quad \frac{L}{L} = 1$$

$$[\Pi_2] = \left[\frac{\sigma}{D^2 \gamma} \right] \quad \text{and} \quad \frac{F}{L} \frac{1}{L^2} \frac{L^3}{F} = 1$$

$$\left. \begin{array}{l} F: f=0 \\ L: e-3f+1=0 \end{array} \right\} \quad \begin{array}{l} e=-1 \end{array}$$

$$\text{Therefore, } \Pi_1 = \frac{\Delta h}{D}$$

$$\Pi_2 = D^g \gamma^h \sigma \text{ and}$$

$$(L)^g \left(\frac{F}{L^3} \right)^h \frac{F}{L} = F^0 L^0 t^0$$

$$\left. \begin{array}{l} F: h+1=0 \\ L: g-3h-1=0 \end{array} \right\} \quad \begin{array}{l} h=-1 \\ g=-2 \end{array}$$

$$\text{Therefore, } \Pi_2 = \frac{\sigma}{D^2 \lambda}$$

Check, using M, L, t dimensions

$$[\Pi_1] = \left[\frac{\Delta h}{D} \right] \quad \text{and} \quad \frac{L}{L} = 1$$

$$[\Pi_2] = \left[\frac{\sigma}{D^2 \gamma} \right] \quad \text{and} \quad \frac{M}{t^2} \frac{1}{L^2} \frac{L^2 t^2}{M} = 1$$

Therefore, both systems of dimensions yield the same dimensionless Π parameters. The predicted functional relationship is

$$\Pi_1 = f(\Pi_2) \quad \text{or} \quad \frac{\Delta h}{D} = f\left(\frac{\sigma}{D^2 \gamma}\right)$$

Notes:

- This result is reasonable on physical grounds. The fluid is static; we would not expect time to be an important dimension.
- We analyzed this problem in Example 2.3, where we found that $\Delta h = 4\sigma \cos(\theta)/\rho g D$ (θ is the contact angle). Hence $\Delta h/D$ is directly proportional to $\sigma/D^2 \gamma$.
- The purpose of this problem is to illustrate use of the dimensional matrix to determine the required number of repeating parameters.

The $n-m$ dimensionless groups obtained from the procedure are independent but not unique. If a different set of repeating parameters is chosen, different groups result. The repeating parameters are so named because they may appear in all the dimensionless groups obtained. Based on experience, viscosity should appear in only one dimensionless parameter. Therefore μ should *not* be chosen as a repeating parameter.

When we have a choice, it usually works out best to choose density ρ (dimensions M/L^3 in the MLt system), speed V (dimensions L/t), and characteristic length L (dimension L) as repeating parameters because experience shows this generally leads to a set of dimensionless parameters that are suitable for correlating a wide range of experimental data; in addition, ρ , V , and L are usually fairly easy to measure or otherwise obtain. The values of the dimensionless parameters obtained using these repeating parameters almost always have a very tangible meaning, telling you the relative strength of various fluid forces (e.g., viscous) to inertia forces—we will discuss several “classic” ones shortly.

It's also worth stressing that, given the parameters you're combining, *we can often determine the unique dimensional parameters by inspection*. For example, if we had repeating parameters ρ , V , and L

and were combining them with a parameter A_f , representing the frontal area of an object, it's fairly obvious that only the combination A_f/L^2 is dimensionless. Experienced fluid mechanicians also know that ρV^2 produces dimensions of stress, so any time a stress or force parameter arises, dividing by ρV^2 or $\rho V^2 L^2$ will produce a dimensionless quantity.

We will find useful a measure of the magnitude of fluid inertia forces, obtained from Newton's second law, $F=ma$; the dimensions of inertia force are thus MLt^{-2} . Using ρ , V , and L to build the dimensions of ma leads to the unique combination $\rho V^2 L^2$.

If $n-m=1$, then a single dimensionless Π parameter is obtained. In this case, the Buckingham Pi theorem indicates that the single Π parameter must be a constant.

7.3 Significant Dimensionless Groups in Fluid Mechanics

Over the years, several hundred different dimensionless groups that are important in engineering have been identified. Following tradition, each such group has been given the name of a prominent scientist or engineer, usually the one who pioneered its use. Several are so fundamental and occur so frequently in fluid mechanics that we should take time to learn their definitions. Understanding their physical significance also gives insight into the phenomena we study.

Forces encountered in flowing fluids include those due to inertia, viscosity, pressure, gravity, surface tension, and compressibility. The ratio of any two forces will be dimensionless. We have previously shown that the inertia force is proportional to $\rho V^2 L^2$.

We can now compare the relative magnitudes of various fluid forces to the inertia force, using the following scheme:

Viscous force ~	$\tau A = \mu \frac{du}{dy} A \propto \mu \frac{V}{L} L^2 = \mu VL$	so	$\frac{\text{viscous}}{\text{inertia}} \sim$	$\frac{\mu VL}{\rho V^2 L^2} = \frac{\mu}{\rho VL}$
Pressure force ~	$\Delta p A \propto \Delta p L^2$	so	$\frac{\text{pressure}}{\text{inertia}} \sim$	$\frac{\Delta p L^2}{\rho V^2 L^2} = \frac{\Delta p}{\rho V^2}$
Gravity force ~	$mg \propto g \rho L^3$	so	$\frac{\text{gravity}}{\text{inertia}} \sim$	$\frac{g \rho L^3}{\rho V^2 L^2} = \frac{gL}{V^2}$
Surface tension ~	σL	so	$\frac{\text{surface tension}}{\text{inertia}} \sim$	$\frac{\sigma L}{\rho V^2 L^2} = \frac{\sigma}{\rho V^2 L}$
Compressibility force ~	$E_v A \propto E_v L^2$	so	$\frac{\text{compressibility force}}{\text{inertia}} \sim$	$\frac{E_v L^2}{\rho V^2 L^2} = \frac{E_v}{\rho V^2}$

All of the dimensionless parameters listed above occur so frequently, and are so powerful in predicting the relative strengths of various fluid forces, that they have been given identifying names.

The first parameter, $\mu/\rho VL$, is by tradition inverted to the form $\rho VL/\mu$, and was actually explored independently of dimensional analysis in the 1880s by Osborne Reynolds, the British engineer, who studied the transition between laminar and turbulent flow regimes in a tube. He discovered that the parameter

$$Re = \frac{\rho \bar{V} D}{\mu} = \frac{\bar{V} D}{\nu}$$

is a criterion by which the flow regime may be determined. Later experiments have shown that the *Reynolds number* is a key parameter for other flow cases as well. Thus, in general,

$$Re = \frac{\rho VL}{\mu} = \frac{VL}{\nu} \quad (7.11)$$

where L is a characteristic length descriptive of the flow field geometry. The Reynolds number is the ratio of inertia forces to viscous forces. Flows with "large" Reynolds number generally are turbulent. Flows in which the inertia forces are "small" compared with the viscous forces are characteristically laminar flows.

In aerodynamic and other model testing, it is convenient to modify the second parameter, $\Delta p/\rho V^2$, by inserting a factor $\frac{1}{2}$ to make the denominator represent the dynamic pressure. The ratio

$$Eu = \frac{\Delta p}{\frac{1}{2}\rho V^2} \quad (7.12a)$$

is formed, where Δp is the local pressure minus the freestream pressure, and ρ and V are properties of the freestream flow. This ratio has been named after Leonhard Euler, the Swiss mathematician who did much early analytical work in fluid mechanics. Euler is credited with being the first to recognize the role of pressure in fluid motion; the Euler equations of Chapter 6 demonstrate this role. The *Euler number* is the ratio of pressure forces to inertia forces. The Euler number is often called the *pressure coefficient*, C_p .

The drag and lift coefficients that we will run into in Chapters 8 and 9 are similar to the Euler coefficient. Instead of pressure, they are formed using the drag force and the lift force. The drag coefficient is defined as

$$C_D = \frac{F_D}{\frac{1}{2}\rho V^2 L^2} \quad (7.12b)$$

And the lift coefficient is defined as

$$C_L = \frac{F_L}{\frac{1}{2}\rho V^2 L^2} \quad (7.12c)$$

In the study of cavitation phenomena, the pressure difference, Δp , is taken as $\Delta p = p - p_v$, where p is the pressure in the liquid stream, and p_v is the liquid vapor pressure at the test temperature. Combining these with ρ and V in the stream yields the dimensionless parameter called the *cavitation number*,

$$Ca = \frac{p - p_v}{\frac{1}{2}\rho V^2} \quad (7.13)$$

The smaller the cavitation number, the more likely cavitation is to occur. This is usually an unwanted phenomenon.

William Froude was a British naval architect. Together with his son, Robert Edmund Froude, he discovered that the parameter

$$Fr = \frac{V}{\sqrt{gL}} \quad (7.14)$$

was significant for flows with free surface effects. Squaring the *Froude number* gives

$$Fr^2 = \frac{V^2}{gL}$$

which may be interpreted as the ratio of inertia forces to gravity forces (it is the inverse of the third force ratio, V^2/gL , that we discussed above). The length, L , is a characteristic length descriptive of the flow field. In the case of open-channel flow, the characteristic length is the water depth; Froude numbers less than unity indicate subcritical flow and values greater than unity indicate supercritical flow. We will have much more to say on this in Chapter 11.

By convention, the inverse of the fourth force ratio, $\sigma/\rho V^2 L$, discussed above, is called the *Weber number*; it indicates the ratio of inertia to surface tension forces

$$We = \frac{\rho V^2 L}{\sigma} \quad (7.15)$$

The value of the Weber number is indicative of the existence of, and frequency of, capillary waves at a free surface.

In the 1870s, the Austrian physicist Ernst Mach introduced the parameter

$$M = \frac{V}{c} \quad (7.16)$$

where V is the flow speed and c is the local sonic speed. Analysis and experiments have shown that the *Mach number* is a key parameter that characterizes compressibility effects in a flow. The Mach number may be written

$$M = \frac{V}{c} = \frac{V}{\sqrt{\frac{dp}{d\rho}}} = \frac{V}{\sqrt{\frac{E_v}{\rho}}} \quad \text{or} \quad M^2 = \frac{\rho V^2 L^2}{E_v L^2} = \frac{\rho V^2}{E_v}$$

which is the inverse of the final force ratio, $E_v/\rho V^2$, discussed above, and can be interpreted as a ratio of inertia forces to forces due to compressibility. For truly incompressible flow, $c = \infty$ so that $M = 0$.

Equations 7.11 through 7.16 are some of the most commonly used dimensionless groupings in fluid mechanics because for any flow pattern they immediately indicate the relative importance of inertia, viscosity, pressure, gravity, surface tension, and compressibility.

7.4 Flow Similarity and Model Studies

To be useful, a model test must yield data that can be scaled to obtain the forces, moments, and dynamic loads that would exist on the full-scale prototype. What conditions must be met to ensure the similarity of model and prototype flows?

Perhaps the most obvious requirement is that the model and prototype must be geometrically similar. *Geometric similarity* requires that the model and prototype be the same shape, and that all linear dimensions of the model be related to corresponding dimensions of the prototype by a constant scale factor.

A second requirement is that the model and prototype flows must be *kinematically similar*. Two flows are kinematically similar when the velocities at corresponding points are in the same direction and differ only by a constant scale factor. Thus two flows that are kinematically similar also have streamline patterns related by a constant scale factor. Since the boundaries form the bounding streamlines, flows that are kinematically similar must be geometrically similar.

In principle, in order to model the performance in an infinite flow field correctly, kinematic similarity would require that a wind tunnel of infinite cross section be used to obtain data for drag on an object. In practice, this restriction may be relaxed considerably, permitting use of equipment of reasonable size.

Kinematic similarity requires that the regimes of flow be the same for model and prototype. If compressibility or cavitation effects, which may change even the qualitative patterns of flow, are not present in the prototype flow, they must be avoided in the model flow.

When two flows have force distributions such that identical types of forces are parallel and are related in magnitude by a constant scale factor at all corresponding points, the flows are *dynamically similar*.

The requirements for dynamic similarity are the most restrictive. Kinematic similarity requires geometric similarity; kinematic similarity is a necessary, but not sufficient, requirement for dynamic similarity.

To establish the conditions required for complete dynamic similarity, all forces that are important in the flow situation must be considered. Thus the effects of viscous forces, of pressure forces, of surface tension forces, and so on, must be considered. Test conditions must be established such that all important forces are related by the same scale factor between model and prototype flows. When dynamic similarity exists, data measured in a model flow may be related quantitatively to conditions in the prototype flow. What, then, are the conditions that ensure dynamic similarity between model and prototype flows?

The Buckingham Pi theorem may be used to obtain the governing dimensionless groups for a flow phenomenon; to achieve dynamic similarity between geometrically similar flows, we must make sure

that each independent dimensionless group has the same value in the model and in the prototype. Then not only will the forces have the same relative importance, but also the dependent dimensionless group will have the same value in the model and prototype.

For example, in considering the drag force on a sphere in Example 7.1, we began with

$$F = f(D, V, \rho, \mu)$$

The Buckingham Pi theorem predicted the functional relation

$$\frac{F}{\rho V^2 D^2} = f_1 \left(\frac{\rho V D}{\mu} \right)$$

In Section 7.3 we showed that the dimensionless parameters can be viewed as ratios of forces. Thus, in considering a model flow and a prototype flow about a sphere the flows are geometrically similar. The flows also will be dynamically similar if the value of the independent parameter, $\rho V D / \mu$, is duplicated between model and prototype, i.e., if

$$\left(\frac{\rho V D}{\mu} \right)_{\text{model}} = \left(\frac{\rho V D}{\mu} \right)_{\text{prototype}}$$

Furthermore, if

$$Re_{\text{model}} = Re_{\text{prototype}}$$

then the value of the dependent parameter, $F / \rho V^2 D^2$, in the functional relationship, will be duplicated between model and prototype, i.e.,

$$\left(\frac{F}{\rho V^2 D^2} \right)_{\text{model}} = \left(\frac{F}{\rho V^2 D^2} \right)_{\text{prototype}}$$

and the results determined from the model study can be used to predict the drag on the full-scale prototype.

The actual force on the object caused by the fluid is not the same for the model and prototype, but the value of its dimensionless group is. The two tests can be run using different fluids, if desired, as long as the Reynolds numbers are matched. For experimental convenience, test data can be measured in a wind tunnel in air and the results used to predict drag in water, as illustrated in Example 7.4.

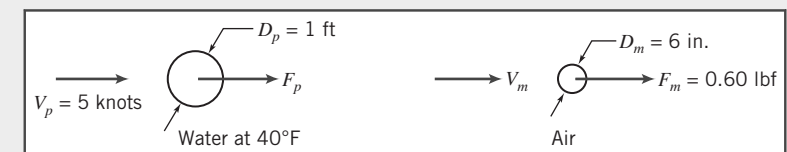
Example 7.4 SIMILARITY: DRAG OF A SONAR TRANSDUCER

The drag of a sonar transducer is to be predicted, based on wind tunnel test data. The prototype, a 1-ft diameter sphere, is to be towed at 5 knots (nautical miles per hour) in seawater at 40°F. The model is 6 in. in diameter. Determine the required test speed in air. If the drag of the model at these test conditions is 0.60 lbf, estimate the drag of the prototype.

Given: Sonar transducer to be tested in a wind tunnel.

Find: (a) V_m .
 (b) F_p .

Solution: Since the prototype operates in water and the model test is to be performed in air, useful results can be expected only if cavitation effects are absent in the prototype flow and compressibility effects are absent from the model test. Under these conditions,



$$\frac{F}{\rho V^2 D^2} = f \left(\frac{\rho V D}{\mu} \right)$$

and the test should be run at

$$Re_{\text{model}} = Re_{\text{prototype}}$$

to ensure dynamic similarity. For seawater at 40°F, $\rho = 1.99 \text{ slug}/\text{ft}^3$ and $\nu \approx 1.69 \times 10^{-5} \text{ ft}^2/\text{s}$. At prototype conditions,

$$V_p = 5 \frac{\text{nmi}}{\text{hr}} \times 6080 \frac{\text{ft}}{\text{nmi}} \times \frac{\text{hr}}{3600 \text{ s}} = 8.44 \text{ ft/s}$$

$$Re_p = \frac{V_p D_p}{\nu_p} = 8.44 \frac{\text{ft}}{\text{s}} \times 1 \text{ ft} \times \frac{\text{s}}{1.69 \times 10^{-5} \text{ ft}^2} = 4.99 \times 10^5$$

The model test conditions must duplicate this Reynolds number. Thus

$$Re_m = \frac{V_m D_m}{\nu_m} = 4.99 \times 10^5$$

For air at STP, $\rho = 0.00238 \text{ slug}/\text{ft}^3$ and $\nu = 1.57 \times 10^{-4} \text{ ft}^2/\text{s}$. The wind tunnel must be operated at

$$V_m = Re_m \frac{\nu_m}{D_m} = 4.99 \times 10^5 \times 1.57 \times 10^{-4} \frac{\text{ft}^2}{\text{s}} \times \frac{1}{0.5 \text{ ft}}$$

$V_m = 157 \text{ ft/s} \leftarrow \overbrace{\phantom{157 \text{ ft/s}}}^{V_m}$

This speed is low enough to neglect compressibility effects.

At these test conditions, the model and prototype flows are dynamically similar. Hence

$$\frac{F}{\rho V^2 D^2} \Big)_m = \frac{F}{\rho V^2 D^2} \Big)_p$$

and

$$F_p = F_m \frac{\rho_p V_p^2 D_p^2}{\rho_m V_m^2 D_m^2} = 0.60 \text{ lbf} \times \frac{1.99}{0.00238} \times \frac{(8.44)^2}{(157)^2} \times \frac{1}{(0.5)^2}$$

$F_p = 5.8 \text{ lbf} \leftarrow \overbrace{\phantom{5.8 \text{ lbf}}}^{F_p}$

If cavitation were expected—if the sonar probe were operated at high speed near the free surface of the seawater—then useful results could not be obtained from a model test in air.

This problem:

- Demonstrates the calculation of prototype values from model test data.
- “Reinvented the wheel”: the results for drag on a smooth sphere are very well known, so we did not need to do a model experiment but instead could have simply read from the graph of Fig. 7.1 the value of $C_D = F_p / (\frac{1}{2} \rho V_p^2 \frac{\pi}{4} D_p^2) \approx 0.1$, corresponding to a Reynolds number of 4.99×10^5 . Then $F_p \approx 5.6 \text{ lbf}$ can easily be computed. We will have more to say on drag coefficients in Chapter 9.

Incomplete Similarity

We have shown that to achieve complete dynamic similarity between geometrically similar flows, it is necessary to duplicate the values of the independent dimensionless groups; by so doing the value of the dependent parameter is then duplicated.

In the simplified situation of Example 7.4, duplicating the Reynolds number value between model and prototype ensured dynamically similar flows. Testing in air allowed the Reynolds number to be duplicated exactly. The drag force on a sphere actually depends on the nature of the boundary-layer flow. Therefore, geometric similarity requires that the relative surface roughness of the model and prototype be the same. This means that relative roughness also is a parameter that must be duplicated between model and prototype situations. If we assume that the model was constructed carefully, measured values of drag from model tests could be scaled to predict drag for the operating conditions of the prototype.

In many model studies, to achieve dynamic similarity requires duplication of several dimensionless groups. In some cases, complete dynamic similarity between model and prototype may not be attainable. Determining the drag force (resistance) of a surface ship is an example of such a situation. Resistance on a surface ship arises from skin friction on the hull (viscous forces) and surface wave resistance (gravity forces). Complete dynamic similarity requires that both Reynolds and Froude numbers be duplicated between model and prototype.

In general it is not possible to predict wave resistance analytically, so it must be modeled. This requires that

$$Fr_m = \frac{V_m}{(gL_m)^{1/2}} = Fr_p = \frac{V_p}{(gL_p)^{1/2}}$$

To match Froude numbers between model and prototype therefore requires a velocity ratio of

$$\frac{V_m}{V_p} = \left(\frac{L_m}{L_p}\right)^{1/2}$$

to ensure dynamically similar surface wave patterns.

Hence for any model length scale, matching the Froude numbers determines the velocity ratio. Only the kinematic viscosity can then be varied to match Reynolds numbers. Thus

$$Re_m = \frac{V_m L_m}{\nu_m} = Re_p = \frac{V_p L_p}{\nu_p}$$

leads to the condition that

$$\frac{\nu_m}{\nu_p} = \frac{V_m}{V_p} \frac{L_m}{L_p}$$

If we use the velocity ratio obtained from matching the Froude numbers, equality of Reynolds numbers leads to a kinematic viscosity ratio requirement of

$$\frac{\nu_m}{\nu_p} = \left(\frac{L_m}{L_p}\right)^{1/2} \frac{L_m}{L_p} = \left(\frac{L_m}{L_p}\right)^{3/2}$$

If $L_m/L_p = \frac{1}{100}$, which a typical length scale for ship model tests, then ν_m/ν_p must be $\frac{1}{1000}$. Figure A.3 shows that mercury is the only liquid with kinematic viscosity less than that of water. However, it is only about an order of magnitude less, so the kinematic viscosity ratio required to duplicate Reynolds numbers cannot be attained.

We conclude that we have a problem in which it is impossible in practice for this model/prototype scale of $\frac{1}{100}$ to satisfy both the Reynolds number and Froude number criteria. At best we will be able to satisfy only one of them. In addition, water is the only practical fluid for most model tests of free-surface flows. To obtain complete dynamic similarity then would require a full-scale test. However, model studies do provide useful information even though complete similarity cannot be obtained. As an example, Fig. 7.2 shows data from a test of a 1:80 scale model of a ship conducted at the U.S. Naval Academy

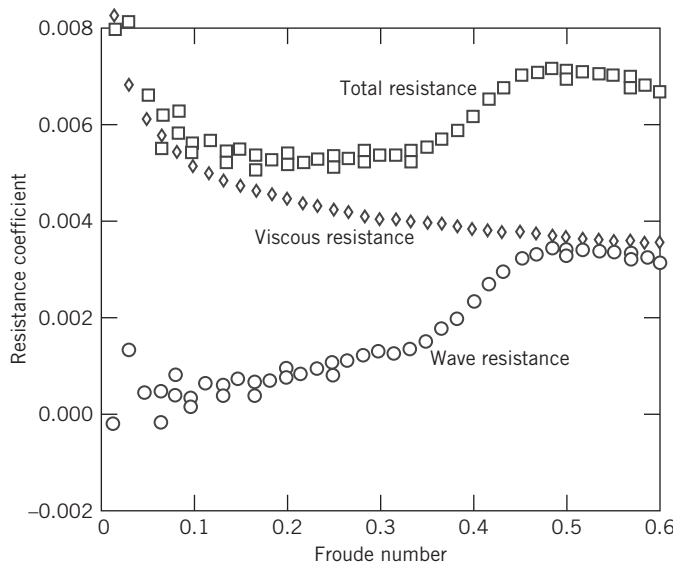


Fig. 7.2 Data from test of 1:80 scale model of U.S. Navy guided missile frigate Oliver Hazard Perry (FFG-7). (Data from U.S. Naval Academy Hydromechanics Laboratory, courtesy of Professor Bruce Johnson.)

Hydromechanics Laboratory. The plot displays “resistance coefficient” data versus Froude number. The square points are calculated from values of total resistance measured in the test. We would like to obtain the corresponding total resistance curve for the full-scale ship.

If you think about it, we can *only* measure the total drag (the square data points). The total drag is due to both wave resistance (dependent on the Froude number) and friction resistance (dependent on the Reynolds number), and it's not possible to determine experimentally how much each contributes. We *cannot* use the total drag curve of Fig. 7.2 for the full-scale ship because, as we have discussed above, we can never set up the model conditions so that its Reynolds number *and* Froude number match those of the full-scale ship. Nevertheless, we would like to extract from Fig. 7.2 the corresponding total drag curve for the full-scale ship. In many experimental situations we need to use a creative “trick” to come up with a solution. In this case, the experimenters used boundary-layer theory (which we discuss in Chapter 9) to *predict* the viscous resistance component of the model (shown as diamonds in Fig. 7.2); then they estimated the wave resistance (not obtainable from theory) by simply subtracting this theoretical viscous resistance from the experimental total resistance, point by point (shown as circles in Fig. 7.2).

Using this idea, Fig. 7.2 therefore gives the wave resistance of the model as a function of Froude number. It is *also* valid for the full-scale ship, because wave resistance depends only on the Froude number! We can now build a graph similar to Fig. 7.2 valid for the full-scale ship: Simply compute from boundary-layer theory the viscous resistance of the full-scale ship and add this to the wave resistance values, point by point. The result is shown in Fig. 7.3. The wave resistance points are identical to those in Fig. 7.2; the viscous resistance points are computed from theory and the predicted total resistance curve for the full-scale ship is finally obtained.

In this example, incomplete modeling was overcome by using analytical computations. The model experiments modeled the Froude number, but not the Reynolds number.

Because the Reynolds number cannot be matched for model tests of surface ships, the boundary-layer behavior is not the same for model and prototype. The model Reynolds number is only $(L_m/L_p)^{3/2}$ as large as the prototype value, so the extent of laminar flow in the boundary layer on the model is too large by a corresponding factor. The method just described assumes that boundary-layer behavior can be scaled. To make this possible, the model boundary layer is “tripped” or “stimulated” to become turbulent

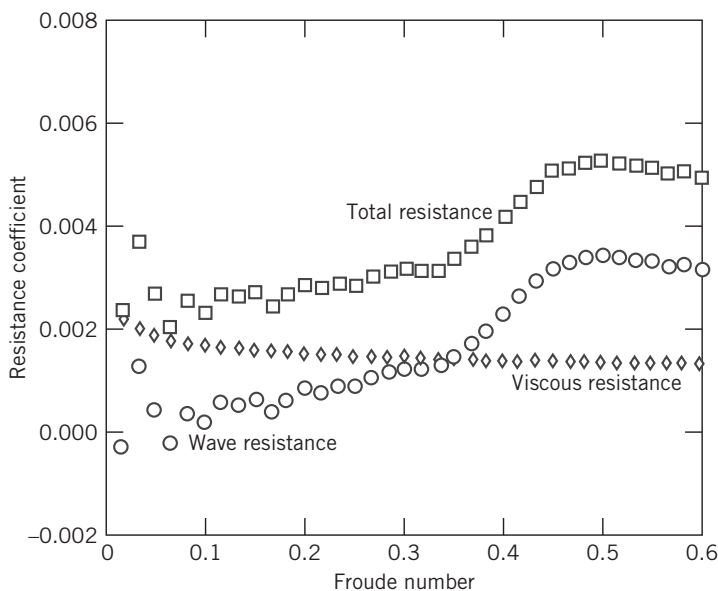


Fig. 7.3 Resistance of full-scale ship predicted from model test results. (Data from U.S. Naval Academy Hydromechanics Laboratory, courtesy of Professor Bruce Johnson.)

at a location that corresponds to the behavior on the full-scale vessel. "Studs" were used to stimulate the boundary layer for the model test results shown in Fig. 7.2.

A correction sometimes is added to the full-scale coefficients calculated from model test data. This correction accounts for roughness, waviness, and unevenness that inevitably are more pronounced on the full-scale ship than on the model. Comparisons between predictions from model tests and measurements made in full-scale trials suggest an overall accuracy within ± 5 percent [5].

As we will see in Chapter 11, the Froude number is an important parameter in the modeling of rivers and harbors. In these situations it is not practical to obtain complete similarity. Use of a reasonable model scale would lead to extremely small water depths, so that viscous forces and surface tension forces would have much larger relative effects in the model flow than in the prototype. Consequently, different length scales are used for the vertical and horizontal directions. Viscous forces in the deeper model flow are increased using artificial roughness elements.

Emphasis on fuel economy has made reduction of aerodynamic drag important for automobiles, trucks, and buses. Most work on development of low-drag configurations is done using model tests. Traditionally, automobile models have been built to $\frac{3}{8}$ scale, at which a model of a full-size automobile has a frontal area of about 0.3 m^2 . Thus testing can be done in a wind tunnel with test section area of 6 m^2 or larger. At $\frac{3}{8}$ scale, a wind speed of about 150 mph is needed to model a prototype automobile traveling at the legal speed limit. Thus there is no problem with compressibility effects, but the scale models are expensive and time-consuming to build.

A large wind tunnel with test section dimensions are 5.4 m high, 10.4 m wide, and 21.3 m long and a maximum air speed of 250 km/hr is used by General Motors to test full-scale automobiles at highway speeds. The large test section allows use of production autos or of full-scale clay mockups of proposed auto body styles. Many other vehicle manufacturers are using comparable facilities; Fig. 7.4 shows a full-size sedan under test in the Volvo wind tunnel. The relatively low speed permits flow visualization using tufts or "smoke" streams. Using full-size "models," stylists and engineers can work together to achieve optimum results.

It is harder to achieve dynamic similarity in tests of trucks and buses; models must be made to smaller scale than those for automobiles. A large scale for truck and bus testing is 1:8. To achieve complete dynamic similarity by matching Reynolds numbers at this scale would require a test speed of 440 mph.



Courtesy of Volvo Cars of North America

Fig. 7.4 Full-scale automobile under test in Volvo wind tunnel, using smoke streaklines for flow visualization.

This would introduce unwanted compressibility effects, and model and prototype flows would not be kinematically similar. Fortunately, trucks and buses are “bluff” objects. Experiments show that above a certain Reynolds number, their nondimensional drag becomes independent of Reynolds number [6]. Figure 7.1 shows that for a sphere, the dimensionless drag is approximately constant for $2000 < Re < 2 \times 10^5$.) Although similarity is not complete, measured test data can be scaled to predict prototype drag forces. The procedure is illustrated in Example 7.5.

Example 7.5 INCOMPLETE SIMILARITY: AERODYNAMIC DRAG ON A BUS

The following wind tunnel test data from a 1:16 scale model of a bus are available:

Air speed (m/s)	18.0	21.8	26.0	30.1	35.0	38.5	40.9	44.1	46.7
Drag force (N)	3.10	4.41	6.09	7.97	10.7	12.9	14.7	16.9	18.9

Using the properties of standard air, calculate and plot the dimensionless aerodynamic drag coefficient,

$$C_D = \frac{F_D}{\frac{1}{2}\rho V^2 A}$$

versus Reynolds number $Re = \rho V w / \mu$, where w is model width. Find the minimum test speed above which C_D remains constant. Estimate the aerodynamic drag force and power requirement for the prototype vehicle at 100 km/hr. (The width and frontal area of the prototype are 8 ft and 84 ft², respectively.)

Given: Data from a wind tunnel test of a model bus. Prototype dimensions are width of 8 ft and frontal area of 84 ft². Model scale is 1:16. Standard air is the test fluid.

Find: (a) Aerodynamic drag coefficient, $C_D = F_D / \frac{1}{2}\rho V^2 A$, versus Reynolds number, $Re = \rho V w / \mu$; plot.
 (b) Speed above which C_D is constant.
 (c) Estimated aerodynamic drag force and power required for the full-scale vehicle at 100 km/hr.

Solution: The model width is

$$w_m = \frac{1}{16} w_p = \frac{1}{16} \times 8 \text{ ft} \times 0.3048 \frac{\text{m}}{\text{ft}} = 0.152 \text{ m}$$

The model area is

$$A_m = \left(\frac{1}{16}\right)^2 A_p = \left(\frac{1}{16}\right)^2 \times 84 \text{ ft}^2 \times (0.305)^2 \frac{\text{m}^2}{\text{ft}^2} = 0.0305 \text{ m}^2$$

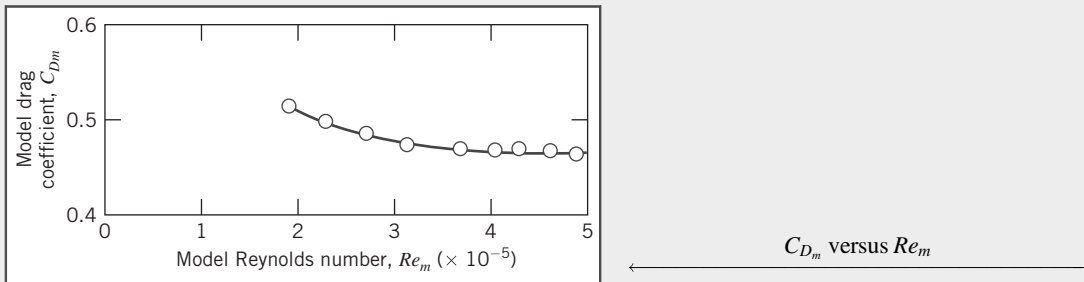
The aerodynamic drag coefficient may be calculated as

$$\begin{aligned} C_D &= \frac{F_D}{\frac{1}{2}\rho V^2 A} \\ &= 2 \times F_D (\text{N}) \times \frac{\text{m}^3}{1.23 \text{ kg}} \times \frac{\text{s}^2}{(\text{V})^2 \text{ m}^2} \times \frac{1}{0.0305 \text{ m}^2} \times \frac{\text{kg} \cdot \text{m}}{\text{N} \cdot \text{s}^2} \\ C_D &= \frac{53.3 F_D (\text{N})}{[\text{V}(\text{m/s})]^2} \end{aligned}$$

The Reynolds number may be calculated as

$$\begin{aligned} Re &= \frac{\rho V w}{\mu} = \frac{V w}{\nu} = V \frac{\text{m}}{\text{s}} \times 0.152 \text{ m} \times \frac{\text{s}}{1.46 \times 10^{-5} \text{ m}^2} \\ Re &= 1.04 \times 10^4 V(\text{m/s}) \end{aligned}$$

The calculated values are plotted in the following figure:



The plot shows that the model drag coefficient becomes constant at $C_{Dm} \approx 0.46$ above $Re_m = 4 \times 10^5$, which corresponds to an air speed of approximately 40 m/s. Since the drag coefficient is independent of Reynolds number above $Re \approx 4 \times 10^5$, then for the prototype vehicle ($Re \approx 4.5 \times 10^6$), $C_D \approx 0.46$. The drag force on the full-scale vehicle is

$$\begin{aligned} F_{D_p} &= C_D \frac{1}{2} \rho V_p^2 A_p \\ &= \frac{0.46}{2} \times 1.23 \frac{\text{kg}}{\text{m}^3} \left(100 \frac{\text{km}}{\text{hr}} \times 1000 \frac{\text{m}}{\text{km}} \times \frac{\text{hr}}{3600 \text{ s}} \right)^2 \times 84 \frac{\text{ft}^2}{\text{ft}^2} \times (0.305)^2 \frac{\text{m}^2}{\text{ft}^2} \times \frac{\text{N} \cdot \text{s}^2}{\text{kg} \cdot \text{m}} \\ F_{D_p} &= 1.71 \text{ kN} \end{aligned}$$

The corresponding power required to overcome aerodynamic drag is

$$\begin{aligned} \mathcal{P}_p &= F_{D_p} V_p \\ &= 1.71 \times 10^3 \text{ N} \times 100 \frac{\text{km}}{\text{hr}} \times 1000 \frac{\text{m}}{\text{km}} \\ &\quad \times \frac{\text{hr}}{3600 \text{ s}} \times \frac{\text{W} \cdot \text{s}}{\text{N} \cdot \text{m}} \\ \mathcal{P}_p &= 47.5 \text{ kW} \end{aligned}$$

This problem illustrates a common phenomenon in aerodynamics: Above a certain minimum Reynolds number the drag coefficient of an object usually approaches a constant—that is, becomes independent of the Reynolds number. Hence, in these situations we do not have to match the Reynolds numbers of the model and prototype in order for them to have the same drag coefficient—a considerable advantage. However, the SAE Recommended Practices [6] suggests $Re \geq 2 \times 10^6$ for truck and bus testing.

For additional details on techniques and applications of dimensional analysis consult [7–10].

Scaling with Multiple Dependent Parameters

In some situations of practical importance there may be more than one dependent parameter. In such cases, dimensionless groups must be formed separately for each dependent parameter.

As an example, consider a typical centrifugal pump. The detailed flow pattern within a pump changes with volume flow rate and speed and these changes affect the pump's performance. Performance parameters of interest include the pressure rise (or head) developed, the power input required, and the machine efficiency measured under specific operating conditions. Performance curves are generated by varying an independent parameter such as the volume flow rate. Thus the independent variables are volume flow rate, angular speed, impeller diameter, and fluid properties. Dependent variables are the several performance quantities of interest.

Finding dimensionless parameters begins from the symbolic equations for the dependence of head, h (energy per unit mass, L^2/t^2), and power, \mathcal{P} , on the independent parameters, given by

$$h = g_1(Q, \rho, \omega, D, \mu)$$

and

$$\mathcal{P} = g_2(Q, \rho, \omega, D, \mu)$$

Straightforward use of the Pi theorem gives the dimensionless *head coefficient* and *power coefficient* as

$$\frac{h}{\omega^2 D^2} = f_1 \left(\frac{Q}{\omega D^3}, \frac{\rho \omega D^2}{\mu} \right) \quad (7.17)$$

and

$$\frac{\mathcal{P}}{\rho \omega^3 D^5} = f_2 \left(\frac{Q}{\omega D^3}, \frac{\rho \omega D^2}{\mu} \right) \quad (7.18)$$

The dimensionless parameter $Q/\omega D^3$ in these equations is called the *flow coefficient*. The dimensionless parameter $\rho \omega D^2/\mu (\propto \rho VD/\mu)$ is a form of Reynolds number.

Head and power in a pump are developed by inertia forces. Both the flow pattern within a pump and the pump performance change with volume flow rate and speed of rotation. Performance is difficult to predict analytically except at the design point of the pump, so it is measured experimentally. Typical characteristic curves plotted from experimental data for a centrifugal pump tested at constant speed are shown in Fig. 7.5 as functions of volume flow rate. The head, power, and efficiency curves in Fig. 7.5 are smoothed through points calculated from measured data. Maximum efficiency usually occurs at the design point.

Complete similarity in pump performance tests would require identical flow coefficients and Reynolds numbers. In practice, it has been found that viscous effects are relatively unimportant when two geometrically similar machines operate under “similar” flow conditions. Thus, from Eqs. 7.17 and 7.18, when

$$\frac{Q_1}{\omega_1 D_1^3} = \frac{Q_2}{\omega_2 D_2^3} \quad (7.19)$$

it follows that

$$\frac{h_1}{\omega_1^2 D_1^2} = \frac{h_2}{\omega_2^2 D_2^2} \quad (7.20)$$

and

$$\frac{\mathcal{P}_1}{\rho_1 \omega_1^3 D_1^5} = \frac{\mathcal{P}_2}{\rho_2 \omega_2^3 D_2^5} \quad (7.21)$$

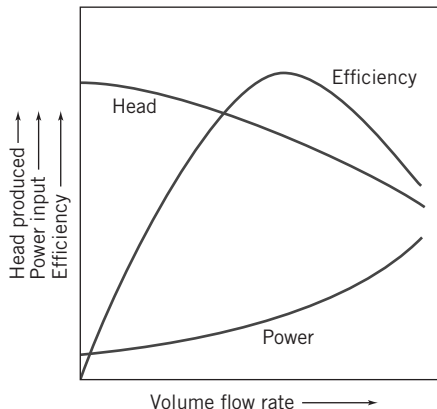


Fig. 7.5 Typical characteristic curves for centrifugal pump tested at constant speed.

The empirical observation that viscous effects are unimportant under similar flow conditions allows use of Eqs. 7.19 through 7.21 to scale the performance characteristics of machines to different operating conditions, as either the speed or diameter is changed. These useful scaling relationships are known as pump or fan “laws.” If operating conditions for one machine are known, operating conditions for any geometrically similar machine can be found by changing D and ω according to Eqs. 7.19 through 7.21. More details on dimensional analysis, design, and performance curves for fluid machinery are presented in Chapter 10.

Another useful pump parameter can be obtained by eliminating the machine diameter from Eqs. 7.19 and 7.20. If we designate $\Pi_1 = Q/\omega D^3$ and $\Pi_2 = h/\omega^2 D^2$, then the ratio $\Pi_1^{1/2}/\Pi_2^{3/4}$ is another dimensionless parameter; this parameter is the *specific speed*, N_s ,

$$N_s = \frac{\omega Q^{1/2}}{h^{3/4}} \quad (7.22a)$$

The specific speed, as defined in Eq. 7.22a, is a dimensionless parameter provided that the head, h , is expressed as energy per unit mass. You may think of specific speed as the speed required for a machine to produce unit head at unit volume flow rate. A constant specific speed describes all operating conditions of geometrically similar machines with similar flow conditions.

Although specific speed is a dimensionless parameter, it is common practice to use a convenient but inconsistent set of units in specifying the variables ω and Q , and to use the energy per unit weight H in place of energy per unit mass h in Eq. 7.22a. When this is done the specific speed,

$$N_{s_{cu}} = \frac{\omega Q^{1/2}}{H^{3/4}} \quad (7.22b)$$

is not a unitless parameter and its magnitude depends on the units used to calculate it. Customary units used in U.S. engineering practice for pumps are rpm for ω , gpm for Q , and feet (energy per unit weight) for H . In these customary U.S. units, “low” specific speed means $500 < N_{s_{cu}} < 4000$ and “high” means $10,000 < N_{s_{cu}} < 15,000$. Example 7.6 illustrates use of the pump scaling laws and specific speed parameter. More details of specific speed calculations and additional examples of applications to fluid machinery are presented in Chapter 10.

Example 7.6 PUMP “LAWS”

A centrifugal pump has an efficiency of 80 percent at its design-point specific speed of 2000 (units of rpm, gpm, and feet). The impeller diameter is 8 in. At design-point flow conditions, the volume flow rate is 300 gpm of water at 1170 rpm. To obtain a higher flow rate, the pump is to be fitted with a 1750 rpm motor. Use the pump “laws” to find the design-point performance characteristics of the pump at the higher speed. Show that the specific speed remains constant for the higher operating speed. Determine the motor size required.

Given: Centrifugal pump with design specific speed of 2000 (in rpm, gpm, and feet units). Impeller diameter is $D = 8$ in. At the pump’s design-point flow conditions, $\omega = 1170$ rpm and $Q = 300$ gpm, with water.

Find: (a) Performance characteristics,
 (b) specific speed, and
 (c) motor size required, for similar flow conditions at 1750 rpm.

Solution: From pump “laws,” $Q/\omega D^3 = \text{constant}$, so

$$Q_2 = Q_1 \frac{\omega_2}{\omega_1} \left(\frac{D_2}{D_1} \right)^3 = 300 \text{ gpm} \left(\frac{1750}{1170} \right) (1)^3 = 449 \text{ gpm} \quad Q_2$$

The pump head is not specified at $\omega_1 = 1170$ rpm, but it can be calculated from the specific speed, $N_{s_{cu}} = 2000$. Using the given units and the definition of $N_{s_{cu}}$,

$$N_{s_{cu}} = \frac{\omega Q^{1/2}}{H^{3/4}} \quad \text{so} \quad H_1 = \left(\frac{\omega_1 Q_1^{1/2}}{N_{s_{cu}}} \right)^{4/3} = 21.9 \text{ ft}$$

Then $H/\omega^2 D^2 = \text{constant}$, so

$$H_2 = H_1 \left(\frac{\omega_2}{\omega_1} \right)^2 \left(\frac{D_2}{D_1} \right)^2 = 21.9 \text{ ft} \left(\frac{1750}{1170} \right)^2 (1)^2 = 49.0 \text{ ft} \xrightarrow{\hspace{10cm}} H_2$$

The pump output power is $\mathcal{P}_1 = \rho g Q_1 H_1$, so at $\omega_1 = 1170$ rpm,

$$\begin{aligned} \mathcal{P}_1 &= 1.94 \frac{\text{slug}}{\text{ft}^3} \times 32.2 \frac{\text{ft}}{\text{s}^2} \times 300 \frac{\text{gal}}{\text{min}} \times 21.9 \text{ ft} \times \frac{\text{ft}^3}{7.48 \text{ gal}} \times \frac{\text{min}}{60 \text{ s}} \times \frac{\text{lbf} \cdot \text{s}^2}{\text{slug} \cdot \text{ft}} \times \frac{\text{hp} \cdot \text{s}}{550 \text{ ft} \cdot \text{lbf}} \\ \mathcal{P}_1 &= 1.66 \text{ hp} \end{aligned}$$

But $\mathcal{P}/\rho \omega^3 D^5 = \text{constant}$, so

$$\mathcal{P}_2 = \mathcal{P}_1 \left(\frac{\rho_2}{\rho_1} \right) \left(\frac{\omega_2}{\omega_1} \right)^3 \left(\frac{D_2}{D_1} \right)^5 = 1.66 \text{ hp} (1) \left(\frac{1750}{1170} \right)^3 (1)^5 = 5.55 \text{ hp} \xrightarrow{\hspace{10cm}} \mathcal{P}_2$$

The required input power may be calculated as

$$\mathcal{P}_{\text{in}} = \frac{\mathcal{P}_2}{\eta} = \frac{5.55 \text{ hp}}{0.80} = 6.94 \text{ hp} \xrightarrow{\hspace{10cm}} \mathcal{P}_{\text{in}}$$

Thus a 7.5-hp motor (the next larger standard size) probably would be specified.

The specific speed at $\omega_2 = 1750$ rpm is

$$N_{s_{cu}} = \frac{\omega Q^{1/2}}{H^{3/4}} = \frac{1750(449)^{1/2}}{(49.0)^{3/4}} = 2000 \xrightarrow{\hspace{10cm}} N_{s_{cu}}$$

This problem illustrates application of the pump “laws” and specific speed to scaling of performance data. Pump and fan “laws” are used widely in industry to scale performance curves for families of machines from a single performance curve, and to specify drive speed and power in machine applications.

Comments on Model Testing

While outlining the procedures involved in model testing, we have tried not to imply that testing is a simple task that automatically gives results that are easily interpreted, accurate, and complete. As in all experimental work, careful planning and execution are needed to obtain valid results. Models must be constructed carefully and accurately, and they must include sufficient detail in areas critical to the phenomenon being measured. Aerodynamic balances or other force measuring systems must be aligned carefully and calibrated correctly. Mounting methods must be devised that offer adequate rigidity and model motion, yet do not interfere with the phenomenon being measured. References [11–13] are considered the standard sources for details of wind tunnel test techniques. More specialized techniques for water impact testing are described in Waugh and Stubstad [14].

Experimental facilities must be designed and constructed carefully. The quality of flow in a wind tunnel must be documented. Flow in the test section should be as nearly uniform as possible (unless the desire is to simulate a special profile such as an atmospheric boundary layer), free from angularity, and with little swirl. If they interfere with measurements, boundary layers on tunnel walls must be removed

by suction or energized by blowing. Pressure gradients in a wind tunnel test section may cause erroneous drag-force readings due to pressure variations in the flow direction.

7.5 Summary and Useful Equations

In this chapter we have:

- ✓ Obtained dimensionless coefficients by nondimensionalizing the governing differential equations of a problem.
- ✓ Stated the Buckingham Pi theorem and used it to determine the independent and dependent dimensionless parameters from the physical parameters of a problem.
- ✓ Defined a number of important dimensionless groups: the Reynolds number, Euler number, cavitation number, Froude number, Weber number, and Mach number, and discussed their physical significance.

We have also explored some ideas behind modeling: geometric, kinematic, and dynamic similarity, incomplete modeling, and predicting prototype results from model tests.

Note: Most of the equations in the table below have a number of constraints or limitations—*be sure to refer to their page numbers for details!*

Useful Equations

Reynolds number (inertia to viscous):	$Re = \frac{\rho VL}{\mu} = \frac{VL}{\nu}$	(7.11)	Page 212
Euler number (pressure to inertia):	$Eu = \frac{\Delta p}{\frac{1}{2}\rho V^2}$	(7.12a)	Page 213
Drag coefficient	$C_D = \frac{F_D}{\frac{1}{2}\rho V^2 L^2}$	(7.12b)	Page 213
Lift coefficient	$C_L = \frac{F_L}{\frac{1}{2}\rho V^2 L^2}$	(7.12c)	Page 213
Cavitation number:	$Ca = \frac{p - p_v}{\frac{1}{2}\rho V^2}$	(7.13)	Page 213
Froude number (inertia to gravity):	$Fr = \frac{V}{\sqrt{gL}}$	(7.14)	Page 213
Weber number (inertia to surface tension):	$We = \frac{\rho V^2 L}{\sigma}$	(7.15)	Page 213
Mach number (inertia to compressibility):	$M = \frac{V}{c}$	(7.16)	Page 214
Centrifugal pump specific speed (in terms of head h):	$N_s = \frac{\omega Q^{1/2}}{h^{3/4}}$	(7.22a)	Page 223
Centrifugal pump specific speed (in terms of head H):	$N_{s_{cu}} = \frac{\omega Q^{1/2}}{H^{3/4}}$	(7.22b)	Page 223

REFERENCES

1. Kline, S. J., *Similitude and Approximation Theory*. New York: McGraw-Hill, 1965.
2. Hansen, A. G., *Similarity Analysis of Boundary-Value Problems in Engineering*. Englewood Cliffs, NJ: Prentice-Hall, 1964.
3. Schlichting, H., *Boundary Layer Theory*, 7th ed. New York: McGraw-Hill, 1979.
4. Buckingham, E., "On Physically Similar Systems: Illustrations of the Use of Dimensional Equations," *Physical Review*, 4, 4, 1914, pp. 345–376.
5. Todd, L. H., "Resistance and Propulsion," in *Principles of Naval Architecture*, J. P. Comstock, ed. New York: Society of Naval Architects and Marine Engineers, 1967.
6. "SAE Wind Tunnel Test Procedure for Trucks and Buses," *Recommended Practice SAE J1252*, Warrendale, PA: Society of Automotive Engineers, 1981.
7. Sedov, L. I., *Similarity and Dimensional Methods in Mechanics*. New York: Academic Press, 1959.
8. Birkhoff, G., *Hydrodynamics—A Study in Logic, Fact, and Similitude*, 2nd ed. Princeton, NJ: Princeton University Press, 1960.
9. Ipsen, D. C., *Units, Dimensions, and Dimensionless Numbers*. New York: McGraw-Hill, 1960.
10. Yalin, M. S., *Theory of Hydraulic Models*. New York: Macmillan, 1971.
11. Pankhurst, R. C., and D. W. Holder, *Wind-Tunnel Technique*. London: Pitman, 1965.
12. Rae, W. H., and A. Pope, *Low-Speed Wind Tunnel Testing*, 2nd ed. New York: Wiley-Interscience, 1984.
13. Pope, A., and K. L. Goin, *High-Speed Wind Tunnel Testing*. New York: Krieger, 1978.
14. Waugh, J. G., and G. W. Stubstad, *Hydroballistics Modeling*. San Diego, CA: U.S. Naval Undersea Center, ca. 1965.
15. L. Prandtl, *Ergebnisse der aerodynamischen, Veersuchsanstalt su Gottingen*, Vol II, 1923.
16. H. Brauer and D. Sucker, "Umstromung von Platten, Zylindern und Kugeln," *Chemie Ingenieur Technik*, 48. Jahrgang, No. 8, 1976, pp. 655–671. Copyright Wiley-VCH Verlag GmbH & Co. KGaA. Reproduced with permission.

Chapter 8 Problems

Laminar versus Turbulent Flow

8.1 For incompressible flow in a circular tube, derive expressions for Reynolds number in terms of (a) volume flow rate and tube diameter and (b) mass flow rate and tube diameter.

8.2 Determine the maximum flow rate of air at laminar conditions in a 4-in.-diameter pipe at an absolute pressure of 30 psia and 100°F? Determine the maximum flow rate when (a) the pressure is raised to 60 psia, and (b) the temperature is raised to 200°F. Describe the reason for the differences in flow rates in terms of the physical mechanisms involved.

Laminar Flow between Parallel Plates

8.3 An incompressible fluid flows between two infinite stationary parallel plates. The velocity profile is given by $u = u_{\max}(Ay^2 + By + C)$, where A , B , and C are constants and y is measured upward from the lower plate. The total gap width is h . Use appropriate boundary conditions to express the constants in terms of h . Develop an expression for volume flow rate per unit depth and evaluate the ratio \bar{V}/u_{\max} .

8.4 A hydraulic jack supports a load of 9000 kg. The following data are given:

Diameter of piston	100 mm
Radial clearance between piston and cylinder	0.05 mm
Length of piston	120 mm

Estimate the rate of leakage of hydraulic fluid past the piston, assuming the fluid is SAE 30 oil at 30°C.

SS 8.5 A horizontal laminar flow occurs between two infinite parallel plates that are 0.3 m apart. The velocity at the centerline is 2.7 m/s. Determine the flow rate through a section 0.9 m wide, the velocity gradient at the surface of the plate, the wall shearing stress, and the pressure drop for a 30 length. The fluid viscosity is 1.44 N s/m².

8.6 A fully developed and laminar flow of oil occurs between parallel plates. The pressure gradient creating the flow is 1.25 kPa/m of length and the channel half-width is 1.5 mm. Calculate the magnitude and direction of the wall shear stress at the upper plate surface. Find the volume flow rate through the channel. The viscosity is 0.50 N s/m².

8.7 A sealed journal bearing is formed from concentric cylinders. The inner and outer radii are 25 and 26 mm, the journal length is 100 mm, and it turns at 2800 rpm. The gap is filled with oil in laminar motion. The velocity profile is linear across the gap. The torque needed to turn the journal is 0.2 N · m. Calculate the viscosity of the oil. Explain why the torque will increase, decrease, or stay the same with time.

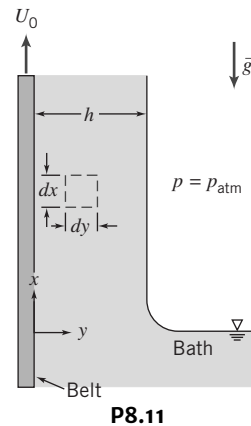
8.8 Two immiscible fluids are of equal thickness are contained between infinite parallel plates separated by a distance $2h$. The lower plate is stationary and the upper plate moves at constant speed of 20 ft/s. The dynamic viscosity of the upper fluid is three times that of the lower fluid. The flow is laminar and the pressure gradient in the direction of flow is zero.

8.9 An incompressible viscous liquid flows steadily down an incline due to gravity. The flow is laminar and the velocity profile, derived in Example 5.9, is $u = \frac{g \sin \theta}{\nu} \left(hy - \frac{y^2}{2} \right)$, where θ is the slope

of the incline and h is the thickness of the film. The fluid kinematic viscosity is 1×10^{-4} m²/s, the slope is 30°, and the film thickness is 0.8 mm. Determine the maximum velocity and the flow rate per meter of width.

8.10 There is a fully developed laminar flow of air between parallel plates. The upper plate moves at 5 ft/s and the spacing between the plates is $a = 0.1$ in. (a) Assume that the air is incompressible and determine the flow rate per unit depth for the case of zero pressure gradient and the shear stress distribution across the channel. (b) Determine the magnitude and direction of the pressure gradient that will give zero shear stress at $y = 0.25a$ and determine the magnitude and direction of the shear stress at both surfaces.

8.11 A continuous belt, passing upward through a chemical bath at speed U_0 , picks up a liquid film of thickness h , density ρ , and viscosity μ . Gravity tends to make the liquid drain down, but the movement of the belt keeps the liquid from running off completely. Assume that the flow is fully developed and laminar with zero pressure gradient, and that the atmosphere produces no shear stress at the outer surface of the film. State clearly the boundary conditions to be satisfied by the velocity at $y = 0$ and $y = h$. Obtain an expression for the velocity profile.



P8.11

Laminar Flow in a Pipe

8.12 Water at 20°C flows in a 1.3 cm diameter pipe that is 30 m long **SS** and discharges to the atmosphere. The pressure at the entrance to the pipe is 0.82 kPa gage. Determine the mass flow rate and Reynolds number.

8.13 Determine the maximum flow rate (kg/s) and corresponding pressure gradient (Pa/m) for which laminar flow would occur for water, SAE 10 W oil, and glycerin. The fluids are at 20°C. Draw some conclusion from your analysis.

8.14 Carbon dioxide flows in a 50-mm-diameter pipe at a velocity of 1.5 m/s, temperature 66°C, and absolute pressure 50 kPa. Determine whether the flow is laminar or turbulent. If the temperature is lowered to 30°C, determine the flow regime. If the pressure is reduced to 20 kPa, determine the flow regime. Explain the differences in answers in terms of the physical mechanisms involved.

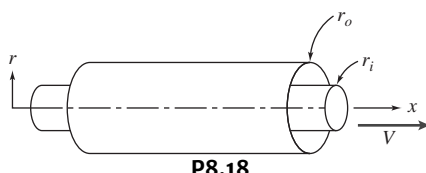
8.15 Oil with a viscosity 1.2 Pa·s and a density of 820 kg/m³ flows in a 0.3 m diameter pipe. The flow is fully established and the velocity at

the center of is 4.5 m/s. Verify that the flow is laminar and calculate the shear stress at the pipe wall, at a radius of 150 mm, and at the centerline.

8.16 Determine the largest diameter of pipeline that may be used to carry 100 gpm of jet fuel (JP-4) at 59°F if the flow is to be laminar.

SS 8.17 A fluid of specific gravity 0.90 flows at a Reynolds number of 1500 in a 0.3-m-diameter pipeline. The velocity 50 mm from the wall is 3 m/s. Calculate the flow rate and the velocity gradient at the wall.

8.18 Consider fully developed laminar flow in the annulus between two concentric pipes. The outer pipe is stationary, and the inner pipe moves in the x direction with speed V . Assume that the axial pressure gradient is zero ($dp/dx = 0$). Obtain a general expression for the shear stress, τ , as a function of the radius, r , in terms of a constant, C_1 . Obtain a general expression for the velocity profile, $u(r)$, in terms of two constants, C_1 and C_2 . Obtain expressions for C_1 and C_2 .



P8.18

Turbulent Velocity Profiles in Fully Developed Pipe Flow

8.19 A fully developed turbulent flow of a fluid in a 3 in. diameter horizontal pipe has a static pressure difference measured between two sections 15 ft apart of 750 psi. Calculate the wall shear stress for the flow.

8.20 For a turbulent flow of a fluid in 0.6 m diameter pipe, the velocity 0.15 m from the wall is 2.7 m/s. Estimate the wall shear stress using the 1/7th expression for the velocity profile.

8.21 The following table gives data for the mean velocity in fully developed turbulent pipe flow at $Re = 50,000$ [5]:

\bar{u}/U	0.996	0.981	0.963	0.937	0.907	0.866	0.831
y/r	0.898	0.794	0.691	0.588	0.486	0.383	0.280
\bar{u}/U	0.792	0.742	0.700	0.650	0.619	0.551	
y/R	0.216	0.154	0.093	0.062	0.041	0.024	

Fit the "power-law" profile for turbulent flow, Eq. 8.22, to the data and obtain a value of n . Plot the data and the correlation on the same graph and verify that Eq. 8.22 is a valid approximation.

8.22 Determine the kinetic energy coefficient α for fully developed laminar flow in a circular tube.

8.23 Using Eqs. 8.24 and 8.27, evaluate the kinetic energy coefficient α for turbulent power law velocity profiles with $n = 1/7$ and $1/10$.

Calculation of Head Loss

8.24 A pipe runs for an elevation of 45 m to an elevation of 115 m. The inlet pressure is 8.5 MPa and the head loss is 6.9 kJ/kg. Calculate the outlet pressure for (a) the inlet at the 45 m elevation and (b) the inlet at the 115 m elevation.

8.25 Water flows in a horizontal 75 mm diameter pipe at an average speed of 5 m/s. The pressure at the pipe inlet is 275 kPa gage and the

outlet is at atmospheric pressure. (a) Determine the head loss in the pipe. Determine the inlet pressure needed to maintain the same flow rate when the pipe is aligned so that (b) the outlet is 15 m above the inlet and (c) the outlet is 15 m below the inlet. (d) Determine how much lower the outlet must be to maintain the same flow rate is maintained if the pressures at both ends of the pipe are atmospheric (i.e., gravity feed).

8.26 A smooth copper tube 50 ft long and 2 1/2 in.-diameter carries a water flow at 60°F of 120 gpm. Determine the pressure drop and head loss for a 50 ft length of tube.

8.27 A reservoir at 300 ft elevation has a 6-in.-diameter discharge pipe located 50 ft below the surface. The pipe is 600 ft long and drops in elevation to 150 ft where the flow discharges to the atmosphere. The pipe is made of riveted steel with a roughness height of 0.005 ft. Determine (a) the flow rate without a head loss and (b) the flow rate with the pipe friction head loss. Since the velocity is not known for part b and the Reynolds number and friction factor depend on velocity, you will need to iterate to find the solution. A good first guess is the velocity from part (a).

8.28 Water flows in a smooth 0.2 m diameter pipeline that is 65 m long. The Reynolds number is 10^6 . Determine the flow rate and pressure drop. After many years of use, minerals deposited on the pipe cause the same pressure drop to produce only one-half the original flow rate. Estimate the size of the relative roughness elements for the pipe.

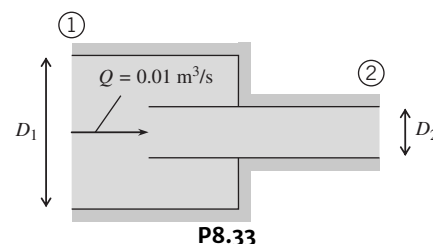
8.29 Two reservoirs are connected by three clean cast-iron pipes in series, $L_1 = 600$ m, $D_1 = 0.3$ m, $L_2 = 900$ m, $D_2 = 0.4$ m, $L_3 = 1500$ m, and $D_3 = 0.45$ m. The flow rate is $0.11 \text{ m}^3/\text{s}$ of water at 15°C. Determine the difference in elevation between the reservoirs.

8.30 A 150-mm-diameter horizontal pipe discharges a $0.05 \text{ m}^3/\text{s}$ flow of water to the atmosphere through a smooth nozzle with a tip diameter of 75 mm diameter. The nozzle loss coefficient is 0.3. Determine the pressure upstream of the nozzle and the head loss assuming (a) the kinetic energy coefficients α are unity and (b) the upstream value of the kinetic energy coefficient is 1.05 and the kinetic energy coefficient of the water in the jet is 1.01. Comment on whether the assumption that the kinetic energy coefficients are unity for turbulent flow is reasonable.

8.31 Water flows through a 2-in.-diameter tube that suddenly contracts to 1 in. diameter. The pressure drop across the contraction is 0.5 psi. Determine the volume flow rate.

8.32 Air at standard conditions flows through a 75 mm diameter circular duct that has a sudden expansion to 225 mm diameter. The pressure downstream is 5 mm of water higher than that upstream. Determine the average speed of the air upstream of the expansion and the volume flow rate.

8.33 Water flows from a larger pipe, diameter $D_1 = 100$ mm, into a smaller one, diameter $D_2 = 50$ mm, by way of a reentrant device. Find the head loss between points (1) and (2).

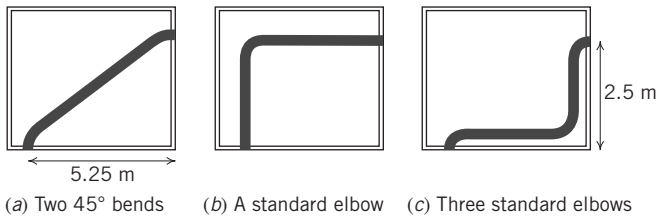


P8.33

Solution of Pipe Flow Problems

8.34 The exhaust duct for a clean room test chamber is 150-mm in diameter and 7 m long. The duct originally had a square-edge entrance, but it was replaced by a well-rounded entrance. The pressure in the chamber is maintained 2.5 mm of water above ambient. Neglect the friction losses in the short duct and determine the volume flow rate for the original square-edge entrance and the well-rounded one.

SS 8.35 A 5-cm-diameter potable water line is to be run through a maintenance room in a commercial building. Three possible layouts for the galvanized iron water line are proposed as shown in the figure. The bends are conventional threaded fittings. Select the option that minimizes losses and determine the pressure drop for a flow of 350 L/min.



P8.35

SS 8.36 A fire hose and nozzle assembly is being designed to deliver 0.75 ft³/s of water. The hose is 3 in. in diameter with a relative roughness of 0.004. The fire hose is made up of four 60 ft sections joined by couplings. The hose connection to the hydrant is square-edged. The nozzle is a gradual contraction with a 90° included angle and an exit diameter of 1 in. Determine the supply pressure required. Under operating conditions two more sections might be coupled to the hose. Determine the flow rate with this situation for the design supply pressure assuming the friction factor is the same as for design conditions.

8.37 Determine the flow rate (gpm) of 0°C water that will be produced in a 75-mm-diameter pipe that is 200 m long for a pressure drop of 425 kPa. The pipe roughness element size is 2.5 mm.

SS 8.38 Water flows steadily in a 125-mm-diameter cast-iron pipe 150 m long. The pressure drop between sections ① and ② is 150 kPa, and section ② is located 15 m above section ①. Find the volume flow rate.

8.39 Hydraulic mining is to be done using water from a lake located 300 m above the mine site. A 900 m long fire hose with an inside diameter of 75 mm and a relative roughness of 0.01 will be used. Couplings are located every 10 m along the hose. The nozzle outlet diameter is 25 mm and its loss coefficient is 0.04 based on the upstream velocity. Estimate the maximum outlet velocity from the hose and the maximum force exerted on a rock face by the water jet.

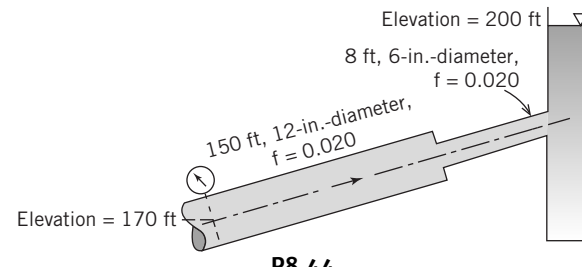
8.40 Two water tanks are connected by a horizontal pipeline. The first tank has a square-edged outlet 3 m below the surface that is connected to a 50-mm-diameter PVC pipe. At 15 m from the tank the pipe is connected to a 100-mm-diameter pipe which runs 30 m to the outlet that is 0.6 m below the surface of the second tank. The water temperature is 20°C. Determine the flow rate through the pipe line.

8.41 Determine the diameter of a smooth steel pipe that will carry 50 cfs of water between a reservoir with a surface at an elevation of 250 ft and one at 100 ft that are located 2 miles apart.

8.42 A 4-ft-diameter cast iron pipeline 4 miles long connects two reservoirs with surface elevations of 500 and 300 ft. It is proposed to increase the flow rate through the line by installing a smooth liner that is just thick enough to cover the roughness elements, reducing the pipe diameter somewhat. Determine the current flow rate and the increase in flow rate using the liner. The water is at 68°F and pipe friction is the dominant loss.

8.43 An industrial plant requires a water flow rate of 5.7 m³/min. **SS** The gage pressure in the water main, located in the street 50 m from the plant, is 800 kPa and the gage pressure required in the plant is 500 kPa. The supply line will require installation of 4 elbows in a total length of 65 m. Determine the smallest size of galvanized iron line that should be installed.

8.44 In the system shown in the figure, the water velocity in the 12 in. diameter pipe is 8 ft/s. Determine the gage reading.

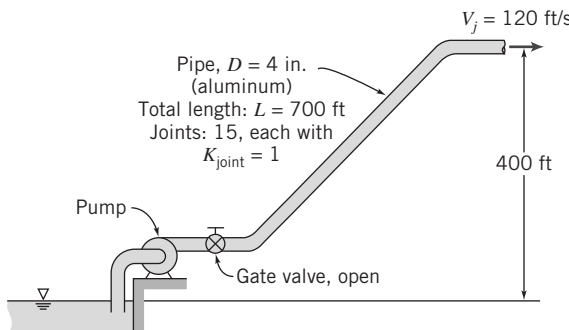


P8.44

8.45 Determine the minimum size smooth rectangular duct with an aspect ratio of 3 that will pass 1 m³/s of 10°C air with a head loss of 25 mm of water per 100 m of duct.

8.46 Determine the diameter of a 175 m long pipe with a roughness of 2.5 mm that will provide a flow of 0.075 m³/s with a 500 kPa pressure drop.

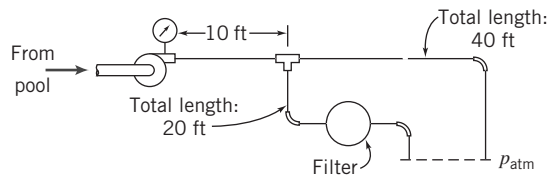
8.47 Cooling water is pumped from a reservoir to rock drills on a construction job using the pipe system shown. The flow rate must be 600 gpm and water must leave the spray nozzle at 120 ft/s. Calculate the minimum pressure needed at the pump outlet. Estimate the required power input if the pump efficiency is 70 percent.



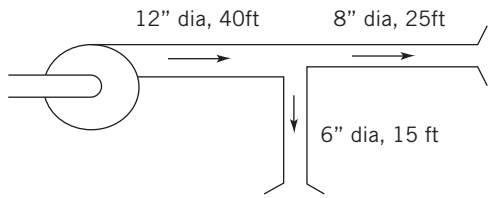
8.48 A new pump is required for the water supply system of a high-rise office building. The system requires 0.06 m³/s of water pumped to a reservoir at the top of the tower 340 m above the street. City water pressure at the street-level pump inlet is 400 kPa gage. The piping is to be commercial steel, the overall length is 20 percent greater than the tower height, and there are fittings every 10 m with loss coefficients of 0.2. Determine the minimum diameter required to keep the average water velocity below 3.5 m/s in the pipe. Calculate the

pressure rise required across the pump and estimate the minimum power needed to drive the pump.

8.49 A swimming pool has a partial-flow filtration system. Water at 75°F is pumped from the pool through the system shown. The pump delivers 30 gpm. The pipe is nominal 3/4-in. PVC (ID = 0.824 in.). The pressure loss through the filter is approximated as $\Delta p = 0.6 Q^2$, where Δp is in psi and Q is in gpm. Determine the pump pressure and the flow rate through each branch of the system.



8.50 An air conditioning system delivers 850 cfm of air at 55°F to two zones as shown in the figure below. The ducts are galvanized steel sheet metal. There are diffusers at the end of the ducts with loss coefficients of 0.8. Estimate the flow rate in each duct, the pressure at the fan exit, and the fan power required. The loss coefficients for the tee, based on the downstream velocity, are 0.13 for the straight-through flow and 1.2 for the turning flow.



8.51 A 75-mm-diameter orifice with D and D/2 taps is used to measure the flow rate of 65°C water in a 150-mm-ID pipe. Determine the pressure difference for a flow rate of 20 L/s.

8.52 A 12 in. \times 6 in. Venturi meter is installed in a horizontal water-line. The pressure gages read 30 and 20 psi. Calculate the flow rate for a water temperature of 68°F and the head loss between the base and throat of the meter. Calculate the flow rate if the pipe is vertical with the throat of the meter 2 ft below the base and the pressure gages read the same values.

8.53 An 8 in. diameter water pipe has a 5.2 in. diameter ASME long-radius nozzle installed for flow metering. The mercury-water manometer used to measure the pressure difference reads 3.2 in. mercury. Determine the mass and volume flow rate for water temperatures of 40°F and 180°F. Because the nozzle coefficient depends on Reynolds number and the flow rate is unknown, you will need to iterate to find the flow rate.

8.54 An air flow of 3.65 m³/s at atmospheric pressure flows in a 0.5 m diameter duct. A 0.35 m diameter ASME long radius nozzle and a water manometer is used to measure the flow rate. Determine the pressure drop across the nozzle in cm of water for air temperatures of 10°C and 40°C.

8.55 A laminar flow meter for measuring air flow is constructed of small diameter (0.2 cm) tubes that are 20 cm long. For an upper limit on the Reynolds number needed to maintain laminar flow of 1800, determine the number of tubes needed for an air flow rate of 0.04 m³/s. Determine the overall pressure drop accounting for the entrance and exit losses of the tubes. Show that the pressure drop is essentially linear with flow rate.

CHAPTER 8

Internal Incompressible Viscous Flow

8.1 Internal Flow Characteristics

Part A Fully Developed Laminar Flow

- 8.2 Fully Developed Laminar Flow Between Infinite Parallel Plates
- 8.3 Fully Developed Laminar Flow in a Pipe

Part B Flow in Pipes and Ducts

- 8.4 Shear Stress Distribution in Fully Developed Pipe Flow

8.5 Turbulent Velocity Profiles in Fully Developed Pipe Flow

- 8.6 Energy Considerations in Pipe Flow
- 8.7 Calculation of Head Loss
- 8.8 Solution of Pipe Flow Problems

Part C Flow Measurement

- 8.9 Restriction Flow Meters for Internal Flows
- 8.10 Summary and Useful Equations

Case Study

“Lab-on-a-Chip”

The power generated by a gasoline or diesel engine depends directly on the mass of air that enters the cylinder chamber. An intake manifold, such as shown in the photograph for a 4-cylinder automobile, is used to transport the air from the ambient to each cylinder and is a critical part of the engine system. Its geometry is important. A short flow length, large diameter, smooth surfaces, and gradual turns all reduce the friction losses and allow the pressure, and thus density, of the air to be close to that of the ambient.

There is a second indirect effect of the geometry on the pressure of the air entering the chamber. Air is sucked into a cylinder

when the intake valve is open. This flow has momentum, and when the intake valve closes the flow stops. The sudden change in momentum results in a pressure rise at the intake valve, which forms a pressure wave that travels back along the manifold to the inlet, where it is then reflected back toward the intake valve. If the inlet valve is opened just when the pressure wave returns, the air pressure is higher and more air enters the chamber, increasing the power.

Unfortunately, such a *tuned intake manifold* is effective only for a narrow band of engine speed. Outside that band, the pressure wave won't arrive in time to increase the pressure at the valve inlet. Depending on the frequency of the pressure wave and engine revolutions, a low pressure wave may arrive at the intake valve and actually reduce the air pressure entering the engine, reducing the power over that with no tuning.

Several modifications have been made to the intake manifold to enhance the effects of these pressure waves. A manifold with short intake pipe lengths allows the pressure wave to travel back-and-forth several times between openings of the inlet valve, increasing the overall speed range. *Variable intake manifolds* with two or more flow lengths can change the pressure wave timing for different engine speeds. Valves are used to direct the flow into passages of different lengths. A further modification is to continuously vary the flow length in time with engine speed. The inlet passages are arranged in a circular shape with a rotor on the inside. The air inlet is on the rotor, which is then turned in synchrony with engine speed to change the flow length. These improvements have resulted in increased power from a given displacement engine over time.



A modern automotive intake manifold.

Cyril Lutsenko/Adobe Stock Photo

Learning Objectives

After completing this chapter, you should be able to

- Describe how laminar and turbulent flows affect the flow in the entrance region.
- Solve a problem with laminar flow through parallel plates and circular tubes using the momentum equation.
- Describe the differences between the laminar and turbulent shear stress distributions.
- Describe the effects of Reynolds number on the fully developed velocity profile for turbulent pipe flow.
- Explain the kinetic energy coefficient and its use.
- Calculate the head loss and pressure drop for single and multiple pipe flow problems.
- Calculate the flow rate using the measurements from a restriction meter.

Flows completely bounded by solid surfaces are called internal flows. Thus internal flows include many important and practical flows such as those through pipes, ducts, nozzles, diffusers, sudden contractions and expansions, valves, and fittings.

Internal flows may be laminar or turbulent. Some laminar flow cases may be solved analytically. In the case of turbulent flow, analytical solutions are generally not possible, and we must rely heavily on semi-empirical theories and on experimental data. The nature of laminar and turbulent flows was discussed in Section 2.6. For internal flows, the flow regime (laminar or turbulent) is primarily a function of the Reynolds number.

In this chapter we will only consider incompressible flows; hence we will study the flow of liquids as well as gases that have negligible heat transfer and for which the Mach number $M < 0.3$. A value of $M = 0.3$ in air corresponds to a speed of approximately 100 m/s. Following a brief introduction, this chapter is divided into the following parts:

Part A Part A discusses fully developed laminar flow of a Newtonian fluid between parallel plates and in a pipe. These two cases can be studied analytically.

Part B Part B is about laminar and turbulent flows in pipes and ducts. The laminar flow analysis follows from Part A; the turbulent flow (which is the most common) is too complex to be analyzed completely so experimental data will be used to develop solution techniques.

Part C Part C is a discussion of methods of flow measurement.

8.1 Internal Flow Characteristics

Laminar versus Turbulent Flow

As discussed previously in Section 2.6, the pipe flow regime (laminar or turbulent) is determined by the Reynolds number, $Re = \rho \bar{V}D/\mu$. One can demonstrate by the classic Reynolds experiment the qualitative difference between laminar and turbulent flows. In this experiment water flows from a large reservoir through a clear tube. A thin filament of dye injected at the entrance to the tube allows visual observation of the flow. At low flow rates (low Reynolds numbers) the dye injected into the flow remains in a single filament along the tube; there is little dispersion of dye because the flow is laminar. A laminar flow is one in which the fluid flows in laminae, or layers and there is no macroscopic mixing of adjacent fluid layers.

As the flow rate through the tube is increased, the dye filament eventually becomes unstable and breaks up into a random motion throughout the tube; the line of dye is stretched and twisted into myriad entangled threads, and it quickly disperses throughout the entire flow field. This behavior of turbulent flow is caused by small, high-frequency velocity fluctuations superimposed on the mean motion of a turbulent flow, as illustrated earlier in Fig. 2.17; the mixing of fluid particles from adjacent layers of fluid results in rapid dispersion of the dye. We mentioned in Chapter 2 an everyday example of the difference between laminar and turbulent flow—when you gently turn on the kitchen faucet. For very low flow rates, the water exits smoothly indicating laminar flow in the pipe; for higher flow rates, the flow is churned up indicating turbulent flow.

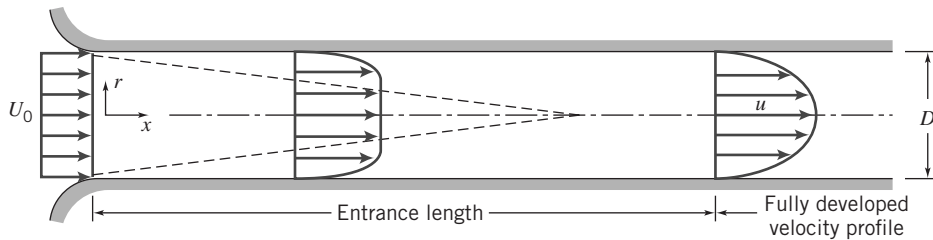


Fig. 8.1 Flow in the entrance region of a pipe.

Under normal conditions, transition to turbulence occurs at $Re \approx 2300$ for flow in pipes. For water flow in a 1-in. diameter pipe, this corresponds to an average speed of 0.3 ft/s. With great care to maintain the flow free from disturbances, and with smooth surfaces, experiments have been able to maintain laminar flow in a pipe to a Reynolds number of about 100,000. However, most engineering flow situations are not so carefully controlled, so we will take $Re \approx 2300$ as our benchmark for transition to turbulence. Transition Reynolds numbers for some other flow situations are given in the examples. Turbulence occurs when the viscous forces in the fluid are unable to damp out random fluctuations in the fluid motion (generated, for example, by roughness of a pipe wall), and the flow becomes chaotic. For example, a high-viscosity fluid such as motor oil is able to damp out fluctuations more effectively than a low viscosity fluid such as water and therefore remains laminar even at relatively high flow rates. On the other hand, a high-density fluid will generate significant inertia forces due to the random fluctuations in the motion, and this fluid will transition to turbulence at a relatively low flow rate.

The Entrance Region

Figure 8.1 illustrates laminar flow in the entrance region of a circular pipe. The flow has uniform velocity U_0 at the pipe entrance. Because of the no-slip condition at the wall, we know that the velocity at the wall must be zero along the entire length of the pipe. A boundary layer (introduced in Section 2.6) develops along the walls of the channel. The solid surface exerts a retarding shear force on the flow; thus the speed of the fluid in the neighborhood of the surface is reduced. At successive sections along the pipe in this entry region, the effect of the solid surface is felt farther out into the flow.

For incompressible flow, mass conservation requires that as the speed close to the wall is reduced the speed in the central frictionless region of the pipe must increase to compensate.

Sufficiently far from the pipe entrance, the boundary layer developing on the pipe wall reaches the pipe centerline and the flow becomes entirely viscous. The velocity profile shape changes until the inviscid core disappears. When the profile shape no longer changes with increasing distance x , the flow is called *fully developed*. The distance downstream from the entrance to the location at which fully developed flow begins is called the *entrance length*. The actual shape of the fully developed velocity profile depends on whether the flow is laminar or turbulent. In Fig. 8.1 the profile is shown qualitatively for a laminar flow.

For laminar flow the entrance length, L , is a function of Reynolds number,

$$\frac{L}{D} \approx 0.06 \frac{\rho \bar{V} D}{\mu} \quad (8.1)$$

where $\bar{V} \equiv Q/A$ is the average velocity. Laminar flow in a pipe may be expected only for Reynolds numbers less than about 2300. Thus the entrance length for laminar pipe flow may be as long as

$$L \approx 0.06 Re D \leq (0.06)(2300)D = 138D$$

or nearly 140 pipe diameters. If the flow is turbulent, enhanced mixing among fluid layers causes more rapid growth of the boundary layer. Experiments show that the mean velocity profile becomes fully developed within 25 to 40 pipe diameters from the entrance. However, the details of the turbulent motion may not be fully developed for 80 or more pipe diameters. We are now ready to study laminar internal flows (Part A), as well as laminar and turbulent flows in pipes and ducts (Part B). For these we will be focusing on what happens after the entrance region, i.e., fully developed flows.

Part A FULLY DEVELOPED LAMINAR FLOW

In this section we consider a few classic examples of fully developed laminar flows. Our intent is to obtain detailed information about the velocity field because knowledge of the velocity field permits calculation of shear stress, pressure drop, and flow rate.

8.2 Fully Developed Laminar Flow Between Infinite Parallel Plates

The flow between parallel plates is the simplest possible, but the question is why *would* there be a flow at all? The answer is that flow could be generated by applying a pressure gradient parallel to the plates, or by moving one plate parallel with respect to the other, or by having a body force (e.g., gravity) parallel to the plates, or by a combination of these driving mechanisms. We will consider all of these possibilities.

Both Plates Stationary

Fluid in high-pressure hydraulic systems, such as the brake system of an automobile, often leaks through the annular gap between a piston and cylinder. For very small gaps (typically 0.005 mm or less), this flow field may be modeled as flow between infinite parallel plates, as indicated in the sketch of Fig. 8.2. To calculate the leakage flow rate, we must first determine the velocity field.

Let us consider the fully developed laminar flow between horizontal infinite parallel plates. The plates are separated by distance a , as shown in Fig. 8.3. The plates are considered infinite in the z direction, with no variation of any fluid property in this direction. The flow is also assumed to be steady and incompressible. Before starting our analysis, what do we know about the flow field? For one thing we know that the x component of velocity must be zero at both the upper and lower plates as a result of the no-slip condition at the wall. The boundary conditions are then

$$\begin{aligned} \text{at } y=0 & \quad u=0 \\ \text{at } y=a & \quad u=0 \end{aligned}$$

Since the flow is fully developed, the velocity cannot vary with x and, hence, depends on y only, so that $u=u(y)$. Furthermore, there is no component of velocity in either the y or z direction ($v=w=0$). In fact, for fully developed flow only the pressure can and will change in the x direction.

In this section we will use a differential control volume to bring out some important features of the fluid mechanics.

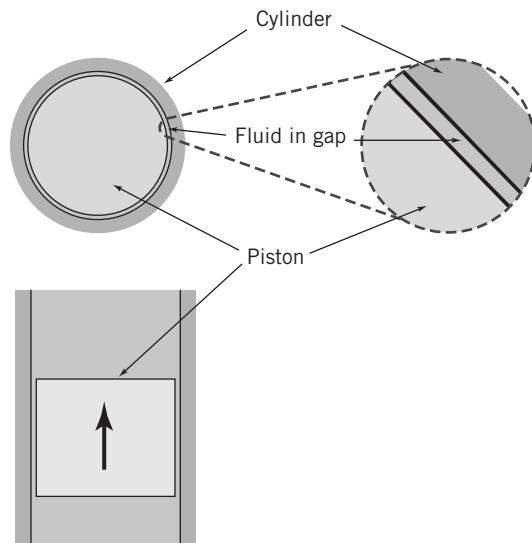


Fig. 8.2 Piston-cylinder approximated as parallel plates.

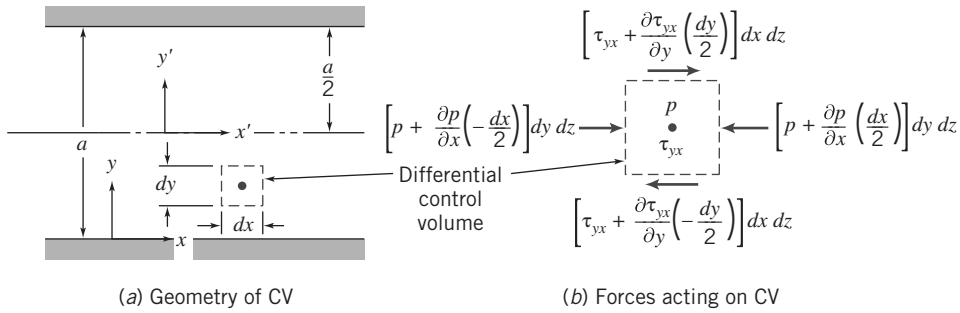


Fig. 8.3 Control volume for analysis of laminar flow between stationary infinite parallel plates.

For our analysis we select a differential control volume of size $dV = dx dy dz$, and apply the x component of the momentum equation.

Basic equation:

$$= 0(3) = 0(1)$$

$$F_{S_x} + \overbrace{F_{B_x}}^{\frac{\partial}{\partial t} \int_{CV} u \rho dV} + \int_{CS} u \rho \vec{V} \cdot d\vec{A} \quad (4.18a)$$

Assumptions:

- 1 Steady flow (given)
 - 2 Fully developed flow (given)
 - 3 $F_{B_x} = 0$ (given)

The very nature of fully developed flow is that the velocity profile is the same at all locations along the flow; hence there is no change in momentum. Equation 4.18a then reduces to the simple result that the sum of the surface forces on the control volume is zero,

$$F_{S_x} = 0 \quad (8.2)$$

The next step is to sum the forces acting on the control volume in the x direction. We recognize that normal forces (pressure forces) act on the left and right faces and tangential forces (shear forces) act on the top and bottom faces.

If the pressure at the center of the element is p , then the pressure force on the left face is

$$dF_L = \left(p - \frac{dp}{dx} \frac{dx}{2} \right) dy dz$$

and the pressure force on the right face is

$$dF_R = - \left(p + \frac{dp}{dx} \frac{dx}{2} \right) dy dz$$

We use the total derivative of pressure with respect to x rather than the partial derivative because we recognize that pressure varies only with x . If the pressure did vary with y then there would be flow in the y -direction. But $v = 0$ everywhere in the fully developed region.

If the shear stress at the center of the element is τ_{vr} , then the shear force on the bottom face is

$$dF_B = - \left(\tau_{yx} - \frac{d\tau_{yx}}{dy} \frac{dy}{2} \right) dx dz$$

and the shear force on the top face is

$$dF_T = \left(\tau_{yx} + \frac{d\tau_{yx}}{dy} \frac{dy}{2} \right) dx dz$$

Note that in expanding the shear stress, τ_{yx} , in a Taylor series about the center of the element, we have used the total derivative rather than a partial derivative. We did this because we recognized that τ_{yx} is only a function of y , since $u = u(y)$.

Using the four surface forces dF_L , dF_R , dF_B , and dF_T in Eq. 8.2, this equation simplifies to

$$\frac{dp}{dx} = \frac{d\tau_{yx}}{dy} \quad (8.3)$$

This equation states that because there is no change in momentum, the net pressure force (which is actually $-dp/dx$) balances the net friction force (which is actually $-d\tau_{yx}/dy$). Equation 8.3 has an interesting feature: The left side is at most a function of x only. This follows immediately from writing the y component of the momentum equation; the right side is at most a function of y only. The flow is fully developed, so it does not change with x . Hence, the only way the equation can be valid for all x and y is for each side to in fact be constant:

$$\frac{d\tau_{yx}}{dy} = \frac{dp}{dx} = \text{constant}$$

Integrating this equation, we obtain

$$\tau_{yx} = \left(\frac{dp}{dx} \right) y + c_1$$

which indicates that the shear stress varies linearly with y . We wish to find the velocity distribution. To do so, we need to relate the shear stress to the velocity field. For a Newtonian fluid we can use Eq. 2.15 because we have a one-dimensional flow

$$\tau_{yx} = \mu \frac{du}{dy} \quad (2.15)$$

so we get

$$\mu \frac{du}{dy} = \left(\frac{dp}{dx} \right) y + c_1$$

Integrating again

$$u = \frac{1}{2\mu} \left(\frac{dp}{dx} \right) y^2 + \frac{c_1}{\mu} y + c_2 \quad (8.4)$$

It is interesting to note that if we had started with the Navier–Stokes equations (Eqs. 5.27) instead of using a differential control volume, after only a few steps (i.e., simplifying and integrating twice) we would have obtained Eq. 8.4. To evaluate the constants, c_1 and c_2 , we must apply the boundary conditions. At $y=0$, $u=0$. Consequently, $c_2=0$. At $y=a$, $u=0$. Hence

$$0 = \frac{1}{2\mu} \left(\frac{dp}{dx} \right) a^2 + \frac{c_1}{\mu} a$$

This gives

$$c_1 = -\frac{1}{2} \left(\frac{dp}{dx} \right) a$$

and hence,

$$u = \frac{1}{2\mu} \left(\frac{dp}{dx} \right) y^2 - \frac{1}{2\mu} \left(\frac{dp}{dx} \right) ay = \frac{a^2}{2\mu} \left(\frac{dp}{dx} \right) \left[\left(\frac{y}{a} \right)^2 - \left(\frac{y}{a} \right) \right] \quad (8.5)$$

At this point we have the velocity profile. This is key to finding other flow properties, as we next discuss.

Shear Stress Distribution

The shear stress distribution is given by

$$\tau_{yx} = \left(\frac{dp}{dx} \right) y + c_1 = \left(\frac{dp}{dx} \right) y - \frac{1}{2} \left(\frac{dp}{dx} \right) a = a \left(\frac{dp}{dx} \right) \left[\frac{y}{a} - \frac{1}{2} \right] \quad (8.6a)$$

Volume Flow Rate

The volume flow rate is given by

$$Q = \int_A \vec{V} \cdot d\vec{A}$$

For a depth l in the z direction,

$$Q = \int_0^a u l dy \quad \text{or} \quad \frac{Q}{l} = \int_0^a \frac{1}{2\mu} \left(\frac{dp}{dx} \right) (y^2 - ay) dy$$

Thus the volume flow rate per unit depth is given by

$$\frac{Q}{l} = -\frac{1}{12\mu} \left(\frac{dp}{dx} \right) a^3 \quad (8.6b)$$

Flow Rate as a Function of Pressure Drop

Since dp/dx is constant, the pressure varies linearly with x and

$$\frac{dp}{dx} = \frac{p_2 - p_1}{L} = \frac{-\Delta p}{L}$$

Substituting into the expression for volume flow rate gives

$$\frac{Q}{l} = -\frac{1}{12\mu} \left[\frac{-\Delta p}{L} \right] a^3 = \frac{a^3 \Delta p}{12\mu L} \quad (8.6c)$$

Average Velocity

The average velocity magnitude, \bar{V} , is given by

$$\bar{V} = \frac{Q}{A} = -\frac{1}{12\mu} \left(\frac{dp}{dx} \right) \frac{a^3 l}{la} = -\frac{1}{12\mu} \left(\frac{dp}{dx} \right) a^2 \quad (8.6d)$$

Point of Maximum Velocity

To find the point of maximum velocity, we set du/dy equal to zero and solve for the corresponding y . From Eq. 8.5

$$\frac{du}{dy} = \frac{a^2}{2\mu} \left(\frac{dp}{dx} \right) \left[\frac{2y}{a^2} - \frac{1}{a} \right]$$

Thus,

$$\frac{du}{dy} = 0 \quad \text{at} \quad y = \frac{a}{2}$$

At

$$y = \frac{a}{2}, \quad u = u_{\max} = -\frac{1}{8\mu} \left(\frac{dp}{dx} \right) a^2 = \frac{3}{2} \bar{V} \quad (8.6c)$$

Transformation of Coordinates

In deriving the above relations, the origin of coordinates, $y = 0$, was taken at the bottom plate. We could just as easily have taken the origin at the centerline of the channel. If we denote the coordinates with origin at the channel centerline as x, y' , the boundary conditions are $u = 0$ at $y' = \pm a/2$.

To obtain the velocity profile in terms of x, y' , we substitute $y = y' + a/2$ into Eq. 8.5. The result is

$$u = \frac{a^2}{2\mu} \left(\frac{dp}{dx} \right) \left[\left(\frac{y'}{a} \right)^2 - \frac{1}{4} \right] \quad (8.7)$$

Equation 8.7 shows that the velocity profile for laminar flow between stationary parallel plates is parabolic, as shown in Fig. 8.4.

Since all stresses were related to velocity gradients through Newton's law of viscosity, and the additional stresses that arise as a result of turbulent fluctuations have not been accounted for, *all of the results in this section are valid for laminar flow only*. Experiments show that laminar flow between stationary parallel plates becomes turbulent for Reynolds numbers (defined as $Re = \rho \bar{V} a / \mu$) greater than approximately 1400. Consequently, the Reynolds number should be checked after using Eqs. 8.6a-d to ensure a valid solution. The calculation of the leakage past a cylinder in an hydraulic system using Eq. 8.6c is shown in Example 8.1.

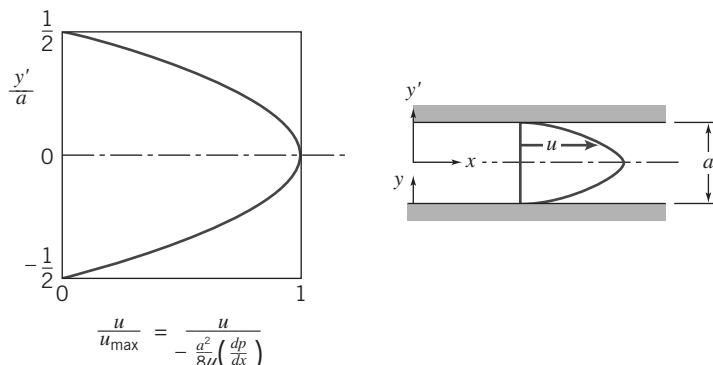


Fig. 8.4 Dimensionless velocity profile for fully developed laminar flow between infinite parallel plates.

Example 8.1 LEAKAGE FLOW PAST A PISTON

A hydraulic system operates at a gage pressure of 20 MPa and 55°C. The hydraulic fluid is SAE 10W oil. A control valve consists of a piston 25 mm in diameter, fitted to a cylinder with a mean radial clearance of 0.005 mm. Determine the leakage flow rate if the gage pressure on the low-pressure side of the piston is 1.0 MPa. The piston is 15 mm long.

Given: Flow of hydraulic oil between piston and cylinder, as shown. Fluid is SAE 10W oil at 55°C.

Find: Leakage flow rate, Q .

Solution: The gap width is very small, so the flow may be modeled as flow between parallel plates. Equation 8.6c may be applied.

Governing equations:

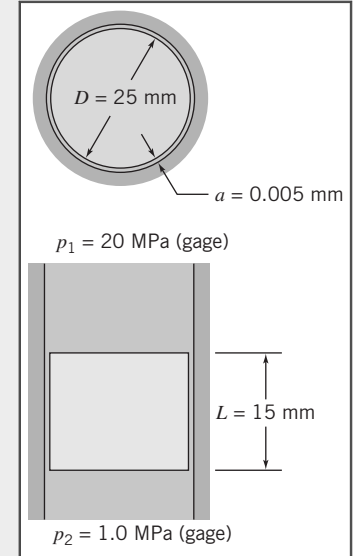
$$\frac{Q}{l} = \frac{a^3 \Delta p}{12\mu L} \quad (8.6c)$$

Assumptions:

- 1 Laminar flow.
- 2 Steady flow.
- 3 Incompressible flow.
- 4 Fully developed flow. (Note $L/a = 15/0.005 = 3000!$)

The plate width, l , is approximated as $l = \pi D$. Thus

$$Q = \frac{\pi D a^3 \Delta p}{12 \mu L}$$



For SAE 10W oil at 55°C, $\mu = 0.018 \text{ kg}/(\text{m} \cdot \text{s})$, from Fig. A.2, Appendix A. Thus

$$Q = \frac{\pi}{12} \times 25 \text{ mm} \times (0.005)^3 \text{ mm}^3 \times (20 - 1) 10^6 \frac{\text{N}}{\text{m}^2} \times \frac{\text{m} \cdot \text{s}}{0.018 \text{ kg}} \times \frac{1}{15 \text{ mm}} \times \frac{\text{kg} \cdot \text{m}}{\text{N} \cdot \text{s}^2}$$

$$Q = 57.6 \text{ mm}^3/\text{s} \leftarrow$$

To ensure that flow is laminar, we also should check the Reynolds number.

$$\bar{V} = \frac{Q}{A} = \frac{Q}{\pi D a} = 57.6 \frac{\text{mm}^3}{\text{s}} \times \frac{1}{\pi} \times \frac{1}{25 \text{ mm}} \times \frac{1}{0.005 \text{ mm}} \times \frac{1}{10^3 \text{ mm}} = 0.147 \text{ m/s}$$

and

$$Re = \frac{\rho \bar{V} a}{\mu} = \frac{SG \rho_{H_2O} \bar{V} a}{\mu}$$

For SAE 10W oil, $SG = 0.92$, from Table A.2, Appendix A. Thus

$$Re = 0.92 \times 1000 \frac{\text{kg}}{\text{m}^3} \times 0.147 \frac{\text{m}}{\text{s}} \times 0.005 \text{ mm} \times \frac{\text{m} \cdot \text{s}}{0.018 \text{ kg}} \times \frac{\text{m}}{10^3 \text{ mm}} = 0.0375$$

Thus flow is surely laminar, since $Re \ll 1400$.

Upper Plate Moving with Constant Speed, U

The second basic way to generate flow between infinite parallel plates is to have one plate move parallel to the other, either with or without an applied pressure gradient. We will next analyze this problem for the case of laminar flow.

Such a flow commonly occurs, for example, in a journal bearing (e.g., the main crankshaft bearings in the engine of an automobile). In such a bearing, an inner cylinder, the journal, rotates inside a stationary member. At light loads, the centers of the two members essentially coincide, and the small clearance gap is symmetric. Since the gap is small, it is reasonable to “unfold” the bearing and to model the flow field as flow between infinite parallel plates, as indicated in the sketch of Fig. 8.5.

Let us now consider a case where the upper plate is moving to the right with constant speed, U . All we have done in going from a stationary upper plate to a moving upper plate is to change one of the boundary conditions. The boundary conditions for the moving plate case are

$$\begin{aligned} u &= 0 && \text{at } y = 0 \\ u &= U && \text{at } y = a \end{aligned}$$

Since only the boundary conditions have changed, there is no need to repeat the entire analysis of the previous section. The analysis leading to Eq. 8.4 is equally valid for the moving plate case. Thus the velocity distribution is given by

$$u = \frac{1}{2\mu} \left(\frac{dp}{dx} \right) y^2 + \frac{c_1}{\mu} y + c_2 \quad (8.4)$$

and our only task is to evaluate constants c_1 and c_2 by using the appropriate boundary conditions.

At $y = 0$, $u = 0$. Consequently, $c_2 = 0$.

At $y = a$, $u = U$. Consequently,

$$U = \frac{1}{2\mu} \left(\frac{dp}{dx} \right) a^2 + \frac{c_1}{\mu} a \quad \text{and thus} \quad c_1 = \frac{U\mu}{a} - \frac{1}{2} \left(\frac{dp}{dx} \right) a$$

Hence,

$$u = \frac{1}{2\mu} \left(\frac{dp}{dx} \right) y^2 + \frac{Uy}{a} - \frac{1}{2\mu} \left(\frac{dp}{dx} \right) ay = \frac{Uy}{a} + \frac{1}{2\mu} \left(\frac{dp}{dx} \right) (y^2 - ay)$$

$$u = \frac{Uy}{a} + \frac{a^2}{2\mu} \left(\frac{dp}{dx} \right) \left[\left(\frac{y}{a} \right)^2 - \left(\frac{y}{a} \right) \right] \quad (8.8)$$

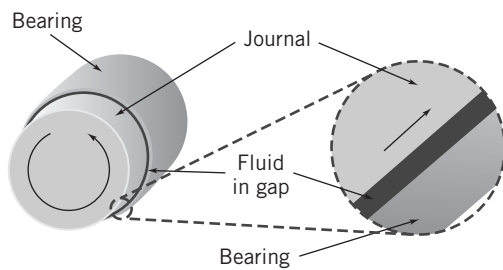


Fig. 8.5 Journal bearing approximated as parallel plates.

It is reassuring to note that Eq. 8.8 reduces to Eq. 8.5 for a stationary upper plate (set $U=0$). From Eq. 8.8, for zero pressure gradient (for $dp/dx=0$) the velocity varies linearly with y . This was the case treated earlier in Chapter 2; this linear profile is called a *Couette* flow, after a 19th-century physicist.

We can obtain additional information about the flow from the velocity distribution of Eq. 8.8.

Shear Stress Distribution

The shear stress distribution is given by $\tau_{yx}=\mu(du/dy)$,

$$\tau_{yx}=\mu \frac{U}{a} + \frac{a^2}{2} \left(\frac{dp}{dx} \right) \left[\frac{2y}{a^2} - \frac{1}{a} \right] = \mu \frac{U}{a} + a \left(\frac{dp}{dx} \right) \left[\frac{y}{a} - \frac{1}{2} \right] \quad (8.9a)$$

Volume Flow Rate

The volume flow rate is given by $Q=\int_A \vec{V} \cdot d\vec{A}$. For depth l in the z direction

$$Q = \int_0^a ul dy \quad \text{or} \quad \frac{Q}{l} = \int_0^a \left[\frac{Uy}{a} + \frac{1}{2\mu} \left(\frac{dp}{dx} \right) (y^2 - ay) \right] dy$$

Thus the volume flow rate per unit depth is given by

$$\frac{Q}{l} = \frac{Ua}{2} - \frac{1}{12\mu} \left(\frac{dp}{dx} \right) a^3 \quad (8.9b)$$

Average Velocity

The average velocity magnitude, \bar{V} , is given by

$$\bar{V} = \frac{Q}{A} = l \left[\frac{Ua}{2} - \frac{1}{12\mu} \left(\frac{dp}{dx} \right) a^3 \right] / la = \frac{U}{2} - \frac{1}{12\mu} \left(\frac{dp}{dx} \right) a^2 \quad (8.9c)$$

Point of Maximum Velocity

To find the point of maximum velocity, we set du/dy equal to zero and solve for the corresponding y . From Eq. 8.8

$$\frac{du}{dy} = \frac{U}{a} + \frac{a^2}{2\mu} \left(\frac{dp}{dx} \right) \left[\frac{2y}{a^2} - \frac{1}{a} \right] = \frac{U}{a} + \frac{a}{2\mu} \left(\frac{dp}{dx} \right) \left[2\left(\frac{y}{a}\right) - 1 \right]$$

Thus,

$$\frac{du}{dy} = 0 \quad \text{at} \quad y = \frac{a}{2} - \frac{U/a}{(1/\mu)(dp/dx)}$$

There is no simple relation between the maximum velocity, u_{\max} , and the mean velocity, \bar{V} , for this flow case.

Equation 8.8 suggests that the velocity profile may be treated as a combination of a linear and a parabolic velocity profile; the last term in Eq. 8.8 is identical to that in Eq. 8.5. The result is a family of velocity profiles, depending on U and $(1/\mu)(dp/dx)$; three profiles are sketched in Fig. 8.6. As shown in Fig. 8.6, some reverse flow—flow in the negative x direction—can occur when $dp/dx > 0$.

Again, all of the results developed in this section are valid for laminar flow only. Experiments show that this flow becomes turbulent for zero pressure gradient at a Reynolds number of approximately 1500,

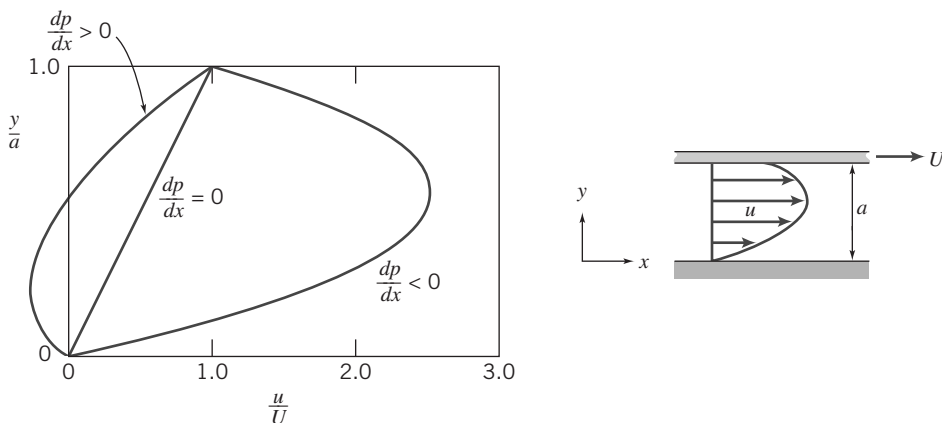


Fig. 8.6 Dimensionless velocity profile for fully developed laminar flow between infinite parallel plates: upper plate moving with constant speed, U .

where $Re = \rho U a / \mu$ for this flow case. Not much information is available for the case where the pressure gradient is not zero. In Example 8.2, the torque and power characteristics of a journal bearing are determined using the parallel plate model.

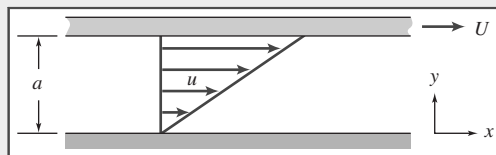
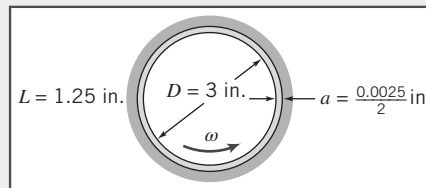
Example 8.2 TORQUE AND POWER IN A JOURNAL BEARING

A crankshaft journal bearing in an automobile engine is lubricated by SAE 30 oil at 210°F . The bearing diameter is 3 in., the diametral clearance is 0.0025 in., and the shaft rotates at 3600 rpm; it is 1.25 in. long. The bearing is under no load, so the clearance is symmetric. Determine the torque required to turn the journal and the power dissipated.

Given: Journal bearing, as shown. Note that the gap width, a , is *half* the diametral clearance. Lubricant is SAE 30 oil at 210°F . Speed is 3600 rpm.

Find: (a) Torque, T .
(b) Power dissipated.

Solution: Torque on the journal is caused by viscous shear in the oil film. The gap width is small, so the flow may be modeled as flow between infinite parallel plates:



Governing equations:

$$\tau_{yx} = \mu \frac{U}{a} + a \left(\frac{dp}{dx} \right) \left[\frac{y}{a} - \frac{1}{2} \right] = 0 \quad (8.9a)$$

Assumptions:

- 1 Laminar flow.
- 2 Steady flow.
- 3 Incompressible flow.
- 4 Fully developed flow.
- 5 Infinite width ($L/a = 1.25/0.00125 = 1000$, so this is a reasonable assumption).
- 6 $dp/dx = 0$ (flow is symmetric in the actual bearing at no load).

Then

$$\tau_{yx} = \mu \frac{U}{a} = \mu \frac{\omega R}{a} = \mu \frac{\omega D}{2a}$$

For SAE 30 oil at 210°F (99°C), $\mu = 9.6 \times 10^{-3} \text{ N} \cdot \text{s/m}^2$ ($2.01 \times 10^{-4} \text{ lbf} \cdot \text{s/ft}^2$), from Fig. A.2, Appendix A. Thus,

$$\begin{aligned}\tau_{yx} &= 2.01 \times 10^{-4} \frac{\text{lbf} \cdot \text{s}}{\text{ft}^2} \times 3600 \frac{\text{rev}}{\text{min}} \times 2\pi \frac{\text{rad}}{\text{rev}} \times \frac{\text{min}}{60 \text{ s}} \times 3 \text{ in.} \times \frac{1}{2} \times \frac{1}{0.00125 \text{ in.}} \\ \tau_{yx} &= 90.9 \text{ lbf/ft}^2\end{aligned}$$

The total shear force is given by the shear stress times the area. It is applied to the journal surface. Therefore, for the torque

$$\begin{aligned}T &= FR = \tau_{yx} \pi DLR = \frac{\pi}{2} \tau_{yx} D^2 L \\ &= \frac{\pi}{2} \times 90.9 \frac{\text{lbf}}{\text{ft}^2} \times (3)^2 \text{ in.}^2 \times \frac{\text{ft}^2}{144 \text{ in.}^2} \times 1.25 \text{ in.} \\ T &= 11.2 \text{ in.} \cdot \text{lbf} \quad \longleftarrow \quad T\end{aligned}$$

The power dissipated in the bearing is

$$\begin{aligned}\dot{W} &= FU = FR\omega = T\omega \\ &= 11.2 \text{ in.} \cdot \text{lbf} \times 3600 \frac{\text{rev}}{\text{min}} \times \frac{\text{min}}{60 \text{ s}} \times 2\pi \frac{\text{rad}}{\text{rev}} \times \frac{\text{ft}}{12 \text{ in.}} \times \frac{\text{hp} \cdot \text{s}}{550 \text{ ft} \cdot \text{lbf}} \\ \dot{W} &= 0.640 \text{ hp} \quad \longleftarrow \quad \dot{W}\end{aligned}$$

To ensure laminar flow, check the Reynolds number.

$$Re = \frac{\rho U a}{\mu} = \frac{SG \rho_{H_2O} U a}{\mu} = \frac{SG \rho_{H_2O} \omega R a}{\mu}$$

Assume, as an approximation, the specific gravity of SAE 30 oil is the same as that of SAE 10W oil. From Table A.2, Appendix A, $SG = 0.92$. Thus

$$\begin{aligned}Re &= 0.92 \times 1.94 \frac{\text{slug}}{\text{ft}^3} \times \frac{(3600)2\pi}{60} \frac{\text{rad}}{\text{s}} \times 1.5 \text{ in.} \times 0.00125 \text{ in.} \\ &\times \frac{\text{ft}^2}{2.01 \times 10^{-4} \text{ lbf} \cdot \text{s}} \times \frac{\text{ft}^2}{144 \text{ in.}^2} \times \frac{\text{lbf} \cdot \text{s}^2}{\text{slug} \cdot \text{ft}}\end{aligned}$$

$$Re = 43.6$$

Therefore, the flow is laminar, since $Re \ll 1500$.

In this problem we approximated the circular-streamline flow in a small annular gap as a linear flow between infinite parallel plates. As we saw in Example 5.10, for the small value of the gap width a to radius R ratio a/R (in this problem $< 1\%$), the error in shear stress is about $\frac{1}{2}$ of this ratio. Hence, the error introduced is insignificant—much less than the uncertainty associated with obtaining a viscosity for the oil.

We have seen how steady, one-dimensional laminar flows between two plates can be generated by applying a pressure gradient, by moving one plate with respect to the other, or by having both driving mechanisms present. To finish our discussion of this type of flow, Example 8.3 examines a *gravity-driven* steady, one-dimensional laminar flow down a vertical wall. Once again, the direct approach would be to start with the two-dimensional rectangular coordinate form of the Navier–Stokes equations (Eqs. 5.27); instead we will use a differential control volume.

Example 8.3 LAMINAR FILM ON A VERTICAL WALL

A viscous, incompressible, Newtonian liquid flows in steady, laminar flow down a vertical wall. The thickness, δ , of the liquid film is constant. Since the liquid free surface is exposed to atmospheric pressure, there is no pressure gradient. For this gravity-driven flow, apply the momentum equation to differential control volume $dx dy dz$ to derive the velocity distribution in the liquid film.

Given: Fully developed laminar flow of incompressible, Newtonian liquid down a vertical wall; thickness, δ , of the liquid film is constant and $dp/dx = 0$.

Find: Expression for the velocity distribution in the film.

Solution: The x component of the momentum equation for a control volume is

$$F_{S_x} + F_{B_x} = \frac{\partial}{\partial t} \int_{CV} u \rho dV + \int_{CS} u \rho \vec{V} \cdot d\vec{A} \quad (4.18a)$$

Under the conditions given we are dealing with a steady, incompressible, fully developed laminar flow.

For steady flow, $\frac{\partial}{\partial t} \int_{CV} u \rho dV = 0$

For fully developed flow, $\int_{CS} u \rho \vec{V} \cdot d\vec{A} = 0$

Thus the momentum equation for the present case reduces to

$$F_{S_x} + F_{B_x} = 0$$

The body force, F_{B_x} , is given by $F_{B_x} = \rho g dV = \rho g dx dy dz$. The only surface forces acting on the differential control volume are shear forces on the vertical surfaces. (Since we have a free-surface flow, with straight streamlines, the pressure is atmospheric throughout; no net pressure forces act on the control volume.)

If the shear stress at the center of the differential control volume is τ_{yx} , then,

$$\text{shear stress on left face is } \tau_{yx_L} = \left(\tau_{yx} - \frac{d\tau_{yx}}{dy} \frac{dy}{2} \right)$$

and

$$\text{shear stress on right face is } \tau_{yx_R} = \left(\tau_{yx} + \frac{d\tau_{yx}}{dy} \frac{dy}{2} \right)$$

The direction of the shear stress vectors is taken consistent with the sign convention of Section 2.3. Thus on the left face, a minus y surface, τ_{yx_L} acts upward, and on the right face, a plus y surface, τ_{yx_R} acts downward.

The surface forces are obtained by multiplying each shear stress by the area over which it acts. Substituting into $F_{S_x} + F_{B_x} = 0$, we obtain

$$-\tau_{yx_L} dx dz + \tau_{yx_R} dx dz + \rho g dx dy dz = 0$$

or

$$-\left(\tau_{yx} - \frac{d\tau_{yx}}{dy} \frac{dy}{2} \right) dx dz + \left(\tau_{yx} + \frac{d\tau_{yx}}{dy} \frac{dy}{2} \right) dx dz + \rho g dx dy dz = 0$$

Simplifying gives

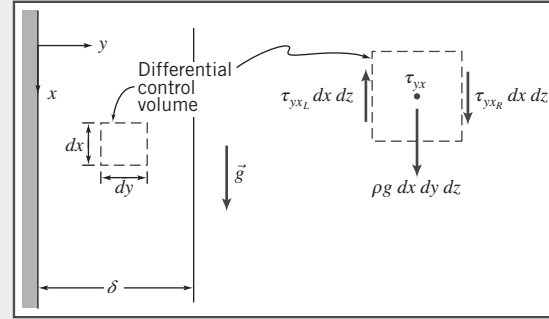
$$\frac{d\tau_{yx}}{dy} + \rho g = 0 \quad \text{or} \quad \frac{d\tau_{yx}}{dy} = -\rho g$$

Since

$$\tau_{yx} = \mu \frac{du}{dy} \quad \text{then} \quad \mu \frac{d^2 u}{dy^2} = -\rho g \quad \text{and} \quad \frac{d^2 u}{dy^2} = -\frac{\rho g}{\mu}$$

Integrating with respect to y gives

$$\frac{du}{dy} = -\frac{\rho g}{\mu} y + c_1$$



Integrating again, we obtain

$$u = -\frac{\rho g}{\mu} \frac{y^2}{2} + c_1 y + c_2$$

To evaluate constants c_1 and c_2 , we apply appropriate boundary conditions:

(i) $y=0, \frac{du}{dy}=0$ (no-slip)

(ii) $y=\delta, \frac{du}{dy}=0$ (neglect air resistance, i.e., assume zero shear stress at free surface)

From boundary condition (i), $c_2=0$

From boundary condition (ii), $0=-\frac{\rho g}{\mu} \delta + c_1$ or $c_1=\frac{\rho g}{\mu} \delta$

Hence,

$$u = -\frac{\rho g}{\mu} \frac{y^2}{2} + \frac{\rho g}{\mu} \delta y \quad \text{or} \quad u = \frac{\rho g}{\mu} \delta^2 \left[\left(\frac{y}{\delta} \right) - \frac{1}{2} \left(\frac{y}{\delta} \right)^2 \right] \xrightarrow{u(y)}$$

Using the velocity profile it can be shown that:

the volume flow rate is $Q/l = \frac{\rho g}{3\mu} \delta^3$

the maximum velocity is $U_{\max} = \frac{\rho g}{2\mu} \delta^2$

the average velocity is $\bar{V} = \frac{\rho g}{3\mu} \delta^2$

Flow in the liquid film is laminar for $Re = \bar{V}\delta/\nu \leq 1000$ [1].

Notes:

- This problem is a special case ($\theta = 90^\circ$) of the inclined plate flow analyzed in Example 5.9 that we solved using the Navier–Stokes equations.
- This problem and Example 5.9 demonstrate that use of the differential control volume approach or the Navier–Stokes equations leads to the same result.

8.3 Fully Developed Laminar Flow in a Pipe

As a final example of fully developed laminar flow, let us consider fully developed laminar flow in a pipe. Here the flow is axisymmetric. Consequently it is most convenient to work in cylindrical coordinates. This is yet another case where we could use the Navier–Stokes equations, this time in cylindrical coordinates (see Example 5.10). Instead we will again take the longer route—using a differential control volume—to bring out some important features of the fluid mechanics. The development will be very similar to that for parallel plates in the previous section. Since the flow is axisymmetric, the control volume will be a differential annulus, as shown in Fig. 8.7. The control volume length is dx and its thickness is dr .

For a fully developed steady flow, the x component of the momentum equation (Eq. 4.18a), when applied to the differential control volume, once again reduces to

$$F_{S_x} = 0$$

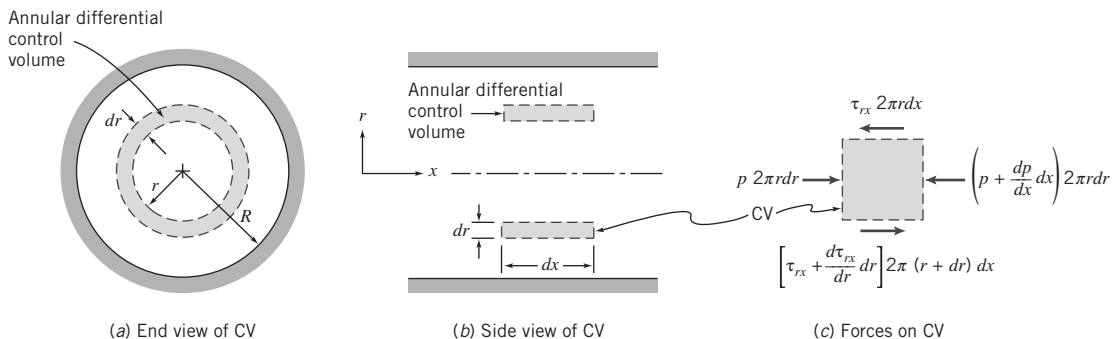


Fig. 8.7 Differential control volume for analysis of fully developed laminar flow in a pipe.

The next step is to sum the forces acting on the control volume in the x direction. We know that normal forces (pressure forces) act on the left and right ends of the control volume, and that tangential forces (shear forces) act on the inner and outer cylindrical surfaces.

If the pressure at the left face of the control volume is p , then the pressure force on the left end is

$$dF_L = p2\pi r dr$$

The pressure force on the right end is

$$dF_R = - \left(p + \frac{dp}{dx} dx \right) 2\pi r dr$$

If the shear stress at the inner surface of the annular control volume is τ_{rx} , then the shear force on the inner cylindrical surface is

$$dF_I = - \tau_{rx} 2\pi r dx$$

The shear force on the outer cylindrical surface is

$$dF_O = \left(\tau_{rx} + \frac{d\tau_{rx}}{dr} dr \right) 2\pi(r+dr)dx$$

The sum of the x components of force, dF_L , dF_R , dF_I , and dF_O , acting on the control volume must be zero. This leads to the condition that

$$-\frac{dp}{dx} 2\pi r dr dx + \tau_{rx} 2\pi dr dx + \frac{d\tau_{rx}}{dr} 2\pi r dr dx = 0$$

Dividing this equation by $2\pi r dr dx$ and solving for dp/dx gives

$$\frac{dp}{dx} = \frac{\tau_{rx}}{r} + \frac{d\tau_{rx}}{dr} = \frac{1}{r} \frac{d(r\tau_{rx})}{dr}$$

Comparing this to the corresponding equation for parallel plates (Eq. 8.3) shows the mathematical complexity introduced because we have cylindrical coordinates. The left side of the equation is at most a function of x only because the pressure is uniform at each section; the right side is at most a function of r only because the flow is fully developed. Hence, the only way the equation can be valid for all x and r is for both sides to in fact be constant:

$$\frac{1}{r} \frac{d(r\tau_{rx})}{dr} = \frac{dp}{dx} = \text{constant} \quad \text{or} \quad \frac{d(r\tau_{rx})}{dr} = r \frac{dp}{dx}$$

We are not quite finished, but already we have an important result: *In a constant diameter pipe, the pressure drops uniformly along the pipe length* (except for the entrance region).

Integrating this equation, we obtain

$$r\tau_{rx} = \frac{r^2}{2} \left(\frac{dp}{dx} \right) + c_1$$

or

$$\tau_{rx} = \frac{r}{2} \left(\frac{dp}{dx} \right) + \frac{c_1}{r} \quad (8.10)$$

Since $\tau_{rx} = \mu du/dr$, we have

$$\mu \frac{du}{dr} = \frac{r}{2} \left(\frac{dp}{dx} \right) + \frac{c_1}{r}$$

and

$$u = \frac{r^2}{4\mu} \left(\frac{dp}{dx} \right) + \frac{c_1}{\mu} \ln r + c_2 \quad (8.11)$$

We need to evaluate constants c_1 and c_2 . We have the one boundary condition that $u=0$ at $r=R$. We also know from physical considerations that the velocity must be finite at $r=0$. The only way that this can be true is for c_1 to be zero. Thus,

$$u = \frac{r^2}{4\mu} \left(\frac{dp}{dx} \right) + c_2$$

The constant, c_2 , is evaluated by using the available boundary condition at the pipe wall: at $r=R$, $u=0$. Consequently,

$$0 = \frac{R^2}{4\mu} \left(\frac{dp}{dx} \right) + c_2$$

This gives

$$c_2 = -\frac{R^2}{4\mu} \left(\frac{dp}{dx} \right)$$

and hence

$$u = \frac{r^2}{4\mu} \left(\frac{dp}{dx} \right) - \frac{R^2}{4\mu} \left(\frac{dp}{dx} \right) = \frac{1}{4\mu} \left(\frac{dp}{dx} \right) (r^2 - R^2)$$

or

$$u = -\frac{R^2}{4\mu} \left(\frac{dp}{dx} \right) \left[1 - \left(\frac{r}{R} \right)^2 \right] \quad (8.12)$$

Since we have the velocity profile, we can obtain a number of additional features of the flow.

Shear Stress Distribution

The shear stress is

$$\tau_{rx} = \mu \frac{du}{dr} = \frac{r}{2} \left(\frac{dp}{dx} \right) \quad (8.13a)$$

The shear stress varies linearly across the flow, with a maximum value at the wall and a value of zero at the centerline.

Volume Flow Rate

The volume flow rate is

$$Q = \int_A \vec{V} \cdot d\vec{A} = \int_0^R u 2\pi r dr = \int_0^R \frac{1}{4\mu} \left(\frac{dp}{dx} \right) (r^2 - R^2) 2\pi r dr$$

$$Q = -\frac{\pi R^4}{8\mu} \left(\frac{dp}{dx} \right) \quad (8.13b)$$

Flow Rate as a Function of Pressure Drop

We have shown that in fully developed flow the pressure gradient, dp/dx , is constant. Therefore, $dp/dx = (p_2 - p_1)/L = -\Delta p/L$. Substituting into Eq. 8.13b for the volume flow rate gives

$$Q = -\frac{\pi R^4}{8\mu} \left[\frac{-\Delta p}{L} \right] = \frac{\pi \Delta p R^4}{8\mu L} = \frac{\pi \Delta p D^4}{128\mu L} \quad (8.13c)$$

for laminar flow in a horizontal pipe. Note that Q is a sensitive function of D ; $Q \sim D^4$, so, for example, doubling the diameter D increases the flow rate Q by a factor of 16.

Average Velocity

The average velocity magnitude, \bar{V} , is given by

$$\bar{V} = \frac{Q}{A} = \frac{Q}{\pi R^2} = -\frac{R^2}{8\mu} \left(\frac{dp}{dx} \right) \quad (8.13d)$$

Point of Maximum Velocity

To find the point of maximum velocity, we set du/dr equal to zero and solve for the corresponding r . From Eq. 8.12

$$\frac{du}{dr} = \frac{1}{2\mu} \left(\frac{dp}{dx} \right) r$$

Thus,

$$\frac{du}{dr} = 0 \quad \text{at} \quad r = 0$$

At $r = 0$,

$$u = u_{\max} = U = -\frac{R^2}{4\mu} \left(\frac{dp}{dx} \right) = 2\bar{V} \quad (8.13e)$$

The velocity profile (Eq. 8.12) may be written in terms of the maximum (centerline) velocity as

$$\frac{u}{U} = 1 - \left(\frac{r}{R} \right)^2 \quad (8.14)$$

The parabolic velocity profile, given by Eq. 8.14 for fully developed laminar pipe flow, was sketched in Fig. 8.1. These laminar flow results are applied to the design of a viscometer in Example 8.4.

Example 8.4 CAPILLARY VISCOMETER

A simple and accurate viscometer can be made from a length of capillary tubing. If the flow rate and pressure drop are measured, and the tube geometry is known, the viscosity of a Newtonian liquid can be computed from Eq. 8.13c. A test of a certain liquid in a capillary viscometer gave the following data:

Flow rate:	$880 \text{ mm}^3/\text{s}$	Tube length:	1 m
Tube diameter:	0.50 mm	Pressure drop:	1.0 MPa

Determine the viscosity of the liquid.

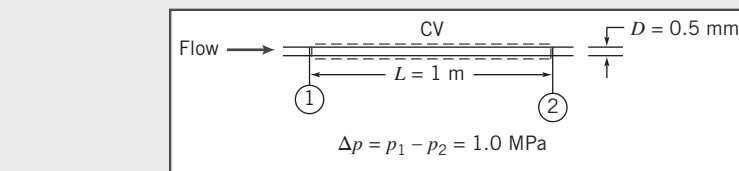
Given: Flow in a capillary viscometer.

The flow rate is $Q = 880 \text{ mm}^3/\text{s}$.

Find: The fluid viscosity.

Solution: Equation 8.13c may be applied.

Governing equation:



$$Q = \frac{\pi \Delta p D^4}{128 \mu L} \quad (8.13c)$$

Assumptions:

- 1 Laminar flow.
- 2 Steady flow.
- 3 Incompressible flow.
- 4 Fully developed flow.
- 5 Horizontal tube.

Then

$$\mu = \frac{\pi \Delta p D^4}{128 L Q} = \frac{\pi}{128} \times 1.0 \times 10^6 \frac{N}{m^2} \times (0.50)^4 mm^4 \times \frac{s}{880 mm^3} \times \frac{1}{1 m} \times \frac{m}{10^3 mm}$$

$$\mu = 1.74 \times 10^{-3} N \cdot s/m^2$$

Check the Reynolds number. Assume the fluid density is similar to that of water, 999 kg/m^3 . Then

$$\bar{V} = \frac{Q}{A} = \frac{4Q}{\pi D^2} = \frac{4}{\pi} \times 880 \frac{mm^3}{s} \times \frac{1}{(0.50)^2 mm^2} \times \frac{m}{10^3 mm} = 4.48 \text{ m/s}$$

and

$$Re = \frac{\rho \bar{V} D}{\mu} = 999 \frac{kg}{m^3} \times 4.48 \frac{m}{s} \times 0.50 mm$$

$$\times \frac{m^2}{1.74 \times 10^{-3} N \cdot s} \times \frac{m}{10^3 mm} \times \frac{N \cdot s^2}{kg \cdot m}$$

$$Re = 1290$$

Consequently, since $Re < 2300$, the flow is laminar.

This problem is a little oversimplified. To design a capillary viscometer the entrance length, liquid temperature, and kinetic energy of the flowing liquid would all need to be considered.

Part B FLOW IN PIPES AND DUCTS

In this section we will be interested in determining the factors that affect the pressure in an incompressible fluid as it flows in a pipe or duct. If we ignore friction for a moment and assume steady flow and consider a streamline in the flow, the Bernoulli equation from Chapter 6 applies,

$$\frac{p}{\rho} + \frac{V^2}{2} + gz = \text{constant} \quad (6.8)$$

From this equation we can see what *tends* to lead to a *pressure decrease* along the streamline in this frictionless flow: a *reduction of area* at some point in the pipe causing an increase in the velocity V , or the pipe having a *positive incline* so z increases. Conversely, the pressure will tend to increase if the flow area is increased or the pipe slopes downward. We say “tends to” because one factor may counteract another; for example, we may have a downward sloping pipe tending to increase pressure with a reduction in diameter tending to decrease pressure.

In reality, flows in pipes and ducts experience significant friction and are often turbulent, so the Bernoulli equation does not apply. It doesn’t even make sense to use V ; instead we will use \bar{V} , to represent the average velocity at a section along the pipe. We will learn that, in effect, friction effects lead to a continual reduction in the value of the Bernoulli constant of Eq. 6.8, representing a “loss” of mechanical energy. We have already seen that, in contrast to the Bernoulli equation, for laminar flow there is a pressure drop even for a horizontal, constant diameter pipe; in this section we will see that turbulent flows experience an even larger pressure drop. We will need to replace the Bernoulli equation with an energy equation that incorporates the effects of friction.

In summary, we can state that *three* factors tend to reduce the pressure in a pipe flow: a decrease in pipe area, an upward slope, and friction. For now we will focus on pressure loss due to friction and so will analyze pipes that are of constant area and that are horizontal.

We have already seen in the previous section that for laminar flow we can deduce the pressure drop. Rearranging Eq. 8.13c to solve for the pressure drop Δp ,

$$\Delta p = \frac{128\mu L Q}{\pi D^4}$$

We would like to develop a similar expression that applies for turbulent flows, but we will see that this is not possible analytically; instead, we will develop expressions based on a combination of theoretical and experimental approaches.

Since circular pipes are most common in engineering applications, the basic analysis will be performed for circular geometries. The results can be extended to other geometries by introducing the hydraulic diameter, which is treated in Section 8.7.

It is conventional to break losses due to friction into two categories: *major losses*, which are losses due to friction in the constant-area sections of the pipe; and *minor losses* (sometimes larger than “major” losses), which are losses due to valves, elbows, and so on. We will consider the friction losses first.

8.4 Shear Stress Distribution in Fully Developed Pipe Flow

We consider again fully developed flow in a horizontal circular pipe, except now we may have laminar or turbulent flow. In Section 8.3 we showed that a force balance between friction and pressure forces leads to Eq. 8.10:

$$\tau_{rx} = \frac{r}{2} \left(\frac{dp}{dx} \right) + \frac{c_1}{r} \quad (8.10)$$

Because we cannot have infinite stress at the centerline, the constant of integration c_1 must be zero, so

$$\tau_{rx} = \frac{r}{2} \frac{dp}{dx} \quad (8.15)$$

Equation 8.15 indicates that *for both laminar and turbulent fully developed flows the shear stress varies linearly across the pipe*, from zero at the centerline to a maximum at the pipe wall. The stress on the wall, τ_w , equal and opposite to the stress in the fluid at the wall, is given by

$$\tau_w = -[\tau_{rx}]_{r=R} = -\frac{R}{2} \frac{dp}{dx} \quad (8.16)$$

For *laminar* flow we used our familiar stress equation $\tau_{rw} = \mu du/dr$ in Eq. 8.15 to eventually obtain the laminar velocity distribution. This led to a set of usable equations, Eq. 8.13a, for obtaining various flow characteristics; e.g., Eq. 8.13c gave a relationship for the flow rate Q , a result first obtained experimentally by Jean Louis Poiseuille, a French physician, and independently by Gotthilf H. L. Hagen, a German engineer, in the 1850s [2].

The stress relations for turbulent flow are more complex than those for laminar flow and are heavily based on experiments.

As we discussed in Section 2.6, and illustrated in Fig. 2.17, turbulent flow is represented at each point by the time-mean velocity \bar{u} plus randomly fluctuating velocity components u' and v' in the x and y directions. These components continuously transfer momentum between adjacent fluid layers, tending to reduce any velocity gradient present. This effect shows up as an apparent stress, first introduced by Osborne Reynolds, and called the *Reynolds stress*. This stress is given by $-\rho \bar{u}' \bar{v}'$, where the overbar indicates a time average. In terms of the distance from the wall, the total stress in turbulent flow can be written as

$$\tau = \tau_{lam} + \tau_{turb} = \mu \frac{d\bar{u}}{dy} - \rho \bar{u}' \bar{v}' \quad (8.17)$$

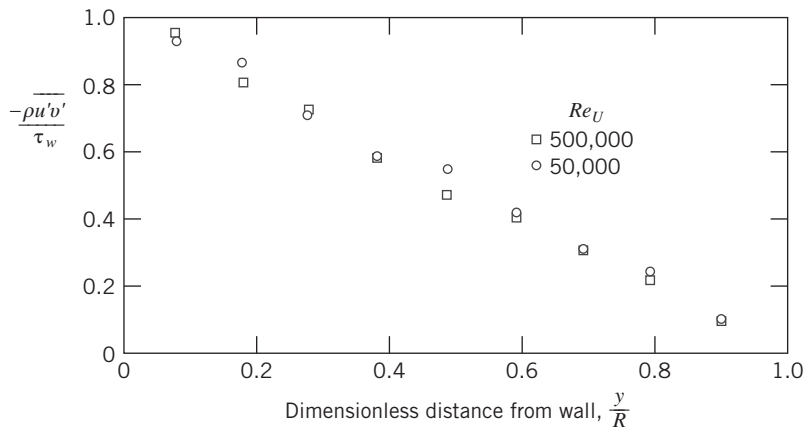


Fig. 8.8 Turbulent shear stress (Reynolds stress) for fully developed turbulent flow in a pipe. (Data from Laufer [3].)

The fluctuations u' and v' are negatively correlated, so that $\tau_{turb} = -\rho \bar{u}' v'$ is positive. In Fig. 8.8, experimental measurements of the Reynolds stress for fully developed turbulent pipe flow at two Reynolds numbers based on the centerline velocity are presented; The turbulent shear stress has been nondimensionalized with the wall shear stress. In Fig. 8.8, we see that the Reynolds stress away from the wall decreases linearly with distance, and that the friction is almost all due to Reynolds stress. Near the wall the Reynolds stress drops to zero. In the region very close to the wall, called the *wall layer*, viscous shear is dominant. In the region between the wall layer and the central portion of the pipe both viscous and turbulent shear are important and in the region far from the wall turbulent friction dominates.

8.5 Turbulent Velocity Profiles in Fully Developed Pipe Flow

Turbulence and turbulent velocity profiles have been extensively studied [4], and the accepted relations developed for internal flows are semi-empirical. We will introduce some simple formulations for turbulent flow that have proved useful. We start with the relation for the total stress in turbulent flow, Eq. 8.17, and divide by the density to yield a more convenient form

$$\frac{\tau}{\rho} = \nu \frac{d\bar{u}}{dy} - \bar{u}' v' \quad (8.18)$$

Prandtl [25] proposed a model for the turbulent viscosity based on mixing in the flow. He hypothesized that the turbulent fluctuations in the mean velocity \bar{u} are a result of a small element of fluid moving upward a small distance ℓ into a region of higher velocity. The fluctuating velocity u' is then negative and given by

$$u' = -\ell \frac{d\bar{u}}{dy}$$

The quantity ℓ is called the *mixing length*. He reasoned that the fluctuation upward of the small element of fluid is caused by a vertical fluctuation in the v -component of velocity, and thus

$$v' = \ell \frac{d\bar{v}}{dx}$$

In homogeneous turbulence, the fluctuations u' and v' are equal and thus the v -component of the fluctuation v' is the same as the u -component, or

$$v' = u' = \ell \frac{d\bar{u}}{dy}$$

The turbulent shear stress is then approximated as

$$\frac{\tau_{turb}}{\rho} = \ell^2 \left(\frac{d\bar{u}}{dy} \right)^2$$

Further, Prandtl hypothesized that the mixing length ℓ increases in proportion to the distance from the wall.

$$\ell = ky$$

Although this is all very approximate and intended mainly to provide some insight into the mechanisms that transfer momentum in a turbulent flow, it has proved very useful in understanding and modeling turbulent flows.

The total shear stress is the sum of the laminar and turbulent shear stresses. Very near the wall the laminar contribution dominates. Further, very near the wall, the shear stress is essentially equal to the value at the wall. In this wall layer, the shear stress is then given by

$$\frac{\tau}{\rho} \approx \frac{\tau_w}{\rho} = \nu \frac{d\bar{u}}{dy}$$

It is convenient to introduce the friction velocity, u_* , which is the square root of the wall shear stress divided by the density, and defined as

$$u_* = \sqrt{\frac{\tau_w}{\rho}}$$

Further, it is convenient to work with wall coordinates u^+ and y^+ defined as

$$u^+ = \frac{\bar{u}}{u_*} \quad \text{and} \quad y^+ = \frac{yu_*}{\nu}$$

The relation for shear stress near the wall can then be written as

$$1 = \frac{du^+}{dy^+}$$

This is readily integrated to yield a linear velocity profile

$$u^+ = y^+ \quad (8.19)$$

In the flow farther from the wall, but still near enough the wall that the total shear stress equals the wall value, the laminar stress is much smaller than the turbulent stress. Neglecting the laminar contribution gives the relation

$$\frac{\tau}{\rho} \approx \frac{\tau_w}{\rho} = k^2 y^2 \left(\frac{d\bar{u}}{dy} \right)^2$$

In wall coordinates u^+ and y^+ , and taking the square root of both sides, the relation becomes

$$1 = ky^+ \frac{du^+}{dy^+}$$

This relation is integrated to yield

$$u^+ = \frac{1}{k} \ln y^+ + C$$

Using experimental data, the constant k , which is called Karman's constant, has been evaluated as 0.4 and the constant C as 5.0. In this region the velocity profile is given as

$$u^+ = \frac{\bar{u}}{u_*} = 2.5 \ln \frac{yu_*}{\nu} + 5.0 \quad (8.20)$$

The velocity profile data for turbulent pipe flow from a large number of investigators is plotted in Fig. 8.9 on semi-logarithmic coordinates. In the region very close to the wall where viscous shear is dominant, called the *viscous sublayer*, the mean velocity profile follows the linear relation given by Eq. 8.19 up to about $y^+ = 5$. This region is called the viscous sublayer and the turbulent friction is negligible compared to the viscous friction. In the region where the viscous effects are negligible, Eq. 8.20 is valid from about $y^+ = 30$ out to the region where the shear stress is no longer constant with distance from

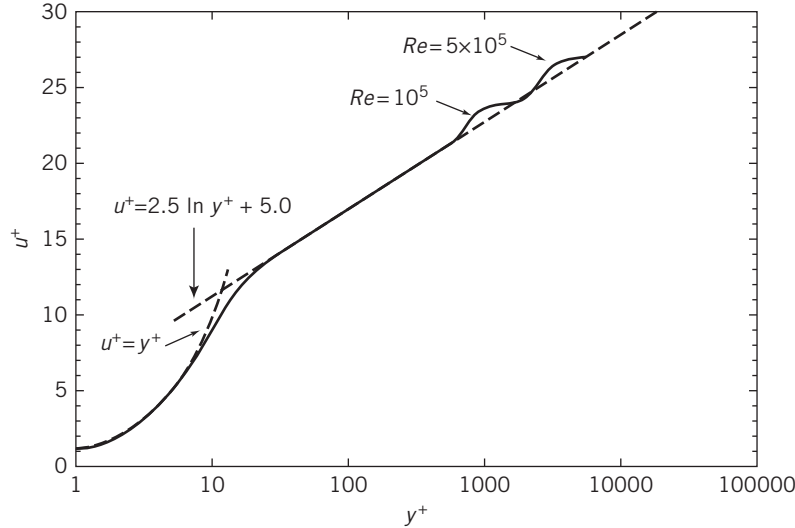


Fig. 8.9 Mean velocity profiles for fully developed turbulent flow in a pipe. Adapted from [24, 25].

the wall. This region is called the *logarithmic layer*. Between $y^+ = 5$ and $y^+ = 30$ is the *buffer layer* where both viscosity and turbulence contribute to the shear stress. Surprisingly, the model proposed by Prandtl nearly 100 years ago has proved valuable in understanding and analyzing turbulent flows.

If Eq. 8.20 is evaluated at the centerline ($y = R$ and $u = U$) and the general expression of Eq. 8.20 is subtracted from the equation evaluated at the centerline, we obtain

$$\frac{U - \bar{u}}{u_*} = 2.5 \ln \frac{R}{y} \quad (8.21)$$

where U is the centerline velocity. Equation 8.21, referred to as the *defect law*, shows that the velocity defect is a function of the distance ratio only and does not depend on the viscosity of the fluid.

The velocity profile for turbulent flow through a smooth pipe may also be approximated by the empirical *power-law* equation

$$\frac{\bar{u}}{U} = \left(\frac{y}{R}\right)^{1/n} = \left(1 - \frac{r}{R}\right)^{1/n} \quad (8.22)$$

where the exponent, n , varies with the Reynolds number. In Fig. 8.10 the data of Laufer [3] are shown on a plot of $\ln y/R$ versus $\ln \bar{u}/U$. If the power-law profile were an accurate representation of the data, all data points would fall on a straight line of slope n . Clearly the data for $Re_U = 5 \times 10^4$ deviate from the best-fit straight line in the neighborhood of the wall.

Hence the power-law profile is not applicable close to the wall ($y/R < 0.04$). Since the velocity is low in this region, the error in calculating integral quantities such as mass, momentum, and energy fluxes at a section is relatively small. The power-law profile gives an infinite velocity gradient at the wall and hence cannot be used in calculations of wall shear stress. Although the profile fits the data close to the centerline, it fails to give zero slope there. Despite these shortcomings, the power-law profile is found to give adequate results in many calculations.

Data from Hinze [5] suggest that the variation of power-law exponent n with Reynolds number (based on pipe diameter, D , and centerline velocity, U) for fully developed flow in smooth pipes is given by

$$n = -1.7 + 1.8 \log Re_U \quad (8.23)$$

for $Re_U > 2 \times 10^4$.

Since the average velocity is $\bar{V} = Q/A$, and

$$Q = \int_A \vec{V} \cdot d\vec{A}$$

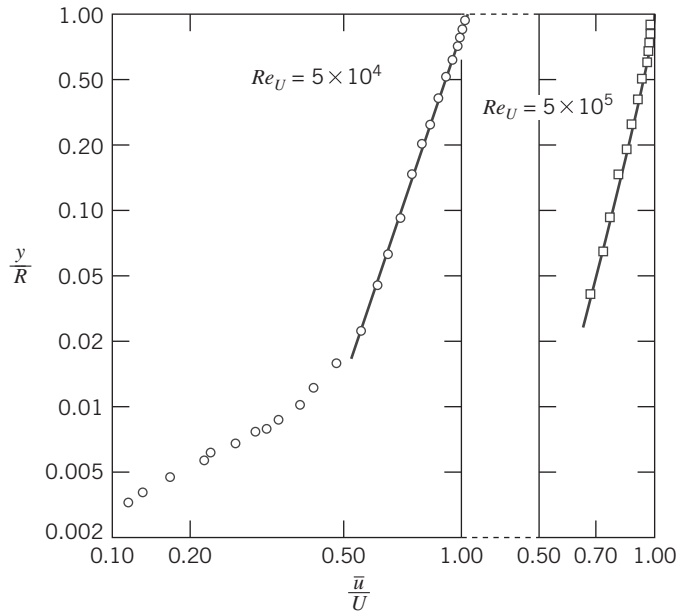


Fig. 8.10 Power-law velocity profiles for fully developed turbulent flow in a smooth pipe. (Data from Laufer [3].)

the ratio of the average velocity to the centerline velocity may be calculated for the power-law profiles of Eq. 8.22 assuming the profiles to be valid from wall to centerline. The result is

$$\frac{\bar{V}}{U} = \frac{2n^2}{(n+1)(2n+1)} \quad (8.24)$$

From Eq. 8.24, we see that as n increases with increasing Reynolds number the ratio of the average velocity to the centerline velocity increases; with increasing Reynolds number the velocity profile becomes more blunt or “fuller” (for $n=6, \bar{V}/U=0.79$ and for $n=10, \bar{V}/U=0.87$). As a representative value, 7 often is used for the exponent; this gives rise to the term “a one-seventh power profile” for fully developed turbulent flow:

$$\frac{\bar{u}}{U} = \left(\frac{y}{R}\right)^{1/7} = \left(1 - \frac{r}{R}\right)^{1/7}$$

Velocity profiles for $n=6$ and $n=10$ are shown in Fig. 8.11. The parabolic profile for fully developed laminar flow is included for comparison. It is clear that the turbulent profile has a much steeper slope near

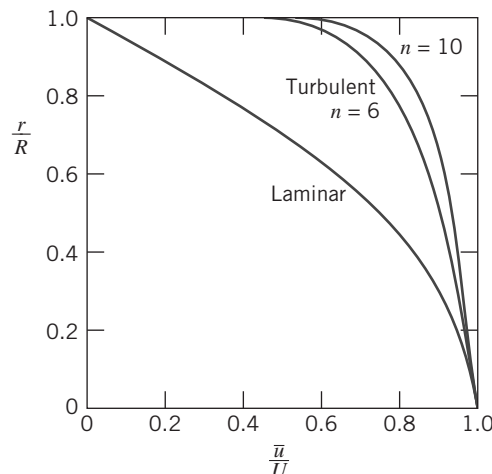


Fig. 8.11 Velocity profiles for fully developed pipe flow.

the wall. This is consistent with our discussion leading to Eq. 8.17—the fluctuating velocity components u' and v' continuously transfer momentum between adjacent fluid layers, tending to reduce the velocity gradient.

8.6 Energy Considerations in Pipe Flow

We have so far used the momentum and conservation of mass equations, in control volume form, to discuss viscous flow. It is obvious that viscous effects will have an important effect on energy considerations. In Section 6.4 we discussed the Energy Grade Line (EGL),

$$EGL = \frac{p}{\rho g} + \frac{V^2}{2g} + z \quad (6.16b)$$

and saw that this is a measure of the total mechanical energy (“pressure,” kinetic and potential, per unit mass) in a flow. We can expect that instead of being constant, which it was for inviscid flow, the EGL will continuously decrease in the direction of flow as friction “eats” the mechanical energy. We can now consider the energy equation to obtain information on the effects of friction.

Consider, for example, steady flow through the piping system, including a reducing elbow, shown in Fig. 8.12. The control volume boundaries are shown as dashed lines. They are normal to the flow at sections ① and ② and coincide with the inside surface of the pipe wall elsewhere.

Basic equation:

$$\begin{aligned} &= 0(1) = 0(2) = 0(1) = 0(3) \\ \dot{Q} - \dot{W}_s - \dot{W}_{shear} - \dot{W}_{other} &= \int_{CV} e \rho dV + \int_{CS} (e + pv) \rho \vec{V} \cdot d\vec{A} \quad (4.56) \\ e &= u + \frac{V^2}{2} + gz \end{aligned}$$

Assumptions:

- 1 $\dot{W}_s = 0, \dot{W}_{other} = 0$.
- 2 $\dot{W}_{shear} = 0$ (although shear stresses are present at the walls of the elbow, the velocities are zero there, so there is no possibility of work).
- 3 Steady flow.
- 4 Incompressible flow.
- 5 Internal energy and pressure uniform across sections ① and ②.

Under these assumptions the energy equation reduces to

$$\begin{aligned} \dot{Q} &= \dot{m}(u_2 - u_1) + \dot{m} \left(\frac{p_2}{\rho} - \frac{p_1}{\rho} \right) + \dot{m}g(z_2 - z_1) \\ &\quad + \int_{A_2} \frac{V_2^2}{2} \rho V_2 dA_2 - \int_{A_1} \frac{V_1^2}{2} \rho V_1 dA_1 \quad (8.25) \end{aligned}$$

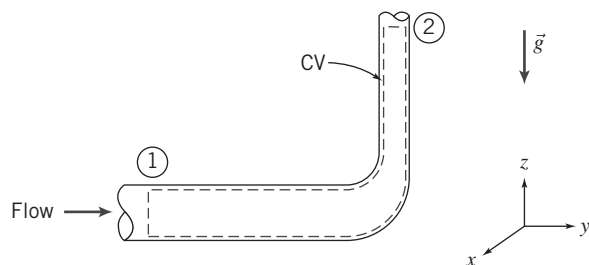


Fig. 8.12 Control volume and coordinates for energy analysis of flow through a 90° reducing elbow.

Note that we have *not* assumed the velocity to be uniform at sections ① and ②, since we know that for viscous flows the velocity at a cross-section cannot be uniform. However, it is convenient to introduce the average velocity into Eq. 8.25 so that we can eliminate the integrals. To do this, we define a kinetic energy coefficient to account for the effect of the variation in velocity on the kinetic energy of the flow.

Kinetic Energy Coefficient

The *kinetic energy coefficient*, α , is defined such that the product of the coefficient and the kinetic energy based on the average velocity equals the actual kinetic energy.

$$\int_A \frac{V^2}{2} \rho V dA = \alpha \int_A \frac{\bar{V}^2}{2} \rho V dA = \alpha \dot{m} \frac{\bar{V}^2}{2} \quad (8.26a)$$

or

$$\alpha = \frac{\int_A \rho V^3 dA}{\dot{m} \bar{V}^2} \quad (8.26b)$$

We can think of α as a correction factor that allows us to use the average velocity \bar{V} in the energy equation to compute the kinetic energy at a cross section.

For laminar flow in a pipe (velocity profile given by Eq. 8.12), $\alpha = 2.0$.

In turbulent pipe flow, the velocity profile is quite flat, as shown in Fig. 8.11. We can use Eq. 8.26b together with Eqs. 8.22 and 8.24 to determine α . Substituting the power-law velocity profile of Eq. 8.22 into Eq. 8.26b, we obtain

$$\alpha = \left(\frac{U}{\bar{V}} \right)^3 \frac{2n^2}{(3+n)(3+2n)} \quad (8.27)$$

Equation 8.24 gives \bar{V}/U as a function of the power-law exponent n ; combining this with Eq. 8.27 leads to a fairly complicated expression in n . The overall result is that in the realistic range of n , from $n = 6$ to $n = 10$ for high Reynolds numbers, α varies from 1.08 to 1.03; for the one-seventh power profile ($n = 7$), $\alpha = 1.06$. Because α is reasonably close to unity for high Reynolds numbers, and because the change in kinetic energy is usually small compared with the dominant terms in the energy equation, *we shall almost always use the approximation $\alpha = 1$ in our pipe flow calculations*.

Head Loss

Using the definition of α , the energy equation (Eq. 8.25) can be written

$$\dot{Q} = \dot{m}(u_2 - u_1) + \dot{m} \left(\frac{p_2}{\rho} - \frac{p_1}{\rho} \right) + \dot{m}g(z_2 - z_1) + \dot{m} \left(\frac{\alpha_2 \bar{V}_2^2}{2} - \frac{\alpha_1 \bar{V}_1^2}{2} \right)$$

Dividing by the mass flow rate gives

$$\frac{\delta Q}{dm} = u_2 - u_1 + \frac{p_2}{\rho} - \frac{p_1}{\rho} + gz_2 - gz_1 + \frac{\alpha_2 \bar{V}_2^2}{2} - \frac{\alpha_1 \bar{V}_1^2}{2}$$

Rearranging this equation, we write

$$\left(\frac{p_1}{\rho} + \alpha_1 \frac{\bar{V}_1^2}{2} + gz_1 \right) - \left(\frac{p_2}{\rho} + \alpha_2 \frac{\bar{V}_2^2}{2} + gz_2 \right) = (u_2 - u_1) - \frac{\delta Q}{dm} \quad (8.28)$$

In Eq. 8.28, the term

$$\left(\frac{p}{\rho} + \alpha \frac{\bar{V}^2}{2} + gz \right)$$

represents the mechanical energy per unit mass at a cross section. Compare it to the EGL expression, Eq. 6.16b, for computing “mechanical” energy, which we discussed at the beginning of this section. The differences are that in the EGL we divide by g to obtain the EGL in units of feet or meters, and here $\alpha\bar{V}^2$ allows for the fact that in a pipe flow we have a velocity profile, not a uniform flow.

The term $u_2 - u_1 - \delta Q/dm$ is equal to the difference in mechanical energy per unit mass between sections ① and ②. It represents the (irreversible) conversion of mechanical energy at section ① to unwanted thermal energy ($u_2 - u_1$) and loss of energy via heat transfer ($-\delta Q/dm$). We identify this group of terms as the total energy loss per unit mass and designate it by the symbol h_{l_T} . The dimensions of energy per unit mass FL/M are equivalent to dimensions of L^2/t^2 . Then

$$\left(\frac{p_1}{\rho} + \alpha_1 \frac{\bar{V}_1^2}{2} + g z_1 \right) - \left(\frac{p_2}{\rho} + \alpha_2 \frac{\bar{V}_2^2}{2} + g z_2 \right) = h_{l_T} \quad (8.29)$$

Equation 8.29 is one of the most important and useful equations in fluid mechanics. It enables us to compute the loss of mechanical energy caused by friction between two sections of a pipe. Now, with friction, Eq. 8.29 indicates that the pressure will change even for a constant-area horizontal pipe—mechanical energy will be continuously changed into thermal energy.

As the empirical science of hydraulics developed during the 19th century, it was common practice to express the energy balance in terms of energy per unit *weight* of flowing liquid (e.g., water) rather than energy per unit *mass*, as in Eq. 8.29. When Eq. 8.29 is divided by the acceleration of gravity, g , we obtain

$$\left(\frac{p_1}{\rho g} + \alpha_1 \frac{\bar{V}_1^2}{2g} + z_1 \right) - \left(\frac{p_2}{\rho g} + \alpha_2 \frac{\bar{V}_2^2}{2g} + z_2 \right) = \frac{h_{l_T}}{g} = H_{l_T} \quad (8.30)$$

Each term in Eq. 8.30 has dimensions of energy per unit weight of flowing fluid. Then the net dimensions of $H_{l_T} = h_{l_T}/g$ are $(L^2/t^2)(t^2/L) = L$, or feet of flowing liquid. Since the term head loss is in common use, we shall use it when referring to either H_{l_T} (with dimensions of energy per unit weight or length) or $h_{l_T} = gH_{l_T}$ (with dimensions of energy per unit mass).

Equation 8.29 (or Eq. 8.30) can be used to calculate the pressure difference between any two points in a piping system, provided the head loss, h_{l_T} (or H_{l_T}), can be determined. We shall consider calculation of head loss in the next section.

8.7 Calculation of Head Loss

Total head loss, h_{l_T} , is regarded as the sum of major losses, h_l , due to frictional effects in fully developed flow in constant-area tubes, and minor losses, h_{l_m} , resulting from entrances, fittings, area changes, and so on. Consequently, we consider the major and minor losses separately.

Major Losses: Friction Factor

The energy balance, expressed by Eq. 8.29, can be used to evaluate the major head loss. For fully developed flow through a constant-area pipe, Eq. 8.29 reduces to

$$\frac{p_1 - p_2}{\rho} = g(z_2 - z_1) + h_l \quad (8.31)$$

If the pipe is horizontal, then $z_2 = z_1$ and

$$\frac{p_1 - p_2}{\rho} = \frac{\Delta p}{\rho} = h_l \quad (8.32)$$

Thus the major head loss can be expressed as the pressure loss for fully developed flow through a horizontal pipe of constant area.

a. Laminar Flow

In laminar flow, we saw in Section 8.3 that the pressure drop may be computed analytically for fully developed flow in a horizontal pipe. Thus, from Eq. 8.13c,

$$\Delta p = \frac{128\mu L Q}{\pi D^4} = \frac{128\mu L \bar{V}(\pi D^2/4)}{\pi D^4} = 32 \frac{L}{D} \frac{\mu \bar{V}}{D}$$

Substituting in Eq. 8.32 gives

$$h_l = 32 \frac{L}{D} \frac{\mu \bar{V}}{\rho D} = \frac{L}{D} \frac{\bar{V}^2}{2} \left(64 \frac{\mu}{\rho \bar{V} D} \right) = \left(\frac{64}{Re} \right) \frac{L}{D} \frac{\bar{V}^2}{2} \quad (8.33)$$

We shall see the reason for writing h_l in this form shortly.

b. Turbulent Flow

In turbulent flow we cannot evaluate the pressure drop analytically; we must resort to experimental results and use dimensional analysis to correlate the experimental data. In fully developed turbulent flow, the pressure drop, Δp , caused by friction in a horizontal constant-area pipe is known to depend on pipe diameter, D , pipe length, L , pipe roughness, e , average flow velocity, \bar{V} , fluid density, ρ , and fluid viscosity, μ . In functional form

$$\Delta p = \Delta p(D, L, e, \bar{V}, \rho, \mu)$$

We applied dimensional analysis to this problem in Example 7.2. The results were a correlation of the form

$$\frac{\Delta p}{\rho \bar{V}^2} = f \left(\frac{\mu}{\rho \bar{V} D}, \frac{L}{D}, \frac{e}{D} \right)$$

We recognize that $\mu/\rho \bar{V} D = 1/Re$, so we can write

$$\frac{\Delta p}{\rho \bar{V}^2} = \phi \left(Re, \frac{L}{D}, \frac{e}{D} \right)$$

Substituting from Eq. 8.32, we see that

$$\frac{h_l}{\bar{V}^2} = \phi \left(Re, \frac{L}{D}, \frac{e}{D} \right)$$

Although dimensional analysis predicts the functional relationship, we must obtain actual values experimentally. Experiments show that the nondimensional head loss is directly proportional to L/D . Hence we can write

$$\frac{h_l}{\bar{V}^2} = \frac{L}{D} \phi_1 \left(Re, \frac{e}{D} \right)$$

By convention the number $\frac{1}{2}$ is introduced into the denominator so that the left side of the equation is the ratio of the head loss to the kinetic energy per unit mass of flow. Then

$$\frac{h_l}{\frac{1}{2} \bar{V}^2} = \frac{L}{D} \phi_2 \left(Re, \frac{e}{D} \right)$$

The unknown function, $\phi_2(Re, e/D)$, is defined as the *friction factor*, f ,

$$f \equiv \phi_2 \left(Re, \frac{e}{D} \right)$$

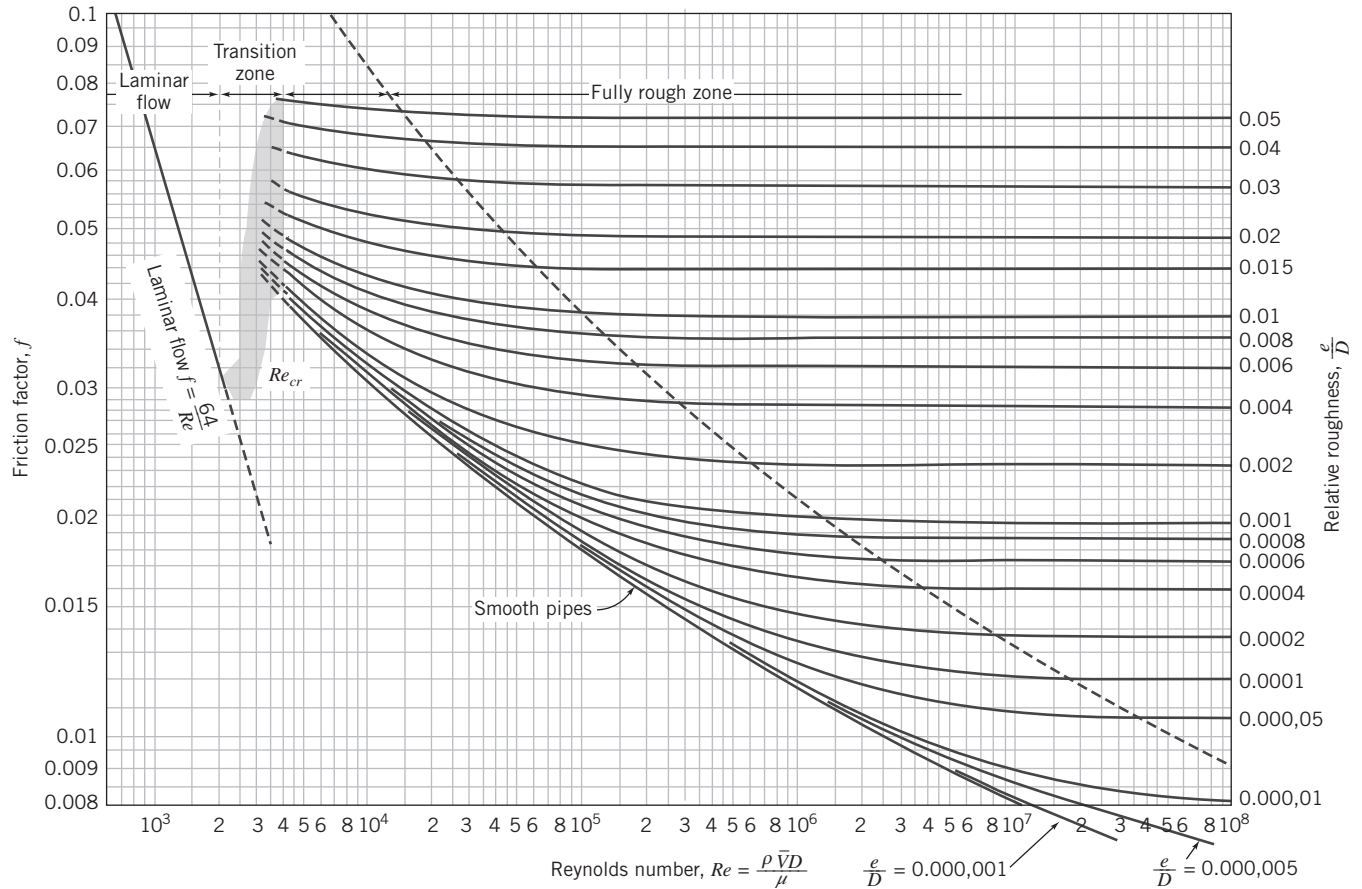


Fig. 8.13 Friction factor for fully developed flow in circular pipes. (Data from Moody [6].)

Using the friction factor

$$h_l = f \frac{L}{D} \frac{\bar{V}^2}{2} \quad (8.34)$$

or

$$H_l = f \frac{L}{D} \frac{\bar{V}^2}{2g} \quad (8.35)$$

The relation between the friction factor and Reynolds number is shown in Fig. 8.13. Figure 8.13 is known as the Moody diagram after L. F. Moody who first presented the data in this fashion [8]. The friction factor taken from Fig. 8.13 is generally considered to be accurate to about 10%. The friction factor defined by Eq. 8.34 is the *Darcy friction factor*. The *Fanning friction factor*, less frequently used, is defined in terms of the wall shear stress. The *Darcy friction factor* is four times the *Fanning friction factor*.

To determine head loss for fully developed flow with known conditions, the Reynolds number is evaluated first. Roughness, e , is obtained from data such as in Table 8.1. Then the friction factor, f , can be read from the appropriate curve in Fig. 8.13, at the known values of Re and e/D . Finally, head loss can be found using Eq. 8.34 or Eq. 8.35.

Table 8.1
Roughness for Pipes of Common Engineering Materials

Pipe	Roughness, e	
	Feet	Millimeters
Riveted steel	0.003–0.03	0.9–9
Concrete	0.001–0.01	0.3–3
Wood stave	0.0006–0.003	0.2–0.9
Cast iron	0.00085	0.26
Galvanized iron or steel	0.0005	0.15
Asphalted or internally coated cast iron	0.0004	0.12
Galvanized steel ductwork	0.00015–0.00035	0.05–0.10
Aluminum ductwork	0.00015–0.0002	0.04–0.06
Commercial steel or wrought iron	0.00015	0.046
Commercially smooth brass, copper, or plastic pipe	0.000005	0.0015

Source: Data from Moody [6].

All of the e values given in Table 8.1 are for new pipes in relatively good condition. Over long periods of service, corrosion takes place and, particularly in hard water areas, lime deposits and rust scale form on pipe walls. Deposit formation increases wall roughness appreciably, and also decreases the effective diameter. These factors combine to cause e/D to increase by factors of 5 to 10 for old pipes. An example is shown in Fig. 8.14.

Several features of Fig. 8.13 require discussion. The friction factor for laminar flow may be obtained by comparing Eqs. 8.33 and 8.34:

$$h_l = \left(\frac{64}{Re} \right) \frac{L}{D} \frac{\bar{V}^2}{2} = f \frac{L}{D} \frac{\bar{V}^2}{2}$$

Consequently, for laminar flow

$$f_{\text{laminar}} = \frac{64}{Re} \quad (8.36)$$

Thus, in laminar flow, the friction factor is a function of Reynolds number only; it is independent of roughness. Although we took no notice of roughness in deriving Eq. 8.33, experimental results verify that the friction factor is a function only of Reynolds number in laminar flow.

As the Reynolds number is increased above the transition value, the velocity profile continues to become fuller, as noted in Section 8.5. For values of relative roughness $e/D \leq 0.001$, the friction factor at first tends to follow the smooth pipe curve, along which friction factor is a function of Reynolds number only. However, as the Reynolds number increases, the velocity profile becomes still fuller. The size of the thin viscous sublayer near the tube wall decreases. As roughness elements begin to poke through this layer, the effect of roughness becomes important, and the friction factor becomes a function of both the Reynolds number and the relative roughness.

At very large Reynolds number, most of the roughness elements on the tube wall protrude through the viscous sublayer. The drag and, hence, the pressure loss, depend only on the size of the roughness elements. This is termed the “fully rough” flow regime; the friction factor depends only on e/D in this regime.

To summarize the preceding discussion, we see that as Reynolds number is increased, the friction factor decreases as long as the flow remains laminar. At transition, f increases sharply. In the turbulent

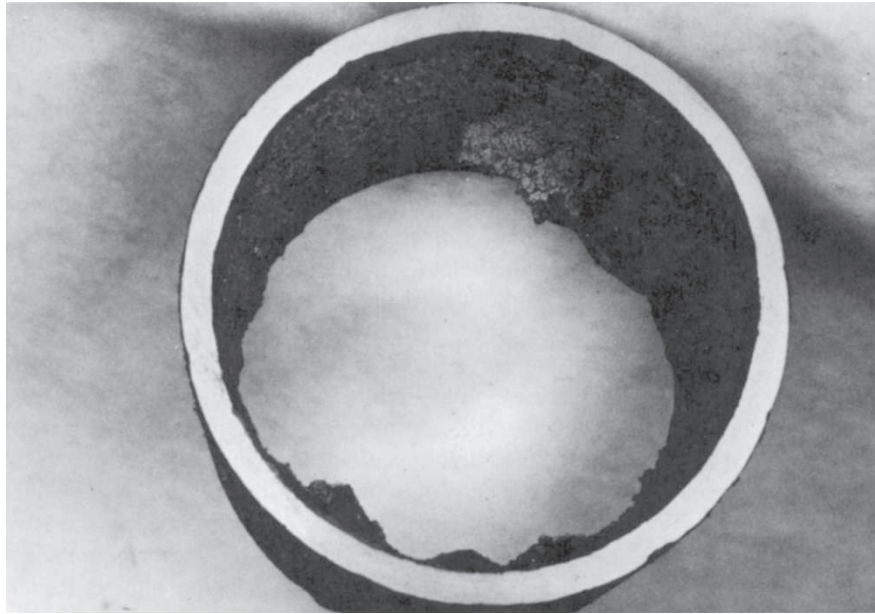


Photo courtesy of Alan T. McDonald

Fig. 8.14 Pipe section removed after 40 years of service as a water line showing formation of scale.

flow regime, the friction factor decreases gradually as Reynolds number increases and levels out at a constant value depending on the relative roughness.

Empirical correlations have been fit to the data. The most widely used formula for friction factor is from Colebrook [7]

$$\frac{1}{\sqrt{f}} = -2.0 \log \left(\frac{e/D}{3.7} + \frac{2.51}{Re \sqrt{f}} \right) \quad (8.37a)$$

Equation 8.37a is implicit in f , and usually requires either iteration of an equation solver to find f . Haaland [27] developed the following equation,

$$\frac{1}{\sqrt{f}} = -1.8 \log \left[\left(\frac{e/D}{3.7} \right)^{1.11} + \frac{6.9}{Re} \right] \quad (8.37b)$$

as an approximation to the Colebrook equation. For $Re > 3000$, it gives results within about 2 percent of the Colebrook equation, without the need to iterate.

For turbulent flow in smooth pipes, the Blasius correlation, valid for $Re \leq 10^5$, is

$$f = \frac{0.316}{Re^{0.25}} \quad (8.38)$$

For $Re > 10^5$, the following relation for smooth pipes is found to be accurate (modified from [26])

$$f = \frac{0.184}{Re^{0.2}} \quad (8.39)$$

Minor Losses

A piping system typically has a variety of fittings, bends, or abrupt changes in area. Additional head losses are encountered, primarily as a result of flow separation. Energy eventually is dissipated by violent mixing in the separated zones. These are termed *minor* losses even though they may be larger than the pipe friction loss, especially for short pipes. Minor losses are computed as

$$h_{l_m} = K \frac{\bar{V}^2}{2} \quad (8.40)$$

where the *loss coefficient*, K , is determined usually experimentally or sometimes with CFD software for each situation. For flow through pipe bends and fittings, the loss coefficient, K , is found to vary with pipe size (diameter) in much the same manner as the friction factor, f , for flow through a straight pipe. The *ASHRAE Handbook—Fundamentals* [9] and websites such as The Engineering Toolbox [22] provide a wealth of data on fitting loss coefficients. The data presented here should be considered as representative for some commonly encountered situations.

a. Inlets and Exits

A poorly designed inlet to a pipe can cause appreciable head loss. If the inlet has sharp corners, flow separation occurs at the corners, and a *vena contracta* is formed. The fluid must accelerate locally to pass through the reduced flow area at the vena contracta. Losses in mechanical energy result from the unconfined mixing as the flow stream decelerates again to fill the pipe. Three basic inlet geometries are shown in Table 8.2. From the table it is clear that the loss coefficient is reduced significantly when the inlet is rounded even slightly. For a well-rounded inlet ($r/D \geq 0.15$) the entrance loss coefficient is almost negligible. Example 8.9 illustrates a procedure for experimentally determining the loss coefficient for a pipe inlet.

The kinetic energy per unit mass is completely dissipated by mixing when flow discharges from a duct into a large reservoir or plenum chamber. The situation corresponds to flow through an abrupt expansion with $AR=0$ (Fig. 8.15). The minor loss coefficient thus equals 1 for turbulent flow. However, the addition of a diffuser can reduce h_{l_m} considerably (see Example 8.10).

b. Enlargements and Contractions

Minor loss coefficients for sudden expansions and contractions in circular ducts are given in Fig. 8.15. Note that both loss coefficients are based on the *larger* value of velocity. Thus losses for a sudden expansion are based on $\bar{V}_1^2/2$, and those for a contraction are based on $\bar{V}_2^2/2$.

Losses caused by area change can be reduced by installing a gradual expansion or contraction between the two sections of straight pipe. Data for contractions are given in Table 8.3. Note that the final column for the included angle $\theta = 180^\circ$ agrees with the data of Fig. 8.15.

Losses in diffusers depend on a number of geometric and flow variables. Diffuser data most commonly are presented in terms of a pressure recovery coefficient, C_p , defined as the ratio of static pressure rise to inlet dynamic pressure,

$$C_p \equiv \frac{P_2 - P_1}{\frac{1}{2}\rho \bar{V}_1^2} \quad (8.41)$$

This shows what fraction of the inlet kinetic energy shows up as a pressure rise. The ideal (frictionless) pressure recovery coefficient is given by

$$C_{p_i} = 1 - \frac{1}{AR^2} \quad (8.42)$$

Table 8.2
Minor Loss Coefficients for Pipe Entrances

Entrance Type	Minor Loss Coefficient, K^a
Reentrant	0.5–1.0 (depending on length of pipe entrance)
Square-edged	0.5
Rounded	r/D 0.02 0.06 ≥ 0.15 K 0.3 0.2 0.04

^a Based on $h_{l_m} = K(\bar{V}^2/2)$, where \bar{V} is the mean velocity in the pipe.

Source: Data from Reference [9].

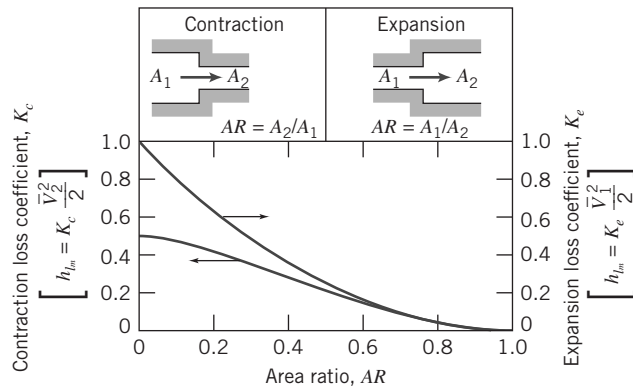


Fig. 8.15 Loss coefficients for flow through sudden area changes. (Data from Streeter [1].)

where AR is the area ratio. Hence, the ideal pressure recovery coefficient is a function only of the area ratio. In reality a diffuser typically has turbulent flow, and the static pressure rise in the direction of flow may cause flow separation from the walls if the diffuser is poorly designed; flow pulsations can even occur. For these reasons the actual C_p will be somewhat less than indicated by Eq. 8.42. Data for conical diffusers with fully developed turbulent pipe flow at the inlet are presented in Fig. 8.16 as a function of geometry. Note that more tapered diffusers (small divergence angle ϕ or large dimensionless length N/R_1) are more likely to approach the ideal constant value for C_p . We can relate the actual C_p to the head loss. If gravity is neglected, and $\alpha_1 = \alpha_2 = 1.0$, the head loss equation, Eq. 8.29, reduces to

Table 8.3
Loss Coefficients (K) for Gradual Contractions: Round and Rectangular Ducts

A_2/A_1	Included Angle, θ , Degrees						
	10	15–40	50–60	90	120	150	180
0.50	0.05	0.05	0.06	0.12	0.18	0.24	0.26
0.25	0.05	0.04	0.07	0.17	0.27	0.35	0.41
0.10	0.05	0.05	0.08	0.19	0.29	0.37	0.43

Note: Coefficients are based on $h_{l_m} = K(\bar{V}_2^2/2)$.

Source: Data from ASHRAE [9].

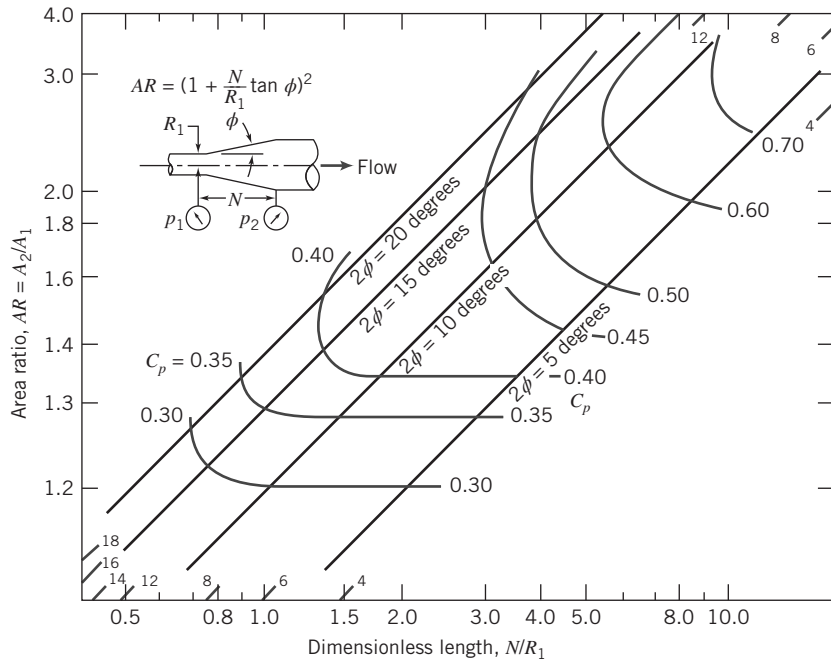


Fig. 8.16 Pressure recovery for conical diffusers with fully developed turbulent pipe flow at inlet. (Data from Cockrell and Bradley [10].)

$$\left[\frac{p_1}{\rho} + \frac{\bar{V}_1^2}{2} \right] - \left[\frac{p_2}{\rho} + \frac{\bar{V}_2^2}{2} \right] = h_{l_T} = h_{l_m}$$

Thus,

$$h_{l_m} = \frac{\bar{V}_1^2}{2} - \frac{\bar{V}_2^2}{2} - \frac{p_2 - p_1}{\rho}$$

$$h_{l_m} = \frac{\bar{V}_1^2}{2} \left[\left(1 - \frac{\bar{V}_2^2}{\bar{V}_1^2} \right) - \frac{p_2 - p_1}{\frac{1}{2}\rho\bar{V}_1^2} \right] = \frac{\bar{V}_1^2}{2} \left[\left(1 - \frac{\bar{V}_2^2}{\bar{V}_1^2} \right) - C_p \right]$$

From continuity, $A_1 \bar{V}_1 = A_2 \bar{V}_2$, so

$$h_{l_m} = \frac{\bar{V}_1^2}{2} \left[1 - \left(\frac{A_1}{A_2} \right)^2 - C_p \right]$$

or

$$h_{l_m} = \frac{\bar{V}_1^2}{2} \left[\left(1 - \frac{1}{(AR)^2} \right) - C_p \right] \quad (8.43)$$

The frictionless result (Eq. 8.42) is obtained from Eq. 8.43 if $h_{l_m} = 0$. We can combine Eqs. 8.42 and 8.43 to obtain an expression for the head loss in terms of the actual and ideal C_p values:

$$h_{l_m} = (C_{p_i} - C_p) \frac{\bar{V}_1^2}{2} \quad (8.44)$$

Diffuser pressure recovery is essentially independent of Reynolds number for inlet Reynolds numbers greater than 7.5×10^4 [11]. Diffuser pressure recovery with uniform inlet flow is somewhat better than that for fully developed inlet flow. Performance maps for plane wall, conical, and annular diffusers for a variety of inlet flow conditions are presented in [12], [14], and [15].

Since static pressure rises in the direction of flow in a diffuser, flow may separate from the walls. For some geometries, the outlet flow is distorted. For wide angle diffusers, vanes or splitters can be used to suppress stall and improve pressure recovery [13].

c. Pipe Bends

The head loss of a bend is larger than for fully developed flow through a straight section of equal length. The additional loss is primarily the result of secondary flow. The loss coefficients for bends of different construction, geometry, and angle are given in Table 8.4. Because they are simple and inexpensive to construct in the field, miter bends often are used in large pipe systems. Miter bends often have turning vanes installed inside them, and, as shown in Table 8.4, the loss is reduced significantly. Bends and fittings in a piping system may have threaded, flanged, or welded connections. For small diameters, threaded joints are most common; large pipe systems frequently have flanged or welded joints.

d. Valves and Fittings

Losses for flow through valves and fittings are also expressed in terms of a loss coefficient. Some representative values are given in Table 8.4.

The resistance for fully open valves is low, but losses increase markedly when valves are partially open. Valve design varies significantly among manufacturers. Whenever possible, loss coefficients furnished by the valve supplier should be used if accurate results are needed.

The values in Table 8.4 are typical, but the loss coefficient for a given pipe fitting depends on the pipe size. In general, the loss coefficient for larger pipe diameters is smaller than that for smaller pipes, and the difference can be as large as a factor of two. The velocity of the fluid has a minor effect, but in general, the loss coefficients are higher for higher velocities than for lower velocities. Further, loss coefficients for fittings and valves may be considerably different from the tabulated values depending on the care used in fabricating and assembling a system. In sizing a pump or fan to meet a given head loss for a piping or duct system, it is common to oversize slightly to account for the uncertainty and variation in the actual value of the pipe and fitting loss coefficients. Reference [12] provides loss coefficients for a wide range of fittings.

Table 8.4
Representative Loss Coefficients for Fittings and Valves

Fitting	Geometry	K	Fitting	Geometry	K
90° elbow	Flanged regular	0.3	Globe valve	Open	10
	Flanged long radius	0.2	Angle valve	Open	5
	Threaded regular	1.5	Gate valve	Open	0.20
	Threaded long radius	0.7		75% open	1.10
	Miter	1.30		50% open	3.6
	Miter with vanes	0.20		25% open	28.8
45° Elbow	Threaded regular	0.4	Ball valve	Open	0.5
	Flanged long radius	0.2		1/3 closed	5.5
Tee, Straight through flow	Threaded	0.9		2/3 closed	200
	Flanged	0.2	Water meter		7
Tee, branching flow	Threaded	2.0	Coupling		0.08
	Flanged	1.0			

Source: Data from References [9] and [21]

Pumps, Fans, and Blowers in Fluid Systems

In many practical flow situations (e.g., the cooling system of an automobile engine, the HVAC system of a building), the driving force for maintaining the flow against friction is a pump for liquids or a fan or blower for gases. Here we will consider pumps, although all the results apply equally to fans and blowers. We generally neglect heat transfer and internal energy changes of the fluid and incorporate them later into the definition of the pump efficiency, so the first law of thermodynamics applied across the pump is

$$\dot{W}_{\text{pump}} = \dot{m} \left[\left(\frac{p}{\rho} + \frac{\bar{V}^2}{2} + gz \right)_{\text{discharge}} - \left(\frac{p}{\rho} + \frac{\bar{V}^2}{2} + gz \right)_{\text{suction}} \right]$$

We can also compute the head Δh_{pump} (energy/mass) produced by the pump,

$$\Delta h_{\text{pump}} = \frac{\dot{W}_{\text{pump}}}{\dot{m}} = \left(\frac{p}{\rho} + \frac{\bar{V}^2}{2} + gz \right)_{\text{discharge}} - \left(\frac{p}{\rho} + \frac{\bar{V}^2}{2} + gz \right)_{\text{suction}} \quad (8.45)$$

In many cases the inlet and outlet diameters (and therefore velocities) and elevations are the same or negligibly different, so Eq. 8.45 simplifies to

$$\Delta h_{\text{pump}} = \frac{\Delta p_{\text{pump}}}{\rho} \quad (8.46)$$

The idea is that in a pump-pipe system the head produced by the pump (Eq. 8.45 or 8.46) is needed to overcome the head loss for the pipe system. Hence, the flow rate in such a system depends on the pump characteristics and the major and minor losses of the pipe system. We will learn in Chapter 10 that the head produced by a given pump is not constant, but varies with flow rate through the pump, leading to the notion of “matching” a pump to a given system to achieve the desired flow rate.

A useful relation is obtained from Eq. 8.46 if we multiply by $\dot{m} = \rho Q$, where Q is the volume flow rate, and recall that $\dot{m}\Delta h_{\text{pump}}$ is the power supplied to the fluid,

$$\dot{W}_{\text{pump}} = Q \Delta p_{\text{pump}} \quad (8.47)$$

We can also define the pump efficiency:

$$\eta = \frac{\dot{W}_{\text{pump}}}{\dot{W}_{\text{in}}} \quad (8.48)$$

where \dot{W}_{pump} is the power reaching the fluid, and \dot{W}_{in} is the power input (usually electrical) to the pump.

When applying the energy equation (Eq. 8.29) to a pipe system, we may include the pump in the system. For these cases we can simply include the head of the pump as a “negative loss”: since it a positive energy gain for the flow.

$$\left(\frac{p_1}{\rho} + \alpha_1 \frac{\bar{V}_1^2}{2} + gz_1 \right) - \left(\frac{p_2}{\rho} + \alpha_2 \frac{\bar{V}_2^2}{2} + gz_2 \right) = h_{l_T} - \Delta h_{\text{pump}} \quad (8.49)$$

Noncircular Ducts

The empirical correlations for turbulent pipe flow also may be used for losses involving noncircular ducts, by introducing the *hydraulic diameter*, provided their cross sections are not too exaggerated.

The hydraulic diameter is defined as

$$D_h \equiv \frac{4A}{P} \quad (8.50)$$

where D_h is used in place of the diameter, D . In Eq. 8.50, A is cross-sectional area, and P is *wetted perimeter*, the length of wall in contact with the flowing fluid at any cross section. The factor 4 is introduced so that the hydraulic diameter will equal the duct diameter for a circular cross section. For a circular duct, $A = \pi D^2/4$ and $P = \pi D$, so that

$$D_h = \frac{4A}{P} = \frac{4\left(\frac{\pi}{4}\right)D^2}{\pi D} = D$$

For a rectangular duct of width b and height h , $A = bh$ and $P = 2(b + h)$, so

$$D_h = \frac{4bh}{2(b+h)}$$

If the *aspect ratio*, ar , is defined as $ar = h/b$, then

$$D_h = \frac{2h}{1+ar}$$

for rectangular ducts. For a square duct, $ar = 1$ and $D_h = h$.

The hydraulic diameter concept can be applied in the approximate range $\frac{1}{4} < ar < 4$. Under these conditions, the turbulent correlations for pipe flow give acceptably accurate results for rectangular ducts. Since such ducts are easy and cheap to fabricate from sheet metal, they are commonly used in air conditioning, heating, and ventilating applications. Extensive data on losses for air flow are available (e.g., see [9, 14]).

Losses caused by secondary flows increase rapidly for more extreme geometries, so the correlations are not applicable to wide, flat ducts, or to ducts of triangular or other irregular shapes. Experimental data must be used when precise design information is required for specific situations.

8.8 Solution of Pipe Flow Problems

Section 8.7 provides us with a complete scheme for solving many different pipe flow problems. For convenience we collect together the relevant computing equations.

The *energy equation*, relating the conditions at any two points 1 and 2 for a single-path pipe system, is

$$\left(\frac{p_1}{\rho} + \alpha_1 \frac{\bar{V}_1^2}{2} + gz_1 \right) - \left(\frac{p_2}{\rho} + \alpha_2 \frac{\bar{V}_2^2}{2} + gz_2 \right) = h_{l_T} = \sum h_l + \sum h_{l_m} \quad (8.29)$$

This equation expresses the fact that there will be a loss of mechanical energy (“pressure,” kinetic and/or potential) in the pipe. Recall that for turbulent flows $\alpha \approx 1$. Note that by judicious choice of points 1 and 2 we can analyze not only the entire pipe system, but also just a certain section of it that we may be interested in. The *total head loss* is given by the sum of the major and minor losses. (Remember that we can also include “negative losses” for any pumps present between points 1 and 2. The relevant form of the energy equation is then Eq. 8.49.)

Each *major loss* is given by

$$h_l = f \frac{L}{D} \frac{\bar{V}^2}{2} \quad (8.34)$$

where the *friction factor* is obtained from

$$f = \frac{64}{Re} \quad \text{for laminar flow } (Re < 2300) \quad (8.36)$$

or

$$\frac{1}{\sqrt{f}} = -2.0 \log \left(\frac{e/D}{3.7} + \frac{2.51}{Re\sqrt{f}} \right) \quad \text{for turbulent flow } (Re \geq 2300) \quad (8.37)$$

and Eqs. 8.36 and 8.37 are presented graphically in the Moody chart (Fig. 8.13).

Each *minor loss* is given by

$$h_{l_m} = K \frac{\bar{V}^2}{2} \quad (8.40)$$

We also note that the flow rate Q is related to the average velocity \bar{V} at each pipe cross section by

$$Q = \pi \frac{D^2}{4} \bar{V}$$

We will apply these equations first to single-path systems.

Single-Path Systems

In single-path pipe problems we generally know the system configuration (type of pipe material and hence pipe roughness, the number and type of elbows, valves, and other fittings, and changes of elevation), as well as the fluid (ρ and μ) we will be working with. Although not the only possibilities, usually the goal is to determine one of the following values:

- (a) The pressure drop Δp , for a given pipe (L and D), and flow rate Q .
- (b) The pipe length L , for a given pressure drop Δp , pipe diameter D , and flow rate Q .
- (c) The flow rate Q , for a given pipe (L and D), and pressure drop Δp .
- (d) The pipe diameter D , for a given pipe length L , pressure drop Δp , and flow rate Q .

Each of these cases often arises in real-world situations. For example, case (a) is a necessary step in selecting the correct size pump to maintain the desired flow rate in a system—the pump must be able to produce the system Δp at the specified flow rate Q . Cases (a) and (b) are computationally straightforward but cases (c) and (d) are more complicated. We will discuss each case, and present an example for each.

The examples present solutions as you might do them using a calculator, but there is also an *Excel* workbook for each. The course website has an *Excel* add-in that once installed will automatically compute f from Re and e/D . The advantage of using a computer application such as an equation solver or a spreadsheet is that the friction factors can be directly obtained and iteration can be efficiently performed. Finally, we can ask “what-if” questions such as if we double the head produced by a pump, how much will the flow rate in a given system increase?

a. Find Δp for a Given L , D , and Q

These types of problems are quite straightforward—the energy equation (Eq. 8.29) can be solved directly for $\Delta p = (p_1 - p_2)$ in terms of known or computable quantities. The flow rate leads to the Reynolds number and hence the friction factor for the flow; tabulated data can be used for minor loss coefficients. The energy equation can then be used to directly obtain the pressure drop. Example 8.5 illustrates this type of problem.

b. Find L for a Given Δp , D , and Q

These types of problems are also straightforward—the energy equation (Eq. 8.29) can be solved directly for L in terms of known or computable quantities. The flow rate again leads to the Reynolds number and hence the friction factor for the flow. Tabulated data can be used for minor loss coefficients. The energy equation can then be rearranged and solved directly for the pipe length. Example 8.6 illustrates this type of problem.

c. Find Q for a Given Δp , L , and D

These types of problems require either manual iteration or use of a computer application. The unknown flow rate or velocity is needed before the Reynolds number and hence the friction factor can be found. To manually iterate we first solve the energy equation directly for \bar{V} in terms of known quantities and the unknown friction factor f . To start the iterative process we make a reasonable guess for f . Then we can compute a Reynolds number and hence obtain a new value for f . We repeat the iteration process $f \rightarrow \bar{V} \rightarrow Re \rightarrow f$ until convergence (usually only two or three iterations are necessary). Example 8.7 illustrates this type of problem.

d. Find D for a Given Δp , L , and Q

These types of problems arise, for example, when we have designed a pump-pipe system and wish to choose the best pipe diameter—the best being the minimum diameter (for minimum pipe cost) that will deliver the design flow rate. As with case c, we need to manually iterate or use a computer application. The unknown diameter is needed before the Reynolds number and relative roughness, and hence the friction factor, can be found. To manually find a solution we make successive guesses for D until the corresponding pressure drop Δp computed from the energy equation matches the design Δp . Example 8.8 illustrates this type of problem.

In choosing a pipe size, it is logical to work with diameters that are available commercially. Pipe is manufactured in a limited number of standard sizes. Some data for standard pipe sizes are given in Table 8.5. For data on extra strong or double extra strong pipes, consult a handbook, e.g., [8] and [22]. Pipe larger than 12 in. nominal diameter is produced in multiples of 2 in. up to a nominal diameter of 36 in. and in multiples of 6 in. for still larger sizes.

Table 8.5

Standard Sizes for Carbon Steel, Alloy Steel, and Stainless Steel Pipe

Nominal Pipe Size (in.)	Inside Diameter (in.)	Nominal Pipe Size (in.)	Inside Diameter (in.)
$\frac{1}{8}$	0.269	$2\frac{1}{2}$	2.469
$\frac{1}{4}$	0.364	3	3.068
$\frac{3}{8}$	0.493	4	4.026
$\frac{1}{2}$	0.622	5	5.047
$\frac{3}{4}$	0.824	6	6.065
1	1.049	8	7.981
$1\frac{1}{2}$	1.610	10	10.020
2	2.067	12	12.000

^a Source: Data from References [8] and [22].

We have solved Examples 8.7 and 8.8 by iteration. Several specialized forms of friction factor versus Reynolds number diagrams are available to solve problems of this type without the need for iteration. For examples of these specialized diagrams, see Daily and Harleman [15] and White [16].

Examples 8.9 and 8.10 illustrate the evaluation of minor loss coefficients and the application of a diffuser to reduce exit kinetic energy from a flow system.

Example 8.5 PIPE FLOW INTO A RESERVOIR: PRESSURE DROP UNKNOWN (CASE A)

A 100-m length of smooth horizontal pipe is attached to a large reservoir. A pump is attached to the end of the pipe to pump water into the reservoir at a volume flow rate of $0.01 \text{ m}^3/\text{s}$. What pressure must the pump produce at the pipe to generate this flow rate? The inside diameter of the smooth pipe is 75 mm.

Given: Water is pumped at $0.01 \text{ m}^3/\text{s}$ through a 75-mm-diameter smooth pipe, with $L = 100 \text{ m}$, into a constant-level reservoir of depth $d = 10 \text{ m}$.

Find: Pump pressure, p_1 , required to maintain the flow.

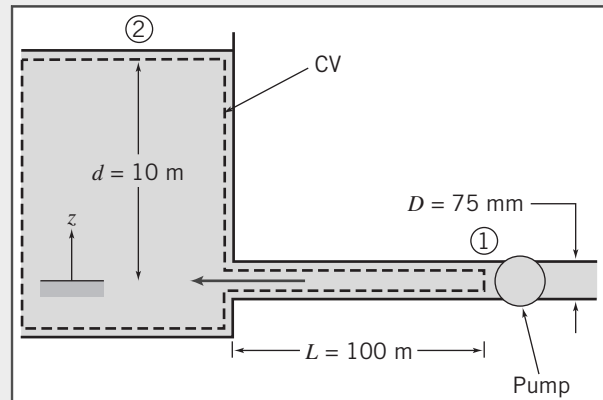
Solution:

Governing equations:

$$\left(\frac{p_1}{\rho} + \alpha_1 \frac{\bar{V}_1^2}{2} + gz_1 \right) - \left(\frac{p_2}{\rho} + \alpha_2 \frac{\bar{V}_2^2}{2} + gz_2 \right) = h_{l_T} = h_l + h_{l_m} \quad (8.29)$$

where

$$h_l = f \frac{L}{D} \frac{\bar{V}^2}{2} \quad (8.34) \quad \text{and} \quad h_{l_m} = K \frac{\bar{V}^2}{2} \quad (8.40a)$$



For the given problem, $p_1 = p_{\text{pump}}$ and $p_2 = 0$ (gage), so $\Delta p = p_1 - p_2 = p_{\text{pump}}$, $\bar{V}_1 = \bar{V}$, $\bar{V}_2 \approx 0$, K (exit loss) = 1.0, and $\alpha_1 \approx 1.0$. If we set $z_1 = 0$, then $z_2 = d$. Simplifying Eq. 8.29 gives

$$\frac{\Delta p}{\rho} + \frac{\bar{V}^2}{2} - gd = f \frac{L}{D} \frac{\bar{V}^2}{2} + \frac{\bar{V}^2}{2} \quad (1)$$

The left side of the equation is the loss of mechanical energy between points ① and ②; the right side is the major and minor losses that contributed to the loss. Solving for the pressure drop, $\Delta p = p_{\text{pump}}$,

$$p_{\text{pump}} = \Delta p = \rho \left(gd + f \frac{L}{D} \frac{\bar{V}^2}{2} \right)$$

Everything on the right side of the equation is known or can be readily computed. The flow rate Q leads to \bar{V} ,

$$\bar{V} = \frac{Q}{A} = \frac{4Q}{\pi D^2} = \frac{4}{\pi} \times 0.01 \frac{\text{m}^3}{\text{s}} \times \frac{1}{(0.075)^2 \text{ m}^2} = 2.26 \text{ m/s}$$

This in turn [assuming water at 20°C, $\rho = 999 \text{ kg/m}^3$, and $\mu = 1.0 \times 10^{-3} \text{ kg/(m}\cdot\text{s)}$] leads to the Reynolds number

$$Re = \frac{\rho \bar{V} D}{\mu} = 999 \frac{\text{kg}}{\text{m}^3} \times 2.26 \frac{\text{m}}{\text{s}} \times 0.075 \text{ m} \times \frac{\text{m} \cdot \text{s}}{1.0 \times 10^{-3} \text{ kg}} = 1.70 \times 10^5$$

For turbulent flow in a smooth pipe ($e=0$), from Eq. 8.37, $f=0.0162$. Then

$$\begin{aligned} p_{\text{pump}} &= \Delta p = \rho \left(gd + f \frac{L}{D} \frac{\bar{V}^2}{2} \right) \\ &= 999 \frac{\text{kg}}{\text{m}^3} \left(9.81 \frac{\text{m}}{\text{s}^2} \times 10 \text{ m} + (0.0162) \times \frac{100 \text{ m}}{0.075 \text{ m}} \times \frac{(2.26)^2 \text{ m}^2}{2 \text{ s}^2} \right) \times \frac{\text{N} \cdot \text{s}^2}{\text{kg} \cdot \text{m}} \end{aligned}$$

$$p_{\text{pump}} = 1.53 \times 10^5 \text{ N/m}^2 (\text{gage})$$

Hence,

$$p_{\text{pump}} = 153 \text{ kPa gage} \quad \text{--- } p_{\text{pump}}$$

This problem illustrates the method for manually calculating pressure drop.

 The Excel workbook for this problem automatically computes Re and f from the given data. It then solves Eq. 1 directly for pressure p_{pump} without having to explicitly solve for it first.

Example 8.6 FLOW IN A PIPELINE: LENGTH UNKNOWN (CASE B)

Crude oil flows through a level section of the Alaskan pipeline at a rate of 1.6 million barrels per day (1 barrel = 42 gal). The pipe inside diameter is 48 in.; its roughness is equivalent to galvanized iron. The maximum allowable pressure is 1200 psi; the minimum pressure required to keep dissolved gases in solution in the crude oil is 50 psi. The crude oil has SG = 0.93; its viscosity at the pumping temperature of 140°F is $\mu = 3.5 \times 10^{-4} \text{ lbf}\cdot\text{s}/\text{ft}^2$. For these conditions, determine the maximum possible spacing between pumping stations. If the pump efficiency is 85 percent, determine the power that must be supplied at each pumping station.

Given: Flow of crude oil through horizontal section of Alaskan pipeline.

$D = 48 \text{ in.}$ (roughness of galvanized iron),
 $\text{SG} = 0.93$, $\mu = 3.5 \times 10^{-4} \text{ lbf}\cdot\text{s}/\text{ft}^2$

Find: (a) Maximum spacing, L .
(b) Power needed at each pump station.

Solution: As shown in the figure, we assume that the Alaskan pipeline is made up of repeating pump-pipe sections. We can draw two control volumes: CV₁, for the pipe flow (state ② to state ①); CV₂, for the pump (state ① to state ②).

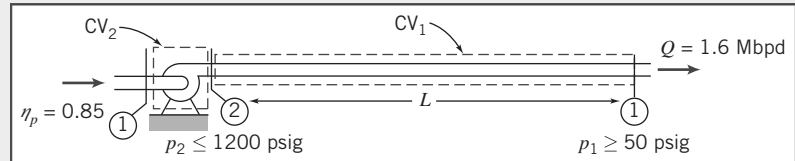
First we apply the energy equation for steady, incompressible pipe flow to CV₁.

Governing equations:

$$\left(\frac{p_2}{\rho} + \alpha_2 \frac{\bar{V}_2^2}{2} + gz_2 \right) - \left(\frac{p_1}{\rho} + \alpha_1 \frac{\bar{V}_1^2}{2} + gz_1 \right) = h_{l_T} = h_l + h_{l_m} \quad (8.29)$$

where

$$h_l = f \frac{L}{D} \frac{\bar{V}^2}{2} \quad (8.34) \quad \text{and} \quad h_{l_m} = K \frac{\bar{V}^2}{2} \quad (8.40a)$$



Assumptions:

- 1 $\alpha_1 \bar{V}_1^2 = \alpha_2 \bar{V}_2^2$.
- 2 Horizontal pipe, $z_1 = z_2$.
- 3 Neglect minor losses.
- 4 Constant viscosity.

Then, using CV₁

$$\Delta p = p_2 - p_1 = f \frac{L}{D} \rho \frac{\bar{V}^2}{2} \quad (1)$$

or

$$L = \frac{2D}{f} \frac{\Delta p}{\rho \bar{V}^2} \text{ where } f = f(Re, e/D)$$

$$Q = 1.6 \times 10^6 \frac{\text{bbl}}{\text{day}} \times 42 \frac{\text{gal}}{\text{bbl}} \times \frac{\text{ft}^3}{7.48 \text{ gal}} \times \frac{\text{day}}{24 \text{ hr}} \times \frac{\text{hr}}{3600 \text{ s}} = 104 \text{ ft}^3/\text{s}$$

so

$$\bar{V} = \frac{Q}{A} = 104 \frac{\text{ft}^3}{\text{s}} \times \frac{4}{\pi(4)^2 \text{ ft}^2} = 8.27 \text{ ft/s}$$

$$Re = \frac{\rho \bar{V} D}{\mu} = (0.93) 1.94 \frac{\text{slug}}{\text{ft}^3} \times 8.27 \frac{\text{ft}}{\text{s}} \times 4 \text{ ft} \times \frac{\text{ft}^2}{3.5 \times 10^{-4} \text{ lbf} \cdot \text{s}} \times \frac{\text{lbf} \cdot \text{s}^2}{\text{slug} \cdot \text{ft}}$$

$$Re = 1.71 \times 10^5$$

From Table 8.1, $e = 0.0005 \text{ ft}$ and hence $e/D = 0.00012$. Then from Eq. 8.37, $f = 0.017$ and thus

$$L = \frac{2}{0.017} \times 4 \text{ ft} \times (1200 - 50) \frac{\text{lbf}}{\text{in.}^2} \times \frac{\text{ft}^3}{(0.93) 1.94 \text{ slug}} \times \frac{\text{s}^2}{(8.27)^2 \text{ ft}^2}$$

$$\times 144 \frac{\text{in.}^2}{\text{ft}^2} \times \frac{\text{slug} \cdot \text{ft}}{\text{lbf} \cdot \text{s}^2} = 6.32 \times 10^5 \text{ ft}$$

$$L = 632,000 \text{ ft} (120 \text{ mi}) \xleftarrow{\hspace{10cm}} L$$

To find the pumping power we can apply the first law of thermodynamics to CV₂. This control volume consists only of the pump, and we saw in Section 8.7 that this law simplifies to

$$\dot{W}_{\text{pump}} = Q \Delta p_{\text{pump}} \quad (8.47)$$

and the pump efficiency is

$$\eta = \frac{\dot{W}_{\text{pump}}}{\dot{W}_{\text{in}}} \quad (8.48)$$

We recall that \dot{W}_{pump} is the power reaching the fluid, and \dot{W}_{in} is the power input. Because we have a repeating system the pressure rise through the pump (i.e., from state ① to state ②) equals the pressure drop in the pipe (i.e., from state ② to state ①),

$$\Delta p_{\text{pump}} = \Delta p$$

so that

$$\dot{W}_{\text{pump}} = Q \Delta p_{\text{pump}} = 104 \frac{\text{ft}^3}{\text{s}} \times \frac{(1200 - 50) \text{lbf}}{\text{in.}^2} \times \frac{144 \text{ in.}^2}{\text{ft}^2} \\ \times \frac{\text{hp} \cdot \text{s}}{550 \text{ ft} \cdot \text{lbf}} \approx 31,300 \text{ hp}$$

and the required power input is

$$\dot{W}_{\text{in.}} = \frac{\dot{W}_{\text{pump}}}{\eta} = \frac{31300 \text{ hp}}{0.85} = 36,800 \text{ hp} \leftarrow \dot{W}_{\text{needed}}$$

This problem illustrates the method for manually calculating pipe length L .

 The Excel workbook for this problem automatically computes Re and f from the given data. It then solves Eq. 1 directly for L without having to explicitly solve for it first.

Example 8.7 FLOW FROM A WATER TOWER: FLOW RATE UNKNOWN (CASE C.)

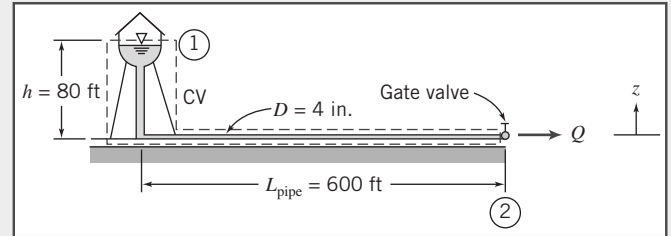
A fire protection system is supplied from a water tower and standpipe 80 ft tall. The longest pipe in the system is 600 ft and is made of cast iron about 20 years old. The pipe contains one gate valve; other minor losses may be neglected. The pipe diameter is 4 in. Determine the maximum rate of flow (gpm) through this pipe.

Given: Fire protection system, as shown.

Find: Q , gpm.

Solution:

Governing equations:



$$\approx 0(2)$$

$$\left(\frac{p_1}{\rho} + \alpha_1 \frac{\bar{V}_1^2}{2} + gz_1 \right) - \left(\frac{p_2}{\rho} + \alpha_2 \frac{\bar{V}_2^2}{2} + gz_2 \right) = h_{l_r} = h_l + h_{l_m} \quad (8.29)$$

where

$$h_l = f \frac{L}{D} \frac{\bar{V}^2}{2} \quad (8.34) \quad \text{and} \quad h_{l_m} = f \frac{L_e}{D} \frac{\bar{V}^2}{2} \quad (8.40b)$$

Assumptions:

$$1 \quad p_1 = p_2 = p_{\text{atm}}$$

$$2 \quad \bar{V}_1 = 0, \text{ and } \alpha_2 \approx 1.0.$$

Then Eq. 8.29 can be written as

$$g(z_1 - z_2) - \frac{\bar{V}_2^2}{2} = h_{l_r} = f \left(\frac{L}{D} + \frac{L_e}{D} \right) \frac{\bar{V}_2^2}{2} \quad (1)$$

For a fully open gate valve, from Table 8.4, $L_e/D = 8$. Thus

$$g(z_1 - z_2) = \frac{\bar{V}_2^2}{2} \left[f \left(\frac{L}{D} + 8 \right) + 1 \right]$$

To manually iterate, we solve for \bar{V}_2 and obtain

$$\bar{V}_2 = \left[\frac{2g(z_1 - z_2)}{f(L/D + 8) + 1} \right]^{1/2} \quad (2)$$

To be conservative, assume the standpipe is the same diameter as the horizontal pipe. Then

$$\frac{L}{D} = \frac{600 \text{ ft} + 80 \text{ ft}}{4 \text{ in.}} \times \frac{12 \text{ in.}}{\text{ft}} = 2040$$

Also

$$z_1 - z_2 = h = 80 \text{ ft}$$

To solve Eq. 2 manually we need to iterate. To start, we make an estimate for f by assuming the flow is fully turbulent (where f is constant). This value can be obtained from solving Eq. 8.37 using a calculator or from Fig. 8.13. For a large value of Re (e.g., 10^8), and a roughness ratio $e/D \approx 0.005$ ($e = 0.00085 \text{ ft}$ for cast iron is obtained from Table 8.1, and doubled to allow for the fact that the pipe is old), we find that $f \approx 0.03$. Thus a first iteration for \bar{V}_2 from Eq. 2 is

$$\bar{V}_2 = \left[2 \times 32.2 \frac{\text{ft}}{\text{s}^2} \times 80 \text{ ft} \times \frac{1}{0.03(2040 + 8) + 1} \right]^{1/2} = 9.08 \text{ ft/s}$$

Now obtain a new value for f :

$$Re = \frac{\rho \bar{V} D}{\mu} = \frac{\bar{V} D}{\nu} = 9.08 \frac{\text{ft}}{\text{s}} \times \frac{\text{ft}}{3} \times \frac{\text{s}}{1.21 \times 10^{-5} \text{ ft}^2} = 2.50 \times 10^5$$

For $e/D = 0.005, f = 0.0308$ from Eq. 8.37. Thus we obtain

$$\bar{V}_2 = \left[2 \times 32.2 \frac{\text{ft}}{\text{s}^2} \times 80 \text{ ft} \times \frac{1}{0.0308(2040 + 8) + 1} \right]^{1/2} = 8.97 \text{ ft/s}$$

The values we have obtained for \bar{V}_2 (9.08 and 8.97 ft/s) differ by less than 2%—an acceptable level of accuracy. If this accuracy had not been achieved we would continue iterating until this, or any other accuracy we desired, was achieved (usually only one or two more iterations at most are necessary for reasonable accuracy). Note that instead of starting with a fully rough value for f , we could have started with a guess value for \bar{V}_2 of, say, 1 or 10 ft/s. The volume flow rate is

$$Q = \bar{V}_2 A = \bar{V}_2 \frac{\pi D^2}{4} = 8.97 \frac{\text{ft}}{\text{s}} \times \frac{\pi}{4} \left(\frac{1}{3}\right)^2 \text{ft}^2 \times 7.48 \frac{\text{gal}}{\text{ft}^3} \times 60 \frac{\text{s}}{\text{min}}$$

$Q = 351 \text{ gpm} \leftarrow$

This problem illustrates the method for manually iterating to calculate flow rate.



The Excel workbook for this problem automatically iterates to solve for the flow rate Q . It solves Eq. 1 without having to solve the explicit equation (Eq. 2) for \bar{V}_2 (or Q) first.

Example 8.8 FLOW IN AN IRRIGATION SYSTEM: DIAMETER UNKNOWN (CASE C)

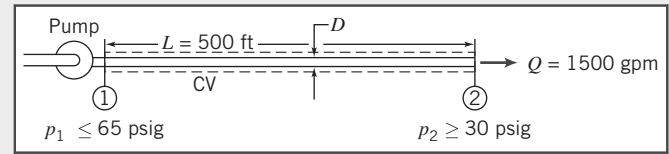
Spray heads in an agricultural spraying system are to be supplied with water through 500 ft of drawn aluminum tubing from an engine-driven pump. In its most efficient operating range, the pump output is 1500 gpm at a discharge pressure not exceeding 65 psig. For satisfactory operation, the sprinklers must operate at 30 psig or higher pressure. Minor losses and elevation changes may be neglected. Determine the smallest standard pipe size that can be used.

Given: Water supply system, as shown.

Find: Smallest standard D .

Solution: Δp , L , and Q are known. D is unknown, so iteration is needed to determine the minimum standard diameter that satisfies the pressure drop constraint at the given flow rate. The maximum allowable pressure drop over the length, L , is

$$\Delta p_{\max} = p_{1\max} - p_{2\min} = (65 - 30) \text{ psi} = 35 \text{ psi}$$



Governing equations:

$$\begin{aligned} \left(\frac{p_1}{\rho} + \alpha_1 \frac{\bar{V}_1^2}{2} + g z_1 \right) - \left(\frac{p_2}{\rho} + \alpha_2 \frac{\bar{V}_2^2}{2} + g z_2 \right) &= h_{l_T} \\ &= 0 \quad (3) \\ h_{l_T} &= h_l + h_{f,m} = f \frac{L}{D} \frac{\bar{V}_2^2}{2} \end{aligned} \quad (8.29)$$

Assumptions:

- 1 Steady flow.
- 2 Incompressible flow.
- 3 $h_{l_T} = h_l$, i.e., $h_{l_m} = 0$.
- 4 $z_1 = z_2$.
- 5 $\bar{V}_1 = \bar{V}_2 = \bar{V}$; $\alpha_1 \approx \alpha_2$.

Then

$$\Delta p = p_1 - p_2 = f \frac{L}{D} \frac{\rho \bar{V}^2}{2} \quad (1)$$

Equation 1 is difficult to solve for D because both \bar{V} and f depend on D ! The best approach is to use a computer application such as *Excel* to automatically solve for D . For completeness here we show the manual iteration procedure. The first step is to express Eq. 1 and the Reynolds number in terms of Q instead of \bar{V} (Q is constant but \bar{V} varies with D). We have $\bar{V} = Q/A = 4Q/\pi D^2$ so that

$$\Delta p = f \frac{L}{D} \frac{\rho}{2} \left(\frac{4Q}{\pi D^2} \right)^2 = \frac{8fL\rho Q^2}{\pi^2 D^5} \quad (2)$$

The Reynolds number in terms of Q is

$$Re = \frac{\rho \bar{V} D}{\mu} = \frac{\bar{V} D}{\nu} = \frac{4Q}{\pi D^2} \frac{D}{\nu} = \frac{4Q}{\pi \nu D}$$

Finally, Q must be converted to cubic feet per second.

$$Q = 1500 \frac{\text{gal}}{\text{min}} \times \frac{\text{min}}{60 \text{ s}} \times \frac{\text{ft}^3}{7.48 \text{ gal}} = 3.34 \text{ ft}^3/\text{s}$$

For an initial guess, take nominal 4 in. (4.026 in. i.d.) pipe:

$$Re = \frac{4Q}{\pi \nu D} = \frac{4}{\pi} \times 3.34 \frac{\text{ft}^3}{\text{s}} \times \frac{\text{s}}{1.21 \times 10^{-5} \text{ ft}^2} \times \frac{1}{4.026 \text{ in.}} \times 12 \frac{\text{in.}}{\text{ft}} = 1.06 \times 10^6$$

For drawn tubing, $e = 5 \times 10^{-6}$ ft (Table 8.1) and hence $e/D = 1.5 \times 10^{-5}$, so $f \approx 0.012$ (Eq. 8.37), and

$$\begin{aligned} \Delta p &= \frac{8fL\rho Q^2}{\pi^2 D^5} = \frac{8}{\pi^2} \times 0.012 \times 500 \text{ ft} \times 1.94 \frac{\text{slug}}{\text{ft}^3} \times (3.34)^2 \frac{\text{ft}^6}{\text{s}^2} \times \frac{1}{(4.026)^5 \text{ in.}^5} \times 1728 \frac{\text{in.}^3}{\text{ft}^3} \times \frac{\text{lbf} \cdot \text{s}^2}{\text{slug} \cdot \text{ft}} \\ \Delta p &= 172 \text{ lbf/in.}^2 > \Delta p_{\max} \end{aligned}$$

Since this pressure drop is too large, try $D = 6$ in. (actually 6.065 in. i.d.):

$$Re = \frac{4}{\pi} \times 3.34 \frac{\text{ft}^3}{\text{s}} \times \frac{\text{s}}{1.21 \times 10^{-5} \text{ ft}^2} \times \frac{1}{6.065 \text{ in.}} \times 12 \frac{\text{in.}}{\text{ft}} = 6.95 \times 10^5$$

For drawn tubing with $D = 6$ in., $e/D = 1.0 \times 10^{-5}$, so $f \approx 0.013$ (Eq. 8.37), and

$$\begin{aligned}\Delta p &= \frac{8}{\pi^2} \times 0.013 \times 500 \text{ ft} \times 1.94 \frac{\text{slug}}{\text{ft}^3} \times (3.34)^2 \frac{\text{ft}^6}{\text{s}^2} \\ &\quad \times \frac{1}{(6.065)^5 \text{ in.}^5} \times (12)^3 \frac{\text{in.}^3}{\text{ft}^3} \times \frac{\text{lbf} \cdot \text{s}^2}{\text{slug} \cdot \text{ft}} \\ \Delta p &= 24.0 \text{ lbf/in.}^2 < \Delta p_{\max}\end{aligned}$$

Since this is less than the allowable pressure drop, we should check a 5 in. nominal pipe with an actual i.d. of 5.047 in.,

$$Re = \frac{4}{\pi} \times 3.34 \frac{\text{ft}^3}{\text{s}} \times \frac{\text{s}}{1.21 \times 10^{-5} \text{ ft}^2} \times \frac{1}{5.047 \text{ in.}} \times 12 \frac{\text{in.}}{\text{ft}} = 8.36 \times 10^5$$

For drawn tubing with $D = 5$ in., $e/D = 1.2 \times 10^{-5}$, so $f \approx 0.0122$ (Eq. 8.37), and

$$\begin{aligned}\Delta p &= \frac{8}{\pi^2} \times 0.0122 \times 500 \text{ ft} \times 1.94 \frac{\text{slug}}{\text{ft}^3} \times (3.34)^2 \frac{\text{ft}^6}{\text{s}^2} \\ &\quad \times \frac{1}{(5.047)^5 \text{ in.}^5} \times (12)^3 \frac{\text{in.}^3}{\text{ft}^3} \times \frac{\text{lbf} \cdot \text{s}^2}{\text{slug} \cdot \text{ft}} \\ \Delta p &= 56.4 \text{ lbf/in.}^2 > \Delta p_{\max}\end{aligned}$$

Thus the criterion for pressure drop is satisfied for a minimum nominal diameter of 6 in. pipe. $\xleftarrow{\hspace{1cm}} D$

This problem illustrates the method for manually iterating to calculate pipe diameter.

 The Excel workbook for this problem automatically iterates to solve for the exact pipe diameter D that satisfies Eq. 1, without having to solve the explicit equation (Eq. 2) for D first. Then the smallest standard pipe size that is equal to or greater than this value needs to be selected. For the given data, $D = 5.58$ in., so the appropriate pipe size is 6 in.

Example 8.9 CALCULATION OF ENTRANCE LOSS COEFFICIENT

Hamilton [22] reports results of measurements made to determine entrance losses for flow from a reservoir to a pipe with various degrees of entrance rounding. A copper pipe 10 ft long, with 1.5 in. i.d., was used for the tests. The pipe discharged to atmosphere. For a square-edged entrance, a discharge of $0.566 \text{ ft}^3/\text{s}$ was measured when the reservoir level was 85.1 ft above the pipe centerline. From these data, evaluate the loss coefficient for a square-edged entrance.

Given: Pipe with square-edged entrance discharging from reservoir as shown.

Find: K_{entrance} .

Solution: Apply the energy equation for steady, incompressible pipe flow.

Governing equations:

$$\begin{aligned}\approx 0(2) &= 0 \\ \frac{p_1}{\rho} + \alpha_1 \frac{\bar{V}_1^2}{2} + g z_1 &= \frac{p_2}{\rho} + \alpha_2 \frac{\bar{V}_2^2}{2} + g z_2 + h_{l_r} \\ h_{l_r} &= f \frac{L}{D} \frac{\bar{V}_2^2}{2} + K_{\text{entrance}} \frac{\bar{V}_2^2}{2}\end{aligned}$$

Assumptions:

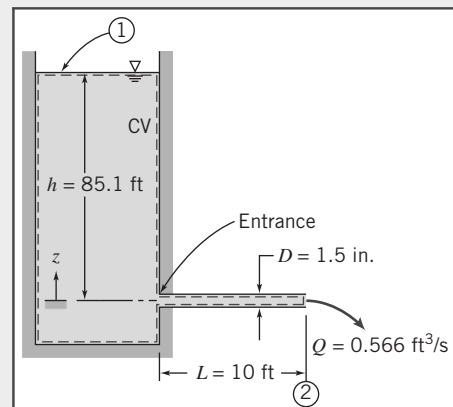
$$1 \ p_1 = p_2 = p_{\text{atm}}.$$

$$2 \ \bar{V}_1 \approx 0.$$

$$\text{Substituting for } h_{l_r} \text{ and dividing by } g \text{ gives } z_1 - h = \alpha_2 \frac{\bar{V}_2^2}{2g} + f \frac{L}{D} \frac{\bar{V}_2^2}{2g} + K_{\text{entrance}} \frac{\bar{V}_2^2}{2g}$$

or

$$K_{\text{entrance}} = \frac{2gh}{\bar{V}_2^2} - f \frac{L}{D} - \alpha_2 \quad (1)$$



The average velocity is

$$\bar{V}_2 = \frac{Q}{A} = \frac{4Q}{\pi D^2}$$

$$\bar{V}_2 = \frac{4}{\pi} \times 0.566 \frac{\text{ft}^3}{\text{s}} \times \frac{1}{(1.5)^2 \text{ in.}^2} \times 1.44 \frac{\text{in.}^2}{\text{ft}^2} = 46.1 \text{ ft/s}$$

Assume $T = 70^\circ\text{F}$, so $\nu = 1.05 \times 10^{-5} \text{ ft}^2/\text{s}$ (Table A.7). Then

$$Re = \frac{\bar{V}D}{\nu} = 46.1 \frac{\text{ft}}{\text{s}} \times 1.5 \text{ in.} \times \frac{\text{s}}{1.05 \times 10^{-5} \text{ ft}^2} \times \frac{\text{ft}}{12 \text{ in.}} = 5.49 \times 10^5$$

For drawn tubing, $e = 5 \times 10^{-6} \text{ ft}$ (Table 8.1), so $e/D = 0.000,04$ and $f = 0.0135$ (Eq. 8.37).

In this problem we need to be careful in evaluating the kinetic energy correction factor α_2 , as it is a significant factor in computing K_{entrance} from Eq. 1. We recall from Section 8.6 and previous examples that we have usually assumed $\alpha \approx 1$, but here we will compute a value from Eq. 8.27:

$$\alpha = \left(\frac{U}{\bar{V}}\right)^3 \frac{2n^2}{(3+n)(3+2n)} \quad (8.27)$$

To use this equation we need values for the turbulent power-law coefficient n and the ratio of centerline to mean velocity U/\bar{V} . For n , from Section 8.5

$$n = -1.7 + 1.8 \log(Re_U) \approx 8.63 \quad (8.23)$$

where we have used the approximation $Re_U \approx Re_{\bar{V}}$. For \bar{V}/U , we have

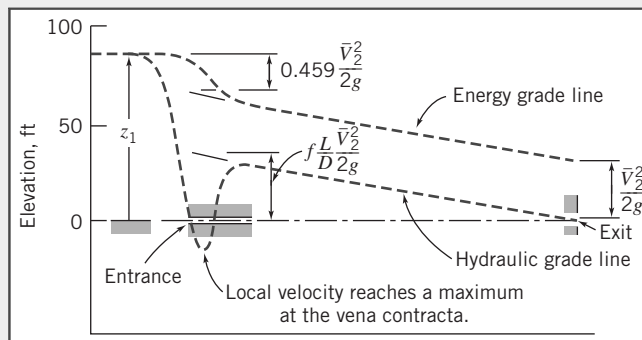
$$\frac{\bar{V}}{U} = \frac{2n^2}{(n+1)(2n+1)} = 0.847 \quad (8.24)$$

Using these results in Eq. 8.27 we find $\alpha = 1.04$. Substituting into Eq. 1, we obtain

$$K_{\text{entrance}} = 2 \times 32.2 \frac{\text{ft}}{\text{s}^2} \times 85.1 \text{ ft} \times \frac{\text{s}^2}{(46.1)^2 \text{ ft}^2} - (0.0135) \frac{10 \text{ ft}}{1.5 \text{ in.}} \times 12 \frac{\text{in.}}{\text{ft}} - 1.04$$

$$K_{\text{entrance}} = 0.459 \xrightarrow{\text{_____}} K_{\text{entrance}}$$

This coefficient compares favorably with that shown in Table 8.2. The hydraulic and energy grade lines are shown below. The large head loss in a square-edged entrance is due primarily to separation at the sharp inlet corner and formation of a vena contracta immediately downstream from the corner. The effective flow area reaches a minimum at the vena contracta, so the flow velocity is a maximum there. The flow expands again following the vena contracta to fill the pipe. The uncontrolled expansion following the vena contracta is responsible for most of the head loss (see Example 8.12).



Rounding the inlet corner reduces the extent of separation significantly. This reduces the velocity increase through the vena contracta and consequently reduces the head loss caused by the entrance. A “well-rounded” inlet almost eliminates flow separation; the flow pattern approaches that shown in Fig. 8.1. The added head loss in a well-rounded inlet compared with fully developed flow is the result of higher wall shear stresses in the entrance length.

This problem:

- Illustrates a method for obtaining the value of a minor loss coefficient from experimental data.
- Shows how the EGL and HGL lines first introduced in Section 6.4 for inviscid flow are modified by the presence of major and minor losses. The EGL line continuously drops as mechanical energy is consumed—quite sharply when, for example, we have a square-edged entrance loss; the HGL at each location is lower than the EGL by an amount equal to the local dynamic head $\bar{V}^2/2g$ —at the vena contracta, for example, the HGL experiences a large drop, then recovers.

Example 8.10 USE OF DIFFUSER TO INCREASE FLOW RATE

Water rights granted to each citizen by the Emperor of Rome gave permission to attach to the public water main a calibrated, circular, tubular bronze nozzle [17]. Some citizens were clever enough to take unfair advantage of a law that regulated flow rate by such an indirect method. They installed diffusers on the outlets of the nozzles to increase their discharge. Assume the static head available from the main is $z_0 = 1.5 \text{ m}$ and the nozzle exit diameter is $D = 25 \text{ mm}$. (The discharge is to atmospheric pressure.) Determine the increase in flow rate when a diffuser with $N/R_1 = 3.0$ and $AR = 2.0$ is attached to the end of the nozzle.

Given: Nozzle attached to water main as shown.

Find: Increase in discharge when diffuser with $N/R_1 = 3.0$ and $AR = 2.0$ is installed.

Solution: Apply the energy equation for steady, incompressible pipe flow.

Governing equation:

$$\frac{p_0}{\rho} + \alpha_0 \frac{\bar{V}_0^2}{2} + gz_0 = \frac{p_1}{\rho} + \alpha_1 \frac{\bar{V}_1^2}{2} + gz_1 + h_{l_T} \quad (8.29)$$

Assumptions:

1 $\bar{V}_0 \approx 0$.

2 $\alpha_1 \approx 1$.

For the nozzle alone,

$$\begin{aligned} &\approx 0(1) \quad \approx 1(2) \quad = 0 \\ \frac{p_0}{\rho} + \alpha_0 \frac{\bar{V}_0^2}{2} + gz_0 &= \frac{p_1}{\rho} + \frac{\bar{V}_1^2}{2} + gz_1 + h_{l_T} \\ h_{l_T} &= K_{\text{entrance}} \frac{\bar{V}_1^2}{2} \end{aligned}$$

Thus

$$gz_0 = \frac{\bar{V}_1^2}{2} + K_{\text{entrance}} \frac{\bar{V}_1^2}{2} = (1 + K_{\text{entrance}}) \frac{\bar{V}_1^2}{2} \quad (1)$$

Solving for the velocity and substituting the value of $K_{\text{entrance}} \approx 0.04$ (from Table 8.2),

$$\bar{V}_1 = \sqrt{\frac{2gz_0}{1.04}} = \sqrt{\frac{2}{1.04} \times 9.81 \frac{\text{m}}{\text{s}^2} \times 1.5 \text{ m}} = 5.32 \text{ m/s}$$

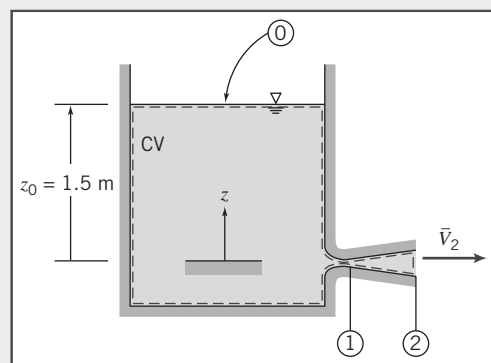
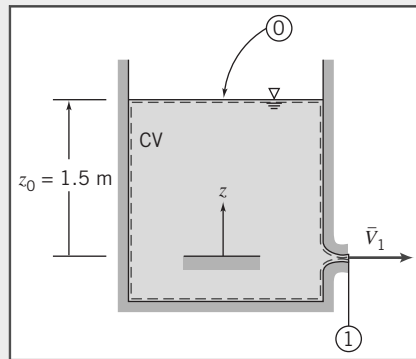
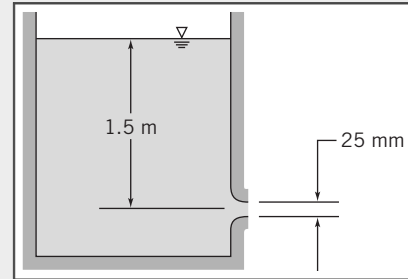
$$Q = \bar{V}_1 A_1 = \bar{V}_1 \frac{\pi D_1^2}{4} = 5.32 \frac{\text{m}}{\text{s}} \times \frac{\pi}{4} \times (0.025)^2 \text{ m}^2 = 0.00261 \text{ m}^3/\text{s} \quad Q$$

For the nozzle with diffuser attached,

$$\begin{aligned} &\approx 0(1) \quad \approx 1(2) \quad = 0 \\ \frac{p_0}{\rho} + \alpha_0 \frac{\bar{V}_0^2}{2} + gz_0 &= \frac{p_2}{\rho} + \frac{\bar{V}_2^2}{2} + gz_2 + h_{l_T} \\ h_{l_T} &= K_{\text{entrance}} \frac{\bar{V}_1^2}{2} + K_{\text{diffuser}} \frac{\bar{V}_2^2}{2} \end{aligned}$$

or

$$gz_0 = \frac{\bar{V}_2^2}{2} + (K_{\text{entrance}} + K_{\text{diffuser}}) \frac{\bar{V}_1^2}{2} \quad (2)$$



From continuity $\bar{V}_1 A_1 = \bar{V}_2 A_2$, so

$$\bar{V}_2 = \bar{V}_1 \frac{A_1}{A_2} = \bar{V}_1 \frac{1}{AR}$$

and Eq. 2 becomes

$$gz_0 = \left[\frac{1}{(AR)^2} + K_{\text{entrance}} + K_{\text{diffuser}} \right] \frac{\bar{V}_1^2}{2} \quad (3)$$

Figure 8.16 gives data for $C_p = \frac{p_2 - p_1}{\frac{1}{2}\rho\bar{V}_1^2}$ for diffusers.

To obtain K_{diffuser} , apply the energy equation from ① to ②.

$$\frac{p_1}{\rho} + \alpha_1 \frac{\bar{V}_1^2}{2} + gz_1 = \frac{p_2}{\rho} + \alpha_2 \frac{\bar{V}_2^2}{2} + gz_2 + K_{\text{diffuser}} \frac{\bar{V}_1^2}{2}$$

Solving, with $\alpha_2 \approx 1$, we obtain

$$K_{\text{diffuser}} = 1 - \frac{\bar{V}_2^2}{\bar{V}_1^2} - \frac{p_2 - p_1}{\frac{1}{2}\rho\bar{V}_1^2} = 1 - \left(\frac{A_1}{A_2} \right)^2 - C_p = 1 - \frac{1}{(AR)^2} - C_p$$

From Fig. 8.16, $C_p = 0.45$, so

$$K_{\text{diffuser}} = 1 - \frac{1}{(2.0)^2} - 0.45 = 0.75 - 0.45 = 0.3$$

Solving Eq. 3 for the velocity and substituting the values of K_{entrance} and K_{diffuser} , we obtain

$$\bar{V}_1^2 = \frac{2gz_0}{0.25 + 0.04 + 0.3}$$

so

$$\bar{V}_1 = \sqrt{\frac{2gz_0}{0.59}} = \sqrt{\frac{2}{0.59} \times 9.81 \frac{\text{m}}{\text{s}^2} \times 1.5 \text{ m}} = 7.06 \text{ m/s}$$

and

$$Q_d = \bar{V}_1 A_1 = \bar{V}_1 \frac{\pi D_1^2}{4} = 7.06 \frac{\text{m}}{\text{s}} \times \frac{\pi}{4} \times (0.025)^2 \text{ m}^2 = 0.00347 \text{ m}^3/\text{s} \quad Q_d$$

The flow rate increase that results from adding the diffuser is

$$\frac{\Delta Q}{Q} = \frac{Q_d - Q}{Q} = \frac{Q_d}{Q} - 1 = \frac{0.00347}{0.00261} - 1 = 0.330 \quad \text{or} \quad 33 \text{ percent} \quad \frac{\Delta Q}{Q}$$

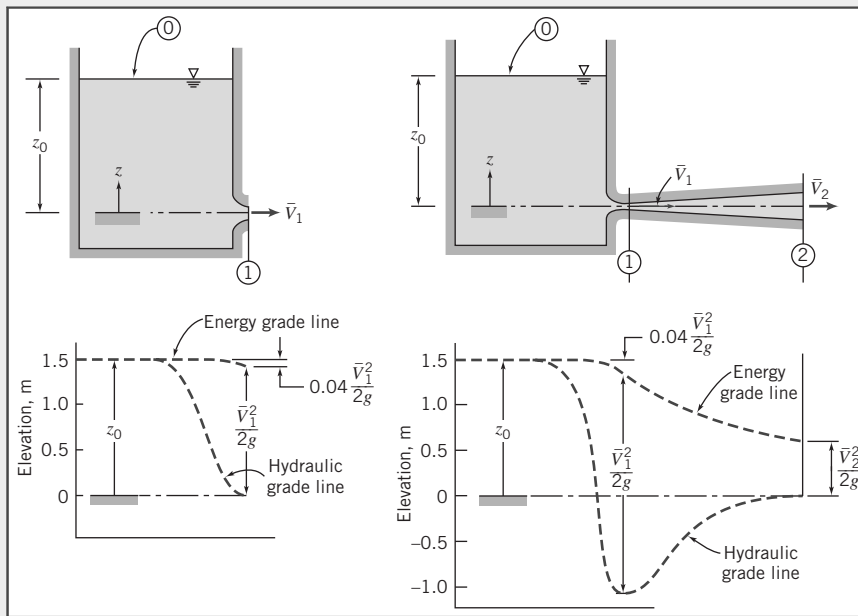
Addition of the diffuser significantly increases the flow rate! There are two ways to explain this.

First, we can sketch the EGL and HGL curves—approximately to scale—as shown below. We can see that, as required, the HGL at the exit is zero for both flows (recall that the HGL is the sum of static pressure and potential heads). However, the pressure rises through the diffuser, so the pressure at the diffuser inlet will be, as shown, quite low (below atmospheric). Hence, with the diffuser, the Δp driving force for the nozzle is much larger than that for the bare nozzle, leading to a much greater velocity, and flow rate, at the nozzle exit plane—it is as if the diffuser acted as a suction device on the nozzle.

Second, we can examine the energy equations for the two flows (for the bare nozzle Eq. 1, and for the nozzle with diffuser Eq. 3). These equations can be rearranged to yield equations for the velocity at the nozzle exit,

$$\bar{V}_1 = \sqrt{\frac{2gz_0}{1 + K_{\text{entrance}}}} \quad (\text{bare nozzle}) \quad \bar{V}_1 = \sqrt{\frac{2gz_0}{\frac{1}{(AR)^2} + K_{\text{diffuser}} + K_{\text{entrance}}}} \quad (\text{nozzle + diffuser})$$

Comparing these two expressions, we see that the diffuser introduces an extra term (its loss coefficient $K_{\text{diffuser}} = 0.3$) to the denominator, tending to reduce the nozzle velocity, but on the other hand we replace the term 1, representing loss of the bare nozzle exit plane kinetic energy, with $1/(AR)^2 = 0.25$, representing a smaller loss, of the diffuser exit plane kinetic energy. The net effect is that we replace 1 in the denominator with $0.25 + 0.3 = 0.55$, leading to a net increase in the nozzle velocity. The resistance to flow introduced by adding the diffuser is more than made up by the fact that we “throw away” much less kinetic energy at the exit of the device (the exit velocity for the bare nozzle is 5.32 m/s, whereas for the diffuser it is 1.77 m/s).



Water Commissioner Frontinus standardized conditions for all Romans in 97 A.D. He required that the tube attached to the nozzle of each customer's pipe be the same diameter for at least 50 lineal feet from the public water main (see Example 8.10).

Multiple-Path Systems

Many real-world pipe systems (e.g., the pipe network that supplies water to the apartments in a large building) consist of a network of pipes of various diameters assembled in a complicated configuration that may contain parallel and series connections. As an example, consider part of a system as shown in Fig. 8.17. Water is supplied at some pressure from a manifold at point 1, and flows through the components shown to the drain at point 5. Some water flows through pipes A, B, C, and D, constituting a *series* of pipes; some flows through A, E, F or G, H, C, and D and the two main branches F and G, which are in *parallel*. We analyze this type of problem in a similar way to how we analyze DC resistor circuits in electrical theory. We apply the conservation of mass principle and the head loss equations.

The simple rules for analyzing piping networks can be expressed in various ways. We will express them as follows:

- 1 The net mass flow out of any node (junction) is zero.
- 2 Each node has a unique pressure head (HGL).

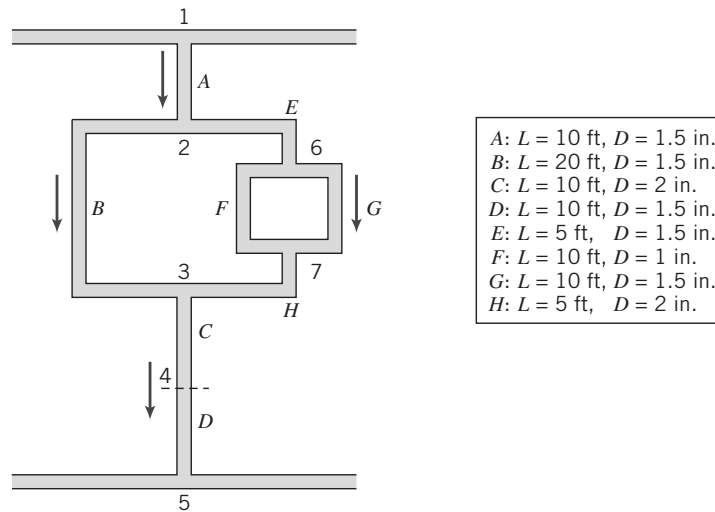


Fig. 8.17 Schematic of part of a pipe network.

For example, in Fig. 8.17 rule 1 means that the flow into node 2 from pipe A must equal the sum of outflows to pipes B and E. Rule 2 means that the pressure head at node 7 must be equal to the head at node 6 less the losses through pipe F or pipe G, as well as equal to the head at node 3 plus the loss in pipe H.

The problems that arise with pipe networks can be as varied as those we discussed when studying single-path systems, but the most common involve finding the flow delivered to each pipe, given an applied pressure difference. We examine this case in Example 8.11. Obviously, pipe networks are much more difficult and time-consuming to analyze than single-path problems, almost always requiring iterative solution methods, and in practice are usually only solved using software. Many engineering consulting companies use proprietary software applications for such analysis.

Example 8.11 FLOW RATES IN A PIPE NETWORK

In the section of a cast-iron water pipe network shown in Fig. 8.17, the static pressure head (gage) available at point 1 is 100 ft of water, and point 5 is a drain (atmospheric pressure). Find the flow rates (gpm) in each pipe.

Given: Pressure head h_{1-5} of 100 ft across pipe network.

Find: The flow rate in each pipe.

Solution:

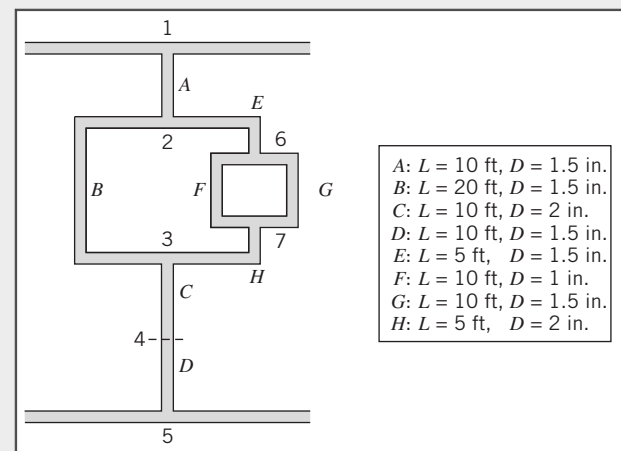
Governing equations:

For each pipe section, we have the relation between flow rate, velocity, and flow area as

$$Q = \bar{V}A$$

The area is related to the diameter as

$$A = \frac{\pi}{4}D^2$$



In addition, we have the energy relation for head loss

$$\left(\frac{p_1}{\rho} + \alpha_1 \frac{\bar{V}_1^2}{2} + g z_1 \right) - \left(\frac{p_2}{\rho} + \alpha_2 \frac{\bar{V}_2^2}{2} + g z_2 \right) = h_{l_T} = h_l + \sum h_{l_m} \quad (8.29)$$

where

$$h_l = f \frac{L \bar{V}^2}{D} \quad (8.34)$$

and f is obtained from either Eq. 8.36 (laminar) or Eq. 8.37 (turbulent). For the cast-iron pipe, Table 8.1 gives a roughness for cast iron of $e = 0.00085$ ft.

Assumptions:

- 1 Ignore gravity effects.
- 2 Ignore minor losses.

Assumption 2 is applied to make the analysis clearer as minor losses can be incorporated easily later.

In addition we have mathematical expressions for the basic rules:

- 1 The net flow out of any node (junction) is zero.
- 2 Each node has a unique pressure head (HGL).

We can apply basic rule 1 to nodes 2 and 6:

$$\text{Node 2: } Q_A = Q_B + Q_E \quad (1)$$

$$\text{Node 6: } Q_E = Q_F + Q_G \quad (2)$$

and we also have the obvious constraints

$$Q_A = Q_C \quad (3)$$

$$Q_A = Q_D \quad (4)$$

$$Q_E = Q_H \quad (5)$$

We can apply basic rule 2 to obtain the following pressure drop constraints:

$$h_{1-5}: \quad h = h_A + h_B + h_C + h_D \quad (6)$$

$$h_{2-3}: \quad h_B = h_E + h_F + h_H \quad (7)$$

$$h_{6-7}: \quad h_F = h_G \quad (8)$$

This set of eight equations, together with the continuity relation and Eqs. 8.29 and 8.34 for each pipe section, must be solved iteratively. If we were to manually iterate, we would use Eqs. 3, 4, and 5 to immediately reduce the number of unknowns and equations to five (Q_A, Q_B, Q_E, Q_F, Q_G). If we were performing the iteration manually, an approach would be to:

- 1 Make a guess for Q_A, Q_B , and Q_F .
- 2 Eqs. 1 and 2 then lead to values for Q_E and Q_G .
- 3 Eqs. 6, 7, and 8 are finally used as a check to see if rule 2 (for unique pressure heads at the nodes) is satisfied.
- 4 If any of Eqs. 6, 7, or 8 are not satisfied, use knowledge of pipe flow to adjust the values of Q_A, Q_B , or Q_F .
- 5 Repeat steps 2 through 5 until convergence occurs.

Equation solving software can be used to efficiently solve the coupled set of equations. Each of the equations is entered and the software does the necessary iterations. This particular solution was obtained using Excel, but other software would be appropriate as well. The flowrates obtained are:

The flow rates are:

$$\begin{aligned} Q_A &= Q_C = Q_D = 167 \text{ gpm} \\ Q_B(\text{gpm}) &= 72 \text{ gpm} \\ Q_E(\text{gpm}) &= Q_H(\text{gpm}) = 95 \text{ gpm} \\ Q_F(\text{gpm}) &= 24 \text{ gpm} \\ Q_G(\text{gpm}) &= 71 \text{ gpm} \end{aligned}$$

This problem illustrates the network approach to solving a complex piping network problem.

Part C FLOW MEASUREMENT

Throughout this text we have referred to the flow rate Q or average velocity \bar{V} in a pipe. The question arises: How does one measure these quantities? We will address this question by discussing the various types of flow meters available.

The choice of a flow meter is influenced by the accuracy required, range, cost, complication, ease of reading or data reduction, and service life. The simplest and cheapest device that gives the desired accuracy should be chosen.

The most obvious way to measure flow rate in a pipe is the *direct method*—simply measure the amount of fluid that accumulates in a container over a fixed time period. Tanks can be used to determine flow rate for steady liquid flows by measuring the volume or mass of liquid collected during a known time interval. If the time interval is long enough to be measured accurately, flow rates may be determined precisely in this way.

Compressibility must be considered in volume measurements for gas flows. The densities of gases generally are too small to permit accurate direct measurement of mass flow rate. However, a volume sample often can be collected by displacing a “bell,” or inverted jar over water (if the pressure is held constant by counterweights). If volume or mass measurements are set up carefully, no calibration is required; this is a great advantage of direct methods.

In specialized applications, particularly for remote or recording uses, *positive displacement* flow meters may be specified, in which the fluid moves a component such as a reciprocating piston or oscillating disk as it passes through the device. Common examples include household water and natural gas meters, which are calibrated to read directly in units of product, or gasoline metering pumps, which measure total flow and automatically compute the cost. Many positive-displacement meters are available commercially. Consult manufacturers’ literature or References (e.g., [18]) for design and installation details.

8.9 Restriction Flow Meters for Internal Flows

Most restriction flow meters for internal flow are based on acceleration of a fluid stream through some form of nozzle, as shown schematically in Fig. 8.18. The idea is that the change in velocity leads to a change in pressure. This Δp can be measured using a pressure gage (electronic or mechanical) or a manometer, and the flow rate inferred using either a theoretical analysis or an experimental correlation for the device.

The most commonly used restriction devices are the orifice, nozzle, and venturi tube. All have similar flow patterns and the flow through a nozzle will be used to illustrate the behavior of the device. Flow separation at the sharp edge of the nozzle throat causes a recirculation zone to form, as shown by

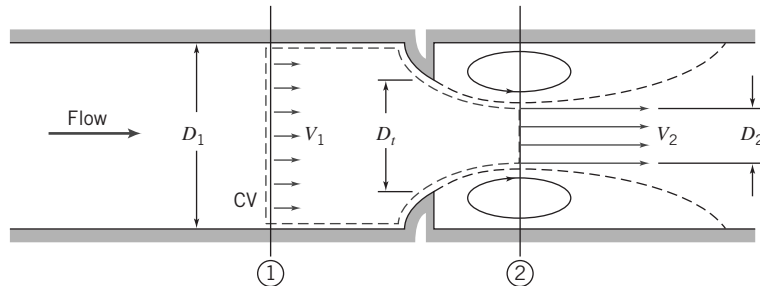


Fig. 8.18 Internal flow through a generalized nozzle showing control volume used for analysis.

the dashed lines downstream from the nozzle. The mainstream flow continues to accelerate from the nozzle throat to form a *vena contracta* at section ② and then decelerates again to fill the duct. At the vena contracta, the flow area is a minimum, the flow streamlines are essentially straight, and the pressure is uniform across the channel section.

The theoretical flow rate may be related to the pressure differential between sections ① and ② by applying the continuity and Bernoulli equations. Then empirical correction factors may be applied to obtain the actual flow rate. The assumptions made are:

- 1 Steady flow.
- 2 Incompressible flow.
- 3 Flow along a streamline.
- 4 No friction.
- 5 Uniform velocity at sections ① and ②.
- 6 No streamline curvature at sections ① or ②, so pressure is uniform across those sections.
- 7 $z_1 = z_2$.

For a fluid with a constant density, the conservation of mass equation is

$$\sum_{\text{CS}} \vec{V} \cdot \vec{A} = 0 \quad (4.13b)$$

and the Bernoulli equation, assuming that the viscous friction is negligible, is

$$\frac{p_1}{\rho} + \alpha_1 \frac{V_1^2}{2} + g z_1 = \frac{p_2}{\rho} + \alpha_2 \frac{V_2^2}{2} + g z_2 \quad (6.8)$$

Assumptions:

Then, from the Bernoulli equation,

$$p_1 - p_2 = \frac{\rho}{2} (V_2^2 - V_1^2) = \frac{\rho V_2^2}{2} \left[1 - \left(\frac{V_1}{V_2} \right)^2 \right]$$

and from continuity

$$(-\rho V_1 A_1) + (\rho V_2 A_2) = 0$$

or

$$V_1 A_1 = V_2 A_2 \quad \text{so} \quad \left(\frac{V_1}{V_2} \right)^2 = \left(\frac{A_2}{A_1} \right)^2$$

Substituting gives

$$p_1 - p_2 = \frac{\rho V_2^2}{2} \left[1 - \left(\frac{A_2}{A_1} \right)^2 \right]$$

Solving for the theoretical velocity, V_2 ,

$$V_2 = \sqrt{\frac{2(p_1 - p_2)}{\rho [1 - (A_2/A_1)^2]}} \quad (8.51)$$

The theoretical mass flow rate is then given by

$$\begin{aligned} \dot{m}_{\text{theoretical}} &= \rho V_2 A_2 \\ &= \rho \sqrt{\frac{2(p_1 - p_2)}{\rho [1 - (A_2/A_1)^2]}} A_2 \end{aligned}$$

or

$$\dot{m}_{\text{theoretical}} = \frac{A_2}{\sqrt{1 - (A_2/A_1)^2}} \sqrt{2\rho(p_1 - p_2)} \quad (8.52)$$

Equation 8.52 shows that, under our set of assumptions, for a given fluid (ρ) and flow meter geometry (A_1 and A_2), the flow rate is directly proportional to the square root of the pressure drop across the meter taps,

$$\dot{m}_{\text{theoretical}} \propto \sqrt{\Delta p}$$

which is the basic idea of these devices. This relationship limits the flow rates that can be measured accurately to approximately a 4:1 range.

Several factors limit the utility of Eq. 8.52 for calculating the actual mass flow rate through a meter. The actual flow area at section ② is unknown when the vena contracta is pronounced (e.g., for orifice plates when D_t is a small fraction of D_1). The velocity profiles approach uniform flow only at large Reynolds numbers. Additionally, the location of pressure taps influences the differential pressure reading.

The theoretical equation is adjusted for Reynolds number and diameter ratio D_t/D_1 by defining an empirical *discharge coefficient* C such that, replacing Eq. 8.52, we have

$$\dot{m}_{\text{actual}} = \frac{CA_t}{\sqrt{1-(A_t/A_1)^2}} \sqrt{2\rho(p_1-p_2)} \quad (8.53)$$

Letting $\beta = D_t/D_1$, then $(A_t/A_1)^2 = (D_t/D_1)^4 = \beta^4$, the general form of the metering equation is

$$\dot{m}_{\text{actual}} = CA_t \sqrt{\frac{2\rho(p_1-p_2)}{1-\beta^4}} \quad (8.54)$$

The value of C depends on the type of meter (orifice, nozzle, or venturi) and the Reynolds number.

In Eq. 8.54, $1/\sqrt{1-\beta^4}$ is the *velocity-of-approach factor*. The discharge coefficient and velocity-of-approach factor are sometimes combined into a single *flow coefficient*,

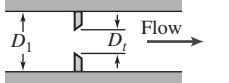
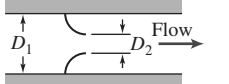
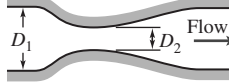
$$K \equiv \frac{C}{\sqrt{1-\beta^4}} \quad (8.55)$$

In terms of this flow coefficient, the actual mass flow rate is expressed as

$$\dot{m}_{\text{actual}} = KA_t \sqrt{2\rho(p_1-p_2)} \quad (8.56)$$

As we have noted, selection of a flow meter depends on factors such as cost, accuracy, need for calibration, and ease of installation and maintenance. Some of these factors are compared for *orifice plate*, *flow nozzle*, and *venturi* meters in Table 8.6. Note that a high head loss means that the running cost of the device is high as it will consume a lot of the fluid energy.

Table 8.6
Characteristics of Orifice, Flow Nozzle, and Venturi Flow Meters

Flow Meter Type	Diagram	Head Loss	Initial Cost
Orifice		High	Low
Flow Nozzle		Intermediate	Intermediate
Venturi		Low	High

Flow meter coefficients reported in the literature have been measured with fully developed turbulent velocity distributions at the meter inlet (Section ①). If a flow meter is to be installed downstream from a valve, elbow, or other disturbance, a straight section of pipe must be placed in front of the meter. Approximately 10 diameters of straight pipe are required for venturi meters, and up to 40 diameters for orifice plate or flow nozzle meters. When a meter has been properly installed, the flow rate may be computed from Eq. 8.54 or 8.56, with an appropriate value for the empirical discharge coefficient, C , or flow coefficient, K , defined in Eqs. 8.53 and 8.55, respectively.

The Orifice Plate

The orifice plate (Fig. 8.19) is a thin plate that may be clamped between pipe flanges. Since its geometry is simple, it is low in cost and easy to install or replace. The sharp edge of the orifice will not foul with scale or suspended matter. However, suspended matter can build up at the inlet side of a concentric orifice in a horizontal pipe; an eccentric orifice may be placed flush with the bottom of the pipe to avoid this difficulty. The primary disadvantages of the orifice are its limited capacity and the high permanent head loss caused by the uncontrolled expansion downstream from the metering element.

Pressure taps for orifices may be placed in several locations, as shown in Fig. 8.19. The standard locations are in the corners of the orifice plate, 1 in. on either side of the orifice plate or one diameter upstream and one-half a diameter downstream of the orifice plate. The value of the discharge coefficient C depends strongly on the location of the taps.

The flow through an orifice is then calculated from the metering equation using the orifice coefficient C_o as

$$\dot{m} = C_o A_t \sqrt{\frac{2\rho(p_1 - p_2)}{1 - \beta^4}} \quad (8.57)$$

The correlating equation recommended for a concentric orifice with one tap located one diameter upstream of the orifice and the second located one-half the diameter downstream (D and $1/2 D$ taps) [23] is

$$C_o = 0.5959 + 0.0321\beta^{2.1} - 0.184\beta^8 + \frac{91.71\beta^{2.5}}{(Re_{D_i} \times 10^{-6})^{0.75}} + 0.0900\left(\frac{L_1}{D}\right)\left[\frac{\beta^4}{1 - \beta^4}\right] - 0.0337\left(\frac{L_2}{D}\right)\beta^3 \quad (8.58)$$

Equation 8.58 predicts orifice discharge coefficients within ± 0.6 percent for $0.2 < \beta < 0.75$ and for $10^4 < Re_{D_i} < 10^7$. The orifice coefficient is plotted in Fig. 8.20. A similar correlating equation is available for orifice plates with corner taps. Flange taps require a different correlation for every line size.

Example 8.12 illustrates the application of flow coefficient data to orifice sizing.

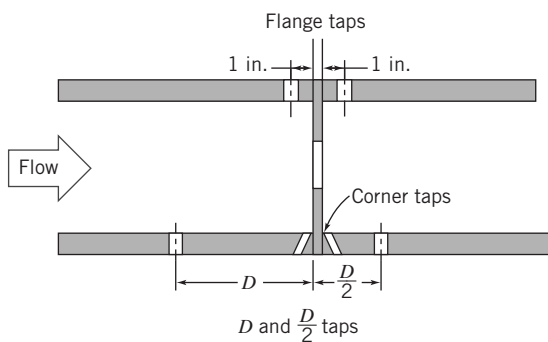


Fig. 8.19 Orifice geometry and pressure tap locations.
(Based on [18].)

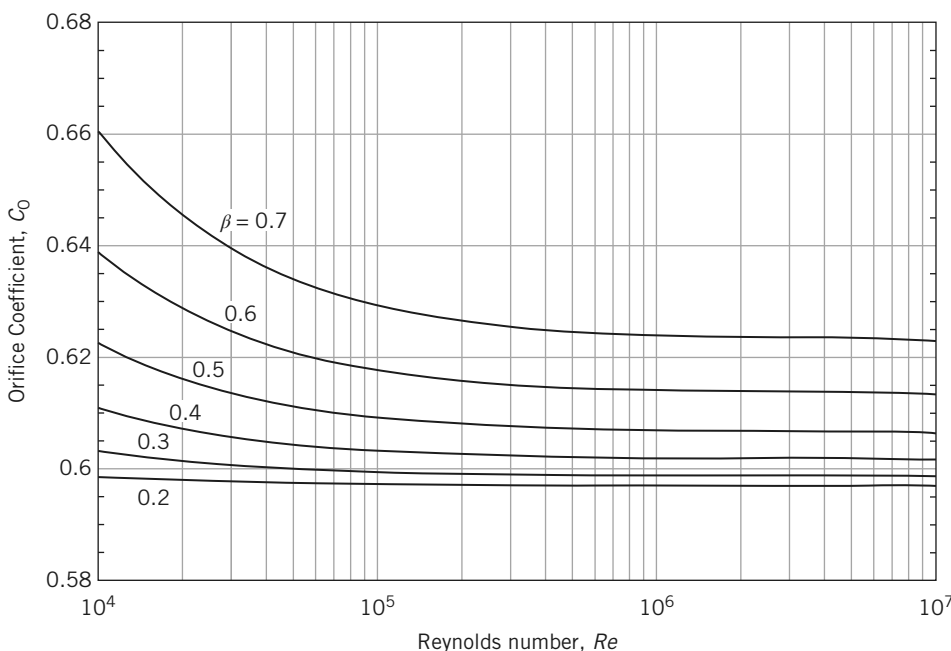


Fig. 8.20 Flow coefficient for concentric orifices with D and $D/2$ taps.

Example 8.12 FLOW THROUGH AN ORIFICE METER

An air flow rate of up to $1 \text{ m}^3/\text{s}$ at standard conditions is expected in a 0.25-m diameter duct. An orifice meter is used to measure the rate of flow. The manometer available to make the measurement has a maximum range of 300 mm of water. Determine the diameter of the orifice plate that should be used with D and $D/2$ pressure taps. Determine the head loss if the flow area at the vena contracta is 0.65 of the orifice diameter.

Given: Flow through duct and orifice as shown.

Find: (a) Orifice diameter for an airflow of $1 \text{ m}^3/\text{s}$ at a pressure difference of 300 mm water.
(b) Head loss for the orifice meter.

Assumptions:

- 1 The air flow is steady.
- 2 The air can be treated as an incompressible fluid.

Solution: The orifice is given by Eq. 8.57 with the orifice coefficient taken from Fig. 8.20.

Governing equation:

$$\dot{m} = C_o A_t \sqrt{\frac{2\rho(p_1 - p_2)}{1 - \beta^4}}$$

In this equation, the maximum mass flow rate is known. The pressure difference will be taken as the maximum (300 mm water) at the maximum flow rate. The unknowns are the orifice coefficient, throat area, and the diameter ratio β . The orifice coefficient C_o depends on the Reynolds number and the diameter ratio. An iterative procedure will be used in which a diameter is selected and the pressure difference determined. If the pressure difference is larger than the criterion of 300 mm water, a larger diameter ratio will be selected.

The pressure difference from Eq. 8.57 is

$$(p_1 - p_2) = \frac{1 - \beta^4}{2\rho} \left(\frac{\dot{m}}{C_o A_t} \right)^2 = \frac{\rho(1 - \beta^4)}{2} \left(\frac{Q}{C_o A_t} \right)^2$$

The air density at standard conditions is 1.23 kg/m^3 , and the air viscosity at standard conditions is $1.46 \cdot 10^{-5} \text{ Pa-s}$.

The Reynolds number is given by

$$\begin{aligned} \text{Re}_{D_1} &= \frac{\rho \bar{V} D_1}{\mu} = \frac{\rho}{\mu} \left(\frac{Q}{A_1} \right) D_1 = \frac{\rho}{\mu} \frac{4Q}{\pi D_1} \\ &= \frac{1.23 \frac{\text{kg}}{\text{m}^3}}{1.46 \times 10^{-5} \text{ Pa-s}} \cdot \frac{4 \cdot 1 \frac{\text{m}^3}{\text{s}}}{\pi \cdot 0.25 \text{ m}} = 3.50 \cdot 10^5 \end{aligned}$$

Our first guess will be for a value of D_t of 0.175 m, which yields a value of β of 0.7. The orifice coefficient from Fig. 8.20 is about 0.625. The pressure difference is then

$$(p_1 - p_2) = \frac{\rho(1 - \beta^4)}{2} \left(\frac{Q}{C_o A_t} \right)^2 = \frac{1.23 \frac{\text{kg}}{\text{m}^3} (1 - 0.7^4)}{2} \left(\frac{1 \frac{\text{m}^3}{\text{s}}}{0.625 \cdot \frac{\pi}{4} \cdot 0.175^2 \text{ m}^2} \right)^2 = 2070 \text{ Pa}$$

The corresponding height of the water column in the manometer is

$$h = \frac{(p_2 - p_1)}{g \rho_{\text{water}}} = \frac{2070 \text{ Pa}}{9.81 \frac{\text{m}}{\text{s}^2} \cdot 998 \frac{\text{kg}}{\text{m}^3}} = 0.211 \text{ m} = 211 \text{ mm} \quad (\text{A})$$

This is lower than the maximum pressure difference and a second guess will be made using a smaller orifice diameter of 0.15 m, which corresponds to a β of 0.6. The orifice coefficient at this diameter ratio is 0.615. The same calculations as above are carried out and the resulting pressure difference and manometer height is

$$(p_1 - p_2) = 4530 \text{ Pa} \quad \text{and} \quad h = 463 \text{ mm}$$

The diameter is too small, but the appropriate diameter is between 0.15 m and 0.175 m. Another guess for the diameter is made and the process repeated. The orifice coefficient at the guess diameter is obtained from linear interpolation between the values for 0.15 m and 0.175 m. Eventually a diameter of 0.165 m is found to yield a pressure of 2830 Pa and a manometer height of 289 mm water, which is close enough to the target value of 300 mm.

The final design is

$$D_t = 0.165 \text{ m} \quad \text{and} \quad \beta = 0.66.$$

To evaluate the permanent head loss, apply Eq. 8.29 between sections ① and ③.

Governing equation:

$$\left(\frac{p_1}{\rho} + \alpha_1 \frac{\bar{V}_1^2}{2} + g z_1 \right) - \left(\frac{p_3}{\rho} + \alpha_3 \frac{\bar{V}_3^2}{2} + g z_3 \right) = h_{l_T} \quad (8.29)$$

Assumptions:

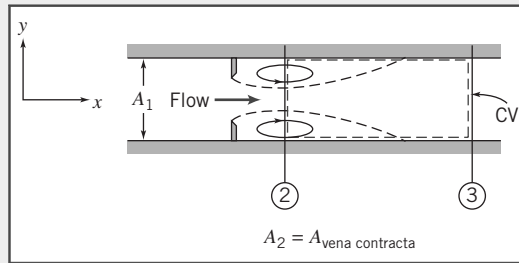
$$3 \quad \alpha_1 \bar{V}_1^2 = \alpha_3 \bar{V}_3^2.$$

4 Neglect Δz .

Then

$$h_{l_T} = \frac{p_1 - p_3}{\rho} = \frac{p_1 - p_2 - (p_3 - p_2)}{\rho} \quad (2)$$

Equation 2 indicates our approach: We will find $p_1 - p_3$ by using $p_1 - p_2 = 289 \text{ mm H}_2\text{O}$, and obtain a value for $p_3 - p_2$ by applying the x component of the momentum equation to a control volume between sections ② and ③.



Governing equation:

$$=0(5)=0(1)$$

$$F_{S_x} + \overset{\nearrow}{F_{B_x}} = \frac{\partial}{\partial t} \int_{\text{CV}} u \rho dV + \int_{\text{CV}} u \rho \vec{V} \cdot d\vec{A} \quad (4.18a)$$

Assumptions:

- 5 $F_{B_x}=0$
- 6 Uniform flow at sections ② and ③.
- 7 Pressure uniform across duct at sections ② and ③.
- 8 Neglect friction force on CV.

Then, simplifying and rearranging,

$$(p_2-p_3)A_1=u_2(-\rho\bar{V}_2A_2)+u_3(\rho\bar{V}_3A_3)=(u_3-u_2)\rho Q=(\bar{V}_3-\bar{V}_2)\rho Q$$

or

$$p_3-p_2=(\bar{V}_2-\bar{V}_3)\frac{\rho Q}{A_1}$$

Now $\bar{V}_3=Q/A_1$, and

$$\bar{V}_2=\frac{Q}{A_2}=\frac{Q}{0.65 A_t}=\frac{Q}{0.65 \beta^2 A_1}$$

Thus,

$$p_3-p_2=\frac{\rho Q^2}{A_1^2}\left[\frac{1}{0.65 \beta^2}-1\right]$$

$$p_3-p_2=1.23 \frac{\text{kg}}{\text{m}^3} \times (1)^2 \frac{\text{m}^6}{\text{s}^2} \times \frac{4^2}{\pi^2} \frac{1}{(0.25)^4 \text{m}^4} \left[\frac{1}{0.65(0.66)^2}-1\right] \frac{\text{N} \cdot \text{s}^2}{\text{kg} \cdot \text{m}}$$

$$p_3-p_2=1290 \text{ N/m}^2$$

Substituting into Eq. 2 gives

$$h_{l_T}=\frac{p_1-p_3}{\rho}=\frac{p_1-p_2-(p_3-p_2)}{\rho}$$

$$h_{l_T}=(2830-1290) \frac{\text{N}}{\text{m}^2} \times \frac{\text{m}^3}{1.23 \text{ kg}}=1250 \text{ N} \cdot \text{m/kg} \quad h_{l_T}$$

The permanent pressure loss as a fraction of the meter differential

$$\frac{p_1-p_3}{p_1-p_2}=\frac{1250 \text{ N/m}^2}{2830 \text{ N/m}^2}=0.44$$

The head loss is about 44 percent of the pressure drop through the orifice. There is then some recovery of the kinetic energy of the fluid in the vena contracta.

This problem illustrates flow meter calculations and shows use of the momentum equation to compute the pressure rise in a sudden expansion.

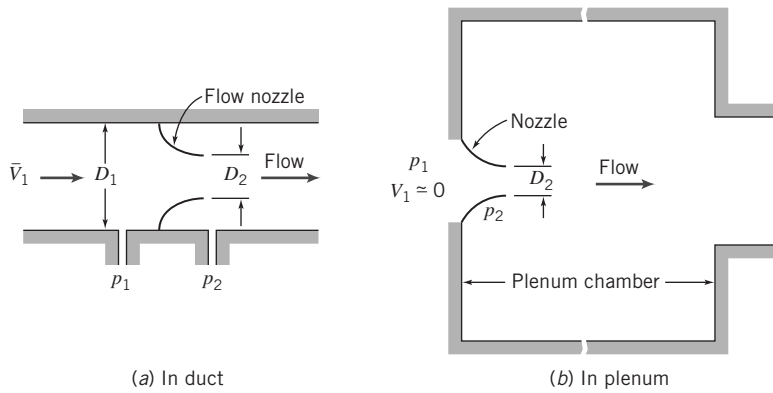


Fig. 8.21 Typical installations of nozzle flow meters.

The Flow Nozzle

Flow nozzles are also commonly used as metering elements. Figure 8.21 shows a schematic of nozzle installation in a duct and in a plenums or ducts.

There are well-established standards for the nozzle shape, pressure tap location, and placement as given in [23]. The nozzle coefficients for the ASME long-radius nozzle are shown in Fig. 8.22. Similar to the orifice, the coefficient is a function of Reynolds number and contraction ratio. However, the losses for a nozzle are less than those of an orifice and the coefficients are correspondingly higher.

The flow rate through a nozzle is given by

$$\dot{m} = C_n A_t \sqrt{\frac{2\rho(p_1 - p_2)}{1 - \beta^4}} \quad (8.59)$$

The correlating equation recommended for an ASME long-radius flow nozzle [18] is

$$C_n = 0.9975 - \frac{6.53\beta^{0.5}}{Re_{D_1}^{0.5}} \quad (8.60)$$

Equation 8.60 is the form for the discharge coefficient C for the flow nozzle; it predicts discharge coefficients for flow nozzles within ± 2.0 percent for $0.25 < \beta < 0.75$ for $10^4 < Re_{D_1} < 10^7$. Some flow coefficients calculated from Eqs. 8.60 and 8.55 are presented in Fig. 8.22.

The Venturi

Venturi meters, as sketched in Table 8.6, are generally made from castings and machined to close tolerances to duplicate the performance of the standard design. As a result, venturi meters are heavy, bulky, and expensive. The conical diffuser section downstream from the throat gives excellent pressure recovery; therefore, overall head loss is low. Venturi meters are also self-cleaning because of their smooth internal contours.

Experimental data show that discharge coefficients for venturi meters range from 0.980 to 0.995 at high Reynolds numbers ($Re_{D_1} > 2 \times 10^5$). Thus $C = 0.99$ can be used to measure mass flow rate within about ± 1 percent at high Reynolds number [18]. Consult manufacturers' literature for specific information at Reynolds numbers below 10^5 .

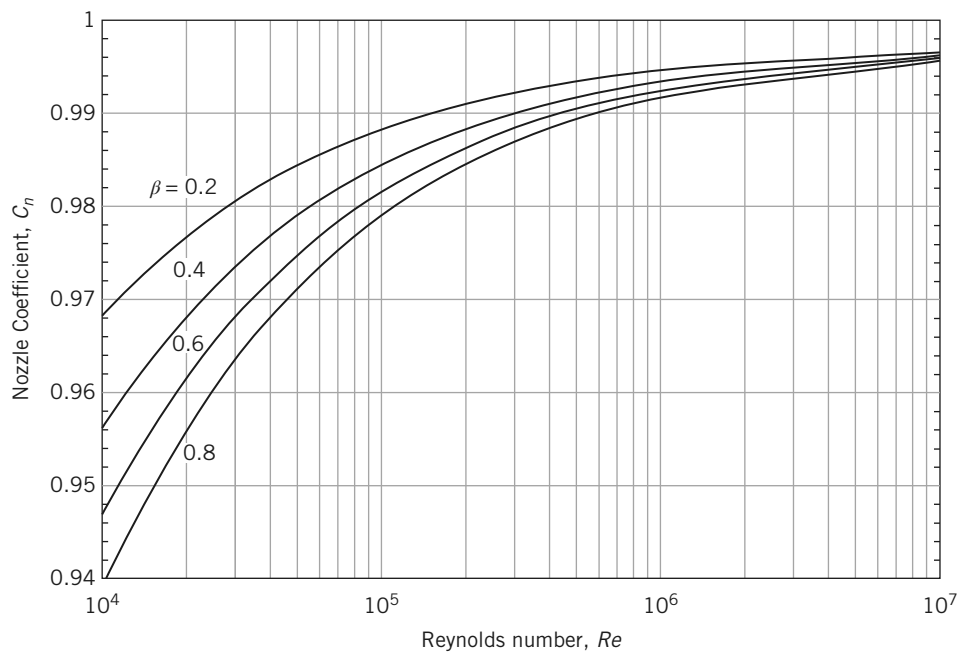


Fig. 8.22 Nozzle coefficients.

The Laminar Flow Element

The *laminar flow element* is designed to produce a pressure differential directly proportional to flow rate. The laminar flow element contains a metering section in which the flow passes through a large number of very small tubes or passages. Each passage is narrow enough so that the flow through each of them is laminar, regardless of the flow conditions in the main pipe. A picture of the internal element in a laminar flow meter is shown in Fig. 8.23. For each passage in the laminar flow element the results of Section 8.3 apply. The flow rate for each tube is given by Eq. 8.13c. The total flow rate is sum of the flow through each passage and also is linearly proportional to the pressure drop. For each laminar flow tube the results of Section 8.3 apply. The flow rate for each tube is then given by Eq. 8.13c, and the total flow rate is then of this form.

$$Q_{\text{tube}} = \frac{\pi D_{\text{tube}}^4}{128\mu L_{\text{tube}}} \Delta p \propto \Delta p \quad (8.13c)$$

The relationship between pressure drop and flow rate for laminar flow also depends on viscosity, which is a strong function of temperature. Therefore, the fluid temperature must be known to obtain accurate metering with a laminar flow meter.

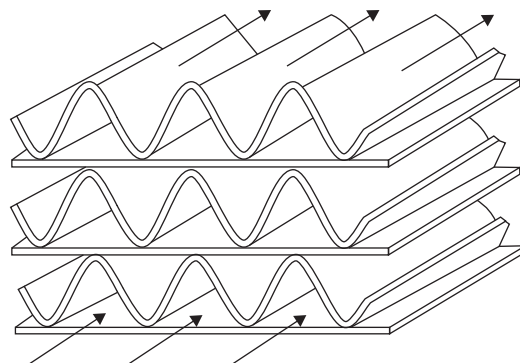


Fig. 8.23 Laminar flow meter element.

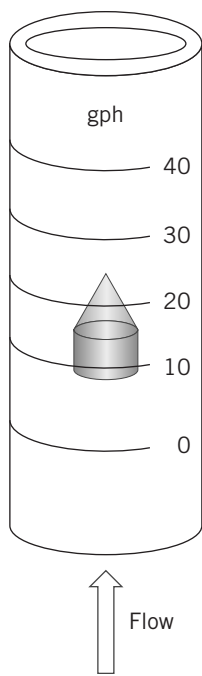


Fig. 8.24 Float-type variable-area flow meter.

Linear Flow Meters

Several flow meter types produce outputs that are directly proportional to flow rate. These meters produce signals without the need to measure differential pressure. The most common linear flow meters are discussed briefly in the following paragraphs.

Float meters may be used to indicate flow rate directly for liquids or gases. An example is shown in Fig. 8.24. In operation, the ball or float is carried upward in the tapered clear tube by the flowing fluid until the drag force and float weight are in equilibrium. Such meters (often called *rotameters*) are available with factory calibration for a number of common fluids and flow rate ranges.

A free-running vaned impeller may be mounted in a cylindrical section of tube (Fig. 8.25) to make a *turbine flow meter*. With proper design, the rate of rotation of the impeller may be made closely proportional to volume flow rate over a wide range.

Rotational speed of the turbine element can be sensed using a magnetic or modulated carrier pickup external to the meter. This sensing method therefore requires no penetrations or seals in the duct. Thus turbine flow meters can be used safely to measure flow rates in corrosive or toxic fluids. The electrical signal can be displayed, recorded, or integrated to provide total flow information.

The *vortex flow meter* takes advantage of the fact that a uniform flow will generate a vortex street when it encounters a bluff body such as a cylinder perpendicular to the flow. A vortex street is a series of alternating vortices shed from the rear of the body; the alternation generates an oscillating sideways force on, and therefore oscillation of, the cylinder. The dimensionless group characterizing this phenomenon is the Strouhal number, $St = fL/V$ (f is the vortex shedding frequency, L is the cylinder diameter, and V is the freestream velocity), and it is approximately constant ($St \approx 0.21$). The velocity is then directly proportional to vortex shedding frequency. Measurement of f thus directly indicates the velocity V . The cylinder used in a flow meter is usually quite short in length—10 mm or less—and placed perpendicular to the flow. The oscillation can be measured using a strain gage or other sensor. Vortex flow meters can be used over a 20:1 range of flow rates.

The *electromagnetic flow meter* uses the principle of magnetic induction. A magnetic field is created across a pipe. When a conductive fluid passes through the field, a voltage is generated at right angles to the field and velocity vectors. Electrodes placed on a pipe diameter are used to detect the resulting signal voltage. The signal voltage is proportional to the average axial velocity when the profile is axisymmetric.

Magnetic flow meters may be used with liquids that have electrical conductivities above 100 microsiemens per meter (1 siemen = 1 ampere per volt). The minimum flow speed should be above about 0.3 m/s, but there are no restrictions on Reynolds number. The flow rate range normally quoted is 10:1.

Ultrasonic flow meters also respond to average velocity at a pipe cross section. Two principal types of ultrasonic meters are common: Propagation time is measured for clean liquids, and reflection frequency shift (Doppler effect) is measured for flows carrying particulates. The speed of an acoustic wave increases in the flow direction and decreases when transmitted against the flow. For clean liquids, an acoustic path inclined to the pipe axis is used to infer flow velocity. Multiple paths are used to estimate the volume flow rate accurately.

Doppler effect ultrasonic flow meters depend on reflection of sonic waves (in the MHz range) from scattering particles in the fluid. When the particles move at flow speed, the frequency shift is proportional to flow speed; for a suitably chosen path, output is proportional to volume flow rate. One or two transducers may be used; the meter may be clamped to the outside of the pipe. Ultrasonic meters may require calibration in place. Flow rate range is 10:1.

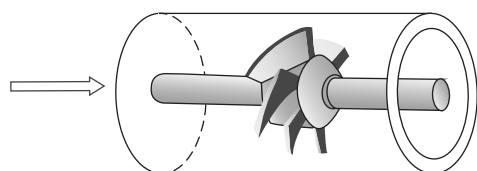


Fig. 8.25 Turbine flow meter.

Traversing Methods

In situations such as in air handling or refrigeration equipment, it may be impractical or impossible to install fixed flow meters. In such cases it may be possible to obtain flow rate data using traversing techniques.

To make a flow rate measurement by traverse, the duct cross section is conceptually subdivided into segments of equal area. The velocity is measured at the center of each area segment using a pitot tube, a total head tube, or a suitable anemometer. The volume flow rate for each segment is approximated by the product of the measured velocity and the segment area. The flow rate through the entire duct is the sum of these segmental flow rates. Details of recommended procedures for flow rate measurements by the traverse method are given in [19].

Use of *pitot* or *pitot-static tubes* for traverse measurements requires direct access to the flow field. Pitot tubes give uncertain results when pressure gradients or streamline curvature are present, and their response times are slow. Two types of anemometers—*thermal anemometers* and *laser Doppler anemometers* (LDAs)—overcome these difficulties partially, although they introduce new complications.

Thermal anemometers use tiny elements (either hot-wire or hot-film elements) that are heated electrically. Sophisticated electronic feedback circuits are used to maintain the temperature of the element constant and to sense the input heating rate needed to do this. The heating rate is related to the local flow velocity by calibration (a higher velocity leads to more heat transfer). The primary advantage of thermal anemometers is the small size of the sensing element. Sensors as small as 0.002 mm in diameter and 0.1 mm long are available commercially. Because the thermal mass of such tiny elements is extremely small, their response to fluctuations in flow velocity is rapid. Thus thermal anemometers are ideal for measuring turbulence quantities. Insulating coatings may be applied to permit their use in conductive or corrosive gases or liquids.

Because of their fast response and small size, thermal anemometers are used extensively for research. Numerous schemes have been published for treating the resulting data [20]. Digital processing techniques, including fast Fourier transforms, can be applied to the signals to obtain mean values and moments, and to analyze frequency content and correlations.

Laser Doppler anemometers are becoming widely used for specialized applications where direct physical access to the flow field is difficult or impossible. One or more laser beams are focused to a small volume in the flow at the location of interest (as shown in Fig. 8.26). Laser light is scattered from particles that are present in the flow (dust or particulates) or introduced for this purpose. A frequency shift is caused by the local flow speed (Doppler effect). Scattered light and a reference beam are collected by receiving optics. The frequency shift is proportional to the flow speed; this relationship may be calculated, so there is no need for calibration. Since velocity is measured directly, the signal is unaffected by changes in temperature, density, or composition in the flow field. The primary disadvantages of LDAs



Courtesy of Dr. Frank W. Chambers

Fig. 8.26 A two-component laser doppler anemometer probe volume.

are that the optical equipment is expensive and fragile, and that extremely careful alignment is needed (as the authors can attest).

8.10 Summary and Useful Equations

In this chapter we have:

- ✓ Defined many terms used in the study of internal incompressible viscous flow, such as: the entrance length, fully developed flow, the friction velocity, Reynolds stress, the kinetic energy coefficient, the friction factor, major and minor head losses, and hydraulic diameter.
- ✓ Analyzed laminar flow between parallel plates and in pipes and observed that we can obtain the velocity distribution analytically, and from this derive: the average velocity, the maximum velocity and its location, the flow rate, the wall shear stress, and the shear stress distribution.
- ✓ Studied turbulent flow in pipes and ducts and learned that semi-empirical approaches are needed, e.g., the power-law velocity profile.
- ✓ Written the energy equation in a form useful for analyzing pipe flows.
- ✓ Discussed how to incorporate pumps, fans, and blowers into a pipe flow analysis.
- ✓ Described various flow measurement devices: direct measurement, restriction devices (orifice plate, nozzle, and venturi), linear flow meters (rotameters, various electromagnetic or acoustic devices, and the vortex flow meter), and traversing devices (pitot tubes and laser-Doppler anemometers).

We have learned that pipe and duct flow problems often need iterative solution—the flow rate Q is not a linear function of the driving force (usually Δp), except for laminar flows. We have also seen that pipe networks can be analyzed using the same techniques as a single-pipe system, with the addition of a few basic rules, and that in practice a computer application such as *Excel* is needed to solve all but the simplest networks.

Note: Most of the equations in the table below have a number of constraints or limitations—*be sure to refer to their page numbers for details!*

Useful Equations

Velocity profile for pressure-driven laminar flow between stationary parallel plates:	$u = \frac{a^2}{2\mu} \left(\frac{\partial p}{\partial x} \right) \left[\left(\frac{y}{a} \right)^2 - \left(\frac{y}{a} \right) \right]$	(8.5)	Page 233
Flow rate for pressure-driven laminar flow between stationary parallel plates:	$\frac{Q}{l} = -\frac{1}{12\mu} \left[\frac{-\Delta p}{L} \right] a^3 = \frac{a^3 \Delta p}{12\mu L}$	(8.6c)	Page 233
Velocity profile for pressure-driven laminar flow between stationary parallel plates (centered coordinates):	$u = \frac{a^2}{2\mu} \left(\frac{\partial p}{\partial x} \right) \left[\left(\frac{y'}{a} \right)^2 - \frac{1}{4} \right]$	(8.7)	Page 234
Velocity profile for pressure-driven laminar flow between parallel plates (upper plate moving):	$u = \frac{Uy}{a} + \frac{a^2}{2\mu} \left(\frac{\partial p}{\partial x} \right) \left[\left(\frac{y}{a} \right)^2 - \left(\frac{y}{a} \right) \right]$	(8.8)	Page 236
Flow rate for pressure-driven laminar flow between parallel plates (upper plate moving):	$\frac{Q}{l} = \frac{Ua}{2} - \frac{1}{12\mu} \left(\frac{\partial p}{\partial x} \right) a^3$	(8.9b)	Page 237
Velocity profile for laminar flow in a pipe:	$u = -\frac{R^2}{4\mu} \left(\frac{\partial p}{\partial x} \right) \left[1 - \left(\frac{r}{R} \right)^2 \right]$	(8.12)	Page 243

Table (Continued)

Flow rate for laminar flow in a pipe:	$Q = -\frac{\pi R^4}{8\mu} \left[\frac{-\Delta p}{L} \right] = \frac{\pi \Delta p R^4}{8\mu L} = \frac{\pi \Delta p D^4}{128\mu L}$	(8.13c)	Page 243
Velocity profile for laminar flow in a pipe (normalized form):	$\frac{u}{U} = 1 - \left(\frac{r}{R} \right)^2$	(8.14)	Page 244
Velocity profile for turbulent flow in a smooth pipe (power-law equation):	$\frac{\bar{u}}{U} = \left(\frac{y}{R} \right)^{1/n} = \left(1 - \frac{r}{R} \right)^{1/n}$	(8.22)	Page 249
Head loss equation:	$\left(\frac{p_1}{\rho} + \alpha_1 \frac{\bar{V}_1^2}{2} + gz_1 \right) - \left(\frac{p_2}{\rho} + \alpha_2 \frac{\bar{V}_2^2}{2} + gz_2 \right) = h_{l_T}$	(8.29)	Page 253
Major head loss equation:	$h_l = f \frac{L \bar{V}^2}{D/2}$	(8.34)	Page 255
Friction factor (laminar flow):	$f_{\text{laminar}} = \frac{64}{Re}$	(8.36)	Page 256
Friction factor (turbulent flow—Colebrook equation):	$\frac{1}{\sqrt{f}} = -2.0 \log \left(\frac{e/D}{3.7} + \frac{2.51}{Re \sqrt{f}} \right)$	(8.37a)	Page 257
Minor loss	$h_{l_m} = K \frac{\bar{V}^2}{2}$	(8.40)	Page 258
Diffuser pressure recovery coefficient:	$C_p \equiv \frac{p_2 - p_1}{\frac{1}{2} \rho \bar{V}_1^2}$	(8.41)	Page 258
Ideal diffuser pressure recovery coefficient:	$C_{p_i} = 1 - \frac{1}{AR^2}$	(8.42)	Page 258
Head loss in diffuser in terms of pressure recovery coefficients:	$h_{l_m} = (C_{p_i} - C_p) \frac{\bar{V}_1^2}{2}$	(8.44)	Page 260
Pump work:	$\dot{W}_{\text{pump}} = Q \Delta p_{\text{pump}}$	(8.47)	Page 262
Pump efficiency:	$\eta = \frac{\dot{W}_{\text{pump}}}{\dot{W}_{\text{in}}}$	(8.48)	Page 262
Hydraulic diameter:	$D_h \equiv \frac{4A}{P}$	(8.50)	Page 263
Mass flow rate equation for a flow meter (in terms of discharge coefficient C):	$\dot{m}_{\text{actual}} = \frac{CA_t}{\sqrt{1-\beta^4}} \sqrt{2\rho(p_1-p_2)}$	(8.54)	Page 281
Mass flow rate equation for a flow meter (in terms of flow coefficient K):	$\dot{m}_{\text{actual}} = KA_t \sqrt{2\rho(p_1-p_2)}$	(8.56)	Page 281

(Continued)

Table (Continued)

Discharge coefficient (as a function of Re):	$C = C_{\infty} + \frac{b}{Re_{D_1}^n}$	(8.57)	Page 282
Flow coefficient (as a function of Re):	$K = K_{\infty} + \frac{1}{\sqrt{1-\beta^4}} \frac{b}{Re_{D_1}^n}$	(8.58)	Page 282

REFERENCES

1. Streeter, V. L., ed., *Handbook of Fluid Dynamics*. New York: McGraw-Hill, 1961.
2. Rouse, H., and S. Ince, *History of Hydraulics*. New York: Dover, 1957.
3. Laufer, J., "The Structure of Turbulence in Fully Developed Pipe Flow," U.S. National Advisory Committee for Aeronautics (NACA), Technical Report 1174, 1954.
4. Tennekes, H., and J. L. Lumley, *A First Course in Turbulence*. Cambridge, MA: The MIT Press, 1972.
5. Hinze, J. O., *Turbulence*, 2nd ed. New York: McGraw-Hill, 1975.
6. Moody, L. F., "Friction Factors for Pipe Flow," *Transactions of the ASME*, 66, 8, November 1944, pp. 671–684.
7. Colebrook, C. F., "Turbulent Flow in Pipes, with Particular Reference to the Transition Region between the Smooth and Rough Pipe Laws," *Journal of the Institution of Civil Engineers, London*, 11, 1938–39, pp. 133–156.
8. ASME Standard B36, ASME, 2 Park Avenue, New York, NY 10016, 2004.
9. ASHRAE *Handbook—Fundamentals*. Atlanta, GA: American Society of Heating, Refrigerating, and Air Conditioning Engineers, Inc., 2017.
10. Cockrell, D. J., and C. I. Bradley, "The Response of Diffusers to Flow Conditions at Their Inlet," Paper No. 5, *Symposium on Internal Flows*, University of Salford, Salford, England, April 1971, pp. A32–A41.
11. McDonald, A. T., and R. W. Fox, "An Experimental Investigation of Incompressible Flow in Conical Diffusers," *International Journal of Mechanical Sciences*, 8, 2, February 1966, pp. 125–139.
12. Runstadler, P. W., Jr., "Diffuser Data Book," Hanover, NH: Creare, Inc., Technical Note 186, 1975.
13. Reneau, L. R., J. P. Johnston, and S. J. Kline, "Performance and Design of Straight, Two-Dimensional Diffusers," *Transactions of the ASME, Journal of Basic Engineering*, 89D, 1, March 1967, pp. 141–150.
14. *Aerospace Applied Thermodynamics Manual*. New York: Society of Automotive Engineers, 1969.
15. Daily, J. W., and D. R. F. Harleman, *Fluid Dynamics*. Reading, MA: Addison-Wesley, 1966.
16. White, F. M., *Fluid Mechanics*, 6th ed. New York: McGraw-Hill, 2016.
17. Herschel, C., *The Two Books on the Water Supply of the City of Rome, from Sextus Julius Frontinus (ca. 40–103 A.D.)*. Boston, 1899.
18. "Flow Measurement", Performance Test Code (PTC) 19.5, New York: American Society of Mechanical Engineers (ASME), 2004.
19. ISO 7145, *Determination of Flowrate of Fluids in Closed Conduits or Circular Cross Sections—Method of Velocity Determination at One Point in the Cross Section*, ISO UDC 532.57.082.25:532.542, 1st ed. Geneva: International Standards Organization, 1982.
20. Bruun, H. H., *Hot-Wire Anemometry—Principles and Signal Analysis*. New York: Oxford University Press, 1995.
21. The Engineering Toolbox, <http://www.EngineeringToolBox.com>.
22. ASTM Standard A999, ASTM, West Conshohocken, PA, 19428-2959 USA, 2014.
23. Taitel, Y. and A. E. Dukler, "A Model for Predicting Flow Regimes Transitions in Horizontal and near Horizontal Gas-Liquid Flow," *AIChE J.* 22, 1, 1976, pp. 47–55.
24. Schetz, J. A., and R. D. W. Bowersox, "Boundary Layer Analysis," *American Institute of Aeronautics and Astronautics*, 2011.
25. Reynolds, A. J., *Turbulent Flows in Engineering*, London: Wiley, 1974.
26. Prandtl, L. "Bericht über Untersuchungen zur ausgebildeten Turbulenz," *Zeitschrift für Angewandte Mathematik und Mechanik*, 5, 1925, pp. 136–139.
27. Haaland, S. E., "Simple and Explicit Formulas for the Friction Factor in Turbulent Flow," *Transactions of ASME, Journal of Fluids Engineering*, 103, 1983, pp. 89–90.

Chapter 9 Problems

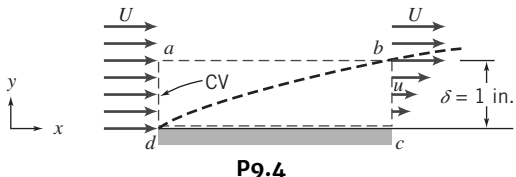
The Boundary-Layer Concept

9.1 A model of a river towboat is to be tested at 1:18 scale. The boat is designed to travel at 3.5 m/s in fresh water at 10°C. Estimate the distance from the bow where transition from a laminar to a turbulent boundary layer occurs. Determine the speed for the model boat so that transition occurs at the same relative position.

9.2 For a flow at 9.0 m/s over a smooth flat plate, estimate the maximum length of the laminar boundary layer for air and for water as the fluid.

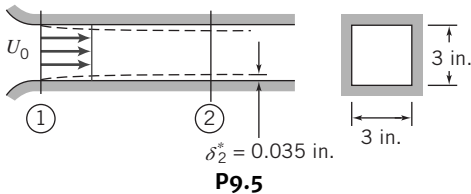
SS 9.3 The velocity profile for a turbulent boundary layer can be approximated by the power law expression $\frac{u}{U} = \left(\frac{y}{\delta}\right)^{1/7}$. Evaluate the displacement thickness $\frac{\delta^*}{\delta}$ and momentum thickness $\frac{\theta}{\delta}$ for the profile. Determine the boundary conditions that are satisfied and not satisfied by this expression.

9.4 A fluid, with density $\rho = 1.5 \text{ slug/ft}^3$, flows at $U = 10 \text{ ft/s}$ over a flat plate 10 ft long and 3 ft wide. At the trailing edge, the boundary-layer thickness is $\delta = 1 \text{ in.}$. Assume that the velocity profile is linear, as shown, and that the flow is two-dimensional (flow conditions are independent of z). Using control volume $abcd$, shown by the dashed lines, compute the mass flow rate across surface ab . Determine the drag force on the upper surface of the plate. Explain how this viscous drag can be computed from the given data even though we do not know the fluid viscosity.



P9.4

9.5 Air flows in the entrance region of a square duct, as shown. The velocity is uniform, $U_0 = 100 \text{ ft/s}$, and the duct is 3 in. square. At a section 1 ft downstream from the entrance, the displacement thickness, δ^* , on each wall measures 0.035 in. Determine the pressure change between sections ① and ②.



P9.5

Laminar Flat-Plate Boundary Layer: Exact Solution

9.6 Plot the Blasius solution for the laminar boundary-layer velocity profile on a flat plate, with $\frac{y}{\delta}$ as the ordinate and $\frac{u}{U}$ as the abscissa.

Plot the approximate parabolic velocity profile $\frac{u}{U} = 2\left(\frac{y}{\delta}\right) - \left(\frac{y}{\delta}\right)^2$ on the same plot and compare the two profiles in terms of shape and boundary conditions.

9.7 For the flow of air over a flat plate, plot on the same graph the laminar boundary-layer thickness as a function of distance along the plate, up to the point of transition, for freestream speeds of 1 m/s, 3 m/s, and 5 m/s. Draw some conclusions from your plot.

9.8 Air at 5 m/s, atmospheric pressure, and 20°C flows over both sides of a flat plate that is 0.8 m long and 0.3 m wide. Determine the total drag force on the plate. Determine the total drag force when the single plate is replaced by two plates each 0.4 m long and 0.3 m wide. Explain why there is a difference in the total drag even though the total surface area is the same.

9.9 Water at a speed of 0.8 m/s and 10°C flows over a flat plate that is 0.35 m long and 1 m wide. The boundary layer on each side of the plate is laminar. Assume that the velocity profile may be approximated as linear and use the momentum integral equation to determine the total drag force on the plate. Compare the drag to that predicted using the results of the Blasius solution.

9.10 Air at standard conditions and 20 m/s flows over one side of a horizontal smooth flat plate that is 1.5 m long and 0.8 m wide. A trip wire is used at the leading edge to ensure that the boundary layer is turbulent. Assume that the velocity profile is represented by a 1/7th power law and evaluate the boundary-layer thickness at the trailing edge of the plate. Determine the wall shear stress at the trailing edge of the plate and the total drag force on the plate.

Pressure Gradients in Boundary-Layer Flow

9.11 Boundary-layer separation occurs when the shear stress at the surface becomes zero. Assume that a polynomial representation for the laminar boundary layer of the form, $u/U = a + b\lambda + c\lambda^2 + d\lambda^3$, where $\lambda = y/\delta$. Specify boundary conditions on the velocity profile at separation. Find appropriate constants, a , b , c , and d , for the separation profile. Calculate the shape factor H at separation. Plot the profile and compare with the parabolic approximate profile.

Drag

9.12 A towboat for river barges is tested in a towing tank. The towboat model is built at a scale ratio of 1:13.5. Dimensions of the model are overall length 3.5 m, beam 1 m, and draft 0.2 m. The model displacement in fresh water is 5500 N. Estimate the average length of wetted surface on the hull. Calculate the skin friction drag force of the prototype at a speed of 7 knots relative to the water.

9.13 A nuclear submarine cruises fully submerged at 27 knots. The hull can be approximated as a circular cylinder with a diameter of 11 m and length of 107 m. Estimate the percentage of the hull length for which the boundary layer is laminar. Determine the skin friction drag on the hull and the power consumed.

9.14 The pilings for a bridge across a river that is 6 ft deep and flows at a maximum speed of 6 mph are made of wood poles 8 in. in diameter buried in the river bed. Estimate the bending moment at the river bed for a piling and discuss the accuracy of the calculation.

9.15 A steel sphere of 0.25 in. diameter has a velocity of 200 ft/s at an altitude of 30,000 ft in the U.S. Standard Atmosphere. Calculate the drag force on this sphere.

9.16 Small oil droplets with a specific gravity of 85 rise in a 30°C water bath. Determine the terminal speed of a droplet as a function of droplet diameter assuming the drag coefficient is given by the

relation for Stokes flow. Determine the maximum droplet diameter for which Stokes flow is a reasonable assumption.

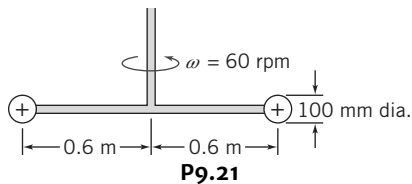
9.17 Atmospheric air is drawn into a low-speed wind tunnel where a 30 cm diameter sphere is mounted on a force balance to measure drag. The oil-filled manometer used to measure the static pressure inside the tunnel reads -40 mm of oil and the oil has a specific gravity of 0.85. Determine the air speed in the tunnel and the drag force on the sphere. Determine the drag force when the air speed is reduced to a manometer reading of -20 mm of oil.

9.18 A water tower consists of a 12-m-diameter sphere on top of a vertical tower 30 m tall and 2 m in diameter. Estimate the bending moment exerted on the base of the tower due to the aerodynamic force imposed by a 100 km/hr wind on a standard day. Neglect interference at the joint between the sphere and tower.

9.19 A 0.5-m-diameter hollow plastic sphere containing pollution test equipment is being dragged through the Hudson River in New York by a diver riding an underwater jet device. The sphere with an effective specific gravity of $SG = 0.30$ is fully submerged, and it is tethered to the diver by a thin 1.5-m-long wire. What is the angle the wire makes with the horizontal if the velocity of the diver and sphere relative to the water is 5 m/s? The water is at 10°C .

9.20 A 0.3 m diameter circular disk is placed normal to a flow stream that has a speed of 5 m/s. Calculate the force and power if the fluid is (a) air and (b) water. If the disk is replaced with a hemisphere with the open end facing downstream, determine the power for the two fluids. Explain why there is a difference for the two geometries even though the frontal area is the same.

SS 9.21 A rotary mixer is constructed from two circular disks as shown. The mixer is rotated at 60 rpm in a large vessel containing a brine solution ($SG = 1.1$). Neglect the drag on the rods and the motion induced in the liquid. Estimate the minimum torque and power required to drive the mixer.



P9.21

9.22 A projectile reduces its speed from 250 m/s to 210 m/s over a horizontal distance of 150 m. The diameter and mass of the projectile are 11 mm and 16 g, respectively. Determine the average drag coefficient for the bullet

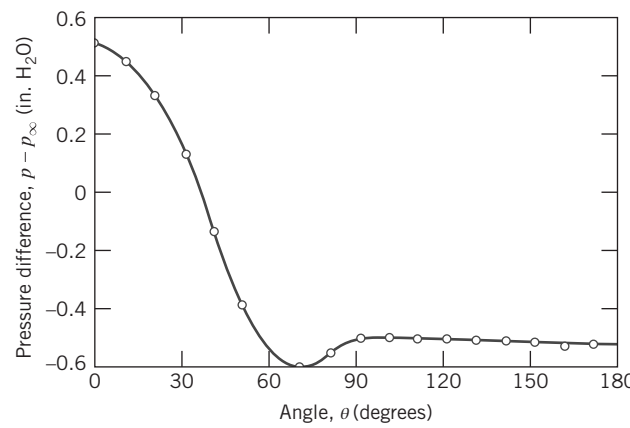
SS 9.23 A typical fully-loaded highway transport truck has a weight of 350 kN, a frontal area of 11.5 m^2 , and a drag coefficient of 0.8. Using drag reduction devices such as a cab top deflector, chassis side skirts, and vortex generators to reduce the wake lowers the drag coefficient to 0.65. Estimate the power requirements for a truck driving 100 km/hr with and without drag reduction devices. The coefficient of rolling friction for the tires is 0.01.

9.24 A fighter airplane is slowed after landing by dual parachutes deployed from the rear. Each parachute is 12 ft in diameter. The plane weighs 32,000 lbf and lands at 160 knots. Estimate the time and distance required to decelerate the aircraft to 100 knots, assuming that the brakes are not used and the drag of the aircraft is negligible.

9.25 A tractor-trailer rig has frontal area $A = 102 \text{ ft}^2$ and drag coefficient $C_D = 0.9$. Rolling resistance is 6 lbf per 1000 lbf of vehicle

weight. The specific fuel consumption of the diesel engine is 0.34 lbm of fuel per horsepower hour, and drivetrain efficiency is 92 percent. The density of diesel fuel is 6.9 lbm/gal. Estimate the fuel economy of the rig at 55 mph if its gross weight is 72,000 lbf. An air fairing system reduces aerodynamic drag 15 percent. The truck travels 120,000 miles per year. Calculate the fuel saved per year by the roof fairing.

9.26 The pressure difference as a function of angle for air flow around a circular cylinder at a Reynolds number of 80,000 is shown in the figure. Numerically integrate the pressure force and estimate the drag coefficient. Compare it to that tabulated in Fig. 9.13. Explain reasons for any difference. **SS**



P9.26

9.27 A rectangular airfoil of 40 ft span and 6 ft chord has lift and drag coefficients of 0.5 and 0.04, respectively, at an angle of attack of 6° . Determine the lift, drag, and horsepower needed to fly this airfoil at 50, 100, and 150 mph horizontally at this angle of attack through still air at 40°F and 13.5 psia.

9.28 The lift and drag coefficients for a rectangular wing with a 10 m chord at takeoff are 1.0 and 0.05, respectively. Determine the span needed to lift 3560 kN at a take-off speed of 282 km/h. Determine the wing drag at this condition.

9.29 A model of wing has a 5 in. chord and 2.5 ft span and is tested at an angle of attack in a wind tunnel at 60 mph with air at 14.5 psia and 70°F . The lift and drag are measured at 6.0 lbf and 0.4 lbf, respectively. Determine the lift and drag coefficients for the wing.

9.30 The mean velocity over the top of a wing with a 1.8 m chord moving through air at 33.5 m/s is 40 m/s, and that over the bottom of the wing is 31 m/s. Determine the lift per meter of span and the lift coefficient.

9.31 A human-powered aircraft has a gross weight of 240 lbf including the pilot. Its wing has a lift coefficient of 1.5 and a lift-to-drag ratio of 70. Estimate the wing area needed and the pilot power that must be provided for this craft to cruise at 15 mph. Assume that the wing profile drag is about 40 percent of the total drag and the propeller efficiency is 80 percent. **SS**

9.32 A model airfoil of chord 6 in. and span 30 in. is placed in a wind tunnel with an air flow of 100 ft/s at 70°F . It is mounted on a cylindrical support rod 1 in. in diameter and 10 in. tall. Instruments at the base of the rod indicate a vertical force of 10 lbf and a horizontal force of 1.5 lbf. Calculate the lift and drag coefficients of the airfoil.

9.33 An airplane with an effective lift area of 25 m^2 is fitted with airfoils of NACA 23012 section (Fig. 9.23). The maximum flap setting that can be used at takeoff corresponds to configuration ② in Fig. 9.23. Determine the maximum gross mass possible for the airplane if its takeoff speed is 150 km/hr at sea level. Find the minimum takeoff speed required for this gross mass if the airplane is instead taking off from Denver (elevation 1.6 km).

SS 9.34 The F-16 fighter aircraft weighs 26,000 lbf fully loaded, has a wing planform area of 300 ft^2 , and a maximum lift coefficient of 1.6. The limit on acceleration during turns in level flight is 5 g. Determine the minimum speed at sea level for which the pilot can produce a 5 g total acceleration. Determine the corresponding flight radius.

9.35 A light airplane has 35-ft effective wingspan and 5.5-ft chord. It was originally designed to use a conventional (NACA 23015) airfoil section. With this airfoil, its cruising speed on a standard

day near sea level is 150 mph. A redesign is proposed in which the current conventional airfoil section is replaced with another conventional airfoil section of the same area, but with aspect ratio $AR = 8$. Determine the cruising speed that could be achieved with this new airfoil for the same power.

9.36 Rotating cylinders have been proposed as a means of ship propulsion as early as 1924. An original design used two rotors, each 10 ft in diameter and 50 ft high, rotating at up to 800 rpm. Calculate the maximum lift and drag forces that act on each rotor in a 30-mph wind. Estimate the power needed to spin the rotors and propel the ship at 800 rpm.

9.37 A baseball pitcher throws a ball 60 ft from the pitcher's mound over home plate at 80 mph. A baseball has a mass of 5 oz and a circumference of 9 in. Determine the spin that should be placed on the ball for maximum horizontal deviation from a straight path and determine the deviation from a straight line.

CHAPTER 9

External Incompressible Viscous Flow

Part A Boundary Layers

- 9.1 The Boundary Layer Concept
- 9.2 Laminar Flat Plate Boundary Layer: Exact Solution
- 9.3 Momentum Integral Equation
- 9.4 Use of the Momentum Integral Equation for Flow with Zero Pressure Gradient

9.5 Pressure Gradients in Boundary Layer Flow

Part B Fluid Flow About Immersed Bodies

- 9.6 Drag
- 9.7 Lift
- 9.8 Summary and Useful Equations

Case Study

The all-electric Tesla Model S depicted in the figure represents a revolutionary advance in automotive design. The 2017 Model S energy consumption has been rated by the EPA as a combined fuel economy of 0.26 kWh/mi, which is equivalent to 104 mpg. The range on a single battery charge is 215 mi. The aerodynamic performance of the vehicle is crucial to achieving fuel consumption and range of the automobile.

Aerodynamic drag on vehicles has been traditionally determined using full-scale prototypes or models tested in wind tunnels. For the Tesla, an in-house computational fluid dynamics (CFD) program was used to determine the effect of modifications in the shape of the body on reducing drag. The drag coefficient, which is a measure of the drag force relative to the kinetic energy of the air flowing over the vehicle, is 0.32 for the current Model S. Further modifications planned by Tesla are expected to reduce the value to 0.21. At speeds above about 30 mph, the aerodynamic drag is the major contributor to fuel use, so aerodynamics are important to the success of the car.

Among the many improvements over conventional car design are the wheels with turbine-style blading that direct the airflow under the car to reduce drag. The underside is flat and smooth with a rear diffuser to reduce the wake. The front end uses a grill shape with rounded edges to control the airflow over the top and sides of the car. Air curtains in the lower fender provide a drag-reducing airstream. Even the door handles are recessed to make for smooth airflow over the sides.

An independent CFD simulation of a model of the Tesla focused on the different components that contribute to the drag. The major contributions came from the front bumper, underside, wheels and housings, and the rear window and trunk. The drag on the front license plate, which is mandatory in many states, was significant. Low pressures on the front hood, windshield, and roof actually reduced the drag somewhat. The low-drag features of the Tesla illustrate the design possibilities using CFD.



A streamlined all-electric automobile.

Herr Loeffler/Adobe Stock Photo

Learning Objectives

After completing this chapter, you should be able to

- Describe a boundary layer and the parameters that characterize it.
- Provide a physical explanation for the terms in the momentum integral equation.
- Compute the boundary layer parameters using the momentum integral equation.
- Explain the effects of pressure gradients on a boundary layer.
- Determine the drag force for flow over different shaped objects.
- Determine the lift force for flow over objects.

External flows are flows over bodies immersed in an unbounded fluid. The flow over a sphere (Fig. 2.14b) and the flow over a streamlined body (Fig. 2.16) are examples of external flows, which were discussed qualitatively in Chapter 2. More interesting examples are the flow fields around such objects as airfoils (Fig. 9.1), automobiles, and airplanes. Our objective in this chapter is to quantify the behavior of viscous, incompressible fluids in external flow.

A number of phenomena that occur in external flow over a body are illustrated in the sketch of viscous flow at high Reynolds number over an airfoil (Fig. 9.1). The freestream flow divides at the stagnation point and flows around the body. Fluid at the surface takes on the velocity of the body as a result of the no-slip condition. Boundary layers form on both the upper and lower surfaces of the body. The boundary-layer thickness on both surfaces in Fig. 9.1 is exaggerated greatly for clarity. The flow in the boundary layers initially is laminar. Transition to turbulent flow occurs at some distance from the stagnation point, depending on freestream conditions, surface roughness, and pressure gradient. The transition points are indicated by “T” in the figure. The turbulent boundary layer following transition grows more rapidly than the laminar layer. A slight displacement of the streamlines of the external flow is caused by the thickening boundary layers on the surface. In a region of increasing pressure (an *adverse pressure gradient*—so called because it opposes the fluid motion, tending to decelerate the fluid particles) flow separation may occur. Separation points are indicated by “S” in the figure. Fluid that was in the boundary layers on the body surface forms the viscous wake behind the separation points.

This chapter has two parts. Part A is a review of boundary-layer flows. Here we discuss in a little more detail the ideas introduced in Chapter 2, and then apply the fluid mechanics concepts we have learned to analyze the boundary layer for flow along a flat plate—the simplest possible boundary layer, because the pressure field is constant. We will be interested in seeing how the boundary-layer thickness grows, what the surface friction will be, and so on. We will explore a classic analytical solution for a laminar boundary layer, and see that we need to resort to approximate methods when the boundary layer is turbulent. We will conclude our introduction to boundary layers by briefly discussing the effect of pressure gradients on boundary-layer behavior.

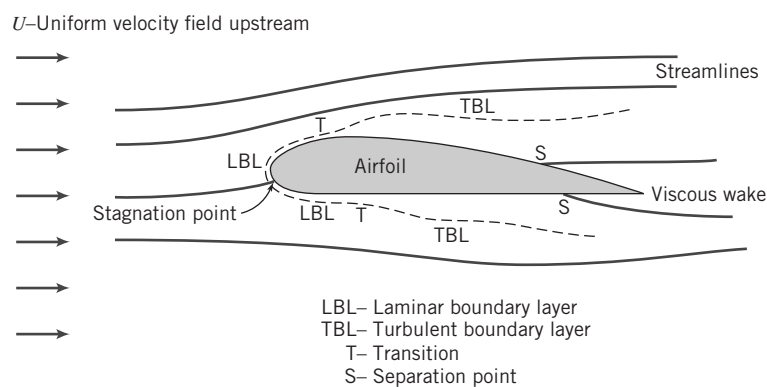


Fig. 9.1 Details of viscous flow around an airfoil.

In Part B we will discuss the force on a submerged body, such as the airfoil of Fig. 9.1. We will see that this force results from both shear and pressure forces acting on the body surface, and that both of these are profoundly affected by the fact that we have a boundary layer, especially when this causes flow separation and a wake. Traditionally the force a body experiences is decomposed into the component parallel to the flow, the *drag*, and the component perpendicular to the flow, the *lift*. Because most bodies do have a point of separation and a wake, it is difficult to use analysis to determine the force components, so we will present approximate analyses and experimental data for various interesting body shapes.

Part A BOUNDARY LAYERS

9.1 The Boundary Layer Concept

The concept of a boundary layer was first introduced by Ludwig Prandtl [1], a German aerodynamicist, in 1904. Prior to Prandtl's historic breakthrough, the science of fluid mechanics had been developing in two rather different directions. *Theoretical hydrodynamics* evolved from Euler's equation of motion for a nonviscous fluid. Since the results of hydrodynamics predicted no drag and contradicted many experimental observations practicing engineers developed their own empirical art of *hydraulics*. This was based on experimental data and differed significantly from the purely mathematical approach of theoretical hydrodynamics.

Although the complete equations describing the motion of a viscous fluid, the Navier–Stokes equations, Eqs. 5.26, were known prior to Prandtl, the mathematical difficulties in solving these equations except for a few simple cases prohibited a theoretical treatment of viscous flows. Prandtl showed [1] that many viscous flows can be analyzed by dividing the flow into two regions, one close to solid boundaries, the other covering the rest of the flow. Only in the thin region adjacent to a solid boundary, termed the boundary layer, is the effect of viscosity important. In the region outside of the boundary layer, the effect of viscosity is negligible and the fluid may be treated as inviscid.

The boundary-layer concept provided the link that had been missing between theory and practice. Furthermore, the boundary-layer concept permitted the solution of viscous flow problems that would have been impossible through application of the Navier–Stokes equations to the complete flow field. Thus the introduction of the boundary-layer concept marked the beginning of the modern era of fluid mechanics.

The development of a boundary layer on a solid surface was discussed in Section 2.6. In the boundary layer both viscous and inertia forces are important. Consequently, it is not surprising that the Reynolds number is significant in characterizing boundary-layer flows. The characteristic length used in the Reynolds number is either the length in the flow direction over which the boundary layer has developed or some measure of the boundary-layer thickness.

As is true for flow in a duct, flow in a boundary layer may be laminar or turbulent. There is no unique value of Reynolds number at which transition from laminar to turbulent flow occurs in a boundary layer. Among the factors that affect boundary-layer transition are pressure gradient, surface roughness, heat transfer, body forces, and freestream disturbances.

In many real flow situations, a boundary layer develops over a long, essentially flat surface. Examples include flow over ship and submarine hulls, aircraft wings, and atmospheric motions over flat terrain. Since the basic features of all these flows are illustrated in the simpler case of flow over a flat plate, we consider this first. The simplicity of the flow over an infinite flat plate is that the velocity U outside the boundary layer is constant, and therefore, because this region is steady, inviscid, and incompressible, the pressure will also be constant. This constant pressure is the pressure felt by the boundary layer—obviously the simplest pressure field possible. This is a *zero pressure gradient flow*.

A qualitative picture of the boundary-layer growth over a flat plate is shown in Fig. 9.2. The boundary layer is laminar for a short distance downstream from the leading edge; transition occurs over a region of the plate rather than at a single line across the plate. The transition region extends downstream to the location where the boundary-layer flow becomes completely turbulent.

For incompressible flow over a smooth flat plate with zero pressure gradient, in the absence of heat transfer, transition from laminar to turbulent flow in the boundary layer can be delayed to a Reynolds

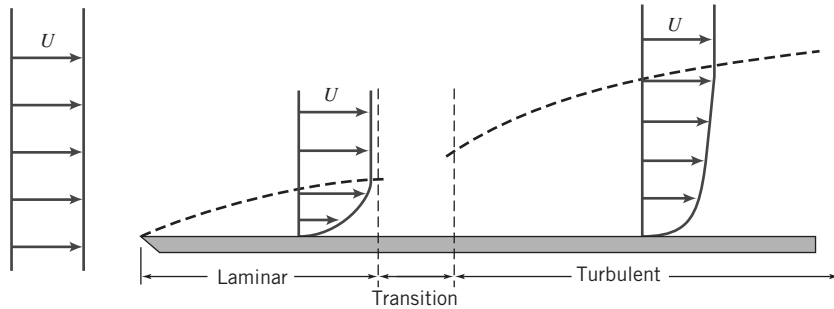


Fig. 9.2 Boundary layer on a flat plate (vertical thickness exaggerated greatly).

number, $Re_x = \rho U x / \mu$, greater than one million if external disturbances are minimized. For calculation purposes, under typical flow conditions, transition usually is considered to occur at a length Reynolds number of 500,000. For air at standard conditions, with freestream velocity $U = 30$ m/s, this corresponds to $x \approx 0.24$ m. In the qualitative picture of Fig. 9.2, we have shown the turbulent boundary layer growing faster than the laminar layer. In later sections of this chapter we shall show that this is indeed true.

The boundary layer is the region adjacent to a solid surface in which viscous stresses are present, as opposed to the free stream where viscous stresses are negligible. These stresses are present because we have shearing of the fluid layers, i.e., a velocity gradient, in the boundary layer. As indicated in Fig. 9.2, both laminar and turbulent layers have such gradients, but the difficulty is that the gradients only asymptotically approach zero as we reach the edge of the boundary layer. Hence, the location of the edge, i.e., of the boundary-layer thickness, is not very obvious and we cannot simply define it as where the boundary-layer velocity u equals the freestream velocity U . Because of this, several boundary-layer definitions have been developed: the boundary layer thickness δ , the displacement thickness δ^* , and the momentum thickness θ .

The most straightforward definition is the boundary layer thickness, δ . This is usually defined as the distance from the surface at which the velocity is within 1 percent of the free stream, $u \approx 0.99U$, as shown in Fig. 9.3b. The other two definitions are based on the notion that the boundary layer retards the fluid, so that the mass flux and momentum flux are both less than they would be in the absence of the boundary layer. We imagine that the flow remains at uniform velocity U , but the surface of the plate is moved upwards to reduce either the mass or momentum flux by the same amount that the boundary layer actually does. The *displacement thickness*, δ^* , is the distance the plate would be moved so that the loss of mass flux due to reduction in uniform flow area is equivalent to the loss the boundary layer causes. The mass flux if we had no boundary layer would be $\int_0^\infty \rho U dy w$, where w is the width of the plate perpendicular to the flow. The actual flow mass flux is $\int_0^\infty \rho u dy w$. Hence, the loss due to the boundary layer is $\int_0^\infty \rho(U-u) dy w$. If we imagine keeping the velocity at a constant U , and instead move the plate up a distance δ^* (as shown in Fig. 9.3a), the loss of mass flux would be $\rho U \delta^* w$. Setting these losses equal to one another gives

$$\rho U \delta^* w = \int_0^\infty \rho(U-u) dy w$$

For incompressible flow, $\rho = \text{constant}$, and

$$\delta^* = \int_0^\infty \left(1 - \frac{u}{U}\right) dy \approx \int_0^\delta \left(1 - \frac{u}{U}\right) dy \quad (9.1)$$

Since $u \approx U$ at $y = \delta$, the integrand is essentially zero for $y \geq \delta$. Application of the displacement-thickness concept is illustrated in Example 9.1.

The *momentum thickness*, θ , is the distance the plate would be moved so that the loss of momentum flux is equivalent to the loss the boundary layer actually causes. The momentum flux if we had the same flow as with the boundary layer but with the momentum of the free stream would be $\int_0^\infty \rho u U dy w$; the actual mass flux with the boundary layer is $\int_0^\infty \rho u dy w$, and the momentum per unit mass flux of the uniform flow is U itself. The actual momentum flux of the boundary layer is $\int_0^\infty \rho u^2 dy w$. Hence, the

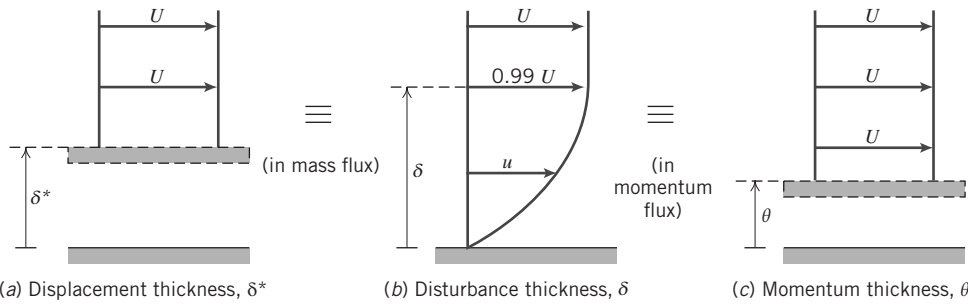


Fig. 9.3 Boundary-layer thickness definitions.

loss of momentum in the boundary layer is $\int_0^\infty \rho u(U-u) dy w$. If we imagine keeping the velocity at a constant U , and instead move the plate up a distance θ (as shown in Fig. 9.3c), the loss of momentum flux would be $\int_0^\theta \rho UU dy w = \rho U^2 \theta w$. Setting these losses equal to one another gives

$$\rho U^2 \theta = \int_0^\infty \rho u(U-u) dy$$

and

$$\theta = \int_0^\infty \frac{u}{U} \left(1 - \frac{u}{U}\right) dy \approx \int_0^\delta \frac{u}{U} \left(1 - \frac{u}{U}\right) dy \quad (9.2)$$

Again, the integrand is essentially zero for $y \geq \delta$.

The displacement and momentum thicknesses, δ^* and θ , are easier to evaluate accurately from experimental data than the boundary-layer thickness, δ . This fact, coupled with their physical significance, accounts for their common use in specifying boundary-layer thickness.

We have seen that the velocity profile in the boundary layer merges into the local freestream velocity asymptotically. Little error is introduced if the slight difference between velocities at the edge of the boundary layer is ignored for an approximate analysis. Simplifying assumptions usually made for engineering analyses of boundary-layer development are:

- 1 $u \rightarrow U$ at $y = \delta$
- 2 $du/dy \rightarrow 0$ at $y = \delta$
- 3 $v \ll U$ within the boundary layer

Results of the analyses developed in the next two sections show that the boundary layer is very thin compared with its development length along the surface. Therefore it is also reasonable to assume:

- 4 Pressure variation across the thin boundary layer is negligible. The freestream pressure distribution is *impressed* on the boundary layer.

Example 9.1 illustrates the use of these boundary parameters in a physical situation.

Example 9.1 BOUNDARY LAYER IN CHANNEL FLOW

A laboratory wind tunnel has a test section that is 305 mm square. Boundary-layer velocity profiles are measured at two cross-sections and displacement thicknesses are evaluated from the measured profiles. At section ①, where the freestream speed is $U_1 = 26 \text{ m/s}$, the displacement thickness is $\delta_1^* = 1.5 \text{ mm}$. At section ②, located downstream from section ①, $\delta_2^* = 2.1 \text{ mm}$. Calculate the change in static pressure between sections ① and ②. Express the result as a fraction of the freestream dynamic pressure at section ①. Assume standard atmosphere conditions.

Given: Flow of standard air in laboratory wind tunnel. Test section is $L = 305$ mm square. Displacement thicknesses are $\delta_1^* = 1.5$ mm and $\delta_2^* = 2.1$ mm. Freestream speed is $U_1 = 26$ m/s.

Find: Change in static pressure between sections ① and ②. (Express as a fraction of freestream dynamic pressure at section ①.)

Solution: The idea here is that at each location the boundary-layer displacement thickness effectively reduces the area of uniform flow, as indicated in the following figures: Location ② has a smaller effective flow area than location ① (because $\delta_2^* > \delta_1^*$). Hence, from mass conservation the uniform velocity at location ② will be higher. Finally, from the Bernoulli equation the pressure at location ② will be lower than that at location ①.

Apply the continuity and Bernoulli equations to freestream flow outside the boundary-layer displacement thickness, where viscous effects are negligible.

Governing equations:

$$= 0(1) \quad (4.12)$$

$$\frac{\partial}{\partial t} \int_{CV} \rho dV + \int_{CS} \rho \vec{V} \cdot d\vec{A} = 0$$

$$\frac{p_1}{\rho} + \frac{V_1^2}{2} + g z_1 = \frac{p_2}{\rho} + \frac{V_2^2}{2} + g z_2 \quad (4.24)$$

Assumptions:

- 1 Steady flow.
- 2 Incompressible flow.
- 3 Flow uniform at each section outside δ^* .
- 4 Flow along a streamline between sections ① and ②.
- 5 No frictional effects in freestream.
- 6 Negligible elevation changes.

From the Bernoulli equation we obtain

$$p_1 - p_2 = \frac{1}{2} \rho (V_2^2 - V_1^2) = \frac{1}{2} \rho (U_2^2 - U_1^2) = \frac{1}{2} \rho U_1^2 \left[\left(\frac{U_2}{U_1} \right)^2 - 1 \right]$$

or

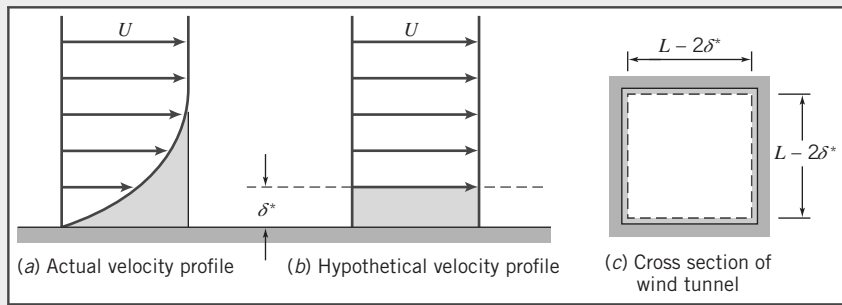
$$\frac{p_1 - p_2}{\frac{1}{2} \rho U_1^2} = \left(\frac{U_2}{U_1} \right)^2 - 1$$

From continuity, $V_1 A_1 = U_1 A_1 = V_2 A_2 = U_2 A_2$, so $U_2/U_1 = A_1/A_2$, where $A = (L - 2\delta^*)^2$ is the effective flow area. Substituting gives

$$\frac{p_1 - p_2}{\frac{1}{2} \rho U_1^2} = \left(\frac{A_1}{A_2} \right)^2 - 1 = \left[\frac{(L - 2\delta_1^*)^2}{(L - 2\delta_2^*)^2} \right]^2 - 1$$

$$\frac{p_1 - p_2}{\frac{1}{2} \rho U_1^2} = \left[\frac{305 - 2(1.5)}{305 - 2(2.1)} \right]^4 - 1 = 0.0161 \text{ or}$$

$$\frac{p_1 - p_2}{\frac{1}{2} \rho U_1^2} = 1.61 \text{ percent} \longleftarrow \frac{p_1 - p_2}{\frac{1}{2} \rho U_1^2}$$



Notes:

- This problem illustrates a basic application of the displacement-thickness concept. It is somewhat unusual in that, because the flow is confined, the reduction in flow area caused by the boundary layer leads to the result that the pressure in the inviscid flow region drops (if only slightly). In most applications the pressure distribution is determined from the inviscid flow and then applied to the boundary layer.
- We saw a similar phenomenon in Section 8.1, where we discovered that the centerline velocity at the entrance of a pipe increases due to the boundary layer “squeezing” the effective flow area.

9.2 Laminar Flat Plate Boundary Layer: Exact Solution

The solution for the laminar boundary layer on a horizontal flat plate was obtained by Prandtl's student H. Blasius [2] in 1908. For two-dimensional, steady, incompressible flow with zero pressure gradient, the governing equations of motion (Eqs. 5.27) reduce to [3]

$$\frac{\partial u}{\partial x} + \frac{\partial v}{\partial y} = 0 \quad (9.3)$$

$$u \frac{\partial u}{\partial x} + v \frac{\partial u}{\partial y} = \nu \frac{\partial^2 u}{\partial y^2} \quad (9.4)$$

with boundary conditions

$$\begin{aligned} \text{at } y=0, \quad u=0, \quad v=0 \\ \text{at } y=\infty, \quad u=U, \quad \frac{\partial u}{\partial y}=0 \end{aligned} \quad (9.5)$$

Equations 9.3 and 9.4, with boundary conditions Eq. 9.5 are a set of nonlinear, coupled, partial differential equations for the unknown velocity field u and v . To solve them, Blasius reasoned that the velocity profile, u/U , should be *similar* for all values of x when plotted versus a nondimensional distance from the wall; the boundary-layer thickness, δ , was a natural choice for nondimensionalizing the distance from the wall. Thus the solution is of the form

$$\frac{u}{U} = g(\eta) \quad \text{where} \quad \eta \propto \frac{y}{\delta} \quad (9.6)$$

Based on the solution of Stokes [4], Blasius reasoned that $\delta \propto \sqrt{\nu x/U}$ and set

$$\eta = y \sqrt{\frac{U}{\nu x}} \quad (9.7)$$

The variable “eta” combines the two variables x and y into one variable. We now introduce the stream function, ψ , where

$$u = \frac{\partial \psi}{\partial y} \quad \text{and} \quad v = -\frac{\partial \psi}{\partial x} \quad (5.4)$$

This substitution satisfies the continuity equation (Eq. 9.3) identically. Substituting for u and v into Eq. 9.4 reduces the momentum equation to one in which ψ is the single dependent variable. Defining a dimensionless stream function as

$$f(\eta) = \frac{\psi}{\sqrt{\nu x U}} \quad (9.8)$$

makes $f(\eta)$ the dependent variable and η the independent variable in Eq. 9.4. With ψ defined by Eq. 9.8 and η defined by Eq. 9.7, we can evaluate each of the terms in Eq. 9.4.

The velocity components are given by

$$u = \frac{\partial \psi}{\partial y} = \frac{\partial \psi}{\partial \eta} \frac{\partial \eta}{\partial y} = \sqrt{\nu x U} \frac{df}{d\eta} \sqrt{\frac{U}{\nu x}} = U \frac{df}{d\eta} \quad (9.9)$$

and

$$v = -\frac{\partial \psi}{\partial x} = -\left[\sqrt{\nu x U} \frac{df}{dx} + \frac{1}{2} \sqrt{\frac{\nu U}{x}} f \right] = -\left[\sqrt{\nu x U} \frac{df}{d\eta} \left(-\frac{1}{2} \eta \frac{1}{x} \right) + \frac{1}{2} \sqrt{\frac{\nu U}{x}} f \right]$$

or

$$v = \frac{1}{2} \sqrt{\frac{\nu U}{x}} \left[\eta \frac{df}{d\eta} - f \right] \quad (9.10)$$

By differentiating the velocity components, it also can be shown that

$$\frac{\partial u}{\partial x} = -\frac{U}{2x}\eta \frac{d^2f}{d\eta^2}$$

$$\frac{\partial u}{\partial y} = U\sqrt{U/\nu x} \frac{d^2f}{d\eta^2}$$

and

$$\frac{\partial^2 u}{\partial y^2} = \frac{U^2}{\nu x} \frac{d^3f}{d\eta^3}$$

Substituting these expressions into Eq. 9.4, we obtain

$$2\frac{d^3f}{d\eta^3} + f \frac{d^2f}{d\eta^2} = 0 \quad (9.11)$$

with boundary conditions:

$$\text{at } \eta = 0, \quad f = \frac{df}{d\eta} = 0$$

$$\text{at } \eta = \infty, \quad \frac{df}{d\eta} = 1 \quad (9.12)$$

The second-order partial differential equations governing the laminar boundary layer on a flat plate (Eqs. 9.3 and 9.4) have been transformed to a nonlinear, third-order ordinary differential equation (Eq. 9.11) with boundary conditions given by Eq. 9.12. It is not possible to solve Eq. 9.11 in closed form; Blasius solved it using a power series expansion and it has been solved more recently using numerical methods [5]. The solution in terms of “eta” is given in Table 9.1.

The velocity profile is sketched in Fig. 9.3b. Velocity profiles measured experimentally are in excellent agreement with the analytical solution. Profiles from all locations on a flat plate collapse to a single profile when plotted in nondimensional coordinates.

From Table 9.1, we see that at $\eta = 5.0$, $u/U = 0.992$. With the boundary-layer thickness, δ , defined as the value of y for which $u/U = 0.99$, Eq. 9.7 gives

$$\delta \approx \frac{5.0}{\sqrt{U/\nu x}} = \frac{5.0x}{\sqrt{Re_x}} \quad (9.13)$$

Table 9.1

The Function $f(\eta)$ for the Laminar Boundary Layer along a Flat Plate at Zero Incidence

$\eta = y\sqrt{\frac{U}{\nu x}}$	f	$f' = \frac{u}{U}$	f''
0	0	0	0.3321
0.5	0.0415	0.1659	0.3309
1.0	0.1656	0.3298	0.3230
1.5	0.3701	0.4868	0.3026
2.0	0.6500	0.6298	0.2668
2.5	0.9963	0.7513	0.2174
3.0	1.3968	0.8460	0.1614
3.5	1.8377	0.9130	0.1078
4.0	2.3057	0.9555	0.0642
4.5	2.7901	0.9795	0.0340
5.0	3.2833	0.9915	0.0159
5.5	3.7806	0.9969	0.0066
6.0	4.2796	0.9990	0.0024
6.5	4.7793	0.9997	0.0008
7.0	5.2792	0.9999	0.0002
7.5	5.7792	1.0000	0.0001
8.0	6.2792	1.0000	0.0000

The wall shear stress may be expressed as

$$\tau_w = \mu \frac{\partial u}{\partial y} \Big|_{y=0} = \mu U \sqrt{U/\nu x} \frac{d^2 f}{d\eta^2} \Big|_{\eta=0}$$

Then

$$\tau_w = 0.332 U \sqrt{\rho \mu U / x} = \frac{0.332 \rho U^2}{\sqrt{Re_x}} \quad (9.14)$$

and the wall shear stress coefficient, C_f , is given by

$$C_f = \frac{\tau_w}{\frac{1}{2} \rho U^2} = \frac{0.664}{\sqrt{Re_x}} \quad (9.15)$$

Each of the results for boundary-layer thickness, δ , wall shear stress, τ_w , and skin friction coefficient, C_f , Eqs. 9.13 through 9.15, depends on the length Reynolds number, Re_x , to the one-half power. The boundary-layer thickness increases as $x^{1/2}$, and the wall shear stress and skin friction coefficient vary as $1/x^{1/2}$. These results characterize the behavior of the laminar boundary layer on a flat plate. In Example 9.2, we evaluate some boundary layer properties using the exact solution.

Example 9.2 LAMINAR BOUNDARY LAYER ON A FLAT PLATE: EXACT SOLUTION

Use the numerical results presented in Table 9.1 to evaluate the following quantities for laminar boundary-layer flow on a flat plate:

- (a) δ^*/δ (for $\eta = 5$ and as $\eta \rightarrow \infty$).
- (b) v/U at the boundary-layer edge.

Given: Numerical solution for laminar flat plate boundary layer, Table 9.1.

Find: (a) The displacement thickness δ^*/δ (for $\eta = 5$ and as $\eta \rightarrow \infty$).
(b) The vertical component of velocity v/U at the boundary-layer edge.
(c) The ratio of the slope of a streamline at the boundary-layer edge to the slope of δ versus x .

Solution: The displacement thickness is defined by Eq. 9.1 as

$$\delta^* = \int_0^\infty \left(1 - \frac{u}{U}\right) dy \approx \int_0^\delta \left(1 - \frac{u}{U}\right) dy$$

In order to use the Blasius exact solution to evaluate this integral, we need to convert it from one involving u and y to one involving $f' (=u/U)$ and η variables. From Eq. 9.7, $\eta = y \sqrt{U/\nu x}$, so $y = \eta \sqrt{\nu x/U}$ and $dy = d\eta \sqrt{\nu x/U}$. Thus,

$$\delta^* = \int_0^{\eta_{\max}} (1-f') \sqrt{\frac{\nu x}{U}} d\eta = \sqrt{\frac{\nu x}{U}} \int_0^{\eta_{\max}} (1-f') d\eta \quad (1)$$

Note: Corresponding to the upper limit on y in Eq. 9.1, $\eta_{\max} = \infty$, or $\eta_{\max} \approx 5$.

From Eq. 9.13,

$$\delta \approx \frac{5}{\sqrt{U/\nu x}}$$

so if we divide each side of Eq. 1 by each side of Eq. 9.13, we obtain (with $f' = df/d\eta$)

$$\frac{\delta^*}{\delta} = \frac{1}{5} \int_0^{\eta_{\max}} \left(1 - \frac{df}{d\eta}\right) d\eta$$

Integrating gives

$$\frac{\delta^*}{\delta} = \frac{1}{5} [\eta - f(\eta)]_0^{\eta_{\max}}$$

Evaluating at $\eta_{\max} = 5$, we obtain

$$\frac{\delta^*}{\delta} = \frac{1}{5} (5.0 - 32833) = 0.343 \xrightarrow{\hspace{10cm}} \frac{\delta^*(\eta=5)}{\delta}$$

The quantity $\eta - f(\eta)$ becomes constant for $\eta > 7$. Evaluating at $\eta_{\max} = 8$ gives

$$\frac{\delta^*}{\delta} = \frac{1}{5} (8.0 - 62792) = 0.344 \xrightarrow{\hspace{10cm}} \frac{\delta^*(\eta \rightarrow \infty)}{\delta}$$

Thus, $\delta_{\eta \rightarrow \infty}^*$ is essentially equal to $\delta_{\eta=5}^*$

From Eq. 9.10, the vertical component of velocity is

$$v = \frac{1}{2} \sqrt{\frac{\nu U}{x}} \left(\eta \frac{df}{d\eta} - f \right), \quad \text{so} \quad \frac{v}{U} = \frac{1}{2} \sqrt{\frac{\nu}{Ux}} \left(\eta \frac{df}{d\eta} - f \right) = \frac{1}{2\sqrt{Re_x}} \left(\eta \frac{df}{d\eta} - f \right)$$

Evaluating at the boundary-layer edge ($\eta = 5$), we obtain

$$\frac{v}{U} = \frac{1}{2\sqrt{Re_x}} [5(0.9915) - 3.2833] = \frac{0.837}{\sqrt{Re_x}} \approx \frac{0.84}{\sqrt{Re_x}} \xrightarrow{\hspace{10cm}} \frac{v}{U}(\eta=5)$$

Thus v is only 0.84 percent of U at $Re_x = 10^4$, and only about 0.12 percent of U at $Re_x = 5 \times 10^5$.

This problem illustrates use of numerical data from the Blasius solution to obtain other information on a flat plate laminar boundary layer.

9.3 Momentum Integral Equation

The exact solution for the laminar boundary layer on a flat plate obtained in Section 9.2 is complex mathematically. It is restricted to a constant free stream velocity with a zero pressure gradient. We will develop a method for analyzing more general cases that include both laminar and turbulent boundary layers in which the freestream velocity and pressure vary along the surface, as for example the curved surface of an airfoil. Our approach will be to apply the basic equations to a control volume.

We will consider the general situation of an incompressible, steady, two-dimensional flow over a solid surface. The boundary-layer thickness, δ , grows with increasing distance, x . For our analysis we choose a differential control volume, of length dx , width w , and height $\delta(x)$, as shown in Fig. 9.4. The freestream velocity is $U(x)$.

We wish to determine the boundary-layer thickness and shear stress as functions of x . There will be mass flow across surfaces ab and cd of differential control volume $abcd$. What about surface bc ? Surface bc is *not* a streamline but is the imaginary boundary that separates the viscous boundary layer and the inviscid freestream flow. Thus there will be mass flow across surface bc . Since control surface ad is

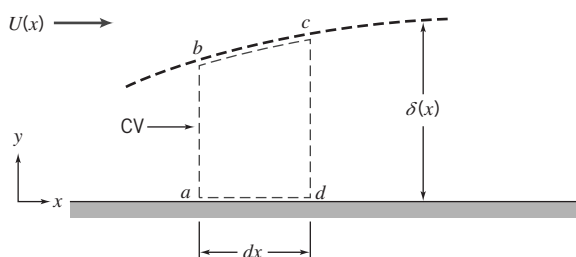


Fig. 9.4 Differential control volume in a boundary layer.

adjacent to a solid boundary, there will not be flow across *ad*. Before considering the forces acting on the control volume and the momentum fluxes through the control surface, let us apply the continuity equation to determine the mass flux through each portion of the control surface.

a. Continuity Equation

Basic equation:

$$=0(1) \quad \frac{\partial}{\partial t} \int_{CV} \rho dV + \int_{CS} \rho \vec{V} \cdot d\vec{A} = 0 \quad (4.12)$$

Assumptions:

- 1 Steady flow.
- 2 Two-dimensional flow.

Then

$$\int_{CS} \rho \vec{V} \cdot d\vec{A} = 0$$

Hence

$$\dot{m}_{ab} + \dot{m}_{bc} + \dot{m}_{cd} = 0$$

or

$$\dot{m}_{bc} = -\dot{m}_{ab} - \dot{m}_{cd}$$

Now let us evaluate these terms for the differential control volume of width *w*:

Surface	Mass Flux
<i>ab</i>	Surface <i>ab</i> is located at <i>x</i> . Since the flow is two-dimensional (no variation with <i>z</i>), the mass flux through <i>ab</i> is
	$\dot{m}_{ab} = - \left\{ \int_0^\delta \rho u dy \right\} w$
<i>cd</i>	Surface <i>cd</i> is located at <i>x+dx</i> . Expanding the \dot{m} in a Taylor series about location <i>x</i> , we obtain
	$\dot{m}_{x+dx} = \dot{m}_x + \left[\frac{\partial \dot{m}}{\partial x} \right]_x dx$
	and hence
	$\dot{m}_{cd} = \left\{ \int_0^\delta \rho u dy + \left[\frac{\partial}{\partial x} \left[\int_0^\delta \rho u dy \right] dx \right] \right\} w$
<i>bc</i>	Thus for surface <i>bc</i> we obtain, from the continuity equation and the above results,
	$\dot{m}_{bc} = - \left\{ \frac{\partial}{\partial x} \left[\int_0^\delta \rho u dy \right] dx \right\} w$

Now let us consider the momentum fluxes and forces associated with control volume *abcd*. These are related by the momentum equation.

b. Momentum Equation

Apply the *x* component of the momentum equation to control volume *abcd*:

Basic equation:

$$=0(3) \quad =0(1) \quad F_{S_x} + F_{B_x} = \frac{\partial}{\partial t} \int_{CV} u \rho dV + \int_{CS} u \rho \vec{V} \cdot d\vec{A} \quad (4.18a)$$

Assumptions:

$$3 \quad F_{B_x} = 0$$

Then

$$F_{S_x} = mf_{ab} + mf_{bc} + mf_{cd}$$

where mf represents the x component of momentum flux.

To apply this equation to differential control volume $abcd$, we must obtain expressions for the x momentum flux through the control surface and also the surface forces acting on the control volume in the x direction. Let us consider the momentum flux first and again consider each segment of the control surface.

Surface	Momentum Flux (mf)
ab	Surface ab is located at x . Since the flow is two-dimensional, the x momentum flux through ab is
	$mf_{ab} = - \left\{ \int_0^\delta u \rho u dy \right\}_w$
cd	Surface cd is located at $x + dx$. Expanding the x momentum flux (mf) in a Taylor series about location x , we obtain
	$mf_{x+dx} = mf_x + \frac{\partial mf}{\partial x} \Big _x dx$
	or
	$mf_{cd} = \left\{ \int_0^\delta u \rho u dy + \frac{\partial}{\partial x} \left[\int_0^\delta u \rho u dy \right] dx \right\}_w$
bc	Since the mass crossing surface bc has velocity component U in the x direction, the x momentum flux across bc is given by
	$mf_{bc} = U \dot{m}_{bc}$
	$mf_{bc} = -U \left\{ \frac{\partial}{\partial x} \left[\int_0^\delta \rho u dy \right] dx \right\}_w$

From the above we can evaluate the net x momentum flux through the control surface as

$$\begin{aligned} \int_{CS} u \rho \vec{V} \cdot d\vec{A} &= - \left\{ \int_0^\delta u \rho u dy \right\}_w + \left\{ \int_0^\delta u \rho u dy \right\}_w \\ &\quad + \left\{ \frac{\partial}{\partial x} \left[\int_0^\delta u \rho u dy \right] dx \right\}_w - U \left\{ \frac{\partial}{\partial x} \left[\int_0^\delta \rho u dy \right] dx \right\}_w \end{aligned}$$

Collecting terms, we find that

$$\int_{CS} u \rho \vec{V} \cdot d\vec{A} = \left\{ \frac{\partial}{\partial x} \left[\int_0^\delta u \rho u dy \right] dx - U \frac{\partial}{\partial x} \left[\int_0^\delta \rho u dy \right] dx \right\}_w$$

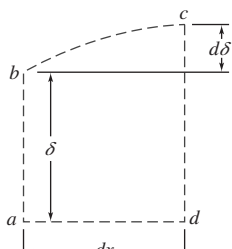


Fig. 9.5 Differential control volume.

Now that we have a suitable expression for the x momentum flux through the control surface, let us consider the surface forces acting on the control volume in the x direction. For convenience the differential control volume has been redrawn in Fig. 9.5. Note that surfaces ab , bc , and cd all experience normal forces (i.e., pressure) that generate force in the x direction. In addition, a shear force acts on surface ad . Since, by definition of the boundary layer, the velocity gradient goes to zero at the edge of the boundary layer, the shear force acting along surface bc is negligible.

Surface	Force
<i>ab</i>	If the pressure at x is p , then the force acting on surface <i>ab</i> is given by
	$F_{ab} = pw\delta$
	The boundary layer is very thin; its thickness has been greatly exaggerated in all the sketches we have made. Because it is thin, pressure variations in the y direction may be neglected, and we assume that within the boundary layer, $p = p(x)$ only.
<i>cd</i>	Expanding in a Taylor series, the pressure at $x + dx$ is given by
	$p_{x+dx} = p + \left. \frac{dp}{dx} \right _x dx$
	The force on surface <i>cd</i> is then given by
	$F_{cd} = - \left(p + \left. \frac{dp}{dx} \right _x dx \right) w(\delta + d\delta)$
<i>bc</i>	The average pressure acting over surface <i>bc</i> is
	$p + \frac{1}{2} \left. \frac{dp}{dx} \right _x dx$
	Then the x component of the normal force acting over <i>bc</i> is given by
	$F_{bc} = \left(p + \frac{1}{2} \left. \frac{dp}{dx} \right _x dx \right) w d\delta$
<i>ad</i>	The average shear force acting on <i>ad</i> is given by
	$F_{ad} = - \left(\tau_w + \frac{1}{2} d\tau_w \right) w dx$

Summing these x components, we obtain the total force acting in the x direction on the control volume,

$$F_{S_x} = \left\{ - \frac{dp}{dx} \delta dx - \frac{1}{2} \frac{dp}{dx} \int_0^\delta dy d\delta - \tau_w dx - \frac{1}{2} d\tau_w dx \right\} w$$

where we note that $dx d\delta \ll \delta dx$ and $d\tau_w \ll \tau_w$, and so neglect the second and fourth terms.

Substituting the expressions, for $\int_{CS} u \rho \vec{V} \cdot d\vec{A}$ and F_{S_x} into the x momentum equation (Eq. 4.18a), we obtain

$$\left\{ - \frac{dp}{dx} \delta dx - \tau_w dx \right\} w = \left\{ \frac{\partial}{\partial x} \left[\int_0^\delta u \rho u dy \right] dx - U \frac{\partial}{\partial x} \left[\int_0^\delta \rho u dy \right] dx \right\} w$$

Dividing this equation by $w dx$ gives

$$-\delta \frac{dp}{dx} - \tau_w = \frac{\partial}{\partial x} \int_0^\delta u \rho u dy - U \frac{\partial}{\partial x} \int_0^\delta \rho u dy \quad (9.16)$$

Equation 9.16 is a “momentum integral” equation that gives a relation between the x components of the forces acting in a boundary layer and the x momentum flux.

The pressure gradient, dp/dx , can be determined by applying the Bernoulli equation to the inviscid flow outside the boundary layer: $dp/dx = -\rho U dU/dx$. If we recognize that $\delta = \int_0^\delta dy$, then Eq. 9.16 can be written as

$$\tau_w = - \frac{\partial}{\partial x} \int_0^\delta u \rho u dy + U \frac{\partial}{\partial x} \int_0^\delta \rho u dy + \frac{dU}{dx} \int_0^\delta \rho U dy$$

Since

$$U \frac{\partial}{\partial x} \int_0^\delta \rho u \, dy = \frac{\partial}{\partial x} \int_0^\delta \rho u U \, dy - \frac{dU}{dx} \int_0^\delta \rho u \, dy$$

we have

$$\tau_w = \frac{\partial}{\partial x} \int_0^\delta \rho u (U - u) \, dy + \frac{dU}{dx} \int_0^\delta \rho (U - u) \, dy$$

and

$$\tau_w = \frac{\partial}{\partial x} U^2 \int_0^\delta \rho \frac{u}{U} \left(1 - \frac{u}{U}\right) \, dy + U \frac{dU}{dx} \int_0^\delta \rho \left(1 - \frac{u}{U}\right) \, dy$$

Using the definitions of displacement thickness, δ^* (Eq. 9.1), and momentum thickness, θ (Eq. 9.2), we obtain

$$\frac{\tau_w}{\rho} = \frac{d}{dx} (U^2 \theta) + \delta^* U \frac{dU}{dx} \quad (9.17)$$

Equation 9.17 is the *momentum integral equation* and is restricted to a steady incompressible two-dimensional flow. This equation will yield an ordinary differential equation for boundary-layer thickness δ as a function of x . To apply the equation we need to provide a suitable expression for the velocity profile u/U and relate the wall stress τ_w to other variables. Once the boundary-layer thickness is determined, expressions for the momentum thickness, displacement thickness, and wall shear stress can then be obtained. As we have not made any specific assumption relating the wall shear stress, τ_w , to the velocity, Eq. 9.17 is valid for either a laminar or turbulent boundary-layer flow. In order to use this equation to estimate the boundary-layer thickness as a function of x , we must first:

- 1 Obtain a first approximation to the freestream velocity distribution, $U(x)$. This is determined from inviscid flow theory (the velocity that would exist in the absence of a boundary layer) and depends on body shape.
- 2 Assume a reasonable velocity-profile shape inside the boundary layer.
- 3 Derive an expression for τ_w using the results obtained from item 2.

To illustrate the application of Eq. 9.17 to boundary-layer flows, we consider first the case of flow with zero pressure gradient over a flat plate. The results can then be compared to the exact Blasius results. The effects of pressure gradients in boundary-layer flow are then discussed in Section 9.5.

9.4 Use of the Momentum Integral Equation for Flow with Zero Pressure Gradient

For the special case of a flat plate (zero pressure gradient) the freestream pressure p and velocity U are both constant.

The momentum integral equation then reduces to

$$\tau_w = \rho U^2 \frac{d\theta}{dx} = \rho U^2 \frac{d}{dx} \int_0^\delta \frac{u}{U} \left(1 - \frac{u}{U}\right) \, dy \quad (9.18)$$

The velocity distribution, u/U , in the boundary layer is assumed to be similar for all values of x and normally is specified as a function of y/δ . Consequently, it is convenient to change the variable of integration from y to y/δ . Defining

$$\eta = \frac{y}{\delta}$$

we get

$$dy = \delta d\eta$$

and the momentum integral equation for zero pressure gradient is written

$$\tau_w = \rho U^2 \frac{d\theta}{dx} = \rho U^2 \frac{d\delta}{dx} \int_0^1 \frac{u}{U} \left(1 - \frac{u}{U}\right) d\eta \quad (9.19)$$

To solve this equation for the boundary-layer thickness as a function of x , we first assume a velocity distribution in the boundary layer, which is of the form

$$\frac{u}{U} = f\left(\frac{y}{\delta}\right)$$

The assumed velocity distribution should satisfy the following approximate physical boundary conditions:

$$\begin{aligned} \text{at } y=0, \quad u &= 0 \\ \text{at } y=\delta, \quad u &= U \\ \text{at } y=\delta, \quad \frac{\partial u}{\partial y} &= 0 \end{aligned}$$

Note that once we have assumed a velocity distribution, from the definition of the momentum thickness (Eq. 9.2), the numerical value of the integral in Eq. 9.19 is simply

$$\int_0^1 \frac{u}{U} \left(1 - \frac{u}{U}\right) d\eta = \frac{\theta}{\delta} = \text{constant} = \beta$$

and the momentum integral equation becomes

$$\tau_w = \rho U^2 \frac{d\delta}{dx} \beta$$

We then an expression for τ_w in terms of δ . This will then permit us to solve for $\delta(x)$, as illustrated below.

Laminar Flow

For laminar flow over a flat plate, a reasonable assumption for the velocity profile is a polynomial in y :

$$u = a + by + cy^2$$

The physical boundary conditions are:

$$\begin{aligned} \text{at } y=0, \quad u &= 0 \\ \text{at } y=\delta, \quad u &= U \\ \text{at } y=\delta, \quad \frac{\partial u}{\partial y} &= 0 \end{aligned}$$

Evaluating constants a , b , and c gives

$$\frac{u}{U} = 2\left(\frac{y}{\delta}\right) - \left(\frac{y}{\delta}\right)^2 = 2\eta - \eta^2 \quad (9.20)$$

The wall shear stress is given by

$$\tau_w = \mu \frac{\partial u}{\partial y} \Big|_{y=0}$$

Substituting the assumed velocity profile, Eq. 9.20, into this expression for τ_w gives

$$\tau_w = \mu \frac{\partial u}{\partial y} \Big|_{y=0} = \mu \frac{U \partial(u/U)}{\delta \partial(y/\delta)} \Big|_{y/\delta=0} = \frac{\mu U}{\delta} \frac{d(u/U)}{d\eta} \Big|_{\eta=0}$$

or

$$\tau_w = \frac{\mu U}{\delta} \frac{d}{d\eta} (2\eta - \eta^2) \Big|_{\eta=0} = \frac{\mu U}{\delta} (2 - 2\eta) \Big|_{\eta=0} = \frac{2\mu U}{\delta}$$

Note that this shows that the wall stress τ_w is a function of x , since the boundary-layer thickness $\delta = \delta(x)$.

Substituting for τ_w and u/U into the momentum integral equation 9.19, we obtain

$$\frac{2\mu U}{\delta} = \rho U^2 \frac{d\delta}{dx} \int_0^1 (2\eta - \eta^2)(1 - 2\eta + \eta^2) d\eta$$

or

$$\frac{2\mu U}{\delta \rho U^2} = \frac{d\delta}{dx} \int_0^1 (2\eta - 5\eta^2 + 4\eta^3 - \eta^4) d\eta$$

Integrating and substituting limits yields

$$\frac{2\mu}{\delta \rho U} = \frac{2}{15} \frac{d\delta}{dx} \quad \text{or} \quad \delta d\delta = \frac{15\mu}{\rho U} dx$$

which is a differential equation for δ . Integrating again gives

$$\frac{\delta^2}{2} = \frac{15\mu}{\rho U} x + c$$

We assume that $\delta = 0$ at $x = 0$ and then $c = 0$, and thus

$$\delta = \sqrt{\frac{30\mu x}{\rho U}}$$

Note that this shows that the laminar boundary-layer thickness δ grows as \sqrt{x} ; it has a parabolic shape. Traditionally this is expressed in dimensionless form:

$$\frac{\delta}{x} = \sqrt{\frac{30\mu}{\rho U x}} = \frac{5.48}{\sqrt{Re_x}} \quad (9.21)$$

Equation 9.21 shows that the ratio of laminar boundary-layer thickness to distance along a flat plate varies inversely with the square root of length Reynolds number. It has the same form as the exact solution and is too large by only about 10 percent. Table 9.2 summarizes corresponding results calculated using other approximate velocity profiles and lists results obtained from the exact solution. The only thing that changes in the analysis when we choose a different velocity profile is the value of β .

The wall shear stress, or “skin friction,” coefficient is defined as

$$C_f \equiv \frac{\tau_w}{\frac{1}{2} \rho U^2} \quad (9.22)$$

Substituting from the velocity profile and Eq. 9.21 gives

$$C_f = \frac{\tau_w}{\frac{1}{2} \rho U^2} = \frac{2\mu(U/\delta)}{\frac{1}{2} \rho U^2} = \frac{4\mu}{\rho U \delta} = 4 \frac{\mu}{\rho U x} \frac{x}{\delta} = 4 \frac{1}{Re_x} \frac{\sqrt{Re_x}}{5.48}$$

Table 9.2

Results of the Calculation of Laminar Boundary-Layer Flow over a Flat Plate at Zero Incidence Based on Approximate Velocity Profiles

Velocity Distribution $\frac{u}{U} = f\left(\frac{y}{\delta}\right) = f(\eta)$	$\beta \equiv \frac{\theta}{\delta}$	$\frac{\delta^*}{\delta}$	$H \equiv \frac{\delta^*}{\theta}$	Constant a in $\frac{\delta}{x} = \frac{a}{\sqrt{Re_x}}$	Constant b in $C_f = \frac{b}{\sqrt{Re_x}}$
$f(\eta) = \eta$	$\frac{1}{6}$	$\frac{1}{2}$	3.00	3.46	0.577
$f(\eta) = 2\eta - \eta^2$	$\frac{2}{15}$	$\frac{1}{3}$	2.50	5.48	0.730
$f(\eta) = \frac{3}{2}\eta - \frac{1}{2}\eta^3$	$\frac{39}{280}$	$\frac{3}{8}$	2.69	4.64	0.647
$f(\eta) = 2\eta - 2\eta^3 + \eta^4$	$\frac{37}{315}$	$\frac{3}{10}$	2.55	5.84	0.685
$f(\eta) = \sin\left(\frac{\pi}{2}\eta\right)$	$\frac{4-\pi}{2\pi}$	$\frac{\pi-2}{\pi}$	2.66	4.80	0.654
Exact	0.133	0.344	2.59	5.00	0.664

Finally,

$$C_f = \frac{0.730}{\sqrt{Re_x}} \quad (9.23)$$

Once the variation of τ_w is known, the viscous drag on the surface can be evaluated by integrating over the area of the flat plate, as illustrated in Example 9.3.

Equation 9.21 can be used to calculate the thickness of the laminar boundary layer at transition. At $Re_x = 5 \times 10^5$, with $U = 30$ m/s, for example, $x = 0.24$ m for air at standard conditions. Thus

$$\frac{\delta}{x} = \frac{5.48}{\sqrt{Re_x}} = \frac{5.48}{\sqrt{5 \times 10^5}} = 0.00775$$

and the boundary-layer thickness is

$$\delta = 0.00775x = 0.00775(0.24 \text{ m}) = 1.86 \text{ mm}$$

The boundary-layer thickness at transition is less than 1 percent of the development length, x . These calculations confirm that viscous effects are confined to a very thin layer near the surface of a body.

The results in Table 9.2 indicate that reasonable results may be obtained with a variety of approximate velocity profiles.

Example 9.3 LAMINAR BOUNDARY LAYER ON A FLAT PLATE: APPROXIMATE SOLUTION USING SINUSOIDAL VELOCITY PROFILE

Consider two-dimensional laminar boundary-layer flow along a flat plate. Assume the velocity profile in the boundary layer is sinusoidal,

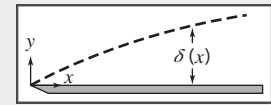
$$\frac{u}{U} = \sin\left(\frac{\pi y}{2\delta}\right)$$

Find expressions for:

- (a) The rate of growth of δ as a function of x .
- (b) The displacement thickness, δ^* , as a function of x .
- (c) The total friction force on a plate of length L and width b .

Given: Two-dimensional, laminar boundary-layer flow along a flat plate. The boundary-layer velocity profile is

$$\frac{u}{U} = \sin\left(\frac{\pi}{2}\frac{y}{\delta}\right) \quad \text{for } 0 \leq y \leq \delta$$



and

$$\frac{u}{U} = 1 \quad \text{for } y > \delta$$

Find: (a) $\delta(x)$.

(b) δ^* .

(c) Total friction force on a plate of length L and width b .

Solution: For flat plate flow, $U = \text{constant}$, $dp/dx = 0$, and

$$\tau_w = \rho U^2 \frac{d\theta}{dx} = \rho U^2 \frac{d\delta}{dx} \int_0^1 \frac{u}{U} \left(1 - \frac{u}{U}\right) d\eta \quad (9.19)$$

Assumptions:

1 Steady flow.

2 Incompressible flow.

Substituting $\frac{u}{U} = \sin\frac{\pi}{2}\eta$ into Eq. 9.19, we obtain

$$\begin{aligned} \tau_w &= \rho U^2 \frac{d\delta}{dx} \int_0^1 \sin\frac{\pi}{2}\eta \left(1 - \sin\frac{\pi}{2}\eta\right) d\eta = \rho U^2 \frac{d\delta}{dx} \int_0^1 \left(\sin\frac{\pi}{2}\eta - \sin^2\frac{\pi}{2}\eta\right) d\eta \\ &= \rho U^2 \frac{d\delta}{dx} \frac{2}{\pi} \left[-\cos\frac{\pi}{2}\eta - \frac{1}{2}\frac{\pi}{2}\eta + \frac{1}{4}\sin\pi\eta \right]_0^1 = \rho U^2 \frac{d\delta}{dx} \frac{2}{\pi} \left[0 + 1 - \frac{\pi}{4} + 0 + 0 - 0 \right] \\ \tau_w &= 0.137 \rho U^2 \frac{d\delta}{dx} = \beta \rho U^2 \frac{d\delta}{dx}; \quad \beta = 0.137 \end{aligned}$$

Now

$$\tau_w = \mu \frac{\partial u}{\partial y} \Big|_{y=0} = \mu \frac{U}{\delta} \frac{\partial(u/U)}{\partial(y/\delta)} \Big|_{y=0} = \mu \frac{U}{\delta} \frac{\pi}{2} \cos\frac{\pi}{2}\eta \Big|_{\eta=0} = \frac{\pi \mu U}{2\delta}$$

Therefore,

$$\tau_w = \frac{\pi \mu U}{2\delta} = 0.137 \rho U^2 \frac{d\delta}{dx}$$

Separating variables gives

$$\delta d\delta = 11.5 \frac{\mu}{\rho U} dx$$

Integrating, we obtain

$$\frac{\delta^2}{2} = 11.5 \frac{\mu}{\rho U} x + c$$

But $c = 0$, since $\delta = 0$ at $x = 0$, so

$$\delta = \sqrt{23.0 \frac{x\mu}{\rho U}}$$

or

$$\frac{\delta}{x} = 4.80 \sqrt{\frac{\mu}{\rho U x}} = \frac{4.80}{\sqrt{Re_x}} \xrightarrow{\delta(x)}$$

The displacement thickness, δ^* , is given by

$$\begin{aligned}\delta^* &= \delta \int_0^1 \left(1 - \frac{u}{U}\right) d\eta \\ &= \delta \int_0^1 \left(1 - \sin \frac{\pi}{2} \eta\right) d\eta = \delta \left[\eta + \frac{2}{\pi} \cos \frac{\pi}{2} \eta \right]_0^1 \\ \delta^* &= \delta \left[1 - 0 + 0 - \frac{2}{\pi} \right] = \delta \left[1 - \frac{2}{\pi} \right]\end{aligned}$$

Since, from part (a),

$$\frac{\delta}{x} = \frac{4.80}{\sqrt{Re_x}}$$

then

$$\frac{\delta^*}{x} = \left(1 - \frac{2}{\pi}\right) \frac{4.80}{\sqrt{Re_x}} = \frac{1.74}{\sqrt{Re_x}} \xrightarrow{\delta^*(x)}$$

The total friction force on one side of the plate is given by

$$F = \int_{A_p} \tau_w dA$$

Since $dA = b dx$ and $0 \leq x \leq L$, then

$$\begin{aligned}F &= \int_0^L \tau_w b dx = \int_0^L \rho U^2 \frac{d\theta}{dx} b dx = \rho U^2 b \int_0^{\theta_L} d\theta = \rho U^2 b \theta_L \\ \theta_L &= \int_0^{\delta_L} \frac{u}{U} \left(1 - \frac{u}{U}\right) dy = \delta_L \int_0^1 \frac{u}{U} \left(1 - \frac{u}{U}\right) d\eta = \beta \delta_L\end{aligned}$$

From part (a), $\beta = 0.137$ and $\delta_L = \frac{4.80L}{\sqrt{Re_L}}$, so

$$F = \frac{0.658 \rho U^2 b L}{\sqrt{Re_L}} \xrightarrow{F}$$

This problem illustrates application of the momentum integral equation to the laminar boundary layer on a flat plate.

Turbulent Flow

For the flat plate, we still have that $U = \text{constant}$. As for the laminar boundary layer, we need to find an approximation for the turbulent velocity profile and an expression for τ_w in order to solve Eq. 9.19. Details of the turbulent velocity profile for boundary layers at zero pressure gradient are very similar to those for turbulent flow in pipes and channels. Data for turbulent boundary layers plot on the universal velocity profile using coordinates of \bar{u}/u_* versus $y u_*/\nu$, as shown in Fig. 8.9. However, this profile is rather complex mathematically for easy use with the momentum integral equation. The momentum integral equation is approximate; hence, an acceptable velocity profile for turbulent boundary layers on smooth flat plates is the empirical power-law profile. An exponent of $\frac{1}{7}$ is typically used to model the turbulent velocity profile. Thus

$$\frac{u}{U} = \left(\frac{y}{\delta}\right)^{1/7} = \eta^{1/7} \quad (9.24)$$

However, this profile does not hold in the immediate vicinity of the wall, since at the wall it predicts $du/dy = \infty$. Consequently, we cannot use this profile in the definition of τ_w to obtain an expression for τ_w in terms of δ as we did for laminar boundary-layer flow. For turbulent boundary-layer flow we adapt the expression developed for pipe flow,

$$\tau_w = 0.0332\rho\bar{V}^2 \left[\frac{\nu}{R\bar{V}} \right]^{0.25} \quad (8.39)$$

For a $\frac{1}{7}$ -power profile in a pipe, Eq. 8.24 gives $\bar{V}/U = 0.817$. Substituting $\bar{V} = 0.817U$ and $R = \delta$ into Eq. 8.39, we obtain

$$\tau_w = 0.0233\rho U^2 \left(\frac{\nu}{U\delta} \right)^{1/4} \quad (9.25)$$

Substituting for τ_w and u/U into Eq. 9.19 and integrating, we obtain

$$0.0233 \left(\frac{\nu}{U\delta} \right)^{1/4} = \frac{d\delta}{dx} \int_0^1 \eta^{1/7} (1 - \eta^{1/7}) d\eta = \frac{7}{72} \frac{d\delta}{dx}$$

Thus we obtain a differential equation for δ :

$$\delta^{1/4} d\delta = 0.240 \left(\frac{\nu}{U} \right)^{1/4} dx$$

Integrating gives

$$\frac{4}{5} \delta^{5/4} = 0.240 \left(\frac{\nu}{U} \right)^{1/4} x + c$$

If we assume that $\delta \simeq 0$ at $x = 0$, which is equivalent to assuming turbulent flow from the leading edge, then $c = 0$ and

$$\delta = 0.382 \left(\frac{\nu}{U} \right)^{1/5} x^{4/5}$$

Note that this shows that the turbulent boundary-layer thickness δ grows as $x^{4/5}$. Expressing the growth in dimensionless form:

$$\frac{\delta}{x} = 0.382 \left(\frac{\nu}{Ux} \right)^{1/5} = \frac{0.382}{Re_x^{1/5}} \quad (9.26)$$

Using Eq. 9.25, we obtain the skin friction coefficient in terms of δ :

$$C_f = \frac{\tau_w}{\frac{1}{2}\rho U^2} = 0.0466 \left(\frac{\nu}{U\delta} \right)^{1/4}$$

Substituting for δ , we obtain

$$C_f = \frac{\tau_w}{\frac{1}{2}\rho U^2} = \frac{0.0594}{Re_x^{1/5}} \quad (9.27)$$

Experiments show that Eq. 9.27 predicts turbulent skin friction on a flat plate very well for $5 \times 10^5 < Re_x < 10^7$. This agreement is remarkable in view of the approximate nature of our analysis.

Application of the momentum integral equation for turbulent boundary-layer flow is illustrated in Example 9.4.

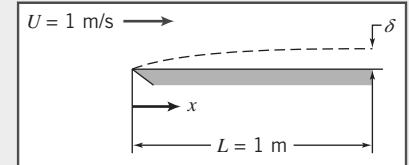
Example 9.4 TURBULENT BOUNDARY LAYER ON A FLAT PLATE: APPROXIMATE SOLUTION USING $\frac{1}{7}$ -POWER VELOCITY PROFILE

Water flows at $U = 1 \text{ m/s}$ past a flat plate with $L = 1 \text{ m}$ in the flow direction. The boundary layer is tripped so it becomes turbulent at the leading edge. Evaluate the disturbance thickness, δ , displacement thickness, δ^* , and wall shear stress, τ_w , at $x = L$. Compare with laminar flow maintained to the same position. Assume a $\frac{1}{7}$ -power turbulent velocity profile.

Given: Flat plate boundary-layer flow; turbulent flow from the leading edge. Assume $\frac{1}{7}$ -power velocity profile.

Find:

- Disturbance thickness, δ_L .
- Displacement thickness, δ_L^* .
- Wall shear stress, $\tau_w(L)$.
- Comparison with results for laminar flow from the leading edge.



Solution: Apply results from the momentum integral equation.

Governing equations:

$$\frac{\delta}{x} = \frac{0.382}{Re_x^{1/5}} \quad (9.26)$$

$$\delta^* = \int_0^\infty \left(1 - \frac{u}{U}\right) dy \quad (9.1)$$

$$C_f = \frac{\tau_w}{\frac{1}{2} \rho U^2} = \frac{0.0594}{Re_x^{1/5}} \quad (9.27)$$

At $x = L$, with $\nu = 1.00 \times 10^{-6} \text{ m}^2/\text{s}$ for water ($T = 20^\circ\text{C}$),

$$Re_L = \frac{UL}{\nu} = 1 \frac{\text{m}}{\text{s}} \times 1 \text{ m} \times \frac{\text{s}}{10^{-6} \text{ m}^2} = 10^6$$

From Eq. 9.26,

$$\delta_L = \frac{0.382}{Re_L^{1/5}} L = \frac{0.382}{(10^6)^{1/5}} \times 1 \text{ m} = 0.0241 \text{ m} \quad \text{or} \quad \delta_L = 24.1 \text{ mm} \quad \underline{\delta_L}$$

Using Eq. 9.1, with $u/U = (y/\delta)^{1/7} = \eta^{1/7}$, we obtain

$$\delta_L^* = \int_0^\infty \left(1 - \frac{u}{U}\right) dy = \delta_L \int_0^1 \left(\frac{u}{U}\right) d\left(\frac{y}{\delta}\right) = \delta_L \int_0^1 (1 - \eta^{1/7}) d\eta = \delta_L \left[\eta - \frac{7}{8} \eta^{8/7} \right]_0^1$$

$$\delta_L^* = \frac{\delta_L}{8} = \frac{24.1 \text{ mm}}{8} = 3.01 \text{ mm} \quad \underline{\delta_L^*}$$

From Eq. 9.27,

$$C_f = \frac{0.0594}{(10^6)^{1/5}} = 0.00375$$

$$\tau_w = C_f \frac{1}{2} \rho U^2 = 0.00375 \times \frac{1}{2} \times 999 \frac{\text{kg}}{\text{m}^3} \times (1)^2 \frac{\text{m}^2}{\text{s}^2} \times \frac{\text{N} \cdot \text{s}^2}{\text{kg} \cdot \text{m}}$$

$$\tau_w = 1.87 \text{ N/m}^2 \quad \underline{\tau_w(L)}$$

For laminar flow, use Blasius solution values. From Eq. 9.13

$$\delta_L = \frac{5.0}{\sqrt{Re_L}} L = \frac{5.0}{(10^6)^{1/2}} \times 1 \text{ m} = 0.005 \text{ m} \quad \text{or} \quad 5.00 \text{ mm}$$

From Example 9.1, $\delta^*/\delta = 0.344$, so

$$\delta^* = 0.344 \quad \delta = 0.344 \times 5.0 \text{ mm} = 1.72 \text{ mm}$$

Use of the momentum integral equation is an approximate technique to predict boundary-layer development; the equation predicts trends correctly. Parameters of the laminar boundary layer vary as $Re_x^{-1/2}$; those for the turbulent boundary layer vary as $Re_x^{-1/5}$. Thus the turbulent boundary layer develops more rapidly than the laminar boundary layer.

Laminar and turbulent boundary layers were compared in Example 9.3. Wall shear stress is much higher in the turbulent boundary layer than in the laminar layer. This is the primary reason for the more rapid development of turbulent boundary layers.

The agreement we have obtained with experimental results shows that use of the momentum integral equation is an effective approximate method that gives us considerable insight into the general behavior of boundary layers.

9.5 Pressure Gradients in Boundary Layer Flow

The boundary layer with a uniform flow along an infinite flat plate is the easiest one to study because the pressure gradient is zero—the fluid particles in the boundary layer are slowed only by shear stresses, leading to boundary-layer growth. We now consider the effects caused by a pressure gradient, which will be present for all bodies except, as we have seen, a flat plate.

A *favorable pressure gradient* is one in which the pressure decreases in the flow direction (i.e., $\partial p/\partial x < 0$); it is called favorable because it tends to overcome the slowing of fluid particles caused by friction in the boundary layer. This pressure gradient arises when the freestream velocity U is increasing with x , for example, in the converging flow field in a nozzle. On the other hand, an *adverse pressure gradient* is one in which pressure increases in the flow direction (i.e., $\partial p/\partial x > 0$); it is called adverse because it will cause fluid particles in the boundary-layer to slow down at a greater rate than that due to boundary-layer friction alone. If the adverse pressure gradient is severe enough, the fluid particles in the boundary layer will actually be brought to rest. When this occurs, the particles will be forced away from the body surface (a phenomenon called *flow separation*) as they make room for following particles, ultimately leading to a *wake* in which flow is turbulent. Examples of this are when the walls of a diffuser diverge too rapidly and when an airfoil has too large an angle of attack.

This description of the adverse pressure gradient and friction in the boundary layer together forcing flow separation certainly makes intuitive sense. The fluid velocity is zero at the surface. Separation would occur when the fluid velocity is zero in the fluid, but this can occur only when $\partial u/\partial y|_{y=0} = 0$. Further, the wall shear stress for laminar and turbulent boundary layers is always positive. We conclude that for uniform flow over a flat plate the flow *never* separates, and we never develop a wake region, whether the boundary layer is laminar or turbulent, regardless of plate length.

Clearly, for flows in which $\partial p/\partial x < 0$ (whenever the freestream velocity is increasing), we can be sure that there will be no flow separation. For flows in which $\partial p/\partial x > 0$ (i.e., adverse pressure gradients) we *could* have flow separation. We should not conclude that an adverse pressure gradient *always* leads to flow separation and a wake but have only concluded that it is a necessary condition for flow separation to occur.

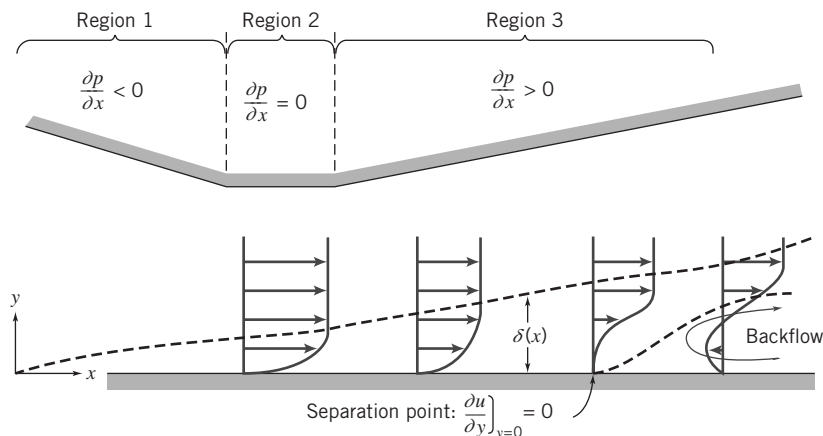


Fig. 9.6 Boundary-layer flow with pressure gradient (boundary-layer thickness exaggerated for clarity).

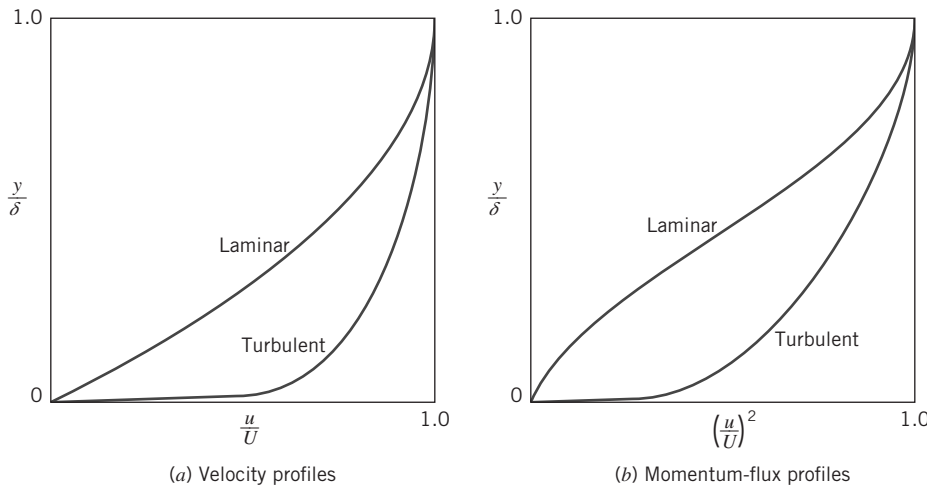


Fig. 9.7 Nondimensional profiles for flat plate boundary-layer flow.

To illustrate these results consider the variable cross-sectional flow shown in Fig. 9.6. Outside the boundary layer the velocity field is one in which the flow accelerates (Region 1), has a constant velocity region (Region 2), and then a deceleration region (Region 3). Corresponding to these, the pressure gradient is favorable, zero, and adverse, respectively, as shown. From our discussions above, we conclude that separation cannot occur in Region 1 or 2, but can occur in Region 3. Could we avoid flow separation in a device like this? Intuitively, we can see that if we make the divergent section less severe, we may be able to eliminate flow separation. In other words, we may eliminate flow separation if we make the adverse pressure gradient $\partial p / \partial x$ small enough. We conclude that flow separation is possible, but not guaranteed, when we have an adverse pressure gradient.

The nondimensional velocity profiles for laminar and turbulent boundary-layer flow over a flat plate are shown in Fig. 9.7a. The turbulent profile is much fuller (more blunt) than the laminar profile. At the same freestream speed, the momentum flux within the turbulent boundary layer is greater than within the laminar layer (Fig. 9.7b). Separation occurs when the momentum of fluid layers near the surface is reduced to zero by the combined action of pressure and viscous forces. As shown in Fig. 9.7b, the momentum of the fluid near the surface is significantly greater for the turbulent profile. Consequently, the turbulent layer is better able to resist separation in an adverse pressure gradient. We shall discuss some consequences of this behavior in Section 9.6.

Adverse pressure gradients cause significant changes in velocity profiles for both laminar and turbulent boundary-layer flows. Approximate solutions for nonzero pressure gradient flow may be obtained from the momentum integral equation

$$\frac{\tau_w}{\rho} = \frac{d}{dx}(U^2 \theta) + \delta^* U \frac{dU}{dx} \quad (9.17)$$

Expanding the first term, we can write

$$\frac{\tau_w}{\rho} = U^2 \frac{d\theta}{dx} + (\delta^* + 2\theta) U \frac{dU}{dx}$$

or

$$\frac{\tau_w}{\rho U^2} = \frac{C_f}{2} = \frac{d\theta}{dx} + (H + 2) \frac{\theta}{U} \frac{dU}{dx} \quad (9.28)$$

where $H = \delta^*/\theta$ is a velocity-profile “shape factor.” The shape factor increases in an adverse pressure gradient. For turbulent boundary-layer flow, H increases from 1.3 for a zero pressure gradient to approximately 2.5 at separation. For laminar flow with zero pressure gradient, $H = 2.6$; at separation $H = 3.5$.

The freestream velocity distribution, $U(x)$, must be known before Eq. 9.28 can be applied. Since $dp/dx = -\rho U dU/dx$, specifying $U(x)$ is equivalent to specifying the pressure gradient. We can obtain a first approximation for $U(x)$ from ideal flow theory for an inviscid flow under the same conditions.

The analytical approach using the momentum equation is limited to fairly simple geometries, and numerical techniques may need to be used to solve the resulting ordinary differential equations. Currently, numerical techniques of CFD are often used to determine the free stream velocity distribution along a surface ([13] and [14]).

Part B FLUID FLOW ABOUT IMMERSED BODIES

Whenever there is relative motion between a solid body and the viscous fluid surrounding it, the body will experience a net force \vec{F} . The magnitude of this force depends on many factors—certainly the relative velocity \vec{V} , but also the body shape and size, and the fluid properties (ρ , μ , etc.). As the fluid flows around the body, it will generate surface stresses on each element of the surface, and it is these that lead to the net force. The surface stresses are composed of tangential stresses due to viscous action and normal stresses due to the local pressure. We might be tempted to think that we can analytically derive the net force by integrating these over the body surface. The first step might be: Given the shape of the body (and assuming that the Reynolds number is high enough that we can use inviscid flow theory), compute the pressure distribution. Then integrate the pressure over the body surface to obtain the contribution of pressure forces to the net force \vec{F} . As we discussed in Chapter 6, this step was developed very early in the history of fluid mechanics; it led to the result that no bodies experience drag. The second step might be: Use this pressure distribution to find the surface viscous stress τ_w (at least in principle, using, for example, Eq. 9.17). Then integrate the viscous stress over the body surface to obtain its contribution to the net force \vec{F} . This procedure sounds conceptually straightforward, but in practice is quite difficult except for the simplest body shapes. In addition, even if possible, it leads to erroneous results in most cases because it takes no account of a very important consequence of the existence of boundary layers—flow separation. This causes a wake, which not only creates a low-pressure region usually leading to large drag on the body, but also radically changes the overall flow field and hence the inviscid flow region and pressure distribution on the body.

For these reasons we must usually resort to experimental or CFD methods to determine the net force for most body shapes. Traditionally the net force \vec{F} is resolved into the drag force, F_D , defined as the component of the force parallel to the direction of motion, and the lift force, F_L defined as the component of the force perpendicular to the direction of motion. In Sections 9.6 and 9.7 we will examine these forces for a number of different body shapes.

9.6 Drag

Drag is the component of force on a body acting parallel to the direction of relative motion. In Chapter 7, we considered the problem of determining the drag force, F_D , on a smooth sphere of diameter d , moving through a viscous, incompressible fluid with speed V . The fluid density and viscosity were ρ and μ , respectively. The drag force, F_D , was written in the functional form

$$F_D = f_1(d, V, \mu, \rho)$$

Application of the Buckingham Pi theorem resulted in two dimensionless Π parameters that were written in functional form as

$$\frac{F_D}{\rho V^2 d^2} = f_2\left(\frac{\rho V d}{\mu}\right)$$

Note that d^2 is proportional to the cross-sectional area ($A = \pi d^2/4$) and therefore we could write

$$\frac{F_D}{\rho V^2 A} = f_3\left(\frac{\rho V d}{\mu}\right) = f_3(Re) \quad (9.29)$$

Although Eq. 9.29 was obtained for a sphere, the form of the equation is valid for incompressible flow over *any* body; the characteristic length used in the Reynolds number depends on the body shape.

The *drag coefficient*, C_D , is defined as

$$C_D \equiv \frac{F_D}{\frac{1}{2}\rho V^2 A} \quad (9.30)$$

The number $\frac{1}{2}$ has been inserted to form the familiar dynamic pressure. Then Eq. 9.29 can be written as

$$C_D = f(Re) \quad (9.31)$$

We have not considered compressibility or free-surface effects in this discussion of the drag force. Had these been included, we would have obtained the functional form

$$C_D = f(Re, Fr, M)$$

We now consider the drag force and drag coefficient for a number of bodies, starting with the simplest: a flat plate parallel to the flow (which has only friction drag); a flat plate normal to the flow (which has only pressure drag); and cylinders and spheres (the simplest 2D and 3D bodies, which have both friction and pressure drag). We will also briefly discuss streamlining.

Pure Friction Drag: Flow over a Flat Plate Parallel to the Flow

This flow situation was considered in detail in Section 9.4. Since the pressure gradient is zero and pressure forces are perpendicular to the plate and do not contribute to drag, the total drag is equal to the friction drag. Thus

$$F_D = \int_{\text{plate surface}} \tau_w dA$$

and

$$C_D = \frac{F_D}{\frac{1}{2}\rho V^2 A} = \frac{\int_{\text{PS}} \tau_w dA}{\frac{1}{2}\rho V^2 A} \quad (9.32)$$

where A is the total surface area in contact with the fluid (i.e., the *wetted area*). The drag coefficient for a flat plate parallel to the flow depends on the shear stress distribution along the plate.

For laminar flow over a flat plate, the shear stress coefficient was given by

$$C_f = \frac{\tau_w}{\frac{1}{2}\rho U^2} = \frac{0.664}{\sqrt{Re_x}} \quad (9.15)$$

The drag coefficient for flow with freestream velocity V , over a flat plate of length L and width b , is obtained by substituting for τ_w from Eq. 9.15 into Eq. 9.32. Thus

$$\begin{aligned} C_D &= \frac{1}{A} \int_A 0.664 Re_x^{-0.5} dA = \frac{1}{bL} \int_0^L 0.664 \left(\frac{V}{\nu}\right)^{-0.5} x^{-0.5} b dx \\ &= \frac{0.664}{L} \left(\frac{\nu}{V}\right)^{0.5} \left[\frac{x^{0.5}}{0.5} \right]_0^L = 1.33 \left(\frac{\nu}{VL}\right)^{0.5} \end{aligned}$$

$$C_D = \frac{1.33}{\sqrt{Re_L}} \quad (9.33)$$

Assuming the boundary layer is turbulent from the leading edge, the shear stress coefficient, based on the approximate analysis of Section 9.4, is given by

$$C_f = \frac{\tau_w}{\frac{1}{2}\rho U^2} = \frac{0.0594}{Re_x^{1/5}} \quad (9.27)$$

Substituting for τ_w from Eq. 9.27 into Eq. 9.32, we obtain

$$\begin{aligned} C_D &= \frac{1}{A} \int_A 0.0594 Re_x^{-0.2} dA = \frac{1}{bL} \int_0^L 0.0594 \left(\frac{V}{\nu}\right)^{-0.2} x^{-0.2} b dx \\ &= \frac{0.0594}{L} \left(\frac{\nu}{V}\right)^{0.2} \left[\frac{x^{0.8}}{0.8}\right]_0^L = 0.0742 \left(\frac{\nu}{VL}\right)^{0.2} \end{aligned}$$

$$C_D = \frac{0.0742}{Re_L^{1/5}} \quad (9.34)$$

Equation 9.34 is valid for $5 \times 10^5 < Re_L < 10^7$.

For $Re_L < 10^9$ the empirical equation given by Schlichting [3]

$$C_D = \frac{0.455}{(\log Re_L)^{2.58}} \quad (9.35)$$

fits experimental data very well.

For a boundary layer that is initially laminar and undergoes transition at some location on the plate, the turbulent drag coefficient must be adjusted to account for the laminar flow over the initial length. The adjustment is made by subtracting the quantity B/Re_L from the C_D determined for completely turbulent flow. The value of B depends on the Reynolds number at transition; B is given by

$$B = Re_{tr}(C_{D_{turbulent}} - C_{D_{laminar}}) \quad (9.36)$$

For a transition Reynolds number of 5×10^5 , the drag coefficient may be calculated by making the adjustment to Eq. 9.34, in which case

$$C_D = \frac{0.0742}{Re_L^{1/5}} - \frac{1740}{Re_L} \quad (5 \times 10^5 < Re_L < 10^7) \quad (9.37a)$$

or to Eq. 9.35, in which case

$$C_D = \frac{0.455}{(\log Re_L)^{2.58}} - \frac{1610}{Re_L} \quad (5 \times 10^5 < Re_L < 10^9) \quad (9.37b)$$

The variation in drag coefficient for a flat plate parallel to the flow is shown in Fig. 9.8.

In the plot of Fig. 9.8, transition was assumed to occur at $Re_x = 5 \times 10^5$ for flows in which the boundary layer was initially laminar. The actual Reynolds number at which transition occurs depends on a combination of factors, such as surface roughness and freestream disturbances. Transition tends to occur at lower Reynolds number as surface roughness or freestream turbulence is increased. For transition at other than $Re_x = 5 \times 10^5$, the constant in the second term of Eqs. 9.37 is modified using Eq. 9.36. Figure 9.8 shows that the drag coefficient is less for a given length of plate when laminar flow is maintained over the longest possible distance. At large $Re_L (> 10^7)$ the contribution of the laminar drag is negligible. Example 9.5 illustrates how the skin friction force due to a turbulent boundary layer is calculated.

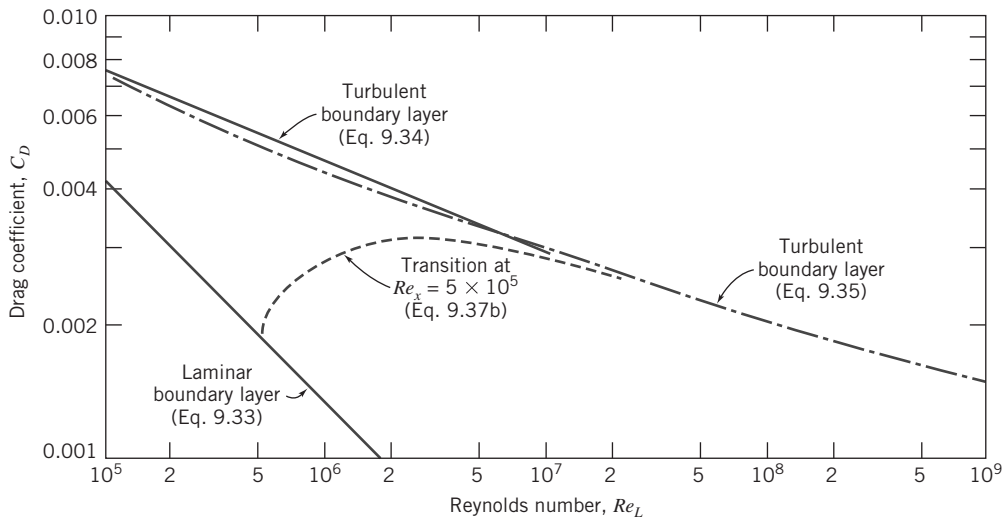


Fig. 9.8 Variation of drag coefficient with Reynolds number for a smooth flat plate parallel to the flow.

Example 9.5 SKIN FRICTION DRAG ON A SUPERTANKER

A supertanker is 360 m long and has a beam width of 70 m and a draft of 25 m. Estimate the force and power required to overcome skin friction drag at a cruising speed of 13 kt in seawater at 10°C.

Given: Supertanker cruising at $U = 13$ kt.

Find: (a) Force.

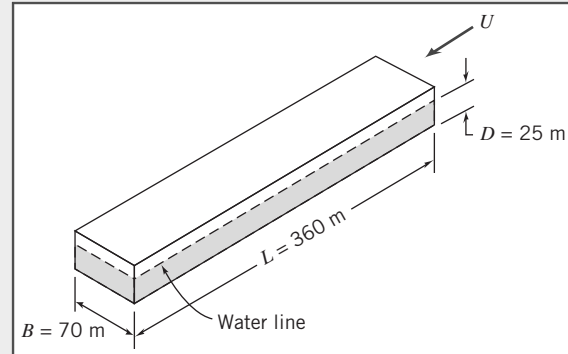
(b) Power required to overcome skin friction drag.

Solution: Model the tanker hull as a flat plate, of length L and width $b = B + 2D$, in contact with water. Estimate skin friction drag from the drag coefficient.

Governing equations:

$$C_D = \frac{F_D}{\frac{1}{2}\rho U^2 A} \quad (9.32)$$

$$C_D = \frac{0.455}{(\log Re_L)^{2.58}} - \frac{1610}{Re_L} \quad (9.37b)$$



The ship speed is 13 kt (nautical miles per hour), so

$$U = 13 \frac{\text{nm}}{\text{hr}} \times 6076 \frac{\text{ft}}{\text{nm}} \times 0.305 \frac{\text{m}}{\text{ft}} \times \frac{\text{hr}}{3600 \text{s}} = 6.69 \text{ m/s}$$

From Appendix A, at 10°C, $\nu = 1.37 \times 10^{-6} \text{ m}^2/\text{s}$ for seawater. Then

$$Re_L = \frac{UL}{\nu} = 6.69 \frac{\text{m}}{\text{s}} \times 360 \text{ m} \times \frac{\text{s}}{1.37 \times 10^{-6} \text{ m}^2} = 1.76 \times 10^9$$

Assuming Eq. 9.37b is valid,

$$C_D = \frac{0.455}{(\log 1.76 \times 10^9)^{2.58}} - \frac{1610}{1.76 \times 10^9} = 0.00147$$

and from Eq. 9.32,

$$F_D = C_D A \frac{1}{2} \rho U^2$$

$$= 0.00147 \times (360 \text{ m})(70 + 50) \text{ m} \times \frac{1}{2} \times 1020 \frac{\text{kg}}{\text{m}^3} \times (6.69)^2 \frac{\text{m}^2}{\text{s}^2} \times \frac{\text{N} \cdot \text{s}^2}{\text{kg} \cdot \text{m}}$$

$$F_D = 1.45 \text{ MN} \leftarrow$$

The corresponding power is

$$\mathcal{P} = F_D U = 1.45 \times 10^6 \text{ N} \times 6.69 \frac{\text{m}}{\text{s}} \times \frac{\text{W} \cdot \text{s}}{\text{N} \cdot \text{m}}$$

$$\mathcal{P} = 9.70 \text{ MW} \leftarrow$$

This problem illustrates application of drag coefficient equations for a flat plate parallel to the flow.

- The power required (about 13,000 hp) is very large because although the friction stress is small, it acts over a substantial area.
- The boundary layer is turbulent for almost the entire length of the ship (transition occurs at $x \approx 0.1 \text{ m}$).

Pure Pressure Drag: Flow over a Flat Plate Normal to the Flow

In flow over a flat plate normal to the flow (Fig. 9.9), the wall shear stress is perpendicular to the flow direction and therefore does not contribute to the drag force. The drag is given by

$$F_D = \int_{\text{surface}} p dA$$

For this geometry the flow separates from the edges of the plate; there is back-flow in the low energy wake of the plate. Although the pressure over the rear surface of the plate is essentially constant, its magnitude cannot be determined analytically. Consequently, we must resort to experiments to determine the drag force.

The drag coefficient for flow over an immersed object usually is based on the *frontal area* (or projected area) of the object. The drag coefficient for a finite plate normal to the flow depends on the ratio of plate width to height and on the Reynolds number. For Re (based on height) greater than about 1000, the drag coefficient is essentially independent of Reynolds number. The variation of C_D with the ratio of plate width to height (b/h) is shown in Fig. 9.10. The ratio b/h is defined as the *aspect ratio* of the plate. For $b/h = 1.0$, the drag coefficient is a minimum at $C_D = 1.18$ this is just slightly higher than for a circular disk ($C_D = 1.17$) at large Reynolds number.

The drag coefficient for all objects with sharp edges is essentially independent of Reynolds number (for $Re \gtrsim 1000$) because the separation points and therefore the size of the wake are fixed by the geometry of the object. Drag coefficients for selected objects are given in Table 9.3.

Friction and Pressure Drag: Flow over a Sphere and Cylinder

We have looked at two special flow cases in which either friction or pressure drag was the sole form of drag present. In the former case, the drag coefficient was a strong function of Reynolds number, while in the latter case, C_D was essentially independent of Reynolds number for $Re \gtrsim 1000$.

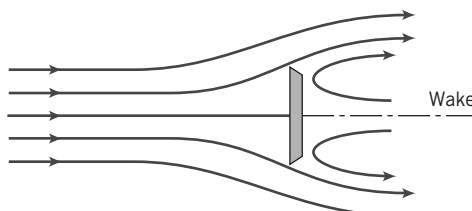


Fig. 9.9 Flow over a flat plate normal to the flow.

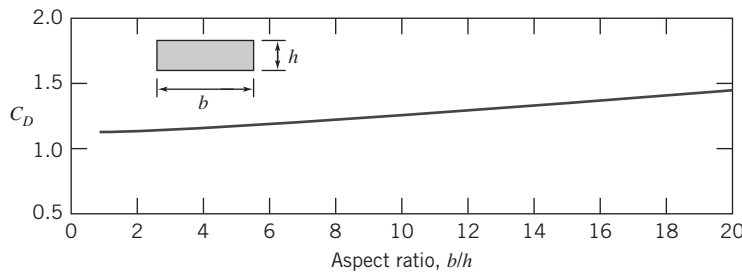
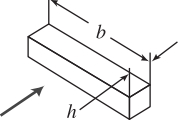
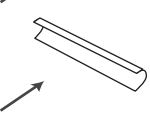
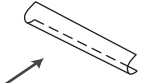


Fig. 9.10 Variation of drag coefficient with aspect ratio for a flat plate of finite width normal to the flow with $Re_h > 1000$ [5].

Table 9.3

Drag Coefficient Data for Selected Objects ($Re \gtrsim 10^3$)^a

Object	Diagram	$C_D(Re \gtrsim 10^3)$
Square prism		$b/h = \infty$ $b/h = 1$ 2.05 1.05
Disk		1.17
Ring		1.20 ^b
Hemisphere (open end facing flow)		1.42
Hemisphere (open end facing downstream)		0.38
C-section (open side facing flow)		2.30
C-section (open side facing downstream)		1.20

^a Data from Hoerner [5].

^b Based on ring area.

In the case of flow over a sphere, both friction drag and pressure drag contribute to total drag. The drag coefficient for flow over a smooth sphere is shown in Fig. 9.11 as a function of Reynolds number.

At very low Reynolds number, $Re \leq 1$, there is no flow separation from a sphere; the wake is laminar and the drag is predominantly friction drag. For very low Reynolds number flows where inertia forces may be neglected, the drag force on a sphere of diameter d , moving at speed V , through a fluid of viscosity μ , is given by

$$F_D = 3\pi\mu Vd$$

The drag coefficient, C_D , defined by Eq. 9.30, is then

$$C_D = \frac{24}{Re}$$

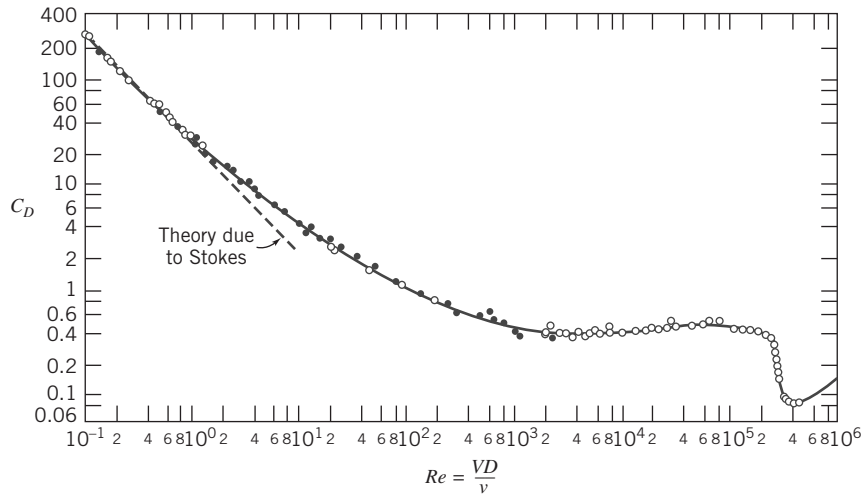


Fig. 9.11 Drag coefficient of a smooth sphere as a function of Reynolds number. (Data from References [3], [16], and [17].)

As shown in Fig. 9.11, this expression agrees with experimental values at low Reynolds number but begins to deviate significantly from the experimental data for $Re > 1.0$.

As the Reynolds number is further increased, the drag coefficient drops continuously up to a Reynolds number of about 1000. A turbulent wake develops and grows at the rear of the sphere as the separation point moves from the rear of the sphere toward the front; this wake is at a relatively low pressure, leading to a large pressure drag. By the time $Re \approx 1000$, about 95 percent of total drag is due to pressure. For $10^3 < Re < 3 \times 10^5$ the drag coefficient is approximately constant. In this range the entire rear of the sphere has a low-pressure turbulent wake, as indicated in Fig. 9.12, and most of the

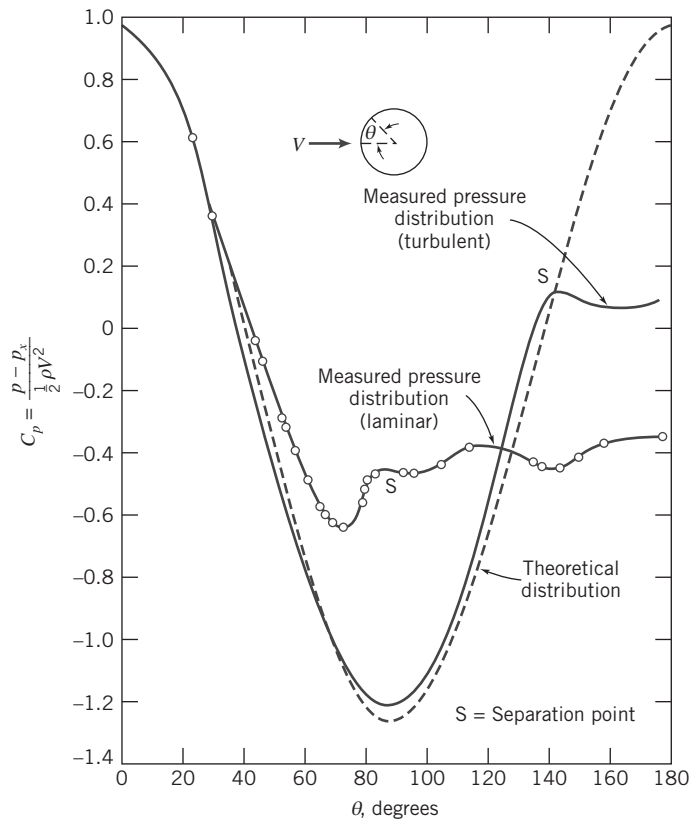


Fig. 9.12 Pressure distribution around a smooth sphere for laminar and turbulent boundary-layer flow, compared with inviscid flow [6].

drag is caused by the front-rear pressure asymmetry. Note that $C_D \propto 1/Re$ corresponds to $F_D \propto V$, and that $C_D \sim \text{const.}$ corresponds to $F_D \propto V^2$, indicating a quite rapid increase in drag.

For Reynolds numbers larger than about 3×10^5 , transition occurs and the boundary layer on the forward portion of the sphere becomes turbulent. The point of separation then moves downstream from the sphere midsection, and the size of the wake decreases. The net pressure force on the sphere is reduced (Fig. 9.12), and the drag coefficient decreases abruptly.

A turbulent boundary layer, since it has more momentum flux than a laminar boundary layer, can better resist an adverse pressure gradient, as discussed in Section 9.5. Consequently, turbulent boundary-layer flow is desirable on a blunt body because it delays separation and thus reduces the pressure drag.

Transition in the boundary layer is affected by roughness of the sphere surface and turbulence in the flow stream. Therefore, the reduction in drag associated with a turbulent boundary layer does not occur at a unique value of Reynolds number. Experiments with smooth spheres in a flow with low turbulence level show that transition may be delayed to a critical Reynolds number, Re_D , of about 4×10^5 . For rough surfaces and/or highly turbulent freestream flow, transition can occur at a critical Reynolds number as low as 50,000.

The drag coefficient of a sphere with turbulent boundary-layer flow is about one-fifth that for laminar flow near the critical Reynolds number. The corresponding reduction in drag force can affect the range of a sphere (e.g., a golf ball) appreciably. The “dimples” on a golf ball are designed to “trip” the boundary layer and, thus, to guarantee turbulent boundary-layer flow and minimum drag.

Adding roughness elements to a sphere also can suppress local oscillations in location of the transition between laminar and turbulent flow in the boundary layer. These oscillations can lead to variations in drag and to random fluctuations in lift (see Section 9.7). In baseball, the “knuckle ball” pitch is intended to behave erratically to confuse the batter. By throwing the ball with almost no spin, the pitcher relies on the seams to cause transition in an unpredictable fashion as the ball moves on its way to the batter. This causes the desired variation in the flight path of the ball.

Figure 9.13 shows the drag coefficient for flow over a smooth cylinder. The variation of C_D with Reynolds number shows the same characteristics as observed in the flow over a smooth sphere, but the values of C_D are about twice as high. The use of Fig. 9.13 to determine the drag force on a chimney is shown in Example 9.6, and the use of the drag coefficient data in Table 9.3 to find the drag of a parachute is given in Example 9.7.

Flow about a smooth circular cylinder may develop a regular pattern of alternating vortices downstream. The *vortex trail*, sometimes called a vortex street, causes an oscillatory lift force on the cylinder perpendicular to the stream motion. Vortex shedding excites oscillations that cause telegraph wires to

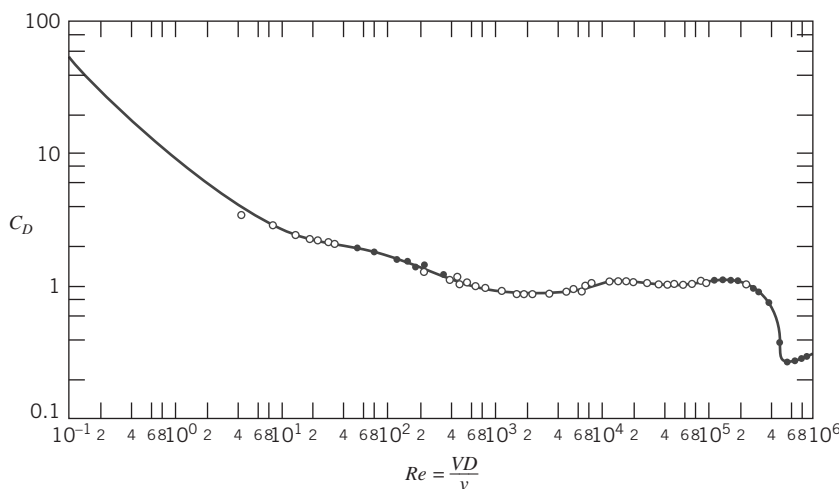


Fig. 9.13 Drag coefficient for a smooth circular cylinder as a function of Reynolds number. (Data from References [3], [16], and [17].)

“sing” and ropes on flag poles to “slap” annoyingly. Sometimes structural oscillations can reach dangerous magnitudes and cause high stresses; they can be reduced or eliminated by applying roughness elements or fins, either axial or helical, that destroy the symmetry of the cylinder and stabilize the flow.

Experimental data show that regular vortex shedding occurs most strongly in the range of Reynolds number from about 60 to 5000. For $Re > 1000$ the dimensionless frequency of vortex shedding, expressed as a Strouhal number, $St = f D/V$, is approximately equal to 0.21 [3].

Roughness affects drag of cylinders and spheres similarly: the critical Reynolds number is reduced by the rough surface, and transition from laminar to turbulent flow in the boundary layers occurs earlier. The drag coefficient is reduced by a factor of about 4 when the boundary layer on the cylinder becomes turbulent.

Example 9.6 AERODYNAMIC DRAG AND MOMENT ON A CHIMNEY

A cylindrical chimney 1 m in diameter and 25 m tall is exposed to a uniform 50 km/hr wind at standard atmospheric conditions. End effects and gusts may be neglected. Estimate the bending moment at the base of the chimney due to wind forces.

Given: Cylindrical chimney, $D = 1 \text{ m}$, $L = 25 \text{ m}$, in uniform flow with

$$V = 50 \text{ km/hr} \quad p = 101 \text{ kPa (abs)} \quad T = 15^\circ\text{C}$$

Neglect end effects.

Find: Bending moment at bottom of chimney.

Solution: The drag coefficient is given by $C_D = F_D / (\frac{1}{2} \rho V^2 A)$, and thus $F_D = C_D A \frac{1}{2} \rho V^2$. Since the force per unit length is uniform over the entire length, the resultant force, F_D , will act at the midpoint of the chimney. Hence the moment about the chimney base is

$$M_0 = F_D \frac{L}{2} = C_D A \frac{1}{2} \rho V^2 \frac{L}{2} = C_D A \frac{L}{4} \rho V^2$$

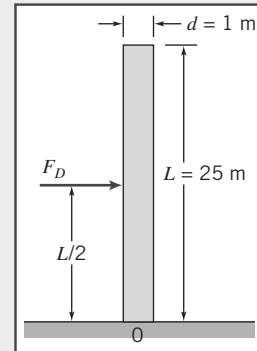
$$V = 50 \frac{\text{km}}{\text{hr}} \times 10^3 \frac{\text{m}}{\text{km}} \times \frac{\text{hr}}{3600 \text{s}} = 13.9 \text{ m/s}$$

For air at standard conditions, $\rho = 1.23 \text{ kg/m}^3$, and $\mu = 1.79 \times 10^{-5} \text{ kg/(m}\cdot\text{s)}$. Thus

$$Re = \frac{\rho V D}{\mu} = 1.23 \frac{\text{kg}}{\text{m}^3} \times 13.9 \frac{\text{m}}{\text{s}} \times 1 \text{ m} \times \frac{\text{m}\cdot\text{s}}{1.79 \times 10^{-5} \text{ kg}} = 9.55 \times 10^5$$

From Fig. 9.13, $C_D \approx 0.35$. For a cylinder, $A = DL$, so

$$\begin{aligned} M_0 &= C_D A \frac{L}{4} \rho V^2 = C_D D L \frac{L}{4} \rho V^2 = C_D D \frac{L^2}{4} \rho V^2 \\ &= \frac{1}{4} \times 0.35 \times 1 \text{ m} \times (25)^2 \text{ m}^2 \times 1.23 \frac{\text{kg}}{\text{m}^3} \times (13.9)^2 \frac{\text{m}^2}{\text{s}^2} \times \frac{\text{N}\cdot\text{s}^2}{\text{kg}\cdot\text{m}} \\ M_0 &= 13.0 \text{ kN}\cdot\text{m} \end{aligned}$$



This problem illustrates application of drag-coefficient data to calculate the force and moment on a structure. We modeled the wind as a uniform flow; more realistically, the lower atmosphere is often modeled as a huge turbulent boundary layer, with a power-law velocity profile, $u \sim y^{1/n}$, where y is the elevation.

Example 9.7 DECELERATION OF AN AUTOMOBILE BY A DRAG PARACHUTE

A dragster weighing 1600 lbf attains a speed of 270 mph in the quarter mile. Immediately after passing through the timing lights, the driver opens the drag chute of area $A = 25 \text{ ft}^2$. Air and rolling resistance of the car may be neglected. Find the time required for the machine to decelerate to 100 mph in standard air.

Given: Dragster weighing 1600 lbf, moving with initial speed $V_0 = 270 \text{ mph}$, is slowed by the drag force on a chute of area $A = 25 \text{ ft}^2$. Neglect air and rolling resistance of the car. Assume standard air.

Find: Time required for the machine to decelerate to 100 mph.

Solution: Taking the car as a system and writing Newton's second law in the direction of motion gives

$$-F_D = ma = m \frac{dV}{dt} \quad \begin{array}{c} F_D \\ \leftarrow \quad \rightarrow \right. \\ \boxed{\text{Car}} \\ \longrightarrow x \end{array} \quad \begin{array}{l} V_0 = 270 \text{ mph} \\ V_f = 100 \text{ mph} \\ \rho = 0.00238 \text{ slug}/\text{ft}^3 \end{array}$$

Since $C_D = \frac{F_D}{\frac{1}{2}\rho V^2 A}$, then $F_D = \frac{1}{2} C_D \rho V^2 A$.

Substituting into Newton's second law gives

$$-\frac{1}{2} C_D \rho V^2 A = m \frac{dV}{dt}$$

Separating variables and integrating, we obtain

$$\begin{aligned} -\frac{1}{2} C_D \rho \frac{A}{m} \int_0^t dt &= \int_{V_0}^{V_f} \frac{dV}{V^2} \\ -\frac{1}{2} C_D \rho \frac{A}{m} t &= -\frac{1}{V} \Big|_{V_0}^{V_f} = -\frac{1}{V_f} + \frac{1}{V_0} = -\frac{(V_0 - V_f)}{V_f V_0} \end{aligned}$$

Finally,

$$t = \frac{(V_0 - V_f)}{V_f V_0} \frac{2 \text{ m}}{C_D \rho A} = \frac{(V_0 - V_f)}{V_f V_0} \frac{2W}{C_D \rho Ag}$$

Model the drag chute as a hemisphere (with open end facing flow). From Table 9.3, $C_D = 1.42$ (assuming $Re > 10^3$). Then, substituting numerical values,

$$\begin{aligned} t &= (270 - 100) \text{ mph} \times 2 \times 1600 \text{ lbf} \times \frac{1}{100 \text{ mph}} \times \frac{\text{hr}}{270 \text{ mi}} \times \frac{1}{1.2} \times \frac{\text{ft}^3}{0.00238 \text{ slug}} \\ &\quad \times \frac{1}{25 \text{ ft}^2} \times \frac{\text{s}^2}{32.2 \text{ ft}} \times \frac{\text{slug} \cdot \text{ft}}{\text{lbf} \cdot \text{s}^2} \times \frac{\text{mi}}{5280 \text{ ft}} \times 3600 \frac{\text{s}}{\text{hr}} \\ t &= 5.05 \text{ s} \end{aligned}$$

Check the assumption on Re :

$$\begin{aligned} Re &= \frac{DV}{\nu} = \left[\frac{4A}{\pi} \right]^{1/2} \frac{V}{\nu} \\ &= \left[\frac{4}{\pi} \times 25 \text{ ft}^2 \right]^{1/2} \times 100 \frac{\text{mi}}{\text{hr}} \times \frac{\text{hr}}{3600 \text{ s}} \times 5280 \frac{\text{ft}}{\text{mi}} \times \frac{\text{s}}{1.57 \times 10^{-4} \text{ ft}^2} \end{aligned}$$

$$Re = 5.27 \times 10^6$$

Hence the assumption is valid.

This problem illustrates application of drag-coefficient data to calculate the drag on a vehicle parachute.

All experimental data presented in this section are for single objects immersed in an unbounded fluid stream. The objective of wind tunnel tests is to simulate the conditions of an unbounded flow. Limitations on equipment size make this goal unreachable in practice. Frequently it is necessary to apply corrections to measured data to obtain results applicable to unbounded flow conditions.

In numerous realistic flow situations, interactions occur with nearby objects or surfaces. Drag can be reduced significantly when two or more objects, moving in tandem, interact. This phenomenon is well known to bicycle riders and automobile racing, where “drafting” is a common practice. Drag reductions of 80 percent may be achieved with optimum spacing [8]. Drag also can be increased significantly when spacing is not optimum.

Drag can be affected by neighbors alongside as well. Small particles falling under gravity travel more slowly when they have neighbors than when they are isolated. This phenomenon has important applications to mixing and sedimentation processes.

Experimental data for drag coefficients on objects must be selected and applied carefully. Due regard must be given to the differences between the actual conditions and the more controlled conditions under which measurements were made.

In addition to the values presented here, the Engineer’s Toolbox [18] has drag coefficients for a wide variety of objects. Additionally, many drag coefficients are now determined using CFD software such as Fluent [19].

Streamlining

The extent of the separated flow region behind many of the objects discussed in the previous section can be reduced or eliminated by streamlining, or fairing, the body shape. We have seen that due to the convergent body shape at the rear of any object the streamlines will diverge, so that the velocity will decrease, and therefore the pressure will increase. Hence, we initially have an adverse pressure gradient at the rear of the body, leading to boundary-layer separation and ultimately to a low-pressure wake leading to large pressure drag. We can reduce the drag on a body by making the rear of the body more tapered, which will reduce the adverse pressure gradient and hence make the turbulent wake smaller. However, we may increase the skin friction drag simply because we have increased the surface area. In practice, there is an optimum amount of fairing or tapering at which the total drag (the sum of pressure and skin friction drag) is minimized.

The pressure gradient around a “teardrop” shape is less severe than that around a cylinder of circular section. The trade-off between pressure and friction drag for this case is shown schematically in Fig. 9.14. The pressure drag increases as the thickness is increased, while the friction drag due to the boundary layer decreases. The total drag is the sum of the two contributions and is a minimum at some value of thickness. This minimum drag is considerably less than that of a cylinder with a diameter equal to this value of thickness. As a result, streamlining of the structural members on aircraft and automobiles leads to significant savings.

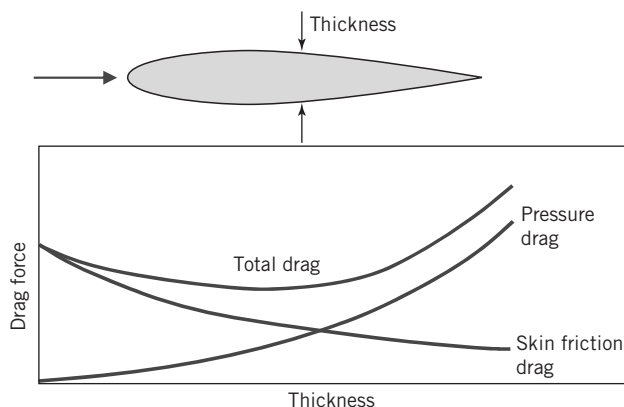


Fig. 9.14 Drag coefficient on a streamlined airfoil as a function of thickness showing contributions of skin friction and pressure to total drag. (Adapted from [7].)

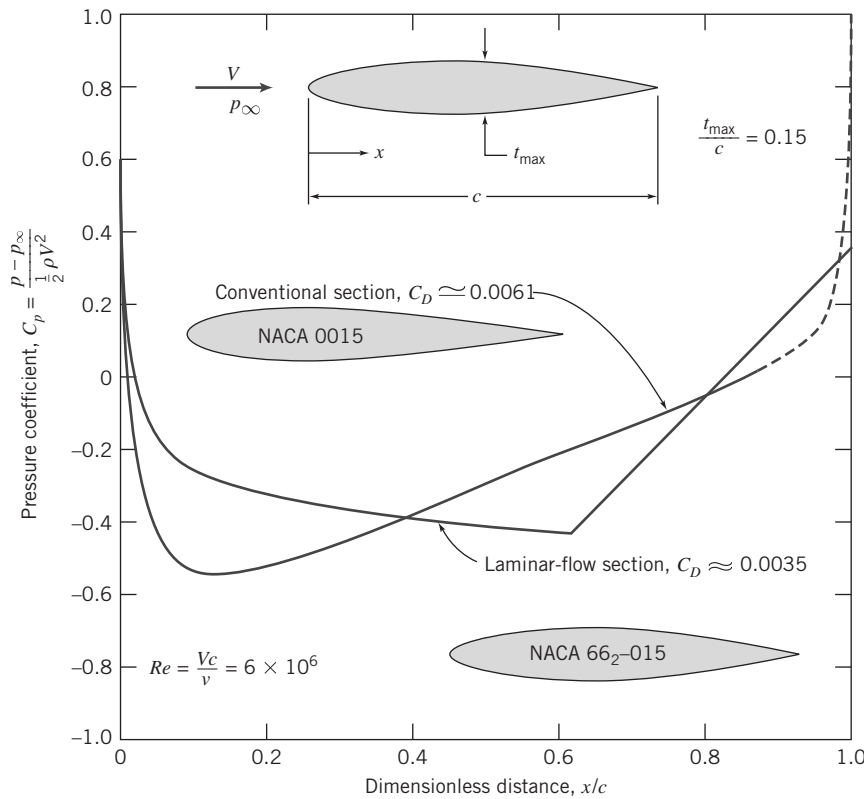


Fig. 9.15 Theoretical pressure distributions at zero angle of attack for two symmetric airfoil sections of 15 percent thickness ratio. (Data from Abbott and von Doenhoff [9].)

The effect of the airfoil shape on the pressure distribution and drag coefficient is shown in Figure 9.15 for two symmetric airfoils of infinite span and 15 percent thickness at zero angle of attack. Transition on the conventional (NACA 0015) airfoil takes place where the pressure gradient becomes adverse, at $x/c = 0.13$, near the point of maximum thickness. Thus most of the airfoil surface is covered with a turbulent boundary layer; the drag coefficient is $C_D \approx 0.0061$. The point of maximum thickness has been moved aft on the airfoil (NACA 66₂-015) designed for laminar flow. The boundary layer is maintained in the laminar regime by the favorable pressure gradient to $x/c = 0.63$. Thus the bulk of the flow is laminar; $C_D \approx 0.0035$ for this section, based on planform area. The drag coefficient based on frontal area is $C_{Df} = C_D/0.15 = 0.0233$, or about 40 percent of the optimum for the shapes shown in Fig. 9.14.

Current airfoil shapes are designed to produce a pressure distribution that prevents separation while maintaining the turbulent boundary layer in a condition that produces negligible skin friction, such as illustrated in Fig. 9.16.

The emphasis on fuel economy and emissions for automobiles and trucks has led to improved aerodynamic designs. Using CFD software to quantify the drag reduction techniques have led to major design innovations such as contouring the exterior to prevent separation, streamlining mirrors and door handles, installing smooth panels covering the underbody, directing air around the wheels, and designing

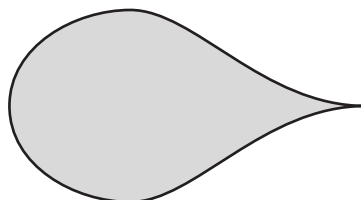


Fig. 9.16 Nearly optimum shape for low-drag strut [11].

the rear to minimize the wake region. The net effect is that drag coefficients for modern automobiles are in the range of 0.25 to 0.3. This represents up to a 50 percent reduction in the drag coefficient over the last two decades.

The trucking industry has also concentrated on changes that improve the fuel economy of vehicles. Long-distance trucks now commonly have a number of drag reduction devices installed, such as a deflector on top of the cab, tractor and trailer side skirts, and boat-tail panels at the rear. These devices reduce the drag coefficient by 15 to 20 percent from the typical value of 0.8 to 1.0.

9.7 Lift

For most objects in relative motion in a fluid, the most significant fluid force is the drag. However, there are some objects, such as airfoils, for which the lift is significant. Lift is defined as the component of fluid force perpendicular to the fluid motion. For an airfoil, the *lift coefficient*, C_L , is defined as

$$C_L \equiv \frac{F_L}{\frac{1}{2} \rho V^2 A_p} \quad (9.38)$$

The lift and drag coefficients are defined as the ratio of an actual force (lift or drag) divided by the product of dynamic pressure and area. This denominator can be viewed as the force that would be generated if the fluid was brought to rest directly on the area. This gives us a “feel” for the meaning of the coefficients.

The lift and drag coefficients for an airfoil are functions of both Reynolds number and angle of attack. The angle of attack, α , is the angle between the airfoil chord and the freestream velocity vector. The *chord* of an airfoil is the straight line joining the leading edge and the trailing edge. The wing section shape is obtained by combining a *mean line* and a thickness distribution [9]. When the airfoil has a symmetric section, the mean line and the chord line both are straight lines, and they coincide. An airfoil with a curved mean line is said to be *cambered*.

The area at right angles to the flow changes with angle of attack. Consequently, the planform area, A_p (the maximum projected area of the wing), is used to define lift and drag coefficients for an airfoil.

The phenomenon of aerodynamic lift is explained by the velocity increase causing pressure to decrease over the top surface of the airfoil and the velocity decrease causing pressure to increase along the bottom surface of the airfoil. Because of the pressure differences relative to atmosphere, the upper surface of the airfoil may be called the *suction surface* and the lower surface the *pressure surface*.

Lift and drag characteristics of modern air craft are usually generated with CFD software and are proprietary. As a result, the airfoil data obtained through wind tunnel testing obtained by NACA, the predecessor to NASA, will be used to illustrate airfoil characteristics [12].

Airfoil stall results when flow separation occurs over a major portion of the upper surface of the airfoil. As the angle of attack is increased, the stagnation point moves back along the lower surface of the airfoil, as shown schematically for the symmetric laminar-flow section in Fig. 9.18a. Flow on the upper surface then must accelerate sharply to round the nose of the airfoil. The effect of angle of attack on the theoretical upper-surface pressure distribution is shown in Fig. 9.18b. The minimum pressure becomes lower, and its location moves forward on the upper surface. A severe adverse pressure gradient appears following the point of minimum pressure; finally, the adverse pressure gradient causes the flow to separate completely from the upper surface and the airfoil stalls. Stall is indicated in Fig. 9.17(a) as the angle of attack for which the lift coefficient decreases sharply.

Movement of the minimum pressure point and accentuation of the adverse pressure gradient are responsible for the sudden increase in C_D for the laminar-flow section, which is apparent in Fig. 9.17. The sudden rise in C_D is caused by early transition from laminar to turbulent boundary-layer flow on the upper surface. Aircraft with laminar-flow sections are designed to cruise in the low-drag region.

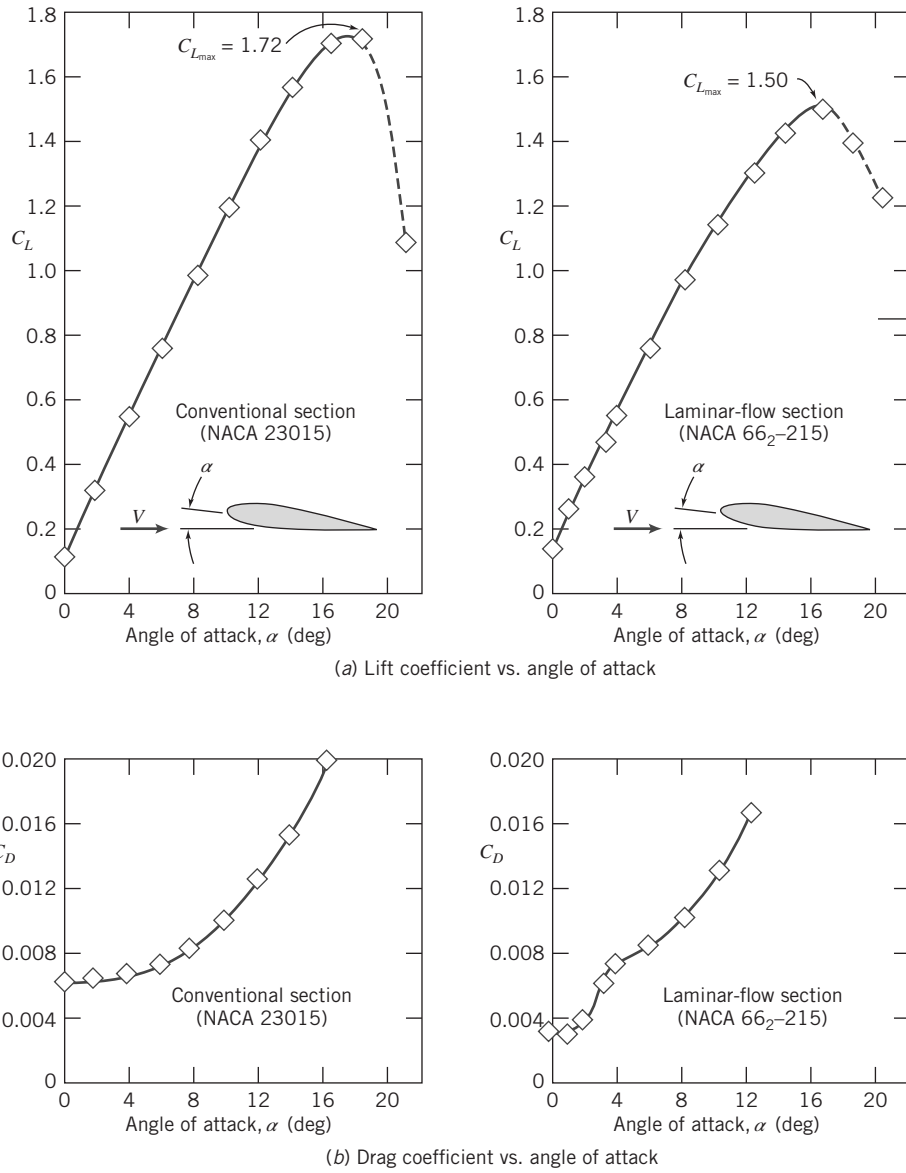


Fig. 9.17 Lift and drag coefficients versus angle of attack for two airfoil sections of 15 percent thickness ratio at $Re_c = 9 \times 10^6$. (Data from Abbott and von Doenhoff [9].)

Because laminar-flow sections have very sharp leading edges, all of the effects we have described are exaggerated, and they stall at lower angles of attack than conventional sections, as shown in Fig. 9.17. The maximum possible lift coefficient, $C_{L_{max}}$, also is less for laminar-flow sections.

Plots of C_L versus C_D (called lift-drag polars) often are used to present airfoil data in compact form. A polar plot is given in Fig. 9.19 for the two sections we have discussed. The lift/drag ratio, C_L/C_D , is shown at the design lift coefficient for both sections. This ratio is very important in the design of aircraft. The lift coefficient determines the lift of the wing and hence the load that can be carried, and the drag coefficient indicates a large part of the drag the airplane engines have to work against in order to generate the needed lift; hence, in general, a high C_L/C_D is the goal, at which the laminar airfoil clearly excels.

Modern modeling and computational capabilities have made it possible to design airfoil sections that develop high lift while maintaining very low drag [10, 11]. Boundary-layer calculation codes are used to develop pressure distributions and the resulting body shapes that postpone transition to the most rearward location possible. The turbulent boundary layer following transition is maintained

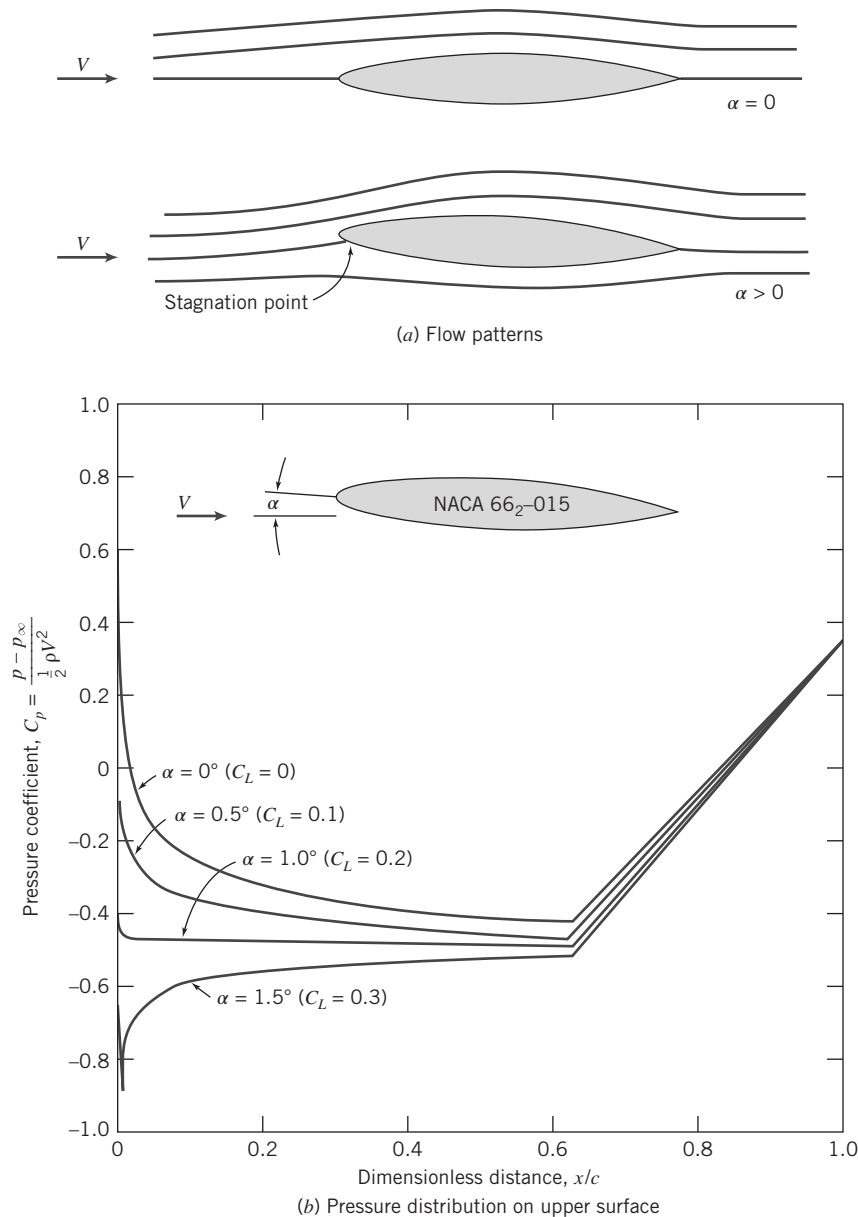


Fig. 9.18 Effect of angle of attack on flowpattern and theoretical pressure distribution for a symmetric laminar-flow airfoil of 15 percent thickness ratio. (Data from Abbott and von Doenhoff [9].)

in a state of incipient separation with nearly zero skin friction by appropriate shaping of the pressure distribution.

All real airfoils are of finite span and have less lift and more drag than their airfoil section data would indicate. There are several ways to explain this. If we consider the pressure distribution near the end of the wing, the low pressure on the upper and high pressure on the lower surface cause flow to occur around the wing tip, leading to *trailing vortices* (as shown in Fig. 9.20), and the pressure difference is reduced, leading to less lift. These trailing vortices can also be explained in terms of circulation. As shown in Section 6.5 circulation around a wing section is present whenever there is lift. Circulation cannot end in the fluid but extends beyond the wing in the form of trailing vortices. Trailing vortices can be very strong and dissipate slowly.

Trailing vortices reduce lift and increase drag because of the loss of pressure difference, called *induced drag*. The “downwash” velocities induced by the vortices mean that the effective angle of attack is reduced and the wing “sees” a flow at approximately the mean of the upstream and downstream

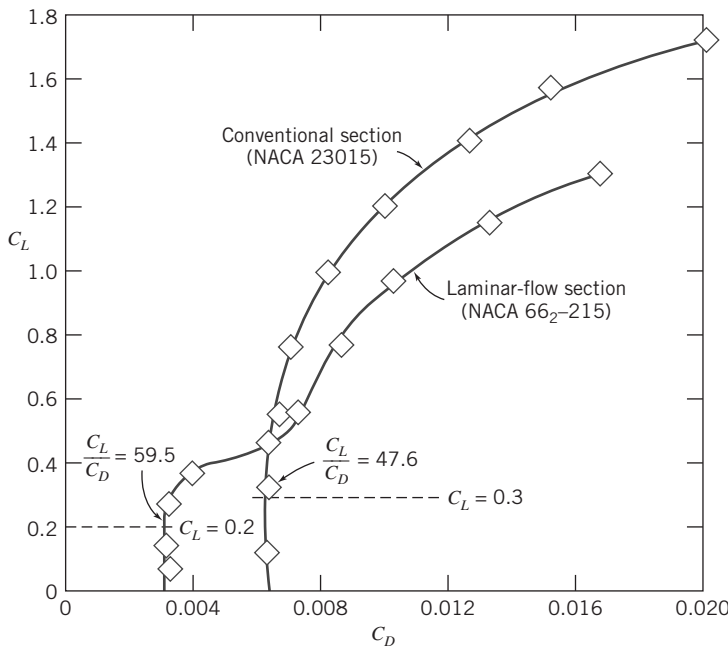


Fig. 9.19 Lift-drag polar for two airfoil sections of 15 percent thickness ratio. (Data from Abbott and von Doenhoff [9].)

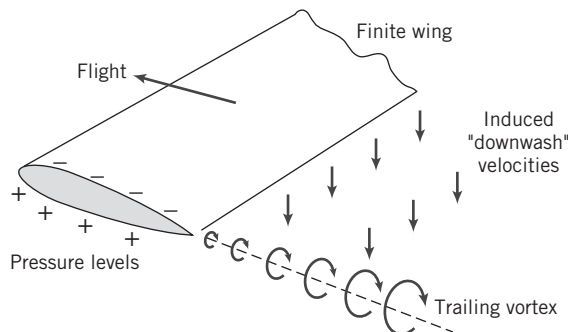


Fig. 9.20 Schematic representation of the trailing vortex system of a finite wing.

directions. This also causes the lift force which is perpendicular to the effective angle of attack to “lean backwards” a little, resulting in some of the lift appearing as drag.

Loss of lift and increase in drag caused by finite-span effects are concentrated near the tip of the wing; hence, it is clear that a short, stubby wing will experience these effects more severely than a very long wing. We should therefore expect the effects to correlate with the wing *aspect ratio*, defined as

$$AR \equiv \frac{b^2}{A_p} \quad (9.39)$$

where A_p is planform area and b is wingspan. For a rectangular planform of wingspan b and chord length c ,

$$AR = \frac{b^2}{A_p} = \frac{b^2}{bc} = \frac{b}{c}$$

The maximum lift/drag ratio for a modern low-drag section may be as high as 400 for infinite aspect ratio. A high-performance sailplane (glider) with $AR = 40$ might have $L/D = 40$, and a typical light plane ($AR \approx 12$) might have $L/D \approx 20$ or so. Variations in aspect ratio are seen in nature. Soaring birds, such as the albatross or California condor, have thin wings of long span. Birds that must maneuver quickly to

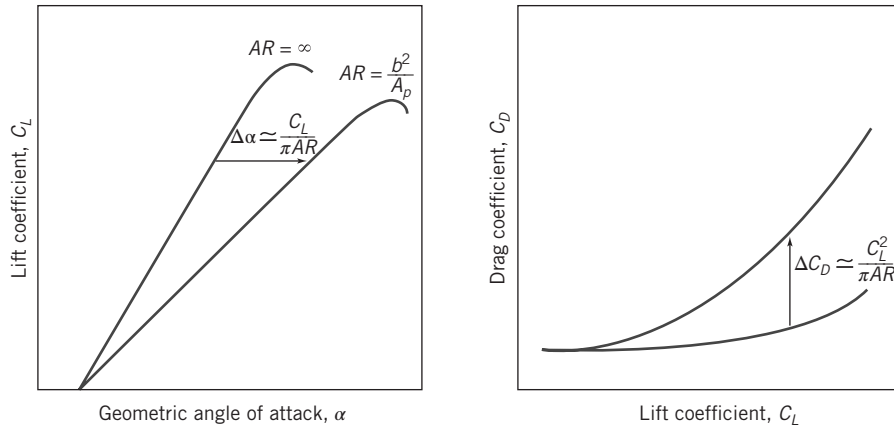


Fig. 9.21 Effect of finite aspect ratio on lift and drag coefficients for a wing.

catch their prey, such as hawks, have wings of relatively short span, but large area, which gives low *wing loading* (ratio of weight to planform area) and thus high maneuverability.

When the angle of attack of a finite wing is increased, the trailing vortices and therefore the downwash increase, leading to loss of lift and to induced drag. The effects of the finite aspect ratio can be characterized as a reduction $\Delta\alpha$ in the effective angle of attack. Theory and experiment indicate that

$$\Delta\alpha \approx \frac{C_L}{\pi AR} \quad (9.40)$$

Compared with an airfoil section ($AR = \infty$), the geometric angle of attack of a wing (finite AR) must be increased by this amount to get the same lift, as shown in Fig. 9.21. It also means that instead of being perpendicular to the motion, the lift force leans angle $\Delta\alpha$ backwards from the perpendicular. The induced drag component of the drag coefficient is

$$\Delta C_D \approx C_L \Delta\alpha \approx \frac{C_L^2}{\pi AR} \quad (9.41)$$

This also is shown in Fig. 9.21.

When written in terms of aspect ratio, the drag of a wing of finite span becomes [9]

$$C_D = C_{D,\infty} + C_{D,i} = C_{D,\infty} + \frac{C_L^2}{\pi AR} \quad (9.42)$$

where $C_{D,\infty}$ is the section drag coefficient at C_L , $C_{D,i}$ is the induced drag coefficient at C_L , and AR is the aspect ratio of the finite-span wing.

Drag on airfoils arises from viscous and pressure forces. Viscous drag changes with Reynolds number but only slightly with angle of attack. These relationships and some commonly used terminology are illustrated in Fig. 9.22.

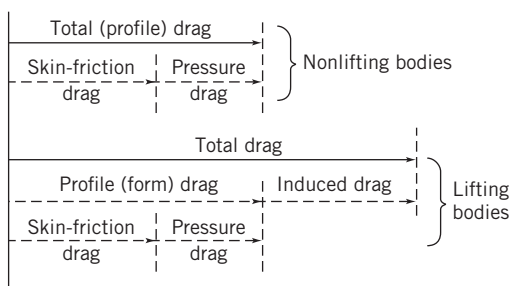


Fig. 9.22 Drag breakdown on nonlifting and lifting bodies.

A useful approximation to the drag polar for a complete aircraft may be obtained by adding the induced drag to the drag at zero lift. The drag at any lift coefficient is obtained from

$$C_D = C_{D,0} + C_{D,i} = C_{D,0} + \frac{C_L^2}{\pi AR} \quad (9.43)$$

where $C_{D,0}$ is the drag coefficient at zero lift and AR is the aspect ratio. The optimum cruising speed of an aircraft brings in these lift and drag relations, as shown in Example 9.8.

Example 9.8 OPTIMUM CRUISE PERFORMANCE OF A JET TRANSPORT

Jet engines burn fuel at a rate proportional to thrust delivered. The optimum cruise condition for a jet aircraft is at maximum speed for a given thrust. In steady level flight, thrust and drag are equal. Hence, optimum cruise occurs at the speed when the ratio of drag force to air speed is minimized.

A Boeing 727-200 jet transport has wing planform area $A_p = 1600 \text{ ft}^2$, and aspect ratio $AR = 6.5$. Stall speed at sea level for this aircraft with flaps up and a gross weight of 150,000 lbf is 175 mph. Below $M = 0.6$, drag due to compressibility effects is negligible, so Eq. 9.43 may be used to estimate total drag on the aircraft. $C_{D,0}$ for the aircraft is constant at 0.0182. Assume sonic speed at sea level is $c = 759 \text{ mph}$.

Evaluate the performance envelope for this aircraft at sea level by plotting drag force versus speed, between stall and $M = 0.6$. Use this graph to estimate optimum cruise speed for the aircraft at sea-level conditions. Comment on stall speed and optimum cruise speed for the aircraft at 30,000 ft altitude on a standard day.

Given: Boeing 727-200 jet transport at sea-level conditions.

$$W = 150,000 \text{ lbf}, \quad A = 1600 \text{ ft}^2, \quad AR = 6.5, \quad \text{and} \quad C_{D,0} = 0.182$$

Stall speed is $V_{\text{stall}} = 175 \text{ mph}$, and compressibility effects on drag are negligible for $M \leq 0.6$ (sonic speed at sea level is $c = 759 \text{ mph}$).

- Find:**
- Drag force as a function of speed from V_{stall} to $M = 0.6$; plot results.
 - Estimate of optimum cruise speed at sea level.
 - Stall speed and optimum cruise speed at 30,000 ft altitude.

Solution: For steady, level flight, weight equals lift and thrust equals drag.

Governing equations:

$$\begin{aligned} F_L &= C_L A \frac{1}{2} \rho V^2 = W & C_D &= C_{D,0} + \frac{C_L^2}{\pi AR} \\ F_D &= C_D A \frac{1}{2} \rho V^2 = T & M &= \frac{V}{c} \end{aligned}$$

At sea level, $\rho = 0.00238 \text{ slug}/\text{ft}^3$, and $c = 759 \text{ mph}$.

Since $F_L = W$ for level flight at any speed, then

$$C_L = \frac{W}{\frac{1}{2} \rho V^2 A} = \frac{2W}{\rho V^2 A}$$

At stall speed, $V = 175 \text{ mph}$, so

$$\begin{aligned} C_L &= 2 \times 150,000 \text{ lbf} \times \frac{\text{ft}^3}{0.00238 \text{ slug}} \left[\frac{\text{hr}}{\text{V mi}} \times \frac{\text{mi}}{5280 \text{ ft}} \times 3600 \frac{\text{s}}{\text{hr}} \right]^2 \frac{1}{1600 \text{ ft}^2} \times \frac{\text{slug} \cdot \text{ft}}{\text{lbf} \cdot \text{s}^2} \\ C_L &= \frac{3.65 \times 10^4}{[\text{V(mph)}]^2} = \frac{3.65 \times 10^4}{(175)^2} = 1.196, \text{ and} \\ C_D &= C_{D,0} + \frac{C_L^2}{\pi AR} = 0.0182 + \frac{(1.196)^2}{\pi(6.5)} = 0.0882 \end{aligned}$$

Then

$$F_D = W \frac{C_D}{C_L} = 150,000 \text{ lbf} \left(\frac{0.0882}{1.19} \right) = 11,100 \text{ lbf}$$

At $M = 0.6, V = Mc = (0.6)759 \text{ mph} = 455 \text{ mph}$, so $C_L = 0.177$ and

$$C_D = 0.0182 + \frac{(0.177)^2}{\pi(6.5)} = 0.0197$$

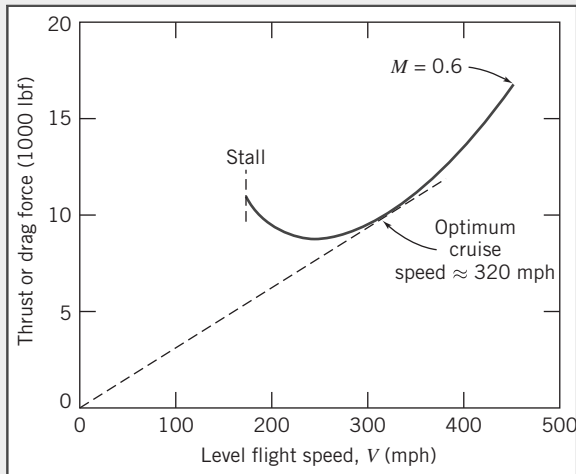
so

$$F_D = 150,000 \text{ lbf} \left(\frac{0.0197}{0.177} \right) = 16,700 \text{ lbf}$$

Similar calculations lead to the following table (computed using Excel):

$V(\text{mph})$	175	200	300	400	455
C_L	1.196	0.916	0.407	0.229	0.177
C_D	0.0882	0.0593	0.0263	0.0208	0.0197
$F_D (\text{lbf})$	11,100	9,710	9,700	13,600	16,700

These data may be plotted as:



From the plot, the optimum cruise speed at sea level is estimated as 320 mph (and using Excel we obtain 323 mph).

At 30,000 ft (9140 m) altitude, the density is only about 0.375 times sea level density, from Table A.3. The speeds for corresponding forces are calculated from

$$F_L = C_L A \frac{1}{2} \rho V^2 \quad \text{or} \quad V = \sqrt{\frac{2F_L}{C_L \rho A}} \quad \text{or} \quad \frac{V_{30}}{V_{SL}} = \sqrt{\frac{\rho_{SL}}{\rho_{30}}} = \sqrt{\frac{1}{0.375}} = 1.63$$

Thus, speeds increase 63 percent at 30,000 ft altitude:

$$\begin{aligned} V_{\text{stall}} &\approx 285 \text{ mph} \\ V_{\text{cruise}} &\approx 522 \text{ mph} \end{aligned}$$

This problem illustrates that high-altitude flight increases the optimum cruising speed—in general this speed depends on aircraft configuration, gross weight, segment length, and winds aloft.

It is possible to increase the *effective* aspect ratio for a wing of given geometric ratio by adding a *winglet* to the wing tip. Winglets are short, aerodynamically contoured wings set perpendicular to the wing at the tip. The winglet blocks the flow from the higher pressure region below the wing tip to the lower pressure region above the wing tip. This reduces the strength of the trailing vortex system and the induced drag. The winglet also produces a small component of force in the flight direction, which

has the effect of further reducing the overall drag of the aircraft. The contour and angle of attack of the winglet are adjusted based on wind tunnel tests to provide optimum results.

As we have seen, aircraft can be fitted with low-drag airfoils to give excellent performance at cruise conditions. However, since the maximum lift coefficient is low for thin airfoils, additional effort must be expended to obtain acceptably low landing speeds. In steady-state flight conditions, lift must equal aircraft weight. Thus,

$$W = F_L = C_L \frac{1}{2} \rho V^2 A$$

Minimum flight speed is therefore obtained when $C_L = C_{L_{\max}}$. Solving for V_{\min} ,

$$V_{\min} = \sqrt{\frac{2W}{\rho C_{L_{\max}} A}} \quad (9.44)$$

According to Eq. 9.44, the minimum landing speed can be reduced by increasing either $C_{L_{\max}}$ or wing area. Two basic techniques are available to control these variables: variable-geometry wing sections such as flaps or boundary-layer control techniques.

Flaps are movable portions of a wing trailing edge that may be extended during landing and takeoff to increase effective wing area. The effects on lift and drag of two typical flap configurations are shown in Fig. 9.23, as applied to the NACA 23012 airfoil section. The maximum lift coefficient for this section is increased from 1.52 in the “clean” condition to 3.48 with double-slotted flaps. From Eq. 9.44, the corresponding reduction in landing speed would be 34 percent.

Figure 9.23 shows that section drag is increased substantially by high-lift devices. From Fig. 9.23b, section drag at $C_{L_{\max}} (C_D \approx 0.28)$ with double-slotted flaps is about 5 times as high as section drag at $C_{L_{\max}} (C_D \approx 0.055)$ for the clean airfoil. Induced drag due to lift must be added to section drag to obtain total drag. Because induced drag is proportional to C_L^2 (Eq. 9.41), total drag rises sharply at low aircraft speeds. At speeds near stall, drag may increase enough to exceed the thrust available from the engines. To avoid this dangerous region of unstable operation, the Federal Aviation Administration (FAA) limits operation of commercial aircraft to speeds above 1.2 times stall speed.

The basic purpose of all boundary-layer control techniques is to delay separation or reduce drag by adding momentum to the boundary layer through blowing or by removing low-momentum boundary-layer fluid by suction. Many examples of practical boundary-layer control systems may be seen on commercial transport aircraft. Two typical systems are shown in Fig. 9.24.

Aerodynamic lift is an important consideration in the design of automobiles. A road vehicle generates lift by virtue of its shape [12]. A representative centerline pressure distribution measured in the

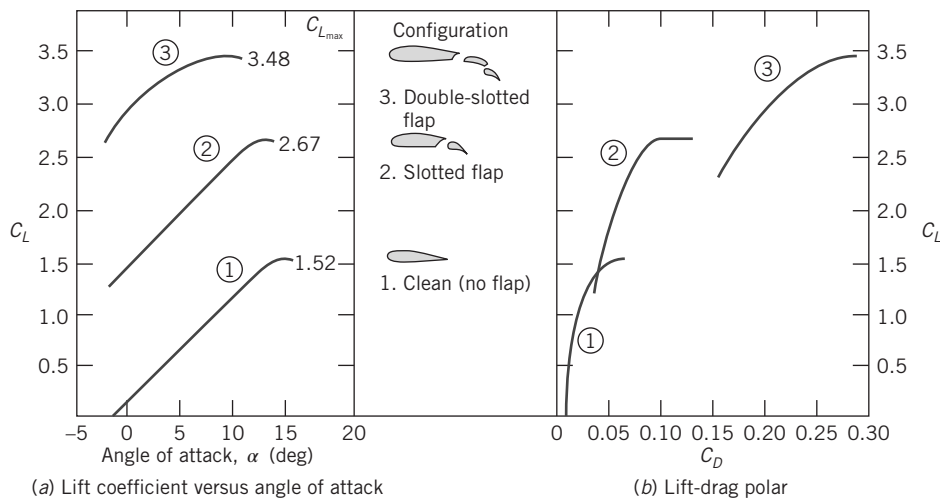


Fig. 9.23 Effect of flaps on aerodynamic characteristics of NACA 23012 airfoil section. (Data from Abbott and von Doenhoff [9].)



Chad Slattery/Getty Images

Fig. 9.24 (a) Application of high-lift boundary-layer control devices to reduce landing speed of a jet transport aircraft. The wing of the Boeing 777 is highly mechanized. In the landing configuration, large slotted trailing-edge flaps roll out from under the wing and deflect downward to increase wing area and camber, thus increasing the lift coefficient. Slats at the leading edge of the wing move forward and down, to increase the effective radius of the leading edge and prevent flow separation, and to open a slot that helps keep air flow attached to the wing's upper surface. After touchdown, spoilers (not shown in use) are raised in front of each flap to decrease lift and ensure that the plane remains on the ground, despite use of the lift-augmenting devices. (This photograph was taken during a flight test. Flow cones are attached to the flaps and ailerons to identify regions of separated flow on these surfaces.)



Jeremy Simms/Getty Images

Fig. 9.24 (b) Application of high-lift boundary-layer control devices to reduce takeoff speed of a jet transport aircraft. This is another view of the Boeing 777 wing. In the takeoff configuration, large slotted trailing-edge flaps deflect to increase the lift coefficient. The low-speed aileron near the wingtip also deflects to improve span loading during takeoff. This view also shows the single-slotted outboard flap, the high-speed aileron, and nearest the fuselage, the double-slotted inboard flap.

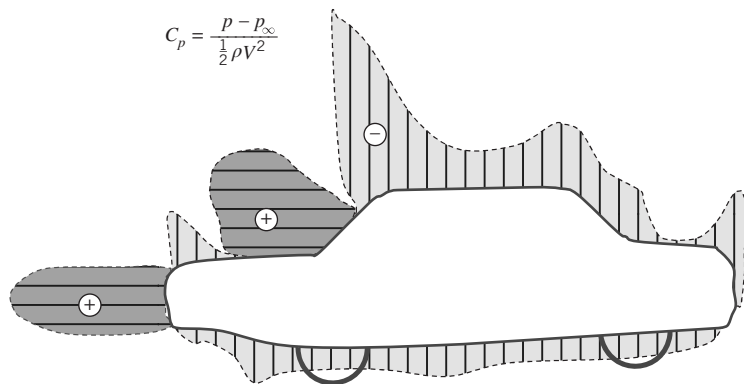


Fig. 9.25 Pressure distribution along the centerline of an automobile. (Based on data from Reference [13].)

wind tunnel for an automobile is shown in Fig. 9.25. The regions of positive and negative pressure coefficient are labeled with + and –, respectively, and indicate the levels of pressure on the automobile surfaces.

The pressure is low around the nose because of streamline curvature as the flow rounds the nose. The pressure reaches a maximum at the base of the windshield, again as a result of streamline curvature. Low-pressure regions also occur at the windshield header and over the top of the automobile. The air speed across the top is approximately 30 percent higher than the freestream air speed. The same effect occurs around the “A-pillars” at the windshield edges. The drag increase caused by an added object, such as an antenna, spotlight, or mirror at that location, thus would be $(1.3)^2 \approx 1.7$ times the drag the object would experience in an undisturbed flow field. Thus the *parasite drag* of an added component can be much higher than would be predicted from its drag calculated for free flow.

At high speeds, aerodynamic lift forces can unload tires, causing serious reductions in steering control and reducing stability to a dangerous extent. Liebeck airfoils [10] are used frequently for high-speed automobiles. Their high lift coefficients and relatively low drag allow downforce equal to or greater than the car weight to be developed at racing speeds. “Ground effect” cars use venturi-shaped ducts under the car and side skirts to seal leakage flows. The net result of these aerodynamic effects is that the downward force generates excellent traction without adding significant weight to the vehicle, allowing faster speeds through curves and leading to lower lap times.

Another method of boundary-layer control is use of moving surfaces to reduce skin friction effects on the boundary layer [14]. Tennis and soccer players use spin to control the trajectory and bounce of a shot. In golf, a drive can leave the tee at 275 ft/s or more, with backspin of 9000 rpm. Spin provides significant aerodynamic lift that substantially increases the carry of a drive. Spin is also largely responsible for hooking and slicing when shots are not hit squarely. Baseball pitchers use spin to throw a curve ball.

Flow about a spinning sphere is shown in Fig. 9.26a. Spin alters the pressure distribution and also affects the location of boundary-layer separation. Separation is delayed on the upper surface of the sphere in Fig. 9.26a, and it occurs earlier on the lower surface. Thus pressure is reduced on the upper surface and increased on the lower surface; the wake is deflected downward as shown. Pressure forces cause a lift in the direction shown; spin in the opposite direction would produce negative lift—a downward force. The force is directed perpendicular to both V and the spin axis.

Lift and drag data for spinning smooth spheres are presented in Fig. 9.26b. The most important parameter is the *spin ratio*, $\omega D / 2V$, the ratio of surface speed to freestream flow speed; Reynolds number plays a secondary role. At low spin ratio, lift is negative in terms of the directions shown in Fig. 9.26a. Only above $\omega D / 2V \approx 0.5$ does lift become positive and continue to increase as spin ratio increases. Lift coefficient levels off at about 0.35. Spin has little effect on sphere drag coefficient, which varies from about 0.5 to about 0.65 over the range of spin ratio shown.

Experimental data for lift and drag coefficients for spinning golf balls are presented in Fig. 9.27 for subcritical Reynolds numbers between 126,000 and 238,000. The lift coefficient on a golf ball with hexagonal dimples is significantly (up to 15 %) higher than on a ball with round dimples. The advantage

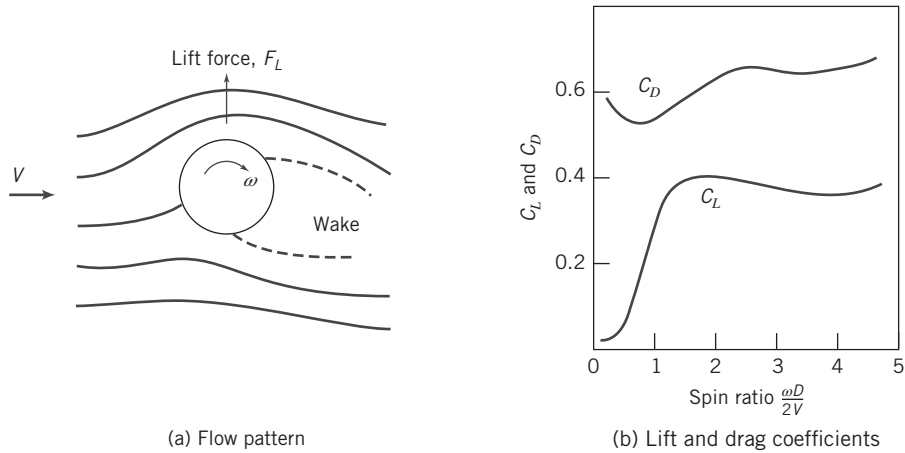


Fig. 9.26 Flow pattern, lift, and drag coefficients for a smooth spinning sphere in uniform flow. (Data from Reference [7].)

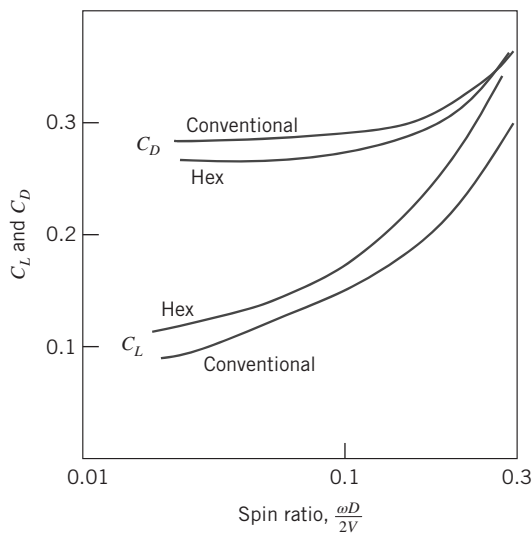


Fig. 9.27 Comparison of conventional and hex-dimpled golf balls. (Based on data from Reference [7].)

for hexagonal dimples continues to the largest spin ratios that were measured. The drag coefficient for a ball with hexagonal dimples is consistently 5 to 7 percent lower than the drag coefficient for a ball with round dimples at low spin ratios, but the difference becomes less pronounced as spin ratio increases.

Example 9.9 LIFT OF A SPINNING BALL

A smooth tennis ball, with 57 g mass and 64 mm diameter, is hit at 25 m/s with topspin of 7500 rpm. Calculate the aerodynamic lift acting on the ball. Evaluate the radius of curvature of its path at maximum elevation in a vertical plane. Compare with the radius for no spin.

Given: Tennis ball in flight, with $m = 57 \text{ g}$ and $D = 64 \text{ mm}$, hit with $V = 25 \text{ m/s}$ and topspin of 7500 rpm.

- Find:**
- Aerodynamic lift acting on ball.
 - Radius of curvature of path in vertical plane.
 - Comparison with radius for no spin.

Solution: Assume ball is smooth.

Use data from Fig. 9.26 to find lift:

$$C_L = f\left(\frac{\omega D}{2V}, Re_D\right).$$

From given data (for standard air, $\nu = 1.46 \times 10^{-5} \text{ m}^2/\text{s}$),

$$\frac{\omega D}{2V} = \frac{1}{2} \times 7500 \frac{\text{rev}}{\text{min}} \times 0.064 \text{ m} \times \frac{\text{s}}{25 \text{ m}} \times 2\pi \frac{\text{rad}}{\text{rev}} \times \frac{\text{min}}{60 \text{ s}} = 1.01$$

$$Re_D = \frac{VD}{\nu} = 25 \frac{\text{m}}{\text{s}} \times 0.064 \text{ m} \times \frac{\text{s}}{1.46 \times 10^{-5} \text{ m}^2} = 1.10 \times 10^5$$

From Fig. 9.26, $C_L \approx 0.3$, so

$$F_L = C_L A \frac{1}{2} \rho V^2$$

$$= C_L \frac{\pi D^2}{4} \frac{1}{2} \rho V^2 = \frac{\pi}{8} C_L D^2 \rho V^2$$

$$F_L = \frac{\pi}{8} \times 0.3 \times (0.064)^2 \text{ m}^2 \times 1.23 \frac{\text{kg}}{\text{m}^3} \times (25)^2 \frac{\text{m}^2}{\text{s}^2} \times \frac{\text{N} \cdot \text{s}^2}{\text{kg} \cdot \text{m}} = 0.371 \text{ N} \quad \text{--- } F_L$$

Because the ball is hit with topspin, this force acts downward.

Use Newton's second law to evaluate the curvature of the path. In the vertical plane,

$$\sum F_z = -F_L - mg = ma_z = -m \frac{V^2}{R} \quad \text{or} \quad R = \frac{V^2}{g + F_L/m}$$

$$R = (25)^2 \frac{\text{m}^2}{\text{s}^2} \left[\frac{1}{9.81 \frac{\text{m}}{\text{s}^2} + 0.371 \text{ N} \times \frac{1}{0.057 \text{ kg}} \times \frac{\text{kg} \cdot \text{m}}{\text{N} \cdot \text{s}^2}} \right]$$

$$R = 38.3 \text{ m (with spin)} \quad \text{--- } R$$

$$R = (25)^2 \frac{\text{m}^2}{\text{s}^2} \times \frac{\text{s}^2}{9.81 \text{ m}} = 63.7 \text{ m (without spin)} \quad \text{--- } R$$

Thus topspin has a significant effect on trajectory of the shot!

Cross flow about a rotating circular cylinder is qualitatively similar to flow about the spinning sphere shown schematically in Fig. 9.26a. If the velocity of the upper surface of a cylinder is in the same direction as the freestream velocity, separation is delayed on the upper surface; it occurs earlier on the lower surface. Thus the wake is deflected and the pressure distribution on the cylinder surface is altered when rotation is present. Pressure is reduced on the upper surface and increased on the lower surface, causing a net lift force acting upward. Spin in the opposite direction reverses these effects and causes a downward lift force.

Lift and drag coefficients for the rotating cylinder are based on projected area, LD . Experimentally measured lift and drag coefficients for subcritical Reynolds numbers between 40,000 and 660,000 are shown as functions of spin ratio in Fig. 9.28. When surface speed exceeds flow speed, the lift coefficient increases to surprisingly high values, while in two-dimensional flow, drag is affected only moderately. Induced drag, which must be considered for finite cylinders, can be reduced by using end disks larger in diameter than the body of the cylinder.

The power required to rotate a cylinder may be estimated from the skin friction drag of the cylinder surface using the tangential surface speed and surface area [15]. The power required to spin the cylinder, when expressed as an equivalent drag coefficient, may represent 20 percent or more of the aerodynamic C_D of a stationary cylinder [7].

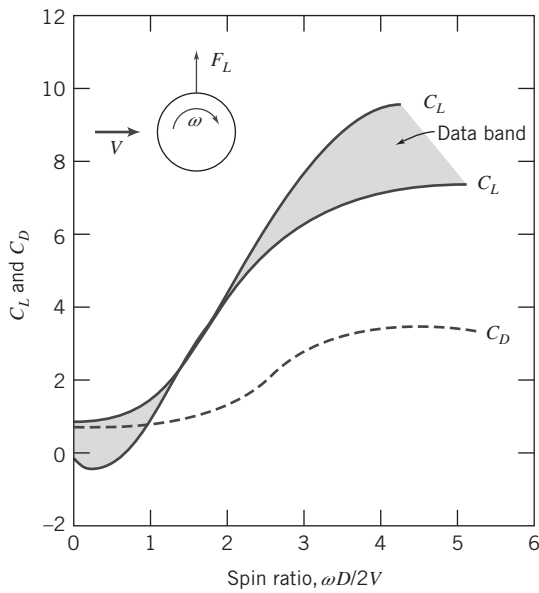


Fig. 9.28 Lift and drag of a rotating cylinder as a function of relative rotational speed; Magnus force. (Data from Reference [15].)

9.8 Summary and Useful Equations

In this chapter we have:

- ✓ Defined and discussed various terms commonly used in aerodynamics, such as: boundary-layer disturbance, displacement and momentum thicknesses; flow separation; streamlining; skin friction and pressure drag and drag coefficient; lift and lift coefficient; wing chord, span and aspect ratio; and induced drag.
- ✓ Derived expressions for the boundary-layer thickness on a flat plate (zero pressure gradient) using exact and approximate methods (using the momentum integral equation).
- ✓ Learned how to estimate the lift and drag from published data for a variety of objects.

While investigating the above phenomena, we developed insight into some of the basic concepts of aerodynamic design, such as how to minimize drag, how to determine the optimum cruising speed of an airplane, and how to determine the lift required for flight.

Note: Most of the equations in the table below have a number of constraints or limitations—*be sure to refer to their page numbers for details!*

Useful Equations

Definition of displacement thickness:	$\delta^* = \int_0^\infty \left(1 - \frac{u}{U}\right) dy \approx \int_0^\delta \left(1 - \frac{u}{U}\right) dy$	(9.1)	Page 296
Definition of momentum thickness:	$\theta = \int_0^\infty \frac{u}{U} \left(1 - \frac{u}{U}\right) dy \approx \int_0^\delta \frac{u}{U} \left(1 - \frac{u}{U}\right) dy$	(9.2)	Page 297
Boundary-layer thickness (laminar, exact—Blasius):	$\delta \approx \frac{5.0}{\sqrt{U/\nu x}} = \frac{5.0x}{\sqrt{Re_x}}$	(9.13)	Table 9.2, Page 300
Wall stress (laminar, exact—Blasius):	$\tau_w = 0.332U \sqrt{\rho \mu U/x} = \frac{0.332 \rho U^2}{\sqrt{Re_x}}$	(9.14)	Page 301

Table (Continued)

Skin friction coefficient (laminar, exact—Blasius):	$C_f = \frac{\tau_w}{\frac{1}{2}\rho U^2} = \frac{0.664}{\sqrt{Re_x}}$	(9.15)	Table 9.2, Page 301
Momentum integral equation:	$\frac{\tau_w}{\rho} = \frac{d}{dx}(U^2 \theta) + \delta^* U \frac{dU}{dx}$	(9.17)	Page 306
Boundary-layer thickness for flat plate (laminar, approximate—polynomial velocity profile):	$\frac{\delta}{x} = \sqrt{\frac{30\mu}{\rho U x}} = \frac{5.48}{\sqrt{Re_x}}$	(9.21)	Page 308
Definition of skin friction coefficient:	$C_f \equiv \frac{\tau_w}{\frac{1}{2}\rho U^2}$	(9.22)	Page 308
Skin friction coefficient for flat plate (laminar, approximate—polynomial velocity profile):	$C_f = \frac{0.730}{\sqrt{Re_x}}$	(9.23)	Page 309
Boundary-layer thickness for flat plate (turbulent, approximate— $\frac{1}{7}$ -power-law velocity profile):	$\frac{\delta}{x} = 0.382 \left(\frac{\nu}{Ux} \right)^{1/5} = \frac{0.382}{Re_x^{1/5}}$	(9.26)	Page 312
Skin friction coefficient for flat plate (turbulent, approximate— $\frac{1}{7}$ -power-law velocity profile):	$C_f = \frac{\tau_w}{\frac{1}{2}\rho U^2} = \frac{0.0594}{Re_x^{1/5}}$	(9.27)	Page 312
Definition of drag coefficient:	$C_D \equiv \frac{F_D}{\frac{1}{2}\rho V^2 A}$	(9.30)	Page 317
Drag coefficient for flat plate (entirely laminar, based on Blasius solution):	$C_D = \frac{1.33}{\sqrt{Re_L}}$	(9.33)	Page 317
Drag coefficient for flat plate (entirely turbulent, based on $\frac{1}{7}$ -power-law velocity profile):	$C_D = \frac{0.0742}{Re_L^{1/5}}$	(9.34)	Page 318
Drag coefficient for flat plate (empirical, $Re_L < 10^9$):	$C_D = \frac{0.455}{(\log Re_L)^{2.58}}$	(9.35)	Page 318
Drag coefficient for flat plate (based on $\frac{1}{7}$ th power-law velocity profile, $5 \times 10^5 \leq Re_L \leq 10^7$):	$C_D = \frac{0.0742}{Re_L^{1/5}} - \frac{1740}{Re_L}$	(9.37a)	Page 318
Drag coefficient for flat plate (empirical, $5 \times 10^5 \leq Re_L \leq 10^9$):	$C_D = \frac{0.455}{(\log Re_L)^{2.58}} - \frac{1610}{Re_L}$	(9.37b)	Page 318
Definition of lift coefficient:	$C_L \equiv \frac{F_L}{\frac{1}{2}\rho V^2 A_p}$	(9.38)	Page 328
Definition of aspect ratio:	$AR \equiv \frac{b^2}{A_p}$	(9.39)	Page 331
Drag coefficient of a wing (finite span airfoil, using $C_{D,\infty}$):	$C_D = C_{D,\infty} + C_{D,i} = C_{D,\infty} + \frac{C_L^2}{\pi AR}$	(9.42)	Page 332
Drag coefficient of a wing (finite span airfoil, using $C_{D,0}$):	$C_D = C_{D,0} + C_{D,i} = C_{D,0} + \frac{C_L^2}{\pi AR}$	(9.43)	Page 333

REF ERENC ES

- 1.** Prandtl, L., "Fluid Motion with Very Small Friction (in German)," *Proceedings of the Third International Congress on Mathematics*, Heidelberg, 1904; English translation available as NACA TM 452, March 1928.
- 2.** Blasius, H., "The Boundary Layers in Fluids with Little Friction (in German)," *Zeitschrift für Mathematik und Physik*, 56, 1, 1908, pp. 1–37; English translation available as NACA TM 1256, February 1950.
- 3.** Schlichting, H. and K. Gersten, *Boundary Layer Theory*, 9th ed. Berlin: Springer-Verlag, 2017.
- 4.** Stokes, G. G., "On the Effect of the Internal Friction of Fluids on the Motion of Pendulums," *Cambridge Philosophical Transactions*, IX, 8, 1851.
- 5.** Hoerner, S. F., *Fluid-Dynamic Drag*, 2nd ed. Midland Park, NJ: Published by the author, 1965.
- 6.** Fage, A., "Experiments on a Sphere at Critical Reynolds Numbers," Great Britain, *Aeronautical Research Council, Reports and Memoranda*, No. 1766, 1937.
- 7.** Goldstein, S., ed., *Modern Developments in Fluid Dynamics*, Vols. I and II. Oxford: Clarendon Press, 1938. (Reprinted in paperback by Dover, New York, 1967.)
- 8.** Morel, T., and M. Bohn, "Flow over Two Circular Disks in Tandem," *Transactions of the ASME, Journal of Fluids Engineering*, 102, 1, March 1980, pp. 104–111.
- 9.** Abbott, I. H., and A. E. von Doenhoff, *Theory of Wing Sections, Including a Summary of Airfoil Data*. New York: Dover, 1959 (paperback).
- 10.** Liebeck, R. H., "Design of Subsonic Airfoils for High Lift," *AIAA Journal of Aircraft*, 15, 9, September 1978, pp. 547–561.
- 11.** Smith, A. M. O., "Aerodynamics of High-Lift Airfoil Systems," in *Fluid Dynamics of Aircraft Stalling*, AGARD CP-102, 1973, pp. 10–1 through 10–26.
- 12.** Carr, G. W., "The Aerodynamics of Basic Shapes for Road Vehicles. Part 3: Streamlined Bodies," The Motor Industry Research Association, Warwickshire, England, Report No. 107/4, 1969.
- 13.** Goetz, H., "The Influence of Wind Tunnel Tests on Body Design, Ventilation, and Surface Deposits of Sedans and Sports Cars," SAE Paper No. 710212, 1971.
- 14.** Moktarian, F., and V. J. Modi, "Fluid Dynamics of Airfoils with Moving Surface Boundary-Layer Control," *AIAA Journal of Aircraft*, 25, 2, February 1988, pp. 163–169.
- 15.** Hoerner, S. F., and H. V. Borst, *Fluid-Dynamic Lift*. Bricktown, NJ: Hoerner Fluid Dynamics, 1975.
- 16.** L. Prandtl, *Ergebnisse der aerodynamischen, Veersuchsanstalt su Gottingen*. Vol II, 1923.
- 17.** H. Brauer, D. Sucker, "Umstromung von Platten, Zylindern und Kugeln," *Chemie Ingenieur Technik*, 48. Jahrgang, No. 8, 1976, p 665–671. Copyright Wiley-VCH Verlag GmbH & Co. KGaA. Reproduced with permission.
- 18.** The Engineering Toolbox, <http://www.EngineeringToolBox.com>.
- 19.** ANSYS Fluent, <https://www.ansys.com/>, 2019.

Chapter 10 Problems

Introduction and Classification of Fluid Machines; Turbomachinery Analysis

10.1 The geometry of a centrifugal water pump is $r_1 = 10\text{ cm}$, $r_2 = 20\text{ cm}$, $b_1 = b_2 = 4\text{ cm}$, $\beta_1 = 30^\circ$, $\beta_2 = 15^\circ$, and it runs at speed 1600 rpm. Estimate the discharge required for axial entry, the power generated in the water in watts, and the head produced.

10.2 The relevant variables for a turbomachine are, D , ω , Q , h , T , and ρ . Find the resulting Π -groups when D , ω , and ρ are the repeating variables. Discuss the meaning of each Π obtained.

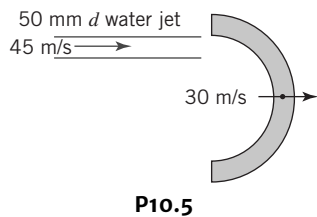
10.3 For the centrifugal pump impeller described in Example 10.1, draw the outlet velocity diagram for a blade angle of 60° . Determine the ideal head rise and mechanical power input and compare to that determined in Example 10.1. Explain the reason for the difference.

10.4 Dimensions of a centrifugal pump impeller are

Parameter	Inlet, Section ①	Outlet, Section ②
Radius, r (in.)	3	9.75
Blade width, b (in.)	1.5	1.125
Blade angle, β (deg)	60	70

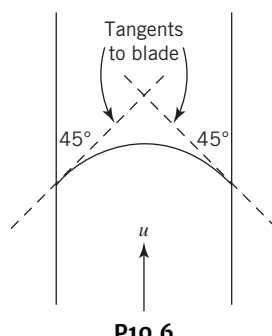
The pump is driven at 1250 rpm while pumping water. Calculate the theoretical head and mechanical power input if the flow rate is 1500 gpm.

10.5 Determine the force exerted by the jet on the single blade of a series of blades. Determine the power produced by the blade.



P10.5

SS 10.6 The absolute velocity of the water decreases from 41.5 m/s to 22.5 m/s as it passes through this blade system shown in the figure. The flow rate is 57 L/s. Determine the blade velocity U , the force on the blade, and the power produced by the blade system.



P10.6

10.7 A centrifugal water pump designed to operate at 1200 rpm has dimensions

Parameter	Inlet	Outlet
Radius, r (mm)	90	150
Blade width, b (mm)	10	7.5
Blade angle, β (deg)	25	45

Determine the flow rate at which the entering velocity has no tangential component. Draw the outlet velocity diagram, and determine the outlet absolute flow angle measured relative to the normal direction at this flow rate. Evaluate the hydraulic power delivered by the pump if its efficiency is 70 percent. Determine the head developed by the pump.

Pumps, Fans, and Blowers

10.8 Data from tests of a water suction pump operated at 2000 rpm with a 12-in.-diameter impeller are

Flow rate, Q (cfm)	36	50	74	88	125
Total head, H (ft)	190	195	176	162	120
Power input, \mathcal{P} (hp)	25	30	35	40	46

Plot the performance curves for this pump; include a curve of efficiency versus volume flow rate. Locate the best efficiency point and specify the pump rating at this point.

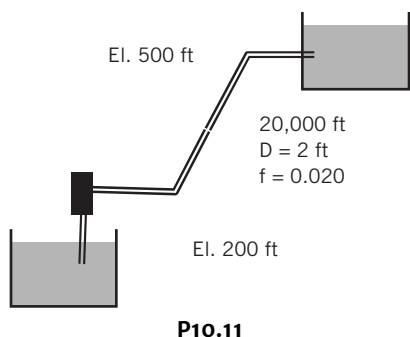
10.9 Data measured during tests of a centrifugal pump driven at 3000 rpm are

Parameter	Inlet, Section ①	Outlet, Section ②
Gage pressure, p (psi)	12.5	
Elevation above datum, z (ft)	6.5	32.5
Average speed of flow, \bar{V} (ft/s)	6.5	15

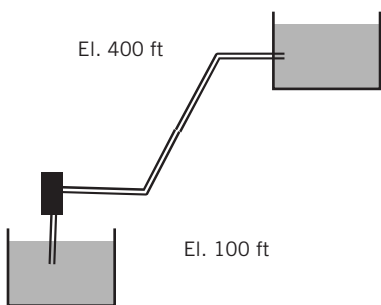
The flow rate is 65 gpm and the torque applied to the pump shaft is 4.75 lbf· ft. The pump efficiency is 75 percent, and the electric motor efficiency is 85 percent. Find (a) the electric power required and (b) the gage pressure at the pump outlet.

10.10 At its best efficiency point ($\eta = 0.87$), a mixed-flow pump, with $D = 16\text{ in.}$, delivers $Q = 2500\text{ cfm}$ of water at $H = 140\text{ ft}$ when operating at $N = 1350\text{ rpm}$. Calculate the specific speed of this pump. Estimate the required power input. Determine the curve-fit parameters of the pump performance curve based on the shutoff point and the best efficiency point. Scale the performance curve to estimate the flow, head, efficiency, and power input required to run the same pump at 820 rpm.

10.11 Using the performance curves in Appendix C, select the smallest diameter Peerless 8AE20G pump operating at 1770 rpm that will deliver a flow of at least 2000 gpm for the pipeline shown. Determine the actual flow rate and the pump electrical power requirement.



- 10.12** A pump (Peerless 8AE20G, Appendix C) with the 20-in impeller operates at 1775 rpm at maximum efficiency. It supplies the pipe-line shown in the figure. Determine the pipeline loss coefficient K in the equation $h_L = KQ^2$, with Q in gpm. Determine the flow rate between the two reservoirs if two of these pumps operate in parallel, assuming the pipeline K value remains unchanged.



- 10.13** Data from tests of a pump with a 12.3-in.-diameter impeller operated at 1450 rpm are

Flow rate, Q (cfm)	20	40	60	80	100	120	140
Net positive suction head required, $NPSHR$ (ft)	7.1	8.0	8.9	10.3	11.8	12.3	16.9

Develop and plot a curve-fit equation for $NPSHR$ versus volume flow rate in the form $NPSHR = a + bQ^2$, where a and b are constants. If the $NPSHA = 20$ ft, estimate the maximum allowable flow rate of this pump.

- 10.14** A four-stage boiler feed pump has suction and discharge lines of 10 cm and 7.5 cm inside diameter. At 3500 rpm, the pump is rated at $0.025 \text{ m}^3/\text{s}$ against a head of 125 m while handling water at 115°C . The inlet pressure gage, located 50 cm below the impeller centerline, reads 150 kPa. The pump is to be factory certified by tests at the same flow rate, head rise, and speed, but using water at 27°C . Calculate the $NPSHA$ at the pump inlet in the field installation. Evaluate the suction head that must be used in the factory test to duplicate field suction conditions.

- 10.15** A centrifugal pump operating at $N = 2265$ rpm lifts water between two reservoirs connected by 300 ft of 6-in.-diameter and 100 ft of 3-in.-diameter cast-iron pipe in series. The gravity lift is 25 ft. Estimate the head requirement, power needed, and hourly cost of electrical energy to pump water at 200 gpm to the higher reservoir. Assume that electricity costs $12\text{¢}/\text{kW}\cdot\text{hr}$ and that the electric motor efficiency is 85 percent. SS

- 10.16** Part of the water supply for the South Rim of Grand Canyon National Park is taken from the Colorado River [54]. A flow rate of 600 gpm taken from the river at elevation 3734 ft is pumped to a storage tank atop the South Rim at 7022 ft elevation. Part of the pipeline is above ground and part is in a hole directionally drilled at angles up to 70° from the vertical; the total pipe length is approximately 13,200 ft. Under steady-flow operating conditions, the frictional head loss is 290 ft of water in addition to the static lift. Estimate the diameter of the commercial steel pipe in the system. Compute the pumping power requirement if the pump efficiency is 61 percent.

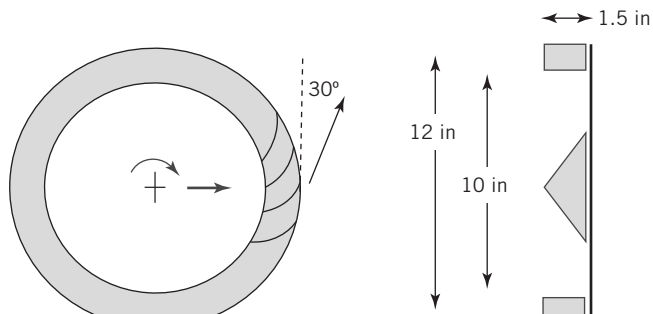
- 10.17** Performance data for a pump are

H (ft)	179	176	165	145	119	84	43
Q (gpm)	0	500	1000	1500	2000	2500	3000

Estimate the delivery when the pump is used to move water between two open reservoirs through 1200 ft of 12-in.-diameter commercial steel pipe containing two 90° elbows and an open gate valve with an elevation increase of 50 ft. Determine the gate valve loss coefficient needed to reduce the volume flow rate by half.

- 10.18** A fire nozzle is supplied through 300 ft of 3-in.-diameter canvas hose with $e = 0.001$ ft. Water from a hydrant is supplied at 50 psig to a booster pump on board the pumper truck. At design operating conditions, the pressure at the nozzle inlet is 100 psig and the pressure drop along the hose is 33 psig per 100 ft of length. Calculate the design flow rate and the maximum nozzle exit speed. Select a pump appropriate for this application, determine its efficiency at this operating condition, and calculate the power required to drive the pump.

- 10.19** A blower has a rotor with 12-in. outside diameter and 10-in. inside diameter with 1.5-in high rotor blades. The flow rate through the blower is $500 \text{ ft}^3/\text{min}$ at a rotor speed of 1800 rpm. The air at blade inlet is in the radial direction and the discharge angle is 30° from the tangential direction. Determine the power required by the blower motor.

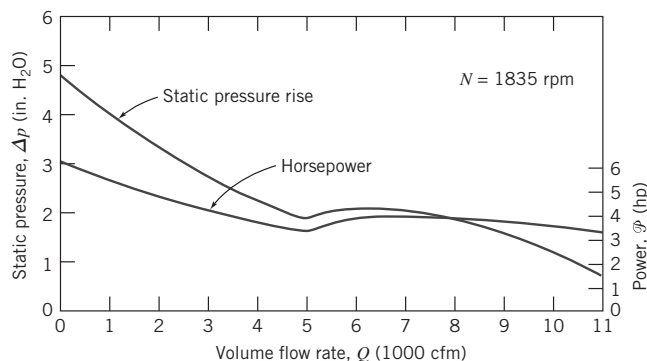


10.20 Performance data for a centrifugal fan of 3-ft diameter tested at 750 rpm are

Volume flow rate, Q (ft³/s)	106	141	176	211	246	282
Static pressure rise, Δp (psi)	0.075	0.073	0.064	0.050	0.033	0.016
Power output, \mathcal{P} (hp)	2.75	3.18	3.50	3.51	3.50	3.22

Plot the performance data versus volume flow rate. Calculate static efficiency, and show the curve on the plot. Find the best efficiency point, and specify the fan rating at this point.

SS 10.21 Performance characteristics of a Howden Buffalo axial flow fan are presented below. The fan is used to power a wind tunnel with 1-ft-square test section. The tunnel consists of a smooth inlet contraction, two screens each with loss coefficient $K = 0.12$, the test section, and a diffuser where the cross section is expanded to 24-in.-diameter at the fan inlet. Flow from the fan is discharged back to the room. Calculate and plot the system characteristic curve of pressure loss versus volume flow rate. Estimate the maximum air flow speed available in this wind tunnel test section.



P10.21

10.22 Experimental test data for an aircraft engine fuel pump are presented below. This gear pump is required to supply jet fuel at 450 pounds per hour and 150 psig to the engine fuel controller. Tests were conducted at 10, 96, and 100 percent of the rated pump speed of 4536 rpm. At each constant speed, the back pressure on the pump was set, and the flow rate was measured. On one graph, plot curves of pressure versus delivery at the three constant speeds. Estimate the pump displacement volume per revolution. Calculate the volumetric efficiency at each test point and sketch contours of constant η_v . Evaluate the energy loss caused by valve throttling at 100 percent speed and full delivery to the engine.

Pump Speed (rpm)	Back Pressure (psig)	Fuel Flow (pph*)	Pump Speed (rpm)	Back Pressure (psig)	Fuel Flow (pph)	Pump Speed (rpm)	Back Pressure (psig)	Fuel Flow (pph)
200	1810		200	1730		200	89	
4536	300	1810	4355	300	1750	453	250	73
(100%)	400	1810	(96%)	400	1735	(10%)	300	58.5
	500	1790		500	1720		350	45
	900	1720		900	1635		400	30

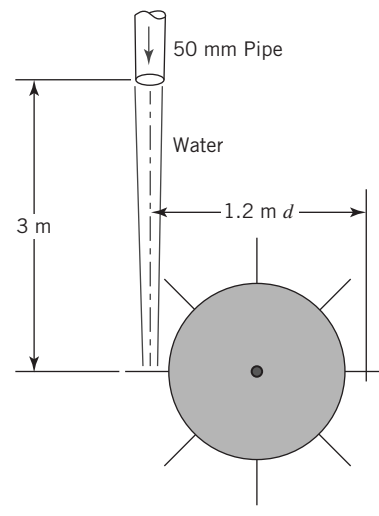
* Fuel flow rate measured in pounds per hour (pph).

Hydraulic Turbines

10.23 Conditions at the inlet to the nozzle of a Pelton wheel are **SS** $p = 700 \text{ psig}$ and $V = 15 \text{ mph}$. The jet diameter is $d = 7.5 \text{ in.}$ and the nozzle loss coefficient is $K_{\text{nozzle}} = 0.04$. The wheel diameter is $D = 8 \text{ ft}$. At this operating condition, $\eta = 0.86$. Calculate (a) the power output, (b) the normal operating speed, (c) the approximate runaway speed, (d) the torque at normal operating speed, and (e) the approximate torque at zero speed.

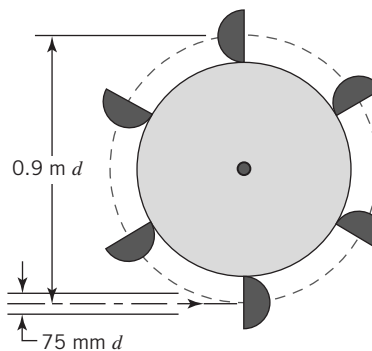
10.24 The runners on the Francis turbines installed at the Grand Coulee Dam on the Columbia River have diameters of 32.6 ft in diameter. At the rated conditions, each turbine develops 820,000 hp at 72 rpm under 285 ft of head at an efficiency of 95 percent. Calculate the specific speed at this condition and estimate the water flow rate through each turbine.

10.25 For a flow rate of 12 L/s and turbine speed of 65 rpm, estimate the power transferred from the jet to the turbine wheel.



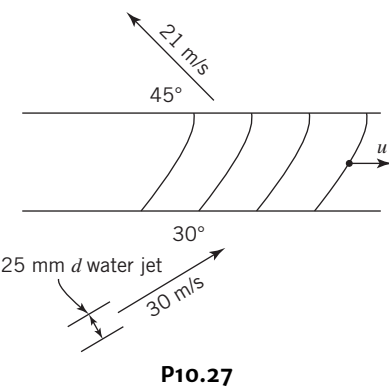
P10.25

10.26 The velocity of the water jet driving this impulse turbine is 45 m/s. The jet has a 75-mm diameter. After leaving the buckets the absolute velocity of the water is observed to be 15 m/s in a direction 60° to that of the original jet. Calculate the mean tangential force exerted by the jet on the turbine wheel and the speed (rpm) of the wheel.



P10.26

10.27 The absolute velocities and directions of the jets entering and leaving the blade system are as shown. Calculate the power transferred from the jet to the blade system and the blade angles required.



P10.27

Propellers and Wind Turbines

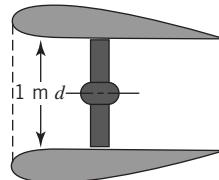
10.28 A fanboat in the Florida Everglades is powered by a propeller with $D = 1.5\text{ m}$ driven at maximum speed, $N = 1800\text{ rpm}$, by a 125 kW engine. Estimate the maximum thrust produced by the propeller at (a) standstill and (b) at boat speed of $V = 12.5\text{ m/s}$.

10.29 The propeller for the Gossamer Condor human-powered aircraft has $D = 12\text{ ft}$ and rotates at $N = 107\text{ rpm}$. The wing loading is 0.4 lbf/ft^2 of wing area, the drag is approximately 6 lbf at 12 mph , the total weight is 200 lbf , and the effective aspect ratio is 17. Estimate the dimensionless performance characteristics and efficiency of this propeller at cruise conditions. Assume the pilot expends 70 percent of maximum power at cruise conditions of 10.7 mph .

10.30 A typical American multiblade farm windmill has $D = 7\text{ ft}$ and is designed to produce maximum power in winds with $V = 15\text{ mph}$. Estimate the rate of water delivery as a function of the height to which the water is pumped. Determine the delivery (gpm) for a height of 25 ft .

SS 10.31 An airplane flies at 200 km/h through still air of specific weight 12 N/m^3 . The propeller is 2.4 m in diameter and its slipstream has a velocity of 290 km/h relative to the fuselage. Calculate (a) the propeller efficiency, (b) the velocity through the plane of the propeller, (c) the power input, (d) the power output, (e) the thrust of the propeller, and (f) the pressure difference across the propeller disk.

10.32 This ducted propeller unit drives a ship through still water at a speed of 4.5 m/s . Within the duct the mean velocity of the water relative to the unit is 15 m/s . Calculate the propulsive force produced by the unit. Calculate the force exerted on the fluid by the propeller. Account for the difference between these forces.



P10.32

10.33 Demonstrate that the ducted propeller system shown in the figure has an efficiency of $\frac{2V_1}{V_4 + V_1}$ when the forward speed is V_1 . For a specific design and operation, the ratios of velocity are $\frac{V_2}{V_1} = \frac{9}{4}$ and $\frac{V_4}{V_2} = \frac{5}{4}$. Determine the fractions of the propulsive force that will be contributed by the propeller and by the duct.

10.34 Determine the maximum power that a wind turbine with a diameter of 130 m can produce in a winds of 35 km/hr and 70 km/hr . If the wind blows at 35 km/hr for 1500 hours and 70 km/hr for 500 hours per year and the turbine efficiency is 0.92, estimate the energy output (kWh) and the number of households consuming 8000 kWh per year it could supply.

10.35 An air compressor with a compression ratio of 7 is designed to take 8.9 kg/s air at 1 atmosphere and 20°C . The design point speed, power requirement, and efficiency are 600 rpm , 5.6 MW , and 80 percent, respectively. A 1:5-scale model of the prototype is built to determine operability for the prototype. Determine the mass flow and power requirement for operation of the model at 80 percent efficiency for air at the same conditions.

10.36 A compressor has been designed for entrance conditions of 14.7 psia and 70°F with a rotating speed of 3200 rpm . The mass flow rate is 125 lbm/s . The compressor is tested on a day when the ambient temperature is 58°F and the inlet pressure is throttled to 8.0 psia . Determine the mass flow rate for the test.

CHAPTER 10

Fluid Machinery

- 10.1 Introduction and Classification of Fluid Machines
- 10.2 Turbomachinery Analysis
- 10.3 Pumps, Fans, and Blowers
- 10.4 Positive Displacement Pumps

- 10.5 Hydraulic Turbines
- 10.6 Propellers and Wind Turbines
- 10.7 Compressible Flow Turbomachines
- 10.8 Summary and Useful Equations

Case Study

Turbochargers have long been used on internal combustion engines as a way to increase the power for racing. Now, the technology is experiencing a revival. Adding a turbocharger such as the one shown in the photograph to an engine offers improved fuel economy, reduced CO₂ emissions, and better performance over a non-turbocharged engine. Turbocharging allows automobile manufacturers to reduce engine size and weight and still provide the power and performance demanded by customers.

A turbocharger consists of a turbine driven by the exhaust stream coupled to a compressor that takes in ambient air and discharges it into the cylinder at a high pressure. Normally, exhaust gases exit an engine at a high temperature and atmospheric pressure. By increasing the discharge pressure, the energy in the exhaust can be used to power a turbine that is coupled to a compressor. The compressor pumps intake air into the cylinders of the engine at a high pressure, and correspondingly density, which allows for more fuel to be injected. The power of the engine is then increased. Because the engine compression ratio determines the exhaust pressure, the exhaust pressure is then increased naturally without a loss of efficiency and the exhaust energy is utilized in the turbocharger.

Turbocharging provides more power under high loads so the engine is acting as a larger engine. For example, a two-liter turbocharged four-cylinder engine can match the output of a three-liter naturally aspirated engine. Under light loads, the turbocharger does not have enough exhaust energy to provide a significant boost, an issue that can be addressed using an electric motor to supplement the turbine at low loads. Adding

the electric motor also reduces the lag, which is the time it takes for the exhaust flow to increase and drive the turbine when the car accelerates.

Emissions are reduced and fuel economy increased because more of the exhaust energy is used to produce work. A smaller, turbocharged engine can increase mileage and lower emissions by 2–6 percent. Turbochargers are becoming more common on truck, car, train, aircraft, and construction equipment engines. As the technology develops further, the performance can be expected to continue to improve.



Oleksandr Moroz/Adobe Stock Photo

An automotive turbocharger.

Learning Objectives

After completing this chapter, you should be able to

- Describe the different types of turbomachines used for power production and moving fluids.
- Determine the performance of a turbomachine using the angular momentum principle.
- Use the performance characteristics of a pump, fan, or blower to determine the operating conditions.

- Determine the operating conditions using the performance characteristics of a positive displacement pump.
- Determine the operating conditions for a hydraulic turbine using the angular momentum principle.
- Determine the performance of a propeller or wind turbine.
- Use the dimensionless parameters to scale compressor performance between operating conditions.

Humans have sought to harness the forces of nature to offset human labor since antiquity. The first fluid machines developed were bucket wheels and screw pumps to lift water. The Romans introduced paddle wheels around 70 B.C.E. to obtain energy from streams [1]. Later, windmills were developed to harness wind power, but the low power density of the wind limited output to a few hundred horsepower. Development of waterwheels made it possible to extract thousands of horsepower at a single site.

Today we take many fluid machines for granted. On a typical day we draw water pressurized by pumps from the tap, drive a car in which fluid pumps operate the lubrication, cooling, and power steering systems, and work in a comfortable environment provided lights and cooling systems powered by electricity produced by steam or gas turbines. The list could be extended indefinitely.

A fluid machine is a device that either performs work on or extracts work from a fluid. This is a very large field of study, so we will limit ourselves mostly to incompressible flows. First the terminology of the field is introduced and machines are classified by operating principle and physical characteristics. We will focus on machines in which energy transfer to or from the fluid is through a rotating element. Basic equations are reviewed and then simplified to forms useful for analysis of fluid machines. Performance characteristics of typical machines are considered. We will use as examples pump and turbine applications in typical systems and then discuss propellers and wind turbines. A discussion of compressible flow machines concludes the chapter.

10.1 Introduction and Classification of Fluid Machines

Fluid machines may be broadly classified as either *positive displacement* or *dynamic*. Dynamic fluid-handling devices that direct the flow with blades or vanes attached to a rotating member are termed *turbomachines*. These devices are very widely used in industry for power generation (e.g., water and steam turbines) and in numerous other applications (e.g., the turbocharger of a high-performance car). In positive-displacement machines, energy transfer is accomplished by volume changes that occur due to movement of the boundary in which the fluid is confined. This includes piston-cylinder arrangements, gear pumps and lobe pumps. We will not analyze these devices but review them briefly. The emphasis in this chapter is on dynamic machines.

A further distinction among types of turbomachines is based on the geometry of the flow path. In *radial-flow* machines, the flow path is essentially radial, with significant changes in radius from inlet to outlet. Such machines sometimes are called *centrifugal* machines. In *axial-flow* machines, the flow path is nearly parallel to the machine centerline, and the radius of the flow path does not vary significantly. In *mixed-flow* machines the flow-path radius changes only moderately.

All work interactions in a turbomachine result from dynamic effects of the rotor on the fluid stream; that is, the transfer of work between the fluid and the rotating machine either increases or decreases the speed of the flow. However, in conjunction with this kinetic energy transfer, machines that include external housings also involve either the conversion of pressure energy to kinetic energy, or vice versa. This acceleration or deceleration of the flow allows for maximum pressure rise in pumps and compressors and for maximum power output from turbines.

Machines for Doing Work on a Fluid

Machines that add energy to a fluid by performing work on it are called *pumps* when the flow is liquid or slurry, and *fans*, *blowers*, or *compressors* for gas- or vapor-handling units, depending on pressure rise. Fans usually have small pressure rise (less than 1 inch of water) and blowers have moderate pressure rise (perhaps 1 inch of mercury); pumps and compressors may have very high pressure rises. Current industrial systems operate at pressures up to 150,000 psi (10^4 atmospheres).

Pumps and compressors consist of a rotating wheel (called an *impeller* or *rotor*, depending on the type of machine) driven by an external power source (e.g., a motor or another fluid machine) to increase

the flow kinetic energy, followed by an element to decelerate the flow, thereby increasing its pressure. This combination is known as a *stage*. These elements are contained within a *housing* or *casing*. A single pump or compressor might consist of several stages within a single housing, depending on the amount of pressure rise required of the machine. The shaft must penetrate the housing in order to receive mechanical work from the external power source. Bearings and seals are needed to minimize frictional (mechanical) losses and prevent leakage of the working fluid.

Three typical centrifugal machines are shown schematically in Fig. 10.1. The rotating element of a centrifugal pump or compressor is frequently called the impeller. Flow enters each machine nearly axially at small radius through the *eye* of the impeller, diagram (a), at radius r_1 . Flow is turned and leaves through the impeller discharge at radius r_2 , where the width is b_2 . As it leaves the impeller the fluid is collected in the *scroll* or *volute*. The increase in flow area reduces the fluid velocity and increases the pressure, as shown in diagram (b). The impeller usually has vanes; it may be *shrouded* (enclosed) as shown in diagram (a), or *open* as shown in diagram (c). The impeller vanes may be relatively straight, or they may be curved. Diagram (c) shows that the diffuser may have vanes to direct the flow between the impeller discharge and the volute; vanes allow for more efficient diffusion. Centrifugal machines are capable of higher pressure ratios than axial machines.

Typical axial- and mixed-flow turbomachines are shown schematically in Fig. 10.2. Figure 10.2a shows a typical axial-flow compressor stage. In these machines the rotating element is referred to as the rotor, and flow diffusion is achieved in the stator. Flow enters nearly parallel to the rotor axis and maintains nearly the same radius through the stage. The mixed-flow pump in diagram (b) shows the flow being turned outward and moving to larger radius as it passes through the stage. Axial flow machines have higher efficiencies and less frontal area than centrifugal machines, but they cannot achieve as high pressure ratios. As a result, axial flow machines are more likely to consist of multiple stages, making

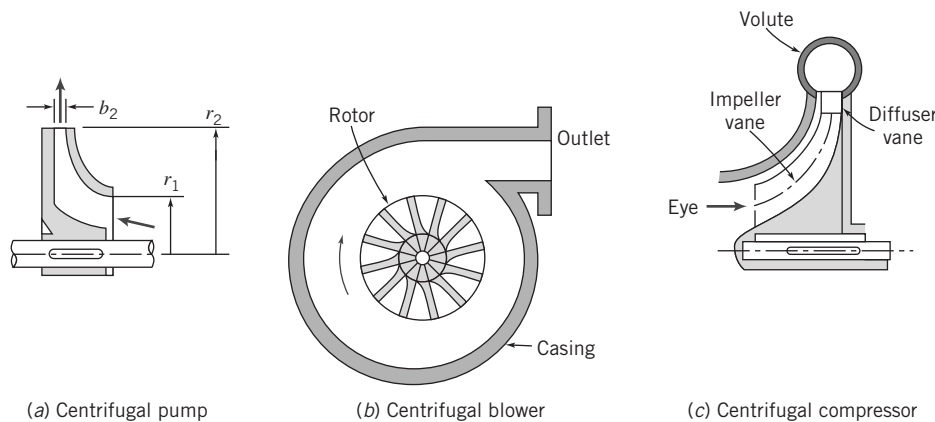


Fig. 10.1 Schematic diagrams of typical centrifugal-flow turbomachines, based on Reference [2].

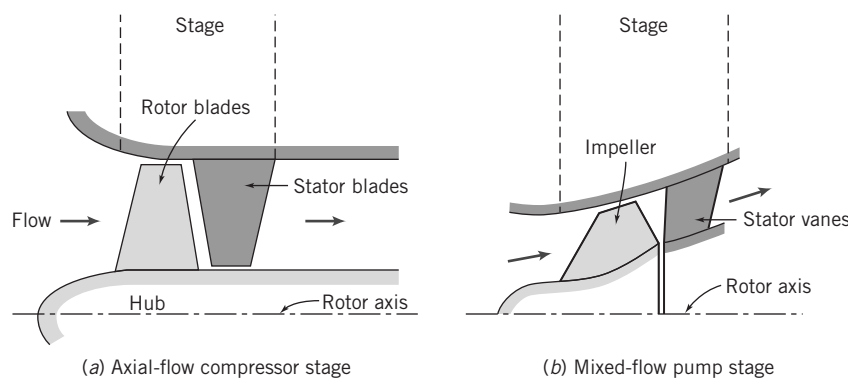
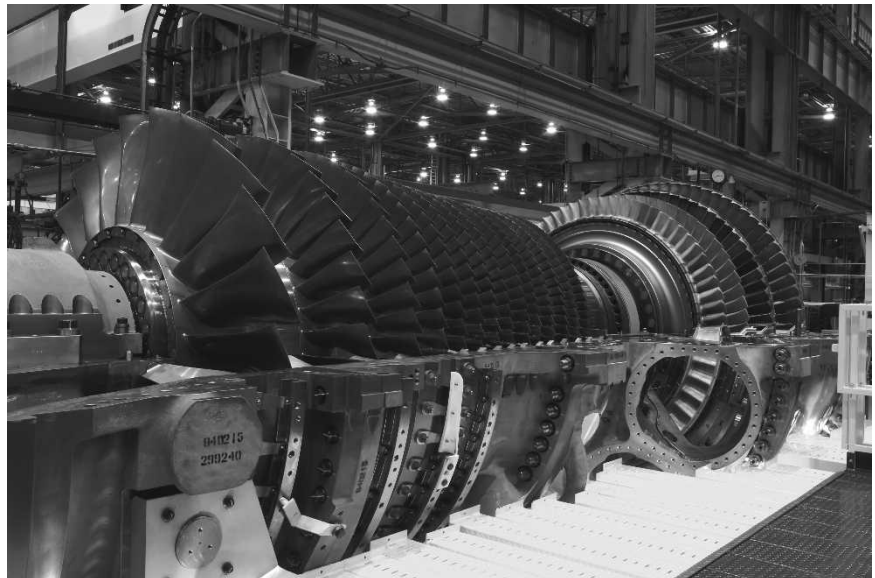


Fig. 10.2 Schematic diagrams of typical axial- and mixed-flow turbomachines, based on reference [2].



Reproduced with permission of General Electric Company

Fig. 10.3 Photograph of a multiple-stage axial-flow compressor rotor for a gas turbine.

them more complex than centrifugal machines. Figure 10.3 shows a multiple-stage axial flow compressor. In this photograph, the outer housing (to which the stator vanes are attached) has been removed, clearly showing the rows of rotor vanes.

The pressure rise that can be achieved efficiently in a single stage is limited, depending on the type of machine. The reason for this limitation can be understood based on the pressure gradients in these machines. In a pump or compressor, the boundary layer subjected to an adverse pressure gradient is not stable so flow is more likely to encounter boundary-layer separation in a compressor or pump. Boundary-layer separation increases the drag on the impeller, resulting in a decrease in efficiency and an increase in work needed.

Propellers are essentially axial-flow devices that operate without an outer housing. Propellers may be designed to operate in gases or liquids. Marine propellers tend to have wide blades compared with their radii, giving high *solidity*. Aircraft propellers tend to have long, thin blades with relatively low solidity. These machines will be discussed in detail in Section 10.6.

Machines for Extracting Work (Power) from a Fluid

Machines that extract energy from a fluid in the form of work are called *turbines*. In *hydraulic turbines*, the working fluid is water, so the flow is incompressible. In *gas turbines* and *steam turbines*, the density of the working fluid may change significantly. In a turbine, a stage normally consists of an element to accelerate the flow, converting some of its pressure energy to kinetic energy, followed by a *rotor*, *wheel*, or *runner* that extracts the kinetic energy from the flow via a set of *vanes*, *blades*, or *buckets* mounted on the wheel.

The two most general classifications of turbines are impulse and reaction turbines. *Impulse turbines* are driven by one or more high-speed free jets. The classic example of an impulse turbine is the water-wheel. In a waterwheel, the jets of water are driven by gravity. The kinetic energy of the water is transferred to the wheel, resulting in work. In more modern forms of impulse turbines, the jet is accelerated in a nozzle external to the turbine wheel. If friction and gravity are neglected, neither the fluid pressure nor speed relative to the runner changes as the fluid passes over the turbine buckets. Thus for an impulse turbine, the fluid acceleration and accompanying pressure drop take place in nozzles external to the blades, and work is extracted as a result of the large momentum change of the fluid.

In *reaction turbines*, part of the pressure change takes place externally and part takes place within the moving blades. The flow is turned to enter the runner in the proper direction as it passes through

nozzles or stationary blades, called *guide vanes* or *wicket gates*. Additional fluid acceleration relative to the rotor occurs within the moving blades, so both the relative velocity and the pressure of the stream change across the runner. Because reaction turbines flow full of fluid, they generally can produce more power for a given overall size than impulse turbines.

Figure 10.4 shows turbines used for different applications. Figure 10.4a shows a Pelton wheel, a type of impulse turbine wheel used in hydroelectric power plants. Figure 10.4b is a photograph of an axial steam turbine rotor, an example of a reaction turbine. Figure 10.4c is a wind turbine farm. A wind turbine is another example of a reaction turbine, but, like a propeller, also operates without an outer housing.

Several typical hydraulic turbines are shown schematically in Fig. 10.5. Figure 10.5a shows an impulse turbine driven by a single jet, which lies in the plane of the turbine runner. Water from the jet strikes each bucket in succession, is turned, and leaves the bucket with relative velocity nearly opposite to that with which it entered the bucket. Spent water falls into the *tailrace* (not shown).

A reaction turbine of the Francis type is shown in Fig. 10.5b. Incoming water flows circumferentially through the turbine casing. It enters the periphery of the stationary guide vanes and flows toward the runner. Water enters the runner nearly radially and is turned downward to leave nearly axially; the flow pattern may be thought of as a centrifugal pump in reverse. Water leaving the runner flows through a diffuser known as a *draft tube* before entering the tailrace. Figure 10.5c shows a propeller turbine of the Kaplan type. The water entry is similar to that in the Francis turbine, but it is turned to flow nearly axially before encountering the turbine runner. Flow leaving the runner may pass through a draft tube.

Thus turbines range from simple windmills to complex gas and steam turbines with many stages of carefully designed blading. These devices also can be analyzed in idealized form by applying the angular-momentum principle.

The allowable amount of pressure drop in a turbine stage is usually greater than the amount of pressure rise allowable in a compressor stage. The difference is due to the favorable pressure gradient that makes boundary-layer separation much less likely than in the case of the compressor.

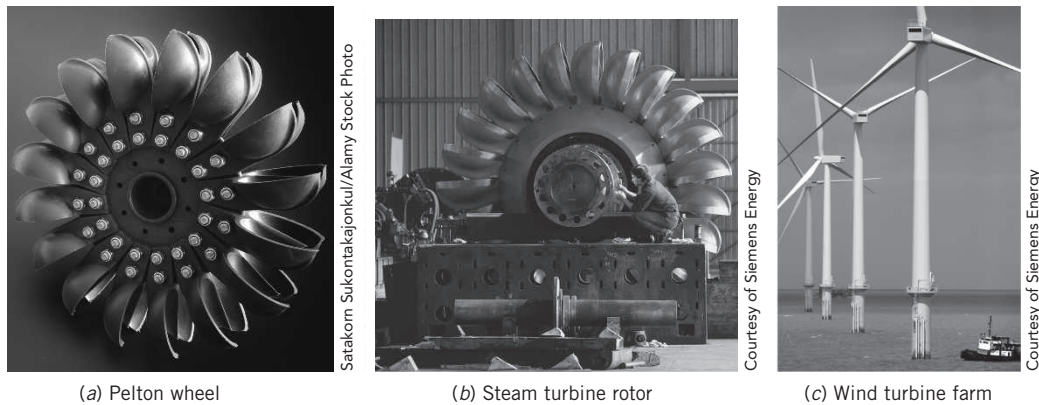


Fig. 10.4 Photograph of turbines used in different applications.

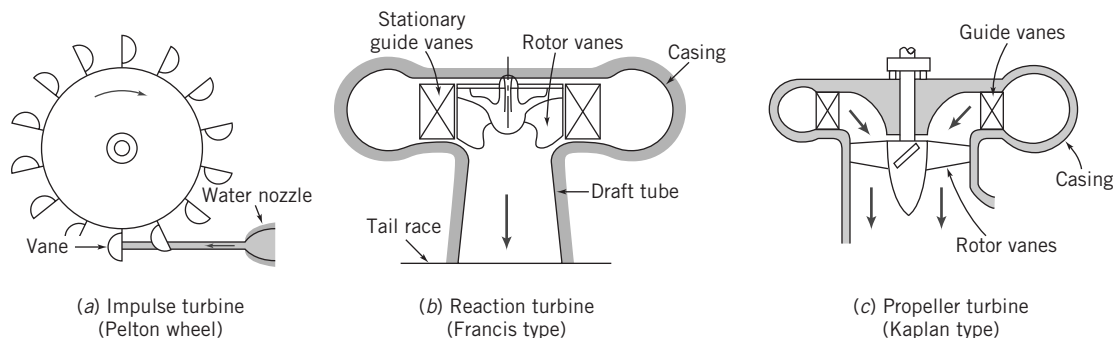


Fig. 10.5 Schematic diagrams of typical hydraulic turbines, based on Reference [2].

Dimensionless parameters, such as *specific speed*, *flow coefficient*, *torque coefficient*, *power coefficient*, and *pressure ratio*, are frequently used to characterize the performance of turbomachines. These are discussed at the end of the appropriate section.

Scope of Coverage

The turbomachinery industry is significant and thus the proper design, construction, selection, and application of pumps and compressors are economically important. Design of actual machines involves diverse technical knowledge, including fluid mechanics, materials, bearings, seals, and vibrations. Our objective here is to present only enough detail to illustrate the analytical basis of fluid flow design and to discuss briefly the limitations on results obtained from simple analytical models. The inherent complexity of the topic means that, on many occasions, we need to resort to empirical results and correlations.

10.2 Turbomachinery Analysis

We will analyze turbomachines using the conservation of mass, momentum, and energy principles applied to a control volume. The analysis that follows applies to machines both for doing work on and extracting work from a fluid flow.

The Angular-Momentum Principle: The Euler Turbomachine Equation

The angular-momentum principle was applied to finite control volumes in Chapter 4. The result was Eq. 4.46.

$$\vec{r} \times \vec{F}_s + \int_{CV} \vec{r} \times \vec{g} \rho dV + \vec{T}_{\text{shaft}} = \frac{\partial}{\partial t} \int_{CV} \vec{r} \times \vec{V} \rho dV + \int_{CV} \vec{r} \times \vec{V} \rho \vec{V} \cdot dA \quad (4.46)$$

Equation 4.46 states that the moment of surface forces and body forces, plus the applied torque, lead to a change in the angular momentum of the flow. The surface forces are due to friction and pressure, the body force is due to gravity, the applied torque could be positive or negative (depending on whether we are doing work on or extracting work from the fluid, respectively), and the angular-momentum change can arise as a change in angular momentum within the control volume or a flux of angular momentum across the control surface.

We will simplify Eq. 4.46 for analysis of turbomachinery. First, it is convenient to choose a fixed control volume enclosing the rotor to evaluate shaft torque. Because we are looking at control volumes for which we expect large shaft torques, as a first approximation torques due to surface forces may be ignored. This means we are neglecting friction and torque generated by pressure changes. The body force may be neglected by symmetry. Then, for steady flow, Eq. 4.46 becomes

$$\vec{T}_{\text{shaft}} = \int_{CV} \vec{r} \times \vec{V} \rho \vec{V} \cdot dA \quad (10.1a)$$

Equation 10.1a states that for a turbomachine with work *input*, the torque *required* causes a change in the fluid angular momentum. For a turbomachine with work *output*, the torque *produced* is due to the change in fluid angular momentum.

As shown in Fig. 10.6, we select a *fixed* control volume enclosing a generalized turbomachine rotor. The fixed coordinate system is chosen with the z -axis aligned with the axis of rotation of the machine. The idealized velocity components are shown in the figure. The fluid enters the rotor at radial location, r_1 , with uniform absolute velocity, \vec{V}_1 ; the fluid leaves the rotor at radial location, r_2 , with uniform absolute velocity \vec{V}_2 . For *uniform flow* into the rotor at Section 10.1, and out of the rotor at Section 10.2, Eq. 10.1a becomes

$$T_{\text{shaft}} \hat{k} = (r_2 V_{t_2} - r_1 V_{t_1}) \dot{m} \hat{k} \quad (10.1b)$$

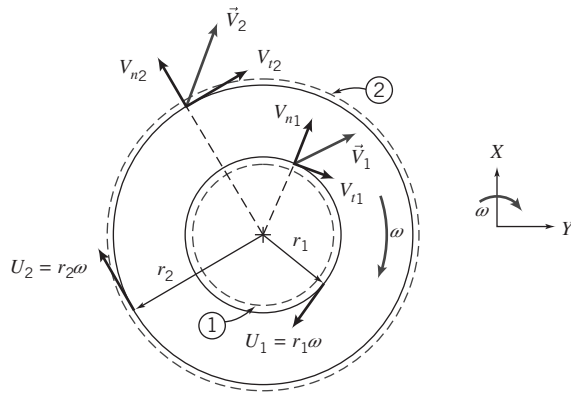


Fig. 10.6 Finite control volume and absolute velocity components for analysis of angular momentum.

For the product $\vec{r} \times \vec{V}$ the position vector \vec{r} is purely radial and only the tangential velocity component V_t counts. In scalar form,

$$T_{\text{shaft}} = (r_2 V_{t_2} - r_1 V_{t_1}) \dot{m} \quad (10.1c)$$

The assumptions we made in deriving this equation are *steady, frictionless flow, uniform flow* at inlet and exit, and *negligible pressure effects*. Equation 10.1c is the basic relationship between torque and angular momentum for all turbomachines and is often called the *Euler turbomachine equation*.

Each velocity that appears in Eq. 10.1c is the tangential component of the absolute velocity of the fluid crossing the control surface. The tangential velocities are chosen positive when in the same direction as the blade speed, U . This sign convention gives $T_{\text{shaft}} > 0$ for pumps, fans, blowers, and compressors and $T_{\text{shaft}} < 0$ for turbines.

The rate of work \dot{W}_m done on a turbomachine rotor is given by the dot product of rotor angular velocity, $\vec{\omega}$, and applied torque, \vec{T}_{shaft} . Using Eq. 10.1b, we obtain

$$\dot{W}_m = \vec{\omega} \cdot \vec{T}_{\text{shaft}} = \omega \hat{k} \cdot T_{\text{shaft}} \hat{k} = \omega \hat{k} \cdot (r_2 V_{t_2} - r_1 V_{t_1}) \dot{m} \hat{k}$$

or

$$\dot{W}_m = \omega T_{\text{shaft}} = \omega (r_2 V_{t_2} - r_1 V_{t_1}) \dot{m} \quad (10.2a)$$

According to Eq. 10.2a, the angular momentum of the fluid is increased by the addition of shaft work. For a pump, $\dot{W}_m > 0$ and the angular momentum of the fluid must increase. For a turbine, $\dot{W}_m < 0$ and the angular momentum of the fluid must decrease.

Equation 10.2a may be written in two other useful forms. Introducing $U = r\omega$, where U is the tangential speed of the rotor at radius r , we have

$$\dot{W}_m = (U_2 V_{t_2} - U_1 V_{t_1}) \dot{m} \quad (10.2b)$$

Dividing Eq. 10.2b by $\dot{m}g$, we obtain a quantity with the dimensions of length, which may be viewed as the theoretical head, or energy per unit weight, added to the flow.

$$H = \frac{\dot{W}_m}{\dot{m}g} = \frac{1}{g} (U_2 V_{t_2} - U_1 V_{t_1}) \quad (10.2c)$$

Equations 10.1 and 10.2 are simplified forms of the angular-momentum equation for a control volume. They all are written for a fixed control volume under the assumptions of steady, uniform flow at each section. The equations show that only the difference in the product rV_t or UV_t , between the outlet and inlet sections, is important in determining the torque applied to the rotor or the mechanical power.

Although $r_2 > r_1$ in Fig. 10.6, no restriction has been made on geometry; the fluid may enter and leave at the same or different radii. Therefore, these equations may be used for axial, radial, or mixed-flow machines.

Velocity Diagrams

The equations that we have derived also suggest the importance of clearly defining the velocity components of the fluid and rotor at the inlet and outlet sections. For this purpose, it is useful to develop *velocity diagrams* for the inlet and outlet flows. Figure 10.7 shows the velocity diagrams and introduces the notation for blade and flow angles. The important notation to remember is that the variable V is typically used to indicate absolute velocity, while the variable W is used to indicate flow velocity relative to the rotating blade.

Machines are designed such that at *design condition* the fluid moves smoothly through the blades. In the idealized situation at the *design speed*, sometimes called shockless entry, flow relative to the rotor is assumed to enter and leave tangent to the blade profile at each section. At speeds other than design speed the fluid may impact the blades at inlet, exit at an angle relative to the blade, or may have significant flow separation, leading to machine inefficiency. Figure 10.7 is representative of a typical radial flow machine. We assume the fluid is moving without major flow disturbances through the machine, as shown in Fig. 10.7a, with blade inlet and exit angles β_1 and β_2 , respectively, relative to the circumferential direction. Note that although angles β_1 and β_2 are both less than 90° in Fig. 10.7, in general they can be less than, equal to, or greater than 90° , and the analysis that follows applies to all of these possibilities.

The runner speed at inlet is $U_1 = r_1\omega$, and therefore it is specified by the impeller geometry and the machine operating speed. The absolute fluid velocity is the vector sum of the impeller velocity and the flow velocity relative to the blade. The absolute inlet velocity may be determined graphically, as shown in Fig. 10.7b. The angle of the absolute fluid velocity, α_1 , is measured from the direction normal to the flow area, as shown. Note that for a given machine, angles α_1 and α_2 will vary with flow rate, Q , (through \vec{V}_1 and \vec{V}_2) and rotor speed, ω (through U_1 and U_2). The tangential component of the absolute velocity, V_{t1} , and the component normal to the flow area, V_{n1} , are also shown in Fig. 10.7b. At each section the normal component of the absolute velocity, V_n , and the normal component of the velocity relative to the blade, W_n , are equal because the blade has no normal velocity. The absolute velocity at the machine entrance depends on whether swirl exists at the entrance. Swirl is the presence of a circumferential velocity component. When the inlet flow is swirl free, the absolute inlet velocity will be purely radial.

The velocity diagram is constructed similarly at the outlet section. The runner speed at the outlet is $U_2 = r_2\omega$, which again is known from the geometry and operating speed of the turbomachine. The relative flow is assumed to leave the impeller tangent to the blades, as shown in Fig. 10.7c. This idealizing assumption of perfect guidance fixes the direction of the relative outlet flow at design conditions.

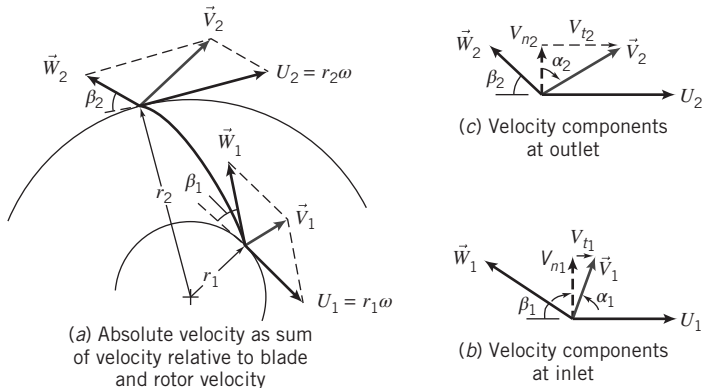


Fig. 10.7 Geometry and notation used to develop velocity diagrams for typical radial-flow machines.

For a centrifugal pump or reaction turbine, the velocity relative to the blade generally changes in magnitude from inlet to outlet. The continuity equation must be applied to determine the normal component of velocity at each section. The normal component together with the outlet blade angle is sufficient to establish the velocity relative to the blade at the impeller outlet for a radial-flow machine. The velocity diagram is completed by the vector addition of the velocity relative to the blade and the wheel velocity, as shown in Fig. 10.7c.

The inlet and outlet velocity diagrams provide all the information needed to calculate the ideal torque or power, absorbed or delivered by the impeller, using Eqs. 10.1 or 10.2. The results represent the performance of a turbomachine under idealized conditions at the design operating point, since we have assumed:

- Negligible torque due to surface forces (viscous and pressure).
- Inlet and exit flow tangent to blades.
- Uniform flow at inlet and exit.

An actual turbomachine is not likely to conform to all of these assumptions, so the results of our analysis represent the upper limit of the performance of actual machines. In Example 10.1 we will use the Euler turbomachine equation to analyze an idealized centrifugal pump.

Example 10.1 IDEALIZED CENTRIFUGAL PUMP

A centrifugal pump is used to pump 150 gpm of water. The water enters the impeller axially through a 1.25-in.-diameter inlet. The inlet velocity is axial and uniform. The impeller outlet diameter is 4 in. Flow leaves the impeller at 10 ft/s relative to the blades, which are radial at the exit. The impeller speed is 3450 rpm. Determine the impeller exit width, b_2 , the torque input, and the power predicted by the Euler turbine equation.

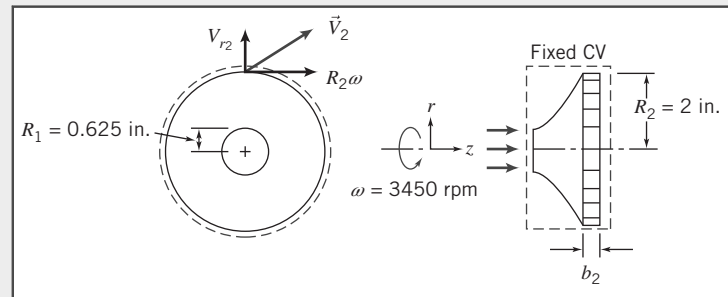
Given: Flow as shown in the figure:

$$V_{r2} = 10 \text{ ft/s}, Q = 150 \text{ gpm}$$

Find: (a) b_2 .
(b) T_{shaft} .
(c) \dot{W}_m .

Solution: Apply the Euler turbomachine equation to a fixed control volume.

Governing equations:



$$T_{\text{shaft}} = (r_2 V_{t2} - r_1 V_{t1}) \dot{m} \quad (10.1c)$$

$$\frac{\partial}{\partial t} \int_{\text{CV}} \rho dV + \int_{\text{CS}} \rho \vec{V} \cdot d\vec{A} = 0 \quad (4.12)$$

Assumptions:

- 1 Neglect torques due to body and surface forces.
- 2 Steady flow.
- 3 Uniform flow at inlet and outlet sections.
- 4 Incompressible flow.

Then, from continuity,

$$(-\rho V_1 \pi R_1^2) + (\rho V_{r2} 2\pi R_2 b_2) = 0$$

or

$$\dot{m} = \rho Q = \rho V_{r_2} 2\pi R_2 b_2$$

so that

$$b_2 = \frac{Q}{2\pi R_2 V_{r_2}} = \frac{1}{2\pi} \times 150 \frac{\text{gal}}{\text{min}} \times \frac{1}{2 \text{ in.}} \times \frac{\text{s}}{10 \text{ ft}} \times \frac{\text{ft}^3}{7.48 \text{ gal}} \times \frac{\text{min}}{60 \text{ s}} \times 12 \frac{\text{in.}}{\text{ft}}$$

$$b_2 = 0.0319 \text{ ft or } 0.383 \text{ in.} \quad \underline{\hspace{10cm}}^{b_2}$$

For an axial inlet the tangential velocity $V_{t_1} = 0$, and for radial exit blades $V_{t_2} = R_2 \omega$, so Eq. 10.1c reduces to

$$T_{\text{shaft}} = R_2^2 \omega \dot{m} = \omega R_2^2 \rho Q$$

where we have used continuity ($\dot{m} = \rho Q$).

Thus,

$$T_{\text{shaft}} = \omega R_2^2 \rho Q = 3450 \frac{\text{rev}}{\text{min}} \times (2)^2 \text{ in.}^2 \times 1.94 \frac{\text{slug}}{\text{ft}^3} \times 150 \frac{\text{gal}}{\text{min}}$$

$$\times 2\pi \frac{\text{rad}}{\text{rev}} \times \frac{\text{min}^2}{3600 \text{ s}^2} \times \frac{\text{ft}^3}{7.48 \text{ gal}} \times \frac{\text{ft}^2}{144 \text{ in.}^2} \times \frac{\text{lbf} \cdot \text{s}^2}{\text{slug} \cdot \text{ft}}$$

$$T_{\text{shaft}} = 6.51 \text{ ft} \cdot \text{lbf} \quad \underline{\hspace{10cm}}^{T_{\text{shaft}}}$$

and

$$\dot{W}_m = \omega T_{\text{shaft}} = 3450 \frac{\text{rev}}{\text{min}} \times 6.51 \text{ ft} \cdot \text{lbf} \times 2\pi \frac{\text{rad}}{\text{rev}} \times \frac{\text{min}}{60 \text{ s}} \times \frac{\text{hp} \cdot \text{s}}{550 \text{ ft} \cdot \text{lbf}}$$

$$\dot{W}_m = 4.28 \text{ hp} \quad \underline{\hspace{10cm}}^{\dot{W}_m}$$

This problem illustrates the application of the Euler turbomachine equation for a fixed control volume to a centrifugal flow machine.

Performance—Hydraulic Power

The torque and power predicted by applying the angular-momentum equation to a turbomachine rotor (Eqs. 10.1c and 10.2a) are idealized values. In practice, rotor power and the rate of change of fluid energy are not equal. Losses are caused by viscous effects, non-uniform flow, mis-matched flow direction and blade angle, and inefficiencies in the diffuser. Energy *dissipation* occurs in seals and bearings and in fluid friction between the rotor and housing of the machine (“windage” losses). Because of these losses, in a pump the actual power delivered to the fluid is less than predicted by the angular-momentum equation. In the case of a turbine, the actual power delivered to the shaft is less than the power given up by the fluid stream.

We can define the power, head, and efficiency of a turbomachine based on whether the machine does work on the fluid or extracts work from the fluid. For a pump, the *hydraulic power* is given by the rate of mechanical energy input to the fluid,

$$\dot{W}_h = \rho Q g H_p \quad (10.3a)$$

where

$$H_p = \left(\frac{p}{\rho g} + \frac{\bar{V}^2}{2g} + z \right)_{\text{discharge}} - \left(\frac{p}{\rho g} + \frac{\bar{V}^2}{2g} + z \right)_{\text{suction}} \quad (10.3b)$$

The mechanical input power needed to drive the pump is greater than that to produce the head rise due to inefficiencies. We define the *pump efficiency* as

$$\eta_p = \frac{\dot{W}_h}{\dot{W}_m} = \frac{\rho Q g H_p}{\omega T} \quad (10.3c)$$

For a hydraulic turbine, the *hydraulic power* is defined as the rate of mechanical energy removal from the flowing fluid stream,

$$\dot{W}_h = \rho Q g H_t \quad (10.4a)$$

where

$$H_t = \left(\frac{p}{\rho g} + \frac{\bar{V}^2}{2g} + z \right)_{\text{inlet}} - \left(\frac{p}{\rho g} + \frac{\bar{V}^2}{2g} + z \right)_{\text{outlet}} \quad (10.4b)$$

For a hydraulic turbine, the power output obtained from the rotor is less than the rate of energy transfer from the fluid to the rotor, because the rotor must overcome friction and windage losses. The mechanical power output obtained from the turbine is related to the hydraulic power by defining *turbine efficiency* as

$$\eta_t = \frac{\dot{W}_m}{\dot{W}_h} = \frac{\omega T}{\rho Q g H_t} \quad (10.4c)$$

Equations 10.4a and 10.4b show that *to obtain maximum power output from a hydraulic turbine, it is important to minimize the mechanical energy in the flow leaving the turbine.* This is accomplished by making the outlet pressure, flow speed, and elevation as small as practical.

Dimensional Analysis and Specific Speed

Dimensional analysis for turbomachines was introduced in Chapter 7, where dimensionless flow, head, and power coefficients were derived in generalized form. The independent parameters were the flow coefficient and a form of Reynolds number. The dependent parameters were the head and power coefficients.

Our objective here is to develop the forms of dimensionless coefficients in common use and to give examples illustrating their use in selecting a machine type, designing model tests, and scaling results. Since we developed an idealized theory for turbomachines, we can gain additional physical insight by developing dimensionless coefficients directly from the resulting computing equations. We will then apply these expressions to scaling of turbomachines through similarity rules in Section 10.3.

The dimensionless *flow coefficient*, Φ , is defined by normalizing the volume flow rate using the exit area and the wheel speed at the outlet. Thus

$$\Phi = \frac{Q}{A_2 U_2} = \frac{V_{n2}}{U_2} \quad (10.5)$$

where V_{n2} is the velocity component perpendicular to the exit area. This component is also referred to as the *meridional velocity* at the wheel exit plane. It appears in true projection in the *meridional plane*, which is any radial cross-section through the centerline of a machine.

A dimensionless head coefficient, Ψ , may be obtained by normalizing the head, H (Eq. 10.2c), with U_2^2/g . Thus

$$\Psi = \frac{gH}{U_2^2} \quad (10.6)$$

A dimensionless torque coefficient, τ , may be obtained by normalizing the torque, T (Eq. 10.1c), with $\rho A_2 U_2^2 R_2$. Thus

$$\tau = \frac{T}{\rho A_2 U_2^2 R_2} \quad (10.7)$$

Finally, the dimensionless power coefficient, Π , is obtained by normalizing the power, \dot{W} (Eq. 10.2b), with $\dot{m}U_2^2 = \rho Q U_2^2$. Thus

$$\Pi = \frac{\dot{W}}{\rho Q U_2^2} = \frac{\dot{W}}{\rho \omega^2 Q R_2^2} \quad (10.8)$$

For pumps, mechanical input power exceeds hydraulic power, and the efficiency is defined as $\eta_p = \dot{W}_h / \dot{W}_m$ (Eq. 10.3c). Hence

$$\dot{W}_m = T\omega = \frac{1}{\eta_p} \dot{W}_h = \frac{\rho Q g H_p}{\eta_p} \quad (10.9)$$

Introducing dimensionless coefficients Φ (Eq. 10.5), Ψ (Eq. 10.6), and τ (Eq. 10.7) into Eq. 10.9, we obtain an analogous relation among the dimensionless coefficients as

$$\tau = \frac{\Psi \Phi}{\eta_p} \quad (10.10)$$

For turbines, mechanical output power is less than hydraulic power, and the efficiency is defined as $\eta_t = \dot{W}_m / \dot{W}_h$ (Eq. 10.4c). Hence

$$\dot{W}_m = T\omega = \eta_t \dot{W}_h = \eta_t \rho Q g H_p \quad (10.11)$$

Introducing dimensionless coefficients Φ , Ψ , and τ into Eq. 10.11, we obtain an analogous relation among the dimensionless coefficients as

$$\tau = \Psi \Phi \eta_t \quad (10.12)$$

The dimensionless coefficients form the basis for designing model tests and scaling the results. The flow coefficient, Φ , is the independent parameter, and the head, torque, and power coefficients are dependent parameters. Under these assumptions, dynamic similarity is achieved when the flow coefficient is matched between model and prototype machines.

A useful parameter called *specific speed* can be obtained by combining the flow and head coefficients and eliminating the machine size. The result is,

$$N_S = \frac{\omega Q^{1/2}}{h^{3/4}} \quad (7.22a)$$

When head is expressed as energy per unit mass (i.e., with dimensions equivalent to L^2/t^2 , or g times head in height of liquid), and ω is expressed in radians per second, the specific speed defined by Eq. 7.22a is dimensionless.

Although specific speed is a dimensionless parameter, it is common practice to use an “engineering” equation form of Eq. 7.22a in which ω and Q are specified in convenient units, and energy per unit mass, h , is replaced with energy per unit weight of fluid, H . When this is done, the specific speed is not a unitless parameter and the magnitude of the specific speed depends on the units used to calculate it. Customary units used in U.S. engineering practice for pumps are rpm for ω , gpm for Q , and feet for H . In practice, the symbol N is used to represent rate of rotation (ω) in rpm. Thus, the dimensional specific speed for pumps, expressed in U.S. customary units, as an “engineering” equation, becomes

$$N_{S_{cu}} = \frac{N(\text{rpm})[Q(\text{gpm})]^{1/2}}{[H(\text{ft})]^{3/4}} \quad (7.22b)$$

For hydraulic turbines, we use the fact that power output is proportional to flow rate and head, $\mathcal{P} \propto \rho Qh$ in consistent units. Substituting $\mathcal{P}/\rho h$ for Q in Eq. 7.22a gives

$$N_S = \frac{\omega}{h^{3/4}} \left(\frac{\mathcal{P}}{\rho h} \right)^{1/2} = \frac{\omega P^{1/2}}{\rho^{1/2} h^{5/4}} \quad (10.13a)$$

as the nondimensional form of the specific speed.

In U.S. engineering practice it is customary to drop the factor $\rho^{1/2}$ because water is invariably the working fluid in the turbines to which the specific speed is applied and to use head H in place of energy per unit mass h . Customary units used in U.S. engineering practice for hydraulic turbines are rpm for ω , horsepower for \mathcal{P} , and feet for H . In practice, the symbol N is used to represent rate of rotation (ω) in rpm. Thus the dimensional specific speed for a hydraulic turbine, expressed in U.S. customary units, as an “engineering” equation, becomes

$$N_{S_{cu}} = \frac{N(\text{rpm})[\mathcal{P}(\text{hp})]^{1/2}}{[H(\text{ft})]^{5/4}} \quad (10.13b)$$

Specific speed may be thought of as the operating speed at which a pump produces unit head at unit volume flow rate (or, for a hydraulic turbine, unit power at unit head). To see this, solve for N in Eqs. 7.22b and 10.13b, respectively. For pumps

$$N(\text{rpm}) = N_{S_{cu}} \frac{[H(\text{ft})]^{3/4}}{[Q(\text{gpm})]^{1/2}}$$

and for hydraulic turbines

$$N(\text{rpm}) = N_{S_{cu}} \frac{[H(\text{ft})]^{5/4}}{[\mathcal{P}(\text{hp})]^{1/2}}$$

Holding specific speed constant describes all operating conditions of geometrically similar machines with similar flow conditions.

It is customary to characterize a machine by its specific speed at the design point. Low specific speeds correspond to efficient operation of radial-flow machines. High specific speeds correspond to efficient operation of axial-flow machines. For a specified head and flow rate, one can choose either a low specific speed machine (which operates at low speed) or a high specific speed machine (which operates at higher speed).

Typical proportions for commercial pump designs and their variation with dimensionless specific speed are shown in Fig. 10.8. In this figure, the size of each machine has been adjusted to give the same head and flow rate for rotation at a speed corresponding to the specific speed. Thus it can be seen that if the machine’s size and weight are critical, one should choose a higher specific speed. Figure 10.8 shows

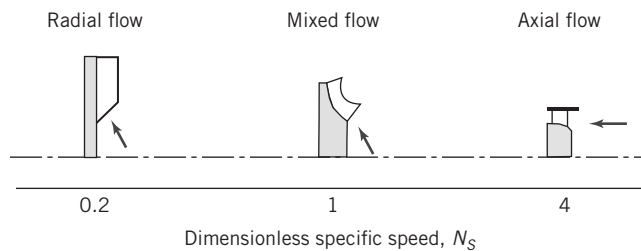


Fig. 10.8 Typical geometric proportions of commercial pumps as a function of dimensionless specific speed, adapted from Reference [3].

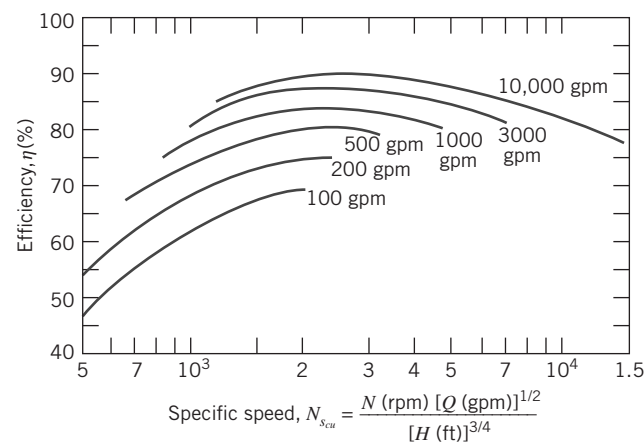


Fig. 10.9 Average efficiencies of commercial pumps as they vary with specific speed and pump size [4].

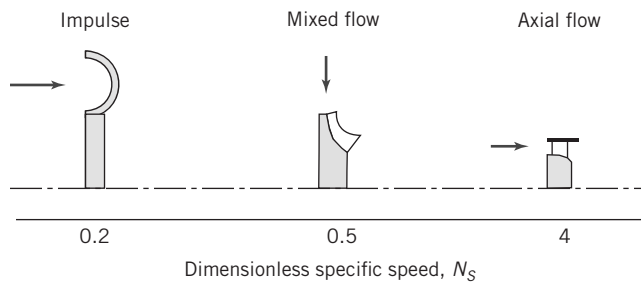


Fig. 10.10 Typical geometric proportions of commercial hydraulic turbines as they vary with dimensionless specific speed, adapted from Reference [3].

the trend from radial (purely centrifugal pumps), through mixed-flow, to axial-flow geometries as specific speed increases.

The corresponding efficiency trends for typical pumps are shown in Fig. 10.9, which shows that pump capacity generally increases as specific speed increases. The figure also shows that at any given specific speed, efficiency is higher for large pumps than for small ones. Physically this scale effect means that viscous losses become less important as the pump size is increased.

Characteristic proportions of hydraulic turbines are also correlated by specific speed, as shown in Fig. 10.10. As in Fig. 10.8, the machine size has been scaled in this illustration to deliver approximately the same power at unit head when rotating at a speed equal to the specific speed. The corresponding efficiency trends for typical turbine types are shown in Fig. 10.11. The most commonly used forms of specific speed for pumps are defined and compared in Example 10.2.

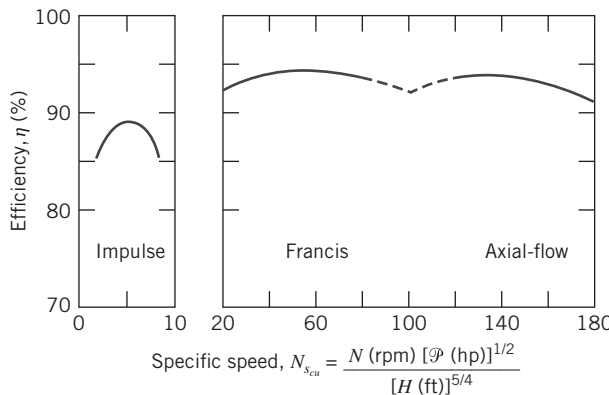


Fig. 10.11 Average efficiencies of commercial hydraulic turbines as they vary with specific speed [4].

Example 10.2 COMPARISON OF SPECIFIC SPEED DEFINITIONS

At the best efficiency point, a centrifugal pump, with impeller diameter $D = 8$ in., produces $H = 21.9$ ft at $Q = 300$ gpm with $N = 1170$ rpm. Compute the corresponding specific speeds using: (a) U.S. customary units, (b) SI units ($\text{rad/s}, \text{m}^3/\text{s}, \text{m}^2/\text{s}^2$), and (c) European units ($\text{rev/s}, \text{m}^3/\text{s}, \text{m}^2/\text{s}^2$). Develop conversion factors to relate the specific speeds.

Given: Centrifugal pump at best efficiency point (BEP). Assume the pump characteristics are $H = 21.9$ ft, $Q = 300$ gpm, and $N = 1170$ rpm.

- Find:** (a) The specific speed in U.S. customary units.
 (b) The specific speed in SI units.
 (c) The specific speed in European units.
 (d) Appropriate conversion factors to relate the specific speeds.

Solution:

$$\text{Governing equations: } N_s = \frac{\omega Q^{1/2}}{h^{3/4}} \quad \text{and} \quad N_{scu} = \frac{N Q^{1/2}}{H^{3/4}}$$

From the given information, the specific speed in U.S. customary units is

$$N_{scu} = 1170 \text{ rpm} \times (300)^{1/2} \text{ gpm}^{1/2} \times \frac{1}{(21.9)^{3/4} \text{ ft}^{3/4}} = 2000 \leftarrow N_{scu}$$

Convert information to SI units:

$$\begin{aligned} \omega &= 1170 \frac{\text{rev}}{\text{min}} \times 2\pi \frac{\text{rad}}{\text{rev}} \times \frac{\text{min}}{60 \text{ s}} = 123 \text{ rad/s} \\ Q &= 300 \frac{\text{gal}}{\text{min}} \times \frac{\text{ft}^3}{7.48 \text{ gal}} \times \frac{\text{min}}{60 \text{ s}} \times (0.305)^3 \frac{\text{m}^3}{\text{ft}^3} = 0.0190 \text{ m}^3/\text{s} \\ H &= 21.9 \text{ ft} \times 0.305 \frac{\text{m}}{\text{ft}} = 6.68 \text{ m} \end{aligned}$$

The energy per unit mass is

$$h = gH = 9.81 \frac{\text{m}}{\text{s}^2} \times 6.68 \text{ m} = 65.5 \text{ m}^2/\text{s}^2$$

The dimensionless specific speed is

$$N_s = 123 \frac{\text{rad}}{\text{s}} \times (0.0190)^{1/2} \frac{\text{m}^{3/2}}{\text{s}^{1/2}} \times \frac{(65.5)^{3/4}}{(0.0190)^{3/4} (6.68)^{3/4}} = 0.736 \leftarrow N_s(\text{SI})$$

Convert the operating speed to hertz:

$$\omega = 1170 \frac{\text{rev}}{\text{min}} \times \frac{\text{min}}{60 \text{ s}} \times \frac{\text{Hz} \cdot \text{s}}{\text{rev}} = 19.5 \text{ Hz}$$

Finally, the specific speed in European units is

$$N_s(\text{Eur}) = 19.5 \text{ Hz} \times (0.0190)^{1/2} \frac{\text{m}^{3/2}}{\text{s}^{1/2}} \times \frac{(\text{s}^2)^{3/4}}{(65.5)^{3/4} (\text{m}^2)^{3/4}} = 0.117 \xleftarrow{N_s(\text{Eur})}$$

To relate the specific speeds, form ratios:

$$\frac{N_{s_{cu}}}{N_s(\text{Eur})} = \frac{2000}{0.117} = 17,100$$

$$\frac{N_{s_{cu}}}{N_s(\text{SI})} = \frac{2000}{0.736} = 2720$$

This problem demonstrates the use of “engineering” equations to calculate specific speed for pumps from each of three commonly used sets of units and to compare the results.

10.3 Pumps, Fans, and Blowers

We will now look at the various types of fluid machines in greater detail. We will begin our discussion with rotating machines that perform work on an incompressible fluid, namely pumps, fans and blowers.

Application of Euler Turbomachine Equation to Centrifugal Pumps

As demonstrated in Example 10.1, the treatment from Section 10.2 may be applied directly to the analysis of centrifugal machines. Figure 10.7 represents the flow through a simple centrifugal pump impeller. If the fluid enters the impeller with a purely radial absolute velocity, then the fluid entering the impeller has no angular momentum and V_{t_1} is identically zero.

With $V_{t_1} = 0$, the increase in head (from Eq. 10.2c) is given by

$$H = \frac{U_2 V_{t_2}}{g} \quad (10.14)$$

From the exit velocity diagram of Fig. 10.7c,

$$V_{t_2} = U_2 - W_2 \cos \beta_2 = U_2 - \frac{V_{n_2}}{\sin \beta_2} \cos \beta_2 = U_2 - V_{n_2} \cot \beta_2 \quad (10.15)$$

Then

$$H = \frac{U_2^2 - U_2 V_{n_2} \cot \beta_2}{g} \quad (10.16)$$

For an impeller of width w , the volume flow rate is

$$Q = \pi D_2 w V_{n_2} \quad (10.17)$$

To express the increase in head in terms of volume flow rate, we substitute for V_{n_2} in terms of Q from Eq. 10.17. Thus

$$H = \frac{U_2^2}{g} - \frac{U_2 \cot \beta_2}{\pi D_2 w g} Q \quad (10.18a)$$

Equation 10.18a is of the form

$$H = C_1 - C_2 Q \quad (10.18b)$$

where constants C_1 and C_2 are functions of *machine geometry and speed*,

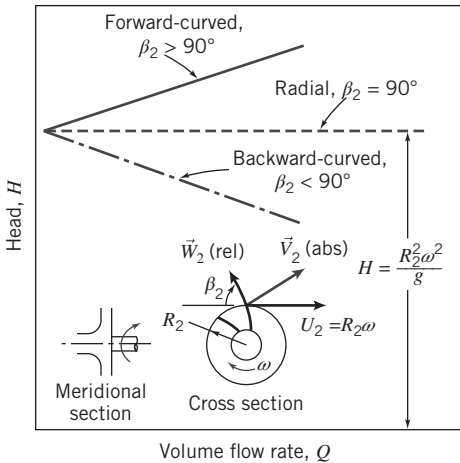


Fig. 10.12 Idealized relationship between head and volume flow rate for centrifugal pump with forward-curved, radial, and backward-curved impeller blades.

$$C_1 = \frac{U_2^2}{g} \quad \text{and} \quad C_2 = \frac{U_2 \cot \beta_2}{\pi D_2 w g}$$

Thus Eq. 10.18a predicts a linear variation of head, H , with volume flow rate, Q . Constant $C_1 = U_2^2/g$ represents the ideal head developed by the pump for zero flow rate and is called the *shutoff head*. The linear relation is an idealized model and actual devices may only approximate linear variation. They may be better modeled with a curve-fitting method based on measured data.

For radial outlet vanes, $\beta_2 = 90^\circ$ and $C_2 = 0$. The tangential component of the absolute velocity at the outlet is equal to the wheel speed and is independent of flow rate. From Eq. 10.18a, the ideal head is independent of flow rate. This characteristic $H-Q$ curve is plotted in Fig. 10.12.

The characteristics of a radial-flow machine can be altered by changing the outlet vane angle. If the vanes are backward curved as shown in Fig. 10.7a, $\beta_2 < 90^\circ$ and $C_2 > 0$. Then the tangential component of the absolute outlet velocity is less than the wheel speed and it decreases in proportion to the flow rate. From Eq. 10.18a, the ideal head decreases linearly with increasing flow rate. The corresponding $H-Q$ curve is plotted in Fig. 10.12.

If the vanes are forward curved, then $\beta_2 > 90^\circ$ and $C_2 < 0$. The tangential component of the absolute fluid velocity at the outlet is greater than the wheel speed, and it increases as the flow rate increases. From Eq. 10.7a, the ideal head increases linearly with increasing flow rate. The corresponding $H-Q$ curve is plotted in Fig. 10.12. Forward-curved vanes are almost never used in practice because they tend to have an unstable operating point.

Application of the Euler Equation to Axial Flow Pumps and Fans

The Euler turbomachine equation developed in Section 10.2 can be used for axial-flow machines with additional assumptions. The most important assumption is that the flow properties at the mean radius (the midpoint of the rotor blades) fully represent the flow at all radii. This is a good assumption provided the ratio of blade height to mean radius is approximately 0.2 or less [5]. At larger ratios a three-dimensional analysis will be necessary. A second assumption is that there is no radial component to the flow velocity. This is a reasonable assumption, since many axial machines incorporate stators or sets of vanes which guide the flow into the machine, removing unwanted radial velocity components. The third assumption is that the flow only varies in the axial direction. This means that the amount of swirl in the flow is constant and does not vary between the blades of the machine [5]. The primary consequence of this model applied to axial-flow machines is that the radius used in Equations (10.1) is constant, i.e.,

$$r_1 = r_2 = R_m \quad (10.19a)$$

Since the angular velocity ω of the rotor is also constant, it follows that

$$U_1 = U_2 = U \quad (10.19b)$$

Therefore, Eqs. 10.1 and 10.2 reduce to:

$$T_{\text{shaft}} = R_m(V_{t_2} - V_{t_1})\dot{m} \quad (10.20)$$

$$\dot{W}_m = U(V_{t_2} - V_{t_1})\dot{m} \quad (10.21)$$

$$H = \frac{\dot{W}_m}{\dot{m}g} = \frac{U}{g}(V_{t_2} - V_{t_1}) \quad (10.22)$$

In Example 10.3 these special versions of the Euler turbomachine equation and velocity diagrams are utilized in the analysis of flow through an axial-flow fan.

Example 10.3 IDEALIZED AXIAL-FLOW FAN

An axial-flow fan operates at 1200 rpm. The blade tip diameter is 1.1 m and the hub diameter is 0.8 m. The inlet and exit angles at the mean blade radius are 30° and 60° , respectively. Inlet guide vanes give the absolute flow entering the first stage an angle of 30° . The fluid is air at standard conditions and the flow may be considered incompressible. There is no change in axial component of velocity across the rotor. Assume the relative flow enters and leaves the rotor at the geometric blade angles and use properties at the mean blade radius for calculations. For these idealized conditions, draw the inlet velocity diagram, determine the volume flow rate of the fan, and sketch the rotor blade shapes. Using the data so obtained, draw the outlet velocity diagram and calculate the minimum torque and power needed to drive the fan.

Given: Flow through rotor of axial-flow fan.

Tip diameter: 1.1 m

Hub diameter: 0.8 m

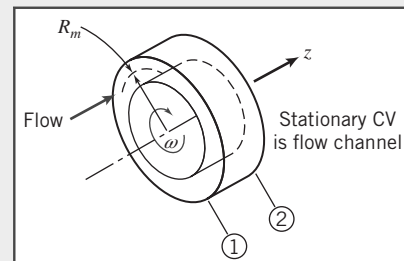
Operating speed: 1200 rpm

Absolute inlet angle: 30°

Blade inlet angle: 30°

Blade outlet angle: 60°

Fluid is air at standard conditions. Use properties at mean diameter of blades.



Find: (a) Inlet velocity diagram.

(b) Volume flow rate.

(c) Rotor blade shape.

(d) Outlet velocity diagram.

(e) Rotor torque.

(f) Power required.

Solution: Apply the Euler turbomachine equation to a fixed control volume.

Governing equations:

$$T_{\text{shaft}} = R_m(V_{t_2} - V_{t_1})\dot{m} = R_m(V_{t_2} - V_{t_1})\rho Q \quad (10.20)$$

Assumptions:

1 Neglect torques due to body or surface forces.

2 Steady flow.

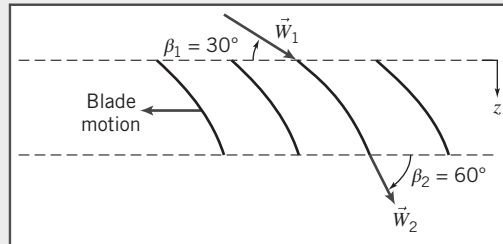
3 Uniform flow at inlet and outlet sections.

4 Incompressible flow.

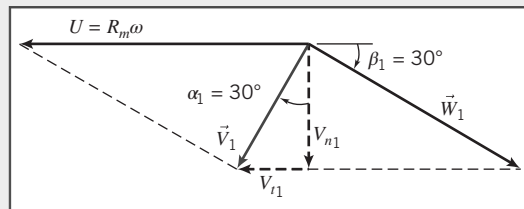
5 No change in axial flow area.

6 Use mean radius of rotor blades, R_m .

The blade shapes are



The inlet velocity diagram is



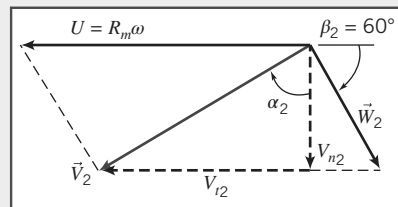
From continuity

$$(-\rho V_{n1} A_1) + (\rho V_{n2} A_2) = 0$$

or

$$Q = V_{n1} A_1 = V_{n2} A_2$$

Since $A_1 = A_2$, then $V_{n1} = V_{n2}$, and the outlet velocity diagram is as shown in the following figure:



At the mean blade radius,

$$U = R_m \omega = \frac{D_m}{2} \omega$$

$$U = \frac{1}{2}(1.1 + 0.8)m \times 1200 \frac{\text{rev}}{\text{min}} \times 2\pi \frac{\text{rad}}{\text{rev}} \times \frac{\text{min}}{60 \text{ s}} = 59.7 \text{ m/s}$$

From the geometry of the inlet velocity diagram,

$$U = V_{n1}(\tan \alpha_1 + \cot \beta_1)$$

so that

$$V_{n1} = \frac{U}{\tan \alpha_1 + \cot \beta_1} = 59.7 \frac{\text{m}}{\text{s}} \times \frac{1}{\tan 30^\circ + \cot 30^\circ} = 25.9 \text{ m/s}$$

Consequently,

$$V_1 = \frac{V_{n_1}}{\cos \alpha_1} = 25.9 \frac{\text{m}}{\text{s}} \times \frac{1}{\cos 30^\circ} = 29.9 \text{ m/s}$$

$$V_{t_1} = V_1 \sin \alpha_1 = 29.9 \frac{\text{m}}{\text{s}} \times \sin 30^\circ = 15.0 \text{ m/s}$$

and

$$W_1 = \frac{V_{n_1}}{\sin \beta_1} = 25.9 \frac{\text{m}}{\text{s}} \times \frac{1}{\sin 30^\circ} = 51.8 \text{ m/s}$$

The volume flow rate is

$$Q = V_{n_1} A_1 = \frac{\pi}{4} V_{n_1} (D_t^2 - D_h^2) = \frac{\pi}{4} \times 25.9 \frac{\text{m}}{\text{s}} [(1.1)^2 - (0.8)^2] \text{m}^2$$

$$Q = 11.6 \text{ m}^3/\text{s} \quad \underline{Q}$$

From the geometry of the outlet velocity diagram,

$$\tan \alpha_2 = \frac{V_{t_2}}{V_{n_2}} = \frac{U - V_{n_2} \cot \beta_2}{V_{n_2}} = \frac{U - V_{n_1} \cot \beta_2}{V_{n_1}}$$

or

$$\alpha_2 = \tan^{-1} \left[\frac{59.7 \frac{\text{m}}{\text{s}} - 25.9 \frac{\text{m}}{\text{s}} \times \cot 60^\circ}{25.9 \frac{\text{m}}{\text{s}}} \right] = 59.9^\circ$$

and

$$V_2 = \frac{V_{n_2}}{\cos \alpha_2} = \frac{V_{n_1}}{\cos \alpha_2} = 25.9 \frac{\text{m}}{\text{s}} \times \frac{1}{\cos 59.9^\circ} = 51.6 \text{ m/s}$$

Finally,

$$V_{t_2} = V_2 \sin \alpha_2 = 51.6 \frac{\text{m}}{\text{s}} \times \sin 59.9^\circ = 44.6 \text{ m/s}$$

Applying Eq. 10.20

$$T_{\text{shaft}} = \rho Q R_m (V_{t_2} - V_{t_1})$$

$$= 1.23 \frac{\text{kg}}{\text{m}^3} \times 11.6 \frac{\text{m}^3}{\text{s}} \times \frac{0.95}{2} \text{m} \times (44.6 - 15.0) \frac{\text{m}}{\text{s}} \times \frac{\text{N} \cdot \text{s}^2}{\text{kg} \cdot \text{m}}$$

$$T_{\text{shaft}} = 201 \text{ N} \cdot \text{m} \quad \underline{T_{\text{shaft}}}$$

Thus the torque *on* the CV is in the same sense as $\vec{\omega}$. The power required is

$$\dot{W}_m = \vec{\omega} \cdot \vec{T} = \omega T_{\text{shaft}} = 1200 \frac{\text{rev}}{\text{min}} \times 2\pi \frac{\text{rad}}{\text{rev}} \times \frac{\text{min}}{60 \text{ s}} \times 201 \text{ N} \cdot \text{m} \times \frac{\text{W} \cdot \text{s}}{\text{N} \cdot \text{m}}$$

$$\dot{W}_m = 25.3 \text{ kW} \quad \underline{\dot{W}_m}$$

This problem illustrates construction of velocity diagrams and application of the Euler turbomachine equation for a fixed control volume to an axial-flow machine under idealized conditions.

Performance Characteristics

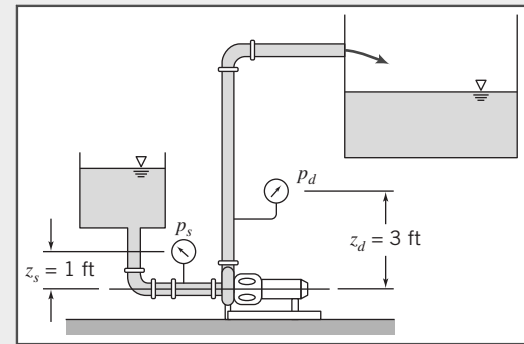
To specify fluid machines for flow systems, the designer must know the pressure rise (or head), torque, power requirement, and efficiency of a machine. For a given machine, each of these characteristics is a function of flow rate and for similar machines depend on size and operating speed. Here we define *performance characteristics* for pumps and turbines and review experimentally measured trends for

typical machines. Measurements are made as flow rate is varied from shutoff (zero flow) to maximum delivery by varying the load from maximum to minimum. Power input to the machine is measured and efficiency is computed as illustrated in Example 10.4. Example 10.5 illustrates curve-fitting for performance results.

Example 10.4 CALCULATION OF PUMP CHARACTERISTICS FROM TEST DATA

The flow system used to test a centrifugal pump at a nominal speed of 1750 rpm is shown. The liquid is water at 80°F, and the suction and discharge pipe diameters are 6 in. Data measured during the test are given in the table. The electric motor is supplied at 460 V, 3-phase, and has a power factor of 0.875 and a constant efficiency of 90 percent.

Rate of Flow (gpm)	Suction Pressure (psig)	Discharge Pressure (psig)	Motor Current (amp)
0	0.65	53.3	18.0
500	0.25	48.3	26.2
800	-0.35	42.3	31.0
1000	-0.92	36.9	33.9
1100	-1.24	33.0	35.2
1200	-1.62	27.8	36.3
1400	-2.42	15.3	38.0
1500	-2.89	7.3	39.0



Calculate the net head delivered and the pump efficiency at a volume flow rate of 1000 gpm. Plot the pump head, power input, and efficiency as functions of volume flow rate.

Given: Pump test flow system and data shown.

Find: (a) Pump head and efficiency at $Q = 1000$ gpm.

(b) Pump head, power input, and efficiency as a function of volume flow rate. Plot the results.

Solution:

Governing equations:

$$\dot{W}_h = \rho Q g H_p \quad \eta_p = \frac{\dot{W}_h}{\dot{W}_m} = \frac{\rho Q g H_p}{\omega T}$$

$$H_p = \left(\frac{p}{\rho g} + \frac{\bar{V}^2}{2g} + z \right)_d - \left(\frac{p}{\rho g} + \frac{\bar{V}^2}{2g} + z \right)_s$$

Assumptions:

- 1 Steady flow.
- 2 Uniform flow at each section.
- 3 $\bar{V}_2 = \bar{V}_1$.
- 4 Correct all heads to the same elevation.

Since $\bar{V}_1 = \bar{V}_2$, the pump head is

$$H_p = \frac{1}{g} \left[\left(\frac{p}{\rho} + gz \right)_d - \left(\frac{p}{\rho} + gz \right)_s \right] = \frac{p_2 - p_1}{\rho g}$$

where the discharge and suction pressures, *corrected to the same elevation*, are designated p_2 and p_1 , respectively.

Correct measured static pressures to the pump centerline:

$$p_1 = p_s + \rho g z_s$$

$$p_1 = -0.92 \frac{\text{lbf}}{\text{in.}^2} + 1.94 \frac{\text{slug}}{\text{ft}^3} \times 32.2 \frac{\text{ft}}{\text{s}^2} \times 1.0 \text{ ft} \times \frac{\text{lbf} \cdot \text{s}^2}{\text{slug} \cdot \text{ft}} \times \frac{\text{ft}^2}{144 \text{ in.}^2} = -0.49 \text{ psig}$$

and

$$p_2 = p_d + \rho g z_d$$

$$p_2 = 36.9 \frac{\text{lbf}}{\text{in.}^2} + 1.94 \frac{\text{slug}}{\text{ft}^3} \times 32.2 \frac{\text{ft}}{\text{s}^2} \times 3.0 \text{ ft} \times \frac{\text{lbf} \cdot \text{s}^2}{\text{slug} \cdot \text{ft}} \times \frac{\text{ft}^2}{144 \text{ in.}^2} = 38.2 \text{ psig}$$

Calculate the pump head:

$$H_p = (p_2 - p_1) / \rho g$$

$$H_p = [38.2 - (-0.49)] \frac{\text{lbf}}{\text{in.}^2} \times \frac{\text{ft}^3}{1.94 \text{ slug}} \times \frac{\text{s}^2}{32.2 \text{ ft}} \times 144 \frac{\text{in.}^2}{\text{ft}^2} \times \frac{\text{slug} \cdot \text{ft}}{\text{lbf} \cdot \text{s}^2} = 89.2 \text{ ft} \quad H_p$$

Compute the hydraulic power delivered to the fluid:

$$\dot{W}_h = \rho Q g H_p = Q(p_2 - p_1)$$

$$= 1000 \frac{\text{gal}}{\text{min}} \times [38.2 - (-0.49)] \frac{\text{lbf}}{\text{in.}^2} \times \frac{\text{ft}^3}{7.48 \text{ gal}} \times \frac{\text{min}}{60 \text{ s}} \times 144 \frac{\text{in.}^2}{\text{ft}^2} \times \frac{\text{hp} \cdot \text{s}}{550 \text{ ft} \cdot \text{lbf}}$$

$$\dot{W}_h = 22.6 \text{ hp}$$

Calculate the motor power output (the mechanical power input to the pump) from electrical information:

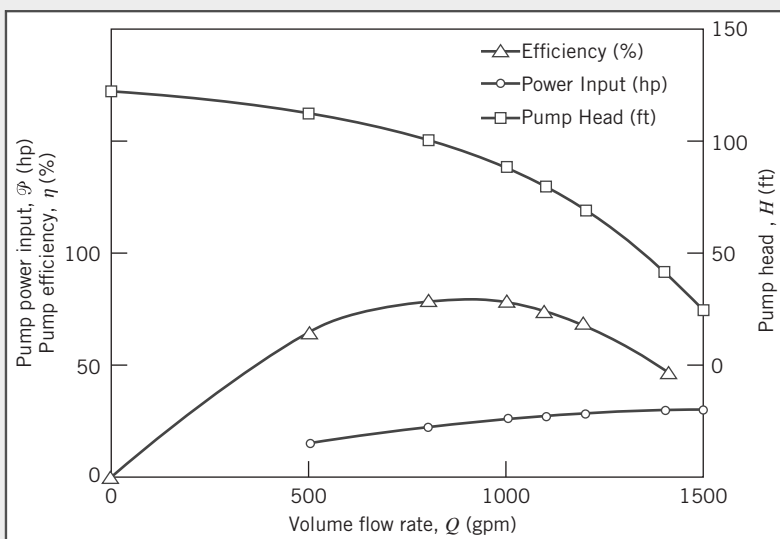
$$\mathcal{P}_{\text{in}} = \eta \sqrt{3} (PF) EI$$

$$\mathcal{P}_{\text{in}} = 0.90 \times \sqrt{3} \times 0.875 \times 460 \text{ V} \times 33.9 \text{ A} \times \frac{\text{W}}{\text{VA}} \times \frac{\text{hp}}{746 \text{ W}} = 28.5 \text{ hp}$$

The corresponding pump efficiency is

$$\eta_p = \frac{\dot{W}_h}{\dot{W}_m} = \frac{22.6 \text{ hp}}{28.5 \text{ hp}} = 0.792 \quad \text{or} \quad 79.2 \text{ percent} \quad \eta_p$$

Results from similar calculations at the other volume flow rates are plotted below:



This problem illustrates the data reduction procedure used to obtain the performance curves for a pump from experimental data. The results calculated and plotted in this problem are typical for a centrifugal pump driven at constant speed:

- The pressure rise is highest at shutoff (zero flow rate).
- Pressure rise decreases steadily as flow rate is increased; compare this typical experimental curve to the linear behavior predicted by Eq. 10.18b, and shown in Fig. 10.12, for idealized backward-curved impeller blades used in most centrifugal pumps.
- Required power input increases with flow rate; the increase is generally nonlinear.
- Efficiency is zero at shutoff, rises to a peak as flow rate is increased, then drops off at larger flow rates; it stays near its maximum over a range of flow rates from about 800 to 1100 gpm.

This problem assumes that the electric motor efficiency is constant. In practice, motor efficiency varies with load.

Example 10.5 CURVE-FIT TO PUMP PERFORMANCE DATA

Pump test data and performance were given in Example 10.4. Fit a parabolic curve, $H = H_0 - AQ^2$, to these calculated pump performance results and compare the fitted curve with the measured data.

Given: Pump test data and performance calculated in Example 10.4.

Find: (a) Parabolic curve, $H = H_0 - AQ^2$, fitted to the pump performance data.
 (b) Comparison of the curve-fit with the calculated performance.

Solution: The curve-fit may be obtained by fitting a linear curve to H versus Q^2 . Tabulating,

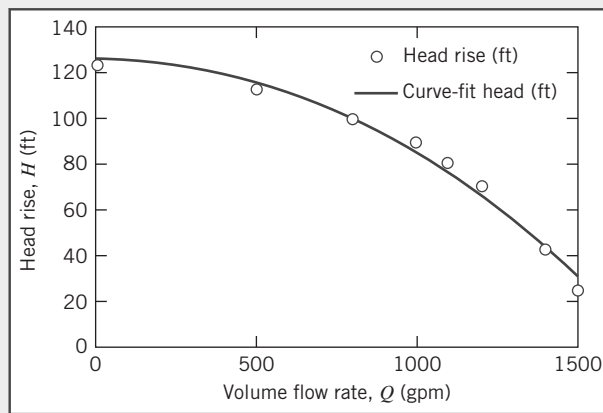
From calculated performance:			From the curve fit:	
Q (gpm)	Q^2 (gpm^2)	H (ft)	H (ft)	Error (%)
0	0	123	127	2.8
500	25×10^4	113	116	3.1
800	64×10^4	100	99.8	-0.5
1000	100×10^4	89.2	84.6	-5.2
1100	121×10^4	80.9	75.7	-6.5
1200	144×10^4	69.8	65.9	-5.6
1400	196×10^4	42.8	43.9	2.5
1500	225×10^4	25.5	31.7	24.2
Intercept = 127				
Slope = -4.23×10^{-5}				
$r^2 = 0.984$				

Using the method of least squares, the equation for the fitted curve is obtained as

$$H(\text{ft}) = 127 - 4.23 \times 10^{-5}[Q(\text{gpm})]^2$$

with coefficient of determination $r^2 = 0.984$. (The closer r^2 is to unity, its maximum possible value, the better the fit.)

Always compare the results of a curve-fit with the data used to develop the fit. The figure shows the curve-fit (the solid line) and the experimental values (the points).



This problem illustrates that the pump test data for Example 10.4 can be fitted quite well to a parabolic curve. As with fitting a curve to any experimental data, our justifications for choosing a parabolic function in this case are:

- Experimental observation—the experimental data looks parabolic.
- Theory or concept—we will see later in this section that similarity rules suggest such a relation between head and flow rate.

Typical characteristic curves for a centrifugal pump tested at constant speed were shown qualitatively in Fig. 7.5. The head versus capacity curve is compared in Fig. 10.13 with characteristics predicted by the idealized analysis. Figure 10.13 shows that the head at any flow rate in the real machine may be significantly lower than is predicted by the idealized analysis. Some of the causes are that at very low flow rate, some fluid recirculates in the impeller, friction loss and leakage loss both increase with flow rate, and "shock loss" results from a mismatch between the direction of the relative velocity and the tangent to the impeller blade at the inlet.

Curves such as those in Figs. 7.5 and 10.13 are measured at constant (design) speed with a single impeller diameter. It is common practice to vary pump capacity by changing the impeller size in a given casing. To present information compactly, data from tests of several impeller diameters may be plotted on a single graph, as shown in Fig. 10.14. Efficiency contours are plotted by joining points having the same constant efficiency. Power-requirement contours are also plotted. Finally, the *NPSH* requirements (discussed later in this section) are shown for the extreme diameters.

The data of Fig. 10.14 are often tabulated for quick access by design software and therefore data are not always presented in the manner shown in this figure. The data of Fig. 10.14 are simplified

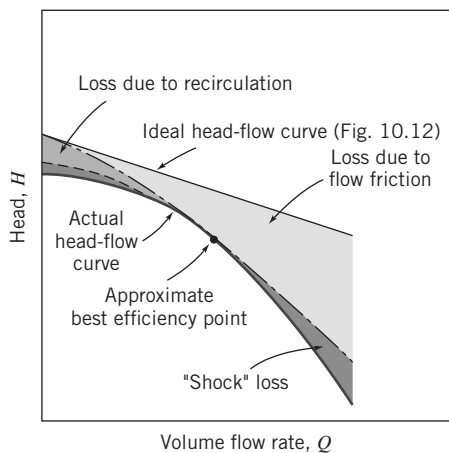


Fig. 10.13 Comparison of ideal and actual head-flow curves for a centrifugal pump with backward-curved impeller blades [10].

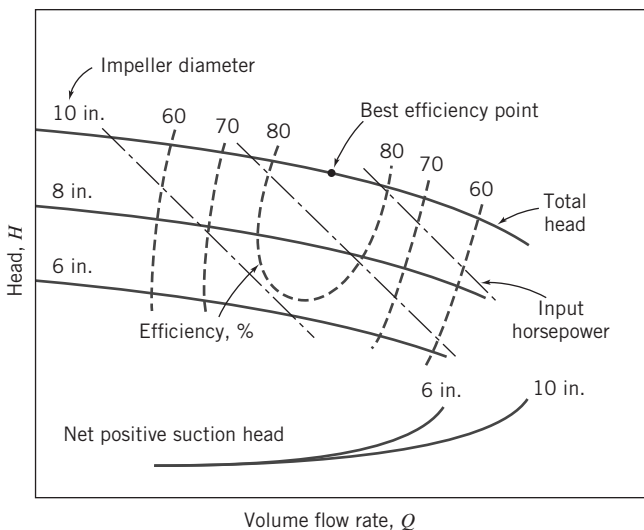


Fig. 10.14 Typical pump performance curves from tests with three impeller diameters at constant speed [6].

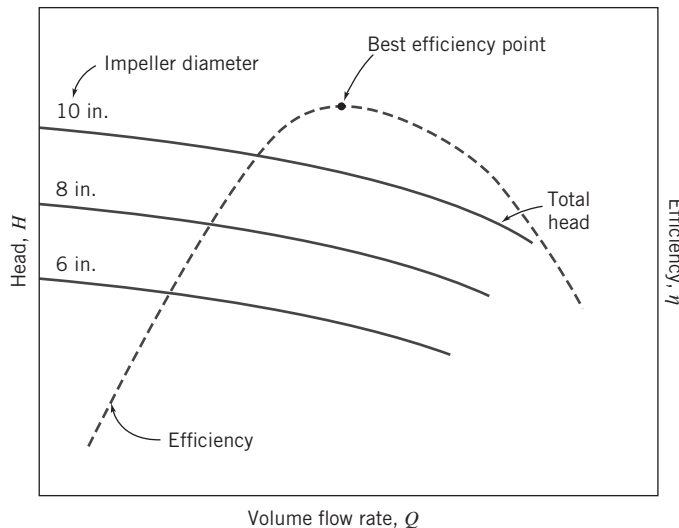


Fig. 10.15 Typical pump performance curves from tests with three impeller diameters at constant speed, showing efficiency as a function of flow rate only [8].

by reporting an average efficiency as a function of the flow rate only, as shown in Fig. 10.15, rather than as a function of flow rate and head. The figures in Appendix C display pump performance in this format.

For this typical machine, head is a maximum at shutoff and decreases continuously as flow rate increases. Input power is minimum at shutoff and increases as delivery is increased. Consequently, to minimize the starting load, it may be advisable to start the pump with the outlet valve closed. Pump efficiency increases with capacity until the *best efficiency point* (BEP) is reached, then decreases as flow rate is increased further. For minimum energy consumption, it is desirable to operate as close to BEP as possible.

Centrifugal pumps may be combined in parallel to deliver greater flow or in series to deliver greater head. A number of manufacturers build multistage pumps, which are essentially several pumps arranged in series within a single casing. Common practice is to drive machines with electric motors at nearly constant speed, but in some system applications energy savings can result from variable-speed operation.

Similarity Rules

The dimensionless parameters developed in Chapter 7 form the basis for predicting changes in performance that result from changes in pump size, operating speed, or impeller diameter. Dynamic similarity requires geometric and kinematic similarity. Assuming similar pumps and flow fields and neglecting viscous effects, we obtain dynamic similarity when the dimensionless flow coefficient is held constant so that two flow conditions satisfy the relation

$$\frac{Q_1}{\omega_1 D_1^3} = \frac{Q_2}{\omega_2 D_2^3} \quad (10.23a)$$

The dimensionless head and power coefficients depend only on the flow coefficient, i.e.,

$$\frac{h}{\omega^2 D^2} = f_1 \left(\frac{Q}{\omega D^3} \right) \quad \text{and} \quad \frac{\mathcal{P}}{\rho \omega^3 D^5} = f_2 \left(\frac{Q}{\omega D^3} \right)$$

We have dynamic similarity when pump characteristics at two conditions satisfy the relation

$$\frac{h_1}{\omega_1^2 D_1^2} = \frac{h_2}{\omega_2^2 D_2^2} \quad (10.23b)$$

and

$$\frac{\mathcal{P}_1}{\rho \omega_1^3 D_1^5} = \frac{\mathcal{P}_2}{\rho \omega_2^3 D_2^5} \quad (10.23c)$$

These scaling relationships may be used to predict the effects of changes in pump operating speed, pump size, or impeller diameter within a given housing.

The simplest situation occurs when the speed of a pump is changed. Geometric similarity is assured, and the flows are dynamically similar when the flow coefficients are equal. For this case of speed change with fixed diameter, Eqs. 10.23 become

$$\frac{Q_2}{Q_1} = \frac{\omega_2}{\omega_1} \quad (10.24a)$$

$$\frac{h_2}{h_1} = \frac{H_2}{H_1} = \left(\frac{\omega_2}{\omega_1} \right)^2 \quad (10.24b)$$

$$\frac{\mathcal{P}_2}{\mathcal{P}_1} = \left(\frac{\omega_2}{\omega_1} \right)^3 \quad (10.24c)$$

In Example 10.5, we showed that a pump performance curve may be modeled within engineering accuracy by the parabolic relationship,

$$H = H_0 - A Q^2 \quad (10.25a)$$

The pump curve for the new operating condition could be derived by scaling any two points from the performance curve measured at the original operating condition. Usually, the *shutoff condition* and the *best efficiency point*, represented by points *B* and *C* in Fig. 10.16, are chosen for scaling.

As shown by Eq. 10.24a, the flow rate increases by the ratio of operating speeds, so

$$Q_{B'} = \frac{\omega_2}{\omega_1} Q_B = 0 \quad \text{and} \quad Q_{C'} = \frac{\omega_2}{\omega_1} Q_C$$

Thus, point *B'* is located directly above point *B*, and point *C'* moves to the right of point *C* (in this example $\omega_2 > \omega_1$).

The head increases by the square of the speed ratio, so

$$H_{B'} = H_B \left(\frac{\omega_1}{\omega_2} \right)^2 \quad \text{and} \quad H_{C'} = H_C \left(\frac{\omega_2}{\omega_1} \right)^2$$

Points *C* and *C'*, where dynamically similar flow conditions are present, are termed *homologous points* for the pump.

We can relate the old operating condition (e.g., running at speed $N_1 = 1170$ rpm, as shown in Fig. 10.16) to the new, primed one (e.g., running at speed $N_2 = 1750$ rpm in Fig. 10.16) using the parabolic relation and Eqs. 10.24a and 10.24b,

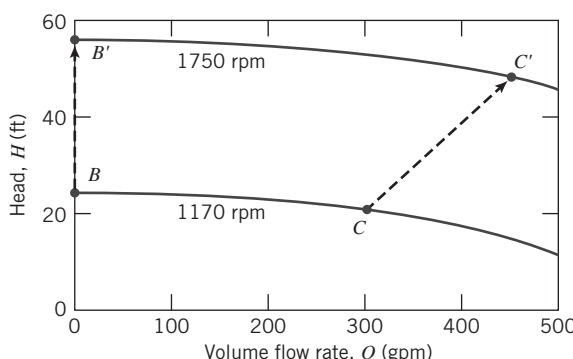


Fig. 10.16 Schematic of a pump performance curve, illustrating the effect of a change in pump operating speed.

$$H = H' \left(\frac{\omega_1}{\omega_2} \right)^2 = H_0 - A Q^2 = H'_0 \left(\frac{\omega_1}{\omega_2} \right)^2 - A Q'^2 \left(\frac{\omega_1}{\omega_2} \right)^2$$

or

$$H' = H'_0 - A Q'^2 \quad (10.25b)$$

so that for a given pump the factor A remains unchanged as we change pump speed, as we will verify in Example 10.6.

Example 10.6 SCALING PUMP PERFORMANCE CURVES

When operated at $N = 1170$ rpm, a centrifugal pump, with impeller diameter $D = 8$ in., has shutoff head $H_0 = 25.0$ ft of water. At the same operating speed, best efficiency occurs at $Q = 300$ gpm, where the head is $H = 21.9$ ft of water. Fit these data at 1170 rpm with a parabola. Scale the results to a new operating speed of 1750 rpm. Plot and compare the results.

Given: Centrifugal pump (with $D = 8$ in. impeller) operated at $N = 1170$ rpm.

Q (gpm)	0	300
H (ft of water)	25.0	21.9

Find: (a) The equation of a parabola through the pump characteristics at 1170 rpm.
(b) The corresponding equation for a new operating speed of 1750 rpm.
(c) Comparison (plot) of the results.

Solution: Assume a parabolic variation in pump head of the form, $H = H_0 - A Q^2$. Solving for A gives

$$A_1 = \frac{H_0 - H}{Q^2} = (25.0 - 21.9) \text{ ft} \times \frac{1}{(300)^2 (\text{gpm})^2} = 3.44 \times 10^{-5} \text{ ft}/(\text{gpm})^2$$

The desired equation is

$$H(\text{ft}) = 25.0 - 3.44 \times 10^{-5} [Q(\text{gpm})]^2$$

The pump remains the same, so the two flow conditions are geometrically similar. Assuming no cavitation occurs, the two flows also will be kinematically similar. Then dynamic similarity will be obtained when the two flow coefficients are matched. Denoting the 1170 rpm condition by subscript 1 and the 1750 rpm condition by subscript 2, we have

$$\frac{Q_2}{\omega_2 D_2^3} = \frac{Q_1}{\omega_1 D_1^3} \quad \text{or} \quad \frac{Q_2}{Q_1} = \frac{\omega_2}{\omega_1} = \frac{N_2}{N_1}$$

since $D_2 = D_1$. For the shutoff condition,

$$Q_2 = \frac{N_2}{N_1} Q_1 = \frac{1750 \text{ rpm}}{1170 \text{ rpm}} \times 0 \text{ gpm} = 0 \text{ gpm}$$

From the best efficiency point, the new flow rate is

$$Q_2 = \frac{N_2}{N_1} Q_1 = \frac{1750 \text{ rpm}}{1170 \text{ rpm}} \times 300 \text{ gpm} = 449 \text{ gpm}$$

The pump heads are related by

$$\frac{h_2}{h_1} = \frac{H_2}{H_1} = \frac{N_2^2 D_2^2}{N_1^2 D_1^2} \quad \text{or} \quad \frac{H_2}{H_1} = \frac{N_2^2}{N_1^2} = \left(\frac{N_2}{N_1} \right)^2$$

since $D_2 = D_1$. For the shutoff condition,

$$H_2 = \left(\frac{N_2}{N_1}\right)^2 H_1 = \left(\frac{1750 \text{ rpm}}{1170 \text{ rpm}}\right)^2 25.0 \text{ ft} = 55.9 \text{ ft}$$

At the best efficiency point,

$$H_2 = \left(\frac{N_2}{N_1}\right)^2 H_1 = \left(\frac{1750 \text{ rpm}}{1170 \text{ rpm}}\right)^2 21.9 \text{ ft} = 49.0 \text{ ft}$$

The curve parameter at 1750 rpm may now be found. Solving for A , we find

$$A_2 = \frac{H_{02} - H_2}{Q_2^2} = (55.9 - 49.0) \text{ ft} \times \frac{1}{(449)^2 (\text{gpm})^2} = 3.44 \times 10^{-5} \text{ ft}/(\text{gpm})^2$$

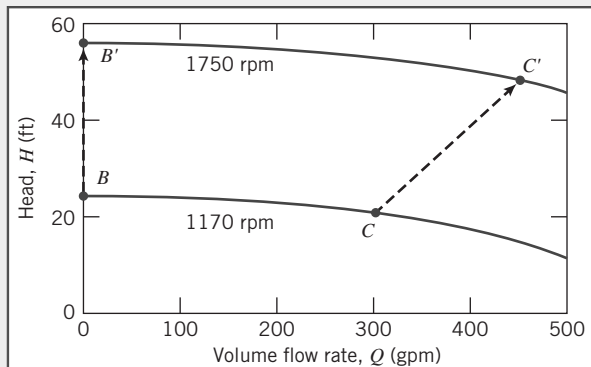
Note that A_2 at 1750 rpm is the same as A_1 at 1170 rpm. Thus we have demonstrated that the coefficient A in the parabolic equation does not change when the pump speed is changed. The “engineering” equations for the two curves are

$$H_1 = 25.0 - 3.44 \times 10^{-5} [Q \text{ (gpm)}]^2 \text{ (at 1170 rpm)}$$

and

$$H_2 = 55.9 - 3.44 \times 10^{-5} [Q \text{ (gpm)}]^2 \text{ (at 1750 rpm)}$$

The pump curves are compared in the following plot:



This problem illustrates the procedures for:

- Obtaining the parabolic “engineering” equation from shutoff head H_0 and best efficiency data on Q and H .
- Scaling pump curves from one speed to another.

Efficiency remains relatively constant between dynamically similar operating points when only the pump operating speed is changed. Application of these ideas is illustrated in Example 10.6.

In principle, geometric similarity would be maintained when pumps of the *same geometry*, differing in size only by a scale ratio, were tested at the *same operating speed*. The flow, head, and power would be predicted to vary with *pump size* as

$$Q_2 = Q_1 \left(\frac{D_2}{D_1}\right)^3, \quad H_2 = H_1 \left(\frac{D_2}{D_1}\right)^2, \quad \text{and} \quad P_2 = P_1 \left(\frac{D_2}{D_1}\right)^5 \quad (10.26)$$

It is impractical to manufacture and test a series of pump models that differ in size by only a scale ratio. Instead it is common practice to test a given pump casing at a fixed speed with several impellers of different diameter [9]. Because pump casing width is the same for each test, impeller width also must be the same; only impeller diameter D is changed. As a result, volume flow rate scales in proportion to D^2 , not to D^3 . Pump input power at fixed speed scales as the product of flow rate and head, so it becomes proportional to D^4 . Using this modified scaling method frequently gives results of acceptable accuracy, as demonstrated in several end-of-chapter problems where the method is checked against measured performance data from Appendix C.

It is not possible to compare the efficiencies at the two operating conditions directly. However, viscous effects should become relatively less important as the pump size increases. Thus efficiency should improve slightly as diameter is increased. Moody [10] suggested an empirical equation that may be used to estimate the maximum efficiency of a prototype pump based on test data from a geometrically similar model of the prototype pump. His equation is written

$$\frac{1-\eta_p}{1-\eta_m} = \left(\frac{D_m}{D_p} \right)^{1/5} \quad (10.27)$$

To develop Eq. 10.27, Moody assumed that only the surface resistance changes with model scale so that losses in passages of the same roughness vary as $1/D^5$. Unfortunately, it is difficult to maintain the same relative roughness between model and prototype pumps. Further, the Moody model does not account for any difference in mechanical losses between model and prototype, nor does it allow determination of off-peak efficiencies. Nevertheless, scaling of the maximum-efficiency point is useful to obtain a general estimate of the efficiency curve for the prototype pump.

Cavitation and Net Positive Suction Head

Cavitation can occur in any machine handling liquid whenever the local static pressure falls below the vapor pressure of the liquid. When this occurs, the liquid can locally flash to vapor, forming a vapor cavity and significantly changing the flow pattern from the noncavitating condition. The vapor cavity changes the effective shape of the flow passage, thus altering the local pressure field. Since the size and shape of the vapor cavity are influenced by the local pressure field, the flow may become unsteady. The unsteadiness may cause the entire flow to oscillate and the machine to vibrate.

As cavitation commences, it reduces the performance of a pump or turbine rapidly. Thus cavitation must be avoided to maintain stable and efficient operation. In addition, local surface pressures may become high when the vapor cavity implodes or collapses, causing erosion damage or surface pitting. The damage may be severe enough to destroy a machine made from a brittle, low-strength material. Obviously cavitation also must be avoided to assure long machine life.

In a pump, cavitation tends to begin at the section where the flow is accelerated into the impeller. Cavitation in a turbine begins where pressure is lowest. The tendency to cavitate increases as local flow speeds increase; this occurs whenever flow rate or machine operating speed is increased.

Cavitation can be avoided if the pressure everywhere in the machine is kept above the vapor pressure of the operating liquid. At constant speed, this requires that a pressure somewhat greater than the vapor pressure of the liquid be maintained at a pump inlet (the *suction*). Because of pressure losses in the inlet piping, the suction pressure may be subatmospheric. Therefore it is important to carefully limit the pressure drop in the inlet piping system.

Net positive suction head (NPSH) is defined as the difference between the absolute stagnation pressure in the flow at the pump suction and the liquid vapor pressure, expressed as head of flowing liquid [11]. Hence the *NPSH* is a measure of the difference between the maximum possible pressure in the given flow and the pressure at which the liquid will start flashing over to a vapor; the larger the *NPSH*, the less likely cavitation is to occur. The *net positive suction head required (NPSHR)* by a specific pump to suppress cavitation varies with the liquid pumped, and with the liquid temperature and pump condition. Typical pump characteristic curves for three impellers tested in the same housing were shown in Fig. 10.14. Experimentally determined *NPSHR* curves for the largest and smallest impeller diameters are plotted near the bottom of the figure.

The *net positive suction head available (NPSHA)* at the pump inlet must be greater than the *NPSHR* to suppress cavitation. Pressure drop in the inlet piping and pump entrance increases as volume flow rate increases. Thus for any system, the *NPSHA* decreases as flow rate is raised. The *NPSHR* of the pump increases as the flow rate is raised. Therefore, as the system flow rate is increased, the curves for *NPSHA*

and $NPSHR$ versus flow rate ultimately cross. Hence, for any inlet system, there is a flow rate that cannot be exceeded if flow through the pump is to remain free from cavitation. Example 10.7 shows the relationships between the $NPSH$, the $NPSHA$, and the $NPSHR$.

Example 10.7 CALCULATION OF NET POSITIVE SUCTION HEAD (NPSH)

A Peerless Type 4AE11 centrifugal pump (Fig. C.3, Appendix C) is tested at 1750 rpm using a flow system with the layout of Example 10.4. The water level in the inlet reservoir is 3.5 ft above the pump centerline; the inlet line consists of 6 ft of 5 in. diameter straight cast-iron pipe, a standard elbow, and a fully open gate valve. Calculate the net positive suction head available ($NPSHA$) at the pump inlet at a volume flow rate of 1000 gpm of water at 80°F. Compare with the net positive suction head required ($NPSHR$) by the pump at this flow rate. Plot $NPSHA$ and $NPSHR$ for water at 80°F and 180°F versus volume flow rate.

Given: A Peerless Type 4AE11 centrifugal pump (Fig. C.3, Appendix C) is tested at 1750 rpm using a flow system with the layout of Example 10.4. The water level in the inlet reservoir is 3.5 ft above the pump centerline; the inlet line has 6 ft of 5 in. diameter straight cast-iron pipe, a standard elbow, and a fully open gate valve.

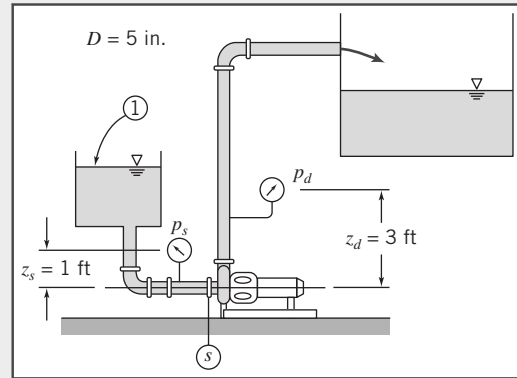
Find: (a) $NPSHA$ at $Q = 1000$ gpm of water at 80°F.
 (b) Comparison with $NPSHR$ for this pump at $Q = 1000$ gpm.
 (c) Plot of $NPSHA$ and $NPSHR$ for water at 80°F and 180°F versus volume flow rate.

Solution: Net positive suction head ($NPSH$) is defined as the difference between the absolute stagnation pressure in the flow at the pump suction and the liquid vapor pressure, expressed as head of flowing liquid. Therefore it is necessary to calculate the head at the pump suction.

Apply the energy equation for steady, incompressible pipe flow to compute the pressure at the pump inlet and thus the $NPSHA$. Denote the reservoir level as ① and the pump suction as ②, as shown above.

Governing equation:

$$p_1 + \frac{1}{2}\rho\bar{V}_1^2 + \rho g z_1 = p_s + \frac{1}{2}\rho\bar{V}_s^2 + \rho g s + \rho h_{\ell_T} \approx 0$$



Assumption: \bar{V}_1 is negligible. Thus

$$p_s = p_1 + \rho g(z_1 - z_s) - \frac{1}{2}\rho\bar{V}_s^2 - \rho h_{\ell_T} \quad (1)$$

The total head loss is

$$h_{\ell_T} = \left(\sum K + \sum f \frac{L_e}{D} + f \frac{L}{D} \right) \frac{1}{2} \rho \bar{V}_s^2 \quad (2)$$

Substituting Eq. 2 into Eq. 1 and dividing by ρg ,

$$H_s = H_1 + z_1 - z_s - \left(\sum K + \sum f \frac{L_e}{D} + f \frac{L}{D} + 1 \right) \frac{\bar{V}_s^2}{2g} \quad (3)$$

Evaluating the friction factor and head loss,

$$f = f(Re, e/D); \quad Re = \frac{\rho \bar{V} D}{\mu} = \frac{\bar{V} D}{\nu}; \quad \bar{V} = \frac{Q}{A}; \quad A = \frac{\pi D^2}{4}$$

For 5 in. (nominal) pipe, $D = 5.047$ in.

$$D = 5.047 \text{ in.} \times \frac{\text{ft}}{12 \text{ in.}} = 0.421 \text{ ft}, \quad A = \frac{\pi D^2}{4} = 0.139 \text{ ft}^2$$

$$\bar{V} = 1000 \frac{\text{gal}}{\text{min}} \times \frac{\text{ft}^3}{7.48 \text{ gal}} \times \frac{1}{0.139 \text{ ft}^2} \times \frac{\text{min}}{60 \text{ s}} = 16.0 \text{ ft/s}$$

From Table A.7, for water at $T = 80^\circ\text{F}$, $\nu = 0.927 \times 10^{-5} \text{ ft}^2/\text{s}$.

The Reynolds number is

$$Re = \frac{\bar{V} D}{\nu} = 16.0 \frac{\text{ft}}{\text{s}} \times 0.421 \text{ ft} \times \frac{\text{s}}{0.927 \times 10^{-5} \text{ ft}^2} = 7.27 \times 10^5$$

From Table 8.1, $e = 0.00085$ ft, so $e/D = 0.00202$. From Eq. 8.37, $f = 0.0237$. The minor loss coefficients are

Entrance	$K = 0.5$
Standard elbow	$\frac{L_e}{D} = 30$
Open gate valve	$\frac{L_e}{D} = 8$

Substituting,

$$\left(\sum K + \sum f \frac{L_e}{D} + f \frac{L}{D} + 1 \right)$$

$$= 0.5 + 0.0237(30 + 8) + 0.0237 \left(\frac{6}{0.421} \right) + 1 = 2.74$$

The heads are

$$H_1 = \frac{p_{\text{atm}}}{\rho g} = 14.7 \frac{\text{lbf}}{\text{in.}^2} \times 144 \frac{\text{in.}^2}{\text{ft}^2} \times \frac{\text{ft}^3}{1.93 \text{ slug}} \times \frac{\text{s}^2}{32.2 \text{ ft}} \times \frac{\text{slug} \cdot \text{ft}}{\text{lbf} \cdot \text{s}^2}$$

$$= 34.1 \text{ ft (abs)}$$

$$\frac{\bar{V}_s}{2g} = \frac{1}{2} \times (16.0)^2 \frac{\text{ft}^2}{\text{s}^2} \times \frac{\text{s}^2}{32.2 \text{ ft}} = 3.98 \text{ ft}$$

Thus,

$$H_s = 34.1 \text{ ft} + 3.5 \text{ ft} - (2.74)3.98 \text{ ft} = 26.7 \text{ ft (abs)}$$

To obtain $NPSHA$, add velocity head and subtract vapor head. Thus

$$NPSHA = H_s + \frac{\bar{V}_s^2}{2g} - H_v$$

The vapor pressure for water at 80°F is $p_v = 0.507$ psia. The corresponding head is $H_v = 1.17$ ft of water. Thus,

$$NPSHA = 26.7 + 3.98 - 1.17 = 29.5 \text{ ft} \xleftarrow{\hspace{10em}} NPSHA$$

This problem illustrates the procedures used for checking whether a given pump is in danger of experiencing cavitation:

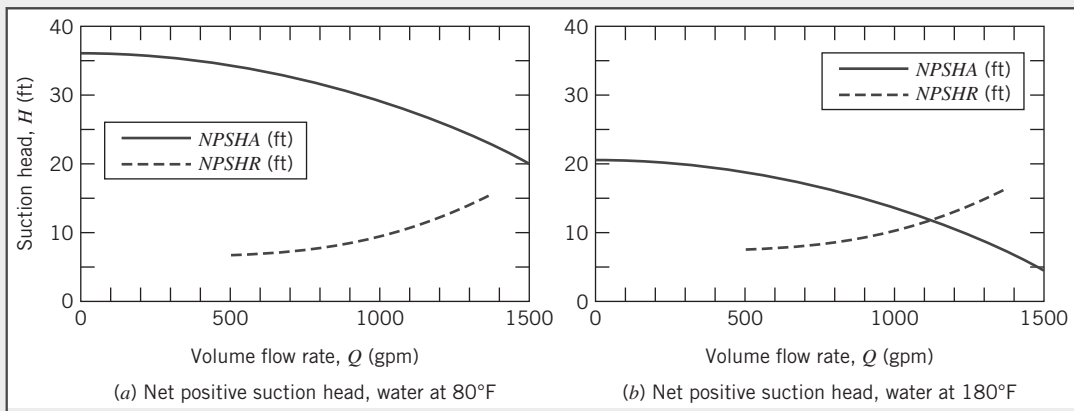
- Equation 3 and the plots show that the $NPSHA$ decreases as flow rate Q (or \bar{V}_s) increases; on the other hand, the $NPSHR$ increases with Q , so if the flow rate is high enough, a pump will likely experience cavitation (when $NPSHA < NPSHR$).
- The $NPSHR$ for any pump increases with flow rate Q because local fluid velocities within the pump increase, causing locally reduced pressures and tending to promote cavitation.
- For this pump, at 80°F , the pump appears to have $NPSHA > NPSHR$ at all flow rates, so it would never experience cavitation; at 180°F , cavitation would occur around 1100 gpm, but from Fig. C.3, the pump best efficiency is around 900 gpm, so it would probably not be run at 1100 gpm—the pump would probably not cavitate even with the hotter water.

The pump curve (Fig. C.3, Appendix C) shows that at 1000 gpm the pump requires

$$NPSHR = 12.0 \text{ ft}$$

$$\underline{NPSHR}$$

Results of similar computations for water at 80°F are plotted in the figure on the left below. (*NPSHR* values are obtained from the pump curves in Fig. C.3, Appendix C.)



Results of computation for water at 180°F are plotted in the figure on the right above. The vapor pressure for water at 180°F is $p_v = 7.51$ psia. The corresponding head is $H_v = 17.3$ ft of water. This high vapor pressure reduces the *NPSHA*, as shown in the plot.

Pump Selection: Applications to Fluid Systems

We define a *fluid system* as the combination of a fluid machine and a network of pipes or channels that convey fluid. The engineering application of fluid machines in an actual system requires matching the machine and system characteristics, while satisfying constraints of energy efficiency, capital economy, and durability.

As we saw in Example 10.4, a typical pump produces a smaller head at higher pressure as the flow rate is increased. In contrast, the head required to maintain flow in a pipe system increases with the flow rate due to increased losses. Therefore, as shown graphically in Fig. 10.17, a pump system will operate at the flow rate at which the pump head rise and required system head match. This is termed the operating point. Figure 10.17 also shows a pump efficiency curve, indicating that, for optimum pump selection, a pump should be chosen that has maximum efficiency near the operating point flow rate.

The required head for a system with no static lift starts at zero flow and head and increases with flow, as shown in Fig. 10.18a. For this system the total head required is the sum of major and minor losses,

$$h_u = \sum h_l + \sum h_m = \sum f \frac{L \bar{V}^2}{D^2} + \sum K \frac{\bar{V}^2}{2}$$

For turbulent flow the friction factors are nearly constant with flow and the minor loss coefficients K are also constant. Hence $h_{l_r} \sim \bar{V}^2 \sim Q^2$ so that the system curve is approximately parabolic. This means the system curve with pure friction becomes steeper as flow rate increases. Pressure change due to elevation difference is independent of flow rate and this component to the head-flow curve is a horizontal straight line. The system head-flow curve is plotted in Fig. 10.18b.

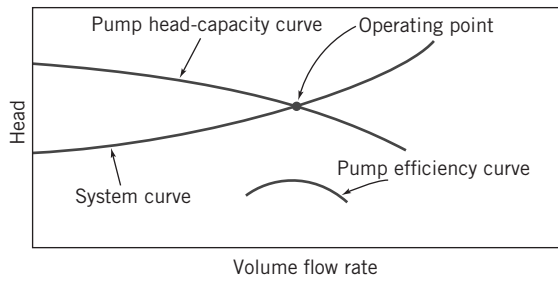


Fig. 10.17 Superimposed system head-flow and pump head-capacity curves.

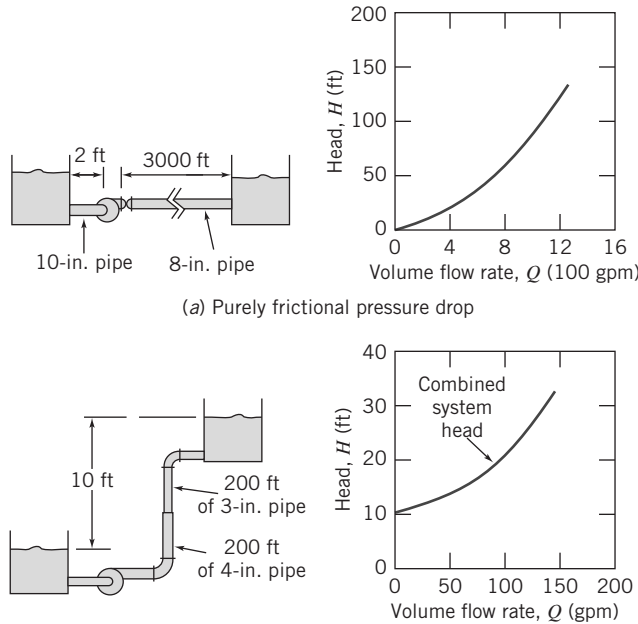


Fig. 10.18 Schematic diagrams illustrating basic types of system head-flow curves (based on Reference [6]).

Whether the resulting system curve is *steep* or *flat* depends on the relative importance of friction and gravity. Friction drop may be relatively unimportant in the water supply to a high-rise building and gravity lift may be negligible in an air-handling system for a one-story building.

In Section 8.7 we obtained a form of the energy equation for a control volume consisting of a pump-pipe system,

$$\left(\frac{p_1}{\rho} + \alpha_1 \frac{\bar{V}_1^2}{2} + gz_1 \right) - \left(\frac{p_2}{\rho} + \alpha_2 \frac{\bar{V}_2^2}{2} + gz_2 \right) = h_{l_T} - \Delta h_{\text{pump}} \quad (8.49)$$

Replacing Δh_{pump} with h_a , representing the head added by any machine that does work on the fluid, and rearranging Eq. 8.4, we obtain a more general expression

$$\frac{p_1}{\rho} + \alpha_1 \frac{\bar{V}_1^2}{2} + gz_1 + h_a = \frac{p_2}{\rho} + \alpha_2 \frac{\bar{V}_2^2}{2} + gz_2 + h_{l_T} \quad (10.28a)$$

Dividing by g gives

$$\frac{p_1}{\rho g} + \alpha_1 \frac{\bar{V}_1^2}{2g} + z_1 + H_a = \frac{p_2}{\rho g} + \alpha_2 \frac{\bar{V}_2^2}{2g} + z_2 + \frac{h_{l_T}}{g} \quad (10.28b)$$

where H_a is the energy per unit weight added by the machine. The procedure used to determine the match point for a pumping system is illustrated in Example 10.8.

Example 10.8 FINDING THE OPERATING POINT FOR A PUMPING SYSTEM

The pump of Example 10.6, operating at 1750 rpm, is used to pump water through the pipe system of Fig. 10.18a. Develop an algebraic expression for the general shape of the system resistance curve. Calculate and plot the system resistance curve. Solve graphically and analytically for the system operating point.

Given: Pump of Example 10.6, operating at 1750 rpm, with $H = H_0 - AQ^2$, where $H_0 = 55.9$ ft and $A = 3.44 \times 10^{-5}$ ft 2 /(gpm) 2 . System of Fig. 10.18a, where $L_1 = 2$ ft of $D_1 = 10$ in. pipe and $L_2 = 3000$ ft of $D_2 = 8$ in. pipe, conveying water between two large reservoirs whose surfaces are at the same level.

- Find:**
- A general algebraic expression for the system head curve.
 - The system head curve by direct calculation.
 - The system operating point using a graphical solution.
 - An *approximate* analytical expression for the system head curve.
 - The system operating point using the analytical expression of part (d).

Solution: Apply the energy equation to the flow system of Fig. 10.18a.

Governing equation:

$$\frac{p_0}{\rho g} + \alpha_0 \frac{\bar{V}_0^2}{2g} + z_0 + H_a = \frac{p_3}{\rho g} + \alpha_3 \frac{\bar{V}_3^2}{2g} + z_3 + \frac{h_{l_T}}{g} \quad (10.24b)$$

where z_0 and z_3 are the surface elevations of the supply and discharge reservoirs, respectively.

Assumptions:

- $p_0 = p_3 = p_{atm}$.
- $\bar{V}_0 = \bar{V}_3 = 0$.
- $z_0 = z_3$ (given).

Simplifying, we obtain

$$H_a = \frac{h_{l_T}}{g} = \frac{h_{IT_{01}}}{g} + \frac{h_{IT_{23}}}{g} = H_{l_T} \quad (1)$$

where sections ① and ② are located just upstream and downstream from the pump, respectively.

The total head losses are the sum of the major and minor losses, so

$$h_{IT_{01}} = K_{ent} \frac{\bar{V}_1^2}{2} + f_1 \frac{L_1}{D_1} \frac{\bar{V}_1^2}{2} = \left(K_{ent} + f_1 \frac{L_1}{D_1} \right) \frac{\bar{V}_1^2}{2}$$

$$h_{IT_{23}} = f_2 \frac{L_2}{D_2} \frac{\bar{V}_2^2}{2} + K_{exit} \frac{\bar{V}_2^2}{2} = \left(f_2 \frac{L_2}{D_2} + K_{exit} \right) \frac{\bar{V}_2^2}{2}$$

From continuity,

$$\bar{V}_1 A_1 = \bar{V}_2 A_2, \text{ so } \bar{V}_1 = \bar{V}_2 \frac{A_2}{A_1} = \bar{V}_2 \left(\frac{D_2}{D_1} \right)^2$$

Hence

$$H_{l_T} = \frac{h_{l_T}}{g} = \left(K_{ent} + f_1 \frac{L_1}{D_1} \right) \frac{\bar{V}_2^2}{2g} \left(\frac{D_2}{D_1} \right)^4 + \left(f_2 \frac{L_2}{D_2} + K_{exit} \right) \frac{\bar{V}_2^2}{2g}$$

or, upon simplifying,

$$H_{l_r} = \left[\left(K_{\text{ent}} + f_1 \frac{L_1}{D_1} \right) \left(\frac{D_2}{D_1} \right)^4 + f_2 \frac{L_2}{D_2} + K_{\text{exit}} \right] \frac{\bar{V}_2^2}{2g} \quad H_{l_r}$$

This is the head loss equation for the system. At the operating point, as indicated in Eq. 1, the head loss is equal to the head produced by the pump, given by

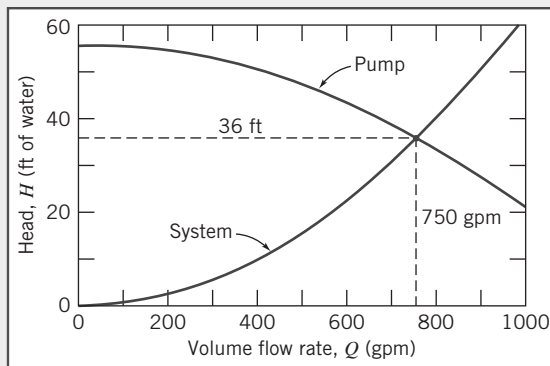
$$H_a = H_0 - A Q^2 \quad (2)$$

where $H_0 = 55.9$ ft and $A = 3.44 \times 10^{-5}$ ft/(gpm)².

The head loss in the system and head produced by the pump can be computed for a range of flow rates:

Q (gpm)	\bar{V}_1 (ft/s)	Re_1 (1000)	f_1 (-)	\bar{V}_2 (ft/s)	Re_2 (1000)	f_2 (-)	H_{l_r} (ft)	H_a (ft)
0	0.00	0	—	0.00	0	—	0.0	55.9
100	0.41	32	0.026	0.64	40	0.025	0.7	55.6
200	0.82	63	0.023	1.28	79	0.023	2.7	54.5
300	1.23	95	0.022	1.91	119	0.023	5.9	52.8
400	1.63	127	0.022	2.55	158	0.022	10.3	50.4
500	2.04	158	0.021	3.19	198	0.022	15.8	47.3
600	2.45	190	0.021	3.83	237	0.022	22.6	43.5
700	2.86	222	0.021	4.47	277	0.022	30.6	39.0
800	3.27	253	0.021	5.11	317	0.022	39.7	33.9
900	3.68	285	0.021	5.74	356	0.021	50.1	28.0
1000	4.09	317	0.021	6.38	396	0.021	61.7	21.5
1100	4.49	348	0.020	7.02	435	0.021	74.4	
1200	4.90	380	0.020	7.66	475	0.021	88.4	
1300	5.31	412	0.020	8.30	515	0.021	103	
1400	5.72	443	0.020	8.94	554	0.021	120	
1500	6.13	475	0.020	9.57	594	0.021	137	

The pump curve and the system resistance curve are plotted below:



The graphical solution is shown on the plot. At the operating point, $H \approx 36$ ft and $Q \approx 750$ gpm.

We can obtain more accuracy from the graphical solution using the following approach: Because the Reynolds number corresponds to the fully turbulent regime, $f \approx \text{const.}$, we can simplify the equation for the head loss and write it in the form

$$H_{l_r} \approx C Q^2 \quad (3)$$

where $C = 8/\pi^2 D_2^4 g$ times the term in square brackets in the expression for H_{l_r} . We can obtain a value for C directly from Eq. 3 by using values for H_{l_r} and Q from the table at a point close to the anticipated operating point. For example, from the $Q = 700$ gpm data point,

$$C = \frac{H_{l_T}}{Q^2} = \frac{30.6 \text{ ft}}{700^2 (\text{gpm})^2} = 6.24 \times 10^{-5} \text{ ft}/(\text{gpm})^2$$

Hence, the approximate analytical expression for the system head curve is

$$H_{l_T} = 6.24 \times 10^{-5} \text{ ft}/(\text{gpm})^2 [Q(\text{gpm})]^2 \xleftarrow{\hspace{10em}} H_{l_T}$$

Using Eqs. 2 and 3 in Eq. 1, we obtain

$$H_0 - AQ^2 = CQ^2$$

Solving for Q , the volume flow rate at the operating point, gives

$$Q = \left[\frac{H_0}{A + C} \right]^{1/2}$$

For this case,

$$Q = \left[55.9 \text{ ft} \times \frac{(\text{gpm})^2}{(3.44 \times 10^{-5} + 6.24 \times 10^{-5}) \text{ ft}} \right]^{1/2} = 760 \text{ gpm} \xleftarrow{\hspace{10em}} Q$$

The volume flow rate may be substituted into either expression for head to calculate the head at the operating point as

$$H = CQ^2 = 6.24 \times 10^{-5} \frac{\text{ft}}{(\text{gpm})^2} \times (760)^2 (\text{gpm})^2 = 36.0 \text{ ft} \xleftarrow{\hspace{10em}} H$$

There is a negligible difference between the two operating points. Both are within the accuracy of the data.

This problem illustrates the procedures used to find the operating point of a pump and flow system.

- Equation 3, for the head loss in the system, must be replaced with an equation of the form $H = Z_o + CQ^2$ when the head H required by the system has a component Z_o due to gravity as well as a component due to head losses.

There are a number of practical issues associated with matching the system and pump characteristic curves. Pump wear reduces delivery and lowers efficiency. For systems with a flat curve, the pump characteristic can intersect the curve at two conditions. This may cause unsteady operation and the pump may “hunt” or oscillate periodically. When a hot liquid with entrained vapor is being pumped, the entrained gas can drastically reduce performance. Fluid viscosity may reduce or increase the performance of a centrifugal pump.

In some systems, such as chilled-water circulation in a building, there may be a wide range in demand with a relatively constant system resistance. Operating constant-speed pumps in series or parallel to supply the system requirements may be the most efficient option. The units are staged with pumps added as demand increases.

For pumps in *series*, the combined performance curve is derived by adding the head rises at each flow rate, as shown in Fig. 10.19. The increase in flow rate gained by operating pumps in series depends on the resistance of the system being supplied. In an actual system, it is not appropriate simply to connect two pumps in series. At a low head requirement when only one pump is sufficient, the flow through the second, unpowered pump would cause additional losses, raising the system resistance. A system of bypasses, valves, and check valves is necessary in an actual installation [9, 12].

Pumps also may be combined in parallel. The resulting performance curve, shown in Fig. 10.20 is obtained by adding the pump capacities at each head. The schematic in Fig. 10.20 shows that the parallel combination may be used most effectively to increase system capacity when the system curve is relatively flat. An actual system installation with parallel pumps also requires control to prevent backflow through the pump that is not powered.

Many other piping arrangements and pump combinations are possible. Pumps of different sizes, heads, and capacities may be combined in series, parallel, or series-parallel arrangements. In many applications the complexity is due to a requirement that the system handle a variety of flow rates. Throttling valves are usually necessary because constant-speed motors drive most pumps, so simply using a

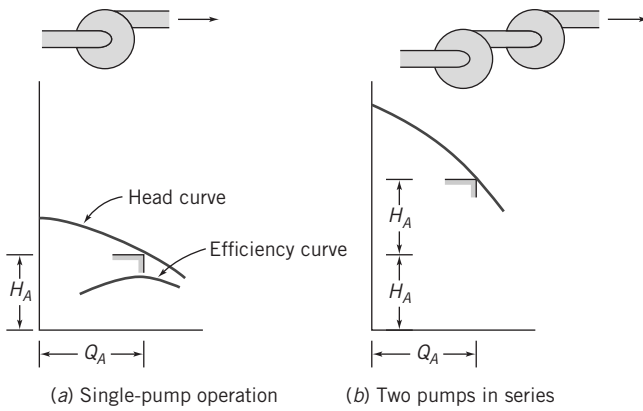


Fig. 10.19 Operation of two centrifugal pumps in series.

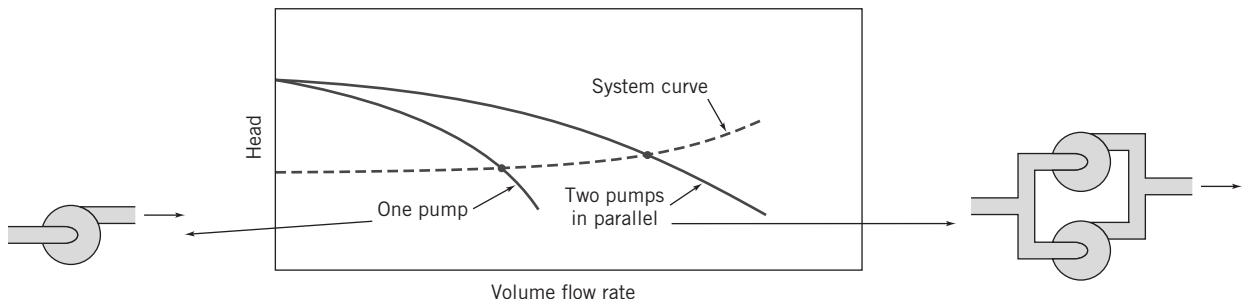


Fig. 10.20 Operation of two centrifugal pumps in parallel.

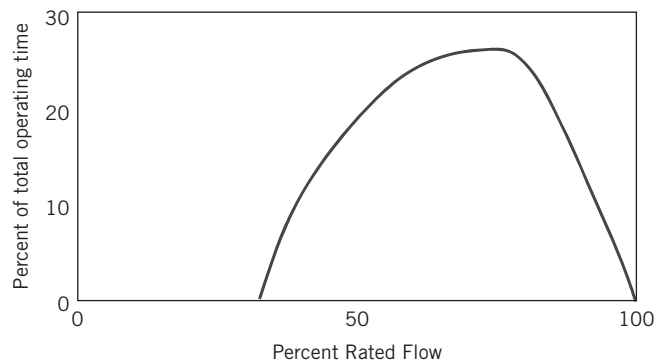


Fig. 10.21 Mean duty cycle for centrifugal pumps in the chemical and petroleum industries, based on Reference [13].

network of pumps without throttling valves allows the flow rate to be varied only in discrete steps. The disadvantage of throttling valves is that they can be a major loss of energy so that a given flow rate will require a larger power supply than would otherwise be the case.

Use of *variable-speed operation* allows infinitely variable control of system flow rate with high energy efficiency and without extra plumbing complexity. A further advantage is that a variable-speed drive system offers much simplified control of system flow rate. The cost savings for variable-speed drive systems can offset the added costs.

The energy and cost savings depend on the specific duty cycle on which the machine operates. Fig. 10.21 is a plot showing the percentage of the time an industrial pump operates at a given flow rate [18]. The plot is typical on many systems and shows that although the system must be designed and installed to deliver full rated capacity, this condition seldom occurs. Instead, more than half the time, the system operates at 70 percent capacity or below.

Blowers and Fans

Fans are designed to handle air or vapor and range from that of the cooling fan in a notebook computer moving a cubic meter of air per hour at a few watts of power to that of the ventilation fans for the Channel Tunnel that move thousands of cubic meters of air per minute and require hundreds of kilowatts of power. Fans are produced in several varieties such as radial-flow (centrifugal) and axial-flow devices. As with pumps, the performance curves for fans depend on the fan type. Some typical curves for centrifugal fans are presented in Appendix C.

A schematic of a centrifugal fan is shown in Fig. 10.22 along with commonly used terminology. The pressure rise produced by fans is several orders of magnitude less than that for pumps and the volume flow rate, since the fluid is a gas, is usually much higher. The machine efficiency may be based on either the static-to-static pressure rise or the static-to-total pressure rise [14] and is frequently plotted on the same characteristic graph as shown in Fig. 10.23. The difference between the total and static pressures is the dynamic pressure, so the vertical distance between these two curves is proportional to the square of the volume flow rate.

There are three general types of centrifugal fans as shown in Fig. 10.24a–c, with backward-curved, radial-tipped, and forward curved blades. All the fans have blades that are curved at their inlet edges to approximate shockless flow between the blade and the inlet flow direction. The forward-curved design illustrated in the figure has very closely spaced blades; it is frequently called a *squirrel-cage fan* because of its resemblance to the exercise wheels found in animal cages. As fans become larger in size and power demand, efficiency becomes more important. The streamlined *airfoil blades* shown in Fig. 10.24d are much less sensitive to inlet flow direction and improve efficiency markedly compared with the thin blades shown in diagrams a through c.

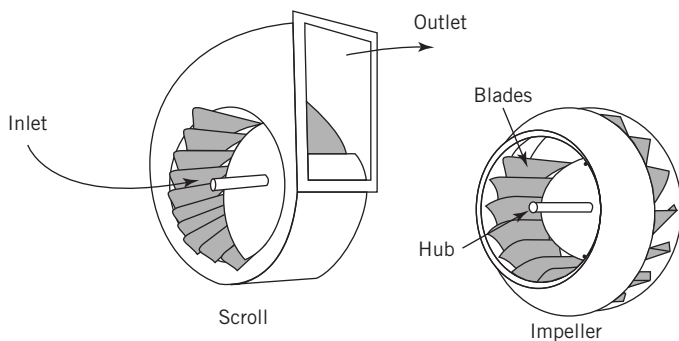


Fig. 10.22 Schematic of a typical centrifugal fan.

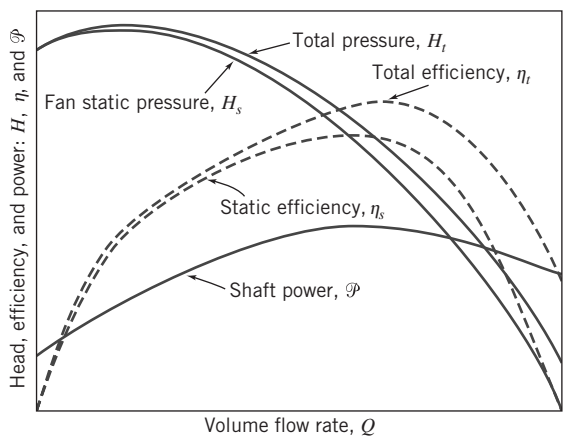


Fig. 10.23 Typical characteristic curves for fan with backward-curved blades.

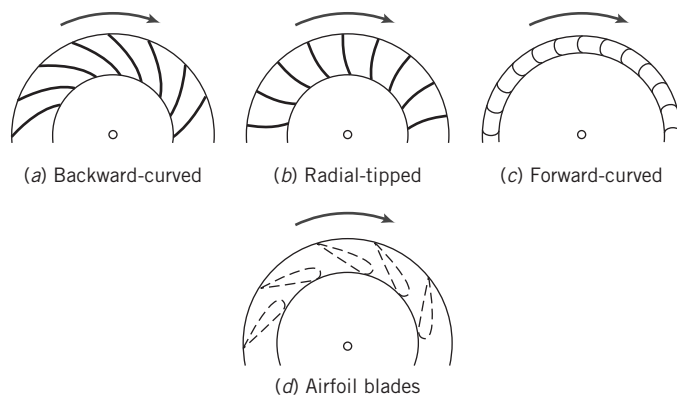


Fig. 10.24 Typical types of blading used for centrifugal fan wheels.

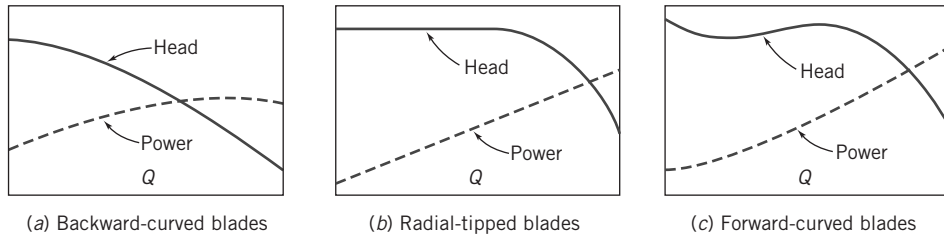


Fig. 10.25 General features of performance curves for centrifugal fans with backward-, radial-, and forward-curved blades.

As is true for pumps, the total pressure rise across a fan is approximately proportional to the absolute velocity of the fluid at the exit from the wheel. The characteristic curves produced by the basic blade shapes tend to differ from each other. The typical curve shapes are as shown in Fig. 10.25, where both pressure rise and power requirements are sketched. Fans with backward-curved blade tips typically have a power curve that reaches a maximum and then decreases as flow rate increases. The power curves for fans with radial and forward-curved blades rise as flow rate increases. Fans with backward-curved blades are best for installations with large power demand and continuous operation. The forward-curved blade fan is preferred where low first cost and small size are important and where service is intermittent. Forward curved blades require lower tip speed to produce a specified head and lower blade tip speed means reduced noise. Thus forward-curved blades may be specified for heating and air conditioning applications to minimize noise.

Characteristic curves for axial-flow (*propeller*) fans differ markedly from those for centrifugal fans. The simple propeller fan is often used for ventilation and it may be free-standing or mounted in an opening, as a window fan, with no inlet or outlet duct work. Modern designs, with airfoil blades, mounted in ducts and often fitted with guide vanes, can deliver large volumes against high resistances with high efficiency [23]. The primary deficiencies are that in certain ranges of flow rate the fan may pulsate and because of the high rotational speeds they can be noisy.

Selection and installation of a fan requires compromise. To minimize energy consumption, it is desirable to operate a fan at its highest efficiency point. To reduce the fan size for a given capacity, it is desirable to operate at higher flow rate than that at maximum efficiency. This tradeoff must be made considering such factors as available space, initial cost, and annual hours of operation. Further, the duct system at both the inlet and the outlet of the fan affect performance.

Fans may be scaled up or down in size or speed using the basic laws developed for fluid machines in Chapter 7. It is possible for two fans to operate with fluids of significantly different density, so

pressure is used instead of head as a dependent parameter. The dimensionless groups appropriate for fan scaling are

$$\Pi_1 = \frac{Q}{\omega D^3}, \quad \Pi_2 = \frac{p}{\rho \omega^2 D^2}, \quad \text{and} \quad \Pi_3 = \frac{\mathcal{P}}{\rho \omega^2 D^5} \quad (10.29)$$

Once again, dynamic similarity is assured when the flow coefficients are matched. Thus when

$$Q' = Q \left(\frac{\omega'}{\omega} \right) \left(\frac{D'}{D} \right)^3 \quad (10.30a)$$

then

$$p' = p \left(\frac{\rho'}{\rho} \right) \left(\frac{\omega'}{\omega} \right)^2 \left(\frac{D'}{D} \right)^2 \quad (10.30b)$$

and

$$\mathcal{P}' = \mathcal{P} \left(\frac{\rho'}{\rho} \right) \left(\frac{\omega'}{\omega} \right)^3 \left(\frac{D'}{D} \right)^5 \quad (10.30c)$$

As a first approximation, the efficiency of the scaled fan is assumed to remain constant, so

$$\eta' = \eta \quad (10.30d)$$

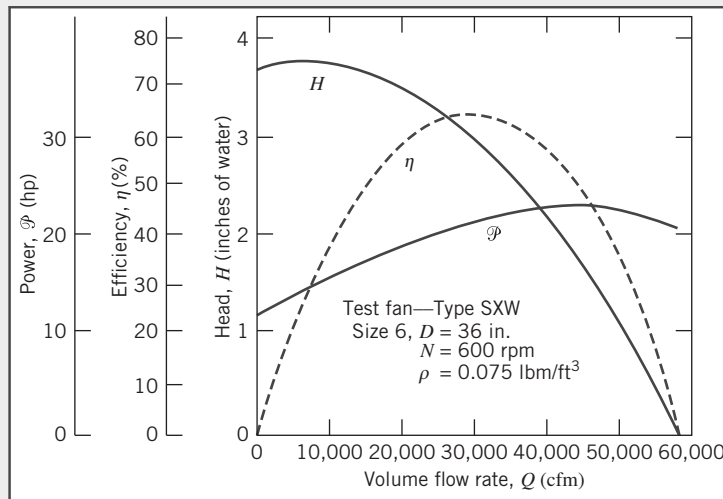
When head is replaced by pressure, and density is included, the expression defining the specific speed of a fan becomes

$$N_S = \frac{\omega Q^{1/2} \rho^{3/4}}{p^{3/4}} \quad (10.31)$$

A fan scale-up with density variation is the subject of Example 10.9.

Example 10.9 SCALING OF FAN PERFORMANCE

Performance curves [14] are given below for a centrifugal fan with $D = 36$ in. and $N = 600$ rpm, as measured on a test stand using cool air ($\rho = 0.075$ lbm/ft³). Scale the data to predict the performance of a similar fan with $D' = 42$ in., $N' = 1150$ rpm, and $\rho' = 0.045$ lbm/ft³. Estimate the delivery and power of the larger fan when it operates at a system pressure equivalent to 7.4 in. of H₂O. Check the specific speed of the fan at the new operating point.



Given: Performance data as shown for centrifugal fan with $D = 36$ in., $N = 600$ rpm, and $\rho = 0.075$ lbm/ft³.

- Find:**
- The predicted performance of a geometrically similar fan with $D' = 42$ in., at $N' = 1150$ rpm, with $\rho' = 0.045$ lbm/ft³.
 - An estimate of the delivery and input power requirement if the larger fan operates against a system resistance of 7.4 in. H₂O.
 - The specific speed of the larger fan at this operating point.

Solution: Develop the performance curves at the new operating condition by scaling the test data point-by-point. Using Eqs. 10.30 and the data from the curves at $Q = 30,000$ cfm, the new volume flow rate is

$$Q' = Q \left(\frac{N'}{N} \right) \left(\frac{D'}{D} \right)^3 = 30,000 \text{ cfm} \left(\frac{1150}{600} \right) \left(\frac{42}{36} \right)^3 = 91,300 \text{ cfm}$$

The fan pressure rise is

$$p' = p \frac{\rho'}{\rho} \left(\frac{N'}{N} \right)^2 \left(\frac{D'}{D} \right)^2 = 2.96 \text{ in. H}_2\text{O} \left(\frac{0.045}{0.075} \right) \left(\frac{1150}{600} \right)^2 \left(\frac{42}{36} \right)^2 = 8.88 \text{ in. H}_2\text{O}$$

and the new power input is

$$\mathcal{P}' = \mathcal{P} \left(\frac{\rho'}{\rho} \right) \left(\frac{N'}{N} \right)^3 \left(\frac{D'}{D} \right)^5 = 21.4 \text{ hp} \left(\frac{0.045}{0.075} \right) \left(\frac{1150}{600} \right)^3 \left(\frac{42}{36} \right)^5 = 195 \text{ hp}$$

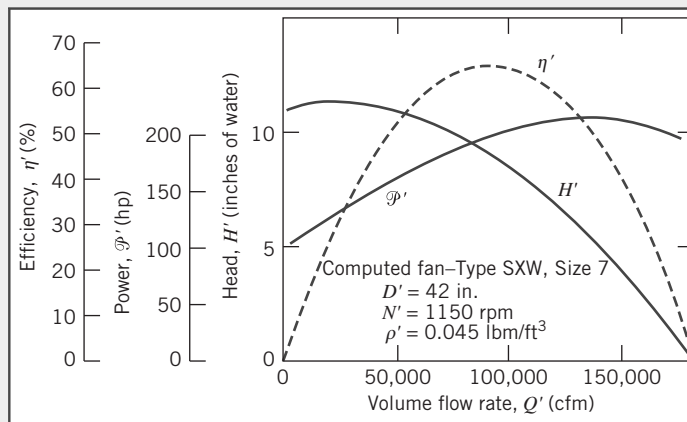
We assume the efficiency remains constant between the two scaled points, so

$$\eta' = \eta = 0.64$$

Similar calculations at other operating points give the results tabulated below:

Q (cfm)	p (in. H ₂ O)	\mathcal{P} (hp)	η (%)	Q' (cfm)	p' (in. H ₂ O)	\mathcal{P}' (hp)
0	3.68	11.1	0	0	11.0	101
10,000	3.75	15.1	37	30,400	11.3	138
20,000	3.50	18.6	59	60,900	10.5	170
30,000	2.96	21.4	65	91,300	8.88	195
40,000	2.12	23.1	57	122,000	6.36	211
50,000	1.02	23.1	34	152,000	3.06	211
60,000	0	21.0	0	183,000	0	192

To allow interpolation among the calculated points, it is convenient to plot the results:



From the head-capacity curve, the larger fan should deliver 110,000 cfm at 7.5 in. H₂O system head, with an efficiency of about 58 percent.

This operating point is only slightly to the right of peak efficiency for this fan, so it is a reasonable point at which to operate the fan. The specific speed of the fan at this operating point (in U.S. customary units) is given by direct substitution into Eq. 10.31:

$$N_{s_{cu}} = \frac{\omega Q^{1/2} \rho^{3/4}}{p^{3/4}} = \frac{(1150 \text{ rpm})(110,000 \text{ cfm})^{1/2} (0.045 \text{ lbm/ft}^3)^{3/4}}{(7.5 \text{ in. H}_2\text{O})^{3/4}}$$

$$= 8223 \xleftarrow[N_{s_{cu}}]{}$$

In nondimensional (SI) units,

$$N_s = \frac{(120 \text{ rad/s})(3110 \text{ m}^3/\text{s})^{1/2} (0.721 \text{ kg/m}^3)^{3/4}}{(1.86 \times 10^3 \text{ N/m}^2)^{3/4}} = 18.5 \xleftarrow[N_s(\text{SI})]$$

This problem illustrates the procedure for scaling performance of fans operating on gases with two different densities.

Three methods are available to control fan delivery: motor speed control, inlet dampers, and outlet throttling. The same benefits of reduced energy usage and noise using speed control that are found with pumps are obtained with fans. Inlet and outlet dampers are effective in controlling flow but they decrease efficiency and increase energy use.

Fans also may be combined in series, parallel, or more complex arrangements to match varying system resistance and flow needs. These combinations may be analyzed using the methods described for pumps [25] and [26].

10.4 Positive Displacement Pumps

Pressure is developed in positive-displacement pumps through volume reductions caused by movement of the boundary in which the fluid is confined. In contrast to turbomachines, positive displacement pumps can develop high pressures at relatively low speeds because the pumping effect depends on volume change instead of dynamic action.

Positive-displacement pumps frequently are used in hydraulic systems at pressures ranging up to 40 MPa (6000 psi). A principal advantage of hydraulic power is the high *power density* (power per unit weight or unit size) that can be achieved. For a given power output, a hydraulic system can be lighter and smaller than a typical electric-drive system. Numerous types of positive-displacement pumps have been developed. Examples include piston pumps, vane pumps, and gear pumps, and may be fixed- or variable-displacement.

The performance characteristics of most positive-displacement pumps are similar. Figure 10.26 is a schematic diagram of a typical gear pump. Oil enters the space between the gears at the bottom of the pump cavity, is carried outward and upward by the teeth of the rotating gears and exits through the outlet port at the top of the cavity. Pressure is generated as the oil is forced toward the pump outlet with leakage and backflow prevented by the closely fitting gear teeth at the center of the pump.

Figure 10.27 is a photo showing the robust housing and bearings needed to withstand the large pressure forces developed within the pump. It also shows pressure-loaded side plates designed to “float” and allow thermal expansion while maintaining the smallest possible side clearance between gears and housing.

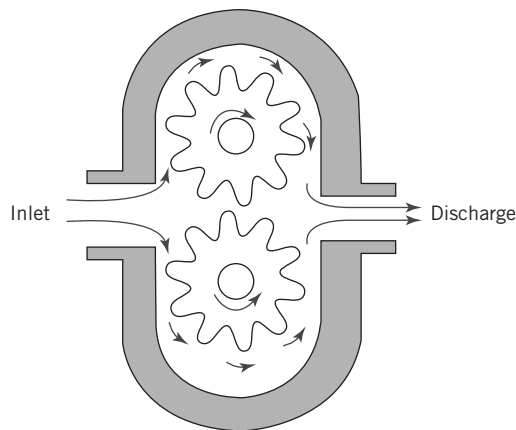


Fig. 10.26 Schematic of typical gear pump.

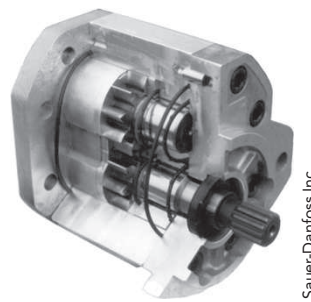


Fig. 10.27 Cutaway photograph of gear pump.
Sauer-Danfoss Inc

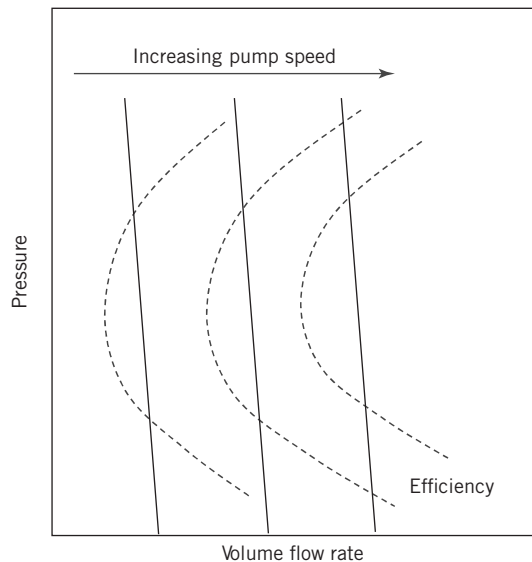


Fig. 10.28 Performance characteristics of typical gear pump.

Schematic performance curves of pressure versus delivery for a medium-duty gear pump are shown in Fig. 10.28. The pump size is specified by its displacement per revolution and the working fluid is characterized by its viscosity and temperature. Curves for three constant speeds are presented in the diagram. At each speed, delivery decreases slightly as pressure is raised. The pump displaces the same volume, but as pressure is raised, both leakage and backflow increase; so delivery decreases slightly.

Overall efficiency, defined as power delivered to the fluid divided by power input, tends to rise and reach a maximum at intermediate pressure as pump speed increases. *Volumetric efficiency* is defined as actual volumetric delivery divided by pump displacement and decreases as pressure is raised or pump speed is reduced.

There are system losses with a fixed-displacement pump compared with losses for variable-displacement and variable-pressure pumps. A fixed-displacement pump will deliver fluid at a fixed flow rate. If the load requires a lower flow the remaining flow must be bypassed back to the reservoir. Variable-displacement pumps modulate delivery to meet the load at lower pressure, reducing loss and increasing efficiency. The best pump choice depends on the operating duty cycle. The performance of constant and variable displacement pumps are compared in Example 10.10.

Example 10.10 PERFORMANCE OF A POSITIVE-DISPLACEMENT PUMP

A hydraulic pump with performance characteristics represented in Fig. 10.28 delivers a flow rate of 48.5 gpm at zero pressure and 46.5 gpm at 1500 psig at a rotating speed of 2000 rpm. The displacement volume is 5.9 in³/revolution. It requires $Q = 20$ gpm at $p = 1500$ psig at one operating condition. Determine the volumetric efficiency at zero pressure. Compute the required pump power input, the power delivered to the load, and the power dissipated by throttling at this condition. Compare with the power dissipated by using (i) a variable-displacement pump at 3000 psig and (ii) a pump with load sensing that operates at 100 psi above the load requirement.

Given: Hydraulic pump, with performance characteristics of Fig. 10.28 operating at 2000 rpm. System requires $Q = 20$ gpm at $p = 1500$ psig.

- Find:**
- (a) The volumetric efficiency at zero pressure.
 - (b) The required pump power input.
 - (c) The power delivered to the load.
 - (d) The power dissipated by throttling at this condition.
 - (e) The power dissipated using:
 - (i) a variable-displacement pump at 3000 psig,
 - (ii) a pump with load sensing that operates at 100 psi above the load pressure requirement.

Solution: The volumetric efficiency at zero pressure is determined using the flow rate of 48.5 gpm. The volume of fluid pumped per revolution is

$$\nabla = \frac{Q}{N} = 48.5 \frac{\text{gal}}{\text{min}} \times \frac{\text{min}}{2000 \text{ rev}} \times 231 \frac{\text{in.}^3}{\text{gal}} = 5.60 \text{ in.}^3/\text{rev} \quad \underline{\nabla}$$

The volumetric efficiency of the pump at maximum flow is

$$\eta_V = \frac{\nabla_{\text{calc}}}{\nabla_{\text{pump}}} = \frac{5.60}{5.9} = 0.949$$

At 1500 psig, the pump delivers 46.5 gpm. The power delivered to the fluid is

$$\begin{aligned} \mathcal{P}_{\text{fluid}} &= \rho Q g H_p = Q \Delta p_p \\ &= 46.5 \frac{\text{gal}}{\text{min}} \times 1500 \frac{\text{lbf}}{\text{in.}^2} \times \frac{\text{ft}^3}{7.48 \text{ gal}} \times \frac{\text{min}}{60 \text{ s}} \times 144 \frac{\text{in.}^2}{\text{ft}^2} \times \frac{\text{hp} \cdot \text{s}}{550 \text{ ft} \cdot \text{lbf}} \\ \mathcal{P}_{\text{fluid}} &= 40.7 \text{ hp} \end{aligned}$$

The pump efficiency at this operating condition is given as $\eta = 0.84$. Therefore the required input power is

$$\mathcal{P}_{\text{input}} = \frac{\mathcal{P}_{\text{fluid}}}{\eta} = \frac{40.7 \text{ hp}}{0.84} = 48 \text{ hp} \quad \underline{\mathcal{P}_{\text{input}}}$$

The power delivered to the load is

$$\begin{aligned} \mathcal{P}_{\text{load}} &= Q_{\text{load}} \Delta p_{\text{load}} \\ &= 20.0 \frac{\text{gal}}{\text{min}} \times 1500 \frac{\text{lbf}}{\text{in.}^2} \times \frac{\text{ft}^3}{7.48 \text{ gal}} \times \frac{\text{min}}{60 \text{ s}} \times 144 \frac{\text{in.}^2}{\text{ft}^2} \times \frac{\text{hp} \cdot \text{s}}{550 \text{ ft} \cdot \text{lbf}} \\ \mathcal{P}_{\text{load}} &= 17.5 \text{ hp} \quad \underline{\mathcal{P}_{\text{load}}} \end{aligned}$$

The power dissipated by throttling is

$$\mathcal{P}_{\text{dissipated}} = \mathcal{P}_{\text{fluid}} - \mathcal{P}_{\text{load}} = 40.7 - 17.5 = 23.2 \text{ hp} \quad \underline{\mathcal{P}_{\text{dissipated}}}$$

The dissipation with the variable-displacement pump is

$$\begin{aligned}\mathcal{P}_{\text{var-disp}} &= Q_{\text{load}}(p_{\text{oper}} - p_{\text{load}}) \\ &= 20.0 \frac{\text{gal}}{\text{min}} \times (3000 - 1500) \frac{\text{lbf}}{\text{in}^2} \times \frac{\text{ft}^3}{7.48 \text{ gal}} \times \frac{\text{min}}{60 \text{ s}} \times 144 \frac{\text{in}^2}{\text{ft}^2} \times \frac{\text{hp} \cdot \text{s}}{550 \text{ ft} \cdot \text{lbf}} \\ \mathcal{P}_{\text{var-disp}} &= 17.5 \text{ hp} \end{aligned}$$

The dissipation with the variable-displacement pump is therefore less than the 23.2 hp dissipated with the constant-displacement pump and throttle. The saving is approximately 6 hp.

The final computation is for the load-sensing pump. If the pump pressure is 100 psi above that required by the load, the excess energy dissipation is

$$\begin{aligned}\mathcal{P}_{\text{var-disp}} &= Q_{\text{load}}(p_{\text{oper}} - p_{\text{load}}) \\ &= 20.0 \frac{\text{gal}}{\text{min}} \times 100 \frac{\text{lbf}}{\text{in}^2} \times \frac{\text{ft}^3}{7.48 \text{ gal}} \times \frac{\text{min}}{60 \text{ s}} \times 144 \frac{\text{in}^2}{\text{ft}^2} \times \frac{\text{hp} \cdot \text{s}}{550 \text{ ft} \cdot \text{lbf}} \\ \mathcal{P}_{\text{var-disp}} &= 1.17 \text{ hp} \end{aligned}$$

This problem contrasts the performance of a system with a pump of constant displacement to that of a system with variable-displacement and load-sensing pumps. The specific savings depend on the system operating point and on the duty cycle of the system.

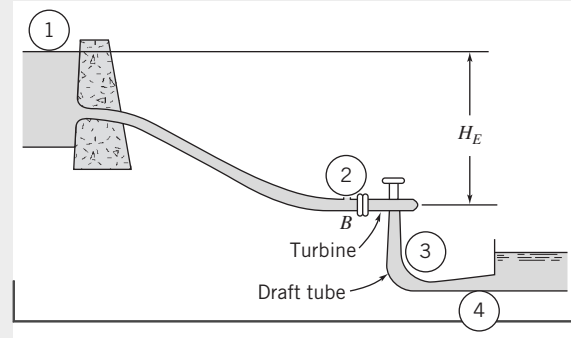
10.5 Hydraulic Turbines

Hydraulic Turbine Theory

The theory for machines extracting work from a fluid is similar to that for pumps with the difference being that torque, work, and power will be negative instead of positive. Example 10.11 illustrates the application of the Euler turbomachine equation to a reaction turbine.

Example 10.11 IDEAL ANALYSIS OF A REACTION TURBINE

In a vertical-shaft Francis turbine the available head at the inlet flange of the turbine is 500 ft and the vertical distance between the runner and the tailrace is 6.5 ft. The runner tip speed is 115 ft/s, the velocity of the water entering the runner is 130 ft/s, and the velocity of the water exiting the runner is constant and equal to 35 ft/s. The flow velocity at the exit of the draft tube is 11.5 ft/s. The hydraulic energy losses estimated from the turbine are equal to 20 ft at the volute, 3.5 ft at the draft tube, and 33.0 ft at the runner. Determine the pressure head (with respect to the tailrace) at the inlet and exit of the runner, the flow angle at the runner inlet, and the efficiency of the turbine.



Given: Flow through a vertical shaft Francis turbine

Head at entrance: 500 ft

Distance between runner and tailrace: 6.5 ft

Runner tip speed: 115 ft/s

Velocity at runner entrance: 130 ft/s

Velocity at runner exit: 35 ft/s

Flow velocity at draft tube exit: 11.5 ft/s

Losses: 20 ft at volute, 3.5 ft at draft tube, 33 ft at runner

Find: (a) Pressure head at inlet and exit of runner.

(b) Flow angle at runner inlet.

(c) Turbine efficiency.

Solution: Apply the energy and Euler turbomachine equations to the control volume.

Governing equations:

$$H = \frac{\dot{W}_m}{\dot{m}g} = \frac{1}{g}(U_2 V_{t2} - U_1 V_{t1}) \quad (10.2c)$$

$$\eta_t = \frac{\dot{W}_m}{\dot{W}_h} = \frac{\omega T}{\rho Q g H_t} \quad (10.4c)$$

$$\frac{p_1}{\rho g} + \alpha_1 \frac{\bar{V}_1^2}{2g} + z_1 + H_a = \frac{p_2}{\rho g} + \alpha_2 \frac{\bar{V}_2^2}{2g} + z_2 + \frac{h_{lt}}{g} \quad (10.28b)$$

Assumptions:

- 1 Steady flow
- 2 Uniform flow at each station
- 3 Turbulent flow; $\alpha = 1$
- 4 Reservoir and tailrace are at atmospheric pressure
- 5 Reservoir is at stagnation condition; $\bar{V}_1 = 0$

(a) If we apply the energy equation between the runner exit and the tailrace:

$$H_3 = \frac{p_3 - p_{atm}}{\rho g} = \frac{\bar{V}_4^2 - \bar{V}_3^2}{2g} + \Delta H_{DT} + z_4$$

$$H_3 = \frac{1}{2} \times \left[\left(11.5 \frac{\text{ft}}{\text{s}} \right)^2 - \left(35 \frac{\text{ft}}{\text{s}} \right)^2 \right] \times \frac{1}{32.2 \frac{\text{ft}}{\text{s}^2}} + 3.5 \text{ ft} - 6.5 \text{ ft} = -19.97 \text{ ft} \xrightarrow{H_3}$$

(negative sign indicates suction)

Next we apply the energy equation between the runner entrance and the tailrace:

$$H_2 = \frac{p_2 - p_{atm}}{\rho g} = H_E - \Delta H_R - \frac{\bar{V}_2^2}{2g}$$

$$H_2 = 500 \text{ ft} - 33.0 \text{ ft} - \frac{1}{2} \times \left(130 \frac{\text{ft}}{\text{s}} \right)^2 \times \frac{1}{32.2 \frac{\text{ft}}{\text{s}^2}} = 205 \text{ ft} \xrightarrow{H_2}$$

(b) Applying the energy equation across the entire system provides the work extraction through the turbine:

$$\frac{p_1}{\rho g} + \alpha_1 \frac{\bar{V}_1^2}{2g} + z_1 + H_a = \frac{p_4}{\rho g} + \alpha_4 \frac{\bar{V}_4^2}{2g} + z_4 + \frac{h_{lt}}{g}$$

If we simplify the expression based on assumptions and solve for the head extracted at the turbine:

$$H_a = \frac{\bar{V}_4^2}{2g} - z_1 + z_4 + \sum \Delta H = \frac{\bar{V}_4^2}{2g} - (H_E + z) + (\Delta H_V + \Delta H_R + \Delta H_{DT})$$

Since station 1 is higher than station 4, we will take the negative of H_a and call that H_T , the head extracted at the turbine:

$$H_T = -\frac{\bar{V}_4^2}{2g} + (H_E + z) - (\Delta H_V + \Delta H_R + \Delta H_{DT})$$

$$= -\frac{1}{2} \times \left(11.5 \frac{\text{ft}}{\text{s}} \right)^2 \times \frac{1}{32.2 \frac{\text{ft}}{\text{s}^2}} + (500 \text{ ft} + 6.5 \text{ ft}) - (20 \text{ ft} + 33 \text{ ft} + 3.5 \text{ ft}) = 448 \text{ ft}$$

Applying the Euler turbomachine equation to this system:

$$-H_T = \frac{U_3 V_{t3} - U_2 V_{t2}}{g}$$

Solving for the tangential velocity at 2:

$$V_{t2} = \frac{g H_T}{U_2} = 32.2 \frac{\text{ft}}{\text{s}^2} \times 448 \text{ ft} \times \frac{1}{115 \text{ ft}} = 125.4 \frac{\text{ft}}{\text{s}}$$

Setting up the velocity triangle:

$$\beta_2 = \tan^{-1} \frac{V_{t2} - U_2}{V_{n2}} = \tan^{-1} \frac{125.4 - 115}{35} = 16.58^\circ \quad \beta_2$$

$$\alpha_2 = \tan^{-1} \frac{V_{t2}}{V_{n2}} = \tan^{-1} \frac{125.4}{10.5} = 85.2^\circ \quad \alpha_2$$

(c) To calculate the efficiency:

$$\eta_t = \frac{\dot{W}_m}{\dot{W}_h} = \frac{gH_T}{gH_E} = \frac{448}{500} = 89.6\% \quad \eta$$

This problem demonstrates the analysis of a hydraulic turbine with head losses and quantifies those effects in terms of a turbine efficiency. In addition, since the head at the turbine exit is below atmospheric, care must be taken to ensure that cavitation does not occur.

Performance Characteristics for Hydraulic Turbines

The impulse turbine is a relatively simple turbomachine and used to illustrate typical test results. Most impulse turbines used today are improved versions of the *Pelton wheel* developed in the 1880s by American mining engineer Lester Pelton. An impulse turbine is supplied with water under high head through a long conduit called a *penstock*. The water is accelerated through a nozzle and discharges as a high-speed free jet at atmospheric pressure. The jet strikes deflecting buckets attached to the rim of a rotating wheel, reducing the jet kinetic energy. Turbine output is controlled by changing the flow rate of water striking the buckets. Water discharged from the wheel at relatively low speed falls into the tailrace.

Figure 10.29 illustrates an impulse-turbine installation. The *gross head* available is the difference between the levels in the supply reservoir and the tailrace. The effective or *net head*, H , used to calculate efficiency, is the total head at the *entrance* to the nozzle measured at the nozzle centerline [7]. Not all of the net head is converted into work at the turbine as some is lost to turbine inefficiency, some in the nozzle itself, and some as residual kinetic energy in the exit flow. The penstock usually is sized so that the net head is 85–95 percent of the gross head. Figure 10.30 shows typical results from tests performed at constant head.

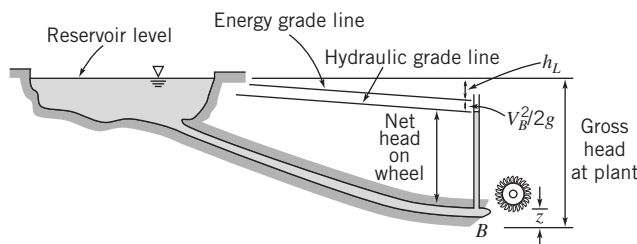


Fig. 10.29 Schematic of impulse-turbine installation, showing definitions of gross and net heads.

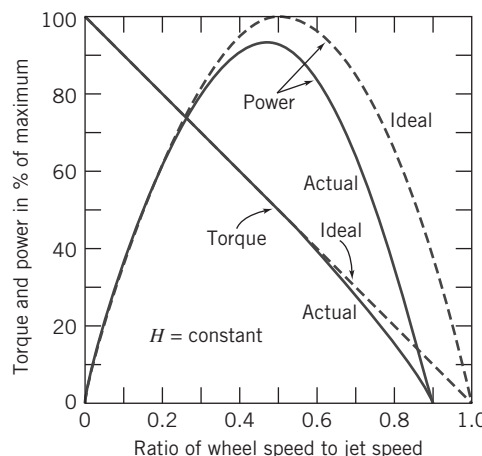


Fig. 10.30 Ideal and actual variable-speed performance for an impulse turbine [4].

The peak efficiency of the impulse turbine corresponds to the peak power, as shown in Example 10.12. For the ideal turbine this occurs when the wheel speed is half the jet speed. At this wheel speed the fluid exits the turbine at the lowest absolute velocity possible, minimizing the loss of kinetic energy at the exit. For large units, overall efficiency may be as high as 88 percent [15].

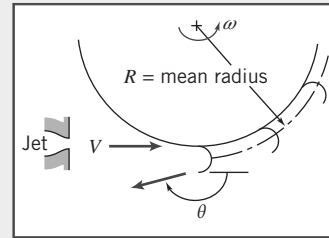
Example 10.12 OPTIMUM SPEED FOR IMPULSE TURBINE

Consider the Pelton wheel and single-jet arrangement shown, in which the jet stream strikes the bucket tangentially and is turned through angle θ . Obtain an expression for the torque exerted by the water stream on the wheel and the corresponding power output. Show that the power is a maximum when the bucket speed, $U = R\omega$, is half the jet speed, V .

Given: Pelton wheel and single jet shown.

Find: (a) Expression for torque exerted on the wheel.
 (b) Expression for power output.
 (c) Ratio of wheel speed U to jet speed V for maximum power.

Solution: As an illustration of its use, we start with the angular-momentum equation, Eq. 4.52, for a rotating CV as shown, rather than the inertial CV form, Eq. 4.46, that we used in deriving the Euler turbomachine equation in Section 10.2.

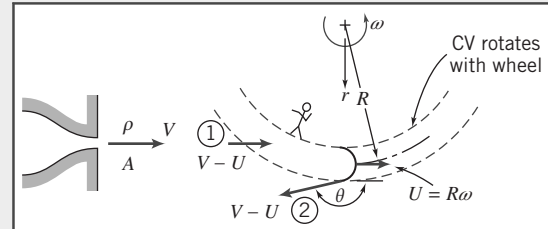


Governing equation:

$$\begin{aligned}
 &= 0(1) &&= 0(2) && \approx 0(3) \\
 \vec{r} \times \vec{F}_s + \int_{CV} \vec{r} \times \vec{g} \rho dV + \vec{T}_{\text{shaft}} - \int_{CV} \vec{r} \times [2\vec{\omega} \times \vec{V}_{xyz} + \vec{\omega} \times (\vec{\omega} \times \vec{r}) + \dot{\vec{\omega}} \times \vec{r}] \rho dV && \\
 &= 0(4) \\
 &= \frac{\partial}{\partial t} \int_{CV} \vec{r} \times \vec{V}_{xyz} \rho dV + \int_{CS} \vec{r} \times \vec{V}_{xyz} \rho \vec{V}_{xyz} \cdot d\vec{A} && (4.52)
 \end{aligned}$$

Assumptions:

- 1 Neglect torque due to surface forces.
- 2 Neglect torque due to body forces.
- 3 Neglect mass of water on wheel.
- 4 Steady flow with respect to wheel.
- 5 All water that issues from the nozzle acts upon the buckets.
- 6 Bucket height is small compared with R , hence $r_1 \approx r_2 \approx R$.
- 7 Uniform flow at each section.
- 8 No change in jet speed relative to bucket.



Then, since all water from the jet crosses the buckets,

$$\begin{aligned}
 \vec{T}_{\text{shaft}} &= \vec{r}_1 \times \vec{V}_1 (-\rho VA) + \vec{r}_2 \times \vec{V}_2 (+\rho VA) \\
 \vec{r}_1 &= R\hat{e}_r & \vec{r}_2 &= R\hat{e}_r \\
 \vec{V}_1 &= (V-U)\hat{e}_\theta & \vec{V}_2 &= (V-U)\cos\theta\hat{e}_\theta + (V-U)\sin\theta\hat{e}_r \\
 \vec{T}_{\text{shaft}} \hat{k} &= R(V-U)\hat{k}(-\rho VA) + R(V-U)\cos\theta\hat{k}(\rho VA)
 \end{aligned}$$

so that finally

$$T_{\text{shaft}} \hat{k} = -R(1-\cos\theta)\rho VA(V-U)\hat{k}$$

This is the external torque of the shaft on the control volume, i.e., on the wheel. The torque exerted by the water on the wheel is equal and opposite,

$$\vec{T}_{\text{out}} = -\vec{T}_{\text{shaft}} = R(1 - \cos \theta)\rho VA(V - U)\hat{k}$$

$$\vec{T}_{\text{out}} = \rho QR(V - U) \times (1 - \cos \theta)\hat{k} \quad \longleftarrow \vec{T}_{\text{out}}$$

The corresponding power output is

$$\dot{W}_{\text{out}} = \vec{\omega} \cdot \vec{T}_{\text{out}} = R\omega(1 - \cos \theta)\rho VA(V - U)$$

$$\dot{W}_{\text{out}} = \rho QU(V - U) \times (1 - \cos \theta) \quad \longleftarrow \dot{W}_{\text{out}}$$

To find the condition for maximum power, differentiate the expression for power with respect to wheel speed U and set the result equal to zero. Thus

$$\frac{d\dot{W}}{dU} = \rho Q(V - U)(1 - \cos \theta) + \rho QU(-1)(1 - \cos \theta) = 0$$

$$\therefore (V - U) - U = V - 2U = 0$$

$$\text{Thus for maximum power, } U/V = \frac{1}{2}U = V/2. \quad \longleftarrow U/V$$

Note: Turning the flow through $\theta = 180^\circ$ would give maximum power with $U = V/2$. Under these conditions, theoretically the *absolute* velocity of the fluid at the exit (computed in the direction of U) would be $U - (V - U) = V/2 - (V - V/2) = 0$, so that the fluid would exit with zero kinetic energy, maximizing the power output. In practice, it is only possible to deflect the jet stream through angles up to 165° . With $\theta = 165^\circ$, $1 - \cos \theta \approx 1.97$, or about 1.5 percent below the value for maximum power.

This problem illustrates the use of the angular-momentum equation for a rotating control volume, Eq. 4.52 (on the web), to analyze flow through an ideal impulse turbine.

- The peak power occurs when the wheel speed is half the jet speed, which is a useful design criterion when selecting a turbine for a given available head.
- This problem also could be analyzed starting with an inertial control volume, i.e., using the Euler turbomachine equation.

Hydraulic turbines usually are run at a constant speed, and output is varied by changing the opening area of the jet nozzle. Nozzle loss increases slightly and mechanical losses become a larger fraction of output as the valve is closed, so efficiency drops sharply at low load, as shown in Fig. 10.31. For this Pelton wheel, efficiency remains above 85 percent from 40 to 113 percent of full load.

For applications in which the head is relatively low, reaction turbines provide better efficiency than impulse turbines. In a reaction turbine, the fluid enters at the periphery and discharges at the inner radial section. Reaction turbines are high-flow, low-head machines. A typical reaction turbine installation is shown schematically in Fig. 10.32.

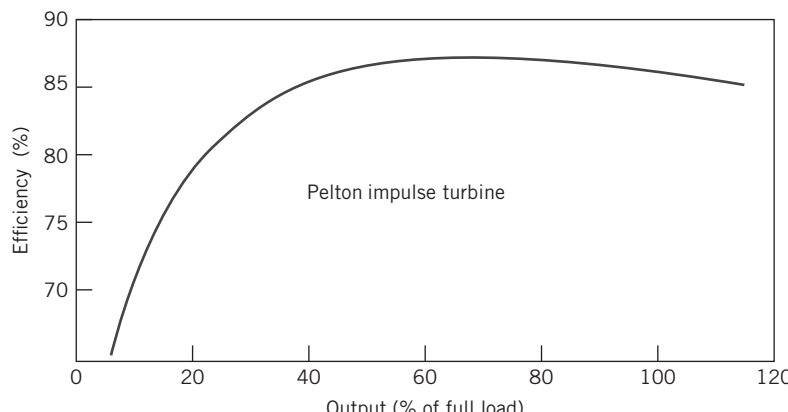


Fig. 10.31 Relation between efficiency and output for a typical Pelton water turbine, based on Reference [15].

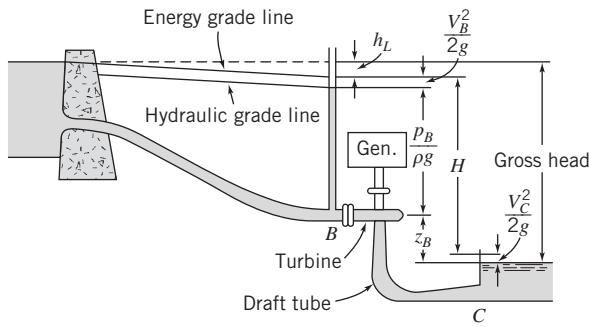


Fig. 10.32 Schematic of typical reaction turbine installation, showing definitions of head terminology.

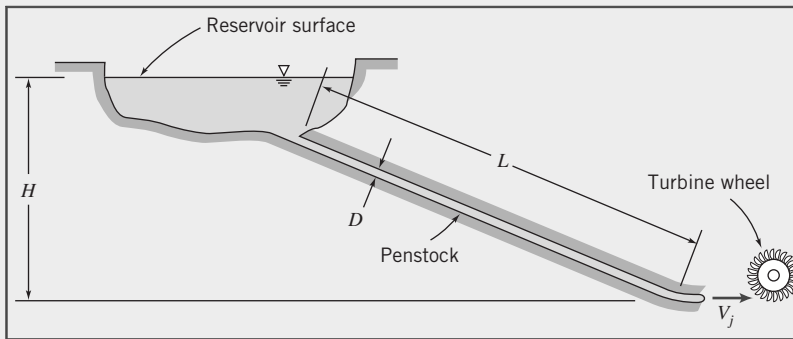
Reaction turbines use a diffuser or draft tube to regain a fraction of the kinetic energy that remains in water leaving the rotor. As shown in Fig. 10.32 the *gross head* available is the difference between the supply reservoir head and the tailrace head. The *effective head* or *net head*, H , used to calculate efficiency, is the difference between the elevation of the energy grade line just upstream of the turbine and that of the draft tube discharge (section C).

A number of other turbine types are sometimes used depending on the application. The *Francis turbine* (Fig. 10.5b) is usually chosen when $15 \text{ m} \leq H \leq 300 \text{ m}$, and the *Kaplan turbine* (Fig. 10.5c) is usually chosen for heads of 15 m or less.

Sizing a turbine for a given application requires a determination of the water flow and head available. The penstock length and diameter are important and need to be designed to accommodate the flow with minimum losses. Example 10.13 illustrates the design process.

Example 10.13 PERFORMANCE AND OPTIMIZATION OF AN IMPULSE TURBINE

Consider the hypothetical impulse turbine installation shown. Analyze flow in the penstock to develop an expression for the optimum turbine output power as a function of jet diameter, D_j . Obtain an expression for the ratio of jet diameter, D_j , to penstock diameter, D , at which output power is maximized. Under conditions of maximum power output, show that the head loss in the penstock is one-third of the available head. Develop a parametric equation for the minimum penstock diameter needed to produce a specified power output, using gross head and penstock length as parameters.



Given: Impulse turbine installation shown.

Find: (a) Expression for optimum turbine output power as a function of jet diameter.
 (b) Expression for the ratio of jet diameter, D_j , to penstock diameter, D , at which output power is maximized.

- (c) Ratio of head loss in penstock to available head for condition of maximum power.
- (d) Parametric equation for the minimum penstock diameter needed to produce a specified output power, using gross head and penstock length as parameters.

Solution: According to the results of Example 10.12, the output power of an idealized impulse turbine is given by $P_{\text{out}} = \rho Q U (V - U)(1 - \cos \theta)$. For optimum power output, $U = V/2 = V_j/2$, and

$$\begin{aligned} P_{\text{out}} &= \rho Q \frac{V}{2} \left(V - \frac{V}{2} \right) (1 - \cos \theta) = \rho A_j V_j \frac{V_j}{2} \frac{V_j}{2} (1 - \cos \theta) \\ P_{\text{out}} &= \rho A_j \frac{V_j^3}{1} (1 - \cos \theta) \end{aligned}$$

Thus output power is proportional to $A_j V_j^3$.

Apply the energy equation for steady incompressible pipe flow through the penstock to analyze V_j^2 at the nozzle outlet. Designate the free surface of the reservoir as section ① there $\bar{V}_1 \approx 0$.

Governing equation:

$$\left(\frac{p_1}{\rho} + \alpha \frac{\bar{V}_1^2}{2} + gz_1 \right)^{\approx 0} - \left(\frac{p_j}{\rho} + \alpha_j \frac{\bar{V}_j^2}{2} + gz_j \right) = h_{l_r} = \left(K_{\text{ent}} + f \frac{L}{D} \right) \frac{\bar{V}_p^2}{2} + K_{\text{nozzle}} \frac{\bar{V}_j^2}{2}$$

Assumptions:

- 1 Steady flow.
- 2 Incompressible flow.
- 3 Fully developed flow.
- 4 Atmospheric pressure at jet exit.
- 5 $\alpha_j = 1$, so $\bar{V}_j = V_j$.
- 6 Uniform flow in penstock, so $\bar{V}_p = V$.
- 7 $K_{\text{ent}} \ll f \frac{L}{D}$.
- 8 $K_{\text{nozzle}} = 1$.

Then

$$g(z_1 - z_j) = gH = f \frac{L V^2}{D 2} + \frac{V_j^2}{2} \quad \text{or} \quad V_j^2 = 2gH - f \frac{L}{D} V^2 \quad (1)$$

Hence the available head is partly consumed in friction in the supply penstock, and the rest is available as kinetic energy at the jet exit—in other words, the jet kinetic energy is reduced by the loss in the penstock. However, this loss itself is a function of jet speed, as we see from continuity:

$$VA = V_j A_j, \text{ so } V = V_j \frac{A_j}{A} = V_j \left(\frac{D_j}{D} \right)^2 \quad \text{and} \quad V_j^2 = 2gH - f \frac{L}{D} V_j^2 \left(\frac{D_j}{D} \right)^4$$

Solving for V_j , we obtain

$$V_j = \left[\frac{2gH}{\left\{ 1 + f \frac{L}{D} \left(\frac{D_j}{D} \right)^4 \right\}} \right]^{1/2} \quad (2)$$

The turbine power can be written as

$$\mathcal{P} = \rho A_j \frac{V_j^3}{4} (1 - \cos \theta) = \rho \frac{\pi}{16} D_j^2 \left[\frac{2gH}{\left\{ 1 + f \frac{L_j}{D} \left(\frac{D_j}{D} \right)^4 \right\}} \right]^{3/2} (1 - \cos \theta)$$

where $C_1 = \rho\pi(2gH)^{3/2}(1 - \cos\theta)/16 = \text{constant}$.

To find the condition for maximum power output, at fixed penstock diameter, D , differentiate with respect to D_j and set equal to zero,

$$\frac{d\mathcal{P}}{dD_j} = 2C_1 D_j \left[1 + f \frac{L}{D} \left(\frac{D_j}{D} \right)^4 \right]^{-3/2} - \frac{3}{2} C_1 D_j^2 \left[1 + f \frac{L}{D} \left(\frac{D_j}{D} \right)^4 \right]^{-5/2} 4f \frac{L}{D} \frac{D_j^3}{D^4} = 0$$

Thus,

$$1 + f \frac{L}{D} \left(\frac{D_j}{D} \right)^4 = 3f \frac{L}{D} \left(\frac{D_j}{D} \right)^4$$

Solving for D_j/D , we obtain

$$\frac{D_j}{D} = \left[\frac{1}{2f \frac{L}{D}} \right]^{1/4} \quad \longleftrightarrow \quad \frac{D_j}{D}$$

At this optimum value of D_j/D , the jet speed is given by Eq. 2 as

$$V_j = \left[\frac{2gH}{\left\{ 1 + f \frac{L}{D} \left(\frac{D_j}{D} \right)^4 \right\}} \right]^{1/2} = \sqrt{\frac{4}{3} g H}$$

The head loss at maximum power is then obtained from Eq. 1 after rearranging

$$h_l = f \frac{L V^2}{D^2} = gH - \frac{V_j^2}{2} = gH - \frac{2}{3}gH = \frac{1}{3}gH$$

and

$$\frac{h_l}{gH} = \frac{1}{3} \leftarrow \frac{h_l}{gH}$$

Under the conditions of maximum power

$$\mathcal{P}_{\max} = \rho V_j^3 \frac{A_j}{4} (1 - \cos\theta) = \rho \left(\frac{4}{3} g H\right)^{3/2} \frac{\pi}{16} \left[\frac{D^5}{2fL}\right]^{1/2} (1 - \cos\theta)$$

Finally, to solve for minimum penstock diameter for fixed output power, the equation may be written in the form

$$D \propto \left(\frac{L}{H}\right)^{1/5} \left(\frac{\mathcal{P}}{H}\right)^{2/5} \quad \longleftrightarrow \quad D$$

This problem illustrates the optimization of an idealized impulse turbine. The analysis determines the minimum penstock diameter needed to obtain a specified power output. In practice, larger diameters than this are used, reducing the frictional head loss below that computed here.

10.6 Propellers and Wind Turbines

Propellers

Propellers and wind turbines such as windmills and wind turbines may be considered axial-flow machines without housings [4]. A propeller produces thrust by imparting linear momentum to a fluid. Thrust production always leaves the stream with some kinetic energy and angular momentum that are not recoverable, so the process is never 100 percent efficient.

The one-dimensional flow model shown schematically in Fig. 10.33 is drawn in absolute coordinates on the left and as seen by an observer moving with the propeller, at speed V , on the right. The wake is modeled as a uniform steady flow as shown. Relative to the propeller, the upstream flow is at speed V and ambient pressure. The axial speed at the propeller is $V + \Delta V/2$, with a corresponding reduction in pressure. Downstream, the speed is $V + \Delta V$ and the pressure returns to ambient. The contraction of the slipstream area to satisfy continuity and the pressure rise across the propeller disk are shown in the figure.

To determine the power produced by a propeller, the x -component of linear momentum is applied to the control volume shown in Fig. 10.40. The fluid is assumed to be incompressible with the flow steady, frictionless, and in the horizontal direction. The Bernoulli equation applied to the control volume from section 1 to 2 is

$$\frac{p_{atm}}{\rho} + \frac{V_1^2}{2} = \frac{p_2}{\rho} + \frac{V_2^2}{2}$$

In terms of gage pressure, the pressure p_2 is

$$p_2 = \rho \left(\frac{V_2^2}{2} - \frac{V_1^2}{2} \right)$$

The Bernoulli equation applied to the control volume from section 3 to 4 is

$$\frac{p_3}{\rho} + \frac{V_3^2}{2} = \frac{p_{atm}}{\rho} + \frac{V_4^2}{2}$$

The pressure p_3 is then

$$p_3 = \rho \left(\frac{V_4^2}{2} - \frac{V_3^2}{2} \right)$$

Using the x -component of the linear momentum equation, and with $V_2 = V_3$, the thrust on the propeller

$$F_T = (p_3 - p_2)A = \frac{1}{2}\rho(V_4^2 - V_1^2)$$

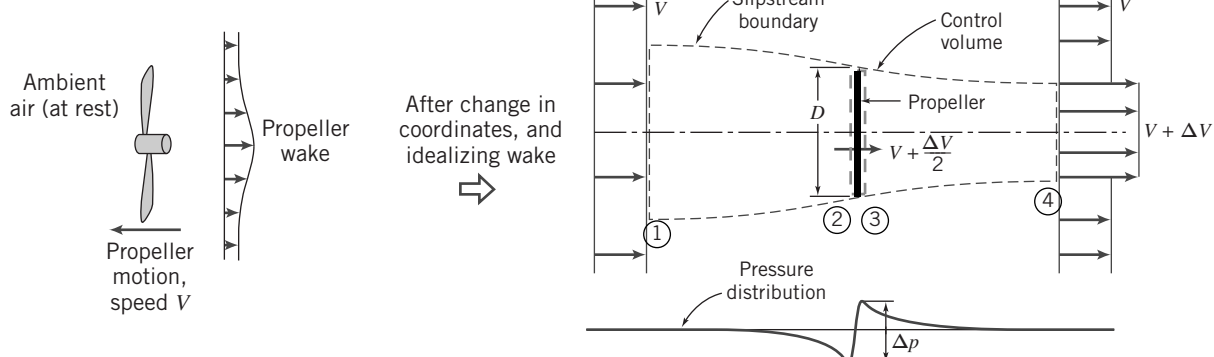


Fig. 10.33 One-dimensional flow model and control volume used to analyze an idealized propeller, based on Reference [4].

The velocity of the fluid at the propeller is V . The continuity equation gives the mass flow through the propeller as

$$\dot{m} = \rho A V$$

Applying the x -component of the momentum equation from section 1 to 4 yields

$$F_T = V_1(-\dot{m}) + V_4(+\dot{m}) = \rho A V (V_4 - V_1) = \rho A V \Delta V \quad (10.32)$$

The power required to increase the kinetic energy of the wind is

$$\mathcal{P}_{\text{input}} = \dot{m} \left[\frac{(V + \Delta V)^2}{2} - \frac{V^2}{2} \right] = \dot{m} \left[\frac{2V\Delta V + (\Delta V)^2}{2} \right] = \dot{m} V \Delta V \left[1 + \frac{\Delta V}{2V} \right] \quad (10.33)$$

The useful power produced is the product of thrust and speed of advance, V , of the propeller. Using Eq. 10.32, this may be written as

$$\mathcal{P}_{\text{useful}} = F_T V = \dot{m} V \Delta V \quad (10.34)$$

Combining Eqs. 10.34 and 10.35, and simplifying, gives the propulsive efficiency as

$$\eta = \frac{\mathcal{P}_{\text{useful}}}{\mathcal{P}_{\text{input}}} = \frac{1}{1 + \frac{\Delta V}{2V}} \quad (10.35)$$

Equations 10.32–10.35 are applicable to any device that creates thrust by increasing the speed of a fluid stream. Thus they apply equally well to propeller-driven or jet-propelled aircraft, boats, or ships.

The lift and drag on a propeller blade can be evaluated. A schematic diagram of an element of a rotating propeller blade is shown in Fig. 10.34. The blade is set at angle θ to the plane of the propeller disk and has a thickness of dr . Lift and drag forces are exerted on the blade perpendicular and parallel to the relative velocity vector V_r , respectively. The angle that V_r makes with the plane of the propeller disk is the *effective pitch angle*, ϕ , and therefore the lift and drag forces are inclined at an angle to the propeller rotation axis and the plane of the propeller disk, respectively. The relative speed of flow, V_r , passing over the blade element depends on both the blade peripheral speed, $r\omega$, and the *speed of advance*, V . Consequently, for a given blade setting, the angle of attack, α , depends on both V and $r\omega$.

For the free-body diagram of the airfoil element of width dr in Fig. 10.34, we find the magnitude of the resultant force dF_r parallel to the velocity vector V :

$$dF_T = dL \cos \phi - dD \sin \phi = q_r c dr (C_L \cos \phi - C_D \sin \phi) \quad (10.36a)$$

In this equation q_r is the dynamic pressure based on the relative velocity V_r ,

$$q_r = \frac{1}{2} \rho V_r^2 \quad (10.38)$$

c is the local chord length, and C_L and C_D are lift and drag coefficients, respectively, for the airfoil. In general, due to twist and taper in the propeller blades, and the radial variation of the blade peripheral speed, C_L, C_D, V_r, c, ϕ , and q_r will all be functions of the radial coordinate r . The torque that must be applied to the propeller is:

$$dT = r(dL \sin \phi + dD \cos \phi) = q_r c dr (C_L \sin \phi + C_D \cos \phi) \quad (10.36b)$$

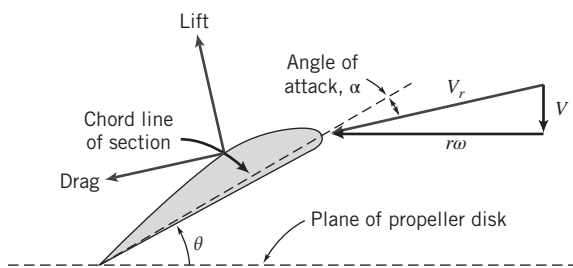


Fig. 10.34 Diagram of blade element and relative flow velocity vector.

These two expressions may be integrated to find the total propulsive thrust and torque, assuming N independent blades mounted on the rotor:

$$F_T = N \int_{r=R_{\text{hub}}}^{r=R} dF_T = qN \int_{R_{\text{hub}}}^R \frac{(C_L \cos \phi - C_D \sin \phi)}{\sin^2 \phi} cdr \quad (10.37a)$$

$$T = N \int_{r=R_{\text{hub}}}^{r=R} dT = qN \int_{R_{\text{hub}}}^R \frac{(C_L \sin \phi - C_D \cos \phi)}{\sin^2 \phi} cdr \quad (10.37b)$$

In these equations, q_r is replaced by $q/\sin^2 \phi$ based on the relationship between V and V_r . We will use the equations above to analyze the startup characteristics of a propeller in Example 10.14.

Example 10.14 PROPELLER STARTUP THRUST AND TORQUE

Use blade element theory to estimate the start-up thrust and torque for a propeller consisting of N independent blades with constant chord length, c , and at a constant angle, θ , with respect to the actuator disk plane.

Given:

Propeller with N independent blades

Chord length c is constant

Angle with respect to actuator disk θ is constant

Find: Expressions for startup thrust and torque

Solution: Apply the equations presented above to the propeller:

Governing equations:

$$dF_T = dL \cos \phi - dD \sin \phi = q_r cdr (C_L \cos \phi - C_D \sin \phi) \quad (10.36a)$$

$$dT = r(dL \sin \phi + dD \cos \phi) = q_r r cd़r (C_L \sin \phi + C_D \cos \phi) \quad (10.36b)$$

$$F_T = qN \int_{R_{\text{hub}}}^R \frac{(C_L \cos \phi - C_D \sin \phi)}{\sin^2 \phi} cdr \quad (10.37a)$$

$$T = qN \int_{R_{\text{hub}}}^R \frac{(C_L \sin \phi + C_D \cos \phi)}{\sin^2 \phi} r cd़r \quad (10.37b)$$

Assumptions:

Local wind velocity V is negligible.

Angular velocity ω is constant.

If at start-up we neglect the local wind velocity V , we find that the integrals in Eqs. 10.37 will be indeterminate since $q=0$ and $\phi=0$. Therefore, we will use the differential thrust and torque expressions given in Eqs. 10.36 and integrate them. At start-up, the relative velocity V_r is simply equal to the local blade element velocity $r\omega$. Therefore, the relative dynamic pressure q_r is equal to:

$$q_r = \frac{1}{2} \rho r^2 \omega^2$$

When $\phi=0$, the differential thrust and torque expressions become

$$dF_T = \frac{1}{2} \rho r^2 \omega^2 cdr (C_L \cos 0 - C_D \sin 0) = \frac{1}{2} \rho \omega^2 c C_L r^2 dr$$

$$dT = \frac{1}{2} \rho r^2 \omega^2 r cd़r (C_L \sin 0 + C_D \cos 0) = \frac{1}{2} \rho \omega^2 c C_D r^3 dr$$

We can then integrate the thrust and torque over the entire actuator disk:

$$F_T = N \int dF_T = \frac{1}{2} \rho \omega^2 c C_L \int_{R_{\text{hub}}}^R r^2 dr = \frac{1}{2} \rho \omega^2 c C_L \times \frac{1}{3} (R^3 - R_{\text{hub}}^3)$$

$$T = N \int dT = \frac{1}{2} \rho \omega^2 c C_D \int_{R_{\text{hub}}}^R r^3 dr = \frac{1}{2} \rho \omega^2 c C_D \times \frac{1}{4} (R^4 - R_{\text{hub}}^4)$$

When we collect terms and simplify we get the following expressions:

$$F_{T_{\text{startup}}} = \frac{\rho \omega^2 c C_L}{6} (R^3 - R_{\text{hub}}^3) \quad F_{T_{\text{startup}}}$$

$$T_{\text{startup}} = \frac{\rho \omega^2 c C_D}{8} (R^4 - R_{\text{hub}}^4) \quad T_{\text{startup}}$$

This problem demonstrates the analysis of a propeller using blade element theory. While the expressions here seem relatively simple, it is important to note that the lift and drag coefficients, C_L and C_D , are functions of the airfoil section being used, as well as the local angle of attack, α , which for $V = 0$ is equal to the blade inclination angle θ . In addition, it should also be noted that when airfoil lift and drag coefficients are presented, such as in Figs. 9.17 or 9.19, they are typically given at high Reynolds numbers, where the flow is fully turbulent and the lift and drag are insensitive to changes in speed. Care needs to be taken to make sure that the lift and drag coefficients used are appropriate for the Reynolds number at startup.

While these expressions may be relatively simple to derive, they are difficult to evaluate. Even if the geometry of the propeller is adjusted to give constant geometric pitch, the flow field in which it operates may not be uniform. Thus, the angle of attack across the blade elements may vary from the ideal, and it can be calculated only with the aid of a comprehensive computer code that can predict local flow directions and speeds. As a result, Eqs. 10.37 are not normally used, and propeller performance characteristics usually are measured experimentally. Figure 10.35 shows typical characteristics for a marine propeller [4] and for an aircraft propeller [17]. The variables used to plot the characteristics are almost dimensionless: by convention, rotational speed, n , is expressed in revolutions per second rather than as ω , in radians per second. The independent variable is the *speed of advance coefficient*, J ,

$$J \equiv \frac{V}{nD} \quad (10.39)$$

Dependent variables are the *thrust coefficient*, C_F , the *torque coefficient*, C_T , the *power coefficient*, C_P , and the *propeller efficiency*, η , defined as

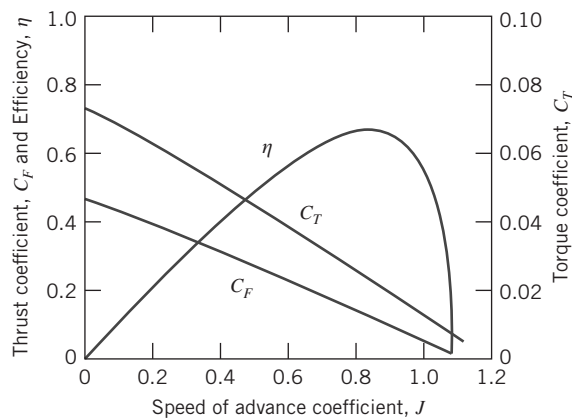
$$C_F = \frac{F_T}{\rho n^2 D^4}, \quad C_T = \frac{T}{\rho n^2 D^5}, \quad C_P = \frac{\mathcal{P}}{\rho n^3 D^5}, \quad \text{and} \quad \eta = \frac{F_T V}{\mathcal{P}_{\text{input}}} \quad (10.40)$$

The performance curves for both propellers show similar trends. Both thrust and torque coefficients are highest, and efficiency is zero, at zero speed of advance. This corresponds to the largest angle of attack for each blade element ($\alpha = \alpha_{\max} = \theta$). Efficiency is zero because no useful work is being done by the stationary propeller. As advance speed increases, thrust and torque decrease smoothly. Efficiency increases to a maximum at an optimum advance speed and then decreases to zero as thrust tends to zero.

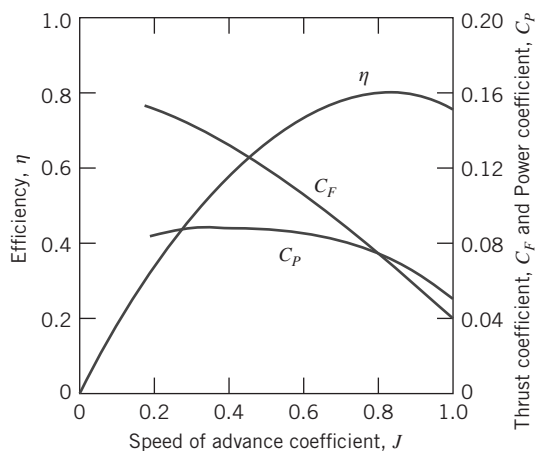
In order to improve performance, some propellers are designed with variable pitch. The performance of a variable-pitch propeller is shown in Fig. 10.36. This figure shows efficiency curves (solid curves) for a propeller set to different pitch angles. As we saw in Fig. 10.35, the propeller exhibits a maximum η at a certain value of J . However, the value of J needed for maximum η varies with θ . If we trace out all of the maxima, the result is the dashed curve in Fig. 10.36. Therefore, if we allow for the variation of θ , we may achieve improved efficiency over a wider range of J than with a fixed-pitch propeller.

Cavitation can be a problem in a liquid and it becomes more prevalent along the blades as the cavitation number,

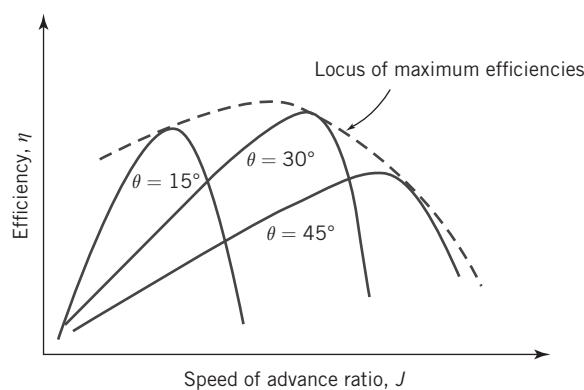
$$Ca = \frac{p - p_v}{\frac{1}{2} \rho V^2} \quad (10.41)$$



(a) Marine propeller, data from Reference [4]



(b) Aircraft propeller, data from Reference [17]

Fig. 10.35 Typical characteristics of two propellers.**Fig. 10.36** Propeller efficiency for a variable-pitch propeller at various overall incidences identified by θ at a fixed radial distance.

is reduced. Eq. 10.41 shows that Ca decreases when pressure is reduced by operating near the free surface or by increasing V .

Compressibility affects aircraft propellers when tip speeds approach the *critical Mach number*, at which the local Mach number approaches $M = 1$ at some point on the blade. Under these conditions, torque increases because of increased drag, thrust drops because of reduced section lift, and efficiency drops drastically.

Wind Turbines

Wind turbines have been used for centuries to harness the power of natural winds. Dutch windmills (Fig. 10.37a) turned slowly so that the power could be used to turn stone wheels for milling grain; hence the name “windmill.” American multi-blade windmills (Fig. 10.37b) were installed on many American farms from about 1850 and many are still in use today.

The emphasis on renewable resources has revived interest in windmill design and optimization. In 2016, wind turbines generated 82 gigawatts of electricity, representing 8 percent of the total electric energy consumption for that year [27]. Wind power accounts for one-third of *all* new generating capacity.

Schematics of wind turbine configurations are shown in Fig. 10.38. In general, wind turbines are classified in two ways. The first classification is the orientation of the turbine axis: horizontal-axis wind turbines (HAWT) and vertical-axis wind turbines (VAWT). Most HAWT designs feature two- or three-bladed propellers mounted on a tower along with its electric generator. The large modern HAWT, shown in Fig. 10.39a, is capable of producing power in any wind above a light breeze and is the type most commonly used in the electrical generation industry. The wind turbine shown in Fig. 10.39b is a VAWT. This device uses a modern symmetric airfoil section for the rotor. Earlier designs of the VAWT, such as the *Darrieus troposkien* shape, suffered from high bending stresses and pulsatory torques. More



Fig. 10.37 Examples of well-known windmills [18].

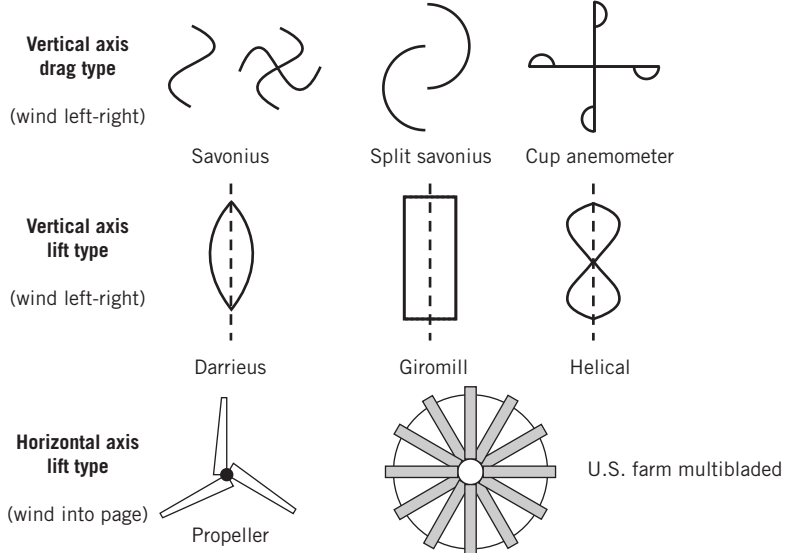


Fig. 10.38 Wind turbine configurations differentiated by axis orientation (horizontal versus vertical) and by nature of force exerted on the active element (lift versus drag).

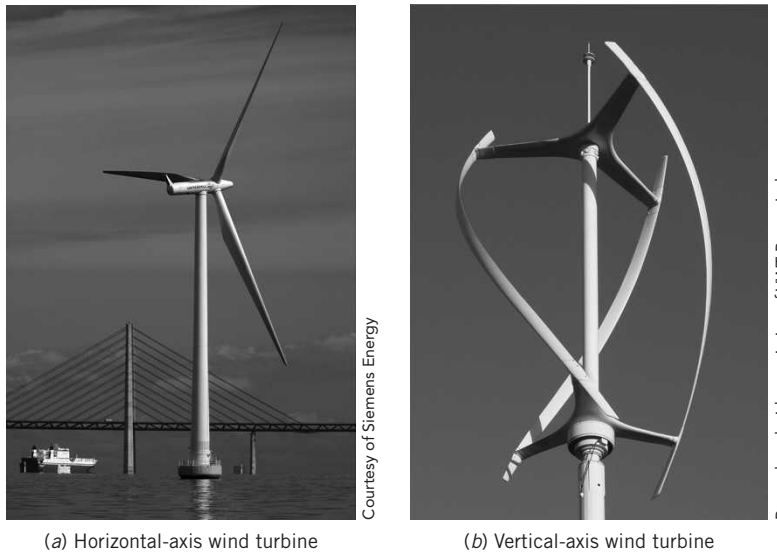


Fig. 10.39 Examples of modern wind turbine designs.

recent designs, such as the one shown in this figure, feature helical airfoils, which distribute the torques more evenly about the central axis. VAWTs feature a ground-mounted electric generator.

The second classification is how the wind energy is harnessed. The first group of turbines collects wind energy through drag forces; these wind turbines are typically of the vertical axis configuration only. The second group collects energy through lift forces. Lift-based wind turbines employ horizontal- or vertical-axis configurations. It is important to note that most of these designs are self-starting. The lift-type VAWT is not capable of starting from rest; it can produce usable power only above a certain minimum angular speed. It is typically combined with a self-starting turbine, such as a Savonius rotor, to provide starting torque [16, 22].

A horizontal-axis wind turbine may be analyzed as a propeller operated in reverse. The Rankine model of one-dimensional flow incorporating an idealized actuator disk is shown in Fig. 10.41. The simplified notation of the figure is frequently used for analysis of wind turbines.

The wind speed far upstream is V . The stream is decelerated to $V(1-a)$ at the turbine disk and to $V(1-2a)$ in the wake of the turbine (a is called the *interference factor*). Thus the stream tube of air captured by the wind turbine is small upstream and its diameter increases as it moves downstream.

Straightforward application of linear momentum to a CV, as shown in Example 10.15, predicts the axial thrust on a turbine of radius R to be

$$F_T = 2\pi R^2 \rho V^2 a(1-a) \quad (10.42)$$

Application of the energy equation assuming no losses gives the power taken from the fluid stream as

$$\mathcal{P} = 2\pi R^2 \rho V^3 a(1-a)^2 \quad (10.43)$$

The efficiency of a wind turbine is most conveniently defined with reference to the kinetic energy flux contained within a stream tube the size of the actuator disk. This kinetic energy flux is

$$KEF = \frac{1}{2} \rho V^3 \pi R^2 \quad (10.44)$$

Combining Eqs. 10.43 and 10.44 gives the efficiency (or alternatively, the *power coefficient* [23]) as

$$\eta = \frac{\mathcal{P}}{KEF} = 4a(1-a)^2 \quad (10.45)$$

Betz [27] was the first to derive this result and to show that the theoretical efficiency is maximized when $a = 1/3$. The maximum theoretical efficiency is $\eta = 0.593$.

If the wind turbine is lightly loaded (a is small), it will affect a large mass of air per unit time, but the energy extracted per unit mass will be small and the efficiency low. Most of the kinetic energy in the initial air stream will be left in the wake and wasted. If the wind turbine is heavily loaded ($a \approx 1/2$), it will affect a much smaller mass of air per unit time. The energy removed per unit mass will be large, but the power produced will be small compared with the kinetic energy flux through the undisturbed area of the actuator disk. Thus a peak efficiency occurs at intermediate disk loadings.

Example 10.15 PERFORMANCE OF AN IDEALIZED WIND TURBINE

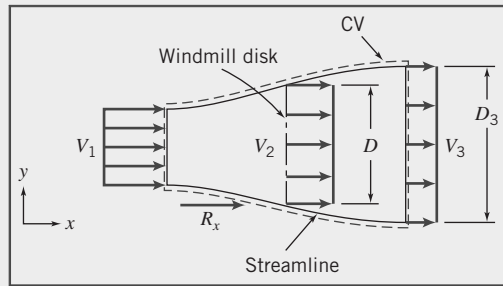
Develop general expressions for thrust, power output, and efficiency of an idealized windmill, as shown in Fig. 10.41. Calculate the thrust, ideal efficiency, and actual efficiency for the Dutch windmill tested by Calvert ($D = 26\text{ m}$, $N = 20\text{ rpm}$, $V = 36\text{ km/hr}$, and $\mathcal{P}_{\text{output}} = 41\text{ kW}$).

Given: Idealized windmill, as shown in Fig. 10.40, and Dutch windmill tested by Calvert:

$$D = 26\text{ m} \quad N = 20\text{ rpm} \quad V = 36\text{ km/hr} \quad \mathcal{P}_{\text{output}} = 41\text{ kW}$$

Find: (a) General expressions for the ideal thrust, power output, and efficiency.
(b) The thrust, power output, and ideal and actual efficiencies for the Dutch windmill tested by Calvert.

Solution: Apply the continuity, momentum (x -component), and energy equations, using the CV and coordinates shown.



Governing equations:

$$\begin{aligned} \frac{\partial}{\partial t} \int_{\text{CV}} \rho dV + \int_{\text{CS}} \rho \vec{V} \cdot d\vec{A} &= 0^{(3)} \\ F_{S_x} + F_{B_x} &= \frac{\partial}{\partial t} \int_{\text{CS}} u \rho dV + \int_{\text{CS}} u \rho \vec{V} \cdot d\vec{A}^{(2)} \\ \dot{Q} - \dot{W}_s &= \frac{\partial}{\partial t} \int_{\text{CV}} e \rho dV + \int_{\text{CS}} \left(e + \frac{p}{\rho} \right) \rho \vec{V} \cdot d\vec{A}^{(7)} \end{aligned}$$

Assumptions:

- 1 Atmospheric pressure acts on CV; $F_{S_x} = R_x$.
- 2 $F_{B_x} = 0$.
- 3 Steady flow.
- 4 Uniform flow at each section.
- 5 Incompressible flow of standard air.
- 6 $V_1 - V_2 = V_2 - V_3 = \frac{1}{2}(V_1 - V_3)$, as shown by Rankine.
- 7 $Q = 0$.
- 8 No change in internal energy for frictionless incompressible flow.

In terms of the interference factor, a , $V_1 = V$, $V_2 = (1-a)V$, and $V_3 = (1-2a)V$.

From continuity, for uniform flow at each cross section, $V_1A_1 = V_2A_2 = V_3A_3$.

From momentum,

$$R_x = u_1(-\rho V_1 A_1) + u_3(+\rho V_3 A_3) = (V_3 - V_1)\rho V_2 A_2 \quad \{u_1 = V_1, u_3 = V_3\}$$

R_x is the external force acting on the control volume. The thrust force exerted by the CV on the surroundings is

$$K_x = -R_x = (V_1 - V_3)\rho V_2 A_2$$

In terms of the interference factor, the equation for thrust may be written in the general form,

$$K_x = \rho V^2 \pi R^2 2a(1-a) \xrightarrow{K_x}$$

(Set dK_x/da equal to zero to show that maximum thrust occurs when $a = \frac{1}{2}$)

The energy equation becomes

$$-\dot{W}_s = \frac{V_1^2}{2}(-\rho V_1 A_1) + \frac{V_3^2}{2}(+\rho V_3 A_3) = \rho V_2 \pi R^2 \frac{1}{2}(V_3^2 - V_1^2)$$

The ideal output power, \mathcal{P} , is equal to \dot{W}_s . In terms of the interference factor,

$$\mathcal{P} = \dot{W}_s = \rho V(1-a)\pi R^2 \left[\frac{V^2}{2} - \frac{V^2}{2}(1-2a)^2 \right] = \rho V^3(1-a) \frac{\pi R^2}{2} [1 - (1-2a)^2]$$

After simplifying algebraically,

$$\mathcal{P}_{\text{ideal}} = 2\rho V^3 \pi R^2 a(1-a)^2 \xrightarrow{\mathcal{P}_{\text{ideal}}}$$

The kinetic energy flux through a stream tube of undisturbed flow, equal in area to the actuator disk, is

$$KEF = \rho V \pi R^2 \frac{V_2}{2} = \frac{1}{2} \rho V^3 \pi R^2$$

Thus the ideal efficiency may be written

$$\eta = \frac{\mathcal{P}_{\text{ideal}}}{KEF} = \frac{2\rho V^3 \pi R^2 a(1-a)^2}{\frac{1}{2} \rho V^3 \pi R^2} = 4a(1-a)^2 \xrightarrow{\eta}$$

To find the condition for maximum possible efficiency, set $d\eta/da$ equal to zero. The maximum efficiency is $\eta = 0.593$, which occurs when $a = 1/3$.

The Dutch windmill tested by Calvert had a tip-speed ratio of

$$X = \frac{NR}{V} = 20 \frac{\text{rev}}{\text{min}} \times 2\pi \frac{\text{rad}}{\text{rev}} \times \frac{\text{min}}{60 \text{ s}} \times 13 \text{ m} \times \frac{\text{s}}{10 \text{ m}} = 2.72 \xrightarrow{X}$$

The maximum theoretically attainable efficiency at this tip-speed ratio, accounting for swirl (Fig. 10.37) would be about 0.53.

The actual efficiency of the Dutch windmill is

$$\eta_{\text{actual}} = \frac{\mathcal{P}_{\text{actual}}}{KEF}$$

Based on Calvert's test data, the kinetic energy flux is

$$\begin{aligned} KEF &= \frac{1}{2} \rho V^3 \pi R^2 \\ &= \frac{1}{2} \times 1.23 \frac{\text{kg}}{\text{m}^3} \times (10)^3 \frac{\text{m}^3}{\text{s}^3} \times \pi \times (13)^2 \text{m}^2 \times \frac{\text{N} \cdot \text{s}^2}{\text{kg} \cdot \text{m}} \times \frac{\text{W} \cdot \text{s}}{\text{N} \cdot \text{m}} \\ KEF &= 3.27 \times 10^5 \text{ W or } 327 \text{ kW} \end{aligned}$$

Substituting into the definition of actual efficiency,

$$\eta_{\text{actual}} = \frac{41 \text{ kW}}{327 \text{ kW}} = 0.125 \xrightarrow{\eta_{\text{actual}}}$$

Thus the actual efficiency of the Dutch windmill is about 24 percent of the maximum efficiency theoretically attainable at this tip-speed ratio.

The actual thrust on the Dutch windmill can only be estimated, because the interference factor, a , is not known. The maximum possible thrust would occur at $a = 1/2$, in which case,

$$\begin{aligned} K_x &= \rho V^2 \pi R^2 2a(1-a) \\ &= 1.23 \frac{\text{kg}}{\text{m}^3} \times (10)^2 \frac{\text{m}^2}{\text{s}^2} \times \pi \times (13)^2 \text{m}^2 \times 2 \left(\frac{1}{2}\right) \left(1 - \frac{1}{2}\right) \times \frac{\text{N} \cdot \text{s}^2}{\text{kg} \cdot \text{m}} \\ K_x &= 3.27 \times 10^4 \text{ N or } 32.7 \text{ kN } \end{aligned}$$

This does not sound like a large thrust force, considering the size ($D = 26 \text{ m}$) of the windmill. However, $V = 36 \text{ km/hr}$ is only a moderate wind. The actual machine would have to withstand much more severe wind conditions during storms.

This problem illustrates application of the concepts of ideal thrust, power, and efficiency for a windmill, and calculation of these quantities for an actual machine.

The Rankine model includes some important assumptions that limit its applicability [23]. First, the wind turbine is assumed to affect only the air contained within the stream tube defined in Fig. 10.40. Second, the kinetic energy produced as swirl behind the turbine is not accounted for. Third, any radial pressure gradient is ignored. Glauert [17] partially accounted for the wake swirl to predict the dependence of ideal efficiency on tip-speed ratio, X ,

$$X = \frac{R\omega}{V} \quad (10.46)$$

as shown in Fig. 10.42 (ω is the angular velocity of the turbine).

As the tip-speed ratio increases, ideal efficiency increases, approaching the peak value ($\eta = 0.593$) asymptotically. Avallone et al. [22] presents a summary of the detailed blade-element theory used to develop the limiting efficiency curve shown in Fig. 10.41. It is necessary to increase the tip-speed ratio

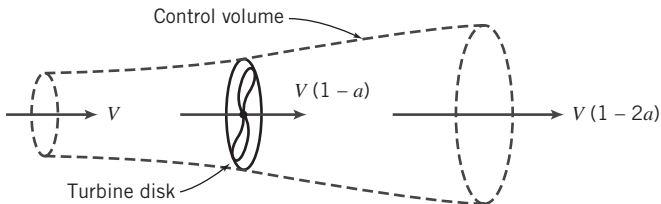


Fig. 10.40 Control volume and simplified notation used to analyze wind turbine performance.

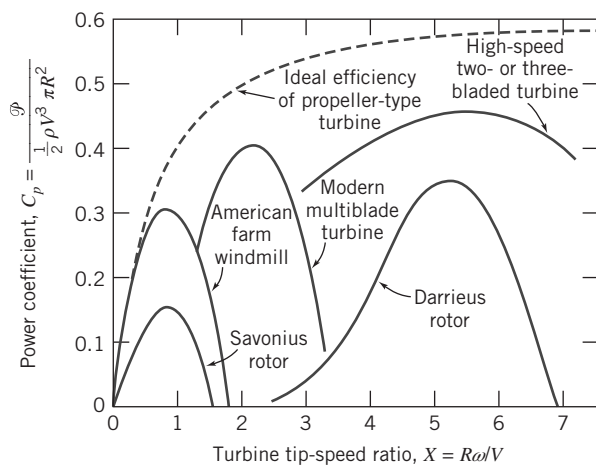


Fig. 10.41 Efficiency trends of wind turbine types versus tip-speed ratio, based on Reference [19].

considerably to reach a more favorable operating range. Modern high-speed wind-turbine designs use carefully shaped airfoils and operate at tip-speed ratios up to 7 [24].

The analysis of a VAWT is slightly different from that of a HAWT. The main reason for this difference can be seen in Fig. 10.42 where a cross section of one airfoil in a Darrieus turbine is shown rotating about the turbine axis. Assuming that the wind emanates from a constant direction, the airfoil angle of attack α will be a function of the azimuthal angle θ . The angle of attack is due to the relation between the effective velocity vector and the rotational direction. As θ varies, α will vary as well until it reaches a maximum value when θ is equal to 90° . In that configuration, the angle of attack is expressed by:

$$\alpha_m = \tan^{-1} \frac{V}{R\omega} \quad (10.47a)$$

In terms of the tip speed ratio X from Eq. 10.46, Eq. 10.47a may then be rewritten as:

$$\alpha_m = \tan^{-1} \frac{1}{X} \quad (10.47b)$$

Since the maximum angle of attack must be less than that for stall ($10^\circ - 15^\circ$ for most typical airfoils), X should be a large number (at least on the order of 6). The lift and drag forces (L and D , respectively) acting on the airfoil can be seen in Fig. 10.42. These aerodynamic forces generate a torque on the rotor. The torque on the rotor at a given value of α is:

$$T = \omega R(L \sin \alpha - D \cos \alpha) \quad (10.48)$$

If the airfoil section is symmetric (zero camber), then the lift coefficient is linearly proportional to the angle of attack [25]:

$$C_L = m\alpha \quad (10.49)$$

In Eq. 10.49, m is the slope of the lift curve, and is specific to the airfoil being used. In addition, the drag coefficient may be approximated by:

$$C_D = C_{D,0} + \frac{C_L^2}{\pi AR} \quad (9.43)$$

In this expression, $C_{D,0}$ is the drag coefficient at zero angle of attack, and AR is the aspect ratio of the airfoil. Decher [16] derived an expression for the efficiency of the rotor based on lift and drag effects,

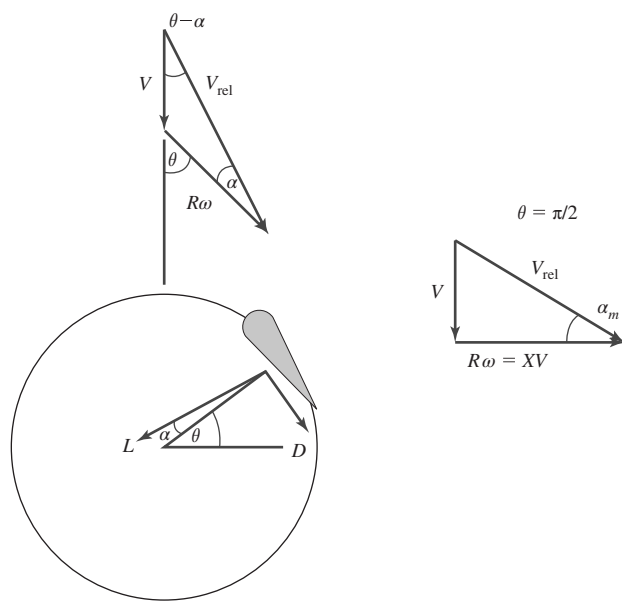


Fig. 10.42 Velocities around a Darrieus rotor blade element at a general azimuthal angle θ , as well as at $\theta = \pi/2$, where the airfoil angle of attack is maximized.

$\eta L/D$. This expression is defined as the useful work out divided by the available power in the wind. In terms of the lift and drag, this expression is:

$$\eta_{L/D} = \frac{R\bar{\omega}(L \sin \alpha - D \cos \alpha)}{V(L \cos \alpha + D \sin \alpha)}$$

The overbars in this equation indicate average values of those quantities. Since the lift and drag forces on the rotor change with θ , a time average of the forces needs to be calculated by integrating. Now once we substitute Eqs. 10.49 and 9.43 into this expression and average over a full revolution of the rotor ($0 \leq \theta \leq 2\pi$), the efficiency becomes:

$$\eta_{L/D} = \frac{1 - C_{D,0} \left(\frac{2}{C_{D,0} AR} + \frac{4X^3}{1 + X^2} \right)}{1 + C_{D,0} \left(\frac{1}{2\pi} + \frac{3}{2C_{D,0} AR X^2} \right)} \quad (10.50)$$

This efficiency modifies the efficiency based on actuator disk theory for an estimate of the overall efficiency of the rotor:

$$\eta \approx \eta_{act\ disk} \eta_{L/D} \quad (10.51)$$

One must keep in mind, however, that in order to determine the efficiency of a complete rotor, one must add the contributions to the torque over the entire rotor. Since different parts of the rotor have different radii (different values of R), they will have different values of X . Based on Eq. 10.50, one might realize that the portions of the rotor with small radii will contribute very little to the torque compared to central portions of the rotor.

10.7 Compressible Flow Turbomachines

The density change of the working fluid is important in gas turbine and steam turbine power generation. The modifications to the governing equations and dimensional analyses necessary in compressible flow applications will be discussed.

Application of the Energy Equation to a Compressible Flow Machine

The first law of thermodynamics for an arbitrary control volume is the energy equation, Eq. 4.56,

$$\dot{Q} - \dot{W}_s - \dot{W}_{shear} - \dot{W}_{other} = \frac{\partial}{\partial t} \int_{CV} epdV + \int_{CS} \left(u + pv + \frac{V^2}{2} + gz \right) \rho \vec{V} \cdot d\vec{A} \quad (4.56)$$

Equation 4.56 can be simplified for compressible flow turbomachinery. First, turbomachines typically run at conditions such that heat transfer with the surroundings are minimized, second, work terms other than shaft work are negligibly small, and third, changes in gravitational potential energy are small. Since enthalpy is defined as $h \equiv u + pv$, for steady flow, Eq. 4.56 becomes

$$\dot{W}_s = - \int_{CS} \left(h + \frac{V^2}{2} \right) \rho \vec{V} \cdot d\vec{A}$$

At this point, we introduce the *stagnation enthalpy* as the sum of the fluid enthalpy and kinetic energy:

$$h_0 = h + \frac{V^2}{2}$$

Therefore, we may rewrite the energy equation as:

$$\dot{W}_s = - \int_{CS} h_0 \rho \vec{V} \cdot d\vec{A} \quad (10.52a)$$

Equation 10.52a states that, for a turbomachine with work *input*, the power *required* causes an increase in the stagnation enthalpy in the fluid; for a turbomachine with work *output*, the power *produced* is due to a decrease in the stagnation enthalpy of the fluid. In this equation, \dot{W}_s is positive when work is being done *by* the fluid (as in a turbine), while \dot{W}_s is negative when work is being done *on* the fluid (as in a compressor).

The integrand on the right side of Eq. 10.52a is the product of the stagnation enthalpy with the mass flow rate at each section. If we make the additional assumption of uniform flow into the machine at section 1, and out of the machine at section 2, Eq. 10.52a becomes

$$\dot{W}_s = -(h_{0_2} - h_{0_1})\dot{m} \quad (10.52b)$$

Compressors

Compressors may be centrifugal or axial, depending on specific speed. Automotive turbochargers, small gas-turbine engines, and natural-gas pipeline boosters usually are centrifugal. Large gas and steam turbines and jet aircraft engines (as seen in Figs. 10.3 and 10.4b) frequently are axial-flow machines.

Since the flow through a compressor will see a change in density, the dimensional analysis presented for incompressible flow is no longer appropriate. Rather, we quantify the performance of a compressor through Δh_{0_s} , the ideal rise in stagnation enthalpy of the flow, the efficiency η , and the power \mathcal{P} . The functional relationship is:

$$\Delta h_{0_s}, \eta, \mathcal{P} = f(\mu, N, D, \dot{m}, \rho_{0_1}, c_{0_1}, k) \quad (10.53)$$

In this relation, the independent variables are, in order, viscosity, rotational speed, rotor diameter, mass flow rate, inlet stagnation density, inlet stagnation speed of sound, and ratio of specific heats.

If we apply the Buckingham Pi theorem to this system, the resulting dimensionless groups are:

$$\begin{aligned} \Pi_1 &= \frac{\Delta h_{0_s}}{(ND)^2} & \Pi_2 &= \frac{\mathcal{P}}{\rho_{0_1} N^3 D^5} \\ \Pi_3 &= \frac{\dot{m}}{\rho_{0_1} ND^3} & \Pi_4 &= \frac{\rho_{0_1} ND^2}{\mu} \\ \Pi_5 &= \frac{ND}{c_{0_1}} \end{aligned}$$

Since the efficiency η and ratio of specific heats k are dimensionless quantities, they can be thought of as Π -terms. The resulting functional relationships are:

$$\frac{\Delta h_{0_s}}{(ND)^2}, \eta, \frac{\mathcal{P}}{\rho_{0_1} N^3 D^5} = f_1 \left(\frac{\dot{m}}{\rho_{0_1} ND^3}, \frac{\rho_{0_1} ND^2}{\mu}, \frac{ND}{c_{0_1}}, k \right) \quad (10.54a)$$

This equation is actually an expression of three separate functions; that is, the terms $\Pi_1 = \Delta h_{0_s}/(ND)^2, \eta$, and $\Pi_2 = \mathcal{P}/\rho_{0_1} N^3 D^5$ are all functions of the other dimensionless quantities. $\Delta h_{0_s}/(ND)^2$ is a measure of the energy change in the flow and is the compressible analog to the head coefficient Ψ (Eq. 10.6). $\mathcal{P}/\rho_{0_1} N^3 D^5$ is a power coefficient, similar to that in Eq. 10.8. $\dot{m}/\rho_{0_1} ND^3$ is a mass flow coefficient, analogous to the incompressible flow coefficient Φ (Eq. 10.5). $\rho_{0_1} ND^2/\mu$ is a Reynolds number based on rotor tip speed, and ND/c_{0_1} is a Mach number based on rotor tip speed. Using the relationships for isentropic processes and for the compressible flow of a perfect gas, we can make some simplifications. As a result, Eq. 10.54a may be rewritten as:

$$\frac{p_{0_2}}{p_{0_1}}, \eta, \frac{\Delta T_0}{T_{0_1}} = f_2 \left(\frac{\dot{m} \sqrt{RT_{0_1}}}{p_{0_1} D^2}, \text{Re}, \frac{ND}{\sqrt{RT_{0_1}}}, k \right) \quad (10.54b)$$

The functional relationships presented here can be used to investigate scaling the performance of similar flow machines. An example of this is presented in Example 10.16.

Example 10.16 SCALING OF A COMPRESSOR

A 1/5 scale model of a prototype air compressor consuming 300 hp and running at a speed of 1000 rpm delivers a flow rate of 20 lbm/s through a pressure ratio of 5. At dynamically and kinematically similar conditions, what would the operating speed, mass flow rate, and power consumption be for the full-scale prototype?

Given: 1/5 scale compressor model

Power: 300 hp

Speed: 1000 rpm

Pressure ratio: 5

Mass flow rate: 50 lbm/s

Find: Prototype speed, mass flow rate, and power consumption at similar conditions.

Solution: Apply the equations presented above and the concepts presented in Chapter 7 on similitude to the compressor:

Governing equations:

$$\left(\frac{ND}{c_{01}}\right)_p = \left(\frac{ND}{c_{01}}\right)_m$$

$$\left(\frac{\dot{m}}{\rho_{01}ND^3}\right)_p = \left(\frac{\dot{m}}{\rho_{01}ND^3}\right)_m$$

$$\left(\frac{\mathcal{P}}{\rho_{01}N^3D^5}\right)_p = \left(\frac{\mathcal{P}}{\rho_{01}N^3D^5}\right)_m$$

Assumption:

Similar entrance conditions for both model and prototype.

Similar entrance conditions would stipulate that the stagnation sound speed and density would be equal for both the model and the prototype. Solving the first equation for the prototype speed:

$$N_p = N_m \frac{D_m c_{01p}}{D_p c_{01m}} = 1000 \text{ rpm} \times \frac{1}{5} \times 1 = 200 \text{ rpm}$$

$N_p = 200 \text{ rpm} \leftarrow$

Solving the second equation for the prototype mass flow rate:

$$\dot{m}_p = \dot{m}_m \frac{\rho_{01p}}{\rho_{01m}} \frac{N_p}{N_m} \left(\frac{D_p}{D_m}\right)^3 = 20 \frac{\text{lbm}}{\text{s}} \times \frac{200}{1000} \times \left(\frac{5}{1}\right)^3 = 500 \frac{\text{lbm}}{\text{s}}$$

$\dot{m}_p = 500 \text{ lbm/s} \leftarrow$

To calculate the power requirement for the prototype:

$$\mathcal{P}_p = \mathcal{P}_m \frac{\rho_{01p}}{\rho_{01m}} \left(\frac{N_p}{N_m}\right)^3 \left(\frac{D_p}{D_m}\right)^5 = 300 \text{ hp} \times \left(\frac{200}{1000}\right)^3 \times \left(\frac{5}{1}\right)^5 = 7500 \text{ hp}$$

$\mathcal{P}_p = 7500 \text{ hp} \leftarrow$

This problem demonstrates the scaling of compressible flow machines. Note that if the working fluid for the two different scale machines were different, e.g., air versus helium, the effects of different gas constants and specific heat ratios would have to be taken into account.

For scaling of compressors operating with the same fluid and at high Reynolds numbers, Eq. 10.54b can be simplified to

$$\frac{p_{0_2}}{p_{0_1}}, \eta, \frac{\Delta T_0}{T_{0_1}} = f_3 \left(\frac{\dot{m} \sqrt{T_{0_1}}}{p_{0_1}}, \frac{N}{\sqrt{T_{0_1}}} \right) \quad (10.54c)$$

This equation is not dimensionless but is still useful in characterizing the performance of a compressor, provided the performance is assessed for a single machine using a single working fluid. The relationship portrayed in Eq. 10.54c is normally expressed in the form of a compressor operability map, as shown in Fig. 10.43. On this map we can see the compression ratio versus mass flow ratio ($\dot{m} \sqrt{T_{0_1}} / p_{0_1}$), with curves of constant normalized speed ($N / \sqrt{T_{0_1}}$) and efficiency. Often, the abscissa is a “corrected mass flow”:

$$\dot{m}_{\text{corr}} = \frac{\dot{m} \sqrt{T_{0_1} / T_{\text{ref}}}}{p_{0_1} / p_{\text{ref}}}$$

and the lines of constant compressor speed are a “corrected speed”:

$$N_{\text{corr}} = \frac{N}{\sqrt{T_{0_1} / T_{\text{ref}}}}$$

In these expressions, T_{ref} and p_{ref} are reference pressure and temperature. This allows the user to read the chart quickly in terms of “real” physical quantities and to be able to make adjustments for varying entrance conditions with a minimum of calculation. The operating line is the locus of points of maximum efficiency for a given mass flow.

This figure shows two of the phenomena that must be avoided in the operation of a compressor. The first is *choking*, which is experienced when the local Mach number at some point in the compressor reaches unity. The maximum possible flow rate for a given rotor speed is reached, and the compressor is choked. It is impossible to increase mass flow without increasing rotor speed.

The second phenomenon is *surge*, which is a cyclic pulsation phenomenon that causes the mass flow rate through the machine to vary, and even reverse. Surge occurs when the pressure ratio in the compressor is raised beyond a certain level for a given mass flow rate. As pressure ratio increases, the adverse pressure gradient across the compressor increases as well. This increase in pressure gradient can cause boundary-layer separation on the rotor surfaces and constrict flow through the space between two adjacent blades. Therefore, the extra flow gets diverted to the next channel between blades. The separation is relieved in the previous channel and moves to the next channel, causing the cyclic pulsation mentioned above. Surge is accompanied by loud noises and can damage the compressor or related components; it too must be avoided. Fig. 10.43 shows the *surge line*, the locus of operating conditions beyond which surge will occur.

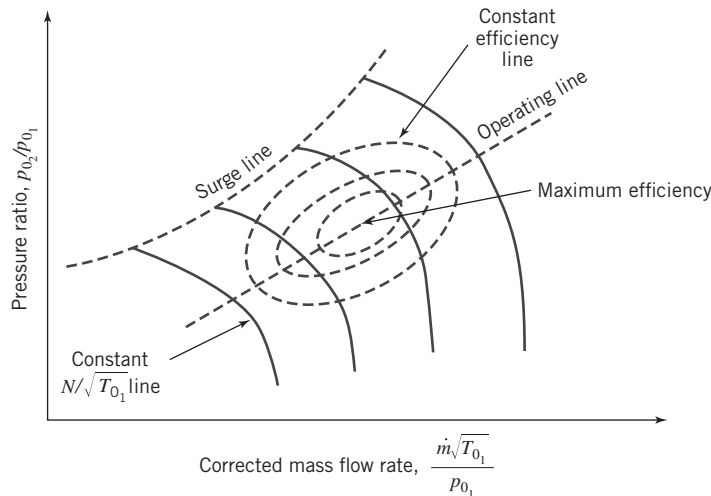


Fig. 10.43 Typical performance map for a compressor.

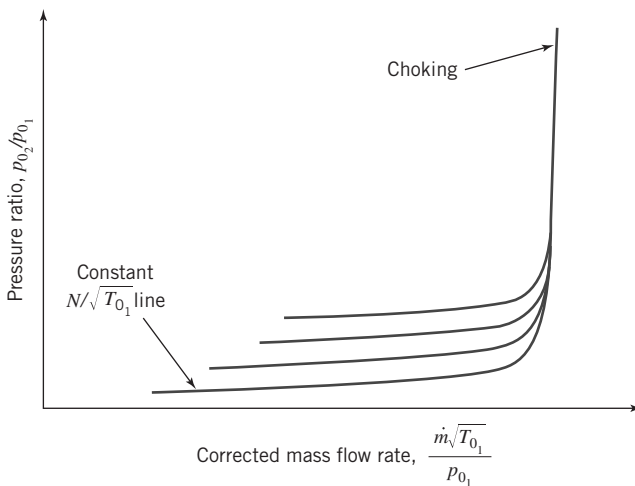


Fig. 10.44 Typical performance map for a compressible flow turbine.

In general, as shown in Fig. 10.43, the higher the performance, the more narrow the range in which the compressor may be operated successfully. Thus a compressor must be carefully matched to its flow system to assure satisfactory operation.

Compressible-Flow Turbines

The flow through a gas turbine is governed by the same general relationship as the compressor. Figure 10.44 shows the performance map for a compressible flow turbine. As in the case for the compressor the turbine map shows lines of constant normalized speed on a graph of pressure ratio versus normalized mass flow rate. The most striking difference between this map and that for the compressor is that the performance is a very weak function of $N/\sqrt{T_{01}}$; the curves are set very close together. The choking of the turbine flow is well-defined on this map. There is a normalized mass flow that cannot be exceeded in the turbine, regardless of the pressure ratio.

10.8 Summary and Useful Equations

In this chapter, we:

- ✓ Defined the two major types of fluid machines: positive displacement machines and turbomachines.
- ✓ Described the various turbomachines: radial, axial, and mixed-flow types of pumps, fans, blowers, compressors, and turbines.
- ✓ Used the angular-momentum equation for a control volume to derive the Euler turbomachine equation.
- ✓ Drew velocity diagrams and applied the Euler turbomachine equation to the analysis of various idealized machines to derive ideal torque, head, and power.
- ✓ Evaluated the performance—head, power, and efficiency—of various actual machines from measured data.
- ✓ Defined and used dimensionless parameters to scale the performance of a fluid machine from one size, operating speed, and set of operating conditions to another.
- ✓ Discussed various defining parameters, such as pump efficiency, turbine efficiency, shutoff head, specific speed, cavitation, $NPSHR$, and $NPSHA$.
- ✓ Matched pumps to pipe systems to obtain the operating point.
- ✓ Discussed and analyzed propellers and wind turbines.
- ✓ Discussed the use and performance of compressible flow turbomachines.

With these concepts and techniques, we learned how to use manufacturers' literature and other data to perform preliminary analyses and make appropriate selections of pumps, fans, hydraulic and wind turbines, and other fluid machines.

Note: Most of the equations in the table below have a number of constraints or limitations—*be sure to refer to their page numbers for details!*

Useful Equations

Euler turbomachine equation:	$T_{\text{shaft}} = (r_2 V_{t_2} - r_1 V_{t_1}) \dot{m}$	(10.1c)	Page 349
Turbomachine theoretical power:	$\dot{W}_m = (U_2 V_{t_2} - U_1 V_{t_1}) \dot{m}$	(10.2b)	Page 349
Turbomachine theoretical head:	$H = \frac{\dot{W}_m}{\dot{m}g} = \frac{1}{g}(U_2 V_{t_2} - U_1 V_{t_1})$	(10.2c)	Page 349
Pump power, head, and efficiency:	$\dot{W}_h = \rho Q g H_p$ $H_p = \left(\frac{p}{\rho g} + \frac{\bar{V}^2}{2g} + z \right)_{\text{discharge}} - \left(\frac{p}{\rho g} + \frac{\bar{V}^2}{2g} + z \right)_{\text{suction}}$ $\eta_p = \frac{\dot{W}_h}{\dot{W}_m} = \frac{\rho Q g H_p}{\omega T}$	(10.3a) (10.3b) (10.3c)	Page 352 Page 353
Turbine power, head, and efficiency:	$\dot{W}_h = \rho Q g H_t$ $H_t = \left(\frac{p}{\rho g} + \frac{\bar{V}^2}{2g} + z \right)_{\text{inlet}} - \left(\frac{p}{\rho g} + \frac{\bar{V}^2}{2g} + z \right)_{\text{outlet}}$ $\eta_t = \frac{\dot{W}_m}{\dot{W}_h} \frac{\omega T}{\rho Q g H_t}$	(10.4a) (10.4b) (10.4c)	Page 353
Dimensionless flow coefficient:	$\Phi = \frac{Q}{A_2 U_2} = \frac{V_{n_2}}{U_2}$	(10.5)	Page 353
Dimensionless head coefficient:	$\Psi = \frac{gH}{U_2^2}$	(10.6)	Page 354
Dimensionless torque coefficient:	$\tau = \frac{T}{\rho A_2 U_2^2 R_2}$	(10.7)	Page 354
Dimensionless power coefficient:	$\Pi = \frac{\dot{W}}{\rho Q U_2^2} = \frac{\dot{W}}{\rho \omega^2 Q R_2^2}$	(10.8)	Page 354
Centrifugal pump specific speed (in terms of head h):	$N_s = \frac{\omega Q^{1/2}}{h^{3/4}}$	(7.22a)	Page 354
Centrifugal pump specific speed (in terms of head H):	$N_{S_{cu}} = \frac{N(\text{rpm})[Q(\text{gpm})]^{1/2}}{[H(\text{ft})]^{3/4}}$	(7.22b)	Page 355
Centrifugal turbine specific speed (in terms of head h):	$N_s = \frac{\omega}{h^{3/4}} \left(\frac{\mathcal{P}}{\rho h} \right)^{1/2} = \frac{\omega \mathcal{P}^{1/2}}{\rho^{1/2} h^{5/4}}$	(10.13a)	Page 355
Centrifugal turbine specific speed (in terms of head H):	$N_{S_{cu}} = \frac{N(\text{rpm})[\mathcal{P}(\text{hp})]^{1/2}}{[H(\text{ft})]^{5/4}}$	(10.13b)	Page 355
Axial-flow turbomachine ideal performance:	$T_{\text{shaft}} = R_m(V_{t_2} - V_{t_1}) \dot{m}$ $\dot{W}_m = U(V_{t_2} - V_{t_1}) \dot{m}$ $H = \frac{\dot{W}_m}{\dot{m}g} = \frac{U}{g}(V_{t_2} - V_{t_1})$	(10.20) (10.21) (10.22)	Page 360

(Continued)

Table (Continued)

Propeller thrust:	$F_T = qN \int_{R_{\text{hub}}}^R \frac{(C_L \cos \phi - C_D \sin \phi)}{\sin^2 \phi} cdr$	(10.37a)	Page 397
Propeller torque:	$T = qN \int_{R_{\text{hub}}}^R \frac{(C_L \sin \phi + C_D \cos \phi)}{\sin^2 \phi} rcdr$	(10.37b)	Page 397
Propeller speed of advance coefficient:	$J \equiv \frac{V}{nD}$	(10.39)	Page 398
Propeller thrust, torque, power, and efficiency coefficients:	$C_F = \frac{F_T}{\rho n^2 D^4}, \quad C_T = \frac{T}{\rho n^2 D^5},$ $C_P = \frac{\mathcal{P}}{\rho n^3 D^5}, \quad \eta = \frac{F_T V}{\mathcal{P}_{\text{input}}}$	(10.40)	Page 398
Cavitation number:	$Ca = \frac{p - p_v}{\frac{1}{2} \rho V^2}$	(10.41)	Page 398
Actuator disk efficiency:	$\eta = \frac{\mathcal{P}}{KEF} = 4a(1-a)^2$	(10.45)	Page 401
Tip-speed ratio	$X = \frac{R\omega}{V}$	(10.46)	Page 404
VAWT efficiency:	$\eta_{L/D} = \frac{1 - C_{D,0} \left(\frac{2}{C_{D,0} AR} + \frac{4X^3}{1+X^2} \right)}{1 + C_{D,0} \left(\frac{1}{2\pi} + \frac{3}{2C_{D,0} AR X^2} \right)}$ $\eta \approx \eta_{act\ disk} \eta_{L/D}$	(10.50) (10.51)	Page 406 Page 406
Energy equation for compressible flow turbomachine:	$\dot{W}_s = -(h_{0_2} - h_{0_1})\dot{m}$	(10.52b)	Page 407
Performance parameters for compressible flow turbomachine:	$\frac{p_{0_2}}{p_{0_1}}, \eta, \frac{\Delta T_0}{T_{0_1}} = f_3 \left(\frac{\dot{m} \sqrt{T_{0_1}}}{p_{0_1}}, \frac{N}{\sqrt{T_{0_1}}} \right)$	(10.54c)	Page 409

REFERENCES

1. Wilson, D. G., "Turbomachinery—From Paddle Wheels to Turbojets," *Mechanical Engineering*, 104, 10, October 1982, pp. 28–40.
2. Logan, E. S., Jr., *Turbomachinery: Basic Theory and Applications*. New York: Dekker, 1981.
3. Sabersky, R. H., A. J. Acosta, E. G. Hauptmann, and E. M. Gates, *Fluid Flow: A First Course in Fluid Mechanics*, 4th ed. Englewood Cliffs, NJ: Prentice-Hall, 1999.
4. Daily, J. W., "Hydraulic Machinery," in Rouse, H., ed., *Engineering Hydraulics*. New York: Wiley, 1950.
5. Dixon, S. L., *Fluid Mechanics and Thermodynamics of Turbomachinery*, 5th ed. Amsterdam: Elsevier, 2005.
6. Peerless Pump, Brochure B-4003, "System Analysis for Pumping Equipment Selection," Indianapolis, IN: Peerless Pump Co., 1979.
7. Daugherty, R. L., J. B. Franzini, and E. J. Finnemore, *Fluid Mechanics with Engineering Applications*, 8th ed. New York: McGraw-Hill, 1985.
8. Peerless Pump Company, RAPID, v 8.25.6, March 23, Indianapolis, IN: Peerless Pump Co., 2007.
9. Hodge, B. K., *Analysis and Design of Energy Systems*, 2nd ed. Englewood Cliffs, NJ: Prentice-Hall, 1990.
10. Moody, L. F., "Hydraulic Machinery," in *Handbook of Applied Hydraulics*, ed. by C. V. Davis. New York: McGraw-Hill, 1942.

11. Hydraulic Institute, *Hydraulic Institute Standards*. New York: Hydraulic Institute, 1969.
12. Hicks, T. G., and T. W. Edwards, *Pump Application Engineering*. New York: McGraw-Hill, 1971.
13. Armintor, J. K., and D. P. Connors, "Pumping Applications in the Petroleum and Chemical Industries," *IEEE Transactions on Industry Applications*, IA-23, 1, January 1987.
14. Air Movement and Control Association, *Laboratory Methods of Testing Fans for Rating*. AMCA Standard 210-74, ASHRAE Standard 51-75. Atlanta, GA: ASHRAE, 1975.
15. Russell, G. E., *Hydraulics*, 5th ed. New York: Henry Holt, 1942.
16. Decher, R., *Energy Conversion: Systems, Flow Physics, and Engineering*. New York: Oxford University Press, 1994.
17. Durand, W. F., ed., *Aerodynamic Theory*, 6 Volumes. New York: Dover, 1963.
18. Putnam, P. C., *Power from the Wind*. New York: Van Nostrand, 1948.
19. Calvert, N. G., *Windpower Principles: Their Application on the Small Scale*. London: Griffin, 1978.
20. American Wind Energy Association, *Annual Wind Industry Report, Year Ending 2008*. Washington, DC: American Wind Energy Association, 2008.
21. "Wind Power in America: Becalmed," *The Economist*, 392, 8642 (August 1, 2009).
22. Eldridge, F. R., *Wind Machines*, 2nd ed. New York: Van Nostrand Reinhold, 1980.
23. Avallone, E. A., T. Baumeister, III, and A. Sadegh, eds., *Marks' Standard Handbook for Mechanical Engineers*, 11th ed. New York: McGraw-Hill, 2007.
24. Migliore, P. G., "Comparison of NACA 6-Series and 4-Digit Airfoils for Darrieus Wind Turbines," *Journal of Energy*, 7, 4, Jul–Aug 1983, pp. 291–292.
25. Anderson, J. D., *Introduction to Flight*, 4th ed. Boston: McGraw-Hill, 2000.
26. White, F. M., *Fluid Mechanics*, 6th ed. New York: McGraw-Hill, 2007.
27. Betz, A. *Introduction to the Theory of Flow Machines*. Oxford: Pergamon Press, 1966.
28. U.S. energy Information Agency, <https://www.eia.gov/>, 2018.

Chapter 11 Problems

Basic Concepts and Definitions

11.1 A pebble is dropped into a stream of water that flows in a rectangular channel at 2 m depth. In one second, a ripple caused by the stone is carried 7 m downstream. Determine the speed of the stream and whether it is subcritical, critical, or supercritical. At another location the ripple moves downstream 11 m. Determine the speed of the stream and whether it is subcritical, critical, or supercritical at that location.

11.2 A water flow rate of 250 cfs flows at a depth of 5 ft in a rectangular channel that is 9 ft wide. Determine whether the flow is sub- or supercritical. For this flow rate, determine the depth for critical flow.

11.3 Determine and plot the relation between water velocity and depth over the range of $V = 0.1 \text{ m/s}$ to 10 m/s for Froude numbers of 0.5 (subcritical), 1.0 (critical), and 2 (supercritical). Explain how the flow can be subcritical, critical, or supercritical for (a) the same velocity and (b) the same depth.

11.4 Capillary waves (ripples) are small amplitude and wavelength waves, commonly seen, for example, when an insect or small particle hits the water surface. They are waves generated due to the interaction of the inertia force of the fluid ρ and the fluid surface tension σ . The wavelength is

$$\lambda = 2\pi \sqrt{\frac{\sigma}{\rho g}}$$

Find the speed of capillary waves in water and mercury.

11.5 Waves on the surface of a tank of water on Earth travel at 5 ft/s. Determine the wave speed if the tank were (a) on the moon, (b) on Jupiter, or (c) on an orbiting space station. Explain your results.

11.6 Verify the equation given in Table 11.1 for the hydraulic radius of a circular channel. Evaluate and plot the ratio R/D for liquid depths between 0 and D .

11.7 A water flow of $10 \text{ m}^3/\text{s}$ in a 5-m-wide rectangular channel with a depth of 2.5 m accelerates under a sluice gate. Determine the depth and Froude number of the accelerated flow.

Energy Equation for Open-Channel Flows

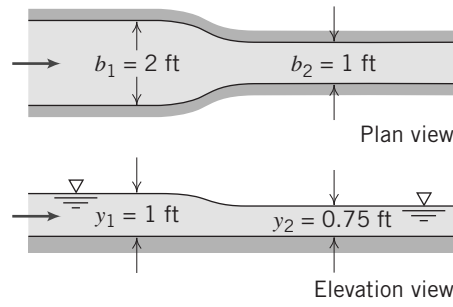
11.8 Find the critical depth for flow at $3 \text{ m}^3/\text{s}$ in a rectangular channel of width 2.5 m.

SS 11.9 Determine the maximum flow rate that may occur in a rectangular channel 2.4 m wide for a specific energy of 1.5 m.

11.10 A rectangular channel carries a discharge of $10 \text{ ft}^3/\text{s}$ per foot of width. Determine the minimum specific energy possible for this flow. Compute the corresponding flow depth and speed.

Localized Effects of Area Change (Frictionless Flow)

11.11 Consider the Venturi flume shown. The bed is horizontal, and the flow may be considered frictionless. The upstream depth is 1 ft, and the downstream depth is 0.75 ft. The upstream breadth is 2 ft, and the breadth of the throat is 1 ft. Estimate the flow rate through the flume.

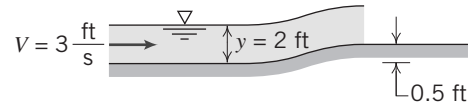


P11.11

11.12 A horizontal rectangular channel 3 ft wide contains a sluice gate. Upstream of the gate the depth is 6 ft and downstream the depth is 0.9 ft. Determine the volume flow rate and the upstream and downstream Froude numbers.

11.13 Determine the depths of an 800 cfs flow in a trapezoidal channel of base width 12 ft and side slopes 1 (vertical) on 3 (horizontal) for a specific energy of 7 ft. SS

11.14 Water, at 3 ft/s and 2 ft depth, approaches a smooth rise in a wide channel. Estimate the stream depth after the 0.5 ft rise.



P11.14

The Hydraulic Jump

11.15 A hydraulic jump occurs in a rectangular channel 4.0 m wide. The water depth before the jump is 0.4 m and after the jump is 1.7 m. Compute the flow rate in the channel, the critical depth, and the head loss in the jump.

11.16 A hydraulic jump occurs in a wide horizontal channel carrying $2 \text{ m}^3/\text{s}$ per meter of width. The upstream depth is 0.5 m. Determine the depth and velocity of the water after the jump.

11.17 A hydraulic jump occurs in a rectangular channel. The flow rate is $200 \text{ ft}^3/\text{s}$, and the depth before the jump is 1.2 ft. Determine the depth behind the jump and the head loss. The channel is 10 ft wide.

11.18 A hydraulic jump occurs on a spillway at a location where depth is 0.9 m and speed is 25 m/s. Determine the depth and speed downstream of the jump. Determine the ratio of the specific energy downstream of the jump to that upstream and determine the head loss. SS

11.19 A hydraulic jump occurs in a rectangular channel. The flow rate is $50 \text{ m}^3/\text{s}$ and the depth before the jump is 2 m. Determine the depth after the jump and the head loss if the channel is 1 m wide.

Uniform Flow

11.20 A 2-m-wide rectangular channel with a bed slope of 0.0005 has a depth of flow of 1.5 m. Manning's roughness coefficient is 0.015. Determine the steady uniform discharge in the channel.

11.21 Determine the uniform flow depth in a rectangular channel 8 ft wide with a slope of 0.0004 that carries a discharge of 90 cfs. Manning's roughness factor is 0.015.

11.22 A rectangular flume built of timber is 3 ft wide. The flume is to handle a flow of 90 ft³/s at a normal depth of 6 ft. Determine the slope required.

11.23 A channel with square cross section is to carry 20 m³/s of water at normal depth on a slope of 0.003. Determine the cross-sectional area and wetted perimeter of the channel required for (a) concrete and (b) masonry.

11.24 Determine the depth for a 4.25 m³/s flow in a rectangular channel 3.6 m wide that is lined with rubble masonry and laid on a slope of 1:4000.

SS 11.25 A semicircular trough of corrugated steel, with diameter $D = 1$ m, carries water at depth $y = 0.25$ m. The slope is 0.01. Find the discharge.

11.26 Determine the slope is necessary to carry 11 m³/s at a depth of 1.5 m in a rectangular channel 3.6 m wide lined with gravel.

11.27 For a trapezoidal shaped channel with $n = 0.014$ and slope $S_b = 0.0002$ with a 20-ft bottom width and side slopes of

1 vertical to 1.5 horizontal, determine the normal depth for a discharge of 1000 cfs.

11.28 A trapezoidal canal lined with brick has side slopes of 2:1 and bottom width of 10 ft. It carries 600 ft³/s at critical speed. Determine the critical slope (the slope at which the depth is critical).

11.29 Determine the discharge for a sharp-crested suppressed weir of length 8.0 ft, crest height of 2.0 ft, and upstream water depth of 3.0 ft. Neglect the velocity of approach head.

11.30 A rectangular sharp-crested weir with end contractions is 1.5 m long. Determine the necessary height of the weir crest to maintain an upstream depth of 2.5 m for a flow rate of 0.5 m³/s.

11.31 Determine the depth of water behind a rectangular sharp-crested weir 1.5 m wide and 1.2 m high for a flow of 0.28 m³/s. Determine the velocity of approach.

11.32 A broad-crested weir 0.9 m high and 6 m long has a flat crest and a coefficient of 1.6. Determine the flow rate for a head of 0.46 m.

11.33 Determine the flow for a 90° V-notch weir for a head of 1.5 ft. Determine the flow rate if the head doubles to 3.0 ft.

CHAPTER 11

Flow in Open Channels

- 11.1 Basic Concepts and Definitions
- 11.2 Energy Equation for Open-Channel Flows
- 11.3 Localized Effect of Area Change (Frictionless Flow)
- 11.4 The Hydraulic Jump

- 11.5 Steady Uniform Flow
- 11.6 Flow with Gradually Varying Depth
- 11.7 Discharge Measurement Using Weirs
- 11.8 Summary and Useful Equations

Case Study

Many flows of liquids in engineering and in nature occur with a free surface. An example of a human-made channel that carries water is shown in the photograph. This is a view of the 190-mile-long Hayden-Rhodes Aqueduct, which is part of the Central Arizona Project (CAP). The CAP is a 336-mile (541 km) diversion canal used to redirect water from the Colorado River into central and southern Arizona. The CAP originates in Lake Havasu on the western border of Arizona, travels through the Phoenix area, and terminates in the San Xavier Indian Reservation southwest of Tucson. It is designed to carry about 1.5 million acre-feet of Colorado River water per year, making it the largest single resource of renewable water supplies in the state of Arizona.

The design of the CAP involved many of the engineering principles we will study in this chapter. Because of the large flow rate of water, the aqueduct was designed as an open channel with a trapezoidal cross section that provided the smallest channel for the desired flow rate. Gravity is the driving force for the flow, and the land was graded to give the correct slope to the channel for the flow. As Lake Havasu is nearly 3000 feet below the

terminus, the final aqueduct design included 15 pumping stations, eight inverted siphons, and three tunnels.



Aqueduct, Central Arizona Project.

Robert Shantz/Alamy Stock Photo

Learning Objectives

After completing this chapter, you should be able to

- Describe the effect of Froude number on the characteristics of open channel flow.
- Determine the relation between flow properties and specific energy.
- Determine the effects of area change.
- Determine the flow properties for a hydraulic jump.
- Determine the flow rate in an open channel using Manning's equation.
- Determine the flow properties due to changes in the channel depth.
- Determine the flow rate in an open channel using weirs.

Free surface flows differ in several important respects from the flows in closed conduits that we studied in Chapter 8. Familiar examples where the free surface of a water flow is exposed to the atmosphere include flows in rivers, aqueducts, irrigation canals, rooftop or street gutters, and drainage ditches. Human-made channels, termed aqueducts, encompass many different types, such as canals, flumes, and culverts. A canal usually is below ground level and may be unlined or lined. Canals generally are long and of very mild slope and are used to carry irrigation or storm water or for navigation. A flume usually is built above ground level to carry water across a depression. A culvert, which usually is designed to flow only part-full, is a short covered channel used to drain water under a highway or railroad embankment.

Figure 11.1 illustrates a typical example of water flowing in an open channel. The channel, often called an aqueduct, carries water from a source, such as a lake, to where the water is needed,



Danita Delimont/Getty Images

Fig. 11.1 A typical example of an open-channel flow of water; located in California's Central Valley with supply pipes visible in background.

often for crop irrigation or as a water supply for a city. As you can see in this figure, the channel is relatively wide with sloped sides and has a gradual slope that allows the water to proceed downhill. Water enters this aqueduct through large corrugated pipes from a higher elevation. Pipes are used because the slope of the hillside is too steep for an open channel. The structure at the entrance to the aqueduct could also house a low head turbine that extracts power from the flowing water.

In this chapter we will introduce some of the basic concepts in open-channel flows. These flows are covered in much more detail in a number of specialized texts [1–8]. We will use the control volume concepts from Chapter 4 to develop the basic theory that describes the behavior and classification of flows in natural and human-made channels. We shall consider:

- *Flows for which the local effects of area change predominate and frictional forces may be neglected.* An example is flow over a bump or depression for which friction is negligible.
- *Flow with an abrupt change in depth.* This occurs during a hydraulic jump in which the water flow goes from fast and shallow to slow and deep in a very short distance.
- *Flow at what is called normal depth.* For this, the flow cross section does not vary in the flow direction. This is analogous to fully developed flow in a pipe.
- *Gradually varied flow.* An example is flow in a channel in which the bed slope varies. The major objective in the analysis of gradually varied flow is to predict the depth of the water.
- *Flow measurement techniques for use in open channels.* Weirs are commonly used for measuring flow in open channels. Weirs are devices placed normal to the channel that cause the flow to go through the critical depth. A depth measurement yields the flow rate.

It is quite common to observe surface waves in flows with a free surface, the simplest example being when an object such as a pebble is thrown into the water. The propagation speed of a surface wave is analogous in many respects to the propagation of a sound wave in a compressible fluid medium (which we discuss in Chapter 12). We shall determine the factors that affect the speed of such surface waves and see that this is an important determinant in whether an open-channel flow is able to gradually adjust to changing conditions downstream or a hydraulic jump occurs.

11.1 Basic Concepts and Definitions

Before analyzing the different types of flows that may occur in an open channel, we will discuss some common concepts and state some simplifying assumptions. There are some important differences between our previous studies of pipes and ducts in Chapter 8 and the study of open-channel flows. One significant difference between flows in pipes and ducts is that the driving force for open channel flows is *gravity*. The gravity force in open-channel flow is opposed by friction force on the solid boundaries of the channel.

Simplifying Assumptions

The flow in an open channel, especially in a natural one such as a river, is often very complex, three-dimensional, and unsteady. However, in most cases, we can obtain useful results by approximating such flows as being:

- *One-dimensional.*
- *Steady.*

A third simplifying assumption is:

- The flow at each section in an open-channel flow is approximated as a *uniform velocity*.

Although the actual velocity in a channel is really not uniform, we will justify this assumption. Figure 11.2 indicates the regions of the maximum velocity in some open-channel flow geometries.

The minimum velocity is zero along the walls because of viscosity. Measurements show that the region of maximum velocity occurs below the free surface. There is a negligible shear stress due to air drag on the free surface, so one would expect the maximum velocity to occur at the free surface. However, secondary flows occur and produce a nonuniform velocity profile with the maximum usually occurring below the surface. Secondary flows also occur when a channel has a bend or curve or has an obstruction, such as a bridge pier. These obstructions can produce vortices that erode the bottom of a natural channel.

Most open-channel flows of water are large in physical scale, so the Reynolds number is generally quite high. Consequently, open-channel flow is seldom laminar, and so we will assume that the flow in open channels is always turbulent. As we saw in earlier chapters, turbulence tends to smooth out the velocity profile. Hence, although there is a velocity profile in an open channel flow, as indicated in Fig. 11.2, we will assume a uniform velocity at each section, as illustrated in Fig. 11.3a.

The next simplifying assumption we make is:

- The pressure distribution is approximated as *hydrostatic*.

This is illustrated in Fig. 11.3b and is a significant difference from the analysis of flows in pipes and ducts of Chapter 8. For these we found that the pressure was uniform at each axial location and varied in the streamwise direction. In open-channel flows, the free surface will be at atmospheric pressure (zero gage), so the pressure at the surface does not vary in the direction of flow. The major pressure variation occurs *across* each section; this will be exactly true if streamline curvature effects are negligible, which is often the case.

We rely on empirical correlations to relate frictional effects to the average velocity of flow. The empirical correlation is included through a head loss term in the energy equation (Section 11.2). Additional complications in many practical cases include the presence of sediment or other particulate matter in the flow, as well as the erosion of earthen channels or structures by water action.

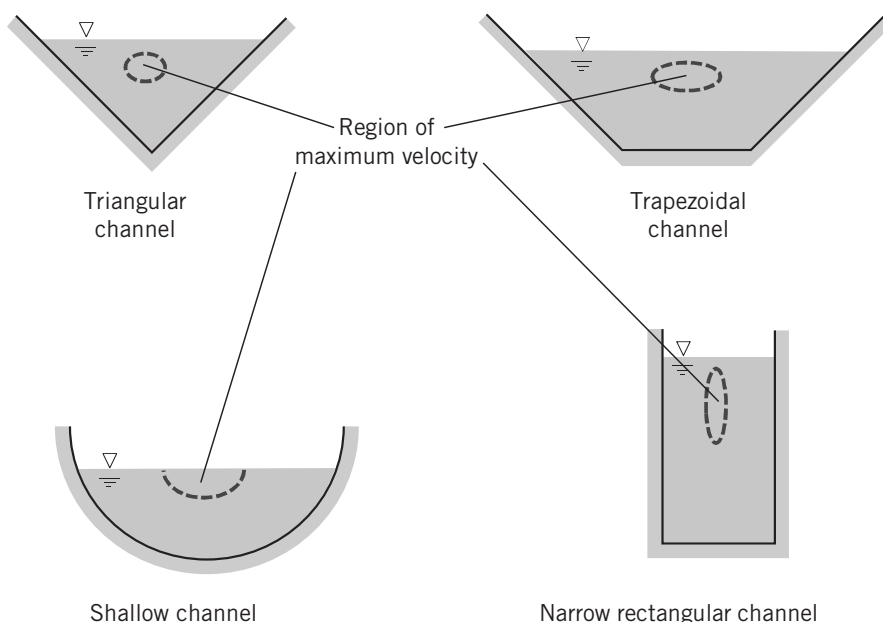
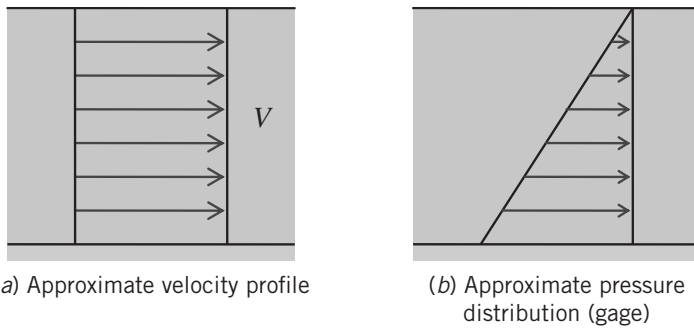


Fig. 11.2 Region of maximum velocity in some typical open-channel geometries. (Based on Chow [1].)

**Fig. 11.3** Approximations for velocity profile and pressure distribution.

Channel Geometry

Channels may be constructed in a variety of cross-sectional shapes and in many cases regular geometric shapes are used. A channel with a constant slope and cross section is termed *prismatic*. Lined canals often are built with rectangular or trapezoidal sections; smaller troughs or ditches sometimes are triangular. Culverts and tunnels generally are circular or elliptical in section. Natural channels are highly irregular and nonprismatic, but often they are approximated using trapezoid or paraboloid sections. Geometric properties of common open-channel shapes are summarized in Table 11.1.

The *depth of flow*, y , is the perpendicular distance measured from the channel bed to the free surface. The *flow area*, A , is the cross section of the flow perpendicular to the flow direction. The *wetted perimeter*, P , is the length of the solid channel cross-section surface in contact with the liquid. The *hydraulic radius*, R_h , is defined as

$$R_h = \frac{A}{P} \quad (11.1)$$

For flow in noncircular closed conduits (Section 8.7), the hydraulic diameter was defined as

$$D_h = \frac{4A}{P} \quad (8.50)$$

Although the hydraulic diameter is used for internal flows, the hydraulic radius, as defined by Eq. 11.1, is commonly used in the analysis of open-channel flows. One reason for this usage is that the hydraulic radius of a wide channel, as seen in Table 11.1, is equal to the actual depth.

For nonrectangular channels, the *hydraulic depth* is defined as

$$y_h = \frac{A}{b_s} \quad (11.2)$$

where b_s is the width at the surface. Hence the hydraulic depth represents the *average depth* of the channel at any cross section. It gives the *depth of an equivalent rectangular channel*.

Table 11.1
Geometric Properties of Common Open-Channel Shapes

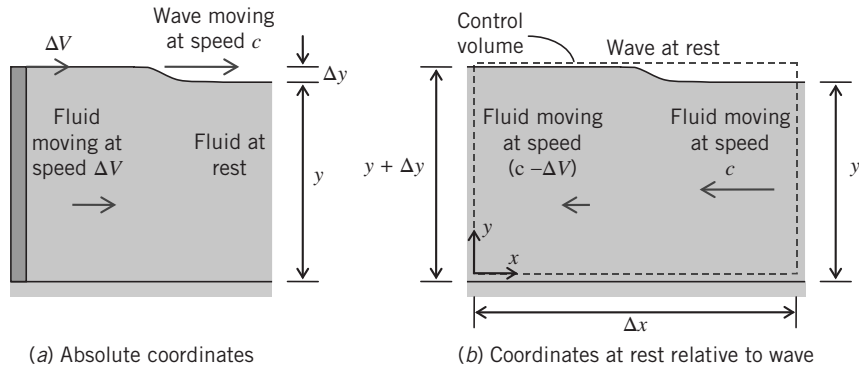
Shape	Section	Flow Area, A	Wetted Perimeter, P	Hydraulic Radius, R_h
Trapezoidal		$y(b + y \cot \alpha)$	$b + \frac{2y}{\sin \alpha}$	$\frac{y(b + y \cot \alpha)}{b + \frac{2y}{\sin \alpha}}$
Triangular		$y^2 \cot \alpha$	$\frac{2y}{\sin \alpha}$	$\frac{y \cos \alpha}{2}$
Rectangular		by	$b + 2y$	$\frac{by}{b + 2y}$
Wide flat		by	b	y
Circular		$(\alpha - \sin \alpha) \frac{D^2}{8}$	$\frac{\alpha D}{2}$	$\frac{D}{4} \left(1 - \frac{\sin \alpha}{\alpha}\right)$

Speed of Surface Waves and the Froude Number

We will learn later in this chapter that the behavior of an open-channel flow as it encounters downstream changes (e.g., a bump of the bed surface, a narrowing of the channel, or a change in slope) is strongly dependent on whether the flow is “slow” or “fast.” A slow flow will have time to gradually adjust to changes downstream, whereas a fast flow will also sometimes gradually adjust but in some situations will do so “violently” (called a hydraulic jump). It turns out that the speed at which surface waves travel along the surface is key to defining more precisely the notions of slow and fast.

To determine the speed (or *celerity*) of surface waves, consider an open channel with movable end wall containing a liquid initially at rest. If the end wall is given a sudden motion, as in Fig. 11.4a, a wave forms and travels down the channel at some speed, c .

If we shift coordinates so that we are traveling with the wave speed, c , we obtain a steady control volume, as shown in Fig. 11.4b. To obtain an expression for c , we will use the continuity and momentum equations for this control volume. We also have the following assumptions:

**Fig. 11.4** Motion of a surface wave.

- 1 Steady flow.
- 2 Incompressible flow.
- 3 Uniform velocity at each section.
- 4 Hydrostatic pressure distribution at each section.
- 5 Frictionless flow.

Assumption **1** is valid for the control volume in shifted coordinates. Assumption **2** is obviously valid for our liquid flow. Assumptions **3** and **4** are commonly used for all channel flows. Assumption **5** is valid in this case because we assume the area on which it acts, $b\Delta x$, is relatively small so the total friction force is negligible.

For an *incompressible* flow with *uniform velocity* at each section, the continuity equation is

$$\sum_{CS} \vec{V} \cdot \vec{A} = 0 \quad (4.13b)$$

Applying Eq. 4.13b to the control volume, we obtain

$$(c - \Delta V)\{(y + \Delta y)b\} - cyb = 0 \quad (11.3)$$

or

$$cy - \Delta Vy + c\Delta y - \Delta V\Delta y - cy = 0$$

Solving for ΔV ,

$$\Delta V = c \frac{\Delta y}{y + \Delta y} \quad (11.4)$$

For the momentum equation, again with the assumption of uniform velocity at each section, we use the following form of the x component of momentum

$$F_x = F_{S_x} + F_{B_x} = \frac{\partial}{\partial t} \int_{CV} u\rho dV + \sum_{CS} u\rho \vec{V} \cdot \vec{A} \quad (4.18d)$$

The unsteady term $\partial/\partial t$ disappears as the flow is *steady*, and the body force F_{B_x} is zero for *horizontal flow*. So we obtain

$$F_{S_x} = \sum_{CS} u\rho \vec{V} \cdot \vec{A} \quad (11.5)$$

The surface force consists of pressure forces on the two ends. By assumption 5, we neglect friction. The gage pressure at the two ends is hydrostatic, as illustrated in Fig. 11.4b. The hydrostatic force F_R on a submerged vertical surface of area A is given by the simple result

$$F_R = p_c A \quad (3.10b)$$

where p_c is the pressure at the centroid of the vertical surface. For the two vertical surfaces of the control volume, then, we have

$$\begin{aligned} F_{S_x} &= F_{R_{\text{left}}} - F_{R_{\text{right}}} = (p_c A)_{\text{left}} - (p_c A)_{\text{right}} \\ &= \left\{ \left(\rho g \frac{y + \Delta y}{2} \right) (y + \Delta y) b \right\} - \left\{ \left(\rho g \frac{y}{2} \right) y b \right\} \\ &= \frac{\rho g b}{2} (y + \Delta y)^2 - \frac{\rho g b}{2} y^2 \end{aligned}$$

Using this result in Eq. 11.5 and evaluating the terms on the right,

$$\begin{aligned} F_{S_x} &= \frac{\rho g b}{2} (y + \Delta y)^2 - \frac{\rho g b}{2} y^2 = \sum_{\text{CS}} u \rho \vec{V} \cdot \vec{A} \\ &= -(c - \Delta V) \rho \{(c - \Delta V)(y + \Delta y) b\} - c \rho \{-cyb\} \end{aligned}$$

The two terms in braces are equal, from continuity as shown in Eq. 11.3, so the momentum equation simplifies to

$$gy\Delta y + \frac{g(\Delta y)^2}{2} = yc\Delta V$$

or

$$g \left(1 + \frac{\Delta y}{2y} \right) \Delta y = c\Delta V$$

Combining this with Eq. 11.4, we obtain

$$g \left(1 + \frac{\Delta y}{2y} \right) \Delta y = c^2 \frac{\Delta y}{y + \Delta y}$$

and solving for c ,

$$c^2 = gy \left(1 + \frac{\Delta y}{2y} \right) \left(1 + \frac{\Delta y}{y} \right)$$

For waves of relatively small amplitude ($\Delta y \ll y$), we can simplify this expression to

$$c = \sqrt{gy} \quad (11.6)$$

Hence the speed of a surface disturbance depends on the local fluid depth. For example, it explains why waves “crash” as they approach the beach. Out to sea, the water depths below wave crests and troughs are approximately the same, and hence so are their speeds. As the water depth decreases on the approach to the beach, the depth of crests start to become significantly larger than trough depths, causing crests to speed up and overtake the troughs.

Note that fluid properties do not enter into the speed. Viscosity is a minor factor and the wave we have described is due to the interaction of gravitational and inertia forces, both of which are linear with density. Equation 11.6 was derived on the basis of one-dimensional motion (x direction); a more realistic model allowing two-dimensional fluid motion (x and y directions) shows that Eq. 11.6 applies for the limiting case of large wavelength waves. Also, there are other types of surface waves, such as capillary waves driven by surface tension, for which Eq. 11.6 does not apply. Example 11.1 illustrates the calculation for the speed of a surface wave that depends only on the depth.

Example 11.1 SPEED OF FREE SURFACE WAVES

You are enjoying a summer's afternoon relaxing in a rowboat on a pond. You decide to find out how deep the water is by splashing your oar and timing how long it takes the wave you produce to reach the edge of the pond. (The pond is artificial; so it has approximately the same depth even to the shore.) From floats installed in the pond, you know you're 20 ft from shore, and you measure the time for the wave to reach the edge to be 1.5 s. Estimate the pond depth. Does it matter if it's a freshwater pond or if it's filled with seawater?

Given: Time for a wave to reach the edge of a pond.

Find: Depth of the pond.

Solution: Use the wave speed equation, Eq. 11.6.

Governing equation: $c = \sqrt{gy}$

The time for a wave, speed c , to travel a distance L , is $\Delta t = \frac{L}{c}$, so $c = \frac{L}{\Delta t}$. Using this and Eq. 11.6,

$$\sqrt{gy} = \frac{L}{\Delta t}$$

where y is the depth, or

$$y = \frac{L^2}{g\Delta t^2}$$

Using the given data

$$y = 20^2 \text{ ft}^2 \times \frac{1}{32.2 \text{ ft}} \frac{\text{s}^2}{\text{ft}} \times \frac{1}{1.5^2} \frac{1}{\text{s}^2} = 5.52 \text{ ft} \quad \leftarrow y$$

The pond depth is about $5\frac{1}{2}$ ft.

The result obtained is independent of whether the water is fresh or saline, because the speed of these surface waves is independent of fluid properties.

The speed of surface disturbances given in Eq. 11.6 provides us with a more useful “litmus test” for categorizing the speed of a flow than the terms “slow” and “fast.” To illustrate this, consider a flow moving at speed V , which experiences a disturbance such as a bump in the channel floor or a barrier. The disturbance will travel upstream at speed c relative to the fluid. If the fluid speed is slow, $V < c$, and the disturbance will travel upstream at absolute speed $(c - V)$. However, if the fluid speed is fast, $V > c$, and the disturbance cannot travel upstream and instead is washed downstream at absolute speed $(V - c)$. This leads to radically different responses of slow and fast flows to a downstream disturbance. Hence, recalling Eq. 11.6 for the speed c , open-channel flows may be classified on the basis of Froude number first introduced in Chapter 7:

$$Fr = \frac{V}{\sqrt{gy}} \quad (11.7)$$

Instead of the rather loose terms “slow” and “fast,” we now have the following criteria:

$Fr < 1$ Flow is *subcritical, tranquil, or streaming*. Disturbances can travel upstream; downstream conditions can affect the flow upstream. The flow can gradually adjust to the disturbance.

$Fr = 1$ Flow is *critical*.

Fr > 1 Flow is *supercritical, rapid, or shooting*. No disturbance can travel upstream; downstream conditions cannot be felt upstream. The flow may “violently” respond to the disturbance because the flow has no chance to adjust to the disturbance before encountering it.

For nonrectangular channels we use the hydraulic depth y_h ,

$$Fr = \frac{V}{\sqrt{gy_h}} \quad (11.8)$$

These regimes of flow behavior are qualitatively analogous to the subsonic, sonic, and supersonic regimes of gas flow that we will discuss in Chapter 12. We will discuss the ramifications of these various Froude number regimes later in this chapter.

11.2 Energy Equation for Open-Channel Flows

In analyzing open-channel flows, we will use the continuity, momentum, and energy equations. As in the case of pipe flow, friction in open-channel flows results in a loss of mechanical energy which is characterized by a head loss. The energy equation for pipe flow derived in Section 8.6 is

$$\left(\frac{p_1}{\rho g} + \alpha_1 \frac{\bar{V}_2^2}{2g} + z_1 \right) - \left(\frac{p_2}{\rho g} + \alpha_2 \frac{\bar{V}_2^2}{2g} + z_2 \right) = \frac{h_{l_T}}{g} = H_{l_T} \quad (8.30)$$

Equation 8.30 was derived using the assumption that the pressure is uniform over each cross-section. In open-channel flow, there is a hydrostatic pressure variation with depth.

To derive an appropriate energy equation we will use the generic control volume shown in Fig. 11.5, with the following assumptions:

- 1 Steady flow.
- 2 Incompressible flow.
- 3 Uniform velocity at a section.
- 4 Gradually varying depth so that pressure distribution is hydrostatic.
- 5 Small bed slope.
- 6 $\dot{W}_s = \dot{W}_{\text{shear}} = \dot{W}_{\text{other}} = 0$.

Assumption 5 simplifies the analysis so that depth, y , is taken to be vertical and speed, V , is taken to be horizontal, rather than normal and parallel to the bed, respectively. Assumption 6 states that there is no shaft work or no work due to fluid shearing at the boundaries. There will still be mechanical energy dissipation within the fluid due to friction.

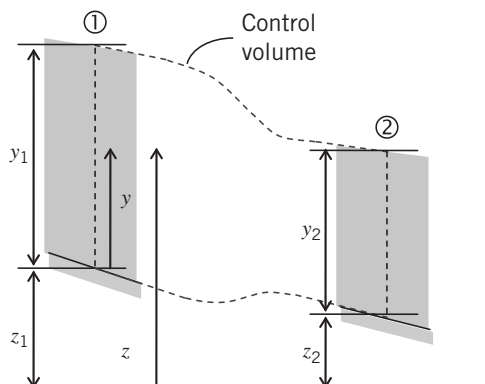


Fig. 11.5 Control volume and coordinates for energy analysis of open-channel flow.

We have chosen a generic control volume so that we can derive a generic energy equation for open-channel flows, that is, an equation that can be applied to a variety of flows such as ones with a variation in elevation, or a hydraulic jump, or a sluice gate, between sections ① and ②. Coordinate z indicates distances measured in the vertical direction; distances measured vertically from the channel bed are denoted by y . Note that y_1 and y_2 are the flow depths at sections ① and ②, respectively, and z_1 and z_2 are the corresponding channel elevations.

The energy equation for a control volume is

$$\begin{aligned} &= 0(6) = 0(6) = 0(6) = 0(1) \\ \dot{Q} - \dot{W}_s - \dot{W}_{\text{shear}} - \dot{W}_{\text{other}} &= \frac{\partial}{\partial t} \int_{\text{CV}} e \rho dV + \int_{\text{CS}} (e + pv) \rho \vec{V} \cdot d\vec{A} \\ e &= u + \frac{V^2}{2} + gz \end{aligned} \quad (4.56)$$

Recall that u is the thermal specific energy and $v = 1/\rho$ is the specific volume. After using assumptions 1 and 6, and rearranging, with $\dot{m} = \int \rho \vec{V} \cdot d\vec{A}$, and $dA = bdy$ where $b(y)$ is the channel width, we obtain

$$\begin{aligned} \dot{Q} &= - \int_1 \left(\frac{p}{\rho} + \frac{V^2}{2} + gz \right) \rho V b dy - \int_1 u \rho V b dy + \int_2 \left(\frac{p}{\rho} + \frac{V^2}{2} + gz \right) \rho V b dy + \int_2 u \rho V b dy \\ &= \int_1 \left(\frac{p}{\rho} + \frac{V^2}{2} + gz \right) \rho V b dy + \int_2 \left(\frac{p}{\rho} + \frac{V^2}{2} + gz \right) \rho V b dy + \dot{m}(u_2 - u_1) \end{aligned}$$

or

$$\int_1 \left(\frac{p}{\rho} + \frac{V^2}{2} + gz \right) \rho V b dy - \int_2 \left(\frac{p}{\rho} + \frac{V^2}{2} + gz \right) \rho V b dy = \dot{m}(u_2 - u_1) - \dot{Q} = \dot{m}h_{l_T} \quad (11.9)$$

This states that the loss in mechanical energies (pressure, kinetic and potential) through the control volume leads to a gain in the thermal energy and/or a loss of heat from the control volume. As in Section 8.6, these thermal effects are collected into the head loss term h_{l_T} .

The surface integrals in Eq. 11.9 can be simplified. The speed, V , is constant at each section by assumption 3. The pressure, p , does vary across sections ① and ②, as does the potential, z . However, by assumption 4, the pressure variation is hydrostatic. Hence, for section ①, using the notation of Fig. 11.5

$$p = \rho g(y_1 - y)$$

and

$$z = (z_1 + y)$$

We see that the pressure *decreases* linearly with y while z *increases* linearly with y , so the two terms together are constant,

$$\left(\frac{p}{\rho} + gz \right)_1 = g(y_1 - y) + g(z_1 + y) = g(y_1 + z_1)$$

Using these results in the first integral in Eq. 11.9,

$$\int_1 \left(\frac{p}{\rho} + \frac{V^2}{2} + gz \right) \rho V b dy = \int_1 \left(\frac{V^2}{2} + g(y_1 + z_1) \right) \rho V b dy = \left(\frac{V_1^2}{2} + gy_1 + gz_1 \right) \dot{m}$$

We find a similar result for section ②, so Eq. 11.9 becomes

$$\left(\frac{V_2^2}{2} + gy_2 + gz_2 \right) - \left(\frac{V_1^2}{2} + gy_1 + gz_1 \right) = h_{l_T}$$

Finally, dividing by g , with $H_l = h_{l_T}/g$, leads to an energy equation for open-channel flow

$$\frac{V_1^2}{2g} + y_1 + z_1 = \frac{V_2^2}{2g} + y_2 + z_2 + H_l \quad (11.10)$$

This can be compared to the corresponding equation for pipe flow, Eq. 8.30, presented at the beginning of this section. Note that we use H_l rather than H_{l_T} ; in pipe flow we can have major and minor losses, justifying T for total, but in open-channel flow we do not make this distinction.

The *total head* or *energy head*, H , at any location in an open-channel flow can be defined from Eq. 11.10 as

$$H = \frac{V^2}{2g} + y + z \quad (11.11)$$

where y and z are the local *flow depth* and *channel bed elevation*, respectively (they no longer represent the coordinates shown in Fig. 11.5). This is a measure of the mechanical energy (kinetic and pressure/potential) of the flow. Using this in the energy equation, we obtain an alternative form

$$H_1 - H_2 = H_l \quad (11.12)$$

From this we see that the loss of total head depends on head loss due to friction.

Specific Energy

We also define the *specific energy* (or *specific head*), denoted by the symbol E ,

$$E = \frac{V^2}{2g} + y \quad (11.13)$$

This is a measure of the mechanical energy of the flow above and beyond that due to channel bed elevation; it essentially indicates *the energy due to the flow's speed and depth*. Using Eq. 11.13 in Eq. 11.10, we obtain another form of the energy equation,

$$E_1 - E_2 + z_1 - z_2 = H_l \quad (11.14)$$

From this we see that the change in specific energy depends on friction and on channel elevation change. While the total head must decrease in the direction of flow (Eq. 11.12), the specific head may decrease, increase, or remain constant, depending on the bed elevation, z .

From continuity, $V = Q/A$, so the specific energy can be written

$$E = \frac{Q^2}{2gA^2} + y \quad (11.15)$$

For all channels the area A increases with depth, causing the first term in Eq. 11.5 to decrease with depth. The energy then is a combination of two terms, one decreasing with depth and one increasing. This is illustrated in Fig. 11.6. For a given flow rate, Q , there is a range of possible flow depths and energies and one depth at which the specific energy is at a minimum. Instead of E versus y Typically we plot y versus E so that the plot corresponds to the flow section, as shown in Fig. 11.7.

A given flow, Q , can have a range of energies, E , and corresponding flow depths, y . Figure 11.7 also reveals some interesting flow phenomena. For a given flow, Q , and specific energy, E , there are two possible flow depths, y ; these are called *alternate depths*. For example, we can have a flow at a large depth that is moving slowly, or a flow that is shallow but fast moving. The plot graphically indicates

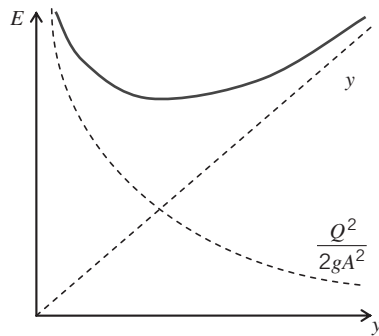


Fig. 11.6 Dependence of specific energy on flow depth for a given flow rate.

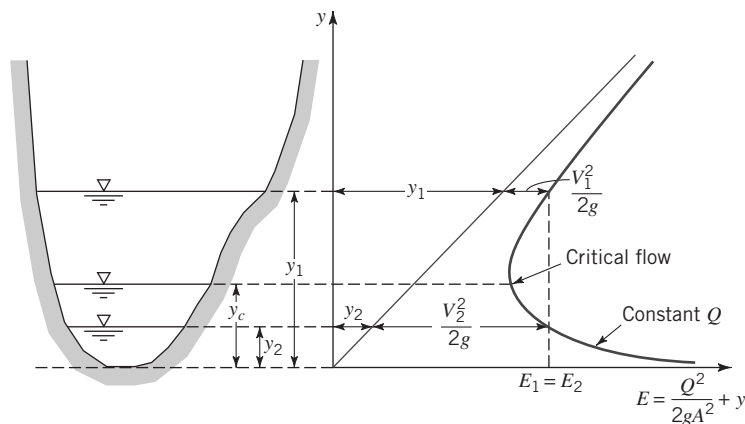


Fig. 11.7 Specific energy curve for a given flow rate.

this: for the first flow, E_1 is made up of a large y_1 and small $V_1^2/2g$; for the second flow, E_2 is made up of a small y_2 and large $V_2^2/2g$. Additionally, for a given Q , there is one flow for which the specific energy is the minimum. We will show that the minimum corresponds to critical conditions.

Critical Depth: Minimum Specific Energy

Example 11.2 treated the case of a rectangular channel. We now consider channels of general cross section. For flow in such a channel we have the specific energy in terms of flow rate Q ,

$$E = \frac{Q^2}{2gA^2} + y \quad (11.15)$$

For a given flow rate Q , to find the depth for minimum specific energy, we differentiate:

$$\frac{dE}{dy} = 0 = -\frac{Q^2}{gA^3} \frac{dA}{dy} + 1 \quad (11.16)$$

For any given cross section we can write

$$dA = b_s dy \quad (11.17)$$

Example 11.2 SPECIFIC ENERGY CURVES FOR A RECTANGULAR CHANNEL

For a rectangular channel of width $b = 10 \text{ m}$, construct a family of specific energy curves for $Q = 0, 2, 5$, and $10 \text{ m}^3/\text{s}$. What are the minimum specific energies for these curves?

Given: Rectangular channel and range of flow rates.

Find: Curves of specific energy. For each flow rate, find the minimum specific energy.

Solution: Use the flow rate form of the specific energy equation (Eq. 11.15) for generating the curves.

Governing equations:

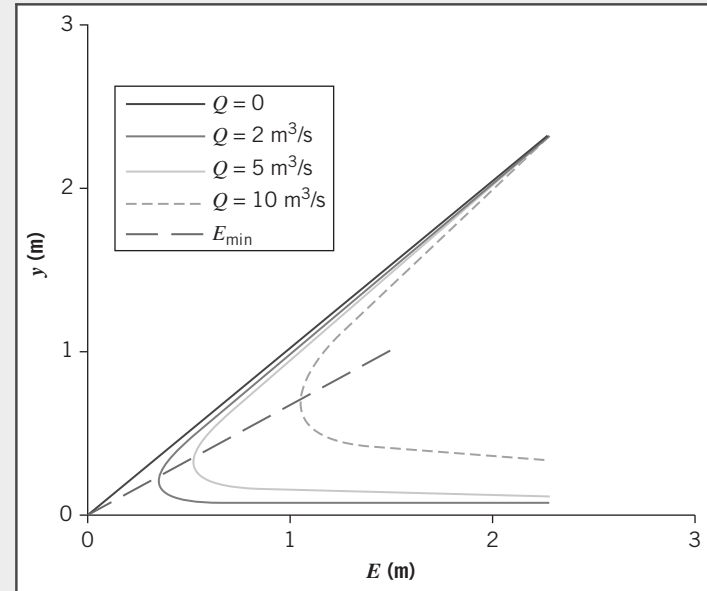
$$E = \frac{Q^2}{2gA^2} + y \quad (11.15)$$

For the specific energy curves, express E as a function of depth, y .

$$E = \frac{Q^2}{2gA^2} + y = \frac{Q^2}{2g(by)^2} + y = \left(\frac{Q^2}{2gb^2}\right)\frac{1}{y^2} + y \quad (1)$$

The table and corresponding graph were generated from this equation using *Excel*.

y (m)	Specific Energy, E (m)			
	$Q = 0$	$Q = 2$	$Q = 5$	$Q = 10$
0.100	0.10	0.92	5.20	20.49
0.125	0.13	0.65	3.39	13.17
0.150	0.15	0.51	2.42	9.21
0.175	0.18	0.44	1.84	6.83
0.200	0.20	0.40	1.47	5.30
0.225	0.23	0.39	1.23	4.25
0.250	0.25	0.38	1.07	3.51
0.275	0.28	0.38	0.95	2.97
0.30	0.30	0.39	0.87	2.57
0.35	0.35	0.42	0.77	2.01
0.40	0.40	0.45	0.72	1.67
0.45	0.45	0.49	0.70	1.46
0.50	0.50	0.53	0.70	1.32
0.55	0.55	0.58	0.72	1.22
0.60	0.60	0.62	0.74	1.17
0.70	0.70	0.72	0.80	1.12
0.80	0.80	0.81	0.88	1.12
0.90	0.90	0.91	0.96	1.15
1.00	1.00	1.01	1.05	1.20
1.25	1.25	1.26	1.28	1.38
1.50	1.50	1.50	1.52	1.59
2.00	2.00	2.00	2.01	2.05
2.50	2.50	2.50	2.51	2.53



To find the minimum energy for a given Q , we differentiate Eq. 1,

$$\frac{dE}{dy} = \left(\frac{Q^2}{2gb^2}\right)\left(-\frac{2}{y^3}\right) + 1 = 0$$

Hence, the depth $y_{E_{\min}}$ for minimum specific energy is

$$y_{E_{\min}} = \left(\frac{Q^2}{gb^2} \right)^{\frac{1}{3}}$$

Using this in Eq. 11.15:

$$\begin{aligned} E_{\min} &= \frac{Q^2}{2gA^2} + y_{E_{\min}} = \frac{Q^2}{2gb^2y_{E_{\min}}^2} + \left[\frac{Q^2}{gb^2} \right]^{\frac{1}{3}} = \frac{1}{2} \left[\frac{Q^2}{gb^2} \right] \left[\frac{gb^2}{Q^2} \right]^{\frac{2}{3}} + \left[\frac{Q^2}{gb^2} \right]^{\frac{1}{3}} = \frac{3}{2} \left[\frac{Q^2}{gb^2} \right]^{\frac{1}{3}} \\ E_{\min} &= \frac{3}{2} \left[\frac{Q^2}{gb^2} \right]^{\frac{1}{3}} = \frac{3}{2} y_{E_{\min}} \end{aligned} \quad (2)$$

Hence for a rectangular channel, we obtain a simple result for the minimum energy. Using Eq. 2 with the given data:

$Q (\text{m}^3/\text{s})$	2	5	10
$E_{\min} (\text{m})$	0.302	0.755	1.51

The depths corresponding to these flows are 0.201 m, 0.503 m, and 1.01 m, respectively.

We will see in the next topic that the depth at which we have minimum energy is the critical depth, y_c , and $E_{\min} = E_{\text{crit}}$.

where, as we saw earlier, b_s is the width at the surface. This is indicated in Fig. 11.8; the incremental increase in area dA due to incremental depth change dy occurs at the free surface, where $b = b_s$.

Using Eq. 11.17 in Eq. 11.16 we find

$$-\frac{Q^2}{gA^3} \frac{dA}{dy} + 1 = -\frac{Q^2}{gA^3} b_s + 1 = 0$$

so

$$Q^2 = \frac{gA^3}{b_s} \quad (11.18)$$

for minimum specific energy. From continuity $V = Q/A$, so Eq. 11.18 leads to

$$V = \frac{Q}{A} = \frac{1}{A} \left[\frac{gA^3}{b_s} \right]^{1/2} = \sqrt{\frac{gA}{b_s}} \quad (11.19)$$

We have previously defined the hydraulic depth,

$$y_h = \frac{A}{b_s} \quad (11.2)$$

Hence, using Eq. 11.2 in Eq. 11.19, we obtain

$$V = \sqrt{gy_h} \quad (11.20)$$

The Froude number is given by

$$Fr = \frac{V}{\sqrt{gy_h}} \quad (11.8)$$

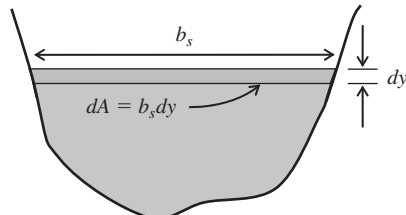


Fig. 11.8 Dependence of flow area change dA on depth change dy .

Hence we see that, for minimum specific energy, $Fr = 1$, which corresponds to critical flow. We obtain the important result that, for flow in any open channel, *the specific energy is at its minimum at critical conditions.*

We collect Eqs. 11.18 and 11.20; for critical flow

$$Q^2 = \frac{gA_c^3}{b_{s_c}} \quad (11.21)$$

$$V_c = \sqrt{gy_{h_c}} \quad (11.22)$$

for $E = E_{\min}$. In these equations, A_c , V_c , b_{s_c} , and y_{h_c} are the critical flow area, velocity, channel surface width, and hydraulic depth, respectively. Equation 11.21 can be used to find the critical depth, y_c , for a given channel cross-section shape, at a given flow rate. The equation is deceptively difficult: A_c and b_{s_c} each depend on flow depth y , often in a nonlinear fashion; so it must usually be iteratively solved for y . Once y_c is obtained, area, A_c , and surface width, b_{s_c} , can be computed, leading to y_{h_c} (using Eq. 11.2). This in turn is used to find the flow speed V_c . Finally, the minimum energy can be computed from Eq. 11.15. Example 11.3 shows how the critical depth is determined for a triangular section channel.

For the particular case of a *rectangular channel*, we have $b_s = b = \text{constant}$ and $A = by$, so Eq. 11.21 becomes

$$Q^2 = \frac{gA_c^3}{b_{s_c}} = \frac{gb^3y_c^3}{b} = gb^2y_c^3$$

so

$$y_c = \left[\frac{Q^2}{gb^2} \right]^{1/3} \quad (11.23)$$

with

$$V_c = \sqrt{gy_c} = \left[\frac{gQ}{b} \right]^{1/3} \quad (11.24)$$

For the rectangular channel, a particularly simple result for the minimum energy is obtained when Eq. 11.24 is used in Eq. 11.15,

$$E = E_{\min} = \frac{V_c^2}{2g} + y_c = \frac{gy_c}{2g} + y_c$$

or

$$E_{\min} = \frac{3}{2}y_c \quad (11.25)$$

This is the same result we found in Example 11.2. The critical state is an important benchmark. It will be used in the next section to help determine what happens when a flow encounters an obstacle such as a bump. Also, near the minimum E , as Fig. 11.7 shows, the depth y changes rapidly with E . This means that for critical flow conditions, even small changes in E , due to channel irregularities or disturbances, can cause pronounced changes in fluid depth.

Example 11.3 CRITICAL DEPTH FOR TRIANGULAR SECTION

A steep-sided triangular section channel ($\alpha = 60^\circ$) has a flow rate of $300 \text{ m}^3/\text{s}$. Find the critical depth for this flow rate. Verify that the Froude number is unity.

Given: Flow in a triangular section channel.

Find: Critical depth; verify that $Fr = 1$.

Solution: Use the critical flow equation, Eq. 11.21

Governing equations:

$$Q^2 = \frac{gA_c^3}{b_{sc}} \quad Fr = \frac{V}{\sqrt{gy_h}}$$

The given data is:

$$Q = 300 \text{ m}^3/\text{s} \quad \alpha = 60^\circ$$

From Table 11.1 we have the following:

$$A = y^2 \cot \alpha$$

and from basic geometry

$$\tan \alpha = \frac{y}{b_s/2} \quad \text{so} \quad b_s = 2y \cot \alpha$$

Using these in Eq. 11.21

$$Q^2 = \frac{gA_c^3}{b_{sc}} = \frac{g[y_c^2 \cot \alpha]^3}{2y_c \cot \alpha} = \frac{1}{2} gy_c^5 \cot^2 \alpha$$

Hence

$$y_c = \left[\frac{2Q^2 \tan^2 \alpha}{g} \right]^{1/5}$$

Using the given data

$$y_c = \left[2 \times 300^2 \left(\frac{\text{m}^3}{\text{s}} \right)^2 \times \tan^2 \left(\frac{60 \times \pi}{180} \right) \times \frac{\text{s}^2}{9.81 \text{ m}} \right]^{1/5} = [5.51 \times 10^4 \text{ m}^5]^{1/5}$$

Finally

$$y_c = 8.88 \text{ m} \xrightarrow{y_c}$$

To verify that $Fr = 1$, we need V and y_h .

From continuity

$$V_c = \frac{Q}{A_c} = \frac{Q}{y_c^2 \cot \alpha} = 300 \frac{\text{m}^3}{\text{s}} \times \frac{1}{8.88^2 \text{ m}^2} \times \frac{1}{\cot \left(\frac{60 \times \pi}{180} \right)} = 6.60 \text{ m/s}$$

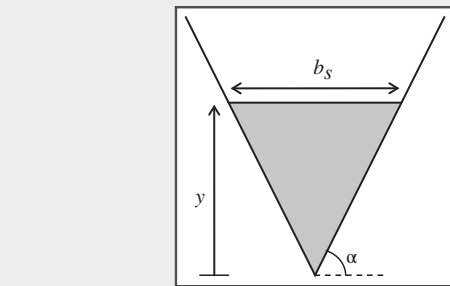
and from the definition of hydraulic depth

$$y_{h_c} = \frac{A_c}{b_{sc}} = \frac{y_c^2 \cot \alpha}{2y_c \cot \alpha} = \frac{y_c}{2} = 4.44 \text{ m}$$

Hence

$$Fr_c = \frac{V_c}{\sqrt{gy_{h_c}}} = \frac{6.60 \frac{\text{m}}{\text{s}}}{\sqrt{9.81 \frac{\text{m}}{\text{s}^2} \times 4.44 \text{ m}}} = 1 \xrightarrow{Fr_c = 1}$$

We have verified that at critical depth the Froude number is unity.



As with the rectangular channel, the triangular section channel analysis leads to an explicit equation for y_c from Eq. 11.21. Other more complicated channel cross sections often lead to an implicit equation that needs to be solved numerically.

11.3 Localized Effect of Area Change (Frictionless Flow)

We will now consider a simple flow case in which the channel bed is horizontal and for which the effects of channel cross section (area change) predominate: flow over a bump. Since this phenomenon takes place over a short distance the effects of friction may be neglected.

The energy equation, Eq. 11.10, with the assumption of no losses due to friction then becomes

$$\frac{V_1^2}{2g} + y_1 + z_1 = \frac{V_2^2}{2g} + y_2 + z_2 = \frac{V^2}{2g} + y + z = \text{const} \quad (11.26)$$

Alternatively, using the definition of specific energy

$$E_1 + z_1 = E_2 + z_2 = E + z = \text{const}$$

We see that the specific energy of a frictionless flow will change only if there is a change in the elevation of the channel bed.

Flow over a Bump

Consider frictionless flow in a horizontal rectangular channel of constant width, b , with a bump in the channel bed, as illustrated in Fig. 11.9. The bump height above the horizontal bed of the channel is $z = h(x)$; the water depth, $y(x)$, is measured from the local channel bottom surface.

We have indicated two possibilities for the free surface behavior: the flow gradually rises over the bump or it gradually dips over the bump. Applying the energy equation (Eq. 11.26) for frictionless flow between an upstream point ① and any point along the region of the bump,

$$\frac{V_1^2}{2g} + y_1 = E_1 = \frac{V^2}{2g} + y + h = E + h(x) = \text{const} \quad (11.27)$$

Equation 11.27 indicates that the specific energy must decrease through the bump, then increase back to its original value (of $E_1 = E_2$),

$$E(x) = E_1 - h(x) \quad (11.28)$$

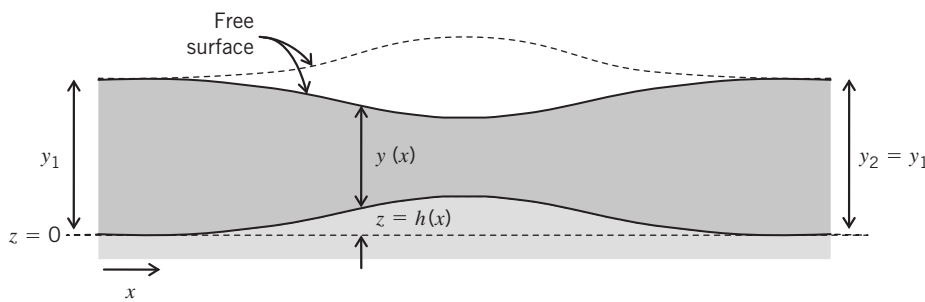


Fig. 11.9 Flow over a bump in a horizontal channel.

From continuity

$$Q = bV_1y_1 = bVy$$

Using this in Eq 11.27

$$\frac{Q^2}{2gb^2y_1^2} + y_1 = \frac{Q^2}{2gb^2y^2} + y + h = \text{const} \quad (11.29)$$

We can obtain an expression for the variation of the free surface depth by differentiating Eq. 11.29:

$$-\frac{Q^2}{gb^2y^3} \frac{dy}{dx} + \frac{dy}{dx} + \frac{dh}{dx} = 0$$

Solving for the slope of the free surface, we obtain

$$\frac{dy}{dx} = \frac{dh/dx}{\left[\frac{Q^2}{gb^2y^3} - 1 \right]} = \frac{dh/dx}{\left[\frac{V^2}{gy} - 1 \right]}$$

Finally,

$$\frac{dy}{dx} = \frac{1}{Fr^2 - 1} \frac{dh}{dx} \quad (11.30)$$

Equation 11.30 leads to the conclusion that the response to a bump very much depends on the local Froude number, Fr .

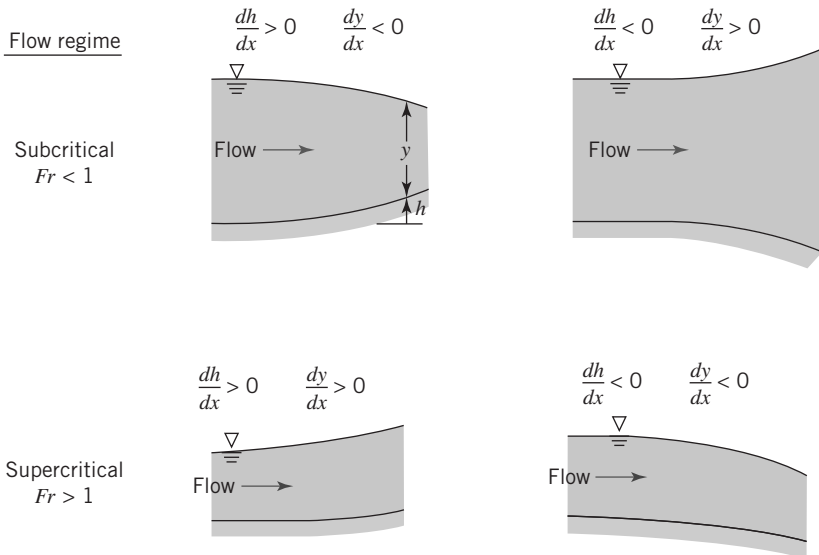
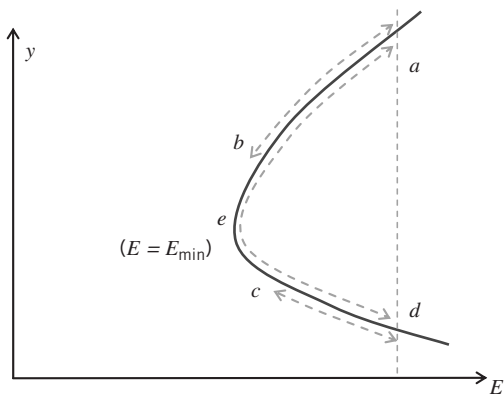
$Fr < 1$ Flow is *subcritical, tranquil, or streaming*. When $Fr < 1$, $(Fr^2 - 1) < 1$ and the slope dy/dx of the free surface has the *opposite* sign to the slope dh/dx of the bump: When the bump elevation increases, the flow dips; when the bump elevation decreases, the flow depth increases. This is the solid free surface shown in Fig. 11.9.

$Fr = 1$ Flow is *critical*. When $Fr = 1$, $(Fr^2 - 1) = 0$. Equation 11.30 predicts an infinite water surface slope, unless dh/dx equals zero at this instant. Since the free surface slope cannot be infinite, then dh/dx must be zero when $Fr = 1$; put another way, if we have $Fr = 1$ it can *only* be at a location where $dh/dx = 0$ (at the crest of the bump, or where the channel is flat). If critical flow *is* attained, then downstream of the critical flow location the flow may be subcritical or supercritical, depending on downstream conditions. If critical flow does *not* occur where $dh/dx = 0$, then flow downstream from this location will be the same type as the flow upstream from the location.

$Fr > 1$ Flow is *supercritical, rapid, or shooting*. When $Fr > 1$, $(Fr^2 - 1) > 1$ and the slope dy/dx of the free surface has the same sign as the slope dh/dx of the bump: when the bump elevation increases, so does the flow depth; when the bump elevation decreases, so does the flow depth. This is the dashed free surface shown in Fig. 11.9.

The general trends for $Fr < 1$ and $Fr > 1$, for either an increasing or decreasing bed elevation, are illustrated in Fig. 11.10. The important point about critical flow ($Fr = 1$) is that, if it does occur, it can do so only where the bed elevation is constant.

An additional visual aid is provided by the specific energy graph of Fig. 11.11. This shows the specific energy curve for a given flow rate, Q . For a subcritical flow that is at state a before it encounters a bump, as the flow moves up the bump toward the bump peak, the specific energy must decrease (Eq. 11.28). Hence we move along the curve to point b . If point b corresponds to the bump peak, then we move back along the curve to a as the flow descends the bump. Alternatively, if the bump continues to increase beyond point b , we continue to move along the curve to the minimum energy point, point e where $E = E_{\min} = E_{\text{crit}}$. As we have discussed, for frictionless flow to exist, point e can only be where $dh/dx = 0$ (the bump peak). For this case, as the flow descends down the bump we can return along the curve to point a , or we can move along the curve to point d . This means that the surface of a subcritical flow that encounters a bump will dip and then *either* return to its original depth *or* if the bump is high enough for the flow to reach critical conditions may continue to accelerate and become shallower until it

**Fig. 11.10** Effects of bed elevation changes.**Fig. 11.11** Specific energy curve for flow over a bump.

reaches the supercritical state corresponding to the original specific energy (point *d*). Which trend occurs depends on downstream conditions. For example, if there is some type of flow restriction, the flow downstream of the bump will return to its original subcritical state. Finally, Fig. 11.11 indicates that a supercritical flow (point *d*) that encounters a bump would increase in depth over the bump (to point *c* at the bump peak), and then return to its supercritical flow at point *d*. We also see that if the bump is high enough a supercritical flow could slow down to critical (point *e*) and then either return to supercritical (point *d*) or become subcritical (point *a*). Which of these possibilities actually occurs obviously depends on the bump shape, but also on upstream and downstream conditions.

Example 11.4 FLOW IN A RECTANGULAR CHANNEL WITH A BUMP OR A NARROWING

A rectangular channel 2 m wide has a flow of $2.4 \text{ m}^3/\text{s}$ at a depth of 1.0 m. Determine whether critical depth occurs at (a) a section where a bump of height $h = 0.20 \text{ m}$ is installed across the channel bed, (b) a side wall constriction (with no bumps) reducing the channel width to 1.7 m, and (c) both the bump and side wall constrictions combined. Neglect head losses of the bump and constriction caused by friction, expansion, and contraction.

Given: Rectangular channel with a bump, a side wall constriction, or both.

Find: Whether critical flow occurs.

Solution: Compare the specific energy to the minimum specific energy for the given flow rate in each case to establish whether critical depth occurs.

Governing equations:

$$E = \frac{Q^2}{2gA^2} + y \quad (11.15) \quad y_c = \left[\frac{Q}{gb^2} \right]^{1/3} \quad (11.23)$$

$$E_{\min} = \frac{3}{2}y_c \quad (11.25) \quad E = E_1 - h \quad (11.28)$$

(a) Bump of height $h = 0.20$ m:

The initial specific energy, E_1 , is

$$\begin{aligned} E_1 &= y_1 + \frac{Q^2}{2gA^2} = y_1 + \frac{Q^2}{2gb^2y_1^2} \\ &= 1.0 \text{ m} + 2.4^2 \left(\frac{\text{m}^3}{\text{s}} \right)^2 \times \frac{1}{2} \times \frac{\text{s}^2}{9.81 \text{ m}} \times \frac{1}{2^2 \text{ m}^2} \times \frac{1}{1^2 \text{ m}^2} \\ E_1 &= 1.073 \text{ m} \end{aligned}$$

Then the specific energy at the peak of the bump, E_{bump} , is obtained from Eq. 11.28

$$\begin{aligned} E_{\text{bump}} &= E_1 - h = 1.073 \text{ m} - 0.20 \text{ m} \\ E_{\text{bump}} &= 0.873 \text{ m} \end{aligned} \quad (1)$$

We compare this to the minimum specific energy for the flow rate Q . First, the critical depth is

$$\begin{aligned} y_c &= \left[\frac{Q^2}{gb^2} \right]^{1/3} = \left[2.4^2 \left(\frac{\text{m}^3}{\text{s}} \right)^2 \times \frac{\text{s}^2}{9.81 \text{ m}} \times \frac{1}{2^2 \text{ m}^2} \right]^{1/3} \\ y_c &= 0.528 \text{ m} \end{aligned}$$

(Note that we have $y_1 > y_c$, so we have a subcritical flow.)

Then the minimum specific energy is

$$E_{\min} = \frac{3}{2}y_c = 0.791 \text{ m} \quad (2)$$

Comparing Eqs. 1 and 2 we see that with the bump we

do not attain critical conditions. \leftarrow

(b) A side wall constriction (with no bump) reducing the channel width to 1.7 m:

In this case the specific energy remains constant throughout ($h = 0$), even at the constriction; so

$$E_{\text{constriction}} = E_1 - h = E_1 = 1.073 \text{ m} \quad (3)$$

However, at the constriction, we have a new value for b , ($b_{\text{constriction}} = 1.7$ m), and so a new critical depth

$$y_{c_{\text{constriction}}} = \left[\frac{Q^2}{gb_{\text{constriction}}^2} \right]^{1/3} = \left[2.4^2 \left(\frac{\text{m}^3}{\text{s}} \right)^2 \times \frac{\text{s}^2}{9.81 \text{ m}} \times \frac{1}{1.7^2 \text{ m}^2} \right]^{1/3}$$

$$y_{c_{\text{constriction}}} = 0.588 \text{ m}$$

Then the minimum specific energy *at the constriction* is

$$E_{\min_{\text{constriction}}} = \frac{3}{2}y_{c_{\text{constriction}}} = 0.882 \text{ m} \quad (4)$$

Comparing Eqs. 3 and 4 we see that with the constriction

we do *not* attain critical conditions. ←

We can determine what constriction *would* cause critical flow. To find this, solve

$$E = 1.073 \text{ m} = E_{\min} = \frac{3}{2}y_c = \frac{3}{2} \left[\frac{Q^2}{gb_c^2} \right]^{1/3}$$

for the critical channel width b_c .

Hence

$$\begin{aligned} \frac{Q^2}{gb_c^2} &= \left[\frac{2}{3}E_{\min} \right]^3 \\ b_c &= \frac{Q}{\sqrt{\frac{8}{27}gE_{\min}^3}} \\ &= \left(\frac{27}{8} \right)^{1/2} \times 2.4 \left(\frac{\text{m}^3}{\text{s}} \right) \times \frac{\text{s}}{9.81^{1/2} \text{ m}^{1/2}} \times \frac{1}{1.073^{3/2} \text{ m}^{3/2}} \\ b_c &= 1.27 \text{ m} \end{aligned}$$

To make the given flow attain critical conditions, the constriction should be 1.27 m; anything wider, and critical conditions are not reached.

(c) For a bump of $h = 0.20 \text{ m}$ and the constriction to $b = 1.7 \text{ m}$:

We have already seen in case (a) that the bump ($h = 0.20 \text{ m}$) was insufficient by itself to create critical conditions. From case (b) we saw that at the constriction the minimum specific energy is $E_{\min} = 0.882 \text{ m}$ rather than $E_{\min} = 0.791 \text{ m}$ in the main flow. When we have both factors present, we can compare the specific energy at the bump and constriction,

$$E_{\text{bump + constriction}} = E_{\text{bump}} = E_1 - h = 0.873 \text{ m} \quad (5)$$

and the minimum specific energy for the flow at the bump and constriction,

$$E_{\min_{\text{constriction}}} = \frac{3}{2}y_{c_{\text{constriction}}} = 0.882 \text{ m} \quad (6)$$

From Eqs. 5 and 6 we see that with both factors the specific energy is actually *less* than the minimum. The fact that we must have a specific energy that is less than the minimum allowable means something has to give. What happens is that the flow assumptions become invalid; the flow may no longer be uniform or one-dimensional, or there may be a significant energy loss, for example due to a hydraulic jump occurring.

Hence the bump and constriction together *are* sufficient to make the flow reach critical state. ←

This problem illustrates how to determine whether a channel bump or constriction, or both, lead to critical flow conditions.

11.4 The Hydraulic Jump

We have shown that open-channel flow may be subcritical ($Fr < 1$) or supercritical ($Fr > 1$). For subcritical flow, disturbances caused by a change in bed slope or flow cross section may move upstream and downstream and the result is a smooth adjustment of the flow. When flow at a section is supercritical the flow velocity exceeds the speed of surface waves and disturbances cannot move upstream. If the

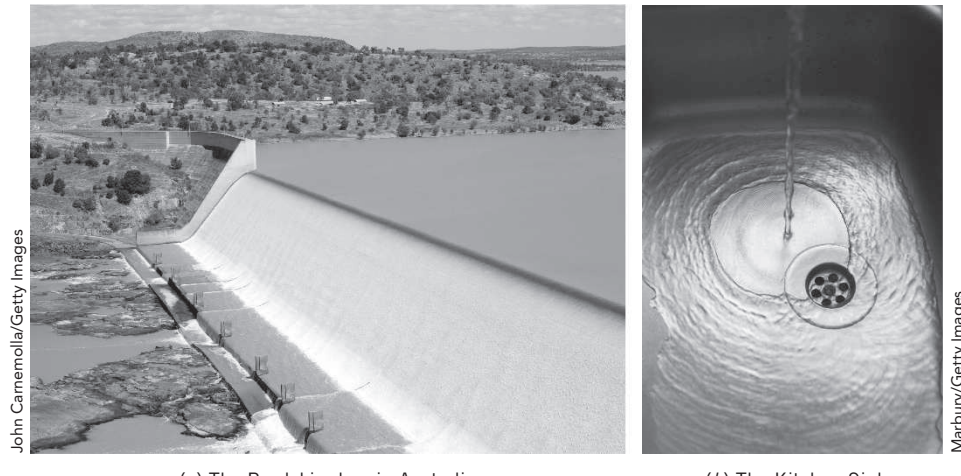


Fig. 11.12 Examples of a hydraulic jump.

(b) The Kitchen Sink
(James Kilfiger)

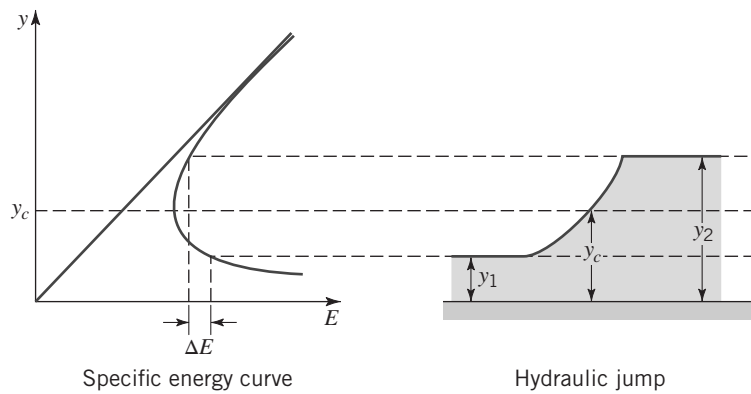


Fig. 11.13 Specific energy curve for flow through a hydraulic jump.

downstream conditions require a change to subcritical flow, a gradual change with a smooth transition through the critical point is not possible. The transition from supercritical to subcritical flow occurs abruptly through a *hydraulic jump*. Hydraulic jumps can occur in canals downstream of regulating sluices, at the foot of spillways (see Fig. 11.12a), and where a steep channel slope suddenly becomes flat. The specific energy curve and general shape of a jump are shown in Fig. 11.13. We will see in this section that the jump always goes from a supercritical depth ($y_1 < y_c$) to a subcritical depth ($y_2 > y_c$) and that there will be a drop ΔE in the specific energy. Unlike the changes due to phenomena such as a bump, the abrupt change in depth involves a significant loss of mechanical energy through turbulent mixing.

We shall analyze the hydraulic jump phenomenon by applying the basic equations to the control volume shown in Fig. 11.14. Experiments show that the jump occurs over a relatively short distance

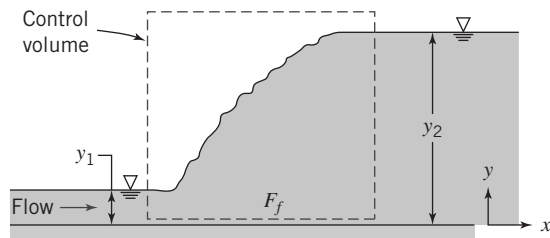


Fig. 11.14 Schematic of hydraulic jump, showing control volume used for analysis.

approximately six times the larger depth (y_2) [9]. In view of this short length, the friction force F_f acting on the control volume is negligible compared to pressure forces. We will assume a horizontal bed and rectangular channel. Hence we have the following assumptions:

- 1 Steady flow.
- 2 Incompressible flow.
- 3 Uniform velocity at each section.
- 4 Hydrostatic pressure distribution at each section.
- 5 Frictionless flow (for the momentum equation).

For an *incompressible* flow with *uniform velocity* at each section, we use the appropriate form of continuity from Chapter 4,

$$\sum_{\text{CS}} \vec{V} \cdot \vec{A} = 0 \quad (4.13b)$$

Applying Eq. 4.13b to the control volume we obtain

$$-V_1 b y_1 + V_2 b y_2 = 0$$

or

$$V_1 y_1 = V_2 y_2 \quad (11.31)$$

This is the continuity equation for the hydraulic jump. For the momentum equation, again with the assumption of uniform velocity at each section, we can use the following form for the x component of momentum

$$F_x = F_{S_x} + F_{B_x} = \frac{\partial}{\partial t} \int_{\text{CV}} u \rho dV + \sum_{\text{CS}} u \rho \vec{V} \cdot \vec{A} \quad (4.18d)$$

The unsteady term $\partial/\partial t$ disappears as the flow is *steady*, and the body force F_{B_x} is zero for *horizontal flow*. So we obtain

$$F_{S_x} = \sum_{\text{CS}} u \rho \vec{V} \cdot \vec{A} \quad (11.32)$$

The surface force consists of pressure forces on the two ends and friction force on the wetted surface. By assumption 5 we neglect friction. The gage pressure at the two ends is hydrostatic, as illustrated in Fig. 11.3b. The hydrostatic force, F_R , on a submerged vertical surface of area, A , is given by the simple result

$$F_R = p_c A \quad (3.10b)$$

where p_c is the pressure at the centroid of the vertical surface. For the two vertical surfaces of the control volume, then, we have

$$\begin{aligned} F_{S_x} &= F_{R_1} - F_{R_2} = (p_c A)_1 - (p_c A)_2 = \{(\rho g y_1) y_1 b\} - \{(\rho g y_2) y_2 b\} \\ &= \frac{\rho g b}{2} (y_1^2 - y_2^2) \end{aligned}$$

Using this result in Eq. 11.32, and evaluating the terms on the right,

$$F_{S_x} = \frac{\rho g b}{2} (y_1^2 - y_2^2) = \sum_{\text{CS}} u \rho \vec{V} \cdot \vec{A} = V_1 \rho \{-V_1 y_1 b\} + V_2 \rho \{V_2 y_2 b\}$$

Rearranging and simplifying

$$\frac{V_1^2 y_1}{g} + \frac{y_1^2}{2} = \frac{V_2^2 y_2}{g} + \frac{y_2^2}{2} \quad (11.33)$$

This is the momentum equation for the hydraulic jump. We have already derived the energy equation for open-channel flows,

$$\frac{V_1^2}{2g} + y_1 + z_1 = \frac{V_2^2}{2g} + y_2 + z_2 + H_l \quad (11.10)$$

For our horizontal hydraulic jump, $z_1 = z_2$, so

$$E_1 = \frac{V_1^2}{2g} + y_1 = \frac{V_2^2}{2g} + y_2 + H_l = E_2 + H_l \quad (11.34)$$

This is the energy equation for the hydraulic jump; the loss of mechanical energy is

$$\Delta E = E_1 - E_2 = H_l$$

The continuity, momentum, and energy equations (Eqs. 11.31, 11.33, and 11.34, respectively) constitute a complete set for analyzing a hydraulic jump.

Depth Increase Across a Hydraulic Jump

To find the downstream or, as it is called, the *sequent* depth in terms of conditions upstream from the hydraulic jump, we first eliminate V_2 from the momentum equation. From continuity, $V_2 = V_1 y_1 / y_2$ (Eq. 11.31), so Eq. 11.33 can be written

$$\frac{V_1^2 y_1}{g} + \frac{y_1^2}{2} = \frac{V_1^2 y_1}{g} \left(\frac{y_1}{y_2} \right) + \frac{y_2^2}{2}$$

Rearranging

$$y_2^2 - y_1^2 = \frac{2V_1^2 y_1}{g} \left(1 - \frac{y_1}{y_2} \right) = \frac{2V_1^2 y_1}{g} \left(\frac{y_2 - y_1}{y_2} \right)$$

Dividing both sides by the common factor $(y_2 - y_1)$, we obtain

$$y_2 + y_1 = \frac{2V_1^2 y_1}{g y_2}$$

Next, multiplying by y_2 and dividing by y_1^2 gives

$$\left(\frac{y_2}{y_1} \right)^2 + \left(\frac{y_2}{y_1} \right) = \frac{2V_1^2}{g y_1} = 2F_r^2 \quad (11.35)$$

Solving for y_2/y_1 using the quadratic formula and ignoring the physically meaningless negative root, we obtain

$$\frac{y_2}{y_1} = \frac{1}{2} \left[\sqrt{1 + 8F_r^2} - 1 \right] \quad (11.36)$$

Hence, the ratio of downstream to upstream depths across a hydraulic jump is only a function of the upstream Froude number. Equation 11.36 has been experimentally verified as shown in Fig. 11.15a. Depths y_1 and y_2 are referred to as *conjugate depths*. From Eq. 11.35, we see that an increase in depth ($y_2 > y_1$) requires an upstream Froude number greater than one ($F_r > 1$).

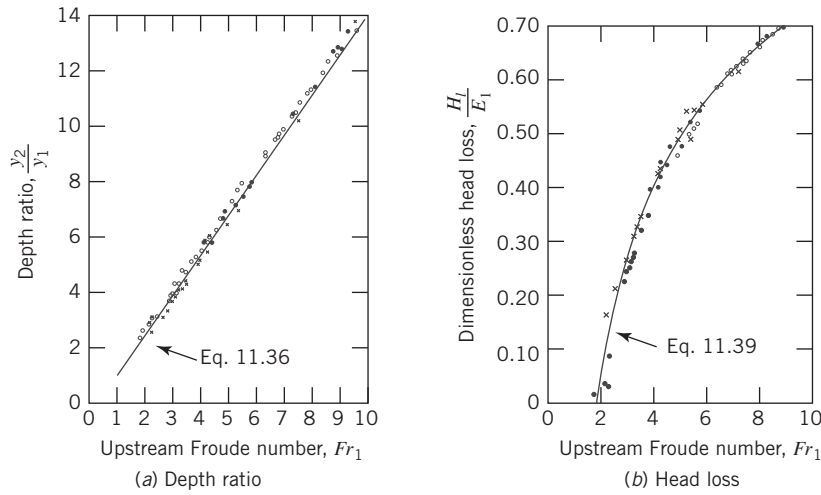


Fig. 11.15 Depth ratio and head loss for a hydraulic jump. (Data from Peterka [9].)

Head Loss Across a Hydraulic Jump

From the energy equation for the jump, Eq. 11.34, we can solve for the head loss

$$H_l = E_1 - E_2 = \frac{V_1^2}{2g} + y_1 - \left(\frac{V_2^2}{2g} + y_2 \right)$$

From continuity, $V_2 = V_1 y_1 / y_2$, so

$$H_l = \frac{V_1^2}{2g} \left[1 - \left(\frac{y_1}{y_2} \right)^2 \right] + (y_1 - y_2)$$

or

$$\frac{H_l}{y_1} = \frac{Fr_1^2}{2} \left[1 - \left(\frac{y_1}{y_2} \right)^2 \right] + \left[1 - \frac{y_2}{y_1} \right] \quad (11.37)$$

Solving Eq. 11.35 for Fr_1 in terms of y_2/y_1 and substituting into Eq. 11.37, we obtain

$$\frac{H_l}{y_1} = \frac{1}{4} \frac{\left[\frac{y_2}{y_1} - 1 \right]^3}{\frac{y_2}{y_1}} \quad (11.38a)$$

The left side is always positive as turbulence must lead to a loss of mechanical energy and so the cubed term must lead to a positive result. Then, from either Eq. 11.35 or Eq. 11.36, we see that we must have $Fr_1 > 1$. An alternative form of this result is obtained after some minor rearranging,

$$H_l = \frac{[y_2 - y_1]^3}{4y_1 y_2} \quad (11.38b)$$

which again shows that $y_2 > y_1$ for real flows ($H_l > 0$). Next, the specific energy, E_1 , can be written as

$$E_1 = \frac{V_1^2}{2g} + y_1 = y_1 \left[\frac{V_1^2}{2gy_1} + 1 \right] = y_1 \frac{(Fr_1^2 + 2)}{2}$$

Nondimensionalizing H_l using E_1 ,

$$\frac{H_l}{E_1} = \frac{1}{2} \frac{\left[\frac{y_2}{y_1} - 1 \right]^3}{\frac{y_2}{y_1} [Fr_1^2 + 2]}$$

The depth ratio in terms of Fr_1 is given by Eq. 11.36. Hence H_l/E_1 , can be written purely as a function of the upstream Froude number. The result, after some manipulation, is

$$\frac{H_l}{E_1} = \frac{\left[\sqrt{1 + 8Fr_1^2} - 3 \right]^3}{8 \left[\sqrt{1 + 8Fr_1^2} - 1 \right] [Fr_1^2 + 2]} \quad (11.39)$$

We see that the head loss, as a fraction of the original specific energy across a hydraulic jump, is only a function of the upstream Froude number. Equation 11.39 is experimentally well verified, as can be seen in Fig. 11.15b. The figure also shows that more than 70 percent of the mechanical energy of the entering stream is dissipated in jumps with $Fr_1 > 9$. Inspection of Eq. 11.39 also shows that if $Fr_1 = 1$, then $H_l = 0$, and that negative values are predicted for $Fr_1 < 1$. Since H_l must be positive in any real flow, this reconfirms that *a hydraulic jump can occur only in supercritical flow. Flow downstream from a jump always is subcritical*. The characteristics of a hydraulic jump are determined in Example 11.5.

Example 11.5 HYDRAULIC JUMP IN A RECTANGULAR CHANNEL FLOW

A hydraulic jump occurs in a rectangular channel 3 m wide. The water depth before the jump is 0.6 m, and after the jump is 1.6 m. Compute (a) the flow rate in the channel, (b) the critical depth, (c) the head loss in the jump.

Given: Rectangular channel with hydraulic jump in which flow depth changes from 0.6 to 1.6 m.

Find: Flow rate, critical depth, and head loss in the jump.

Solution: Use the equation that relates depths y_1 and y_2 in terms of the Froude number (Eq. 11.36); then use the Froude number (Eq. 11.7) to obtain the flow rate; use Eq. 11.23 to obtain the critical depth; and finally compute the head loss from Eq. 11.38b.

Governing equations:

$$\frac{y_2}{y_1} = \frac{1}{2} \left[-1 + \sqrt{1 + 8Fr_1^2} \right] \quad (11.36)$$

$$Fr = \frac{V}{\sqrt{gy}} \quad (11.7)$$

$$y_c = \left[\frac{Q^2}{gb^2} \right]^{1/3} \quad (11.23)$$

$$H_l = \frac{[y_2 - y_1]^3}{4y_1 y_2} \quad (11.38b)$$

(a) From Eq. 11.36

$$\begin{aligned} Fr_1 &= \sqrt{\frac{\left(1 + 2 \frac{y_2}{y_1}\right)^2 - 1}{8}} \\ &= \sqrt{\frac{\left(1 + 2 \times \frac{1.6 \text{ m}}{0.6 \text{ m}}\right)^2 - 1}{8}} \\ Fr_1 &= 2.21 \end{aligned}$$

As expected, $Fr_1 > 1$ (supercritical flow). We can now use the definition of Froude number for open-channel flow to find V_1

$$Fr_1 = \frac{V_1}{\sqrt{gy_1}}$$

Hence

$$V_1 = Fr_1 \sqrt{gy_1} = 2.21 \times \sqrt{\frac{9.81 \text{ m}}{\text{s}^2} \times 0.6 \text{ m}} = 5.36 \text{ m/s}$$

From this we can obtain the flow rate, Q .

$$\begin{aligned} Q &= by_1 V_1 = 3.0 \text{ m} \times 0.6 \text{ m} \times \frac{5.36 \text{ m}}{\text{s}} \\ Q &= 9.65 \text{ m}^3/\text{s} \end{aligned} \quad \underline{\hspace{10cm}} \quad Q$$

(b) The critical depth can be obtained from Eq. 11.23.

$$\begin{aligned} y_c &= \left[\frac{Q^2}{gb^2} \right]^{1/3} \\ &= \left(9.65^2 \frac{\text{m}^6}{\text{s}^2} \times \frac{\text{s}^2}{9.81 \text{ m}} \times \frac{1}{3.0^2 \text{ m}^2} \right)^{1/3} \\ y_c &= 1.02 \text{ m} \end{aligned} \quad \underline{\hspace{10cm}} \quad y_c$$

Note that as illustrated in Fig. 11.13, $y_1 < y_c < y_2$.

(c) The head loss can be found from Eq. 11.38b.

$$\begin{aligned} H_l &= \frac{[y_2 - y_1]^3}{4y_1 y_2} \\ &= \frac{1}{4} \frac{[1.6 \text{ m} - 0.6 \text{ m}]^3}{1.6 \text{ m} \times 0.6 \text{ m}} = 0.260 \text{ m} \end{aligned} \quad \underline{\hspace{10cm}} \quad H_l$$

As a verification of this result, we use the energy equation directly,

$$H_l = E_1 - E_2 = \left(y_1 + \frac{V_1^2}{2g} \right) - \left(y_2 + \frac{V_2^2}{2g} \right)$$

with $V_2 = Q/(by_2) = 2.01 \text{ m/s}$,

$$\begin{aligned} H_l &= \left(0.6 \text{ m} + 5.36^2 \frac{\text{m}^2}{\text{s}^2} \times \frac{1}{2} \times \frac{\text{s}^2}{9.81 \text{ m}} \right) \\ &\quad - \left(1.6 \text{ m} + 2.01^2 \frac{\text{m}^2}{\text{s}^2} \times \frac{1}{2} \times \frac{\text{s}^2}{9.81 \text{ m}} \right) \\ H_l &= 0.258 \text{ m} \end{aligned}$$

This problem illustrates computation of flow rate, critical depth, and head loss, for a hydraulic jump.

11.5 Steady Uniform Flow

Steady uniform flow occurs for channels of constant slope and cross section. Figs. 11.1 and 11.2 show examples of this kind of flow. A fully developed flow is one for which the channel is *prismatic*, that is, a channel with constant slope and cross section that flows at constant depth. This depth, y_n , is termed the

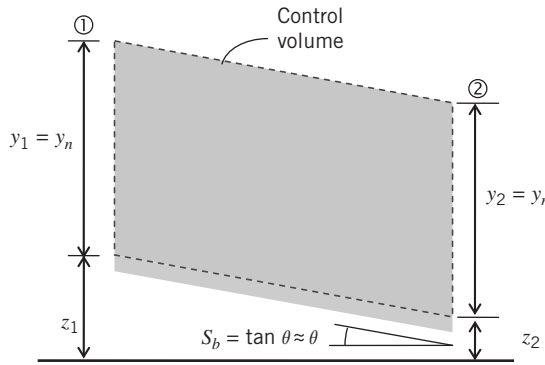


Fig. 11.16 Control volume for uniform channel flow.

normal depth and the flow is termed a *uniform flow*. Hence the expression *uniform flow* in this chapter has a different meaning than in earlier chapters. In earlier chapters it meant that the *velocity* was uniform *at a section* of the flow. In this chapter the velocity is uniform and in the *flow* is the same *at all sections*. Hence for the flow shown in Fig. 11.16, we have $A_1 = A_2 = A$ (cross-section areas), $Q_1 = Q_2 = Q$ (flow rates), $V_1 = V_2 = V$ (average velocity, $V = Q/A$), and $y_1 = y_2 = y_n$ (flow depth).

We make the following assumptions:

- 1 Steady flow.
- 2 Incompressible flow.
- 3 Uniform velocity at a section.
- 4 Gradually varying depth so that pressure distribution is hydrostatic.
- 5 Bed slope is small.
- 6 $\dot{W}_s = \dot{W}_{\text{shear}} = \dot{W}_{\text{other}} = 0$.

Assumption 5 means that we can approximate the flow depth y to be vertical and flow speed horizontal. The continuity equation is.

$$Q = V_1 A_1 = V_2 A_2 = VA$$

For the momentum equation, again with the assumption of uniform velocity at each section, we can use the following form for the x component of momentum

$$F_x = F_{S_x} + F_{B_x} = \frac{\partial}{\partial t} \int_{CV} u \rho dV + \sum_{CS} u \rho \vec{V} \cdot \vec{A} \quad (4.18d)$$

The unsteady term $\partial/\partial t$ disappears as the flow is steady, and the control surface summation is zero because $V_1 = V_2$; hence the right-hand side is zero as there is no change of momentum for the control volume. The body force $F_{B_x} = W \sin \theta$ where W is the weight of fluid in the control volume; θ is the bed slope, as shown in Fig. 11.16. The surface force consists of the hydrostatic force on the two end surfaces at ① and ② and the friction force F_f on the wetted surface of the control volume. However, because we have the same pressure distributions at ① and ②, the net x component of pressure force is zero. Using all these results in Eq. 4.18d we obtain

$$-F_f + W \sin \theta = 0$$

or

$$F_f = W \sin \theta \quad (11.40)$$

We see that for flow at normal depth, the component of the gravity force driving the flow is just balanced by the friction force acting on the channel walls. The friction force may be expressed as the product of an

average wall shear stress, τ_w , and the channel wetted surface area, PL (where L is the channel length), on which the stress acts

$$F_f = \tau_w PL \quad (11.41)$$

The component of gravity force can be written as

$$W \sin \theta = \rho g AL \sin \theta \approx \rho g AL \theta \approx \rho g A L S_b \quad (11.42)$$

where S_b is the channel bed slope. Using Eqs. 11.41 and 11.42 in Eq. 11.40,

$$\tau_w PL = \rho g A L S_b$$

or

$$\tau_w = \frac{\rho g A S_b}{P} = \rho g R_h S_b \quad (11.43)$$

where we have used the hydraulic radius, $R_h = A/P$ as defined in Eq. 11.1. In Chapter 9 we introduced a skin friction coefficient,

$$C_f = \frac{\tau_w}{\frac{1}{2} \rho V^2} \quad (9.22)$$

Using this in Eq. 11.43

$$\frac{1}{2} C_f \rho V^2 = \rho g R_h S_b$$

so, solving for V

$$V = \sqrt{\frac{2g}{C_f}} \sqrt{R_h S_b} \quad (11.44)$$

The Manning Equation for Uniform Flow

Equation 11.44 gives the flow velocity V as a function of the hydraulic radius, R_h , the slope, S_b , and the skin friction coefficient, C_f . This latter term is difficult to obtain experimentally or theoretically as it depends on a number of factors such as bed roughness, fluid properties, and the velocity. We will combine these terms and define a new quantity,

$$C = \sqrt{\frac{2g}{C_f}}$$

so that Eq. 11.44 becomes

$$V = C \sqrt{R_h S_b} \quad (11.45)$$

Equation 11.45 is termed the *Chezy equation*, and C is referred to as the *Chezy coefficient*. Experimental values of C were obtained by Manning [10]. He suggested that

$$C = \frac{1}{n} R_h^{1/6} \quad (11.46)$$

where n is a roughness coefficient having different values for different types of boundary roughness. Some representative values of n are listed in Table 11.2. The range of values given in the table reflects the importance of surface characteristics. For the same material, the value of n can vary 20 to 30 percent depending on the finish of the channel surface. Substituting C from Eq. 11.46 into Eq. 11.45 results in the *Manning equation* for the velocity for flow at normal depth

$$V = \frac{1}{n} R_h^{2/3} S_b^{1/2} \quad (11.47a)$$

Table 11.2
Representative Manning's Roughness Coefficients

Channel Type	Condition	Manning's n
Constructed, unlined	Smooth earth	0.016–0.020
	Bare earth	0.018–0.022
	Gravel	0.022–0.030
	Rocky	0.025–0.035
	Plastic	0.009–0.011
	Asphalt	0.013–0.016
	Concrete	0.013–0.015
	Brick	0.014–0.017
	Wood	0.011–0.015
	Masonry	0.025–0.030
Constructed, lined	Corrugated metal	0.022–0.024
	Stream, clean	0.025–0.035
	Major river, clean	0.030–0.040
Natural	Major river, sluggish	0.040–0.080

Source: Data taken from References [1,3,7,11,12].

Equation 11.47 is not dimensionally consistent and is valid only for SI units. Manning's equation in SI units can also be expressed as

$$Q = \frac{1}{n} A R_h^{2/3} S_b^{1/2} \quad (11.48a)$$

For V in ft/s and R_h in feet (English Engineering units), Eq. 11.47a becomes

$$V = \frac{1.49}{n} R_h^{2/3} S_b^{1/2} \quad (11.47b)$$

and Eq. 11.48a in English Engineering units is

$$Q = \frac{1.49}{n} A R_h^{2/3} S_b^{1/2} \quad (11.48b)$$

where A is in square feet. These equations are “engineering” equations; that is, *the user needs to be aware of the required units of each term in the equation*.

The relationship among variables in Eqs. 11.48a can be viewed in a number of ways. For example, it shows that the volume flow rate through a prismatic channel of given slope and roughness is a function of both channel size and channel shape. This is illustrated in Examples 11.6 and 11.7.

Example 11.6 FLOW RATE IN A RECTANGULAR CHANNEL

An 8-ft-wide rectangular channel with a bed slope of 0.0004 ft/ft has a depth of flow of 2 ft. Assuming steady uniform flow, determine the discharge in the channel. The Manning roughness coefficient is $n = 0.015$.

Given: Geometry of rectangular channel and flow depth.

Find: Flow rate Q .

Solution: Use the appropriate form of Manning's equation. For a problem in English Engineering units, this is Eq. 11.48b.

Governing equations:

$$Q = \frac{1.49}{n} A R_h^{2/3} S_b^{1/2} \quad R_h = \frac{by}{b+2y} \quad (\text{Table 11.1})$$

Using this equation with the given data

$$\begin{aligned} Q &= \frac{1.49}{n} A R_h^{2/3} S_b^{1/2} \\ &= \frac{1.49}{0.015} \times (8 \text{ ft} \times 2 \text{ ft}) \times \left(\frac{8 \text{ ft} \times 2 \text{ ft}}{8 \text{ ft} + 2 \times 2 \text{ ft}} \right)^{2/3} \times \left(0.004 \frac{\text{ft}}{\text{ft}} \right)^{1/2} \\ Q &= 38.5 \text{ ft}^3/\text{s} \end{aligned}$$

This problem demonstrates use of Manning's equation to solve for flow rate, Q . Note that because this is an "engineering" equation, the units do not cancel.

Example 11.7 FLOW VERSUS AREA THROUGH TWO CHANNEL SHAPES

Open channels, of square and semicircular shapes, are being considered for carrying flow on a slope of $S_b = 0.001$; the channel walls are to be poured concrete with $n = 0.015$. Evaluate the flow rate delivered by the channels for maximum dimensions between 0.5 and 2.0 m. Compare the channels on the basis of volume flow rate for given cross-sectional area.

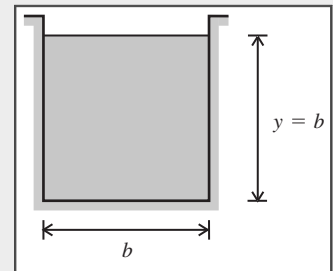
Given: Square and semicircular channels; $S_b = 0.001$ and $n = 0.015$. Sizes between 0.5 and 2.0 m across.

Find: Flow rate as a function of size. Compare channels on the basis of volume flow rate, Q , versus cross-sectional area, A .

Solution: Use the appropriate form of Manning's equation. For a problem in SI units, this is Eq. 11.68a.

Governing equations:

$$Q = \frac{1}{n} A R_h^{2/3} S_b^{1/2} \quad (11.48a)$$



Assumption: Flow at normal depth.

For the square channel,

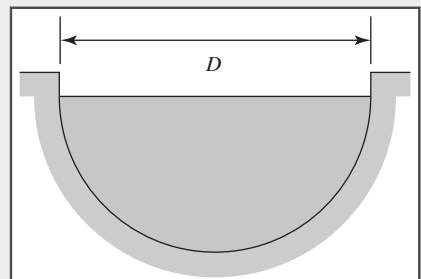
$$P = 3b \quad \text{and} \quad A = b^2 \quad \text{so} \quad R_h = \frac{b}{3}$$

Using this in Eq. 11.48a

$$Q = \frac{1}{n} A R_h^{2/3} S_b^{1/2} = \frac{1}{n} b^2 \left(\frac{b}{3} \right)^{2/3} S_b^{1/2} = \frac{1}{3^{2/3} n} S_b^{1/2} b^{8/3}$$

For $b = 1 \text{ m}$,

$$Q = \frac{1}{3^{2/3} (0.015)} (0.001)^{1/2} (1)^{8/3} = 1.01 \text{ m}^3/\text{s} \quad Q$$



Tabulating for a range of sizes yields

$b \text{ (m)}$	0.5	1.0	1.5	2.0
$A \text{ (m}^2\text{)}$	0.25	1.00	2.25	4.00
$Q \text{ (m}^3/\text{s)\text{)}$	0.160	1.01	2.99	6.44

For the semicircular channel,

$$P = \frac{\pi D}{2} \quad \text{and} \quad A = \frac{\pi D^2}{8}$$

$$\text{so} \quad R_h = \frac{\pi D^2}{8} \cdot \frac{2}{\pi D} = \frac{D}{4}$$

Using this in Eq. 11.48a

$$Q = \frac{1}{n} A R_h^{2/3} S_b^{1/2} = \frac{1}{n} \frac{\pi D^2}{8} \left(\frac{D}{4} \right)^{2/3} S_b^{1/2}$$

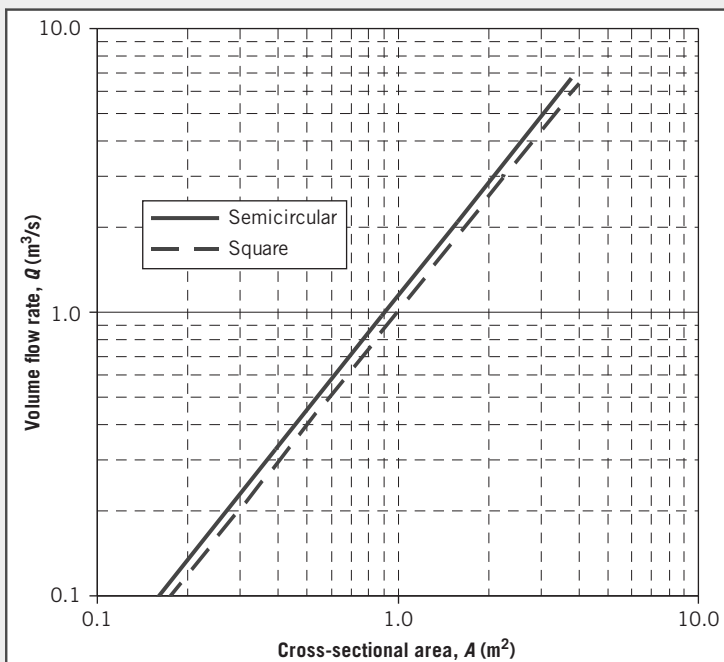
$$= \frac{\pi}{4^{5/3}(2)n} S_b^{1/2} D^{8/3}$$

For $D = 1 \text{ m}$,

$$Q = \frac{\pi}{4^{5/3}(2)(0.015)} (0.001)^{1/2} (1)^{8/3} = 0.329 \text{ m}^3/\text{s} \quad \text{--- } Q$$

Tabulating for a range of sizes yields

$D \text{ (m)}$	0.5	1.0	1.5	2.0
$A \text{ (m}^2)$	0.0982	0.393	0.884	1.57
$Q \text{ (m}^3/\text{s})$	0.0517	0.329	0.969	2.09



For both channels, volume flow rate varies as

$$Q \sim L^{8/3} \quad \text{or} \quad Q \sim A^{4/3}$$

since $A \sim L^2$. The plot of flow rate versus cross-sectional area shows that the semicircular channel is more “efficient.”

Performance of the two channels may be compared at any specified area. At $A = 1 \text{ m}^2$, $Q/A = 1.01 \text{ m/s}$ for the square channel. For the semicircular channel with $A = 1 \text{ m}^2$, then $D = 1.60 \text{ m}$, and $Q = 1.15 \text{ m}^3/\text{s}$; so $Q/A = 1.15 \text{ m/s}$. Thus the semicircular channel carries approximately 14 percent more flow per unit area than the square channel.

The comparison on cross-sectional area is important in determining the amount of excavation required to build the channel. The channel shapes also could be compared on the basis of perimeter, which would indicate the amount of concrete needed to finish the channel.

The relationships given by Eqs. 11.48 mean that, for normal flow, the flow rate depends on the channel size and shape. For a specified flow rate through a prismatic channel of given slope and roughness, the depth of uniform flow is a function of both channel size and shape and in addition the slope. There is only one depth for uniform flow at a given flow rate and it may be greater than, less than, or equal to the critical depth. This is illustrated in Examples 11.8 and 11.9.

Example 11.8 NORMAL DEPTH IN A RECTANGULAR CHANNEL

Determine the normal depth (for uniform flow) if the channel described in Example 11.6 has a flow rate of 100 cfs.

Given: Geometric data on rectangular channel of Example 11.6.

Find: Normal depth for a flow rate $Q = 100 \text{ ft}^3/\text{s}$.

Solution: Use the appropriate form of Manning's equation. For a problem in English Engineering units, this is Eq. 11.48b.

Governing equations:

$$Q = \frac{1.49}{n} A R_h^{2/3} S_b^{1/2} \quad R_h = \frac{by_n}{b+2y_n} \quad (\text{Table 11.1})$$

Combining these equations

$$Q = \frac{1.49}{n} A R_h^{2/3} S_b^{1/2} = \frac{1.49}{n} (by_n) \left(\frac{by_n}{b+2y_n} \right)^{2/3} S_b^{1/2}$$

Hence, after rearranging

$$\left(\frac{Qn}{1.49b^{5/3}S_b^{1/2}} \right)^3 (b+2y_n)^2 = y_n^5$$

Substituting $Q = 100 \text{ ft}^3/\text{s}$, $n = 0.015$, $b = 8 \text{ ft}$, and $S_b = 0.0004$ and simplifying

$$3.89(8+2y_n)^2 = y_n^5$$

This nonlinear equation can be solved for y_n using a numerical method to yield

$$y_n = 3.97 \text{ ft} \leftarrow$$

There are five roots, but four of them are mathematically correct but physically meaningless.

- This problem demonstrates the use of Manning's equation for finding the normal depth.
- This relatively simple physical problem still involved solving a nonlinear algebraic equation.

Example 11.9 DETERMINATION OF FLUME SIZE

An above-ground flume, built from timber, is to convey water from a mountain lake to a small hydroelectric plant. The flume is to deliver water at $Q = 2 \text{ m}^3/\text{s}$; the slope is $S_b = 0.002$ and $n = 0.013$. Evaluate the required flume size for (a) a rectangular section with $y/b = 0.5$ and (b) an equilateral triangular section.

Given: Flume to be built from timber, with $S_b = 0.002$, $n = 0.013$, and $Q = 2.00 \text{ m}^3/\text{s}$.

Find: Required flume size for:

- Rectangular section with $y/b = 0.5$.
- Equilateral triangular section.

Solution: Assume flume is long, so flow is uniform at normal depth. Then Eq. 11.48a applies.

Governing equations:

$$Q = \frac{1}{n} A R_h^{2/3} S_b^{1/2} \quad (11.48a)$$

The choice of channel shape fixes the relationship between R_h and A ; so Eq. 11.48a may be solved for normal depth, y_n , thus determining the channel size required.

(a) Rectangular section

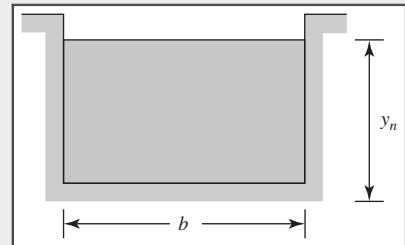
$$\begin{aligned} P &= 2y_n + b; \quad y_n/b = 0.5 \text{ so } b = 2y_n \\ P &= 2y_n + 2y_n = 4y_n \quad A = y_n b = y_n(2y_n) = 2y_n^2 \\ \text{so } R_h &= \frac{A}{P} = \frac{2y_n^2}{4y_n} = 0.5y_n \end{aligned}$$

Using this in Eq. 11.48a,

$$Q = \frac{1}{n} A R_h^{2/3} S_b^{1/2} = \frac{1}{n} (2y_n^2) (0.5y_n)^{2/3} S_b^{1/2} = \frac{2(0.5)^{2/3}}{n} y_n^{8/3} S_b^{1/2}$$

Solving for y_n

$$y_n = \left[\frac{nQ}{2(0.5)^{2/3} S_b^{1/2}} \right]^{3/8} = \left[\frac{0.013(2.00)}{2(0.5)^{2/3} (0.002)^{1/2}} \right]^{3/8} = 0.748 \text{ m}$$



The required dimensions for the rectangular channel are

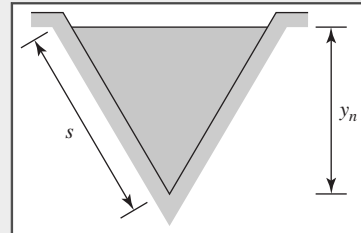
$$y_n = 0.748 \text{ m} \quad A = 1.12 \text{ m}^2$$

$$b = 1.50 \text{ m} \quad p = 3.00 \text{ m} \quad \text{Flume size}$$

(b) Equilateral triangle section

$$P = 2s = \frac{2y_n}{\cos 30^\circ} \quad A = \frac{y_n s}{2} = \frac{y_n^2}{2 \cos 30^\circ}$$

$$\text{so } R_h = \frac{A}{P} = \frac{y_n}{4}$$



Using this in Eq. 11.48a,

$$Q = \frac{1}{n} A R_h^{2/3} S_b^{1/2} = \frac{1}{n} \left(\frac{y_n^2}{2 \cos 30^\circ} \right) \left(\frac{y_n}{4} \right)^{2/3} S_b^{1/2} = \frac{1}{2 \cos 30^\circ (4)^{2/3} n} y_n^{8/3} S_b^{1/2}$$

Solving for y_n

$$y_n = \left[\frac{2 \cos 30^\circ (4)^{2/3} n Q}{S_b^{1/2}} \right]^{3/8} = \left[\frac{2 \cos 30^\circ (4)^{2/3} (0.013)(2.00)}{(0.002)^{1/2}} \right]^{3/8} = 1.42 \text{ m}$$

The required dimensions for the triangular channel are

$$y_n = 1.42 \text{ m} \quad A = 1.16 \text{ m}^2$$

$$b_s = 1.64 \text{ m} \quad p = 3.28 \text{ m} \quad \text{Flume size}$$

Note that for the triangular channel

$$V = \frac{Q}{A} = 2.0 \frac{\text{m}^3}{\text{s}} \times \frac{1}{1.16 \text{ m}^2} = 1.72 \text{ m/s}$$

and

$$Fr = \frac{V}{\sqrt{8y_h}} = \frac{V}{\sqrt{gA/b_s}}$$

$$Fr = 1.72 \frac{\text{m}}{\text{s}} \times \frac{1}{\left[9.81 \frac{\text{m}}{\text{s}^2} \times 1.16 \text{ m}^2 \times \frac{1}{1.64 \text{ m}} \right]^{1/2}} = 0.653$$

Hence this normal flow is subcritical (as is the flow in the rectangular channel).

Comparing results, we see that the rectangular flume would be cheaper to build as its perimeter is about 8.5 percent less than that of the triangular flume.

This problem shows the effect of channel shape on the size required to deliver a given flow at a specified bed slope and roughness coefficient. At specified S_b and n , flow may be subcritical, critical, or supercritical, depending on Q .

Energy Equation for Uniform Flow

To complete our discussion of normal flows, we consider the energy equation. The energy equation derived in Section 11.2. is

$$\frac{V_1^2}{2g} + y_1 + z_1 = \frac{V_2^2}{2g} + y_2 + z_2 + H_l \quad (11.10)$$

For normal flow we obtain, with $V_1 = V_2 = V$, and $y_1 = y_2 = y_n$,

$$z_1 = z_2 + H_l$$

or

$$H_l = z_1 - z_2 = LS_b \quad (11.49)$$

where S_b is the slope of the bed and L is the distance between points ① and ②. Hence we see that for flow at normal depth, *the head loss due to friction is equal to the change in elevation of the bed*. The specific energy, E , is the same at all sections,

$$E = E_1 = \frac{V_1^2}{2g} + y_1 = E_2 = \frac{V_2^2}{2g} + y_2 = \text{const}$$

We can also compute the energy grade line EGL and hydraulic grade line HGL. From Section 6.4

$$EGL = \frac{p}{\rho g} + \frac{V^2}{2g} + z_{\text{total}} \quad (6.16b)$$

and

$$HGL = \frac{p}{\rho g} + z_{\text{total}} \quad (6.16c)$$

where $z_{\text{total}} = z + y$. Hence at any point on the free surface (recall that we are using gage pressures),

$$EGL = \frac{V^2}{2g} + z + y \quad (11.50)$$

and

$$HGL = z + y \quad (11.51)$$

Hence, using Eqs. 11.50 and 11.51 in Eqs. 11.10, between points ① and ② we obtain

$$EGL_1 - EGL_2 = H_l = z_1 - z_2$$

and (because $V_1 = V_2$)

$$HGL_1 - HGL_2 = H_l = z_1 - z_2$$

For normal flow, the energy grade line, the hydraulic grade line, and the channel bed are all parallel. The trends for the energy grade line, hydraulic grade line, and specific energy, are shown in Fig. 11.17.

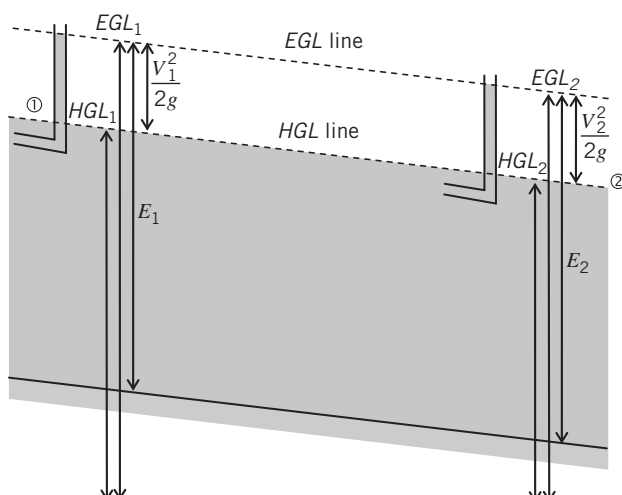


Fig. 11.17 Energy grade line, hydraulic grade line, and specific energy for uniform flow.

Optimum Channel Cross Section

For given slope and roughness, the optimum channel cross section is that for which we need the smallest channel for a given flow rate; this is when Q/A is maximized. From Eq. 11.48a

$$\frac{Q}{A} = \frac{1}{n} R_h^{2/3} S_b^{1/2} \quad (11.52)$$

Thus the optimum cross section has maximum hydraulic radius, R_h . Since $R_h = A/P$, R_h is maximum when the wetted perimeter is minimum. Solving Eq. 11.52 for A (with $R_h = A/P$) then yields

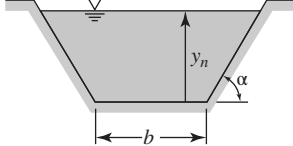
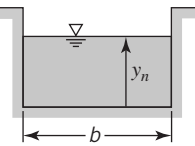
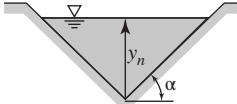
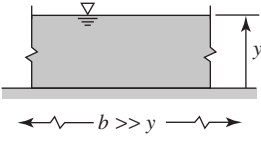
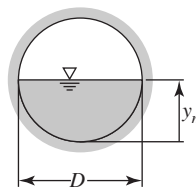
$$A = \left[\frac{nQ}{S_b^{1/2}} \right]^{3/5} P^{2/5} \quad (11.53)$$

From Eq. 11.53, the flow area will be a minimum when the wetted perimeter is a minimum.

Wetted perimeter, P , is a function of channel shape. For any given prismatic channel shape (rectangular, trapezoidal, triangular, circular, etc.), the channel cross section can be optimized. Optimum cross sections for common channel shapes are given in Table 11.3.

Once the optimum cross section for a given channel shape has been determined, expressions for normal depth, y_n , and area, A , as functions of flow rate can be obtained from Eq. 11.48a. These expressions are included in Table 11.3.

Table 11.3
Properties of Optimum Open-Channel Sections (SI Units)

Shape	Section	Optimum Geometry	Normal Depth, y_n	Cross-Sectional Area, A
Trapezoidal		$\alpha = 60^\circ$ $b = \frac{2}{\sqrt{3}} y_n$	$0.968 \left[\frac{Qn}{S_b^{1/2}} \right]^{3/8}$	$1.622 \left[\frac{Qn}{S_b^{1/2}} \right]^{3/4}$
Rectangular		$b = 2y_n$	$0.917 \left[\frac{Qn}{S_b^{1/2}} \right]^{3/8}$	$1.682 \left[\frac{Qn}{S_b^{1/2}} \right]^{3/4}$
Triangular		$\alpha = 45^\circ$	$1.297 \left[\frac{Qn}{S_b^{1/2}} \right]^{3/8}$	$1.682 \left[\frac{Qn}{S_b^{1/2}} \right]^{3/4}$
Wide Flat		None	$1.00 \left[\frac{(Q/b)n}{S_b^{1/2}} \right]^{3/8}$	—
Circular		$D = 2y_n$	$1.00 \left[\frac{Qn}{S_b^{1/2}} \right]^{3/8}$	$1.583 \left[\frac{Qn}{S_b^{1/2}} \right]^{3/4}$

11.6 Flow with Gradually Varying Depth

Most human-made channels are designed to have uniform flow. However, a channel can have nonuniform flow, that is, a flow for which the depth, and hence speed, vary along the channel for a number of reasons. Examples include when an open-channel flow encounters a change in bed slope, geometry, or roughness, or is adjusting itself back to normal depth after experiencing an upstream change such as a sluice gate. We have already studied rapid, localized changes, such as that occurring in a hydraulic jump, but here we assume flow depth changes gradually. Flow with gradually varying depth is analyzed by applying the energy equation to a differential control volume. The result is a differential equation that relates changes in depth to distance along the flow. The resulting equation may be solved analytically or, more typically numerically, if we approximate the head loss at each section as being the same as that for flow at normal depth, using the velocity and hydraulic radius of the section. Water depth and channel bed height are assumed to change slowly. As in the case of flow at normal depth, velocity is assumed uniform, and the pressure distribution is assumed hydrostatic at each section.

The energy equation (Eq. 11.10) for open-channel flow was applied to a finite control volume in Section 11.2,

$$\frac{V_1^2}{2g} + y_1 + z_1 = \frac{V_2^2}{2g} + y_2 + z_2 + H_l \quad (11.10)$$

We apply this equation to the differential control volume, of length dx , shown in Fig. 11.18. The *energy grade line*, *hydraulic grade line*, and *channel bottom* all have different slopes, unlike for the uniform flow of the previous section!

The energy equation becomes

$$\frac{V^2}{2g} + y + z = \frac{V^2}{2g} + d\left(\frac{V^2}{2g}\right) + y + dy + z + dz + dH_l$$

or after simplifying and rearranging

$$-d\left(\frac{V^2}{2g}\right) - dy - dz = dH_l \quad (11.54)$$

The differential loss of mechanical energy equals the differential head loss. From channel geometry

$$dz = -S_b dx \quad (11.55)$$

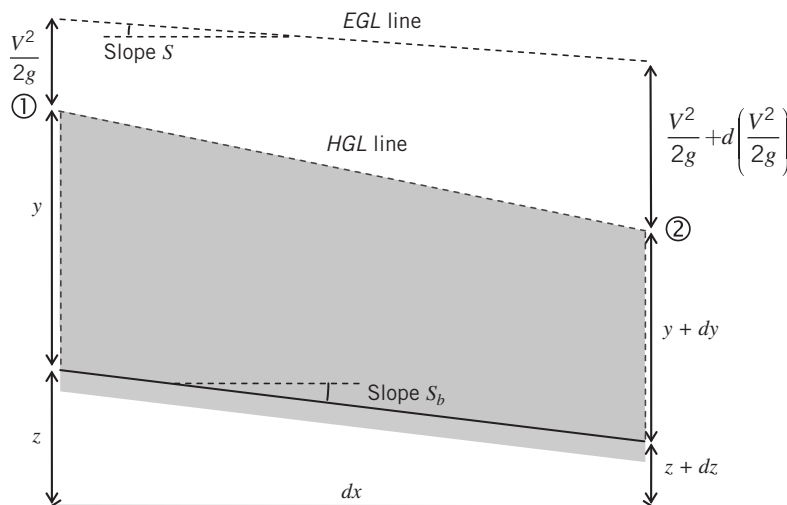


Fig. 11.18 Control volume for energy analysis of gradually varying flow.

We also have the approximation that the head loss can be approximated by the head loss that uniform flow would have at the same flow rate, Q , at the section. Hence the differential head loss is approximated by

$$dH_l = Sdx \quad (11.56)$$

where S is the slope of the EGL (see Fig. 11.18). Using Eqs. 11.55 and 11.56 in Eq. 11.54, dividing by dx , and rearranging, we obtain

$$\frac{d}{dx} \left(\frac{V^2}{2g} \right) + \frac{dy}{dx} = S_b - S \quad (11.57)$$

To eliminate the velocity derivative, we differentiate the continuity equation, $Q = VA = \text{const}$, to obtain

$$\frac{dQ}{dx} = 0 = A \frac{dV}{dx} + V \frac{dA}{dx}$$

or

$$\frac{dV}{dx} = -\frac{V}{A} \frac{dA}{dx} = -\frac{Vb_s}{A} \frac{dy}{dx} \quad (11.58)$$

where we have used $dA = b_s dy$ (Eq. 11.17), where b_s is the channel width at the free surface. Using Eq. 11.58 in Eq. 11.57, after rearranging

$$\frac{d}{dx} \left(\frac{V^2}{2g} \right) + \frac{dy}{dx} = \frac{V}{g} \frac{dV}{dx} + \frac{dy}{dx} = -\frac{V^2 b_s}{gA} \frac{dy}{dx} + \frac{dy}{dx} = S_b - S \quad (11.59)$$

Next, we recognize that

$$\frac{V^2 b_s}{gA} = \frac{V^2}{g} \frac{b_s}{A} = \frac{V^2}{g y_h} = Fr^2$$

where y_h is the hydraulic depth (Eq. 11.2). Using this in Eq. 11.59, we finally obtain our desired form of the *energy equation for gradually varying flow*

$$\frac{dy}{dx} = \frac{S_b - S}{1 - Fr^2} \quad (11.60)$$

This equation indicates how the depth y of the flow varies. Whether the flow becomes deeper $dy/dx > 0$ or shallower $(dy/dx < 0)$ depends on the sign of the right-hand side. For example, consider a channel that has a horizontal section ($S_b = 0$):

$$\frac{dy}{dx} = -\frac{S}{1 - Fr^2}$$

Because of friction the EGL always decreases, so $S > 0$. If the incoming flow is subcritical ($Fr < 1$), the flow depth will gradually decrease ($dy/dx < 0$); if the incoming flow is supercritical ($Fr > 1$), the flow depth will gradually increase ($dy/dx > 0$). Note also that for critical flow ($Fr = 1$), the equation leads to a singularity, and gradually flow is no longer sustainable.

Calculation of Surface Profiles

Equation 11.60 can be used to solve for the free surface shape $y(x)$. It is difficult to solve because the bed slope, S_b , the local Froude number, Fr , and S , the EGL slope equivalent to uniform flow at rate Q , will in general all vary with location, x . For S , we use the results obtained in Section 11.5, specifically

$$Q = \frac{1}{n} A R_h^{2/3} S^{1/2} \quad (11.48a)$$

or for English Engineering units

$$Q = \frac{1.49}{n} A R_h^{2/3} S^{1/2} \quad (11.48b)$$

Note that we have used S rather than S_b in Eq. 11.48 as we are using the equation to obtain an *equivalent* value of S for a uniform flow at rate Q . Solving for S ,

$$S = \frac{n^2 Q^2}{A^2 R_h^{4/3}} \quad (11.61a)$$

or for English Engineering units

$$S = \frac{n^2 Q^2}{1.49^2 A^2 R_h^{4/3}} \quad (11.61b)$$

We can also express the Froude number as a function of Q ,

$$Fr = \frac{V}{\sqrt{gy_h}} = \frac{Q}{A \sqrt{gy_h}} \quad (11.62)$$

Using Eqs. 11.61a (or 11.61b) and 11.62 in Eq. 11.60

$$\frac{dy}{dx} = \frac{S_b - S}{1 - Fr^2} = \frac{\frac{S_b - \frac{n^2 Q^2}{A^2 R_h^{4/3}}}{1 - \frac{Q^2}{A^2 gy_h}}}{1 - \frac{Q^2}{A^2 gy_h}} \quad (11.63a)$$

or for English Engineering units

$$\frac{dy}{dx} = \frac{\frac{S_b - \frac{n^2 Q^2}{1.49^2 A^2 R_h^{4/3}}}{1 - \frac{Q^2}{A^2 gy_h}}}{1 - \frac{Q^2}{A^2 gy_h}} \quad (11.63b)$$

For a given channel (slope, S_b , and roughness coefficient, n , both of which may vary with x) and flow rate Q , the area A , hydraulic radius R_h , and hydraulic depth y_h are all functions of depth y (see Section 11.1). Hence Eqs. 11.63 are usually best solved using a suitable numerical integration scheme. Example 11.10 shows such a calculation for the simplest case, that of a rectangular channel.

Example 11.10 CALCULATION OF FREE SURFACE PROFILE

Water flows in a 5-m-wide rectangular channel made from unfinished concrete with $n = 0.015$. The channel contains a long reach on which S_b is constant at $S_b = 0.020$. At one section, flow is at depth $y_1 = 1.5$ m, with speed $V_1 = 4.0$ m/s. Calculate and plot the free surface profile for the first 100 m of the channel, and find the final depth.

Given: Water flow in a rectangular channel.

Find: Plot of free surface profile; depth at 100 m.

Solution: Use the appropriate form of the equation for flow depth, Eq. 11.63a.

Governing equations:

$$\frac{dy}{dx} = \frac{S_b - \frac{n^2 Q^2}{A^2 R_h^{4/3}}}{1 - \frac{Q^2}{A^2 gy_h}} \quad (11.63a)$$

We use Euler's method to convert the differential equation to a difference equation. In this approach, the differential is converted to a difference,

$$\frac{dy}{dx} \approx \frac{\Delta y}{\Delta x} \quad (1)$$

where Δx and Δy are small but finite changes in x and y , respectively. Combining Eqs. 11.63a and 1, and rearranging,

$$\Delta y = \Delta x \left(\frac{S_b - \frac{n^2 Q^2}{A^2 R_h^{4/3}}}{1 - \frac{Q^2}{A^2 g y_h}} \right)$$

Finally, we let $\Delta y = y_{i+1} - y_i$, where y_i and y_{i+1} are the depths at point i and a point $(i+1)$ distance Δx further downstream,

$$y_{i+1} = y_i + \Delta x \left(\frac{S_{b_i} - \frac{n_i^2 Q^2}{A_i^2 R_{h_i}^{4/3}}}{1 - \frac{Q^2}{A_i^2 g y_{h_i}}} \right) \quad (2)$$

Equation 2 computes the depth, y_{i+1} , given data at point i . In the current application, S_b and n are constant, but A , R_h , and y_h will, of course, vary with x because they are functions of y . For a rectangular channel we have the following:

$$\begin{aligned} A_i &= b y_i \\ R_{h_i} &= \frac{b y_i}{b + 2 y_i} \\ y_{h_i} &= \frac{A_i}{b_s} = \frac{A_i}{b} = \frac{b y_i}{b_s} = y_i \end{aligned}$$

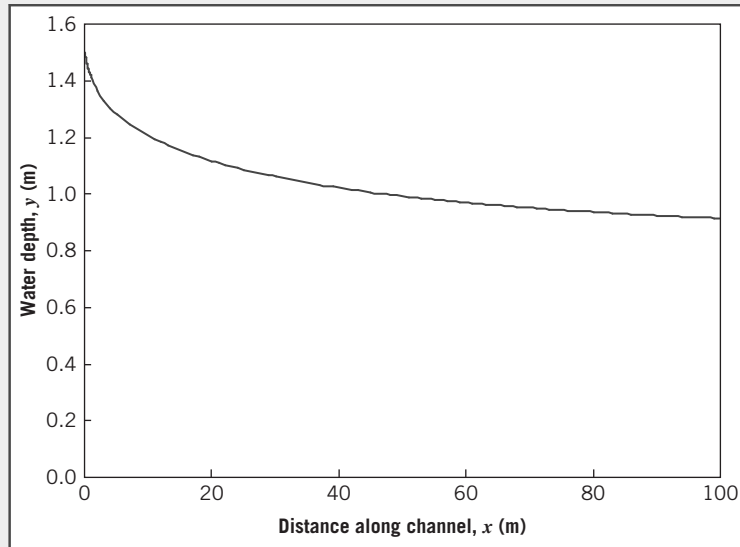
The calculations are conveniently performed and results plotted using *Excel*. Note that partial results are shown in the table, and that for the first meter, over which there is a rapid change in depth, the step size is $\Delta x = 0.05$.

i	x (m)	y (m)	A (m^2)	R_h (m)	y_h (m)
1	0.00	1.500	7.500	0.938	1.500
2	0.05	1.491	7.454	0.934	1.491
3	0.10	1.483	7.417	0.931	1.483
4	0.15	1.477	7.385	0.928	1.477
5	0.20	1.471	7.356	0.926	1.471
⋮	⋮	⋮	⋮	⋮	⋮
118	98	0.916	4.580	0.670	0.916
119	99	0.915	4.576	0.670	0.915
120	100	0.914	4.571	0.669	0.914

The depth at location $x = 100$ m is seen to be 0.914 m.

$$y(100 \text{ m}) = 0.914 \text{ m} \quad \xleftarrow{\hspace{1cm}} \quad y(100 \text{ m})$$

Note (following the solution procedure of Example 11.8) that the normal depth for this flow is $y_n = 0.858$ m; the flow depth is asymptotically approaching this value. In general, this is one of several possibilities, depending on the values of the initial depth and the channel properties (slope and roughness). A flow may approach normal depth, become deeper and deeper, or eventually become shallower and experience a hydraulic jump.



The accuracy of the results obtained obviously depends on the numerical model used; for example, a more accurate model is the RK4 method. Also, for the first meter or so, there are rapid changes in depth, bringing into question the validity of several assumptions, for example, uniform flow and hydrostatic pressure.

11.7 Discharge Measurement Using Weirs

A *weir* is a device that is placed normal to the direction of flow. The weir essentially backs up water so that, in flowing over the weir, the water goes through critical depth. Weirs have been used for the measurement of water flow in open channels for many years. Weirs can generally be classified as *sharp-crested weirs* and *broad-crested weirs*. Weirs are discussed in detail in Bos [13], Brater [14], and Repleglo [15].

A *sharp-crested weir* is basically a thin plate mounted perpendicular to the flow with the top of the plate having a beveled, sharp edge, which makes the nappe spring clear from the plate (see Fig. 11.19).

The rate of flow is determined by measuring the head, typically in a stilling well (see Fig. 11.20) at a distance upstream from the crest.

Suppressed Rectangular Weir

These sharp-crested weirs are as wide as the channel and the width of the nappe is the same length as the crest. Referring to Fig. 11.20, consider an elemental area $dA = bdh$ and assume the velocity is $V = \sqrt{2gh}$; then the elemental flow is

$$dQ = bdh\sqrt{2gh} = b\sqrt{2gh}^{1/2}dh$$

The discharge is expressed by integrating this over the area above the top of the weir crest:

$$Q = \int_0^H dQ = \sqrt{2gb} \int_0^H h^{1/2} dh = \frac{2}{3}\sqrt{2gb}H^{3/2} \quad (11.64)$$

Friction effects have been neglected in the derivation of Eq. 11.64. The drawdown effect shown in Fig. 11.19 and the crest contraction indicate that the streamlines are not parallel or normal to the area in the plane. To account for these effects, a coefficient of discharge C_d is used, so that

$$Q = C_d \frac{2}{3}\sqrt{2gb}H^{3/2}$$

where C_d is approximately 0.62. This is the basic equation for a suppressed rectangular weir, which can be expressed more generally as

$$Q = C_w b H^{3/2} \quad (11.65)$$

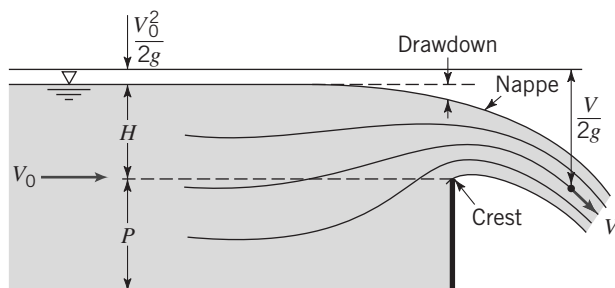


Fig. 11.19 Flow over sharp-crested weir.

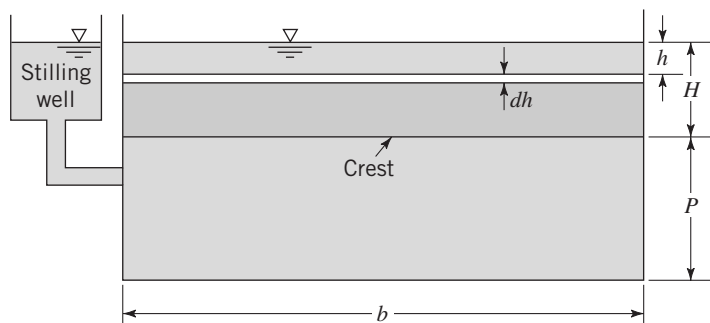


Fig. 11.20 Rectangular sharp-crested weir without end contraction.

where the C_w is the weir coefficient, $C_w = \frac{2}{3}C_d\sqrt{2g}$. For English Engineering units, $C_w \approx 3.33$, and for SI units, $C_w \approx 1.84$.

If the velocity of approach, V_a , where H is measured is appreciable, then the integration limits are

$$Q = \sqrt{2gb} \int_{V_a^2/2g}^{H+V_a^2/2g} h^{1/2} dh = C_w b \left[\left(H + \frac{V_a^2}{2g} \right)^{3/2} - \left(\frac{V_a^2}{2g} \right)^{3/2} \right] \quad (11.66)$$

When $(V_a^2/2g)^{3/2} \approx 0$ Eq. 11.66 can be simplified to

$$Q = C_w b \left(H + \frac{V_a^2}{2g} \right)^{3/2} \quad (11.67)$$

Contracted Rectangular Weirs

A *contracted horizontal weir* is another sharp-crested weir with a crest that is shorter than the width of the channel and one or two beveled end sections so that water contracts both horizontally and vertically. This forces the nappe width to be less than b . The effective crest length is

$$b' = b - 0.1 nH$$

where $n = 1$ if the weir is placed against one side wall of the channel so that the contraction on one side is suppressed and $n = 2$ if the weir is positioned so that it is not placed against a side wall.

Triangular Weir

Triangular or *V-notch* weirs are sharp-crested weirs that are used for relatively small flows but that have the advantage that they can also function for reasonably large flows as well. Referring to Fig. 11.21, the rate of discharge through an elemental area, dA , is

$$dQ = C_d \sqrt{2gh} dA$$

where $dA = 2xdh$, and $x = (H-h)\tan(\theta/2)$; so $dA = 2(H-h)\tan(\theta/2)dh$. Then

$$dQ = C_d \sqrt{2gh} \left[2(H-h)\tan\left(\frac{\theta}{2}\right) dh \right]$$

and

$$\begin{aligned} Q &= C_d 2 \sqrt{2g} \tan\left(\frac{\theta}{2}\right) \int_0^H (H-h) h^{1/2} dh \\ &= C_d \left(\frac{8}{15}\right) \sqrt{2g} \tan\left(\frac{\theta}{2}\right) H^{5/2} \\ Q &= C_w H^{5/2} \end{aligned}$$

The value of C_w for a value of $\theta = 90^\circ$, the most common, is $C_w = 1.38$ for SI units and $C_w = 2.50$ for English Engineering units.

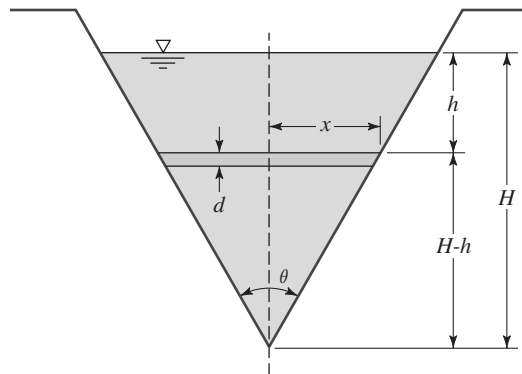


Fig. 11.21 Triangular sharp-crested weir.

Broad-Crested Weir

Broad-crested weirs (Fig. 11.22) are essentially critical-depth weirs in that if the weirs are high enough, critical depth occurs on the crest of the weir. For critical flow conditions $y_c = (Q^2/gb^2)^{1/3}$ (Eq. 11.23) and $E = 3y_c/2$ (Eq. 11.25) for rectangular channels:

$$Q = b\sqrt{gy_c^3} = b\sqrt{g\left(\frac{2}{3}E\right)^3} = b\left(\frac{2}{3}\right)^{3/2}\sqrt{gE^{3/2}}$$

or, assuming the approach velocity is negligible:

$$\begin{aligned} Q &= b\left(\frac{2}{3}\right)^{3/2}\sqrt{gH^{3/2}} \\ Q &= C_w b H^{3/2} \end{aligned}$$

Figure 11.23 illustrates a broad-crested weir installation in a trapezoidal canal.

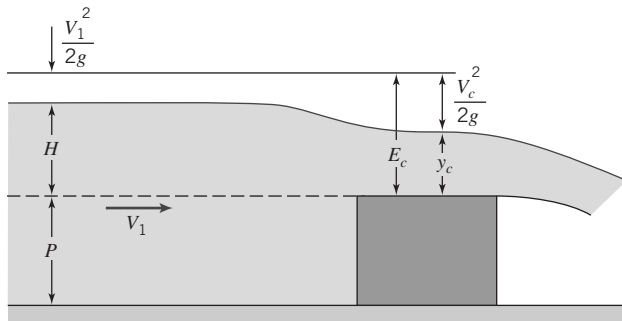


Fig. 11.22 Broad-crested weir.

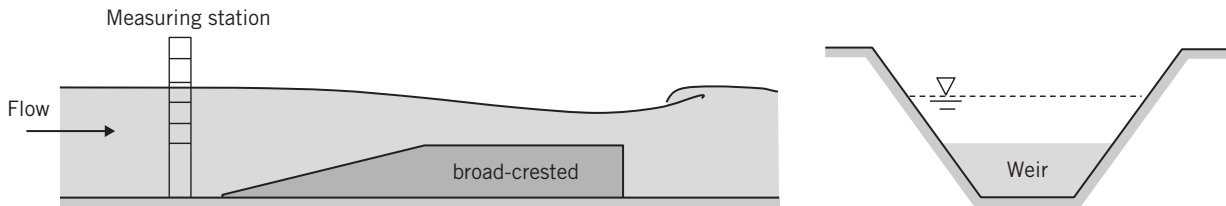


Fig. 11.23 Broad-crested weir in trapezoidal canal.

Example 11.11 shows the process for calculating the flow over a sharp-crested weir. The procedure for other weir geometries is basically the same as for this specific geometry.

Example 11.11 DISCHARGE FROM A RECTANGULAR SHARP-CRESTED SUPPRESSED WEIR

A rectangular, sharp-crested suppressed weir 3 m long is 1 m high. Determine the discharge when the head is 150 mm.

Given: Geometry and head of a rectangular sharp-crested suppressed weir.

Find: Discharge (flow rate), Q .

Solution: Use the appropriate weir discharge equation.

Governing equation:

$$Q = C_w b H^{3/2} \quad (11.65)$$

In Eq. 11.65 we use $C_w \approx 1.84$, and the given data, $b = 3 \text{ m}$ and $H = 150 \text{ mm} = 0.15 \text{ m}$, so

$$\begin{aligned} Q &= 1.84 \times 3 \text{ m} \times (0.15 \text{ m})^{3/2} \\ Q &= 0.321 \text{ m}^3/\text{s} \end{aligned}$$

Note that Eq. 11.65 is an “engineering” equation; so we do not expect the units to cancel.

This problem illustrates use of one of a number of weir discharge equations.

11.8 Summary and Useful Equations

In this chapter, we:

- ✓ Derived an expression for the speed of surface waves and developed the notion of the specific energy of a flow, and derived the Froude number for determining whether a flow is subcritical, critical, or supercritical.
- ✓ Investigated rapidly varied flows, especially the hydraulic jump.
- ✓ Investigated steady uniform flow in a channel, and used energy and momentum concepts to derive Chezy's and Manning's equations.
- ✓ Investigated some basic concepts of gradually varied flows.

We also learned how to use many of the important concepts mentioned above in analyzing a range of real-world open-channel flow problems.

Note: Most of the equations in the table below have a number of constraints or limitations—*be sure to refer to their page numbers for details!*

Useful Equations

Hydraulic radius:	$R_h = \frac{A}{P}$	(11.1)	Page 418
Hydraulic depth:	$y_h = \frac{A}{b_s}$	(11.2)	Page 418
Speed of surface wave:	$c = \sqrt{gy}$	(11.6)	Page 421
Froude number:	$Fr = \frac{V}{\sqrt{gy}}$	(11.7)	Page 422
Energy equation for open-channel flow:	$\frac{V_1^2}{2g} + y_1 + z_1 = \frac{V_2^2}{2g} + y_2 + z_2 + H_l$	(11.10)	Page 425
Total head:	$H = \frac{V^2}{2g} + y + z$	(11.11)	Page 425
Specific energy:	$E = \frac{V^2}{2g} + y$	(11.13)	Page 425
Critical flow:	$Q^2 = \frac{gA_c^3}{b_{s_c}}$	(11.21)	Page 429
Critical velocity:	$V_c = \sqrt{gy_{h_c}}$	(11.22)	Page 429
Critical depth (rectangular channel):	$y_c = \left[\frac{Q^2}{gb^2} \right]^{1/3}$	(11.23)	Page 429
Critical velocity (rectangular channel):	$V_c = \sqrt{gy_c} = \left[\frac{gQ}{b} \right]^{1/3}$	(11.24)	Page 429
Minimum specific energy (rectangular channel):	$E_{min} = \frac{3}{2}y_c$	(11.25)	Page 429
Hydraulic jump conjugate depths:	$\frac{y_2}{y_1} = \frac{1}{2} \left[\sqrt{1 + 8Fr_1^2} - 1 \right]$	(11.36)	Page 438
Hydraulic jump head loss:	$H_l = \frac{[y_2 - y_1]^3}{4y_1 y_2}$	(11.38b)	Page 439

Table (Continued)

Hydraulic jump head loss (in terms of Fr_1):	$\frac{H_l}{E_1} = \frac{\left[\sqrt{1 + 8Fr_1^2} - 3 \right]^3}{8 \left[\sqrt{1 + 8Fr_1^2} - 1 \right] [Fr_1^2 + 2]}$	(11.39)	Page 440
Chezy equation:	$V = C\sqrt{R_h S_b}$	(11.45)	Page 443
Chezy coefficient:	$C = \frac{1}{n} R_h^{1/6}$	(11.46)	Page 443
Manning equation for velocity (SI units)	$V = \frac{1}{n} R_h^{2/3} S_b^{1/2}$	(11.47a)	Page 443
Manning equation for flow (SI units)	$Q = \frac{1}{n} A R_h^{2/3} S_b^{1/2}$	(11.48a)	Page 444
Manning equation for velocity (English Engineering units)	$V = \frac{1.49}{n} R_h^{2/3} S_b^{1/2}$	(11.47b)	Page 444
Manning equation for flow (English Engineering units)	$Q = \frac{1.49}{n} A R_h^{2/3} S_b^{1/2}$	(11.48b)	Page 444
Energy Grade Line	$EGL = \frac{V^2}{2g} + z + y$	(11.50)	Page 449
Hydraulic Grade Line	$HGL = z + y$	(11.51)	Page 449
Energy equation (gradually varying flow):	$\frac{dy}{dx} = \frac{S_b - S}{1 - Fr^2}$	(11.60)	Page 452

REFERENCES

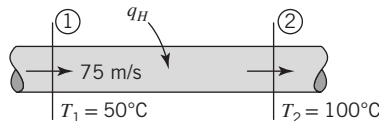
1. Chow, V. T., *Open-Channel Hydraulics*. New York: McGraw-Hill, 1959.
2. Henderson, F. M., *Open-Channel Flow*. New York: Macmillan, 1966.
3. "Manning's Roughness Coefficient," The Engineer's Toolbox, http://www.engineeringtoolbox.com/mannings-roughness-d_799.html (accessed September 22, 2014).
4. Townson, J. M., *Free-Surface Hydraulics*. London: Unwin Hyman, 1991.
5. Chaudhry, M. H., *Open-Channel Flow*. Englewood Cliffs, NJ: Prentice Hall, 1993.
6. Jain, S. C., *Open Channel Flow*. New York: Wiley, 2001.
7. "Design Charts for Open Channel Flow," HDS 3, Federal Highway Association, 1961, <http://www.fhwa.dot.gov/engineering/hydraulics/pubs/hds3.pdf>.
8. Mays, L. W., *Water Resources Engineering*, 2005 ed. New York: Wiley, 2005.
9. Peterka, A. J., "Hydraulic Design of Stilling Basins and Energy Dissipators," U.S. Department of the Interior, Bureau of Reclamation, Engineering Monograph No. 25 (Revised), July 1963.
10. Manning, R., "On the Flow of Water in Open Channels and Pipes." *Transactions Institute of Civil Engineers of Ireland*, vol. 20, pp. 161–209, Dublin, 1891; Supplement, vol. 24, pp. 179–207, 1895.
11. Linsley, R. K., J. B. Franzini, D. L. Freyberg, and G. Tchobanoglous, *Water Resources Engineering*. New York: McGraw-Hill, 1991.
12. Chen, Y. H., and G. K. Cotton, *Design of Roadside Channels with Flexible Linings*, Hydraulic Engineering Circular 15, FHWA-IP-87-7, Federal Highway Administration, McClean, VA, 1988.
13. Bos, M. G., J. A. Replogle, and A. J. Clemmens, *Flow Measuring Flumes for Open Channel System*. New York: John Wiley & Sons, 1984.
14. Brater, E. F., H. W. King, J. E. Lindell, and C. Y. Wei, *Handbook of Hydraulics*, 7th ed. New York: McGraw-Hill, 1996.
15. Replogle, J. A., A. J. Clemmens, and C. A. Pugh, "Hydraulic Design of Flow Measuring Structures." *Hydraulic Design Handbook*, L. W. Mays, ed. New York: McGraw-Hill, 1999.

Chapter 12 Problems

Review of Thermodynamics

12.1 Air is expanded in a steady flow process through a turbine. Initial conditions are 1300°C and 2.0 MPa absolute. Final conditions are 500°C and atmospheric pressure. Show this process on a Ts diagram. Evaluate the changes in internal energy, enthalpy, and specific entropy for this process.

12.2 Hydrogen flows as a perfect gas without friction in the pipe shown in the figure. Determine the outlet velocity when $7.5 \times 10^5 \text{ J/kg}$ of heat is added.



P12.2

12.3 Air enters a turbine in steady flow at 0.5 kg/s with negligible velocity. Inlet conditions are 1300°C and 2.0 MPa absolute. The air is expanded through the turbine to atmospheric pressure. If the actual temperature and velocity at the turbine exit are 500°C and 200 m/s , determine the power produced by the turbine. Label state points on a Ts diagram for this process.

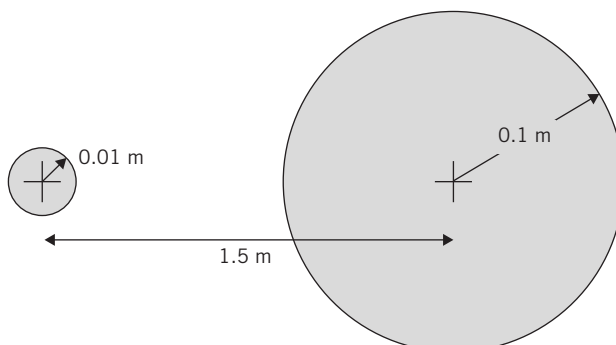
12.4 Carbon dioxide at 150°C and 120 kPa absolute flows at a speed of 10 m/s in a pipe and discharges through a nozzle where the exit velocity is 50 m/s . Determine the temperature and pressure leaving the nozzle. Assume that this is an adiabatic flow of a perfect gas.

Propagation of Sound Waves

12.5 Calculate the speed of sound at 20°C for (a) hydrogen, (b) helium, (c) methane, (d) nitrogen, (e) carbon dioxide and (f) air. Draw some conclusion from the results.

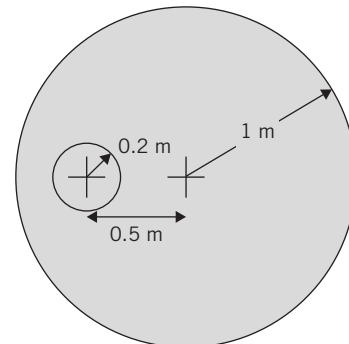
12.6 An airplane flies at 550 km/hr at 1500 m altitude on a standard day. The plane climbs to $15,000 \text{ m}$ and flies at 1200 km/h . Calculate the Mach number of flight in both cases.

12.7 An object traveling in atmospheric air emits two pressure waves at different times. At an instant in time, the waves appear as in the figure. Determine the velocity and Mach number of the object and its current location.



P12.7

12.8 An object traveling in atmospheric air emits two pressure waves at different times. At an instant in time, the waves appear as in the figure. Determine the velocity and Mach number of the object and its current location.



P12.8

12.9 A photograph of a bullet shows a Mach angle of 32° . Determine the speed of the bullet for standard air.

12.10 An aircraft flying at a Mach number of 1.5 passes overhead at 3 km altitude. Determine the air speed of the aircraft. If a headwind blows at 30 m/s , determine how long after the aircraft passes directly overhead that its sound reaches a point on the ground. Assume that the air temperature is constant at 20°C .

12.11 Determine the air density in the undisturbed air and at the stagnation point of an aircraft flying at 400 m/s in air at 28 kPa and 5°C . Determine the percentage increase in density and whether the deceleration process can be approximated as an incompressible flow.

Reference State: Local Isentropic Stagnation Properties

12.12 A supersonic wind tunnel test section is designed to have $M = 2.5$ at 15°C and 35 kPa absolute. The fluid is air. Determine the required inlet stagnation conditions, T_0 and p_0 . Calculate the required mass flow rate for a test section area of 0.175 m^2 .

12.13 Oxygen flows in a duct at a pressure of 25 psia. The pressure and temperature on the nose of a small object in the flow are 28 psia and 150°F , respectively. Determine the velocity in duct.

12.14 Consider steady, adiabatic flow of air through a long straight pipe with $A = 0.05 \text{ m}^2$. At the inlet section ① the air is at 200 kPa absolute, 60°C , and 146 m/s . Downstream at section ②, the air is at 95.6 kPa absolute and 280 m/s . Determine p_{01} , p_{02} , T_{01} , T_{02} , and the entropy change for the flow. Show static and stagnation state points on a Ts diagram. SS

12.15 Air passes through a normal shock in a supersonic wind tunnel. Upstream conditions are $M_1 = 1.8$, $T_1 = 270 \text{ K}$, and $p_1 = 10.0 \text{ kPa}$ absolute. Downstream conditions are $M_2 = 0.6165$, $T_2 = 413.6 \text{ K}$, and $p_2 = 36.13 \text{ kPa}$ absolute. (Four significant figures are given to minimize roundoff errors.) Evaluate local isentropic stagnation conditions (a) upstream from, and (b) downstream from, the normal shock. Calculate the change in specific entropy across the shock. Plot static and stagnation state points on a Ts diagram.

SS **12.16** Air flows from the atmosphere into an evacuated tank through a convergent nozzle of 38-mm tip diameter. If atmospheric pressure and temperature are 101.3 kPa and 15°C, respectively, determine the vacuum that must be maintained in the tank to produce sonic velocity in the jet. Determine the flow rate and the flow rate when the vacuum is 254 mm of mercury.

12.17 Oxygen discharges from a tank through a convergent nozzle. The temperature and velocity in the jet are -20°C and 270 m/s, respectively. Determine the temperature in the tank and the temperature on the nose of a small object in the jet.

Critical Conditions

12.18 The hot gas stream at the turbine inlet of a JT9-D jet engine is at 1500°C, 140 kPa absolute, and $M = 0.32$. Calculate the critical conditions (temperature, pressure, and flow speed) that correspond to these conditions. Assume the fluid properties of pure air.

12.19 Carbon dioxide discharges from a tank through a convergent nozzle with a diameter of 4 mm into the atmosphere. If the tank temperature and gage pressure are 38°C and 140 kPa, respectively, determine the jet temperature, pressure, and velocity and the mass flow rate. Barometric pressure is 101.3 kPa.

12.20 Air at 100°F and 100 psia in a large tank flows into a 6-in.-diameter pipe, from which it discharges to the atmosphere at 15.0 psia through a convergent nozzle of 4-in. tip-diameter. Calculate pressure, temperature, and velocity in the pipe.

12.21 Air at a pressure and temperature of 100 in. of mercury absolute and 100°F, respectively, discharges at a rate of 5 lbm/s from a tank through a convergent-divergent nozzle into another tank maintained at a pressure of 20 in. of mercury. Determine the nozzle throat and exit diameters for full expansion. Determine the pressure, temperature, velocity in the throat, and the Mach number at the nozzle exit.

Isentropic Flow—Area Variation

SS **12.22** Air flows adiabatically through a duct. At the entrance, the static temperature and pressure are 310 K and 200 kPa, respectively. At the exit, the static and stagnation temperatures are 294 K and 316 K, respectively, and the static pressure is 125 kPa. Find (a) the Mach numbers of the flow at the entrance and exit and (b) the area ratio A_2/A_1 .

12.23 Air flows isentropically through a converging nozzle into a receiver where the pressure is 250 kPa absolute. If the pressure is 350 kPa absolute and the speed is 150 m/s at the nozzle location where the Mach number is 0.5, determine the pressure, speed, and Mach number at the nozzle throat.

12.24 Air flows isentropically through a converging nozzle attached to a large tank, where the absolute pressure is 171 kPa and the

temperature is 27°C. At the inlet section the Mach number is 0.2. The nozzle discharges to the atmosphere; the discharge area is 0.015 m². Determine the magnitude and direction of the force that must be applied to hold the nozzle in place.

12.25 Air enters a converging-diverging nozzle with an area of 20 cm² at 2 MPa absolute and 313°K. At the exit of the nozzle, the pressure is 200 kPa absolute. Determine the area at the nozzle exit and the mass flow rate of the air.

12.26 A converging nozzle is bolted to the side of a large tank. Air inside the tank is maintained at a constant 50 psia and 100°F. The inlet area of the nozzle is 10 in.² and the exit area is 1 in.² The nozzle discharges to the atmosphere. For isentropic flow in the nozzle, determine the total force on the bolts, and indicate whether the bolts are in tension or compression.

12.27 A converging-diverging nozzle with a throat area of 2 in.² is connected to a large tank in which air is kept at a pressure of 80 psia and a temperature of 60°F. If the nozzle is to operate at design conditions and the ambient pressure outside the nozzle is 12.9 psia, calculate the exit area of the nozzle and the mass flow rate. Assume the flow is isentropic.

Normal Shocks

12.28 A total-pressure probe is placed in a supersonic wind tunnel where $T = 530^\circ\text{R}$ and $M = 2.0$. A normal shock stands in front of the probe. Behind the shock, $M_2 = 0.577$ and $p_2 = 5.76$ psia. Find (a) the downstream stagnation pressure and stagnation temperature and (b) all fluid properties upstream from the shock. Show static and stagnation state points and the process path on a T_s diagram.

12.29 A normal shock wave exists in an airflow. The absolute pressure, velocity, and temperature just upstream from the wave are 207 kPa, 610 m/s, and -17.8°C, respectively. Calculate the pressure, velocity, temperature, and sonic velocity just downstream from the shock wave.

12.30 Air approaches a normal shock at $M_1 = 2.5$, with $T_{01} = 1250^\circ\text{R}$ and $p_1 = 20$ psia. Determine the speed and temperature of the air leaving the shock and the entropy change across the shock.

12.31 The stagnation temperature in an airflow is 149°C upstream and downstream from a normal shock wave. The absolute stagnation pressure downstream from the shock wave is 229.5 kPa. Through the wave the absolute pressure rises from 103.4 to 138 kPa. Determine the velocities upstream and downstream from the wave.

12.32 A supersonic aircraft cruises at $M = 2.2$ at 12 km altitude. A pitot tube is used to sense pressure for calculating air speed. A normal shock stands in front of the tube. Evaluate the local isentropic stagnation conditions in front of the shock. Estimate the stagnation pressure sensed by the pitot tube. Show static and stagnation state points and the process path on a T_s diagram.

CHAPTER 12

Introduction to Compressible Flow

- 12.1 Review of Thermodynamics
- 12.2 Propagation of Sound Waves
- 12.3 Reference State: Local Isentropic Stagnation Properties
- 12.4 Critical Conditions

- 12.5 Basic Equations for One-Dimensional Compressible Flow
- 12.6 Isentropic Flow of an Ideal Gas: Area Variation
- 12.7 Normal Shocks
- 12.8 Supersonic Channel Flow with Shocks
- 12.9 Summary and Useful Equations

Case Study

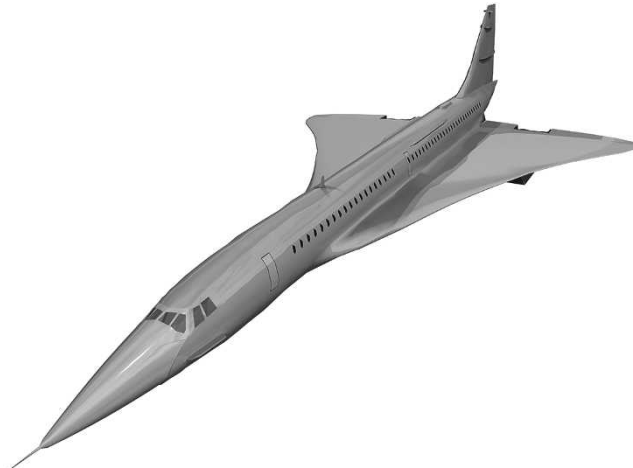
Supersonic passenger transportation has long been a goal of the aviation industry. An airplane flying at supersonic speeds has the potential to shorten international travel time significantly, reducing the discomforts of long-distance travel. The Concorde was the first commercially successful supersonic airplane and cruised at Mach 2.04, over four times the speed of conventional airplanes. The Concorde flew transatlantic routes from 1976 to 2000, when a tragic accident killed all of the passengers on a flight leaving Paris and terminated the program.

A supersonic passenger airplane as depicted in the figure has a number of design features that differ from conventional subsonic planes. To keep the aerodynamic drag low the wingspan is minimized. The delta wing, shown here, has a short wingspan and also generates a vortex that energizes the airflow on the upper surface at high speeds and attack angles. This delays flow separation and gives the aircraft a very high stall angle. During landing at subsonic speeds, the aircraft needs to be "nose high", and designs such as the Concorde had a droop nose that angled down during landing.

The heat generated by air friction is a major issue. To reduce weight, most supersonic designs use aluminum alloys that lose their strength quickly at high temperatures. This limits maximum speed to around Mach 2.2. The engine air intake design is especially critical and needs to provide low distortion levels (to prevent engine surge) and high efficiency for all likely ambient temperatures to be met in cruise. Additionally, adequate subsonic performance at take-off is required. Turbofan engines that pass

additional cold air around the engine core to increase fuel efficiency are the most suitable.

One of the largest hurdles is the sonic boom created by supersonic airplanes. The boom hasn't been completely eradicated from current designs and it's currently illegal to fly at supersonic speeds above US soil. The latest iterations of supersonic technology are attacking this problem.



A supersonic passenger aircraft design.

Ericus/Adobe Stock Photo

Learning Objectives

After completing this chapter, you should be able to:

- Compute properties using the ideal gas relations.
- Determine flow characteristics as a function of Mach number.
- Determine the reference state and flow properties for isentropic flow.
- Determine the flow properties at critical conditions.
- Describe the equations that govern one-dimensional compressible flow.
- Determine the flow properties for one-dimensional isentropic flow with changes in flow area.
- Determine the flow properties for a normal shock.

In Chapter 2 we briefly discussed the two most important questions we must ask before analyzing a fluid flow: whether or not the flow is viscous, and whether or not the flow is compressible. We subsequently considered *incompressible, inviscid* flows (Chapter 6) and *incompressible, viscous* flows (Chapters 8 and 9). We are now ready to study flows that experience compressibility effects. Because this is an introductory text, our focus will be mainly on *one-dimensional compressible, inviscid* flows, although we will also review some important *compressible, viscous* flow phenomena.

We first need to establish what we mean by a “compressible” flow. This is a flow in which there are significant changes in fluid density. Just as inviscid fluids do not actually exist, incompressible fluids do not actually exist. For example, in this text we have treated water as an incompressible fluid, although in fact the density of seawater increases by 1 percent for each mile or so of depth. Hence, whether or not a given flow can be treated as incompressible is a judgment call: Liquid flows will almost always be considered incompressible, but gas flows could easily be either incompressible or compressible. We will learn in Example 12.5 that for Mach numbers M less than about 0.3, the change in gas density due to the flow will be less than 3 percent; this change is small enough in most engineering applications for the following rule: *A gas flow can be considered incompressible when $M < 0.3$.*

The consequences of compressibility are not limited simply to density changes. Density changes mean that we can have significant compression or expansion work on a gas, so the thermodynamic state of the fluid will change, meaning that in general *all* properties such as temperature, internal energy, and entropy, can change. In particular, density changes create a mechanism for exchange of energy between “mechanical” energies (kinetic, potential, and “pressure”) and the thermal internal energy. For this reason, we begin with a review of the thermodynamics needed to study compressible flow.

After we cover the basic concepts of compressible flow, we will discuss one-dimensional compressible flow in more detail. We will look at the changes in the fluid properties caused by a variation in the flow area or by a normal shock. In addition to these basic phenomena, a real flow is likely to experience friction on the walls of the flow passage, heating or cooling of the flow, and two-dimensional effects such as oblique shock and expansion waves. We will only introduce the basic ideas of compressible flow in this text, and provide material on the more complicated aspects as supplements on the Instructor website. We more hope that our coverage will provide you with a foundation for further study of this important topic.

12.1 Review of Thermodynamics

The pressure, density, temperature and other properties of a substance are related through an equation of state. Although many substances are complex in behavior, most gases of engineering interest, at moderate pressure and temperature, are well represented by the ideal gas equation of state. A review of thermodynamic relations is given in Moran et al. [1].

$$p = \rho RT \quad (12.1)$$

where R is a unique constant for each gas; For air, $R = 287 \text{ N} \cdot \text{m}/(\text{kg} \cdot \text{K}) = 53.3 \text{ ft} \cdot \text{lbf}/(\text{lbm} \cdot {}^\circ \text{R})$. R is given by

$$R = \frac{R_u}{M_m}$$

where R_u is the universal gas constant, $R_u = 8314 \text{ N} \cdot \text{m}/(\text{kgmole} \cdot \text{K}) = 1544 \text{ ft} \cdot \text{lbf}/(\text{lbmole} \cdot {}^\circ\text{R})$ and M_m is the molecular mass of the gas. Although the ideal gas equation is derived using a model that assumes that the gas molecules (a) take up zero volume (i.e., they are point masses) and (b) do not interact with one another, many real gases conform to Eq. 12.1, especially if the pressure is “low” enough and/or temperature “high” enough. For example, at room temperature, as long as the pressure is less than about 30 atm, Eq. 12.1 models the air density to better than 1 percent accuracy; similarly, Eq. 12.1 is accurate for air at 1 atm for temperatures that are greater than about -130°C (-200°F).

In general, the *internal energy* of a simple substance may be expressed as a function of any two independent properties, e.g., $u = u(v, T)$, where $v \equiv 1/\rho$ is the *specific volume*. Then

$$du = \left(\frac{\partial u}{\partial T} \right)_v dT + \left(\frac{\partial u}{\partial v} \right)_T dv$$

The *specific heat at constant volume* is defined as $c_v \equiv (\partial u / \partial T)_v$, so that

$$du = c_v dT + \left(\frac{\partial u}{\partial v} \right)_T dv$$

For an ideal gas the internal energy, u , is a function of temperature only, so $(\partial u / \partial v)_T = 0$, and

$$du = c_v dT \quad (12.2)$$

Furthermore, since $u = u(T)$, then from Eq. 12.2, $c_v = c_v(T)$.

The *enthalpy* of any substance is defined as $h \equiv u + p/\rho$. For an ideal gas, $p = \rho RT$, and so $h = u + RT$. Since $u = u(T)$ for an ideal gas, h also must be a function of temperature alone.

We can obtain a relation between h and T by recalling once again that for a simple substance any property can be expressed as a function of any two other independent properties, e.g., $h = h(v, T)$ as we did for u , or $h = h(p, T)$. We choose the latter in order to develop a useful relation,

$$dh = \left(\frac{\partial h}{\partial T} \right)_p dT + \left(\frac{\partial h}{\partial p} \right)_T dp$$

Since the *specific heat at constant pressure* is defined as $c_p \equiv (\partial h / \partial T)_p$,

$$dh = c_p dT + \left(\frac{\partial h}{\partial p} \right)_T dp$$

We have shown that for an ideal gas h is a function of T only. Consequently, $(\partial h / \partial T)_T = 0$ and

$$dh = c_p dT \quad (12.3)$$

Since h is a function of T alone, Eq. 12.3 requires that c_p be a function of T only for an ideal gas.

Although specific heats for an ideal gas are functions of temperature, their difference is a constant for each gas. To see this, from

$$h = u + RT$$

we can write

$$dh = du + RdT$$

Combining this with Eqs. 12.2 and 12.3, we can write

$$dh = c_p dT = du + RdT = c_v dT + RdT$$

Then

$$c_p - c_v = R \quad (12.4)$$

The *ratio of specific heats* is defined as

$$k \equiv \frac{c_p}{c_v} \quad (12.5)$$

Using the definition of k , we can solve Eq. 12.4 for either c_p or c_v in terms of k and R . Thus,

$$c_p = \frac{kR}{k-1} \quad (12.6a)$$

and

$$c_v = \frac{R}{k-1} \quad (12.6b)$$

Although the specific heats of an ideal gas may vary with temperature, for moderate temperature ranges they vary only slightly, and can be treated as constant, so

$$u_2 - u_1 = \int_{u_1}^{u_2} du = \int_{T_1}^{T_2} c_v dT = c_v(T_2 - T_1) \quad (12.7a)$$

$$h_2 - h_1 = \int_{h_1}^{h_2} dh = \int_{T_1}^{T_2} c_p dT = c_p(T_2 - T_1) \quad (12.7b)$$

Data for M_m , c_p , c_v , R , and k for common gases are given in Table A.6 of Appendix A.

We will find the property *entropy* to be extremely useful in analyzing compressible flows. State diagrams, particularly the temperature-entropy (Ts) diagram, are valuable aids in the physical interpretation of analytical results.

Entropy is defined by the equation

$$\Delta S \equiv \int_{\text{rev}} \frac{\delta Q}{T} \quad \text{or} \quad dS = \left(\frac{\delta Q}{T} \right)_{\text{rev}} \quad (12.8)$$

where the subscript signifies *reversible*.

The inequality of Clausius, deduced from the second law, states that

$$\oint \frac{\delta Q}{T} \leq 0$$

As a consequence of the second law, we can write

$$dS \geq \frac{\delta Q}{T} \quad \text{or} \quad T dS \geq \delta Q \quad (12.9a)$$

For *reversible* processes, the equality holds, and

$$T ds = \frac{\delta Q}{m} \quad (\text{reversible process}) \quad (12.9b)$$

The inequality holds for *irreversible* processes, and

$$T ds > \frac{\delta Q}{m} \quad (\text{irreversible process}) \quad (12.9c)$$

For an *adiabatic* process, $\delta Q/m = 0$. Thus

$$ds = 0 \quad (\text{reversible adiabatic process}) \quad (12.9d)$$

and

$$ds > 0 \quad (\text{irreversible adiabatic process}) \quad (12.9e)$$

Thus a process that is *reversible and adiabatic* is also *isentropic*; the entropy remains constant during the process. Inequality 12.9e shows that entropy must *increase* for an adiabatic process that is irreversible. Equations 12.9 show that any two of the restrictions—reversible, adiabatic, or isentropic—imply the third. For example, a process that is isentropic and reversible must also be adiabatic.

A useful relationship among properties (p, v, T, s, u) can be obtained by considering the first and second laws together. The result is the Gibbs, or $T ds$, equation

$$T ds = du + p dv \quad (12.10a)$$

This is a differential relationship among properties, valid for any process between any two equilibrium states. An alternative form of Eq. 12.10a can be obtained by substituting

$$du = d(h - p\nu) = dh - p d\nu - \nu dp$$

to obtain

$$T ds = dh - \nu dp \quad (12.10b)$$

For an ideal gas, entropy change can be evaluated from the $T ds$ equations as

$$ds = \frac{du}{T} + \frac{p}{T} d\nu = c_v \frac{dT}{T} + R \frac{d\nu}{\nu}$$

$$ds = \frac{dh}{T} - \frac{\nu}{T} dp = c_p \frac{dT}{T} - R \frac{dp}{p}$$

For constant specific heats, these equations can be integrated to yield

$$s_2 - s_1 = c_v \ln \frac{T_2}{T_1} + R \ln \frac{\nu_2}{\nu_1} \quad (12.11a)$$

$$s_2 - s_1 = c_p \ln \frac{T_2}{T_1} - R \ln \frac{p_2}{p_1} \quad (12.11b)$$

and also

$$s_2 - s_1 = c_v \ln \frac{p_2}{p_1} + c_p \ln \frac{\nu_2}{\nu_1} \quad (12.11c)$$

Equation 12.11c can be obtained from either Eq. 12.11a or 12.11b using Eq. 12.4 and the ideal gas equation, Eq. 12.1, written in the form $p\nu = RT$, to eliminate T . Example 12.1 shows use of the above governing equations (the $T ds$ equations) to evaluate property changes during a process.

Example 12.1 PROPERTY CHANGES IN COMPRESSIBLE DUCT FLOW

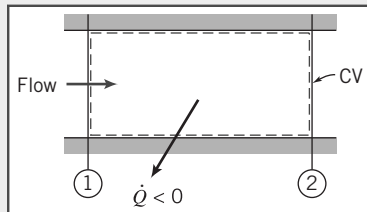
Air flows through a long duct of constant area at 0.15 kg/s. A short section of the duct is cooled by liquid nitrogen that surrounds the duct. The rate of heat loss in this section is 15.0 kJ/s from the air. The absolute pressure, temperature, and velocity entering the cooled section are 188 kPa, 440 K, and 210 m/s, respectively. At the outlet, the absolute pressure and temperature are 213 kPa and 351 K. Compute the duct cross-sectional area and the changes in enthalpy, internal energy, and entropy for this flow.

Given: Air flows steadily through a short section of constant-area duct that is cooled by liquid nitrogen.

$$T_1 = 440 \text{ K}$$

$$p_1 = 188 \text{ kPa (abs)}$$

$$V_1 = 210 \text{ m/s}$$



$$T_2 = 351 \text{ K}$$

$$p_2 = 213 \text{ kPa (abs)}$$

- Find:** (a) Duct area.
 (b) Δh .
 (c) Δu .
 (d) Δs .

Solution: The duct area may be found from the continuity equation.

Governing equations:

$$\frac{\partial}{\partial t} \int_{CV} \rho dV + \int_{CV} \rho \vec{V} \cdot d\vec{A} = 0 \quad (4.12)$$

Assumptions:

- 1 Steady flow.
- 2 Uniform flow at each section.
- 3 Ideal gas with constant specific heats.

Then

$$(-\rho_1 V_1 A_1) + (\rho_2 V_2 A_2) = 0$$

or

$$\dot{m} = \rho_1 V_1 A = \rho_2 V_2 A$$

since $A = A_1 = A_2 = \text{constant}$. Using the ideal gas relation, $p = \rho RT$, we find

$$\rho_1 = \frac{p_1}{RT_1} = 1.88 \times 10^5 \frac{\text{N}}{\text{m}^2} \times \frac{\text{kg} \cdot \text{K}}{287 \text{ N} \cdot \text{m}} \times \frac{1}{440 \text{ K}} = 1.49 \text{ kg/m}^3$$

From continuity,

$$A = \frac{\dot{m}}{\rho_1 V_1} = 0.15 \frac{\text{kg}}{\text{s}} \times \frac{\text{m}^3}{1.49 \text{ kg}} \times \frac{\text{s}}{210 \text{ m}} = 4.79 \times 10^{-4} \text{ m}^2 \quad A$$

For an ideal gas, the change in enthalpy is

$$\Delta h = h_2 - h_1 = \int_{T_1}^{T_2} c_p dT = c_p (T_2 - T_1) \quad (12.7b)$$

$$\Delta h = 1.00 \frac{\text{kJ}}{\text{kg} \cdot \text{K}} \times (351 - 440) \text{ K} = -89.0 \text{ kJ/kg} \quad \Delta h$$

Also, the change in internal energy is

$$\Delta u = u_2 - u_1 = \int_{T_1}^{T_2} c_v dT = c_v (T_2 - T_1) \quad (12.7a)$$

$$\Delta u = 0.717 \frac{\text{kJ}}{\text{kg} \cdot \text{K}} \times (351 - 440) \text{ K} = -63.8 \text{ kJ/kg} \quad \Delta u$$

The entropy change may be obtained from Eq. 12.11b,

$$\begin{aligned} \Delta s &= s_2 - s_1 = c_p \ln \frac{T_2}{T_1} - R \ln \frac{p_2}{p_1} \\ &= 1.00 \frac{\text{kJ}}{\text{kg} \cdot \text{K}} \times \ln \left(\frac{351}{440} \right) - 0.287 \frac{\text{kJ}}{\text{kg} \cdot \text{K}} \times \ln \left(\frac{2.13 \times 10^5}{1.88 \times 10^5} \right) \\ \Delta s &= -0.262 \text{ kJ/(kg} \cdot \text{K}) \quad \Delta s \end{aligned}$$

We see that entropy may decrease for a nonadiabatic process in which the gas is cooled.

This problem illustrates the use of the governing equations for computing property changes of an ideal gas during a process.

For an ideal gas with constant specific heats, we can use Eqs. 12.11 to obtain relations valid for an isentropic process. From Eq. 12.11a

$$s_2 - s_1 = 0 = c_v \ln \frac{T_2}{T_1} + R \ln \frac{\nu_2}{\nu_1}$$

Then, using Eqs. 12.4 and 12.5,

$$\left(\frac{T_2}{T_1} \right) \left(\frac{\nu_2}{\nu_1} \right)^{R/c_v} = 1 \quad \text{or} \quad T_2 \nu_2^{k-1} = T_1 \nu_1^{k-1} = T \nu^{k-1} = \text{constant}$$

where states 1 and 2 are arbitrary states of the isentropic process. Using $\nu = 1/\rho$,

$$T \nu^{k-1} = \frac{T}{\rho^{k-1}} = \text{constant} \quad (12.12a)$$

We can apply a similar process to Eqs. 12.11b and 12.11c, respectively, and obtain the following useful relations:

$$T p^{1-k/k} = \text{constant} \quad (12.12b)$$

$$p \nu^k = \frac{p}{\rho^k} = \text{constant} \quad (12.12c)$$

Equations 12.12 are for an ideal gas undergoing an isentropic process. To complete our review of the thermodynamic fundamentals, we evaluate the slopes of lines of constant pressure and of constant volume on the Ts diagram in Example 12.2.

Example 12.2 CONSTANT-PROPERTY LINES ON A Ts DIAGRAM

For an ideal gas, find the equations for lines of (a) constant volume and (b) constant pressure in the Ts plane.

Find: Equations for lines of (a) constant volume and (b) constant pressure in the Ts plane for an ideal gas.

Solution:

(a) We are interested in the relation between T and s with the volume ν held constant. This suggests use of Eq. 12.11a,

$$s_2 - s_1 = c_v \ln \frac{T_2}{T_1} + R \ln \frac{\nu_2}{\nu_1} = 0 \quad (12.8)$$

We relabel this equation so that state 1 is now reference state 0, and state 2 is an arbitrary state,

$$s - s_0 = c_v \ln \frac{T}{T_0} \quad \text{or} \quad T = T_0 e^{(s-s_0)/c_v} \quad (1)$$

Hence, we conclude that constant volume lines in the Ts plane are exponential.

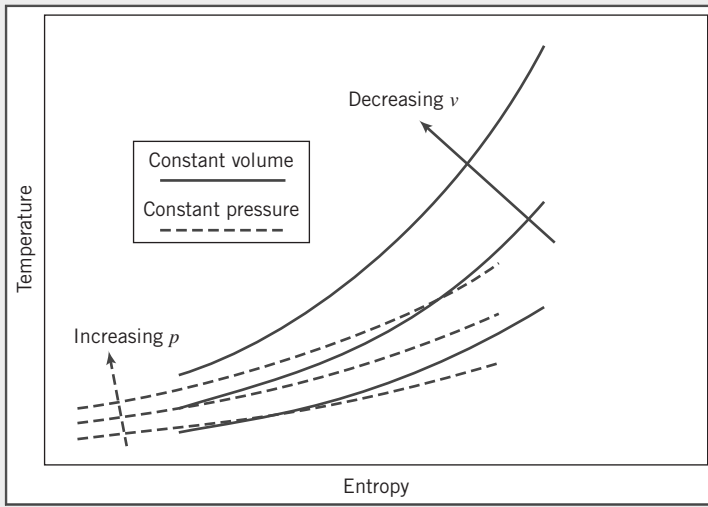
(b) We are interested in the relation between T and s with the pressure p held constant. This suggests use of Eq. 12.11b, and using a similar approach to case (a), we find

$$T = T_0 e^{(s-s_0)/c_p} \quad (2)$$

Hence, we conclude that constant pressure lines in the Ts plane are also exponential.

What about the slope of these curves? Because $c_p > c_v$ for all gases, we can see that the exponential, and therefore the slope, of the constant pressure curve, Eq. 2, is smaller than that for the constant volume curve, Eq. 1.

This is shown in the sketch below:



This problem illustrates use of governing equations to explore relations among properties.

12.2 Propagation of Sound Waves

Speed of Sound

The speed of sound, c , is an important property in compressible fluid flow. Flows with speeds less than the speed of sound are called subsonic and those with speeds greater are called supersonic flows. The behaviors of subsonic and supersonic flows are completely different. We will summarize some of the important aspects of sub- and supersonic flows in this chapter. References [2] and [3] describe compressible fluid flow behavior in more detail.

We have previously defined the Mach number M of a flow as

$$M \equiv \frac{V}{c} \quad (12.13)$$

where V is the speed of the fluid. The speed of sound is important in fluid mechanics because this is the speed at which “signals” can travel through the medium. As an object moves, it generates disturbances (infinitesimal pressure waves, which are sound waves) that emanate from the object in all directions. These waves travel out at the speed of sound and cumulatively “signal” the air and redirect it around the body as it approaches.

Consider propagation of a sound wave of infinitesimal strength into an undisturbed medium, as shown in Fig. 12.1a. We are interested in relating the speed of wave propagation, c , to fluid property changes across the wave. If pressure and density in the undisturbed medium ahead of the wave are denoted by p and ρ , passage of the wave will cause them to undergo infinitesimal changes to become $p + dp$ and $\rho + d\rho$. Since the wave propagates into a stationary fluid, the velocity ahead of the wave, V_x , is zero. The magnitude of the velocity behind the wave, $V_x + dV_x$, then will be simply dV_x ; in Fig. 12.1a, the direction of the motion behind the wave has been assumed to the left.

The flow of Fig. 12.1a appears unsteady to a stationary observer, viewing the wave motion from a fixed point on the ground. However, the flow appears steady to an observer located *on* an inertial control volume moving with a segment of the wave, as shown in Fig. 12.1b. The velocity approaching the control volume is then c , and the velocity leaving is $c - dV_x$.

The basic equations may be applied to the differential control volume shown in Fig. 12.1b (we use V_x for the x component of velocity to avoid confusion with internal energy, u).

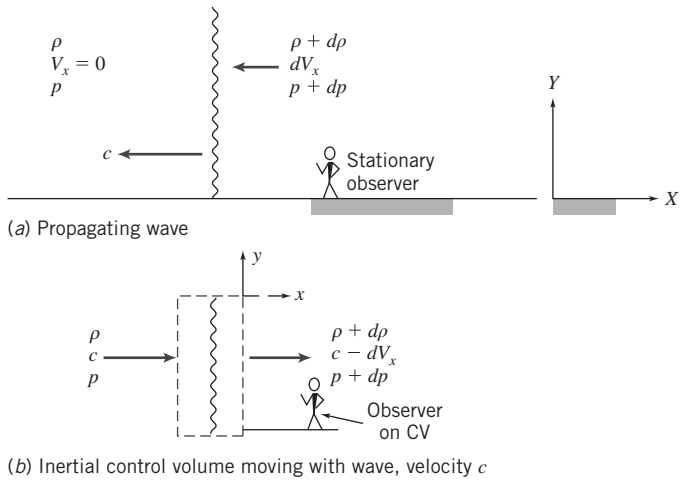


Fig. 12.1 Propagating sound wave showing control volume chosen for analysis.

a. Continuity Equation

Governing equations:

$$\frac{\partial}{\partial t} \int_{CV} \rho dV + \int_{CS} \rho \vec{V} \cdot d\vec{A} = 0 \quad (4.12)$$

Assumptions:

- 1 Steady flow.
- 2 Uniform flow at each section.

Then

$$(-\rho c A) + \{(\rho + d\rho)(c - dV_x)A\} = 0 \quad (12.14a)$$

or

$$-\rho c A + \rho c A - \rho dV_x A + d\rho c A - d\rho dV_x A \approx 0$$

or

$$dV_x = \frac{c}{\rho} d\rho \quad (12.14b)$$

b. Momentum Equation

Governing equation:

$$F_{S_x} + F_{B_x} = \frac{\partial}{\partial t} \int_{CV} V_x \rho dV + \int_{CS} V_x \rho \vec{V} \cdot d\vec{A} = 0 \quad (4.18a)$$

Assumption:

$$3 \quad F_{B_x} = 0$$

The only surface forces acting in the x direction on the control volume of Fig. 12.1b are due to pressure. The upper and lower surfaces have zero friction because the areas are infinitesimal.

$$F_{S_x} = pA - (p + dp)A = -A dp$$

Substituting into the governing equation gives

$$-A dp = c(-\rho c A) + (c - dV_x)\{(\rho + d\rho)(c - dV_x)A\}$$

Using the continuity equation (Eq. 12.14a), this reduces to

$$\begin{aligned}-A dp &= c(-\rho c A) + (c - dV_x)(\rho c A) = (-c + c - dV_x)(\rho c A) \\ -A dp &= -\rho c A dV_x\end{aligned}$$

or

$$dV_x = \frac{1}{\rho c} dp \quad (12.14c)$$

Combining Eqs. 12.14b and 12.14c, we obtain

$$dV_x = \frac{c}{\rho} d\rho = \frac{1}{\rho c} dp$$

from which

$$dp = c^2 d\rho$$

or

$$c^2 = \frac{dp}{d\rho} \quad (12.15)$$

Equation 12.15 indicates that the speed of sound depends on how the pressure and density of the medium are related. To obtain the speed of sound in a medium we could measure the time a sound wave takes to travel a prescribed distance, or instead we could apply a small pressure change dp to a sample, measure the corresponding density change $d\rho$, and evaluate c from Eq. 12.15. For example, an *incompressible* medium would have $d\rho = 0$ for any dp , so $c \rightarrow \infty$. We can anticipate that solids and liquids whose densities are difficult to change will have relatively high c values, and gases whose densities are easy to change will have relatively low c values. For a simple substance, each property depends on any two independent properties. For a sound wave, by definition we have an infinitesimal pressure change (i.e., it is *reversible*), and it occurs very quickly, so there is no time for any heat transfer to occur (i.e., it is *adiabatic*). Thus the sound wave propagates *isentropically*. Hence, if we express p as a function of density and entropy, $p = p(\rho, s)$, then

$$dp = \left(\frac{\partial p}{\partial \rho} \right)_s d\rho + \left(\frac{\partial p}{\partial s} \right)_\rho ds = \left(\frac{\partial p}{\partial \rho} \right)_s d\rho$$

so Eq. 12.15 becomes

$$c^2 = \frac{dp}{d\rho} = \left(\frac{\partial p}{\partial \rho} \right)_s$$

and

$$c = \sqrt{\left(\frac{\partial p}{\partial \rho} \right)_s} \quad (12.16)$$

We can now apply Eq. 12.16 to solids, liquids, and gases. For *solids* and *liquids* data are usually available on the bulk modulus E_ν , which is a measure of how a pressure change affects a relative density change,

$$E_\nu = \frac{dp}{d\rho/\rho} = \rho \frac{dp}{d\rho}$$

For these media

$$c = \sqrt{E_\nu / \rho} \quad (12.17)$$

For an *ideal gas*, the pressure and density in isentropic flow are related by

$$\frac{p}{\rho^k} = \text{constant} \quad (12.12c)$$

Taking logarithms and differentiating, we obtain

$$\frac{dp}{p} - k \frac{d\rho}{\rho} = 0$$

Therefore,

$$\left. \frac{\partial p}{\partial \rho} \right)_s = k \frac{p}{\rho}$$

But $p/\rho = RT$, so finally

$$c = \sqrt{kRT} \quad (12.18)$$

for an ideal gas. The speed of sound in air has been measured precisely by numerous investigators [4]. The results agree closely with the theoretical prediction of Eq. 12.18.

The important feature of sound propagation in an ideal gas, as shown by Eq. 12.18, is that the *speed of sound is a function of temperature only*. Example 12.3 shows the use of Eqs. 12.17 and 12.18 in determining the speed of sound in different media.

Example 12.3 SPEED OF SOUND IN STEEL, WATER, SEAWATER, AND AIR

Find the speed of sound in (a) steel ($E_v \approx 200 \text{ GN/m}^2$), (b) water (at 20°C), (c) seawater (at 20°C), and (d) air at sea level on a standard day.

Find: Speed of sound in (a) steel ($E_v \approx 200 \text{ GN/m}^2$), (b) water (at 20°C), (c) seawater (at 20°C), and (d) air at sea level on a standard day.

Solution:

(a) For steel, a solid, we use Eq. 12.17, with ρ obtained from Table A.1(b),

$$c = \sqrt{E_v/\rho} = \sqrt{E_v/SG\rho_{H_2O}}$$

$$c = \sqrt{200 \times 10^9 \frac{\text{N}}{\text{m}^2} \times \frac{1}{7.83} \times \frac{1 \text{ m}^3}{1000 \text{ kg}} \times \frac{\text{kg} \cdot \text{m}}{\text{N} \cdot \text{s}^2}} = 5050 \text{ m/s} \quad c_{\text{steel}}$$

(b) For water we also use Eq. 12.17, with data obtained from Table A.2,

$$c = \sqrt{E_v/\rho} = \sqrt{E_v/SG\rho_{H_2O}}$$

$$c = \sqrt{2.24 \times 10^9 \frac{\text{N}}{\text{m}^2} \times \frac{1}{0.998} \times \frac{1 \text{ m}^3}{1000 \text{ kg}} \times \frac{\text{kg} \cdot \text{m}}{\text{N} \cdot \text{s}^2}} = 1500 \text{ m/s} \quad c_{\text{water}}$$

(c) For seawater we again use Eq. 12.17, with data obtained from Table A.2,

$$c = \sqrt{E_v/\rho} = \sqrt{E_v/SG\rho_{H_2O}}$$

$$c = \sqrt{2.42 \times 10^9 \frac{\text{N}}{\text{m}^2} \times \frac{1}{1.025} \times \frac{1 \text{ m}^3}{1000 \text{ kg}} \times \frac{\text{kg} \cdot \text{m}}{\text{N} \cdot \text{s}^2}} = 1540 \text{ m/s} \quad c_{\text{seawater}}$$

(d) For air we use Eq. 12.18, with the sea level temperature obtained from Table A.3,

$$c = \sqrt{kRT}$$

$$c = \sqrt{1.4 \times 287 \frac{\text{N} \cdot \text{m}}{\text{kg} \cdot \text{K}} \times 288 \text{ K} \times \frac{\text{kg} \cdot \text{m}}{\text{N} \cdot \text{s}^2}} = 340 \text{ m/s} \quad c_{\text{air}(288 \text{ K})}$$

This problem illustrates the relative magnitudes of the speed of sound in typical solids, liquids, and gases ($c_{\text{solids}} > c_{\text{liquids}} > c_{\text{gases}}$). Do not confuse the speed of sound with the attenuation of sound—the rate at which internal friction of the medium reduces the sound level—generally, solids and liquids attenuate sound much more rapidly than do gases.

Types of Flow—The Mach Cone

Flows for which $M < 1$ are *subsonic*, while those with $M > 1$ are *supersonic*. Flow fields that have both subsonic and supersonic regions are termed *transonic*. The transonic regime occurs for Mach numbers between about 0.9 and 1.2. Although most flows within our experience are subsonic, there are important practical cases where $M \geq 1$ occurs in a flow field. Perhaps the most obvious are supersonic aircraft and transonic flows in aircraft compressors and fans. Yet another flow regime, *hypersonic* flow ($M \gtrsim 5$), is of interest in missile and reentry-vehicle design. Some important qualitative differences between subsonic and supersonic flows can be deduced from the properties of a simple moving sound source.

Consider a point source of sound that emits a pulse every Δt seconds. Each pulse expands outwards from its origination point at the speed of sound c , so at any instant t the pulse will be a sphere of radius ct centered at the pulse's origination point. We want to investigate what happens if the point source itself is moving. There are four possibilities, as shown in Fig. 12.2:

- (a) $V = 0$. The point source is *stationary*. Figure 12.2a shows conditions after $3\Delta t$ seconds. The first pulse has expanded to a sphere of radius $c(3\Delta t)$, the second to a sphere of radius $c(2\Delta t)$, and the third to a sphere of radius $c(\Delta t)$; a new pulse is about to be emitted. The pulses constitute a set of ever-expanding concentric spheres.
- (b) $0 < V < c$. The point source moves to the left at *subsonic* speed. Figure 12.2b shows conditions after $3\Delta t$ seconds. The source is shown at times $t = 0, \Delta t, 2\Delta t$, and $3\Delta t$. The first pulse has expanded to a sphere of radius $c(3\Delta t)$ centered where the source was originally, the second to a sphere of radius $c(2\Delta t)$ centered where the source was at time Δt , and the third to a sphere of radius $c(\Delta t)$ centered where the source was at time $2\Delta t$; a new pulse is about to be emitted. The pulses again constitute a set of ever-expanding spheres, except now they are not concentric. The pulses are all expanding at

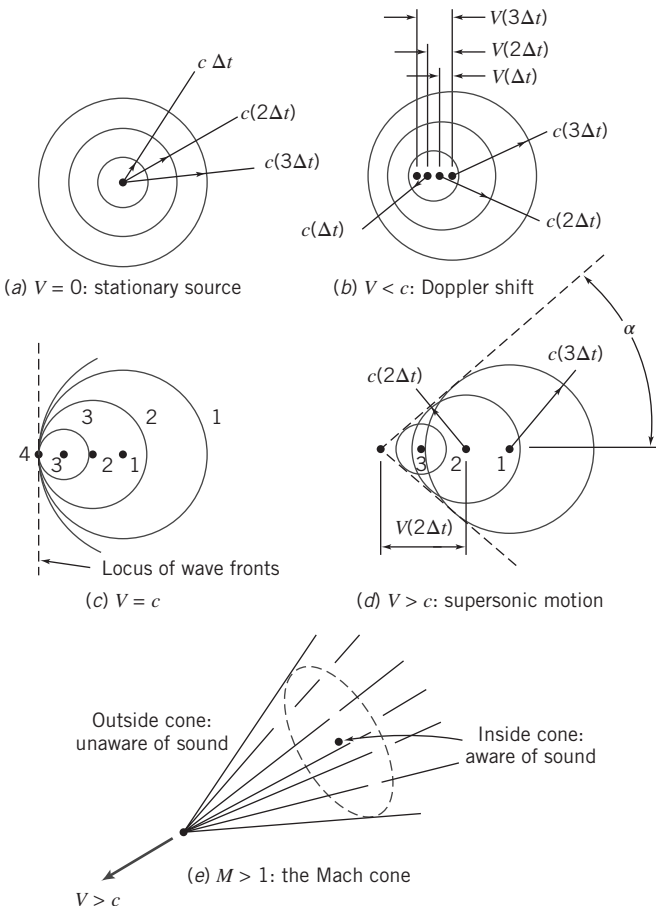


Fig. 12.2 Propagation of sound waves from a moving source: The Mach cone.

constant speed c . We make two important notes: First, we can see that an observer who is ahead of the source (or whom the source is approaching) will hear the pulses at a higher frequency rate than will an observer who is behind the source. This is the Doppler effect that occurs when a vehicle approaches and passes. Second, an observer ahead of the source hears the source *before* the source itself reaches the observer.

- (c) $V = c$. The point source moves to the left at *sonic* speed. Figure 12.2c shows conditions after $3\Delta t$ seconds. The source is shown at times $t = 0$ (point 1), Δt (point 2), $2\Delta t$ (point 3), and $3\Delta t$ (point 4). The first pulse has expanded to sphere 1 of radius $c(3\Delta t)$ centered at point 1, the second to sphere 2 of radius $c(2\Delta t)$ centered at point 2, and the third to sphere 3 of radius $c(\Delta t)$ centered around the source at point 3. We can see once more that the pulses constitute a set of ever-expanding spheres, except now they are tangent to one another on the left. The pulses are all expanding at constant speed c , but the source is also moving at speed c , with the result that the source and all its pulses are traveling together to the left. We again make two important notes: First, we can see that an observer who is ahead of the source will *not* hear the pulses before the source reaches the observer. Second, over time an unlimited number of pulses will accumulate at the front of the source, leading to a sound wave of unlimited amplitude.
- (d) $V > c$. The point source moves to the left at *supersonic* speed. Figure 12.2d shows conditions after $3\Delta t$ seconds. We can see once more that the pulses constitute a set of ever-expanding spheres, except now the source is moving so fast it moves ahead of each sphere that it generates. For supersonic motion, the spheres generate what is called a *Mach cone* tangent to each sphere. In this case, an observer who is ahead of the source will not hear the pulses until after the source passes the observer. The region inside the cone is called the *zone of action* and that outside the cone the *zone of silence*, as shown in Fig. 12.2e. From geometry, we see from Fig. 12.2d that

$$\sin \alpha = \frac{c}{V} = \frac{1}{M}$$

or

$$\alpha = \sin^{-1} \left(\frac{1}{M} \right) \quad (12.19)$$

Figure 12.3 shows an image of an F/A-18 Hornet just as it accelerates to supersonic speed. The visible vapor pattern is due to the sudden increase in pressure as a shock wave washes over the aircraft. The Mach cone, which is not visible, emanates from the nose of the aircraft and passes through the periphery of the vapor disk. In Example 12.4, the properties of the Mach cone are used in analyzing a bullet trajectory.

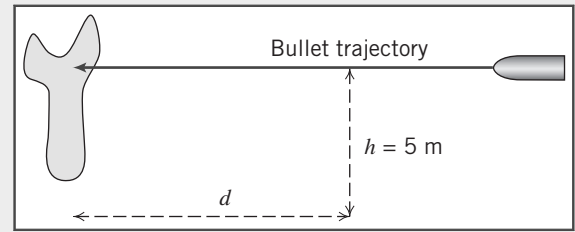


Conspicuous/Alamy Stock Photo

Fig. 12.3 An F/A-18 Hornet as it breaks the sound barrier.

Example 12.4 MACH CONE OF A BULLET

In tests of a protective material, we wish to photograph a bullet as it impacts a jacket made of the material. A camera is set up a perpendicular distance $h = 5 \text{ m}$ from the bullet trajectory. We wish to determine the perpendicular distance d from the target plane at which the camera must be placed such that the sound of the bullet will trigger the camera at the impact time. Note: The bullet speed is measured to be 550 m/s ; the delay time of the camera is 0.005 s .



Find: Location of camera for capturing impact image.

Solution: The correct value of d is that for which the bullet hits the target 0.005 s before the Mach wave reaches the camera. We must first find the Mach number of the bullet; then we can find the Mach angle; finally, we can use basic trigonometry to find d .

Assuming sea level conditions, from Table A.3 we have $T = 288 \text{ K}$. Hence Eq. 12.18 yields

$$c = \sqrt{kRT} \\ c = \sqrt{1.4 \times 287 \frac{\text{N} \cdot \text{m}}{\text{kg} \cdot \text{K}} \times 288 \text{ K} \times \frac{\text{kg} \cdot \text{m}}{\text{N} \cdot \text{s}^2}} = 340 \text{ m/s}$$

Then we can find the Mach number,

$$M = \frac{V}{c} = \frac{550 \text{ m/s}}{340 \text{ m/s}} = 1.62$$

From Eq. 12.19 we can next find the Mach angle,

$$\alpha = \sin^{-1} \left(\frac{1}{M} \right) = \sin^{-1} \left(\frac{1}{1.62} \right) = 38.2^\circ$$

The distance x traveled by the bullet while the Mach wave reaches the camera is then

$$x = \frac{h}{\tan(\alpha)} = \frac{5 \text{ m}}{\tan(38.2^\circ)} = 6.35 \text{ m}$$

Finally, we must add to this the time traveled by the bullet while the camera is operating, which is $0.005 \text{ s} \times 550 \text{ m/s}$,

$$d = 0.005 \text{ s} \times \frac{550 \text{ m}}{\text{s}} + 6.35 \text{ m} = 2.75 \text{ m} + 6.35 \text{ m} \\ d = 9.10 \text{ m} \quad \text{---} \quad d$$

12.3 Reference State: Local Isentropic Stagnation Properties

In our study of compressible flow, we will discover that, in general, *all* properties (p, T, ρ, u, s, V) may be changing as the flow proceeds. We need to obtain reference conditions that we can use to relate conditions in a flow from point to point. For any flow, a reference condition is obtained when the fluid is brought to rest either in reality or conceptually. We will call this the *stagnation condition*, and the property values ($p_0, T_0, \rho_0, u_0, h_0, s_0$) at this state the *stagnation properties*. The stagnation state is defined by an isentropic process, in which there is no friction, no heat transfer, and no “violent” events. Hence, the properties we obtain will be the *local isentropic stagnation properties* and, each point in the flow will have its own, or local, isentropic stagnation properties. This is illustrated in Fig. 12.4, showing a flow from some state ① to some new state ②. The local isentropic stagnation properties for each state,

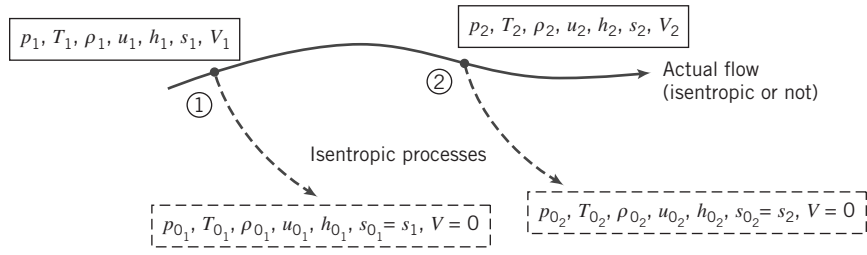


Fig. 12.4 Local isentropic stagnation properties.

obtained by isentropically bringing the fluid to rest, are also shown. Hence, $s_{01} = s_1$ and $s_{02} = s_2$. If the flow *is* isentropic, $s_1 = s_2 = s_{01} = s_{02}$, so the stagnation states are identical; if it is *not* isentropic, then $s_{01} \neq s_{02}$. We will see that changes in local isentropic stagnation properties will provide useful information about the flow.

We can obtain information on the reference isentropic stagnation state for *incompressible* flows by recalling the Bernoulli equation from Chapter 6

$$\frac{p}{\rho} + \frac{V^2}{2} + gz = \text{constant} \quad (6.8)$$

valid for a steady, incompressible, frictionless flow along a streamline. Equation 6.8 is valid for an incompressible isentropic process because it is reversible (frictionless and steady) and adiabatic. As we saw in Section 6.2, the Bernoulli equation leads to

$$p_0 = p + \frac{1}{2}\rho V^2 \quad (6.11)$$

The gravity term drops out because we assume the reference state is at the same elevation as the actual state, and in any event in external flows it is usually much smaller than the other terms. In Example 12.6 we compare isentropic stagnation conditions obtained assuming incompressibility (Eq. 6.11), and allowing for compressibility.

Local Isentropic Stagnation Properties for the Flow of an Ideal Gas

For a compressible flow we can derive the isentropic stagnation relations by applying the mass conservation and momentum equations to a differential control volume, and then integrating. For the process shown schematically in Fig. 12.4, we can depict the process from state ① to the corresponding stagnation state by imagining the control volume shown in Fig. 12.5. Consider first the continuity equation.

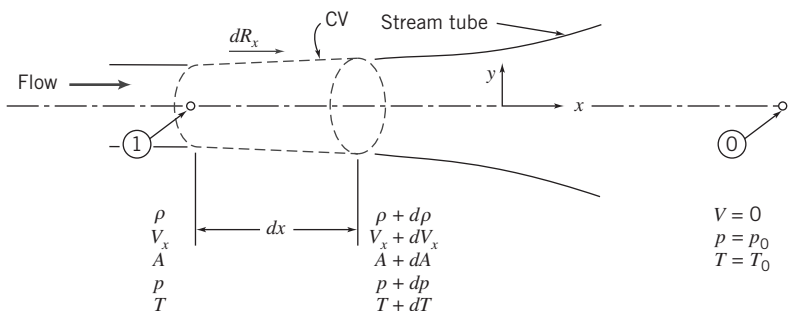


Fig. 12.5 Compressible flow in an infinitesimal stream tube.

a. Continuity Equation

Governing equation:

$$\frac{\partial}{\partial t} \int_{CV} \rho dV + \int_{CS} \rho \vec{V} \cdot d\vec{A} = 0 \quad (4.12)$$

Assumptions:

- 1 Steady flow.
- 2 Uniform flow at each section.

Then

$$(-\rho V_x A) + \{(\rho + d\rho)(V_x + dV_x)(A + dA)\} = 0$$

or

$$\rho V_x A = (\rho + d\rho)(V_x + dV_x)(A + dA) \quad (12.20a)$$

b. Momentum Equation

Governing equation:

$$F_{S_x} + F_{B_x} = \frac{\partial}{\partial t} \int_{CV} V_x \rho dV + \int_{CS} V_x \rho \vec{V} \cdot d\vec{A} \quad (4.18a)$$

Assumptions:

- 3 $F_{B_x} = 0$
- 4 Frictionless flow.

The surface forces acting on the infinitesimal control volume are

$$F_{S_x} = dR_x + pA - (p + dp)(A + dA)$$

The force dR_x is applied along the stream tube boundary, as shown in Fig. 12.5, where the average pressure is $p + dp/2$, and the area component in the x direction is dA . There is no friction. Thus,

$$F_{S_x} = \left(p + \frac{dp}{2} \right) dA + pA - (p + dp)(A + dA)$$

or

$$F_{S_x} \approx p dA + \frac{dp dA}{2} + pA - pA - dpA - pdA - dp dA \approx -dpA$$

Substituting this result into the momentum equation gives

$$-dpA = V_x \{-\rho V_x A\} + (V_x + dV_x) \{(\rho + d\rho)(V_x + dV_x)(A + dA)\}$$

which may be simplified using Eq. 12.20a to obtain

$$-dpA = (-V_x + V_x + dV_x)(\rho V_x A)$$

Finally,

$$dp = -\rho V_x dV_x = -\rho d \left(\frac{V_x^2}{2} \right)$$

or

$$\frac{dp}{\rho} + d \left(\frac{V_x^2}{2} \right) = 0 \quad (12.20b)$$

Equation 12.20b is a relation among properties during the deceleration process. In developing this relation, we have specified a frictionless deceleration process. Before we can integrate between the initial state and final stagnation state, we must specify the relation that exists between pressure, p , and density, ρ , along the process path.

Since the deceleration process is isentropic, then p and ρ for an ideal gas are related by the expression

$$\frac{p}{\rho^k} = \text{constant} \quad (12.12c)$$

Along the stagnation streamline there is only a single component of velocity; V_x is the magnitude of the velocity. Hence we can drop the subscript in Eq. 12.20b.

From $p/\rho^k = \text{constant} = C$, we can write

$$p = C\rho^k \quad \text{and} \quad \rho = p^{1/k}C^{-1/k}$$

Then, from Eq. 12.20b,

$$-d\left(\frac{V^2}{2}\right) = \frac{dp}{\rho} = p^{-1/k}C^{1/k}dp$$

We can integrate this equation between the initial state and the corresponding stagnation state

$$-\int_V^0 d\left(\frac{V^2}{2}\right) = C^{1/k} \int_p^{p_0} p^{-1/k} dp$$

to obtain

$$\begin{aligned} \frac{V^2}{2} &= C^{1/k} \frac{k}{k-1} \left[p^{(k-1)/k} \right]_p^{p_0} = C^{1/k} \frac{k}{k-1} \left[p_0^{(k-1)/k} - p^{(k-1)/k} \right] \\ \frac{V^2}{2} &= C^{1/k} \frac{k}{k-1} p^{(k-1)/k} \left[\left(\frac{p_0}{p} \right)^{(k-1)/k} - 1 \right] \end{aligned}$$

Since $C^{1/k} = p^{1/k}/\rho$,

$$\begin{aligned} \frac{V^2}{2} &= \frac{k}{k-1} \frac{p^{1/k}}{\rho} p^{(k-1)/k} \left[\left(\frac{p_0}{p} \right)^{(k-1)/k} - 1 \right] \\ \frac{V^2}{2} &= \frac{k}{k-1} \frac{p}{\rho} \left[\left(\frac{p_0}{p} \right)^{(k-1)/k} - 1 \right] \end{aligned}$$

Since we seek an expression for stagnation pressure, we can rewrite this equation as

$$\left(\frac{p_0}{p} \right)^{(k-1)/k} = 1 + \frac{k-1}{k} \frac{\rho V^2}{2}$$

and

$$\frac{p_0}{p} = \left[1 + \frac{k-1}{k} \frac{\rho V^2}{2} \right]^{k/(k-1)}$$

For an ideal gas, $p = \rho RT$, and hence

$$\frac{p_0}{p} = \left[1 + \frac{k-1}{2} \frac{V^2}{kRT} \right]^{k/(k-1)}$$

Also, for an ideal gas the sonic speed is $c = \sqrt{kRT}$, and thus

$$\begin{aligned} \frac{p_0}{p} &= \left[1 + \frac{k-1}{2} \frac{V^2}{c^2} \right]^{k/(k-1)} \\ \frac{p_0}{p} &= \left[1 + \frac{k-1}{2} M^2 \right]^{k/(k-1)} \end{aligned} \quad (12.21a)$$

Equation 12.21a enables us to calculate the local isentropic stagnation pressure at any point in a flow field of an ideal gas, provided that we know the static pressure and Mach number at that point.

We can readily obtain expressions for other isentropic stagnation properties by applying the relation

$$\frac{p}{\rho^k} = \text{constant}$$

between end states of the process. Thus

$$\frac{p_0}{p} = \left(\frac{\rho_0}{\rho} \right)^k \quad \text{and} \quad \frac{\rho_0}{\rho} = \left(\frac{p_0}{p} \right)^{1/k}$$

For an ideal gas, then,

$$\frac{T_0}{T} = \frac{p_0 \rho}{p \rho_0} = \frac{p_0}{p} \left(\frac{p_0}{p} \right)^{-1/k} = \left(\frac{p_0}{p} \right)^{(k-1)/k}$$

Using Eq. 12.21a, we can summarize the equations for determining local isentropic stagnation properties of an ideal gas as

$$\frac{p_0}{p} = \left[1 + \frac{k-1}{2} M^2 \right]^{k/(k-1)} \quad (12.21a)$$

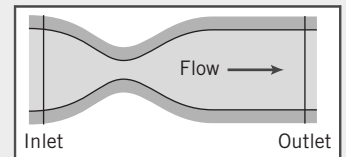
$$\frac{T_0}{T} = 1 + \frac{k-1}{2} M^2 \quad (12.21b)$$

$$\frac{\rho_0}{\rho} = \left[1 + \frac{k-1}{2} M^2 \right]^{1/(k-1)} \quad (12.21c)$$

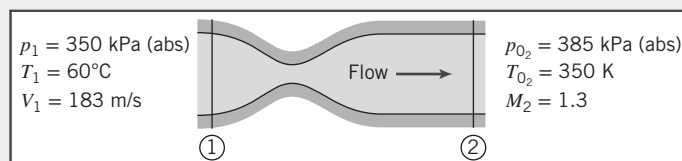
From Eqs. 12.21, the ratio of each local isentropic stagnation property to the corresponding static property at any point in a flow field for an ideal gas can be found if the local Mach number is known. We will usually use Eqs. 12.21 in lieu of the continuity and momentum equations for relating the properties at a state to that state's stagnation properties, but it is important to remember that we derived Eqs. 12.21 using these equations *and* the isentropic relation for an ideal gas. Appendix D.1 lists flow functions for property ratios T_0/T , p_0/p , and ρ_0/ρ , in terms of M for isentropic flow of an ideal gas. A table of values, as well as a plot of these property ratios is presented for air ($k = 1.4$) for a limited range of Mach numbers. The calculation procedure is illustrated in Example 12.5. The Mach number range for validity of the assumption of incompressible flow is investigated in Example 12.6.

Example 12.5 LOCAL ISENTROPIC STAGNATION CONDITIONS IN CHANNEL FLOW

Air flows steadily through the duct shown from 350 kPa (abs), 60°C, and 183 m/s at the inlet state to $M = 1.3$ at the outlet, where local isentropic stagnation conditions are known to be 385 kPa (abs) and 350 K. Compute the local isentropic stagnation pressure and temperature at the inlet and the static pressure and temperature at the duct outlet. Locate the inlet and outlet static state points on a T_s diagram, and indicate the stagnation processes.



Given: Steady flow of air through a duct as shown in the sketch.



- Find:**
- p_{0_1} .
 - T_{0_1} .
 - p_2 .
 - T_2 .
 - State points ① and ② on a Ts diagram; indicate the stagnation processes.

Solution: To evaluate local isentropic stagnation conditions at section ①, we must calculate the Mach number, $M_1 = V_1/c_1$. For an ideal gas, $c = \sqrt{kRT}$. Then

$$c_1 = \sqrt{kRT_1} = \left[1.4 \times 287 \frac{\text{N} \cdot \text{m}}{\text{kg} \cdot \text{K}} \times (273 + 60) \text{ K} \times \frac{\text{kg} \cdot \text{m}}{\text{N} \cdot \text{s}^2} \right]^{1/2} = 366 \text{ m/s}$$

and

$$M_1 = \frac{V_1}{c_1} = \frac{183}{366} = 0.5$$

Local isentropic stagnation properties can be evaluated from Eqs. 12.21. Thus

$$\begin{aligned} p_{0_1} &= p_1 \left[1 + \frac{k-1}{2} M_1^2 \right]^{k/(k-1)} = 350 \text{ kPa} [1 + 0.2(0.5)^2]^{3.5} = 415 \text{ kPa (abs)} \xrightarrow[p_{0_1}]{T_{0_1}} \\ T_{0_1} &= T_1 \left[1 + \frac{k-1}{2} M_1^2 \right] = 333 \text{ K} [1 + 0.2(0.5)^2] = 350 \text{ K} \xrightarrow[T_{0_1}]{ } \end{aligned}$$

At section ②, Eqs. 12.21 can be applied again. Thus from Eq. 12.21a,

$$p_2 = \frac{p_{0_2}}{\left[1 + \frac{k-1}{2} M_2^2 \right]^{k/(k-1)}} = \frac{385 \text{ kPa}}{[1 + 0.2(1.3)^2]^{3.5}} = 139 \text{ kPa (abs)} \xrightarrow[p_2]{ }$$

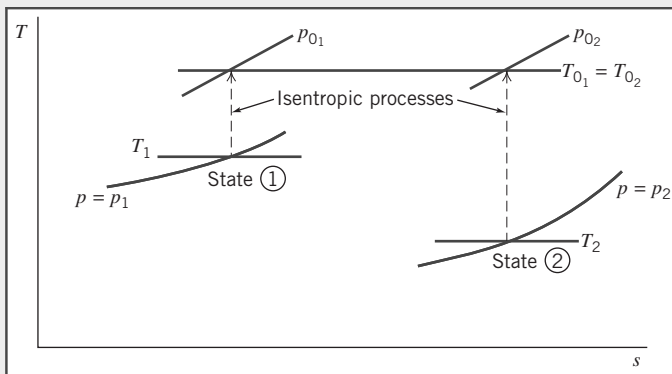
From Eq. 12.21b,

$$T_2 = \frac{T_{0_2}}{1 + \frac{k-1}{2} M_2^2} = \frac{350 \text{ K}}{1 + 0.2(1.3)^2} = 262 \text{ K} \xrightarrow[T_2]{ }$$

To locate states ① and ② in relation to one another, and sketch the stagnation processes on the Ts diagram, we need to find the change in entropy $s_2 - s_1$. At each state we have p and T , so it is convenient to use Eq. 12.11b,

$$\begin{aligned} s_2 - s_1 &= c_p \ln \frac{T_2}{T_1} - R \ln \frac{p_2}{p_1} \\ &= 1.00 \frac{\text{kJ}}{\text{kg} \cdot \text{K}} \times \ln \left(\frac{262}{333} \right) - 0.287 \frac{\text{kJ}}{\text{kg} \cdot \text{K}} \times \ln \left(\frac{139}{350} \right) \\ s_2 - s_1 &= 0.0252 \text{ kJ}/(\text{kg} \cdot \text{K}) \end{aligned}$$

Hence in this flow we have an increase in entropy. Perhaps there is irreversibility (e.g., friction), or heat is being added, or both. (We will see in Chapter 13 that the fact that $T_{0_1} = T_{0_2}$, for this particular flow means that actually we have an adiabatic flow.) We also found that $T_2 < T_1$ and that $p_2 < p_1$. We can now sketch the Ts diagram, and as we saw in Example 12.2 that isobars (lines of constant pressure) in Ts space are exponential.



This problem illustrates use of the local isentropic stagnation properties (Eqs. 12.21) to relate different points in a flow.

Example 12.6 MACH-NUMBER LIMIT FOR INCOMPRESSIBLE FLOW

We have derived equations for p_0/p for both compressible and incompressible flows. By writing both equations in terms of Mach number, compare their behavior. Find the Mach number below which the two equations agree within engineering accuracy.

Given: The incompressible and compressible forms of the equations for stagnation pressure, p_0 .

$$\text{Incompressible} \quad p_0 = p + \frac{1}{2}\rho V^2 \quad (6.11)$$

$$\text{Compressible} \quad \frac{p_0}{p} = \left[1 + \frac{k-1}{2}M^2 \right]^{k/(k-1)} \quad (12.21a)$$

Find: (a) Behavior of both equations as a function of Mach number.

(b) Mach number below which calculated values of p_0/p agree within engineering accuracy.

Solution: First, let us write Eq. 6.11 in terms of Mach number. Using the ideal gas equation of state and $c^2 = kRT$,

$$\frac{p_0}{p} = 1 + \frac{\rho V^2}{2p} = 1 + \frac{V^2}{2RT} = 1 + \frac{kV^2}{2kRT} = 1 + \frac{kV^2}{2c^2}$$

Thus,

$$\frac{p_0}{p} = 1 + \frac{k}{2}M^2 \quad (1)$$

for “incompressible” flow.

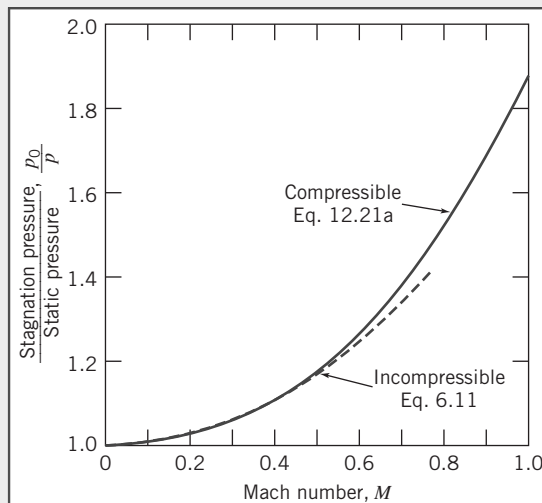
Equation 12.21a may be expanded using the binomial theorem,

$$(1+x)^n = 1 + nx + \frac{n(n-1)}{2!}x^2 + \dots, |x| < 1$$

For Eq. 12.21a, $x = [(k-1)/2]M^2$, and $n = k/(k-1)$. Thus the series converges for $[(k-1)/2]/M^2 < 1$, and for compressible flow,

$$\begin{aligned} \frac{p_0}{p} &= 1 + \left(\frac{k}{k-1} \right) \left[\frac{k-1}{2}M^2 \right] + \left(\frac{k}{k-1} \right) \left(\frac{k}{k-1} - 1 \right) \frac{1}{2!} \left[\frac{k-1}{2}M^2 \right]^2 \\ &\quad + \left(\frac{k}{k-1} \right) \left(\frac{k}{k-1} - 1 \right) \left(\frac{k}{k-1} - 2 \right) \frac{1}{3!} \left[\frac{k-1}{2}M^2 \right]^3 + \dots \\ &= 1 + \frac{k}{2}M^2 + \frac{k}{8}M^4 + \frac{k(2-k)}{48}M^6 + \dots \\ \frac{p_0}{p} &= 1 + \frac{k}{2}M^2 \left[1 + \frac{1}{4}M^2 + \frac{(2-k)}{24}M^4 + \dots \right] \end{aligned} \quad (2)$$

In the limit, as $M \rightarrow 0$, the term in brackets in Eq. 2 approaches 1.0. Thus, for flow at low Mach number, the incompressible and compressible equations give the same result. The variation of p_0/p with Mach number is shown below. As Mach number is increased, the compressible equation gives a larger ratio, p_0/p .



Equations 1 and 2 may be compared quantitatively most simply by writing

$$\frac{p_0}{p} - 1 = \frac{k}{2} M^2 \text{ ("incompressible")}$$

$$\frac{p_0}{p} - 1 = \frac{k}{2} M^2 \left[1 + \frac{1}{4} M^2 + \frac{(2-k)}{24} M^4 + \dots \right] \text{ (compressible)}$$

12.4 Critical Conditions

Stagnation conditions are useful as reference conditions for thermodynamic properties. A useful reference value for velocity is the *critical speed*, which is the speed V we attain when a flow is either accelerated or decelerated isentropically until $M = 1$. Even if there is no point in a given flow field where the Mach number is equal to unity, such a hypothetical condition still is useful as a reference condition.

Using asterisks to denote conditions at $M = 1$, by definition

$$V^* \equiv c^*$$

At critical conditions, Eqs. 12.21 for isentropic stagnation properties become

$$\frac{p_0}{p^*} = \left[\frac{k+1}{2} \right]^{k/(k-1)} \quad (12.22a)$$

$$\frac{T_0}{T^*} = \frac{k+1}{2} \quad (12.22b)$$

$$\frac{\rho_0}{\rho^*} = \left[\frac{k+1}{2} \right]^{1/(k-1)} \quad (12.22c)$$

The critical speed may be written in terms of either critical temperature, T^* , or isentropic stagnation temperature, T_0 .

For an ideal gas, $c^* = \sqrt{kRT^*}$, and thus $V^* = \sqrt{kRT^*}$. Since, from Eq. 12.22b,

$$T^* = \frac{2}{k+1} T_0$$

we have

$$V^* = c^* = \sqrt{\frac{2k}{k+1} RT_0} \quad (12.23)$$

We shall use both stagnation conditions and critical conditions as reference conditions when we consider a variety of compressible flows.

12.5 Basic Equations for One-Dimensional Compressible Flow

We will develop general equations for a one-dimensional flow that express the basic laws *mass conservation* (continuity), *momentum*, the *first law of thermodynamics*, the *second law of thermodynamics*, and an *equation of state*. To do so, we will use the fixed control volume shown in Fig. 12.6. We initially assume that the flow is affected by area change, friction, and heat transfer. Then, for each individual phenomenon we will simplify the equations to obtain useful results.

As shown in Fig. 12.6, the properties at sections ① and ② are labeled with corresponding subscripts. R_x is the x component of surface force from friction and pressure on the sides of the channel. There will also be surface forces from pressures at surfaces ① and ②. Note that the x component of body force is zero, so it is not shown. \dot{Q} is the heat transfer.

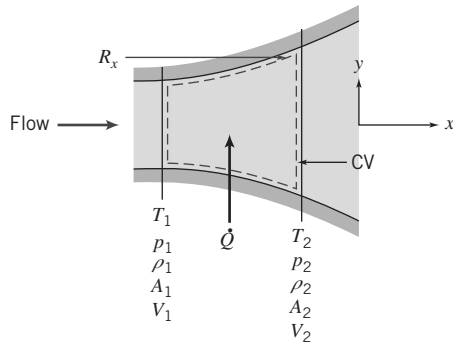


Fig. 12.6 Control volume for analysis of a general one-dimensional flow.

Continuity Equation

Basic equation:

$$\frac{\partial}{\partial t} \int_{CV} \rho dV + \int_{CS} \rho \vec{V} \cdot d\vec{A} = 0 \quad (4.12)$$

Assumptions:

- 1 Steady flow.
- 2 One-dimensional flow.

Then

$$(-\rho_1 V_1 A_1) + (\rho_2 V_2 A_2) = 0$$

or

$$\rho_1 V_1 A_1 = \rho_2 V_2 A_2 = \rho V A = \dot{m} = \text{constant} \quad (12.24a)$$

Momentum Equation

Basic equation:

$$F_{S_x} + F_{B_x} = \frac{\partial}{\partial t} \int_{CV} V_x \rho dV + \int_{CS} V_x \rho \vec{V} \cdot d\vec{A} \quad (4.18a)$$

Assumption:

- 3 $F_{B_x} = 0$

The surface force is caused by pressure forces at surfaces ① and ②, and by the friction and distributed pressure force, R_x , along the channel walls. Substituting gives

$$R_x + p_1 A_1 - p_2 A_2 = V_1 (-\rho_1 V_1 A_1) + V_2 (\rho_2 V_2 A_2)$$

Using continuity, we obtain

$$R_x + p_1 A_1 - p_2 A_2 = \dot{m} V_2 - \dot{m} V_1 \quad (12.24b)$$

First Law of Thermodynamics

Basic equation:

$$\dot{Q} - \dot{W}_s - \dot{W}_{\text{shear}} - \dot{W}_{\text{other}} = \frac{\partial}{\partial t} \int_{CV} e \rho dV + \int_{CS} (e + pv) \rho \vec{V} \cdot d\vec{A} \quad (4.56)$$

where

$$e = u + \frac{V^2}{2} + gz \stackrel{\simeq 0(6)}{\nearrow}$$

Assumptions:

- 4 $\dot{W}_s = 0$.
- 5 $\dot{W}_{\text{shear}} = \dot{W}_{\text{other}} = 0$.
- 6 Effects of gravity are negligible.

Note that even if we have friction, there is no friction *work* at the walls because with friction the velocity at the walls must be zero from the no-slip condition. Under these assumptions, the first law reduces to

$$\dot{Q} = \left(u_1 + p_1 v_1 + \frac{V_1^2}{2} \right) (-\rho_1 V_1 A_1) + \left(u_2 + p_2 v_2 + \frac{V_2^2}{2} \right) (\rho_2 V_2 A_2)$$

This can be simplified by using $h \equiv u + p\nu$, and continuity (Eq. 12.24a),

$$\dot{Q} = \dot{m} \left[\left(h_2 + \frac{V_2^2}{2} \right) - \left(h_1 + \frac{V_1^2}{2} \right) \right]$$

We can write the heat transfer on a per unit mass rather than per unit time basis:

$$\frac{\delta Q}{dm} = \frac{1}{m} \dot{Q}$$

so

$$\frac{\delta Q}{dm} + h_1 + \frac{V_1^2}{2} = h_2 + \frac{V_2^2}{2} \quad (12.24c)$$

Equation 12.24c expresses the fact that heat transfer changes the total energy (the sum of thermal energy h , and kinetic energy $V^2/2$) of the flowing fluid. This combination, $h + V^2/2$, occurs often in compressible flow, and is called the *stagnation enthalpy*, h_0 . This is the enthalpy obtained if a flow is brought adiabatically to rest.

Hence, Eq. 12.24c can also be written

$$\frac{\delta Q}{dm} = h_{02} - h_{01}$$

We see that heat transfer causes the stagnation enthalpy, and hence, stagnation temperature, T_0 , to change.

Second Law of Thermodynamics

Basic equation:

$$\frac{\partial}{\partial t} \int_{CV} s \rho dV + \int_{CS} s \rho \vec{V} \cdot d\vec{A} \stackrel{=0(1)}{\geq} \int_{CS} \frac{1}{T} \left(\frac{\dot{Q}}{A} \right) dA \quad (4.58)$$

or

$$s_1(-\rho_1 V_1 A_1) + s_2(\rho_2 V_2 A_2) \stackrel{=0(1)}{\geq} \int_{CS} \frac{1}{T} \left(\frac{\dot{Q}}{A} \right) dA$$

and, again using continuity,

$$\dot{m}(s_2 - s_1) \stackrel{=0(1)}{\geq} \int_{CS} \frac{1}{T} \left(\frac{\dot{Q}}{A} \right) dA \quad (12.24d)$$

Equation of State

The equation of state for a simple substance can be expressed as a function of any two other independent properties. For example, we could write $h = h(s, p)$, or $\rho = \rho(s, p)$, and so on. We will primarily be concerned with ideal gases with constant specific heats, and for these we can write Eqs. 12.1 and 12.7b (renumbered for convenient use in this section),

$$p = \rho RT \quad (12.24e)$$

and

$$\Delta h = h_2 - h_1 = c_p \Delta T = c_p (T_2 - T_1) \quad (12.24f)$$

For ideal gases with constant specific heats, the change in entropy, $\Delta s = s_2 - s_1$, for any process can be computed from any of Eqs. 12.11. For example, Eq. 12.11b (renumbered here for convenience) is

$$\Delta s = s_2 - s_1 = c_p \ln \frac{T_2}{T_1} - R \ln \frac{P_2}{P_1} \quad (12.24g)$$

We now have a basic set of equations for analyzing one-dimensional compressible flows of an ideal gas with constant specific heats:

$$\rho_1 V_1 A_1 = \rho_2 V_2 A_2 = \rho V A = \dot{m} = \text{constant} \quad (12.24a)$$

$$R_x + p_1 A_1 - p_2 A_2 = \dot{m} V_2 - \dot{m} V_1 \quad (12.24b)$$

$$\frac{\delta Q}{dm} + h_1 + \frac{V_1^2}{2} = h_2 + \frac{V_2^2}{2} \quad (12.24c)$$

$$\dot{m}(s_2 - s_1) \geq \int_{\text{CS}} \frac{1}{T} \left(\frac{\dot{Q}}{A} \right) dA \quad (12.24d)$$

$$p = \rho RT \quad (12.24e)$$

$$\Delta h = h_2 - h_1 = c_p \Delta T = c_p (T_2 - T_1) \quad (12.24f)$$

$$\Delta s = s_2 - s_1 = c_p \ln \frac{T_2}{T_1} - R \ln \frac{P_2}{P_1} \quad (12.24g)$$

Note that Eq. 12.24e applies only if we have an ideal gas; Equations 12.24f and 12.24g apply only if we have an ideal gas with constant specific heats. We can simplify this set of equations for each of the phenomena that can affect the flow:

- Flow with varying area.
- Normal shock.
- Flow in a channel with friction.
- Flow in a channel with heating or cooling.

12.6 Isentropic Flow of an Ideal Gas: Area Variation

The first phenomenon is one in which the flow is changed only by area variation without heat transfer, friction, or shocks. The absence of heat transfer, friction, and shocks means the flow will be reversible and adiabatic, so Eq. 12.24d becomes

$$\dot{m}(s_2 - s_1) = \int_{\text{CS}} \frac{1}{T} \left(\frac{\dot{Q}}{A} \right) dA = 0$$

or

$$\Delta s = s_2 - s_1 = 0$$

so such a flow is *isentropic*. This means that Eq. 12.24g leads to the result we saw previously,

$$T_1 p_1^{(1-k)/k} = T_2 p_2^{(1-k)/k} = T p^{(1-k)/k} = \text{constant} \quad (12.12b)$$

or its equivalent, which can be obtained by using the ideal gas equation of state in Eq. 12.12b to eliminate temperature,

$$\frac{p_1}{\rho_1^k} = \frac{p_2}{\rho_2^k} = \frac{p}{\rho^k} = \text{constant} \quad (12.12c)$$

Hence, the basic set of equations (Eqs. 12.24) becomes:

$$\rho_1 V_1 A_1 = \rho_2 V_2 A_2 = \rho V A = \dot{m} = \text{constant} \quad (12.25a)$$

$$R_x + p_1 A_1 - p_2 A_2 = \dot{m} V_2 - \dot{m} V_1 \quad (12.25b)$$

$$h_{0_1} = h_1 + \frac{V_1^2}{2} = h_2 + \frac{V_2^2}{2} = h_{0_2} = h_0 \quad (12.25c)$$

$$s_2 = s_1 = s \quad (12.25d)$$

$$p = \rho R T \quad (12.25e)$$

$$\Delta h = h_2 - h_1 = c_p \Delta T = c_p (T_2 - T_1) \quad (12.25f)$$

$$\frac{p_1}{\rho_1^k} = \frac{p_2}{\rho_2^k} = \frac{p}{\rho^k} = \text{constant} \quad (12.25g)$$

Equations 12.25c, 12.25d, and 12.25f provide insight into how this process appears on an *hs* diagram and on a *Ts* diagram. From Eq. 12.25c, the total energy, or stagnation enthalpy h_0 , of the fluid is constant; the enthalpy and kinetic energy may vary along the flow, but their sum is constant. This means that if the fluid accelerates, its temperature must decrease, and vice versa. Equation 12.25d indicates that the entropy remains constant. These results are shown for a typical process in Fig. 12.7.

Equation 12.25f indicates that the temperature and enthalpy are linearly related; hence, processes plotted on a *Ts* diagram will look very similar to that shown in Fig. 12.7 except for the vertical scale.

Equations 12.25 could be used to analyze isentropic flow in a channel of varying area. For example, if we know conditions at section ① (i.e., p_1 , ρ_1 , T_1 , s_1 , h_1 , V_1 , and A_1) we could use these equations to find conditions at some new section ② where the area is A_2 . We would have seven equations and seven unknowns (p_2 , ρ_2 , T_2 , s_2 , h_2 , V_2 , and R_x).

We can gain insight into the isentropic process by reviewing the results we obtained previously when we analyzed a differential control volume (Fig. 12.5). The momentum equation for this was

$$\frac{dp}{\rho} + d\left(\frac{V^2}{2}\right) = 0 \quad (12.20b)$$

Then

$$dp = -\rho V dV$$

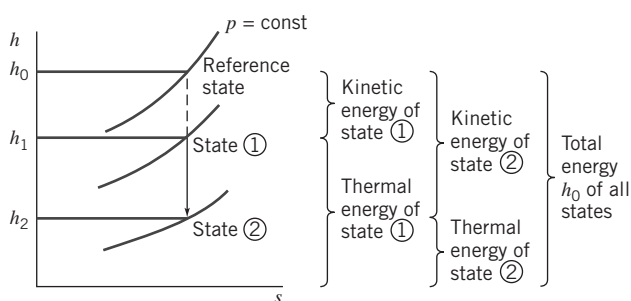


Fig. 12.7 Isentropic flow in the *hs* plane.

Dividing by ρV^2 , we obtain

$$\frac{dp}{\rho V^2} = -\frac{dV}{V} \quad (12.26)$$

A convenient differential form of the continuity equation can be obtained from Eq. 12.25a, in the form

$$\rho A V = \text{constant}$$

Differentiating and dividing by $\rho A V$ yields

$$\frac{d\rho}{\rho} + \frac{dA}{A} + \frac{dV}{V} = 0 \quad (12.27)$$

Solving Eq. 12.27 for dA/A gives

$$\frac{dA}{A} = -\frac{dV}{V} - \frac{d\rho}{\rho}$$

Substituting from Eq. 12.26 gives

$$\frac{dA}{A} = \frac{dp}{\rho V^2} - \frac{d\rho}{\rho}$$

or

$$\frac{dA}{A} = \frac{dp}{\rho V^2} \left[1 - \frac{V^2}{dp/d\rho} \right]$$

Now recall that for an isentropic process, $dp/d\rho = \partial p/\partial \rho)_s = c^2$, so

$$\frac{dA}{A} = \frac{dp}{\rho V^2} \left[1 - \frac{V^2}{c^2} \right] = \frac{dp}{\rho V^2} [1 - M^2]$$

or

$$\frac{dp}{\rho V^2} = \frac{dA}{A} \frac{1}{[1 - M^2]} \quad (12.28)$$

Substituting from Eq. 12.26 into Eq. 12.28, we obtain

$$\frac{dV}{V} = -\frac{dA}{A} \frac{1}{[1 - M^2]} \quad (12.29)$$

Note that for an isentropic flow there can be no friction. Equations 12.28 and 12.29 confirm that for this case, from a momentum point of view we expect an increase in pressure to cause a decrease in speed, and vice versa. Although we cannot use them for computations because we have not so far determined how M varies with A , Eqs. 12.28 and 12.29 give us insights into how the pressure and velocity change as we change the area of the flow. Three possibilities are discussed below.

Subsonic Flow, $M < 1$

For $M < 1$, the factor $1/[1 - M^2]$ in Eqs. 12.28 and 12.29 is positive, so that a positive dA leads to a positive dp and a negative dV . These mathematical results mean that in a *divergent* section ($dA > 0$) the flow must experience an *increase* in pressure ($dp > 0$) and the velocity must *decrease* ($dV < 0$). Hence a *divergent channel is a subsonic diffuser* that decelerates a flow.

On the other hand, a negative dA leads to a negative dp and a positive dV . These mathematical results mean that in a *convergent* section ($dA < 0$) the flow must experience a *decrease* in pressure ($dp < 0$) and the velocity must *increase* ($dV > 0$). Hence a *convergent channel is a subsonic nozzle* that accelerates a flow.

These results are consistent with our everyday experience. For example, recall the venturi meter in Chapter 8, in which a reduction in area at the throat of the venturi led to a local increase in velocity, and

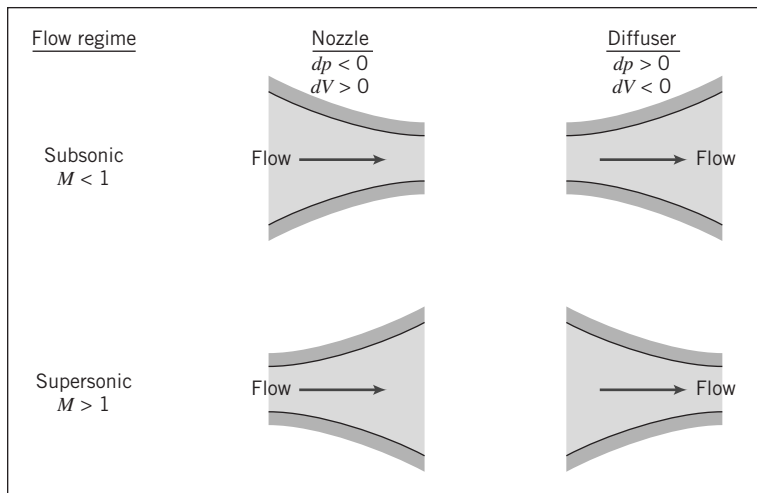


Fig. 12.8 Nozzle and diffuser shapes as a function of initial Mach number.

because of the Bernoulli principle, to a pressure drop, and the divergent section led to pressure recovery and flow deceleration. The subsonic diffuser and nozzle are also shown in Fig. 12.8.

Supersonic Flow, $M > 1$

For $M > 1$, the factor $1/[1 - M^2]$ in Eqs. 12.28 and 12.29 is negative, so that a positive dA leads to a negative dp and a positive dV . These mathematical results mean that in a *divergent* section ($dA > 0$) the flow must experience a *decrease* in pressure ($dp < 0$) and the velocity must *increase* ($dV > 0$). Hence a *divergent channel is a supersonic nozzle*.

On the other hand, a negative dA leads to a positive dp and a negative dV . These mathematical results mean that in a *convergent* section ($dA < 0$) the flow must experience an *increase* in pressure ($dp > 0$) and the velocity must *decrease* ($dV < 0$). Hence a *convergent channel is a supersonic diffuser*.

These results are inconsistent with our everyday experience the opposite of what we saw in the venturi meter. The supersonic nozzle and diffuser are also shown in Fig. 12.8.

These somewhat counterintuitive results can be understood when we realize that we are used to assuming that $\rho = \text{constant}$, but we are now in a flow regime where the fluid density is a function of flow conditions. From Eq. 12.27,

$$\frac{dV}{V} = -\frac{dA}{A} - \frac{dp}{\rho}$$

For example, in a supersonic diverging flow (dA positive) the flow actually accelerates (dV also positive) because the density drops sharply ($d\rho$ is negative and large, with the net result that the right side of the equation is positive).

Sonic Flow, $M = 1$

As we approach $M = 1$, from either a subsonic or supersonic state, the factor $1/[1 - M^2]$ in Eqs. 12.28 and 12.29 approaches infinity, implying that the pressure and velocity changes also approach infinity. This is obviously unrealistic, so we must look for some other way for the equations to make physical sense. The only way we can avoid these singularities in pressure and velocity is if we require that $dA \rightarrow 0$ as $M \rightarrow 1$. Hence, for an isentropic flow, sonic conditions can only occur where the area is constant. We can imagine approaching $M = 1$ from either a subsonic or a supersonic state. A subsonic flow ($M < 1$) would need to be accelerated using a subsonic nozzle, which we have learned is a converging section; a supersonic flow ($M > 1$) would need to be decelerated using a supersonic diffuser, which is also a converging section. Hence, sonic conditions are limited not just to a location of constant area, but one that is a minimum area. The important result is that *for isentropic flow the sonic condition $M = 1$ can only be attained at a throat, or section of minimum area*.

We can see that to isentropically accelerate a fluid from rest to supersonic speed we would need to have a subsonic nozzle (converging section) followed by a supersonic nozzle (diverging section), with $M = 1$ at the throat. This device is called a *converging-diverging nozzle* (C-D nozzle). Of course, to create a supersonic flow we need more than just a C-D nozzle: We must also generate and maintain a pressure difference between the inlet and exit.

We must be careful in our discussion of isentropic flow, especially deceleration, because real fluids can experience nonisentropic phenomena such as boundary-layer separation and shock waves. In practice, supersonic flow cannot be decelerated to exactly $M = 1$ at a throat because sonic flow near a throat is unstable in a rising (adverse) pressure gradient. It turns out that disturbances that are always present in a real subsonic flow propagate upstream, disturbing the sonic flow at the throat, causing shock waves to form and travel upstream, where they may be disgorged from the inlet of the supersonic diffuser.

The throat area of a real supersonic diffuser must be slightly larger than that required to reduce the flow to $M = 1$. Under the proper downstream conditions, a weak normal shock forms in the diverging channel just downstream from the throat. Flow leaving the shock is subsonic and decelerates in the diverging channel. Thus deceleration from supersonic to subsonic flow cannot occur isentropically in practice, since the weak normal shock causes an entropy increase. Normal shocks will be analyzed in Section 12.7.

For accelerating flows (favorable pressure gradients), the idealization of isentropic flow is generally a realistic model of the actual flow behavior. For decelerating flows, the idealization of isentropic flow may not be realistic because of the adverse pressure gradients and the attendant possibility of flow separation, as discussed for incompressible boundary-layer flow in Chapter 9.

Reference Stagnation and Critical Conditions for Isentropic Flow of an Ideal Gas

As we discussed at the beginning of this section, in principle we could use Eqs. 12.25 to analyze one-dimensional isentropic flow of an ideal gas, but the computations would be somewhat tedious. Instead, because the flow is isentropic, we can use the results of Sections 12.3 (reference stagnation conditions) and 12.4 (reference critical conditions). The idea is illustrated in Fig. 12.9: Instead of using Eqs. 12.25 to compute, for example, properties at state ② from those at state ①, we can use state ① to determine two reference states (the stagnation state and the critical state), and then use these to obtain properties at state ②. We need two reference states because the reference stagnation state does not provide area information.

We will use Eqs. 12.21 (renumbered for convenience),

$$\frac{p_0}{p} = \left[1 + \frac{k-1}{2} M^2 \right]^{k/(k-1)} \quad (12.30a)$$

$$\frac{T_0}{T} = 1 + \frac{k-1}{2} M^2 \quad (12.30b)$$

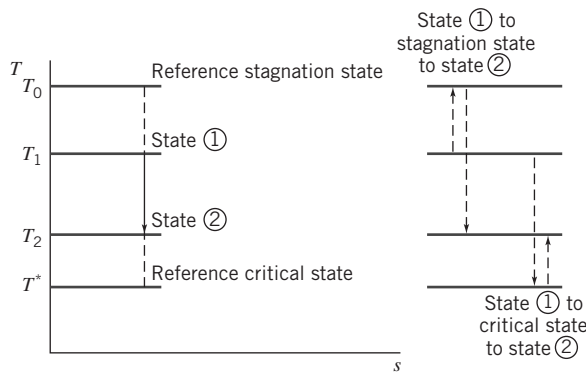


Fig. 12.9 Example of stagnation and critical reference states in the T_s plane.

$$\frac{\rho_0}{\rho} = \left[1 + \frac{k-1}{2} M^2 \right]^{1/(k-1)} \quad (12.30c)$$

We note that *the stagnation conditions are constant throughout the isentropic flow*. The critical conditions ($M = 1$) were related to stagnation conditions in Section 12.4,

$$\frac{p_0}{p^*} = \left[\frac{k+1}{2} \right]^{k/(k-1)} \quad (12.22a)$$

$$\frac{T_0}{T^*} = \frac{k+1}{2} \quad (12.22b)$$

$$\frac{\rho_0}{\rho^*} = \left[\frac{k+1}{2} \right]^{1/(k-1)} \quad (12.22c)$$

$$V^* = c^* = \sqrt{\frac{2k}{k+1}} RT_0 \quad (12.23)$$

Although a particular flow may never attain sonic conditions, as in the example in Fig. 12.9, we will still find the critical conditions useful as reference conditions. Equations 12.30a, 12.30b, and 12.30c relate local properties (p , ρ , T , and V) to stagnation properties (p_0 , ρ_0 , and T_0) via the Mach number M , and Eqs. 12.22 and 12.23 relate critical properties (p^* , ρ^* , T^* , and V^*) to stagnation properties (p_0 , ρ_0 , and T_0) respectively, but we have yet to obtain a relation between areas A and A^* . To do this we start with continuity (Eq. 12.25a) in the form

$$\rho A V = \text{constant} = \rho^* A^* V^*$$

Then

$$\begin{aligned} \frac{A}{A^*} &= \frac{\rho^* V^*}{\rho V} = \frac{\rho^* c^*}{\rho M c} = \frac{1}{M} \frac{\rho^*}{\rho} \sqrt{\frac{T^*}{T}} \\ \frac{A}{A^*} &= \frac{1}{M} \frac{\rho^* \rho_0}{\rho_0 \rho} \sqrt{\frac{T^*/T_0}{T/T_0}} \\ \frac{A}{A^*} &= \frac{1}{M} \frac{\left[1 + \frac{k-1}{2} M^2 \right]^{1/(k-1)}}{\left[\frac{k+1}{2} \right]^{1/(k-1)}} \left[\frac{1 + \frac{k-1}{2} M^2}{\frac{k+1}{2}} \right]^{1/2} \\ \frac{A}{A^*} &= \frac{1}{M} \left[\frac{1 + \frac{k-1}{2} M^2}{\frac{k+1}{2}} \right]^{(k+1)/2(k-1)} \end{aligned} \quad (12.30d)$$

Equations 12.30 form a set that is convenient for analyzing isentropic flow of an ideal gas with constant specific heats, which we usually use instead of the basic equations, Eqs. 12.25. For convenience we list Eqs. 12.30 together:

$$\frac{p_0}{p} = \left[1 + \frac{k-1}{2} M^2 \right]^{k/(k-1)} \quad (12.30a)$$

$$\frac{T_0}{T} = 1 + \frac{k-1}{2} M^2 \quad (12.30b)$$

$$\frac{\rho_0}{\rho} = \left[1 + \frac{k-1}{2} M^2 \right]^{1/(k-1)} \quad (12.30c)$$

$$\frac{A}{A^*} = \frac{1}{M} \left[\frac{1 + \frac{k-1}{2} M^2}{\frac{k+1}{2}} \right]^{(k+1)/2(k-1)} \quad (12.30d)$$

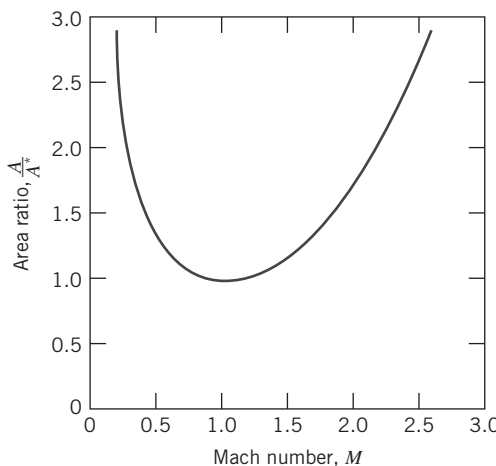


Fig. 12.10 Variation of A/A^* with Mach number for isentropic flow of an ideal gas with $k = 1.4$.

Equations 12.30 provide property relations in terms of the local Mach number, the stagnation conditions, and critical conditions. These equations are readily programmed (e.g. [5] and [6]). While they are somewhat complicated algebraically, they have the advantage over the basic equations, Eq. 12.25, that they are not coupled. Each property can be found directly from its stagnation value and the Mach number.

Equation 12.30d shows the relation between Mach number M and area A . The critical area A^* is used to normalize area A . For each Mach number M we obtain a unique area ratio, but as shown in Fig. 12.10 each A/A^* ratio (except 1) has two possible Mach numbers—one subsonic, the other supersonic. The shape shown in Fig. 12.10 looks like a converging-diverging section for accelerating from a subsonic to a supersonic flow (with, as necessary, $M = 1$ only at the throat), but in practice this is not the shape to which such a passage would be built. For example, the diverging section usually will have a much less severe angle of divergence to reduce the chance of flow separation.

Appendix D.1 lists flow functions for property ratios T_0/T , p_0/p , ρ_0/ρ , and A/A^* in terms of M for isentropic flow of an ideal gas. A table of values, as well as a plot of these property ratios, is presented for air ($k = 1.4$) for a limited range of Mach numbers.

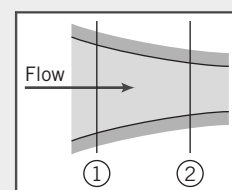
Example 12.7 demonstrates use of some of the above equations. As shown in Fig. 12.9, we can use the equations to relate a property at one state to the stagnation value and then from the stagnation value to a second state, but note that we can accomplish this in one step—for example, p_2 can be obtained from p_1 by writing $p_2 = (p_2/p_0)(p_0/p_1)p_1$, where the pressure ratios come from Eq. 12.30a evaluated at the two Mach numbers.

Example 12.7 ISENTROPIC FLOW IN A CONVERGING CHANNEL

Air flows isentropically in a channel. At section ①, the Mach number is 0.3, the area is 0.001 m^2 , and the absolute pressure and the temperature are 650 kPa and 62°C , respectively. At section ②, the Mach number is 0.8. Sketch the channel shape, plot a T_s diagram for the process, and evaluate properties at section ②. Verify that the results agree with the basic equations, Eqs. 12.25.

Given: Isentropic flow of air in a channel. At sections ① and ②, the following data are given:
 $M_1 = 0.3$, $T_1 = 62^\circ\text{C}$, $p_1 = 650 \text{ kPa}$ (abs), $A_1 = 0.001 \text{ m}^2$, and $M_2 = 0.8$.

Find: (a) The channel shape.
(b) A T_s diagram for the process.
(c) Properties at section ②.
(d) Show that the results satisfy the basic equations.



Solution: To accelerate a subsonic flow requires a converging nozzle. The channel shape must be as shown.

On the Ts plane, the process follows an $s = \text{constant}$ line. Stagnation conditions remain fixed for isentropic flow.

Consequently, the stagnation temperature at section ② can be calculated (for air, $k = 1.4$) from Eq. 12.30b.

$$T_{0_2} = T_{0_1} = T_1 \left[1 + \frac{k-1}{2} M_1^2 \right] \\ = (62 + 273) \text{ K} \left[1 + 0.2(0.3)^2 \right] \\ T_{0_2} = T_{0_1} = 341 \text{ K} \xrightarrow{T_{0_1}, T_{0_2}}$$

For p_{0_2} , from Eq. 12.30a,

$$p_{0_2} = p_{0_1} = p_1 \left[1 + \frac{k-1}{2} M_1^2 \right]^{k/(k-1)} = 650 \text{ kPa} [1 + 0.2(0.3)^2]^{3.5} \\ p_{0_2} = 692 \text{ kPa (abs)} \xrightarrow{p_{0_2}}$$

For T_2 , from Eq. 12.30b,

$$T_2 = T_{0_2} \left/ \left[1 + \frac{k-1}{2} M_2^2 \right] \right. = 341 \text{ K} / [1 + 0.2(0.8)^2] \\ T_2 = 302 \text{ K} \xrightarrow{T_2}$$

For p_2 , from Eq. 12.30a,

$$p_2 = p_{0_2} \left/ \left[1 + \frac{k-1}{2} M_2^2 \right] \right.^{k/k-1} = 692 \text{ kPa} / [1 + 0.2(0.8)^2]^{3.5} \\ p_2 = 454 \text{ kPa} \xrightarrow{p_2}$$

Note that we could have directly computed T_2 from T_1 because $T_0 = \text{constant}$:

$$\frac{T_2}{T_1} = \frac{T_2}{T_0} \left/ \frac{T_0}{T_1} \right. = \left[1 + \frac{k-1}{2} M_1^2 \right] \left/ \left[1 + \frac{k-1}{2} M_2^2 \right] \right. = [1 + 0.2(0.3)^2] \left/ [1 + 0.2(0.8)^2] \right. \\ \frac{T_2}{T_1} = \frac{0.8865}{0.9823} = 0.9025$$

Hence,

$$T_2 = 0.9025 T_1 = 0.9025(273 + 62) \text{ K} = 302 \text{ K}$$

Similarly, for p_2 ,

$$\frac{p_2}{p_1} = \frac{p_2}{p_0} \left/ \frac{p_0}{p_1} \right. = 0.8865^{3.5} \left/ 0.9823^{3.5} \right. = 0.6982$$

Hence,

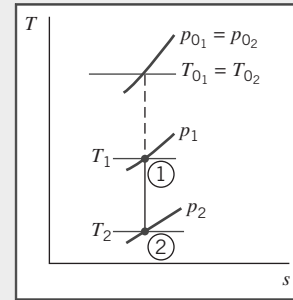
$$p_2 = 0.6982 p_1 = 0.6982(650 \text{ kPa}) = 454 \text{ kPa}$$

The density ρ_2 at section ② can be found from Eq. 12.30c using the same procedure we used for T_2 and p_2 , or we can use the ideal gas equation of state, Eq. 12.25e,

$$\rho_2 = \frac{p_2}{RT_2} = 4.54 \times 10^5 \frac{\text{N}}{\text{m}^2} \times \frac{\text{kg} \cdot \text{K}}{287 \text{ N} \cdot \text{m}} \times \frac{1}{302 \text{ K}} = 5.24 \text{ kg/m}^3 \xrightarrow{\rho_2}$$

and the velocity at section ② is

$$V_2 = M_2 c_2 = M_2 \sqrt{kRT_2} = 0.8 \times \sqrt{1.4 \times 287 \frac{\text{N} \cdot \text{m}}{\text{kg} \cdot \text{K}} \times 302 \text{ K} \times \frac{\text{kg} \cdot \text{m}}{\text{s}^2 \cdot \text{N}}} = 279 \text{ m/s} \xrightarrow{V_2}$$



The area A_2 can be computed from Eq. 12.30d, noting that A^* is constant for this flow,

$$\begin{aligned}\frac{A_2}{A_1} &= \frac{A_2 A^*}{A^* A_1} = \frac{1}{M_2} \left[\frac{1 + \frac{k-1}{2} M_2^2}{\frac{k+1}{2}} \right]^{(k+2)/2(k-1)} \Bigg/ \frac{1}{M_1} \left[\frac{1 + \frac{k-1}{2} M_1^2}{\frac{k+1}{2}} \right]^{(k+1)/2(k-1)} \\ &= \frac{1}{0.8} \left[\frac{1 + 0.2(0.8)^2}{1.2} \right]^3 \Bigg/ \frac{1}{0.3} \left[\frac{1 + 0.2(0.3)^2}{1.2} \right]^3 = \frac{1.038}{2.035} = 0.5101\end{aligned}$$

Hence,

$$A_2 = 0.5101 A_1 = 0.5101 (0.001 \text{ m}^2) = 5.10 \times 10^{-4} \text{ m}^2 \xrightarrow{\hspace{10cm}} A_2$$

Note that $A_2 < A_1$ as expected.

Let us verify that these results satisfy the basic equations.

We first need to obtain ρ_1 and V_1 :

$$\rho_1 = \frac{p_1}{RT_1} = 6.5 \times 10^5 \frac{\text{N}}{\text{m}^2} \times \frac{\text{kg} \cdot \text{K}}{287 \text{ N} \cdot \text{m}} \times \frac{1}{335 \text{ K}} = 6.76 \text{ kg/m}^3$$

and

$$V_1 = M_1 c_1 = M_1 \sqrt{kRT_1} = 0.3 \times \sqrt{1.4 \times 287 \frac{\text{N} \cdot \text{m}}{\text{kg} \cdot \text{K}} \times 335 \text{ K} \times \frac{\text{kg} \cdot \text{m}}{\text{s}^2 \cdot \text{N}}} = 110 \text{ m/s}$$

The mass conservation equation is

$$\rho_1 V_1 A_1 = \rho_2 V_2 A_2 = \rho V A = \dot{m} = \text{constant} \quad (12.25a)$$

$$\dot{m} = 6.76 \frac{\text{kg}}{\text{m}^3} \times 110 \frac{\text{m}}{\text{s}} \times 0.001 \text{ m}^2 = 5.24 \frac{\text{kg}}{\text{m}^3} \times 279 \frac{\text{m}}{\text{s}} \times 0.00051 \text{ m}^2 = 0.744 \text{ kg/s} \quad (\text{Check!})$$

We cannot check the momentum equation (Eq. 12.25b) because we do not know the force R_x produced by the walls of the device (we could use Eq. 12.25b to compute this if we wished). The energy equation is

$$h_{0_1} = h_1 + \frac{V_1^2}{2} = h_2 + \frac{V_2^2}{2} = h_{0_2} = h_0 \quad (12.25c)$$

We will check this by replacing enthalpy with temperature using Eq. 13.2f,

$$\Delta h = h_2 - h_1 = c_p \Delta T = c_p (T_2 - T_1) \quad (12.25f)$$

so the energy equation becomes

$$c_p T_1 + \frac{V_1^2}{2} = c_p T_2 + \frac{V_2^2}{2} = c_p T_0$$

Using c_p for air from Table A.6,

$$c_p T_1 + \frac{V_1^2}{2} = 1004 \frac{\text{J}}{\text{kg} \cdot \text{K}} \times 335 \text{ K} + \frac{(110)^2}{2} \left(\frac{\text{m}}{\text{s}} \right)^2 \times \frac{\text{N} \cdot \text{s}^2}{\text{kg} \cdot \text{m}} \times \frac{\text{J}}{\text{N} \cdot \text{m}} = 342 \text{ kJ/kg}$$

$$c_p T_2 + \frac{V_2^2}{2} = 1004 \frac{\text{J}}{\text{kg} \cdot \text{K}} \times 302 \text{ K} + \frac{(278)^2}{2} \left(\frac{\text{m}}{\text{s}} \right)^2 \times \frac{\text{N} \cdot \text{s}^2}{\text{kg} \cdot \text{m}} \times \frac{\text{J}}{\text{N} \cdot \text{m}} = 342 \text{ kJ/kg}$$

$$c_p T_0 = 1004 \frac{\text{J}}{\text{kg} \cdot \text{K}} \times 341 \text{ K} = 342 \text{ kJ/kg} \quad (\text{Check!})$$

The final equation we can check is the relation between pressure and density for an isentropic process (Eq. 12.25g),

$$\frac{p_1}{\rho_1^k} = \frac{p_2}{\rho_2^k} = \frac{p}{\rho^k} = \text{constant} \quad (\text{Check!})$$

$$\frac{p_1}{\rho_1^{1.4}} = \frac{650 \text{ kPa}}{\left(6.76 \frac{\text{kg}}{\text{m}^3} \right)^{1.4}} = \frac{p_2}{\rho_2^{1.4}} = \frac{454 \text{ kPa}}{\left(5.24 \frac{\text{kg}}{\text{m}^3} \right)^{1.4}} = 44.7 \frac{\text{kPa}}{\left(\frac{\text{kg}}{\text{m}^3} \right)^{1.4}} \quad (\text{Check!})$$

The basic equations are satisfied by our solution.

This problem illustrates:

- Use of the isentropic equations, Eqs. 12.30
- That the isentropic equations are consistent with the basic equations, Eqs. 12.25
- That the computations can be quite laborious without using preprogrammed isentropic relations (available, for example, in the Excel add-ins on the website)!

Isentropic Flow in a Converging Nozzle

Now that we have our computing equations (Eqs. 12.30) for analyzing isentropic flows, we are ready to see how we could obtain flow in a nozzle, starting from rest. We first look at the converging nozzle, and then the C-D nozzle. In either case, to produce a flow we must provide a pressure difference. For example, as illustrated in the converging nozzle shown in Fig. 12.11a, we can do this by providing the gas from a reservoir (or “plenum chamber”) at p_0 and T_0 , and using a vacuum pump/valve combination to create a low pressure, the “back pressure,” p_b . We are interested in what happens to the gas properties as the gas flows through the nozzle, and also in knowing how the mass flow rate increases as we progressively lower the back pressure.

Let us call the pressure at the exit plane p_e . The results we obtain as we progressively open the valve from a closed position are shown in Figs. 12.11b and 12.11c. We consider each of the cases shown.

When the valve is closed, there is no flow through the nozzle. The pressure is p_0 throughout, as shown by condition (i) in Fig. 12.11a.

If the back pressure, p_b , is now reduced to slightly less than p_0 , there will be flow through the nozzle with a decrease in pressure in the direction of flow, as shown by condition (ii). Flow at the exit plane will be subsonic with the exit-plane pressure equal to the back pressure.

As we continue to decrease the back pressure the flow rate will continue to increase, and the exit-plane pressure will continue to decrease, as shown by condition (iii) in Fig. 12.11a. As we progressively lower the back pressure the flow rate increases, and so do the velocity and Mach number at the exit plane.

The maximum flow rate occurs when we have sonic conditions at the exit plane, when $M_e = 1$, and $p_e = p_b = p^*$, the critical pressure. This is shown as condition (iv) in Fig. 12.11a, and is called a “choked flow,” beyond which the flow rate cannot be increased. From Eq. 12.30a with $M = 1$ (or from Eq. 12.21a),

$$\left. \frac{p_e}{p_0} \right|_{\text{choked}} = \frac{p^*}{p_0} = \left(\frac{2}{k+1} \right)^{k/(k-1)} \quad (12.31)$$

For air, $k = 1.4$, so $p_e/p_0|_{\text{choked}} = 0.528$. For example, if we wish to have sonic flow at the exit of a nozzle from a plenum chamber that is at atmospheric pressure, we would need to maintain a back pressure of about 7.76 psia, or about 6.94 psig vacuum. For the maximum, or choked, mass flow rate we have

$$\dot{m}_{\text{choked}} = \rho^* V^* A^*$$

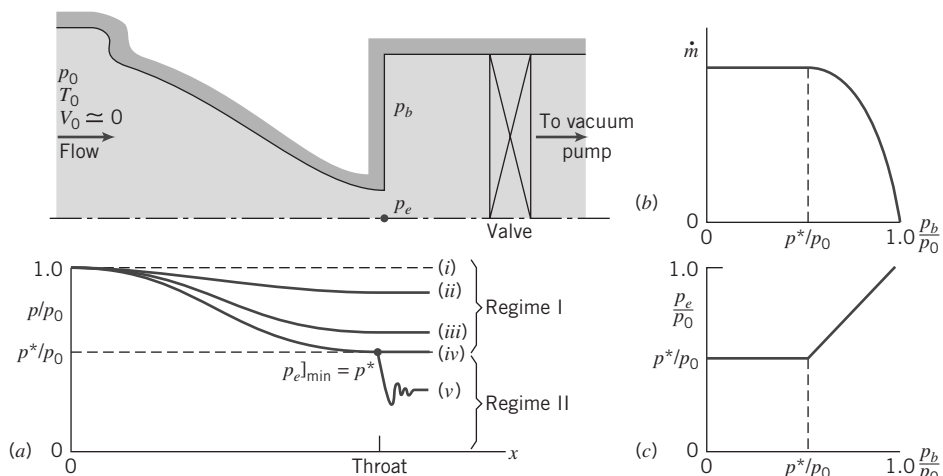


Fig. 12.11 Converging nozzle operating at various back pressures.

Using the ideal gas equation of state, Eq. 12.25e, and the stagnation to critical pressure and temperature ratios, Eqs. 12.30a and 12.30b respectively, with $M = 1$ (or Eqs. 12.21a and 12.21b, respectively), with $A^* = A_e$, it can be shown that this becomes

$$\dot{m}_{\text{choked}} = A_e p_0 \sqrt{\frac{k}{RT_0}} \left(\frac{2}{k+1} \right)^{(k+1)/2(k-1)} \quad (12.32a)$$

Note that for a given gas (k and R), the maximum flow rate in the converging nozzle depends *only* on the size of the exit area (A_e) and the conditions in the reservoir (p_0 , T_0).

For air, for convenience we write an “engineering” form of Eq. 12.32a,

$$\dot{m}_{\text{choked}} = 0.04 \frac{A_e p_0}{\sqrt{T_0}} \quad (12.32b)$$

with \dot{m}_{choked} in kg/s, A_e in m^2 , p_0 in Pa, and T_0 in K, and

$$\dot{m}_{\text{choked}} = 76.6 \frac{A_e p_0}{\sqrt{T_0}} \quad (12.32c)$$

with \dot{m}_{choked} in lbm/s, A_e in ft^2 , p_0 in psia, and T_0 in $^{\circ}\text{R}$.

If we continue to lower the back pressure, the flow remains choked. The mass flow rate does not increase, as shown in Fig. 12.11b, and the pressure distribution in the nozzle remains unchanged, with $p_e = p^* > p_b$, as shown in condition (v) in Figs. 12.11a and 12.11c. After exiting, the flow adjusts down to the applied back pressure, but does so in a nonisentropic, three-dimensional manner in a series of expansion waves and shocks, and for this part of the flow our one-dimensional, isentropic flow concepts no longer apply. We will return to this discussion in Section 12.8.

This idea of choked flow can be explained in at least two ways. First, we have already discussed that to increase the mass flow rate beyond choked would require $M_e > 1$, which is not possible. Second, once the flow reaches sonic conditions, it becomes “deaf” to downstream conditions: Any change (i.e., a reduction) in the applied back pressure propagates in the fluid at the speed of sound in all directions, so it gets “washed” downstream by the fluid which is moving at the speed of sound at the nozzle exit.

Flow through a converging nozzle may be divided into two regimes:

- 1 In Regime I, $1 \geq p_b/p_0 \geq p^*/p_0$. Flow to the throat is isentropic and $p_e = p_b$.
- 2 In Regime II, $p_b/p_0 < p^*/p_0$. Flow to the throat is isentropic, and $M_e = 1$. A nonisentropic expansion occurs in the flow leaving the nozzle and $p_e = p^* > p_b$ (entropy increases because this is adiabatic but irreversible).

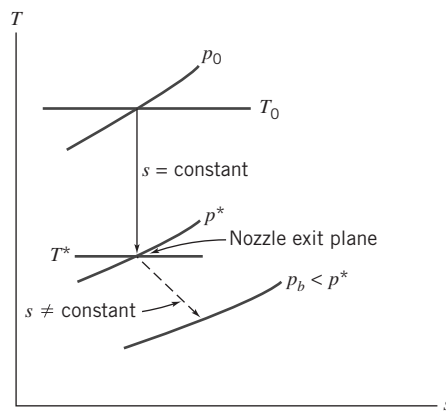


Fig. 12.12 Schematic Ts diagram for choked flow through a converging nozzle.

Although isentropic flow is an idealization, it often is a very good approximation for the actual behavior of nozzles. Since a nozzle is a device that accelerates a flow, the internal pressure gradient is favorable. This tends to keep the wall boundary layers thin and to minimize the effects of friction. The flow processes corresponding to Regime II are shown on a *Ts* diagram in Fig. 12.12. Two problems involving converging nozzles are solved in Examples 12.8 and 12.9.

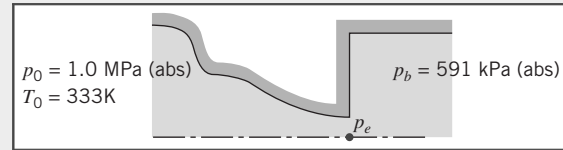
Example 12.8 ISENTROPIC FLOW IN A CONVERGING NOZZLE

A converging nozzle, with a throat area of 0.001 m^2 , is operated with air at a back pressure of 591 kPa (abs). The nozzle is fed from a large plenum chamber where the absolute stagnation pressure and temperature are 1.0 MPa and 60°C . The exit Mach number and mass flow rate are to be determined.

Given: Air flow through a converging nozzle at the conditions shown:

Flow is isentropic.

Find: (a) M_e .
(b) \dot{m} .

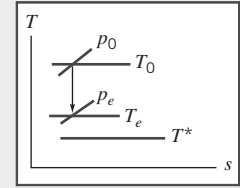


Solution: The first step is to check for choking. The pressure ratio is

$$\frac{p_b}{p_0} = \frac{5.91 \times 10^5}{1.0 \times 10^6} = 0.591 > 0.528$$

so the flow is *not* choked. Thus $p_b = p_e$, and the flow is isentropic, as sketched on the *Ts* diagram.

Since $p_0 = \text{constant}$, M_e may be found from the pressure ratio,



Solving for M_e , since $p_e = p_b$, we obtain

$$1 + \frac{k-1}{2} M_e^2 = \left(\frac{p_0}{p_b} \right)^{(k-1)/k}$$

and

$$M_e = \left\{ \left[\left(\frac{p_0}{p_b} \right)^{(k-1)/k} - 1 \right] \frac{2}{k-1} \right\}^{1/2} = \left\{ \left[\left(\frac{1.0 \times 10^6}{5.91 \times 10^5} \right)^{0.286} - 1 \right] \frac{2}{1.4-1} \right\}^{1/2} = 0.90 \quad M_e$$

The mass flow rate is

$$\dot{m} = \rho_e V_e A_e = \rho_e M_e c_e A_e$$

We need T to find ρ_e and c_e . Since $T_0 = \text{constant}$,

$$\frac{T_0}{T_e} = 1 + \frac{k-1}{2} M_e^2$$

or

$$T_e = \frac{T_0}{1 + \frac{k-1}{2} M_e^2} = \frac{(273 + 60)\text{K}}{1 + 0.2(0.9)^2} = 287 \text{ K}$$

$$c_e = \sqrt{kRT_e} = \left[1.4 \times 287 \frac{\text{N} \cdot \text{m}}{\text{kg} \cdot \text{K}} \times 287 \text{ K} \times \frac{\text{kg} \cdot \text{m}}{\text{N} \cdot \text{s}^2} \right]^{1/2} = 340 \text{ m/s}$$

and

$$\rho_e = \frac{p_e}{RT_e} = 5.91 \times 10^5 \frac{\text{N}}{\text{m}^2} \times \frac{\text{kg} \cdot \text{K}}{287 \text{ N} \cdot \text{m}} \times \frac{1}{287 \text{ K}} = 7.18 \text{ kg/m}^3$$

Finally,

$$\begin{aligned}\dot{m} &= \rho_e M_e c_e A_e = 7.18 \frac{\text{kg}}{\text{m}^3} \times 0.9 \times 340 \frac{\text{m}}{\text{s}} \times 0.0001 \text{ m}^2 \\ &= 2.20 \text{ kg/s} \end{aligned}$$

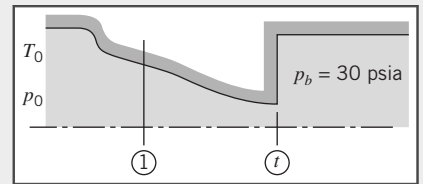
This problem illustrates use of the isentropic equations, Eqs. 12.30a for a flow that is not choked.

Example 12.9 CHOKED FLOW IN A CONVERGING NOZZLE

Air flows isentropically through a converging nozzle. At a section where the nozzle area is 0.013 ft^2 , the local pressure, temperature, and Mach number are 60 psia, 40°F , and 0.52, respectively. The back pressure is 30 psia. The Mach number at the throat, the mass flow rate, and the throat area are to be determined.

Given: Air flow through a converging nozzle at the conditions shown:

$$\begin{aligned}M_1 &= 0.52 \\T_1 &= 40^\circ\text{F} \\p_1 &= 60 \text{ psia} \\A_1 &= 0.013 \text{ ft}^2\end{aligned}$$



Find: (a) M_t . (b) \dot{m} . (c) A_t .

Solution:

First we check for choking, to determine if flow is isentropic down to p_b . To check, we evaluate the stagnation conditions.

$$p_0 = p_1 \left[1 + \frac{k-1}{2} M_1^2 \right]^{k/(k-1)} = 60 \text{ psia} [1 + 0.2(0.52)^2]^{3.5} = 72.0 \text{ psia}$$

The back pressure ratio is

$$\frac{p_b}{p_0} = \frac{30.0}{72.0} = 0.417 < 0.528$$

so the flow is choked. For choked flow,

$$M_t = 1.0$$

The T_s diagram is

The mass flow rate may be found from conditions at section ①, using $\rho_1 V_1 A_1$.

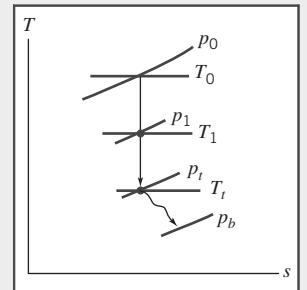
$$V_1 = M_1 c_1 = M_1 \sqrt{kRT_1}$$

$$= 0.52 \left[1.4 \times 53.3 \frac{\text{ft} \cdot \text{lbf}}{\text{lbm} \cdot {}^\circ\text{R}} \times (460 + 40) {}^\circ\text{R} \times 32.2 \frac{\text{lbm}}{\text{slug}} \times \frac{\text{slug} \cdot \text{ft}}{\text{lbf} \cdot \text{s}^2} \right]^{1/2}$$

$$V_1 = 570 \text{ ft/s}$$

$$\rho_1 = \frac{p_1}{RT_1} = 60 \frac{\text{lbf}}{\text{in.}^2} \times \frac{\text{lbm} \cdot {}^\circ\text{R}}{53.3 \text{ ft} \cdot \text{lbf}} \times \frac{1}{500 {}^\circ\text{R}} \times 144 \frac{\text{in.}^2}{\text{ft}^2} = 0.324 \text{ lbm/ft}^3$$

$$\dot{m} = \rho_1 V_1 A_1 = 0.324 \frac{\text{lbm}}{\text{ft}^3} \times 570 \frac{\text{ft}}{\text{s}} \times 0.013 \text{ ft}^2 = 2.40 \text{ lbm/s}$$



From Eq. 12.29,

$$\frac{A_1}{A^*} = \frac{1}{M_1} \left[\frac{1 + \frac{k-1}{2} M_1^2}{\frac{k+1}{2}} \right]^{(k+1)/2(k-1)} = \frac{1}{0.52} \left[\frac{1 + 0.2(0.52)^2}{1.2} \right]^{3.00} = 1.303$$

For choked flow, $A_t = A^*$. Thus,

$$A_t = A^* = \frac{A_1}{1.303} = \frac{0.013 \text{ ft}^2}{1.303}$$

$$A_t = 9.98 \times 10^{-3} \text{ ft}^2$$

This problem illustrates use of the isentropic equations, Eqs. 12.30a for a flow that is choked.

- Because the flow is choked, we could also have used Eq. 12.32a for \dot{m} (after finding T_0).

Isentropic Flow in a Converging-Diverging Nozzle

Having considered isentropic flow in a converging nozzle, we turn now to isentropic flow in a converging-diverging (C-D) nozzle. As in the previous case, flow through the converging-diverging passage of Fig. 12.13 is induced by a vacuum pump downstream, and is controlled by the valve shown; upstream stagnation conditions are constant. Pressure in the exit plane of the nozzle is p_e ; the nozzle discharges to back pressure p_b . As for the converging nozzle, we wish to see, among other things, how the flow rate varies with the driving force, the applied pressure difference ($p_0 - p_b$). Consider the effect of gradually reducing the back pressure. The results are illustrated graphically in Fig. 12.13. Let us consider each of the cases shown.

With the valve initially closed, there is no flow through the nozzle; the pressure is constant at p_0 . Opening the valve slightly (p_b slightly less than p_0) produces pressure distribution curve (i). If the flow rate is low enough, the flow will be subsonic and essentially incompressible at all points on this curve. Under these conditions, the C-D nozzle will behave as a venturi, with flow accelerating in the converging portion until a point of maximum velocity and minimum pressure is reached at the throat, then decelerating in the diverging portion to the nozzle exit.

As the valve is opened further and the flow rate is increased, a more sharply defined pressure minimum occurs, as shown by curve (ii). Although compressibility effects become important, the flow is still subsonic everywhere, and flow decelerates in the diverging section. Finally, as the valve is opened completely, curve (iii) results. At the section of minimum area the flow finally reaches $M = 1$, and the nozzle is choked. The flow rate is the maximum possible for the given nozzle and stagnation conditions.

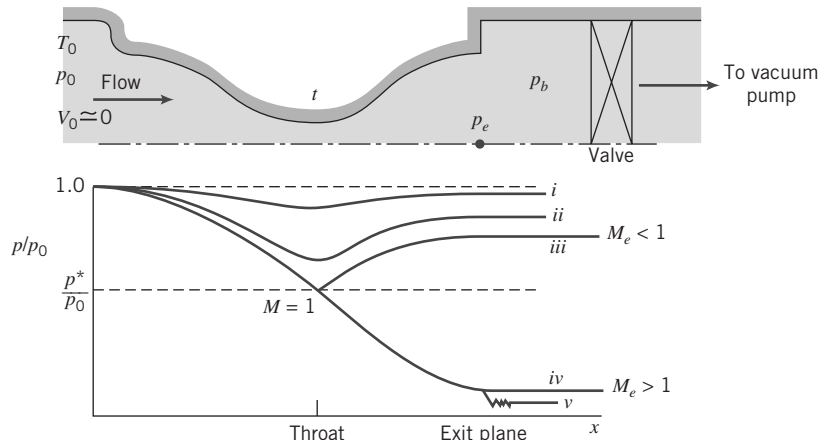


Fig. 12.13 Pressure distributions for isentropic flow in a converging-diverging nozzle.

All flows with pressure distributions (i), (ii), and (iii) are isentropic; as we progress from (i) to (ii) to (iii) we are generating increasing mass flow rates. Finally, when curve (iii) is reached, critical conditions are present at the throat. For this flow rate, the flow is choked, and

$$\dot{m} = \rho^* V^* A^*$$

where $A^* = A_t$, just as it was for the converging nozzle, and for this maximum possible flow rate Eq. 12.32a applies (with A_e replaced with the throat area A_t),

$$\dot{m}_{\text{choked}} = A_t p_0 \sqrt{\frac{k}{RT_0}} \left(\frac{2}{k+1} \right)^{(k+1)/2(k-1)} \quad (12.33a)$$

For a given gas (k and R), the maximum flow rate in the C-D nozzle depends *only* on the size of the throat area (A_t) and the conditions in the reservoir (p_0 , T_0).

As with the converging nozzle, for air we write an “engineering” form of Eq. 12.33a,

$$\dot{m}_{\text{choked}} = 0.04 \frac{A_t p_0}{\sqrt{T_0}} \quad (12.33b)$$

with \dot{m}_{choked} in kg/s, A_t in m^2 , p_0 in Pa, and T_0 in K, and

$$\dot{m}_{\text{choked}} = 76.6 \frac{A_t p_0}{\sqrt{T_0}} \quad (12.33c)$$

with \dot{m}_{choked} in lbm/s, A_t in ft^2 , p_0 in psia, and T_0 in °R. We again have Eqs. 12.32b and 12.32c, with the exit area A_e now replaced by the throat area A_t .

Any attempt to increase the flow rate by further lowering the back pressure will fail, for the two reasons we discussed earlier: once we attain sonic conditions, downstream changes can no longer be transmitted upstream; and we cannot exceed sonic conditions at the throat, because this would require passing through the sonic state somewhere in the converging section, which is not possible in isentropic flow.

With sonic conditions at the throat, we consider what *can* happen to the flow in the diverging section. We have previously discussed (see Fig. 12.8) that a diverging section will decelerate a subsonic flow ($M < 1$) but will accelerate a supersonic flow ($M > 1$). The flow in the diverging section can be either subsonic or supersonic, depending on the back pressure. We have already seen subsonic flow behavior [curve (iii)]: the applied back pressure leads to a gradual downstream pressure increase, decelerating the flow. We now consider accelerating the choked flow.

To accelerate flow in the diverging section requires a pressure decrease. This condition is illustrated by curve (iv) in Fig. 12.13. The flow will accelerate isentropically in the nozzle provided the exit pressure is set at p_{iv} . Thus, we see that with a throat Mach number of unity, there are two possible isentropic flow conditions in the converging-diverging nozzle. This is consistent with the results of Fig. 12.10, where we found two Mach numbers for each A/A^* in isentropic flow.

Lowering the back pressure below condition (iv), say to condition (v), has no effect on flow in the nozzle. The flow is isentropic from the plenum chamber to the nozzle exit [as in condition (iv)] and then it undergoes a three-dimensional irreversible expansion to the lower back pressure. A nozzle operating under these conditions is said to be *underexpanded*, since additional expansion takes place outside the nozzle.

A converging-diverging nozzle generally is intended to produce supersonic flow at the exit plane. If the back pressure is set at p_{iv} , flow will be isentropic through the nozzle, and supersonic at the nozzle exit. Nozzles operating at $p_b = p_{iv}$ [corresponding to curve (iv) in Fig. 12.13] are said to operate at *design conditions*.

Flow leaving a C-D nozzle is supersonic when the back pressure is at or below nozzle design pressure. The exit Mach number is fixed once the area ratio, A_e/A^* , is specified. All other exit plane

properties are uniquely related to stagnation properties by the fixed exit plane Mach number. The assumption of isentropic flow for a real nozzle at design conditions is a reasonable one. However, the one-dimensional flow model is inadequate for the design of relatively short nozzles.

Rocket-propelled vehicles use C-D nozzles to accelerate the exhaust gases to the maximum possible speed to produce high thrust. A propulsion nozzle is subject to varying ambient conditions during flight through the atmosphere, so it is impossible to attain the maximum theoretical thrust over the complete operating range. Because only a single supersonic Mach number can be obtained for each area ratio, nozzles for developing supersonic flow in wind tunnels often are built with interchangeable test sections, or with variable geometry.

For a converging-diverging nozzle operating with back pressure in the range $p_{iii} > p_b > p_{iv}$, the flow cannot expand isentropically to p_b . Under these conditions a shock occurs somewhere within the flow.

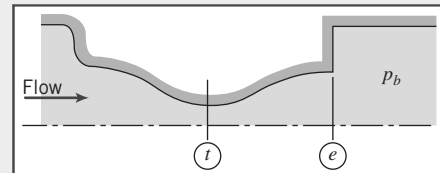
Nozzles operating with $p_{iii} > p_b > p_{iv}$ are said to be *overexpanded* because the pressure at some point in the nozzle is less than the back pressure. Obviously, an overexpanded nozzle could be made to operate at a new design condition by removing a portion of the diverging section. In Example 12.10, we consider isentropic flow in a C-D nozzle and in Example 12.11, we consider choked flow in a C-D nozzle.

Example 12.10 ISENTROPIC FLOW IN A CONVERGING-DIVERGING NOZZLE

Air flows isentropically in a converging-diverging nozzle, with exit area of 0.001 m^2 . The nozzle is fed from a large plenum where the stagnation conditions are 350 K and 1.0 MPa (abs). The exit pressure is 954 kPa (abs) and the Mach number at the throat is 0.68 . Fluid properties and area at the nozzle throat and the exit Mach number are to be determined.

Given: Isentropic flow of air in C-D nozzle as shown:

$$\begin{aligned} T_0 &= 350 \text{ K} \\ p_0 &= 1.0 \text{ MPa (abs)} \\ p_b &= 954 \text{ kPa (abs)} \\ M_t &= 0.68 \quad A_e = 0.001 \text{ m}^2 \end{aligned}$$



Find: (a) Properties and area at nozzle throat.

(b) M_e .

Solution: Stagnation temperature is constant for isentropic flow. Thus, since

$$\frac{T_0}{T} = 1 + \frac{k-1}{2} M^2$$

then

$$T_t = \frac{T_0}{1 + \frac{k-1}{2} M_t^2} = \frac{350 \text{ K}}{1 + 0.2(0.68)^2} = 320 \text{ K} \xrightarrow{T_t}$$

Also, since p_0 is constant for isentropic flow, then

$$\begin{aligned} p_t &= p_0 \left(\frac{T_t}{T_0} \right)^{k/(k-1)} = p_0 \left[\frac{1}{1 + \frac{k-1}{2} M_t^2} \right]^{k/(k-1)} \\ p_t &= 1.0 \times 10^6 \text{ Pa} \left[\frac{1}{1 + 0.2(0.68)^2} \right]^{3.5} = 734 \text{ kPa (abs)} \xrightarrow{p_t} \end{aligned}$$

so

$$\rho_t = \frac{p_t}{RT_t} = 7.34 \times 10^5 \frac{\text{N}}{\text{m}^2} \times \frac{\text{kg} \cdot \text{K}}{287 \text{ N} \cdot \text{m}} \times \frac{1}{320 \text{ K}} = 7.99 \text{ kg/m}^3 \xrightarrow{\rho_t}$$

and

$$V_t = M_t c_t = M_t \sqrt{kRT_t}$$

$$V_t = 0.68 \left[14 \times 287 \frac{\text{N} \cdot \text{m}}{\text{kg} \cdot \text{K}} \times 320 \text{ K} \times \frac{\text{kg} \cdot \text{m}}{\text{N} \cdot \text{s}^2} \right]^{1/2} = 244 \text{ m/s} \xrightarrow{V_t}$$

From Eq. 12.30d we can obtain a value of A_t/A^*

$$\frac{A_t}{A^*} = \frac{1}{M_t} \left[\frac{1 + \frac{k-1}{2} M_t^2}{\frac{k+1}{2}} \right]^{(k+1)/2(k-1)} = \frac{1}{0.68} \left[\frac{1 + 0.2(0.68)^2}{1.2} \right]^{3.00} = 1.11$$

but at this point A^* is not known.

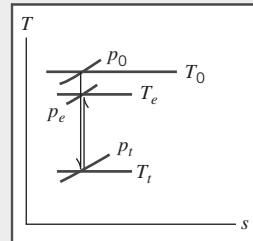
Since $M_t < 1$, flow at the exit must be subsonic. Therefore, $p_e = p_b$. Stagnation properties are constant, so

$$\frac{p_0}{p_e} = \left[1 + \frac{k-1}{2} M_e^2 \right]^{k/(k-1)}$$

Solving for M_e gives

$$M_e = \left\{ \left[\left(\frac{p_0}{p_e} \right)^{(k-1)/k} - 1 \right] \frac{2}{k-1} \right\}^{1/2} = \left\{ \left[\left(\frac{1.0 \times 10^6}{9.54 \times 10^5} \right)^{0.286} - 1 \right] (5) \right\}^{1/2} = 0.26 \xrightarrow{M_e}$$

The Ts diagram for this flow is



Since A_e and M_e are known, we can compute A^* . From Eq. 12.30d

$$\frac{A_e}{A^*} = \frac{1}{M_e} \left[\frac{1 + \frac{k-1}{2} M_e^2}{\frac{k+1}{2}} \right]^{(k+1)/2(k-1)} = \frac{1}{0.26} \left[\frac{1 + 0.2(0.26)^2}{1.2} \right]^{3.00} = 2.317$$

Thus,

$$A^* = \frac{A_e}{2.317} = \frac{0.001 \text{ m}^2}{2.317} = 4.32 \times 10^{-4} \text{ m}^2$$

and

$$A_t = 1.110 A^* = (1.110)(4.32 \times 10^{-4} \text{ m}^2)$$

$$= 4.80 \times 10^{-4} \text{ m}^2 \xrightarrow{A_t}$$

This problem illustrates use of the isentropic equations, Eqs. 12.30a for flow in a C-D nozzle that is not choked.

- Note that use of Eq. 12.30d allowed us to obtain the throat area without needing to first compute other properties.

Example 12.11 ISENTROPIC FLOW IN A CONVERGING-DIVERGING NOZZLE: CHOKED FLOW

The nozzle of Example 12.10 has a design back pressure of 87.5 kPa (abs) but is operated at a back pressure of 50.0 kPa (abs). Assume flow within the nozzle is isentropic. Determine the exit Mach number and mass flow rate.

Given: Air flow through C-D nozzle as shown:

$$T_0 = 350 \text{ K}$$

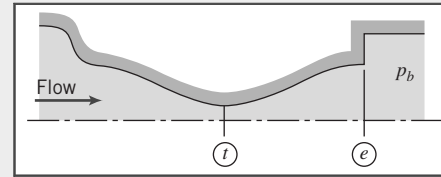
$$p_0 = 1.0 \text{ MPa (abs)}$$

$$p_e(\text{design}) = 87.5 \text{ kPa (abs)}$$

$$p_b = 50.0 \text{ kPa (abs)}$$

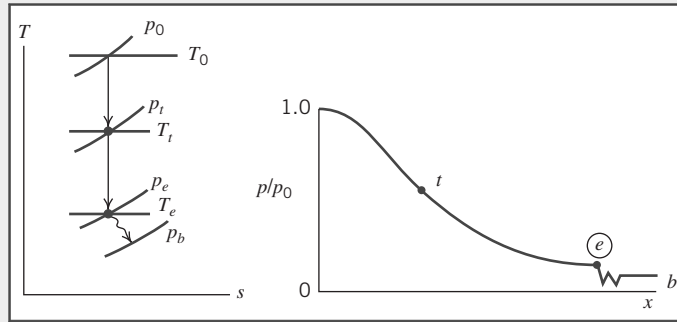
$$A_e = 0.001 \text{ m}^2$$

$$A_t = 4.8 \times 10^{-4} \text{ m}^2 \text{ (Example 12.10)}$$



Find: (a) M_e .
(b) \dot{m} .

Solution: The operating back pressure is *below* the design pressure. Consequently, the nozzle is underexpanded, and the Ts diagram and pressure distribution will be as shown:



Flow *within* the nozzle will be isentropic, but the irreversible expansion from p_e to p_b will cause an entropy increase; $p_e = p_e(\text{design}) = 87.5 \text{ kPa (abs)}$.

Since stagnation properties are constant for isentropic flow, the exit Mach number can be computed from the pressure ratio. Thus

$$\frac{p_0}{p_e} = \left[1 + \frac{k-1}{2} M_e^2 \right]^{k/(k-1)}$$

or

$$M_e = \sqrt{\frac{\left(\frac{p_0}{p_e} \right)^{(k-1)/k} - 1}{\frac{2}{k-1}}} = \sqrt{\frac{\left(\frac{1.0 \times 10^6}{8.75 \times 10^4} \right)^{0.286} - 1}{0.4}} = 2.24$$

Because the flow is choked we can use Eq. 12.33b for the mass flow rate,

$$\dot{m}_{\text{choked}} = 0.04 \frac{A_t p_0}{\sqrt{T_0}} \quad (12.33b)$$

(with \dot{m}_{choked} in kg/s, A_t in m^2 , p_0 in Pa, and T_0 in K), so

$$\dot{m}_{\text{choked}} = 0.04 \times 4.8 \times 10^{-4} \times 1 \times 10^6 / \sqrt{350}$$

$$\dot{m} = \dot{m}_{\text{choked}} = 1.04 \text{ kg/s} \quad \dot{m}$$

This problem illustrates use of the isentropic equations, Eqs. 12.30a for flow in a C-D nozzle that is choked.
• Note that we used Eq. 12.33b, an “engineering equation”—that is, an equation containing a coefficient that has units.

12.7 Normal Shocks

We mentioned normal shocks in the previous section in the context of flow through a nozzle. In practice, these irreversible discontinuities can occur in any supersonic flow field, in either internal flow or external flow. Knowledge of property changes across shocks and of shock behavior is important in understanding the design of supersonic diffusers, e.g., for inlets on high performance aircraft, and supersonic wind tunnels.

Before applying the basic equations to normal shocks, it is important to form a clear physical picture of the shock itself. Although it is physically impossible to have discontinuities in fluid properties, the normal shock is nearly discontinuous. The thickness of a shock is about $0.2 \mu\text{m}$ (10^{-5} in.), or roughly 4 times the mean free path of the gas molecules. Large changes in pressure, temperature, and other properties occur across this small distance. Fluid particle decelerations through the shock reach tens of millions of gs . These considerations justify treating the normal shock as an abrupt discontinuity; we are interested in changes occurring across the shock rather than in the details of its structure.

Consider the short control volume surrounding a normal shock standing in a passage of arbitrary shape shown in Fig. 12.14. As for isentropic flow with area variation (Section 12.6), our starting point in analyzing this normal shock is the set of basic equations (Eqs. 12.24), describing one-dimensional motion that may be affected by several phenomena: area change, friction, and heat transfer. These are

$$\rho_1 V_1 A_1 = \rho_2 V_2 A_2 = \rho V A = \dot{m} = \text{constant} \quad (12.24a)$$

$$R_x + p_1 A_1 - p_2 A_2 = \dot{m} V_2 - \dot{m} V_1 \quad (12.24b)$$

$$\frac{\delta Q}{dm} + h_1 + \frac{V_1^2}{2} = h_2 + \frac{V_2^2}{2} \quad (12.24c)$$

$$\dot{m}(s_2 - s_1) \geq \int_{\text{CS}} \frac{1}{T} \left(\frac{\dot{Q}}{A} \right) dA \quad (12.24d)$$

$$p = \rho R T \quad (12.24e)$$

$$\Delta h = h_2 - h_1 = c_p \Delta T = c_p (T_2 - T_1) \quad (12.24f)$$

$$\Delta s = s_2 - s_1 = c_p \ln \frac{T_2}{T_1} - R \ln \frac{p_2}{p_1} \quad (12.24g)$$

We recall that Equation 12.24a is *continuity*, Eq. 12.24b is a *momentum equation*, Eq. 12.24c is an *energy equation*, Eq. 12.24d is the *second law of thermodynamics*, and Eqs. 12.24e, 12.24f, and 12.24g are useful *property relations* for an ideal gas with constant specific heats.

Basic Equations for a Normal Shock

We can now simplify Eqs. 12.24 for flow of an ideal gas with constant specific heats through a normal shock. The most important simplifying feature is that the width of the control volume is infinitesimal (in reality about $0.2 \mu\text{m}$), so $A_1 \approx A_2 \approx A$, the force due to the walls $R_x \approx 0$ because the control volume wall surface area is infinitesimal, and the heat exchange with the walls $\delta Q/dm \approx 0$, for the same reason. Hence, for this flow our equations become

$$\rho_1 V_1 = \rho_2 V_2 = \frac{\dot{m}}{A} = \text{constant} \quad (12.34a)$$

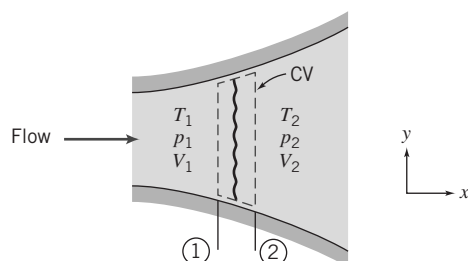


Fig. 12.14 Control volume used for analysis of normal shock.

$$p_1 A - p_2 A = \dot{m} V_2 - \dot{m} V_1$$

or, using Eq. 12.34a,

$$p_1 + \rho_1 V_1^2 = p_2 + \rho_2 V_2^2 \quad (12.34b)$$

$$h_{01} = h_1 + \frac{V_1^2}{2} = h_2 + \frac{V_2^2}{2} = h_{02} \quad (12.34c)$$

$$s_2 > s_1 \quad (12.34d)$$

$$p = \rho R T \quad (12.34e)$$

$$\Delta h = h_2 - h_1 = c_p \Delta T = c_p (T_2 - T_1) \quad (12.34f)$$

$$\Delta s = s_2 - s_1 = c_p \ln \frac{T_2}{T_1} - R \ln \frac{p_2}{p_1} \quad (12.34g)$$

Equations 12.34 can be used to analyze flow through a normal shock. For example, if we know conditions before the shock, at section ① (i.e., p_1 , ρ_1 , T_1 , s_1 , h_1 , and V_1), we can use these equations to find conditions after the shock, at section ②. We have six equations (not including the constraint of Eq. 12.34d) and six unknowns (p_2 , ρ_2 , T_2 , s_2 , h_2 , and V_2). Hence, for given upstream conditions there is a single unique downstream state. To analyze a shock, we need to solve this set of *nonlinear coupled algebraic* equations. We have shown that changes in a one-dimensional flow can be caused by area variation, friction, or heat transfer, but in deriving Eqs. 12.34 we have eliminated all three causes. In the absence of area change, friction, and heat transfer, flow properties will not change *except* in a very abrupt, irreversible manner, for which the entropy increases. In fact, all properties except T_0 change through the shock.

A normal shock can occur only when the incoming flow is supersonic. Fluid flows will generally gradually adjust to downstream conditions (e.g., an obstacle in the flow) as the pressure field redirects the flow (e.g., around the object). However, if the flow is moving at such a speed that the pressure field cannot propagate upstream (when the flow speed, V , is greater than the local speed of sound, c , or in other words $M > 1$), then the fluid has to “violently” adjust to the downstream conditions. The pressure suddenly increases through the shock, so that, at the instant a particle is passing through the shock, there is a very large negative pressure gradient. This pressure gradient causes a dramatic reduction in speed, V , and hence a rapid rise in temperature, T , as kinetic energy is converted to internal thermal energy, and the density, ρ , increases through the shock. Because the shock is adiabatic but highly irreversible, entropy, s , increases through the shock. Finally, we see that as speed, V , decreases and the speed of sound, c , increases (because temperature, T , increases) through the normal shock, the Mach number, M , decreases; in fact, we will see later that it always becomes subsonic. These results are shown graphically in Fig. 12.15 and in tabular form in Table 12.1.

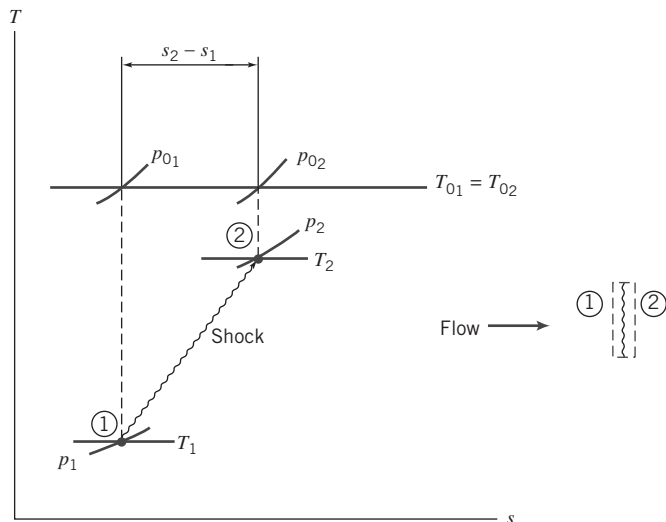


Fig. 12.15 Schematic of normal-shock process on the Ts plane.

Table 12.1

Summary of Property Changes Across a Normal Shock

Property	Effect	Obtained from:
Stagnation temperature	$T_0 = \text{Constant}$	Energy equation
Entropy	$s \uparrow$	Second law
Stagnation pressure	$p_0 \downarrow$	T_s diagram
Temperature	$T \uparrow$	T_s diagram
Velocity	$V \downarrow$	Energy equation, and effect on T
Density	$\rho \uparrow$	Continuity equation, and effect on V
Pressure	$p \uparrow$	Momentum equation, and effect on V
Mach number	$M \downarrow$	$M = V/c$, and effects on V and T

Normal-Shock Flow Functions for One-Dimensional Flow of an Ideal Gas

The basic equations, Eqs. 12.34, can be used to analyze flows that experience a normal shock. However, it is often more convenient to use Mach number-based equations, in this case based on the incoming Mach number, M_1 . This involves three steps: First, we obtain property ratios (e.g., T_2/T_1 and p_2/p_1) in terms of M_1 and M_2 , then we develop a relation between M_1 and M_2 , and finally, we use this relation to obtain expressions for property ratios in terms of upstream Mach number, M_1 .

The temperature ratio can be expressed as

$$\frac{T_2}{T_1} = \frac{T_2}{T_{02}} \frac{T_{02}}{T_{01}} \frac{T_{01}}{T_1}$$

Since stagnation temperature is constant across the shock, we have

$$\frac{T_2}{T_1} = \frac{1 + \frac{k-1}{2} M_1^2}{1 + \frac{k-1}{2} M_2^2} \quad (12.35)$$

A velocity ratio may be obtained by using

$$\frac{V_2}{V_1} = \frac{M_2 c_2}{M_1 c_1} = \frac{M_2 \sqrt{kRT_2}}{M_1 \sqrt{kRT_1}} = \frac{M_2}{M_1} \sqrt{\frac{T_2}{T_1}}$$

or

$$\frac{V_2}{V_1} = \frac{M_2}{M_1} \left[\frac{1 + \frac{k-1}{2} M_1^2}{1 + \frac{k-1}{2} M_2^2} \right]^{1/2}$$

A ratio of densities may be obtained from the continuity equation

$$\rho_1 V_1 = \rho_2 V_2 \quad (12.34a)$$

so that

$$\frac{\rho_2}{\rho_1} = \frac{V_1}{V_2} = \frac{M_1}{M_2} \left[\frac{1 + \frac{k-1}{2} M_2^2}{1 + \frac{k-1}{2} M_1^2} \right]^{1/2} \quad (12.36)$$

Finally, we have the momentum equation,

$$p_1 + \rho_1 V_1^2 = p_2 + \rho_2 V_2^2 \quad (12.34b)$$

Substituting $\rho = p/RT$, and factoring out pressures, gives

$$p_1 \left[1 + \frac{V_1^2}{RT_1} \right] = p_2 \left[1 + \frac{V_2^2}{RT_2} \right]$$

Since

$$\frac{V^2}{RT} = k \frac{V^2}{kRT} = kM^2$$

then

$$p_1 [1 + kM_1^2] = p_2 [1 + kM_2^2]$$

Finally,

$$\frac{p_2}{p_1} = \frac{1 + kM_1^2}{1 + kM_2^2} \quad (12.37)$$

To solve for M_2 in terms of M_1 , we must obtain another expression for one of the property ratios given by Eqs. 12.35 through 12.37.

From the ideal gas equation of state, the temperature ratio may be written as

$$\frac{T_2}{T_1} = \frac{p_2/\rho_2 R}{p_1/\rho_1 R} = \frac{p_2 \rho_1}{p_1 \rho_2}$$

Substituting from Eqs. 12.36 and 12.37 yields

$$\frac{T_2}{T_1} = \left[\frac{1 + kM_1^2}{1 + kM_2^2} \right] \frac{M_2}{M_1} \left[\frac{1 + \frac{k-1}{2} M_1^2}{1 + \frac{k-1}{2} M_2^2} \right]^{1/2} \quad (12.38)$$

Equations 12.35 and 12.38 are two equations for T_2/T_1 . We can combine them and solve for M_2 in terms of M_1 . Combining and canceling gives

$$\left[\frac{1 + \frac{k-1}{2} M_1^2}{1 + \frac{k-1}{2} M_2^2} \right]^{1/2} = \frac{M_2}{M_1} \left[\frac{1 + kM_1^2}{1 + kM_2^2} \right]$$

Squaring, we obtain

$$\frac{1 + \frac{k-1}{2} M_1^2}{1 + \frac{k-1}{2} M_2^2} = \frac{M_2^2}{M_1^2} \left[\frac{1 + 2kM_1^2 + k^2 M_1^4}{1 + 2kM_2^2 + k^2 M_2^4} \right]$$

which may be solved explicitly for M_2^2 . Two solutions are obtained:

$$M_2^2 = M_1^2 \quad (12.39a)$$

and

$$M_2^2 = \frac{M_1^2 + \frac{2}{k-1}}{\frac{2k}{k-1} M_1^2 - 1} \quad (12.39b)$$

Obviously, the first of these is trivial. The second expresses the unique dependence of M_2 on M_1 .

Now, having a relationship between M_2 and M_1 , we can solve for property ratios across a shock. Knowing M_1 , we obtain M_2 from Eq. 12.39b; the property ratios can be determined subsequently from Eqs. 12.35 through 12.37.

Since the stagnation temperature remains constant, the stagnation temperature ratio across the shock is unity. The ratio of stagnation pressures is evaluated as

$$\frac{p_{0_2}}{p_{0_1}} = \frac{p_{0_2} p_2 p_1}{p_2 p_1 p_{0_1}} = \frac{p_2}{p_1} \left[\frac{1 + \frac{k-1}{2} M_2^2}{1 + \frac{k-1}{2} M_1^2} \right]^{k/(k-1)} \quad (12.40)$$

Combining Eqs. 12.37 and 12.39b, we obtain (after considerable algebra)

$$\frac{p_2}{p_1} = \frac{1 + kM_1^2}{1 + kM_2^2} = \frac{2k}{k+1} M_1^2 - \frac{k-1}{k+1} \quad (12.41)$$

Using Eqs. 12.39b and 12.41, we find that Eq. 12.40 becomes

$$\frac{p_{0_2}}{p_{0_1}} = \frac{\left[\frac{k+1}{2} M_1^2 \right]^{k/(k-1)}}{\left[\frac{2k}{k+1} M_1^2 - \frac{k-1}{k+1} \right]^{1/(k-1)}} \quad (12.42)$$

After substituting for M_2^2 from Eq. 12.39b into Eqs. 12.35 and 12.36, we summarize the set of Mach number-based equations (renumbered for convenience) for use with an ideal gas passing through a normal shock:

$$M_2^2 = \frac{M_1^2 + \frac{2}{k-1}}{\frac{2k}{k-1} M_1^2 - 1} \quad (12.43a)$$

$$\frac{p_{0_2}}{p_{0_1}} = \frac{\left[\frac{k+1}{2} M_1^2 \right]^{k/(k-1)}}{\left[\frac{2k}{k+1} M_1^2 - \frac{k-1}{k+1} \right]^{1/(k-1)}} \quad (12.43b)$$

$$\frac{T_2}{T_1} = \frac{\left(1 + \frac{k-1}{2} M_1^2 \right) \left(k M_1^2 - \frac{k-1}{2} \right)}{\left(\frac{k+1}{2} \right)^2 M_1^2} \quad (12.43c)$$

$$\frac{p_2}{p_1} = \frac{2k}{k+1} M_1^2 - \frac{k-1}{k+1} \quad (12.43d)$$

$$\frac{\rho_2}{\rho_1} = \frac{V_1}{V_2} = \frac{\frac{k+1}{2} M_1^2}{1 + \frac{k-1}{2} M_1^2} \quad (12.43e)$$

Equations 12.43 are useful for analyzing flow through a normal shock. Note that all changes through a normal shock depend only on the incoming Mach number M_1 and the ratio of specific heats, k . The equations are usually preferable to the original equations, Eq. 12.34, because they provide explicit, uncoupled expressions for property changes; Eqs. 12.34 are occasionally useful too. Note that Eq. 12.43d requires $M_1 > 1$ for $p_2 > p_1$, which agrees with our previous discussion. The ratio p_2/p_1 is known as the *strength* of the shock; the higher the incoming Mach number, the stronger (more violent) the shock.

Equations 12.43, while quite complex algebraically, provide explicit property relations in terms of the incoming Mach number, M_1 . They are easily programmed and there are also interactive websites that make them available (e.g. [5] and [6]). The equations can also be programmed in *Excel* and

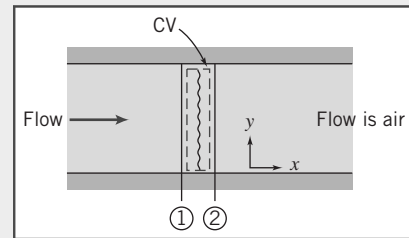
spreadsheets are available from the website; with the add-ins, functions are available for computing M_2 , and the stagnation pressure, temperature, pressure, and density/velocity ratios, from M_1 , and M_1 from these ratios. Appendix D.2 lists flow functions for M_2 and property ratios p_{02}/p_{01} , T_2/T_1 , p_2/p_1 , and $\rho_2/\rho_1(V_1/V_2)$ in terms of M_1 for normal-shock flow of an ideal gas. A table of values, as well as a plot of these property ratios, is presented for air ($k = 1.4$) for a limited range of Mach numbers. A problem involving a normal shock is solved in Example 12.12.

Example 12.12 NORMAL SHOCK IN A DUCT

A normal shock stands in a duct. The fluid is air, which may be considered an ideal gas. Properties upstream from the shock are $T_1 = 5^\circ\text{C}$, $p_1 = 65.0 \text{ kPa (abs)}$, and $V_1 = 668 \text{ m/s}$. Determine properties downstream and $s_2 - s_1$. Sketch the process on a Ts diagram.

Given: Normal shock in a duct as shown:

$$\begin{aligned} T_1 &= 5^\circ\text{C} \\ P_1 &= 65.0 \text{ kPa (abs)} \\ V_1 &= 668 \text{ m/s} \end{aligned}$$



Find: (a) Properties at section ②.
(b) $s_2 - s_1$.
(c) Ts diagram.

Solution: First compute the remaining properties at section ①. For an ideal gas,

$$\begin{aligned} \rho_1 &= \frac{P_1}{RT_1} = 6.5 \times 10^4 \frac{\text{N}}{\text{m}^2} \times \frac{\text{kg} \cdot \text{K}}{287 \text{ N} \cdot \text{m}} \times \frac{1}{278 \text{ K}} = 0.815 \text{ kg/m}^3 \\ c_1 &= \sqrt{kRT_1} = \left[1.4 \times 287 \frac{\text{N} \cdot \text{m}}{\text{kg} \cdot \text{K}} \times 278 \text{ K} \times \frac{\text{kg} \cdot \text{m}}{\text{N} \cdot \text{s}^2} \right]^{1/2} = 334 \text{ m/s} \end{aligned}$$

Then $M_1 = \frac{V_1}{c_1} = \frac{668}{334} = 2.00$, and (using isentropic stagnation relations, Eqs. 12.21b and 12.21a)

$$\begin{aligned} T_{01} &= T_1 \left(1 + \frac{k-1}{2} M_1^2 \right) = 278 \text{ K} [1 + 0.2(2.0)^2] = 500 \text{ K} \\ p_{01} &= p_1 \left(1 + \frac{k-1}{2} M_1^2 \right)^{k/(k-1)} = 65.0 \text{ kPa} [1 + 0.2(2.0)^2]^{3.5} = 509 \text{ kPa (abs)} \end{aligned}$$

From the normal-shock flow functions, Eqs. 12.43, at $M_1 = 2.0$,

M_1	M_2	p_{02}/p_{01}	T_2/T_1	p_2/p_1	V_2/V_1
2.00	0.5774	0.7209	1.687	4.500	0.3750

From these data

$$\begin{aligned} T_2 &= 1.687T_1 = (1.687)278 \text{ K} = 469 \text{ K} & T_2 \\ p_2 &= 4.500p_1 = (4.500)65.0 \text{ kPa} = 293 \text{ kPa (abs)} & p_2 \\ V_2 &= 0.3750V_1 = (0.3750)668 \text{ m/s} = 251 \text{ m/s} & V_2 \end{aligned}$$

For an ideal gas,

$$\rho_2 = \frac{p_2}{RT_2} = 2.93 \times 10^5 \frac{\text{N}}{\text{m}^2} \times \frac{\text{kg} \cdot \text{K}}{287 \text{ N} \cdot \text{m}} \times \frac{1}{469 \text{ K}} = 2.18 \text{ kg/m}^3 \xrightarrow{\hspace{10cm}} \rho_2$$

Stagnation temperature is constant in adiabatic flow. Thus

$$T_{02} = T_{01} = 500 \text{ K} \xrightarrow{\hspace{10cm}} T_{02}$$

Using the property ratios for a normal shock, we obtain

$$p_{02} = p_{01} \frac{p_{02}}{p_{01}} = 509 \text{ kPa (0.7209)} = 367 \text{ kPa (abs)} \xrightarrow{\hspace{10cm}} p_{02}$$

For the change in entropy (Eq. 12.34g),

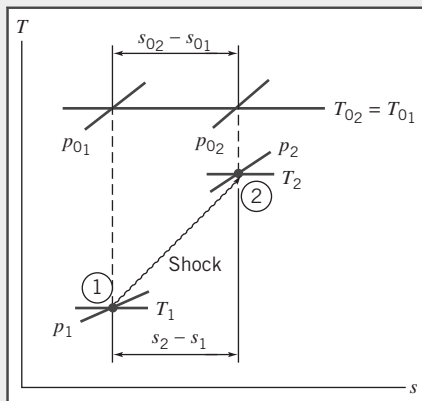
$$s_2 - s_1 = c_p \ln \frac{T_2}{T_1} - R \ln \frac{p_2}{p_1}$$

But $s_{02} - s_{01} = s_2 - s_1$, so

$$s_{02} - s_{01} = s_2 - s_1 = c_p \ln \frac{T_{02}}{T_{01}} - R \ln \frac{p_{02}}{p_{01}} = -0.287 \frac{\text{kJ}}{\text{kg} \cdot \text{K}} \times \ln(0.7209) \xrightarrow{\hspace{10cm}} s_2 - s_1$$

$$s_2 - s_1 = 0.0939 \text{ kJ/(kg} \cdot \text{K})$$

The Ts diagram is



This problem illustrates the use of the normal shock relations, Eqs. 12.43, for analyzing flow of an ideal gas through a normal shock.

12.8 Supersonic Channel Flow with Shocks

Supersonic flow is a necessary condition for a normal shock to occur and the possibility of a normal shock must be considered in any supersonic flow. Sometimes a shock *must* occur to match a downstream pressure condition; it is desirable to determine if a shock will occur and the shock location when it does occur.

In this section isentropic flow in a converging-diverging nozzle (Section 12.6) is extended to include shocks and complete our discussion of flow in a converging-diverging nozzle operating under varying back pressures. The pressure distribution through a nozzle for different back pressures is shown in Fig. 12.16.

Four flow regimes are possible. In Regime I the flow is subsonic throughout. The flow rate increases with decreasing back pressure. At condition (iii), which forms the dividing line between Regimes I and II, flow at the throat is sonic, and $M_t = 1$.

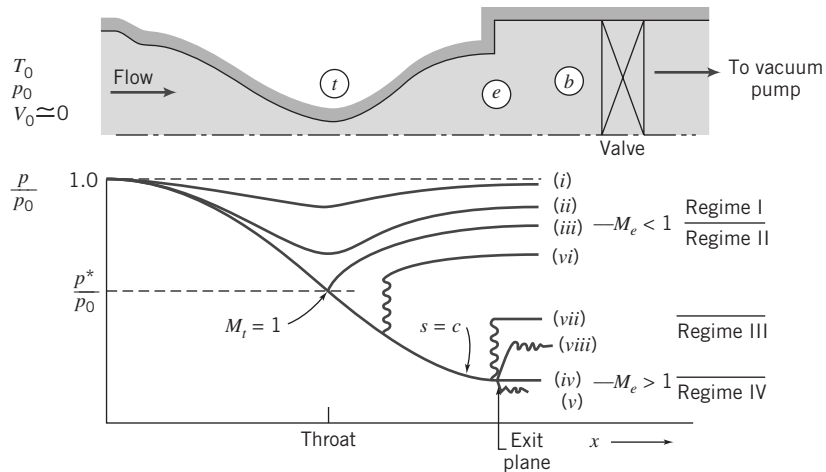


Fig. 12.16 Pressure distributions for flow in a converging–diverging nozzle for different back pressures.

As the back pressure is lowered below condition (iii), a normal shock appears downstream from the throat, as shown by condition (vi). There is a pressure rise across the shock. Since the flow is subsonic ($M < 1$) after the shock, the flow decelerates, with an accompanying increase in pressure, through the diverging channel. As the back pressure is lowered further, the shock moves downstream until it appears at the exit plane (condition vii). In Regime II, as in Regime I, the exit flow is subsonic, and consequently $p_e = p_b$. Since flow properties at the throat are constant for all conditions in Regime II, the flow rate in Regime II does not vary with back pressure.

In Regime III, as exemplified by condition (viii), the back pressure is higher than the exit pressure, but not high enough to sustain a normal shock in the exit plane. The flow adjusts to the back pressure through a series of oblique compression shocks outside the nozzle; these oblique shocks cannot be treated by one-dimensional theory.

As previously noted in Section 12.6, condition (iv) represents the design condition. In Regime IV the flow adjusts to the lower back pressure through a series of oblique expansion waves outside the nozzle; these oblique expansion waves cannot be treated by one-dimensional theory.

The Ts diagram for converging-diverging nozzle flow with a normal shock is shown in Fig. 12.17; state ① is located immediately upstream from the shock and state ② is immediately downstream. The entropy increase across the shock moves the subsonic downstream flow to a new isentropic line. The critical temperature is constant, so p_2^* is lower than p_1^* . Since $\rho^* = p^*/RT^*$, the critical density downstream also is reduced. To carry the same mass flow rate, the downstream flow must have a larger critical area. From continuity (and the equation of state), the critical area ratio is the inverse of the critical pressure ratio, i.e., across a shock, $p^*A^* = \text{constant}$.

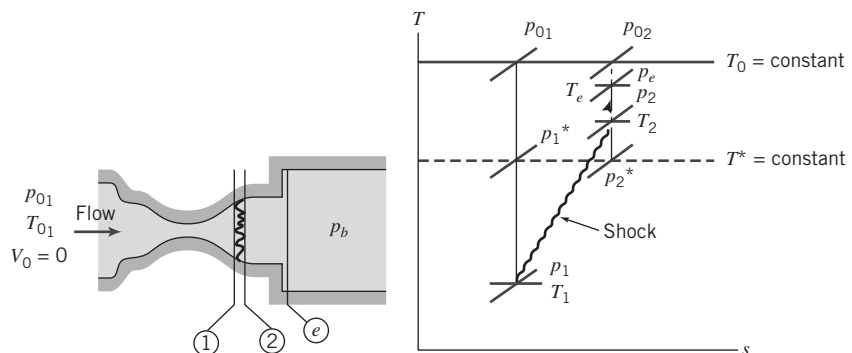


Fig. 12.17 Schematic Ts diagram for flow in a converging–diverging nozzle with a normal shock.

If the Mach number (or position) of the normal shock in the nozzle is known, the exit-plane pressure can be calculated directly. In the more realistic situation, the exit-plane pressure is specified, and the position and strength of the shock are unknown. The subsonic flow downstream must leave the nozzle at the back pressure, so $p_b = p_e$. Then

$$\frac{p_b}{p_{0_1}} = \frac{p_e}{p_{0_1}} = \frac{p_e}{p_{0_2}} \frac{p_{0_2}}{p_{0_1}} = \frac{p_e}{p_{0_2}} \frac{A_1^*}{A_2^*} = \frac{p_e}{p_{0_2}} \frac{A_t}{A_e} \frac{A_e}{A_2^*} \quad (12.44)$$

Because we have isentropic flow from state ② (after the shock) to the exit plane, $A_2^* = A_e^*$ and $p_{0_2} = p_{0_e}$. Then from Eq. 12.44 we can write

$$\frac{p_e}{p_{0_1}} = \frac{p_e}{p_{0_2}} \frac{A_t}{A_e} \frac{A_e}{A_2^*} = \frac{p_e}{p_{0_e}} \frac{A_t}{A_e} \frac{A_e}{A_e^*}$$

Rearranging,

$$\frac{p_e}{p_{0_1}} \frac{A_e}{A_t} = \frac{p_e}{p_{0_e}} \frac{A_e}{A_e^*} \quad (12.45)$$

In Eq. 12.45 the left side contains known quantities, and the right side is a function of the exit Mach number M_e only. The pressure ratio is obtained from the stagnation pressure relation (Eq. 12.21a); the area ratio is obtained from the isentropic area relation (Eq. 12.30d). Finding M_e from Eq. 12.45 usually requires iteration. The magnitude and location of the normal shock can be found once M_e is known by rearranging Eq. 12.45 (remembering that $p_{0_2} = p_{0_e}$),

$$\frac{p_{0_2}}{p_{0_1}} = \frac{A_t}{A_e} \frac{A_e}{A_e^*} \quad (12.46)$$

In Eq. 12.46 the right side is known (the first area ratio is given and the second is a function of M_e only), and the left side is a function of the Mach number before the shock, M_1 , only. Hence, M_1 can be found. The area at which this shock occurs can then be found from the isentropic area relation (Eq. 12.30d, with $A^* = A_t$) for isentropic flow between the throat and state ①.

In this introductory chapter on compressible flow, we have covered some of the basic flow phenomena and presented the equations that allow us to evaluate the flow properties in some of the simpler flow situations. There are many more complex compressible flow situations and we have provided an introduction to some of these advanced topics on the Instructor website.

12.9 Summary and Useful Equations

In this chapter, we:

- ✓ Reviewed the basic equations used in thermodynamics, including isentropic relations.
- ✓ Introduced some compressible flow terminology, such as definitions of the Mach number and subsonic, supersonic, transonic, and hypersonic flows.
- ✓ Learned about several phenomena having to do with the speed of sound.
- ✓ Learned the two useful reference states for a compressible flow: the isentropic stagnation condition, and the isentropic critical condition.
- ✓ Developed a set of governing equations for one-dimensional flow of a compressible fluid as it may be affected by area change, friction, heat exchange, and normal shocks.
- ✓ Developed the equations for isentropic flow affected only by area change.
- ✓ Developed the relations for a normal-shock.

While investigating the above flows we developed insight into some interesting compressible flow phenomena, including:

- ✓ Use of Ts plots in visualizing flow behavior.
- ✓ The necessary shape of, subsonic and supersonic nozzles and diffusers.
- ✓ The phenomenon of choked flow in converging nozzles and C-D nozzles, and the circumstances under which shock waves develop in C-D nozzles.

Note: Most of the equations in the table below have a number of constraints or limitations. Be sure to refer to their page numbers for details! In particular, most of them assume an ideal gas, with constant specific heats.

Useful Equations

Definition of Mach number M :	$M \equiv \frac{V}{c}$	(12.13)	Page 467
Speed of sound c :	$c = \sqrt{\left(\frac{\partial p}{\partial \rho}\right)_s}$	(12.16)	Page 469
Speed of sound c (solids and liquids):	$c = \sqrt{E_v/\rho}$	(12.17)	Page 469
Speed of sound c (ideal gas):	$c = \sqrt{kRT}$	(12.18)	Page 470
Mach cone angle α :	$\alpha = \sin^{-1} \left(\frac{1}{M} \right)$	(12.19)	Page 472
Isentropic pressure ratio (ideal gas, constant specific heats):	$\frac{p_0}{p} = \left[1 + \frac{k-1}{2} M^2 \right]^{k/(k-1)}$	(12.21a)	Page 477
Isentropic temperature ratio (ideal gas, constant specific heats):	$\frac{T_0}{T} = 1 + \frac{k-1}{2} M^2$	(12.21b)	Page 477
Isentropic density ratio (ideal gas, constant specific heats):	$\frac{\rho_0}{\rho} = \left[1 + \frac{k-1}{2} M^2 \right]^{1/(k-1)}$	(12.21c)	Page 477
Critical pressure ratio (ideal gas, constant specific heats):	$\frac{p_0}{p_*} = \left[\frac{k+1}{2} \right]^{k/(k-1)}$	(12.22a)	Page 480
Critical temperature ratio (ideal gas, constant specific heats):	$\frac{T_0}{T_*} = \frac{k+1}{2}$	(12.22b)	Page 480
Critical density ratio (ideal gas, constant specific heats):	$\frac{\rho_0}{\rho_*} = \left[\frac{k+1}{2} \right]^{1/(k-1)}$	(12.22c)	Page 480
Critical velocity V^* (ideal gas, constant specific heats):	$V^* = c_* = \sqrt{\frac{2k}{k+1} RT_0}$	(12.23)	Page 480
One-dimensional flow equations:	$\rho_1 V_1 A_1 = \rho_2 V_2 A_2 = \rho V A = \dot{m} = \text{constant}$ $R_x + p_1 A_1 - p_2 A_2 = \dot{m} V_2 - \dot{m} V_1$ $\frac{\delta Q}{dm} + h_1 + \frac{V_1^2}{2} = h_2 + \frac{V_2^2}{2}$ $\dot{m}(s_2 - s_1) \geq \int_{CS} \frac{1}{T} \left(\frac{\dot{Q}}{A} \right) dA$ $p = \rho RT$ $\Delta h = h_2 - h_1 = c_p \Delta T = c_p (T_2 - T_1)$ $\Delta s = s_2 - s_1 = c_p \ln \frac{T_2}{T_1} - R \ln \frac{p_2}{p_1}$	(12.24a) (12.24b) (12.24c) (12.24d) (12.24e) (12.24f) (12.24g)	Page 483
Isentropic relations: These equations are listed and tabulated and plotted for air in Appendix D.	$\frac{p_0}{p} = f(M)$ $\frac{T_0}{T} = f(M)$ $\frac{\rho_0}{\rho} = f(M)$ $\frac{A}{A^*} = f(M)$	(12.30a) (12.30b) (12.30c) (12.30d)	Page 488
Pressure ratio for choked converging nozzle, $p_e/p_0 _{\text{choked}}$:	$\left. \frac{p_e}{p_0} \right _{\text{choked}} = \frac{p_*}{p_0} = \left(\frac{2}{k+1} \right)^{k/(k-1)}$	(12.31)	Page 492

Table (Continued)

Mass flow rate for choked converging nozzle:	$\dot{m}_{\text{choked}} = A_e p_0 \sqrt{\frac{k}{RT_0}} \left(\frac{2}{k+1} \right)^{(k+1)/2(k-1)}$	(12.32a)	Page 493
Mass flow rate for choked converging nozzle (SI units):	$\dot{m}_{\text{choked}} = 0.04 \frac{A_e p_0}{\sqrt{T_0}}$	(12.32b)	Page 493
Mass flow rate for choked converging nozzle (English Engineering units):	$\dot{m}_{\text{choked}} = 76.6 \frac{A_e p_0}{\sqrt{T_0}}$	(12.32c)	Page 493
Mass flow rate for choked converging-diverging nozzle:	$\dot{m}_{\text{choked}} = A_t p_0 \sqrt{\frac{k}{RT_0}} \left(\frac{2}{k+1} \right)^{(k+1)/2(k-1)}$	(12.33a)	Page 497
Mass flow rate for choked converging-diverging nozzle (SI units):	$\dot{m}_{\text{choked}} = 0.04 \frac{A_t p_0}{\sqrt{T_0}}$	(12.33b)	Page 497
Mass flow rate for choked converging-diverging nozzle (English Engineering units):	$\dot{m}_{\text{choked}} = 76.6 \frac{A_t p_0}{\sqrt{T_0}}$	(12.33c)	Page 497
Normal shock relations: These equations are listed and tabulated and plotted for air in Appendix D.	$M_2 = f(M_1)$ $\frac{p_{02}}{p_{01}} = f(M_1)$ $\frac{T_2}{T_1} = f(M_1)$ $\frac{p_2}{p_1} = f(M_1)$ $\frac{\rho_2}{\rho_1} = \frac{V_1}{V_2} = f(M_1)$	(12.43a) (12.43b) (12.43c) (12.43d) (12.43e)	Page 505
Useful relations for determining the normal shock location in converging-diverging nozzle:	$\frac{p_e}{p_{01}} \frac{A_e}{A_t} = \frac{p_e}{p_{0e}} \frac{A_e}{A_e^*}$ $\frac{p_{02}}{p_{01}} = \frac{A_t}{A_e} \frac{A_e}{A_e^*}$	(12.45) (12.46)	Page 509

REFERENCES

1. Moran, M. J., H. N. Shapiro, D. D. Boettner, and M. B. Bailey, *Fundamentals of Engineering Thermodynamics*, 8th ed. John Wiley and Sons, ISBN: ES8-1-118-41293-0, 20, 2014.
2. Shapiro, A. *The Dynamics and Thermodynamics of Compressible Fluid Flow*, Volume 1, John Wiley and Sons, ISBN: 978-0-471-06691-0, 1953.
3. Rathakrishnan, E. *Applied Gas Dynamics*, 2nd ed. John Wiley and Sons, ISBN: 978-1-119-50045-2, 2019.
4. Wong, G. S. K., Speed of Sound in Standard Air, *J. Acoustical Society America*, 79, 5, May 1986, pp. 1359–1366.
5. National Aeronautics and Space Administration, <https://www.grc.nasa.gov/www/k-12/airplane/isentrop.html>, 2019.
6. Devenport, W., *Isentropic Calculator*, Virginia Polytechnic Institute and State University, <http://www.aoe.vt.edu/aoe3114/calc.html>, 2014.

APPENDIX A

Fluid Property Data

A.1 Specific Gravity

Specific gravity data for several common liquids and solids are presented in Fig. A.1*a* and *b* and in Tables A.1 and A.2. For liquids specific gravity is a function of temperature. (Density data for water and air are given as functions of temperature in Tables A.7 through A.10.) For most liquids specific gravity decreases as temperature increases. Water is unique: It displays a maximum density of 1000 kg/m³(1.94 slug/ft³) at 4°C (39°F). The maximum density of water is used as a reference value to calculate specific gravity. Thus

$$SG \equiv \frac{\rho}{\rho_{H_2O} \text{ (at } 4^\circ\text{C)}}$$

Consequently, the maximum SG of water is exactly unity.

Specific gravities for solids are relatively insensitive to temperature; values given in Table A.1 were measured at 20°C.

The specific gravity of seawater depends on both its temperature and salinity. A representative value for ocean water is SG = 1.025, as given in Table A.2.

A-2 Appendix A Fluid Property Data

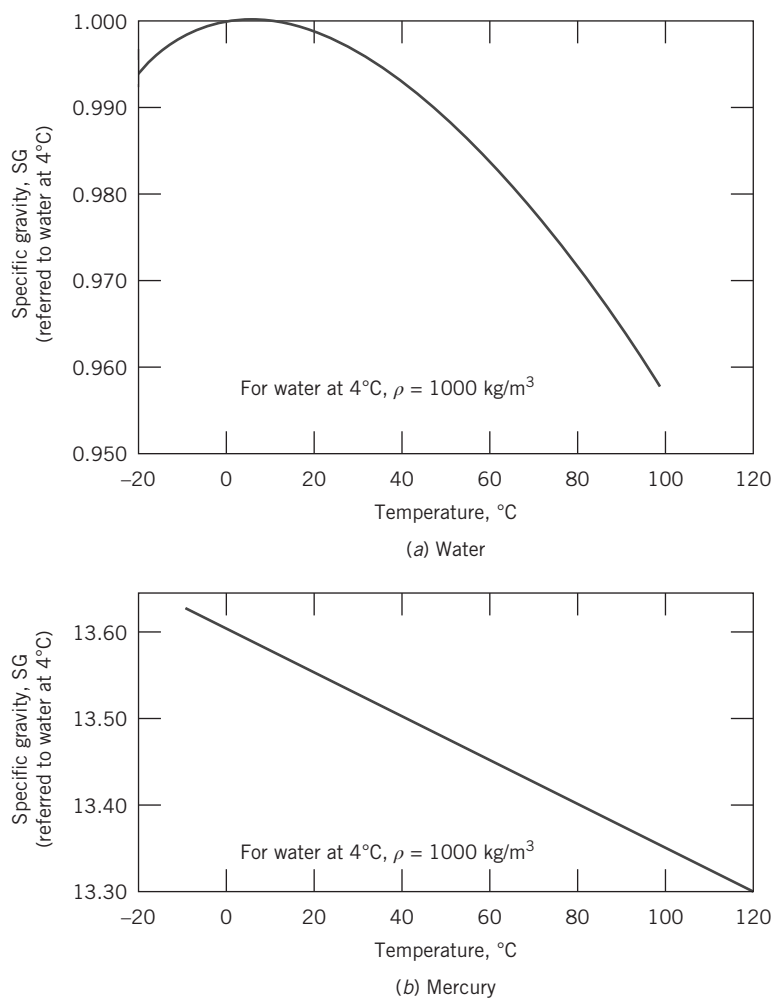


Fig. A.1 Specific gravity of water and mercury as functions of temperature. (Data from Reference [1].) (The specific gravity of mercury varies linearly with temperature. The variation is given by $SG = 13.60 - 0.00240 T$ when T is measured in $^{\circ}\text{C}$.)

Table A.1
Specific Gravities of Selected Engineering Materials

(a) Common Manometer Liquids at 20°C	
Liquid	Specific Gravity
E.V. Hill blue oil	0.797
Meriam red oil	0.827
Benzene	0.879
Dibutyl phthalate	1.04
Monochloronaphthalene	1.20
Carbon tetrachloride	1.595
Bromoethylbenzene (Meriam blue)	1.75
Tetrabromoethane	2.95
Mercury	13.55

Source: Data from References [1–3].

Table A.1
Specific Gravities of Selected Engineering Materials (*Continued*)

(b) Common Materials	
Material	Specific Gravity (—)
Aluminum	2.64
Balsa wood	0.14
Brass	8.55
Cast Iron	7.08
Concrete (cured)	2.4 ^a
Concrete (liquid)	2.5 ^a
Copper	8.91
Ice (0°C)	0.917
Lead	11.4
Oak	0.77
Steel	7.83
Styrofoam (1 pcf ^b)	0.0160
Styrofoam (3 pcf)	0.0481
Uranium (depleted)	18.7
White pine	0.43

Source: Data from Reference [4].

^adepending on aggregate.

^bpounds per cubic foot.

Table A.2
Physical Properties of Common Liquids at 20°C

Liquid	Isentropic Bulk Modulus ^a (GN/m ²)	Specific Gravity (—)
Benzene	1.48	0.879
Carbon tetrachloride	1.36	1.595
Castor oil	2.11	0.969
Crude oil	—	0.82–0.92
Ethanol	—	0.789
Gasoline	—	0.72
Glycerin	4.59	1.26
Heptane	0.886	0.684
Kerosene	1.43	0.82
Lubricating oil	1.44	0.88
Methanol	—	0.796
Mercury	28.5	13.55
Octane	0.963	0.702
Seawater ^b	2.42	1.025
SAE 10W oil	—	0.92
Water	2.24	0.998

Source: Data from References [1, 5, 6].

^aCalculated from speed of sound; 1 GN/m² = 10⁹ N/m² (1 N/m² = 1.45 × 10⁻⁴ lbf/in.²).

^bDynamic viscosity of seawater at 20°C is $\mu = 1.08 \times 10^{-3}$ N·s/m². (Thus, the kinematic viscosity of seawater is about 5 percent higher than that of freshwater.)

Table A.3
Properties of the U.S. Standard Atmosphere

Geometric Altitude (m)	Temperature (K)	p/p_{SL} (—)	ρ/ρ_{SL} (—)
-500	291.4	1.061	1.049
0	288.2	1.000 ^a	1.000 ^b
500	284.9	0.9421	0.9529
1,000	281.7	0.8870	0.9075
1,500	278.4	0.8345	0.8638
2,000	275.2	0.7846	0.8217
2,500	271.9	0.7372	0.7812
3,000	268.7	0.6920	0.7423
3,500	265.4	0.6492	0.7048
4,000	262.2	0.6085	0.6689
4,500	258.9	0.5700	0.6343
5,000	255.7	0.5334	0.6012
6,000	249.2	0.4660	0.5389
7,000	242.7	0.4057	0.4817
8,000	236.2	0.3519	0.4292
9,000	229.7	0.3040	0.3813
10,000	223.3	0.2615	0.3376
11,000	216.8	0.2240	0.2978
12,000	216.7	0.1915	0.2546
13,000	216.7	0.1636	0.2176
14,000	216.7	0.1399	0.1860
15,000	216.7	0.1195	0.1590
16,000	216.7	0.1022	0.1359
17,000	216.7	0.08734	0.1162
18,000	216.7	0.07466	0.09930
19,000	216.7	0.06383	0.08489
20,000	216.7	0.05457	0.07258
22,000	218.6	0.03995	0.05266
24,000	220.6	0.02933	0.03832
26,000	222.5	0.02160	0.02797
28,000	224.5	0.01595	0.02047
30,000	226.5	0.01181	0.01503
40,000	250.4	0.002834	0.003262
50,000	270.7	0.0007874	0.0008383
60,000	255.8	0.0002217	0.0002497
70,000	219.7	0.00005448	0.00007146
80,000	180.7	0.00001023	0.00001632
90,000	180.7	0.000001622	0.000002588

Source: Data from Reference [7].

^a $p_{SL} = 1.01325 \times 10^5 \text{ N/m}^2$ (abs) (= 14.696 psia).

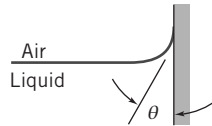
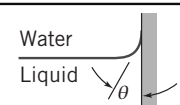
^b $\rho_{SL} = 1.2250 \text{ kg/m}^3$ (= 0.002377 slug/ft³).

A.2 Surface Tension

The values of surface tension, σ , for most organic compounds are remarkably similar at room temperature; the typical range is 25 to 40 mN/m. Water is higher, at about 73 mN/m at 20°C. Liquid metals have values in the range between 300 and 600 mN/m; mercury has a value of about 480 mN/m at 20°C. Surface tension decreases with temperature; the decrease is nearly linear with absolute temperature. Surface tension at the critical temperature is zero.

Values of σ are usually reported for surfaces in contact with the pure vapor of the liquid being studied or with air. At low pressures both values are about the same.

Table A.4
Surface Tension of Common Liquids at 20°C

Liquid	Surface Tension, σ (mN/m) ^a	Contact Angle, θ (degrees)
(a) In contact with air		
Benzene	28.9	
Carbon tetrachloride	27.0	
Ethanol	22.3	
Glycerin	63.0	
Hexane	18.4	
Kerosene	26.8	
Lube oil	25–35	
Mercury	484	140
Methanol	22.6	
Octane	21.8	
Water	72.8	~0
Source: Data from References [1, 5, 8, 9].		
(b) In contact with water		
Benzene	35.0	
Carbon tetrachloride	45.0	
Hexane	51.1	
Mercury	375	140
Methanol	22.7	
Octane	50.8	

Source: Data from References [1, 5, 8, 9].

^a 1 mN/m = 10⁻³ N/m.

A.3 The Physical Nature of Viscosity

Viscosity is a measure of internal fluid friction, i.e., resistance to deformation. The mechanism of gas viscosity is reasonably well understood, but the theory is poorly developed for liquids. We can gain some insight into the physical nature of viscous flow by discussing these mechanisms briefly.

The viscosity of a Newtonian fluid is fixed by the state of the material. Thus, $\mu = \mu(T, p)$. Temperature is the more important variable, so let us consider it first. Excellent empirical equations for viscosity as a function of temperature are available.

Effect of Temperature on Viscosity

a. Gases

All gas molecules are in continuous random motion. When there is bulk motion due to flow, the bulk motion is superimposed on the random motions. It is then distributed throughout the fluid by molecular collisions. Analyses based on kinetic theory predict

$$\mu \propto \sqrt{T}$$

The kinetic theory prediction is in fair agreement with experimental trends, but the constant of proportionality and one or more correction factors must be determined; this limits practical application of this simple equation.

A-6 Appendix A Fluid Property Data

If two or more experimental points are available, the data may be correlated using the empirical Sutherland correlation [7]

$$\mu = \frac{bT^{1/2}}{1 + S/T} \quad (\text{A.1})$$

Constants b and S may be determined most simply by writing

$$\mu = \frac{bT^{3/2}}{S+T}$$

or

$$\frac{T^{3/2}}{\mu} = \left(\frac{1}{b}\right)T + \frac{S}{b}$$

(Compare this with $y = mx + c$.) From a plot of $T^{3/2}/\mu$ versus T , one obtains the slope, $1/b$, and the intercept, S/b . For air,

$$b = 1.458 \times 10^{-6} \frac{\text{kg}}{\text{m} \cdot \text{s} \cdot \text{K}^{1/2}}$$

$$S = 110.4 \text{ K}$$

These constants were used with Eq. A.1 to compute viscosities for the standard atmosphere in [7], the air viscosity values at various temperatures shown in Table A.10, and using appropriate conversion factors, the values shown in Table A.9.

b. Liquids

Viscosities for liquids cannot be estimated well theoretically. The phenomenon of momentum transfer by molecular collisions is overshadowed in liquids by the effects of interacting force fields among the closely packed liquid molecules.

Liquid viscosities are affected drastically by temperature. This dependence on absolute temperature may be represented by the empirical equation

$$\mu = Ae^{B/(T-C)} \quad (\text{A.2})$$

or the equivalent form

$$\mu = A10^{B/(T-C)} \quad (\text{A.3})$$

where T is absolute temperature.

Equation A.3 requires at least three points to fit constants A , B , and C . In theory, it is possible to determine the constants from measurements of viscosity at just three temperatures. It is better practice to use more data and to obtain the constants from a statistical fit to the data.

However a curve-fit is developed, always compare the resulting line or curve with the available data. The best way is to critically inspect a plot of the curve-fit compared with the data. In general, curve-fit results will be satisfactory only when the quality of the available data and that of the empirical relation are known to be excellent.

Data for the dynamic viscosity of water are fitted well using constant values $A = 2.414 \times 10^{-5}$ N·s/m², $B = 247.8$ K, and $C = 140$ K. Reference [10] states that using these constants in Eq. A.3 predicts water viscosity within ± 2.5 percent over the temperature range from 0°C to 370°C. Equation A.3 and *Excel* were used to compute the water viscosity values at various temperatures shown in Table A.8, and using appropriate conversion factors, the values shown in Table A.7.

Note that the viscosity of a liquid decreases with temperature, while that of a gas increases with temperature.

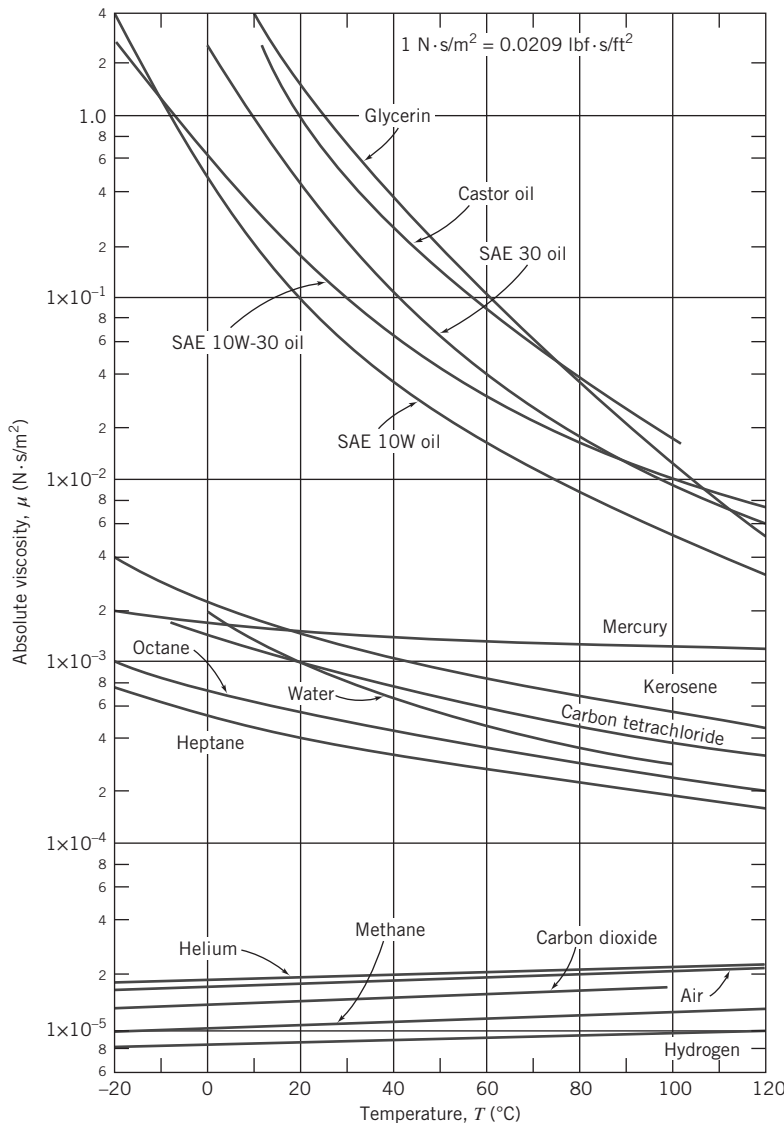


Fig. A.2 Dynamic (absolute) viscosity of common fluids as a function of temperature. (Data from References [1, 6, 10].)

Effect of Pressure on Viscosity

a. Gases

The viscosity of gases is essentially independent of pressure between a few hundredths of an atmosphere and a few atmospheres. However, viscosity at high pressures increases with pressure (or density).

b. Liquids

The viscosities of most liquids are not affected by moderate pressures, but large increases have been found at very high pressures. For example, the viscosity of water at 10,000 atm is twice that at 1 atm. More complex compounds show a viscosity increase of several orders of magnitude over the same pressure range.

More information may be found in Reid and Sherwood [11].

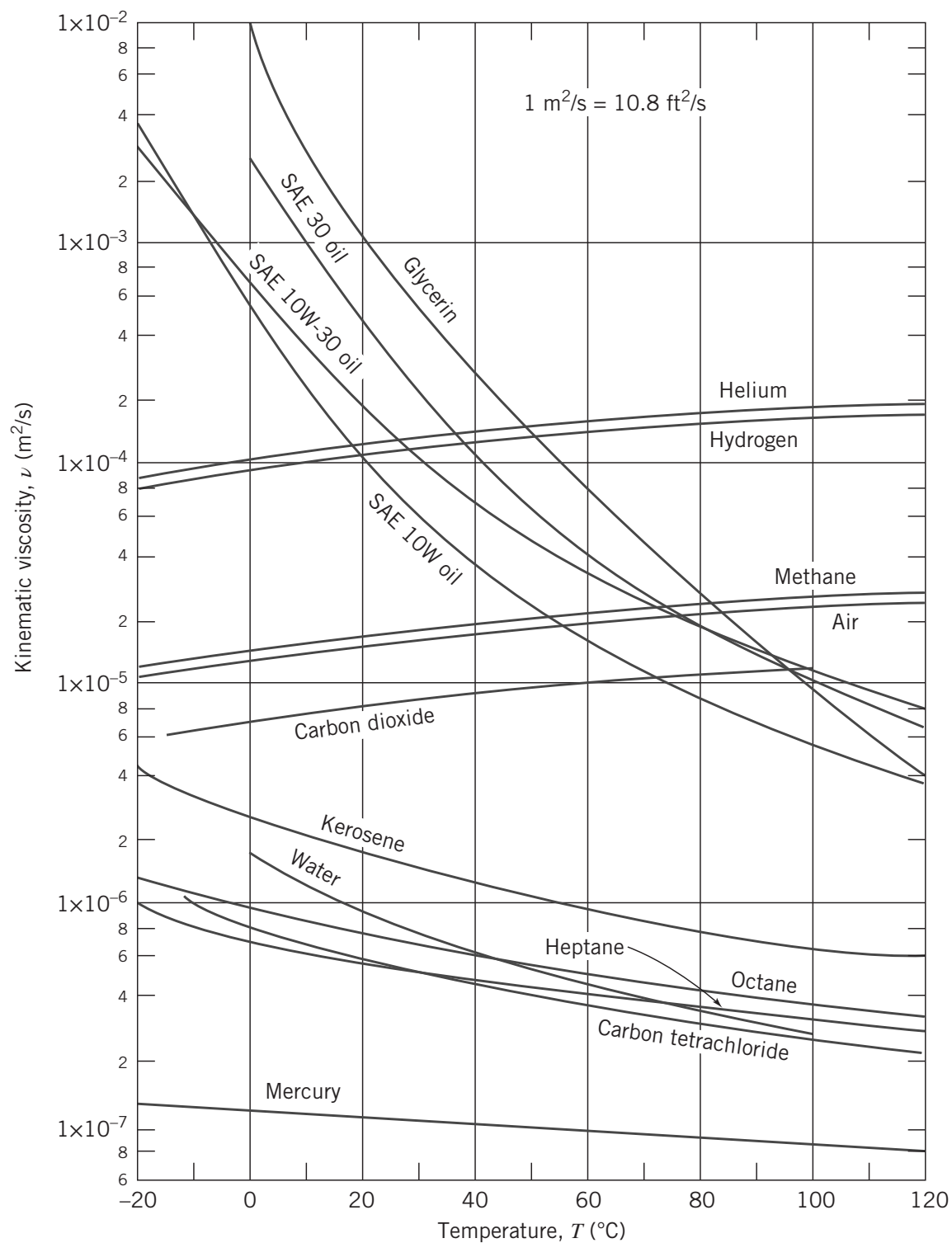


Fig. A.3 Kinematic viscosity of common fluids (at atmospheric pressure) as a function of temperature. (Data from References [1, 6, 10].)

A.4 Lubricating Oils

Engine and transmission lubricating oils are classified by viscosity according to standards established by the Society of Automotive Engineers [12]. The allowable viscosity ranges for several grades are given in Table A.5.

Viscosity numbers with W (e.g., 20W) are classified by viscosity at 0°F. Those without W are classified by viscosity at 210°F.

Multigrade oils (e.g., 10W-40) are formulated to minimize viscosity variation with temperature. High polymer “viscosity index improvers” are used in blending these multigrade oils. Such additives are highly non-Newtonian; they may suffer permanent viscosity loss caused by shearing.

Special charts are available to estimate the viscosity of petroleum products as a function of temperature. The charts were used to develop the data for typical lubricating oils plotted in Figs. A.2 and A.3. For details, see [15].

Table A.5
Allowable Viscosity Ranges for Lubricants

Engine Oil	SAE Viscosity Grade	Max. Viscosity (cP) ^a at Temp. (°C)	Viscosity (cSt) ^b at 100°C	
			Min	Max
	0W	3250 at -30	3.8	—
	5W	3500 at -25	3.8	—
	10W	3500 at -20	4.1	—
	15W	3500 at -15	5.6	—
	20W	4500 at -10	5.6	—
	25W	6000 at -5	9.3	—
	20	—	5.6	<9.3
	30	—	9.3	<12.5
	40	—	12.5	<16.3
	50	—	16.3	<21.9
Axe and Manual Transmission Lubricant	SAE Viscosity Grade	Max. Temp. (°C) for Viscosity of 150,000 cP	Viscosity (cSt) at 100°C	
			Min	Max
			4.1	—
			4.1	—
			7.0	—
			11.0	—
			13.5	<24.0
			24.0	<41.0
Automatic Transmission Fluid (Typical)	Maximum Viscosity (cP)	Temperature (°C)	Viscosity (cSt) at 100°C	
			Min	Max
			6.5	8.5
			6.5	8.5
			6.5	8.5

Source: Data from References [12–14].

^a centipoise = 1 cP = 1 mPa · s = 10^{-3} Pa · s ($= 2.09 \times 10^{-5}$ lbf · s/ft²).

^b centistoke = 10^{-6} m²/s ($= 1.08 \times 10^{-5}$ ft²/s).

A.5 Properties of Common Gases, Air, and Water

Table A.6Thermodynamic Properties of Common Gases at STP^a

Gas	Chemical Symbol	Molecular Mass, M_m	$\left(\frac{R^b}{\text{kg} \cdot \text{K}}\right)$	$\left(\frac{c_p}{\text{kg} \cdot \text{K}}\right)$	$\left(\frac{c_v}{\text{kg} \cdot \text{K}}\right)$	$k = \frac{c_p}{c_v}$	$\left(\frac{R^b}{\text{lbm} \cdot \text{R}}\right)$	$\left(\frac{c_p}{\text{Btu}}\right)$	$\left(\frac{c_v}{\text{Btu}}\right)$
Air	—	28.98	286.9	1004	717.4	1.40	53.33	0.2399	0.1713
Carbon dioxide	CO ₂	44.01	188.9	840.4	651.4	1.29	35.11	0.2007	0.1556
Carbon monoxide	CO	28.01	296.8	1039	742.1	1.40	55.17	0.2481	0.1772
Helium	He	4.003	2077	5225	3147	1.66	386.1	1.248	0.7517
Hydrogen	H ₂	2.016	4124	14,180	10,060	1.41	766.5	3.388	2.402
Methane	CH ₄	16.04	518.3	2190	1672	1.31	96.32	0.5231	0.3993
Nitrogen	N ₂	28.01	296.8	1039	742.0	1.40	55.16	0.2481	0.1772
Oxygen	O ₂	32.00	259.8	909.4	649.6	1.40	48.29	0.2172	0.1551
Steam ^c	H ₂ O	18.02	461.4	~2000	~1540	~1.30	85.78	~0.478	~0.368

Source: Data from References [7, 16, 17].

^a STP = standard temperature and pressure, $T = 15^\circ\text{C} = 59^\circ\text{F}$ and $p = 101.325 \text{ kPa (abs)} = 14.696 \text{ psia}$.

^b $R \equiv R_u/M_m; R_u = 8314.3 \text{ J/(kgmol} \cdot \text{K}) = 1545.3 \text{ ft} \cdot \text{lbf}/(\text{lbmol} \cdot \text{R})$; 1 Btu = 778.2 ft · lbf.

^c Water vapor behaves as an ideal gas when superheated to 55°C (100°F) or more.

Table A.7

Properties of Water (U.S. Customary Units)

Temperature, T ($^\circ\text{F}$)	Density, ρ (slug/ft ³)	Dynamic Viscosity, μ (lbf · s/ft ²)	Kinematic Viscosity, ν (ft ² /s)	Surface Tension, σ (lbf/ft)	Vapor Pressure, p_v (psia)	Bulk Modulus, E_v (psi)
32	1.94	3.68E-05	1.90E-05	0.00519	0.0886	2.92E + 05
40	1.94	3.20E-05	1.65E-05	0.00514	0.122	
50	1.94	2.73E-05	1.41E-05	0.00509	0.178	
59	1.94	2.38E-05	1.23E-05	0.00504	0.247	
60	1.94	2.35E-05	1.21E-05	0.00503	0.256	
68	1.94	2.10E-05	1.08E-05	0.00499	0.339	
70	1.93	2.05E-05	1.06E-05	0.00498	0.363	3.20E + 05
80	1.93	1.80E-05	9.32E-06	0.00492	0.507	
90	1.93	1.59E-05	8.26E-06	0.00486	0.699	
100	1.93	1.43E-05	7.38E-06	0.00480	0.950	
110	1.92	1.28E-05	6.68E-06	0.00474	1.28	
120	1.92	1.16E-05	6.05E-06	0.00467	1.70	3.32E + 05
130	1.91	1.06E-05	5.54E-06	0.00461	2.23	
140	1.91	9.70E-06	5.08E-06	0.00454	2.89	
150	1.90	8.93E-06	4.70E-06	0.00448	3.72	
160	1.89	8.26E-06	4.37E-06	0.00441	4.75	
170	1.89	7.67E-06	4.06E-06	0.00434	6.00	
180	1.88	7.15E-06	3.80E-06	0.00427	7.52	
190	1.87	6.69E-06	3.58E-06	0.00420	9.34	
200	1.87	6.28E-06	3.36E-06	0.00413	11.5	3.08E + 05
212	1.86	5.84E-06	3.14E-06	0.00404	14.7	

Table A.8

Properties of Water (SI Units)

Temperature, <i>T</i> (°C)	Density, <i>ρ</i> (kg/m ³)	Dynamic Viscosity, <i>μ</i> (N·s/m ²)	Kinematic Viscosity, <i>ν</i> (m ² /s)	Surface Tension, <i>σ</i> (N/m)	Vapor Pressure, <i>p_v</i> (kPa)	Bulk Modulus, <i>E_v</i> (GPa)
0	1000	1.76E-03	1.76E-06	0.0757	0.661	2.01
5	1000	1.51E-03	1.51E-06	0.0749	0.872	
10	1000	1.30E-03	1.30E-06	0.0742	1.23	
15	999	1.14E-03	1.14E-06	0.0735	1.71	
20	998	1.01E-03	1.01E-06	0.0727	2.34	2.21
25	997	8.93E-04	8.96E-07	0.0720	3.17	
30	996	8.00E-04	8.03E-07	0.0712	4.25	
35	994	7.21E-04	7.25E-07	0.0704	5.63	
40	992	6.53E-04	6.59E-07	0.0696	7.38	
45	990	5.95E-04	6.02E-07	0.0688	9.59	
50	988	5.46E-04	5.52E-07	0.0679	12.4	2.29
55	986	5.02E-04	5.09E-07	0.0671	15.8	
60	983	4.64E-04	4.72E-07	0.0662	19.9	
65	980	4.31E-04	4.40E-07	0.0654	25.0	
70	978	4.01E-04	4.10E-07	0.0645	31.2	
75	975	3.75E-04	3.85E-07	0.0636	38.6	
80	972	3.52E-04	3.62E-07	0.0627	47.4	
85	969	3.31E-04	3.41E-07	0.0618	57.8	
90	965	3.12E-04	3.23E-07	0.0608	70.1	2.12
95	962	2.95E-04	3.06E-07	0.0599	84.6	
100	958	2.79E-04	2.92E-07	0.0589	101	

Table A.9

Properties of Air at Atmospheric Pressure (U.S. Customary Units)

Temperature, <i>T</i> (°F)	Density, <i>ρ</i> (slug/ft ³)	Dynamic Viscosity, <i>μ</i> (lbf·s/ft ²)	Kinematic Viscosity, <i>ν</i> (ft ² /s)
40	0.00247	3.63E-07	1.47E-04
50	0.00242	3.69E-07	1.52E-04
59	0.00238	3.74E-07	1.57E-04
60	0.00237	3.74E-07	1.58E-04
68	0.00234	3.79E-07	1.62E-04
70	0.00233	3.80E-07	1.63E-04
80	0.00229	3.85E-07	1.68E-04
90	0.00225	3.91E-07	1.74E-04
100	0.00221	3.96E-07	1.79E-04
110	0.00217	4.02E-07	1.86E-04
120	0.00213	4.07E-07	1.91E-04
130	0.00209	4.12E-07	1.97E-04
140	0.00206	4.18E-07	2.03E-04
150	0.00202	4.23E-07	2.09E-04
160	0.00199	4.28E-07	2.15E-04
170	0.00196	4.33E-07	2.21E-04
180	0.00193	4.38E-07	2.27E-04
190	0.00190	4.43E-07	2.33E-04
200	0.00187	4.48E-07	2.40E-04

Table A.10
Properties of Air at Atmospheric Pressure (SI Units)

Temperature, T (°C)	Density, ρ (kg/m ³)	Dynamic Viscosity, μ (N·s/m ²)	Kinematic Viscosity, ν (m ² /s)
0	1.29	1.72E-05	1.33E-05
5	1.27	1.74E-05	1.37E-05
10	1.25	1.76E-05	1.41E-05
15	1.23	1.79E-05	1.45E-05
20	1.21	1.81E-05	1.50E-05
25	1.19	1.84E-05	1.54E-05
30	1.17	1.86E-05	1.59E-05
35	1.15	1.88E-05	1.64E-05
40	1.13	1.91E-05	1.69E-05
45	1.11	1.93E-05	1.74E-05
50	1.09	1.95E-05	1.79E-05
55	1.08	1.98E-05	1.83E-05
60	1.06	2.00E-05	1.89E-05
65	1.04	2.02E-05	1.94E-05
70	1.03	2.04E-05	1.98E-05
75	1.01	2.06E-05	2.04E-05
80	1.00	2.09E-05	2.09E-05
85	0.987	2.11E-05	2.14E-05
90	0.973	2.13E-05	2.19E-05
95	0.960	2.15E-05	2.24E-05
100	0.947	2.17E-05	2.29E-05

REFERENCES

1. *Handbook of Chemistry and Physics*, 62nd ed. Cleveland, OH: Chemical Rubber Publishing Co., 1981–1982.
2. “Meriam Standard Indicating Fluids,” Pamphlet No. 920GEN: 430-1, The Meriam Instrument Co., 10920 Madison Avenue, Cleveland, OH 44102.
3. E. Vernon Hill, Inc., P.O. Box 7053, Corte Madera, CA 94925.
4. Avallone, E. A., and T. Baumeister, III, eds., *Marks' Standard Handbook for Mechanical Engineers*, 11th ed. New York: McGraw-Hill, 2007.
5. *Handbook of Tables for Applied Engineering Science*. Cleveland, OH: Chemical Rubber Publishing Co., 1970.
6. Vargaftik, N. B., *Tables on the Thermophysical Properties of Liquids and Gases*, 2nd ed. Washington, DC: Hemisphere Publishing Corp., 1975.
7. *The U.S. Standard Atmosphere (1976)*. Washington, DC: U.S. Government Printing Office, 1976.
8. Trefethen, L., “Surface Tension in Fluid Mechanics,” in *Illustrated Experiments in Fluid Mechanics*. Cambridge, MA: The M.I.T. Press, 1972.
9. Streeter, V. L., ed., *Handbook of Fluid Dynamics*. New York: McGraw-Hill, 1961.
10. Tououloukian, Y. S., S. C. Saxena, and P. Hestermans, *Thermophysical Properties of Matter, the TPRC Data Series. Vol. 11—Viscosity*. New York: Plenum Publishing Corp., 1975.
11. Reid, R. C., and T. K. Sherwood, *The Properties of Gases and Liquids*, 2nd ed. New York: McGraw-Hill, 1966.
12. “Engine Oil Viscosity Classification—SAE Standard J300 Jun86,” *SAE Handbook*, 1987 ed. Warrendale, PA: Society of Automotive Engineers, 1987.
13. “Axe and Manual Transmission Lubricant Viscosity Classification—SAE Standard J306 Mar85,” *SAE Handbook*, 1987 ed. Warrendale, PA: Society of Automotive Engineers, 1987.
14. “Fluid for Passenger Car Type Automatic Transmissions—SAE Information Report J311 Apr86,” *SAE Handbook*, 1987 ed. Warrendale, PA: Society of Automotive Engineers, 1987.
15. ASTM Standard D 341-77, “Viscosity-Temperature Charts for Liquid Petroleum Products,” American Society for Testing and Materials, 1916 Race Street, Philadelphia, PA 19103.
16. NASA, *Compressed Gas Handbook (Revised)*. Washington, DC: National Aeronautics and Space Administration, SP-3045, 1970.
17. ASME, *Thermodynamic and Transport Properties of Steam*. New York: American Society of Mechanical Engineers, 1967.

APPENDIX B

Videos for Fluid Mechanics

OC Referenced in the text are the following videos available in the enhanced ebook.

Chapter 2

- Streamlines
- Streaklines
- Capillary Rise
- Boundary Layer Flow
- Streamlined Flow over an Airfoil
- Internal Laminar Flow in a Tube
- Streamlines around a Car
- Laminar and Turbulent Flow

Pipe Flow: Transitional

- The Glen Canyon Dam: A Turbulent Pipe Flow

Chapter 4

- Mass Conservation: Filling a Tank
- Momentum Effect: A Jet Impacting a Surface

Chapter 9

- Flow around an Airfoil
- Flow Separation on an Airfoil
- Effect of Viscosity on Boundary Layer Growth
- Examples of Boundary Layer Growth
- Flow Separation: Airfoil
- Flow about a Sports Car
- Plate Normal to the Flow
- An Object with a High Drag Coefficient
- Examples of Flow around a Sphere
- Vortex Trail behind a Cylinder
- Flow Past an Airfoil ($\alpha = 0^\circ$)
- Flow Past an Airfoil ($\alpha = 10^\circ$)
- Flow Past an Airfoil ($\alpha = 20^\circ$)
- Wing Tip Vortices
- Leading Edge Slats

Chapter 5

- An Example of Streamlines/Streaklines
- Particle Motion in a Channel
- Linear Deformation
- Flow Past a Cylinder

Chapter 10

- Flow in an Axial Flow Compressor (Animation)

Chapter 7

- Geometric, Not Dynamic, Similarity: Flow Past a Block 1
- Geometric, Not Dynamic, Similarity: Flow Past a Block 2

Chapter 11

- A Laminar Hydraulic Jump

Chapter 8

- The Reynolds Transition Experiment
- Pipe Flow: Laminar

Chapter 12

- Shock Waves due to a Projectile
- Shock Waves over a Supersonic Airplane

The following videos were developed by the National Committee for Fluid Mechanics Films (NCFMF) and may be viewed at <http://web.mit.edu/hml/ncfmf.html>. Each of these videos goes into the subject in more depth than may be appropriate for an undergraduate class. However, selected segments of the videos are useful in bringing out important fluids phenomena.

These videos are supplied by:

Encyclopaedia Britannica Educational Corporation
331 North La Salle Street
Chicago, IL 60654

Aerodynamic Generation of Sound (44 min, principals: M. J. Lighthill, J. E. Ffowcs-Williams)
Cavitation (31 min, principal: P. Eisenberg)
Channel Flow of a Compressible Fluid (29 min, principal: D. E. Coles)
Deformation of Continuous Media (38 min, principal: J. L. Lumley)
Eulerian and Lagrangian Descriptions in Fluid Mechanics (27 min, principal: J. L. Lumley)
Flow Instabilities (27 min, principal: E. L. Mollo-Christensen)
Flow Visualization (31 min, principal: S. J. Kline)
The Fluid Dynamics of Drag (4 parts, 120 min, principal: A. H. Shapiro)
Fundamentals of Boundary Layers (24 min, principal: F. H. Abernathy)
Low-Reynolds-Number Flows (33 min, principal: Sir G. I. Taylor)
Magnetohydrodynamics (27 min, principal: J. A. Shercliff)
Pressure Fields and Fluid Acceleration (30 min, principal: A. H. Shapiro)
Rarefied Gas Dynamics (33 min, principals: F. C. Hurlbut, F. S. Sherman)
Rheological Behavior of Fluids (22 min, principal: H. Markovitz)
Rotating Flows (29 min, principal: D. Fultz)
Secondary Flow (30 min, principal: E. S. Taylor)
Stratified Flow (26 min, principal: R. R. Long)
Surface Tension in Fluid Mechanics (29 min, principal: L. M. Trefethen)
Turbulence (29 min, principal: R. W. Stewart)
Vorticity (2 parts, 44 min, principal: A. H. Shapiro)
Waves in Fluids (33 min, principal: A. E. Bryson)

Another source of fluid mechanics videos is a CD entitled “Multimedia Fluid Mechanics” by Homsy et al. It is available from Cambridge University Press, 32 Avenue of the Americas, New York, NY 10013-2473, ISBN 9780521721691. This CD contains a very large number of videos that illustrate different phenomena in fluid flow.

APPENDIX C

Selected Performance Curves for Pumps and Fans

C.1 Introduction

Many firms, worldwide, manufacture fluid machines in numerous standard types and sizes. Each manufacturer publishes complete performance data to allow application of its machines in systems. This appendix contains selected performance data for use in solving pump and fan system problems. Two pump types and one fan type are included.

Choice of a manufacturer may be based on established practice, location, or cost. Once a manufacturer is chosen, machine selection is a three-step process:

1. Select a machine type, suited to the application, from a manufacturer's full-line catalog, which gives the ranges of pressure rise (head) and flow rate for each machine type.
2. Choose an appropriate machine model and driver speed from a master selector chart, which superposes the head and flow rate ranges of a series of machines on one graph.
3. Verify that the candidate machine is satisfactory for the intended application, using a detailed performance curve for the specific machine.

It is wise to consult with experienced system engineers, either employed by the machine manufacturer or in your own organization, before making a final purchase decision.

Many manufacturers currently use computerized procedures to select a machine that is most suitable for each given application. Such procedures are simply automated versions of the traditional selection method. Use of the master selector chart and the detailed performance curves is illustrated below for pumps and fans, using data from one manufacturer of each type of machine. Literature of other manufacturers differs in detail but contains the necessary information for machine selection.

C.2 Pump Selection

Representative data are shown in Figs. C.1 through C.10 for Peerless horizontal split case single-stage (series AE) pumps and in Figs. C.11 and C.12 for Peerless multi-stage (series TU and TUT) pumps [1].

Figures C.1 and C.2 are master pump selector charts for series AE pumps at 3500 and 1750 nominal rpm. On these charts, the model number (e.g., 6AE14) indicates the discharge line size (6 in. nominal pipe), the pump series (AE), and the maximum impeller diameter (approximately 14 in.).

Figures C.3 through C.10 are detailed performance charts for individual pump models in the AE series.

Figures C.11 and C.12 are master pump selector charts for series TU and TUT pumps at 1750 nominal rpm. Data for two-stage pumps are presented in Fig. C.11, while Fig. C.12 contains data for pumps with three, four, and five stages.

Each pump performance chart contains curves of total head versus volume flow rate; curves for several impeller diameters—tested in the same casing—are presented on a single graph. Each performance chart also contains curves showing pump efficiency and driver power; the net positive suction head (*NPSH*) requirement, as it varies with flow rate, is shown by the curve at the bottom of each chart. The best efficiency point (BEP) for each impeller may be found using the efficiency curves.

Use of the master pump selector chart and detailed performance curves is illustrated in Example C.1.

Example C.1 PUMP SELECTION PROCEDURE

Select a pump to deliver 1750 gpm of water at 120 ft total head. Choose the appropriate pump model and driver speed. Specify the pump efficiency, driver power, and *NPSH* requirement.

Given: Select a pump to deliver 1750 gpm of water at 120 ft total head.

Find:

- (a) Pump model and driver speed.
- (b) Pump efficiency.
- (c) Driver power.
- (d) *NPSH* requirement.

Solution: Use the pump selection procedure described in Section C-1. (The numbers below correspond to the numbered steps given in the procedure.)

1. Select a machine type suited to the application. (This step actually requires a manufacturer's full-line catalog, which is not reproduced here. The Peerless product line catalog specifies a maximum delivery and head of 2500 gpm and 660 ft for series AE pumps. Therefore the required performance can be obtained; assume the selection is to be made from this series.)
2. Consult the master pump selector chart. The desired operating point is not within any pump contour on the 3500 rpm selector chart (Fig. C.1). From the 1750 rpm chart (Fig. C.2), select a model 6AE14 pump. From the performance curve for the 6AE14 pump (Fig. C.6), choose a 13-in. impeller.
3. Verify the performance of the machine using the detailed performance chart. On the performance chart for the 6AE14 pump, project up from the abscissa at $Q = 1750$ gpm. Project across from $H = 120$ ft on the ordinate. The intersection is the pump performance at the desired operating point:

$$\eta \approx 85.8 \text{ percent} \quad \mathcal{P} \approx 64 \text{ hp}$$

From the operating point, project down to the *NPSH* requirement curve. At the intersection, read $NPSH \approx 17$ ft.

This completes the selection process for this pump. One should consult with experienced system engineers to verify that the system operating condition has been predicted accurately and the pump has been selected correctly.

C.3 Fan Selection

Fan selection is similar to pump selection. A representative master fan selection chart is shown in Fig. C.13 for a series of Howden Buffalo axial-flow fans. The chart shows the efficiency of the entire series of fans as a function of total pressure rise and flow rate. The series of numbers for each fan indicates the fan diameter in inches, the hub diameter in inches, and the fan speed in revolutions per minute. For instance, a 54-26-870 fan has a fan diameter of 54 in., a hub diameter of 26 in., and should be operated at 870 rpm.

Normally, final evaluation of suitability of the fan model for the application would be done using detailed performance charts for the specific model. Instead, we use the efficiencies from Fig C.13, which are indicated by the shading of the different zones on the map. To calculate the power requirement for the fan motor, we use the following equation:

$$\mathcal{P}(\text{hp}) = \frac{Q(\text{cfm}) \times \Delta p(\text{in. H}_2\text{O})}{6350 \times \eta}$$

A sample fan selection is presented in Example C.2.

Example C.2 FAN SELECTION PROCEDURE

Select an axial flow fan to deliver 30,000 cfm of standard air at 1.25 in. H₂O total pressure. Choose the appropriate fan model and driver speed. Specify the fan efficiency and driver power.

Given: Select an axial flow fan to deliver 30,000 cfm of standard air at 1.25 in. H₂O total head.

Find:

- (a) Fan size and driver speed.
- (b) Fan efficiency.
- (c) Driver power.

Solution: Use the fan selection procedure described in Section C-1. (The numbers below correspond to the numbered steps given in the procedure.)

1. Select a machine type suited to the application. (This step actually requires a manufacturer's full-line catalog, which is not reproduced here. Assume the fan selection is to be made from the axial fan data presented in Fig. C.13.)
2. Consult the master fan selector chart. The desired operating point is within the contour for the 48-21-860 fan on the selector chart (Fig. C.13). To achieve the desired performance requires driving the fan at 860 rpm.
3. Verify the performance of the machine using a detailed performance chart. To determine the efficiency, we consult Fig. C.13 again. We estimate an efficiency of 85 percent. To determine the motor power requirement, we use the equation given above:

$$\mathcal{P} = \frac{Q \times \Delta p}{6350 \times \eta} = \frac{30,000 \text{ cfm} \times 1.25 \text{ in. H}_2\text{O}}{6350 \times 0.85} = 6.95 \text{ hp}$$

This completes the fan selection process. Again, one should consult with experienced system engineers to verify that the system operating condition has been predicted accurately and the fan has been selected correctly.

A-18 Appendix C Selected Performance Curves for Pumps and Fans

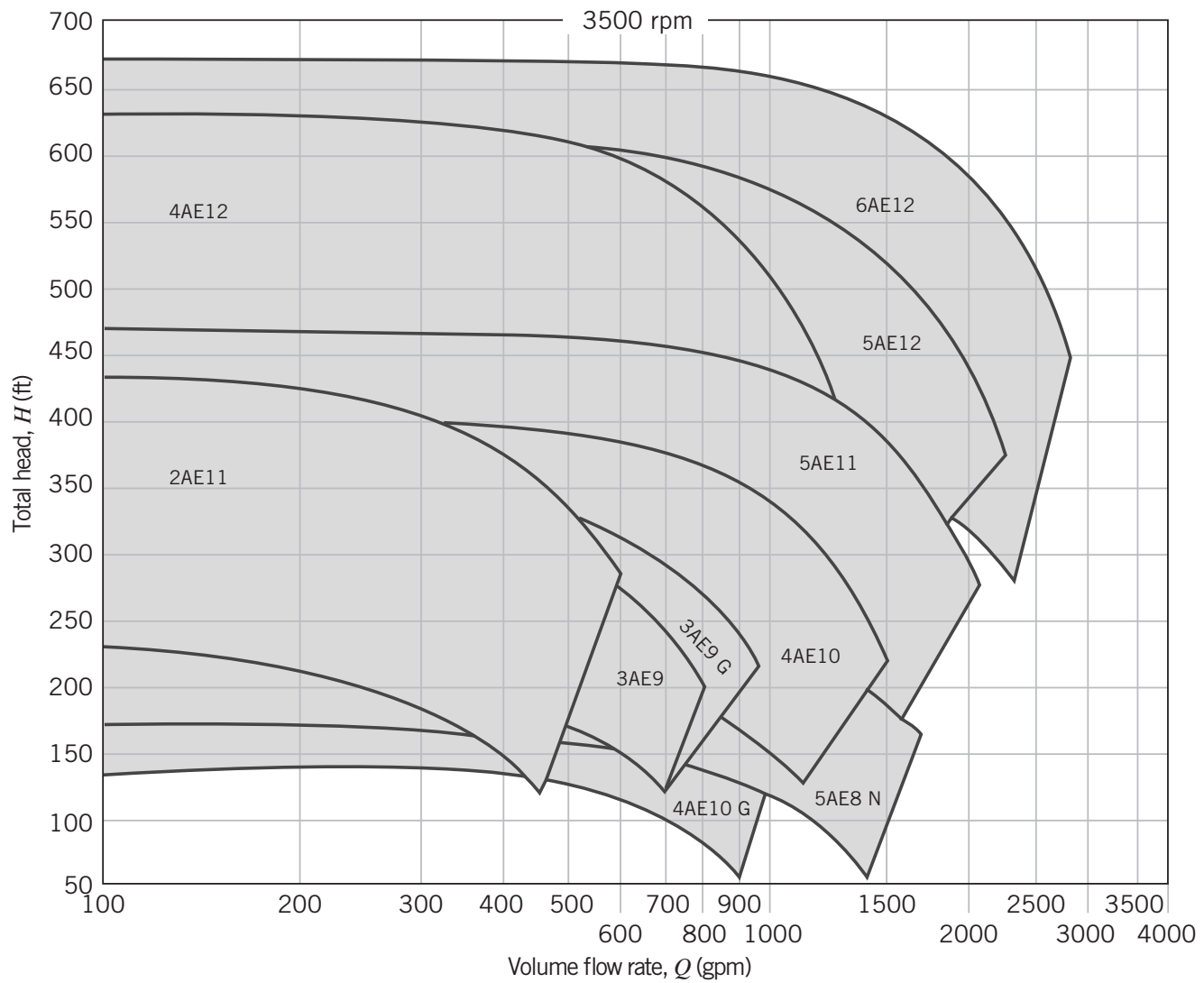


Fig. C.1 Selector chart for Peerless horizontal split case (series AE) pumps at 3500 nominal rpm.

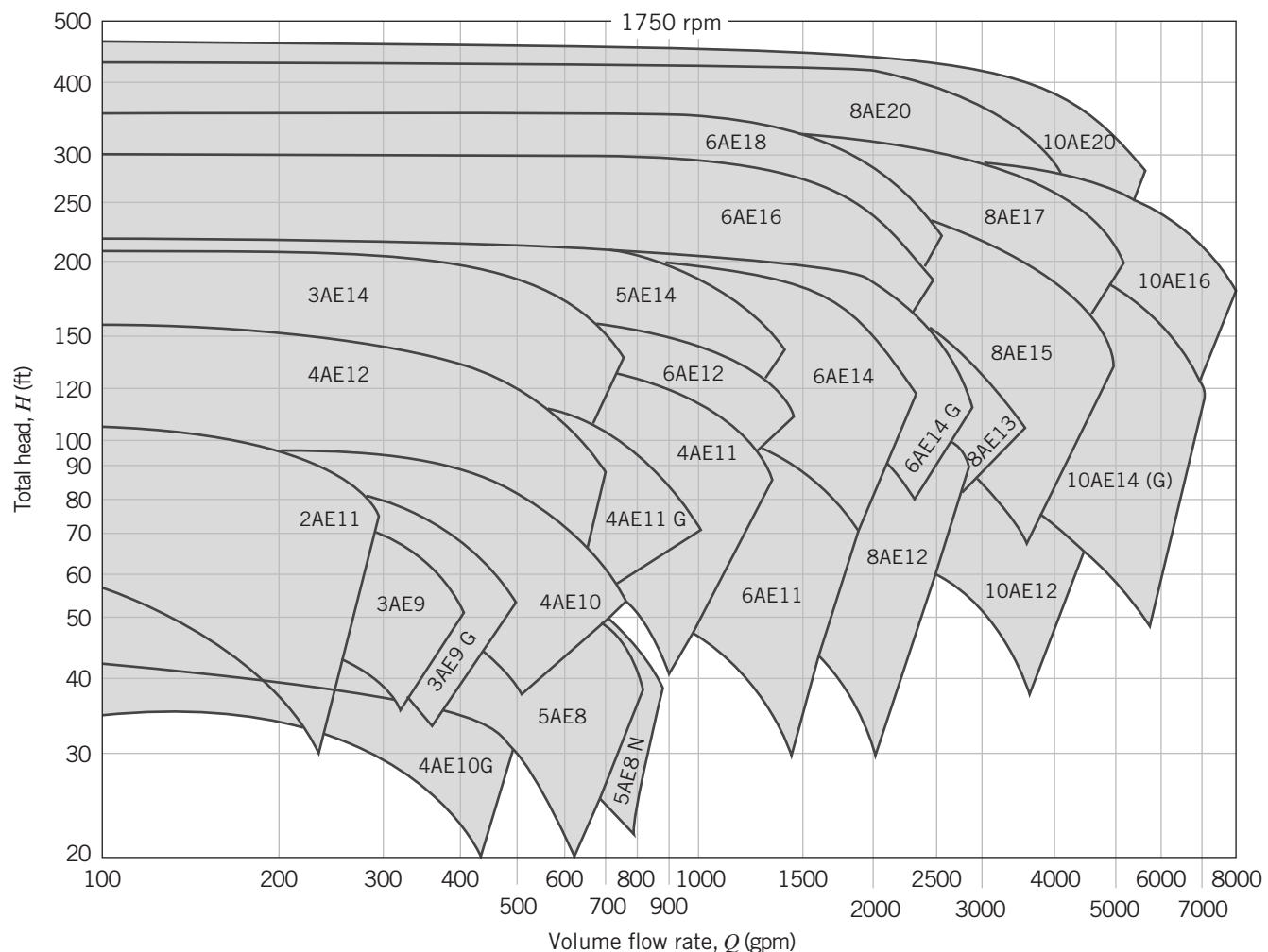


Fig. C.2 Selector chart for Peerless horizontal split case (series AE) pumps at 1750 nominal rpm.

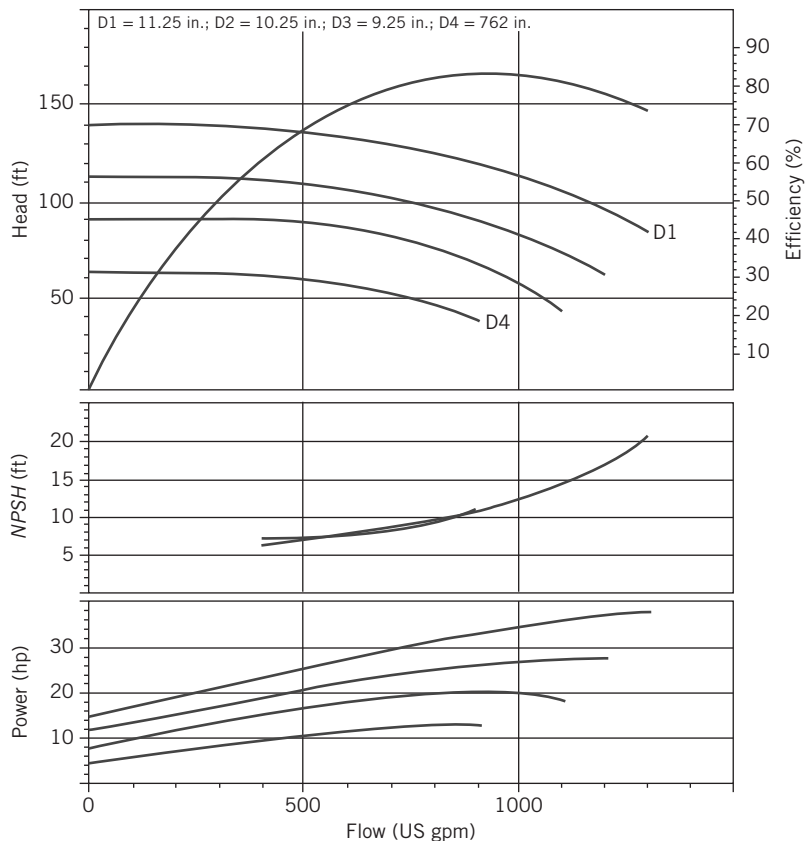


Fig. C.3 Performance curve for Peerless 4AE11 pump at 1750 rpm.

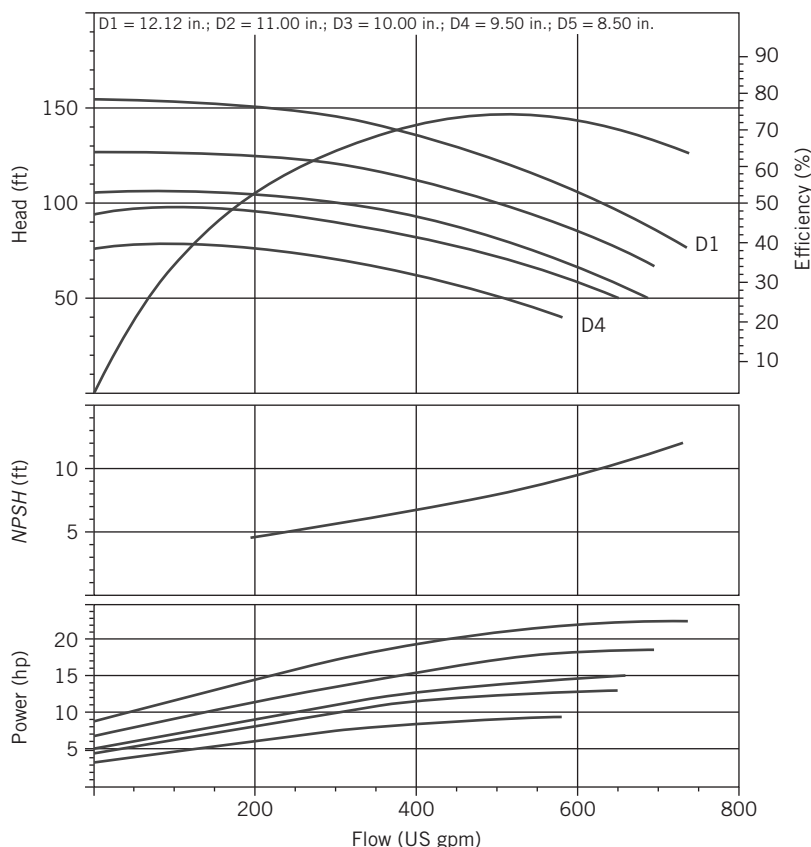


Fig. C.4 Performance curve for Peerless 4AE12 pump at 1750 rpm.

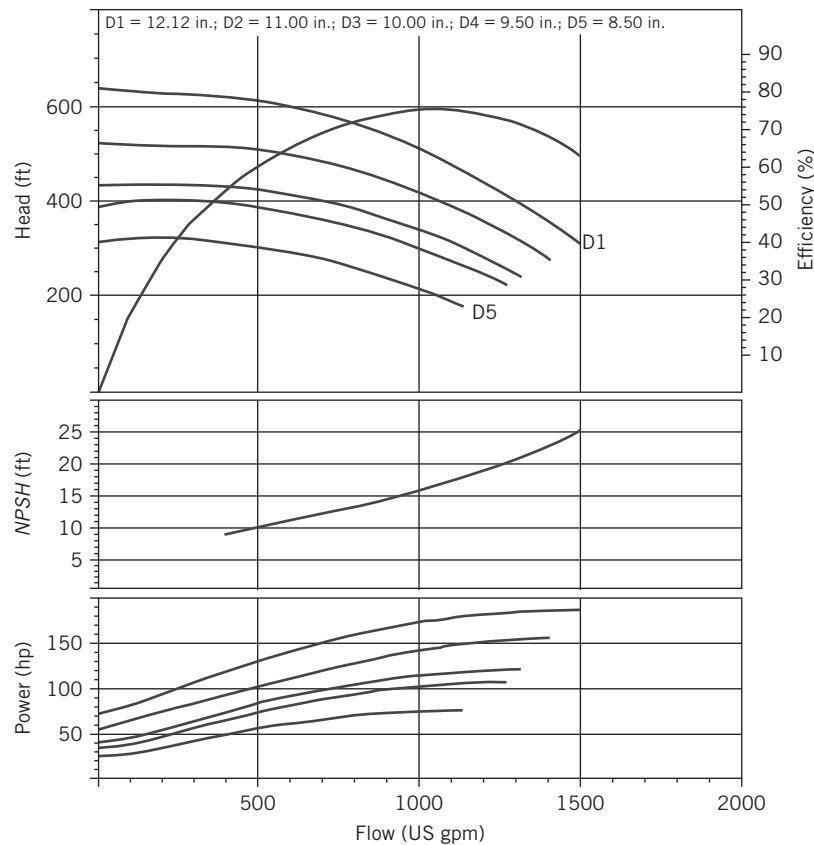


Fig. C.5 Performance curve for Peerless 4AE12 pump at 3550 rpm.

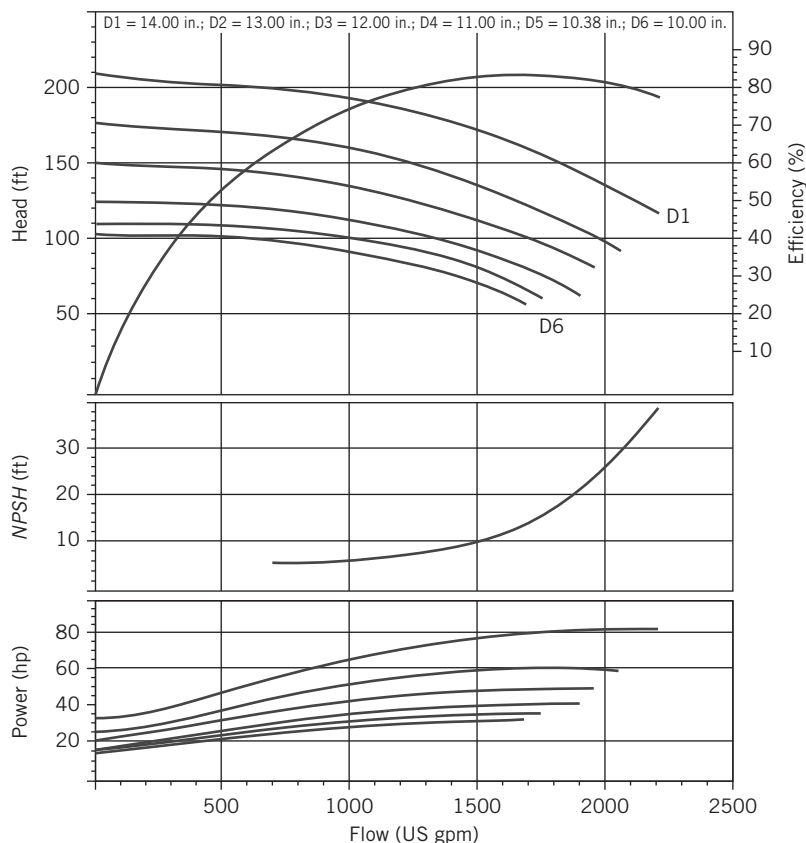


Fig. C.6 Performance curve for Peerless 6AE14 pump at 1750 rpm.

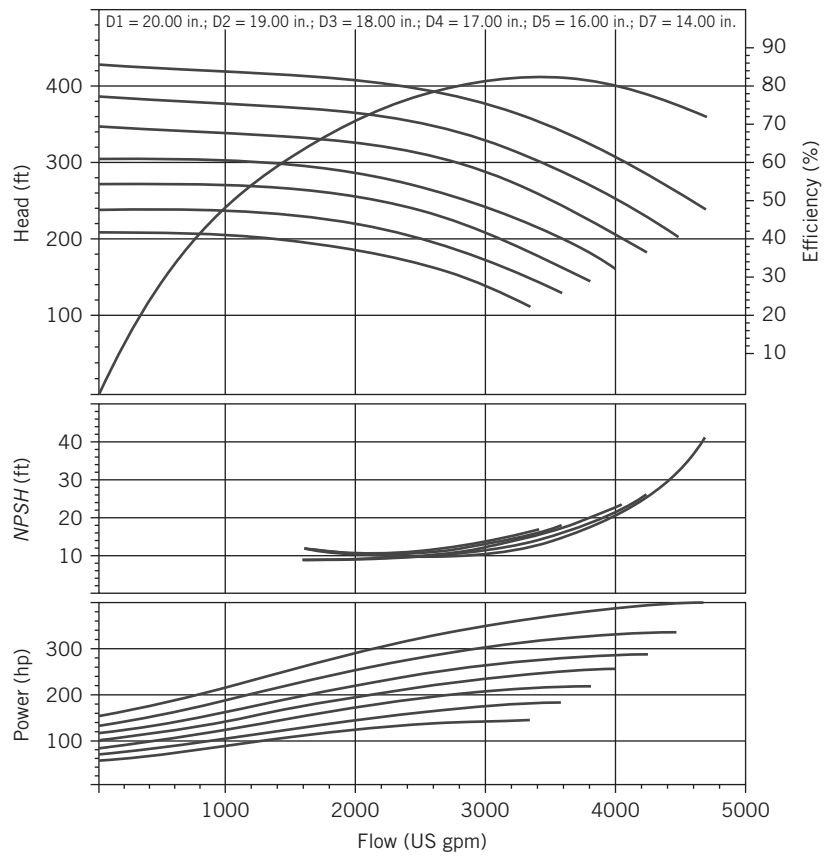


Fig. C.7 Performance curve for Peerless 8AE20G pump at 1770 rpm.

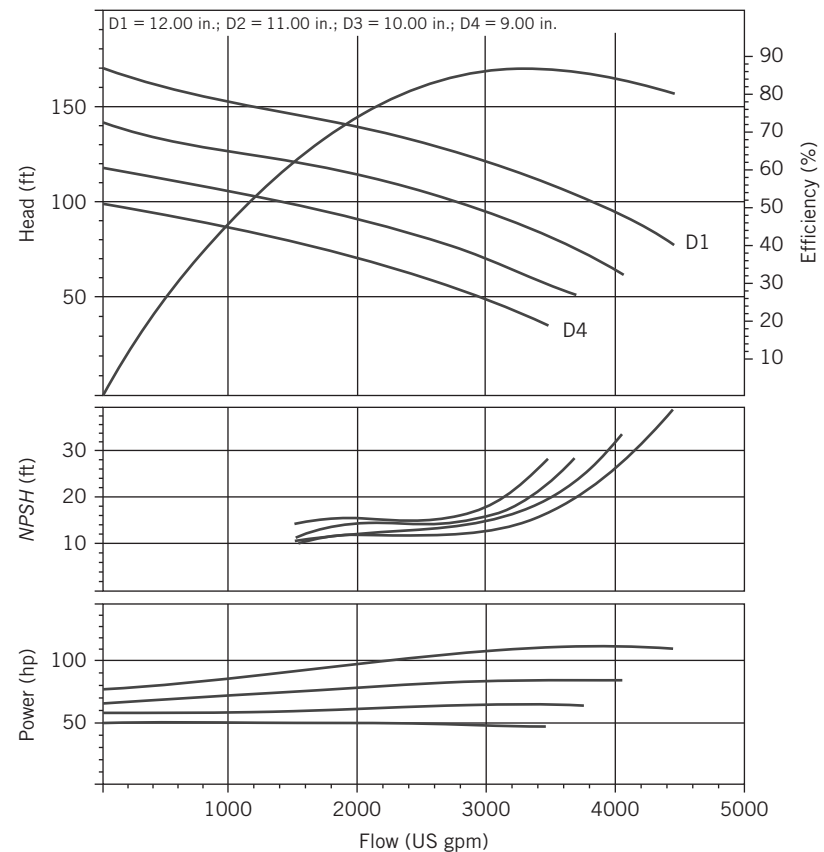


Fig. C.8 Performance curve for Peerless 10AE12 pump at 1760 rpm.

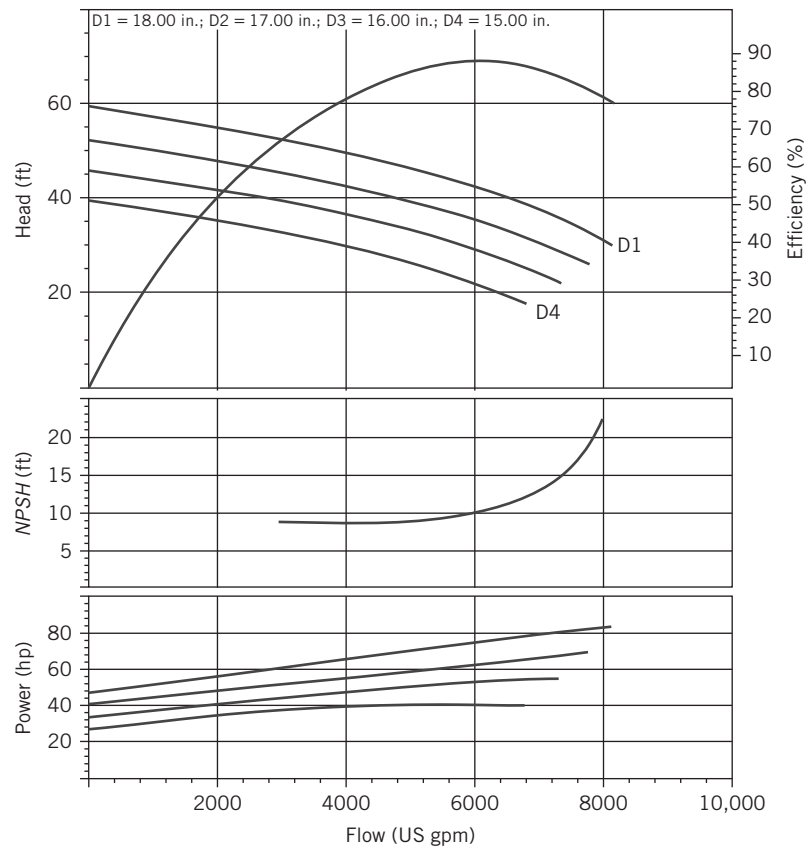


Fig. C.9 Performance curve for Peerless 16A18B pump at 705 rpm.

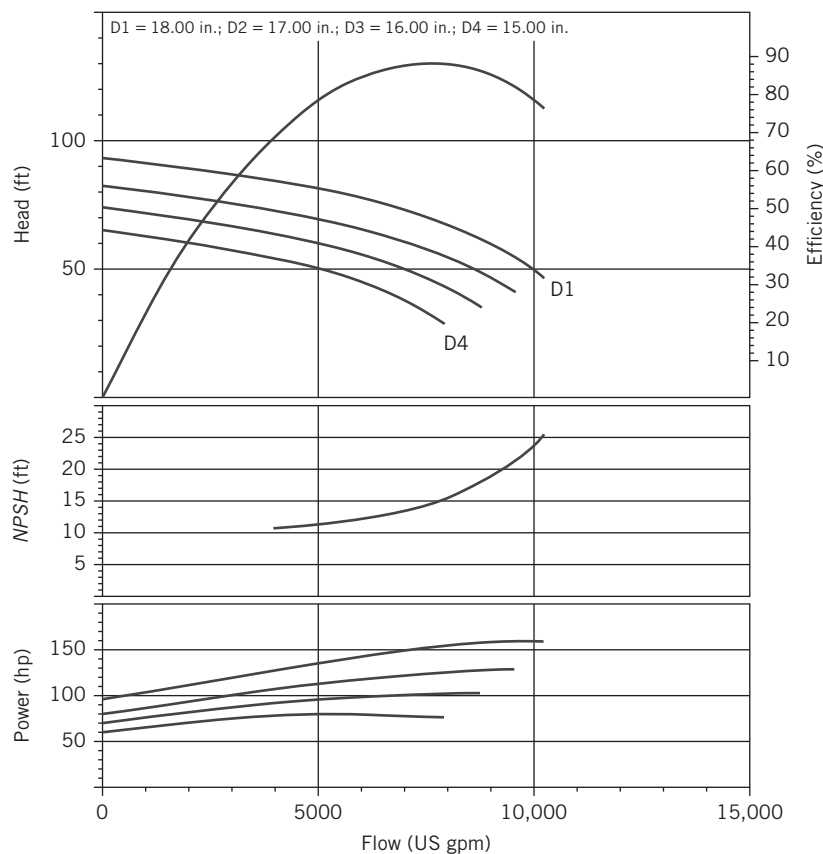


Fig. C.10 Performance curve for Peerless 16A18B pump at 880 rpm.

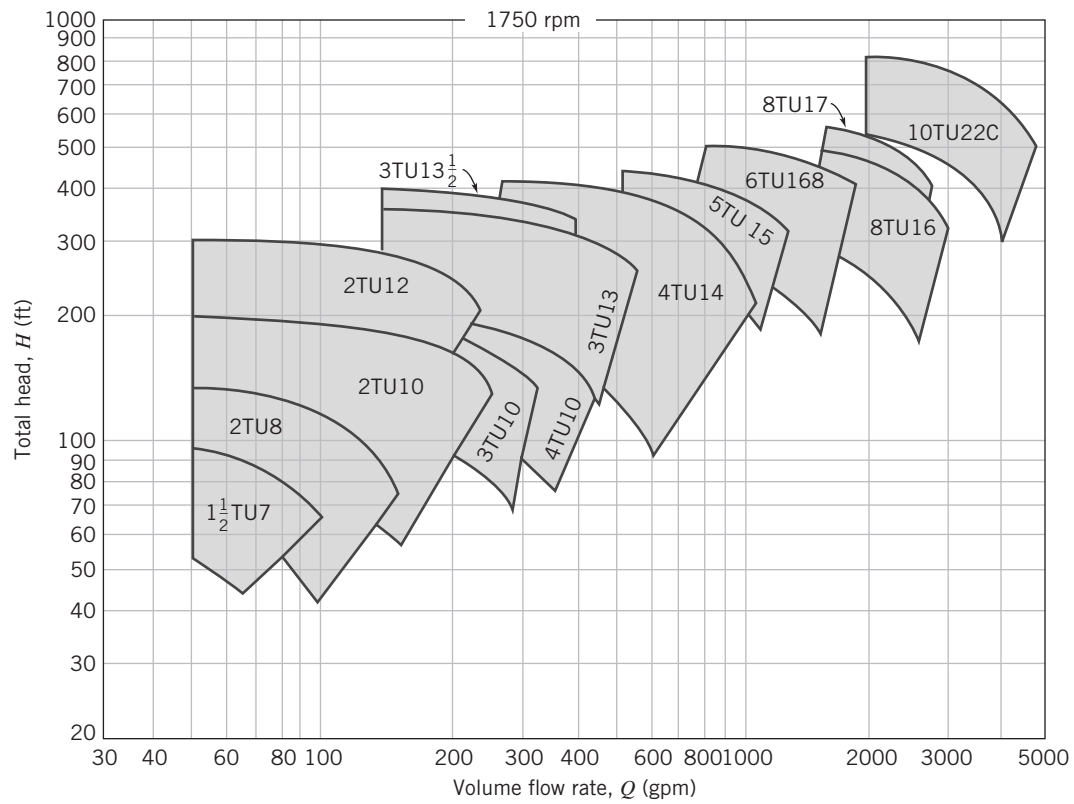


Fig. C.11 Selector chart for Peerless two-stage (series TU and TUT) pumps at 1750 nominal rpm.

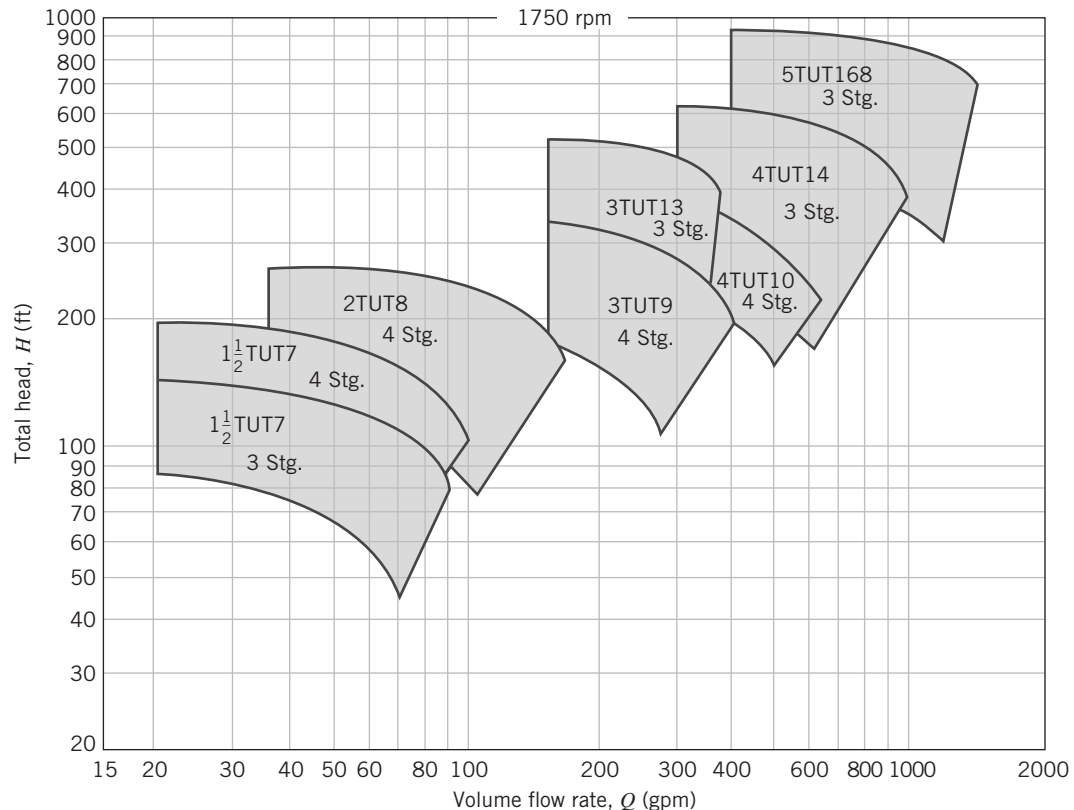


Fig. C.12 Selector chart for Peerless multi-stage (series TU and TUT) pumps at 1750 nominal rpm.

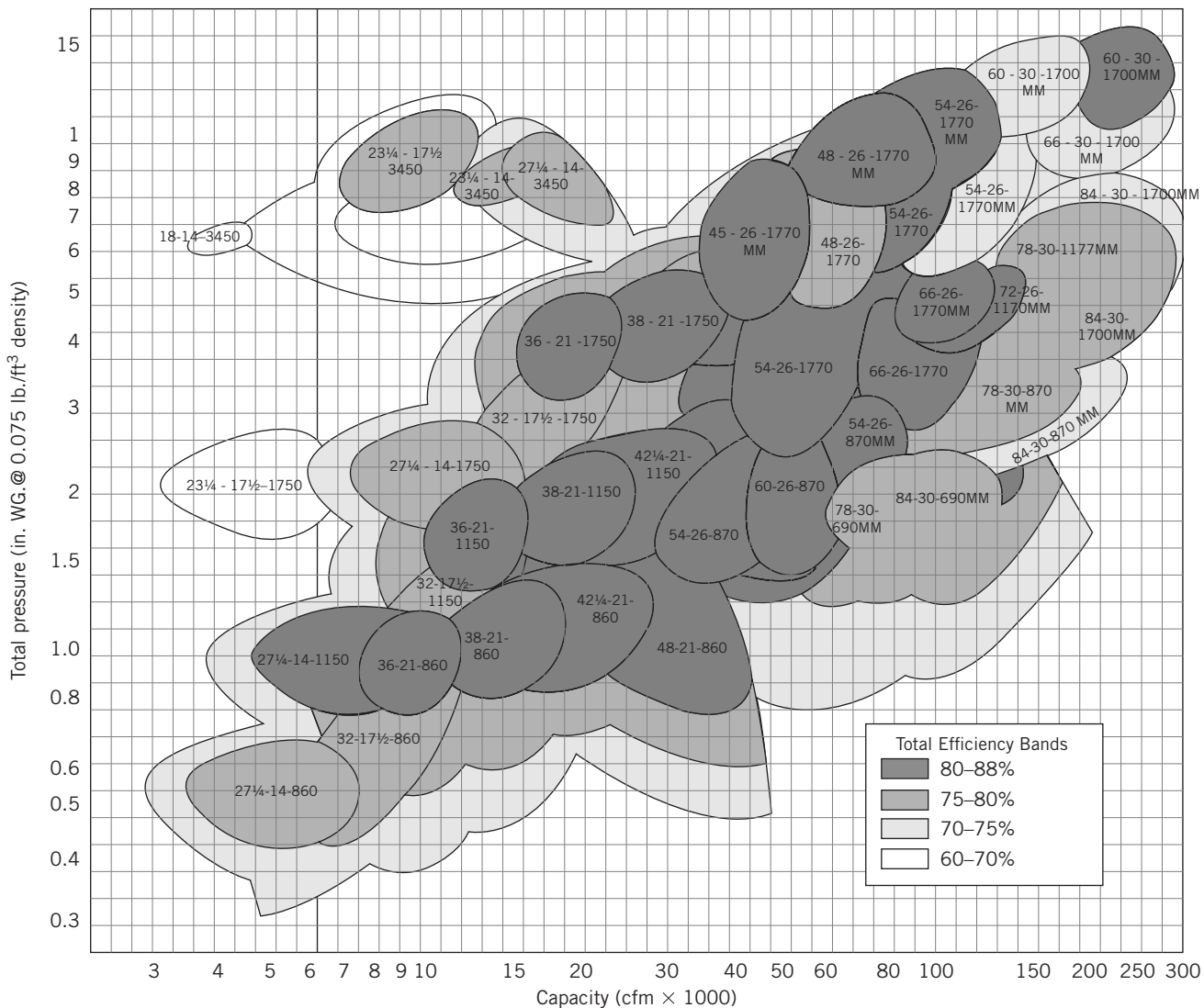


Fig. C.13 Master fan selection chart for Howden Buffalo axial fans.

REFERENCES

1. Peerless Pump literature:
 - Horizontal Split Case Single Stage Double Suction Pumps, Series AE, Brochure B-1200, 2003.
 - Horizontal Split Case, Multistage Single Suction Pumps, Types TU, TUT, 60 Hertz, Performance Curves, Brochure B-1440, 2003.
 - RAPID v8.25.6, March 2007.
 - Peerless Pump Company, P.O. Box 7026, Indianapolis, IN 46207-7026.
2. Buffalo Forge literature:
 - Axivane Axial Fan Optimum Efficiency Selection Chart, n.d.
3. Howden Buffalo Inc., 2029 W. DeKalb St., Camden, SC 29020.

APPENDIX D

Flow Functions for Computation of Compressible Flow

D.1 *Isentropic Flow*

Isentropic flow functions are computed using the following equations:

$$\frac{p_0}{p} = \left[1 + \frac{k-1}{2} M^2 \right]^{k/(k-1)} \quad (12.21a/12.30a)$$

$$\frac{T_0}{T} = 1 + \frac{k-1}{2} M^2 \quad (12.21b/12.30b)$$

$$\frac{\rho_0}{\rho} = \left[1 + \frac{k-1}{2} M^2 \right]^{1/(k-1)} \quad (12.21c/12.30c)$$

$$\frac{A}{A^*} = \frac{1}{M} \left[\frac{1 + \frac{k-1}{2} M^2}{\frac{k+1}{2}} \right]^{(k+1)/2(k-1)} \quad (12.30d)$$

Representative values of the isentropic flow functions for $k = 1.4$ are presented in Table D.1 and plotted in Fig. D.1. These functions can also be calculated using the Excel worksheets available on the website.

Table D.1
Isentropic Flow Functions (one-dimensional flow, ideal gas, $k = 1.4$)

M	T/T_0	p/p_0	ρ/ρ_0	A/A^*
0.00	1.0000	1.0000	1.0000	∞
0.50	0.9524	0.8430	0.8852	1.340
1.00	0.8333	0.5283	0.6339	1.000
1.50	0.6897	0.2724	0.3950	1.176
2.00	0.5556	0.1278	0.2301	1.688
2.50	0.4444	0.05853	0.1317	2.637
3.00	0.3571	0.02722	0.07623	4.235
3.50	0.2899	0.01311	0.04523	6.790
4.00	0.2381	0.006586	0.02766	10.72
4.50	0.1980	0.003455	0.01745	16.56
5.00	0.1667	0.001890	0.01134	25.00

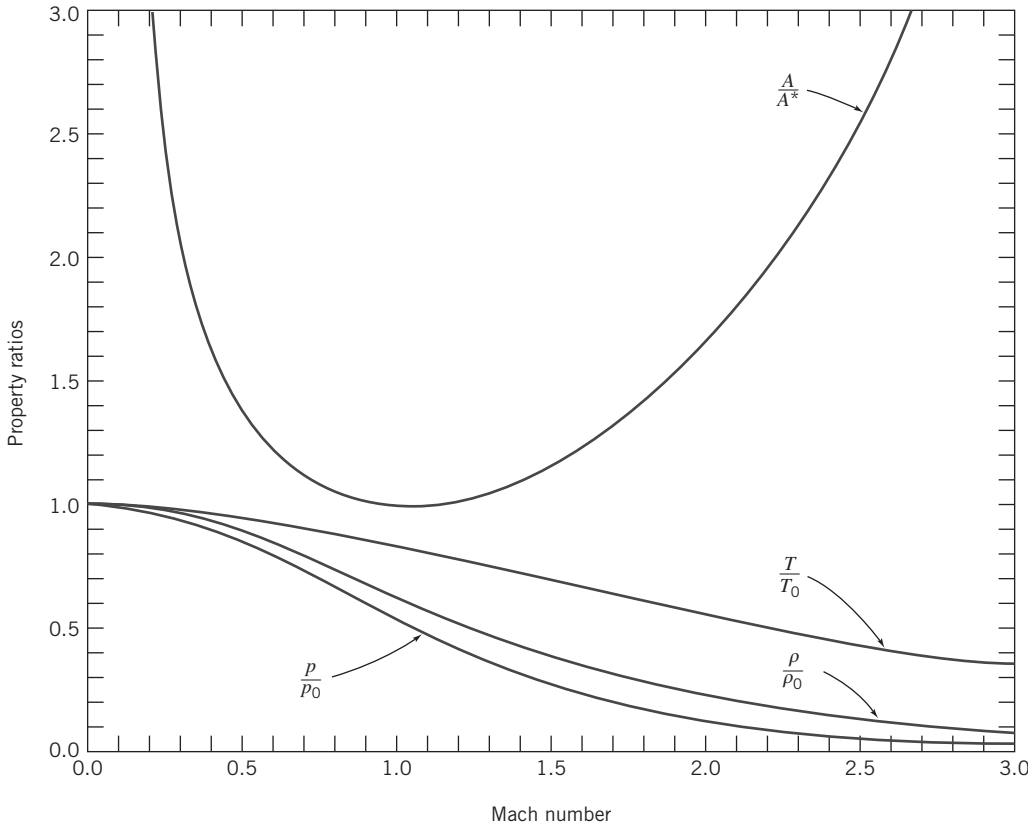


Fig. D.1 Isentropic flow functions.

D.2 Normal Shock

Normal-shock flow functions are computed using the following equations:

$$M_2^2 = \frac{M_1^2 + \frac{2}{k-1}}{\frac{2k}{k-1}M_1^2 - 1} \quad (12.43a)$$

$$\frac{p_{0_2}}{p_{0_1}} = \frac{\left[\frac{k+1}{2} M_1^2 \right]^{k/(k-1)}}{\left[1 + \frac{k-1}{2} M_1^2 \right]^{k/(k-1)}} \quad (12.43b)$$

$$\frac{T_2}{T_1} = \frac{\left(1 + \frac{k-1}{2} M_1^2 \right) \left(k M_1^2 - \frac{k-1}{2} \right)}{\left(\frac{k+1}{2} \right)^2 M_1^2} \quad (12.43c)$$

$$\frac{p_2}{p_1} = \frac{2k}{k+1} M_1^2 - \frac{k-1}{k+1} \quad (12.43d)$$

$$\frac{\rho_2}{\rho_1} = \frac{V_1}{V_2} = \frac{\frac{k+1}{2} M_1^2}{1 + \frac{k-1}{2} M_1^2} \quad (12.43e)$$

Representative values of the normal-shock flow functions for $k = 1.4$ are presented in Table D.2 and plotted in Fig. D.2.

Table D.2
Normal-Shock Flow Functions (one-dimensional flow, ideal gas, $k = 1.4$)

M_1	M_2	p_{02}/p_{01}	T_2/T_1	p_2/p_1	ρ_2/ρ_1
1.00	1.000	1.000	1.000	1.000	1.000
1.50	0.7011	0.9298	1.320	2.458	1.862
2.00	0.5774	0.7209	1.687	4.500	2.667
2.50	0.5130	0.4990	2.137	7.125	3.333
3.00	0.4752	0.3283	2.679	10.33	3.857
3.50	0.4512	0.2130	3.315	14.13	4.261
4.00	0.4350	0.1388	4.047	18.50	4.571
4.50	0.4236	0.09170	4.875	23.46	4.812
5.00	0.4152	0.06172	5.800	29.00	5.000

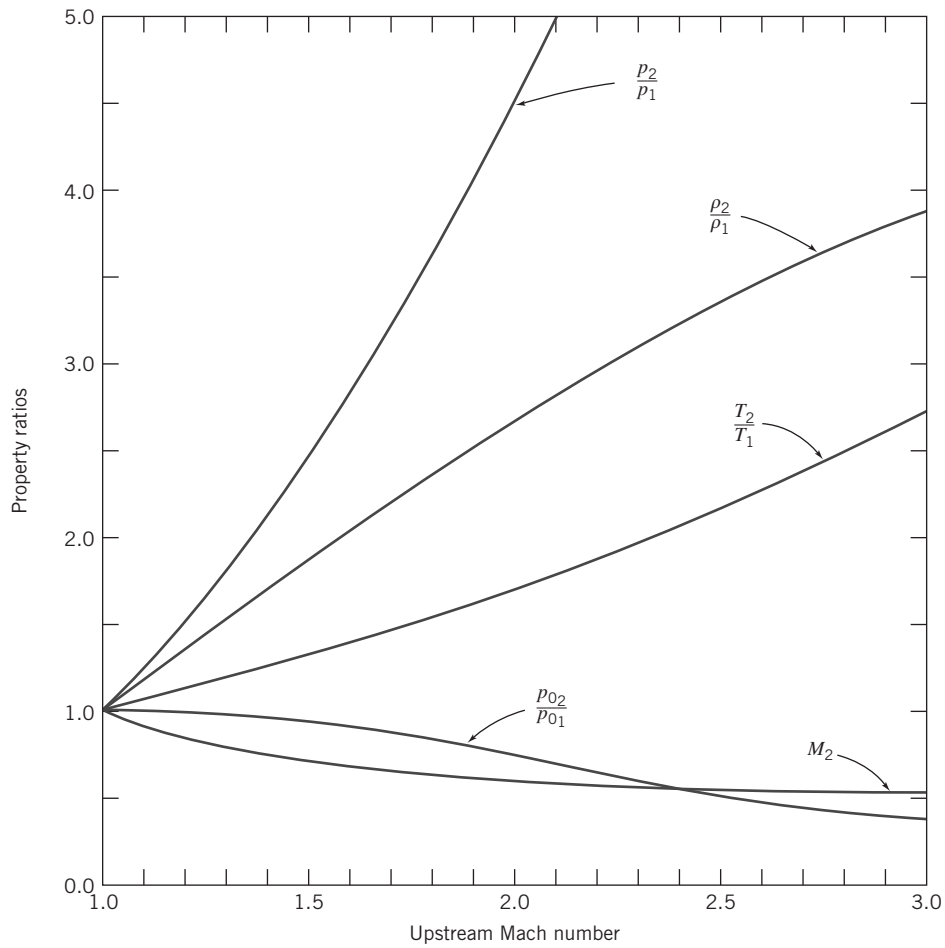


Fig. D.2 Normal-shock flow functions.

APPENDIX E

Analysis of Experimental Uncertainty

E.1 Introduction

Experimental data often are used to supplement engineering analysis as a basis for design. Not all data are equally good; the validity of data should be documented before test results are used for design. Uncertainty analysis is the procedure used to quantify data validity and accuracy. Analysis of uncertainty also is useful during experiment design. Careful study may indicate potential sources of unacceptable error and suggest improved measurement methods. An error analysis is often relevant to simulations in which there is uncertainty in the input parameters. It is important that any results presented have an indication of their accuracy and uncertainty.

E.2 Types of Error

Errors always are present when experimental measurements are made. Aside from gross blunders by the experimenter, experimental error may be of two types. Fixed (or systematic) error causes repeated measurements to be in error by the same amount for each trial. Fixed error is the same for each reading and can be removed by proper calibration or correction. Random error (nonrepeatability) is different for every reading and hence cannot be removed. The factors that introduce random error are uncertain by their nature. The objective of uncertainty analysis is to estimate the probable random error in experimental results.

We assume that equipment has been constructed correctly and calibrated properly to eliminate fixed errors. We assume that instrumentation has adequate resolution and that fluctuations in readings are not excessive. We assume also that care is used in making and recording observations so that only random errors remain.

E.3 Estimation of Uncertainty

Our goal is to estimate the uncertainty of experimental measurements and calculated results due to random errors. The procedure has three steps:

1. Estimate the uncertainty interval for each measured quantity.
2. State the confidence limit on each measurement.
3. Analyze the propagation of uncertainty into results calculated from experimental data.

Below we outline the procedure for each step and illustrate applications with examples.

Step 1 Estimate the measurement uncertainty interval. Designate the measured variables in an experiment as x_1, x_2, \dots, x_n . One possible way to find the uncertainty interval for each variable would be to repeat each measurement many times. The result would be a distribution of data for each variable. Random errors in measurement usually produce a *normal (Gaussian)* frequency distribution of measured values. The data scatter for a normal distribution is characterized by the standard deviation, σ . The uncertainty interval for each measured variable, x_i , may be stated as $\pm n\sigma_i$, where $n = 1, 2, \text{ or } 3$.

However, the most typical situation in engineering work is a “single-sample” experiment, where only one measurement is made for each point [1]. A reasonable estimate of the measurement uncertainty due to random error in a single-sample experiment usually is plus or minus half the smallest scale division (the *least count*) of the instrument. However, this approach also must be used with caution, as illustrated in the following example.

Example E.1 UNCERTAINTY IN BAROMETER READING

The observed height of the mercury barometer column is $h = 752.6$ mm. The least count on the vernier scale is 0.1 mm, so one might estimate the probable measurement error as ± 0.05 mm.

A measurement probably could not be made this precisely. The barometer sliders and meniscus must be aligned by eye. The slider has a least count of 1 mm. As a conservative estimate, a measurement could be made to the nearest millimeter. The probable value of a single measurement then would be expressed as 752.6 ± 0.5 mm. The relative uncertainty in barometric height would be stated as

$$u_h = \pm \frac{0.5 \text{ mm}}{752.6 \text{ mm}} = \pm 0.000664 \quad \text{or} \quad \pm 0.0664 \text{ percent}$$

Comments:

1. An uncertainty interval of ± 0.1 percent corresponds to a result specified to three significant figures; this precision is sufficient for most engineering work.
2. The measurement of barometer height was precise, as shown by the uncertainty estimate. But was it accurate? At typical room temperatures, the observed barometer reading must be reduced by a temperature correction of nearly 3 mm! This is an example of a fixed error that requires a correction factor.

When repeated measurements of a variable are available, they are usually normally distributed data, for which over 99 percent of measured values of x_i lie within $\pm 3\sigma_i$ of the mean value, 95 percent lie within $\pm 2\sigma_i$, and 68 percent lie within $\pm \sigma_i$ of the mean value of the data set [2]. Thus it would be possible to quantify expected errors within any desired *confidence limit* if a statistically significant set of data were available.

The method of repeated measurements usually is impractical. In most applications it is impossible to obtain enough data for a statistically significant sample owing to the excessive time and cost involved. However, the normal distribution suggests several important concepts:

1. Small errors are more likely than large ones.
2. Plus and minus errors are about equally likely.
3. No finite maximum error can be specified.

Step 2 *State the confidence limit on each measurement.* The uncertainty interval of a measurement should be stated at specified odds. For example, one may write $h = 752.6 \pm 0.5$ mm (20 to 1). This means that one is willing to bet 20 to 1 that the height of the mercury column actually is within ± 0.5 mm of the stated value. It should be obvious [3] that "... the specification of such odds can only be made by the experimenter based on ... total laboratory experience. There is no substitute for sound engineering judgment in estimating the uncertainty of a measured variable."

The confidence interval statement is based on the concept of standard deviation for a normal distribution. Odds of about 370 to 1 correspond to $\pm 3\sigma$; 99.7 percent of all future readings are expected to fall within the interval. Odds of about 20 to 1 correspond to $\pm 2\sigma$ and odds of 3 to 1 correspond to $\pm \sigma$ confidence limits. Odds of 20 to 1 typically are used for engineering work.

Step 3 *Analyze the propagation of uncertainty in calculations.* Suppose that measurements of independent variables, x_1, x_2, \dots, x_n , are made in the laboratory. The relative uncertainty of each independently measured quantity is estimated as u_i . The measurements are used to calculate some result, R , for the experiment. We wish to analyze how errors in the x_i 's propagate into the calculation of R from measured values.

In general, R may be expressed mathematically as $R = R(x_1, x_2, \dots, x_n)$. The effect on R of an error in measuring an individual x_i may be estimated by analogy to the derivative of a function [4]. A variation, δx_i , in x_i would cause variation δR_i in R ,

$$\delta R_i = \frac{\partial R}{\partial x_i} \delta x_i$$

The relative variation in R is

$$\frac{\delta R_i}{R} = \frac{1}{R} \frac{\partial R}{\partial x_i} \delta x_i = \frac{x_i}{R} \frac{\partial R}{\partial x_i} \frac{\delta x_i}{x_i} \quad (\text{E.1})$$

Equation E.1 may be used to estimate the relative uncertainty in the result due to uncertainty in x_i . Introducing the notation for relative uncertainty, we obtain

$$u_{R_i} = \frac{x_i}{R} \frac{\partial R}{\partial x_i} u_{x_i} \quad (\text{E.2})$$

How do we estimate the relative uncertainty in R caused by the combined effects of the relative uncertainties in all the x_i s? The random error in each variable has a range of values within the uncertainty interval. It is unlikely that all errors will have adverse values at the same time. It can be shown [1] that the best representation for the relative uncertainty of the result is

$$u_R = \pm \left[\left(\frac{x_1}{R} \frac{\partial R}{\partial x_1} u_1 \right)^2 + \left(\frac{x_2}{R} \frac{\partial R}{\partial x_2} u_2 \right)^2 + \cdots + \left(\frac{x_n}{R} \frac{\partial R}{\partial x_n} u_n \right)^2 \right]^{1/2} \quad (\text{E.3})$$

Example E.2 UNCERTAINTY IN VOLUME OF CYLINDER

Obtain an expression for the uncertainty in determining the volume of a cylinder from measurements of its radius and height. The volume of a cylinder in terms of radius and height is

$$\mathcal{V} = \mathcal{V}(r, h) = \pi r^2 h$$

Differentiating, we obtain

$$d\mathcal{V} = \frac{\partial \mathcal{V}}{\partial r} dr + \frac{\partial \mathcal{V}}{\partial h} dh = 2\pi r h dr + \pi r^2 dh$$

since

$$\frac{\partial \mathcal{V}}{\partial r} = 2\pi r h \quad \text{and} \quad \frac{\partial \mathcal{V}}{\partial h} = \pi r^2$$

From Eq. E.2, the relative uncertainty due to radius is

$$u_{\mathcal{V}, r} = \frac{\delta \mathcal{V}_r}{\mathcal{V}} = \frac{r}{\mathcal{V}} \frac{\partial \mathcal{V}}{\partial r} u_r = \frac{r}{\pi r^2 h} (2\pi r h) u_r = 2u_r$$

and the relative uncertainty due to height is

$$u_{\mathcal{V}, h} = \frac{\delta \mathcal{V}_h}{\mathcal{V}} = \frac{h}{\mathcal{V}} \frac{\partial \mathcal{V}}{\partial h} u_h = \frac{h}{\pi r^2 h} (\pi r^2) u_h = u_h$$

The relative uncertainty in volume is then

$$u_{\mathcal{V}} = \pm [(2u_r)^2 + (u_h)^2]^{1/2} \quad (\text{E.4})$$

Comment:

The coefficient 2, in Eq. E.4, shows that the uncertainty in measuring cylinder radius has a larger effect than the uncertainty in measuring height. This is true because the radius is squared in the equation for volume.

E.4 Applications to Data

Applications to data obtained from laboratory measurements are illustrated in the following examples.

Example E.3 UNCERTAINTY IN LIQUID MASS FLOW RATE

The mass flow rate of water through a tube is to be determined by collecting water in a beaker. The mass flow rate is calculated from the net mass of water collected divided by the time interval,

$$\dot{m} = \frac{\Delta m}{\Delta t} \quad (\text{E.5})$$

where $\Delta m = m_f - m_e$. Error estimates for the measured quantities are

$$\begin{aligned} \text{Mass of full beaker, } m_f &= 400 \pm 2 \text{ g (20 to 1)} \\ \text{Mass of empty beaker, } m_e &= 200 \pm 2 \text{ g (20 to 1)} \\ \text{Collection time interval, } \Delta t &= 10 \pm 0.2 \text{ s (20 to 1)} \end{aligned}$$

The relative uncertainties in measured quantities are

$$u_{m_f} = \pm \frac{2 \text{ g}}{400 \text{ g}} = \pm 0.005$$

$$u_{m_e} = \pm \frac{2 \text{ g}}{200 \text{ g}} = \pm 0.01$$

$$u_{\Delta t} = \pm \frac{0.2 \text{ s}}{10 \text{ s}} = \pm 0.02$$

The relative uncertainty in the measured value of net mass is calculated from Eq. E.3 as

$$\begin{aligned} u_{\Delta m} &= \pm \left[\left(\frac{m_f}{\Delta m} \frac{\partial \Delta m}{\partial m_f} u_{m_f} \right)^2 + \left(\frac{m_e}{\Delta m} \frac{\partial \Delta m}{\partial m_e} u_{m_e} \right)^2 \right]^{1/2} \\ &= \pm \{ [(2)(1)(\pm 0.005)]^2 + [(1)(-1)(\pm 0.01)]^2 \}^{1/2} \\ u_{\Delta m} &= \pm 0.0141 \end{aligned}$$

Because $\dot{m} = \dot{m}(\Delta m, \Delta t)$, we may write Eq. E.3 as

$$u_{\dot{m}} = \pm \left[\left(\frac{\Delta m}{\dot{m}} \frac{\partial \dot{m}}{\partial \Delta m} u_{\Delta m} \right)^2 + \left(\frac{\Delta t}{\dot{m}} \frac{\partial \dot{m}}{\partial \Delta t} u_{\Delta t} \right)^2 \right]^{1/2} \quad (\text{E.6})$$

The required partial derivative terms are

$$\frac{\Delta m}{\dot{m}} \frac{\partial \dot{m}}{\partial \Delta m} = 1 \quad \text{and} \quad \frac{\Delta t}{\dot{m}} \frac{\partial \dot{m}}{\partial \Delta t} = -1$$

Substituting into Eq. E.6 gives

$$u_{\dot{m}} = \pm \{ [(1)(\pm 0.0141)]^2 + [(-1)(\pm 0.02)]^2 \}^{1/2}$$

$$u_{\dot{m}} = \pm 0.0245 \quad \text{or} \quad \pm 2.45 \text{ percent (20 to 1)}$$

Comment:

The 2 percent uncertainty interval in time measurement makes the most important contribution to the uncertainty interval in the result.

Example E.4 UNCERTAINTY IN THE REYNOLDS NUMBER FOR WATER FLOW

The Reynolds number is to be calculated for flow of water in a tube. The computing equation for the Reynolds number is

$$Re = \frac{4\dot{m}}{\pi\mu D} = Re(\dot{m}, D, \mu) \quad (\text{E.7})$$

We have considered the uncertainty interval in calculating the mass flow rate. What about uncertainties in μ and D ? The tube diameter is given as $D = 6.35$ mm. Do we assume that it is exact? The diameter might be measured to the nearest 0.1 mm. If so, the relative uncertainty in diameter would be estimated as

$$u_D = \pm \frac{0.05 \text{ mm}}{6.35 \text{ mm}} = \pm 0.00787 \quad \text{or} \quad \pm 0.787 \text{ percent}$$

The viscosity of water depends on temperature. The temperature is estimated as $T = 24 \pm 0.5^\circ\text{C}$. How will the uncertainty in temperature affect the uncertainty in μ ? One way to estimate this is to write

$$u_{\mu(T)} = \pm \frac{\delta\mu}{\mu} = \frac{1}{\mu} \frac{d\mu}{dT} (\pm \delta T) \quad (\text{E.8})$$

The derivative can be estimated from tabulated viscosity data near the nominal temperature of 24°C . Thus

$$\begin{aligned} \frac{d\mu}{dT} &\approx \frac{\Delta\mu}{\Delta T} = \frac{\mu(25^\circ\text{C}) - \mu(23^\circ\text{C})}{(25 - 23)^\circ\text{C}} = (0.000890 - 0.000933) \frac{\text{N}\cdot\text{s}}{\text{m}^2} \times \frac{1}{2^\circ\text{C}} \\ \frac{d\mu}{dT} &= -2.15 \times 10^{-5} \text{ N}\cdot\text{s}/(\text{m}^2 \cdot {}^\circ\text{C}) \end{aligned}$$

It follows from Eq. E.8 that the relative uncertainty in viscosity due to temperature is

$$\begin{aligned} u_{\mu(T)} &= \frac{1}{0.000911} \frac{\text{m}^2}{\text{N}\cdot\text{s}} \times -2.15 \times 10^{-5} \frac{\text{N}\cdot\text{s}}{\text{m}^2 \cdot {}^\circ\text{C}} \times (\pm 0.5^\circ\text{C}) \\ u_{\mu(T)} &= \pm 0.0118 \quad \text{or} \quad \pm 1.18 \text{ percent} \end{aligned}$$

Tabulated viscosity data themselves also have some uncertainty. If this is ± 1.0 percent, an estimate for the resulting relative uncertainty in viscosity is

$$u_\mu = \pm [(\pm 0.01)^2 + (\pm 0.0118)^2]^{1/2} = \pm 0.0155 \quad \text{or} \quad \pm 1.55 \text{ percent}$$

The uncertainties in mass flow rate, tube diameter, and viscosity needed to compute the uncertainty interval for the calculated Reynolds number now are known. The required partial derivatives, determined from Eq. E.7, are

$$\begin{aligned} \frac{\dot{m}}{Re} \frac{\partial Re}{\partial \dot{m}} &= \frac{\dot{m}}{Re} \frac{4}{\pi\mu D} = \frac{Re}{Re} = 1 \\ \frac{\mu}{Re} \frac{\partial Re}{\partial \mu} &= \frac{\mu}{Re} (-1) \frac{4\dot{m}}{\pi\mu^2 D} = -\frac{Re}{Re} = -1 \\ \frac{D}{Re} \frac{\partial Re}{\partial D} &= \frac{D}{Re} (-1) \frac{4\dot{m}}{\pi\mu D^2} = -\frac{Re}{Re} = -1 \end{aligned}$$

Substituting into Eq. E.3 gives

$$\begin{aligned} u_{Re} &= \pm \left\{ \left[\frac{\dot{m}}{Re} \frac{\partial Re}{\partial \dot{m}} u_{\dot{m}} \right]^2 + \left[\frac{\mu}{Re} \frac{\partial Re}{\partial \mu} u_\mu \right]^2 + \left[\frac{D}{Re} \frac{\partial Re}{\partial D} u_D \right]^2 \right\}^{1/2} \\ u_{Re} &= \pm \left\{ [(1)(\pm 0.0245)]^2 + [(-1)(\pm 0.0155)]^2 + [(-1)(\pm 0.00787)]^2 \right\}^{1/2} \\ u_{Re} &= \pm 0.0300 \quad \text{or} \quad \pm 3.00 \text{ percent} \end{aligned}$$

Comment:

Examples E.3 and E.4 illustrate two points important for experiment design. First, the mass of water collected, Δm , is calculated from two measured quantities, m_f and m_e . For any stated uncertainty interval in the measurements of m_f and m_e , the *relative* uncertainty in Δm can be decreased by making Δm larger. This might be accomplished by using larger containers or a longer measuring interval, Δt , which also would reduce the relative uncertainty in the measured Δt . Second, the uncertainty in tabulated property data may be significant. The data uncertainty also is increased by the uncertainty in measurement of fluid temperature.

Example E.5 UNCERTAINTY IN AIR SPEED

Air speed is calculated from pitot tube measurements in a wind tunnel. From the Bernoulli equation,

$$V = \left(\frac{2gh\rho_{\text{water}}}{\rho_{\text{air}}} \right)^{1/2} \quad (\text{E.9})$$

where h is the observed height of the manometer column.

The only new element in this example is the square root. The variation in V due to the uncertainty interval in h is

$$\frac{h}{V} \frac{\partial V}{\partial h} = \frac{h}{V} \frac{1}{2} \left(\frac{2gh\rho_{\text{water}}}{\rho_{\text{air}}} \right)^{-1/2} \frac{2g\rho_{\text{water}}}{\rho_{\text{air}}}$$

$$\frac{h}{V} \frac{\partial V}{\partial h} = \frac{h}{V} \frac{1}{2} \frac{1}{V} \frac{2g\rho_{\text{water}}}{\rho_{\text{air}}} = \frac{1}{2} \frac{V^2}{V^2} = \frac{1}{2}$$

Using Eq. E.3, we calculate the relative uncertainty in V as

$$u_V = \pm \left[\left(\frac{1}{2} u_h \right)^2 + \left(\frac{1}{2} u_{\rho_{\text{water}}} \right)^2 + \left(-\frac{1}{2} u_{\rho_{\text{air}}} \right)^2 \right]^{1/2}$$

If $u_h = \pm 0.01$ and the other uncertainties are negligible,

$$u_V = \pm \left\{ \left[\frac{1}{2} (\pm 0.01) \right]^2 \right\}^{1/2}$$

$$u_V = \pm 0.00500 \text{ or } \pm 0.500 \text{ percent}$$

Comment:

The square root reduces the relative uncertainty in the calculated velocity to half that of u_h .

E.5 Summary

A statement of the probable uncertainty of data is an important part of reporting experimental results completely and clearly. Many journals require that manuscripts include an adequate statement of uncertainty of experimental data [5]. Estimating uncertainty in experimental results requires care, experience, and judgment, in common with many endeavors in engineering. We have emphasized the need to quantify the uncertainty of measurements. More information is available in References [4, 6, 7]. We urge you to consult them when designing experiments or analyzing data.

REFERENCES

1. Kline, S. J., and F. A. McClintock, "Describing Uncertainties in Single-Sample Experiments," *Mechanical Engineering*, 75, 1, January 1953, pp. 3–9.
2. Pugh, E. M., and G. H. Winslow, *The Analysis of Physical Measurements*. Reading, MA: Addison-Wesley, 1966.
3. Doebelin, E. O., *Measurement Systems*, 4th ed. New York: McGraw-Hill, 1990.
4. Young, H. D., *Statistical Treatment of Experimental Data*. New York: McGraw-Hill, 1962.
5. Rood, E. P., and D. P. Telionis, "JFE Policy on Reporting Uncertainties in Experimental Measurements and Results," *Transactions of ASME, Journal of Fluids Engineering*, 113, 3, September 1991, pp. 313–314.
6. Coleman, H. W., and W. G. Steele, *Experimentation and Uncertainty Analysis for Engineers*. New York: Wiley, 1989.
7. Holman, J. P., *Experimental Methods for Engineers*, 5th ed. New York: McGraw-Hill, 1989.

APPENDIX F

Introduction to Computational Fluid Dynamics

F.1 Introduction to Computational Fluid Dynamics

In this section we will discuss in a very basic manner the ideas behind *computational fluid dynamics* (CFD). We will first review some very basic ideas in numerically solving an ordinary and a partial differential equation with a couple of examples. After studying these, the reader will be able to numerically solve a range of simple CFD problems. Then, for those with further interest in CFD, we will review in more detail some concepts behind numerical methods, particularly CFD. This review will highlight some of the advantages and pitfalls of CFD. We will apply some of these concepts to a simple 1D model, but these concepts are so fundamental that they are applicable to almost any CFD calculation. As we apply the CFD solution procedure to the model, we will comment on the extension to the general case. Our goal is to help the reader understand what CFD entails and the power of it to solve fluid problems.

The Need for CFD

As discussed in Section 5.4, the equations describing fluid flow can be a bit intimidating. For example, even though we may limit ourselves to incompressible flows for which the viscosity is constant, we still end up with the following equations from Chapter 5:

$$\frac{\partial u}{\partial x} + \frac{\partial v}{\partial y} + \frac{\partial w}{\partial z} = 0 \quad (5.1c)$$

$$\rho \left(\frac{\partial u}{\partial t} + u \frac{\partial u}{\partial x} + v \frac{\partial u}{\partial y} + w \frac{\partial u}{\partial z} \right) = \rho g_x - \frac{\partial p}{\partial x} + \mu \left(\frac{\partial^2 u}{\partial x^2} + \frac{\partial^2 u}{\partial y^2} + \frac{\partial^2 u}{\partial z^2} \right) \quad (5.27a)$$

$$\rho \left(\frac{\partial v}{\partial t} + u \frac{\partial v}{\partial x} + v \frac{\partial v}{\partial y} + w \frac{\partial v}{\partial z} \right) = \rho g_y - \frac{\partial p}{\partial y} + \mu \left(\frac{\partial^2 v}{\partial x^2} + \frac{\partial^2 v}{\partial y^2} + \frac{\partial^2 v}{\partial z^2} \right) \quad (5.27b)$$

$$\rho \left(\frac{\partial w}{\partial t} + u \frac{\partial w}{\partial x} + v \frac{\partial w}{\partial y} + w \frac{\partial w}{\partial z} \right) = \rho g_z - \frac{\partial p}{\partial z} + \mu \left(\frac{\partial^2 w}{\partial x^2} + \frac{\partial^2 w}{\partial y^2} + \frac{\partial^2 w}{\partial z^2} \right) \quad (5.27c)$$

Equation 5.1c is the continuity equation (mass conservation) and Eqs. 5.27 are the Navier–Stokes equations (momentum), expressed in Cartesian coordinates. In principle, we can solve these equations for the velocity field $\vec{V} = \hat{i}u + \hat{j}v + \hat{k}w$ and pressure field p , given sufficient initial and boundary conditions. Note that in general, u, v, w , and p all depend on x, y, z , and t . In practice, there is no general analytic solution to these equations, for the combined effect of a number of reasons (none of which is insurmountable by itself):

- 1 They are coupled. The unknowns, u, v, w , and p , appear in all the equations (p is not in Eq. 5.1c) and we cannot manipulate the equations to end up with a single equation for any one of the unknowns. Hence we must solve for all unknowns simultaneously.
- 2 They are nonlinear. For example, in Eq. 5.27a, the convective acceleration term, $u \frac{\partial u}{\partial x} + v \frac{\partial u}{\partial y} + w \frac{\partial u}{\partial z}$, has products of u with itself as well as with v and w . The consequence of this is that we cannot combine one solution of the equations with a second solution to obtain a third solution.
- 3 They are second-order partial differential equations. For example, in Eq. 5.27a, the viscous term, $\mu(\frac{\partial^2 u}{\partial x^2} + \frac{\partial^2 u}{\partial y^2} + \frac{\partial^2 u}{\partial z^2})$, is second-order in u . These are obviously of a different order of complexity than, say, a first-order ordinary differential equation.

These difficulties have led engineers, scientists, and mathematicians to adopt several approaches to the solution of fluid mechanics problems. For relatively simple physical geometries and boundary or initial conditions, the equations can often be reduced to a solvable form. We saw two examples of this in Examples 5.9 and 5.10 (for cylindrical forms of the equations). If we can neglect the viscous terms, the resulting incompressible, inviscid flow can often be successfully analyzed. This is the entire topic of Chapter 6. Most incompressible flows of interest do not have simple geometries and are not inviscid. The only option remaining is to use numerical methods to analyze problems. It is possible to obtain approximate computer-based solutions to the equations for a variety of engineering problems. This is the main subject matter of CFD.

Applications of CFD

CFD is employed in a variety of applications and is now widely used in various industries. As examples of CFD simulations, Figure F.1 shows the paths taken by selected fluid particles around a Formula 1 car. By studying such pathlines and other flow attributes, engineers gain insights into how to design the car so as to reduce drag and enhance performance. The flow through a catalytic converter, a device used to clean automotive exhaust gases, is shown in Figure F.2. This image shows path lines colored by velocity magnitude. CFD helps engineers develop more effective catalytic converters by allowing them to study how different chemical species mix and react in the device. Figure F.3 presents contours of static pressure in a backward-inclined centrifugal fan used in ventilation applications. Fan performance characteristics obtained from the CFD simulations compared well with results from physical tests.

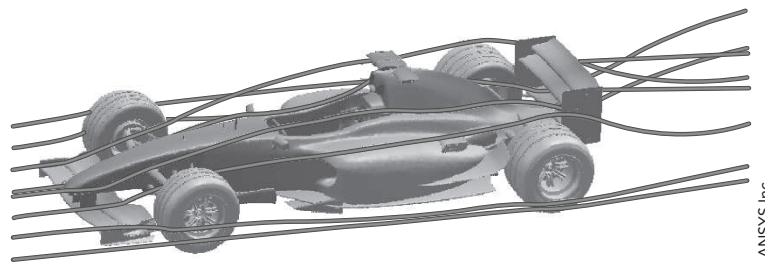


Fig. F.1 Pathlines around a Formula 1 car.



Fig. F.2 Flow through a catalytic converter.

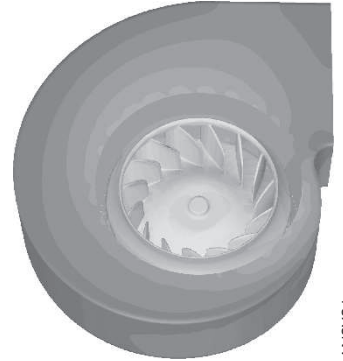


Fig. F.3 Static pressure contours for flow through a centrifugal fan.

F.2 Finite Difference Approach to CFD

We will introduce the approach of CFD using a finite difference approximation to represent the differential equations that describe fluid motion. By using finite differences, we reduce a problem from one of solving differential equations to one of solving algebraic equations. This is a significant advantage that, coupled with the advent of high-speed computing equipment, makes solvable problems that were previously intractable.

We will use as an example the flow between two stationary parallel plates, Section 8.2, where we have only one differential equation and have the exact solution for comparison. For this situation, the analytical solution for the velocity is given by Eq. 8.5 as

$$u = \frac{a^2}{2\mu} \left(\frac{dp}{dx} \right) \left[\left(\frac{y}{a} \right)^2 - \left(\frac{y}{a} \right) \right] \quad (8.5)$$

And the shear stress distribution is given by

$$\tau_{yx} = \mu \left(\frac{dp}{dx} \right) \left[\frac{y}{a} - \frac{1}{2} \right] \quad (8.6a)$$

The shear stress is related to the velocity through Newton's law of viscosity

$$\tau_{yx} = \mu \frac{du}{dy} \quad (2.15)$$

To illustrate the numerical integration process, we will solve for the velocity profile numerically using equations 8.6a and 2.15 and then compare to the exact solution, Eq. 8.5. We first divide the flow up into a grid. Since the velocity is one-dimensional and varies only in the y -direction, we divide the y coordinate into a number of horizontal layers spaced the distance Δy apart. The grid, with the final results for the velocity profile plotted, is shown in Figure F.4. We identify the velocity at a location $y = n$ as u_n , and the next location at $y + \Delta y = n + 1$ as u_{n+1} . We will recast Eq. 2.15 in a simple finite difference form by representing the derivative as a finite difference. The finite difference approximates the derivative as

$$\frac{du}{dy} \approx \frac{\Delta u}{\Delta y} = \frac{u_{n+1} - u_n}{\Delta y}$$

Using the finite difference approximation, we combine Eqs 8.6a and 2.15 as

$$\tau_{yx} = \mu \frac{du}{dy} \approx \mu \frac{u_{n+1} - u_n}{\Delta y} = \mu \left(\frac{dp}{dx} \right) \left[\frac{y_n}{a} - \frac{1}{2} \right]$$

Solving this relation for the velocity at $n = 1$ in terms of the velocity at n , we have

$$u_{n+1} = u_n + \frac{\mu}{\mu} \left(\frac{dp}{dx} \right) \left[\frac{y_n}{a} - \frac{1}{2} \right] \Delta y \quad (F.1)$$

Equation F.1 is now an algebraic *finite difference* equation that represents the velocity at a new y -location in terms of the velocity at a previous location. This simple representation is termed Euler's method. It bases the next value of u only on the previous value and thus there is an error. More sophisticated finite difference formulations reduce the error.

We will illustrate the numerical integration process. We will write Eq. F.1 in terms of the variable y/a and combine the constant terms into a coefficient C :

$$u_{n+1} = u_n + \frac{a^2}{\mu} \left(\frac{dp}{dx} \right) \left[\frac{y_n}{a} - \frac{1}{2} \right] \Delta \left(\frac{y_n}{a} \right) = u_n + C \left[\left(\frac{y_n}{a} \right) - \frac{1}{2} \right] \Delta \left(\frac{y_n}{a} \right) \quad (F.2)$$

We will solve for the velocity profile for a value of $C = -4$ m/s and $a = 1$ cm. The value of C is negative because the pressure gradient is negative. To solve Eq. F.2, we create a table as shown below with values of n , y/a , and u . The coordinate y starts at the wall where the value of u is 0 m/s. We have chosen a relatively large increment of $\Delta y = 0.1$ cm to illustrate the process.

n	y/a	u (m/s)	n	y/a	u (m/s)
1	0		7	0.6	
2	0.1		8	0.7	
3	0.2		9	0.8	
4	0.3		10	0.9	
5	0.4		11	1.0	
6	0.5				

The value of u_2 at $n = 2$ and $y = 0.1$ is calculated as follows:

$$u_2 = u_1 + C \left[\frac{y_1}{a} - \frac{1}{2} \right] \frac{\Delta y}{a} = 0 - 4 \cdot \left[0 - \frac{1}{2} \right] \cdot 0.1 = 0.2 \frac{m}{s}$$

The value of u_3 is calculated similarly

$$u_3 = u_2 + C \left[\frac{y_2}{a} - \frac{1}{2} \right] \Delta y = 0.2 - 4 \cdot \left[0.1 - \frac{1}{2} \right] \cdot 0.1 = 0.36 \frac{m}{s}$$

The process proceeds and the final values are shown in the table below.

n	y/a	u (m/s)	n	y/a	u (m/s)
1	0	0	7	0.6	0.6
2	0.1	0.2	8	0.7	0.56
3	0.2	0.36	9	0.8	0.48
4	0.3	0.48	10	0.9	0.36
5	0.4	0.56	11	1.0	0.2
6	0.5	0.6			

The results for the velocity profile using an increment of $\Delta y/a$ of 0.1 are plotted in Figure F.4. Also shown are values for the same Euler calculation procedure but with a value of $\Delta y/a$ of 0.01. For comparison, the profile obtained analytically, Eq. 8.5 is plotted. The results demonstrate that even a relatively crude grid produces the general shape of the velocity profile. As the number of grid points is increased from 11 to 101, the accuracy becomes much better.

This example illustrates a number of important issues relating to the numerical computation of flow problems. First, for this relatively simple example, we needed a large number of grid points, on the order of 100, to get an accurate answer. Even so, there is still some error and the Euler method does not meet the no-slip condition at the upper wall. The calculated velocity there is small, but nonzero.

More sophisticated numerical techniques such as Crank-Nicholson or Runge-Kutta methods would increase accuracy and allow fewer grid points. These methods involve more complicated calculations and often iteration at each step. For nonlinear equations, there is also the issue of stability and the solutions may not converge or be reasonable if the grid spacing is too large. The calculation time may be increased even though the number of grid points is reduced. Reference [3] describes some of the most widely used finite difference approaches to solving fluid problems.

If we had been interested in solving the developing flow problem for this parallel plate example, we would have also needed a grid that extended downstream. Laminar flow develops on the order of

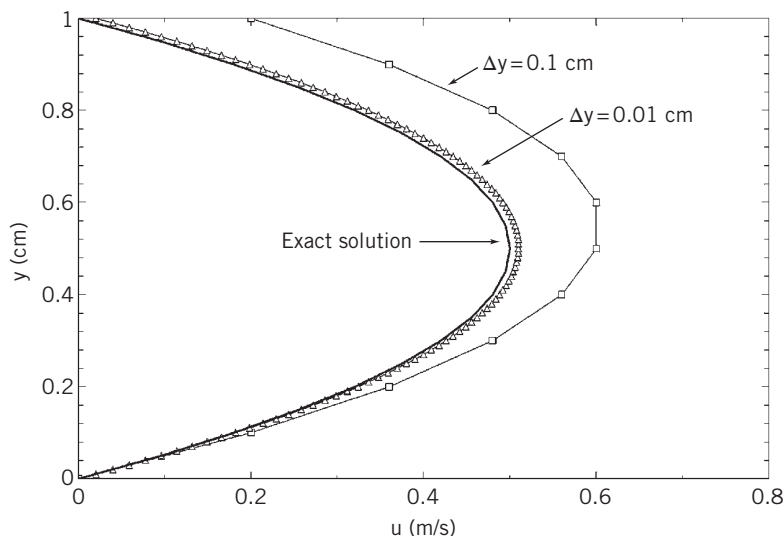


Fig. F.4 Comparison of finite difference and analytical solutions.

100 diameters, and so we would then have needed on the order of 100 times the 100 grid points downstream for each of the grid points across the flow, or on the order of 10,000 downstream grid points. The number of calculations is increased dramatically for more complex flow patterns.

To solve the entry length problem, we would also need more than the steady state relation between the shear stress and pressure gradient. We would need to put the continuity equation and momentum equation in finite difference form. These are coupled equations and the momentum equation is nonlinear and second order and they would need to be solved for u and v simultaneously at each grid point. The calculation time would then be significant.

Another fundamental problem is that finite difference solutions do not necessarily satisfy the conservation equations. This means that there is possibly not a balance between the forces and momentum flows for any one fluid element, leading to errors in the solution.

Lastly, the example problem is for laminar flow. Much of the interest in fluid mechanics is in turbulent flow, which requires accurate models for turbulence. A simple mixing length model for turbulence was presented in Section 8.5. This semi-empirical model is valid for many flows, but complicated flow patterns such as the flow over an automobile or in a combustion chamber require a much more sophisticated turbulence model. Such models exist and are described in [1] and [2], but they often bring in more equations that also need to be solved simultaneously with the continuity and momentum equations.

The general conclusion to draw from this discussion is that finite difference techniques are useful, but not as amenable to complex flow problems as other approaches. Modern CFD codes usually employ other formulations as discussed in the next section.

Techniques of CFD

All CFD approaches employ the same approach of modeling the flow field by using a mesh consisting of cells or elements as illustrated in Figure F.5. This mesh is constructed with a finer structure in the regions of greatest interest and/or the regions with the largest changes in properties. As shown in the figure, the mesh is very fine near the surface of the airfoil and in the wake region and becomes coarse farther from the airfoil.

In the *finite element method* applied to fluid problems, the flow field is also divided up into sub-domains, with the relevant equations applied to each subdomain [4]. For example, a flow field might be divided up into the boundary layer region and the inviscid free stream. The finite element method eliminates the spatial derivatives by approximating the partial differential equations locally with a set of algebraic equations for steady state problems. The equations for the elements are then relatively simple equations that locally approximate the original complex partial differential equations with algebraic equations that describe the flow. The error in this approximation is minimized by fitting trial functions into the partial differential equations and using variational methods to minimize the error. In this step, the conservation equations are satisfied.

Finite element analysis is suitable for analyzing problems over complicated domains such as the flow over a complex shape. In order to simulate a given flow field, a mesh consisting of up to millions of small elements that form the shape of the flow field is created. The calculations are made for each element and the individual results combined to describe the whole flow field. The approximation is due to representing the solution over each mesh by a polynomial. This yields the values of the variable, for example, velocity, at certain points within the element but not at every point.

The *finite volume method* is another commonly used approach for CFD software [5]. The basis for this method is the integral conservation law. The approach is to approximate the conservation law on each of the many control volumes represented by the mesh. The governing partial differential equations are then solved over a finite control volume rather than between grid points. Using the finite volume method guarantees that mass, momentum, and energy fluxes through a particular control volume are conserved.

An advantage of the finite element and finite volume methods over finite difference methods is that a structured mesh is not required. The finite volume method is possibly preferable to other methods in its application of boundary conditions because the values of the conserved variables are determined within the volume element and not at nodes or surfaces.

As in the finite difference methods, models for turbulence are essential to modeling real flows. A number of turbulence models of increasing sophistication have been developed. A number of them are described in References [1] and [2].

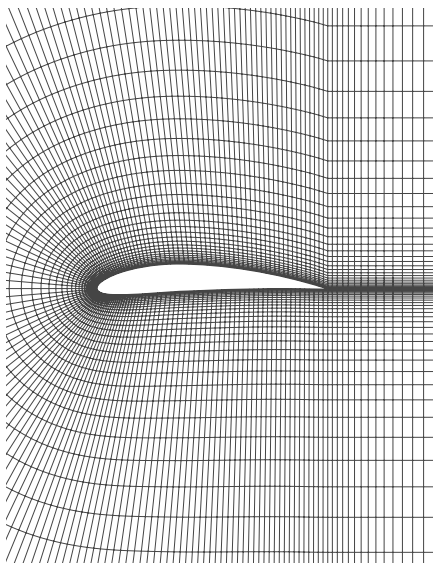


Fig. F.5 Example of CFD mesh used to study the flow over an airfoil.

Computational fluid dynamics is now widely used. The powerful software developed by ANSYS called Fluent [6] is widely used in academic, research, and industrial settings to model complex flow problems. Simulations are commonly used in conjunction with limited laboratory experiments in both basic research and production. There is a reduction in cost and time, as experiments can be expensive and time-consuming to set up, while CFD simulations are relatively inexpensive and fast. In industry, this allows a quick assessment of design variations, with engineering data to be introduced early in the design process. For researchers, CFD can be used to explore new flow situations. The results provide information at any location in the region of interest, rather than being confined to discrete locations as in experiments.

There are several caveats to using CFD codes for analyzing a new situation. The simulation necessitates incorporating many engineering approximations, modeling shortcuts, and real-world variabilities. Turbulence modeling is especially critical. These limitations produce uncertainty in the accuracy of the solution and force the user to determine if the degree of uncertainty is acceptable enough to be useful. Experience is essential as an untrained user has the tendency to believe that the CFD results are true. Carefully constructed experiments may be necessary to validate the CFD solution. The white paper by Linfield and Mudry [7] succinctly summarizes the advantages and limitations of CFD.

REFERENCES

1. Cebeci, T., *Turbulence Models and Their Application*, Horizons Publishing Inc., Long Beach, CA; Springer-Verlag, Berlin, New York, 2004. ISMN 0-9668461-6-8 and ISBN 3-54040288-8
2. Ferzinger, J. H. and M. Peric', *Computational Methods for Fluid Dynamics*, 2nd edition," Springer-Verlag, Heidleberg, New York, 1999, ISBN 3-540-65373-2
3. Patankar, S. V., *Numerical Heat Transfer and Fluid Flow*, Hemisphere Publishing CO., New York, 1980.
4. Myers, G. E., *Analytical methods in conduction heat transfer*, McGraw-Hill Book Company, New York, 1971. Available for Amazon and the Wiley online library <https://onlinelibrary.wiley.com/>
5. Sharma, A., *Introduction to Computational Fluid Dynamics*, John Wiley and Sons, New York, 2017, ISBN 978-11-1900-299-4
6. Fluent, ANSYS, Inc., 2600 ANSYS Drive, Canonsburg, PA 15317, 2019
7. K. W. Linfield, K. W. and R. G. Mudry, *Pros and Cons of CFD and Physical Flow Modeling, A White Papery*, Airflow Sciences Corporation, 2008. <http://www.airflowsciences.com/sites/default/files/docs/Pros-and-Cons-of-CFD-and-Physical-Flow-Modeling.pdf>

Index

- Absolute metric (system of units), 10
Absolute pressure, 42
Absolute viscosity, 27
Acceleration
 convective, 141
 gravitational, 11
 local, 141
 of particle in velocity field, 140, 142
 cylindrical coordinates, 147
 rectangular coordinates, 152
Adiabatic process, 463
Adverse pressure gradient, 33, 176, 314, 323, 326, 328, 346, 409, 487
Alternate depths, 425
Anemometer
 laser Doppler, 289
 thermal, 289
Angle of attack, 314, 327, 328, 396, 405
Angular deformation, 138, 144, 147–149
Angular-momentum principle, 72, 347, 348
 fixed control volume, 110–114
A-pillars, 337
Apparent shear stress, 246
Apparent viscosity, 29
Aqueduct, 415
Archimedes' principle, 61
Area, centroid of, 51
 second moment of, 52
Area ratio, 259
 isentropic flow, 489
Aspect ratio
 airfoil, 331, 405
 flat plate, 320
 rectangular duct, 263
Atmosphere, standard, 42, 48
Average velocity, 78, 229
 open channel, 417
 parallel plates, 234, 238
 pipe, 244, 279, 288

Barometer, 30, 48
Barotropic fluid, 35
Basic equation of fluid statics, 39–42
Basic equations for control volume, 77
 angular-momentum principle, for inertial control volume, 110
 for Euler turbomachine, 348
 conservation of mass, 77–82
 first law of thermodynamics, 118–125
Newton's second law (linear momentum),
 for control volume moving with constant velocity, 97
 for control volume with rectilinear acceleration, 99–105

for differential control volume, 93–96
for nonaccelerating control volume, 83
second law of thermodynamics, 125
Basic laws for system, 71–73
 angular-momentum principle, 72
 conservation of mass, 71–72
 first law of thermodynamics, 72–73
 Newton's second law (linear momentum), 72
 differential form, 151
 second law of thermodynamics, 73
Basic pressure-height relation, 43
Bernoulli equation, 11, 95, 167
 applications, 171–176
 cautions on use of, 176–177
 interpretation as an energy equation, 177–181
 irrotational flow, 185–200
 restrictions on use of, 95, 167, 177
Best efficiency point (BEP), 367
Betz's law, 1, 401
Bingham plastic, 29
Blower, 262, 344, 358, 380
Body force, 23, 72
Boundary layer, 33, 199, 229
 control, 335, 336
 displacement thickness, 296
 effect of pressure gradient on, 314
 flat plate, 296
 laminar, approximate solution, 309–311
 momentum-flux profiles, 315
 momentum integral equation for, 302–306
 momentum thickness, 297
 pressure gradients, 314–316
 separation, 314
 shape factor, 315
 thickness, 296
 transition, 296
 turbulent, 312
 velocity profiles, 315
British Gravitational systems of units, 11
Broad-crested weirs, 457
Buckingham Pi theorem, 203, 407
Buffer layer, 249
Bulk (compressibility) modulus, 35, 469
Buoyancy force, 61

Camber, 328
Capillary effect, 30, 210–211
Capillary rise, 30
Capillary viscometer, 244–245
Cavitation, 35, 213, 371
Cavitation number, 213, 398

Celerity, 419
Center of pressure, 50, 52
Centrifugal pump, 358
CFD, *see* Computational fluid dynamics (CFD)
Chezy equation, 443
Choked flow, 492
Chord, 328, 331
Circulation, 146, 192, 330
Closed system, 5
Compressible flow, 34–35, 406–410, 479
 basic equations for, 480–483
 property changes, 464–465
Compressor, 344, 407
Computational fluid dynamics (CFD), 3, 128, 293, 546
 and Navier–Stokes equations, 154
Conical diffuser, 259, 286
Conjugate depth, 438
Conservation
 of energy, *see* First law of thermodynamics
 of mass, 77–82
 cylindrical coordinates, 133–135
 rectangular coordinates, 129–133
Consistency index, 28
Contact angle, 29
Continuity, *see* Conservation, of mass
Continuity equation, 77
 differential form, 132–133
 cylindrical coordinates, 133
 rectangular coordinates, 131
Continuum, 16
Contracted horizontal weir, 456
Control surface, 6
Control volume, 5, 6, 71
 rate of work done by, 119–121
Convective acceleration, 141
Converging-diverging nozzle, *see* Nozzle
Converging nozzle, *see* Nozzle
Couette flow, 237
Critical conditions, compressible flow, 480
Critical depth, 426–430
Critical flow in open channel, 422, 426–429, 432
Critical pressure ratio, 480, 492
Critical speed
 compressible flow, 480
 open-channel flow, 426
Curl, 145
Cylinder
 drag coefficient, 323
inviscid flow around, 192, 194–196

I-2 Index

- D'Alembert paradox, 32, 33, 199
Deformation
 angular, 138, 144, 147–149
 linear, 149–150
 rate of, 4, 26, 149
Del operator
 cylindrical coordinates, 131, 186
 rectangular coordinates, 131
Density, 4, 16
Density field, 17
Derivative, substantial, 141
Design conditions, *see* Nozzle
Differential equation, nondimensionalizing, 204–206
Differential momentum equation, 152
Diffuser, 258, 274, 347
 optimum geometries, 258
 pressure recovery in, 258, 261
 supersonic, 486
Dilatant, 29
Dilation, volume, 149
Dimensional analysis, 202
Dimensional homogeneity, 9, 10
Dimensions of flow field, 20
Discharge coefficient, 281
 flow nozzle, 281
 orifice plate, 281
 venturi meter, 286
 weir, 456
Displacement thickness, 296
Disturbance thickness, *see* Boundary layer
Doppler effect, 288, 472
Doublet, 189
 strength of, 191
Downwash, 330
Draft tube, 347, 387, 392
Drag, 32, 295
 form, 32, 332
 friction and pressure drag, 320–326
 induced, 330
 parasite, 337
 profile, 332
 pure friction drag, 317–320
 pure pressure drag, 320
 streamlining, 326–328
Drag coefficient, 203, 317
 airfoil, 328, 329
 complete aircraft, 333
 cylinder, 323
 rotating, 339
 flat plate normal to flow, 320
 flat plate parallel to flow, 318
 golf balls, 337
 induced, 330
 selected objects, 320
 sphere, 321
 spinning, 337
 streamlined strut, 327
 supertanker, 319–320
 vehicle, 311
Duct flows, 35
Dynamic pressure, 169, 170
Dynamic similarity, 214
Dynamic viscosity, 26
Dyne, 10
Efficiency, 221
 hydraulic turbine, 353
 propeller, 396
 propulsive, 396
 pump, 222, 262, 351
Elastic, 4, 25
Electric truck, 70
Elementary plane flows, *see* Potential flow theory
End-plate, 334
Energy equation, for pipe flow, 251, 262,
 see also First law of thermodynamics
Energy grade line (EGL), 181–183,
 251, 449
English Engineering (system of units), 10
Enthalpy, 124, 462
Entrance length, 229
Entropy, 463
Equations of motion, *see* Navier–Stokes equations
Equation of state, 4, 483–485
 ideal gas, 4, 461
Euler equations, 163
 along streamline, 165
 cylindrical coordinates, 163
 normal to streamline, 165
 rectangular coordinates, 163
 streamline coordinates, 164
Eulerian method of description, 9, 142
Euler number, 213
Euler's equations, 205
Euler turbomachine equation, 348
Experimental uncertainty, 13
Extensive property, 73
External flow, 35–36
Fan, 262, 344, 358, 380
 “laws,” 223, 382
 specific speed, 382
Federal Aviation Administration (FAA), 335
Field representation, 17
Finite systems, 7
First law of thermodynamics, 72–73,
 118–125
Fittings, losses in, *see* Head loss, in valves and fittings
Flap, 335
Flat plate, flow over, 295
Float-type flow meter, 288
Flow behavior index, 28
Flow coefficient, 222, 281
 flow nozzle, 281
 orifice plate, 281
turbomachine, 353
venturi, 281
Flow field, dimensions of, 18
Flow measurement, 279
 internal flow, 279–290
 linear flow meters, 288
 electromagnetic, 288
 float-type, 288
 rotameter, 288
 turbine, 288
 ultrasonic, 288
 vortex shedding, 288
 traversing methods, 289–290
 laser Doppler anemometer, 289
 thermal anemometer, 289
open-channel flow, 455
restriction flow meters
 flow nozzle, 281
 laminar flow element, 287
 orifice plate, 281
 venturi, 286
Flow meter, *see* Flow measurement
Flow nozzle, 281
Flow similarity. *see* Similarity
Flow visualization, 19, 219
Flow work, 121
Fluid, 3
Fluid machinery
 fan, 344
 performance characteristics, 363
 positive displacement, 344, 384
 propeller, 381
 pump, 344, 384
 turbine, 344, 346
Fluid particle, 9, 18
 forces acting on, 151–152
Fluid rotation, 144–147
Fluid statics
 basic equation of, 39–42
 pressure-height relation, 41
Fluid system, 262, 374
Force
 body, 23, 39
 buoyancy, 60
 compressibility, 212
 drag, 316–328
 gravity, 212
 hydrostatic, 50
 on curved submerged surface, 57
 on plane submerged surface, 50–57
inertia, 206, 212
lift, 316, 328–340
pressure, 32, 39, 212, 316
shear, 317
surface, 23, 40
surface tension, 29, 212
viscous, 212
Forced vortex, 146
Francis turbine, 347, 357, 392
Free-body diagram (FBD), 5, 56

- Free vortex, 145
 Friction drag, *see* Drag
 Friction factor, 253–257
 compressible adiabatic, *see*
 Isentropic flow
 Darcy, 255
 data correlation for, 254
 Fanning, 255
 laminar flow, 256
 smooth pipe correlation, 257
 Frictionless flow, incompressible, 163
 Friction velocity, 248
 Froude number, 213, 216, 419–423
 Fully developed flow, 229
 laminar, 230–245
 turbulent, 246
 Fully rough flow regime, 256
 Gage pressure, 42
 Gas constant
 ideal gas equation of state, 4, 461
 universal, 462
 g_c , 10, 11
 Geometric similarity, 214
 Gibbs equations, 179, 463
 Grade line, 181
 energy, 181–183, 251, 276
 hydraulic, 181–183, 276
 Gradient, 40
 Gradually varied flow, 451
 Ground effect, 337
 Guide vanes, 347
 Head, 182, 349
 gross, 389
 net, 389, 392
 pump, 262, 353, 375
 shutoff, 359
 Head coefficient, 222, 354, 407
 Head loss, 252–253
 in diffusers, 258
 in enlargements and contractions, 258–261
 in exits, 258
 in gradual contractions, 259
 hydraulic jump, 439–441
 in inlets, 258
 major, 253–257
 minor, 258–261
 in miter bends, 261
 in nozzles, 258
 in open-channel flow, 423–430
 in pipe bends, 261
 in pipe entrances, 259
 in pipes, 261
 in sudden area changes, 259
 total, 253
 in valves and fittings, 261
 Head loss coefficient, 258
 Hydraulic depth, 418, 423
 Hydraulic diameter, 246, 262, 418
 Hydraulic grade line, 182, 273, 449
 Hydraulic jump, 419, 435
 basic equation for, 438–439
 depth increase across, 438–439
 head loss across, 439–440
 Hydraulic power, 352, 384
 Hydraulic radius, 418
 Hydraulic turbine, 346, 387
 Hydrostatic force, 50
 on curved submerged surfaces, 57
 on plane submerged surfaces, 50–57
 Hydrostatic pressure distribution, 54
 Hydrostatic pressure force, 90–92
 Hypersonic flow, 471
 Ideal fluid, 187, 199
 Ideal gas, 4, 461
 Impeller, 344, 380
 Incomplete similarity, 216–221
 Incompressible flow, 34–35, 78, 131, 135
 Incompressible fluid, 32
 Individual fluid particle, 71
 Induced drag, 330
 Inertial control volume, 82–99
 Inertial coordinate system, 83, 103
 Infinitesimal systems, 7
 Intensive property, 73
 Internal energy, 461
 Internal flow, 35–36, 228
 Inviscid flow, 32–34, 146
 Irreversible process, 463
 Iрротational flow, 146, 185–200
 Iрротationality condition, 185
 Iрротational vortex, 146, 191
 Isentropic flow
 basic equations for, ideal gas, 476, 488
 converging-diverging nozzle, 496–500
 in converging nozzle, 492–496
 effect of area variation on, 483–500
 flow functions for computation of, 477
 in hs plane, 484
 reference conditions for, 473, 488
 Isentropic process, 466
 Isentropic stagnation properties, 473–480
 Journal bearing, 236
 Kaplan turbine, 347, 392
 Kinematic similarity, 214
 Kinematics of fluid motion
 fluid deformation, 147–150
 fluid rotation, 144–147
 fluid translation, 138–143
 Kinematic viscosity, 27
 Kinetic energy coefficient, 252
 Lagrangian method of description, 142–143
 Laminar boundary layer, 294, 308
 exact solution, 299–302
 flat plate approximate solution, 309–311
 Laminar flow, 34, 228
 between infinite parallel plates, 230–241
 in pipe, 241–245
 Laminar flow element (LFE), 287
 Laplace's equation, 187–189
 Lift, 295, 316, 328–340
 Lift coefficient, 328
 airfoil, 328
 Darrieus rotor blade, 405
 rotating cylinder, 340
 spinning golf ball, 337
 spinning sphere, 337
 Lift/drag ratio, 329
 Lift-induced drag, 15
 Linear deformation, 149–150
 Linear momentum, *see* Newton's second law of motion
 Local oscillations, 323
 Loss coefficient, *see* Head loss
 Loss, major and minor, *see* Head loss
 Mach cone, 471–473
 Mach number, 35, 214, 467
 Magnus effect, 340
 Major loss, *see* Head loss
 Manning
 equation, 443–444
 roughness coefficient, 444
 Manometer, 30, 43
 capillary effect in, 30
 multiple liquid, 47
 reservoir, 45
 sensitivity, 44
 U-tube, 44
 Material derivative, 141
 Measurement, flow, *see* Flow measurement
 Mechanical energy, 179, 245, 251, 263
 Mechanical flow meter, *see* Flow measurement
 Mechanical power, 349
 Meniscus, 30, 210
 Meridional plane, 353
 Meridional velocity, 353
 Meter, flow, *see* Flow measurement
 Methods of description
 Eulerian, 9, 142
 Lagrangian, 7, 142–143
 Minor loss, *see* Head loss
 Minor loss coefficient, *see* Head loss coefficient
 Model studies, 214–225
 Model test facilities, 224–225
 Modulus of elasticity, 35
 Molecular mass, 462
 Momentum
 angular, *see* Angular-momentum principle
 linear, *see* Newton's second law of motion

I-4 Index

- Momentum equation, 101, 151
for control volume moving with constant velocity, 97
for control volume with rectilinear acceleration, 99–105
for differential control volume, 93–96
differential form, 151
for inertial control volume, 82–99
for inviscid flow, 163
Momentum flux, 94
Momentum integral equation, 302–306
for zero pressure gradient flow, 295
Momentum thickness, 297
Moody diagram, 255
Multiple dependent parameters, 221–224
- Nappe, 455
Navier-Stokes equations, 152–159, 204
Negligible pressure effects, 349
Net positive suction head, 366, 371–372
Network, pipe, 276
Newton, 10
Newtonian fluid, 26, 152–159
Newton's second law of motion, 5, 72
Noncircular duct, 262–263
Non-Newtonian fluid, 26, 28–29
apparent viscosity, 29
consistency index, 28
flow behavior index, 28
power-law model, 28
pseudoplastic, 29
rheoplectic, 29
thixotropic, 29
time-dependent, 29
viscoelastic, 29
Normal depth, 442
Normal shock, 501
basic equations for, 501–503
flow functions for computation of, 503–507
supersonic channel flow with, 507–509
Ts diagram, 506
Normal stress, 23, 39, 119–120
No-slip condition, 4, 18, 33, 199, 229
Nozzle, 172, 176, 485
choked flow in, 493, 497
converging, 485, 492–496
converging-diverging, 487, 507
design conditions, 497, 508
incompressible flow through, 175, 372, 486
normal shock in, 507
- Oblique shock, 508
One-dimensional compressible flow, basic equations
continuity equation, 481
equation of state, 483
first law of thermodynamics, 481–482
momentum equation, 481
- second law of thermodynamics, 482
One-dimensional flow, 18–19
Open-channel flow, 36, 419
critical flow, 422, 426–429
energy equation for, 423–429
geometric properties, 419
gradually varied depth, 419–420, 451
hydraulic jump, 419, 435
measurements in, 455
normal depth, 442
rapidly varied flow, 423, 432
steady uniform flow, 441–444
total head, 425
- Open system, 5
Orifice plate, 281
- Parasite drag, 337
Particle derivative, 141
Pathline, 19, 20
Pelton wheel, 347, 392
Pipe
head loss, *see* Head loss
laminar flow in, 212, 229, 241–245
noncircular, 262–263
roughness, 254, 255
standard sizes, 265
turbulent flow in, 228, 246
- Pipe flow, 35
pressure drop, 208–209
- Pipe systems, 261, 276
networks, 276
pumps in, 262, 374
- Pitch, 396, 398
Pi theorem, 203
Pitot-static tube, 171
Pitot tube, 171
Planform area, 327
Poise, 27
Polar plot, lift-drag, 329
Potential flow theory, 187
elementary plane flows
doublet, 191
sink, 191
source, 191
uniform flow, 192
vortex, 191
functions for five elementary two-dimensional flows, 189
- Potential function, 186
Potential, velocity, 186–187
Power coefficient, 222, 348, 354, 367
Power-law model, non-Newtonian fluid, 28
Power-law velocity profile, 250
Prandtl boundary layer equations, 249
Pressure, 39
absolute, 42
center of, 52
dynamic, 169–171, 258
gage, 42
stagnation, 169–171
- static, 169–171
thermodynamic, 121, 153, 169
- Pressure coefficient, 213, 337
Pressure distribution, 316
airfoil, 320
automobile, 337
converging-diverging nozzle, 487, 508
converging nozzle, 493
cylinder, 339
cylinder, inviscid flow, 192, 195
diffuser, 258, 314
sphere, 33, 337
wing, 7
- Pressure drag, *see* Drag
- Pressure field, 39
- Pressure force, 40
- Pressure gradient, 40, 294
effect on boundary layer, 320
- Pressure recovery coefficient, 258
- Pressure tap, 169, 182, 281
- Primary dimension, 9, 207
- Profile, velocity, *see* Velocity profile
- Propeller, 346, 381, 395
actuator disk, 397
efficiency, 396
pitch, 398
power coefficient, 398
propulsive efficiency, 396
solidity, 346
speed of advance coefficient, 398
thrust coefficient, 398
torque coefficient, 398
- Propulsive efficiency, 396
- Pseudoplastic, 29
- Pump, 344
in fluid system, 262, 344
“laws,” 223
operating point, 350
parallel operation, 367, 378
positive displacement, 384–387
series operation, 367, 378
specific speed, 353
variable-speed operation, 367, 379
- Rate of deformation, 4, 26, 149
Reentrant entrance, 259
Reference frame, noninertial, 100
Repeating parameter, 208
Restriction flow meters, 279–290
Reversible process, 463
Reynolds experiment, 228
Reynolds number, 32, 205, 212
critical, *see* Transition
Reynolds stress, 246
Reynolds transport theorem, 76
Rheoplectic, 29
Rotating control volume, 113–118
Rotor, 345
Roughness coefficient, Manning, 444
Roughness, pipe, 254, 255

- Secondary dimension, 10
 Secondary flow, 261
 Second law of thermodynamics, 73, 125, 126
 Separation, 258, 294
 Separation point, 33
 Sequent depth, 438
 Shaft work, 119
 Shape factor, velocity profile, 315
 Sharp-crested weirs, 455
 Shear rate, 26
 Shear stress, 3, 23, 138
 distribution in pipe, 243
 Shear work, 120
 Shockless entry flow, 350
 Shock, normal, *see* Normal shock
 Shock, oblique, *see* Oblique shock
 Shutoff head, 359
 Significant figures, 3
 Similarity
 dynamic, 214
 geometric, 214
 incomplete, 216–221
 kinematic, 214
 rules, 367–369
 Similar velocity profiles, 299
 Sink, 189
 Skin friction coefficient, 308, 443
 Slope, bed, 419
 Slug, 10
 Sluice gate, 90–92, 174–175, 424
 Solidity, 346
 Sonic flow, 486–487
 Sound waves, propagation
 Mach cone, 471–473
 speed of sound
 continuity equation, 468
 momentum equation, 468–470
 Source, strength of, 189
 Span, wing, 327, 330
 Specific energy, 425–426
 Specific gravity, 17
 Specific heat
 constant pressure, 462
 constant volume, 462
 Specific heat ratio, 462
 Specific speed, 223, 348, 353, 382
 Specific volume, 121, 424, 462
 Specific weight, 17
 Speed of advance coefficient, 398
 Speed of sound, 467–470
 ideal gas, 469
 solid and liquid, 469
 Sphere
 drag coefficient, 322
 flow around, 33
 pressure distribution, 322
 Spin ratio, 337
 Stability, 60–63
 Stage, 345
 Stagnation enthalpy, 406, 482
 Stagnation point, 33, 195, 197, 294
 Stagnation pressure, 169–171
 isentropic, *see* Isentropic stagnation properties
 Stagnation pressure probe, 170
 Stagnation properties, *see* Isentropic stagnation properties
 Stagnation state, 474
 Stagnation temperature, 480
 Standard atmosphere, 42
 Standard pipe sizes, 265
 Static fluid, pressure variation in, 43–50
 Static pressure, 169
 Static pressure probe, 169
 Static pressure tap, 170
 Steady flow, 18, 79, 131, 442
 Stoke, 27
 Stokes' theorem, 147
 STP (standard temperature and pressure), 16, 216
 Streakline, 19
 Stream function, 135–137
 Streamline, 19, 33
 coordinates, 164, 167
 curvature, 165, 337
 equation of, 20, 21, 136
 Stream tube, 93, 177
 Stress, 23
 components, 24, 152
 compressive, 40
 Newtonian fluid, 153
 normal, 23, 121, 152
 notation, 24
 shear, 23, 159
 sign convention, 24
 yield, 28, 29
 Stress field, 23–25
 Strouhal number, 288, 324
 Subsonic flow, 485–486
 Substantial derivative, 141
 Sudden expansion, 258
 Superposition, of elementary plane flows, 191–199
 direct method of, 192
 inverse method of, 199
 Supersonic flow, 486
 Supersonic passenger aircraft design, 460
 Supersonic passenger transportation, 460
 Surface force, 23
 Surface tension, 29
 Surface waves, speed of, 419–423
 System derivative, 73
 relation to control volume, 76
 System head curves, 375
 Systems, 6
 of dimensions, 9–10
 of units, 10–11
 System volume, 5
 Taylor series expansion, 39, 129, 133, 144, 147, 151, 232, 303
Tds equations, 463
 Theoretical hydrodynamics, 295
 Thermodynamic pressure, *see* Pressure
 Thermodynamics, review of, 461–467
 Thixotropic, 29
 Three-dimensional flow, 18–19
 Throat, nozzle, 487, 498
 Thrust coefficient, 398
 Time-independent behavior, 28
 Timeline, 19
 Torque coefficient, 348, 354, 398
 Total head tube, 170
 Trailing vortex, 331, 334
 Transition, 212, 256, 294, 323
 Transonic flow, 471
Ts diagram, 463, 484, 494
 constant-property lines, 466–467
 Turbine, 346
 hydraulic, 346, 356, 387
 impulse, 347, 389, 392
 reaction, 347, 387, 392
 specific speed, 348, 353, 382
 wind, 347, 395, 400
 Turbine flow meter, 288
 Turbofan engines, 460
 Turbomachine, 344
 axial flow, 344, 359–362
 centrifugal, 344
 fan, 344, 358
 flow coefficient, 222, 348, 353, 357
 head coefficient, 222, 354
 mixed flow, 344
 power coefficient, 222, 353, 366, 402, 407
 pump, 344
 radial flow, 344, 350, 359
 scaling laws for, 223
 specific speed, 223, 353–358
 stage, 345
 torque coefficient, 348, 354, 398
 Turbulent boundary layer, flat plate, 312
 Turbulent flow, 34, 228
 Turbulent pipe flow, 247
 fluctuating velocity, 247
 mean velocity, 247, 248
 shear stress distribution, 246
 velocity profile, 247–251
 Two-dimensional flow, 20
 Uncertainty, experimental, 13
 Underexpanded nozzle, 497
 Uniform flow
 in open channel, 441–444
 at a section, 18, 79
 Uniform flow field, 197
 Units, 9
 Universal gas constant, 462
 Unsteady flow, 20, 82

I-6 Index

- Vapor pressure, 35
Vector, differentiation of, 131, 134, 142
Velocity diagram, 350–351
Velocity field, 17
Velocity measurement, *see* Flow measurement
Velocity potential, 186–187
Velocity profile, 27, 243, 247–251
Vena contracta, 258, 273, 280
Venturi flowmeter, 281, 286
Viscoelastic, 4, 29
Viscometer, capillary, 244–245
Viscosity, 4, 29
 absolute (or dynamic), 27
 apparent, 29
 kinematic, 27
Viscous flow, 4, 25, 32–34
Viscous sublayer, 248
Visualization, flow, 19, 219
V-notch weirs, 456
Volume dilation, 149
Volume flow rate, 78
Vortex, 146, 197
 irrotational, 146, 191
 shedding, 288, 323
 strength of, 190
 trailing, 330, 332
Vorticity, 146
Wake, 33, 314, 316
Wall shear stress, 247, 255, 301, 313, 314
Water hammer, 35
Waves, capillary, 30
Weber number, 214
Weir, 455
 broad crested, 455, 457
 coefficient, 455
 contracted rectangular, 456
 suppressed rectangular, 455–456
 triangular, 456
Wetted area, 317
Wetted perimeter, 263, 418, 450
Windmill, 344, 400
Wind power, 344, 347, 400
Wind tunnel, 215, 219, 224
Wind turbines, 1, 347
Winglet, 334
Wing loading, 332
Wing span, 330
Work, rate of, 119–121
 shaft, 119
 shear, 120
 sign convention for, 73, 119
Yield stress, 28
Zero pressure gradient flow, 295
 laminar flow, 307–311
 turbulent flow, 311–314
Zone of action, 472
 of silence, 472

WILEY END USER LICENSE AGREEMENT

Go to www.wiley.com/go/eula to access Wiley's ebook EULA.